

DEEP-SEA RESEARCH PART II

Topical Studies in Oceanography

Special Issue: Understanding Ecosystem Processes
in the Eastern Bering Sea II

Guest Editors: Carin J. Ashjian, H. Rodger Harvey, Michael W. Lomas,
Jeffrey M. Napp, Michael F. Sigler, Phyllis J. Stabeno,
and Thomas I. Van Pelt

Volume 94, 2013

CONTENTS

Editorial	1	Appreciation
Introduction H. Rodger Harvey and M.F. Sigler	2	An introduction to the Bering Sea Project: Volume II
Special Issue Articles M.S. Baumann, S.B. Moran, R.P. Kelly, M.W. Lomas and D.H. Shull	7	^{234}Th balance and implications for seasonal particle retention in the eastern Bering Sea
C. Tsukazaki, K.-I. Ishii, R. Saito, K. Matsuno, A. Yamaguchi and I. Imai	22	Distribution of viable diatom resting stage cells in bottom sediments of the eastern Bering Sea shelf
L.W. Cooper, M.G. Sexson, J.M. Grebmeier, R. Gradinger, C.W. Mordy and J.R. Lovvorn	31	Linkages between sea-ice coverage, pelagic–benthic coupling, and the distribution of spectacled eiders: Observations in March 2008, 2009 and 2010, northern Bering Sea
R. Ohashi, A. Yamaguchi, K. Matsuno, R. Saito, N. Yamada, A. Iijima, N. Shiga and I. Imai	44	Interannual changes in the zooplankton community structure on the southeastern Bering Sea shelf during summers of 1994–2009
E.B. Sherr, B.F. Sherr and C. Ross	57	Microzooplankton grazing impact in the Bering Sea during spring sea ice conditions

(Continued on inside back cover)

For a full and complete Guide for Authors, please go to <http://www.elsevier.com/locate/dsr2>.

Available online at www.sciencedirect.com

ScienceDirect



0967-0645(20131001)94:C;1-P

94

DEEP-SEA RESEARCH II Vol. 94 (2013) 1–342

Bering Sea

ELSEVIER



Volume 94

1 October 2013

ISSN 0967-0645

DEEP-SEA RESEARCH PART II

Editor:
John D. Milliman

Guest Editors

Carin J. Ashjian
H. Rodger Harvey
Michael W. Lomas
Jeffrey M. Napp
Michael F. Sigler
Phyllis J. Stabeno
Thomas I. Van Pelt

Understanding Ecosystem Processes
in the Eastern Bering Sea II



www.elsevier.com/locate/dsr2

DEEP-SEA RESEARCH II

<http://www.elsevier.com/locate/dsr2>

Editor

PROFESSOR JOHN D. MILLIMAN: *Virginia Institute of Marine Science, School of Marine Science, The College of William and Mary, P.O. Box 1346, Gloucester Point, VA 23062-1346, USA*
E-mail: milliman@vims.edu

Associate Editors

J.W. MURRAY (*Chemistry*): *School of Oceanography, WB-10, University of Washington, Seattle, WA 98195, U.S.A.* E-mail: jmurray@ocean.washington.edu

SHARON L. SMITH: *The Rosenstiel School, University of Miami, 4600 Rickenbacker Causeway, Miami, FL 33149, USA.* E-mail: ssmith@rsmas.miami.edu

Founder Editor: DR. MARY SEARS

Publication information: *Deep-Sea Research II* (ISSN 0967-0645). For 2013, volumes 85–98 (14 issues) are scheduled for publication. Subscription prices are available upon request from the Publisher or from the Elsevier Customer Service Department nearest you or from this journal's website (<http://www.elsevier.com/locate/dsr2>). Further information is available on this journal and other Elsevier products through Elsevier's website (<http://www.elsevier.com>). Subscriptions are accepted on a prepaid basis only and are entered on a calendar year basis. Issues are sent by standard mail (surface within Europe, air delivery outside Europe). Priority rates are available upon request. Claims for missing issues should be made within six months of the date of dispatch.

Orders, claims, and journal inquiries: please contact the Elsevier Customer Service Department nearest you:

St. Louis: Elsevier Customer Service Department, 3251 Riverport Lane, Maryland Heights, MO 63043, USA; phone: (877) 8397126 [toll free within the USA]; (+1) (314) 4478878 [outside the USA]; fax: (+1) (314) 4478077; e-mail: JournalCustomerService-usa@elsevier.com

Oxford: Elsevier Customer Service Department, The Boulevard, Langford Lane, Kidlington, Oxford OX5 1GB, UK; phone: (+44) (1865) 843434; fax: (+44) (1865) 843970; e-mail: JournalsCustomerServiceEMEA@elsevier.com

Tokyo: Elsevier Customer Service Department, 4F Higashi-Azabu, 1-Chome Bldg, 1-9-15 Higashi-Azabu, Minato-ku, Tokyo 106-0044, Japan; phone: (+81) (3) 5561 5037; fax: (+81) (3) 5561 5047; e-mail: JournalsCustomerServiceJapan@elsevier.com

Singapore: Elsevier Customer Service Department, 3 Killiney Road, #08-01 Winsland House I, Singapore 239519; phone: (+65) 63490222; fax: (+65) 67331510; e-mail: JournalsCustomerServiceAPAC@elsevier.com

Author inquiries: For enquiries relating to the submission of articles (including electronic submission) please visit this journal's homepage at <http://www.elsevier.com/locate/dsr2>. For detailed instructions on the preparation of electronic artwork, please visit <http://www.elsevier.com/artworkinstructions>. Contact details for questions arising after acceptance of an article, especially those relating to proofs, will be provided by the publisher. You can track accepted articles at <http://www.elsevier.com/trackarticle>. You can also check our Author FAQs at <http://www.elsevier.com/authorFAQ> and/or contact Customer Support via <http://support.elsevier.com>.

Advertising information: If you are interested in advertising or other commercial opportunities please e-mail Commercialsales@elsevier.com and your enquiry will be passed to the correct person who will respond to you within 48 hours.

Printed by Henry Ling Ltd., Dorchester, United Kingdom

© The paper used in this publication meets the requirements of ANSI/NISO Z39.48-1992 (Permanence of Paper)

DEEP-SEA RESEARCH II, Vol. 94, 2013

(Continued from outside back cover)

- | | | |
|---|-----|---|
| L. Gemery, T.M. Cronin, L.W. Cooper and J.M. Grebmeier | 68 | Temporal changes in benthic ostracode assemblages in the Northern Bering and Chukchi Seas from 1976 to 2010 |
| M.E.S. Esch, D.H. Shull, A.H. Devol and S.B. Moran | 80 | Regional patterns of bioturbation and iron and manganese reduction in the sediments of the southeastern Bering Sea |
| R.E.A. Horak, H. Whitney, D.H. Shull, C.W. Mordy and A.H. Devol | 95 | The role of sediments on the Bering Sea shelf N cycle: Insights from measurements of benthic denitrification and benthic DIN fluxes |
| G.V. Khen, E.O. Basyuk, N.S. Vanin and V.I. Matveev | 106 | Hydrography and biological resources in the western Bering Sea |
| A.J. Hermann, G.A. Gibson, N.A. Bond, E.N. Curchitser, K. Hedstrom, W. Cheng, M. Wang, P.J. Stabeno, L. Eisner and K.D. Cieciel | 121 | A multivariate analysis of observed and modeled biophysical variability on the Bering Sea shelf: Multidecadal hindcasts (1970–2009) and forecasts (2010–2040) |
| E.C. Siddon, R.A. Heintz and F.J. Mueter | 140 | Conceptual model of energy allocation in walleye pollock (<i>Theragra chalcogramma</i>) from age-0 to age-1 in the southeastern Bering Sea |
| R.A. Heintz, E.C. Siddon, E.V. Farley Jr. and J.M. Napp | 150 | Correlation between recruitment and fall condition of age-0 pollock (<i>Theragra chalcogramma</i>) from the eastern Bering Sea under varying climate conditions |
| T. Wilderbuer, W. Stockhausen and N. Bond | 157 | Updated analysis of flatfish recruitment response to climate variability and ocean conditions in the Eastern Bering Sea |
| B.A. Agler, G.T. Ruggerone, L.I. Wilson and F.J. Mueter | 165 | Historical growth of Bristol Bay and Yukon River, Alaska chum salmon (<i>Oncorhynchus keta</i>) in relation to climate and inter- and intraspecific competition |
| A. Harding, R. Paredes, R. Suryan, D. Roby, D. Irons, R. Orben, H. Renner, R. Young, C. Barger, I. Dorresteijn and A. Kitaysky | 178 | Does location really matter? An inter-colony comparison of seabirds breeding at varying distances from productive oceanographic features in the Bering Sea |
| S. Vincenzi and M. Mangel | 192 | Linking food availability, body growth and survival in the black-legged kittiwake <i>Rissa tridactyla</i> |
| T.I. Smart, E.C. Siddon and J.T. Duffy-Anderson | 201 | Vertical distributions of the early life stages of walleye pollock (<i>Theragra chalcogramma</i>) in the Southeastern Bering Sea |
| S.L. Parker-Stetter, J.K. Horne, E.V. Farley, D.H. Barbee, A.G. Andrews III, L.B. Eisner and J.M. Nomura | 211 | Summer distributions of forage fish in the eastern Bering Sea |
| S. Kotwicki and R.R. Lauth | 231 | Detecting temporal trends and environmentally-driven changes in the spatial distribution of bottom fishes and crabs on the eastern Bering Sea shelf |
| N.A. Friday, A.N. Zerbini, J.M. Waite, S.E. Moore and P.J. Clapham | 244 | Cetacean distribution and abundance in relation to oceanographic domains on the eastern Bering Sea shelf, June and July of 2002, 2008, and 2010 |

(Continued on last page)

Cover Image: Encountering pancake sea ice as the icebreaker USCGC *Healy* steams northward into the seasonal ice of the Bering Sea, March 2009. (Photo by Thomas Van Pelt).

DEEP-SEA RESEARCH

PART II

Topical Studies in Oceanography

Understanding Ecosystem Processes in the Eastern Bering Sea II

Guest Editors

Carin J. Ashjian

Woods Hole Oceanographic Institution
Woods Hole, Massachusetts

H. Rodger Harvey

Ocean, Earth, and Atmospheric Sciences
Old Dominion University
Norfolk, Virginia

Michael W. Lomas

Bigelow Laboratory for Ocean Sciences,
East Boothbay, Maine

Jeffrey M. Napp

Alaska Fisheries Science Center
NOAA
Seattle, Washington

Michael F. Sigler

Alaska Fisheries Science Center
NOAA
Juneau, Alaska

Phyllis J. Stabeno

Pacific Marine Environmental Laboratory
NOAA
Seattle, Washington

Thomas I. Van Pelt*

North Pacific Research Board
Anchorage, Alaska

*Managing Guest Editor
E-mail address: tvanpelt@nprb.org



ELSEVIER

Amsterdam • Boston • London • New York • Oxford • Paris • Philadelphia • San Diego • St. Louis

STATEMENT POLICY

Deep-Sea Research Part II: Topical Studies in Oceanography Publishes the topical issues arising from the many international and interdisciplinary projects which are undertaken.

Shorter research papers are welcomed for *Deep-Sea Research Part I: Oceanographic Research Papers*. Acceptable topics for papers include:

- (1) **the results of original scientific research**
- (2) **theoretical work of evident oceanographic applicability**
- (3) **the solution of some instrumental or laboratory problem with evidence of its successful use, and**
- (4) **applications of oceanography.**

Papers dealing with research on continental shelves (water depths shallower than 100–200 m) in most cases should be submitted to our sister journal *Continental Shelf Research*.

Progress reports and review articles may be invited by the Editor but these are generally more appropriate for *Progress in Oceanography*.

© 2013 Elsevier Ltd. All rights reserved.

This journal and the individual contributions contained in it are protected under copyright by Elsevier Ltd, and the following terms and conditions apply to their use:

Photocopying

Single photocopies of single articles may be made for personal use as allowed by national copyright laws. Permission of the publisher and payment of a fee is required for all other photocopying, including multiple or systematic copying, copying for advertising or promotional purposes, resale, and all forms of document delivery. Special rates are available for educational institutions that wish to make photocopies for non-profit educational classroom use.

For information on how to seek permission visit www.elsevier.com/permissions or call: (+44) 1865 843830 (UK) / (+ 1) 215 239 3804 (USA).

Derivative Works

Subscribers may reproduce tables of contents or prepare lists of articles including abstracts for internal circulation within their institutions. Permission of the publisher is required for resale or distribution outside the institution.

Permission of the publisher is required for all other derivative works, including compilations and translations (please consult www.elsevier.com/permissions).

Electronic Storage or Usage

Permission of the Publisher is required to store electronically any material contained in this journal, including any article or part of an article (please consult www.elsevier.com/permissions).

Except as outlined above, no part of this publication may be reproduced, stored in a retrieval system or transmitted in any form or by any means, electronic, mechanical, photocopying, recording or otherwise, without prior written permission of the publisher.

Notice

No responsibility is assumed by the Publisher for any injury and/or damage to persons or property as a matter of products liability, negligence or otherwise, or from any use or operation of any methods, products, instructions or ideas contained in the material herein. Because of rapid advances in the medical sciences, in particular, independent verification of diagnoses and drug dosages should be made.

Although all advertising material is expected to conform to ethical (medical) standards, inclusion in this publication does not constitute a guarantee or endorsement of the quality or value of such product or of the claims made of it by its manufacturer.

Funding body agreements and policies

Elsevier has established agreements and developed policies to allow authors whose articles appear in journals published by Elsevier to comply with potential manuscript archiving requirements as specified as conditions of their grant awards. To learn more about existing agreements and policies please visit <http://www.elsevier.com/fundingbodies>.

Abstracted/indexed in *BIOBASE*, *BIOSIS databases/Zoological Records*, *CAB International*, *Chemical Abstracts Service*, *Current Awareness in Biological Sciences*, *Current Contents ASCA/Engineering Technology & Applied Science/Science Citation Index/SCISEARCH Data*, *Current Contents/Agriculture, Biology & Environmental Sciences*, *Current Contents/Physics, Chemical, & Earth Sciences*, *Engineering Index*, *Environmental Periodicals Bibliograph, Bib & Index*, *INSPEC Data/Cam Sci Abstr*, *Marine Literature Review*, *Meteorological and Geostrophysical Abstracts*, *Oceanbase*, *Oceanographic Literature Review*, *Research Alert*, *Scisearch*. Also covered in the abstract and citation database *SciVerse SCOPUS®*. Full text available on *SciVerse ScienceDirect®*.



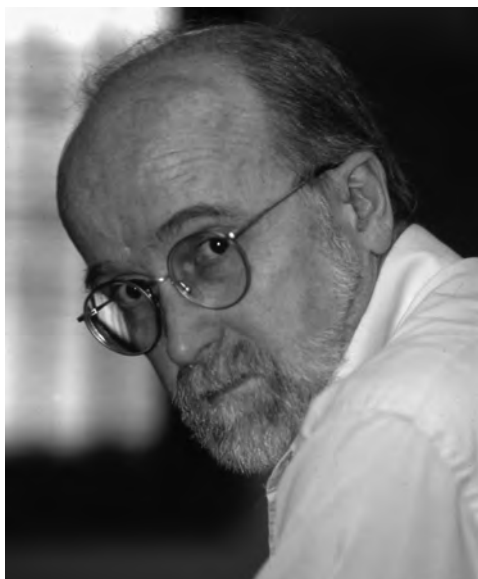
Contents lists available at ScienceDirect

Deep-Sea Research II

journal homepage: www.elsevier.com/locate/dsr2



Appreciation



We – the Science Advisory Board and the community of participants in the Bering Sea Project – dedicate the second special issue to Dr. William J. Wiseman, Jr., with appreciation and gratitude. We wish to recognize him for his vision, to thank him for facilitating the Bering Sea Project, and to admire his tireless efforts on behalf of this project and the many others he supported in the U.S. Arctic.

Bill Wiseman has been the Program Director for the Arctic Natural Sciences Program within the Office of Polar Programs at the National Science Foundation since 2003. His leadership and collaboration with Dr. Clarence Pautzke, former Executive Director of the North Pacific Research Board, was what created and sustained this collaborative program in the eastern Bering Sea. His promotion of integration among disciplines and projects is resulting in synthetic products that exemplify the success of the Program.



Introduction

An introduction to the Bering Sea Project: Volume II

1. Introduction

As one of the most productive marine ecosystems in the world, the Bering Sea is a region particularly sensitive to climate. Seasonal ice cover acts as a major organizing driver, and in winter, geology, latitude, and circulation combine to produce ice cover extending south an estimated 1700 km, that is unmatched elsewhere in the northern hemisphere. In the spring and summer seasons, the retreating ice, longer daylight hours, and nutrient-rich ocean waters forced onto the shallow continental shelf result in intense marine productivity, sustaining nearly half of the U.S. annual commercial fish landings and providing food and cultural value to thousands of coastal and island residents. The predicted major changes in ice cover in the coming decades (Overland et al., 2012) have intensified concern over the future of this economically and culturally important region.

In response to these ongoing observations of a changing region, the North Pacific Research Board (NPRB) and the National Science Foundation (NSF) created an important partnership to support the study of how climate change affects the Bering Sea ecosystem from lower trophic level organisms (e.g. plankton) to humans. The “Bering Sea Project” integrates two research programs, the NSF Bering Ecosystem Study (BEST) and the NPRB Bering Sea Integrated Ecosystem Research Program (BSIERP), with substantial in-kind contributions from National Oceanic and Atmospheric Administration and the U.S. Fish and Wildlife Service. The program spans the Eastern Bering Sea shelf and slope from the Alaska Peninsula to the border of the U.S. Economic Exclusive Zone with Russia. Over the 6 year program and its ongoing synthesis, the Bering Sea Project has provided new insights into the functioning of the eastern Bering Sea ecosystem, particularly in the northern domain where data sets and temporal coverage have been sparse.

The first special volume of DSR II which presented the results of the Bering Sea program included twenty four papers that described new information on this ecosystem, placed new results in their historical context, and assessed their implications for the future of Bering Sea ecosystem as a whole. It coalesced a rich series of new information that explored the ecosystem and the complex linkages of trophic interactions and functions. Each of these papers addressed one or more of the core program hypotheses which guided the field program and ongoing synthesis activities. These hypotheses include (1) physical forcing and its modification by climate affects food availability; (2) ocean conditions structure trophic relationships through bottom-up processes; (3) ecosystem controls are dynamic; (4) location matters; and (5) commercial and subsistence fisheries reflect climate. The papers in the first issue were largely results gained from individual investigator or

small study teams, testing these hypotheses and extending their analyses to consider the observed variability that typifies this dynamic system. The papers in this second issue of *Deep Sea Research II* continue to present new information gained from various projects and data sets, but also extend to include several synthetic results. This issue is organized to reflect these hypotheses, and many papers include comparative results across seasons and domains. This issue also incorporates several papers from parallel studies conducted through related programs in the region including the Ecosystem Studies of Sub-Arctic Seas (ESSAS) Program, which addresses the need to understand how climate change will affect the marine ecosystems of the sub-arctic seas and their sustainability. Finally, we note the ongoing efforts to recognize the complex heterogeneity of the Eastern Bering Sea system and need for tools to support spatially explicit modeling.

2. Physics structure trophic relationships

These first two hypotheses of the Bering Sea Program reflect the role of physical environment on ecosystem structure and the complex response of all trophic levels driven by spatial and temporal changes in primary production. A climate-induced change in physical forcing was hypothesized to modify the availability and partitioning of food for all trophic levels through bottom-up processes. Primary production is the dominant source of organic matter on the Eastern Bering shelf as with other productive shelf systems. While a portion of this primary production is consumed in the water column, the rapid onset of primary production experienced in the Eastern Bering Sea in spring and its export to the shallow sediments which underlie much of the region is a hallmark of the system. Using ^{234}Th measures in the water column and sediments, Baumann et al. (2013), examined the export and retention of particles and sediments over a wide range of locations in the eastern Bering Sea. They observed elevated amounts of ^{234}Th in sediments which they attributed to the rapid removal of material following blooms and associated particles in the marginal ice zone during the spring sea-ice retreat. They also found that particles appear to be largely retained on the shelf with little transport to deeper slope/oceanic regions, in contrast to previous models. While much of this material is detrital, some fraction of this vertical export appears to include living material as discussed by Tsukazaki et al. (2013), who showed evidence for the widespread appearance of viable diatom resting cells in bottom sediments across the region.

The importance of phytoplankton derived material to the benthos was also documented by Cooper et al. (2013) in early season sampling in the region of St. Lawrence Island. They

observed low water column chlorophyll values prior to the onset of the spring bloom, but significant sedimentation of chlorophyll containing material. The remineralization of detrital material in sediments showed significant regeneration of ammonium and its release to the water column. They concluded that organic matter recycling is closely linked to areas of increased benthic biomass which in turn leads to preferred areas for feeding by apex diving predators such as the speckled eider.

In the Bering Sea large crustacean zooplankters are an important component of the ecosystem and considered an essential element of the trophic link between primary production and fisheries resources. The response of macrozooplankton to climate, however, remains uncertain and led Ohashi and coauthors to use summer samples collected from 1994 through 2009 to examine community structure and composition (Ohashi et al., 2013). Copepod abundance varied dramatically over the period as did biomass, with higher abundance and biomass seen in cold years. These changes were due to alterations of the copepod community between the warm and cold periods. Strong links to primary production and its timing appear to be an important control which in turn has implications for recruitment of fish, such as walleye pollock. Zooplankton grazing on the phytoplankton community, however is not limited to larger macrozooplankton as shown by Sherr et al. (2013) who found significant rates of microzooplankton herbivory in spring with large heterotrophic dinoflagellates and ciliates as the primary consumers of phytoplankton. Microzooplankton grazing was significant in both non-bloom and bloom conditions, and could account for a substantial fraction of phytoplankton growth. These experiments and others point out that multiple consumers may regulate phytoplankton stocks in these polar waters, with microzooplankton playing a significant role in the recycling of materials prior to sediment incorporation.

While rapid oscillations in ocean surface conditions have been seen in the eastern Bering Sea over the last 30 years (1st DSR II volume), the impact on benthic processes has not been studied in detail. Gemery et al. (2013) analyzed long-term benthic ostracod assemblages from the northern Bering and the Chukchi Seas, to examine species distributions and the impact of climatic and oceanographic changes. They found evidence that decadal-scale environmental changes were reflected in population distributions which impacted both northern and transitional species. These results suggest that both pelagic and benthic assemblages have been impacted by climatic shifts seen in the region. Esch et al. (2013) investigated broader questions of carbon remineralization in sediments, in particular the role of iron and manganese reduction in sediments and the impact of benthic bioturbation. Their results indicate that Fe oxide reduction is a significant pathway for carbon remineralization in the northern and middle-shelf regions, where organic matter deposition rates and benthic biomass are high. The iron was also implicated as a possible source of bioavailable iron for phytoplankton. In contrast Mn oxide reduction was of minor significance, accounting for no more than 5% of total carbon oxidation in any of the regions. In addition to carbon, sedimentary nitrogen cycling on the shelf was examined by Horak et al., (2013), who quantified benthic fluxes of N_2 and dissolved inorganic nitrogen (DIN), together with the extent of coupled nitrification/denitrification. They observed widespread sedimentary denitrification over the shelf which was fueled mostly through coupled nitrification/denitrification. Rates suggested that total nitrogen loss from the Bering Sea shelf was significantly larger than previously estimated. Sediments were not a significant source of remineralized nitrogen returned for primary production over the shelf, further reducing available nitrogen over the ecosystem.

While the Bering Sea Project has a strong focus over the eastern Bering shelf, Khen and colleagues expanded the examination to a

multi-decadal summary of environmental variables observed across the western Bering Sea (Khen et al., 2013). They observed large-scale similarities between the two regions, but also noted differences to the eastern Bering region. Water exchange was seen to be more variable than expected with a slight weakening of vertical exchange over recent years and increased phosphate concentrations. Several of these changes appeared associated with climatic trends and were accompanied by shifts in the fish assemblage.

An important component of the overall program is the use of multiscale modeling to integrate observations and link lower trophic processes with fisheries and humans. Those synthesis efforts are underway and the paper by Hermann and colleagues (Hermann et al., 2013) used a multivariate statistical approach to explore the bottom-up and top-down effects of climate change on the spatial structure of the region. Empirical Orthogonal Function analysis was used to extract the emergent properties of a coupled physical/biological hindcast of the Bering Sea for the 36 year period of 1970–2009, which includes multiple episodes of warming and cooling. The model was used to replicate environmental conditions and explore the relationships of temperature and large crustacean zooplankton on the southeastern Bering Sea shelf. Model results were able to replicate the observed relationships among temperature and salinity, as well as the observed inverse correlation between temperature and large crustacean zooplankton on the southeastern Bering Sea shelf.

3. Bottom-up and top-down control

The Oscillating Control Hypothesis states that later spring phytoplankton blooms as a result of early ice retreat will increase zooplankton production, thereby resulting in increased abundances of juvenile piscivorous fish (pollock, cod and arrowtooth flounder). The recruitment success of these juvenile fish is initially high, until the point when the adult fish inflict heavy pre-recruitment mortality on the larval and juvenile stages and the community is controlled by top-down processes.

The third Bering Sea Project hypothesis addresses the influence of bottom-up and top-down control of the Bering Sea ecosystem. Later spring blooms were hypothesized to increase zooplankton abundance and, with successive warm years and delayed blooms, to lead to increased abundance of piscivorous species and switch from a community controlled by bottom-up production to a community controlled by top-down processes. The original premise that warm years would lead to higher recruitment rates and increased abundance of piscivorous species has been shown to be incorrect (Hunt et al., 2011; Coyle et al., 2011), and Bering Sea Project research provided the understanding of why this was the case. Two papers in this volume examine how young pollock accumulate energy reserves and how young pollock must be fat before their first winter for good survival to occur. Siddon et al. devised a conceptual model of energy allocation in walleye pollock from larvae to age-1. Energy densities remained relatively low during the larval phase in spring, consistent with energy allocation to somatic growth and development. Lipid acquisition rates increased rapidly after transformation to the juvenile form with energy allocation to lipid storage leading to higher energy densities in late summer. Siddon et al. (2013) proposed that the time after the end of larval development and before the onset of winter represents a short, critical period for energy storage in age-0 walleye pollock, and that overwinter survival depends on accumulating sufficient stores the previous growing season and consequently may be an important determinant of recruitment success. Heintz et al. (2013) considered the relationship between the condition of young-of-the-year (YOY) pollock in fall and their

survival to age-1 by characterizing their energy density by season and also the nutritional composition of their prey. They concluded that recruitment to age-1 can be predicted by the condition of YOY pollock prior to their first winter, and that survival is favored by cold conditions in the eastern Bering Sea.

The abundance of arrowtooth flounder, a piscivorous flatfish, has been increasing in the Bering Sea, and the third Bering Sea Project hypothesis identified the competitive effect of their increase to negatively affect abundance of their prey and other piscivorous species in the Bering Sea. Wilderbuer et al. (2013) examined whether climate variability and density-dependence affect recruitment of arrowtooth flounder as well as northern rock sole and flathead sole. For arrowtooth flounder, they found that the Arctic Oscillation was an important indicator of arrowtooth flounder productivity, but were not able to identify a more specific physical factor. In contrast, they found that wind-forced, on-shelf transport during spring led to advection of northern rock sole and flathead sole larvae to favorable nursery grounds and coincided with years of good recruitment. They also forecast the future impacts of climate on northern rock sole productivity which gave an unexpected result. IPCC (Intergovernmental Panel on Climate Change) future springtime wind scenarios were used to model the impact of climate change on northern rock sole productivity. Model results indicated that a moderate increase in recruitment might be expected because the current climate change projections favor on-shelf transport. Density-dependence effects were predicted to dampen this increase such that northern rock sole abundance will not be substantially affected by climate change. This demonstrates the importance of considering both physical and biological processes in climate change predictions.

Agler et al. (2013) also examined the relationships of climate indices and physical factors on other commercially important species in the Bering Sea. While not a Bering Sea Project focal species, chum salmon are an important subsistence and commercial fishery species in western Alaska. Agler et al. (2013) found that both sea temperature and climate indices were related to chum growth which also was affected by high Asian chum salmon abundance and high Russian pink salmon abundance.

4. Location matters

This hypothesis proposes that climate and ocean conditions which influence circulation patterns and domain boundaries will affect the distribution, frequency and persistence of fronts and other prey-concentrating features, and thus the foraging success of marine birds and mammals largely through bottom-up processes. The concern is that climate-ocean changes will displace predictably located, abundant prey necessary for successful foraging by central place foragers such as seabirds and fur seals while nurturing young as well as hot spot foragers dependent on concentrated prey such as baleen whales and walrus. As a result, these central place foragers will shift their diet, foraging locations or rookery locations to optimize foraging opportunities based on differential foraging success. Harding et al. (2013) examined the foraging strategies of thick-billed murres at three colonies. They hypothesized that close proximity of the breeding colony to productive oceanographic features is beneficial for seabird reproduction. Instead, murres in this study exhibited a remarkable degree of plasticity in foraging strategy among nearby breeding colonies, and high breeding performance regardless of colony proximity to productive oceanographic features. In the context of hypothesis four, this result indicates that breeding murres are resilient to a wide range of foraging conditions. Vincenzi and Mangel (2013) modeled the effect of climate-induced changes in the physical environment on another central place forager, the black-legged kittiwake. They examined reproductive tradeoffs these seabirds may

make in the face of variation in environment and energy resources. In their model, they found that tradeoffs in growth rate and nesting duration can be made that compensate for climate variation and thus maintain their potential productivity, at least on the individual level of productivity. Both papers, one using direct evidence and one using modeled scenarios, support the conclusion that these seabird species can adjust their breeding and foraging strategies to compensate for poor foraging conditions and maintain productivity.

The next four papers together address the distributions of fish, crab and whale species and how climate variation affects their distributions. Smart et al. (2013) examined vertical distributions of the early life stages of walleye pollock in the southeastern Bering Sea to assess ontogenetic and diel vertical migration in relation to development, area, and prey resources. Eggs occurred deepest in the water column and early juveniles occurred shallowest. Their results suggest that vertical distributions and diel migration potentially are driven by prey availability at sufficient light levels for preflexion larvae to feed and a trade-off between prey access and predation risk for late larvae. Parker-Stetter et al. (2013) assessed forage fish density distributions in late-summer 2006 to 2010 including age-0 pollock, age-0 cod, and capelin. Pollock and cod were most abundant. Age-0 pollock vertical distributional changes occurred between 2006–2007 and 2009–2010. Previous to this assessment, high midwater densities of age-0 pollock had not been observed. These may be related to the increasingly colder water temperatures that occurred during the latter period. Kotwicki and Lauth (2013) used a 30-year time series of bottom fish and crab shelf surveys to examine the effects of the cold pool and population density on spatial distributions. Results clearly show that the size of the cold pool partly drives the short-term interannual variability in patterns of spatial distribution. Despite inclusion of data from the extended cold period lasting from 2006–2010, populations that previously responded with a northward shift during warm periods did not retract during the recent cold period. There continued to be a broad-scale community-wide temporal northward shift over the 30-year time series. Friday et al. (2013) conducted cetacean surveys to describe distribution and estimate abundance on the eastern Bering Sea shelf. Estimates for the Bering Sea Project focal whale species, humpback and fin whales, increased from 2002 to 2010, but it is likely that changes in estimated abundance are due at least in part to shifts in distribution and not just changes in overall population size. Humpback whales were consistently concentrated in coastal waters north of Unimak Pass whereas fin whales were broadly distributed in the outer domain in 2008 and 2010, but sightings were sparse in 2002.

The last paper in this section connects fur seals to oceanography by determining how well oceanographic data collected by free-ranging animals compared to those from traditional ship-board vertical sampling. Nordstrom et al. (2013) found similar patterns in the temperature fields produced by ships and instrumented seals despite the differences in sampling frequency and distribution. However, the fur seal dataset was of higher temporal and spatial resolution and could therefore be used to visualize finer detail with less estimated error than ship-derived data, particularly in dynamic areas. Fur seals also collected 4700 additional profiles post-cruise which documented a ≥ 1 °C warming of the upper 100 m through mid-September, including regions where ship sampling has traditionally been sparse.

5. Commercial and subsistence fisheries, LTK

The fifth Bering Sea Project hypothesis addresses the effect of climate change on commercial and subsistence fisheries and the communities that depend on them. The related papers in this

volume focus on subsistence harvests and Bering Sea coastal communities. Fall et al. (2013) examined harvest surveys spaced approximately twenty years apart including recent surveys during 2008–2010. These surveys documented relatively high and diverse subsistence harvests, consistent with earlier research that demonstrated the continuing economic, social, and cultural importance of subsistence uses of wild resources. So far, as in the past, families and communities have adapted to changing economic, social, and environmental conditions, but the future is less clear if such changes intensify or accelerate.

Subsistence harvests typically are depicted in terms of subsistence use areas: the places where harvests and associated travel occur. The first of three papers by Huntington et al. (2013) took another way to consider this interaction by examining seasonal subsistence use areas, lifetime subsistence use areas, and “calorie-sheds,” or the area over which harvested species range. Each perspective offers useful information concerning not only the nature of human–environment interactions, but also the scope for potential conflict with other human activity and the means by which such conflicts could be reduced, avoided, or otherwise addressed. Fienup-Riordan et al. (2013) focused on the coastal community of Emmonak, Alaska and placed the subsistence survey and interview data (like that collected by Fall et al. (2013) in 2013) into an ethnographic and historical context. Taking examples from salmon fishing, seal harvesting, and local understandings of place, they argue that a comprehensive ethnographic approach, including both local and traditional knowledge and cultural history, is essential in understanding contemporary Bering Sea coastal communities. An ethnographic approach could also describe the linkage between people and the Bering Sea, which underlines an overall goal of the Bering Sea Project, to understand the interconnectedness in the system, including humans.

The second paper by Huntington et al. (2013) focused on a pair of coastal communities, trying to understand environmental influences on walrus hunting success, combining community and scientific knowledge to tackle this question. Information from

hunters, harvest monitors, and previous studies suggested that ice concentration and wind were among the environmental factors influencing harvest levels. For the period 1996–2009, they used ice concentrations based on satellite data, wind speed and direction based on a high-resolution atmospheric reanalysis to specify physical conditions each day during spring, and daily walrus harvests provided by U.S. Fish and Wildlife Service records for the villages of Gambell and Savoonga, Alaska on St. Lawrence Island and found that that other factors (e.g., fog, fuel prices, socioeconomic conditions) collectively cause a greater share of variability than ice and wind. Nonetheless, the findings suggest that environmental change is also likely to influence future harvest levels, and that climate models which yield appropriately scaled data on ice and wind around the island may be of use in determining the magnitude and direction of those influences. The final paper by Huntington et al. (2013) surveyed elders, hunters, and fishers from five coastal communities along the eastern Bering Sea to learn what if any changes they observed in this ecosystem. The observations described a complex and dynamic ecosystem with many more responses of change in the south, than the north.

6. Beyond the hypotheses; managing the heterogeneity of the Eastern Bering Sea

One challenge of this large research program is the breadth of its geographic scope and the need for consistent and coherent ways of comparing data sets. This is particularly important for a large, heterogeneous area like the eastern Bering Sea shelf. A panel led by Ivonne Ortiz developed a tool for use by Bering Sea Project scientists, which is described in a dataset available in the Bering Sea Project Data Archive (Ortiz et al., 2012). This tool divides the eastern Bering Sea into a spatially explicit set of marine regions with specific boundaries (see Fig. 1). For example, the freshwater influenced, well-mixed, inner domain was separated from the

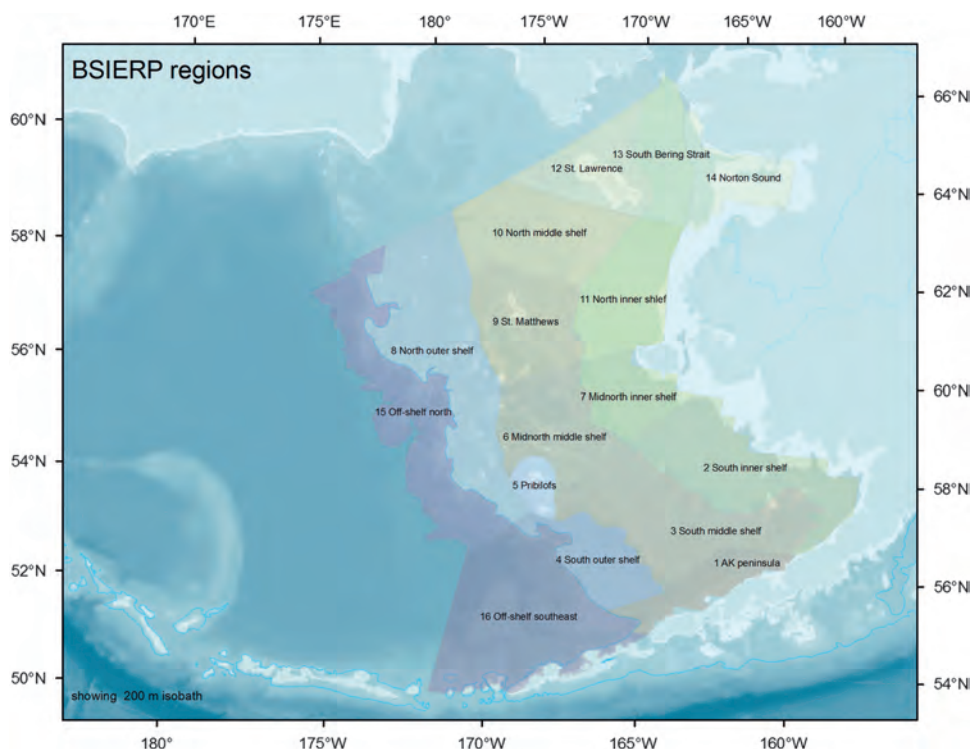


Fig. 1. Map illustrating the 16 marine regions based on observed physical, environmental, and biotic variables seen across the Eastern Bering Sea Project area. A detailed description of the process used to delineate these areas by consensus panel recommendation is described by Ortiz et al. (2012).

two-layered (during summer) middle domain. The development of the tool was initiated by the Bering Sea Project modeling group, whose goal was to develop a consensus approach of spatial scales which could be used to compare model predictions to observations. It should be emphasized that the regions were defined strictly in a qualitative way through discussion and general consensus of Bering Sea Project scientists. Although, based on the experience and information available to panelists, it should be considered only a solid starting point for further exploration for Bering Sea system and the models being developed.

Acknowledgments

This second issue and broader program has greatly benefited from the contributions of the additional members of the scientific advisory board of the Bering Sea Program (Carin Ashjian, Mike Lomas, Jeffrey Napp and Phyllis Stabeno) and editor Tom Van Pelt, who also provided thoughtful reviews to this introduction. This is best BEST-BSIERP Bering Sea Project publication number 101 and NPRB publication number 424.

References

- Agler, B.A., Ruggerone, G.T., Wilson, L.I., Mueter, F., 2013. Historical growth of Bristol Bay and Yukon River, Alaska chum salmon (*Oncorhynchus keta*) in relation to climate and inter- and intraspecific competition. *Deep Sea Res. II Top. Stud. Oceanogr.* 94, 165–177.
- Baumann, M.S., Moran, S.B., Kelly, R.P., Lomas, M.W., Shull, D.H., 2013. ²³⁴Th balance and implications for seasonal particle retention in the eastern Bering Sea. *Deep Sea Res. II Top. Stud. Oceanogr.* 94, 7–21.
- Cooper, L.W., Sexson, M.G., Grebmeier, J.M., Gradinger, R., Mordy, C.W., Lovvorn, J.R., 2013. Linkages between sea-ice coverage, pelagic-benthic coupling, and the distribution of spectacled eiders: observations in March 2008, 2009 and 2010, Northern Bering Sea. *Deep Sea Res. II Top. Stud. Oceanogr.* 94, 31–43.
- Coyle, K.O., Eisner, L.B., Mueter, F.J., Pinchuk, A.I., Janout, M.A., Cieciel, K.D., Farley, E. V., Andrews, A.G., 2011. Climate change in the southeastern Bering Sea: impacts on pollock stocks and implications for the oscillating control hypothesis. *Fish. Oceanogr.* 20 (2), 139–156.
- Esch, M.E.S., Shull, D.H., Devol, A.H., Moran, B., 2013. Regional patterns of bioturbation and iron and manganese reduction in the sediments of the southeastern Bering Sea. *Deep Sea Res. II Top. Stud. Oceanogr.* 94, 80–94.
- Fall, J.A., Braem, N.S., Brown, C.L., Hutchinson-Scarborough, L.B., Koster, D.S., Krieg, T.M., 2013. Continuity and change in subsistence harvests in five Bering Sea communities: Akutan, Emmonak, Savoonga, St. Paul, and Togiak. *Deep Sea Res. II Top. Stud. Oceanogr.* 94, 274–291.
- Fienup-Riordan, A., Brown, C., Braem, N.M., 2013. The value of ethnography in times of change: the story of Emmonak. *Deep Sea Res. II Top. Stud. Oceanogr.* 94, 301–311.
- Friday, N.A., Zerbini, A.N., Waite, J.M., Moore, S.E., Clapham, P.J., 2013. Cetacean distribution and abundance in relation to oceanographic domains on the eastern Bering Sea shelf, June and July of 2002, 2008, and 2010. *Deep Sea Res. II Top. Stud. Oceanogr.* 94, 244–256.
- Gemery, L., Cronin, T.M., Cooper, L.W., Grebmeier, J.M., 2013. Temporal changes in benthic ostracode assemblages in the Northern Bering and Chukchi Seas from 1976 to 2010. *Deep Sea Res. II Top. Stud. Oceanogr.* 94, 68–79.
- Harding, A., Paredes, R., Suryan, R., Roby, D., Irons, D., Orben, R., Renner, H., Young, R., Barger, C., Dorresteijn, I., Kitaysky, A., 2013. Does location really matter? An inter-colony comparison of seabirds breeding at varying distances from productive oceanographic features in the Bering Sea. *Deep Sea Res. II Top. Stud. Oceanogr.* 94, 178–191.
- Heintz, R.A., Siddon, E.C., Farley Jr., E.V., Napp, J.M., 2013. Correlation between recruitment and fall condition of age-0 pollock (*Theragra chalcogramma*) from the eastern Bering Sea under varying climate conditions. *Deep Sea Res. II Top. Stud. Oceanogr.* 94, 150–156.
- Hermann, A.J., Gibson, G.A., Bond, N.A., Curchitser, E.N., Hedstrom, K., Cheng, W., Wang, M., Stabeno, P.J., Eisner, L., Cieciel, K.D., 2013. A multivariate analysis of observed and modeled biophysical variability on the Bering Sea shelf: multi-decadal hindcasts (1970–2009) and forecasts (2010–2040). *Deep Sea Res. II Top. Stud. Oceanogr.* 94, 121–139.
- Horak, R.E.A., Whitney, H., Shull, D.H., Mordy, C.W., Devol, A.H., 2013. The role of sediments on the Bering Sea shelf N cycle: insights from measurements of benthic denitrification and benthic DIN fluxes. *Deep Sea Res. II Top. Stud. Oceanogr.* 94, 95–105.
- Hunt Jr., G.L., Coyle, K.O., Eisner, L.B., Farley, E.V., Heintz, R.A., Mueter, F., Napp, J.M., Overland, J.E., Ressler, P.H., Salo, S., Stabeno, P.J., 2011. Climate impacts on eastern Bering Sea foodwebs: a synthesis of new data and an assessment of the Oscillating Control Hypothesis ICES. *J. Mar. Sci.* 68 (6), 1230–1243.
- Huntington, H.P., Noongwook, G., Bond, N.A., Benter, B., Snyder, J.A., Zhang, J., 2013. The influence of wind and ice on spring walrus hunting success on St. Lawrence Island, Alaska. *Deep Sea Res. II Top. Stud. Oceanogr.* 94, 312–322.
- Huntington, H.P., Ortiz, I., Noongwook, G., Fidel, M., Childers, D., Morse, M., Beaty, J., Alessa, L., Kliskey, A., 2013. Mapping human interaction with the Bering Sea ecosystem: comparing seasonal use areas, lifetime use areas, and “calorie-sheds”. *Deep Sea Res. II Top. Stud. Oceanogr.* 94, 292–300.
- Huntington, H.P., Braem, N.M., Brown, C.L., Hunn, E., Krieg, T.M., Lestenkof, P., Noongwook, G., Sepez, J., Sigler, M.F., Wiese, F.K., Zavadil, P., 2013. Local and traditional knowledge regarding the Bering Sea ecosystem: selected results from five indigenous communities. *Deep Sea Res. II Top. Stud. Oceanogr.* 94, 323–332.
- Khen, G.V., Basyuk, E.O., Vanin, N.S., Matveev, V.I., 2013. Hydrography and biological resources in the western Bering Sea. *Deep Sea Res. II Top. Stud. Oceanogr.* 94, 106–120.
- Kotwicki, S., Lauth, R.R., 2013. Detecting temporal trends and environmentally-driven changes in the spatial distribution of bottom fishes and crabs on the eastern Bering Sea shelf. *Deep Sea Res. II Top. Stud. Oceanogr.* 94, 231–243.
- Nordstrom, C.A., Benoit-Bird, K.J., Battaile, B.C., Trites, A.W., 2013. Northern fur seals augment ship-derived ocean temperatures with higher temporal and spatial resolution data in the eastern Bering Sea. *Deep Sea Res. II Top. Stud. Oceanogr.* 94, 257–273.
- Ohashi, R., Yamaguchi, A., Matsuno, K., Saito, R., Yamada, N., Iijima, A., Shiga, N., Imai, I., 2013. Interannual changes in the zooplankton community structure on the southeastern Bering Sea shelf during summers of 1994–2009. *Deep Sea Res. II Top. Stud. Oceanogr.* 94, 44–56.
- Ortiz, I.; Weise, F. Greig, A. 2012. Marine Regions Boundary Data for the Bering Sea Shelf and Slope. UCAR/NCAR - EOL/ Computing, Data, and Software Facility. <http://dx.doi.org/10.5065/D6DF6P6C>.
- Overland, J.E., et al., 2012. Recent Bering Sea warm and cold events in a 95-year context. *Deep Sea Res. II Top. Stud. Oceanogr.* 65–70, 6–13.
- Parker-Stetter, S.L., Horne, J.K., Farley, E.V., Barbee, D.H., Andrews, A.G., Eisner, L.B., Nomura, J.M., 2013. Summer distributions of forage fish in the eastern Bering Sea. *Deep Sea Res. II Top. Stud. Oceanogr.* 94, 211–230.
- Sherr, E.B., Sherr, B.F., Ross, C., 2013. Microzooplankton grazing impact in the Bering Sea during spring sea ice conditions. *Deep Sea Res. II Top. Stud. Oceanogr.* 94, 57–67.
- Smart, T.I., Siddon, E.C., Duffy-Anderson, J.T., 2013. Vertical distributions of the early life stages of walleye pollock (*Theragra chalcogramma*) in the Southeastern Bering Sea. *Deep Sea Res. II Top. Stud. Oceanogr.* 94, 201–210.
- Siddon, E.C., Heintz, R.A., Mueter, F.J., 2013. Conceptual model of energy allocation in walleye pollock (*Theragra chalcogramma*) from age-0 to age-1 in the southeastern Bering Sea. *Deep Sea Res. II Top. Stud. Oceanogr.* 94, 140–149.
- Tsukazaki, C., Ishii, K., Saito, R., Matsuno, K., Yamaguchi, A., Imai, I., 2013. Distribution of viable diatom resting stage cells in bottom sediments of the eastern Bering Sea shelf. *Deep Sea Res. II Top. Stud. Oceanogr.* 94, 22–30.
- Vincenzi, S., Mangel, M., 2013. Linking food availability, body growth and survival in the black-legged Kittiwake *Rissa tridactyla*. *Deep Sea Res. II Top. Stud. Oceanogr.* 94, 192–200.
- Wilderbuer, T., Stockhausen, W., Bond, N., 2013. Updated analysis of flatfish recruitment response to climate variability and ocean conditions in the Eastern Bering Sea. *Deep Sea Res. II Top. Stud. Oceanogr.* 94, 157–164.

H. Rodger Harvey*

Department of Ocean, Earth and Atmospheric Sciences, Old Dominion University, Norfolk, VA 23529, USA
E-mail address: rharvey@odu.edu

Michael F. Sigler

Alaska Fisheries Science Center, National Oceanic and Atmospheric Administration, 17109 Point Lena Loop Road, Juneau, AK 99801, USA
E-mail address: Mike.Sigler@noaa.gov

Available online 29 April 2013

* Corresponding author.



^{234}Th balance and implications for seasonal particle retention in the eastern Bering Sea



M.S. Baumann^{a,*}, S.B. Moran^{a,1}, R.P. Kelly^{a,2}, M.W. Lomas^{b,3}, D.H. Shull^{c,4}

^a Graduate School of Oceanography, University of Rhode Island, Narragansett, RI 02882-1197, USA

^b Bigelow Laboratory for Ocean Sciences, 60 Bigelow Drive, East Boothbay Harbor, ME 04544, USA

^c Department of Environmental Sciences, Western Washington University, Bellingham, WA 98225, USA

ARTICLE INFO

Available online 14 March 2013

Keywords:

Bering Sea

^{234}Th

Particle transport

Sediment

ABSTRACT

As part of the Bering Ecosystem Study-Bering Sea Integrated Ecosystem Research Program (BEST-BSIERP), distributions of ^{234}Th in the water column and sediments were measured at approximately 60 stations over the shelf and slope/oceanic regions of the eastern Bering Sea during spring and summer of 2009 and 2010. During this study period, the inventory of sediment excess ^{234}Th ($^{234}\text{Th}_{\text{xs}}$) on the shelf was determined to be $\sim 1/3$ of the total ^{234}Th deficit in the overlying water column; the average focusing factor ($FF_{\text{Th}} = \text{sediment } ^{234}\text{Th}_{\text{xs}} / \text{water column } ^{234}\text{Th deficit}$) was 0.34 ± 0.23 . In addition, the export flux of ^{234}Th from the shelf to the slope/oceanic region was determined to be on average $\sim 30\%$ of the total production of ^{234}Th throughout the shelf. Taken together, these results indicate that ^{234}Th and associated particles are largely retained on the shelf, and that shelf sediments represent a sink for particles. In contrast, the FF_{Th} in the slope/oceanic region was higher, averaging 1.52 ± 1.34 . The higher FF_{Th} at the slope is attributed primarily to enhanced scavenging removal and sediment deposition of ^{234}Th associated with periods of high biogenic particle flux at the marginal ice zone during the spring sea-ice retreat. A more general conclusion is that the ocean margin of the eastern Bering Sea may serve as an accumulation area for particles and associated reactive chemicals.

Published by Elsevier Ltd.

1. Introduction

Continental shelves represent only 10% of the world ocean, yet these regions account for $\sim 20\%$ of global primary production (Walsh, 1988). Ocean margins are recognized to be effective areas for the enhanced removal of reactive chemicals via particle scavenging and for the transfer of organic matter from continental shelves to the deep ocean. These processes are thought to play an important role in shelf–basin exchange of organic carbon and the sediment accumulation of particle-reactive pollutants on a global basis. A significant challenge is quantifying the rates and mechanisms of particle transport in shelf/slope systems.

Uranium-series radionuclides are proven tracers of particle transport processes in aquatic environments. In particular, previous studies have utilized long-lived radionuclides, such as ^{210}Pb

($t_{1/2} = 22.3$ yr), ^{230}Th ($t_{1/2} = 75, 200$ yr), and ^{231}Pa ($t_{1/2} = 32, 500$ yr) to investigate particle transport in shelf regions on decadal and longer time-scales (e.g., Anderson et al., 1994; Bacon et al., 1994; Nozaki et al., 1997; Roy-Barman, 2009; Smith et al., 2003). Over the past several decades, the short-lived, particle-reactive radionuclide ^{234}Th ($t_{1/2} = 24.1$ d) has been increasingly used as a tracer of POC export from the upper ocean (e.g., Buesseler, 1998; Buesseler et al., 1998; Charette et al., 2001; Lalonde et al., 2007; Moran and Buesseler, 1993; Moran et al., 2003; Savoye et al., 2004). In addition to its utility in quantifying POC export from the upper water column, the disequilibrium between ^{234}Th and its soluble parent ^{238}U in seawater and sediments has significant potential in quantifying seasonal particle transport and retention in shelf systems; for example, in a manner similar to that described for ^{210}Pb (e.g., Bacon et al., 1994).

As part of the Bering Ecosystem Study-Bering Sea Integrated Ecosystem Research Program (BEST-BSIERP), measurements of the water column deficit of ^{234}Th and sediment excess inventory ($^{234}\text{Th}_{\text{xs}}$) are presented from 2009 and 2010 over the eastern Bering Sea shelf and slope (Fig. 1). These data have been used to investigate several aspects of particle transport, including: seasonal particle retention over the shelf, export of POC, and enhanced particle export and deposition associated with the marginal ice zone (MIZ). Results indicate that $\sim 30\%$ of ^{234}Th produced over the

* Corresponding author. Tel.: +1 401 874 6259; fax: +1 401 874 6811.

E-mail addresses: matthew_baumann@my.uri.edu (M.S. Baumann), sbmoran@mail.uri.edu (S.B. Moran), rokelly@mail.uri.edu (R.P. Kelly), mlomas@bigelow.org (M.W. Lomas), david.shull@wwu.edu (D.H. Shull).

¹ Tel.: +1 401 874 6530.

² Tel.: +1 401 874 6273.

³ Tel.: +1 202 747 3255x311.

⁴ Tel.: +1 360 650 3690.

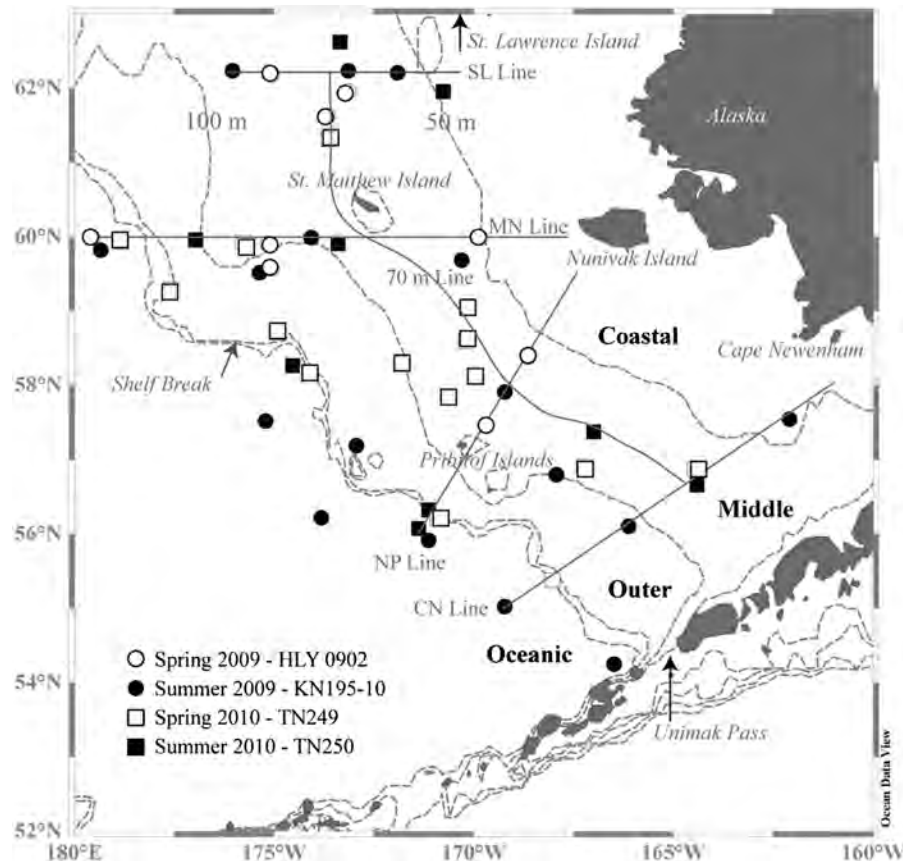


Fig. 1. Map of the eastern Bering Sea identifying the major transects during the BEST-BSIERP field program and station locations where water column and sediment samples were collected.

shelf is exported to the ocean interior, implying that ^{234}Th and, by inference, associated particles in this system are largely retained over the shelf on a seasonal basis. In addition, relatively large inventories of $^{234}\text{Th}_{\text{xs}}$ observed in the slope and deep ocean sediments during summer are suggested to result from enhanced scavenging removal and deposition of ^{234}Th associated with the MIZ during the spring sea-ice retreat, and possibly augmented by boundary scavenging removal of ^{234}Th at the ocean margin.

1.1. Study area

The broad (~500 km) and extensive (> 500,000 km²) seasonally ice-free eastern Bering Sea shelf is bordered on the south by the Alaska Peninsula and to the east by the Alaska mainland (Fig. 1). The shelf break, located approximately at the 170 m isobath, extends northwestward from Unimak Pass and encompasses the Pribilof Islands, St. Matthew Island, Nunivak Island, and St. Lawrence Island. During the ice-free months, the shelf waters may be subdivided into three cross-shelf domains, separated by three fronts (Coachman, 1986; McRoy et al., 1986). The Inner Front, located near the 50 m isobath, separates the shallow, well-mixed Coastal Domain (0–50 m) from the two-layered Middle Domain (50–100 m) (Kachel et al., 2002; McRoy et al., 1986). The Coastal Domain is well-mixed because the wind and tidally mixed layers overlap. The Middle Domain, characterized by the strongest stratification and the presence of a summer cold pool (Fig. 2; summer temperature section), is isolated from the Outer Domain by the Middle Front, which overlies the 100 m isobath. Recent observations (Stabeno et al., 2002) have indicated north–south variability within the Middle Domain, though these trends are less pronounced than cross-shelf variability. The Outer Domain (100 m

– shelf break) is characterized by surface and bottom mixed layers, though is separated by a structured middle layer (Stabeno et al., 1999). The Shelf Break Front separates the Outer Domain from the Oceanic Domain. These fronts affect lateral advection and diffusion, property exchange rates, and mixing between the water masses.

2. Materials and methods

Water column and sediment core samples were collected in the eastern Bering Sea during spring and summer cruises as part of the 2009 and 2010 BEST-BSIERP field program (Fig. 1). A series of transects were completed during each cruise aboard the USCGC *Healy* (March 31 to May 12, 2009), *R/V Knorr* (June 14 to July 13, 2009), and *R/V Thomas G. Thompson* (May 9 to June 14, 2010, and June 16 to July 13, 2010) (Table 1). Because the 2010 spring cruise was delayed until May and early June it is referred to as ‘late’ spring, compared to 2009. Major transects from south to north are as follows: CN (Cape Newenham), NP (Nunivak Island–St. Paul Island), MN (St. Matthew Island–Nunivak Island), SL (St. Lawrence Island) and the 70 m isobath line running from CN northward to SL (Fig. 1).

2.1. Water column ^{234}Th sampling and analysis

^{234}Th water column profiles were obtained via small volume (4 L) water samples collected from CTD-rosette casts ($n=27$ and 29 profiles collected in 2009 and $n=29$ and 19 profiles collected in 2010, during spring and summer, respectively). Samples were analyzed for total (dissolved+particulate) ^{234}Th at high vertical

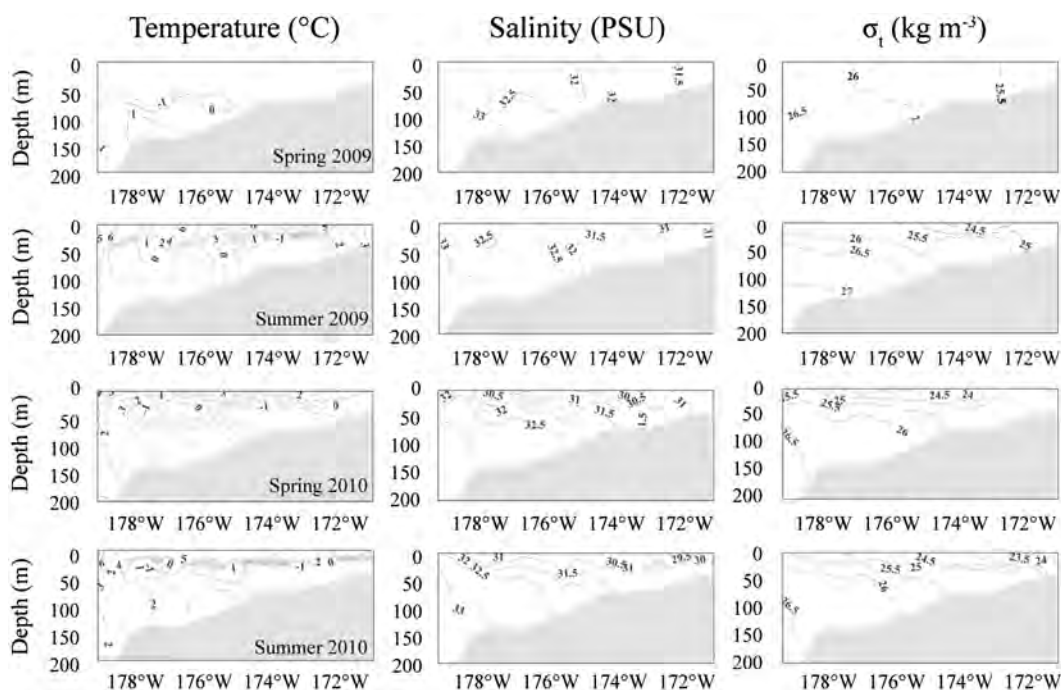


Fig. 2. Temperature ($^{\circ}\text{C}$), salinity (PSU), and density (kg m^{-3}) sections along the MN line for spring and summer 2009–2010.

Table 1

Sampling dates during the 2009 and 2010 BEST-BSIERP field program.

Cruise	Vessel	Dates
HLY 0902	USCGC Healy	March 31–May 12, 2009
KN195-10	R/V Knorr	June 14–July 13, 2009
TN249	R/V Thompson	May 9–June 14, 2010
TN250	R/V Thompson	June 16–July 13, 2010

resolution (~ 10 m) throughout the upper water column to encompass the entire photic zone. On the shelf, the entire water column was sampled. In the slope/oceanic region, profiles extend to a depth of ~ 500 m. ^{234}Th was extracted via co-precipitation with MnO_2 (Benitez-Nelson et al., 2001; Buesseler et al., 2001). Briefly, the pH of the sample was raised by the drop-wise addition of concentrated ammonium hydroxide followed by the addition of 0.2 M KMnO_4 (25 μL) and 1.0 M MnCl_2 (11.5 μL) to generate the MnO_2 precipitate. After one hour of equilibration, each sample was vacuum filtered onto a 25 mm diameter 1 μm pore size glass microfiber filter (GM/F). Deep samples (> 1000 m) were collected as a check for detector efficiency. Samples were spiked with a known ^{230}Th activity as an internal standard of ^{234}Th scavenging efficiency ($n=52$). After ^{234}Th analysis (described below), Th was radiochemically purified and ^{230}Th was measured by alpha particle emission (Lepore et al., 2007). Scavenging efficiencies for the small volume ^{234}Th method were determined to be $91 \pm 4.5\%$ (1 σ).

The total ^{234}Th in water column samples was quantified by measurement of the beta emission of $^{234\text{m}}\text{Pa}$ ($E_{\text{max}}=2.19$ MeV; $t_{1/2}=1.2$ min) using a low-background beta detector (RISØ National Laboratory, Roskilde, Denmark), with an average detector efficiency of $44 \pm 3\%$ determined at sea. Prior to analysis, each sample was mounted on an acrylic planchet and covered with clear plastic wrap and aluminum foil to shield low-level beta and alpha emitters. Samples were counted several times over the first six half-lives of ^{234}Th , with the first count at least 3 days after collection to allow for the decay of short lived isotopes. After 144 days (six half-lives of ^{234}Th), the activity of ^{234}Th decayed below the detection limit and samples were counted to establish background levels. Data were

fitted to the ^{234}Th decay curve and corrected to yield ^{234}Th activity at the time of collection.

^{238}U activities were calculated from salinity according to $^{238}\text{U}=0.07081 \times S$ (‰) (Chen et al., 1986).

2.2. Sediment core ^{234}Th sampling and analysis

Sediment cores were collected during each cruise in 2009 and 2010 ($n=19$ and 19 profiles collected in 2009 and $n=21$ and 17 profiles collected in 2010, during spring and summer, respectively) using an Oceans Instruments MC-800 eight-tube multicorer. Cores were sectioned into 0.5 cm increments in the upper 2 cm, and into 1 cm increments for depths of 2–5 cm. Sediment samples were dried at 60 $^{\circ}\text{C}$ in 125 mL jars, ground, and homogenized prior to analysis. The sediment density ($\rho=\rho_D(1-\phi)$) of each sample analyzed was calculated using an assumed solid particle density (ρ_D) of 2.65 g cm^{-3} (Burdige, 2006) and sediment porosities (ϕ) determined in the laboratory from measurements of wet and dry sediment weight.

Samples were analyzed for ^{234}Th using a sea-going Canberra pure Ge planar type detector (GCW3023, 2000 mm^2) or on a shore-based Canberra pure Ge well type detector (GL20203, 150 cm^3) calibrated for the specific sample geometry. Sample activities were determined by gamma emission at 63.3 keV and decay corrected to the mid-point of collection. Supported levels of ^{234}Th (^{234}Th produced in the sediment column) were measured after 144 days and subtracted from the total ^{234}Th activity. Self-absorption corrections were applied according to the method described by Cutshall et al. (1983). Detector efficiencies were determined to be $10.8 \pm 0.3\%$ and $52.1 \pm 1.0\%$ for ^{234}Th at 63.3 keV for the planar and well type detectors, respectively.

3. Results

3.1. Water column ^{234}Th – ^{238}U disequilibrium

The ^{234}Th – ^{238}U activity ratio (AR) provides a quantitative measure of the removal of ^{234}Th relative to ^{238}U from the water column via particle scavenging and export. During spring 2009,

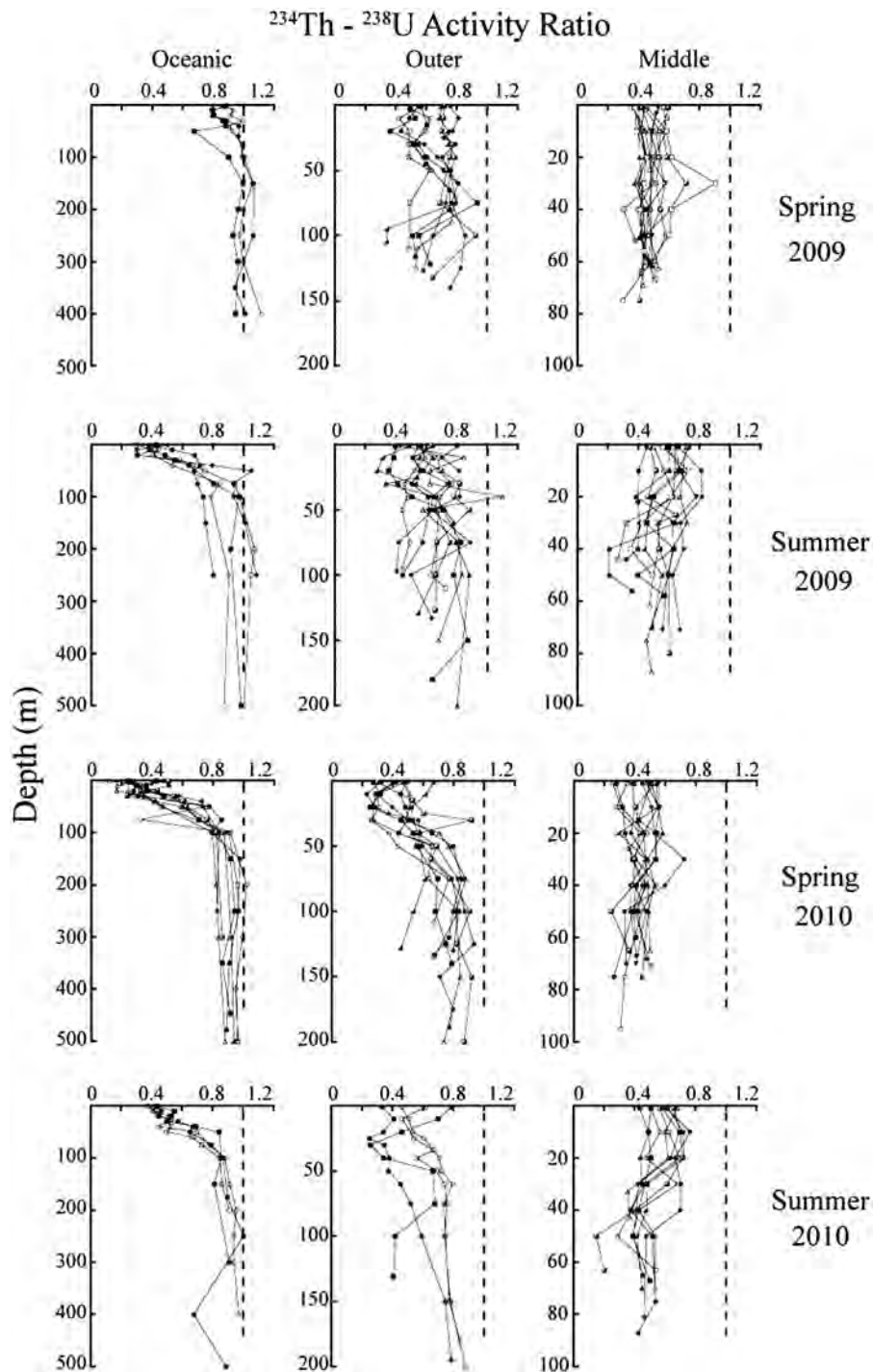


Fig. 3. Depth profiles of ^{234}Th - ^{238}U activity ratios according to season and domain. Slope–Oceanic Domain profiles plotted to a maximum depth of 500 m. Middle and Outer shelf profiles plotted to sea floor.

activity ratios ranged from ~ 0.4 to 0.8 on the shelf, whereas secular equilibrium ($AR=1$) was observed in the slope/oceanic water column (Fig. 3). In summer 2009, ARs measured in the shelf domains indicate a similar degree of ^{234}Th - ^{238}U disequilibrium ($AR < 1$) compared to spring. Unlike spring, however, ^{234}Th - ^{238}U disequilibrium was observed during summer in the upper water column of the Oceanic Domain. In 2010, ARs on the shelf indicate a deficiency of ^{234}Th in the water column consistent with 2009 (Fig. 3). In contrast to the previous spring, disequilibrium was observed in the water column of the Oceanic Domain during late spring 2010 down to depths of ~ 200 m. Cross-shelf ^{234}Th - ^{238}U activity ratios along the MN Line (Fig. 4) indicate

that disequilibrium is also similar between late spring and summer over the shelf and at the shelf break. The difference in water column ARs between spring 2009 and spring 2010 may be attributed to the temporal offset in sampling dates.

3.2. Sediment excess ^{234}Th

Sediment excess ^{234}Th ($^{234}\text{Th}_{xs}$) is defined as the ^{234}Th unsupported by decay of the parent ^{238}U , and which is supplied by particle scavenging of ^{234}Th from the overlying water column to

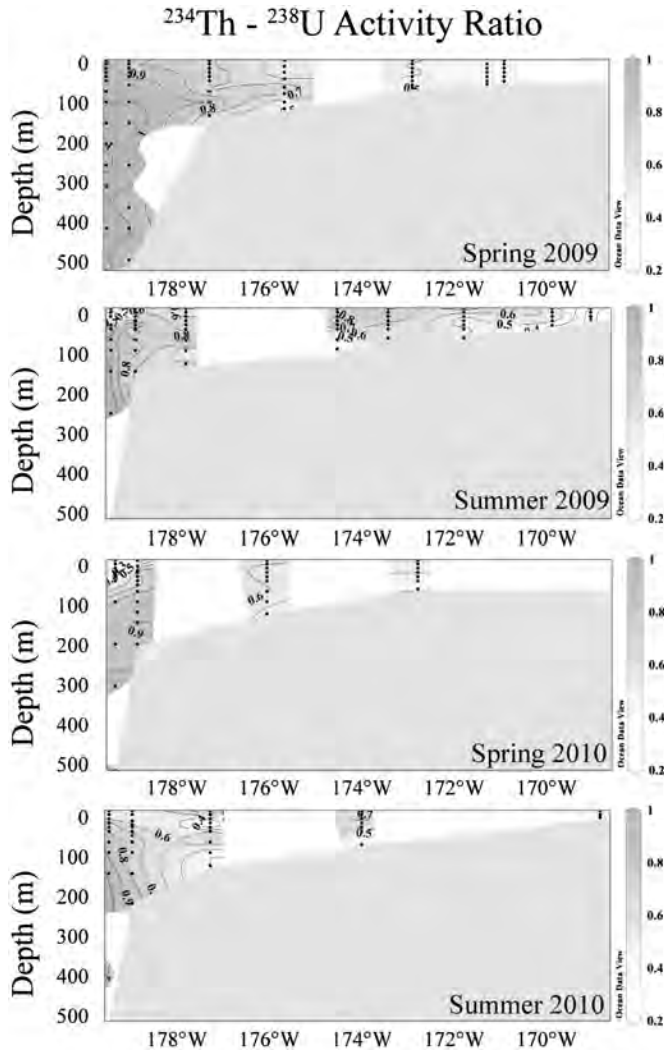


Fig. 4. Seasonal variability in ^{234}Th – ^{238}U activity ratio (AR) along the MN Line.

the sediments:

$$^{234}\text{Th}_{\text{xs}} = ^{234}\text{Th}_{\text{tot}} - ^{234}\text{Th}_{\text{supp}} \quad (1)$$

$^{234}\text{Th}_{\text{xs}}$ was observed in nearly all sediment cores, typically confined to the upper 1.5 cm (Fig. 5). Sediment cores were not obtained for the Coastal Domain because coring was not possible due to sandy sediment. Sediment excess ^{234}Th activities measured in shelf sediments indicate high spatial variability; though do not exceed ~ 40 dpm g^{-1} at the surface of the sediment column. The highest $^{234}\text{Th}_{\text{xs}}$ activities were observed during summer in the slope/oceanic region sediments, where activities of up to 135 dpm g^{-1} were measured. Water column ^{234}Th and ^{238}U (dpm L^{-1}) and sediment ^{234}Th activity (dpm g^{-1}) data are listed in the Appendix.

3.3. Water column deficits of ^{234}Th

^{234}Th deficits in the water column are calculated by difference of depth integrated ^{234}Th and ^{238}U activity profiles:

$$^{234}\text{Th deficit} = \int_0^z (A_U - A_{\text{Th}}) dz \quad (2)$$

where A_U is the activity of ^{238}U , A_{Th} is the activity of ^{234}Th and z is the depth of the water column. For the shelf regions ($z < 200$ m), ^{234}Th and ^{238}U activities were integrated over the entire water

column. For the slope/oceanic regions, the water column was integrated to the depth where ^{234}Th and ^{238}U reached secular equilibrium (~ 200 – 400 m).

For spring 2009, average ^{234}Th deficits over the Middle and Outer shelf were 7.3 ± 0.7 and 9.4 ± 1.9 dpm cm^{-2} (1σ), respectively. The Oceanic Domain yielded an average ^{234}Th deficit of 3.1 ± 3.6 dpm m^{-2} (Fig. 6; Table 2). ^{234}Th deficits over the eastern Bering Sea during summer 2009 were 6.2 ± 1.1 in the Middle, 10.0 ± 1.7 dpm cm^{-2} in the Outer, and 10.7 ± 5.2 dpm cm^{-2} in the Oceanic domains, respectively. During late spring 2010, average deficits of ^{234}Th over the Middle and Outer shelf increased to 8.8 ± 1.7 and 11.5 ± 1.4 dpm cm^{-2} , respectively, though large standard error within the data sets prevent statistical differentiation between seasons. Furthermore, the late spring 2010 average deficit in the oceanic water column was 16.9 ± 3.6 dpm cm^{-2} , which is an approximate five-fold increase from earlier in spring of 2009. Average water column deficits in the summer of 2010 were 7.2 ± 1.3 in the Middle, 14.7 ± 3.3 in the Outer, and 13.0 ± 2.2 dpm cm^{-2} in the Oceanic domains, respectively (Fig. 6; Table 2).

3.4. Sediment inventories of excess ^{234}Th

Because $^{234}\text{Th}_{\text{xs}}$ is typically observed in the upper 1.5 cm of the sediment core, sediment profiles are integrated to this depth to yield the excess ^{234}Th inventory:

$$\text{Excess } ^{234}\text{Th inventory} = \int_0^z (^{234}\text{Th}_{\text{tot}} - ^{234}\text{Th}_{\text{supp}}) dz = \int_0^z ^{234}\text{Th}_{\text{xs}} dz \quad (3)$$

In spring 2009, average $^{234}\text{Th}_{\text{xs}}$ inventories were 2.8 ± 1.1 (Middle Domain), 4.1 ± 2.7 (Outer Domain), and 2.3 ± 1.0 dpm cm^{-2} (Oceanic Domain) (Fig. 6; Table 2). For summer 2009, average excess inventories were 2.7 ± 2.0 , 2.3 ± 1.0 , and 3.6 ± 1.8 dpm cm^{-2} for the Middle, Outer, and Oceanic domains, respectively. Average $^{234}\text{Th}_{\text{xs}}$ inventories in late spring 2010 are not differentiable from either season in 2009: 2.1 ± 1.0 (Middle Domain), 3.2 ± 1.7 (Outer Domain), and 4.0 ± 1.2 (Oceanic Domain) dpm cm^{-2} . In summer 2010, the highest inventories were observed in the summer Oceanic Domain, while this relative increase is not observed over the shelf: 3.3 ± 1.8 in the Middle, 3.9 ± 3.4 in the Outer, and 30.6 ± 18.8 dpm cm^{-2} in the Oceanic domains, respectively.

4. Discussion

4.1. ^{234}Th balance over the eastern Bering Sea shelf

The radiochemical balance of ^{234}Th over the eastern Bering Sea shelf can be used to provide insight into particle transport, including the seasonal retention of particles in shelf sediments. Specifically, particle retention can be evaluated by establishing the balance between the export flux of ^{234}Th from the water column and the flux of ^{234}Th into the sediments. This approach follows that described by Bacon et al. (1994), who used ^{210}Pb to evaluate the transport of particles on a decadal time-scale in the Middle Atlantic Bight (MAB). Fig. 7 illustrates the balance between the supply and removal of ^{234}Th over the eastern Bering Sea shelf. Assuming a steady-state, the radiochemical balance of ^{234}Th over the shelf is defined as:

$$\lambda A_U + V \times \Delta \text{Th}_{\text{CS}} = \lambda A_{\text{Th}} + T \times \Delta \text{Th}_{\text{AS}} + J_{\text{sed}} + J_{\text{exp}} \quad (4)$$

Eq. (4) represents the balance between the supply of ^{234}Th via *in situ* production from ^{238}U decay, λA_U (^{234}Th decay constant; $\lambda = 0.0288$ d^{-1}), and the net flux of ^{234}Th from the Oceanic to the

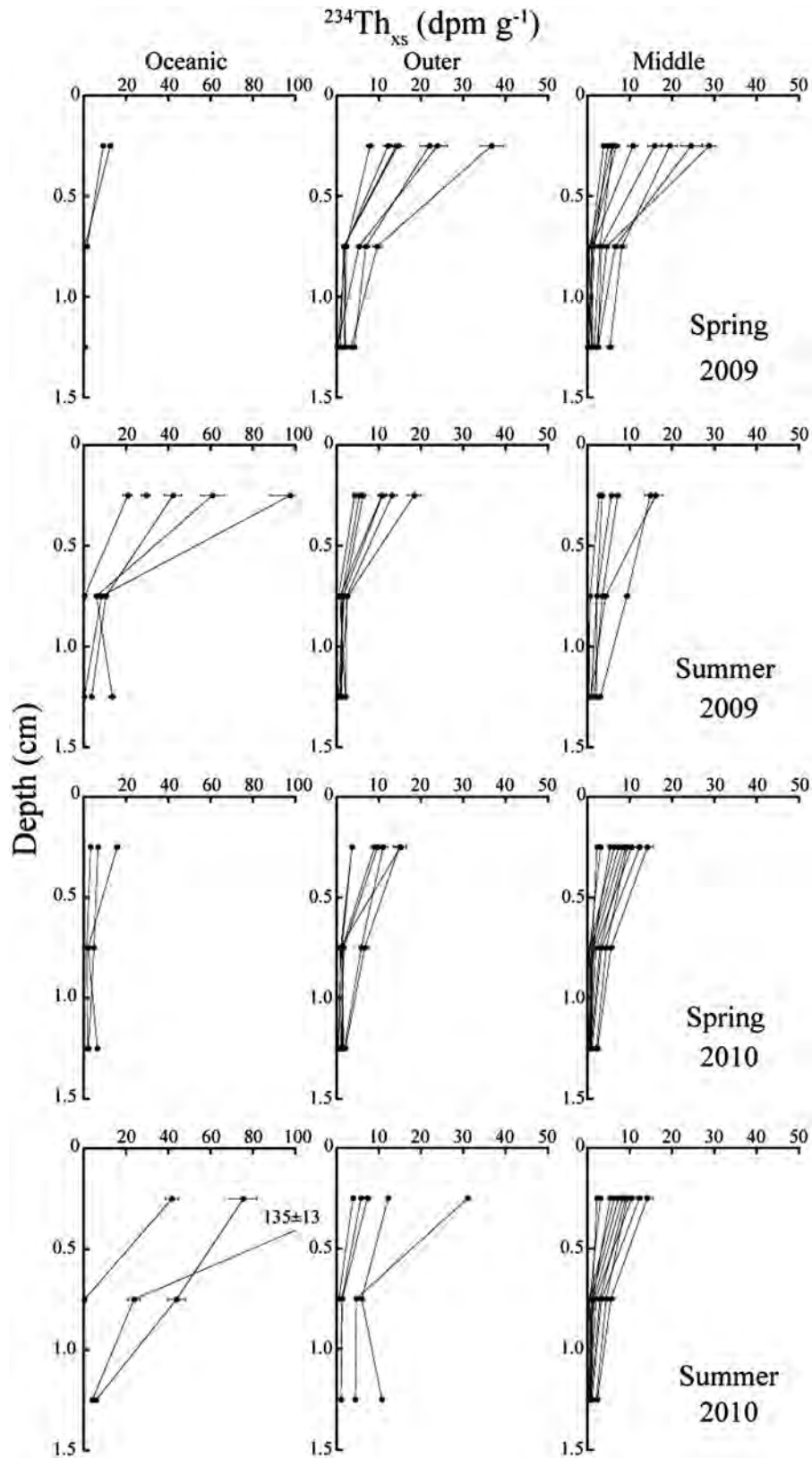


Fig. 5. Depth profiles of sediment $^{234}\text{Th}_{\text{xs}}$ (dpm g^{-1}). Profiles are plotted to a maximum depth of 1.5 cm (1.25 cm mid-point), which correlates with integration depth.

Outer shelf waters, $V \times \Delta Th_{\text{CS}}$ ($\text{dpm cm}^{-2} \text{d}^{-1}$), where V ($\text{m}^2 \text{s}^{-1}$) is the horizontal cross-front exchange rate and ΔTh_{CS} (dpm m^{-4}) represents the cross-shelf ^{234}Th activity gradient between the Oceanic and Outer domains (ΔTh_{CS} can be represented by dTh/dy , where y represents the cross-shelf direction). The removal

terms include the *in situ* decay of ^{234}Th , λA_{Th} , and the along-shelf transport of ^{234}Th , $T \times \Delta Th_{\text{AS}}$ ($\text{dpm cm}^{-2} \text{d}^{-1}$), where T (m s^{-1}) represents the along-shelf water volume transport and ΔTh_{AS} (dpm m^{-3}) is defined as ^{234}Th activity difference between the northern and southern regions. The term J_{sed} represents the net

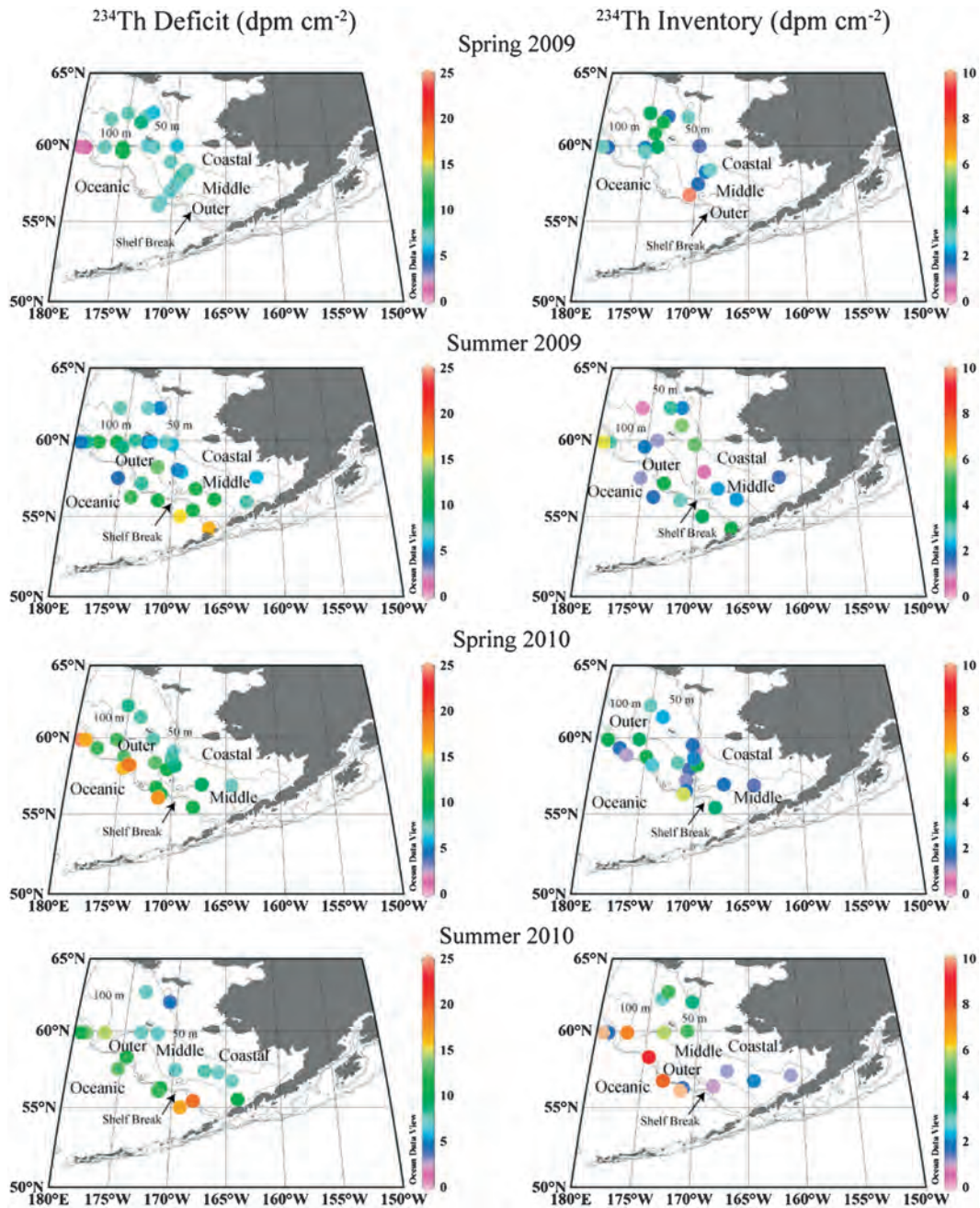


Fig. 6. Maps of water column ^{234}Th deficit and sediment $^{234}\text{Th}_{\text{ss}}$ inventory. Note that two Oceanic sediment $^{234}\text{Th}_{\text{ss}}$ inventories for summer 2010 are off-scale and indicated by lightly shaded symbols.

flux of ^{234}Th to the sediments, and J_{exp} is the net ^{234}Th export from the shelf to the ocean interior. Note that this equation does not explicitly include diffusive transport of ^{234}Th over the shelf. It is assumed that the contribution of diffusion is negligible in the radiochemical balance for ^{234}Th , which is justified below. Also, this balance neglects ^{234}Th input from rivers because ^{234}Th activities in freshwater are negligible and riverine supply to the Middle and Outer shelf regions is insignificant.

4.1.1. Diffusive and advective fluxes of ^{234}Th

The net exchange of ^{234}Th from the Oceanic Domain to the Outer shelf can be quantified as the product of the exchange rate (V) across the shelf break and the ^{234}Th activity gradient between the Oceanic and Outer domains (ΔTh_{CS}). A similar approach was used to examine the diffusive flux of ^{210}Pb across the MAB frontal zone to

the shelf (Bacon et al., 1994). In their study, strong cross-shelf gradients of ^{210}Pb and a significant correlation between ^{210}Pb activity and salinity were used to estimate the flux of ^{210}Pb from the deep ocean to the shelf. For the eastern Bering Sea, however, there is not a significant correlation between ^{234}Th and salinity for any season ($r^2=0.01\text{--}0.36$). The calculated cross-shelf gradient in ^{234}Th (ΔTh_{CS}) between the Oceanic and Outer domains ranged from -0.0005 ± 0.0013 to 0.0057 ± 0.0017 (mean = 0.0018 ± 0.0028) $\text{dpm m}^{-3} \text{m}^{-1}$ of the approximately 100 km width of the Outer Domain. The cross-front exchange rate (V) for the shelf break was determined to be $0.46 \text{ m}^2 \text{ s}^{-1}$ based on a reported net on-shelf water mass transport rate of $14,500 \text{ km}^3 \text{ yr}^{-1}$ (Aagaard et al., 2006) and a shelf length of approximately 1000 km. This value is similar to cross-front exchange rates recently reported for the Middle Front at the 100 m isobath (Danielson et al., 2012). Using these values, the cross-shelf exchange of ^{234}Th from the Oceanic Domain to the Outer

Table 2Water column ^{234}Th deficit, sediment excess inventory ($^{234}\text{Th}_{\text{xs}}$), focusing factor (FF_{Th}), and residence time of total ^{234}Th (τ_t) for the eastern Bering Sea during 2009 and 2010.

Station	Latitude °N	Longitude °W	Bottom depth (m)	^{234}Th deficit (dpm cm $^{-2}$)	$^{234}\text{Th}_{\text{xs}}$ (dpm cm $^{-2}$)	FF_{Th}	τ_t (d)
<i>Spring, March 31–May 12, 2009</i>							
<i>Middle Domain (z=50–100 m)</i>							
1-NP7	57.90	169.32	66	7.71 ± 0.41	nd	nd	25.9
2-NP6.5	58.04	169.23	67	8.01 ± 0.43	nd	nd	26.6
3-Ice/process 1	58.23	169.12	72	nd	1.93 ± 0.35	nd	nd
9-MN4.5	59.97	169.86	55	6.32 ± 0.34	1.41 ± 0.32	0.22 ± 0.02	25.4
10-MN5	58.90	170.40	62	7.38 ± 0.39	nd	nd	25.4
14-MN8	59.91	172.18	72	7.54 ± 0.52	nd	nd	34.1
32-SL12	62.20	175.14	80	6.87 ± 0.74	3.22 ± 0.38	0.47 ± 0.06	50.3
35-SL9	61.97	173.24	62	7.26 ± 0.60	1.85 ± 0.35	0.26 ± 0.03	25.3
39-SL6	61.93	171.22	51	nd	2.96 ± 0.47	nd	nd
54-NP5	58.37	168.73	68	7.63 ± 0.66	2.76 ± 0.45	0.36 ± 0.04	28.2
58-NP9	57.45	169.75	67	7.01 ± 0.50	1.67 ± 0.29	0.24 ± 0.02	33.2
66-NP11	56.98	170.28	75	6.87 ± 0.61	nd	nd	40.3
83-ICE 3	60.81	174.39	91	nd	4.05 ± 0.45	nd	nd
92-MN-SL5	61.57	173.71	72	8.47 ± 0.52	4.79 ± 0.58	0.57 ± 0.04	28.4
93-BN1	62.25	172.51	57	6.06 ± 0.39	nd	nd	29.3
98-SL12	62.18	175.15	81	7.69 ± 0.69	3.74 ± 0.35	0.49 ± 0.05	41.1
120-70M42	60.00	172.73	64	6.62 ± 0.56	nd	nd	38.7
			Average (± 1σ)	7.2 ± 0.7	2.8 ± 1.1	0.37 ± 0.14	32.3 ± 7.7
<i>Outer Domain (z=100–200 m)</i>							
17-MN11	59.90	173.99	104	nd	3.64 ± 0.44	nd	nd
19-MN13	59.86	175.22	120	10.12 ± 1.11	2.05 ± 0.31	0.20 ± 0.03	55.6
22-MN16	59.90	176.99	136	7.37 ± 1.55	nd	nd	107.6
29-MN-SL4	61.78	176.80	113	7.68 ± 1.16	nd	nd	72.8
60-ST	56.27	171.08	142	6.70 ± 1.80	nd	nd	131.7
65-NP12	56.72	170.53	109	nd	9.75 ± 0.96	nd	nd
69-BL1	59.56	175.20	133	10.30 ± 1.34	5.31 ± 0.64	0.52 ± 0.07	61.3
73-BL4	59.59	175.08	129	9.85 ± 1.35	2.62 ± 0.34	0.27 ± 0.04	63.5
90-BL20	59.55	175.15	132	12.30 ± 0.98	2.47 ± 0.34	0.20 ± 0.02	36.0
116-BL15	59.56	175.15	130	10.53 ± 1.38	2.91 ± 0.38	0.28 ± 0.04	61.0
			Average (± 1σ)	9.4 ± 1.9	4.1 ± 2.7	0.29 ± 0.13	73.7 ± 30.9
<i>Oceanic Domain (z > 200 m)</i>							
25-MN19	59.89	178.90	705	1.26 ± 0.14	1.57 ± 0.23	1.25 ± 0.17	–
26-MN20	59.92	179.45	2714	0.71 ± 0.08	2.96 ± 0.51	4.17 ± 0.59	–
61-NP15	56.05	171.30	2760	7.23 ± 5.91	nd	nd	–
			Average (± 1σ)	3.1 ± 3.6	2.3 ± 1.0	2.71 ± 2.07	–
<i>Summer, June 14–July 13, 2009</i>							
<i>Middle Domain (z=50–100 m)</i>							
10-UAP3	55.96	163.14	90	7.85 ± 0.76	nd	nd	44.0
17-CN2	57.56	162.13	51	5.75 ± 0.32	1.49 ± 0.35	0.26 ± 0.03	23.4
45-NP7	57.90	169.24	70	5.97 ± 0.60	0.64 ± 0.09	0.11 ± 0.01	44.3
89-XB6	59.71	170.32	66	5.82 ± 0.56	5.34 ± 0.77	0.92 ± 0.11	40.8
100-MN6	59.90	171.00	70	7.19 ± 0.65	nd	nd	39.4
104-MN9	59.90	172.80	77	4.62 ± 0.86	nd	nd	83.2
130-XB2-4	61.00	171.76	65	nd	5.51 ± 0.45	nd	nd
137-SL6	62.20	171.89	51	5.20 ± 0.34	2.09 ± 0.33	0.40 ± 0.04	29.3
140-SL9	62.20	173.11	62	7.06 ± 0.41	3.21 ± 0.42	0.45 ± 0.03	25.8
147-SL16	62.20	175.98	95	7.73 ± 0.88	0.75 ± 0.06	0.10 ± 0.01	52.5
165-70M41	59.91	172.42	70	5.68 ± 0.75	nd	nd	61.2
181-70M25	58.05	169.65	68	5.19 ± 0.45	nd	nd	38.4
			Average (± 1σ)	6.2 ± 1.1	2.7 ± 2.0	0.37 ± 0.30	43.8 ± 17.1
<i>Outer Domain (z=100–200 m)</i>							
22-CN12	56.13	166.13	113	10.04 ± 0.95	2.18 ± 0.27	0.22 ± 0.02	43.1
25-CN17	55.43	168.06	203	10.61 ± 2.57	nd	nd	115.1
32-CNN6	56.80	167.87	104	10.86 ± 0.81	2.19 ± 0.41	0.20 ± 0.02	33.1
60-SB7	56.28	173.84	196	12.63 ± 2.20	1.72 ± 0.33	0.14 ± 0.03	80.5
79-XB16	57.16	172.95	121	8.14 ± 1.36	4.10 ± 0.48	0.50 ± 0.09	72.7
106-MN11	60.00	174.00	105	8.14 ± 1.07	1.12 ± 0.23	0.14 ± 0.02	58.4
109-MN14	59.90	175.80	132	11.98 ± 1.34	nd	nd	51.4
112-MN17	59.90	177.60	140	10.73 ± 1.49	nd	nd	64.3
113-MN19	59.90	178.74	152	8.29 ± 1.92	3.10 ± 0.46	0.37 ± 0.09	–
122-XB2-12	59.56	175.20	136	8.49 ± 1.57	1.94 ± 0.32	0.23 ± 0.05	84.8
			Average (± 1σ)	10.0 ± 1.7	2.3 ± 1.0	0.26 ± 0.13	67.0 ± 24.7
<i>Oceanic Domain (z > 200 m)</i>							
1-U1	54.25	166.56	1246	15.96 ± 2.80	4.51 ± 0.4748	0.28 ± 0.05	92.0
27-CN20	55.02	169.22	2343	15.38 ± 3.87	3.79 ± 0.4348	0.25 ± 0.07	124.2
53-NP15	56.06	171.34	2800	10.65 ± 4.34	2.99 ± 0.348	0.28 ± 0.12	193.9

Table 2 (continued)

Station	Latitude °N	Longitude °W	Bottom depth (m)	^{234}Th deficit (dpm cm $^{-2}$)	$^{234}\text{Th}_{\text{xs}}$ (dpm cm $^{-2}$)	FF_{Th}	τ_{r} (d)
66-P14-7	58.23	171.59	2090	13.29 ± 3.30	nd	nd	142.5
67-P14-10	57.50	175.24	3492	4.19 ± 0.46	1.11 ± 0.181	0.26 ± 0.04	–
115-MN20	59.89	179.37	2779	4.87 ± 3.78	6.02 ± 0.4668	1.24 ± 0.97	–
Average (± 1σ)				10.7 ± 5.2	3.7 ± 1.8	0.46 ± 0.43	138.1 ± 42.7
<i>Spring, May 9–June 14, 2010</i>							
<i>Middle Domain (z=50–100 m)</i>							
15-Z6	57.90	170.65	80	10.63 ± 0.46	1.51 ± 0.27	0.14 ± 0.01	19.0
24-Z15	58.35	171.80	99	13.01 ± 0.63	3.04 ± 0.44	0.23 ± 0.02	21.6
66-NZ4.5	59.07	170.17	67	6.96 ± 0.45	0.99 ± 0.29	0.14 ± 0.02	29.3
71-HBR1	56.92	167.32	78	9.14 ± 0.51	1.76 ± 0.37	0.19 ± 0.02	24.5
80-AL2	57.18	170.87	85	nd	1.27 ± 0.24	nd	nd
81-70M26	58.17	169.91	72	8.77 ± 0.41	4.22 ± 0.60	0.48 ± 0.03	23.0
99-70M4	56.85	164.51	73	7.30 ± 0.56	1.42 ± 0.23	0.20 ± 0.02	33.6
121-70M26	58.15	169.92	71	8.74 ± 0.42	nd	nd	21.2
124-70M29	58.62	170.28	72	8.11 ± 0.51	2.05 ± 0.36	0.25 ± 0.02	28.4
147-70M52	61.41	173.74	75	7.85 ± 0.58	2.20 ± 0.35	0.28 ± 0.03	33.4
156-SL12	62.19	175.15	80	8.22 ± 0.65	2.90 ± 0.31	0.35 ± 0.03	35.9
175-MN8	59.90	172.20	73	7.72 ± 0.56	nd	nd	33.1
178-AL4	59.52	170.50	68	nd	1.66 ± 0.30	nd	nd
Average (± 1σ)				8.8 ± 1.7	2.1 ± 1.0	0.25 ± 0.11	27.5 ± 5.9
<i>Outer Domain (z=100–200 m)</i>							
2-NP14	56.28	171.05	141	8.96 ± 1.51	nd	nd	83.8
6-NP13	56.51	170.80	122	nd	1.83 ± 0.31	nd	nd
7-NP12	56.73	171.57	109	11.71 ± 0.93	nd	nd	37.7
35-ZC8	58.74	174.90	146	13.16 ± 1.40	4.62 ± 0.60	0.35 ± 0.04	49.8
39-IE1	59.33	177.61	138	12.71 ± 1.33	1.80 ± 0.31	0.14 ± 0.02	49.6
54-AL1	58.86	176.86	126	nd	1.08 ± 0.24	nd	nd
84-CN17	55.44	168.06	200	12.36 ± 2.25	nd	nd	88.0
87-CN17	55.43	168.06	204	11.24 ± 2.50	3.52 ± 0.46	0.31 ± 0.08	108.1
161-MN19	59.90	178.91	206	10.12 ± 2.61	nd	nd	125.1
169-MN14	59.90	175.81	130	12.75 ± 1.21	3.68 ± 0.50	0.29 ± 0.03	44.3
190-NP14	56.28	171.06	188	10.65 ± 1.42	5.94 ± 0.64	0.56 ± 0.08	62.5
Average (± 1σ)				11.5 ± 1.4	3.2 ± 1.7	0.33 ± 0.15	72.1 ± 30.7
<i>Oceanic Domain (z > 200 m)</i>							
49-MN19	59.90	178.91	489	13.65 ± 5.44	4.92 ± 0.72	0.36 ± 0.15	203.7
52-MN20	59.90	179.44	2699	12.55 ± 5.51	nd	nd	225.6
55-NZ11.5	58.20	174.24	381	16.41 ± 5.32	2.64 ± 0.42	0.16 ± 0.06	163.7
56-P14-3	58.00	174.85	3014	15.80 ± 5.42	nd	nd	173.0
57-NZ11.5	58.22	174.35	440	18.83 ± 5.34	nd	nd	137.8
162-MN20	59.90	179.44	2672	24.44 ± 4.79	nd	nd	99.1
163-MN19	59.89	178.90	656	16.54 ± 3.80	4.54 ± 0.55	0.27 ± 0.07	112.6
195-NP15	56.05	171.30	2740	17.28 ± 5.33	nd	nd	155.1
Average (± 1σ)				16.9 ± 3.6	4.0 ± 1.2	0.27 ± 0.10	158.8 ± 42.9
<i>Summer, June 16–July 13, 2010</i>							
<i>Middle Domain (z=50–100 m)</i>							
8-UAP5	55.53	163.98	91	9.85 ± 0.69	nd	nd	31.3
15-UAP2	57.06	161.04	74	nd	1.16 ± 0.17	nd	nd
20-CN8	56.71	164.51	76	7.20 ± 0.65	2.07 ± 0.30	0.29 ± 0.03	39.8
34-CNN4	57.35	167.04	72	7.88 ± 0.52	1.15 ± 0.26	0.15 ± 0.02	29.7
47-NP9	57.44	169.82	66	6.94 ± 0.53	nd	nd	34.0
74-W7	60.00	171.06	70	nd	5.10 ± 0.66	nd	nd
91-MN10	59.90	173.40	86	7.20 ± 0.79	5.74 ± 0.76	0.80 ± 0.10	51.0
122-ML3	61.97	170.78	50	4.62 ± 0.37	3.38 ± 0.43	0.73 ± 0.07	37.1
134-SL11	62.20	173.93	64	nd	2.76 ± 0.35	nd	nd
145-BN3	62.67	173.38	66	7.30 ± 0.51	5.08 ± 0.62	0.70 ± 0.06	32.2
167-70M39	59.83	171.77	75	7.02 ± 0.62	nd	nd	40.5
197-70M9	57.26	165.75	70	7.16 ± 0.57	nd	nd	35.3
Average (± 1σ)				7.2 ± 1.3	3.3 ± 1.8	0.53 ± 0.29	36.8 ± 6.5
<i>Outer Domain (z=100–200 m)</i>							
25-CN17	55.43	168.06	198	19.28 ± 1.89	nd	nd	46.4
31-CNN7	56.35	168.29	130	nd	0.94 ± 0.15	nd	nd
53-TD2	56.25	171.11	190	11.50 ± 2.14	1.61 ± 0.23	0.14 ± 0.03	91.2
58-SB5	56.72	173.02	132	nd	7.76 ± 0.68	nd	nd
97-MN16	59.90	177.00	136	14.38 ± 1.17	7.33 ± 0.97	0.51 ± 0.05	37.4
100-TD4	59.90	178.85	225	13.43 ± 2.76	1.79 ± 0.28	0.13 ± 0.03	97.5
Average (± 1σ)				14.6 ± 3.3	3.9 ± 3.4	0.26 ± 0.22	68.1 ± 30.6

Table 2 (continued)

Station	Latitude °N	Longitude °W	Bottom depth (m)	^{234}Th deficit (dpm cm^{-2})	$^{234}\text{Th}_{\text{ss}}$ (dpm cm^{-2})	FF_{Th}	τ_t (d)
Oceanic Domain ($z > 200$ m)							
26-CN20	55.02	169.22	2332	16.52 ± 5.38	nd	nd	163.7
54-NP15	56.06	171.32	2785	12.71 ± 5.66	39.69 ± 3.77	3.12 ± 1.42	223.3
62-P14N-10	57.50	175.24	3473	13.08 ± 5.62	nd	nd	215.0
63-P14N-7	58.27	174.56	2112	12.25 ± 2.46	9.00 ± 0.74	0.73 ± 0.15	97.3
102-MN20	59.90	179.40	2705	10.62 ± 5.71	43.24 ± 4.45	4.07 ± 2.23	273.5
Average ($\pm 1\sigma$)				13.0 ± 2.2	30.6 ± 18.8	2.64 ± 1.72	194.6 ± 66.9

shelf was estimated to range from -0.0018 ± 0.0051 to 0.0226 ± 0.0069 (mean = 0.0069 ± 0.0100) $\text{dpm cm}^{-2} \text{d}^{-1}$ spread over the approximate width of the Outer shelf (Table 3). These low average lateral fluxes imply that the cross-shelf exchange of ^{234}Th from the deep ocean to the Outer shelf is a minor component in the ^{234}Th balance for the eastern Bering Sea shelf (Fig. 8).

Because of the separation imposed by the Middle Front and the difference in water mass circulation, the along-shelf transport of ^{234}Th may vary for the Outer and Middle domains. Sub-tidal water transport over the Middle and Outer shelf is small relative to boundary currents, (Coachman, 1986) and along-shelf ^{234}Th activity differences between the northern and southern regions of the eastern Bering Sea shelf are negligible. Therefore, T is small and variable and ΔTh_{AS} is zero, implying that the along-shelf transport of ^{234}Th over the shelf is negligible in the ^{234}Th budget.

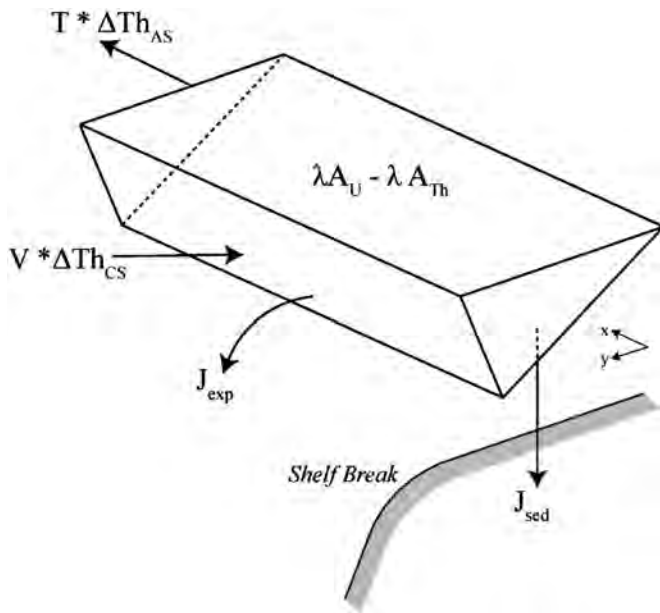


Fig. 7. Illustration of the supply and removal terms responsible for the radiochemical balance of ^{234}Th over the eastern Bering Sea shelf. Terms defined in Table 3.

Table 3

Seasonal ^{234}Th budget for the Middle and Outer domains of the eastern Bering Sea shelf (all units in $\text{dpm cm}^{-2} \text{d}^{-1}$).

Process	Term	Spring 2009	Summer 2009	Spring 2010	Summer 2010	Average	Fraction λU	
Input	Production by <i>in situ</i> decay of ^{238}U	λU	0.55 ± 0.21	0.59 ± 0.24	0.64 ± 0.30	0.61 ± 0.32	0.59 ± 0.27	
	Cross-front exchange of ^{234}Th	$V \times \Delta Th_{\text{CS}}$	0.023 ± 0.007	-0.001 ± 0.006	-0.002 ± 0.005	0.008 ± 0.006	0.007 ± 0.006	0.01 ± 0.01
Output	Loss by <i>in situ</i> decay of ^{234}Th	λTh	0.32 ± 0.18	0.36 ± 0.19	0.36 ± 0.26	0.34 ± 0.23	0.34 ± 0.21	0.58 ± 0.44
	Along-shore transport	$T \times \Delta Th_{\text{AS}}$	0	0	0	0	0	
	Decay of ^{234}Th in sediments	J_{sed}	0.10 ± 0.06	0.07 ± 0.04	0.07 ± 0.04	0.10 ± 0.07	0.09 ± 0.05	0.15 ± 0.11
Excess	Shelf export flux of ^{234}Th	J_{exp}	0.16 ± 0.28	0.16 ± 0.31	0.21 ± 0.40	0.18 ± 0.40	0.17 ± 0.35	0.29 ± 0.60

A further argument for the negligible transport of ^{234}Th by advection and diffusion lies in the length scale over which these processes are significant for the relevant spatial and temporal scales. Physical transport of water over the Middle and Outer shelf of the eastern Bering Sea is predominantly due to cross-shelf tidal currents (Coachman, 1982, 1986). The eastern Bering Sea experiences mixed semi-diurnal tides, with M_2 tidal current velocities of $15\text{--}30 \text{ cm s}^{-1}$ and the K_1 constituent contributing $10\text{--}20 \text{ cm s}^{-1}$ (Coachman, 1986). The length scale (L_a) over which advective transport of ^{234}Th is significant can be determined using (e.g., Lepore et al., 2007):

$$L_a = U_h t \quad (5)$$

where U_h is the tidal velocity (15 cm s^{-1}) and t is the mean life of ^{234}Th (35 d). Using these values, L_a is approximately 450 km. However, because daily current velocities are a function of both ebb and flood tides, the net daily cross-shelf water flux over the Middle and Outer shelves is small. Thus, the net advective transport of ^{234}Th by tides is a minor component in the radiochemical balance of ^{234}Th .

To examine horizontal diffusion as a mechanism for the transport of ^{234}Th , the mean diffusive path length in the absence of ^{234}Th scavenging is calculated as (e.g., Lepore et al., 2007; Moran et al., 1997):

$$L_d = \sqrt{2K_H t} \quad (6)$$

Coachman (1982) determined eddy diffusion (K_H) to range from ~ 1 to $5 \times 10^6 \text{ cm}^2 \text{ s}^{-1}$, depending on depth, location, and time of

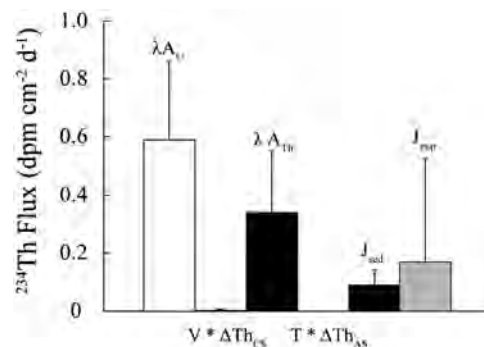


Fig. 8. Seasonally averaged supply (white bar), removal (black bars), and off-shelf export (gray bar) of ^{234}Th over the eastern Bering Sea shelf.

year for the Middle and Outer shelf areas of the eastern Bering Sea. An average K_H of $2.6 \times 10^6 \text{ cm}^2 \text{ s}^{-1}$ provides an L_d of $\sim 40 \text{ km}$. Over transit scales of $> 40 \text{ km}$, ingrowth of ^{234}Th would tend to obscure the scavenging signature for a particular parcel of water. Note also that, assuming a shelf length of 1000 km and average depth of 170 m , the net cross-shelf water flux to the Outer shelf averaged over the entire shelf break is 85 km yr^{-1} , or 8 km over the mean-life of ^{234}Th . Therefore, because L_a , L_d , and the imported signal of ^{234}Th from the deep ocean are small compared to spatial sampling, the flux of ^{234}Th from advective transport by tidal currents, horizontal diffusion, and on-shelf transport over the mean-life of ^{234}Th are insignificant over the relevant spatial and temporal time scales of this study.

4.1.2. Production, decay, and sediment flux of ^{234}Th over the shelf

Because advection and diffusion of ^{234}Th has been determined to be insignificant, the radiochemical balance of ^{234}Th (Eq. (4)) for the Middle and Outer domains of the eastern Bering Sea simplifies to an equation dependent on the *in situ* water column production and decay of ^{234}Th , the flux of ^{234}Th into the sediments, and the net particle export flux of ^{234}Th from the shelf:

$$\lambda A_U = \lambda A_{Th} + J_{sed} + J_{exp} \quad (7)$$

The production and decay terms are evaluated using spatially averaged, depth integrated activities of ^{234}Th and ^{238}U . On a seasonal basis, the areal production of ^{234}Th by ^{238}U decay in the water column ranges from 0.55 ± 0.21 to 0.64 ± 0.30 (mean = 0.59 ± 0.04) $\text{dpm cm}^{-2} \text{ d}^{-1}$. The areal decay of ^{234}Th in the water column is smaller than production, ranging from 0.32 ± 0.18 to 0.36 ± 0.23 (mean = 0.34 ± 0.02) $\text{dpm cm}^{-2} \text{ d}^{-1}$ (Table 3). The difference between the production and decay rates of ^{234}Th ($\lambda(A_U - A_{Th})$) is equal to the total particle removal flux ($J_{sed} + J_{exp}$).

At steady-state, the flux of ^{234}Th into the shelf sediments must be balanced by decay in the sediment column. Thus, J_{sed} is quantified as the product of the average excess sediment inventory of ^{234}Th and the ^{234}Th decay constant (Bacon et al., 1994):

$$J_{sed} = \lambda \int_0^z {}^{234}\text{Th}_{xs} dz \quad (8)$$

The seasonal decay of ^{234}Th in shelf sediments of the eastern Bering Sea ranges from 0.07 ± 0.04 to 0.10 ± 0.07 (mean = 0.09 ± 0.02) $\text{dpm cm}^{-2} \text{ d}^{-1}$ (Table 3). By comparison, decay of excess ^{234}Th in the sediments represents 0.15 ± 0.11 of ^{234}Th production in the water column (Table 3). The implication is that shelf sediments are an important sink in the scavenging removal of ^{234}Th from the overlying water column.

4.1.3. Off-shelf export of ^{234}Th

The radiochemical balance of ^{234}Th in the eastern Bering Sea is summarized in Table 3. The seasonal export flux of ^{234}Th from the shelf to the ocean interior (J_{exp}) can be calculated from the difference between the supply and removal fluxes of ^{234}Th (Eq. (7)). For spring and summer, J_{exp} represents on average 0.29 ± 0.60 of the total production of ^{234}Th (Fig. 8), implying that on a seasonal basis ^{234}Th is largely retained (i.e., $\sim 70\%$ of ^{234}Th production) over the eastern Bering Sea shelf. This result is consistent with a previous study conducted in the MAB using ^{210}Pb , which demonstrated that $\sim 20\%$ of the total ^{210}Pb supplied to that shelf is removed by particle export into the interior ocean on a time-scale of decades (Bacon et al., 1994). From the present data set, however, it is not possible to define a mechanism responsible for the transport and removal of ^{234}Th and associated particles off the shelf over seasonal time-scales. It is interesting to note that Bacon et al. (1994) propose that particles are removed from the shelf by a

deposition-bioturbation-resuspension-redeposition loop over decadal time-scales, and it is possible that such a mechanism exists for the eastern Bering Sea.

In addition, J_{exp} can be used to place an upper bound on the seasonal export flux of POC. Using the average J_{exp} value (Table 3; $0.17 \pm 0.35 \text{ dpm cm}^{-2} \text{ d}^{-1}$) and an average POC/ ^{234}Th ratio of $11 \pm 9 \text{ } \mu\text{mol C dpm}^{-1}$ at 100 m measured in sediment trap material collected in spring and summer of 2008–2010 (Baumann et al., 2012) yields a POC export flux of $18 \pm 41 \text{ mmol C m}^{-2} \text{ d}^{-1}$. Despite the inherent uncertainty in this estimate, this POC export flux is similar to values of $10 \pm 8 \text{ mmol C m}^{-2} \text{ d}^{-1}$ determined using ^{234}Th – ^{238}U disequilibrium and sediment traps in 2008 (Moran et al., 2012), and $19 \pm 17 \text{ mmol C m}^{-2} \text{ d}^{-1}$ recorded in sediment traps in spring and summer of 2008–2010 (Baumann et al., 2012). The estimated POC export flux should be regarded as an upper estimate, due to the uncertainty in converting J_{exp} to a POC export flux using an imputed POC/ ^{234}Th ratio, which can vary considerably (e.g., Moran et al., 2003), and to possible preferential remineralization of POC.

4.2. Residence time of ^{234}Th in the water column

The residence time of total ^{234}Th (τ_t) can be used to further assess the time-scale of particle retention over the eastern Bering Sea shelf. Specifically, the residence time of total ^{234}Th provides a quantitative measure of the efficiency of scavenging and transport of ^{234}Th within the shelf and upper water column of the Oceanic region. A one-dimensional, irreversible scavenging model is used for the estimation of total water column ^{234}Th residence time, which as justified above, sets advective and diffusive transport of ^{234}Th to zero (Coale and Bruland, 1987; Wei and Murray, 1992):

$$\frac{\partial A_{Th}}{\partial t} = \lambda A_U - \lambda A_{Th} - \lambda_c A_{Th} \quad (9)$$

where λ_c is the first-order rate scavenging constant for ^{234}Th . Eq. (9) describes the balance between ^{234}Th production, decay, and particle scavenging. Assuming steady-state, Eq. (9) simplifies to:

$$\lambda_c = \lambda \frac{\int_0^z (A_U - A_{Th}) dz}{\int_0^z A_{Th} dz} \quad (10)$$

where z is the depth of integration. The residence time of total ^{234}Th can be estimated for the entire water column by the relationship:

$$\tau_t = \frac{1}{\lambda_c} \quad (11)$$

Water column ^{234}Th residence times exhibit a gradient off the shelf during spring and summer (Fig. 9; Table 2). For the Middle and Outer shelves, ^{234}Th residence time averages $49 \pm 26 \text{ d}$, which is similar to other coastal systems, such as Dabob Bay, Washington State (4–70 d) (Wei and Murray, 1992) and the inner region of the Gulf of Maine (34–143 d) (Moran and Buesseler, 1993). In the Oceanic region, residence times increase to 5–6 months, which are similar to those reported for the outer reaches of the Gulf of Maine (Moran and Buesseler, 1993) and Funka Bay, Japan (Wei and Murray, 1992). By comparison, estimates of water transport onto the shelf of the eastern Bering Sea and flow through the Bering Strait were used to determine water mass residence times of ~ 3 – 7 yr for the shelf region (Aagaard et al., 2006). Shelf water residence times are much longer than the average τ_t , which is consistent with the largely seasonal retention of ^{234}Th and associated particles over the eastern Bering Sea shelf.

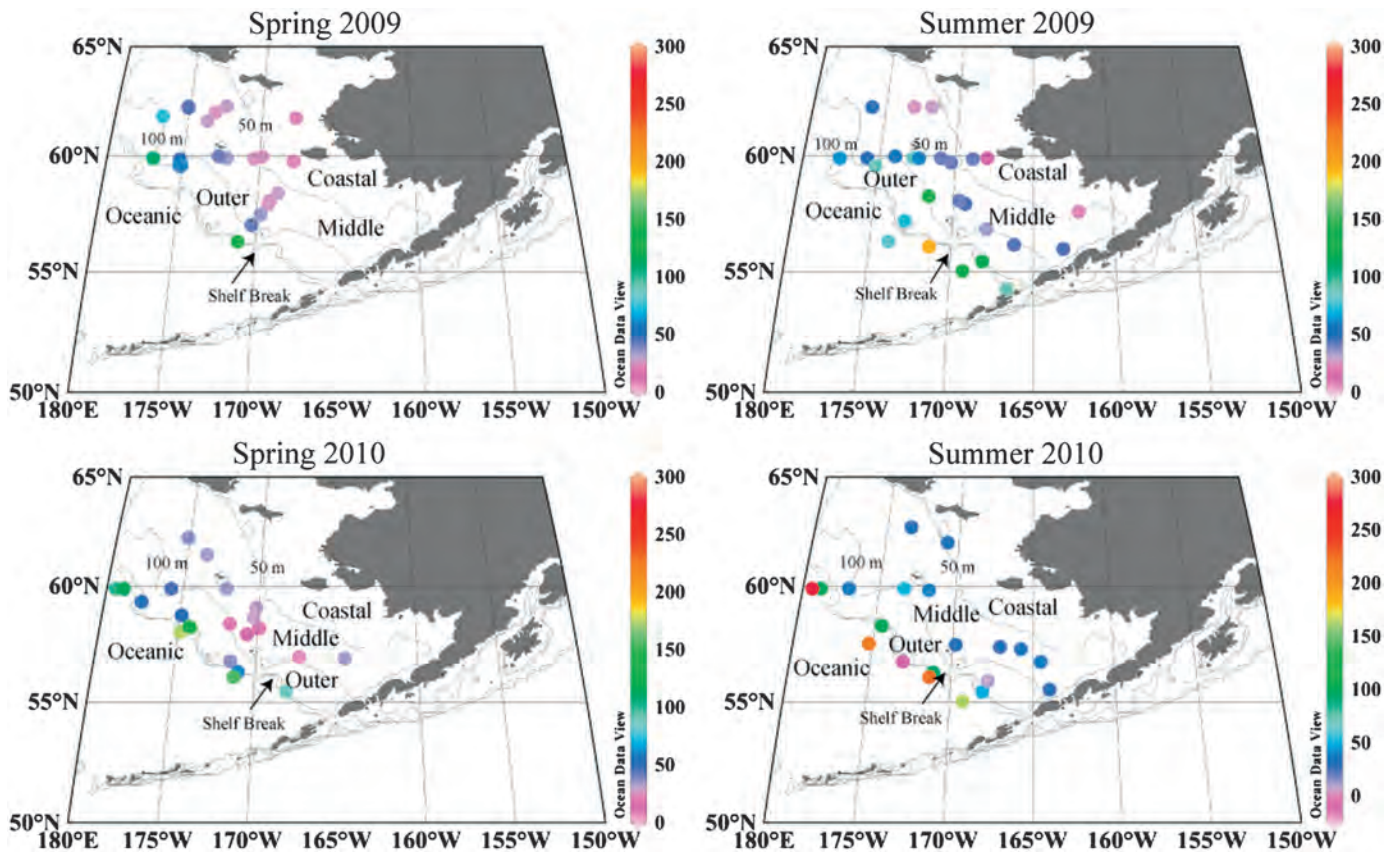


Fig. 9. Distributions of total ^{234}Th residence time (τ_r , d) in the eastern Bering Sea.

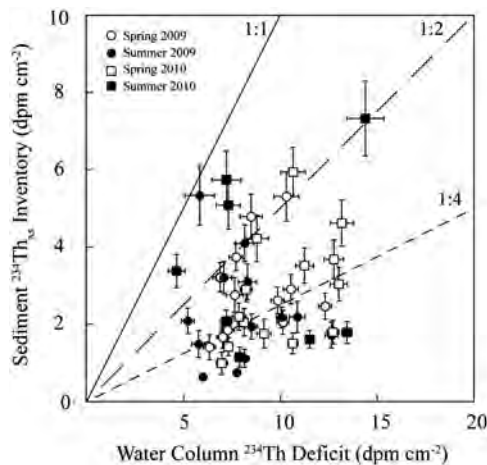


Fig. 10. Plot of sediment $^{234}\text{Th}_{\text{xs}}$ inventory against water column deficit of ^{234}Th for the eastern Bering Sea shelf. Data plotted only for the Middle and Outer shelf regions.

4.3. ^{234}Th focusing factors

To further establish the extent to which there is a net seasonal retention of particles over the shelf, the exchange of ^{234}Th between the water column and sediments can be evaluated on a station-by-station basis. The relationship between the ^{234}Th deficit in the water column and $^{234}\text{Th}_{\text{xs}}$ inventory (Table 2) on the eastern Bering Sea shelf is illustrated in Fig. 10. This comparison indicates that for $\sim 65\%$ of stations sampled over the shelf, $^{234}\text{Th}_{\text{xs}}$ inventories are within a factor of ~ 1.5 –4 of the measured water column deficits of ^{234}Th . This observation is consistent with the conclusion that the flux of ^{234}Th into the

sediment represents an important sink for ^{234}Th produced over the shelf.

The ^{234}Th focusing factor (FF_{Th}) can be used to further quantify the exchange of ^{234}Th between the water column and sediment. In particular, the FF_{Th} is an empirical relationship that defines the efficiency of ^{234}Th transport from the water column to the underlying sediment (Cochran et al., 1990). The sediment $^{234}\text{Th}_{\text{xs}}$ inventory is related to the water column deficit by the relationship (Cochran et al., 1990; Lepore et al., 2007)

$$FF_{\text{Th}} = \frac{\int_0^z {}^{234}\text{Th}_{\text{xs}} dz}{\int_0^z (A_{238\text{U}} - A_{234\text{Th}}) dz} \quad (12)$$

$FF_{\text{Th}}=1$ implies that the sediment inventory is in balance with water column removal of ^{234}Th over seasonal time scales. FF_{Th} greater, or less, than 1 indicates the redistribution of ^{234}Th into, or away from, a specific sampling location, respectively.

Evaluation of individual FF_{Th} values over the entire geographical area of the eastern Bering Sea provides insight into the shelf-wide, seasonal retention of ^{234}Th (Fig. 11). For the Middle Domain, seasonally averaged FF_{Th} values range from 0.25 ± 0.11 to 0.53 ± 0.29 (mean = 0.38 ± 0.11), whereas values in the Outer Domain range from 0.26 ± 0.22 to 0.33 ± 0.15 (mean = 0.29 ± 0.03) (Fig. 12; Table 2). Elevated (> 1) FF_{Th} values are observed to a lesser extent in the oceanic/slope areas, where seasonal averages range from 0.27 ± 0.10 to 2.71 ± 2.07 in both years (mean = 1.52 ± 1.34) (Figs. 11 and 12), though fewer stations were occupied in the deeper slope water stations.

The observation that FF_{Th} values range from ~ 0.25 – 0.50 implies that shelf sediments are an important sink for ^{234}Th scavenged from the water column on a seasonal time-scale (Figs. 10–12; Table 4). Based on these results, vertical processes of sedimentation must be efficient at retaining particulate ^{234}Th , thereby working against lateral processes that would otherwise largely

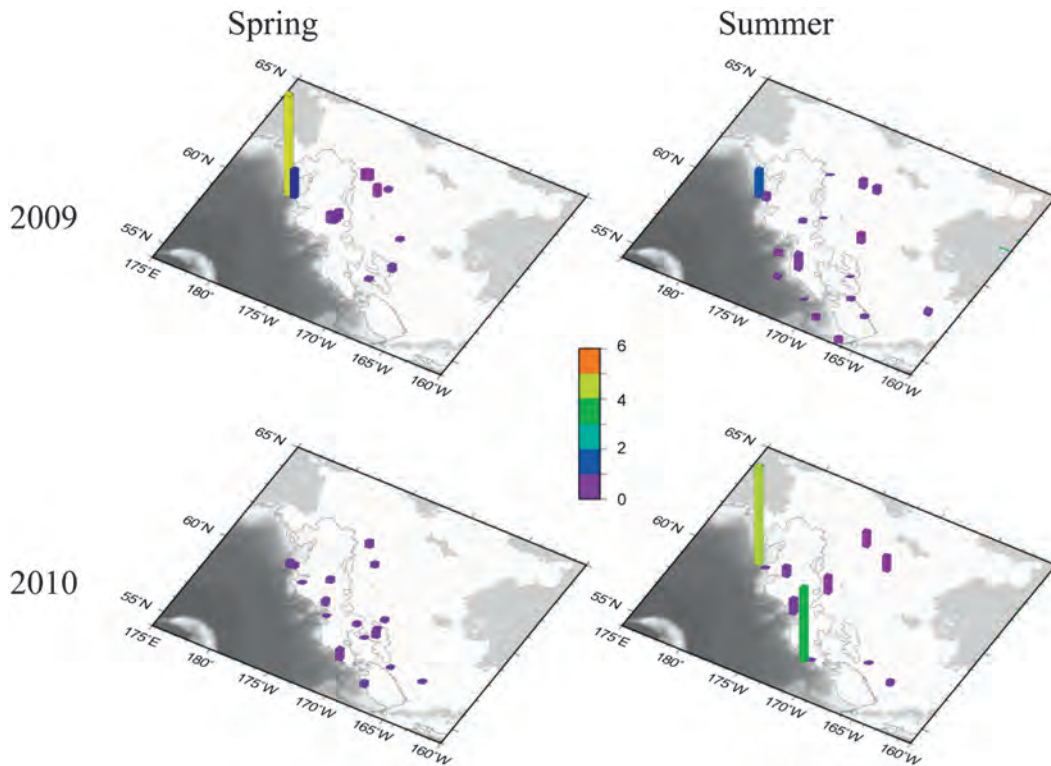


Fig. 11. ^{234}Th focusing factors (FF_{Th}) determined in the eastern Bering Sea.

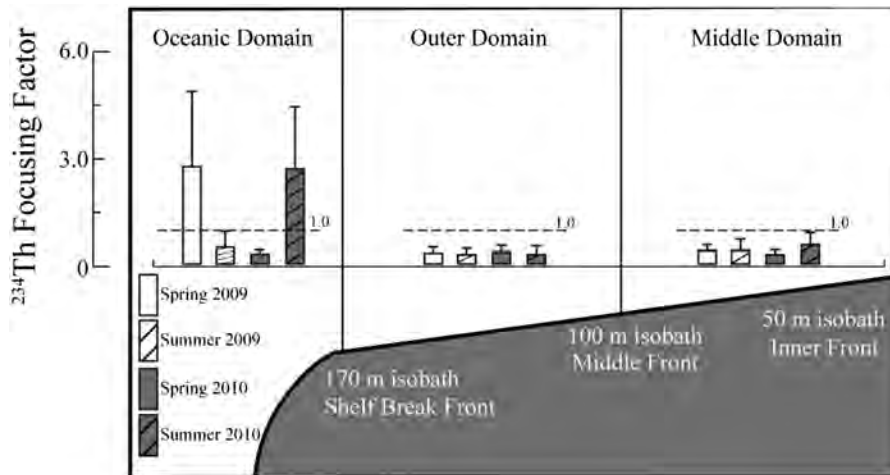


Fig. 12. Average FF_{Th} calculated according to season and domain. Uncertainties represent 1σ .

Table 4

Shelf averages (Middle and Outer domains) of the water column ^{234}Th deficit and sediment $^{234}\text{Th}_{xs}$ inventory. FF_{Th} s were calculated from average deficits and inventories.

Season	^{234}Th deficit dpm cm^{-2}	$^{234}\text{Th}_{xs}$ dpm cm^{-2}	FF_{Th}
Spring 2009	8.01 ± 1.60	3.36 ± 1.97	0.42 ± 0.26
Summer 2009	8.00 ± 2.37	2.53 ± 1.55	0.32 ± 0.22
Spring 2010	10.01 ± 2.09	2.53 ± 1.38	0.25 ± 0.15
Summer 2010	9.52 ± 4.07	3.53 ± 2.41	0.37 ± 0.30
Average	8.79 ± 2.61	2.97 ± 1.85	0.34 ± 0.23

export ^{234}Th (J_{exp}) off the shelf into the interior ocean. As noted above, this result is consistent with a previous study using ^{210}Pb in the MAB, which indicated a net retention of particles on the shelf for up to several decades (Bacon et al., 1994).

4.4. Implications for particle transport and retention

There are several possible qualitative interpretations that may account for the elevated FF_{Th} values observed in the slope/oceanic region (Figs. 11 and 12). In particular, surface water chlorophyll (Chl *a*) distributions indicate events of high autotrophic production at the MIZ associated with retreating sea-ice at the shelf break during late spring. High levels of Chl *a* persist into early summer at the shelf break and are clearly visible from satellite aqua MODIS chlorophyll distributions in May 2009 and 2010 (<http://oceancolor.gsfc.nasa.gov/>). Spring blooms of primary production appear coincident with the locations of the high FF_{Th} values along the shelf break. Thus, elevated FF_{Th} values in deeper water sediments may be attributed to the scavenging removal and deposition of ^{234}Th associated with biogenic particle blooms. Furthermore, there exists a temporal lag between the upper water column deficit

and the high $^{234}\text{Th}_{\text{xs}}$ observed in the sediments in late spring 2010 and summer 2010 (Table 2). Assuming a settling speed of 80–150 m d⁻¹ (Berelson, 2002) for particles sinking through a 2000 m water column, 13–25 days would be required for particles to sink from the surface waters to the underlying sediments. This suggests that vertically exported ^{234}Th from spring autotrophic blooms near the MIZ would settle to the deeper sediments after approximately several weeks.

In addition, the spatial distribution of the elevated FF_{Th} values is consistent with removal of ^{234}Th from high activity, open ocean water to the underlying deep slope sediments. This process is commonly referred to as boundary scavenging, which has been identified as important for a number of other long-lived radiochemical tracers, including ^{210}Pb , ^{230}Th , and ^{231}Pa (e.g., Anderson et al., 1994; Roy-Barman, 2009). In particular, because FF_{Th} values are > 1 in summer at several stations located seaward of the Shelf Break Front, and ^{234}Th export from the shelf is relatively small, the elevated FF_{Th} values are consistent with boundary scavenging removal of ^{234}Th . The source of ^{234}Th that results in the elevated sediment $^{234}\text{Th}_{\text{xs}}$ and hence high FF_{Th} values in the slope/oceanic sediments may be attributed to ^{234}Th -rich off-shore water that is transported to areas of high particle flux, such as near MIZ blooms. Therefore, boundary scavenging provides an additional explanation for the observation of large FF_{Th} values in the slope/oceanic region of the eastern Bering Sea.

Finally, post-depositional transport of surficial, shelf or slope-derived sediments could result in large FF_{Th} values in deep water sediments. Many of the deep water (> 2000 m) cores were extracted from submarine canyons, such as the Pribilof and Zhemchug canyons, which may accumulate sediments from large areas of the shelf and slope.

5. Conclusion

The results reported in this study provide important new insights regarding our understanding of particle transport processes, water column–sediment interaction, and the magnitude of off-shelf export of particles and associated reactive chemicals in a highly dynamic Arctic shelf environment. Prior studies in the northern Bering Sea have reported dramatic shifts in benthic productivity and water column–benthic coupling in the context of a changing climate (Grebmeier et al., 2006a, 2006b). The present study utilizes a geochemical tracer method to evaluate the fate of particles over the southeastern Bering Sea shelf, which has broader applicability in quantifying particle transport processes in other complex shelf systems.

Specifically, based on comprehensive measurements of ^{234}Th in the water column and sediments, it has been determined that on a seasonal basis roughly 2/3 of the supply of ^{234}Th is balanced by decay and sediment burial over the eastern Bering Sea shelf. Furthermore, the off-shelf export flux of ^{234}Th (J_{exp}) represents ~30% of the total ^{234}Th supply, implying that ^{234}Th and associated particles are largely retained on the shelf, rather than exported to the ocean interior. While it not possible to define the mechanism (s) responsible for off-shelf export of ^{234}Th , it is suggested that this may involve a particle deposition–bioturbation–resuspension–re-deposition loop, as described for the off-shelf transport of particles in the MAB (Bacon et al., 1994). In addition, the results of this study have been used to provide an upper estimate of seasonal POC export from the shelf water column of 18 ± 41 mmol C m⁻² d⁻¹. The short average residence time of ^{234}Th in the water column (49 ± 26 d) and average FF_{Th} of 0.34 ± 0.23 on the shelf is further indicative of the net shelf-retention of ^{234}Th in this region. Specifically, the mean residence time of total ^{234}Th is much shorter than mean water mass residence times estimated for

the entire shelf, and the average FF_{Th} of ~0.3 suggests that a significant fraction of ^{234}Th removed from the water column is retained in shelf sediments. In contrast, elevated sediment $^{234}\text{Th}_{\text{xs}}$ and relatively high average FF_{Th} values of 1.52 ± 1.34 observed in the slope/oceanic region of the eastern Bering Sea are attributed to enhanced particle scavenging associated with bloom events in the MIZ region during spring sea-ice retreat. In addition, these high $^{234}\text{Th}_{\text{xs}}$ and FF_{Th} values may also result from boundary scavenging removal of ^{234}Th supplied from high activity, open ocean water transported to areas of high particle flux at the slope, and post depositional transport of material to deeper sediments. It is concluded that ^{234}Th scavenged from the water column, and by inference particles, particulate organic carbon, and other reactive chemicals supplied to the eastern Bering Sea, are largely retained over the shelf on a seasonal time-scale.

Acknowledgments

We thank the Chief Scientists, officers, and crew of the USCGC *Healy*, *R/V Knorr*, and *R/V Thompson* for their efforts. We thank John Karavias of Walt Whitman High School (Queens, NY) and Jason Pavlich of Red Hook High School (Red Hook, NY) for their assistance as part of the ARMADA project. We thank Seth Danielson (UAF) for his input regarding physical transport processes over the eastern Bering Sea shelf. We also thank the hydrographic team from NOAA-PMEL for providing hydrographic data and assisting in sample collection, accessible through the EOL data archive supported by NSF and NOAA. Constructive reviews by three anonymous reviewers are greatly appreciated. This research was supported by awards ARC-0732680 and NPRB-B56 to S.B.M., ARC-0732359 to M.W.L., and ARC-0612380 to D.H.S. This is BEST-BSIERP Bering Sea Project publication number 86.

Appendix A. Supplementary Information

Supplementary data associated with this article can be found in the online version at <http://dx.doi.org/10.1016/j.dsr2.2013.03.008>.

References

- Aagaard, K., Weingartner, T.J., Danielson, S.L., Woodgate, R.A., Johnson, G.C., Whitledge, T.E., 2006. Some controls on flow and salinity in Bering Strait. *Geophys. Res. Lett.* 33 (19), L19602. [10.1029/2006gl026612](https://doi.org/10.1029/2006gl026612).
- Anderson, R.F., Fleisher, M.Q., Biscaye, P.E., Kumar, N., Ditrich, B., Kubik, P., Suter, M., 1994. Anomalous boundary scavenging in the Middle Atlantic Bight: evidence from Th-230, Pa-231, Be-10 and Pb-210. *Deep-Sea Res.* II 41 (2–3), 537–561.
- Bacon, M.P., Belastock, R.A., Bothner, M.H., 1994. Pb-210 balance and implications for particle-transport on the continental-shelf, US Middle Atlantic Bight. *Deep-Sea Res.* II 41 (2–3), 511–535.
- Baumann, M.S., Moran, S.B., Lomas, M.W., Kelly, R.P., Bell, D.W., 2012. Seasonal decoupling of primary production and POC export in relation to sea-ice extent at the shelf break of the eastern Bering Sea. 2013 Aquatic Sciences Meeting (Abstract).
- Benitez-Nelson, C., Buesseler, K.O., Rutgers van der Loeff, M., Andrews, J., Ball, L., Crossin, G., Charette, M., 2001. Testing a new small-volume technique for determining ^{234}Th in seawater. *J. Radioanal. Nucl. Chem.* 248 (3), 795–799.
- Berelson, W.M., 2002. Particle settling rates increase with depth in the ocean. *Deep-Sea Res.* II 49 (1–3), 237–251.
- Buesseler, K.O., 1998. The decoupling of production and particulate export in the surface ocean. *Global Biogeochem. Cycle* 12, 297–310.
- Buesseler, K.O., Ball, L., Andrews, J., Benitez-Nelson, C., Belastock, R., Chai, F., Chao, Y., 1998. Upper ocean export of particulate organic carbon in the Arabian Sea derived from thorium-234. *Deep-Sea Res.* II 45, 2461–2487.
- Buesseler, K.O., Benitez-Nelson, C., Rutgers van der Loeff, M., Andrews, J., Ball, L., Crossin, G., Charette, M.A., 2001. An intercomparison of small-and large-volume techniques for thorium-234 in seawater. *Mar. Chem.* 74, 15–28.
- Burdige, D.J., 2006. *Geochemistry of Marine Sediments*. Princeton University Press, Princeton, NJ.

- Charette, M.A., Moran, S.B., Pike, S.M., Smith, J.N., 2001. Investigating the carbon cycle in the Gulf of Maine using the natural tracer thorium-234. *J. Geophys. Res.* 106, 11,553–11,579.
- Chen, J.H., Edwards, R.L., Wasserburg, G.J., 1986. U-238, U-234 and Th-232 in seawater. *Earth Planet. Sci. Lett.* 80 (3–4), 241–251.
- Coachman, L.K., 1982. Flow convergence over a broad, flat continental shelf. *Cont. Shelf Res.* 1 (1), 1–14.
- Coachman, L.K., 1986. Circulation, water masses, and fluxes on the southeastern Bering Sea shelf. *Cont. Shelf Res.* 5 (1–2), 23–108.
- Coale, K.H., Bruland, K.W., 1987. Oceanic stratified euphotic zone as elucidated by $^{234}\text{Th}/^{238}\text{U}$ disequilibria. *Limnol. Oceanogr.* 32 (1), 189–200.
- Cochran, J.K., Mckibbin-Vaughan, T., Dornblaser, M.M., Hirschberg, D., Livingston, H. D., Buesseler, K.O., 1990. Pb-210 scavenging in the North-Atlantic and North Pacific oceans. *Earth Planet. Sci. Lett.* 97 (3–4), 332–352.
- Cutshall, N.H., Larsen, I.L., Olsen, C.R., 1983. Direct analysis of ^{210}Pb in sediment samples: self-absorption corrections. *Nucl. Instrum. Methods* 206 (1–2), 309–312.
- Danielson, S., Hedstrom, K., Aagaard, K., Weingartner, T., Curchitser, E., 2012. Wind-induced reorganization of the Bering shelf circulation. *Geophys. Res. Lett.* 39 (8), L08601, <http://dx.doi.org/10.1029/2012GL051231>.
- Grebmeier, J.M., Cooper, L.W., Feder, H.M., Sirenko, B.I., 2006a. Ecosystem dynamics of the Pacific-influenced northern Bering and Chukchi seas in the Amerasian Arctic. *Prog. Oceanogr.* 71, 331–361.
- Grebmeier, J.M., Overland, J.E., Moore, S.E., Farley, E.V., Carmack, E.C., Cooper, L.W., Frey, K.E., Helle, J.H., McLaughlin, F.A., McNutt, S.L., 2006b. A major ecosystem shift in the northern Bering Sea. *Science* 311, 1461–1464.
- Kachel, N.B., Hunt, G.L., Salo, S.A., Schumacher, J.D., Stabeno, P.J., Whitedge, T.E., 2002. Characteristics and variability of the inner front of the southeastern Bering Sea. *Deep-Sea Res.* II 49, 5889–5909.
- Lalande, C., Lepore, K., Cooper, L.W., Grebmeier, J.M., Moran, S.B., 2007. Export fluxes of particulate organic carbon in the Chukchi Sea: a comparative study using $^{234}\text{Th}/^{238}\text{U}$ disequilibria and drifting sediment traps. *Mar. Chem.* 103, 185–196.
- Lepore, K., Moran, S.B., Grebmeier, J.M., Cooper, L.W., Lalande, C., Maslowski, W., Hill, V., Bates, N.R., Hansell, D.A., Mathis, J.T., Kelly, R.P., 2007. Seasonal and interannual changes in particulate organic carbon export and deposition in the Chukchi Sea. *J. Geophys. Res.* 112, C10024.
- McRoy, C.P., Hood, D.W., Coachman, L.K., Walsh, J.J., Goering, J.J., 1986. Processes and Resources of the Bering Sea Shelf (PROBES): the development and accomplishments of the project. *Cont. Shelf Res.* 5 (1–2), 5–21.
- Moran, S.B., Buesseler, K.O., 1993. Size-fractionated ^{234}Th in continental shelf waters off New England: implications for the role of colloids in oceanic trace metal scavenging. *J. Mar. Res.* 51, 893–922.
- Moran, S.B., Ellis, K.M., Smith, J.N., 1997. Th-234/U-238 disequilibrium in the central Arctic Ocean: implications for particulate organic carbon export. *Deep-Sea Res.* II 44 (8), 1593–1606.
- Moran, S.B., Lomas, M.W., Kelly, R.P., Gradinger, R., Iken, K., Mathis, J.T., 2012. Seasonal succession of net primary productivity, particulate organic carbon export, and autotrophic community composition in the eastern Bering Sea. *Deep-Sea Res.* II 65–70, 84–97.
- Moran, S.B., Weinstein, S.E., Edmonds, H.N., Smith, J.N., Kelly, R.P., Pilson, M.E.Q., Harrison, W.G., 2003. Does $^{234}\text{Th}/^{238}\text{U}$ disequilibrium provide an accurate record of the export flux of particulate organic carbon from the upper ocean? *Limnol. Oceanogr.* 48 (3), 1018–1029.
- Nozaki, Y., Zhang, J., Takeda, A., 1997. Pb-210 and Po-210 in the equatorial Pacific and the Bering Sea: the effects of biological productivity and boundary scavenging. *Deep-Sea Res.* II 44 (9–10), 2203–2220.
- Roy-Barman, M., 2009. Modelling the effect of boundary scavenging on thorium and protactinium profiles in the ocean. *Biogeosciences* 6 (12), 3091–3107.
- Savoye, N., Buesseler, K.O., Cardinal, D., Dehairs, F., 2004. ^{234}Th deficit and excess in the Southern Ocean during spring 2001: particle export and remineralization. *Geophys. Res. Lett.* 31 (12), L12301.
- Smith, J.N., Moran, S.B., Macdonald, R.W., 2003. Shelf-basin interactions in the Arctic Ocean based on ^{210}Pb and Ra isotope tracer distributions. *Deep-Sea Res.* I 50, 397–416.
- Stabeno, P.J., Kachel, N.B., Sullivan, M., Whitedge, T.E., 2002. Variability of physical and chemical characteristics along the 70-m isobath of the southeastern Bering Sea. *Deep-Sea Res.* II 49, 5931–5943.
- Stabeno, P.J., Schumacher, J.D., Ohtani, K., 1999. The physical oceanography of the Bering Sea. In: Loughlin, T.R., Ohtani, K. (Eds.), *A Summary of Physical, Chemical, and Biological Characteristics, and a Synopsis of Research on the Bering Sea*. North Pacific Marine Science Organization (PICES), Univ. of Alaska Sea, pp. 1–28, Grant, AK-SG-99-03.
- Walsh, J.J., 1988. *On the Nature of Continental Shelves*. Academic Press.
- Wei, C.-L., Murray, J.W., 1992. Temporal variations of ^{234}Th activity in the water column of Dabob Bay: particle scavenging. *Limnol. Oceanogr.* 37 (2), 296–314.



Distribution of viable diatom resting stage cells in bottom sediments of the eastern Bering Sea shelf



Chiko Tsukazaki^{a,*}, Ken-Ichiro Ishii^b, Rui Saito^a, Kohei Matsuno^a, Atsushi Yamaguchi^a, Ichiro Imai^{a,*}

^a Graduate School of Fisheries Sciences, Hokkaido University, 3-1-1 Minato-cho, Hakodate, Hokkaido 041-8611, Japan

^b Graduate School of Agriculture, Kyoto University, Oiwake-cho, Kitashirakawa, Sakyo-ku, Kyoto 606-8502, Japan

ARTICLE INFO

Available online 19 March 2013

Keywords:

Diatom
Resting stage cells
Resting spore
Resting cell
Ice algae
Phytoplankton bloom
Overwintering
Life cycle strategy

ABSTRACT

Information on diatom resting stages is fundamentally important to understanding the population dynamics of diatoms including bloom formation. The distribution of viable diatom resting stage cells in bottom sediments of the eastern Bering Sea in July 2009 was investigated by the most probable number (MPN) method. The abundances of diatom resting stage cells ranged from 1.7×10^3 to 1.2×10^6 MPN cells cm^{-3} wet sediment, comparable to those in shallow eutrophic areas where diatom blooms frequently occur. Common species during the spring phytoplankton bloom in the eastern Bering Sea were also dominant in sediments as resting stage cells. It should be noted that relatively high numbers of ice algae species, especially ribbon-shaped chain forming pennate diatoms, were found in the sediments. The life cycle strategy using resting stage cells allows planktonic and ice algal species to survive unfavorable environmental conditions such as the dark winter season, and potentially contribute to form blooms of several types (subsurface of ice, ice edge, plankton) through vertical mixing.

© 2013 Elsevier Ltd. All rights reserved.

1. Introduction

Diatoms are important primary producers within marine ecosystems, and contribute to efficient primary production. Many diatom species are large and often form colonies in chains. Diatom blooms occur extensively in the spring and fall along the coastal areas of middle to high latitudes. It is well known that many diatoms, especially coastal planktonic species, form resting stage cells associated with unfavorable conditions such as low nitrogen concentration and low light intensity (Durbin, 1978; Garrison, 1984; Hargraves and French, 1975; Hollibaugh et al., 1981; McQuoid and Hobson, 1996). Vegetative cells of these diatom species temporarily disappear from the water column, and then reappear and bloom again after some period. The life cycle including resting stages ensures they survive variable coastal environments, leading to domination among phytoplankton populations.

High abundances of diatom resting stage cells ($\sim 10^6$ MPN cells cm^{-3} wet sediment) have been reported from bottom sediments of temperate coastal areas such as the Seto Inland Sea, Japan (Imai et al., 1990; Itakura et al., 1997). The distribution of resting stage cells in sediments is likely related to the distribution of phytoplankton populations in the water column (Pitcher, 1990).

Viable resting stage cells potentially affect the occurrence of autochthonous plankton species in the water column (Itakura et al., 1997). Therefore information, for example distribution and abundance, on resting stage cells is fundamentally important in determining the spatial distribution of diatoms population dynamics and species succession (McQuoid, 2002).

The eastern Bering Sea shelf is the widest continental sea shelf outside the Arctic. The wide shallow shelf, more than 500 km wide, is seasonally covered by sea ice in all years. This is a region well known for high productivity of upper trophic level organisms including crabs, fish, birds, and mammals (McRoy et al., 1986). The annual increase in primary production usually begins with the growth of ice algae on the underside of sea ice (e.g. *Acnathes taeniata*, *Fragilaria striatula*, *Fragilariopsis cylindrus*, *Fragilariopsis oceanica*; Saito and Taniguchi, 1978), followed by a phytoplankton bloom in the water column in the ice front zone (e.g. *Thalassiosira gravida*, *Thalassiosira hyalina*, *Thalassiosira nordenskiöldii*; Saito and Taniguchi, 1978), and the conventional spring bloom in the water column upon thermal stratification (e.g. *Chaetoceros convolutus*, *Chaetoceros debilis*, *Chaetoceros furcellatus*, *Chaetoceros diadema*, dinoflagellates; McRoy and Goering, 1976; Saito and Taniguchi, 1978). When the ice retreats early in late winter, the open water bloom begins in late spring in the stratified water columns due to solar heating without ice associated spring bloom (Eslinger and Iverson, 2001; Hunt et al., 2002; Stabeno et al., 1998, 2001).

The southeastern Bering Sea shelf is separated into distinguishable hydrographic domains by three fronts, and these domains have different circulation features with distinct temperature,

* Corresponding author. Tel.: +81 138 40 5541; fax: +81 138 40 5542.

E-mail addresses: tskzkuai@gmail.com (C. Tsukazaki), imai1ro@fish.hokudai.ac.jp (I. Imai).

salinity and stratification properties (Coachman et al., 1980; Coachman, 1986). In the coastal shelf domain (CSD: < 50 m isobath), the water column tends to be vertically homogeneous due to the overlapping of wind and tidal mixing energies. The middle shelf domain (MSD: $50 < H < 100$ m isobaths) water column is generally homogeneous during fall and winter. Throughout late spring and summer, the surface wind mixed layer is separated from the tidally mixed bottom layer by a pronounced thermocline. The outer shelf domain (OSD: $100 < H < 170$ m isobaths) is a zone of little or no mixing energy characterized by persistent fine structuring of properties between the surface wind mixed layer and tidally mixed bottom layer. The shelf break front separating shelf water from basin water along the shelf edge zone, the Bering Slope Current (Kinder et al., 1975; Schumacher and Reed 1992), is an important physical feature (Springer et al., 1996).

The life cycle of diatoms, including resting stages, is considered essential to their survival and dominance over the Bering Sea shelf, similar to the situation of temperate coastal areas where there is a mutually intimate interaction between water column and sea bottom. In this manuscript, we report on the distribution of viable resting stage cells of diatoms in the eastern Bering Sea shelf bottom sediments, and discuss the dynamics of diatom populations.

2. Materials and methods

Sampling was conducted at 22 stations in the eastern Bering Sea shelf from 8 to 15 July 2009 during a cruise OS202 of the T/S Oshoro-Maruo of Hokkaido University (Fig. 1). A CTD cast was made at each station to measure water column temperature, salinity, density and collect discrete samples for nutrient analysis. Major nutrient concentrations were measured with a Technicon auto-analyzer basically employing the methods reported by Parsons et al. (1984) and Matsunaga et al. (1990). Sediment sampling was carried out at 17 stations using a Smith-McIntyre grab sampler or a gravity core sampler. The top 3 cm of sediment core was extruded and stored in darkness at 2°C for more than 3 months for the purpose of eliminating vegetative cells. Sediment samples were analyzed following the procedure of the most probable number (MPN) method (Imai et al., 1984, 1990) to estimate the abundance of viable resting stage cells in sediments. Homogenized sediment samples were suspended in sterile filtered seawater at a concentration of $0.1\text{ g wet weight mL}^{-1}$ (10^0 dilution). This 10^0 dilution of suspension was used to prepare a 10^{-1} – 10^{-6} dilution series with modified SWM-3 culture medium (Chen et al., 1969; Imai et al., 1996a). Five aliquots (1 mL) of each dilution series were incubated using tissue culture microplates under an illumination of $30\ \mu\text{mol photons m}^{-2}\text{ s}^{-1}$ and a 14:10 h light:dark cycle at a temperature of 5°C on the assumption of representing the sea surface environmental conditions. Appearance of vegetative cells was measured for each well of the microplates, and species or taxonomic groups identified using inverted microscopy every 3 days until the end of incubation at 7–14 days. Wells in which vegetative cells were identified were scored as positive. MPN of viable diatom resting stage cells (MPN cells g^{-1} wet sediment) was estimated according to statistical tables (Itoh and Imai, 1987; Throndsen, 1978), based upon the number of positive scores in the five wells of each dilution. MPN per cubic centimeter of wet sediment was calculated with the apparent specific gravity of wet sediment determined according to Kamiyama (1996).

Water samples were collected from the sea surface at each station and from several depths at St. 11 and St. 18 for phytoplankton and chlorophyll *a* analyses. Water samples were sequentially filtered through $20\ \mu\text{m}$ mesh, a membrane filter ($2\ \mu\text{m}$) and a GF/F filter, then analyzed for chlorophyll *a* using a Turner Designs fluorometer (Suzuki and Ishimaru, 1990). Phytoplankton samples

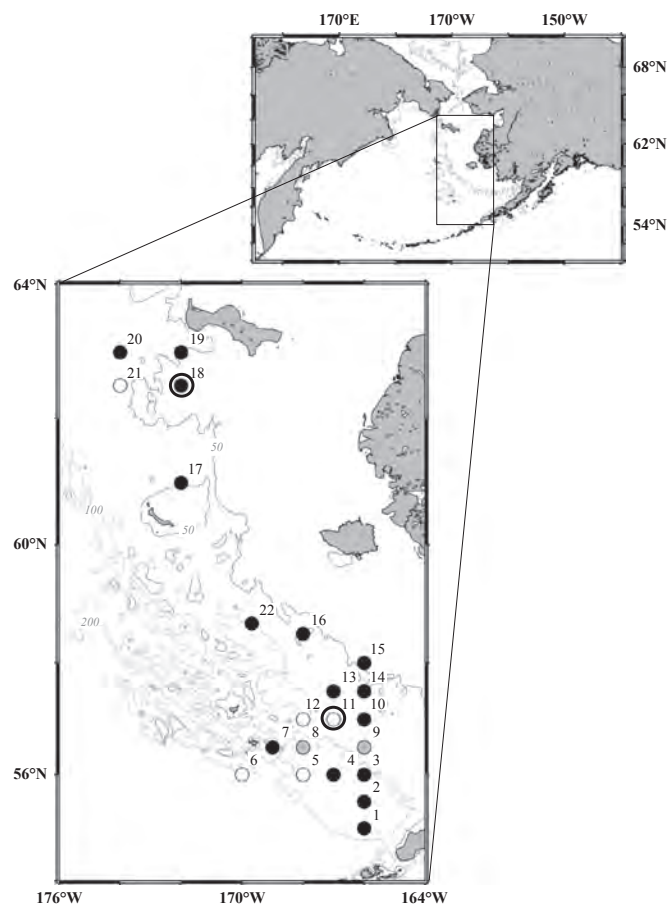


Fig. 1. Sampling stations in the eastern Bering Sea. •: stations for collection of sediment core and surface water, ◉: sediment core, ◊: surface water, ⊙: water samples from several depths.

were preserved with glutaraldehyde at a final concentration of 1% and then settled and concentrated to ten to twenty fold. Appropriate aliquots (0.2–1 mL) of concentrated samples were transferred to a slide glass and phytoplankton cells counted using an inverted microscope. Species were further identified using a light microscope at $1000\times$ magnification and a scanning electron microscope.

3. Results

3.1. Hydrography

According to the theory of Coachman et al. (1980), stations were divided into three distinct depth domains. Thermoclines were generally found at 20–30 m in the MSD during the cruise (Fig. 2A). The pycnocline was exceptionally clear at stations with about 20 m depth in the Saint Laurence Island Polynya region (Smith et al., 1990) (Fig. 2B). These stations were separated from other MSD stations by characteristics of bottom temperature. Surface nutrients were depleted over the eastern Bering Sea shelf during the cruise (Table 1).

3.2. Distribution of phytoplankton

High surface chlorophyll *a* concentrations (St. 5; $6.1\ \mu\text{g L}^{-1}$, St. 7; $4.7\ \mu\text{g L}^{-1}$) and phytoplankton cell abundances (6.1×10^5 – 1.8×10^6 cells L^{-1}) were patchy at stations along the shelf edge. The dominant species was *Pseudo-nitzschia cf. delicatissima* (St. 5; 85%, St. 7; 45%).

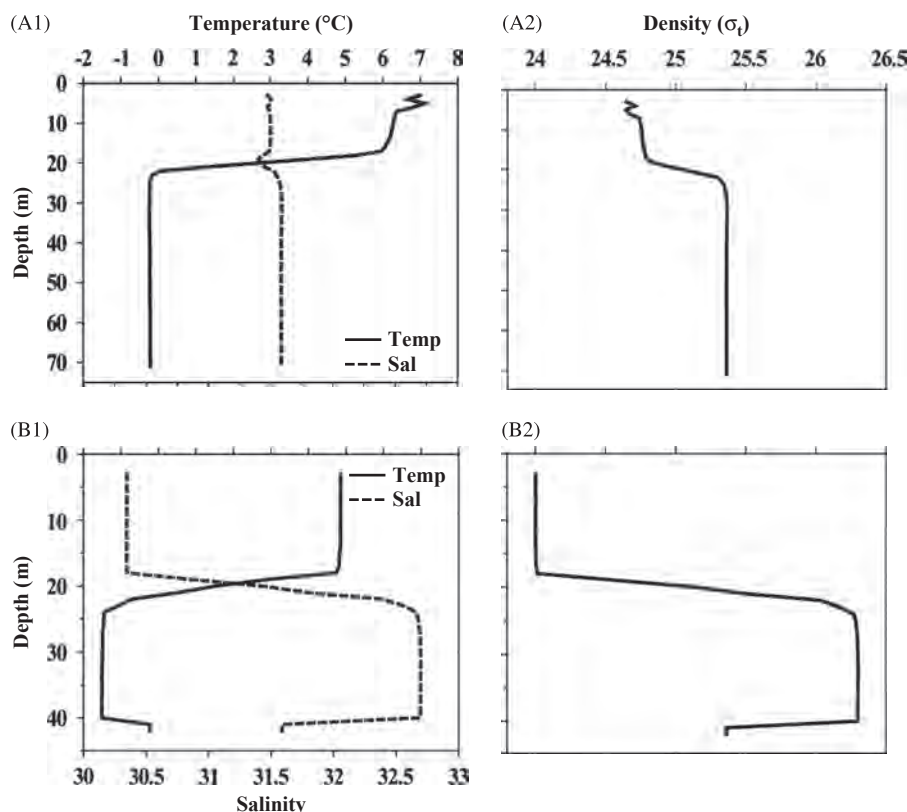


Fig. 2. Vertical profiles of temperature and salinity at station 11 (A-1) and station 18 (B-1), and density profiles at station 11 (A-2) and station 18 (B-2) in water columns of the eastern Bering Sea during the cruise in July 2009.

Table 1

Surface nutrient ($\text{NO}_3 + \text{NO}_2, \text{SiO}_2, \text{PO}_4$) concentration (μM) in the Bering Sea in July 2009. Stations were divided into four domains, OSD (outer shelf domain: $100 < H < 170$ m isobaths), MSD (middle shelf domain: $50 < H < 100$ m isobaths), CSD (coastal shelf domain: < 50 m isobaths) and SLIP (St. Lawrence Island Polynya region).

St.	Domain	Depth (m)	Day (July 2009)	$\text{NO}_3 + \text{NO}_2$ (μM)	SiO_2 (μM)	PO_4 (μM)
1	OSD	135	8	14.25	28.34	1.25
2	OSD	121	8	1.74	13.20	0.55
3	OSD	113	9	0.58	10.35	0.50
4	OSD	133	9	0.40	7.58	0.29
5	OSD	136	9	1.62	20.85	0.59
6	OSD	220	9	6.28	24.77	0.88
7	OSD	102	10	0.37	16.92	0.29
8	OSD	115	10	0.09	2.03	0.22
9	MSD	84	10	0.10	1.83	0.16
10	MSD	70	10	0.08	2.42	0.41
11	MSD	75	10	0.05	1.30	0.15
12	MSD	77	11	0.05	1.30	0.15
13	MSD	70	11	0.09	1.71	0.57
14	MSD	64	11	0.08	2.36	0.41
22	MSD	70	15	0.03	1.06	0.18
15	CSD	54	11	0.06	1.59	0.48
16	CSD	45	11	0.08	2.42	0.48
17	SLIP	55	12	0.09	4.36	0.57
18	SLIP	45	13	0.11	2.12	0.32
19	SLIP	53	13	0.03	3.18	0.43
20	SLIP	74	13	0.06	5.71	0.37
21	SLIP	68	14	0.31	4.06	0.42

In the southern region (St. 11; MSD), there was a maximum in chlorophyll *a* concentration ($1.62 \mu\text{g L}^{-1}$) and cell abundance ($1.1 \times 10^5 \text{ cells L}^{-1}$) above the pycnocline (Fig. 3). The small phytoplankton size fractions ($< 20 \mu\text{m}$) contributed to high chlorophyll *a* concentrations, and were dominated by small dinoflagellates and microflagellates (78–92%). Diatoms dominated below the pycnocline,

but chlorophyll *a* concentrations and cell abundances were relatively low. In the northern region (St. 18; Polynya region), there was a maximum of chlorophyll *a* concentration ($1.3 \mu\text{g L}^{-1}$) and cell abundance ($3.8 \times 10^5 \text{ cells L}^{-1}$) below the pycnocline dominated by large ($> 20 \mu\text{m}$) diatoms (71–95%). At this station, dinoflagellates and microflagellates dominated in the abundance in the upper layer but chlorophyll *a* concentrations and cell abundances were relatively low.

Fig. 4 illustrates the vertical distributions of diatoms at St. 11 and St. 18. Vegetative cells of *Chaetoceros* spp. were observed in the upper layer, and resting spores of *Chaetoceros* spp., especially *C. furcellatus*, were abundant in the lower layer of both stations. The diatom species characteristically found in the water column were *Paralia sulcata* at St. 11, and *T. nordenskiöldii* and *Porosira glacialis* at St. 18.

3.3. Abundances of resting stage cells in sediments estimated by the MPN method

The numbers of resting stage cells in bottom sediments estimated by the MPN method were in the range of 1.7×10^3 (St. 1) to 1.2×10^6 (St. 20) MPN cells cm^{-3} wet sediment (Fig. 5). Eighteen centric diatom taxa and 4 pennate diatom taxa were observed as vegetative cells after the incubation for the MPN method (Table 2). Almost all species were already reported as species found in the Bering Sea (Goering and Iverson, 1981; Motoda and Minoda, 1974; Saito and Taniguchi, 1978; Schandelmeier and Alexander, 1981). Dinoflagellate cysts were also estimated ($\sim 1.2 \times 10^3$ MPN cells cm^{-3} wet sediment). The highest concentrations were found south of St. Lawrence Island (St. 20). The number of viable cells ranged from 6.1×10^4 to 9.2×10^5 MPN cells cm^{-3} wet sediment (average 2.4×10^5) in the MSD and CSD. There were small numbers of resting stage cells in the OSD and shelf edges where the bottom depths were greater

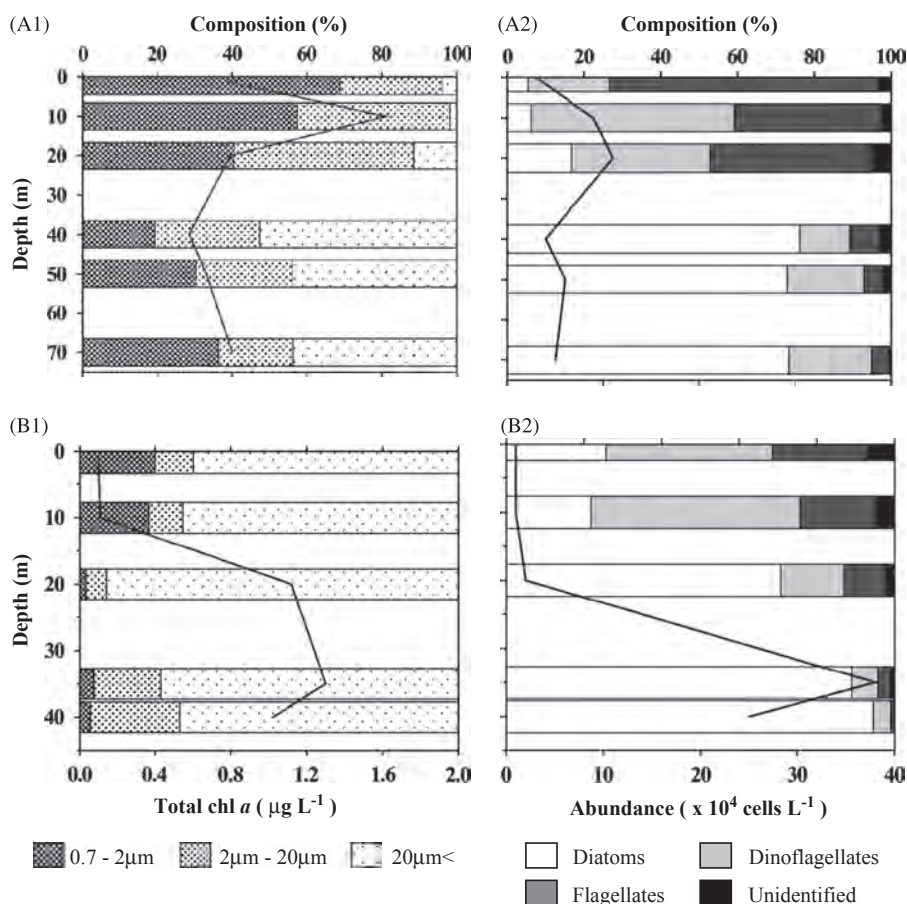


Fig. 3. Vertical profiles of chlorophyll *a* concentrations ($\mu\text{g L}^{-1}$) of three size fractions at station 11 (A-1) and station 18 (B-1), and cell abundances ($\times 10^4$ cells L^{-1}) and taxonomic group composition of phytoplankton at station 11 (A-2) and station 18 (B-2) in water columns of the eastern Bering Sea in July 2009.

than 100 m, and the numbers ranged from 1.7×10^3 to 6.8×10^4 MPN cells cm^{-3} wet sediment (average 2.1×10^4).

Fig. 6 shows the dominant diatom species of viable resting stage cells in sediments. The numbers of resting stage cells in the southern region and south of St. Lawrence Island are summarized in Table 2. *Chaetoceros* spp. ($\sim 1.3 \times 10^5$ MPN cells cm^{-3} wet sediment), *Thalassiosira* spp. ($\sim 1.8 \times 10^5$ MPN cells cm^{-3} wet sediment) and *Attheya longicornis* ($\sim 8.7 \times 10^5$ MPN cells cm^{-3} wet sediment) were the dominant taxa. *C. diadema* ($\sim 6.8 \times 10^4$ MPN cells cm^{-3} wet sediment), *Chaetoceros socialis* ($\sim 6.3 \times 10^4$ MPN cells cm^{-3} wet sediment) and *C. furcellatus* ($\sim 2.4 \times 10^4$ MPN cells cm^{-3} wet sediment) were abundant species of the genus *Chaetoceros*. *T. nordenskiöldii* ($\sim 1.8 \times 10^5$ MPN cells cm^{-3} wet sediment) and *T. gravida* ($\sim 5.5 \times 10^4$ MPN cells cm^{-3} wet sediment) were abundant species of the genus *Thalassiosira*. *P. sulcata* was detected at high abundances in the southern region ($\sim 6.3 \times 10^4$ MPN cells cm^{-3} wet sediment). *Skeletonema* spp. and *Odontella* spp. were also identified but the abundances were relatively low. Other species with high abundances were the pennate diatoms of ribbon-shaped colony forming species, *F. cylindrus*, *F. oceanica*, *Fragilaria* cf. *capucina*, *Fragilaria oblonga*, *Pauliera taeniata* ($\sim 1.1 \times 10^5$ MPN cells cm^{-3} wet sediment) and solitary *Navicula* spp. ($\sim 3.6 \times 10^4$ MPN cells cm^{-3} wet sediment).

4. Discussion

4.1. Phase of phytoplankton populations during the study cruise

Phytoplankton populations were changing from a phase dominated by diatoms to one dominated by flagellates during this

sampling period. The phase transition was observed above the pycnocline and low latitudes (St. 11). Surface nutrient concentrations were depleted when surface stratification developed, and chlorophyll concentrations declined to low levels over the eastern Bering Sea shelf (Whitledge et al., 1986). Observed phytoplankton assemblages suggest that the study period was near the end of a diatom bloom. High abundances of *Chaetoceros* spp. resting spores were observed in the lower layer whereas the vegetative cell abundances were low in the upper layer (Fig. 4). This result strongly suggests that diatom resting stage cells would have formed before the cruise and had been sinking near the end of the bloom.

It is well known that there is a current of water originating at the Bering Sea shelf edge that is rich in nutrients and plankton (Springer et al., 1996). During this cruise, relatively high chlorophyll *a* concentrations and phytoplankton (diatoms) cell abundances were observed only at the shelf edge, suggesting the contribution to primary productivity in summer season.

4.2. Distribution of resting stage cells in the bottom sediments

The viable resting stage cells in sediments are potentially important seed banks for planktonic blooms. The population size of resting stage cells distributed in the eastern Bering Sea shelf was comparable to that distributed in the Seto Inland Sea of Japan ($\sim 10^6$ MPN cells cm^{-3} wet sediment: Imai et al., 1990; Itakura et al., 1997, 1999), and that in the coastal Swedish fjord ($\sim 5.7 \times 10^4$ MPN cells g^{-1} wet sediment: McQuoid et al. 2002). The study area of the Seto Inland Sea and coastal Swedish fjord are mostly inshore areas (shallower than depth of 30 m) where

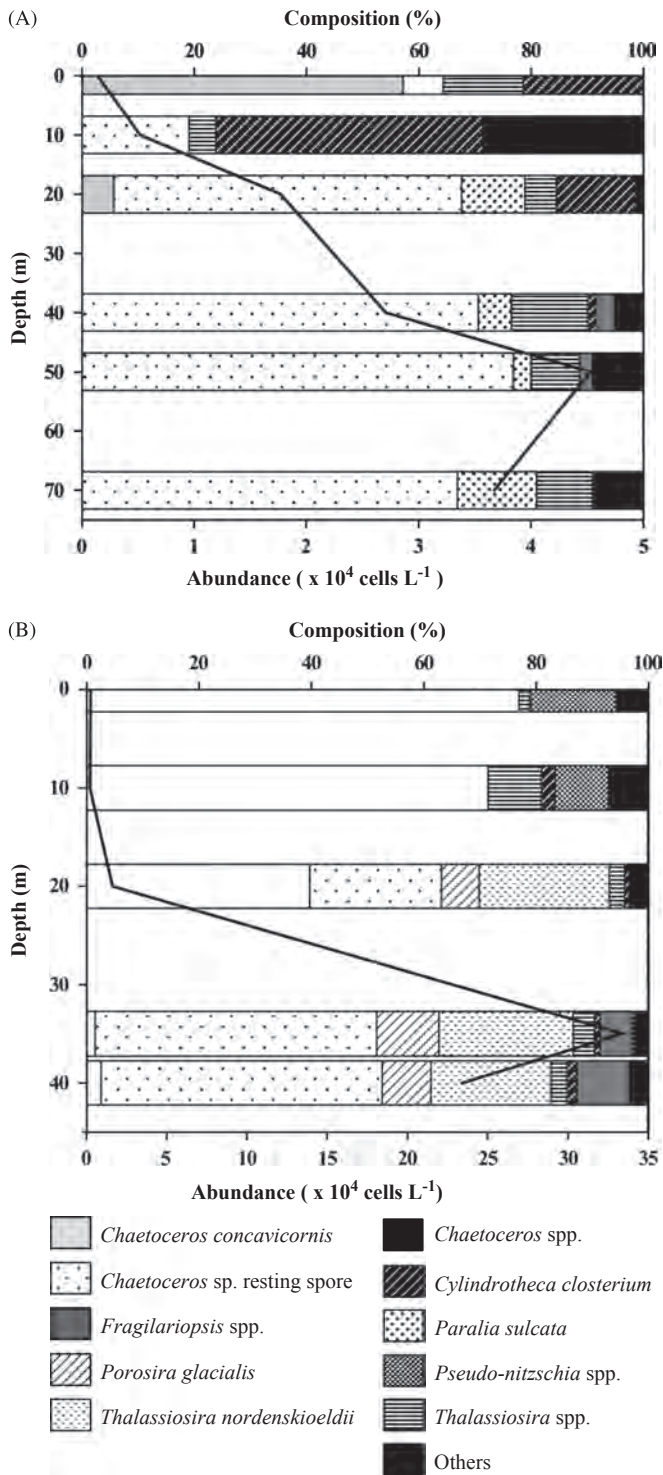


Fig. 4. Vertical distributions of cell abundance ($\times 10^4$ cells L⁻¹) and species composition of the dominant diatoms in water columns at station 11 (A) and station 18 (B).

intercommunication of diatoms between water column and sea bottom is capable and frequent. Although the study area of the Bering Sea shelf was offshore and a deeper depth (average 83 m), the diatom resting stage cells also appeared abundantly in sediments.

Plankton biomass largely influences the population size of the diatom resting stage cells (Itakura et al., 1999; McQuoid, 2002). High abundances of resting stage cells in sediments are believed to reflect dense bloom of diatoms predominant among the plankton

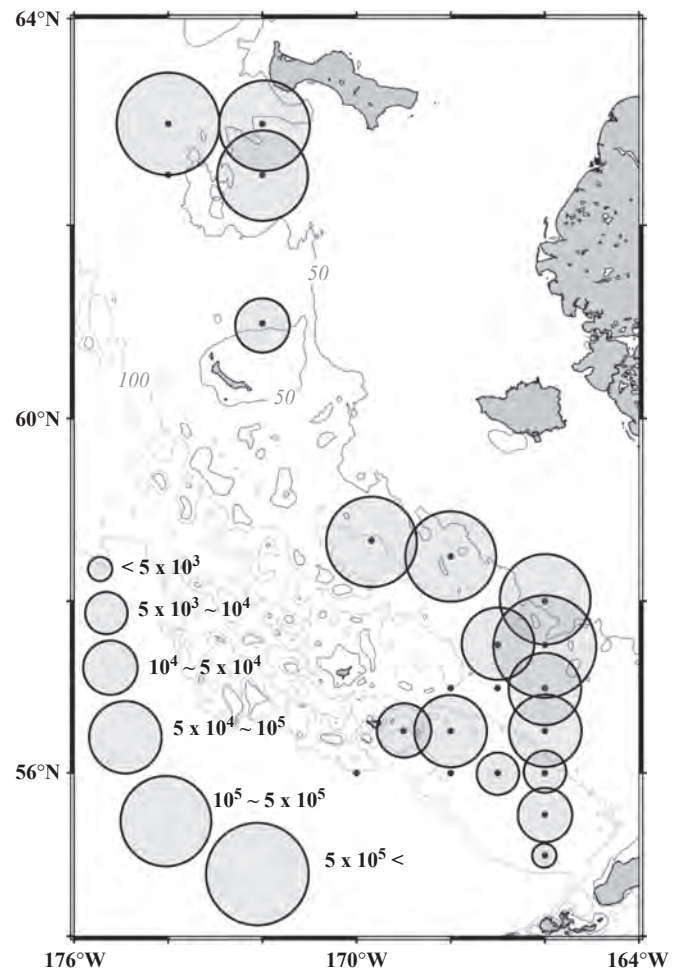


Fig. 5. Spatial distribution of total diatom resting stage cells (MPN cells cm⁻³ wet sediment) in surface sediments (top 3 cm depth) of the study area. Stations without circle indicate no data.

community on the Bering Sea shelf. There is a relationship between the dominant phytoplankton species in the water columns and resting stage cells in sediments. Similarities in species composition of the resting stages and typical plankton populations reveal that resting stage cells were formed locally after the blooms in the water columns.

Viable resting stage cells of *Skeletonema* spp. were most abundant in the bottom sediments of the Seto Inland Sea and coastal Swedish Fjord, but less so over the Bering Sea shelf. *Skeletonema* spp. usually occurs in high abundance in eutrophic to extremely eutrophic regions (Yamada et al., 1980); therefore, the supply of resting stage cells from the water column is presumably low in the Bering Sea where the degree of anthropogenic eutrophication is limited.

P. sulcata grows primarily at the sea bottom of shallow areas, but this species is sometimes found with high cell abundances in the water column (Abrantes, 1988; Hobson and McQuoid, 1997) presumably due to physical forces such as strong winds or tidal mixings (Blasco et al., 1980; Oh and Koh, 1995). In this study, *P. sulcata* cells were abundant in bottom sediments at MSD and CSD, and the lower water column at St. 11 (MSD). Cells of *P. sulcata* were also distributed at the surface of CSD in the study period. This fact suggests that cells were transported from bottom to surface layer by physical forces such as storms and strong tidal action at the bottom.

Chaetoceros concavicornis and *Ch. convolutus*, both dominant species in summer in the Bering Sea, were found in the water

Table 2
Abundance ranges and means (MPN cells cm⁻³ wet sediment) of diatom resting stage cells and dinoflagellate cysts in bottom sediments of the study area.

Species	Southeastern Bering Sea		St. Lawrence Island Polynya region	
	min–max	mean	min–max	mean
Class Bacillariophyceae				
Order Centrales				
<i>Actinopterychus senarius</i>	N. D.~2.6 × 10 ³	2.9 × 10 ²	N. D.	
<i>Attheya longicornis</i>	N. D.~5.6 × 10 ⁵	5.0 × 10 ⁴	7.2 × 10 ² –8.7 × 10 ⁵	2.3 × 10 ⁵
Total <i>Chaetoceros</i> spp.	N. D.~6.9 × 10 ⁴	1.6 × 10 ⁴	3.1 × 10 ³ –1.3 × 10 ⁵	7.5 × 10 ⁴
<i>Chaetoceros curvisetus</i>	N. D.		N. D.~2.5 × 10 ³	6.3 × 10 ²
<i>Chaetoceros diadema</i>	N. D.~3.3 × 10 ⁴	5.0 × 10 ³	N. D.~6.8 × 10 ⁴	2.6 × 10 ⁴
<i>Chaetoceros didymus</i>	N. D.~2.8 × 10 ³	2.7 × 10 ²	N. D.~2.7 × 10 ³	6.9 × 10 ²
<i>Chaetoceros mitra</i>	N. D.~1.0 × 10 ⁴	8.0 × 10 ²	N. D.	
<i>Chaetoceros socialis</i>	N. D.~2.6 × 10 ⁴	5.7 × 10 ³	3.1 × 10 ³ –6.3 × 10 ⁴	3.4 × 10 ⁴
<i>Chaetoceros furcellatus</i>	N. D.~2.4 × 10 ⁴	3.9 × 10 ³	N. D.~1.7 × 10 ³	4.4 × 10 ²
<i>Chaetoceros lacinius</i>	N. D.~1.6 × 10 ³	1.2 × 10 ²	N. D.	
<i>Chaetoceros debilis</i>	N. D.~3.2 × 10 ³	2.5 × 10 ²	N. D.	
Other <i>Chaetoceros</i> spp.	N. D.~7.1 × 10 ²	5.4 × 10 ¹	N. D.~5.1 × 10 ⁴	1.3 × 10 ⁴
<i>Detonula</i> spp.	N. D.~1.0 × 10 ⁴	1.6 × 10 ³	N. D.~1.9 × 10 ⁴	4.9 × 10 ³
<i>Skeletonema</i> spp.	N. D.~6.9 × 10 ³	1.4 × 10 ³	N. D.~3.2 × 10 ²	8.1 × 10 ¹
Total <i>Thalassiosira</i> spp.	N. D.~1.1 × 10 ⁵	1.7 × 10 ⁴	N. D.~1.8 × 10 ⁵	9.0 × 10 ⁴
<i>Thalassiosira nordenskiöldii</i>	N. D.~7.4 × 10 ⁴	7.4 × 10 ³	N. D.~1.8 × 10 ⁵	7.7 × 10 ⁴
<i>Thalassiosira gravida</i>	N. D.~5.5 × 10 ⁴	9.1 × 10 ³	N. D.~3.7 × 10 ⁴	1.3 × 10 ⁴
Other <i>Thalassiosira</i> spp.	N. D.~7.7 × 10 ³	7.2 × 10 ²	N. D.	
<i>Paralia sulcata</i>	N. D.~6.3 × 10 ⁴	1.1 × 10 ⁴	N. D.~3.6 × 10 ²	1.7 × 10 ²
<i>Porosira glacialis</i>	N. D.~3.3 × 10 ³	5.4 × 10 ²	N. D.	
<i>Odontella</i> spp.	N. D.~1.6 × 10 ³	4.1 × 10 ²	N. D.~2.7 × 10 ³	9.6 × 10 ²
<i>Delphineis</i> spp.	N. D.~6.0 × 10 ³	8.2 × 10 ²	N. D.	
<i>Navicula</i> spp.	N. D.~1.8 × 10 ⁴	2.1 × 10 ⁴	N. D.~3.6 × 10 ⁴	1.2 × 10 ⁴
Pennate species (ribbon forming)	N. D.~9.6 × 10 ⁴	1.9 × 10 ⁴	3.6 × 10 ² –1.1 × 10 ⁵	2.8 × 10 ⁴
<i>Fragilaria</i> spp.	N. D.~2.3 × 10 ⁴	1.1 × 10 ⁴	N. D.	
<i>Fragilariopsis</i> spp.	N. D.~9.4 × 10 ⁴	1.7 × 10 ⁴	N. D.~1.1 × 10 ⁵	2.8 × 10 ⁴
<i>Pauliera taeniata</i>	N. D.		N. D.~3.6 × 10 ²	9.1 × 10 ¹
Class Dinophyceae	N. D.~2.8 × 10 ²	1.5 × 10 ²	N. D.	
Total	1.74 × 10 ³ –9.2 × 10 ⁵	1.4 × 10 ⁵	1.0 × 10 ⁴ –1.2 × 10 ⁶	4.9 × 10 ⁵

N. D. : not detected.

samples during this study. However, we could not detect the appearance of them after incubation of the sediments with the MPN treatment. These *Chaetoceros* species appear to have a life strategy different from those forming resting stage cells.

There is no report of resting stage cells for *Pseudo-nitzschia* spp. Although *Pseudo-nitzschia* spp. were dominant at the shelf edge during the study period, they are presumably unable to overwinter in the Bering Sea without resting stages due to poor light conditions. It is considered that they are allochthonous populations transported by the current from the southern areas to the Bering Sea.

There are several pennate diatom species forming resting stage cells (McQuoid and Hobson, 1996). The pennate species found in sediments in high abundance were ribbon-shaped colony forming species (*F. cylindrus*, *F. oceanica*, *Fragilaria* cf. *capunica*, *P. taeniata*) and solitary *Navicula* spp. They frequently comprise the ice algae populations. These species are known to grow at the subsurface of sea ice in late winter to early spring in the Bering Sea (Saito and Taniguchi, 1978; Schandelmeier and Alexander, 1981; Goering and Iverson, 1981). Benthic *Delphineis* species were also observed in the sediments, but already attaching to the substrata such as sand grains with several cells before incubation. Resembling the centric diatom species, ice algae species form resting stage cells, and they survive in bottom sediments after sinking from sea ice melted during the warm season and then serve as a source of seed stock for ice algae was suggested to be sediments (Horner and Schrader, 1982). The present study confirmed the existence of resting stage cells of ice algae species in the bottom sediments during summer season. The resting stage cells presumably play an important role as a seed population in developing large biomass of ice algae when they were resuspended and incorporated into the ice during freeze-up.

Attheya sp. were usually found in the plankton associated with *Chaetoceros* species (Crawford et al., 1994) and from undersurface of sea ice (Melnikov et al., 2002; Schandelmeier and Alexander, 1981; von Quillfeldt, 2000; Werner et al., 2007). They possibly contribute to primary productivity as plankton and also as ice algae. High abundances of resting stage cells in sediments indicate the importance of the genus *Attheya* as primary producers in the Bering Sea.

4.3. Contribution of resting stage cells to bloom formation

Germination and rejuvenation of diatom resting stage cells are generally affected by light (Hargraves and French 1983; Hollibaugh et al., 1981; Imai et al., 1996b), and hence the resting stage cells in the sea bottom need to be resuspended to the euphotic zone where they can germinate or rejuvenate and resultant vegetative cells commence to grow (Itakura et al., 1997). In regions of upwelling, the prevalence of resting spores of the genus *Chaetoceros* in newly upwelled waters (Abrantes, 1988; Pitcher, 1990) indicate that upwelling events have enough energy to resuspend the resting stage cells from the benthos into the water column (Pitcher et al., 1991). In the Funka Bay of Japan, the resting spores of *Chaetoceros* spp. in the bottom layer were brought back into the euphotic zone during the vertical mixing of the water column (Odate and Maita, 1990), implying that vertical mixing also has sufficient energy to resuspend the resting stage cells into the water column. It was reported that artificial stirring of stable water columns led to larger cell size diatom blooms in marine environment (Eppley et al., 1978).

In a study of the Bering Sea (Sambrotto et al., 1986; Eslinger and Iverson, 2001), the spring phytoplankton bloom onset occurred when the water column was vertically mixed to the sea bottom,

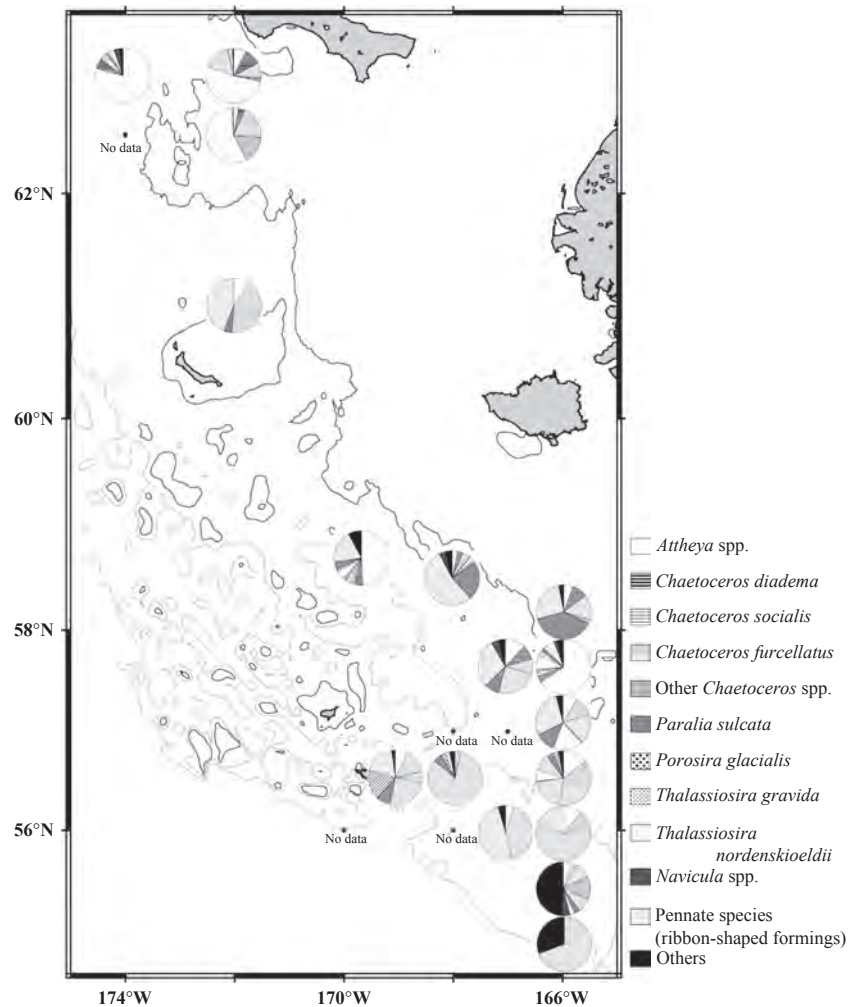


Fig. 6. Species composition of the diatom resting stage cells observed in surface sediments (top 3 cm depth) of the study area detected with the most probable number (MPN) method. The stations without circle indicate no data.

and chlorophyll maxima were associated with the shoaling of the mixed layer. Blooms often tend to appear suddenly because vegetative cells originated from resting stage cells are supposed to divide rapidly with the organic matter already stored in the cells (Shakshaug, 1989). Hence, the trigger of the spring bloom was not only supply of inorganic nutrients, but also probably the resuspension of resting stage cells into the euphotic layer.

As is the case in temperate seas, the seasonal decrease in atmospheric temperature and increase turbulence enhance the vertical mixing in fall and winter in the Bering Sea shelf. When the sea surface was covered with ice, wind driven mixing ceases but the convective mixing layer deepens to a depth about 50–100 m in response to brine drainage of freezing ice (Ikeya and Kawanobe, 2002; Ohtani, 1969, 1973; Sullivan et al., 1988). Upwelling plumes of circulation cell have also been observed at the ice edges in the Bering Sea (Alexander and Niebauer, 1981; Okkonen and Niebauer, 1995). These physical processes have the potential to mix resting stage cells from the benthos to the water column. A cold water mass (−1.7 to 0°C) remained under the pycnocline in the southern part of the St. Lawrence Island Polynya and MSD during the study period suggesting that the sea ice possibly formed in that region and the vertical convection reached the benthos.

Fig. 7 gives a schematic representation of the life cycles of ice algae and phytoplankton in the eastern Bering Sea shelf. Horner and Schrader (1982) reported that microalgae were present in the sea ice as soon as it formed in the fall and generally were scattered throughout the ice thickness. In the winter period, resting stage

cells of ribbon-shaped pennate species and solitary *Navicula* spp. would be mixed to the water column from the bottom by convection. If those species are incorporated or attached to the sea ice, they would develop in ice algae. Similarities in composition of benthic and ice algae species (Matheke and Horner, 1974) support this hypothesis. As an alternate explanation, plankton species could survive the winter period as resting stage cells and be resuspended in the water column the following spring and bloom, when they are successfully trapped to the euphotic layer. Resting stage cells probably are resuspended non-selectively, but the germination/ rejuvenation in response to favorable light and temperature conditions (French and Hargraves, 1985; Hollibaugh et al., 1981; Imai et al., 1996b) will affect vegetative growth, and so initiation and composition of bloom.

In a past study, benthic *P. sulcata* cells existed in the sea ice (Schandelmeier and Alexander, 1981), suggesting that cells suspended from the sea bottom were incorporated into ice. Resting spores of *C. socialis* and *F. oceanica* were also found in the ice (von Quillfeldt, 1997). There is a strong possibility that the resting stage cells of plankton species are incorporated into the sea ice together with ice algae species. Those resting stage cells of plankton species could germinate in the upper layer when the sea ice is melting, and probably contribute to the ice edge bloom accompanied with ice algae species. When the water column is vertically mixed to the sea bottom by the process of wind and tidal mixing, the resting stages of planktonic species probably contribute to the open water bloom after the water has stabilized.

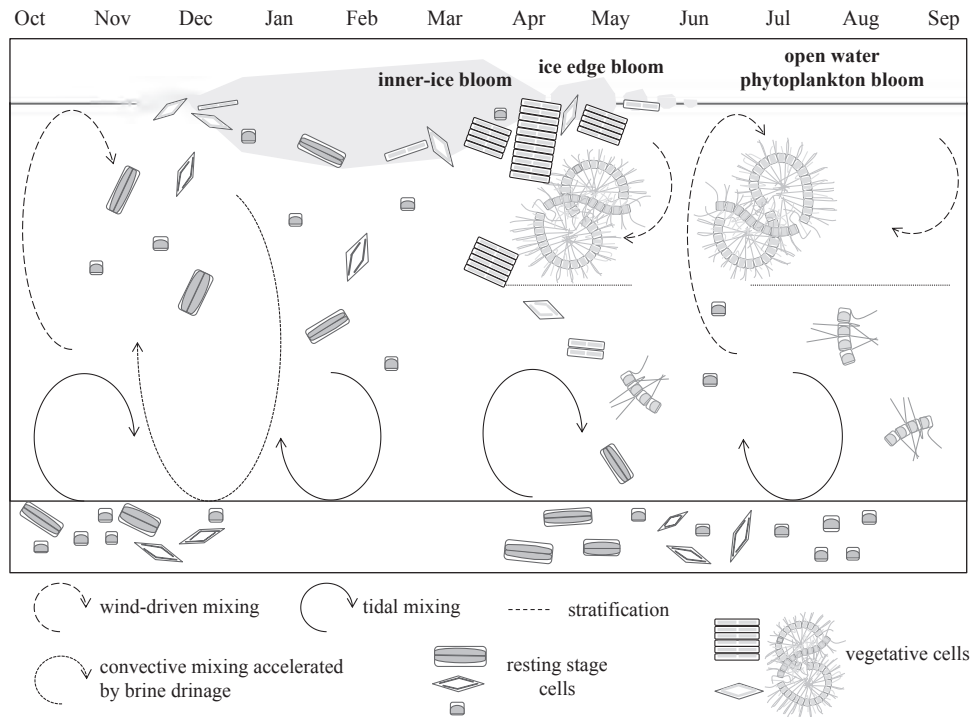


Fig. 7. Schematic representation of the life cycles of ice algae and planktonic diatoms in the eastern Bering Sea shelf based on the present study and partially following Coachman et al. (1980), Sullivan et al. (1988) and Ikeya and Kawanobe (2002).

Under conditions that favor extensive spatial and temporal extent of sea ice, more resting stage cells could be incorporated into the ice as seed populations and contribute to a rich bloom. In contrast, when sea ice has limited spatial and temporal extent, there is insufficient light to support a bloom (Hunt et al., 2002) and a smaller seed population to contribute to a bloom. Thus there is a possibility that year to year variations in ice extent and duration have large effects in the scale and period of the spring blooms in the Bering Sea.

5. Conclusion

Diatom species of plankton and ice algae employ resting stages as survival strategies in the Bering Sea as is the case of the resting stages of many diatoms in temperate waters. It is strongly suggested that resting stage cells play a crucially important role in overwintering of diatoms in the Bering Sea, where vegetative cells are exposed to extremely severe conditions (low temperature, sea ice formation, extreme light limitation) in winter, and in supplying a seed populations for spring blooms through germination and/or rejuvenation in water columns and sea ice.

Acknowledgments

We are grateful to Professor Kenshi Kuma (Graduate School of Environmental Science, Hokkaido University), Associate Professor Jun Yamamoto (Graduate School of Environmental Science, Hokkaido University), and to the captain, officers and crew of T/S Oshoro-Maruo of Hokkaido University for cooperation in sampling. We also thank Professor Kenshi Kuma (Graduate School of Fisheries Sciences, Hokkaido University) and members of his laboratory for supplying the environmental data.

References

- Abrantes, F., 1988. Diatom assemblages as upwelling indicators in surface sediments off Portugal. *Mar. Geol.* 85, 15–39.
- Alexander, V., Niebauer, H., J., 1981. Oceanography of the eastern Bering Sea ice-edge zone in spring. *Limnol. Oceanogr.* 26, 1111–1125.
- Blasco, D., Estrada, M., Jones, B., 1980. Relationship between the phytoplankton distribution and composition and the hydrography in the Northwest African upwelling region near Cabo Carvoeiro. *Deep-Sea Res.* 27A, 799–821.
- Chen, L.C.M., Edelman, T., McLachlan, J., 1969. *Bonnemaisonia hamifera* Hariot in nature and culture. *J. Phycol.* 5, 211–220.
- Coachman, L.K., 1986. Circulation, water masses, and fluxes on the southeastern Bering Sea shelf. *Cont. Shelf Res.* 5, 23–108.
- Coachman, L. K., Kinder, T. H., Schumacher, J. D., Tripp, R. B., 1980. Frontal systems of the southeastern Bering Sea strait. In: Carstens, T., McClimans, T. (Eds.), *Stratified Flows, Second IAH Symposium, Trondheim, June 1980*. Tapir, Trondheim, pp. 917–933.
- Crawford, R.M., Gardner, C., Medlin, L.K., 1994. The genus *Attheya*. I. A description of four new taxa, and the transfer of *Gonioceros septentrionalis* and *G. armadas*. *Diatom Res.* 9, 27–51.
- Durbin, E.G., 1978. Aspects of the biology of resting spores of *Thalassiosira nordenskiöldii* and *Detonula confervacea*. *Mar. Biol.* 45, 31–37.
- Eppley, R.W., Koeller, P., Wallace, G.T., 1978. Stirring influences the phytoplankton composition within enclosed columns of coastal sea water. *J. Exp. Mar. Biol. Ecol.* 32, 219–239.
- Eslinger, D.L., Iverson, R.L., 2001. The effects of convective and wind-driven mixing on spring phytoplankton dynamics in the Southeastern Bering Sea middle shelf domain. *Cont. Shelf Res.* 21, 627–650.
- French, F.W., Hargraves, P.E., 1985. Spore formation in the life cycles of the diatoms *Chaetoceros diadema* and *Leptocylindrus danicus*. *J. Phycol.* 21, 477–484.
- Garrison, D.L., 1984. Planktonic diatoms. In: Steidinger, K.A., Walker, L.M. (Eds.), *Marine Plankton Life Cycle Strategies*. CRC Press, Boca Raton, Florida, pp. 1–17.
- Goering, J.J., Iverson, R.L., 1981. Phytoplankton distribution on the southeastern Bering Sea shelf. In: Hood, D.W., Calder, J.A. (Eds.), *The Eastern Bering Sea shelf: Oceanography and Resources vol. 2, Marine Pollution Assessment*. University of Washington Press, Seattle, pp. 933–946.
- Hargraves, P.E., French, F.W., 1975. Observations on the survival of diatom resting spores. *Beih. Nova Hedw.* 53, 229–238.
- Hargraves, P.E., French, F.W., 1983. Diatom resting spores: significance and strategies. In: Fryxell, G.A. (Ed.), *Survival strategies of the algae*. Cambridge University Press, Cambridge, pp. 49–68.
- Hobson, L.A., McQuoid, M.R., 1997. Temporal variation among planktonic diatom assemblages in a turbulent environment of the southern Strait of Georgia, British Columbia, Canada. *Mar. Ecol. Prog. Ser.* 150, 263–274.
- Hollibaugh, J.T., Seibert, D.L.R., Thomas, W.H., 1981. Observations on the survival and germination of resting spores of three *Chaetoceros* (Bacillariophyceae) species. *J. Phycol.* 17, 1–9.

- Horner, R., Schrader, G.C., 1982. Relative contributions of ice algae, phytoplankton, and benthic microalgae to primary production in nearshore regions of the Beaufort Sea. *Arctic* 35, 485–503.
- Hunt Jr., G.L., Stabeno, P., Walters, G., Sinclair, E., Brodeur, R.D., Napp, J.M., Bond, N. A., 2002. Climate change and control of the southeastern Bering Sea pelagic ecosystem. *Deep-Sea Res. II* 49, 5821–5853.
- Ikeya, T., Kawanobe, K., 2002. Phytoplankton under the sea ice (in Japanese). *Gekkan Kaiyo (Marine Science Monthly) Gougai* 30, 139–144.
- Imai, I., Itakura, S., Itoh, K., 1990. Distribution of diatom resting cells in sediments of Harima-Nada and northern Hiroshima Bay, the Seto Inland Sea, Japan (in Japanese with English abstract). *Bull. Coastal Oceanogr.* 28, 75–84.
- Imai, I., Itakura, S., Matsuyama, Y., Yamaguchi, M., 1996a. Selenium requirement for growth of a novel red tide flagellate *chattonella verruculosa* (Raphidophyceae) in culture. *Fish. Sci.* 62, 834–835.
- Imai, I., Itakura, S., Yamaguchi, M., Honjo, T., 1996b. Selective germination of *Heterosigma akashiwo* (Raphidophyceae) cysts in bottom sediments under low light conditions: a possible mechanism of red tide initiation. In: Yasumoto, T., Oshima, Y., Fukuyo, Y. (Eds.), *Harmful and Toxic Algal Blooms*. International Oceanographic Commission of UNESCO, Paris, pp. 197–200.
- Imai, I., Itoh, K., Anraku, M., 1984. Extinction dilution method for enumeration of dormant cells of red tide organisms in marine sediments. *Bull. Plankton Soc. Jpn.* 31, 123–124.
- Itakura, S., Imai, I., Itoh, K., 1997. “Seed bank” of coastal planktonic diatoms in bottom sediments of Hiroshima Bay, Seto Inland Sea, Japan. *Mar. Biol.* 128, 497–508.
- Itakura, S., Nagasaki, K., Yamaguchi, M., Imai, I., 1999. Abundance and spatial distribution of viable resting stage cells of planktonic diatoms in bottom sediments of the Seto Inland Sea, Japan. In: Mayama, S., Idei, M., Koizumi, I. (Eds.), *Proceedings of the 14th International Diatom Symposium 1996*. Koeltes Scientific Books, Koenigstein, pp. 213–226.
- Itoh, K., Imai, I., 1987. *Rafido-so* (Raphidophyceae). In: *Japan Fisheries Resource Conservation Association (Ed.), A Guide for Studies of Red Tide Organisms*. Shuwa, Tokyo, pp. 122–130.
- Kamiyama, T., 1996. Determination of the abundance of viable tintinnid cysts in marine sediments in Hiroshima Bay, the Seto Inland Sea of Japan, using a modified MPN method. *J. Plankton Res.* 18, 1253–1259.
- Kinder, T.H., Coachman, L.K., Galt, J.A., 1975. The Bering Slope Current System. *J. Phys. Oceanogr.* 5, 231–244.
- Matheke, G.E.M., Horner, R., 1974. Primary productivity of the benthic microalgae in the Chukchi Sea near Barrow, Alaska. *J. Fish. Res. Board Can.* 31, 1779–1786.
- Matsunaga, K., Abe, K., Kuma, K., Hasebe, K., 1990. Measurement of reagent blanks for the determination of ammonia and silicate. *Bull. Fac. Fish., Hokkaido Univ.* 41, 51–55.
- McQuoid, M.R., 2002. Pelagic and benthic environmental controls on the spatial distribution of a viable diatom propagule bank on the Swedish west coast. *J. Phycol.* 38, 881–893.
- McQuoid, M.R., Hobson, L.A., 1996. Diatom resting stages. *J. Phycol.* 32, 889–902.
- McQuoid, M.R., Godhe, A., Nordberg, K., 2002. Viability of phytoplankton resting stages in the sediments of a coastal Swedish fjord. *Eur. J. Phycol.* 37, 191–201.
- McRoy, C.P., Goering, J.J., 1976. Annual budget of primary production in the Bering Sea. *Mar. Sci. Commun.* 2, 255–267.
- McRoy, C.P., Hood, D.W., Coachman, L.K., Walsh, J.J., Goering, J.J., 1986. Processes and resources of the Bering Sea shelf (PROBES): the development and accomplishments of the project. *Cont. Shelf Res.* 5, 5–21.
- Melnikov, I.A., Kolosova, E.G., Welch, H.E., Zhitina, L.S., 2002. Sea ice biological communities and nutrient dynamics in the Canada Basin of the Arctic Ocean. *Deep-Sea Res. I* 49, 1623–1649.
- Motoda, S., Minoda, T., 1974. Plankton of the Bering Sea. In: Hood, D.W., Kelly, E.J. (Eds.), *Oceanography of the Bering Sea*. Institute of the Marine Science, University of Alaska, Fairbanks, pp. 207–241.
- Okkonen, S., Niebauer, H.J., 1995. Ocean circulation in the Bering Sea marginal ice edge zone from Acoustic Doppler Current Profiler observations. *Cont. Shelf Res.* 15, 1879–1902.
- Odate, T., Maita, Y., 1990. Seasonal distribution and vertical flux of resting spores of *Chaetoceros* (Bacillariophyceae) species in the Neritic Water of Funka Bay, Japan. *Bull. Fac. Fish., Hokkaido Univ.* 41, 1–7.
- Oh, S.-H., Koh, C.-H., 1995. Distribution of diatoms in the surficial sediments of the Mangyung-Dongjin tidal flat, west coast of Korea (Eastern Yellow Sea). *Mar. Biol.* 122, 487–496.
- Ohtani, K., 1969. On the oceanographic structure and the ice formation on the continental shelf in the Bering Sea (in Japanese with English abstract). *Bull. Fac. Fish., Hokkaido Univ.* 10, 94–117.
- Ohtani, K., 1973. Oceanographic structure in the Bering Sea. *Mem. Fac. Fish., Hokkaido Univ.* 21, 65–106.
- Parsons, T.R., Maita, Y., Lalli, C.M., 1984. *A Manual of Chemical and Biological Methods for Seawater Analysis*. Pergamon Press, New York 173 pp.
- Pitcher, G.C., 1990. Phytoplankton seed populations of the Cape Peninsula upwelling plume, with particular reference to resting spores of *Chaetoceros* (Bacillariophyceae) and their role in seeding upwelling waters. *Estuarine Coast. Shelf Sci.* 31, 283–301.
- Pitcher, G.C., Walker, D.R., Mitchell-Innes, B.A., Moloney, C.L., 1991. Short-term variability during an anchor station study in the southern Benguela upwelling system: phytoplankton dynamics. *Prog. Oceanogr.* 28, 39–64.
- Saito, K., Taniguchi, A., 1978. Phytoplankton communities in the Bering Sea and adjacent seas II. Spring and summer communities in seasonally ice-covered areas. *Astarte* 11, 27–35.
- Shakshaug, E., 1989. The physiological ecology of polar phytoplankton. In: *Proceedings of the Six Conference of the Comité Arctique International*, 13–15 May 1985. In: Rey, L., Alexander, V. (Eds.), pp. 61–89.
- Sambrotto, R.N., Niebauer, H.J., Goering, J.J., Iverson, R.L., 1986. Relationships among vertical mixing, nitrate uptake, and phytoplankton growth during the spring bloom in the southeast Bering Sea middle shelf. *Cont. Shelf Res.* 5, 161–198.
- Schandelmeier, L., Alexander, V., 1981. An analysis of the influence of ice on spring phytoplankton population structure in the southeast Bering Sea. *Limnol. Oceanogr.* 26, 935–943.
- Schumacher, J.D., Reed, R.K., 1992. Characteristics of currents over the continental slope of the eastern Bering Sea. *J. Geophys. Res.* 97, 9423–9433.
- Smith, S.D., Muench, R.D., Pease, C.H., 1990. Polynyas and leads: an overview of physical processes and environment. *J. Geophys. Res.* 95, 9461–9479.
- Springer, A.M., Mcroy, C., Flint, M.V., 1996. The Bering Sea Green Belt: shelf-edge processes and ecosystem production. *Fish. Oceanogr.* 5, 205–223.
- Stabeno, P.J., Schumacher, J.D., Davis, R.F., Napp, J.M., 1998. Under-ice observations of water column temperature, salinity, and spring phytoplankton dynamics: eastern Bering Sea shelf. *J. Mar. Res.* 56, 239–255.
- Stabeno, P.J., Bond, N.A., Kachel, N.B., Salo, S.A., Schumacher, J.D., 2001. On the temporal variability of the physical environment over the southeastern Bering Sea. *Fish. Oceanogr.* 10, 81–98.
- Sullivan, C.W., McClain, C.R., Comiso, J.C., Smith Jr., W.O., 1988. Phytoplankton standing crops within an Antarctic ice edge assessed by satellite remote sensing. *J. Geophys. Res.* 93, 12487–12498.
- Suzuki, R., Ishimaru, T., 1990. An improved method for the determination of phytoplankton chlorophyll using N,N-dimethyl-formamide. *J. Oceanogr. Soc. Jpn.* 46, 190–194.
- Thronsdon, J., 1978. The dilution-culture method. In: Sournia, A. (Ed.), *Phytoplankton Manual*. UNESCO, Paris, pp. 218–224.
- von Quillfeldt, C.H., 1997. Distribution of diatoms in Northeast Water Polynya, Greenland. *J. Mar. Syst.* 10, 211–240.
- von Quillfeldt, C.H., 2000. Common diatom species in Arctic spring blooms: their distribution and abundance. *Bot. Mar.* 43, 499–516.
- Werner, I., Ikavalko, J., Schunemann, H., 2007. Sea-ice algae in Arctic pack ice during late winter. *Polar Biol.* 30, 1493–1504.
- Whitledge, T.E., Reeburgh, W.S., Walsh, J.J., 1986. Seasonal inorganic nitrogen distributions and dynamics in the southeastern Bering Sea. *Cont. Shelf Res.* 5, 109–132.
- Yamada, M., Tsuruta, A., Yoshida, Y., 1980. A list of phytoplankton as eutrophic level indicator (in Japanese with English abstract). *Bull. Jpn. Soc. Sci. Fish.* 46, 1435–1438.



Linkages between sea-ice coverage, pelagic–benthic coupling, and the distribution of spectacled eiders: Observations in March 2008, 2009 and 2010, northern Bering Sea



L.W. Cooper^{a,*}, M.G. Sexson^b, J.M. Grebmeier^a, R. Gradinger^c, C.W. Mordy^d, J.R. Lovvorn^e

^a Chesapeake Biological Laboratory, University of Maryland Center for Environmental Science, PO Box 38, Solomons, MD 20688, USA

^b US Geological Survey, Alaska Science Center, 4210 University Drive, Anchorage, AK 99508, USA

^c School of Fisheries and Ocean Science, University of Alaska Fairbanks, Fairbanks, AK 99775, USA

^d Joint Institute for the Study of the Atmosphere and Ocean, University of Washington, 3737 Brooklyn Ave NE, Box 355672, Seattle, WA 98105-5672, USA

^e Department of Zoology and Center for Ecology, Southern Illinois University, Carbondale, IL 62901, USA

ARTICLE INFO

Available online 7 March 2013

Keywords:

Bering Sea

Spectacled eider

Sea ice

Pelagic–benthic coupling

Organic sedimentation

ABSTRACT

Icebreaker-based sampling in the northern Bering Sea south of St. Lawrence Island in March of 2008, 2009, and 2010 has provided new data on overall ecosystem function early in the annual productive cycle. While water-column chlorophyll concentrations ($<25 \text{ mg m}^{-2}$ integrated over the whole water column) are two orders of magnitude lower than observed during the spring bloom in May, sea-ice algal inventories of chlorophyll are high (up to 1 g m^{-3} in the bottom 2-cm of sea-ice). Vertical fluxes of chlorophyll as measured in sediment traps were between 0.3 and $3.7 \text{ mg m}^{-2} \text{ d}^{-1}$ and were consistent with the recent deposition (days' to weeks' time scale) of chlorophyll to the surface sediments ($0\text{--}25 \text{ mg m}^{-2}$ present at $0\text{--}1 \text{ cm}$). Sediment oxygen respiration rates were lower than previous measurements that followed the spring bloom, but were highest in areas of known high benthic biomass. Early spring release of sedimentary ammonium occurs, particularly southeast of St. Lawrence Island, leading to bottom-water ammonium concentrations of $>5 \mu\text{M}$. These data, together with other physical, biological, and nutrient data, are presented here in conjunction with observed sea-ice dynamics and the distribution of an apex predator, the Spectacled Eider (*Somateria fischeri*). Sea-ice dynamics in addition to benthic food availability, as determined by sedimentation processes, play a role in the distribution of spectacled eiders, which cannot always access the greatest biomass of their preferred bivalve prey. Overall, the data and observations indicate that the northern Bering Sea is biologically active in late winter, but with strong atmospheric and hydrographic controls. These controls pre-determine nutrient and chlorophyll distributions, water-column mixing, as well as pelagic–benthic coupling.

© 2013 Elsevier Ltd. All rights reserved.

1. Introduction

The northern Bering Sea, which we define as the continental shelf north of St. Matthew Island extending to the Bering Strait, is a large-scale ecotone between the pelagic-dominated southeast Bering Sea and more Arctic waters found north of the Bering Strait. In the region around St. Lawrence Island (SLI), nutrient distributions are controlled by the course and extent of the Anadyr Current (AC) from the western side of the Bering Sea (reviewed by Cooper et al., 2012). The AC has its origin in the deep Bering Sea and consists of waters that upwell onto the Bering shelf from the Bering Slope Current (Kinder et al., 1975; Wang et al., 2009). A branch of the AC passes south of SLI, although the main flow is

northward through Anadyr Strait (Clement et al., 2005; Danielson et al., 2006, 2011; Grebmeier and Cooper, 1995).

To the east of SLI, the Bering Sea is dominated by Alaska Coastal Water (ACW), which is nutrient-poor compared to the AC to the west. Prior to the initiation of seasonal biological production, however, the contrast in nutrient concentration across the northern Bering Sea is smaller than observed during the open water season when a drawdown occurs due to biological productivity. In summer, generally nutrient-poor runoff from rivers in Alaska also creates a west-to-east gradient of decreasing salinity across the northern Bering Sea.

The alignment of high productivity by water mass and the shallow shelf of the Bering Sea result in a large proportion of high-quality organic carbon being deposited to the continental shelf, which in turn supports highly productive benthic communities (reviewed by Grebmeier, 2012; Grebmeier et al., 2006). Benthic communities in turn support apex predators such as the Pacific

* Corresponding author. Tel.: +1 410 326 7359; fax: +1 410 326 7341.

E-mail address: cooper@umces.edu (L.W. Cooper).

Walrus (*Odobenus rosmarus divergens*), Bearded Seal (*Erignathus barbatus*), Gray Whale (*Eschrichtius robustus*), several sea duck species (Subfamily Merginae), and other organisms that forage on benthic food sources. Despite high benthic biomass and evidence for recent ecosystem-scale declines in biomass and shifts in biological community structure (Grebmeier, 2012), there has been limited sampling in this region during periods of ice cover (e.g. Clement et al., 2004; Cooper et al., 2002, 2012; Danielson et al., 2006), which is typically present from November until May or June. Information regarding ecosystem dynamics in the northern Bering Sea during the late winter period (March) is critical for understanding the initiation of the productive biological spring bloom as solar radiation increases sufficiently to initiate biological production. However, opportunities to document pre-seasonal conditions have been limited by seasonal (e.g., sea ice and extreme cold temperatures) and logistical (e.g., icebreaker-based instrumentation) constraints.

We present observations of hydrographic and biological conditions present on three research cruises in March 2008, March 2009, and March 2010. Specifically, we present mapped water mass boundaries (derived from salinity, oxygen isotopes and inorganic nutrients), water column nutrients and chlorophyll, the vertical flux of sea ice algal and phytoplankton pigments, and an inventory of recently deposited chlorophyll (days to weeks) on the sea floor.

We discuss measured physical and biogeochemical processes, particularly organic sedimentation that drives high benthic biomass in the context of a case study of the distribution of one apex predator that uses this region, the Spectacled Eider (*Somateria fischeri*). While our study was not focused on benthic community structure and dynamics, we use known distributions of benthic invertebrates as a means to explore the interplay between sea ice coverage, benthic invertebrate distribution, and the distribution of eiders.

Spectacled eiders are medium-sized sea ducks (spring adults: 1275–1850 g) that nest in coastal areas of northern and western Alaska, and northern Russia, yet spend most of the annual cycle at non-breeding (i.e., fall molting, wintering, and spring staging) areas in the near-shore East Siberian, Chukchi, Beaufort, and northern Bering Seas (Petersen et al., 2000). As a result of rapid population decline (up to 96% from 1952 to 1993) within the western Alaska breeding population, the species was designated 'threatened' under the US Endangered Species Act in 1993 (Ely et al., 1994; Stehn et al., 1993; US Fish and Wildlife Service, 1993). Subsequently, critical habitat was designated throughout the species' range, including an area encompassing the primary wintering site in the northern Bering Sea south of SLI (73,530 km²; US Fish and Wildlife Service, 2001).

2. Methods

A suite of samples were collected and observations made during two cruises of the USCGC *Healy* (Cruise 08-01, 13–26 March 2008 and Cruise 09-01, 10–31 March 2009) and one cruise of the USCGC *Polar Sea* (Cruise 10-01, 7 March–7 April 2010) while sea ice was continuing to form under late winter conditions (Tables 1–3). A majority of sampling stations had been previously occupied for water column and benthic biological studies dating back to 1990 and earlier. Other stations were selected in situ to document localized water column conditions and prey available to spectacled eiders and Pacific walrus observed at the time of the cruise. Data relevant to the distribution of spectacled eiders are presented here; Pacific walrus data are in preparation (C. Jay, personal communication).

The conductivity, temperature, and depth (CTD) instrument used aboard both *Healy* and *Polar Sea* consisted of a 12-place rosette with 30-L Niskin bottles and a Sea-Bird Electronics Model

Table 1
HLY0801 station information.

Station number	Station name	Date (m/dd/yyyy)	Latitude °N	Longitude °W	Depth (m)
1	VNG1	3/16/2008	61.974	−175.050	79
2	NWC5	3/16/2008	62.048	−175.201	80
3	NWC4	3/17/2008	62.381	−174.567	72
4	VNG3.5	3/17/2008	62.568	−173.579	68
5	SWC2	3/17/2008	62.915	−172.298	60
6	NWC2.5	3/18/2008	63.033	−173.446	70
7	NWC3	3/18/2008	62.799	−173.929	70
8	NWC4a	3/18/2008	62.578	−174.165	70
9	DLN3	3/19/2008	62.879	−174.538	72
10	NWC2	3/19/2008	63.119	−173.122	71
11	POP3a	3/20/2008	62.550	−172.320	60
12	SIL3	3/20/2008	62.438	−172.300	60
13	SEC2.5	3/20/2008	62.483	−171.848	60
14	POP4	3/21/2008	62.400	−172.705	60
15	FD1	3/21/2008	62.482	−172.464	55
16	SEC2	3/21/2008	62.601	−170.968	45
17	NEC2	3/21/2008	62.424	−170.113	39
18	WAL1	3/21/2008	62.387	−169.362	33
19	WAL2	3/22/2008	62.394	−169.381	36
20	WAL3	3/22/2008	62.367	−168.976	36
21	WAL4	3/22/2008	62.562	−169.318	34
22	WAL5	3/22/2008	62.522	−169.635	30
23	WAL6	3/22/2008	62.404	−169.720	34
24	MK10A	3/23/2008	62.192	−169.010	36
25	NEC1	3/23/2008	62.754	−169.594	42
26	JGR1	3/23/2008	62.711	−170.167	43
27	SEC1	3/23/2008	62.992	−170.289	40
28	JGR2	3/23/2008	62.988	−170.800	40
29	JGR3	3/23/2008	63.158	−170.921	37
30	JGR4	3/23/2008	63.116	−171.301	46

911+ CTD system. Salinities were standardized with a Guideline Autosol salinometer with international seawater standards. The electronics system was calibrated before and after the cruises at the Sea-Bird manufacturing facility in Bellevue, Washington. Niskin bottles were closed at selected depths during the up-cast, usually 0, 10, 20, 30, 40 and 50 m below the surface and a final bottle closed at 5–10 m above the sea floor (bottom water) as determined by an altimeter installed on the CTD.

The stable oxygen isotope composition of water samples was also measured in surface water samples to assess freshwater contributions from runoff relative to melted sea ice. Isotopic analyses were performed via equilibration with carbon dioxide within a Thermo Delta Plus Gas Bench and stable isotope mass spectrometer used in a continuous flow mode at the University of Maryland Center for Environmental Science with internal and international standards used for calibration. Data are reported for oxygen isotopes of these surface waters, as well as carbon isotopes of marine algal sediment trap samples (methodology described below), in the delta notation, where

$$\delta X = [(R_{\text{sample}}/R_{\text{standard}}) - 1] \times 1000$$

where X is ¹⁸O or ¹³C of the sample and R is the corresponding ratio ¹⁸O/¹⁶O or ¹³C/¹²C. Analytical precision was ±0.1‰.

Nutrient samples were collected from all CTD casts during the cruise and analyzed for nitrate, nitrite, ammonium, phosphate and silicate. Samples were collected in a 60-ml syringe after three complete seawater rinses, and filtered through a 45-µm cellulose acetate membrane directly into acid washed 25-ml high-density polyethylene bottles rinsed three times with unfiltered seawater. Samples were then frozen at −80 °C until analyzed. Nutrient analysis was carried out at the Pacific Marine Environmental Laboratory (PMEL) following the protocols of Gordon et al. (1994), including reagent preparation, equipment calibration, preparation of primary and secondary standards, and corrections for

Table 2
 HLY0901 station information.

Station number	Station name	Date (m/dd/yyyy)	Latitude °N	Longitude °W	Depth (m)
1	VNG1	3/14/2009	62.016	−175.071	79
2	NWC5	3/14/2009	62.055	−175.197	80
3	NWC4	3/14/2009	62.381	−174.536	71
4	SWC3	3/15/2009	62.558	−173.087	62
5	NWC2.5A	3/16/2009	62.970	−173.384	71
6	DLN2	3/16/2009	63.278	−173.737	74
7	NWC2	3/17/2009	63.104	−173.146	70
8	NWC1	3/17/2009	63.487	−172.317	50
9	VNG3.5	3/18/2009	62.566	−173.568	67
	VNG3.5	3/18/2009	62.563	−173.559	67
10	SIL2	3/19/2009	62.762	−171.654	50
11	SEC2	3/19/2009	62.590	−170.962	45
12	CD2	3/20/2009	62.530	−172.122	51
13	SEC1.5	3/20/2009	62.812	−170.645	45
14	NEC1	3/21/2009	62.758	−169.586	42
15	SEC1	3/21/2009	62.986	−170.266	40
16	SIL1	3/21/2009	63.100	−171.295	47
17	JGR3	3/21/2009	63.160	−170.941	40
18	WAL7	3/22/2009	62.743	−169.316	38
19	WAL8	3/22/2009	62.627	−169.636	40
20	WAL9	3/22/2009	62.668	−169.140	40
21	MK1	3/22/2009	62.728	−168.951	40
22	WAL10	3/23/2009	62.521	−168.970	33
23	WAL11	3/23/2009	62.255	−169.638	40
24	WAL12	3/24/2009	62.067	−169.272	40
25	XSL1	3/24/2009	62.073	−169.762	40
26	XSL2	3/24/2009	62.068	−170.252	45
27	NEC3	3/24/2009	62.067	−170.621	50
28	XSL3	3/24/2009	62.046	−171.118	50
29	SLP1	3/24/2009	62.374	−170.371	41
30	SLP1A	3/25/2009	62.493	−170.482	40
31	SLP2	3/25/2009	62.631	−170.502	42
32	SLP3	3/25/2009	62.870	−170.634	43
33	JGR3	3/25/2009	63.156	−170.918	40
34	SEC1	3/25/2009	62.977	−170.270	40
35	NEC1	3/25/2009	62.754	−169.589	40
36	MK1B	3/25/2009	62.725	−169.017	36
37	WAL13	3/26/2009	62.859	−169.016	35
38	SEC1.5	3/27/2009	62.811	−170.648	43
39	SIL2.5	3/27/2009	62.632	−171.991	50
40	CD1	3/27/2009	62.676	−173.372	70
41	NWC3	3/27/2009	62.760	−173.816	72
42	POP4	3/28/2009	62.388	−172.700	60
43	SWC4A	3/28/2009	62.239	−173.741	60

blanks and refractive index. Silicate analysis was conducted a second time at least 1 day after thawing to minimize complications due to polymerization (Macdonald et al., 1986).

During the two *Healy* cruises, water column chlorophyll *a* was measured by filtering 250-mL water samples through 25-mm GF/F filters. The filters were initially frozen (~1 h) to fracture cell walls, and then stored in 10 mL of 90% acetone at 4 °C for 24 h in the dark. This storage temperature was used because it is close to in situ water temperatures and presumably results in low rates of chlorophyll degradation. Chlorophyll *a* was extracted and measured using the Welschmeyer (1994) method with a Turner Designs 10-AU field fluorometer. The fluorometer was calibrated with a Turner Design Part no. 10-850 chlorophyll standard before and after all sampling, with the use of a secondary solid standard (Part no. 10-AU-904) during sampling to identify any possible instrument drift. Integrated chlorophyll *a* was calculated for individual stations from ocean surface to sediments on a square meter basis, as most stations were 40–60 m in depth.

A similar procedure was used during the *Polar Sea* cruise to measure chlorophyll *a*. In addition, replicate samples were collected, filtered onto 25-mm GF/F filters, placed into 1.5-mL microcentrifuge tubes and stored at −80 °C, and returned frozen

to PMEL for post-cruise analysis. Filters were stored in 10 mL of 90% acetone at 4 °C for 24 h in the dark, and then analyzed on a Turner Designs 10-AU field fluorometer using the Welschmeyer method. Replicates were collected to evaluate the impacts of freezing and storing the filters prior to measuring chlorophyll.

Ice sampling occurred in 2009 and 2010 at stations (Table 4) selected according to ice and weather conditions, and overall cruise planning. Sampling occurred during daytime around solar noon on ice floes considered representative for a given area. We sampled ice floes of sufficient thickness for safe field work (>0.25 m), whereas new ice (e.g. pancake, grease, nilas) was not sampled.

Ice cores were taken with a 9-cm diameter ice corer. Cores were sectioned into 1 to 20-cm long segments and stored in coolers in the dark for transport. Core segments were melted directly in a dark and cold room (2–4 °C) and split into 5 to 250-ml subsamples. One subsample was filtered onto Whatman GF/F filters, and frozen for algal pigment analysis. A second subsample was filtered onto pre-combusted GF/F filters to later analyze the stable isotope composition ($\delta^{13}\text{C}$, $\delta^{15}\text{N}$) of organic material and quantify particulate organic carbon and nitrogen (POC, PON; data to be presented elsewhere). Filters for algal pigment analysis were extracted with 7 ml of 90% acetone for 24 h (Gradinger et al., 2005) and analysis was conducted fluorometrically with a Turner Designs fluorometer (Arar and Collins, 1997).

Filters containing organic matter were dried 1–2 d and HCl-fumed to remove carbonates. Filters were analyzed at the University of Alaska Fairbanks Stable Isotope Facility using an elemental analyzer coupled to a Thermo Delta stable isotope mass spectrometer operated in a continuous flow mode. Organic carbon isotope ratios are expressed in the conventional delta notation as described previously for oxygen isotope composition of surface waters.

An ice saw was used to cut holes in the ice, through which sediment traps were deployed for 2–6 h below ice floes at depths of 5 and 20 m. Traps were filled with 0.7- μm filtered seawater prior to deployment. Upon recovery, samples were parsed and treated using the same methods used to process ice samples. Live macroorganisms were manually removed from all samples.

Sediment samples (0–1 cm) were collected on all cruises for assessment of chlorophyll *a* surface sediment, as well as other sediment characteristics (e.g. total organic carbon, C:N ratios, grain size) reported elsewhere. Sediment samples were collected using a multi- or single-HAPS benthic corer (133 cm²; Kannevorf and Nicolaisen, 1973) or from the top of a van Veen grab (0.1 m²). In prior studies we determined that bioturbation is high on a month–annual scale and the less disturbed nature of surface sediments collected by corers relative to grabs is negated for these shelf sediments (Cooper et al., 1998; Pirtle-Levy et al., 2009). We also assumed that the 0–1 cm sediment depth increment predominantly contained chlorophyll deposited on a week–month time scale, based on the findings that surface sediment chlorophyll inventories in the northern Bering Sea vary in response to seasonally variable primary production in the ice and water column (Cooper et al., 2002).

Duplicate sediment cores for shipboard incubations were collected using a HAPS benthic corer with removable Plexiglas® insert sleeves (133-cm² surface area as described above). Under optimal conditions, the resultant cores were approximately 15-cm deep, with a low degree of apparent disturbance. Apparent disturbance was determined to be low if clear water was present at the sediment–water interface, flocculent materials such as fecal pellets were present at the base of benthic burrows at the sediment surface, and filtering activity was exhibited by macrobenthic invertebrates. Sediment–flux measurements for dissolved oxygen followed the methods of Grebmeier and McRoy (1989). Bottom water for these experiments was collected from the CTD

Table 3
Polar Sea 10-01 station information.

Station number	Station name	Date (m/dd/yyyy)	Latitude °N	Longitude °W	Depth (m)
1	VNG1	3/13/2010	62.018	-175.050	83
2	NWC5	3/13/2010	62.051	-175.200	84
2	NWC5	3/13/2010	62.047	-175.196	84
3	NWC4	3/14/2010	62.401	-174.527	74
4	NWC4A	3/15/2010	62.562	-174.210	73
5	VNG3	3/15/2010	62.555	-173.841	71
6	VNG35	3/16/2010	62.577	-173.624	70
7	CD1	3/16/2010	62.676	-173.367	70
8	VNG4	3/16/2010	62.756	-173.410	78
8	VNG4	3/16/2010	62.762	-173.435	71
9	NWC2.5	3/17/2010	63.033	-173.423	75
10	VNG5	3/17/2010	62.968	-172.986	70
11	SWC3A	3/17/2010	62.762	-172.710	65
12	POP3A	3/18/2010	62.576	-172.310	85
13	SIL3	3/18/2010	62.442	-172.312	55
14	SEC2.5	3/18/2010	62.496	-171.853	50
15	CD2	3/18/2010	62.531	-172.119	50
15	CD2	3/18/2010	62.560	-172.179	50
16	CD08	3/19/2010	62.653	-172.236	56
17	SIL2	3/19/2010	62.751	-171.664	50
18	SIL2.5	3/19/2010	62.630	-171.987	50
19	CD10C	3/20/2010	62.371	-172.383	56
20	CD10B	3/20/2010	62.258	-172.282	56
21	CD10A	3/20/2010	62.151	-172.178	55
22	SEC4	3/20/2010	61.924	-172.218	60
23	SEC3	3/20/2010	62.281	-171.563	52
24	NEC3	3/21/2010	62.059	-170.650	55
25	MK11	3/21/2010	62.178	-169.465	40
26	NEC2	3/21/2010	62.429	-170.057	40
27	NEC1	3/22/2010	62.759	-169.592	44
28	NEC1.1	3/22/2010	62.853	-169.887	46
29	NEC1.2	3/22/2010	62.648	-170.314	45
30	SEC2	3/22/2010	62.606	-170.955	47
31	SEC1.8	3/22/2010	62.692	-170.764	46
32	SEC1.5	3/23/2010	62.809	-170.646	45
33	SEC1.1	3/23/2010	62.887	-170.431	45
34	SEC1	3/23/2010	62.993	-170.267	42
35	CDF	3/23/2010	62.934	-170.928	46
36	CDF1.4	3/23/2010	62.860	-171.030	47
37	CD10D	3/23/2010	62.614	-171.385	50
38	POP4	3/24/2010	62.399	-172.686	46
39	SWC4	3/24/2010	62.226	-173.768	46
39	SWC4	3/24/2010	62.224	-173.776	65
40	SWC4A	3/25/2010	62.418	-173.411	65
41	NWC3	3/26/2010	62.748	-173.871	74
42	DLN3	3/26/2010	62.894	-174.515	80
43	DLN2	3/27/2010	63.264	-173.735	82
44	CD81.1	3/27/2010	62.632	-172.266	55
45	CD81.5	3/28/2010	62.719	-171.839	54
46	SWC2	3/28/2010	62.908	-172.275	60
47	NWC2	3/28/2010	63.131	-173.123	72
48	CDF	3/29/2010	62.920	-170.947	46
49	70M58	3/30/2010	62.199	-174.752	79
50	70M56	3/21/2010	61.950	-174.372	77
51	70M55	3/21/2010	61.860	-174.102	77
52	70M54	3/21/2010	61.738	-173.874	77
53	70M52	3/21/2010	61.419	-173.734	79
54	70M50	3/21/2010	61.074	-173.843	84
55	70M48	4/1/2010	60.749	-173.670	76
56	70M47	4/1/2010	60.571	-173.633	72
57	70M46	4/1/2010	60.429	-173.593	70
58	70M45	4/1/2010	60.265	-173.531	73
59	70M44	4/1/2010	60.101	-173.297	75
60	70M43	4/1/2010	60.042	-173.004	71
61	70M42	4/1/2010	59.962	-172.723	73
62	70M41	4/2/2010	59.911	-172.436	78
63	70M40	4/2/2010	59.904	-172.203	76
64	70M39	4/2/2010	59.884	-171.655	76
65	70M38	4/2/2010	59.779	-171.428	77
66	70M37	4/2/2010	59.709	-171.137	76
67	70M36	4/2/2010	59.591	-170.917	75
68	70M35	4/2/2010	59.450	-170.915	76
69	70M34	4/2/2010	59.335	-170.648	73
70	70M32	4/3/2010	59.113	-170.260	70
71	70M30	4/3/2010	58.789	-170.301	75

Table 3 (continued)

Station number	Station name	Date (m/dd/yyyy)	Latitude °N	Longitude °W	Depth (m)
72	70M28	4/3/2010	58.449	−170.153	77
73	70M26	4/3/2010	58.146	−169.917	77
74	70M24	4/3/2010	57.918	−169.512	73
75	70M22	4/3/2010	57.848	−168.899	75
76	70M20	4/4/2010	57.614	−168.729	74
77	70M17	4/4/2010	57.505	−168.009	75
78	70M14	4/4/2010	57.520	−167.049	75
79	70M11	4/4/2010	57.328	−166.351	74
80	70M08	4/4/2010	57.110	−165.611	75
81	70M04	4/5/2010	56.796	−164.582	77

Table 4

Sea ice sampling stations, 2009–2010.

Cruise	Station	Date (m/dd/yy)	Latitude °N	Longitude °W	Ice thickness (cm)	Snow depth (cm)
HLY0901	DLN2	3/16/09	63.267	−173.695	86	15
HLY0901	NWC1	3/17/09	63.485	−172.317	65	25
HLY0901	SEC2	3/19/09	62.594	−170.959	95	24
HLY0901	MK1	3/22/09	62.729	−168.952	87	14
HLY0901	WAL12	3/23/09	62.112	−169.256	67	16
HLY0901	MK1B	3/25/09	62.699	−169.024	68	34
HLY0901	NWC3	3/27/09	62.682	−173.388	109	33
PSea1001	NWC5	3/13/10	62.050	−175.199	53	3
PSea1001	VNG4	3/16/10	62.756	−173.411	53	2
PSea1001	CD2	3/18/10	62.532	−172.121	49	3
PSea1001	SWC4	3/24/10	62.225	−173.770	57	7
PSea1001	NWC3	3/25/10	62.754	−173.854	56	7
PSea1001	DLN2	3/26/10	63.263	−173.736	55.5	5
PSea1001	NWC2	3/28/10	63.131	−173.123	41.5	5

rosette. Enclosed sediment cores with motorized paddles were maintained in the dark at in situ bottom temperatures for approximately 12–24 h. Point measurements were made at the start and end of the experiment, and flux measurements were calculated, based on the concentration differences adjusted to a daily flux per m². Previous shipboard measurements indicated a steady decline in oxygen values in the overlying water during the course of incubation. Sediments were sieved after completing the experiment to determine faunal composition (data to be reported elsewhere).

Surface sediment chlorophyll *a* inventories were measured on all cruises using a Turner Designs fluorometer without acidification (Welschmeyer method) using a standardized method that includes a 12 h dark incubation in 90% acetone at 4 °C (Cooper et al., 2002). Surface sediment inventories reported are the mean of two independent determinations.

Satellite telemetry was used to collect weekly geo-referenced locations from adult and juvenile spectacled eiders. In 2008–2010, spectacled eiders were captured at coastal sites in western and northern Alaska. A veterinarian implanted a satellite transmitter (Model PTT 100, Microwave Telemetry Inc.) in the coelom of 92 individuals using standard surgical methods (Korschgen et al., 1996; Mulcahy and Esler, 1999). Permits for eider capture and transmitter deployment were obtained from the US Fish and Wildlife Service and the Alaska Department of Fish and Game, with capture and surgical protocols reviewed and approved by the USGS Alaska Science Center and the University of Alaska Fairbanks animal care and use committees. Satellite transmitters were programmed to provide location data every 4–7 days over a 2-year period. Location, body temperature, and voltage data were received from each transmitter through the Collecte Localisation Satellites Argos system (CLS America, Lanham, Maryland). Prior to analysis, we excluded location data from dead individuals and other poor quality data locations. The Douglas Argos-Filter Algorithm and associated software (Douglas, 2010) was used to

synthesize multiple locations into the single most likely location received from each individual during each transmission period. Near-real time locations were used during research cruises in 2009 and 2010 to guide aerial surveys for spectacled eiders and document sea ice conditions in used areas.

We assessed general spatiotemporal patterns in the distribution of spectacled eiders at the species' primary wintering area, south of St. Lawrence Island in the northern Bering Sea, constraining analysis to an area south of 63°47'N and between 175° and 168° W. Within the primary wintering area, we assessed overlap in the distribution of spectacled eiders in September–May between 2008 and 2009, 2009 and 2010, and 2010 and 2011. We also compared all locations from winters 2008–2011 to similar telemetry data collected in 1993–1997 (Petersen et al., 1999). We used Geospatial Modeling Environment (Version 0.6.0.0, Beyer, 2012) to calculate kernel densities and 50% and 95% isopleths for each set of locations, using least squares cross-validation to calculate kernel smoothing parameters. We used ArcMap 10 (ArcGIS, ESRI, Redlands, CA) to calculate the percent overlap of paired isopleths (ESRI, 2010). We also used ArcMap to extract depth values at each location in the data set using the General Bathymetric Chart of the Oceans (The GEBCO_08 Grid, version 20100927, <http://www.gebco.net>).

Density of major bivalve prey of eiders at each sampling station was mapped based on van Veen grab samples taken in March–April 2001 and May–June 2006. Benthic samples collected contemporaneously with the eider telemetry data were being analyzed at the time of manuscript preparation. However, we expect more recently collected data will not fundamentally alter our understanding of where benthic biomass is greatest; see Grebmeier (2012) for a more detailed description of long-term changes in benthic community composition southwest of SLI. Furthermore, bivalves must be several years old to reach size classes considered preferred for eiders (Lovvorn et al., 2003). Therefore, we assumed that the dispersion of these prey in 2009 resembled dispersion in 2006. Maps of prey density were overlain

with maps of percent ice cover (in tenths) on 2 March 2001 and 2009, the same months in which eiders were collected for body condition and diet studies (J. Lovvorn, unpublished data). Ice cover percentages were derived from National Ice Center digital Ice Analysis charts, which are based on data sources (and spatial resolution) including RADARSAT 2 (100 m), ASAR (150 m), ENVISAT GMM (1 km), MODIS (0.25–1 km), AVHRR (1.1–2.9 km), and OLS (0.5–2.4 km).

3. Results and discussion

3.1. Hydrography, nutrients and chlorophyll fields

During our early spring observations in the northern Bering Sea in 2008, 2009, and 2010, the water column was highly mixed,

partly a result of brine rejection (i.e. exclusion of salt from ice during sea ice formation). Temperatures were isothermal and near the freezing point ($-1.8\text{ }^{\circ}\text{C}$) although salinity varied spatially if not vertically. Horizontal gradients in bottom salinity were generally the result of brine rejection south of SLI relative to less saline water present to the south and west (Fig. 1). This pattern differed from that observed during open-water seasons with salinity greater (>32.5) in the west (i.e. Anadyr water) and declining significantly to the east (<31) (e.g. Walsh et al., 1989). Some distinctions in water masses were observed based on the nutrient concentration. At this early point in the seasonal cycle, there was limited runoff in the Alaska coastal water to the east of SLI. For example, the stable oxygen isotope data (Fig. 2), as well as salinity (Fig. 1) showed negligible runoff relative to published early summer data (e.g. Cooper et al., 1997). Therefore, we concluded that salinity variation is primarily driven at this time by the

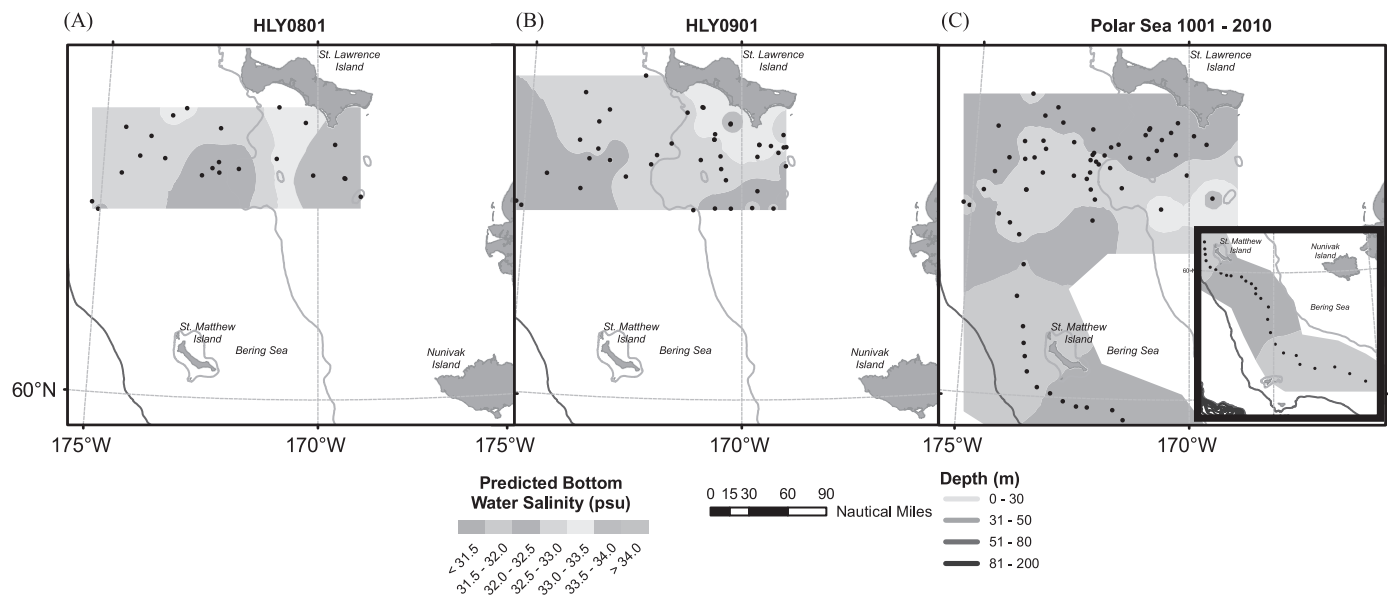


Fig. 1. Bottom water salinity in March 2008 (A), March 2009 (B) and March 2010 (C) south of St. Lawrence Island. Symbols correspond to the available data; color gradations are estimated (predicted) interpolations and are created using inverse distance weighting method (default settings) of Geospatial Analyst Extension for ArcMap 9.3 (ESRI, Redlands, CA) (For interpretation of the references to color in this figure legend, the reader is referred to the web version of this article.)

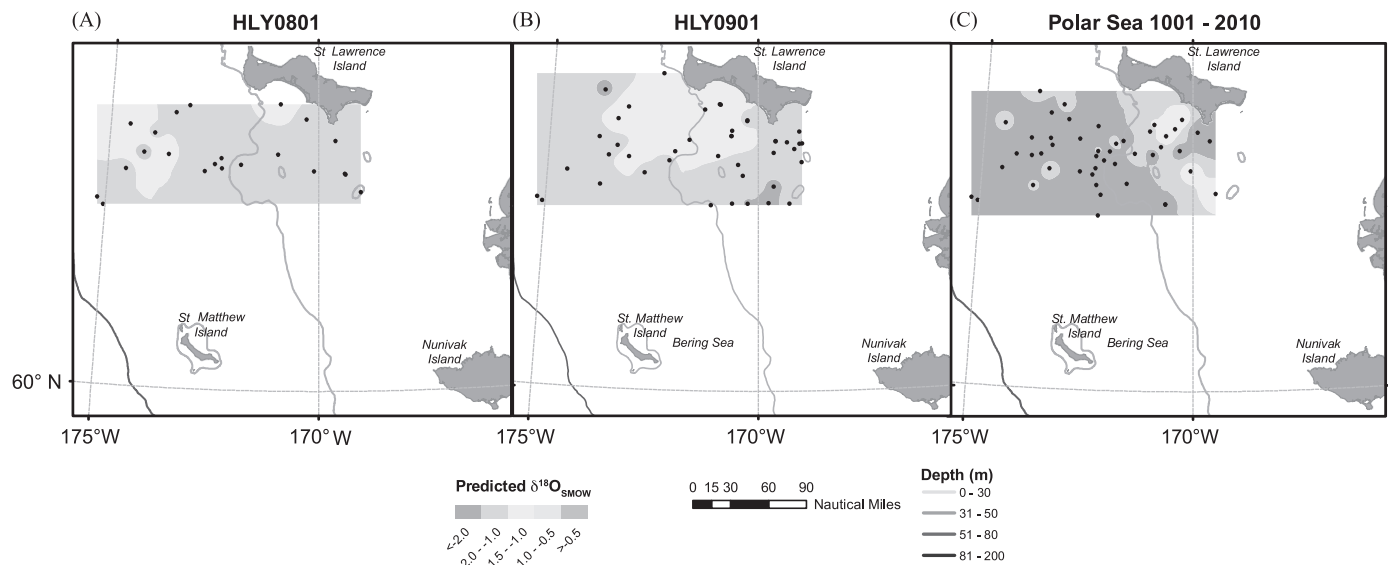


Fig. 2. Surface water $\delta^{18}\text{O}$ values in March 2008 (A), March 2009 (B) and March 2010 (C) south of St. Lawrence Island. Symbols correspond to the available data; color gradations are estimated interpolations using inverse distance weighting method (default settings) of Geospatial Analyst Extension for ArcMap 9.3 (ESRI, Redlands, CA) (For interpretation of the references to color in this figure legend, the reader is referred to the web version of this article.)

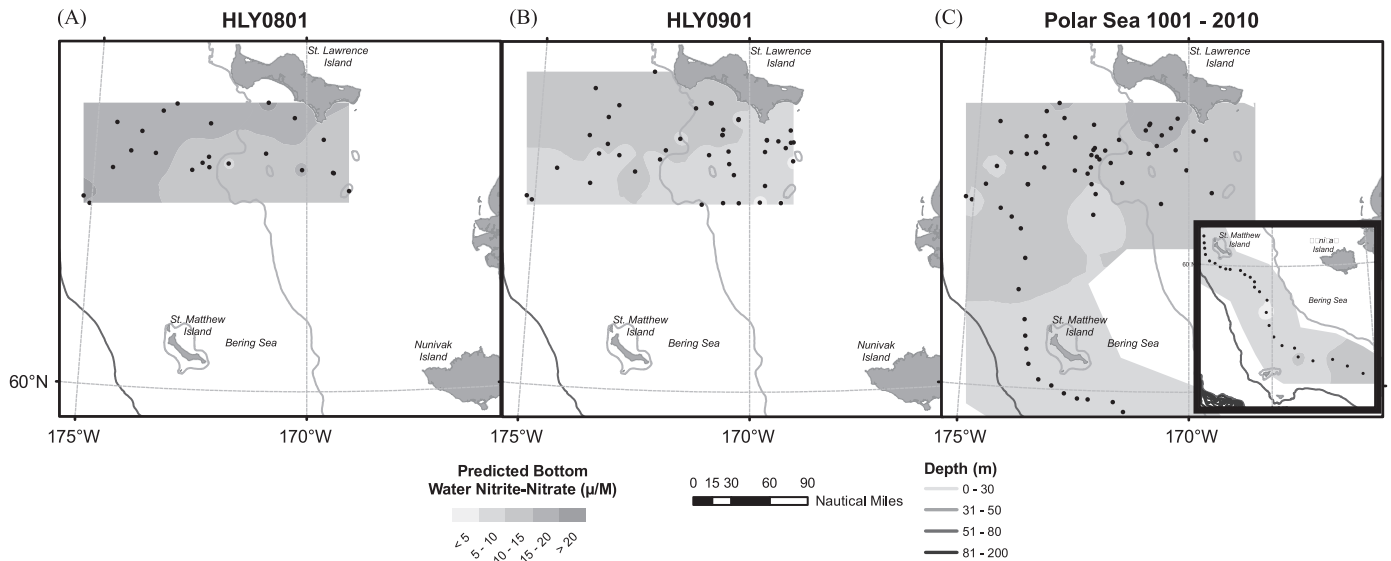


Fig. 3. Bottom water nitrate + nitrite (μM) in March 2008 (A), March 2009 (B) and March 2010 (C) south of St. Lawrence Island. Symbols correspond to the available data; color gradations are estimated interpolations as in Fig. 1. (For interpretation of the references to color in this figure legend, the reader is referred to the web version of this article.)

injection or rejection of brine from sea ice rather than differences between Anadyr water and Alaska coastal water. The greatest salinities were observed south and southeast of the island, resulting from brine rejected waters originating from the formation of sea ice in the polynya south of SLI (e.g. Fig. 1B). More saline waters were then advected south and apparently entrained into north-easterly flowing water on the Bering Shelf, as described in Danielson et al. (2006) and Cooper et al. (2012) (Fig. 1A and C). We also observed an elevation of $\delta^{18}\text{O}$ values in surface waters south of SLI to $\sim 0.5\%$ to -1.0% (an enrichment of $\sim 1\%$, see Fig. 2), particularly in 2009 and 2010. Enrichments do not mirror salinity variations (Fig. 1) driven by water mass. Therefore, we think the pattern in oxygen isotope variability indicated the presence of a small freshwater component originating from melted sea ice. Freshwater is isotopically heavier ($\sim 2\%$) than the seawater from which it forms due to isotopic fractionation during ice formation. This suggests that at early stages of sea ice formation, such as when frazil or grease ice forms in the polynya south of SLI, some of the newly formed ice may subsequently pass back into a liquid phase, releasing a freshwater fraction isotopically more enriched in ^{18}O than other surface waters. Therefore, at early stages of sea ice formation, or in regions of active sea ice formation, there may be an isotopic signal present in surface waters that traces recent sea ice formation. To our knowledge, these patterns of isotopic enrichment of ^{18}O in surface waters in a polynya have not been reported previously.

Well-documented differences in water masses in the northern Bering Sea (e.g. Walsh et al., 1989) were apparent according to nutrient concentrations. A west-to-east decrease in bottom water nitrate+nitrite was unambiguously observed in 2 of the 3 years (Fig. 3A and B). In 2010, the greatest bottom water nitrate+nitrite concentrations ($>20 \mu\text{M}$) were observed immediately south of SLI, which may actually reflect a branch of the AC that flows south of the island (Danielson et al., 2006; Grebmeier and Cooper, 1995). However, placement of sampling stations in 2010 may have precluded clear mapping of the east-to-west increasing concentrations of nitrate+nitrite due to the influence of Anadyr water. Surface water concentrations of nitrate+nitrite were equally as high as bottom waters (data not shown) indicating biological production had not significantly impacted inorganic nutrients at this point in the seasonal cycle. Silica and phosphate varied in a similar spatial pattern as nitrate+nitrite (data not shown), meaning water mass differences in nutrients were present early in the season, but differences among

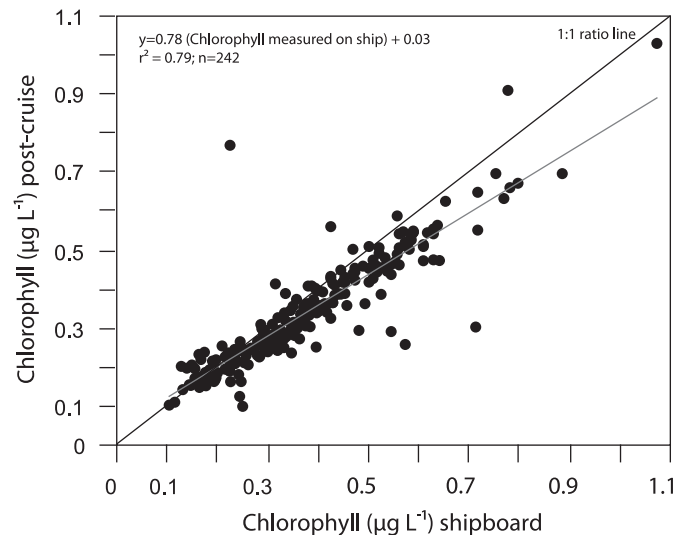


Fig. 4. Chlorophyll *a* concentrations in replicate water samples collected and analyzed during the Polar Sea 10–01 cruise (x-axis) versus frozen filters analyzed post-cruise (y-axis). The black regression line shows the expected 1:1 ratio for replicate samples. The red line shows the actual regression between the two sets of samples, indicating that chlorophyll *a* concentration determined shipboard, was on average 19% greater than replicate samples analyzed post-cruise from frozen filters. (For interpretation of the references to color in this figure legend, the reader is referred to the web version of this article.)

water masses were not as great as observed following extensive water column production later in the season.

Systematic differences were observed between chlorophyll *a* measured shipboard and using frozen filters analyzed later (Fig. 4). Chlorophyll *a* concentrations determined shipboard using the Welschmeyer method shortly after sampling were on average $\sim 19\%$ greater than concentrations reported for samples from the same rosette bottles determined in the lab from frozen filters, otherwise using the same methods. This suggests degradation influenced the concentration of chlorophyll stored on frozen filters. Therefore, we used the shipboard chlorophyll determinations in our data analysis. However, further work is needed to assess the relative importance of various sources of chlorophyll degradation on frozen filters measured post-cruise (e.g. time until acetone extraction, storage temperature, etc.).

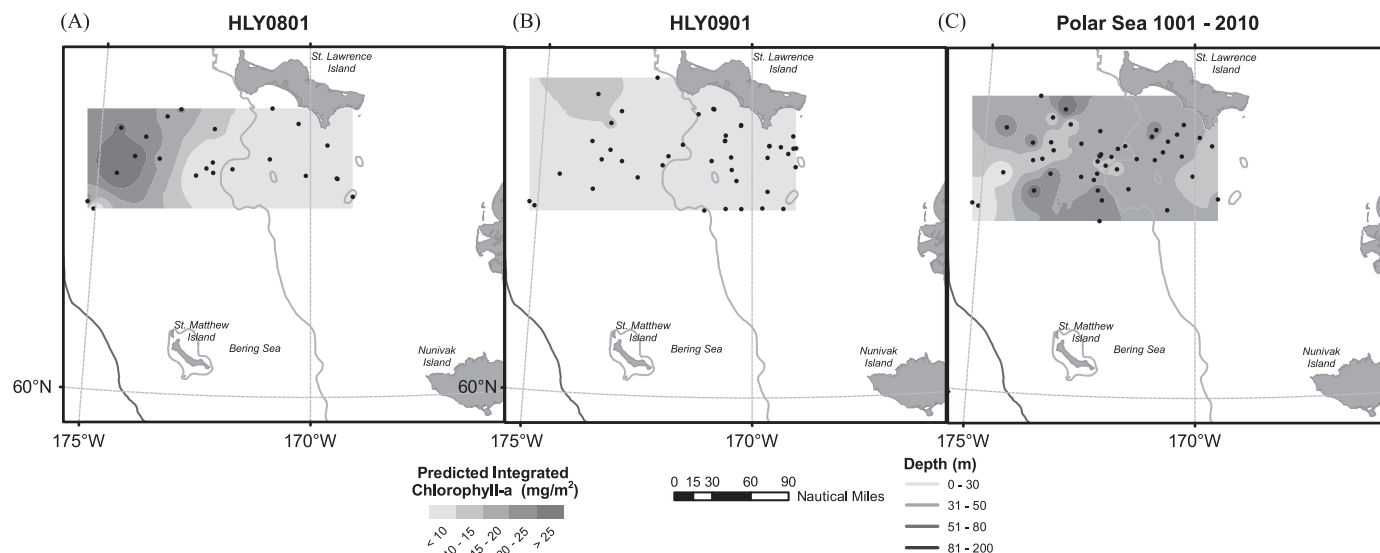


Fig. 5. Integrated chlorophyll *a* inventories (mg m^{-2}) in March 2008 (A), March 2009 (B) and March 2010 (C) south of St. Lawrence Island. The integrated chlorophyll *a* inventories are based on bottle measurements of chlorophyll *a* concentrations at discrete depths, which were summed from surface to seafloor. Symbols correspond to the available data; color gradations are estimated interpolations as in Fig. 1. (For interpretation of the references to color in this figure legend, the reader is referred to the web version of this article.)

Concentrations of chlorophyll *a* in the water column were integrated over the entire water column (Fig. 5). The higher integrated chlorophyll inventories tend to match the nitrate + nitrite bottom water concentrations driven by water mass (Fig. 3), although there was more complexity apparent in 2010 (Fig. 3C). In 2008 and 2009, a decreasing trend in integrated water column chlorophyll *a* was observed from west to east. The maximum integrated chlorophyll values ($\sim 25 \text{ mg chlorophyll } a \text{ m}^{-2}$, or on volume basis: 0.5 mg m^{-3}) are consistent with previous measurements made in this region of the Bering Sea in April 1999 and March 2001 (Clement et al., 2004). However, these concentrations are also as much as two orders of magnitude lower than observations made during the peak of the spring bloom in May–June, with values of up to 1000 mg m^{-2} or more (Cooper et al., 2002, 2012). The sharp contrast in water column concentrations between March–April and May–June is clearly tied to sea ice break-up and rapid development of an ice-associated bloom. This ice edge initiated bloom includes sea ice obligate organisms such as pennate diatoms, but also cryophilic water column phytoplankton such as *Fragilariopsis* spp.

3.2. Sea ice measurements

Ice floe thickness in 2009 and 2010 varied between 42 and 109 cm and snow depth between 2 and 34 cm (Fig. 6A and B). Ice floes in 2009 were significantly ($p < 0.001$, Mann–Whitney U-test) thicker than 2010 and covered with significantly ($p < 0.001$, Mann–Whitney U-test) more snow. In both sea ice (bottom 1-cm) and the water column, algal pigment concentrations (Fig. 6C) were significantly greater in 2010 compared to 2009 ($p < 0.001$, Mann–Whitney U-test), indicating thicker sea ice and snow in 2009 was associated with lower chlorophyll biomass. Overall sea ice chlorophyll concentrations significantly ($p < 0.001$, Mann–Whitney U-test) exceeded phytoplankton values by about three orders of magnitude.

3.3. Sediment trap measurements

The vertical flux of chlorophyll *a* (Fig. 6E) varied between 0.3 and $3.7 \text{ mg chlorophyll } a \text{ m}^{-2} \text{ d}^{-1}$ with a median value of $1.1 \text{ mg chlorophyll } a \text{ m}^{-2} \text{ d}^{-1}$. We did not observe a significant difference between years (Mann–Whitney U-test $p > 0.8$) or

between concentrations in the 5 and 20-m sediment traps (Mann–Whitney U-test, $p > 0.8$). However, the $\delta^{13}\text{C}$ ratio (Fig. 6F) of the sinking material was significantly ($p < 0.05$, Mann–Whitney U-test) more positive in 2010 compared to 2009 with an overall median value of -23.4% . More positive $\delta^{13}\text{C}$ values in 2010 are consistent with greater light conditions under thinner ice and snow, greater photosynthetic rates, and reduced discrimination against ^{13}C during photosynthesis.

Observed export fluxes of chlorophyll *a* are similar in magnitude to observations from other first year ice regions in the Arctic (e.g. Michel et al., 2006) and are also consistent with inventories of chlorophyll in surface sediments during this early season sampling. Chlorophyll *a* extracted from surface sediments ranged from zero to upwards of 20 mg m^{-2} in each of the 3 years of the study (Fig. 7). In May–July, as primary production reaches a peak in the water column, more widely distributed and greater inventories in surface sediments are often observed (Cooper et al., 2002, 2012). Similarity, the order of magnitude of vertical fluxes (median of $1.1 \text{ mg m}^{-2} \text{ d}^{-1}$) observed in the early season sampling compared with the inventory present in surface sediments (up to 20 mg m^{-2}) does not suggest steady-state conditions for deposition of chlorophyll to the surface sediments, but rather slow burial and/or consumption that occurs at a rate slower than sedimentation rates (see also discussion by Grebmeier and Barry, 2007).

3.4. Bottom water ammonium

Additional evidence of active early season biological activity included elevated ammonium concentrations observed in bottom water (Fig. 8) particularly in 2008 and 2009 to the southeast of SLI. Increased ammonium in bottom waters subsequent to spring production has been observed in other portions of the eastern Bering Sea shelf (Mordy et al., 2012; Whitedge et al., 1986). In 2010, this pattern of elevated ammonium in bottom waters southeast of SLI was not observed. However, extended sampling along the 70-m isobath (not sampled in 2008 and 2009) showed relatively high ammonium concentrations in bottom water further to the south and southeast. Areas of high ammonium concentrations were generally not located in mud dominated areas where high oxygen utilization by benthic macrofauna have been observed in the past (Grebmeier et al., 2006), implying the importance of bacterial processes involved

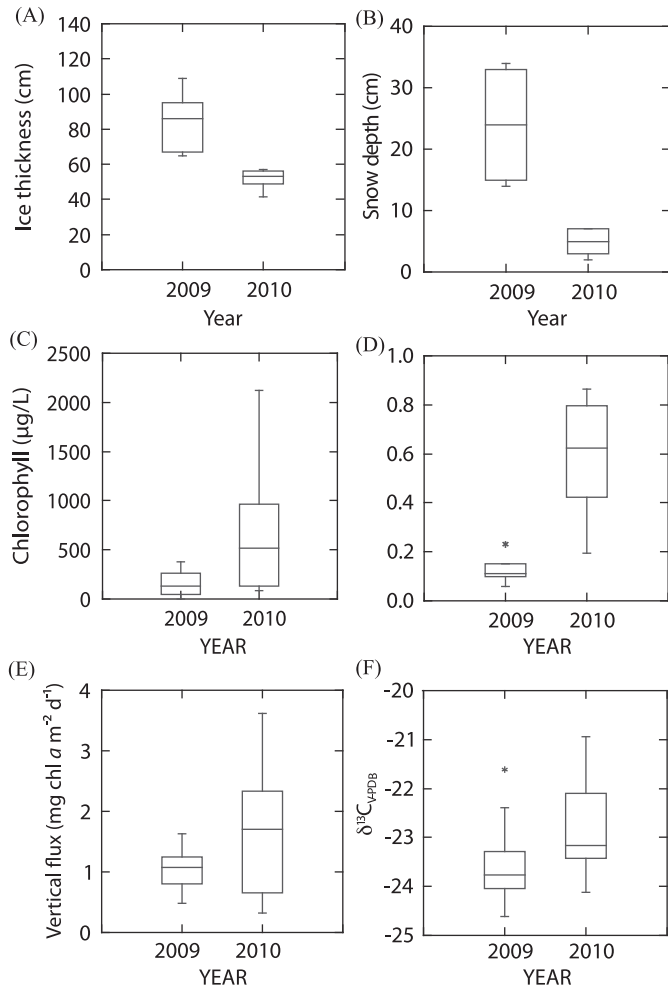


Fig. 6. (A) Sea ice thicknesses in 2009 and 2010 at sampled ice stations; (B) snow thickness on top of sea ice in 2009 and 2010 at sampled ice stations; (C) chlorophyll *a* concentrations in lowest 2 cm of sea ice in 2009 and 2010 at sampled ice stations; (D) chlorophyll *a* concentrations in water column in 2009 and 2010 at sampled ice stations; (E) vertical flux in chlorophyll *a* determined from short-term deployments of sediment traps anchored beneath the ice; (F) carbon isotope composition of organic matter collected in short-term sediment traps.

in regenerating inorganic nitrogen. Greater ammonium bottom water concentrations were also observed to the southeast of SLI where nitrate + nitrite tended to be lower (Fig. 3). Based on the expectations of slow southeastern movement of bottom waters away from SLI during sea ice formation (Danielson et al., 2006, 2011), bottom waters in contact with the sediments immediately south of the SLI may contribute ammonium and potentially regenerated nitrate through nitrification.

3.5. Sedimentation oxygen uptake

The rate of sediment oxygen uptake was as high as 16 mmol O₂ m⁻² d⁻¹, centered on an area of high benthic biomass (described by Grebmeier, 2012; Grebmeier et al., 2006) to the southwest of SLI (Fig. 9). Rates of oxygen uptake rates were much lower than have been observed historically or at other times of year southwest of SLI (25–30 O₂ m⁻² d⁻¹) when there is greater productivity in the water column (Cooper et al., 2012; Grebmeier, 2012; Grebmeier and Cooper, 1995; Grebmeier et al., 2006). The lower oxygen uptake rates we observed during this study are consistent with lower benthic biological activity prior to the peak of the bloom in May–June, but nevertheless indicate significant metabolic activity early in the season.

3.6. Spectacled eider distribution

Over winters 2008–2009, 2009–2010, and 2010–2011, we received 3229 high quality locations from tagged spectacled eiders within the primary wintering area (Fig. 10). Mean water depth at wintering locations was 42±13 m. Nearly all locations received during each winter originated from the primary wintering area, and concurrent aerial surveys and population estimates (approximately 380,000 individuals; W. Larned, personal communication) suggested that nearly the entire population of spectacled eiders winters in this area annually.

Eiders arrived at the wintering area as early as the last week of September and departed no later than the last week of May, constituting a maximum duration of approximately 9 months. Within each winter, we observed a complete spatiotemporal shift in the distribution of eiders. In general, eiders occupied an area approximately 45 km southwest of Southeast Cape on SLI in

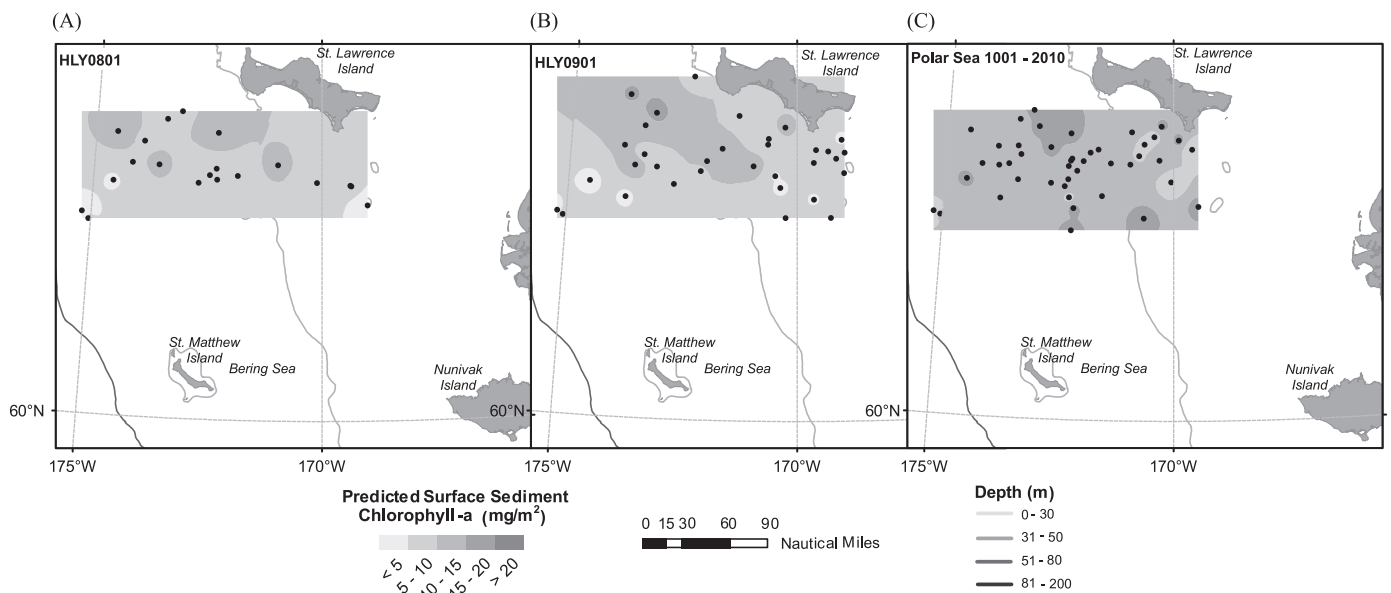


Fig. 7. Chlorophyll *a* inventories (mg m⁻²) in surface (0–1 cm) sediments March 2008 (A), March 2009 (B) and March 2010 (C) south of St. Lawrence Island. Symbols correspond to the available data; color gradations are estimated interpolations as in Fig. 1. (For interpretation of the references to color in this figure legend, the reader is referred to the web version of this article.)

October–November. In December, eiders shifted to an area approximately 70 km to the west-southwest where most remained through April (Figs. 11A and 12A). The reasons for this shift are not understood; sea ice had not developed potentially forcing eiders to move, and benthic resources were likely not exhausted in the area used in early winter. However, the latter area is well matched with the greatest biomass of benthic bivalves (Grebmeier, 2012; Grebmeier et al., 2006), and among spectaclered eiders collected in this area in 2001, almost 100% of esophageal contents were bivalve *Nuculana radiata* (Lovvorn et al., 2003).

Pair-wise percent overlap of 50% kernel isopleths between winters 2008 and 2009, 2009 and 2010, and 2010 and 2011 ranged from 16.9% to 58.5%, indicating interannual use of similar core wintering areas (Fig. 11A). Pair-wise percent overlap of 95% kernel isopleths ranged from 65.7% to 77.4%, indicating eiders generally used the same primary wintering area in all years (Fig. 12B). Within each winter, the distribution and location of eiders appeared to respond to sea ice concentration. Eider locations were

more concentrated during periods of greater ice density. However, additional analysis is needed to quantify eider movement in response to the density and movement of ice.

Percent overlap of 50% and 95% kernel isopleths between winters 1993–1997 and 2008–2011 was 21.7% and 44.8%, respectively, indicating eiders generally used the same areas during each period (Fig. 12A and B). The 50% isopleth representing the distribution of eiders in December–April in 2008–2011 was approximately 50 km northeast of the distribution in 1993–1997, suggesting a possible shift in the late winter distribution of spectaclered eiders in recent years. However, substantial differences in the number and quality of locations received during each period introduce considerable uncertainty to comparison between sampling periods.

Based on the previous models of foraging energetics, the average abundance of the preferred bivalve *Nuculana radiata* must exceed 90 m^{-2} for spectaclered eiders to maintain positive energy balance throughout winter (Lovvorn et al., 2009). Near the site where eiders were collected on 19 March 2001, adequate prey

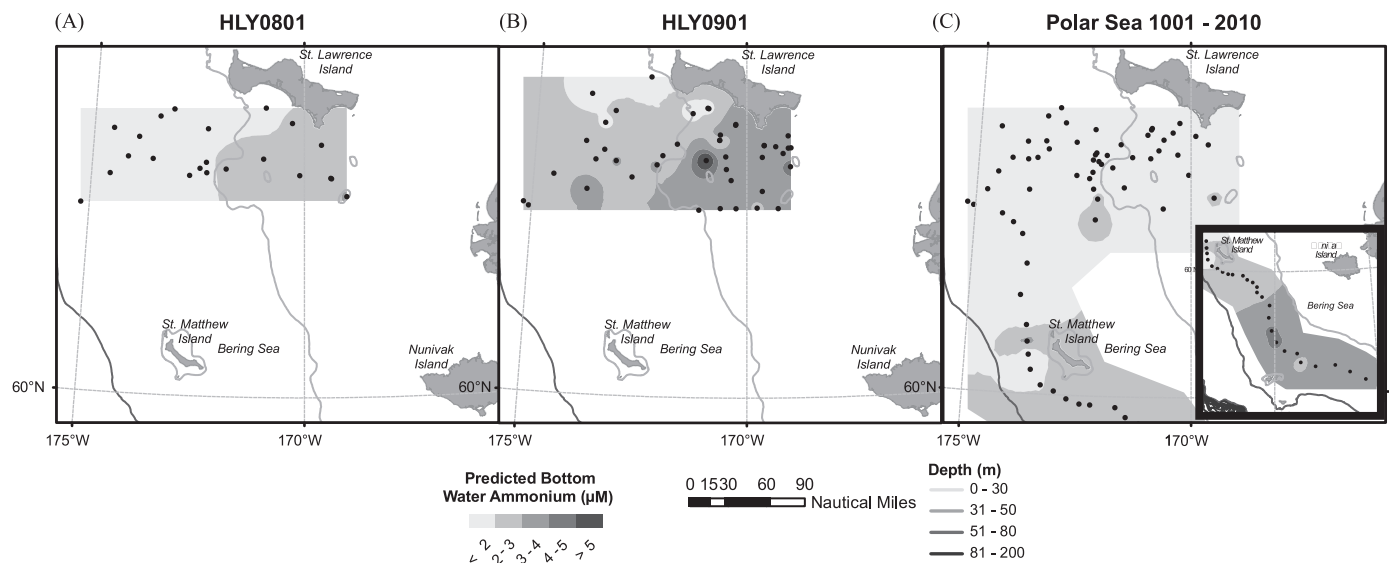


Fig. 8. Bottom water ammonium in March 2008 (A), March 2009 (B) and March 2010 (C) south of St. Lawrence Island. Symbols correspond to the available data; color gradations are estimated (predicted) interpolations and are estimated interpolations as in Fig. 1. (For interpretation of the references to color in this figure legend, the reader is referred to the web version of this article.)

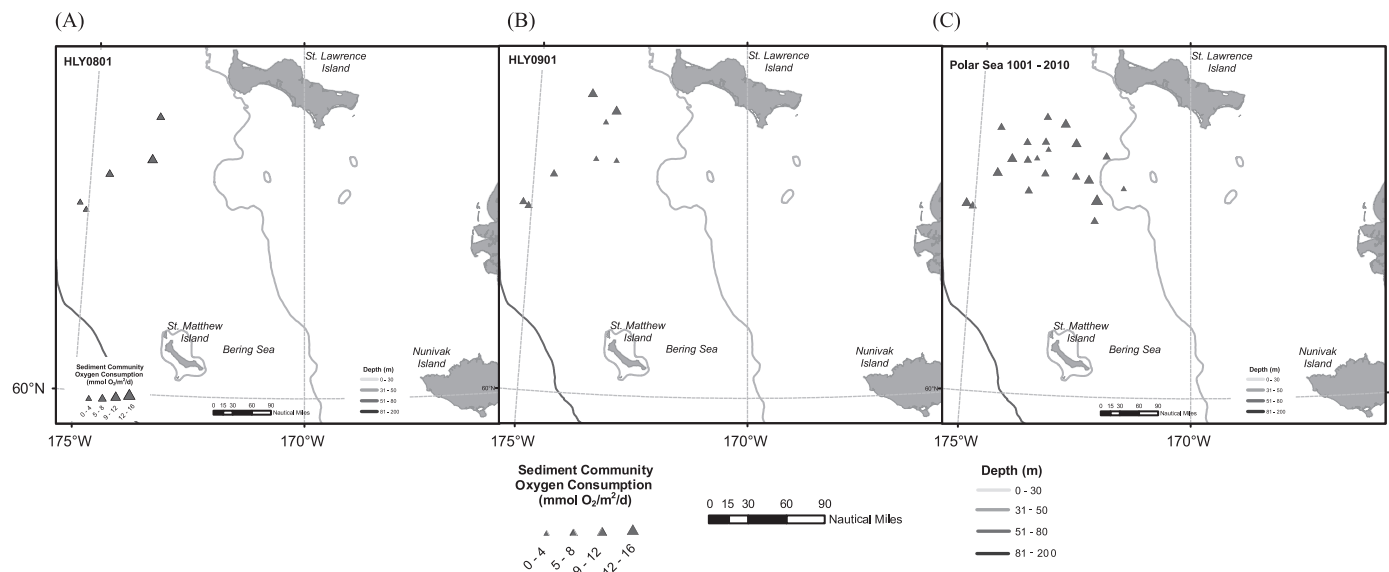


Fig. 9. Sediment oxygen consumption as measured in duplicate 133 cm^2 cores incubated shipboard for 12–24 h in March 2008 (A), March 2009 (B), and March 2010 (C). Symbols correspond to the available data; because of relatively limited sampling, no color interpolations are shown.

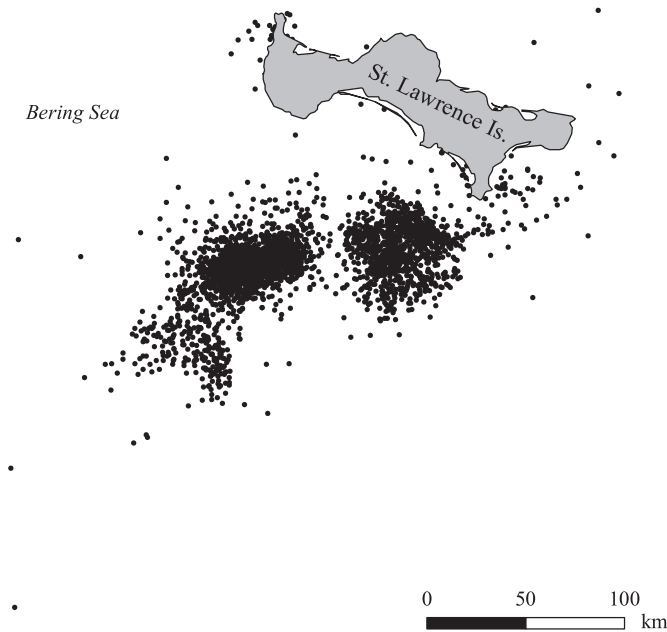


Fig. 10. Spectaclered eider satellite telemetry locations ($n=3229$) received from the primary wintering area in the Bering Sea south of St. Lawrence Island, Alaska, in September–May in 2008–2009, 2009–2010, and 2010–2011.

densities were distributed mostly in a large contiguous region with many openings in the ice that allowed eiders access to those prey (Fig. 13). In contrast, areas with sufficient prey densities in 2009 were more scattered and covered with mostly continuous ice with few openings. Visual observations during helicopter surveys from 14 to 22 March 2009 revealed very few leads in the region where eiders had been collected on 19–22 March 2001. Near the collection site in 2009, leads were few, small, and contained very high densities of eiders, i.e., numbers of birds per spatial area of open-water. Further analyses revealed that severe ice conditions in 2009 had prevailed for most of winter. While benthic biomass and productivity in the northern Bering Sea are very well documented (e.g. Grebmeier, 2012; Grebmeier et al., 2006), our assessment of the interaction between eiders and benthic sources of prey should be treated with caution until benthic samples collected contemporaneously with the eider telemetry data (2009–2010) are fully analyzed (Grebmeier and Cooper, unpublished data). The major complexity is that while the distribution and overall biomass of the clam prey base are established, the size distribution varies annually, and spectacled eiders have specific size preferences (Lovvorn et al., 2003).

The fat content of spectacled eiders collected in late March was 33–35% lower in 2009 (Lovvorn, unpublished data) than in 2001, likely as a result of conditions in 2009 that were not encountered in 2001 namely thicker and more extensive ice that limited access to benthic foods. Female spectacled eiders lay eggs soon after arrival on

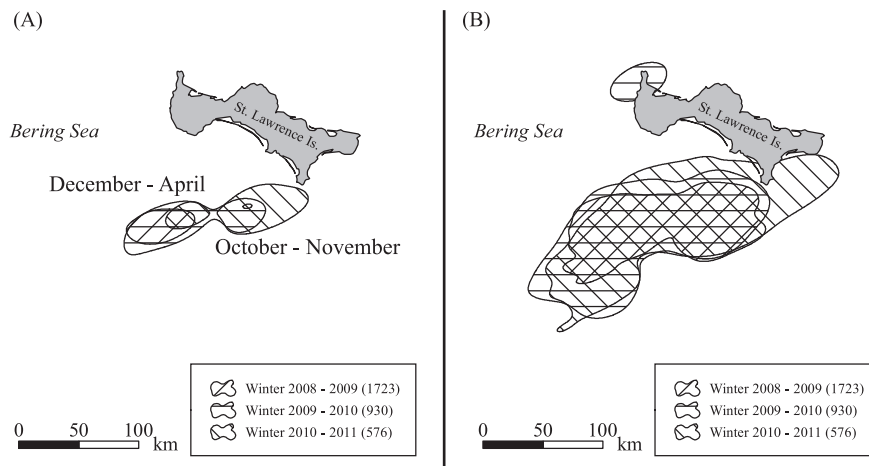


Fig. 11. Fifty percent (A) and 95% (B) kernel isopleths representing the distributional density of spectaclered eider locations in the primary wintering area in the Bering Sea south of St. Lawrence Island, Alaska, in September–May in 2008–2009, 2009–2010, and 2010–2011. Samples sizes used to calculate each isopleth are in parentheses.

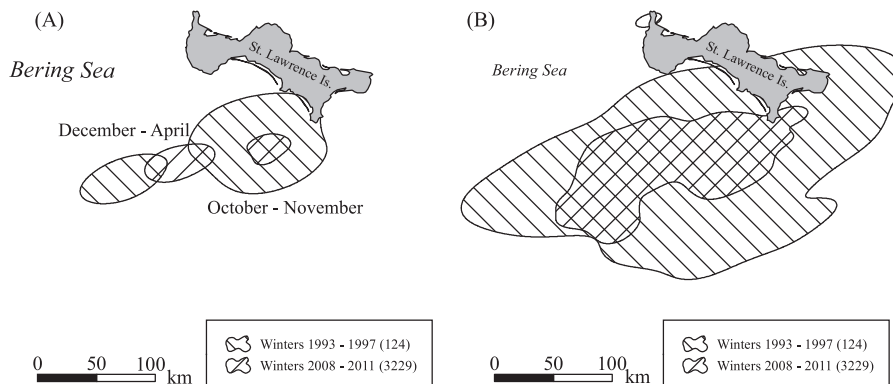


Fig. 12. Fifty percent (A) and 95% (B) kernel isopleths representing the distributional density of spectaclered eider locations in the primary wintering area in the Bering Sea south of St. Lawrence Island, Alaska, in winters 1993–1997 and 2008–2011. Samples sizes used to calculate each isopleth are in parentheses.

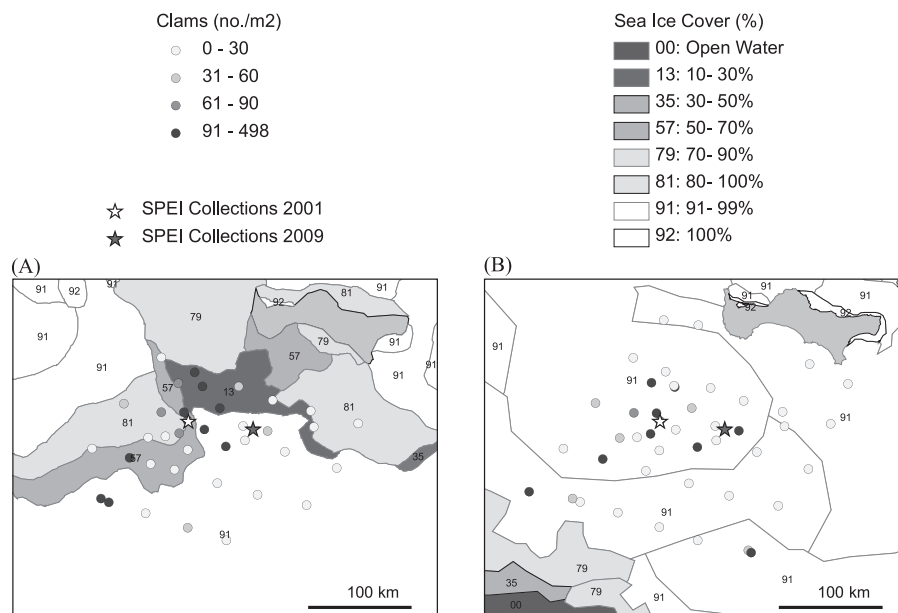


Fig. 13. Densities (number/m²) of the primary prey of spectacled eiders (the bivalve *Nuculana radiata*) at sampling stations in (A) March–April 2001 and (B) May–June 2006, and the dispersion of percent ice cover on 2 March in (A) 2001 and (B) 2009, south of St. Lawrence Island in the Bering Sea. Collection sites for spectacled eiders on 19–22 March in 2001 (white stars) and 2009 (red stars) are shown. (For interpretation of the references to color in this figure legend, the reader is referred to the web version of this article.)

breeding areas in coastal Alaska and Russia, so females must carry enough stored nutrients to produce all eggs and accommodate loss of about 500 g of body mass by the end of incubation (Lovvorn et al., 2003; Petersen et al., 2000). Therefore, breeding propensity and/or success likely depend on stored reserves before arrival (Coulson, 1984; Oosterhuis and Van Dijk, 2002). However, prey densities on migration routes to some breeding sites appear to be quite low compared to the wintering area (Feder et al., 1994; Lovvorn et al., 2009). Our observations in 2009 suggested that when wintering sites with adequate prey densities are covered with dense sea ice, spectacled eiders may have difficulty achieving sufficient reserves before spring migration and breeding.

The movement of nutrient rich water through the northern Bering Sea, the rate of deposition of chlorophyll to northern Bering Sea sediments, and mixing throughout the water column suggests an abundance of nutrient and planktonic resources for benthic bivalves, thereby supporting locally high densities of prey for eiders and other apex predators. However, intra-annual movement of eiders within the primary wintering area in response to sea ice concentration and flow suggested that in some winters ice may control the distribution of wintering eiders. Furthermore, eiders were observed roosting on the surface of sea ice adjacent to water during aerial surveys, suggesting that sea ice might also play a positive role in the winter ecology of the species. However, the ecology of spectacled eiders in the northern Bering Sea remains poorly understood. Unknown aspects include the frequency of foraging bouts, and the relative importance of sea ice as a barrier to food or as a platform for resting or heat conservation out of water.

4. Conclusions

Observations of hydrographic and biological conditions in March 2008, 2009, and 2010 indicated that the northern Bering Sea is biologically active during the late winter–early spring transition in part due to the presence of significant populations of apex predators, including almost the entire world population of

spectacled eiders. Chlorophyll stocks in the water column however are relatively low, and fluxes are less on an areal basis than surface sediment inventories, suggesting seasonal accumulation of organic matter on the sea floor despite significant metabolic activity (e.g. oxygen respiration) in the sediments. Chlorophyll is concentrated on the bottom of the sea ice, and high nutrient concentrations throughout the water column and up to the surface sustain growth of these sea ice algal communities. West-to-east decreases in salinity, nutrients and water-column chlorophyll readily apparent in the open water season (e.g. Walsh et al., 1989) are muted at this time because biological production has not reached high enough levels to significantly impact inorganic nutrient or chlorophyll concentrations. Salinity variation is more influenced by brine injection than water mass differences, which is corroborated by the stable oxygen isotope data from surface waters. We also observed distributions of the stable isotope ¹⁸O that suggest potential use of the isotope as a tracer of new ice production in polynyas.

Finally, we were able to document the interannual distribution of spectacled eiders within these waters, which are clearly important for this species due to the high concentrations of benthic foods. Aggregations of spectacled eiders were associated with open leads and high benthic food resources. However, eiders were forced into presumably less productive waters when sea ice precluded use of areas with greater benthic biomass. Therefore, the balance between food availability and abiotic variables, such as sea ice extent and lead formation, is a likely important controlling factor for eiders and other apex predators in the northern Bering Sea. In years of heavy ice cover, the spatiotemporal distribution of spectacled eiders within the primary wintering area appears to be controlled by the formation and movement of sea ice, in addition to sources of food as determined by biological productivity.

Acknowledgments

The field sampling would not have been possible without strong support from the commanding officers, crew and officers

of both the USCGC *Healy* on the 2008 and 2009 cruises, and during the apparently final science mission of the USCGC *Polar Sea* in 2010. Shipboard support for water column collections and data management was provided by Steve Roberts, Tom Bolmer, Matt Durham, Ben Gire, Sigrid Salo, Peter Proctor, Mark Bradford, John Allison, and Scott Hiller. Also at sea, we thank Markus Janout, Boris Sirenko, Craig Casemod, Deanna Wheeler, Rebecca Neumann, Sarah Story, Joe Bump, Perry Pungowiyi, Gay Sheffield, Marisa Guarinello, Regan Simpson, Krista Hoff, Maria Ceballos, Linton Beaven, Cynthia Yeung, Laura Gemery, Nathalie Morata, Jared Weems, Brenna McConnell, Marjorie Brooks, Steve Fenske, Dawn Sechler, Martin Schuster, and Edward Davis for their help in collecting the data presented here. Alynne Bayard and Ariel Rowan provided GIS expertise with drafting some of the figures and Dana Biasatti made the oxygen isotope determinations. We thank two anonymous reviewers and guest editor Mike Lomas for their efforts in reviewing earlier versions of the manuscript. Financial support was provided in part by the North Pacific Research Board. The Office of Polar Programs of the National Science Foundation also supported this work, through ARC-0732767 to RG, ARC-0732430 to CM, and ARC-082290 to L.C. and J.G. The spectacled eider telemetry efforts were supported by the Bureau of Ocean Energy Management, the Bureau of Land Management, the National Fish and Wildlife Foundation, the US Fish and Wildlife Service, ConocoPhillips-Alaska, Inc., the Columbus Zoo and Aquarium, the Mesker Park Zoo & Botanic Garden, and the Point Defiance Zoo & Aquarium. Use of trade names is for descriptive purposes only and does not imply endorsement by the US Geological Survey or the US Government. This study was also in part funded by the Joint Institute for the Study of the Atmosphere and Ocean (JISAO) under NOAA Cooperative Agreement no. NA17RJ1232. This work is Contribution 3854 to NOAA's Pacific Environmental Laboratory, 2041 to JISAO, EcoFOCI-0786 to NOAA's Fisheries-Oceanography Coordinated Investigations, and Contribution 87 to the BEST-BSERP program.

References

- Arar, E.J., Collins, G.B., 1997. Method 445.0. In Vitro Determination of Chlorophyll *a* and Pheophytin *a* in Marine and Freshwater Algae by Fluorescence, Revision 1.2. National Exposure Research Laboratory Office of Research and Development U.S. Environmental Protection Agency Cincinnati, Cincinnati, OH 45268, p. 22.
- Beyer, H.L., 2012. Geospatial Modelling Environment (Version 0.6.0.0). (software). URL: (<http://www.spatialecology.com/gme>).
- Clement, J.L., Cooper, L.W., Grebmeier, J.M., 2004. Late winter water column and sea ice conditions in the northern Bering Sea. *J. Geophys. Res.* 109, C3, <http://dx.doi.org/10.1029/2003JC002047>, C03022.
- Clement, J.L., Maslowski, W., Cooper, L.W., Grebmeier, J.M., Walczowski, W., 2005. Ocean circulation and exchanges through the northern Bering Sea—1979–2001 model results. *Deep-Sea Res.* II 52, 3509–3540.
- Cooper, L.W., Whitley, T.E., Grebmeier, J.M., Weingartner, T., 1997. The nutrient, salinity, and stable oxygen isotope composition of Bering and Chukchi Seas waters in and near the Bering Strait. *J. Geophys. Res.* 102, 12563–12573.
- Cooper, L.W., Grebmeier, J.M., Larsen, I.L., Dolvin, S., Reed, A.J., 1998. Inventories and distribution of radiocesium in arctic marine sediments: influence of biological and physical processes. *Chem. Ecol.* 15, 27–46.
- Cooper, L.W., Grebmeier, J.M., Larsen, I.L., Egorov, V.G., Theodorakis, C., Kelly, H.P., Lovvorn, J.R., 2002. Seasonal variation in sedimentation of organic materials in the St. Lawrence Island polynya region, Bering Sea. *Mar. Ecol. Prog. Ser.* 226, 13–26.
- Cooper, L.W., Janout, M.A., Frey, K.E., Pirtle-Levy, R., Guarinello, M.L., Grebmeier, J.M., Lovvorn, J.R., 2012. The relationship between sea ice break-up, water mass variation, chlorophyll biomass, and sedimentation in the northern Bering Sea. *Deep Sea Research Part II* 65, 141–162, <http://dx.doi.org/10.1016/j.dsr2.2012.02.002>.
- Coulson, J.C., 1984. The population dynamics of the eider duck *Somateria mollissima* and evidence of extensive non-breeding by adult ducks. *Ibis* 126, 525–543.
- Danielson, S., Aagaard, K., Weingartner, T., Martin, S., Winsor, P., Gawarkiewicz, G., Quadfasel, D., 2006. The St. Lawrence polynya and the Bering shelf circulation: new observations and a model comparison. *J. Geophys. Res.* 111, C09023.
- Danielson, S., Eisner, L., Weingartner, T., Aagaard, K., 2011. Thermal and haline variability over the central Bering Sea shelf: Seasonal and interannual perspectives. *Conti. Shelf Res* 31 (6), 539–554.
- Douglas, D., 2010. The Douglas Argos-Filter Algorithm, Version 7.03 (Software). USGS Alaska Science Center. Available at: (<http://alaska.usgs.gov/science/biology/spatial/douglas.html>).
- Ely, C.R., Dau, C.P., Babcock, C.A., 1994. Decline in a Population of Spectacled Eiders Nesting on the Yukon-Kuskokwim Delta, Alaska. *Northwestern Naturalist* 75 (3), 81–87.
- ESRI, 2010. ArcGIS Desktop: Release 10 (Software). Environmental Systems Research Institute, Redlands, CA.
- Feder, H.M., Foster, N.R., Jewett, S.C., Weingartner, T.J., Baxter, R., 1994. Mollusks in the northeastern Chukchi Sea. *Arctic* 47, 145–163.
- Gordon, L., Jennings, J., Ross, A., Krest, J., 1994. A Suggested Protocol for Continuous Flow Analysis of Seawater Nutrients (Phosphate, Nitrate, Nitrite, and Silicic Acid) in the WOCE Hydrographic Program and the Joint Global Ocean Fluxes Study. WHP Office Report.
- Gradinger, R., Meiners, K., Plumley, G., Zhang, Q., Bluhm, B.A., 2005. Abundance and composition of the sea-ice meiofauna in off-shore pack ice of the Beaufort Gyre in summer 2002 and 2003. *Polar Biol.* 28, 171–181.
- Grebmeier, J.M., 2012. Biological community shifts in Pacific Arctic and sub-Arctic seas. *Ann. Rev. Mar. Sci.* 4, 63–78 [10.1146/annurev-marine-120710-100926](http://dx.doi.org/10.1146/annurev-marine-120710-100926).
- Grebmeier, J.M., McRoy, C.P., 1989. Pelagic-benthic coupling on the shelf of the northern Bering and Chukchi Seas. III. Benthic food supply and carbon cycling. *Mar. Ecol.: Prog. Ser.* 53, 79–91.
- Grebmeier, J.M., Cooper, L.W., 1995. Influence of the St. Lawrence Island Polynya upon the Bering Sea Benthos. *J. Geophys. Res.* 100, 4439–4460.
- Grebmeier, J.M., Cooper, L.W., Feder, H.M., Sirenko, B.I., 2006. Ecosystem dynamics of the Pacific influenced Northern Bering and Chukchi Seas. *Prog. Oceanogr.* 71, 331–361.
- Grebmeier, J.M., Barry, J.P., 2007. Benthic processes in polynyas. In: W.O. Smith, Jr., D.G. Barber (Eds.), *Polynyas: Windows to the World*, Elsevier Oceanography Series, vol. 74, pp. 363–390.
- Kannevorff, E., Nicolaisen, W., 1973. The “HAPS”: a frame supported bottom corer. *Ophelia Supplement* 10, 119–129.
- Kinder, T.H., Coachman, L.K., Galt, J.A., 1975. The Bering slope current system. *J. Phys. Oceanogr.* 5, 231–244.
- Korschgen, C.E., Kenow, K.P., Gendron-Fitzpatrick, A., Green, W.L., Dein, F.J., 1996. Implanting intra-abdominal radiotransmitters with external whip antennas in ducks. *J. Wildl. Manage.* 60, 132–137.
- Lovvorn, J.R., Richman, S.E., Grebmeier, J.M., Cooper, L.W., 2003. Diet and body condition of spectacled eiders wintering in pack ice of the Bering Sea. *Polar Biol.* 26, 259–267.
- Lovvorn, J.R., Grebmeier, J.M., Cooper, L.W., Bump, J.K., Richman, S.E., 2009. Modeling marine protected areas for threatened eiders in a climatically changing Bering Sea. *Ecol. Appl.* 19, 1596–1613.
- Macdonald, R.W., McLaughlin, F.A., Wong, C.S., 1986. The storage of reactive silicate samples by freezing. *Limnol. Oceanogr.* 31, 1139–1142.
- Michel, C., Ingram, R.G., Harris, L.R., 2006. Variability in oceanographic and ecological processes in the Canadian Arctic Archipelago. *Prog. Oceanogr.* 71, 379–401.
- Mordy, C.W., Cokelet, E.D., Ladd, C., Menzia, F.A., Proctor, P., Stabeno, P.J., Wisegarver, E., 2012. Net community production on the middle shelf of the eastern Bering Sea. *Deep-Sea Res.* II 65–70, 110–125.
- Mulcahy, D.M., Esler, D., 1999. Surgical and immediate postrelease mortality of Harlequin Ducks implanted with abdominal radio transmitters with percutaneous antennae. *J. Zoo Wildlife Med.* 30, 397–401.
- Oosterhuis, R., Van Dijk, K., 2002. Effect of food shortage on the reproductive output of common eiders *Somateria mollissima* breeding at Griend (Wadden Sea). *Atlantic Seabirds* 4, 29–38.
- Petersen, M.R., Larned, W.W., Douglas, D.C., 1999. At-sea distribution of Spectacled Eiders: a 120-year-old mystery resolved. *Auk* 116, 1009–1020.
- Petersen, M.R., Grand, J.B., Dau, C.P., 2000. Spectacled eider (*Somateria fischeri*). In: Poole, A., Gill, F. (Eds.), *The Birds of North America*, No. 547. The Birds of North America, Inc., Philadelphia, PA.
- Pirtle-Levy, R., Grebmeier, J.M., Cooper, L.W., Larsen, I.L., 2009. Seasonal variation of chlorophyll *a* in Arctic sediments implies long persistence of plant pigments. *Deep-Sea Res.* II 56, 1326–1338.
- Stehn, R.A., Dau, C.P., Conant, R., Butler Jr., W.I., 1993. Decline of spectacled eiders nesting in western Alaska. *Arctic* 46, 264–277.
- US Fish and Wildlife Service, 1993. Final rule to list the spectacled eider as threatened. *Federal Register* 58, 27374–27480.
- U.S. Fish and Wildlife Service, 2001. Endangered and threatened wildlife and plants; final determination of critical habitat for the spectacled eider. *Federal Register* 66, 9146–9185.
- Wang, J., Hu, H., Mizobata, K., Saitoh, S., 2009. Seasonal variations of sea ice and ocean circulation in the Bering Sea: a model-data fusion study. *J. Geophys. Res.* 114, C02011.
- Walsh, J.J., McRoy, C.P., Coachman, L.K., Goering, J.J., Nihoul, J.J., Whitley, T.E., Blackburn, T.H., Parker, P.L., Wirick, C.D., Shuert, P.G., Grebmeier, J.M., Springer, A.M., Tripp, R.D., Hansell, D.A., Djenidi, S., Deleersnijder, E., Henriksen, K., Lund, B.A., Andersen, P., Müller-Karger, F.E., Dean, K., 1989. Carbon and nitrogen cycling within the Bering/Chukchi Seas: source regions for organic matter effecting AOU demands of the Arctic Ocean. *Prog. Oceanogr.* 22, 277–359.
- Welschmeyer, N.A., 1994. Fluorometric analysis of chlorophyll *a* in the presence of chlorophyll *b* and pheopigments. *Limnol. Oceanogr.* 39, 1985–1992.
- Whitley, T.E., Reeburgh, W.S., Walsh, J.J., 1986. Seasonal inorganic nitrogen distributions and dynamics in the southeastern Bering Sea. *Conti. Shelf Res.* 5, 109–132.



Interannual changes in the zooplankton community structure on the southeastern Bering Sea shelf during summers of 1994–2009



Rie Ohashi^a, Atsushi Yamaguchi^{a,*}, Kohei Matsuno^a, Rui Saito^a, Nao Yamada^b,
Anai Iijima^c, Naonobu Shiga^d, Ichiro Imai^a

^a Graduate School of Fisheries Sciences, Hokkaido University, 3-1-1 Minato, Hakodate, Hokkaido 041-8611, Japan

^b Hokkaido Hakodate Fisheries High School, 2-15-3 Nanaehama, Hokuto, Hokkaido 049-0111, Japan

^c Donan Research Branch, Salmon and Freshwater Fisheries Research Institute, Hokkaido Research Organization, 189-43 Kumaishi Ayukawacho, Yakumocho, Futami, Hokkaido 043-0402, Japan

^d Hakodate Junior College, 52-1 Takaokacho, Hakodate, Hokkaido 042-0955, Japan

ARTICLE INFO

Available online 15 March 2013

Keywords:

Annual variations
Abundance
Biomass
Zooplankton
Community composition
Species diversity

ABSTRACT

On the southeastern Bering Sea shelf, mesozooplankton plays an important role in material transfer between primary producers and fisheries resources. The biomass of mesozooplankton in this region is known to vary annually, but little is known about annual changes in community structure and species composition. In the present study, regional and long-term changes in abundance, biomass and community structure of copepods and chaetognaths on the shelf were evaluated based on NORPAC net samples collected during summers of 1994–2009. During the study period, regime shifts occurred from high interannual variability regime (1994–1999) to low interannual variability regime with high temperature (2000–2005), then to a low interannual variability regime with low temperature (2007–2009). A total of 24 calanoid copepod species belonging to 21 genera were identified from samples. Copepod abundance ranged from 150 to 834,486 inds. m⁻², was greatest on the Middle shelf, and was higher in cold years, than in warm years. Copepod biomass ranged from 0.013 to 150 g DM m⁻², and was also higher in cold years than in warm years. Based on the results of cluster analysis, the copepod community was divided into six groups (A–F). The regional and interannual distributions of each group were distinct. Interannual changes in abundance of the dominant copepod on the Outer shelf and Middle shelf were highly significant ($p < 0.0001$), and their abundances were negatively correlated with temperature and salinity. Interannual changes in copepod community that occurred between cold and warm years are thought to have been caused by differences in the magnitude and timing of the spring phytoplankton bloom between the two regimes. Abundance and biomass of the chaetognath *Parasagitta elegans* ranged from 30 to 15,180 inds. m⁻² and from 11 to 1559 mg DM m⁻², respectively. Chaetognath abundance was significantly correlated with the abundance of the dominant copepods ($p < 0.0001$). Differences in cold and warm years may also affect recruitment of walleye pollock. We conclude that on the southeastern Bering Sea shelf, the magnitude and timing of primary production, which is related to climate change, may significantly affect how it is transferred through the food web.

© 2013 Elsevier Ltd. All rights reserved.

1. Introduction

The southeastern Bering Sea shelf is characterized by high biological productivity, has large amounts of phytoplankton, zooplankton, benthos, fishes, seabirds and marine mammals, and is an important fishing ground of walleye pollock (*Theragra chalcogramma*) (Springer, 1992; Springer et al., 1996). Recently, this region has undergone large biological/environmental changes (Jin et al., 2009; Stabeno et al., 2010). In 1997, a coccolithophore (*Emiliania huxleyi*) bloom was observed (Napp and Hunt, 2001;

Stockwell et al., 2001; Sukhanova and Flint, 1998), and mass mortality of short-tailed shearwaters (*Puffinus tenuirostris*) occurred near the Pribilof Islands (Baduini et al., 2001). In 1998, a climate regime shift was reported (McFarlane et al., 2000), and the biomass of the jellyfish *Chrysaora melanaster* was observed to peak (Brodeur et al., 2008). To describe the effect of climate regime shifts on lower to higher trophic levels, Hunt et al. (2002) proposed the Oscillation Control Hypothesis (OCH). In 2006, a climate regime shift from a warm period to cold period was reported, and the OCH was revised based on observations during this period (Hunt et al., 2011).

In the Bering Sea ecosystem, mesozooplankton are important because they connect primary production to higher trophic level production. In the mesozooplankton fauna of this region, the

* Corresponding author. Tel.: +81 138 40 5543; fax: +81 138 40 5542.

E-mail address: a-yama@fish.hokudai.ac.jp (A. Yamaguchi).

dominant taxon is Copepoda, and various studies have been conducted on their biology and ecology. They include studies of seasonal variations of community structure during spring and summer (Smith and Vidal, 1986), interannual variations in their total wet-weight biomass (Hunt et al., 2008; Napp et al., 2002; Sugimoto and Tadokoro, 1997, 1998), seasonal and spatial variations in community structure (Kang et al., 2006), and the effects of El Niño and La Niña on biomass and production (Coyle and Pinchuk, 2002). However, most studies of long-term variations in mesozooplankton have treated only wet-weight biomass data without examining the species caught or separating sub-regions or domains. In studies of species and zooplankton community structure, the study areas have been narrow, and the study periods have been short. Consequently, information on long-term changes in mesozooplankton community and their species composition is extremely scarce.

The second most abundant taxonomic group in the Bering Sea mesozooplankton biomass is chaetognaths (Coyle and Pinchuk, 2002). They are carnivores, prey upon small zooplankton and fish larvae, contribute to vertical fluxes to deep water (Brodeur and Terazaki, 1999), and sometimes account for nearly 50% of the prey of walleye pollock larvae (Brodeur and Wilson, 1996). Thus, chaetognaths are important because of their role linking lower to higher trophic levels. However, little is known about their long-term variation in the Bering Sea.

In the present study, regional and long-term changes in abundance, biomass and community structure of copepods and chaetognaths are evaluated based on samples collected over the southeastern Bering Sea shelf during the summers of 1994–2009. Long-term data on copepods and chaetognaths are compared with hydrographic data, and we discuss possible mechanisms controlling interannual variations in mesozooplankton community structures and species composition.

Table 1

Calanoid copepod species collected in the southeastern Bering Sea during summers of 1994–2009. Major region of occurrence is also shown for each species. •: Large oceanic copepods that have a diapause phase in deep layer (Miller et al., 1984). Region abbreviations are: I: Inner shelf, M: Middle shelf, O: Outer shelf, S: Slope and B: Basin. *: Rare species (occurred only < 2% of the whole stations) omitted from data for cluster analysis (cf. Fig. 4).

Species	Major region of occurrence
<i>Acartia longiremis</i> (Lilljeborg, 1853)	I, M, O
<i>A. tumida</i> Willey, 1920	M, O
* <i>Aetideopsis rostrata</i> Sars, 1903	B
* <i>Aetideus pacificus</i> Brodsky, 1950	B
<i>Calanus</i> spp.	M, O, S, B
<i>Candacia columbiae</i> Campbell, 1929	S, B
<i>Centropages abdominalis</i> Sato, 1913	I, M
<i>Epilabidocera amphitrites</i> (McMurrich, 1916)	I
* <i>Eucalanus bungii</i> Giesbrecht, 1892	O, S, B
<i>Eurytemora herdmanni</i> Thompson and Scott, 1897	I
<i>Gaetanus intermedius</i> Wolfenden, 1905	S, B
<i>G. simplex</i> Brodsky, 1950	S, B
<i>Heterorhabdus tanneri</i> (Giesbrecht, 1895)	S, B
<i>Metridia pacifica</i> Brodsky, 1950	O, S, B
<i>Microcalanus pygmaeus</i> (Sars, 1900)	M, O
* <i>Neocalanus cristatus</i> (Krøyer, 1848)	O, S, B
* <i>N. flemingeri</i> Miller, 1988	O, S, B
* <i>N. plumchrus</i> (Marukawa, 1921)	O, S, B
<i>Paraeuchaeta elongata</i> (Esterly, 1913)	B
<i>Pleuromamma scutullata</i> Brodsky, 1950	S, B
<i>Pseudocalanus</i> spp.	I, M, O, S, B
* <i>Racovitzanus antarcticus</i> Giesbrecht, 1902	B
<i>Scolecithricella minor</i> (Brady, 1883)	O, S, B
* <i>S. ovata</i> (Farran, 1905)	B
<i>Tortanus discaudatus</i> (Thompson and Scott, 1897)	I
<i>Undinopsis pacificus</i> Brodsky, 1950	O, S

2. Material and methods

2.1. Field sampling

Sampling was conducted over the southeastern Bering Sea shelf during 1994–2009 between 24 June and 8 August on board the T/S Oshoro-Maru of the Faculty of Fisheries, Hokkaido University. For each year, samples were collected within a two week period. Zooplankton samples were collected by vertical hauls of flowmeter-equipped NORPAC nets (45 cm mouth diameter, 0.335 mm mesh; Motoda, 1957) from 150 m depth or near the bottom (where the depth was shallower than 150 m) to the surface. Zooplankton samples were immediately preserved with 5% formaldehyde-seawater buffered with sodium tetraborate. In addition, temperature and salinity were measured with a CTD (Neil Brown, Mark IIIB during 1994–2001 and Seabird SBE-911plus during 2002–2009). Water samples from the CTD rosette were filtered through GF/F filters, extracted with acetone or DMF and chlorophyll *a* concentration was measured using a fluorometer (Turner Designs, Inc.).

The number of sampling stations in any one year was 9–49 (total=96), and the total number of samples was 428 (Fig. 1). Based on the bottom depth, the southeastern Bering Sea shelf was divided into three regions: Inner shelf (< 50 m), Middle shelf (50–100 m) and Outer shelf (100–200 m) (Coachman and Charnell, 1979; Coachman, 1986). Areas with depth of 200–1000 m and > 1000 m were classified as Slope and Basin, respectively. Six stations on the Outer shelf and six on the Middle shelf were sampled every year of the study (Fig. 1), so only the data from these twelve stations were used to analyze long-term changes.

2.2. Sample analysis

Based on the biomass of the samples, subsamples were created with a Motoda plankton splitter (Motoda, 1959), and the subsamples were examined under a stereomicroscope.

Copepods were staged and identified to the lowest possible taxonomic level. For copepods, the most important genus in this region (*Calanus*) is reported to be mixture of *Calanus glacialis* and *Calanus marshallae* (Nelson et al., 2009). We could not distinguish

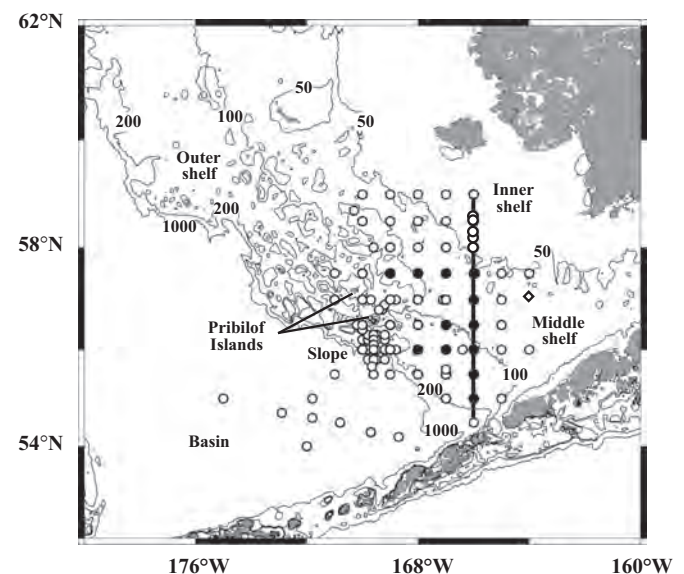


Fig. 1. Location of the sampling stations in the southeastern Bering Sea during the summers of 1994–2009 (circles). Solid symbols denote stations where sampling was conducted in all years from 1994–2009, providing the data used for annual comparisons. Line indicates 166°W transect where the hydrographic data were analyzed (cf. Fig. 2).

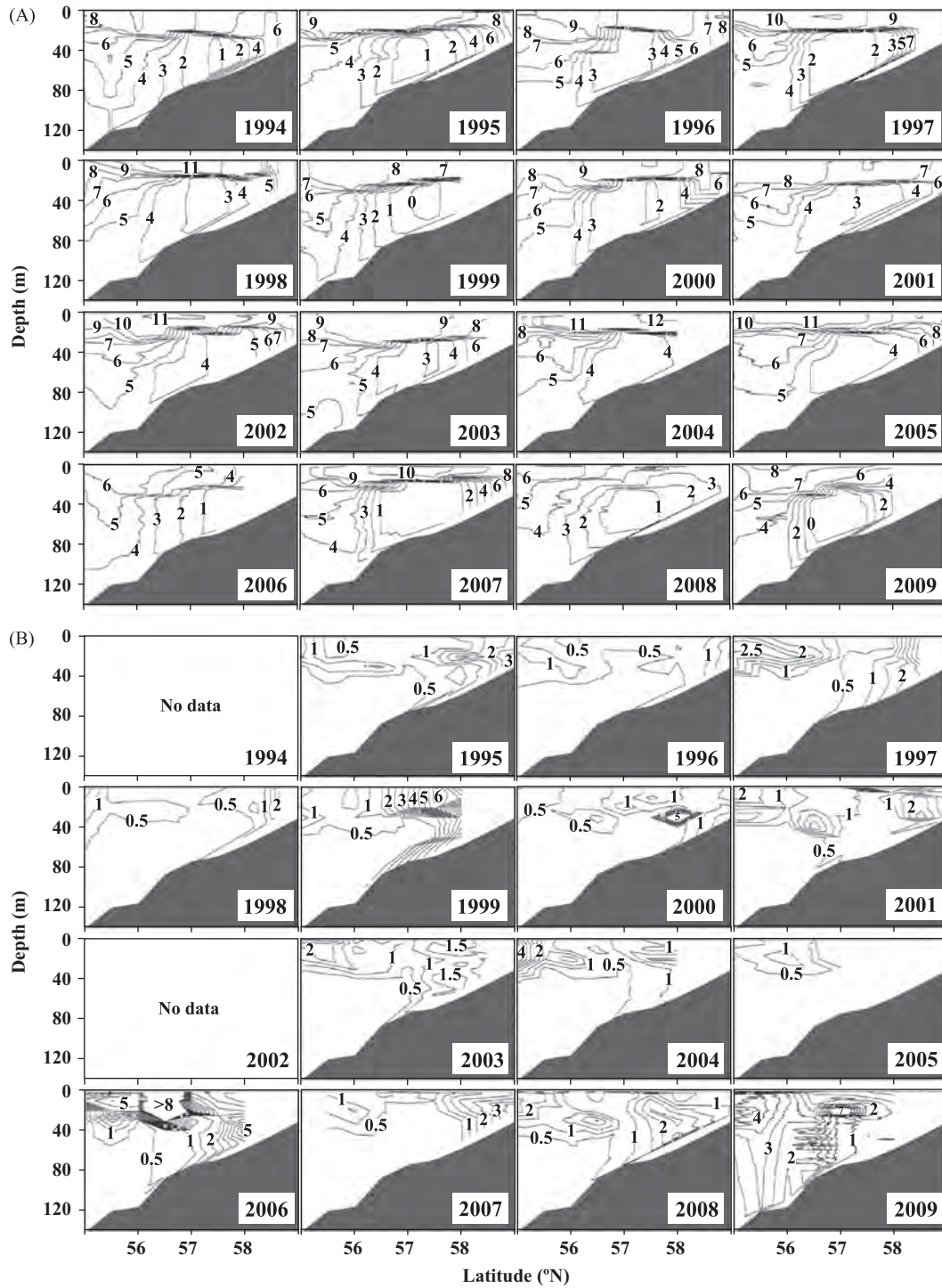


Fig. 2. (A) Temperature and (B) chlorophyll *a* stations along 166°W during summers of 1994–2009.

the two species and treated them as “*Calanus* spp.”. For biomass estimation, copepods were separated into four groups: *Calanus* spp., *Neocalanus* spp., *Eucalanus bungii* and other copepods. One hundred individuals in each group were chosen randomly for measurement of total lengths (TL, μm) by ocular micrometer. Dry mass (DM, μg) was estimated using the following equations derived for organisms from the Oyashio region (Imao, 2005):

$$\text{Calanus and Neocalanus spp. (less lipids)} \\ \log_{10} \text{ DM} = 2.48 \log_{10} \text{ TL} - 6.00 \quad (1)$$

$$\text{Calanus and Neocalanus spp. (more lipids)} \\ \log_{10} \text{ DM} = 3.00 \log_{10} \text{ TL} - 7.70 \quad (2)$$

$$E. \text{ bungii} \quad \log_{10} \text{ DM} = 3.16 \log_{10} \text{ TL} - 9.16 \quad (3)$$

$$\text{Other copepods} \quad \log_{10} \text{ DM} = 2.62 \log_{10} \text{ TL} - 6.40 \quad (4)$$

For *Calanus* spp. and *Neocalanus* spp., lipid accumulation was separated into two: less lipids (<20% of prosome volume) and more lipids ($\geq 20\%$ of prosome volume). Then Eqs. (1) and (2) were applied for less and more lipid specimens, respectively. The total

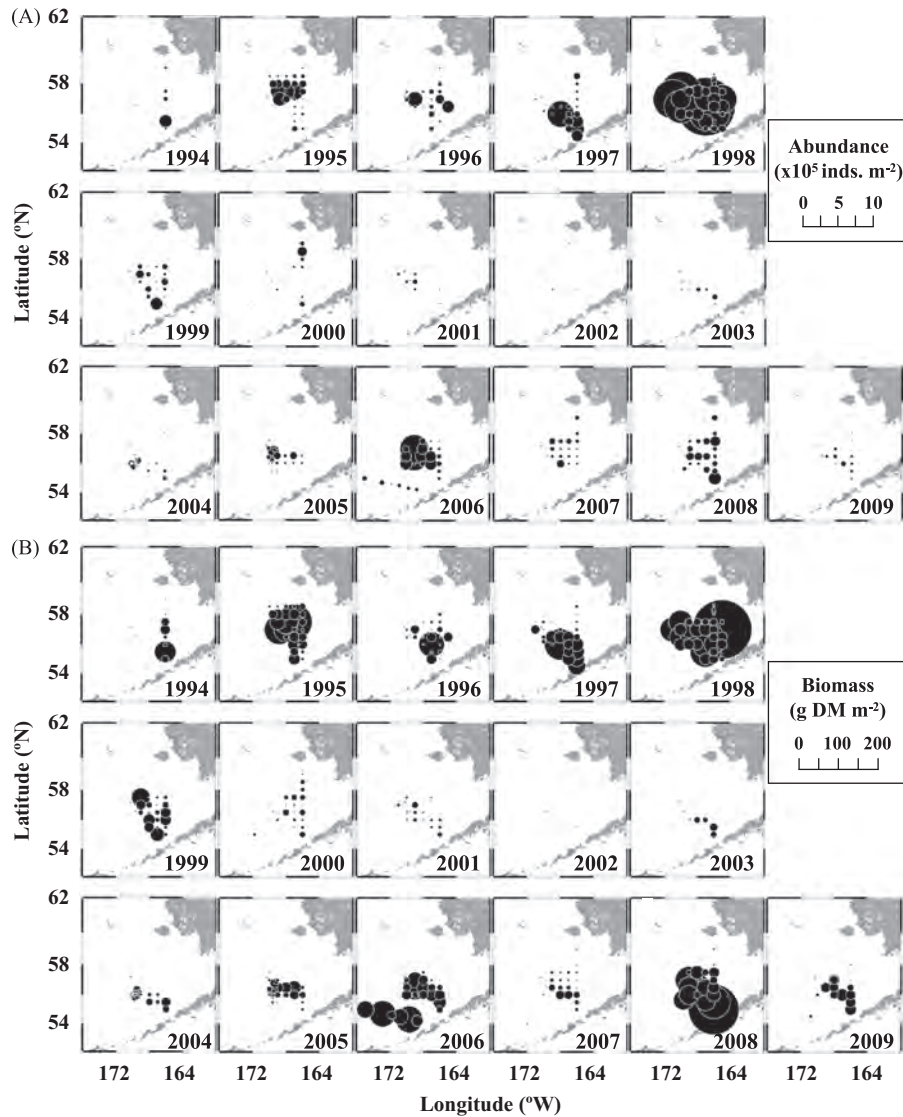


Fig. 3. Regional variations in (A) copepod abundance and (B) biomass in the southeastern Bering Sea during summers of 1994–2009.

biomass of copepods (mg DM m^{-2}) was estimated by multiplying the average individual mass (mg DM inds.^{-1}) by the abundance (inds. m^{-2}).

Chaetognaths were identified to species based on the samples collected during 1996–2009. The total length (TL, mm) of the dominant chaetognath, *P. elegans*, was measured using a ruler for large individuals ($\text{TL} \geq 10$ mm) and an ocular micrometer for small specimens ($\text{TL} < 10$ mm). Specimens were classified according to McLaren (1969), Sameoto (1973) and Zo (1973): Stage I (juveniles), Stage II (immature) and Stage III (mature). To estimate DM, ash-free dry mass (AFDM, mg) was estimated from the TL using the following equation (Mumm, 1991):

$$\text{AFDM} = 0.0002\text{TL}^{2.6924} \quad (5)$$

Dry mass was estimated as $\text{DM} = \text{AFDM}/0.9$ (Båmstedt, 1986).

2.3. Data analysis

Zooplankton samples were collected day and night. Since the depths of most sampling stations were < 150 m and the sampling was conducted throughout the water column, day–night differences in abundance and biomass were expected to be small. There

were no significant differences between day and night abundance or biomass of copepods and chaetognaths for all years ($p = 0.06$ – 0.93 , *U*-test). Thus, no day–night conversions were done for abundance or biomass.

To examine community structure, we conducted cluster analysis and nonmetric multidimensional scaling (NMDS) ordination. Abundance data (X : inds. m^{-2}) of each species were transformed to $\log_{10}(X+1)$ prior to analysis to reduce the bias of abundant species. Rare species which occurred only $< 2\%$ of the whole stations were eliminated from the data for analysis (cf. Table 1). Similarities between samples were examined by Bray–Curtis index (Bray and Curtis, 1957) according to the differences in species composition. For grouping the samples, the similarity indices were coupled with hierarchical agglomerative clustering with a complete linkage method. The NMDS ordination was carried out to delineate the sample groups on the two-dimensional map. All of these analyses were carried out using BIOSTAT II software (Sigma Soft).

To evaluate environmental factors that may have influenced sample groups determined by cluster analysis, nonmetric multidimensional scaling (NMDS) ordination was carried out to delineate the sample groups in two-dimensional space. We then

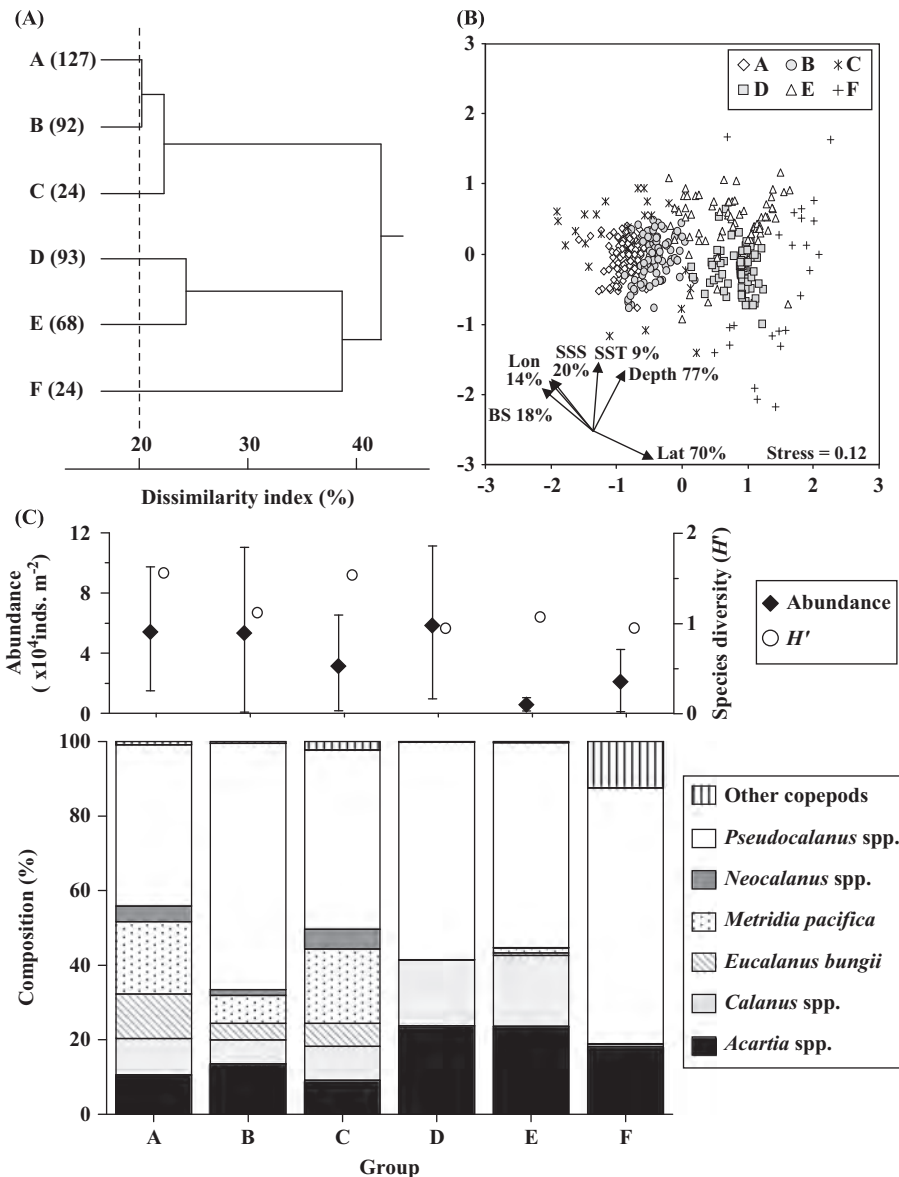


Fig. 4. Copepod assemblages: (A) dendrograms from the cluster analysis based on copepod abundance. Six groups (A–F) were identified with dissimilarity at 20% (dashed line). Numbers in the parentheses indicate quantity of stations included in each group. (B) Nonmetric multidimensional scaling plots of the six groups, with arrows and percentages indicating directions of environmental parameters and coefficient of determinations (r^2), respectively. Lat: latitude, Lon: longitude, SSS: sea surface salinity, SST: sea surface temperature, BS: bottom salinity. (C) Mean abundance with standard deviations and species diversity (H') (upper) and taxonomic composition of each group (lower).

conducted multiple-regression analysis ($Y = aX_1 + bX_2 + c$) with the hydrographic data (Y : latitude, longitude, depth, sea surface and bottom temperature and sea surface and bottom salinity) are the dependent variables and two-dimensional NMDS as independent variables (thus, axis 1 as X_1 and axis 2 as X_2) (a , b , c are fitted constants). Shannon's diversity index (H') in each group was calculated using the equation:

$$H' = -\sum n_i/N \times \ln n_i/N \quad (6)$$

where n_i is the abundance (inds. m^{-2}) of the i th species, and N is the total copepod abundance (inds. m^{-2}) in the group (Shannon and Weaver, 1949).

To evaluate factors affecting the variability of copepod abundance, two-way ANOVA with year and station as independent variables was used. To determine which factors controlled annual changes in copepod abundance, correlation analysis was done between the abundance of dominant copepods and three factors: water

temperature (throughout whole water column, in upper layer and in lower layer), salinity and chlorophyll a (whole water column).

For *P. elegans*, cohort analysis was done based on the TL histogram data from the Middle shelf using Microsoft Excel Solver (Aizawa and Takiguchi, 1999).

To evaluate what factors controlled the interannual changes in chaetognath abundance, we tested for correlations between the chaetognath abundance for the Outer shelf and Middle shelf and four factors: water temperature (whole water column, upper and lower layer), salinity (whole water column), chlorophyll a (whole water column) and abundance of the dominant copepods.

3. Results

3.1. Hydrography

In all years, a thermocline was present 20–30 m, and the bottom temperature of Middle shelf ranged between 0 and 4 °C, but was

higher for the Inner and Outer shelves (Fig. 2A). The Middle shelf, bottom temperature was about 4°C during 2001–2005, and lower (0–3 °C) during 2007–2009. Owing to Stabeno et al. (2012), there were three regimes in depth-averaged ocean temperature: cold; 1995, 1997, 1999, 2007–2009, average; 1996, 2000, 2006, and warm; 1998, 2001–2005. Our results confirmed this pattern (Fig. 2A).

The peak of summer chlorophyll *a* at each station varied between 0.5 and 25.4 mg m⁻³, and chlorophyll *a* was high above the thermocline and on the Inner shelf (Fig. 2B). The peak of chlorophyll *a* was low (ca. 1 mg m⁻³) during the warm regime (2001–2005).

3.2. Copepods

Regional and interannual changes in total copepod abundance and biomass were observed (Fig. 3). Copepod abundance ranged from 150 to 834,486 inds. m⁻², and was greatest on the Middle shelf (Fig. 3A). Copepod abundance was high during cold years (1995, 1997, 1999 and 2007–2009), and low in warm years (2001–2005) (Fig. 3A). Copepod biomass ranged from 0.013 to 150 g DM m⁻², and was highest on the Outer and Middle shelves (Fig. 3B). The biomass peak occurred in more oceanic waters than

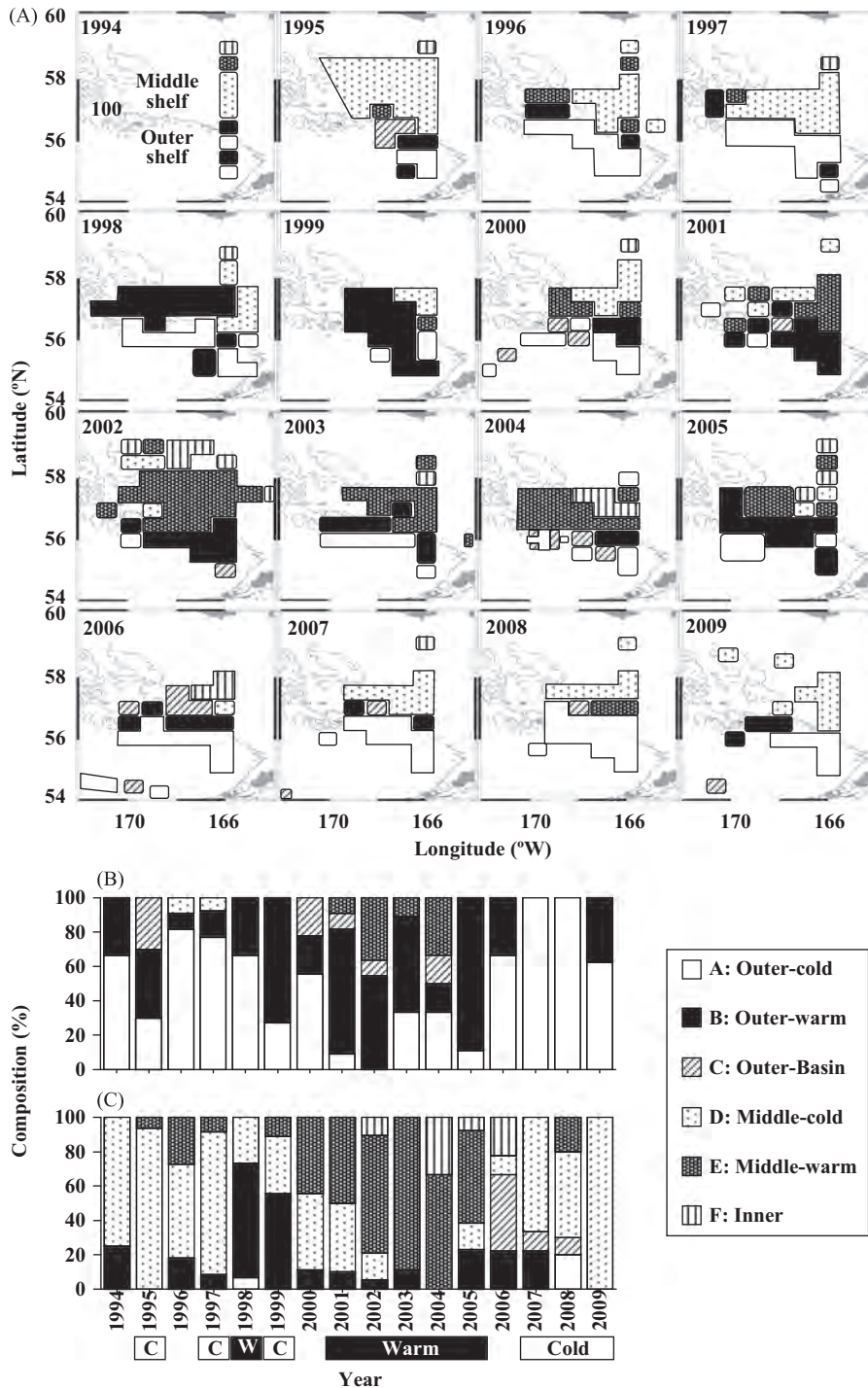


Fig. 5. (A) Spatial and temporal distribution of six copepod communities identified from Bray–Curtis dissimilarity analysis. Annual distribution of groups on the (B) Outer shelf and (C) Middle shelf.

the abundance peak due to the dominance of large-sized oceanic copepods. Copepod biomass and abundance were both high in cold years and low in warm years.

Throughout the study period, 24 calanoid copepod species from 21 genera were identified (Table 1). *Pseudocalanus* spp. was the most numerous, and *Calanus* spp. was dominated the copepod biomass. Large-sized oceanic copepods that diapause at depth (i.e., *E. bungii*, *Metridia pacifica*, *Neocalanus cristatus*, *Neocalanus flemingeri* and *Neocalanus plumchrus*) were collected on the Outer shelf, on the Slope and in the Basin (Table 1).

Based on abundance of each species, cluster analysis divided the copepod community into six groups (A–F). The groups contained 24–127 stations (Fig. 4A). From multiple-regression analysis, environmental factors that were significantly related with the group separation were latitude, longitude, depth, sea surface temperature, sea surface salinity and bottom salinity. The most important factors were latitude and depth; they determined 70–77% of the variability of the copepod community (Fig. 4B). Mean copepod abundance was highest in group D and lowest in group E (Fig. 4C). Species diversity was higher in groups A and C ($H' = 1.6$) than in groups B, D, E and F ($H' = 1.0$ – 1.1). These group-specific differences in species diversity were caused by their species composition. For groups A–C, *Pseudocalanus* spp. and large, oceanic

copepods (*M. pacifica*, *E. bungii*, *Neocalanus* spp.) were abundant (Fig. 4C). For groups D and E, species diversity was lower, and the species compositions were similar; they were comprised of *Pseudocalanus* spp. (55–58%), *Acartia* spp. (24%) and *Calanus* spp. (18–19%). In group F, the proportion of *Calanus* spp. decreased, and the main species were *Pseudocalanus* spp. (69%), and *Acartia* spp. (18%). Endemic species, such as *Epilabidocera amphitrites*, *Eurytemora herdmani* and *Tortanus discaudatus*, were also observed (Fig. 4C, Table 1).

The regional and interannual distributions of each group were clearly separated (Fig. 5A). Composition of group A was greater in cold years (1995, 1997, 1999 and 2007–2009) on the Outer shelf, and that of group B was greater in warm years (1998, 2001–2005) on the Outer shelf, and group C was seen mainly on the Outer shelf and in the Basin, but also on the Middle shelf in 2006–2008 (Fig. 5B). Group D was mainly observed in cold years on the Middle shelf, group E was seen in warm years on the Middle shelf, and group F was centered on the Inner shelf (Fig. 5A).

Two-way analysis of variance (ANOVA) on annual and geographical differences in abundance of the dominant copepods showed significant interannual changes for *Acartia* spp., *M. pacifica* and *Neocalanus* spp. on the Outer shelf (Table 2). Significant station-to-station differences were detected only for *Calanus* spp. on the Middle shelf. All dominant copepods on the Middle shelf (*Acartia* spp., *Calanus* spp. and *Pseudocalanus* spp.) showed highly significant interannual changes in abundance ($p < 0.0001$, Table 2).

Correlation analysis was used to evaluate which environmental parameters were related to the interannual changes in copepod abundance. Abundances of the three dominant copepods on the Middle shelf, which all showed high interannual variability, were strongly negatively correlated with temperature and salinity (Table 3).

Table 2

Variance analysis (two-way ANOVA) on year-to-year and station-to-station differences in abundance (inds. m^{-2}) of dominant copepod taxa on Outer and Middle shelf of the southeastern Bering Sea during summers of 1994–2009.

Domain	Species	F-value df_1, df_2	
		Year _{15,30}	Station _{2,30}
Outer shelf	<i>Acartia</i> spp.	2.136*	1.215 ^{ns}
	<i>Calanus</i> spp.	1.259 ^{ns}	3.027 ^{ns}
	<i>Eucalanus bungii</i>	1.402 ^{ns}	2.610 ^{ns}
	<i>Metridia pacifica</i>	2.060*	1.464 ^{ns}
	<i>Neocalanus</i> spp.	5.228***	1.956 ^{ns}
	<i>Pseudocalanus</i> spp.	1.190 ^{ns}	0.194 ^{ns}
Middle shelf	<i>Acartia</i> spp.	6.574****	2.798 ^{ns}
	<i>Calanus</i> spp.	6.026****	3.745*
	<i>Pseudocalanus</i> spp.	5.791****	0.195 ^{ns}

ns: not significant.

* $p < 0.05$.

*** $p < 0.001$.

**** $p < 0.0001$.

3.3. Chaetognaths

Two chaetognath species (*P. elegans* and *Eukrohnia hamata*) were collected. *P. elegans* dominated the chaetognath fauna, composing 84% of the total chaetognath abundance and 89% of the chaetognath abundance on the Middle shelf. For this reason, *E. hamata* was not included in the subsequent analysis of chaetognaths.

P. elegans abundance ranged from 30 to 15,180 inds. m^{-2} , and was highest on the Middle shelf (Fig. 6A). Abundance was low during 2000–2004 and high during 1996–1999 and 2005–2009. *P. elegans* biomass varied from 11 to 1559 mg DM m^{-2} (Fig. 6B). Biomass was low during 2002–2004 and high during 1996–1999 and 2005–2009. Differences in the timing of the abundance and

Table 3

Correlation coefficients (r) between abundance of dominant copepods and various environmental parameters in the southeastern Bering Sea during summers of 1994–2009.

Domain	Species	Temperature ($n=91$)			Salinity ($n=91$)	Chlorophyll a ($n=45$)
		Whole water column	Upper layer	Lower layer	Whole water column	Whole water column
Outer shelf	<i>Acartia</i> spp.	0.207*	0.149	0.186	–0.140	0.067
	<i>Calanus</i> spp.	–0.423****	–0.101	–0.406****	–0.294**	0.192
	<i>Eucalanus bungii</i>	0.138	–0.143	0.307**	0.517****	0.071
	<i>Metridia pacifica</i>	–0.231*	–0.258*	–0.105	0.076	0.370*
	<i>Neocalanus</i> spp.	–0.285**	–0.404****	–0.108	0.252*	0.369*
	<i>Pseudocalanus</i> spp.	–0.159	–0.142	–0.044	–0.028	0.341*
Middle shelf	<i>Acartia</i> spp.	–0.410****	–0.146	–0.431****	–0.506****	–0.111
	<i>Calanus</i> spp.	–0.448****	–0.340**	–0.457****	–0.407****	–0.126
	<i>Pseudocalanus</i> spp.	–0.567****	–0.292**	–0.539****	–0.484****	–0.037

* $p < 0.05$.

** $p < 0.01$.

*** $p < 0.001$.

**** $p < 0.0001$.

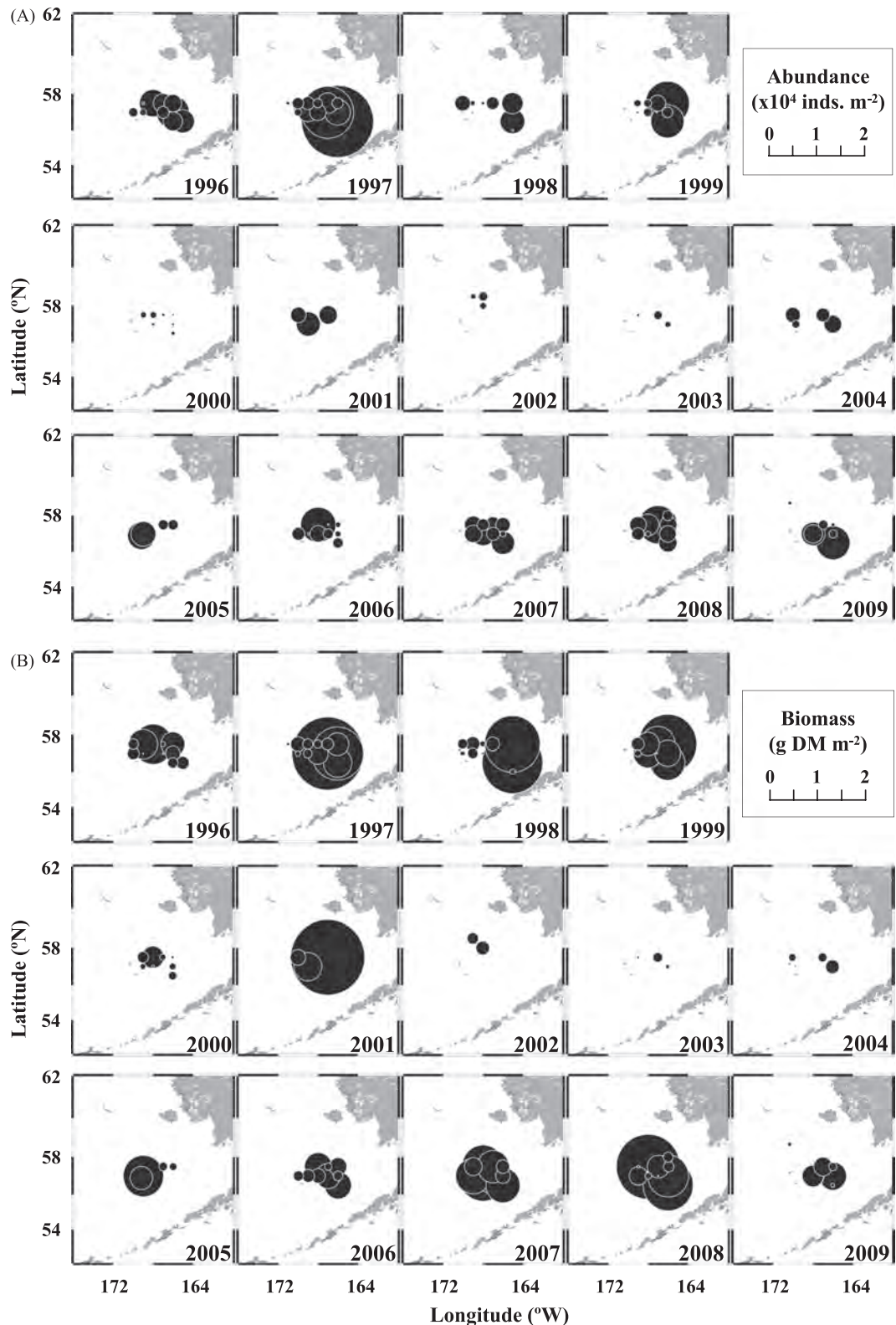


Fig. 6. Regional variations in *Parasagitta elegans*: (A) abundance and (B) biomass during summers of 1996–2009.

biomass peaks might have been caused by interannual changes in *P. elegans* body-size composition.

In every year, *P. elegans* TL composition on the Middle shelf had two or three cohorts (Fig. 7). The small-sized cohort was dominated by Stage I (juveniles), the middle-sized cohort by Stage II (immature), and the large-sized cohort by Stage III (mature)

individuals. Stage III was not observed in 2003 or 2004 (Fig. 7). The average TL of the small-sized cohort (Stage I) was significantly larger (3.5–8.5 mm) during 1996–2005 than those (2.5–5.5 mm) during 2006–2009 (Fig. 7) ($p < 0.05$, *U*-test).

P. elegans abundance on the Outer shelf was positively correlated with dominant copepod abundance (*Acartia* spp., *Calanus*

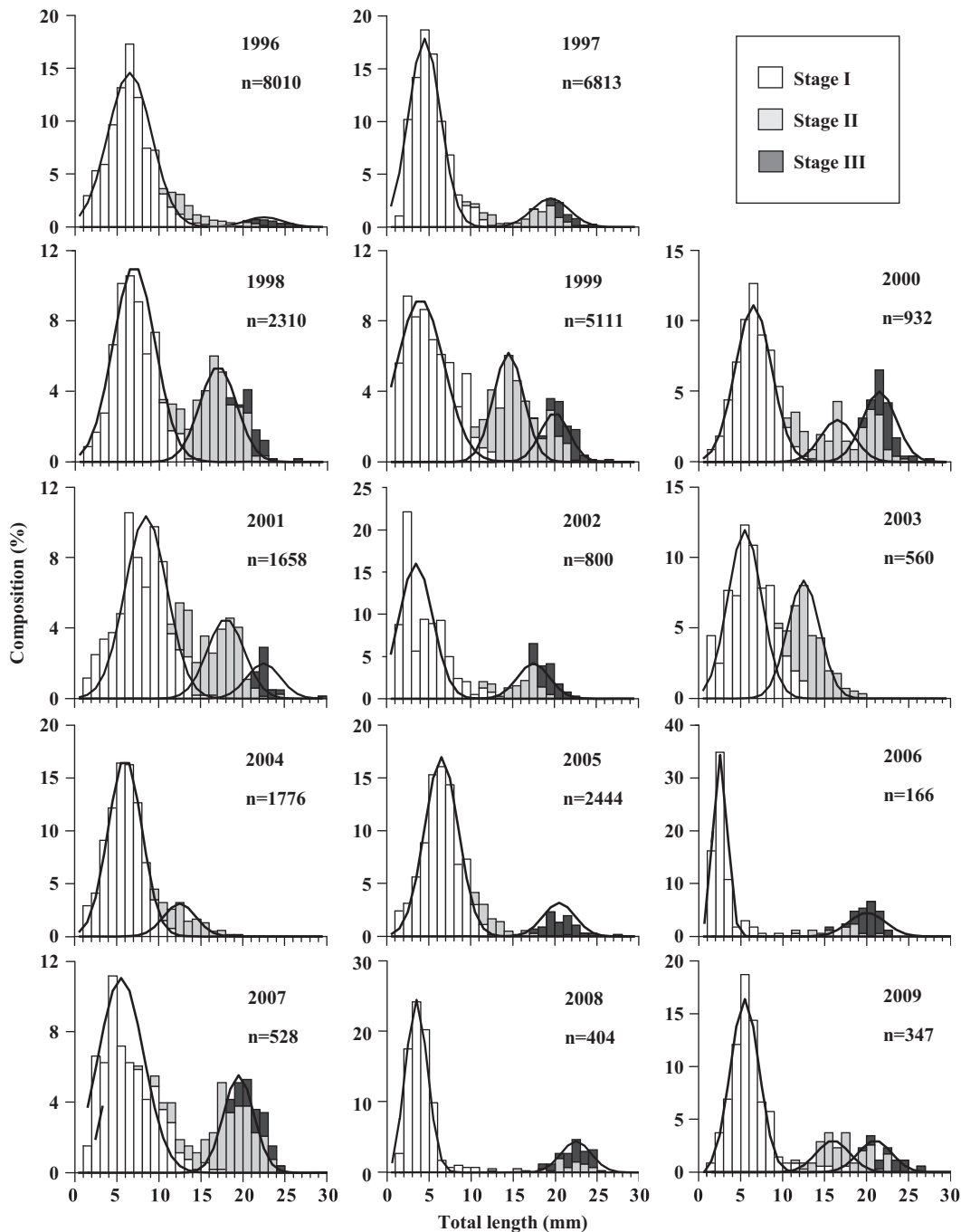


Fig. 7. Annual patterns of *Parasagitta elegans* length frequency on Middle shelf during summers of 1996–2009. *n*: number of measured specimens.

spp. and *Pseudocalanus* spp.), but not with environmental factors (Table 4). On the Middle shelf, *P. elegans* had a highly significant positive correlation with dominant copepod abundance ($p < 0.0001$) and significant negative correlations with temperature and salinity. Thus on the Middle shelf, *P. elegans* abundance was high when temperature and salinity were low, and low when temperature and salinity were high, which is similar to the pattern observed in copepod abundance (Table 4).

4. Discussion

The copepod community on the Bering Sea shelf showed large interannual differences across the shelf (Fig. 5A). The major environmental factors that were related to the copepod

community were latitude and depth (Fig. 4B), and species diversity was highest on the Outer shelf because of the occurrence of the oceanic copepods in addition to the shelf copepods (Fig. 4C). These findings correspond well with the horizontal distribution of copepod community structure reported by Cooney and Coyle (1982). These cross-shelf differences in copepod species may be related to the occurrence of frontal structures (Coachman and Charnell, 1979; Coachman, 1986). The large number of oceanic species on the Middle shelf in 1998 (Fig. 5C) may be caused by the transportation of oceanic copepods by strong cross-shelf advection (Stabeno et al., 2001) (Fig. 1). Stabeno et al. (2012) also reported the transport of oceanic species during warm years.

Long-term changes in zooplankton on the southeastern Bering Sea shelf based upon wet-weight biomass have been reported (Sugimoto and Tadokoro, 1997, 1998; Napp et al., 2002). Recently,

Table 4

Correlation coefficients (r) between abundance of chaetognath *Parasagitta elegans* and various parameters (water temperature, salinity and copepod abundance) on the Outer shelf and Middle shelf in the southeastern Bering Sea during summers of 1996–2009.

Parameters	Outer shelf	Middle shelf
<i>Temperature</i>		
Whole water column	–0.137	–0.519****
Upper layer	–0.057	–0.301**
Lower layer	–0.057	–0.547****
<i>Salinity</i>		
Whole water column	–0.172	–0.513****
<i>Copepods</i>		
<i>Acartia</i> spp.	0.343**	0.563****
<i>Calanus</i> spp.	0.431****	0.503****
<i>Eucalanus bungii</i>	0.129	–
<i>Metridia pacifica</i>	0.195	–
<i>Neocalanus</i> spp.	0.093	–
<i>Pseudocalanus</i> spp.	0.291**	0.566****

–: not applicable.

** $p < 0.01$.

**** $p < 0.0001$.

Hunt et al. (2008) also reported that the zooplankton wet mass was lower in the early 2000s than in the late 1990s. This corresponds with the interannual changes in copepod abundance and biomass observed in the present study (Fig. 3). In the present study, the copepod community greatly varied between cold years (1995, 1997, 1999 and 2007–2009) and warm years (1998, 2001–2005) on both the Outer and Middle shelves. In warm years, oceanic species decreased on the Outer shelf, but showed no change on the Middle shelf, and the abundance of all copepod species drastically decreased on both the Outer and Middle shelf (Fig. 5). Thus, these findings clearly indicate that both the wet mass and copepod community structure showed interannual changes on the southeastern Bering Sea shelf (Fig. 8).

Physical and biological changes have occurred in the southeastern Bering Sea shelf over the last two decades (Fig. 8). During the 1997 El Niño/Southern Oscillation (ENSO) event, there were anomalous atmospheric conditions over the southeastern Bering Sea shelf (Overland et al., 2001), a warm surface layer, a bloom of the coccolithophorid *E. huxleyi* (Sukhanova and Flint, 1998) and mass mortality of short-tailed shearwaters (*P. tenuirostris*) (Baduini et al., 2001). Short-tailed shearwaters prey on large zooplankton, especially adult euphausiids (Hunt et al., 1996), and the starvation of shearwaters that occurred during the summer of 1997 may have been due to low densities of adult euphausiids (Stockwell et al., 2001) or difficulty in finding prey patches due to low water transparency caused by the coccolithophore blooms (Lovvorn et al., 2001). Thus, the mass mortality of short-tailed shearwaters may not have been related with the pattern of mesozooplankton abundance and biomass described in this study.

Coccolithophore (*E. huxleyi*) blooms in recent times were first observed in this region in September 1997 (Vance et al., 1998). Large-scale coccolithophore blooms were also observed in June 1998 and 2000 (Sukhanova and Flint, 1998; Iida et al., 2002, 2008, 2012). As an ecological consequence of coccolithophores, negative effect for short-tailed shearwaters and their nutritional values for copepods should be considered. Information in the literature regarding ingestion of coccolithophores by copepods is contradictory. For example, Huskin et al. (2000) state that *E. huxleyi* is difficult to digest and has low nutritional value, it is not a preferred food item for *Calanus* species. However, Nejtgaard et al. (1997) reported that about 75% of the carbon consumed by *Calanus finmarchicus* during an *E. huxleyi* bloom came from *E. huxleyi* ($> 30 \times 10^6$ cells L^{-1}), and high abundance of *Calanus* spp. was

observed on the Inner shelf during a coccolithophore bloom (Coyle and Pinchuk, 2002). The latter observations suggest that coccolithophore production may have little effect on *Calanus* spp. In fact, years of coccolithophore blooms (1997, 1998 and 2000) did not correspond with years of low copepod abundance or biomass (Fig. 8B). This discrepancy between coccolithophore blooms and copepod abundance could be explained if coccolithophorids are ingested by *Calanus* species (Nejtgaard et al., 1997) and have some nutritional value. As the other possible cause, turbid waters of coccolithophore bloom may provide copepods refuge from visual predators (Lovvorn et al., 2001).

During the study period, there were cold (1995, 1997, 1999, 2007–2010), average (1996, 2000, 2006) and warm years (1998, 2001–2005) (Fig. 2A). During cold and warm years, the timing and magnitude of the spring bloom differ (Stabeno et al., 2001; Hunt et al., 2002, 2011). During cold years, the sea ice remains during the severe winter storms, and ice-edge blooms occur. In warm years, the sea ice melts before the spring storms, and strong wind mixing delays the start of the bloom until stratification occurs when the thermocline develops. From long-term (1960–2005) simulation modeling, Jin et al. (2009) reported that in cold years ($PDO < -1$), phytoplankton blooms start early, last long and are large, while in warm years ($PDO > 1$), they occur later with short pulses and are small. These differences in bloom timing between cold and warm years have also been recorded in mooring observations in this region (Hunt et al., 2011).

Copepod abundance and biomass on both the Outer shelf and Middle shelf were high during cold years (1995, 1997, 1999 and 2007–2009) and low during warm years except 1998 (2001–2005) (Fig. 3, Table 3). The dominant copepod, *Calanus* spp., has an extended spawning period; it starts well before the spring phytoplankton bloom (February) and ends in May; however the survival rate of early developmental stages depends on whether they encounter a phytoplankton bloom or not, and recruitment of copepodid stages increases if they encounter early ice associated blooms, which are highly productive (Baier and Napp, 2003). Low temperatures in cold years may also lead to greater abundance of the small copepods *Pseudocalanus* spp. and *Acartia* spp. especially in the Middle shelf (Table 3). Cold temperature may provide the longer growing season and high primary productivity of ice-edge blooms, sufficient food condition for copepods, resulting in increased abundance of both large and small copepods.

In this study, copepod abundance on both the Outer and Middle shelf was negatively correlated with temperature (Table 3). In contrast, on the Inner shelf, positive correlations were reported between spring temperatures and the abundance of three copepods (*Calanus* spp., *Pseudocalanus* spp. and *Acartia* spp.), and between summer temperatures and two copepods (*Pseudocalanus* spp. and *Acartia* spp.) (Coyle and Pinchuk, 2002). This suggests that the response of copepods to temperature may vary between the Outer-Middle shelf (negative, this study), and the Inner shelf (positive, Coyle and Pinchuk, 2002). In this study, differences between cold and warm years on the Middle shelf were observed in copepod abundance, but not in species composition (groups D and E in Fig. 4C). This is partly because both large and small copepods were abundant in cold years and less abundant in warm years (Table 3). Coyle et al. (2008) compared the summer zooplankton community on the Middle shelf between a cold (1999) and warm year (2004), and reported that the dominant species shifted from large species in the cold year to small species in the warm year. However, this phenomenon was not observed during the 16 years of the present study. Our results showed that both large- and small-sized copepods showed a clear negative correlation with habitat temperature (Table 3).

Similar to copepods, the biomass of the jellyfish *C. melanaster* is high in cold years and low in warm years (Brodeur et al., 2008).

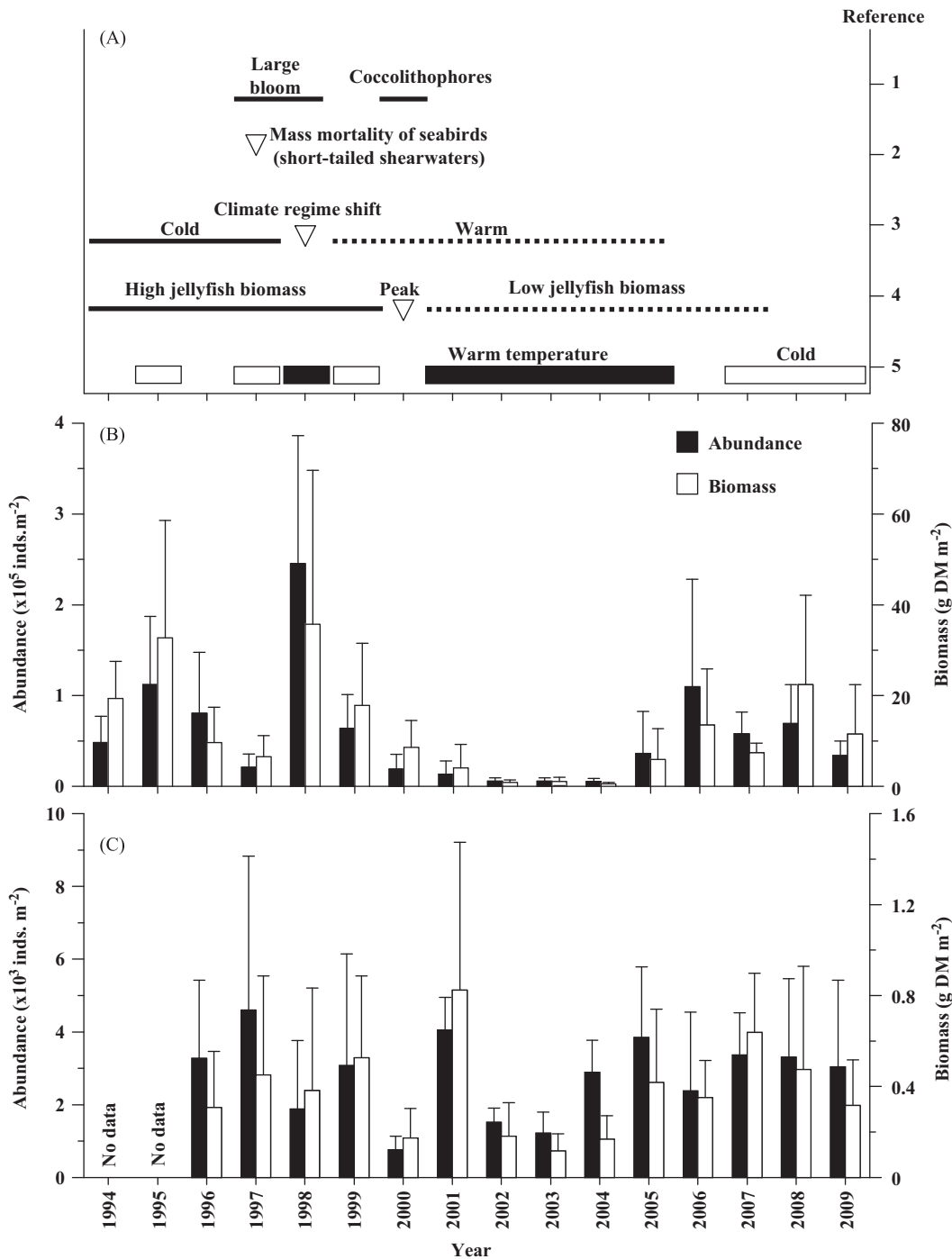


Fig. 8. (A) Annual changes in biological/environmental conditions, (B) copepod abundance and biomass and (C) chaetognath (*Parasagitta elegans*) abundance and biomass on Middle shelf of the southeastern Bering Sea during summers of 1994–2009. Values are means and error bars indicate standard deviations. For references in (A), 1: Sukhanova and Flint (1998), Iida et al. (2002,2008), 2: Baduini et al. (2001), 3: McFarlane et al. (2000), 4: Brodeur et al. (2008), Hunt et al. (2010), 5: Stabeno et al. (2012).

The increase in cold years may be due to improved feeding conditions for polyps (mass sinking of phytoplankton after ice-edge bloom), and subsequent abundant food (copepods) for pelagic medusae may improve survival and growth (Brodeur et al., 2008). In contrast, oceanic blooms in warm years are less productive and provide less food (sinking phytoplankton) for polyps, as well as less food (copepods) for planktonic medusae, resulting in low growth and survival of polyps and medusae.

Interannual changes in chaetognath abundance and biomass were somewhat similar to the changes in copepods (Fig. 8). This may be an example of bottom-up control on predatory

chaetognath abundance by prey (copepods) abundance. Chaetognaths in this region change their food items and size at maturity between cold and warm years; in cold years, they prey on large *Calanus* spp. and mature at large size, while in warm years, they feed on small *Pseudocalanus* spp. and mature at small size (Baier and Terazaki, 2005). The TL of most mature (Stage III) individuals in the present study was > 20 mm in cold years (1997, 1999 and 2007–2009), and < 20 mm in warm years (1998, 2001, 2002 and 2005), and no mature individuals were observed in the warm years 2003 and 2004 (Fig. 7). These facts support the finding of Baier and Terazaki (2005), who reported that sufficient food

conditions in cold years result in a large size at maturity, while food limitation in warm years induces small size at maturity.

For the early life history stages of walleye pollock, an important fisheries resource in this region, food conditions differ between cold and warm years (Napp et al., 2000; Hunt et al., 2011). In cold years, there may be a mismatch between the production of pollock larvae and their prey (Napp et al., 2000), but an early start of the ice-edge bloom and high abundance of lipid-rich prey for age-0 fish (copepods and euphausiids) results in high survival rates and low cannibalism (Hunt et al., 2011). In warm years, the late start of the open-water bloom results in a low abundance of lipid-rich prey for the age-0 pollock and chaetognaths. Under this food-limited condition, growth and survival of walleye pollock juveniles decrease, and the proportion of cannibalism may increase. This results in a decrease in recruitment (Hunt et al., 2011, Heintz et al., 2013). Thus, the timing and magnitude of primary production related with climate change affects production through the entire food web structure on the southeastern Bering Sea shelf.

Acknowledgments

We thank Dr. J.R. Bower of Hokkaido University for his comments on the manuscript. All samples and hydrographic data used in this study were collected by the T/S *Oshoro-Maru*. We are grateful to the captain and crew for their help. Some of the chaetognath data were collected by Mr. N. Hagimoto. This study was supported by Grant-in-Aid for Scientific Research (A) 24248032 and Grant-in-Aid for Scientific Research on Innovative Areas 24110005 from the Japan Society for the Promotion of Science (JSPS).

References

- Aizawa, Y., Takiguchi, N., 1999. Consideration of the methods for estimating the age-composition from the length frequency data with MS-Excel. *Bull. Jpn. Soc. Fish. Oceanogr.* 63, 205–214, in Japanese.
- Baduini, C.L., Hyrenbach, K.D., Coyle, K.O., Pinchuk, A., Mendenhall, V., Hunt Jr., G.L., 2001. Mass mortality of short-tailed shearwaters in the south-eastern Bering Sea during summer 1997. *Fish. Oceanogr.* 10, 117–130.
- Baier, C.T., Napp, J.M., 2003. Climate-induced variability in *Calanus marshallae* populations. *J. Plankton Res.* 25, 771–782.
- Baier, C.T., Terazaki, M., 2005. Interannual variability in a predator-prey interaction: climate, chaetognaths and copepods in the southeastern Bering Sea. *J. Plankton Res.* 27, 1113–1125.
- Båmstedt, U., 1986. Chemical composition and energy content. In: Corner, E.D.S., O'Hara, S.C.M. (Eds.), *The Biological Chemistry of Marine Copepods*. Clarendon Press, Oxford, pp. 1–58.
- Bray, J.R., Curtis, J.T., 1957. An ordination of the upland forest communities of southern Wisconsin. *Ecol. Monogr.* 27, 325–349.
- Brodeur, R.D., Decker, M.B., Ciannelli, L., Purcell, J.E., Bond, N.A., Stabeno, P.J., Acuna, E., Hunt Jr., G.L., 2008. Rise and fall of jellyfish in the eastern Bering Sea in relation to climate regime shifts. *Prog. Oceanogr.* 77, 103–111.
- Brodeur, R.D., Terazaki, M., 1999. Springtime abundance of chaetognaths in the shelf region of the northern Gulf of Alaska, with observations on the vertical distribution and feeding of *Sagitta elegans*. *Fish. Oceanogr.* 8, 93–103.
- Brodeur, R.D., Wilson, M.T., 1996. A review of the distribution, ecology and population dynamics of age-0 walleye pollock in the Gulf of Alaska. *Fish. Oceanogr.* 5, 148–166.
- Coachman, L.K., 1986. Circulation, water masses, and fluxes on the southeastern Bering Sea shelf. *Cont. Shelf Res.* 5, 23–108.
- Coachman, L.K., Charnell, R.L., 1979. On lateral water mass interaction—a case study, Bristol Bay, Alaska. *J. Phys. Oceanogr.* 6, 278–297.
- Cooney, R.T., Coyle, K.O., 1982. Trophic implications of cross-shelf copepod distributions in the southeastern Bering Sea. *Mar. Biol.* 70, 187–196.
- Coyle, K.O., Pinchuk, A.L., 2002. Climate-related differences in zooplankton density and growth on the inner shelf of the southeastern Bering Sea. *Prog. Oceanogr.* 55, 177–194.
- Coyle, K.O., Pinchuk, A.L., Eisner, L.B., Napp, J.M., 2008. Zooplankton species composition, abundance and biomass on the eastern Bering Sea shelf during summer: the potential role of water-column stability and nutrients in structuring the zooplankton community. *Deep-Sea Res.* II 55, 1775–1791.
- Hunt Jr., G.L., Allen, B.M., Angliss, R.P., Baker, T., Bond, N., Buck, G., Byrd, G.V., Coyle, K.O., Devol, A., Eggers, D.M., Eisner, L., Feely, R., Fitzgerald, S., Fritz, L.W., Gritsai, E.V., Ladd, C., Lewis, W., Mathis, J., Mordy, C.W., Mueter, F., Napp, J., Sherr, E., Shull, D., Stabeno, P., Stepanenko, M.A., Strom, S., Whitedge, T.E., 2010. Status and trends of the Bering Sea region, 2003–2008. In: McKinnell, S.M., Dagg, M.J. (Eds.), *Marine Ecosystems of the North Pacific Ocean, 2003–2008*, 4. PICES Special Publication, pp. 196–267.
- Hunt Jr., G.L., Coyle, K.O., Eisner, L.B., Farley, E.V., Heintz, R.A., Mueter, F., Napp, J.F., Overland, J.E., Ressler, P.H., Salo, S., Stabeno, P.J., 2011. Climate impacts on eastern Bering Sea food webs: a synthesis of new data and an assessment of the Oscillating Control Hypothesis. *ICES J. Mar. Sci.* 68, 1230–1243.
- Hunt Jr., G.L., Coyle, K.O., Hoffman, S., Decker, M.B., Flint, E.N., 1996. Foraging ecology of short-tailed shearwaters near the Pribilof Islands, Bering Sea. *Mar. Ecol. Prog. Ser.* 141, 1–11.
- Hunt Jr., G.L., Stabeno, P.J., Strom, S., Napp, J.M., 2008. Patterns of spatial and temporal variation in the marine ecosystem of the southeastern Bering Sea, with special reference to the Pribilof Domain. *Deep-Sea Res.* II 55, 1919–1944.
- Hunt Jr., G.L., Stabeno, P., Walters, G., Sinclair, E., Brodeur, R.D., Napp, J.M., Bond, N.A., 2002. Climate changes and control of the southeastern Bering Sea pelagic ecosystem. *Deep-Sea Res.* II 49, 5821–5853.
- Huskin, I., Anadón, R., Álvarez-Marqués, F., Harris, R.P., 2000. Ingestion, fecal pellet and egg production rates of *Calanus helgolandicus* feeding coccolithophorid versus non-coccolithophorid diets. *J. Exp. Mar. Biol. Ecol.* 248, 239–254.
- Iida, T., Mizobata, K., Saitoh, S.-I., 2008. Temporal and spatial variability of phytoplankton in the Bering Sea—from diatom bloom in spring to coccolithophore bloom in summer and fall. *Kaiyo Mon. Extra* 50, 127–137. (in Japanese).
- Iida, T., Mizobata, K., Saitoh, S.-I., 2012. Interannual variability of coccolithophore *Emiliania huxleyi* blooms in response to changes in water column stability in the eastern Bering Sea. *Cont. Shelf Res.* 34, 7–17.
- Iida, T., Saitoh, S.-I., Miyamura, T., Toratani, M., Fukushima, H., Shiga, N., 2002. Temporal and spatial variability of coccolithophore blooms in the eastern Bering Sea, 1998–2001. *Prog. Oceanogr.* 55, 165–177.
- Imao, F., 2005. Zooplankton Community Structure and Their Functional Role in Carbon Cycle in the Oyashio Region, Western Subarctic Pacific. Master Thesis, Hokkaido University, 42 pp.
- Jin, M., Deal, C., Wang, J., McRoy, C.P., 2009. Response of lower trophic level production to long-term climate change in the southeastern Bering Sea. *J. Geophys. Res.* 114, C04010, <http://dx.doi.org/10.1029/2008JC005105>.
- Kang, Y., Kim, S., Lee, W., 2006. Seasonal and spatial variations of zooplankton in the central and southeastern Bering Sea during the mid-1990s. *Deep-Sea Res.* I 53, 795–803.
- Lovvorn, J.R., Baduini, C.L., Hunt Jr., G.L., 2001. Modeling underwater visual and filter feeding by planktivorous shearwaters in unusual sea conditions. *Ecology* 82, 2342–2356.
- McFarlane, G.A., King, J.R., Beamish, R.J., 2000. Have there been recent changes in climate? Ask the fish. *Prog. Oceanogr.* 47, 147–169.
- McLaren, I.A., 1969. Population and production ecology of zooplankton in Ogac Lake, a landlocked fjord on Baffin Island. *J. Fish. Res. Bd. Canada* 26, 1485–1559.
- Miller, C.B., Frost, B.W., Batchelder, H.P., Clemons, M.J., Conway, R.E., 1984. Life histories of large, grazing copepods in a Subarctic Ocean Gyre: *Neocalanus plumchrus*, *Neocalanus cristatus*, and *Eucalanus bungii* in the Northeast Pacific. *Prog. Oceanogr.* 13, 201–243.
- Motoda, S., 1957. North Pacific standard plankton net. *Inf. Bull. Planktol. Jpn.* 4, 13–15.
- Motoda, S., 1959. Devices of simple plankton apparatus. *Mem. Fac. Fish. Hokkaido Univ.* 7, 73–94.
- Mumm, N., 1991. On the summer distribution of mesozooplankton in the Nansen Basin, Arctic Ocean. *Rep. Polar Res.* 92, 1–146.
- Napp, J.M., Baier, C.T., Brodeur, R.D., Coyle, K.O., Shiga, N., Mier, K., 2002. Interannual and decadal variability in zooplankton communities of the south-east Bering Sea shelf. *Deep-Sea Res.* II 49, 5991–6008.
- Napp, J.M., Hunt, G.L., 2001. Anomalous conditions in the south-eastern Bering Sea 1997: linkage among climate, weather, ocean, and biology. *Fish. Oceanogr.* 10, 61–68.
- Napp, J.M., Kendall Jr., A.W., Schumacher, J.D., 2000. A synthesis of biological and physical processes affecting the feeding environment of larval walleye pollock (*Theragra chalcogramma*) in the eastern Bering Sea. *Fish. Oceanogr.* 9, 147–162.
- Nejstgaard, J.C., Gismervik, I., Solberg, P.T., 1997. Feeding and reproduction by *Calanus finmarchicus*, and microzooplankton grazing during mesocosm blooms of diatoms and the coccolithophore *Emiliania huxleyi*. *Mar. Ecol. Prog. Ser.* 147, 197–217.
- Nelson, R.J., Carmack, E.C., McLaughlin, F.A., Cooper, G.A., 2009. Penetration of Pacific zooplankton into the western Arctic Ocean tracked with molecular population genetics. *Mar. Ecol. Prog. Ser.* 381, 129–138.
- Overland, J.E., Bond, N.A., Adams, J.M., 2001. North Pacific atmospheric and SST anomalies in 1997: links to ENSO? *Fish. Oceanogr.* 10, 69–80.
- Sameoto, D.D., 1973. Annual life cycle and production of the chaetognath *Sagitta elegans* in Bedford Basin, Nova Scotia. *J. Fish. Res. Bd. Canada* 30, 333–344.
- Shannon, C.E., Weaver, W., 1949. *The Mathematical Theory of Communication*. The University of Illinois Press, Urbana.
- Smith, S.L., Vidal, J., 1986. Variations in the distribution, abundance, and development of copepods in the southeastern Bering Sea in 1980 and 1981. *Cont. Shelf Res.* 5, 215–239.
- Springer, A.M., 1992. A review: Walleye pollock in the North Pacific—how much difference do they really make? *Fish. Oceanogr.* 1, 80–96.
- Springer, A.M., McRoy, C.P., Flint, M.V., 1996. The Bering Sea Green Belt: shelf-edge processes and ecosystem production. *Fish. Oceanogr.* 5, 205–223.
- Stabeno, P.J., Bond, N.A., Kachel, N.B., Salo, S.A., Schumacher, J.D., 2001. On the temporal variability of the physical environment over the south-eastern Bering Sea. *Fish. Oceanogr.* 10, 81–98.
- Stabeno, P.J., Napp, J., Mordy, C., Whitedge, T., 2010. Factors influencing physical structure and lower trophic levels of the eastern Bering Sea shelf in 2005: ice, tides and winds. *Prog. Oceanogr.* 85, 180–196.

- Stabeno, P.J., Kachel, N.B., Moore, S.E., Napp, J.M., Sigler, M., Yamaguchi, A., Zerbini, A.N., 2012. Comparison of warm and cold years on the southeastern Bering Sea shelf and some implications for the ecosystem. *Deep-Sea Res. II* 65–70, 31–45.
- Stockwell, D.A., Whitley, T.E., Zeeman, S.I., Coyle, K.O., Napp, J.M., Brodeur, R.D., Pinchuk, A.I., Hunt Jr., G.L., 2001. Anomalous conditions in the south-eastern Bering Sea, 1997: nutrients, phytoplankton and zooplankton. *Fish. Oceanogr.* 10, 99–116.
- Sugimoto, T., Tadokoro, K., 1997. Interannual–interdecadal variations in zooplankton biomass, chlorophyll concentration and physical environment in the subarctic Pacific and Bering Sea. *Fish. Oceanogr.* 6, 74–93.
- Sugimoto, T., Tadokoro, K., 1998. Interdecadal variations of plankton biomass and physical environment in the North Pacific. *Fish. Oceanogr.* 7, 289–299.
- Sukhanova, I.N., Flint, M.V., 1998. Anomalous blooming of coccolithophorids over the eastern Bering Sea shelf. *Oceanology* 38, 502–505.
- Vance, T.C., Schumacher, J.D., Stabeno, P.J., Baier, C.T., Wyllie-Echeverria, T., Tynan, C.T., Brodeur, R.D., Napp, J.M., Coyle, K.O., Decker, M.B., Hunt Jr., G.L., Stockwell, D., Whitley, T.E., Jump, M., Zeeman, S., 1998. Aquamarine waters recorded for first time in Eastern Bering Sea. *Eos Trans. Am. Geophys. Union* 79, 121–126.
- Zo, Z., 1973. Breeding and growth of the chaetognath *Sagitta elegans* in Bedford Basin. *Limnol. Oceanogr.* 18, 750–756.



Microzooplankton grazing impact in the Bering Sea during spring sea ice conditions



Evelyn B. Sherr*, Barry F. Sherr, Celia Ross

College of Earth, Ocean, and Atmospheric Sciences, Oregon State University, Corvallis, OR 97331-5503, USA

ARTICLE INFO

Available online 14 March 2013

Keywords:

Microzooplankton
Herbivory
Dilution assay
Phytoplankton growth
Bering Sea

ABSTRACT

Microzooplankton grazing impact on phytoplankton in the Bering Sea during spring was assessed in 2008, 2009 and 2010 using two-point dilution assays. Forty-nine experiments were completed in a region encompassing shelf to slope waters, including the 70 m line along the edge of the shelf. A variety of conditions were encountered, with a concomitant range of trophic states, from pre-bloom low chlorophyll-a (Chl-a) $< 3 \mu\text{g l}^{-1}$ during heavy ice cover to late spring open water diatom blooms with Chl-a up to $40 \mu\text{g l}^{-1}$. Microzooplankton biomass was dominated by large heterotrophic dinoflagellates and ciliates. Both athecate and thecate dinoflagellates, as well as some species of ciliates, fed on diatom cells and chains. Other types of protists, notably thecate amoebae and parasitoid flagellates, were also observed preying on diatoms. Total microzooplankton biomass ranged from 0.1 to $109 \mu\text{g C l}^{-1}$ and was positively related to Chl-a concentration. Significant rates of microzooplankton herbivory were found in 55% of dilution experiments. Maximum grazing rate was 0.49 d^{-1} , and average grazing rate, including experiments with no significant grazing, was $0.09 \pm 0.10 \text{ d}^{-1}$. Phytoplankton intrinsic growth rates varied from slightly negative growth to $> 0.4 \text{ d}^{-1}$. Microzooplankton grazing was significant in both non-bloom and bloom conditions, averaging $46 \pm 75\%$ of phytoplankton daily growth. Based on the amount of phytoplankton carbon consumed, we estimated potential microzooplankton community growth rates of up to 1.3 d^{-1} . Our results confirm the importance of protist grazers in planktonic food webs of high latitude ecosystems. We also conclude that our finding of significant grazing by microzooplankton on spring blooms in the Bering Sea does not support theories about phytoplankton bloom formation based on escape from grazing, due either to predation resistance or to slow growth of herbivorous protists at cold temperature.

© 2013 Elsevier Ltd. All rights reserved.

1. Introduction

Microzooplankton, which include ciliates and heterotrophic dinoflagellates from $\sim 12 \mu\text{m}$ to $200 \mu\text{m}$ in size, are dominant herbivores in planktonic food webs (Sherr and Sherr, 2002, 2007; Calbet and Landry, 2004; Calbet, 2008; Buitenhuis et al., 2010). Protists in this size class are also a significant food resource for mesozooplankton (Levinsen and Nielsen, 2002; Calbet and Saiz, 2005; Olsen et al., 2006; Campbell et al., 2009; Löder et al., 2011) and for fish larvae (Howell-Kübler et al., 1996; Lessard et al., 1996; Montagnes et al., 2010). Phagotrophic ciliates and dinoflagellates are known to be abundant in arctic and sub-arctic marine systems (Howell-Kübler et al., 1996; Levinsen et al., 1999; Levinsen and Nielsen, 2002; Olson and Strom, 2002; Strom and Fredrickson, 2008; Sherr et al., 2009). However, the quantitative

roles of microzooplankton in the food webs of high latitude regions are not well constrained.

The Bering Sea is highly productive, supporting major commercial and subsistence fisheries, and is also highly sensitive to climate variability (Hunt et al., 2008, 2010; Hunt Jr. et al., 2011). Extent of winter sea ice, and timing of sea ice retreat during the spring bloom season, have crucial impacts on the magnitude and fate of primary production in this region (Hunt Jr. et al., 2011; Lomas et al., 2012; Stabeno et al., 2012). The partitioning of production between plankton and benthos is thought to be directly related to presence or absence of ice during spring, with impacts on water temperature, stratification, and light available to phytoplankton. Late sea ice retreat results in early season, ice-associated diatom blooms that sink to the benthos, while early sea ice retreat promotes late season planktonic diatom blooms that are more efficiently grazed by crustacean zooplankton (Hunt et al., 2002; Hunt Jr. et al., 2011).

Prior to our study, herbivory by microzooplankton in the Bering Sea had not been evaluated during the critical spring bloom season. Previous research on microzooplankton grazing in

* Corresponding author. Tel.: +1 541 757 1032; fax: +1 541 737 2064.
E-mail address: sherre@coas.oregonstate.edu (E.B. Sherr).

this region has been confined to summer, after sea ice melt (Liu et al., 2002; Olson and Strom, 2002; Strom and Fredrickson, 2008). The goals of our project were to estimate the flux of spring bloom production through the microzooplankton in this productive subarctic region, and to compare the importance of microzooplankton and mesozooplankton as herbivores (R. Campbell and C. Ashjian unpublished). During the three years of this study, the Bering Sea experienced a cold climate regime, with extensive sea ice, cold water temperatures, and ice-edge blooms during spring (Stabeno et al., 2012). Our results thus quantify microzooplankton grazing in spring under cold regime conditions in the Bering Sea.

The results of this study are relevant to a more general issue: the extent to which marine phytoplankton blooms, and especially diatom blooms, result from temporary escape from microzooplankton grazing mortality. Two such theories have been suggested. Irigoien et al. (2005) proposed that bloom-forming phytoplankton are species that chemically or mechanically inhibit microzooplankton predation: the 'loophole' hypothesis. Rose and Caron (2007) surveyed literature on growth rates for monospecific cultures of marine phytoplankton and phagotrophic protists over a range of temperatures, and concluded that at $< \sim 10^\circ\text{C}$, maximum growth rates of herbivorous protists were less than those of phytoplankton, while at higher temperatures herbivorous protist growth rates were as high, or higher, than those of phytoplankton. Rose and Caron suggested that temperature constraint on growth rates, and thus potential grazing rates, of microzooplankton is a factor in the initiation and development of mass phytoplankton blooms in high latitude, cold water regions of the ocean. We observed high microzooplankton grazing impact on phytoplankton at low seawater temperatures in the Bering Sea. These observations suggest that our data do not support the ideas that the diatom blooms were initiated either due to predation escape by cell defenses, or to cold temperatures differentially inhibiting microzooplankton growth. Rather, the blooms occurred because light and nutrient availability in spring allowed diatoms to initially grow faster than co-occurring microzooplankton, which were food limited until the blooms attained higher biomass (Banse, 1982; Sherr and Sherr, 2009).

2. Methods

2.1. Sampling

Microzooplankton herbivory was assessed as part of the Bering Sea Ecosystem Study (BEST) during April/May cruises in 2008 and 2009, and a May/June cruise in 2010. Grazing experiments were carried out at a subset of stations occupied during these cruises along established transects from shelf to slope, including along the 70 m isobath at the edge of the shelf (Fig. 1 and Table 1). Water for the dilution assays was collected using a CTD in 30-liter Niskin bottles at a pre-determined depth, either the Chl-a maximum or a depth in the upper mixed layer at the 15%, 25% or 50% light level, corresponding to one of the depths sampled for phytoplankton production just prior to our cast (Lomas et al., 2012). Sampling for dilution experiments was coordinated with sampling for rates of primary production (Lomas et al., 2012) and for mesozooplankton grazing experiments (R. Campbell and C. Ashjian unpublished). In addition, water samples were taken from 6 depths from primary production profile casts for analysis of microzooplankton community composition and biomass. We also acquired samples for microzooplankton analysis from an early spring cruise (from mid-March to mid-April, 2010) in the BEST study area. These samples were collected from bottle casts at 15 or 20 m depth and preserved using the same protocol as in our

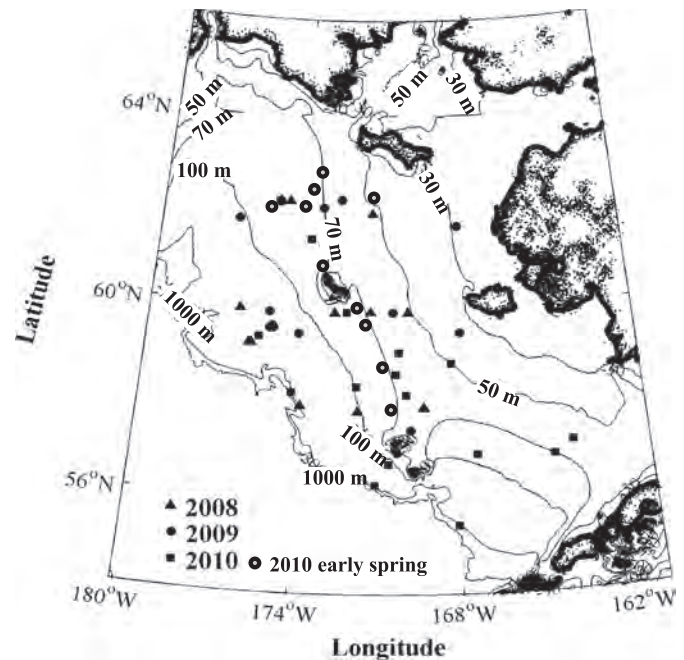


Fig. 1. Location of stations sampled in the eastern Bering Sea. Solid symbols denote stations at which water was collected to set up dilution assay experiments during the three spring BEST process cruises. Dotted circles denote stations for which microzooplankton biomass was sampled in early spring 2010.

spring cruises. Data on bottom depth, seawater temperature, and nitrate concentration at the depths sampled were provided courtesy of the BEST service team. Percent of sea surface covered by sea ice was visually estimated and recorded by the CTD operator at the time of sampling.

2.2. Dilution assays

A two-point dilution assay, consisting of 10% and 100% whole seawater treatments, were carried out following the general protocol of Landry et al. (2008). In this modification of the dilution assay, two equations are solved for the unknowns: phytoplankton intrinsic growth rate, μ , and microzooplankton grazing mortality, m :

$$m = (kd - k)/(1 - x) \quad (1)$$

$$\mu = k + m \quad (2)$$

where kd is the Chl-a based growth rate in the diluted treatment, k is the Chl-a based growth rate in the whole water treatment, and x is the fractional dilution used in the diluted treatment, in this case $x=0.1$. Strom and Fredrickson (2008) compared results using the traditional multi-point dilution series and the two-point protocol in experiments in the southeastern Bering Sea, and found no significant between-method difference in estimates of phytoplankton growth or grazing mortality.

Considerations regarding the dilution technique have been discussed by Gifford (1988), Gallegos (1989), Landry (1993), Neuer and Cowles (1994), Dolan et al. (2000), and Olson and Strom (2002). Two common manipulations in the method are to pre-screen whole seawater to exclude grazers $> 200 \mu\text{m}$, and to add nutrients to the dilution series to minimize potential nutrient limitation of phytoplankton growth (Landry, 1993). For these experiments, we elected not to pre-screen whole water, since during blooms large diatom cells and chains could have been retained on the screen. We did add nutrients to initial water for

Table 1

Summary of dates, station locations, bottom depths, ice extent as visually estimated percent of sea surface cover, sampling depth, water temperature and nitrate concentration at the sampling depth, and light level during incubation as percent of incident light, for dilution assay experiments conducted during BEST spring cruises. In 2010, no quantitative assessment of ice cover was made, however notes were made as to no ice cover observed, when sampling was done at the ice edge (edge), or when ice floes were present (floes). Nitrate concentrations were provided by the BEST service team. nd=No data.

Date	Latitude °N	Longitude °W	Bottom depth (m)	Ice cover (%)	Sample depth (m)	Temp. (°C)	Nitrate (µM)	Light (% I ₀)
4/2/2008	57.895	169.246	67	90	15	-1.3	12.8	15
4/5/2008	59.892	169.791	53	90	16	-0.1	nd	Dark
4/7/2008	59.878	172.680	76	100	10	-0.1	nd	Dark
4/8/2008	59.900	176.432	141	90	2	-1.6	20.8	15
4/11/2008	62.204	175.099	80	70	10	-1.6	16.4	15
4/13/2008	61.964	171.223	53	9	14	-0.8	10.1	15
4/16/2008	59.904	171.257	74	80	2	-1.0	9.7	25
4/18/2008	57.914	169.230	69	30	10	-1.3	11.9	25
4/21/2008	57.827	171.734	101	0	14	1.8	8.9	25
4/23/2008	57.929	173.877	165	0	10	-0.4	19.0	15
4/25/2008	59.206	175.906	139	0	20	-0.3	16.0	25
4/28/2008	59.196	175.982	139	0	10	nd	14.8	25
4/29/2008	62.199	174.698	73	100	10	-1.6	14.3	25
4/8/2009	59.902	170.39	62	80	10	-1.4	5.0	25
4/10/2009	59.867	175.256	120	90	20	-0.5	16.6	15
4/12/2009	59.901	178.905	504	90	16	-1.3	23.9	15
4/14/2009	61.778	176.789	113	6	10	-1.1	17.9	15
4/16/2009	62.077	173.275	60	10	10	-1.0	11.2	15
4/18/2009	61.697	167.742	28	90	10	-1.0	4.2	15
4/20/2009	59.457	167.786	38	60	10	-0.6	0.9	25
4/22/2009	57.441	169.745	66	70	10	-0.7	15.4	15
4/24/2009	56.974	170.273	72	0	10	0.6	17.0	25
4/26/2009	59.529	175.203	137	0	7	-1.0	11.5	50
4/27/2009	59.540	175.077	130	0	7	-0.8	6.0	50
4/29/2009	59.584	175.125	132	0	5	-1.1	2.4	50
4/30/2009	59.546	175.143	133	0	5	-1.1	3.7	50
5/2/2009	62.255	172.543	59	80	10	-1.4	8.5	25
5/4/2009	62.183	175.131	80	90	10	-1.2	14.4	25
5/6/2009	59.433	174.076	115	0	15	-0.1	0.0	25
5/12/2010	56.283	171.051	140	0	15	3.5	9.4	15
5/13/2010	56.727	170.573	115	Edge	40	-0.4	6.9	15
5/15/2010	58.351	171.791	102	0	18	0.6	0.6	15
5/17/2010	59.329	175.606	142	Edge	27.5	2.0	17.5	15
5/19/2010	59.899	178.898	485	0	5	1.3	0.2	15
5/21/2010	58.204	174.236	381	0	24	2.6	12.5	15
5/23/2010	59.072	170.170	67	Floes	19	0.2	2.7	15
5/25/2010	56.917	167.317	78	0	22	1.8	7.0	15
5/27/2010	58.171	169.898	72	0	28.5	1.5	1.8	15
5/29/2010	55.432	168.061	204	0	12	3.4	9.7	15
5/30/2010	57.131	163.798	67	0	25	2.2	8.2	15
5/31/2010	56.853	164.506	73	0	15	1.9	0.1	15
6/2/2010	58.612	170.285	72	0	15	1.3	0.5	15
6/4/2010	61.411	173.735	76	0	25	2.6	1.0	15
6/5/2010	62.189	175.152	79	0	27	2.7	0.1	15
6/7/2010	59.893	178.898	666	0	17	3.6	10.1	15
6/9/2010	59.900	172.200	73	0	25	1.8	0.1	15
6/10/2010	58.830	168.159	46	0	35	2.3	0.1	15

experiments in which on-board nutrient analysis indicated that in situ nitrate and phosphate concentrations might be limiting. We were not able to include both nutrient-addition and control non-nutrient addition whole water treatments in our assays.

All carboys, bottles, and tubing used in setting up dilution assays were pre-soaked in 5% HCl and thoroughly rinsed with deionized water. Nitex gloves were worn during experimental set-up. Seawater was gently transferred from Niskin bottles into 50l carboys through silicon tubing; care was taken to avoid bubbles in the tubing as the carboys were filled. After collection of seawater, all other preparation steps were carried out in a temperature-controlled environmental chamber set at -1 to 0 °C under dim light (approximately 0.1% of incident light). For dilutions, particle-free seawater was prepared by gravity filtration through a Pall 0.2 µm filter presoaked in 5% HCl and thoroughly rinsed with deionized water. Five liters of seawater were passed through the 0.2 µm filter before beginning collection of particle-free water for the dilutions.

Experimental bottles were filled within two to three hours of sample collection. Particle-free water was added to 2-l polycarbonate bottles to yield 10% whole seawater. As needed to ensure non-nutrient limited growth of phytoplankton, ammonium nitrate and sodium phosphate were added to experimental bottles to yield concentrations of 5 µM N and 0.25 µM P. A carboy filled with whole seawater was gently mixed for several minutes using a plexiglass rod with a small plexiglass disc attached to the end. Then, while the carboy continued to be gently mixed, whole seawater was siphoned out of the carboy to fill triplicate 10% and 100% whole water experimental bottles and an additional 2-l bottle for initial samples. Parafilm was placed on top of each bottle prior to securing the cap, in order to minimize air bubbles in the bottles, as protist cells can lyse on contact with air (Gifford, 1988).

The experimental bottles were wrapped with combinations of neutral density Scrim and blue plastic film to mimic the approximate in situ light intensity and quality of the water depths sampled (Table 1) and mounted onto a plankton wheel on-deck

incubator cooled with flowing seawater. Temperature in the on-deck incubator was continually monitored using a Hobo temperature recorder immersed in the plankton wheel incubator. Average temperatures during the 24-h incubations varied from -1.6 to 3.6 °C (Table 1).

Initial samples were taken from whole seawater for determination of Chl-a concentration, and for microscopic enumeration of microzooplankton abundance, biomass, and general taxonomic composition. Depending on the phytoplankton concentration, from 25 to 300 ml quadruplicate volumes were settled via vacuum filtration onto GFF filters in dim light. The filters were extracted in 6 ml of 90% acetone in 13×100 mm² glass culture tubes at -20 °C for 18 to 24 h. At the end of the extraction period, the filter was carefully removed from each tube, and the Chl-a concentration determined using a calibrated Turner Designs fluorometer outfitted with filter sets for the non-acidification protocol of Welschmeyer (1994). A solid chlorophyll standard was used to check for fluorometer drift at the beginning of each reading of Chl-a samples. Additional Chl-a measurements from primary production profile samples were provided by M. Lomas using the acidification protocol of Parsons et al. (1984) (Lomas et al., 2012). A cross-comparison of samples using these two methods carried out during the spring cruises showed good replication of Chl-a values.

For determination of microzooplankton biomass and abundance, 200 ml subsamples were preserved with 5% final concentration acid Lugol solution for inverted microscopy. Separate subsamples were preserved for inspection via epifluorescence microscopy with a three-step alkaline Lugol-sodium thiosulfate-2% final concentration formalin fixation protocol (Sherr and Sherr, 1993). Formalin-preserved samples were held at 2 °C for 12 to 24 h, and then settled onto 0.8 μ m or 3.0 μ m black membrane filters, stained with DAPI (5 μ g ml⁻¹ final concentration), and mounted onto glass slides that were stored at temperatures of -20 °C or lower until analysis. At the end of the dilution incubations, final samples were taken from each bottle for Chl-a concentration. Depending on the initial phytoplankton concentration and dilution, from 25 to 500 ml triplicate subsamples were filtered for chlorophyll-a determination.

2.3. Calculation of phytoplankton growth and grazing rates

Phytoplankton growth rates in 10% and 100% whole water treatments were calculated by change in Chl-a. Initial Chl-a concentrations in the 10% dilutions were calculated from whole seawater Chl-a concentrations. Phytoplankton growth rates (k_d and k) were determined for each experimental bottle using an exponential growth equation based on initial and final Chl-a concentrations in the 10% dilution and WW treatments:

$$k_d \text{ or } k = (\ln \text{ final Chl-a} - \ln \text{ Initial Chl-a}) d^{-1}$$

these growth rates were then used in the two-step dilution equations to calculate values for μ and m (Eqs. (1) and (2)).

In order to estimate daily phytoplankton growth and grazing loss in terms of carbon biomass, we first calculated the daily phytoplankton intrinsic biomass production, and estimated the amount of daily production consumed by microzooplankton, in terms of Chl-a l⁻¹ d⁻¹: \ln WW Chl-a daily intrinsic production = $[\ln \text{ initial WW Chl-a} + \mu] - \ln \text{ initial WW Chl-a}$; Chl-a grazed per day = $[\text{initial Chl-a} + \text{calculated Chl-a intrinsic production}] - \text{final WW Chl-a}$. We then converted the Chl-a values to daily increase or consumption of phytoplankton carbon biomass (mg C m⁻³ d⁻¹) using an average C:Chl-a ratio of 50 empirically determined during the 2008–2009 Bering Sea cruises (Lomas et al., 2012).

Significance of relationships between intrinsic growth rates and grazing rates estimated in the dilution experiments was assessed by two-sample t -test assuming unequal variances.

2.4. Post-cruise sample analysis

Microzooplankton abundance and biomass were determined in initial whole seawater samples for 36 of the experiments and at 6 depths from 100% to 1% light levels for selected primary production casts during the three spring cruises (Lomas et al. (2012)), for a total of 125 single-depth samples. In addition, in order to evaluate early spring microzooplankton stocks, we also inspected 10 samples collected at depths of 15 or 20 m in the eastern Bering Sea from 13 March to 3 April 2010 by L. Cooper. From 15 to 50 ml of Lugol-preserved samples were settled for a minimum of 24 h and then the whole slide inspected by inverted light microscopy. A Nikon inverted microscope mated to a computer digitizing system via a drawing tube was used to identify and measure microzooplankton cells and to convert linear dimensions to cell volumes using equations appropriate for individual cell shapes (Roff and Hopcroft, 1986). All ciliate and dinoflagellate cells in each sample were counted, sized, and categorized into the general taxonomic groups of choreotrichous ciliates, oligotrichous ciliates, didinid ciliates, tintinnids, athecate dinoflagellates, and thecate dinoflagellates. Ciliate and dinoflagellate cells ranged in size from ~ 12 – 15 μ m to 200 μ m in size. From 60 to 400 protist cells were counted and sized in each sample inspected. Samples on slides preserved for epifluorescence microscopy were inspected using an Olympus epifluorescence microscope equipped with a multi-wavelength filter set to determine whether dinoflagellates counted in Lugol-preserved samples were heterotrophic or autotrophic; only heterotrophic dinoflagellate morphotypes were included in the microzooplankton data. Cell biomass for dinoflagellates was estimated using an algorithm of Menden-Deuer and Lessard (2000) and for ciliates was estimated using the 0.19 pg C μ m⁻³ value of Putt and Stoecker (1989). Ratios of heterotrophic dinoflagellate biomass, and of > 40 μ m sized microzooplankton biomass, as a fraction of total microzooplankton biomass were also calculated. For primary production profiles, integrated microzooplankton biomass (mg C m⁻²) was determined over the depth interval sampled, from 0–17 to 0–40 m, and compared to integrated phytoplankton biomass assuming a C:Chl-a ratio of 50 (Lomas et al., 2012).

2.5. Microzooplankton biomass-specific grazing rates and potential microzooplankton growth rates

Biomass-specific grazing rates (d⁻¹) of the microzooplankton community were calculated as the amount of phytoplankton carbon grazed by the microzooplankton community during the dilution assays (μ g C l⁻¹ d⁻¹, see Section 2.2), divided by the initial standing stock of microzooplankton (μ g C l⁻¹). Potential microzooplankton growth rates were estimated using the exponential growth equation:

$$\mu = (\ln B_f - \ln B_o) d^{-1}$$

where B_o is the initial microzooplankton biomass (μ g C l⁻¹) and B_f the $B_o + (\text{phytoplankton C grazed}) \times 0.3$, assuming an average gross growth efficiency for the protist community of 30% (Straille, 1997; Landry and Calbet, 2004; Chen and Liu, 2011). Doubling times (days) for the microzooplankton community were calculated from the growth rates: doubling time = $\ln 2 / \mu$.

Statistical procedures were done using the NCSS-2001 software package.

Table 2

Summary of results for dilution assay experiments conducted during BEST spring cruises. Where calculated MZP grazing rates were negative, i.e., $k > kd$, we assumed a grazing rate of 0.

Date	Sample site	Chl-a ($\mu\text{g l}^{-1}$)	Phyto. μ (d^{-1})	MZP, m (d^{-1})	Significance	μ (m)
4/2/2008	NP-7	0.22	0.10	0.21	$P < 0.04$	2.2
4/5/2008	MN-4	0.15	0.04	0	ns	0
4/7/2008	MN-8.5	0.11	0.08	0	ns	0
4/8/2008	MN-15	1.0	0.14	0.50	$P < 0.06$	3.6
4/11/2008	SL-12	1.6	0.19	0.12	$P < 0.04$	0.64
4/13/2008	SL-6	0.8	0.12	0	ns	0
4/16/2008	W7.5	0.15	0.14	0	ns	0
4/18/2008	NP7	0.30	0.27	0	ns	0
4/21/2008	BS1	21.4	0.31	0	ns	0
4/23/2008	BS2	7.0	0.30	0	ns	0
4/25/2008	ZZ14	6.4	0.23	0.08	$P < 0.02$	0.36
4/28/2008	ZZ27	9.7	0.12	0.10	$P < 0.02$	0.31
4/29/2008	70m58	8.5	0.06	0.05	ns	0
4/8/2009	MN5	0.3	0	0	ns	0
4/10/2009	MN13	0.4	0.09	0	ns	0
4/12/2009	MN19	0.9	0.25	0	ns	0
4/14/2009	MN-SL4	0.2	0	0	ns	0
4/16/2009	SL9	0.5	0.36	0.18	$P < 0.02$	0.51
4/18/2009	SL1	0.3	0.10	0.08	$P < 0.01$	0.77
4/20/2009 ^a	NP1	0.3	0	0.03	ns	0
4/22/2009	NP9	1.1	0.15	0.03	ns	0
4/24/2009	NP11	2.9	0.43	0.02	ns	0
4/26/2009	BL1	10.3	0.38	0.14	$P < 0.02$	0.36
4/27/2009 ^a	BL4	23.6	0.27	0.14	$P < 0.02$	0.54
4/29/2009 ^a	BL15	20.9	0.47	0.17	$P < 0.01$	0.36
4/29/2009 ^a	BL15	20.9	0.40	0.08	$P < 0.01$	0.21
4/30/2009 ^a	BL20	21.4	0.27	0.07	$P < 0.06$	0.26
4/30/2009 ^a	BL20	21.4	0.31	0.10	$P < 0.02$	0.30
5/2/2009 ^a	BN-1	1.9	0.42	0.16	$P < 0.06$	0.39
5/4/2009 ^a	SL-12	0.6	0.36	0.27	$P < 0.01$	0.76
5/6/2009 ^a	B-21	38.1	0.18	0.17	$P < 0.02$	0.91
5/12/2010	NP-14	14.8	0.20	0.07	$P < 0.06$	0.35
5/13/2010	NP-12	8.1	0.16	0.09	$P < 0.001$	0.57
5/15/2010 ^a	Z-15	11.0	0.11	0	ns	0
5/17/2010	IE-1	10.5	0.35	0.33	$P < 0.002$	0.93
5/19/2010 ^a	MN-19	24.3	0.15	0.15	$P < 0.01$	1.0
5/21/2010	NZ 11.5	1.2	0.18	0	ns	0
5/23/2010 ^a	NZ 4.5	11.1	0.10	0.08	$P < 0.01$	0.75
5/25/2010 ^a	HBR1	31.6	0.04	0	ns	0
5/27/2010 ^a	70m26	5.6	0.10	0.15	$P < 0.01$	1.6
5/29/2010	CN17	7.8	0.38	0	ns	0
5/30/2010 ^a	CN 5	3.5	0.06	0	ns	0
5/31/2010 ^a	70m4	7.5	0.24	0	ns	0
6/2/2010 ^a	70m29	0.5	0.39	0.14	$P < 0.001$	0.36
6/4/2010 ^a	70m52	14.9	0.15	0.13	$P < 0.04$	0.87
6/5/2010 ^a	SL12	2.0	0.00	0	ns	0
6/7/2010 ^a	MN-19	7.9	0.16	0.07	$P < 0.03$	0.45
6/9/2010	MN8	0.4	0.24	0.05	$P < 0.02$	0.22
6/10/2010 ^a	NP-3	1.2	0.07	0.21	$P < 0.07$	3.0

^a Experiments in which nutrients were added.

3. Results

3.1. General conditions

The BEST spring process cruises focused on the ice-covered continental shelf and ice-edge outer shelf and shelf break. Stations on the 70 m isobath along the outer shelf, which has been the focus of time series and mooring sampling efforts (Stabeno et al., 2002, 2012), were occupied during all three cruises. A variety of conditions were encountered, from heavy sea ice cover over the shelf during early to mid-April, to ice melt and open water in late April to early June (Table 1). All phases of the Bering Sea spring bloom were encountered: pre-bloom and post-bloom conditions in which Chl-a was $< 3 \mu\text{g l}^{-1}$, growth of sea ice diatoms in March and April, and ice-edge planktonic diatom blooms with Chl-a of > 3 and up to $40 \mu\text{g l}^{-1}$ during April–June (Table 2). Qualitative assessment of phytoplankton communities by microscopic inspection of samples indicated that

pennate diatom species characteristic of sea ice, notably *Fragilaria* spp., *Navicula* spp., and *Nitzschia* spp., were often an important component of algae in the water column. However, ice edge and open water blooms were characterized by pelagic centric diatoms, dominated by species of *Chaetoceros*, *Thalassiosira*, and *Cylindrotheca*.

3.2. Dilution assay results

A total of 49 dilution assays were completed at 47 stations (Tables 1 and 2). Initial Chl-a concentrations in the experiments varied from $\sim 0.1 \mu\text{g l}^{-1}$ in early April 2008 to $38 \mu\text{g l}^{-1}$ in May 2009 (Table 2). There was a significant microzooplankton grazing rate in over half (27 out of 49) of the dilution assays (Table 2). Phytoplankton intrinsic growth rates varied from highest values of 0.30 to 0.47 d^{-1} to lowest values of $< 0.1 \text{ d}^{-1}$ (Table 2). We were not able to compare phytoplankton growth in treatments with and without added nutrients, so growth rates for

Table 3

Mean seawater temperature, Chl-a concentration, phytoplankton production and microzooplankton grazing rate as $\text{mg C m}^{-3} \text{d}^{-1}$, and percent of phytoplankton production grazed by microzooplankton during spring; mean values \pm one standard deviation. At bloom stations Chl-a concentrations were $> 3.0 \mu\text{g l}^{-1}$. All data, including experiments with non-significant grazing, were included.

Year	Surface seawater temp ($^{\circ}\text{C}$)	Chl-a ($\mu\text{g l}^{-1}$)	Phyto. prod. rate ($\text{mg C m}^{-3} \text{d}^{-1}$)	Microzoop. grazing rate ($\text{mg C m}^{-3} \text{d}^{-1}$)	Percent of Chl-a grazed (d^{-1})	Percent of phyto. prod. grazed (d^{-1})
Spring 2008						
Non-bloom	-1.0 ± 0.6	0.6 ± 0.6	2.7 ± 3.0	4.6 ± 8.6	11 ± 17	86 ± 140
Bloom	-0.4 ± 1.0	10.6 ± 6.2	135 ± 144	16 ± 13	4 ± 4	31 ± 31
Spring 2009						
Non-bloom	-1.0 ± 0.3	0.8 ± 0.8	14 ± 25	4.1 ± 6.6	9 ± 12	26 ± 32
Bloom	-0.6 ± 0.7	22.4 ± 8.2	410 ± 127	67 ± 103	11 ± 10	45 ± 23
Spring 2010						
Non-bloom	2.2 ± 0.6	1.1 ± 0.6	6.7 ± 5.2	4.6 ± 8.6	9 ± 10	69 ± 120
Bloom	1.9 ± 1.3	12.2 ± 7.8	104 ± 67	57 ± 72	9 ± 11	50 ± 50

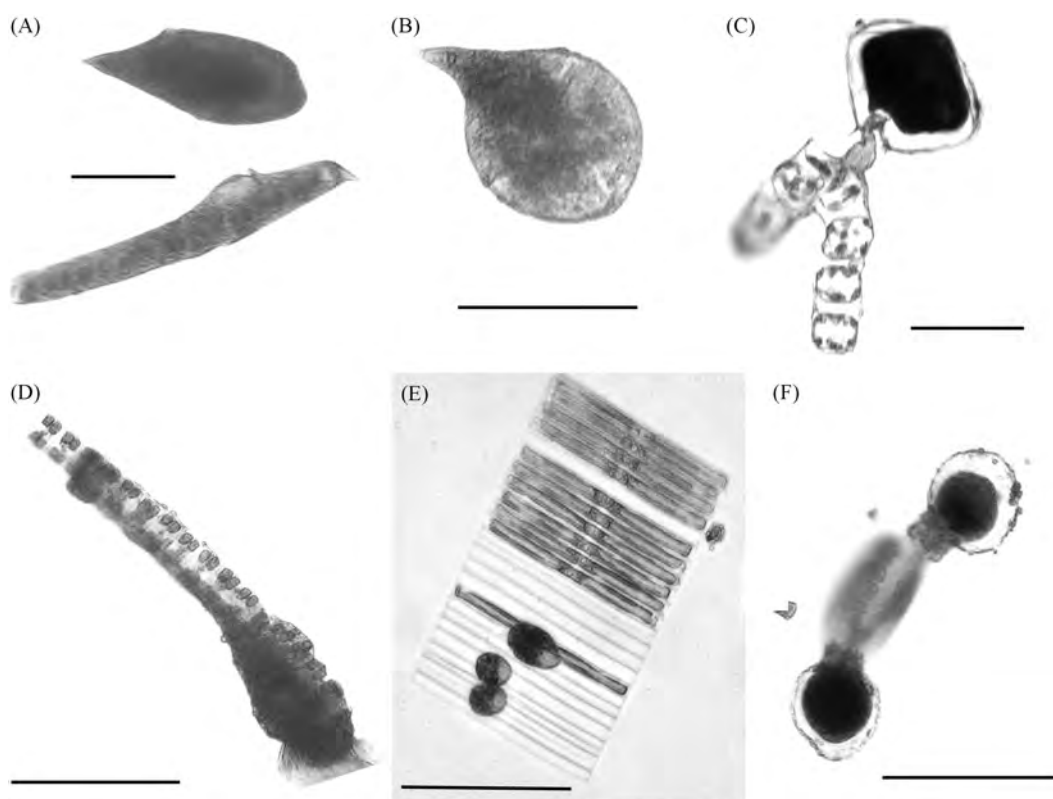


Fig. 2. Examples of protists observed feeding on diatoms in the Bering Sea during spring. (A) heterotrophic athecate dinoflagellates, cf. *Gyrodinium* sp., upper cell with no ingested prey, lower cell distended with ingested diatom chain, (B) heterotrophic gyrodinoid dinoflagellate cell distended with ingested centric diatom, (C) heterotrophic thecate dinoflagellate, cf. *Protoperidinium* sp., attached to a diatom chain by an extruded pallium, (D) spirotrichous ciliate with ingested diatom chain, (E) three parasitoid heterotrophic flagellates on a pennate diatom chain, empty frustules suggest prior feeding by the flagellates, and (F) two testate amoebae feeding on a centric diatom cell. Scale bars = 50 μm .

stations with low initial nutrients may be higher than in situ rates. Grazing mortality as a fraction of phytoplankton growth ranged from zero to a grazing mortality two- to three-fold greater than phytoplankton growth rate (Table 2). Microzooplankton grazing rate was not significantly correlated to phytoplankton growth rate or to Chl-a concentration. Phytoplankton production and microzooplankton grazing impact were converted to units of $\text{mg C m}^{-3} \text{d}^{-1}$ to facilitate comparison of microzooplankton and mesoplankton herbivory (Table 3).

Because of the wide variability in phytoplankton stocks encountered during spring, we separated our data into 'non-bloom' versus 'bloom' conditions, using $3.0 \mu\text{g Chl-a l}^{-1}$

as the cut-off value. About half of our experiments (24) had initial Chl-a concentrations less than this value, and the rest had Chl-a concentrations of 3.5 to $38 \mu\text{g Chl-a l}^{-1}$. All data, including results of experiments with non-significant grazing, were included in this analysis. During the three cruises, under non-bloom conditions ($\text{Chl-a} < 3 \mu\text{g C l}^{-1}$) microzooplankton grazing averaged 26% to 86% of phytoplankton production, and under bloom conditions, with average Chl-a concentrations of 11 to $22 \mu\text{g C l}^{-1}$, 31% to 59% of production (Table 3). The daily amount of Chl-a standing stock consumed by microzooplankton averaged from 4% to 11% over the three years (Table 3).

Table 4

Values under non-bloom ($\text{Chl-a} < 3.0 \mu\text{g l}^{-1}$) and bloom ($\text{Chl-a} > 3.0 \mu\text{g l}^{-1}$) conditions during the three BEST spring cruises for Chl-a concentration, microzooplankton (MZP) biomass, fraction of MZP biomass composed of heterotrophic dinoflagellates (HDino), and fraction of MZP biomass composed of cells $> 40 \mu\text{m}$ in longest linear dimension. Values are means \pm one standard deviation, with range of values in parentheses.

	Chl-a ($\mu\text{g l}^{-1}$)	MZP biomass ($\mu\text{g C l}^{-1}$)	HDino fraction of MZP biomass	$> 40 \mu\text{m}$ fraction of MZP biomass
Dilution initial MZP depths				
Non-bloom	0.86 ± 0.72	9.2 ± 7.8	0.65 ± 0.12	0.49 ± 0.21
17 Stations	(0.15–2.9)	(2.0–27)	(0.42–0.84)	(0.19–0.80)
Bloom	16 ± 9	42 ± 22	0.67 ± 0.14	0.66 ± 0.17
21 Stations	(5.6–38)	(15–109)	(0.45–0.86)	(0.31–0.85)
Phytoplankton production profiles, 6 depths per profile				
Non-bloom	0.86 ± 0.83	11 ± 17	0.75 ± 0.13	0.51 ± 0.23
16 Stations	(0.06–2.95)	(0.2–71)	(0.43–0.93)	(0.14–0.88)
Bloom	15 ± 9	23 ± 22	0.72 ± 0.13	0.62 ± 0.13
15 Stations	(3.5–40)	(5.5–100)	(0.40–0.93)	(0.33–0.86)
Early spring, March 12–April 3 2010				
Pre-bloom	0.28 ± 0.14	3.2 ± 0.8	0.81 ± 0.08	0.52 ± 0.13
10 Stations	(0.17–0.59)	(2.0–4.4)	(0.40–0.93)	(0.37–0.77)

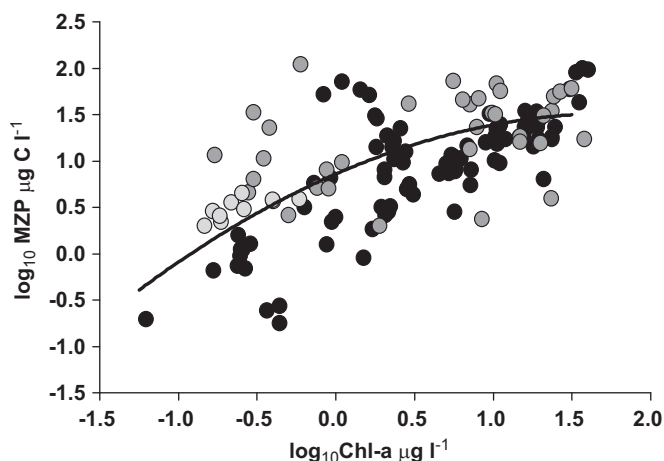


Fig. 3. Log–log relation of microzooplankton biomass (MZP, $\mu\text{g C l}^{-1}$) to Chl-a ($\mu\text{g l}^{-1}$). Dark gray symbols represent initial water samples collected for dilution assays, black symbols water samples from primary production profile depths, light gray symbols water samples from a 2010 early spring (from 13 March to 3 April) cruise. Polynomial curve equation: $\log_{10} \text{MZP} = 0.86 + 0.74 \log_{10} \text{Chl-a} - 0.21(\log_{10} \text{Chl-a})^2$, $R^2 = 0.44$.

3.3. Microzooplankton composition and biomass

Microzooplankton biomass and general taxonomic composition were analyzed for initial water samples from the dilution experiments for which significant grazing was found, and also for selected primary production profiles. The protist community was in general similar to that found in the Bering Sea during summer (Strom and Fredrickson, 2008) and in the Western Arctic Ocean (Sherr et al., 2009). Ciliates were dominated by naked spirotrichs, including species in the genera *Strombidium*, *Strobilidium*, *Leagardiella*, and *Laboea*. A few tintinnid species were observed, the most common of which was a *Ptychocyclus* sp. Heterotrophic dinoflagellates, including thecate and athecate forms (examples in Fig. 2A–C), were abundant and were frequently found with ingested diatoms, including very large cells and chains. We also observed several other types of protists feeding on diatom cells. These included spirotrich ciliates with ingested diatom chains (Fig. 2D) or large

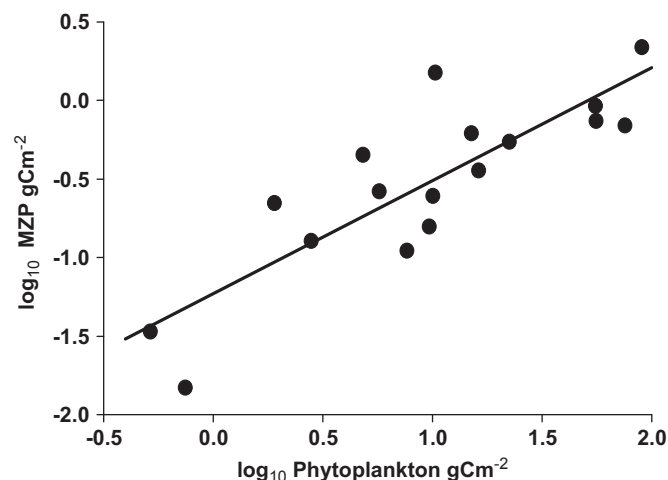


Fig. 4. Log–log relation of depth integrated microzooplankton biomass (MZP, g C m^{-2}) to integrated phytoplankton biomass (g C m^{-2}) for primary production casts. Regression equation: $\log_{10} \text{MZP} = -1.23 + 0.72 \log_{10} \text{phytoplankton}$, $R^2 = 0.72$.

Table 5

Values under non-bloom and bloom conditions during the three BEST spring cruises for microzooplankton biomass-specific grazing rate, potential microzooplankton growth rates, and microzooplankton community doubling times. Values are means \pm one standard deviation, with range of values in parentheses.

	MZP specific grazing rate (d^{-1})	Potential growth rate (d^{-1})	Doubling time days ^a
Non-bloom	1.0 ± 1.6	0.33 ± 0.50	3.3 ± 3.5
17 Stations	(0–4.8)	(0–1.45)	(0.5–8.5)
Bloom	2.0 ± 1.6	0.43 ± 0.37	2.2 ± 1.7
21 Stations	(0–5.4)	(0–1.14)	(0.6–6.0)

^a Doubling times only calculated for stations for which microzooplankton had non-zero potential growth rates.

single pennate diatom cells (not shown), parasitoid flagellates feeding on pennate diatom chains (Fig. 2E), and what we identified as a species of testate amoeba that exclusively fed on single centric diatom cells (Fig. 2F).

For all initial water samples collected for dilution assays, total microzooplankton protist biomass varied from $2.0 \mu\text{g C l}^{-1}$ to $109 \mu\text{g C l}^{-1}$, averaging $8.4 \pm 6.6 \mu\text{g C l}^{-1}$ under non-bloom conditions and $45 \pm 27 \mu\text{g C l}^{-1}$ under bloom conditions. For all of the primary production profiles analyzed, microzooplankton protist biomass varied from $0.2 \mu\text{g C l}^{-1}$ to $100 \mu\text{g C l}^{-1}$, averaging $11.2 \pm 17.2 \mu\text{g C l}^{-1}$ under non-bloom conditions and $23 \pm 23 \mu\text{g C l}^{-1}$ under bloom conditions. Average values of these parameters under non-bloom and bloom conditions for individual years are presented in Table 4. Heterotrophic dinoflagellates composed, on average, from 65% to 75%, and cells $> 40 \mu\text{m}$ in size 49% to 66%, of total microzooplankton biomass. Epifluorescence microscopic inspection of samples confirmed that the dinoflagellates enumerated did not have chloroplasts, and thus were not autotrophic. Using the Chl-a concentrations we measured in initial dilution assay samples, and Chl-a values determined by Lomas et al. (2012) for the primary production profiles and by L. Cooper (personal communication) for the early spring samples, we found a positive log–log relation between protist biomass and Chl-a concentration, although there was high variability between the two parameters at Chl-a concentrations < 3 ($\log 0.5$) $\mu\text{g l}^{-1}$ (Fig. 3). Integrated microzooplankton biomass for the production profiles was also variable, ranging from 0.11 to 2.17 g C m^{-2} . There was a significant positive relation between integrated microzooplankton and phytoplankton biomass (Fig. 4),

Table 6

Comparison of phytoplankton growth and microzooplankton grazing rates, and percent of phytoplankton production grazed, found in this study with values for these parameters determined by the dilution technique in another Arctic system, and in general geographic regions of the world ocean. Values are means \pm one standard deviation.

Region	Temp. (°C)	Chl-a ($\mu\text{g l}^{-1}$)	Phyto. growth μ (d^{-1})	MZP grazing g (d^{-1})	% Phyto growth grazed	Reference
Arctic/sub-arctic						
Barents Sea—early summer	−0.2–7.4	0.66 \pm 0.20	0.32 \pm 0.13	0.24 \pm 0.11	77 \pm 8	Verity et al. (2002)
Western Arctic Ocean—spring	−1.6 \pm 0.1	2.1 \pm 2.5	0.21 \pm 0.15	0.07 \pm 0.06	17 \pm 21	Sherr et al. (2009)
Western Arctic Ocean—summer	−0.4 \pm 2.0	3.4 \pm 5.4	0.11 \pm 0.13	0.06 \pm 0.05	27 \pm 33	Sherr et al. (2009)
Southeastern Bering Sea—summer 1999	11.1 \pm 1.1	1.4 \pm 1.1	0.53 \pm 0.21	0.43 \pm 0.28	90 \pm 56	Olson and Strom (2002)
Southern Bering Sea—summer 1999	6.6 \pm 0.9	1.2 \pm 0.5	0.47 \pm 0.15	0.27 \pm 0.14	58 \pm 31	Liu et al. (2002)
Southeastern Bering Sea—summer 2004	6.8 \pm 1.8	1.4 \pm 1.0	0.35 \pm 0.30	0.13 \pm 0.09	49	Strom and Fredrickson (2008)
Eastern Bering Sea—spring, non-bloom	−0.3 \pm 1.4	0.8 \pm 0.7	0.17 \pm 0.14	0.08 \pm 0.12	52 \pm 100	This study
Eastern Bering Sea—spring, bloom	0.8 \pm 1.7	14 \pm 9	0.21 \pm 0.12	0.09 \pm 0.08	42 \pm 42	This study
Other ocean regions						
Oceanic		0.58 \pm 0.03	0.59 \pm 0.02	0.39 \pm 0.01	70 \pm 2	Calbet and Landry (2004)
Tropical/subtropical		1.01 \pm 0.21	0.72 \pm 0.02	0.50 \pm 0.02	74 \pm 2	Calbet and Landry (2004)
Temperate/subpolar		5.18 \pm 0.66	0.69 \pm 0.03	0.41 \pm 0.02	61 \pm 2	Calbet and Landry (2004)
Polar (Southern Ocean)		0.62 \pm 0.06	0.44 \pm 0.05	0.41 \pm 0.16	59 \pm 3	Calbet and Landry (2004)

with integrated microzooplankton C biomass averaging from 1 to 15% (average 4.3%) of integrated phytoplankton C biomass.

3.4. Microzooplankton specific grazing rates, potential growth rates, and doubling times

These rates were averaged for non-bloom and bloom conditions (Table 5), with Chl-a concentrations the same as in Table 4. There were no significant differences (Student's *t*-test) between these rate values for bloom versus non-bloom Chl-a conditions. Specific grazing rates varied from 0 in dilution assays with no herbivory, to 10.9 d^{-1} , averaging about 2 d^{-1} during bloom and 1 d^{-1} during non-bloom conditions. Potential growth rates also showed a wide range, from 0 to 1.45 d^{-1} , with average μ of 0.3 to 0.4 (Table 5). Doubling times calculated for positive growth rates varied from 0.5 to 8.5 d. On average the microzooplankton community had a doubling time of 2–3 d.

4. Discussion

4.1. Phytoplankton growth rates

Algal biomass and primary production in the Bering Sea during spring is dominated by sea ice and planktonic diatoms $> 5 \mu\text{m}$ in size (Sukhanova et al., 1999; Moran et al., 2012; Lomas et al., 2012). The variety of stages of diatom bloom formation sampled during the three years in this study resulted in high variability in measured phytoplankton intrinsic growth rates (μ). Extensive sea ice cover in April and early May, at the beginning of the bloom season (Table 1) resulted in low phytoplankton biomass due to light limitation: 1.1 \pm 1.9 $\mu\text{g Chl-a l}^{-1}$ for ice cover from 30% to 100%, compared to Chl-a concentrations of 11.6 \pm 1.9 $\mu\text{g l}^{-1}$ for ice-free conditions in May and June. Even so, high phytoplankton growth rates from 0.2 to 0.4 d^{-1} were observed at some stations during April/May with significant sea ice cover. The presence of diatom species common in sea ice communities in samples collected at these stations suggested that ice algae were capable of active growth in the water column.

Intrinsic phytoplankton growth rate for all stations at which Chl-a was $< 3 \mu\text{g l}^{-1}$ was, on average, 0.18 \pm 0.14 d^{-1} . Ice edge and open water diatom blooms encountered in May and June had

an equally wide range of growth rates, from 0.045 d^{-1} at the station with highest phytoplankton biomass, 38 $\mu\text{g Chl-a l}^{-1}$, to 0.47 d^{-1} at a station with a developed bloom of 20 $\mu\text{g Chl-a l}^{-1}$. For all dilution assays in which Chl-a was $> 3 \mu\text{g l}^{-1}$, growth rate averaged 0.22 \pm 0.12 d^{-1} . These values are similar to the average phytoplankton growth rate, 0.21 \pm 0.15 d^{-1} , found in the Western Arctic Ocean during spring (Sherr et al., 2009), under similar conditions of low temperatures and extensive ice cover. Phytoplankton growth rates in the Bering Sea and in the Barents Sea during summer, when temperatures are higher and light is less limiting, average from 0.3 to 0.5 d^{-1} (Table 6).

4.2. Microzooplankton grazing impact in the eastern Bering Sea during spring

The main fates of bloom production in the Bering Sea are export to the benthos or consumption in the water column (Moran et al., 2012). A central issue addressed by this study, coupled with the estimates of grazing on phytoplankton by mesozooplankton, was the extent to which planktonic grazers consume algal production in the Bering Sea during spring sea ice conditions.

Microzooplankton exert a significant grazing impact on phytoplankton biomass and primary production in all regions of the world ocean, including eutrophic ecosystems (Calbet and Landry, 2004). A prevailing idea about plankton grazers is that microzooplankton mainly consume phytoplankton $< 5 \mu\text{m}$ in size (pico- to small nano-sized cells), while mesozooplankton are dominant herbivores of phytoplankton $> 5 \mu\text{m}$ in size, especially of bloom-forming diatoms. However, it is now apparent that protistan herbivores, and in particular heterotrophic dinoflagellates, are voracious predators of bloom-forming diatoms and are as, or more, significant as mesozooplankton in consuming diatom production in the sea (Jeong et al., 2004; Sherr and Sherr, 2007; Aberle et al., 2007; Campbell et al., 2009; Löder et al., 2011). Our results underscore this new understanding.

Microzooplankton grazing rates, like phytoplankton growth rates, were highly variable during spring in the Bering Sea. Protist herbivores consumed, on average, from 26% to 86% of phytoplankton growth at stations with lowest algal biomass ($\sim 1 \mu\text{g Chl-a l}^{-1}$) and from 31% to 50% of growth at stations with significant blooms (~ 10 – $20 \mu\text{g Chl-a l}^{-1}$) (Table 3). These grazing rates are higher than the

average microzooplankton grazing impact of about 17% to 22% of daily phytoplankton growth previously reported in the Western Arctic Ocean, but in the range of average grazing impacts on phytoplankton growth in the Barents Sea and in the Bering Sea during summer (Table 6). However, in these prior studies, the average Chl-a concentrations were lower than that of the spring bloom conditions observed in our study, and water temperatures were warmer.

4.3. Microzooplankton biomass and composition

At present, more is known about the biomass, species composition, and distribution of mesozooplankton compared to microzooplankton in marine systems, even though the latter is indisputably more important as planktonic herbivores (Calbet and Landry, 2004; Calbet, 2008). Irigoien et al. (2004) summarized data on the distribution of phytoplankton and zooplankton, including microzooplankton, in the sea. They found that the maximum biomass of marine microzooplankton, when both ciliates and phagotrophic dinoflagellates were included, was about $100 \mu\text{g C l}^{-1}$, and that the log–log relation between microzooplankton and phytoplankton biomass was saturated, i.e., leveled off, at phytoplankton biomass greater than $100 \mu\text{g C l}^{-1}$, equivalent to $\sim 2 \mu\text{g Chl-a l}^{-1}$ assuming a C:Chl-a ratio of 50.

Microzooplankton biomass in the Bering Sea often reaches the global maximum value reported by Irigoien et al. (2004). Strom and Fredrickson (2008) reported microzooplankton biomass of up to $118 \mu\text{g C l}^{-1}$, averaging $38 \mu\text{g C l}^{-1}$, in the Bering Sea around the Pribilof Islands during summer 2004. Olson and Strom (2002) found an even greater range in microzooplankton biomass, 18 to $164 \mu\text{g C l}^{-1}$, in the southeast Bering Sea in 1999 when coccolithophorids dominated the phytoplankton community. Our data match these earlier observations, with spring microzooplankton biomass as high as $109 \mu\text{g C l}^{-1}$ and averaging $42 \mu\text{g C l}^{-1}$ in initial water samples for dilution assays in which Chl-a was $> 3 \mu\text{g l}^{-1}$ (Table 4).

Strom and Fredrickson (2008) reported a generally positive relation between microzooplankton biomass and Chl-a concentrations from 0.2 to $5 \mu\text{g l}^{-1}$ during the summer of 1999. In this study, we found a positive log–log relation between these two parameters, over a broader range of Chl-a values from 0.1 to $38 \mu\text{g l}^{-1}$ (Fig. 3). There was a degree of leveling off, or saturation, in the log–log relation at the highest Chl-a concentrations, but not as apparent as that found by Irigoien et al. (2004) for a larger combined data set. Comparison of the depth-integrated microzooplankton and phytoplankton biomass resulted in a linear relationship (Fig. 4), although phytoplankton biomass was one to two orders of magnitude greater.

We also confirmed the results of the earlier studies in the Bering Sea that the biomass of herbivorous protists was dominated by heterotrophic dinoflagellates (Table 4). Heterotrophic dinoflagellates ranged from two-thirds to three-quarters of total microzooplankton biomass. The importance of phagotrophic dinoflagellates in marine pelagic systems cannot be overemphasized (Sherr and Sherr, 2007; Jeong et al., 2010). Heterotrophic dinoflagellates often compose $> 60\%$ of total microzooplankton biomass in both oligotrophic and eutrophic conditions (Sherr and Sherr, 2009). In this study, we observed thecate, gymnodinoid dinoflagellates with ingested diatom chains and single diatom cells, which usually greatly distended the dinoflagellate cell (e.g., Fig. 2A and B). Heterotrophic gymnodinoid dinoflagellates are frequently observed during diatom blooms, and have been implicated as important consumers of phytoplankton production, in arctic and subarctic marine systems (Putland, 2000; Levinsen and Nielsen, 2002; Hansen et al., 2003; Strom and Fredrickson, 2008; Suffrian et al., 2008; Sherr et al., 2009; Ardyna et al., 2011). Thecate heterotrophic dinoflagellates were also common and

occasionally seen attached to a diatom cell or chain with an extruded pseudopodial pallium (Fig. 2C).

A surprising observation in our study was that of spirotrichous ciliates with ingested diatom chains (Fig. 2D), or single pennate diatom cells, so large that they distorted the cell. Although benthic ciliates are known to feed on diatoms, pelagic spirotrichous ciliates, e.g., in the genera *Strombidium* and *Strombidinopsis*, are generally considered to consume prey cells much smaller than themselves, mainly nanoflagellates. Smetacek (1981) was the first to report marine pelagic ciliates with ingested large-sized diatoms, in the Kiel Bight, Germany. Subsequently Aberle et al. (2007) found that $> 50 \mu\text{m}$ sized *Strombidium* and *Strombidinopsis* spp. ciliates, rather than heterotrophic dinoflagellates, were the main protist herbivores during mesocosm diatom blooms using water from the Kiel Bight. In their study, the ciliates ingested both diatom chains and single diatom cells equal to, or greater than, the length of the ciliate cell. Johansson et al. (2004) also suggested that ciliates could be significant predators of spring bloom diatoms in the Baltic Sea. Spirotrichous ciliates have additionally been observed with ingested diatom chains in a Brazilian lagoon (Abreu and Odebrecht, 1997). Thus the phenomenon of pelagic ciliates preying on large-sized diatoms may be widespread in the sea.

Other types of protists in our samples were found feeding on diatoms. A variety of heterotrophic flagellates parasitize marine diatoms (Raven and Waite, 2004) and have been suggested to cause significant mortality in diatom blooms in European coastal waters (Tillmann et al., 1999) and in the Bering Sea in summer (Sukhanova et al., 1999). We observed putative parasitoid flagellates feeding on pennate diatom chains during spring (Fig. 2E). We also found thecate amoebae attached to, and apparently sucking out the contents of, centric diatoms in some samples (Fig. 2F). Similar thecate amoebae were reported preying on centric diatoms, mainly *Chaetoceros* sp., during a mesocosm study in the North Sea (Löder et al., 2011).

We also separately assessed the biomass of heterotrophic nanoflagellates via epifluorescence inspection of preserved DAPI-stained samples collected on $0.8 \mu\text{m}$ membrane filters (Sherr et al., 1993) during the 2009 and 2010 cruises (Sherr, unpublished). The average cell size of these flagellates was 2–3 μm , too small to feed on bloom-forming diatoms unless they were parasitoid species. The average biomass of heterotrophic nanoflagellates was 2–4 $\mu\text{g C l}^{-1}$, about 10% of the average biomass of the microzooplankton. These nano-sized protists would be mainly consuming bacteria and other pico-sized prey, and would not be expected to contribute significantly to herbivory in the Bering Sea during spring.

4.4. Specific microzooplankton grazing and growth rates

In situ growth rates of microzooplankton protists are not well constrained, as it is difficult to assess this parameter at natural food abundances and at low in situ temperatures (Sherr and Sherr, 2009). Determining growth rates by change in in situ protist cell abundance is challenging because microzooplankton abundance is typically too low for statistically accurate counts, and because different protist species may be growing at different rates. While we did carry out several long-term (6–10 d) protist growth experiments in the ship's environmental chamber during our cruises, we were able to document positive growth for only a few morphological types of protists, including gymnodinoid dinoflagellates, a *Ptychocylis* sp. tintinnid ciliate, and the testate amoeba.

An alternate method of estimating growth rates for the overall microzooplankton community is to scale carbon-based phytoplankton consumption to microzooplankton biomass (Strom and Fredrickson, 2008). Our specific grazing rates (μg phytoplankton C

per μg MZPC per d) averaged 1.0 d^{-1} for stations with $\text{Chl-a} < 3\ \mu\text{g l}^{-1}$, and 2.0 d^{-1} for stations with $\text{Chl-a} > 3\ \mu\text{g l}^{-1}$ (Table 5). These specific grazing rates are greater than those reported by Strom and Fredrickson (2008) for microzooplankton in the Bering Sea in summer 2004, with average Chl-a of $1.4 \pm 1.0\ \mu\text{g l}^{-1}$. When a C:Chl-a ratio of 50 was assumed, the same ratio used in our calculation, they found average specific rates of about 0.2 to 0.6 d^{-1} . The high rates we estimated for bloom stations are due, in part, to higher phytoplankton biomass, which allowed for higher protist specific ingestion rates.

Based on biomass-specific consumption of phytoplankton carbon, and assuming a gross growth efficiency of 30%, we determined microzooplankton community growth rates of $0.33 \pm 0.50\text{ d}^{-1}$ for dilution experiments for stations with $\text{Chl-a} < 3\ \mu\text{g l}^{-1}$, and $0.43 \pm 0.37\text{ d}^{-1}$ for stations with $\text{Chl-a} > 3\ \mu\text{g l}^{-1}$ (Table 5). The mean estimated growth rate for microzooplankton at non-bloom stations was not significantly different from growth rates at bloom stations due to the limited amount of data and high variability in estimated growth rates. Growth rates of over 1 d^{-1} were found at some stations. These estimated microzooplankton growth rates are in the range of phytoplankton growth rates determined from dilution assays in our study (Table 2).

4.5. Role of microzooplankton in controlling phytoplankton blooms at cold water temperatures

The fact that microzooplankton graze a significant fraction of diatom production in the Bering Sea during spring (Table 3) argues against the 'loophole' hypothesis of Irigoien et al. (2005). Heterotrophic dinoflagellates, as well as other protists, were able to feed on the dominate diatom species composing the spring blooms (examples shown in Fig. 2).

The hypothesis of Rose and Caron (2007) of lower protist growth rates at cold temperature is hampered by lack of relevant data. Their comparison of the maximum growth rates (μ_{Max}) of phytoplankton (mainly diatoms) and of herbivorous protists at cold water temperature was limited to data on growth rates of a laboratory-cultured filter-feeding ciliate and a nanoflagellate grown on algae $< 20\ \mu\text{m}$ in size. These protists are not representative of microzooplankton grazers, predominately heterotrophic dinoflagellates, which prey on large-sized and chain-forming diatoms. In addition, phagotrophic protists living in cold water habitats may be physiologically adapted to low temperature.

Our study showed that growth rates of the microzooplankton community were potentially equivalent to phytoplankton growth rates at the cold temperatures ($< 4\text{ }^\circ\text{C}$) characteristic of the Bering Sea in spring (Table 5). During blooms, while average phytoplankton growth rate was only 0.22 d^{-1} , microzooplankton growth rates were higher, averaging 0.43 d^{-1} . The rates of microzooplankton growth we estimated are similar to the rate, 0.3 d^{-1} , empirically determined by Bjørnsen and Kuparinen (1991) for herbivorous dinoflagellates, *Gymnodinium* spp., in the Southern Ocean at water temperatures of $< 0\text{ }^\circ\text{C}$. Levinsen and Nielsen (2002) also found that heterotrophic dinoflagellates could grow rapidly during spring diatom blooms in Disko Bay, Greenland, with water temperatures of -1.8 to $6\text{ }^\circ\text{C}$. These findings do not support the hypothesis of Rose and Caron (2007) of lower protist growth rates compared to phytoplankton growth rates at temperatures $< 10\text{ }^\circ\text{C}$ in high-latitude marine systems.

We have previously argued that hypotheses about the initiation of diatom blooms as a result of escape from microzooplankton grazing have largely ignored the well-known relationship between protist grazing and growth rates and prey abundance (Sherr and Sherr, 2009). A main reason that microzooplankton are not likely to prevent the initiation of a diatom bloom is due to the disparity in growth rates of diatoms and herbivorous protists in the early stages

of a bloom. At the beginning of a bloom, when phytoplankton biomass is low, diatom cells grow at the maximum rate at which nutrient supply, light, and temperature allow. The growth rate of herbivorous protists, however, is related to prey biomass by a functional response curve in which growth rates are much less than μ_{Max} at low food abundance, and only approach μ_{Max} when prey biomass is high. While protist μ_{Max} may vary by two- to four-fold over a range of environmental temperatures, as shown by Rose and Caron (2007), at any one temperature the specific growth rate can vary over more than an order of magnitude depending on how much prey food is available (Sherr and Sherr, 2009). The result of this functional relationship is very low growth rates, and thus potential grazing rates, of herbivorous protists at the beginning of a bloom when phytoplankton biomass is low. Phytoplankton blooms, and in particular diatom blooms, occur because autotrophic cells have intrinsically higher growth rates compared to protist predators in the early stages of bloom development. Microzooplankton grazers can, however, limit biomass accumulation by cropping a portion of daily production as the bloom matures.

Growth rates of microzooplankton grazers do respond positively to higher water temperature in both arctic and temperate habitats (Levinsen and Nielsen, 2002; Aberle et al., 2007; Hunt et al., 2010). However, bottom-up (prey abundance) and top-down (predation mortality) factors are likely to supersede temperature effect on growth rates of protistan herbivores in cold temperature marine ecosystems. Modeling the grazing impact of microzooplankton in the Bering Sea as climate change affects sea ice extent and water temperature will not be straightforward.

4.6. Conclusions

During spring sea ice conditions in the Bering Sea, both phytoplankton growth rate and microzooplankton grazing impact was highly variable. Microzooplankton grazing averaged about 40–50% of daily phytoplankton production, higher than that previously reported for the Western Arctic Ocean (Sherr et al., 2009), but lower than microzooplankton herbivory in the Bering Sea during summer (Table 6). An unexpected variety of protists were observed feeding on bloom-forming diatom chains and cells, including athecate and thecate dinoflagellates, species of spirotrichous ciliate, parasitoid flagellates, and a thecate amoeba. Microzooplankton biomass was high and was positively related to phytoplankton stocks. Growth rates estimated for the microzooplankton community, based on amount of phytoplankton carbon consumed, were in the same range as phytoplankton growth rates. Microzooplanktonic protists have a central role in pelagic food webs during spring diatom blooms in the Bering Sea, and should be incorporated into ecosystem models of this region.

Acknowledgments

We are indebted to the captain and crew of the U.S. Coast Guard Healy for their expert support during the BEST cruises, to Calvin Mordy and the BEST CTD service group for their help in collecting seawater samples for experiments and for nutrient analyses, and to Julie Arrington for technical help at sea. Funding for this project was provided by NSF grant 0124892-OPP to B. and E. Sherr. This is BEST-BSIERP Bering Sea Project publication number 103.

References

- Aberle, N., Lengfellner, K., Sommer, U., 2007. Spring bloom succession, grazing impact and herbivore selectivity of ciliate communities in response to winter warming. *Oecologia* 150, 668–681.

- Abreu, P.C., Odebrecht, C., 1997. Bacteria and protozooplankton. In: Seeliger, U., Odebrecht, C., Castello, J.P. (Eds.), *Subtropical Convergence Environments, the Coast and Sea in the Southwestern Atlantic*. Springer, Berlin, pp. 37–39.
- Ardaya, M., Gosselin, M., Michel, C., Poulin, M., Tremblay, J.E., 2011. Environmental forcing of phytoplankton community structure and function in the Canadian High Arctic: contrasting oligotrophic and eutrophic regions. *Mar. Ecol. Prog. Ser.* 442, 37–57.
- Banse, K., 1982. Cell volume, maximal growth rates of unicellular algae and ciliates, and the role of ciliates in the marine pelagial. *Limnol. Oceanogr.* 27, 1059–1071.
- Bjørnsen, P.K., Kuparinen, J., 1991. Growth and herbivory by heterotrophic dinoflagellates in the Southern Ocean, studied by microcosm experiments. *Mar. Biol.* 109, 397–405.
- Buitenhuis, E.T., Rivkin, R.B., Sailley, S., Le Quéré, C., 2010. Biogeochemical fluxes through microzooplankton. *Global Biogeochem. Cycles* 24, GB4015, <http://dx.doi.org/10.1029/2009GB003601>.
- Calbet, A., 2008. The trophic roles of microzooplankton in marine systems. *ICES J. Mar. Sci.* 65, 325–331.
- Calbet, A., Landry, M.R., 2004. Phytoplankton growth, microzooplankton grazing, and carbon cycling in marine systems. *Limnol. Oceanogr.* 40, 51–57.
- Calbet, A., Saiz, E., 2005. The ciliate–copepod link in marine ecosystems. *Aquat. Microb. Ecol.* 38, 157–167.
- Campbell, R.G., Sherr, E.B., Ashjian, C.J., Plourde, S., Sherr, B.F., Hill, V., Stockwell, D.A., 2009. Mesozooplankton prey preference and grazing impact in the Western Arctic Ocean. *Deep-Sea Res. II* 56, 1274–1289.
- Chen, M., Liu, H., 2011. Experimental simulation of trophic interactions among omnivorous copepods, heterotrophic dinoflagellates and diatoms. *J. Exp. Mar. Biol. Ecol.* 403, 65–74.
- Dolan, J.R., Gallegos, C.L., Moigis, A., 2000. Dilution effects on microzooplankton in dilution grazing experiments. *Mar. Ecol. Prog. Ser.* 200, 127–139.
- Gallegos, C.L., 1989. Microzooplankton grazing on phytoplankton in the Rhode River, Maryland: nonlinear feeding kinetics. *Mar. Ecol. Prog. Ser.* 57, 23–33.
- Gifford, D.J., 1988. Impact of grazing by microzooplankton in the Northwest Arm of Halifax Harbour, Nova Scotia. *Mar. Ecol. Prog. Ser.* 47, 249–258.
- Hansen, A.S., Nielsen, T.G., Levensen, H., Madsen, S.D., Thingstad, T.F., Hansen, B.W., 2003. Impact of changing ice cover on pelagic productivity and food web structure in Disko Bay, West Greenland: a dynamic model approach. *Deep-Sea Res.* 1 50, 171–187.
- Howell-Kübler, A.N., Lessard, E.J., Napp, J.M., 1996. Springtime microprotozoan abundance and biomass in the southeastern Bering Sea and Shelikof Strait, Alaska. *J. Plankton Res.* 18, 731–745.
- Hunt, G.L., Stabeno, P., Walters, G., Sinclair, E., Brodeur, R.D., Napp, J.M., Bond, N.A., 2002. Climate change and control of the southeastern Bering Sea pelagic ecosystem. *Deep-Sea Res. II* 49, 5821–5853.
- Hunt, G.L., Stabeno, P., Strom, S., Napp, J.M., 2008. Patterns of spatial and temporal variation in the marine ecosystem of the southeastern Bering Sea, with special reference to the Pribilof Domain. *Deep-Sea Res. II* 55, 1919–1944.
- Hunt, G.L., Allen, B.M., Angliss, R.P., Baker, T., Bond, N., Buck, G., Byrd, G.V., Coyle, K.O., Devol, A., Eggers, D.M., Eisner, L., Feely, R., Fitzgerald, S., Fritz, L.W., Gritsai, E.V., Ladd, C., Lewis, W., Mathis, J., Mordy, C.W., Mueter, F., Napp, J., Sherr, E., Shull, D., Stabeno, P., Stepanenko, M.A., Strom, S., Whitledge, T.E., 2010. Status and trends of the Bering Sea region, 2003–2008. In: McKinnell, S.M., Dagg, M.J. (Eds.), *The Marine Ecosystems of the North Pacific Ocean; Status and Trends, 2003–2008*. ICES, pp. 196–267.
- Hunt Jr., G.L., Coyle, K.O., Eisner, L., Farley, E.V., Heintz, R., Mueter, F., Napp, J.M., Overland, J.E., Ressler, P.H., Salo, S., Stabeno, P.J., 2011. Climate impacts on eastern Bering Sea food webs: a synthesis of new data and an assessment of the oscillating control hypothesis. *ICES J. Mar. Sci.*, <http://dx.doi.org/10.1093/icesjms/fsr036>.
- Irigoin, X., Huisman, J., Harris, R.P., 2004. Global biodiversity patterns of marine phytoplankton and zooplankton. *Nature* 429, 863–867.
- Irigoin, X., Flynn, K.J., Harris, R.P., 2005. Phytoplankton blooms: a 'loophole' in microzooplankton grazing impact? *J. Plankton Res.* 27, 313–321.
- Jeong, H.J., Yoo, Y.D., Kim, S.T., Kang, N.S., 2004. Feeding by the heterotrophic dinoflagellate *Protoperidinium bipes* on the diatom *Skeletonema costatum*. *Aquat. Microb. Ecol.* 36, 171–179.
- Jeong, H.J., Yoo, Y.D., Kim, J.S., Seong, K., Ah Kang, N.S., Kim, T.H., 2010. Growth, feeding and ecological roles of the mixotrophic and heterotrophic dinoflagellates in marine planktonic food webs. *Ocean Sci. J.* 45, 65–91.
- Johansson, M., Gorokhova, E., Larsson, U., 2004. Annual variability in ciliate community structure, potential prey and predators in the open northern Baltic Sea proper. *J. Plankton Res.* 26, 67–80.
- Landry, M.R., 1993. Estimating rates of growth and grazing mortality of phytoplankton by the dilution method. In: Kemp, P.F., Sherr, B.F., Sherr, E.B., Cole, J.J. (Eds.), *Handbook of Methods in Aquatic Microbial Ecology*. Lewis Publ., Boca Raton, FL, pp. 715–722.
- Landry, M.R., Calbet, A., 2004. Microzooplankton production in the oceans. *ICES J. Mar. Sci.* 61, 501–507.
- Landry, M.R., Brown, S.L., Rii, Y.M., Selph, K.E., Bidigare, R.R., Yang, E.J., Simmons, M.P., 2008. Depth-stratified phytoplankton dynamics in Cyclone Opal, a subtropical mesoscale eddy. *Deep-Sea Res. II* 55, 1348–1359.
- Lessard, E.J., Martin, M.P., Montagnes, D.J.S., 1996. A new method for live-staining protists with DAPI and its application as a tracer of ingestion by walleye pollock (*Theragra chalcogramma*) larvae. *J. Exp. Mar. Biol. Ecol.* 204, 43–57.
- Levensen, H., Nielsen, T.G., 2002. The trophic role of marine pelagic ciliates and heterotrophic dinoflagellates in arctic and temperate coastal ecosystems: a cross-latitude comparison. *Limnol. Oceanogr.* 47, 427–439.
- Levensen, H., Nielsen, T.G., Hansen, B.W., 1999. Plankton community structure and carbon cycling on the western coast of Greenland during the stratified summer situation. II. Heterotrophic dinoflagellates and ciliates. *Aquatic Microb. Ecol.* 16, 217–232.
- Liu, H., Suzuki, K., Saino, T., 2002. Phytoplankton growth and microzooplankton grazing in the subarctic Pacific Ocean and the Bering Sea during summer 1999. *Deep-Sea Res.* I 49, 363–375.
- Löder, M.G., Meunier, C., Wiltshire, K.H., Boersma, M., Aberle, N., 2011. The role of ciliates, heterotrophic dinoflagellates and copepods in structuring spring plankton communities at Helgoland Roads, North Sea. *Mar. Biol.* 158, 1551–1580.
- Lomas, M.W., Moran, S.B., Casey, J.R., Bell, D.W., Tiahlo, M., Whitefield, J., Kelly, R.P., Mathis, J.T., Cokelet, E.D., 2012. Spatial and seasonal variability of primary production on the Eastern Bering Sea shelf. *Deep-Sea Res.* II 65–70, 126–140.
- Menden-Deuer, S., Lessard, E., 2000. Carbon to volume relationships for dinoflagellates, diatoms, and other protist plankton. *Limnol. Oceanogr.* 45, 569–579.
- Montagnes, D.J.S., Dower, J.F., Figueiredo, G.M., 2010. The protozooplankton–ichthyoplankton trophic link: an overlooked aspect of aquatic food webs. *J. Eukaryot. Microbiol.* 57, 223–228.
- Moran, S.B., Lomas, M.W., Kelly, R.P., Iken, K., Gradinger, R., Mathis, J.T., 2012. Seasonal succession of net primary productivity, particulate organic carbon export, and autotrophic community composition in the eastern Bering Sea. *Deep-Sea Res.* II 65–70, 84–97.
- Neuer, S., Cowles, T.J., 1994. Protist herbivory in the Oregon upwelling system. *Mar. Ecol. Prog. Ser.* 113, 147–162.
- Olsen, Y., Anderson, T., Gismervik, I., Vladstein, O., 2006. Protozoan and metazoan zooplankton-mediated carbon flows in nutrient-enriched coastal planktonic communities. *Mar. Ecol. Prog. Ser.* 331, 67–83.
- Olson, M.B., Strom, S.L., 2002. Phytoplankton growth, microzooplankton herbivory and community structure in the southeast Bering Sea: insight into the formation and temporal persistence of an *Emiliania huxleyi* bloom. *Deep-Sea Res.* II 49, 5969–5990.
- Parsons, T., Maita, Y., Lalli, C., 1984. *A Manual of Chemical and Biological Methods for Seawater Analysis*. Pergamon Press, New York.
- Putland, J.N., 2000. Microzooplankton herbivory and bacterivory in Newfoundland coastal waters during spring, summer, and winter. *J. Plankton Res.* 22, 253–277.
- Putt, M., Stoecker, D.K., 1989. An experimentally determined carbon: volume ratio for marine "oligotrichous" ciliates from estuarine and coastal waters. *Limnol. Oceanogr.* 34, 1097–1103.
- Raven, J.A., Waite, A.M., 2004. The evolution of silicification in diatoms: inescapable sinking and sinking as escape? *New Phytol.* 162, 45–61.
- Roff, J.C., Hopcroft, R.R., 1986. High precision microcomputer based measuring system for ecological research. *Can. J. Fish. Aquat. Sci.* 43, 2044–2048.
- Rose, J.M., Caron, D.A., 2007. Does low temperature constrain the growth rate of heterotrophic protists? Evidence and implications for algal blooms in cold waters. *Limnol. Oceanogr.* 52, 886–895.
- Sherr, E.B., D.A. Caron, and B.F. Sherr. 1993. Staining of heterotrophic protists for visualization via epifluorescence microscopy. p. 213–228. In: P. Kemp, B. Sherr, E. Sherr, and J. Cole (eds), *Current Methods in Aquatic Microbial Ecology*, Lewis Publ., NY.
- Sherr, E.B., Sherr, B.F., 2002. Significant of predation by protists in aquatic microbial food webs. *Antonie van Leeuwenhoek Int. J. Gen. Mol. Microbiol.* 81, 293–308.
- Sherr, E.B., Sherr, B.F., 2007. Heterotrophic dinoflagellates: a significant component of microzooplankton biomass and major grazers of diatoms in the sea. *Mar. Ecol. Prog. Ser.* 352, 187–197.
- Sherr, E.B., Sherr, B.F., 2009. Capacity of herbivorous protists to control initiation and development of mass phytoplankton blooms. *Aquat. Microb. Ecol.* 57, 253–262.
- Sherr, E.B., Sherr, B.F., Hartz, A.J., 2009. Microzooplankton grazing impact in the Western Arctic Ocean. *Deep-Sea Res. II* 56, 1264–1273.
- Smetacek, V., 1981. The annual cycle of protozooplankton in the Kiel Bight. *Mar. Biol.* 63, 1–11.
- Stabeno, P.J., Kachel, N.B., Sullivan, M., Whitledge, T.E., 2002. Variability of physical and chemical characteristics along the 70-m isobath of the southeast Bering Sea. *Deep-Sea Res. II* 49, 5931–5943.
- Stabeno, P., Kachel, N., Moore, S., Napp, J., Sigler, M., Zerbini, A.N., 2012. Comparison of warm and cold years on the southeastern Bering Sea shelf and some implications for the ecosystem. *Deep Sea Res. II* 65–70, 31–45.
- Straile, D., 1997. Gross growth efficiencies of protozoan and metazoan zooplankton and their dependence on food concentration, predator–prey weight ratio, and taxonomic group. *Limnol. Oceanogr.* 42, 1375–1385.
- Strom, S.L., Fredrickson, K.A., 2008. Intense stratification leads to phytoplankton nutrient limitation and reduced microzooplankton grazing in the southeastern Bering Sea. *Deep-Sea Res.* 55, 1761–1774.
- Suffrian, K., Simonelli, P., Nejtgaard, J.C., Putzeys, S., Carotenuto, Y., Antia, A.N., 2008. Microzooplankton grazing and phytoplankton growth in marine mesocosms with increased CO₂ levels. *Biogeosciences* 5, 1145–1156.
- Sukhanova, I., Semina, H., Venttsel, M., 1999. Spatial distribution and temporal variability of phytoplankton in the Bering Sea. In: Loughlin, T., Ohtani, K. (Eds.), *Dynamics of the Bering Sea*. University of Alaska Sea Grant, Fairbanks, pp. 453–484.
- Tillmann, U., Hesse, K.-J., Tillmann, A., 1999. Large-scale parasitic infection of diatoms in the Northfrisian Wadden Sea. *J. Sea Res.* 42, 255–261.
- Verity, P.G., Wassmann, P., Frischer, M.E., Howard-Jones, M.H., Allen, A.E., 2002. Grazing of phytoplankton by microzooplankton in the Barents Sea during early summer. *J. Mar. Syst.* 38, 109–123.
- Welschmeyer, N.A., 1994. Fluorometric analysis of chlorophyll a in the presence of chlorophyll b and pheopigments. *Limnol. Oceanogr.* 39, 1985–1992.



Temporal changes in benthic ostracode assemblages in the Northern Bering and Chukchi Seas from 1976 to 2010



L. Gemery^{a,b,*}, T.M. Cronin^a, L.W. Cooper^{b,c}, J.M. Grebmeier^{b,c}

^a USGS National Center, 12201 Sunrise Valley Drive, Reston, VA 20192, USA

^b Marine, Estuarine and Environmental Science Graduate Program, University of Maryland, College Park, MD, USA

^c Chesapeake Biological Laboratory, University of Maryland Center for Environmental Science, PO Box 38, Solomons, MD, USA

ARTICLE INFO

Available online 14 March 2013

Keywords:

Bering Sea
Chukchi Sea
Benthic
Ecosystem change
Ostracodes
Meiofauna

ABSTRACT

We analyzed living ostracode assemblages from the northern Bering Sea, collected between 1976 and 2010, and from the Chukchi Sea, collected in 2009 and 2010, to examine how climatic and oceanographic changes are affecting modern ostracode species distributions. Totals of 21 and 28 ostracode species were identified, respectively, from Bering and Chukchi Sea surface sediment samples. The Bering Sea assemblage is largely transitional in species composition between those inhabiting western Arctic continental shelves and the subarctic Gulf of Alaska. Temporal changes in the Bering Sea assemblage provide evidence that decadal temperature changes have affected species composition. For example, the proportion of *Normanicythere leioderma*, a predominantly Arctic species, decreased from 70% of the total assemblage population in 1999 to 15% by 2006. This decrease coincided with a shift in the Arctic Oscillation toward a positive mode and warmer Bering sea-surface temperatures (SST) beginning in the early 2000s. In contrast, the more temperate species, *Pectocythere janae* (also known as *Kotoracythere arctoborealis*) made up less than 4% of the Bering assemblage prior to 2000 but increased in abundance to as much as 30% as Bering Sea temperatures rose from 2001 to 2006. This pattern has reversed since 2006 when cooler temperatures led to a decline in *P. janae* and return in the prominence of *N. leioderma*. Our results support the idea that recent ocean temperature changes and a reduced sea-ice season in the Bering–Chukchi Sea region are changing species composition in benthic ecosystems.

Published by Elsevier Ltd.

1. Introduction

As surface temperatures rise in the Arctic Ocean and sub-polar seas, satellite observations document a corresponding reduction in the extent, thickness, and duration of seasonal sea-ice cover (Stroeve et al., 2008) and a potential increase in primary production as a result of greater light penetration into sea ice-free waters (Pabi et al., 2008). In recent years, Arctic multi-year ice has declined by almost 50% in extent, and fall freeze-up occurs later in the year (Serreze et al., 2007; Stroeve et al., 2008). Model results indicate these trends will continue, and that the Arctic Ocean might become predominantly ice-free in summer in a few decades (Wang and Overland, 2009). Sea-ice retreat has been particularly dramatic in the Arctic Ocean just north of the Bering Strait; sea-ice retreats in 2007 and 2009 lengthened the

open-water season by about four weeks compared with a decade ago (Grebmeier et al., 2010).

While these patterns of sea-ice decline are well documented, much less is known about the responses of biological communities to ice cover changes. According to Yasuhara et al. (2012a) sea-ice cover is an important factor controlling benthic faunal distributions and species diversity. Here we present new data on benthic ostracode distributions from the Chukchi Sea continental shelf, the Chirikov Basin of the northern Bering Sea, and the area south of St. Lawrence Island (Fig. 1). Ostracodes have environmentally sensitive distributions, and water temperature is one of the most influential factors controlling reproduction, survival, geographic distribution and diversity (Hutchins, 1947; Smith and Horne, 2002; Yasuhara et al., 2009). Ostracodes are meio-benthic, bivalved Crustacea, and have several distinct advantages for retrospective ecosystem studies. Their calcium carbonate shells are preserved in marine sediments enabling species identification from shell morphology, even after their soft parts decompose. Unlike macrofaunal species, which cannot be analyzed quantitatively in sediment cores because of their size and scarcity, adult ostracodes range in size from 0.5 mm to 2 mm and can be quantified in small samples available from individual grab and/or

* Corresponding author at: USGS National Center, 12201 Sunrise Valley Drive, Reston, VA 20192, USA. Tel.: +1 703 648 6021; fax: +1 703 648 6032.

E-mail addresses: lgemery@usgs.gov (L. Gemery), tcronin@usgs.gov (T.M. Cronin), cooper@umces.edu (L.W. Cooper), jgrebmei@umces.edu (J.M. Grebmeier).

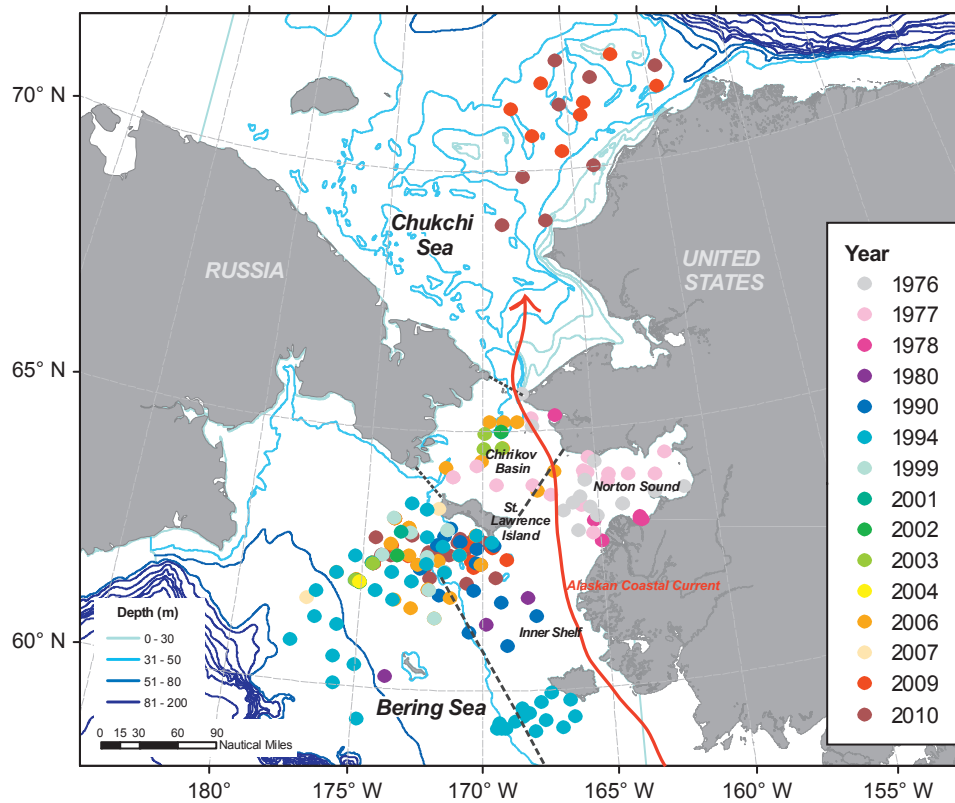


Fig. 1. Bathymetry of the Bering and Chukchi seas and locations of 225 Bering Sea and 18 Chukchi Sea surface sediments analyzed in this study, color-coded by year of collection.

core samples. Moreover, marine ostracode species have biogeographical and ecological limits controlled by temperature, salinity, or nutrient/food availability (Cronin et al., 2010a; Stepanova et al., 2007; Yasuhara et al., 2012a). Consequently, these crustaceans are used extensively in paleoecology and paleoclimatology to document climatically driven changes in ocean temperature, circulation, salinity, and ocean productivity (e.g.; Cronin et al., 1994, 1996, 2005, 2010b; Didié and Bauch, 2000; Yasuhara et al., 2012a, 2012b). In this study, we sought to determine whether recent changes in temperature and ice cover in the Bering Sea have affected species distributions. To the best of our knowledge, this is the first published report on modern ostracode fauna from the northern Bering shelf. Adjacent areas where ostracode data are available include the Arctic Ocean (Cronin et al., 2010b) including the Chukchi/Beaufort Seas to the north of Bering Strait (Joy and Clark, 1977) and the Gulf of Alaska to the south of the Bering Sea (Brouwers, 1990; 1993; 1994).

1.1. Environmental setting

The Bering and Chukchi Seas are among the world's most productive ecosystems supporting high, seasonal primary productivity that exceeds $1 \text{ gC m}^{-2} \text{ d}^{-1}$ during the spring bloom (Brown et al., 2011; Springer et al., 1996) as well as diverse invertebrate, fish, seabird, and marine mammal populations (National Research Council, 1996). About 50% of the Bering Sea is a wide continental shelf to the north and east, which is less than 200 m in depth (Brown et al., 2011). This shelf extends through the Bering Strait into the Chukchi continental shelf in the western Arctic Ocean.

The Bering Sea is located in a transition region between a generally cold, dry Arctic air mass to the north and moist, relatively warm air to the south (Mantua and Hare, 2002). Hunt and Stabeno

(2002) concluded that the southeastern Bering Sea climate is jointly influenced by both the Pacific Decadal Oscillation (PDO) and the Arctic Oscillation (AO). The PDO is a multi-decadal pattern of Pacific climate variability involving air–ocean interactions that create current and sea surface temperature changes in the North Pacific (Mantua and Hare, 2002). In contrast, the northern Bering Sea, which we define as the shelf north of St. Matthew Island (approximately 61–65°N), and the Chukchi Sea are more directly influenced by the AO (Grebmeier et al., 2006a, 2006b). The state of the AO is determined by the atmospheric pressure gradient in the high Arctic, and it alternates between negative (high pressure over the North Pole) and positive (low pressure) modes. This coupled air–sea interaction is closely linked to the strength and position of the Beaufort Gyre in the Arctic Ocean. From 1989 to 2006, the AO was predominantly in a positive mode, causing lower Arctic air pressure and higher sea surface temperatures in the Arctic Ocean (Overland et al., 2008). NOAA's Climate Prediction Center (<http://www.cpc.ncep.noaa.gov/>) indicates that the AO has been in a negative mode for the period 2009–2010 but has exhibited an overall positive trend since 1989.

These air–sea interactions, and also anthropogenic factors, have contributed to interannual and decadal changes in temperature and sea ice in the North American Arctic over the last several decades (Overland et al., 2008; Serreze et al., 2007). These changes have happened in the context of general circulation in the Bering and Chukchi Seas, which is influenced by three northward flowing water masses arrayed east to west: less saline and nutrient-poor Alaska coastal water (Fig. 1); a mixed, more saline Bering Shelf water mass to the west; and a seasonally cold and even more saline Anadyr water mass further to the west (Stabeno et al., 2007; Belkin et al., 2009). As these water masses extend into the Chukchi Sea, the differences between the mixed shelf water and Anadyr water become less distinct; and there are also

differences in temperature, nutrients and salinity depending upon the season when N. Bering Sea water passes through Bering Strait (Cooper et al., 2013).

One example of recent change is the duration of the open water season. The Chirikov Basin, located to the north of St. Lawrence Island and extending to Bering Strait, has had an open-water season increase of 25 days during the past 25 years (Fig. 2). (The Chirikov Basin is bounded by St. Lawrence Island to the south, the Chukotka peninsula to the west, the Seward peninsula to the east, and Bering Strait to the north.) This has changed not only the timing of when primary productivity peaks but may also increase production due to a longer, sustained bloom (Arrigo et al., 2008; Brown et al., 2011; Brown and Arrigo, 2012). In the Bering and Chukchi Sea region, ecosystem reorganization (also called a regime shift, Bluhm and Gradinger, 2008; Hare and Mantua, 2000) may be related to changing seasonal sea-ice conditions, which can alter benthic-pelagic ecosystem processes and cause a cascade of consequences through the food web (Grebmeier et al., 2006a). Biological observations in these areas have documented changes in species composition and northward range extensions for zooplankton, bottom-dwelling organisms and fish that may collectively signify a large, climate-driven ecosystem reorganization (Grebmeier, 2012; Mueter and Litzow, 2008).

Despite these changes in the northern Bering Sea and Chukchi Sea, it is important to note that similar sea-ice changes are not being consistently observed further to the south in the Bering Sea

(Stabeno et al., 2012). In winter, the southern margin of sea-ice coverage in the Bering Sea reaches an annual maximum by March, but sea ice is in part uncoupled from sea-ice retreat to the north because of the semi-enclosed nature of the marginal sea. Ice duration in the southern Bering Sea and along the continental margin, although varying from year to year, has not consistently changed over the time period we consider here (Fig. 2; Brown et al., 2011).

2. Materials and methods

2.1. Ostracode sampling

A total of 225 northern Bering Sea surface sediment samples containing 5972 ostracode valves and carapaces were collected during a number of cruises from 1976 to 2010 (Table 1). Most samples came from the central and northern Bering Sea continental shelf, with additional samples from Norton Sound collected in 1976–1978 (Fig. 1). The 1977 cruise also included sampling locations in the Chirikov Basin, immediately north of St. Lawrence Island. Sixteen surface sediment samples from the Chukchi shelf contained 1198 specimens. Samples were collected from water depths ranging from 10 to 110 m and were taken from

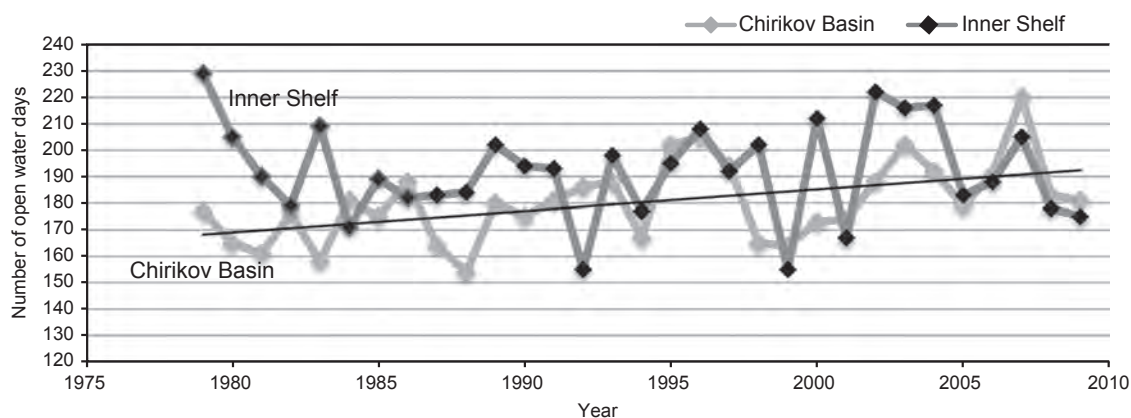


Fig. 2. Number of open water days (reflecting length of ice-free period) in the Chirikov Basin (blue line) and along the Inner shelf (red line), 1979–2009. The trend line shows open water duration in the Chirikov Basin (north of St. Lawrence Island) has increased over these three decades, accounting for an ice loss of $\sim 77 \pm 37$ km² of ice per year, with ice exiting by mid-June (Brown et al., 2011). “Open water” is defined as a satellite-derived sea-ice concentration below 10%. (For interpretation of the references to color in this figure caption, the reader is referred to the web version of this article.)

Table 1

Listing of research cruises by year, month, ship, and region, from which samples for this study were collected.

Year	Month	Ship	Region
2010	March	USCGC Polar Sea	South of St. Lawrence Island
2009	March	USCGC Healy	South of St. Lawrence Island
2007	May–June	USCGC Healy	Chirikov and South of St. Lawrence Island
2006	May–June	USCGC Healy	Chirikov and South of St. Lawrence Island
2004	July	CCGS Sir Wilfrid Laurier	Chirikov and South of St. Lawrence Island
2003	July	CCGS Sir Wilfrid Laurier	Chirikov and South of St. Lawrence Island
2002	July	CCGS Sir Wilfrid Laurier	Chirikov and South of St. Lawrence Island
2001	July	CCGS Sir Wilfrid Laurier	Chirikov and South of St. Lawrence Island
1999	April	USCGC Polar Sea	South of St. Lawrence Island
1994	May–June	RV Alpha Helix	South of St. Lawrence Island
1990	June	RV Alpha Helix	South of St. Lawrence Island
1980	August	Samuel Phillips Lee	South of St. Lawrence Island
1978	August–September	Sea Sounder	Norton Sound, Bering
1978	July	Karluk	Norton Sound, Bering
1977	July–August	Sea Sounder	Chirikov and Norton Sound
1976	March	Sea Sounder	Chirikov and Norton Sound
2009	July–August	RV Alpha Helix	Chukchi
2010	July–August	RV Moana Wave	Chukchi

the top of Van Veen grabs before the grab was opened, or from the top of HAPS (a frame-supported bottom corer) and box corers.

Sediments ranged from silty clay to sand. Ostracodes were generally more abundant in silty clay sediments than in coarser sandy sediments, which likely results from slower deposition in more hydrodynamically active areas.

We assume that ostracode assemblages preserved in continental shelf surface sediments in this region are organisms that were living at or shortly before the time of collection. This assumption is supported by ^{7}Be data in sediment cores that were collected from the Canadian Coast Guard Service vessel Sir Wilfrid Laurier in July 1998 at six stations in the Chukchi Sea north of Bering Strait that have been incorporated into a Distributed Biological Observatory for the Pacific Arctic region (Grebmeier et al., 2010). These data indicate that this atmospherically derived radionuclide (^{7}Be , half-life 53d) is present in the surface 0–1 cm sediments and was not detected at all at depths of 4 cm or greater (L.W. Cooper, unpublished data).

With a few exceptions, the ostracode data we report here involved spring and summer cruise collections. Sometimes the shells of molts or dead specimens from prior years are also recovered. In the case of Bering Sea ostracodes, most assemblages included adult specimens and juvenile molts, and 60% of the specimens were articulated carapaces, or carapaces with chitinous appendages. A few samples contained Rose bengal-stained specimens. Rose bengal stains cytoplasm, so this method can help distinguish specimens that were alive at the time of collection. A few reworked specimens from prior years, identified by broken or abraded specimens, are expected in a continental shelf setting. Thus, we consider the faunal data presented here to be largely representative of the live species assemblages present at the time that the ostracode samples were collected. We expect that these species assemblage data will be useful for detecting decadal and, in some cases, large interannual changes in the ecosystem.

2.2. Sample processing

Ostracodes were separated from 20 to 100 g sediment aliquots by washing the samples with tap water through a 63- μm sieve. Samples were then dried in a convection oven at 50 °C for 12–24 h. The > 63- μm size fraction includes adults and most juvenile molts of all species. Ostracodes were picked from the > 125 μm sediment size fractions with a fine, damp brush under a light microscope and placed on slides. The > 125 μm fraction is conventionally used because ostracode carapaces are usually larger than this, with the exception of some early instars. Species were identified primarily following the taxonomy and scanning electron microscope (SEM) imagery provided in Stepanova et al. (2007) and Brouwers (1990, 1993, 1994). Identification is based primarily on physical features such as carapace morphology (shape and size), pore size, and pore distribution, hinge characteristics, and shell ornamentation.

Species abundances (relative frequencies), which we define as the percentage of each species of the total ostracode assemblage, were calculated for each sample. Abundances were computed by dividing the number of individual species found in each sample by the total number of specimens found in that sample and then multiplying the result by 100 to convert to percent. Density was calculated by dividing the total number of ostracode specimens found in each sample by the dry sediment weight (grams) of that sample.

2.3. Sources of temperature and sea-ice data

Mean summer Sea Surface Temperature (SST) data (1982–2009) for the Chirikov Basin and Inner Shelf regions are based on the Reynolds Optimum Interpolation SST (OISST) Version 2 product

derived from the Advanced Very High Resolution Radiometer (AVHRR) at 0.25° resolution available from NOAA (Brown et al., 2011). We used the geographic boundaries for the Chirikov Basin and Inner Shelf regions defined in Brown et al., 2011, Fig. 1. For these two regions, depth averages between 0 and 50 m. “Summer” is defined as July, August and September. Annual mean Bering Sea summer bottom water temperatures (BWT) and May SST (Fig. 5A) were obtained from the Bering Climate and Ecosystem data archive (<http://www.beringclimate.noaa.gov/data/>). BWT data were collected from bottom trawl surveys across the eastern Bering Sea shelf from early June to early August, during the years 1982–2007. The spatial coverage spans approximately latitudes 54.5–62°N and longitudes 179–158°W, with stations gridded at roughly 20 nautical miles distance (248–317 stations/yr).

The May SST data from the southeastern Bering Sea (defined as 54.3–60.0°N, 161.2–172.5°W) is probably the best long-term regional water temperature data set. These data were summarized in the NCEP/NCAR Reanalysis project (Kalnay et al., 1996). Index values of the data are defined as deviations from the mean value (2.48 °C) for the 1961–2000 period normalized by the standard deviation (0.73 °C). We recognize that the northern and southern Bering Sea regions have different temperature histories, with more seasonality in the north due to greater surface warming from the influence of Alaska Coastal water (Fig. 1). Because the central-northern Bering Sea is shallow (< 50 m) and well mixed, SST and BWT patterns generally show broad decadal patterns but do not provide year- and site-specific temperature data for our study region or precise temperature ranges that ostracode species require. Nonetheless, the southeastern Bering record is the best available annual spring–summer record covering the study period and appears to represent regional temperature patterns for the last few decades.

2.4. Statistical analyses

All statistical tests were performed with PAST (PALEontological Statistics; Hammer et al., 2001). PAST is a comprehensive statistics package that runs a range of standard numerical analysis and operations used in quantitative paleontology and many sub-fields of earth science. Several multivariate techniques (cluster, detrended correspondence and canonical correspondence analyses) were used to provide a consistent way to search for distributional patterns.

3. Results

3.1. Bering Sea assemblage composition

A total of 21 species (Fig. 3) were identified in the Bering Sea representing a mixture of Arctic and subarctic species. The dominant taxa were *Normanicythere leioderma*, *Sarsicytheridea bradii*, *Semicytherura complanata*, and *Pectocythere janae*. While varying in relative abundance from year-to-year, these four species cumulatively make up 72% of all specimens identified. During the 34-year time span of this study, average ostracode density was 3.18 specimens per gram of dry sediment. The number of individuals fluctuated widely from sample to sample, from a few specimens to several hundred.

3.2. Cluster analysis

We used PAST to perform an R-mode cluster analysis with a Euclidean similarity measure to sort species with similar patterns of abundance into separate groups (Fig. 3). Using all samples ($n=225$), a dendrogram grouped the two most dominant species,

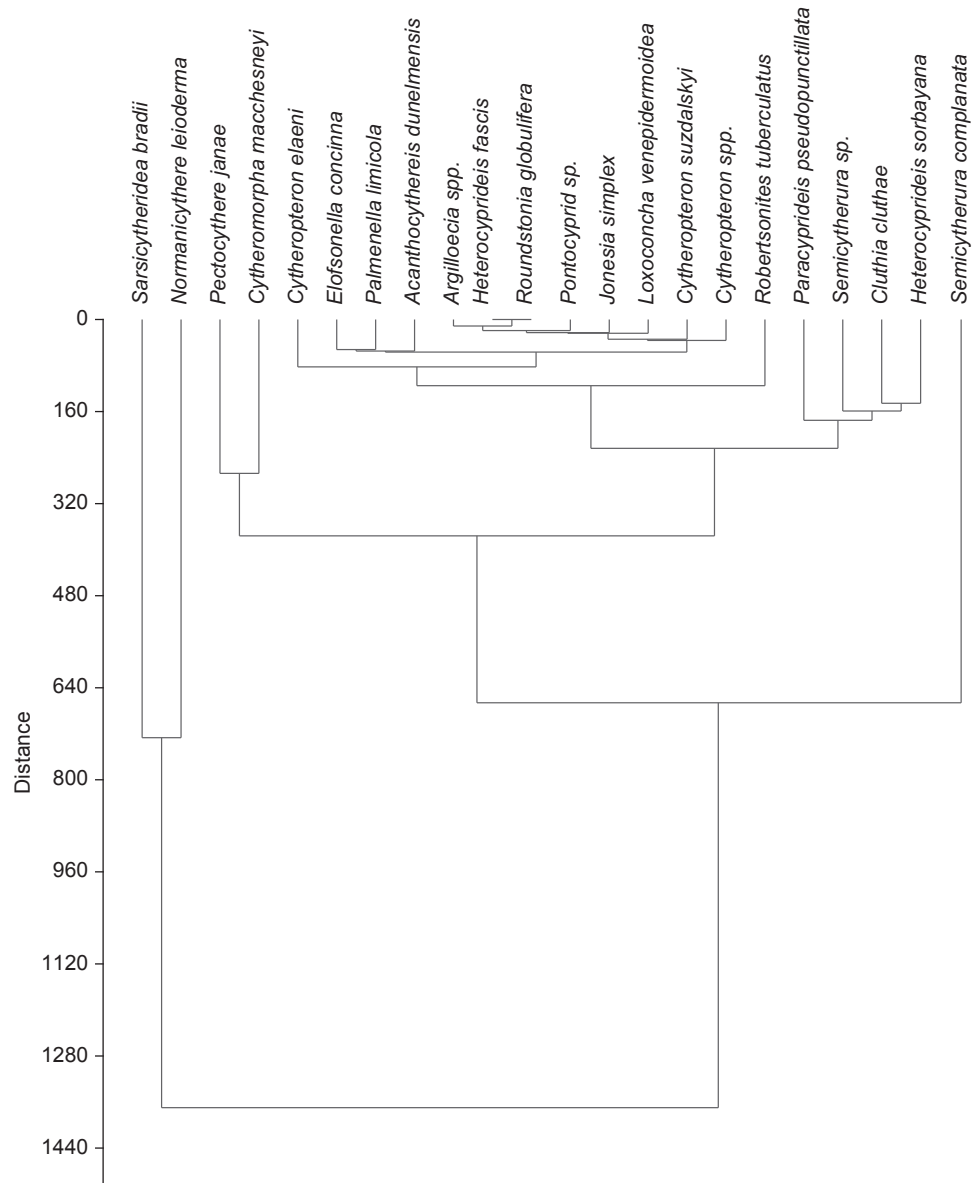


Fig. 3. Cluster analysis with a Euclidean similarity measure of 21 species of ostracodes in the northern Bering Sea, 1976–2010. (*Loxoconcha* was very rare in a few samples and is not included in the total species count of 21.) This grouping sorts species with similar patterns of abundance.

N. leioderma and *S. bradlii*, as a single separate node, based upon similar abundance patterns. Another cluster is linked from this one node to a second grouping, which includes some euryhaline species, such as *Heterocyprideis fascis* and *Paracyprideis pseudopunctillata*. *P. janae* and *C. macchesneyi* also grouped together. Finally, several relatively uncommon species clustered together including *Cytheropteron elaeni* and *Robertsonites tuberculatus*.

3.3. Distributions of dominant taxa in the Arctic Ocean and North Pacific

The dominant taxa we found in the northern Bering Sea have been identified living in other areas of the Arctic, as well as subarctic and temperate regions. We used the ~700-sample Modern Arctic Ostracode Database (Cronin et al., 2010a; 2010b) collected over the past 50 years to provide some context for our collections. *N. leioderma*, *S. bradlii* and *S. complanata* are polar species and are found on continental shelves along the Chukchi–Beaufort and

Laptev–Kara Sea margins (Fig. 4A–C). The most abundant species observed in all years in the northern Bering Sea (except 2004, when only limited samples were available) was *N. leioderma*. Compared to the Bering Sea, it also occurs with less frequency in the Chukchi–Beaufort Sea region at water depths of 10–80 m, comprising up to 30% of the ostracode fauna there. *S. complanata* is relatively rare in the western Beaufort and Chukchi Sea and is more common along Siberian shelves (Stepanova et al., 2007). *S. bradlii* occurs in the Chukchi and Beaufort Seas, usually comprising between 20% and 40% of the assemblage at depths of 0–50 m.

In contrast, *Pectocythere* is primarily a more temperate genus that inhabits subarctic regions in the Pacific Ocean, such as the Gulf of Alaska (Brouwers, 1990). *P. janae* inhabits the Bering Sea in varying abundances depending on the year, occurring in higher abundances during relatively warmer temperatures. It has been reported in the high Arctic only in low numbers in a few samples in the western Beaufort Sea collected in 1969 and 1970 and in the East Siberian Sea in Chaunskaya Bight Inlet, a warm refugium inhabited by a number of species common to the Bering Sea (E.

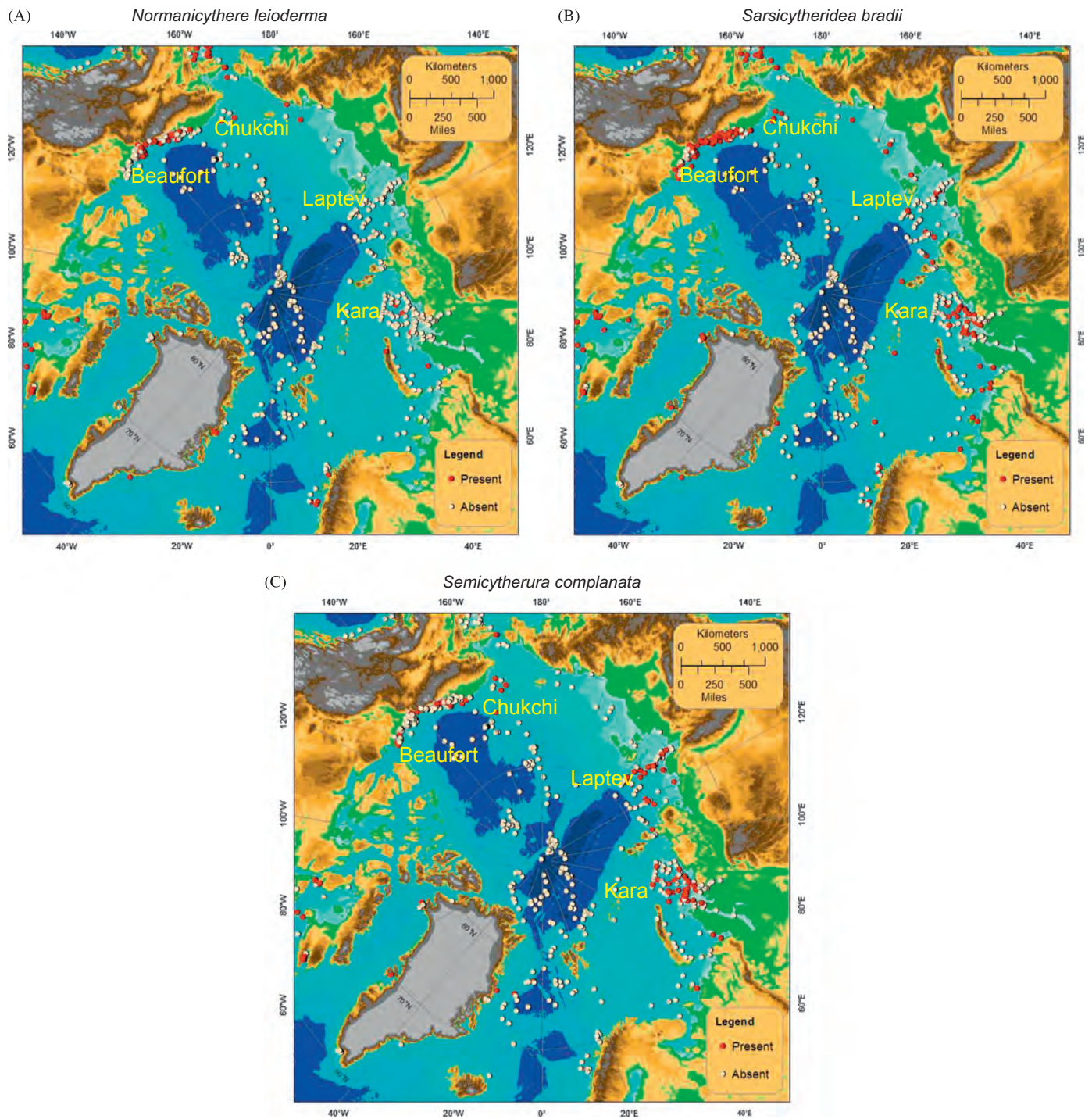


Fig. 4. (A–C) Modern Arctic distribution and abundance of three key cryophilic species, *Normanicocythere leioderma* (a), *Sarsicytheridea bradii* (b), and *Semicytherura complanata* (c), based on a ~700-core-top sediment sample database (the Modern Arctic Ostracode Database, MAOD). The red circles indicate species presence, white circles absence. The MAOD provides census data for approximately 100 species of benthic marine Ostracoda from modern surface sediments collected over the last 50 years from the Arctic Ocean and adjacent seas (Cronin et al., 2010b).

Schornikov, personal communication, 2012). *P. janae* is absent in other parts of the East Siberian Sea (E. Schornikov, personal communication). It has not been reported in the Laptev, Kara, Barents, Norwegian, or Greenland Seas. Although its precise temperature tolerance is not constrained, this species is clearly not a circum-Arctic, cryophilic species like others found in the Bering Sea assemblages, and is only found in the Bering and the Arctic (Chukchi–Beaufort and Eastern Siberian Seas) during

periods with warmer water temperatures. We note here that W.M. Briggs (personal communications) considers *P. janae* to be a synonym of *Kotorocythere arctoborealis*.

3.4. Temporal trends in Bering Sea indicator species

We plot the relative proportions (percent abundance of each species out of the total assemblage) for four key species for each

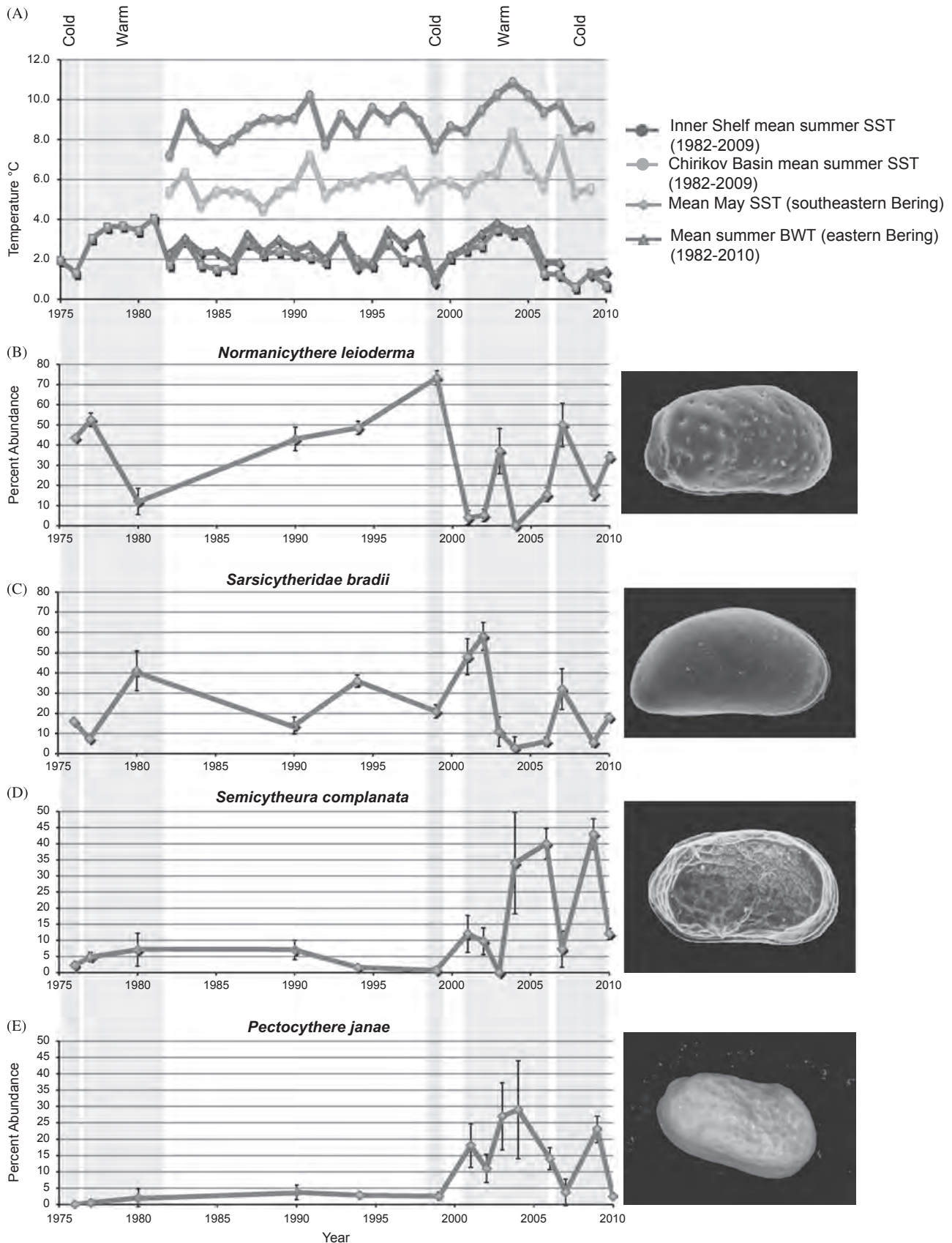


Fig. 5. (A) Chirikov Basin and Inner Shelf mean summer sea-surface temperature (SST) from 1982 to 2009 (purple and green lines). In order to have a temperature record that encompassed the study's time period, we include May SST (blue line) for the southeastern Bering since 1975 and summer BWT (red line) for the eastern Bering since 1982. Because the central-northern Bering Sea is shallow (< 50 m) and well mixed, SST and BWT patterns generally show similar decadal patterns but do not provide year- and site-specific temperature data for our exact study region or precise temperature range that ostracode species require. May SST and BWT data are correlated ($r^2 = 0.82$; $p < 0.001$) for the period 1982–2003. (Data from <http://www.beringclimate.noaa.gov/data/>). (B–E) Plots of abundances of the four most common species in the Bering Sea, 1976–2010. (Photos courtesy of A. Stepanova and *Pectocythere* photo by L. Gemery.) Results represent the relative abundance of the major taxa out of the entire population for each year. (For interpretation of the references to color in this figure caption, the reader is referred to the web version of this article.)

year in which samples were available from 1976 to 2010 (Fig. 5B–E). (Samples from the Norton Sound area in 1978 were not plotted in this analysis because these samples were collected in a river plume and are not representative of the central Bering area assemblage.) These abundance data were evaluated with respect to averaged BWT and May SST data (Fig. 5A). May SST is a good predictor for the summer bottom temperature, based upon a regression analysis of the two variables, ($r^2 = 0.82$; $p < 0.001$) for the period 1982–2003. Confidence limits on ostracode abundance data were generated using the binomial methods of Buzas (1990).

N. leioderma (Fig. 5B) comprised 40–50% of the Bering assemblages in 1976–1977 before declining to 10% during warming in the late 1970s/early 1980s. *N. leioderma* increased in abundance during the 1980s and 1990s, peaking at $> 70\%$ abundance during the cold year of 1999. This species decreased to a minimum in the early 2000s, as temperatures warmed between 2000 and 2005 and then increased again in abundance during the cooler period since 2006.

S. bradii (Fig. 5C) comprised between 8% and 60% of Bering Sea ostracode assemblages from 1976 to 2002, followed by a sharp decline in 2003–2006, apparently in response to warmer temperatures. The decline, however, lagged the near-immediate decline of *N. leioderma* by a year or two.

Based on our observations of morphological variability in *S. complanata* (Fig. 5D) throughout the Arctic and subarctic, it appears that this is a species that may include several subspecies living in cold temperate to Arctic regions, with each having a different temperature tolerance. Bering Sea populations of *S. complanata* comprised $< 10\%$ of assemblages during the late 1970s through 1999, followed by an increase to 30–40% during 2004–2006.

In contrast to some of the cryophilic species discussed above, *P. janae* is typically absent to very rare ($< 4\%$ of assemblages) in the northern Bering Sea from 1976 to 1999 (Fig. 5E). During the interval 2001–2006, it increased to 10–30% of northern Bering assemblages as water temperatures increased.

3.5. Canonical correspondence analysis for Bering Sea species

A canonical correspondence analysis (CCA) is a standard form of correspondence analysis that allows environmental data to be incorporated into the analysis. It was used to examine the frequencies of ostracode species in relation to several environmental variables that may influence their overall abundance (Fig. 6; Park and Cohen, 2011; Torres Saldarriaga and Martínez, 2010). The five most abundant species were evaluated in the context of the following variables: (1) surface air temperature (SAT, the air temperature at 2m height above the ocean surface, as derived from the NCEP/NCAR reanalysis model) in the Chirikov Basin (Z. Brown, personal communication); (2) SAT along the Inner Shelf (Z. Brown, personal communication); (3) the Arctic Oscillation Index (<http://www.beringclimate.noaa.gov/data/>); (4) May SST in the southeastern Bering Sea (<http://www.beringclimate.noaa.gov/data/>), and (5) the number of open water days in the Chirikov Basin and Inner Shelf (Brown et al., 2011). Only samples containing ≥ 20 total specimens ($n=77$) were used in this analysis (see Buzas, 1990 for sample size reasoning). Considering that ostracode density was low, we decided that a criterion of ≥ 20 specimens per sample would provide a sufficient indication of the dominant species living in the area. Our reasoning was that a higher cutoff would have eliminated too many sample sites from the available data pool and would have prevented a broader regional characterization. We concluded that the 20-specimen threshold optimally balances the competing demands of describing representative population structure and geographic coverage. We recognize that due to this threshold, not all the rare species are enumerated statistically, but the number of samples ($n=77$, 4923 specimens) in the study vicinity helps to validate general community composition. Finally, we note that the 1978 data were excluded from the CCA because those samples were collected from shoreline locations and corresponded to much lower salinity conditions.

The CCA shows that the frequency of *P. janae* is associated with high SATs, or in general, warmer temperatures, indicating a

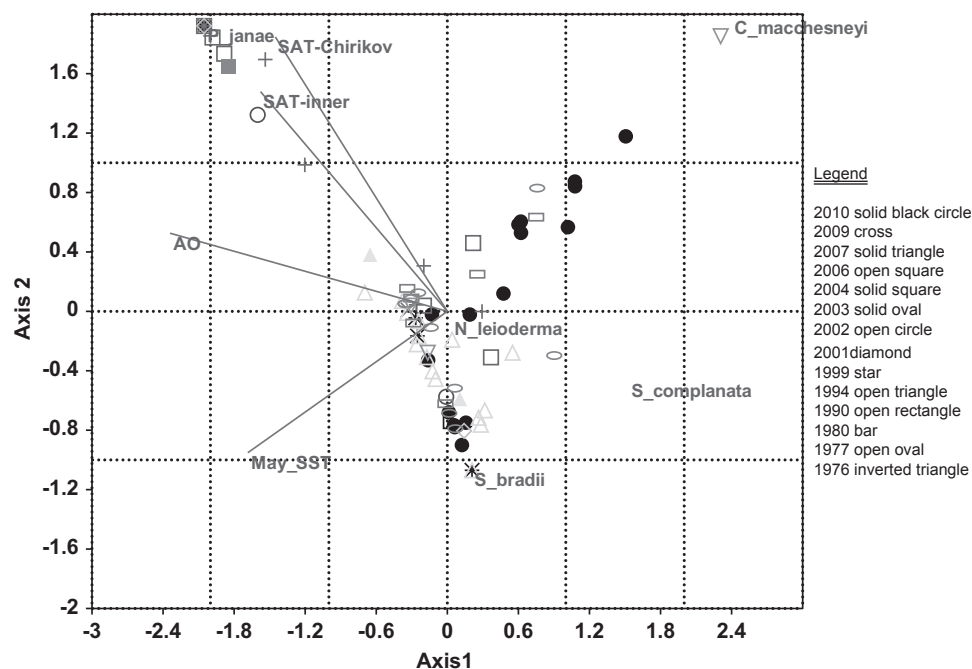


Fig. 6. Canonical correspondence analysis (CCA) results of five dominant Bering Sea ostracode species frequencies ($n=77$) in relation to several environmental variables (surface air temperature [SAT] in the Chirikov Basin, SAT along the Inner Shelf, the Arctic Oscillation Index, May sea surface temperature [SST] in the southeastern Bering Sea) that may influence their overall abundance and distribution. The green vector lines show the environmental variables and the quadrant and samples with which they are associated. (For interpretation of the references to color in this figure caption, the reader is referred to the web version of this article.)

distinct ecological niche for *P. janae* because of the high degree of separation within its own quadrant in the CCA plot. Samples from the year 2010 (maroon circles) are in the opposite quadrant from the SAT vectors and *P. janae*, consistent with colder water temperatures in 2010. Samples from 1994 (light gray circles) cluster together because in that year *S. bradii* and *N. leioderma* represented 36% and 49% of the total ostracode population, respectively. A few samples from 1977 and 1976 (pink and army green circles) are located in lower salinity waters of Norton Sound and correspondingly group with *C. macchesneyi*, a species that can tolerate reduced salinity. Several samples in 2010 (maroon circles) contained higher proportions of *C. macchesneyi* as well. Data corresponding to *N. leioderma* is centrally distributed in the plot, meaning that it is abundant in many of the samples in most years. Computed eigenvalues show that axis one (80%) and axis two (15%) account for a combined 94% of the variance in this analysis.

3.6. Chukchi Sea ostracode assemblages

In the Chukchi Sea, we identified a total of 28 species from eight surface sediment samples collected in 2009 and eight samples from 2010, representing a mixture of Arctic and subarctic species (Fig. 7). The most abundant species in the Chukchi Sea were *P. pseudopunctillata* (17% in 2009 and 16% in 2010) and *S. bradii* (27% in 2009 and 8.4% in 2010). Although the Chukchi shelf has many species in common with the Bering Sea, *N. leioderma* was less abundant in the Chukchi (0.8% in 2009 and 11% in 2010); *P. janae* comprised 7.8% in 2009 and 5.1% in 2010. Ostracode density averaged 1.6 ostracodes per dry gram of sample.

3.7. Detrended Correspondence Analysis (DCA) of ostracodes from the Bering, Chukchi, Beaufort, Laptev, and Kara Seas

We performed a detrended correspondence analysis (DCA) of ostracode samples from Bering Sea and Arctic Ocean shelf surface sediments in order to evaluate the similarity of Bering Sea ostracode assemblages to those living on Arctic continental shelves. DCA is commonly used to analyze similarities and dissimilarities among faunal and floral assemblages. We used the PAST DCA software application and included surface samples from our Chukchi and Bering Seas study and samples from the Beaufort, Kara, and Laptev Seas contained in the MAOD database (Cronin et al., 2010a; 2010b). A total of 306 samples containing 43,220 ostracode specimens were used in the DCA. We excluded samples with < 20 specimens and samples from water depths ≥ 200 m to constrain the analysis to continental shelf samples.

The plot of the first and second principal components, which accounts for 51% of the variance, shows a distinct clustering of the Bering Sea samples and a clustering of the Arctic samples (Fig. 8). These results indicate that the Bering Sea samples differ from the Arctic samples in having larger proportions of *N. leioderma* and *S. bradii* and much lower proportions of *P. pseudopunctillata*.

4. Discussion

During the 34-year time span of this study, we found that two primary assemblages inhabited the northern Bering Sea. One assemblage is dominated by Arctic species (i.e. *N. leioderma*, *S. bradii*), and the other has greater proportions of temperate-subarctic species (i.e. *P. janae*). These two end-members are evident in Fig. 9A–D during the relatively cool years 1994 and 1999 and warm years 2000–2006. These data suggest that *P. janae*

and *S. complanata* prefer warmer conditions (Fig. 9A and B). The CCA (Fig. 6) further suggests that *P. janae* has a distinct warmer temperature preference, as it plots in its own quadrant and is positively correlated with SAT. We hypothesize that *P. janae* survive and possibly migrate, with the help of strong northward currents, in the Bering Sea in greater numbers during these warm periods. Marine ostracode species migrate in response to climatic changes, including changes in ocean temperatures and water masses over glacial–interglacial and millennial timescales (Didié and Bauch, 2000). However, the rates at which populations can migrate in response to short term temperature changes (i.e. interannual to decadal) is poorly known. Our data suggest that populations of *P. janae* and perhaps other species may have been able to increase in population, either through migration, higher

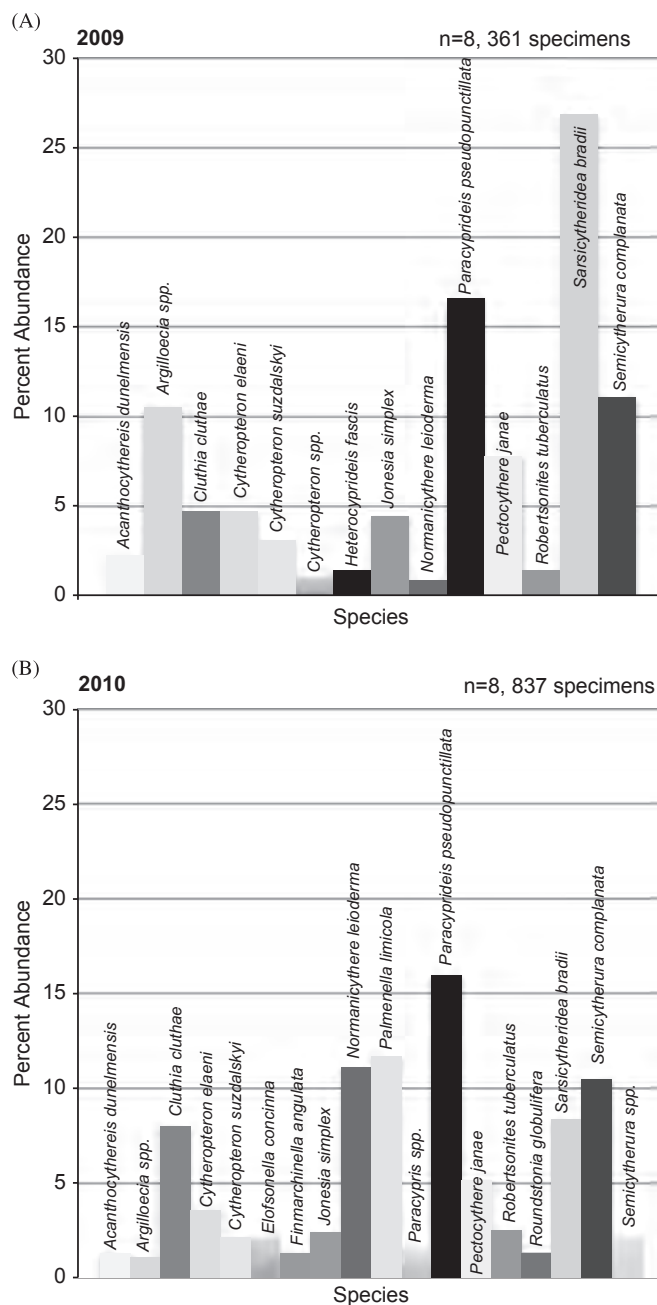


Fig. 7. The Chukchi Sea ostracode assemblages in 2009 and 2010. Bar plots include species that composed > 1% of the total population.

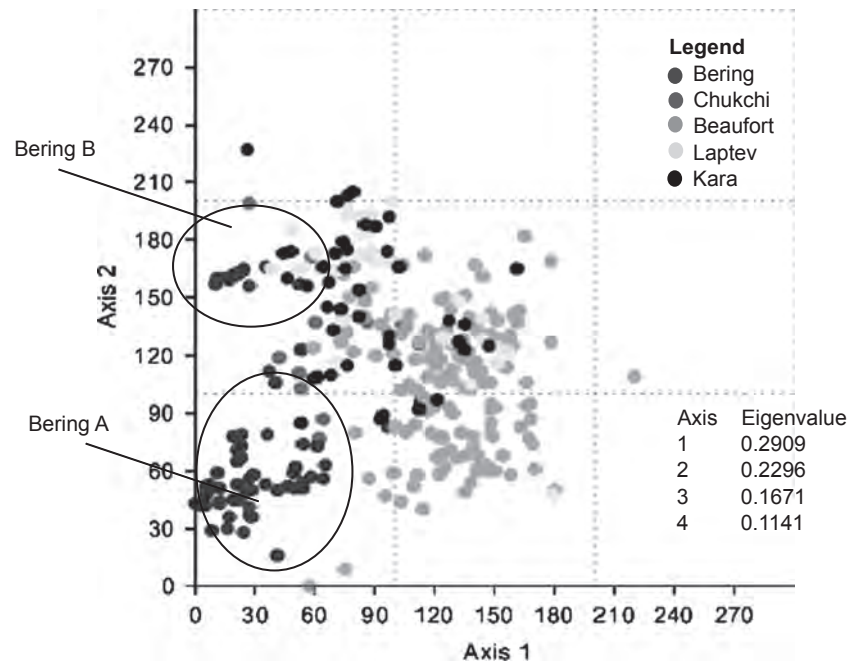


Fig. 8. Detrended correspondence analysis (DCA) results on shallow-water ostracode abundances in samples from the Bering (blue dots) and Arctic (Chukchi [red dots], Beaufort [green dots], Laptev [yellow dots], and Kara [black dots]) ($n=306$, 43,200 specimens). (For interpretation of the references to color in this figure caption, the reader is referred to the web version of this article.)

reproduction rates or alternately enhanced survival in parts of the Bering Sea over relatively short timescales. Additional study is needed to clarify the mechanisms for increased abundance of particular species. For example, *P. janae* may have higher reproduction rates with warmer temperatures, leading to higher abundance during warm years. During 2004–2006, *S. complanata* reached a maximum of 40% abundance of the total ostracode population, suggesting a preference for warmer water and/or minimal sea ice (Fig. 5C). Further work is needed to establish the significance of this variation in *S. complanata* abundance with respect to Bering Sea oceanographic patterns.

In contrast, *N. leioderma* and *S. bradii* clearly decline in abundance in warm years (Fig. 9C,D). These patterns support prior studies that show water temperatures are critical for survival and reproduction in many marine ostracodes (Brouwers, 1988; Hazel, 1970).

This study also provides insight into the ostracode faunal composition of shallow, continental shelf areas in the Bering Sea and Arctic Ocean proper. The subarctic Bering Sea assemblage (Fig. 8, blue circles) contains different dominant species than the Arctic assemblages in the Chukchi, Beaufort, Laptev and Kara Seas, which had many more species in common. Fig. 8 further reflects that the Chukchi assemblage (red circles) is intermediate in position between the subarctic and Arctic assemblages, representing some mixing of species.

The greater proportion of *N. leioderma* found in the Bering Sea is the key difference between subarctic and Arctic populations. Although Stepanova et al. (2010) found this species in a few shallow samples in the Kara Sea, occurring at depths of less than 50 m, *N. leioderma* is present outside the Arctic and seems to prefer subarctic ecosystems. For example, it occurs in shallow coastal waters of the Atlantic and Atlantic-influenced Arctic: Gulf of St. Lawrence (Norman, 1869), Iceland (Elofson, 1941), eastern Ellesmere Island (Brady and Norman, 1896), western Greenland (Stephensen, 1938), St. Margaret's Bay, Nova Scotia (Levings, 1975) and the Gulf of Maine (Blake, 1933). Hazel (1970) classified *N. leioderma* as an amphi-Atlantic species (i.e. a species that occurs on both eastern and western margins of the Atlantic) ranging in depth from 3 to 150 m in the frigid-cold climate zone,

which coincides with the Arctic–Nova Scotian biogeographic province. Hazel (1970) specifically noted that summer survival and reproductive temperatures control *N. leioderma*'s population. This agrees with our data showing a decline in *N. leioderma* during warmer periods in the northern Bering Sea.

Additionally, the DCA plot indicates separation between two groups of the Bering Sea samples, which we term as “Bering B” and “Bering A”. Bering A samples plot low on axis two due to larger proportions of *N. leioderma* and *S. bradii*. Together these two species comprised up to 94% of the total Bering Sea ostracode assemblage during colder years between 1976 and 2010. They were less common during years in which northern Bering Sea summer bottom temperatures were $>0-2^{\circ}\text{C}$. *S. bradii*, which reaches $>50\%$ of the community composition in the Bering Sea, was less common in the Chukchi Sea (27% maximum in 2009 and 8.4% in 2010) as was *N. leioderma* (0.8% in 2009 and 11% in 2010). In contrast to the Beaufort Sea and Chukchi Sea where it is common (17% in 2009 and 16% in 2010), *P. pseudopunctillata* comprised only 2% of the total Bering Sea assemblage. The Bering B group contained larger proportions of *S. complanata* in samples collected in 2006 and 2009.

5. Conclusions

This study provides the first faunal survey and time-series examination of ostracode assemblages in the Bering Sea. We conclude that the relative dominance of Arctic and subarctic species in the Bering Sea has changed during the last several decades as ocean temperatures fluctuated, illustrating the potential use of ostracodes to characterize ocean water mass changes in the region. We hypothesize that these faunal changes reflect either the direct effects of temperature or other temperature-related factors, such as reduced sea ice. Data from the two research cruises that collected Chukchi Sea ostracodes are not extensive enough to assess temporal change, but can serve as a baseline for future study.

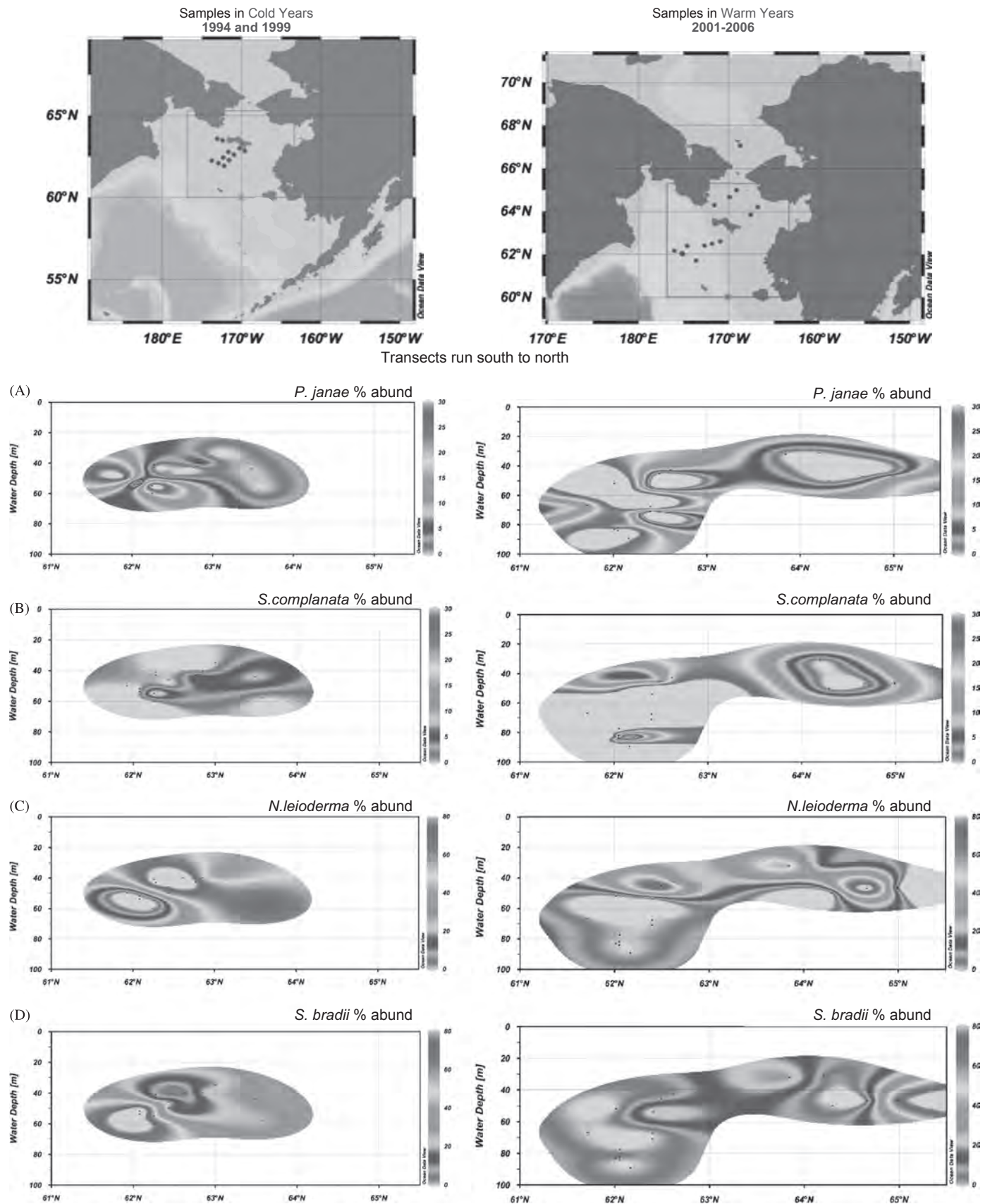


Fig. 9. A–D: Contour plots comparing species abundance in cold years (1994 and 1999) vs. warm years (2001–2006) north and south of St. Lawrence Island. Maps (top) show central-northern Bering shelf study area (red square) and locations of samples (blue dots) in the years represented. Contour plots show abundance of key taxa from a south–north transect. (For interpretation of the references to color in this figure caption, the reader is referred to the web version of this article.)

Acknowledgments

We thank W.M. Briggs and E.I. Schornikov for meaningful discussions and identification regarding *Kotorocythere arctoborealis* vs. *Pectocythere janae*, A. Bayard and R. Marzen for assisting with mapping graphics, E.M. Brouwers, H. Nelson, K. McDougall, B. Casey for sediment samples, Z. Brown for sea-ice extent data and manuscript critique and improvements, Christina Riesselman, Moriaki Yasuhara, Anna Stepanova and Walter Boynton for helpful reviews of the original manuscript. We are grateful for lab assistance from R. Lindsay, R. Marzen, D. Reed, J. Farmer and B. Gordon. Financial support was provided in part by NSF ARC 0802290 and the USGS Climate and Land Use Change Program. This is contribution #85 to the BEST-BSIERP Bering Sea Project publication.

References

- Arrigo, K.R., van Dijken, G., Pabi, S., 2008. Impact of a shrinking Arctic ice cover on marine primary production. *Geophys. Res. Lett.* 35, L19603, <http://dx.doi.org/10.1029/2008GL035028>.
- Belkin, I.M., Cornillon, P.C., Sherman, K., 2009. Fronts in large marine ecosystems. *Prog. Ocean* 81, 223–236.
- Blake, C., 1933. The Mount Desert region Ostracoda in Biological Survey of the Mount Desert Region. Wistar Institute of Anatomy and Biology, Philadelphia, pp. 229–241.
- Bluhm, B., Gradinger, R., 2008. Regional Variability In Food Availability For Arctic Marine Mammals. *Ecological Applications* 18, S77–S96.
- Brady, G.S., Norman, A.M., 1896. A monograph of the marine and freshwater Ostracoda of the North Atlantic and of Northwestern Europe. Sections 2–4: Myodocopa, Cladocopa, Platycopta. *Sci. Trans. R. Dublin Soc. Ser. 2* (5), 353–374.
- Brown, Z.W., Arrigo, K.R., 2012. Contrasting trends in sea ice and primary production in the Bering Sea and Arctic Ocean. *ICES J. Mar. Sci.: J. Conseil* 69 (7), 1180–1193.
- Brown, Z.W., van Dijken, G.L., Arrigo, K.R., 2011. A reassessment of primary production and environmental change in the Bering Sea. *J. Geophys. Res.* 116, C08014, <http://dx.doi.org/10.1029/2010JC006766>.
- Brouwers, E.M., 1994. Systematic Paleontology of Quaternary Ostracode Assemblages from the Gulf of Alaska: Part 3. Family Cytheruridae, U.S. Geol. Surv. Prof. Pap. No. 1544, pp.1–43.
- Brouwers, E.M., 1993. Systematic Paleontology of Quaternary Ostracode Assemblages from the Gulf of Alaska: Part 2. Families Trachyleberididae, Hemicytheridae, Loxoconchidae, Paracytheridae, U.S. Geol. Surv. Prof. Pap. No. 1531, pp.1–40.
- Brouwers, E.M., 1990. Systematic Paleontology of Quaternary Ostracode Assemblages from the Gulf of Alaska: Part 1. Families Cytherellidae, Bairdiidae, Cytheridae, Leptocytheridae, Limnocytheridae, Eucytheridae, Crithidae, Cushmanideidae. U.S. Geol. Surv. Prof. Pap. No. 1510, 1–40.
- Brouwers, E.M., 1988. Palaeobathymetry on the continental shelf based on examples using Ostracods from the Gulf of Alaska. In: DeDecker, P., Colin, J.-P., Peypouquet, J.P. (Eds.), *Ostracoda in the Earth Sciences*. Elsevier, pp. 55–76.
- Buzas, M., 1990. Another look at confidence limits for species proportions. *J. Paleont.* 64 (5), 842–843.
- Cooper, L.W., Sexton, M.G., Grebmeier, J.M., Gradinger, R., Mordy, C.W., Lovvorn, J.R., 2013. Linkages between sea ice coverage, Pelagic-Benthic coupling and the distribution of spectated eiders: observations in March 2008, 2009 and 2010 from the Northern Bering Sea. *Deep-Sea Res. II* 94, 31–43.
- Cronin, T.M., Gemery, L.J., Briggs Jr., W.M., Jakobsson, M., Polyak, L., Brouwers, E.M., 2010a. Quaternary Sea-ice history in the Arctic Ocean based on a new Ostracode sea-ice proxy. *Quat. Sci. Rev.* 29 (25–26), 3415–3429.
- Cronin, T.M., Gemery, L., Brouwers, E.M., Briggs Jr., W.M., Wood, A., Stepanova, A., Schornikov, E.I., Farmer, J., Smith, K.E.S., 2010b. Modern Arctic Ostracode Database. IGBP PAGES/WDCa Contribution Series Number, 2010–2081. <ftp://ftp.ncdc.noaa.gov/pub/data/paleo/contributions_by_author/cronin2010/cronin2010.txt>.
- Cronin, T.M., Dowsett, H.J., Dwyer, G.S., Baker, P.A., Chandler, M.A., 2005. Mid-Pliocene deep-sea bottom-water temperatures based on ostracode Mg/Ca ratios. *Mar. Micropaleontol.* 54, 249–261.
- Cronin, T.M., Raymo, M.E., Kyle, K.P., 1996. Pliocene (3.2–2.4 Ma) ostracode faunal cycles and deep ocean circulation, North Atlantic Ocean. *Geology* 24, 695–698.
- Cronin, T.M., Holtz, T.R., Whatley, R.C., 1994. Quaternary paleoceanography of the deep Arctic Ocean based on quantitative analysis of Ostracoda. *Mar. Geol.* 119 (3–4), 305–332.
- Didié, C., Bauch, H.A., 2000. Species composition and glacial-interglacial variations in the ostracode fauna of the northeast Atlantic during the past 200,000 years. *Mar. Micropaleontol.* 40, 105–129.
- Elofson, O., 1941. Zur kenntnis der marinen Ostracoden Schwedens, mit besonderer berucksichtigung des skagerrads. *Zool. Bidr. fran Uppsala* 19, 215–534.
- Grebmeier, J.M., 2012. Shifting patterns of life in the Pacific Arctic and Sub-Arctic seas. *Ann. Rev. Mar. Sci.* 4 (16), 1–16.
- Grebmeier, J.M., Moore, S.E., Overland, J.E., Frey, K.E., Gradinger, R.R., 2010. Biological response to recent Pacific Arctic sea-ice retreats. *Eos Trans. AGU* 91, 161–168.
- Grebmeier, J.M., Overland, J.E., Moore, S.E., Farley, E.V., Carmack, E.C., Cooper, L.W., Frey, K.E., Helle, J.H., McLaughlin, F.A., McNutt, S.L., 2006a. A major ecosystem shift in the northern Bering Sea. *Science* 311, 1461–1464.
- Grebmeier, J.M., Cooper, L.W., Feder, H.M., Sirenko, B.I., 2006b. Ecosystem dynamics of the Pacific-influenced North Bering and Chukchi Seas in the Amerasian Arctic. *Prog. Ocean* 71, 331–361.
- Hammer, Ø., Harper, D.A.T., Ryan, P.D., 2001. PAST: paleontological statistics software package for education and data analysis. *Palaeontol. Electron.* 4 (1), 9 <http://palaeo-electronica.org/2001_1/past/issue1_01.htm>.
- Hare, S.R., Mantua, N.J., 2000. Empirical Evidence for North Pacific Regime Shifts in 1977 and 1989. *Progress in Oceanography* 47, 103–145.
- Hazel, J.E., 1970. Atlantic Continental Shelf and Slope of United States—Ostracode Zoogeography in the Southern Nova Scotian and Northern Virginian Faunal Provinces. U.S. Geol. Surv. Prof. Pap. No. 529-E, E1–E21.
- Hunt, G.L., Stabeno, P.J., 2002. Climate change and the control of energy flow in the southeastern Bering Sea. *Prog. Ocean* 55 (1–2), 5–22.
- Hutchins, L.W., 1947. The bases for temperature zonation in geographical distribution. *Ecol. Mono.* 17, 325–335.
- Joy, J.J., Clark, D.L., 1977. The distribution, ecology and systematics of the Benthic Ostracoda of the Central Arctic Ocean. *Micropaleontology* 23 (2), 129–154.
- Kalnay, E., Kanamitsu, M., Kistler, R., Collins, W., Deaven, D., Gandin, L., Iredell, M., Saha, S., White, G., Woollen, J., Zhu, Y., Leetmaa, A., Reynolds, R., 1996. The NCEP/NCAR 40-year reanalysis project. *Bull. Am. Meteor. Soc.* 77, 437–471.
- Levings, N.D., 1975. Analyses of temporal variation in the structure of a shallow-water benthic community in Nova Scotia. *Int. Rev. Gesamten Hydrobiol. Hydrographieol.* 60 (4), 1522–2632.
- Mantua, N.J., Hare, S.R., 2002. The Pacific Decadal Oscillation. *J. Ocean* 58 (1), 35–44.
- Mueter, F.J., Litzow, M.A., 2008. Sea ice retreat alters biogeography of the Bering Sea Continental Shelf. *Ecol. Appl.* 18, 309–320.
- National Research Council, 1996. The Bering Sea Ecosystem. National Academy Press, Washington, D.C. 324 pp.
- Norman, A.M., 1869. Shetland Final Dredging Report, Part II on the Crustacea, Tunicata, Polyzoa, Echinodermata, Actinozoa, Hydrozoa, & Porifera. *Rep. Brit. Ass.* 38, Norwich, 247–336, Supplement pp.341–2 [Ostracoda pp. 289–95].
- Overland, J.E., Wang, M., Salo, S., 2008. The recent Arctic warm period. *Tellus* 60A, 589–597.
- Pabi, S., van Dijken, G.L., Arrigo, K.R., 2008. Primary production in the Arctic Ocean, 1998–2006. *J. Geophys. Res.* 113, C08005.
- Park, L.E., Cohen, A.S., 2011. Paleocological response of ostracods to early Late Pleistocene lake-level changes in Lake Malawi, East Africa. *Palaeogeogr. Palaeoclim. Palaeoecol.* 303, 71–80.
- Serreze, M.C., Holland, M.M., Stroeve, J., 2007. Perspectives on the Arctic's shrinking sea-ice cover. *Science* 315, 1533–1536.
- Smith, A.J., Horne, D.J., 2002. Ecology of Marine, Marginal Marine and Non-marine Ostracodes. In: Holmes, J.A., Chivas, A.R. (Eds.), *The Ostracoda: Applications in Quaternary Research*. Geophy. Mono. Ser., vol. 131. AGU, Washington, DC, pp. 37–64.
- Springer, A.M., McRoy, C.P., Flint, M.V., 1996. The Bering Sea Green belt: shelf-edge processes and ecosystem production. *Fish. Oceanogr.* 5, 205–223.
- Stabeno, P., Moore, S.E., Napp, J.M., Sigler, M., Zerbini, A., 2012. Comparison of warm and cold years on the Southeastern Bering Sea shelf and some implications for the ecosystem. *Deep-Sea Res. II* 65–70, 31–45.
- Stabeno, P.J., Bond, N.A., Salo, S.A., 2007. On the recent warming of the southeastern Bering Sea Shelf. *Deep-Sea Res. II* 54, 2599–2618.
- Stephensen, K., 1938. Marine Ostracoda and Cladocera. In: *Zoology of Iceland III*. Copenhagen and Reykjavik, pp.1–19.
- Stepanova, A.Y., Taldenkova, E.E., Bauch, H.A., 2010. Arctic Quaternary Ostracods and Their Use in Paleoreconstructions. *Paleont. J.* 44 (1), 41–48.
- Stepanova, A.Y., Taldenkova, E.E., Bauch, H.A., 2007. Comparison study of the modern ostracod associations in the Kara and Laptev seas: ecological aspects. *Mar. Micropaleontol.* 63, 111–142.
- Stroeve, J.C., Serreze, M.C., Drobot, S., Gearheard, S., Holland, M.M., Maslanik, J., Meier, W., Scambos, T., 2008. Arctic sea ice extent plummets in 2007. *Eos Trans. AGU* 89, 13–20.
- Torres Saldarriaga, A., Martínez, J.I., 2010. Ecology of non-marine ostracoda from La Fe reservoir (El Retiro, Antioquia) and their potential application in paleoenvironmental studies. *Rev. Acad. Col. Cienc.* 34 (132), 397–409.
- Wang, M., Overland, J.E., 2009. A sea-ice free summer Arctic within 30 years? *Geophys. Res. Lett.* 36, L07502.
- Yasuhara, M., Hunt, G., Cronin, T.M., Okahashi, H., 2009. Temporal latitudinal-gradient dynamics and tropical instability of deep-sea species diversity. *Proc. Nat. Acad. Sci. USA* 106, 21717–21720.
- Yasuhara, M., Hunt, G., van Dijken, G., Arrigo, K.R., Cronin, T.M., Wollenburg, J.E., 2012a. Patterns and controlling factors of species diversity in the Arctic Ocean. *J. Biogeogr.* <http://dx.doi.org/10.1111/j.1365-2699.2012.02758>.
- Yasuhara, M., G. Hunt, G., Cronin, T.M., Hokanishi, N., Kawahata, H., Tsujimoto, A., Ishitake, M., 2012b. Climatic forcing of Quaternary deep-sea benthic communities in the North Pacific Ocean. *Paleobiology* 38, 162–179.



Regional patterns of bioturbation and iron and manganese reduction in the sediments of the southeastern Bering Sea



Margaret E.S. Esch^{a,*}, David H. Shull^a, Allan H. Devol^b, S. Bradley Moran^c

^a Department of Environmental Sciences, Western Washington University, 516 High Street, Bellingham, WA 98225, USA

^b School of Oceanography, University of Washington, Seattle, WA 98195, USA

^c Graduate School of Oceanography, University of Rhode Island, 215 South Ferry Road, Narragansett, RI 02882-1197, USA

ARTICLE INFO

Available online 10 April 2013

Keywords:

USA
Alaska
Bering Sea
Continental shelves
Benthos
Iron oxide reduction
Bioturbation

ABSTRACT

Regional patterns of iron (Fe) and manganese (Mn) reduction rates across the shelf and slope of the southeastern Bering Sea, as well as the relative importance of these pathways in sedimentary organic matter remineralization, were investigated during the spring and summer of 2009. Reduction rates of Fe and Mn were calculated using depth profiles of solid-phase iron and manganese oxide concentrations and bioturbation coefficients, D_b , determined from profiles of excess ^{234}Th . Iron reduction was found to be a significant pathway for carbon mineralization across the shelf, with an average rate of $1.74 \text{ mmol m}^{-2} \text{ d}^{-1}$. However, Fe reduction rates higher than $6 \text{ mmol m}^{-2} \text{ d}^{-1}$ were calculated, and a significant regional pattern was observed, with highest rates found on the northern shelf, and dropping toward the south and offshore. Conversely, Mn oxide reduction was found to be of minor significance, with low reduction rates in all regions, averaging only $0.09 \text{ mmol m}^{-2} \text{ d}^{-1}$ across the shelf, and accounting for no more than 5% of total carbon oxidation in any region. These results indicate that Fe oxide reduction is a significant pathway for carbon remineralization in the northern and middle-shelf regions, where organic matter deposition rates and benthic biomass are high. Additionally, this work provides insight into the potential role of sedimentary iron reduction as a source of bioavailable Fe in this region.

© 2013 Elsevier Ltd. All rights reserved.

1. Introduction

The shelf region of the Bering Sea is productive, with iron (Fe)-replete surface waters, whereas the off-shelf region has been described as an Fe-limited, high-nutrient low-chlorophyll regime (Aguilar-Islas et al., 2007; Hurst et al., 2010). Studies have shown the importance of Fe in controlling productivity in these environments (Hutchins and Bruland, 1998; Moore et al., 2002), and Fe availability likely limits primary production in the oceanic region of the Bering Sea (Aguilar-Islas et al., 2007; Sambrotto et al., 2008). On the shelf however, primary production is limited by nitrogen availability after the spring bloom (Rho et al., 2005; Aguilar-Islas et al., 2007). Thus, it is of interest to investigate potential sources of Fe to shelf region of the Bering Sea. There are limited data regarding riverine inputs of Fe to the southeastern Bering shelf, namely by the Yukon river. Still, Feely et al. (1981), found a depletion of Fe offshore, relative to the Yukon River estuary. Likewise, more recently it was suggested that strong frontal systems along the 30 m isobath can prevent the cross-

shelf spreading of coastal waters (Danielson et al., 2011). This would likely trap much of the Yukon River outflow, preventing transport onto the shelf. Excluding riverine input, the sediment is a probable source of Fe to the bottom waters on the shelf, and due to the relatively shallow water depths, could also be a source of surface-water Fe. Fairly recent studies have discussed the role of sediment resuspension as a dominant source of Fe on continental shelves (Johnson et al., 1999; Chase et al., 2005). Additionally, the flux of reduced Fe out of the sediment may be a significant source of bioavailable Fe (Berelson et al., 2003; Elrod et al., 2004). Within the sediment, particulate Fe oxides become soluble once reduced. This reduced Fe^{2+} can then be re-oxidized and re-cycled within the sediment or it may escape re-oxidation and be mobilized out of the sediment into bottom waters. Hurst et al. (2010) suggested that the benthic efflux of Fe^{2+} , followed by its rapid oxidation in the well-oxygenated bottom waters might explain elevated concentrations of leachable, particulate Fe in the benthic boundary layer. Subsequently this Fe could be transported to surface waters through various mixing processes. However, studies investigating Fe reduction on the Bering shelf are scarce, if not entirely lacking. Consequently, in order to determine whether the sediments could be a source of bioavailable Fe, rates of Fe reduction in Bering Sea sediments must be measured.

The southeastern Bering Sea shelf is broad (> 500 km) and makes up approximately half of the total area of the Bering Sea,

* Corresponding author. Present address: Department of Marine Sciences, The University of Georgia, 220 Marine Sciences Building, Athens, GA 30602, USA. Tel.: +1 706 542 6549.

E-mail addresses: eschm@uga.edu (M.E.S. Esch), David.Shull@uw.edu (D.H. Shull), devol@ocean.washington.edu (A.H. Devol), sbmoran@mail.uri.edu (S.B. Moran).

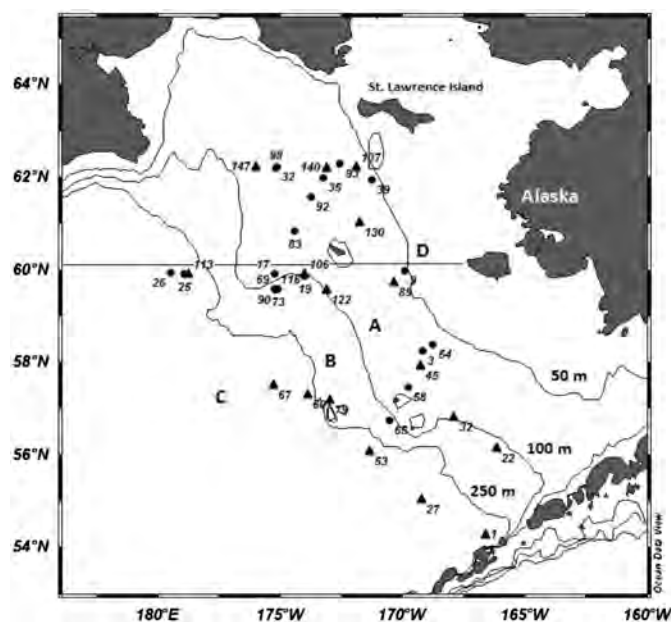


Fig. 1. Map showing locations sampled on both the spring and summer research cruises. Circles represent spring (HLY0902) stations and triangles represent summer (KN195-10) stations. Bathymetry lines indicate the locations of oceanographic fronts that separate the shelf into the middle (A) and outer (B) domains. Past the shelf break is the off-shelf region (C) and the northern region (D) is located above 60° latitude. Chart created using Ocean Data View (Schlitzer, 2008).

with the rest consisting of a deep basin, referred to here as the off-shelf region (Hood, 1981; Fig. 1). The northern-shelf region lies above 60° latitude (Stabeno et al., 2012), whereas south of 60° latitude the shelf waters can be separated into three domains during ice-free conditions; the coastal (0–50 m), middle (50–100 m) and outer (100–200 m) domains. Distinct oceanographic fronts separate each of these shelf regions. The inner front separates the coastal and middle domains, the outer front separates the middle and outer domains and the shelf-break separates the outer domain from the off-shelf waters (Stabeno et al., 2001; Hunt et al., 2002). These fronts greatly reduce cross-shelf advection of nutrient-rich waters during the summer months, significantly impacting primary production and ecosystem structure (Stabeno and Hunt, 2002). Furthermore, weakened cross-shelf circulation between the middle and outer domains due to the outer front can constrain zooplankton biomass to the outer shelf domain, lowering grazing in the middle shelf domain, and allowing for higher carbon export to the benthos, compared to the outer shelf (Walsh and McRoy, 1986; Coyle et al., 2007). Annual primary production for the Bering shelf has been estimated from between 94 Tg C yr⁻¹ (Rho and Whitledge, 2007) to 152 Tg C yr⁻¹ (Lomas et al., 2012). However, these rates are highly variable across the shelf domains as well as seasonally (Lomas et al., 2012). Additionally, the northern region experiences an annual advance and retreat of sea ice which influences the surface water productivity and sedimentation of organic material to the benthos (Stabeno et al., 2012). High rates of primary production have been observed in the northern region (Cooper et al., 2002), where high quality, nitrogen-rich OM reaches the sediment surface (Grebmeier et al., 1988). Recent work by Moran et al. (2012) also supports this general observation. They found relatively high rates of net primary production and carbon export at marginal ice zones in the northern region, generally decreasing southward and toward the shelf break.

Based on this observed ecosystem structure, we expected carbon export to vary regionally across the shelf, and be highest in the northern region and decrease seaward as water depth

increases. Specifically, the following order is expected: northern region > middle domain > outer domain > off-shelf region. Also, if greater OM input to the sediment promotes an increase in sediment oxygen consumption rates, we expected anaerobic remineralization pathways to account for a greater percentage of total OM oxidation in regions with higher OM supply rates. As the redox chemistry and sedimentary cycling of Mn is similar to that of Fe, we also investigated rates of manganese (Mn) reduction across the shelf. We hypothesized that reduction rates of both Fe and Mn and the percentage of total OM oxidation by these pathways would follow the same regional pattern expected for carbon export. Here, we present the patterns of Fe and Mn reduction rates in the sediments of the southeastern Bering Sea.

2. Sampling and methods

Samples were collected over the course of two research cruises during the spring of 2009 (April 1–May 13), aboard the USCGC Healy (HLY0902), and during the summer of the same year (June 12–July 13), aboard the R/V Knorr (KN195-10). Twenty stations were sampled in spring and 19 stations were sampled during the summer cruise (Fig. 1). As many as 16 polycarbonate cores, 10 cm in diameter and up to 40 cm in length, were collected at each site using an Oceans Instruments MC-800 eight-tube multicore. Up to seven of the collected cores were used specifically in this study.

2.1. Whole core incubations

Up to three cores per station were incubated for the determination of oxygen consumption rates. These were subcored using 8-cm diameter polycarbonate tubes. The cores were stored in the dark at near in situ temperature (2 °C), uncapped, for approximately 24 h, after which they were sealed with silicone stoppers equipped with magnetic stirrers. Pre-inserted into each silicone stopper were two lengths of nylon tubing, fitted with two-way valves. One length of tubing was connected to a reservoir of bottom water collected during the time of sampling. This reservoir allowed for samples of overlying water to be collected without the introduction of air bubbles. The cores were incubated for a period of 2–5 days during which time a series of samples from the overlying water was taken. Oxygen concentrations in each sample were determined using an optode optical microsensor (PreSens Microx TX3), calibrated before and after each reading. A 32 ppm salt solution equilibrated with the atmosphere and kept at in situ temperature was used for 100% saturation of oxygen, and a solution of sodium sulfite in seawater was used to zero the optode. Oxygen fluxes were corrected using an empirical formula ($y = 1.125x + 3.365$, where y is the corrected flux and x is the uncorrected flux) for the slow leakage of oxygen from the silicone stoppers used during incubations (Davenport et al., 2012).

2.2. Pore-water oxygen penetration depth

At each station, vertical oxygen pore-water profiles were also taken, on a separate core, using a Unisense Clark-type microelectrode (Revsbech, 1989). These profiles were used to determine the depth at which pore-water oxygen concentrations reached zero. Through the use of a micromanipulator, the probe was lowered into the sediment in 0.5-mm intervals. A two-point calibration was used to convert picoamperes to dissolved oxygen concentrations. A 32 ppm salt solution equilibrated with the atmosphere and kept at in situ temperature was used for 100% saturation of oxygen, whereas the zero oxygen reading was determined from the bottom of the dissolved oxygen profile.

2.3. Pore-water profiles of nitrate, iron and manganese

At each station, two cores were collected for vertical pore-water profiles. These cores were sectioned at the following depths: 0–0.5, 0.5–1, 1–1.5, 1.5–2, 2–3, 3–4, 5–6, 7–8, 9–10, 12–14, 14–16, and 19–20 cm. Approximately 3 mL of sediment from each depth was saved and frozen in a 12 × 75 mm² tube for porosity measurements. Remaining sediment from each depth was packed into plastic, acid-washed centrifuge tubes and centrifuged at 10,000 rpm for 20 min to separate the pore-water from the solid phase. After centrifugation, the pore-water was decanted into a 10 mL Luer-lok™ syringe and filtered through a 0.45-μm filter into a 20 mL high-density, polyethylene scintillation vial. Centrifuge tubes were opened and all filtration was completed under a nitrogen-gas atmosphere in a glove bag. Pore-water nitrate analysis was completed using reagents described by Gordon et al. (1994), but these methods were modified for use on a Smartchem discrete autoanalyzer (Westco Scientific), with cadmium reduction to nitrite (precision for nitrate analysis=1.1%). After the completion of nutrient analyses, remaining pore-water was frozen for later Fe and Mn analysis in the lab. These frozen samples were allowed to slowly thaw under refrigeration at approximately 4 °C just prior to analysis and then diluted with nitric acid to achieve a 1.5% or 2% solution of HNO₃, depending on sample volume. Acidified samples were analyzed using flame atomic absorption spectrophotometry (Varian SpectrAA 220FS). Standards (Fisher Scientific, 1000 ppm Fe/Mn in 1.5% nitric acid) and blanks were run with each set of samples, along with continuing calibration verifications and blanks to ensure measurements were within 3% error and stable over time.

2.4. Thorium-234 profiles

At each station one core was selected for the analysis of ²³⁴Th, which was used as the tracer to determine rates of bioturbation (described in Section 2.7.1). This core was sectioned in 0.5-cm increments to 2 cm and 1-cm increments to 5 cm. Each section was placed into a 125-mL polypropylene jar and dried for approximately 24 h at approximately 70 °C. Approximately 15 mL of the dried sediment was ground and placed into a clean 125-mL jar, and total ²³⁴Th activity was determined using a high-purity germanium gamma spectrometer (Canberra GL2820R), at the 63.3 keV energy peak. The first three depths of each station were counted aboard the ship until the counting error reduced to 10%, or approximately 24 h. Remaining depths were counted on shore at the end of the cruise. Counts were corrected for background, and detector efficiencies were determined by counting a standard created by adding reference-grade 0.05% Uranium pitchblende (U.S. Dept. of Energy) to sediment from the study site. At least 5 months after the initial total ²³⁴Th counts, the samples were recounted to determine supported activity. These values were subtracted from the total ²³⁴Th activities to determine excess ²³⁴Th activity (dpm g⁻¹).

2.5. Solid-phase iron and manganese

Sediment samples for solid-phase iron and manganese analysis were taken from the same core as pore-water samples. This core was sectioned in 0.5-cm increments to 2 cm and then in 1-cm increments to 10 cm. Subsamples of sediment from each depth were placed into 20-mL high-density polyethylene scintillation vials. Samples were stored frozen and then freeze-dried and powdered using a mortar and pestle.

Iron and manganese oxides were extracted from freeze-dried sediment with acidified ammonium-oxalate (0.2 M ammonium oxalate/0.1 M oxalic acid, pH=3). This extraction method has been shown to dissolve Fe oxyhydroxides without attacking silicates or crystalline goethite (Robbins et al., 1984; Phillips and Lovely, 1987).

Concentrations of Fe and Mn oxides were determined using flame absorption spectrophotometry, as previously described.

2.6. Sediment porosity

Sediment collected for porosity measurements was stored frozen until analysis. Samples were then thawed, weighed wet, dried at 65 °C for 48 h, and then reweighed.

Porosities were corrected for pore-water salt content.

2.7. Calculating rates

Since Fe and Mn oxides are particulate electron acceptors, particle-mixing has a significant role in the sedimentary cycling of these metal oxides. Bioturbation, or the mixing and displacement of sediment particles by benthic infauna (Richter, 1952), is the mechanism by which Fe and Mn oxides are transported and cycled within the sediment. Hence, the diagenetic model we used to calculate Fe and Mn reduction rates required the calculation of D_b , the biodiffusion coefficient.

2.7.1. Bioturbation

The naturally occurring radionuclide, ²³⁴Th, has a half-life of 24.1 days and was used as the tracer for determining bioturbation rates (Aller and Cochran, 1976). Profiles of excess ²³⁴Th (Appendix Table A1) were used to quantify bioturbation rates using the following equation:

$$\frac{\partial A}{\partial t} = D_b \frac{\partial^2 A}{\partial z^2} - \omega \frac{\partial A}{\partial z} - \lambda A \quad (1)$$

where

A = excess ²³⁴Th activity (dpm g⁻¹ dry weight)

z = depth (cm)

D_b = bioturbation or particle mixing rate (cm² yr⁻¹)

ω = sedimentation rate (cm yr⁻¹)

λ = the first-order radioactive decay coefficient for ²³⁴Th (10.5 yr⁻¹).

Published sedimentation rates for the Bering Sea, range from 10⁻³ cm yr⁻¹ (Grebmeier et al., 1988) to 10⁻² cm yr⁻¹ (Sharma, 1974). We estimated the relative importance of bioturbation and sedimentation by calculating Peclet numbers (Boudreau, 1997), given this range of sedimentation rates, our calculated biodiffusion coefficients and an average bioturbation depth of 10 cm (Boudreau, 1998). Peclet numbers ranged from 8 × 10⁻⁴ to 6.7 × 10⁻¹. We therefore assumed that bioturbation rates were large relative to sedimentation, reducing Eq. (1) to:

$$\frac{\partial A}{\partial t} = D_b \frac{\partial^2 A}{\partial z^2} - \lambda A \quad (2)$$

Assuming steady-state conditions and constant porosity and with the boundary conditions of $A=A_0$ at $Z=0$ and $A=0$ at $Z=\infty$, the solution to Eq. (2) is:

$$A = A_0 e^{-\sqrt{(\lambda/D_b)}z} \quad (3)$$

Rates of bioturbation were then estimated from the slope of the linear regression of $\ln(A)$ versus depth. Here, we assumed that the zone of bioturbation extended to the base of the ²³⁴Th profiles, based on the work by Boudreau (1998) demonstrating that mixed layer depths average 10 cm, and are rarely shallower than 5 cm within the range of water depths in our study region. However, the method of using radioactive tracers to quantify rates of particle mixing in sediments has both strengths and weaknesses, which are discussed in Section 4.1.

2.7.2. Iron and manganese reduction

Since Fe and Mn oxides exist naturally as components of the sediment-particle matrix, but are also deposited to the sediment surface through sorption onto sinking particles or from precipitation of dissolved species, we used excess concentrations of Fe and Mn oxides in the sediment, which represent the microbially reducible portion of these elements, to calculate Fe and Mn reduction rates. Excess concentrations are defined here as the concentrations of Fe or Mn greater than the minimum concentration first reached with depth in each vertical profile (Aller, 1994).

In order to calculate Fe and Mn reduction rates, a polynomial (2–4 order) was fitted to each profile of excess solid-phase Fe and Mn (Appendix Table A1). Since particle transport was dominated by bioturbation, assuming steady-state, the rate of Fe or Mn oxide reduction was calculated using the following relation:

$$\Sigma R_{(z)} = D_b \frac{\partial^2 C}{\partial z^2} \quad (4)$$

where:

C = excess concentrations of Fe or Mn ($\mu\text{mol cm}^{-3}$)

ΣR = general reaction term for Fe or Mn reduction ($\mu\text{mol cm}^{-3} \text{yr}^{-1}$)

D_b = particle mixing rate ($\text{cm}^2 \text{yr}^{-1}$)

Over the depth in the sediment being considered, D_b was assumed constant. Additionally, ΣR represents net Fe or Mn reduction, and therefore the integrated reduction rate can be defined as the depth-integrated sum of reactions, expressed as:

$$\int_{z_1}^{z_2} \Sigma R_{(z)} dz = D_b \int_{z_1}^{z_2} \frac{d^2 C}{dz^2} dz \quad (4)$$

The second derivative of the fitted profiles was integrated over the zone of metal reduction. For Fe, this zone was defined as the region from the bottom of the pore-water nitrate penetration depth (z_1) to the depth where excess Fe-oxide concentrations reached zero (z_2); and for Mn, from the bottom of the pore-water oxygen penetration depth (z_1) to the depth where excess Mn concentrations reached zero (z_2). This quantity was multiplied by the bioturbation rate determined from the ^{234}Th profile from the same station to calculate the Fe and Mn reduction rate. For Fe, three stations (Table 2) had no usable pore-water nitrate profile, in which case the bottom of the Mn reduction zone was used for z_1 . These depths were the same or very similar for nearly all stations. An inherent assumption made here is that the mixed-layer depth extends to the base of the excess Fe and Mn profiles. Again, this has been shown to be reasonable (Boudreau, 1998).

Table 1
Bioturbation rates for each sampling location in the Bering Sea.

Date	Station	Location	Depth (m)	D_b ($\text{cm}^2 \text{yr}^{-1}$)
Northern shelf region				
4/16/09	HLY 32	62° 11.924°N 175° 8.463°W	80	4.36
4/16/09	HLY 35	61° 57.693°N 173° 14.382°W	62	11.09
4/17/09	HLY 39	61° 56.049°N 171° 12.878°W	51	6.30
4/28/09	HLY 83	60° 48.78°N 174° 23.38°W	91	2.04
5/1/09	HLY 92	61° 34.3°N 173° 42.75°W	72	5.69
5/2/09	HLY 93	62° 15.98°N 172° 31.04°W	57	5.27
5/4/09	HLY 98	62° 10.94°N 175° 8.69°W	81	1.59
7/6/09	KNR 130	61° 0.003°N 171° 45.324°W	65	5.55
7/7/09	KNR 137	62° 12.063°N 171° 53.391°W	51	11.83
7/7/09	KNR 140	62° 12.076°N 173° 6.379°W	62	9.22
7/8/09	KNR 147	62° 11.983°N 175° 58.513°W	95	2.02
Middle shelf region				
4/7/09	HLY 9	59° 58.193°N 169° 51.856°W	55	7.75
4/21/09	HLY 54	58° 22.093°N 168° 43.91°W	68	1.14
4/22/09	HLY 58	57° 27.08°N 169° 45.194°W	67	5.41
6/22/09	KNR 45	57° 53.93°N 169° 14.49°W	70	2.04
6/30/09	KNR 89	59° 42.86°N 170° 19.27°W	66	2.16
Outer shelf region				
4/9/09	HLY 17	59° 54.23°N 173° 59.23°W	104	1.17
4/10/09	HLY 19	59° 51.305°N 175° 13.41°W	120	7.30
4/23/09	HLY 65	56° 43.41°N 170° 31.86°W	109	2.17
4/26/09	HLY 69	59° 33.79°N 175° 12.05°W	133	3.04
4/27/09	HLY 73	59° 35.428°N 175° 4.62°W	129	1.37
4/30/09	HLY 90	59° 32.75°N 175° 8.95°W	132	0.63
5/16/09	HLY 116	59° 33.709°N 175° 9.17°W	130	2.83
6/18/09	KNR 22	56° 7.694°N 166° 7.836°W	113	3.04
6/20/09	KNR 32	56° 48.154°N 167° 52.25°W	104	3.75
6/25/09	KNR 60	57° 16.747°N 173° 50.522°W	196	0.15
6/29/09	KNR 79	57° 9.839°N 172° 56.764°W	121	1.27
7/2/09	KNR 106	59° 54.00°N 173° 59.981°W	105	2.02
7/3/09	KNR 113	59° 53.683°N 178° 44.589°W	152	1.62
7/5/09	KNR 122	59° 33.803°N 175° 11.998°W	136	3.55
Off shelf region				
4/12/09	HLY 25	59° 53.55°N 178° 54.198°W	705	0.65
4/12/09	HLY 26	59° 55.059°N 179° 27.253°W	2714	0.90
6/14/09	KNR 1	54° 14.744°N 166° 33.838°W	1246	1.23
6/19/09	KNR 27	55° 1.394°N 169° 13.02°W	2343	0.35
6/23/09	KNR 53	56° 3.817°N 171° 20.268°W	2800	4.79
6/26/09	KNR 67	57° 29.751°N 175° 14.567°W	3492	0.31

The relative contribution of Fe or Mn oxide reduction to OM remineralization was estimated using the calculated Fe or Mn reduction rates and measured oxygen flux rates from incubation cores. Total carbon oxidation rates were estimated from sediment oxygen consumption rates, based on Redfield ratio $C_{org}:O_2=106:138$. The fraction of OM remineralized by Fe or Mn oxide reduction was then determined by using the stoichiometric ratios of 4Fe: C_{org} and 2Mn:1 C_{org} (Froelich et al., 1979).

Using sediment oxygen consumption as a proxy for the depth-integrated carbon oxidation rate necessitates the assumption that the various biogeochemical pathways of sediment respiration are closely coupled. That is, that all oxygen consumed is either directly or indirectly linked to carbon mineralization via aerobic respiration or through the reoxidation of reduced terminal electron acceptors. In some environments, the occurrence of significant denitrification and the burial or non-steady-state reoxidation of reduced compounds (e.g.: Fe sulfides) could weaken this link (Burdige, 2012). Rates of denitrification have been shown to be small relative to oxygen consumption in Bering shelf sediments (Horak et al., 2013); however, we do not have estimates on the burial of reduced compounds such as Fe sulfides in this environment. Thus, we acknowledge that this could be a potential source of error that may lead to the underestimation of carbon oxidation

rates; still, we consider the oxygen consumption rates to be our best approximation of organic-carbon oxidation rates.

2.8. Statistical analyses

To determine the extent to which rates of both Fe and Mn oxide reduction positively covaried with sediment oxygen consumption rates, linear regressions were performed on full datasets. Both Fe and Mn reduction rate datasets failed to meet the requirements of normality for regression analysis ($W=0.72$, p -value= 4.32×10^{-6} ; and $W=0.66$, p -value= 5.11×10^{-7} , for Fe and Mn, respectively). To address this Fe and Mn reduction rates were log transformed prior to statistical analysis. The linear regressions shown are significant at the $\alpha=0.05$ level (Figs. 6 and 7).

Additionally, Jonckheere's test for ordered alternatives was used to test the hypothesis of no difference among shelf regions against the ordered alternative, $\tau_1 > \tau_2 > \tau_3 > \tau_4$ (Hollander and Wolfe, 1973). That is, regions will follow the predicted order: northern region > middle domain > outer domain > off-shelf region, with the highest rates in the northern region, where the highest carbon export is expected.

Table 2

Summary of measured sediment properties as well as calculated metal reduction rates. Percent of total organic carbon oxidation in parentheses. "No fit" indicates Fe/Mn profiles for which an appropriate model fit could not be found. Fe_{xs} and Mn_{xs} are excess Fe and Mn concentrations, respectively.

Station	O_2 flux ($mmol\ m^{-2}\ d^{-1}$)	O_2 penetration depth (cm)	NO_3^- penetration depth (cm)	Total C_{oxid}^a ($mmol\ m^{-2}\ d^{-1}$)	Fe red. rate ($mmol\ m^{-2}\ d^{-1}$)	Mn red. rate ($mmol\ m^{-2}\ d^{-1}$)	Surface Fe_{xs} ($\mu mol\ cm^{-3}$)	Surface Mn_{xs} ($\mu mol\ cm^{-3}$)
Northern-shelf region								
HLY 32	5.96	0.75	2.50	4.58	0.89 (4.84)	0.34 (3.76)	9.27	0.69
HLY 35	8.41	1.15	5.50	6.46	9.46 (36.59)	0.59 (4.59)	5.04	1.16
HLY 39	6.22	0.65	1.75	4.78	5.08 (26.59)	0.08 (0.86)	22.43	1.65
HLY 83	8.73	0.75	1.25	6.71	1.59 (5.91)	0.07 (0.50)	22.05	0.67
HLY 92	7.61	1.05	1.25	5.84	4.30 (18.41)	0.22 (1.84)	38.36	1.31
HLY 93	8.20	0.50	2.50	6.30	No fit	0.03 (0.21)	10.00	0.63
HLY 98	10.03	0.95	1.25	7.71	1.00 (3.25)	0.01 (0.04)	24.84	0.46
KNR 130	16.57	0.45	0.75	12.73	6.31 (12.40)	0.09 (0.37)	31.25	1.91
KNR 140	9.75	0.55	1.75	7.49	No fit	No fit	7.01	0.72
KNR 147	10.38	0.50	1.25	7.97	1.97 (6.18)	0.02 (0.11)	43.16	0.30
Middle-shelf region								
HLY 9	7.61	1.35	2.5	5.85	3.46 (14.80)	0.39 (3.31)	52.47	1.89
HLY 54	10.19	1.25	–	7.83	1.75 (5.58)	0.01 (0.06)	49.10	0.96
HLY 58	7.83	0.60	–	6.01	No fit	0.04 (0.34)	28.48	0.43
KNR 45	11.46	0.50	–	8.80	1.07 (3.03)	0.02 (0.13)	32.24	0.87
KNR 89	7.90	0.80	1.75	6.07	0.96 (3.95)	0.12 (1.01)	43.88	1.53
Outer-shelf region								
HLY 17	5.41	1.25	1.25	4.15	0.93 (5.62)	0.00 (0.05)	11.67	0.87
HLY 19	6.99	1.05	1.75	5.37	0.90 (4.21)	No fit	12.86	0.22
HLY 65	4.50	1.25	1.75	3.45	0.31 (2.25)	0.02 (0.34)	15.09	0.35
HLY 69	4.76	0.85	5.50	3.65	No fit	0.04 (0.60)	35.97	0.42
HLY 73	5.98	1.10	1.25	4.60	0.87 (4.76)	0.00 (0.01)	19.58	0.24
HLY 90	5.78	1.55	1.75	4.44	0.11 (0.62)	0.00 (0.01)	24.09	0.23
HLY 116	6.68	0.95	5.50	5.13	1.46 (7.10)	0.04 (0.41)	20.99	0.23
KNR 22	9.38	0.70	3.50	4.94	0.31 (1.07)	No fit	13.40	0.15
KNR 32	7.88	0.65	1.75	6.06	3.65 (15.07)	0.10 (0.82)	20.08	1.24
KNR 60	5.83	0.30	–	4.47	0.04 (0.25)	0.00 (0.02)	1.90	0.52
KNR 79	10.54	1.15	1.75	8.10	0.48 (1.48)	0.02 (0.10)	15.38	0.48
KNR 106	11.89	0.60	3.50	9.13	No fit	0.01 (0.04)	15.17	0.13
KNR 113	6.10	1.15	1.75	4.69	0.53 (2.84)	0.01 (0.11)	14.40	0.18
KNR 122	8.62	0.85	2.50	6.62	1.14 (4.30)	No fit	13.73	0.06
Off-shelf region								
HLY 25	3.70	0.50	0.75	2.84	0.45 (3.98)	No fit	11.17	0.09
HLY 26	3.25	0.50	7.50	2.49	No fit	0.03 (0.58)	18.77	3.75
KNR 1	1.24	0.55	2.50	0.96	0.08 (2.22)	0.01 (0.34)	4.62	0.18
KNR 27	6.44	0.80	2.50	4.94	0.22 (1.10)	No fit	6.30	1.90
KNR 53	5.33	0.85	2.50	4.09	0.95 (5.82)	0.26 (3.22)	8.78	2.00
KNR 67	4.38	0.90	2.00	3.37	0.11 (0.83)	0.01 (0.21)	6.87	5.64

^a Total carbon oxidation rates based on oxygen flux rates.

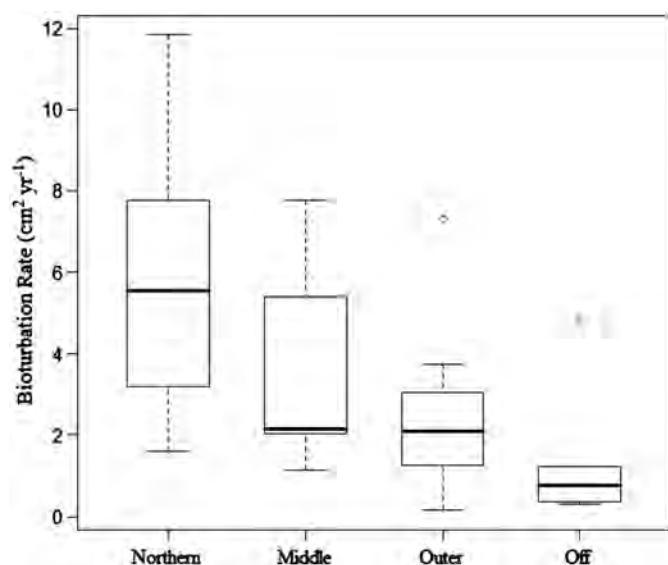


Fig. 2. Box and whisker plot showing bioturbation rates separated by shelf region. Each box encompasses the middle 50% of the data with the horizontal line representing the median. The vertical, dashed line extends to the minimum of either the maximum value or 1.5 times the middle 50% of the data. Individual points fall outside this range.

3. Results

3.1. Bioturbation

Bioturbation rates, determined from excess ^{234}Th profiles (Appendix Table A1) varied regionally across the shelf (Table 1, Fig. 2). The northern region contained the highest calculated rates, averaging $5.91 \pm 3.53 \text{ cm}^2 \text{ yr}^{-1}$ ($1.59\text{--}11.83 \text{ cm}^2 \text{ yr}^{-1}$, $N=11$). Rates decreased moving to the middle shelf domain, which averaged $3.70 \pm 2.78 \text{ cm}^2 \text{ yr}^{-1}$ ($1.14\text{--}7.75 \text{ cm}^2 \text{ yr}^{-1}$, $N=5$). The outer shelf rates were similar to but slightly lower than the middle shelf, averaging $2.42 \pm 1.78 \text{ cm}^2 \text{ yr}^{-1}$ ($0.15\text{--}7.30 \text{ cm}^2 \text{ yr}^{-1}$, $N=14$), and the off-shelf region had the lowest average bioturbation rate of $1.37 \pm 1.71 \text{ cm}^2 \text{ yr}^{-1}$ ($0.31\text{--}4.79 \text{ cm}^2 \text{ yr}^{-1}$, $N=6$).

The decreasing trend in regional bioturbation rates across the shelf in the seaward direction significantly followed the predicted order based on Jonckheere's test for ordered alternatives ($J^* = -3.63$, $p < 0.0001$).

3.2. Solid-phase iron and manganese

Depth distributions of solid-phase Fe and Mn were somewhat variable across the shelf (Appendix Table A1). Generally, Fe oxide concentrations decreased with depth, with or without a subsurface peak, while Mn profiles either showed a steep, shallow gradient just below the sediment-water interface, or a more gradual decline with depth. As the oxidation of organic carbon by Fe and Mn oxides results in the reduction of these metals to their soluble phase, the increase of Fe^{2+} and Mn^{2+} in pore-water provided another indication of Fe and Mn oxide reduction. At stations where both solid-phase and pore-water Fe and Mn profiles were available, comparisons showed that the depth range over which oxide concentrations decreased was consistent with the depth range over which Fe and Mn pore-water concentrations increased, thereby confirming the relative depth distributions of Fe or Mn reduction (Fig. 3, Appendix Table A1).

Pore-water nitrate profiles were also compared to profiles of pore-water Fe and Mn, enabling us to relate the zone of denitrification to the zones of both Fe and Mn reduction (Fig. 3).

Typically, over the depth range where nitrate concentrations decreased, there was a concurrent increase in pore-water Mn. Peaks in reduced Fe tended to occur deeper than the depth of depletion of pore-water nitrate. Additionally, the subsurface gradient observed in both Fe^{2+} and Mn^{2+} profiles suggests a potential flux of reduced Fe or Mn out of the sediment. These comparisons also indicated that the depth range of positive Fe and Mn pore-water gradients corresponded to the depth range of Fe and Mn reduction determined from profiles of excess Fe and Mn oxides, dissolved oxygen and nitrate.

Rates of sedimentary Fe reduction showed a regional trend similar to that of bioturbation rates (Fig. 4, Table 2). Highest rates were in the northern region, where the average was $3.82 \text{ mmol m}^{-2} \text{ d}^{-1}$ ($0.89\text{--}9.46 \text{ mmol m}^{-2} \text{ d}^{-1}$, $N=8$). Rates were lower in the middle shelf domain, averaging $1.81 \text{ mmol m}^{-2} \text{ d}^{-1}$ ($0.96\text{--}3.46 \text{ mmol m}^{-2} \text{ d}^{-1}$, $N=4$). The average Fe reduction rate for the outer shelf was $0.89 \text{ mmol m}^{-2} \text{ d}^{-1}$ ($0.04\text{--}3.65 \text{ mmol m}^{-2} \text{ d}^{-1}$, $N=12$), and the lowest rates were in the off-shelf region where the mean was $0.36 \text{ mmol m}^{-2} \text{ d}^{-1}$ ($0.08\text{--}0.95 \text{ mmol m}^{-2} \text{ d}^{-1}$, $N=5$). This ordering was also found to be significant based on Jonckheere's test for ordered alternatives, which resulted in the rejection of the null hypothesis of no difference among shelf regions for both Fe reduction rates ($J^* = -4.05$, $p < 0.0001$) and the percentage of OM remineralized by Fe reduction ($J^* = -3.06$, $p = 0.0011$).

Fe reduction rates across the shelf were also compared to oxygen flux. This analysis was used to determine how Fe reduction rates vary with organic carbon mineralization rates, as oxygen consumption estimates sedimentary organic carbon mineralization. A linear regression analysis found a significant relationship between these two variables ($p = 0.003$; Fig. 6). However, oxygen flux can only account for approximately 26% of the variation in Fe reduction ($R^2 = 0.265$).

In contrast to Fe, rates of Mn oxide reduction were consistently low across the shelf (Fig. 5, Table 2). Mean rates of Mn reduction were highest in the northern and middle-shelf regions with averages of $0.16 \text{ mmol m}^{-2} \text{ d}^{-1}$ and $0.12 \text{ mmol m}^{-2} \text{ d}^{-1}$, respectively ($0.01\text{--}0.59 \text{ mmol m}^{-2} \text{ d}^{-1}$, $N=9$; $0.01\text{--}0.39 \text{ mmol m}^{-2} \text{ d}^{-1}$, $N=5$, respectively). Unlike Fe reduction rates, however, the off-shelf region had slightly higher Mn reduction rates than the outer shelf domain ($\mu = 0.08 \text{ mmol m}^{-2} \text{ d}^{-1}$, $0.01\text{--}0.26 \text{ mmol m}^{-2} \text{ d}^{-1}$, $N=4$; $\mu = 0.02 \text{ mmol m}^{-2} \text{ d}^{-1}$, $0.00\text{--}0.10 \text{ mmol m}^{-2} \text{ d}^{-1}$, $N=11$, respectively). However, Jonckheere's test for ordered alternatives showed that Mn reduction rates were also significantly ordered as predicted ($J^* = -2.04$, $p = 0.0207$), but the percentages of OM remineralized by Mn reduction were not found to significantly differ among regions ($J^* = -1.21$, $p = 0.1131$). These percentages were also extremely low across the shelf, and were not above 5% in any region. Additionally, linear regression analysis comparing Mn reduction rates to sediment oxygen consumption rates showed no significant relationship (Fig. 7).

4. Discussion

The energetics of metal reduction, along with denitrification and sulfate reduction typically results in these processes occurring in a given sequence in the sediment. In most continental margin sediments, Fe reduction occurs below that of Mn reduction and denitrification, which have been shown to overlap (Burdige, 1993; Emerson and Hedges, 2003). Historically, Fe and Mn oxide reduction have been thought of as minor contributors to OM remineralization; however, more recent studies have shown that Fe and Mn oxide reduction can be important components of carbon respiration in some marine sediment environments (Canfield et al., 1993; Kostka et al., 1999; Nickel et al., 2008). The

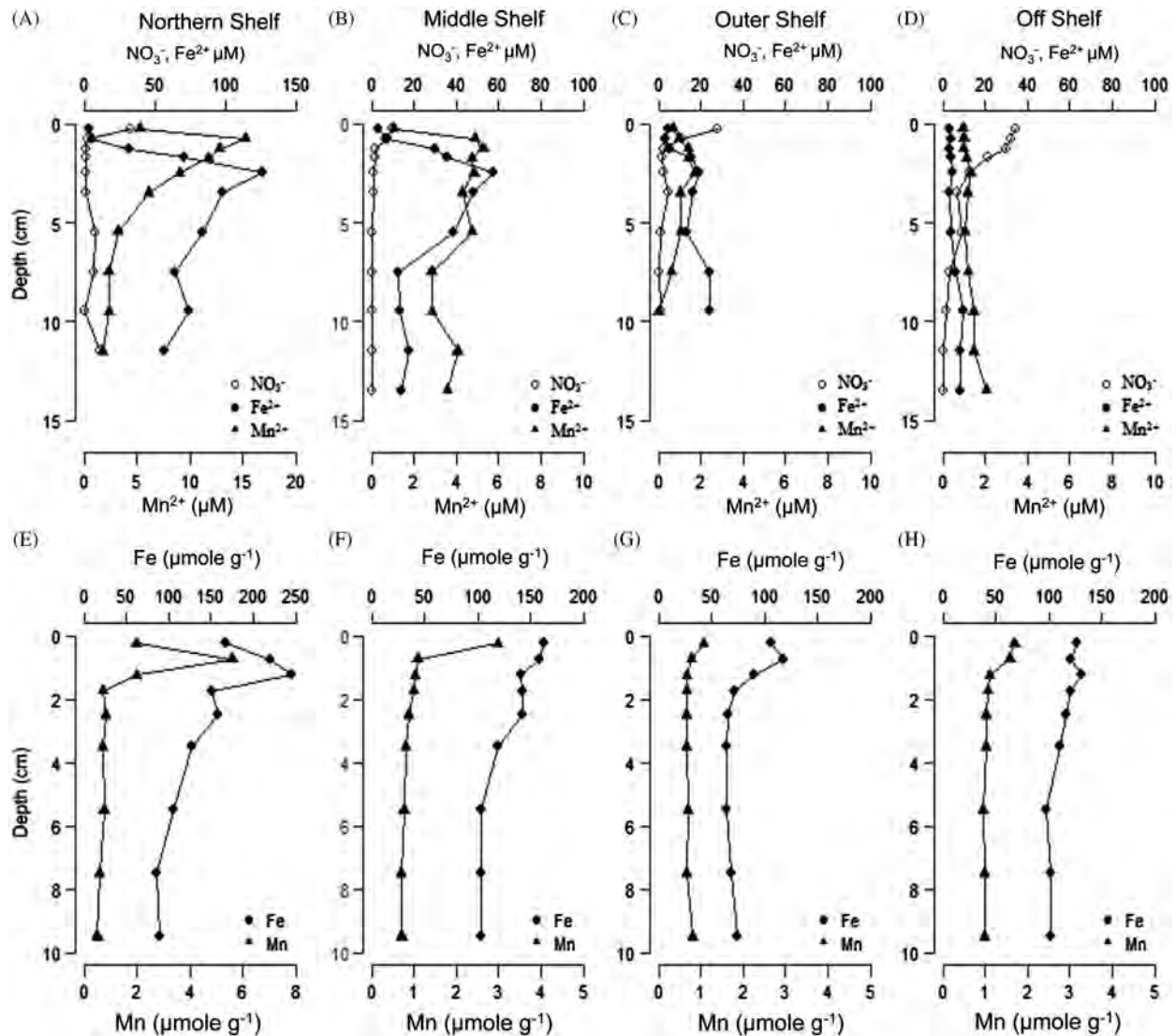


Fig. 3. Depth profiles showing pore-water Fe^{2+} , Mn^{2+} and NO_3^- (A–D) and Fe and Mn oxides (E–H). A station representing each domain is pictured, ordered from left to right as; HLY 32 (A,E), KNR 89 (B,F), HLY 90 (C,G) and KNR 1 (D,F). Note the difference in the x-axis scaling in profiles (A) and (E).

depth profiles of Fe^{2+} , Mn^{2+} , and NO_3^- seen here are typical of those observed in other hemipelagic or continental margin sediments, providing additional support for the potential significance of Fe reduction in sediments (Emerson and Hedges, 2003). The input and lability of OM often regulates the rate of metal reduction, whereas the relative significance of Fe or Mn reduction in total carbon remineralization is likely regulated by their respective sediment oxide concentrations (Roden and Wetzel, 2002; Canfield et al., 2005). However, rapid internal cycling of these metals can increase the significance of metal reduction under low input conditions. Nonetheless, we expected to see regional variation in Fe and Mn reduction rates that were similar to that which has been observed of carbon export (Moran et al., 2012). That is, rates should be highest in the northern region and decrease in the seaward direction (northern region > middle domain > outer domain > off-shelf region). Consistent with this hypothesis, rates of both Fe reduction varied as expected. In contrast, the cross-shelf variation in Mn reduction rates did not show as strong a pattern. Additionally, bioturbation rates varied similarly to carbon export and Fe reduction rates.

4.1. Bioturbation

The method of quantifying bioturbation rates by fitting a diffusive model to the profile of a particle-reactive radionuclide tracer requires several assumptions (Meysman et al., 2003; Burdige, 2006). First, the calculation of a biodiffusion coefficient (D_b) requires that particle mixing be spatially random and occur over a small scale, analogous to diffusive transport. That is, the distance over which particle movement occurs is shorter than the tracer's mixing length. Second, the frequency of mixing events must be more frequent than the decay rate of the tracer. Short-lived radioisotopes, such as ^{234}Th , may violate these assumptions resulting in an overestimate of bioturbation rate, a phenomenon termed "tracer dependence". Tracer dependence has been shown to be of greater significance in sediments with low mixing rates. Lacroart et al. (2010) argued that in environments with bioturbation rates greater than $2 \text{ cm}^2 \text{ yr}^{-1}$, tracer dependence is absent and ^{234}Th is suitable to quantify values of D_b . Bioturbation rates calculated in this study meet that condition in all the regions of the Bering Sea, except for the off-shelf region, which had an average bioturbation rate of $1.37 \text{ cm}^2 \text{ yr}^{-1}$, the lowest of all the

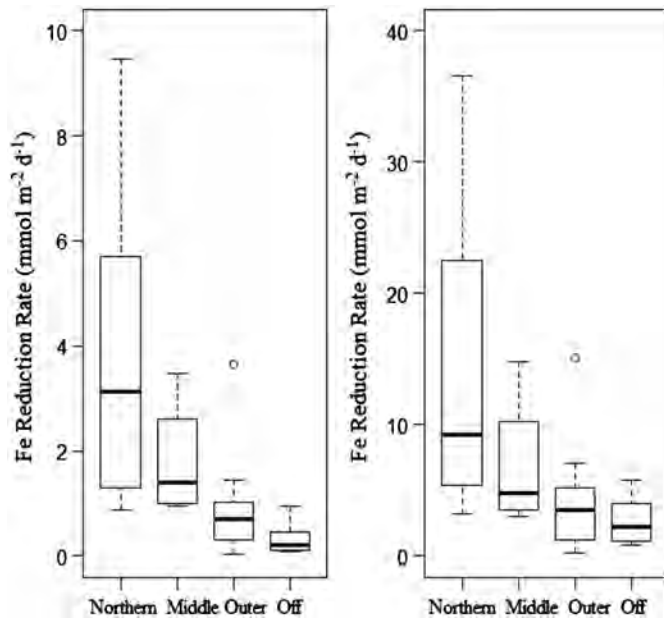


Fig. 4. Box and whisker plots of iron reduction rates by region and as a percentage of total carbon oxidation rates based on oxygen consumption rates. Each box encompasses the middle 50% of the data with the horizontal line representing the median. The vertical, dashed line extends to the minimum of either the maximum value or 1.5 times the middle 50% of the data. Individual points fall outside this range.

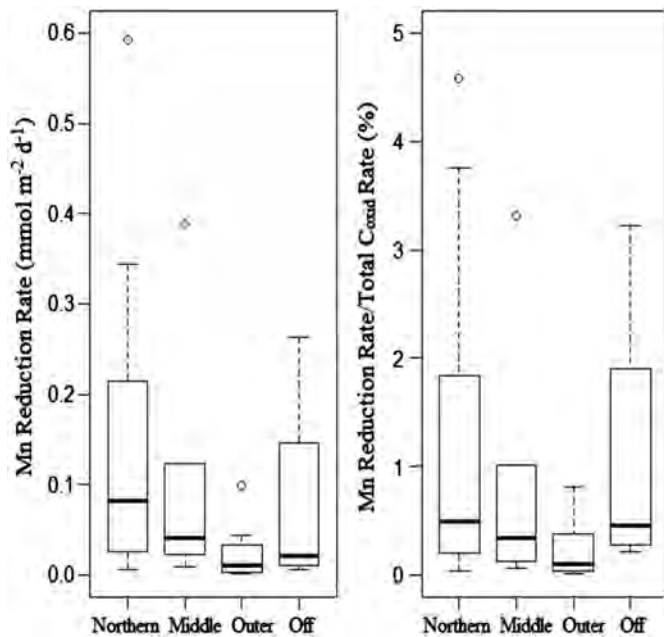


Fig. 5. Box and whisker plots showing Mn reduction rates by region and as a percentage of total carbon oxidation rates, based on oxygen consumption rates. Each box encompasses the middle 50% of the data with the horizontal line representing the median. The vertical, dashed line extends to the minimum of either the maximum value or 1.5 times the middle 50% of the data. Individual points fall outside this range.

regions. Thus, it is likely that the very low values of D_b calculated for the off-shelf region are overestimates of bioturbation. Since D_b was used in the calculation of Fe and Mn reduction rates, many of the calculated rates in the off-shelf region are likely overestimated as well. Regardless, D_b is still a good indicator of variation in bioturbation, even in the off-shelf region.

The highest bioturbation rates calculated were in the northern region, consistent with past observations of a high rate of supply of

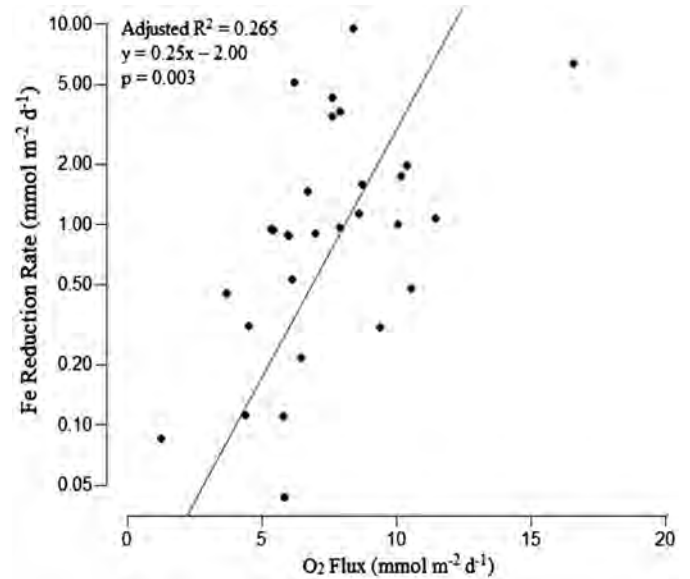


Fig. 6. Rates of iron oxide reduction plotted as a function of total oxygen consumption rates across the southeastern Bering Sea shelf. Iron oxide reduction rates are plotted on a log scale.

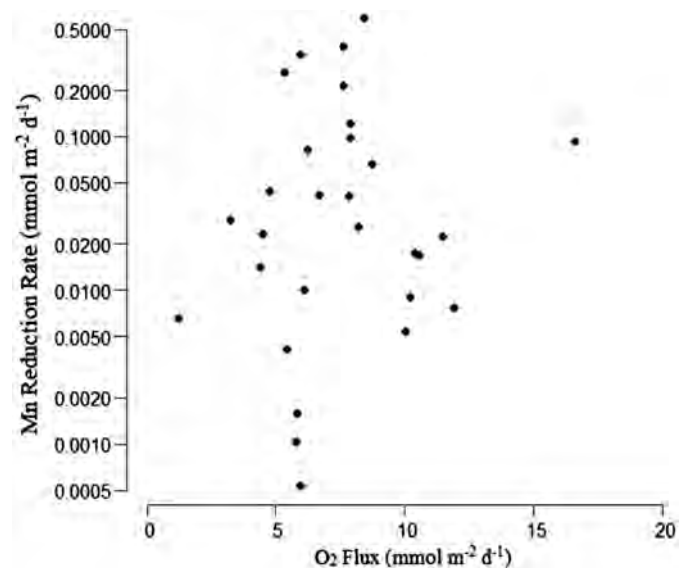


Fig. 7. Rates of manganese oxide reduction plotted as a function of total oxygen consumption rates across the southeastern Bering Sea shelf. Manganese oxide reduction rates are plotted on a log scale.

OM to the sediment and high benthic biomass in this region (Grebmeier et al., 1988, 2006). The range of bioturbation rates in the middle domain included rates similar to those found in the northern region (Fig. 2), pointing to comparable environmental conditions. For instance, Moran et al. (2012) showed comparable carbon export rates between the northern and middle regions. However, this is in contrast to the outer shelf where pelagic grazing dominates and less OM is delivered to the sediment surface (Grebmeier et al., 1988). This could serve as an explanation for the low rates of bioturbation in this region compared to the northern and middle-shelf regions.

4.2. Iron reduction

High rates of Fe reduction corresponded to the regions of the Bering shelf where we would expect greater carbon export to the

Table A1

Table showing porosity values, excess ^{234}Th profiles, solid-phase and pore-water Fe and Mn profiles. Pore-water profiles for stations marked with (†) represent average values from duplicate cores.

Station	Avg. depth (cm)	Porosity	Excess Th-234 (dpm g^{-1})	Fe concentration ($\mu\text{mol g}^{-1}$)	Mn concentration ($\mu\text{mol g}^{-1}$)	Pore water Fe (μM)	Pore water Mn (μM)
HLY 9	0.25	0.71	5.88 (± 0.46)	143.07	2.58	–	–
	0.75	0.58	0.50 (± 0.19)	138.29	0.93	–	–
	1.25	0.61	–0.56 (± 0.14)	106.46	0.62	–	–
	1.75	0.61	0.70 (± 0.23)	85.99	0.58	–	–
	2.5	0.63	–	86.54	0.53	–	–
	3.5	0.63	–	84.50	0.67	–	–
	5.5	0.57	–	88.94	0.58	–	–
	7.5	0.55	–	81.14	0.56	–	–
	9.5	0.44	–	67.45	0.55	–	–
†HLY 17	0.25	0.87	22.07 (± 1.87)	170.04	2.37	3.87	0.62
	0.75	0.78	4.94 (± 0.52)	213.93	1.58	3.45	1.53
	1.25	0.76	–0.40 (± 0.20)	161.55	1.06	34.93	3.64
	1.75	0.76	–	138.60	1.04	62.96	4.05
	2.5	0.76	–	152.33	1.04	71.52	4.73
	3.5	0.73	–	136.32	1.16	75.83	3.75
	5.5	0.75	–	130.58	1.15	59.19	3.17
	7.5	0.70	–	114.14	1.00	54.26	2.03
	9.5	0.72	–	127.41	1.16	45.62	2.01
†HLY 19	0.25	0.81	5.07 (± 0.63)	111.29	1.07	3.05	0.25
	0.75	0.76	1.43 (± 0.28)	118.74	0.89	4.26	0.95
	1.25	0.74	1.53 (± 0.33)	113.47	0.96	9.43	1.48
	1.75	0.75	–	99.54	0.91	20.55	1.84
	2.5	0.75	–	92.45	0.80	39.10	2.05
	3.5	0.75	–	90.46	0.82	45.85	1.83
	5.5	0.73	–	85.22	0.62	33.21	1.53
	7.5	0.71	–	96.34	0.66	65.23	1.37
	9.5	0.71	–	72.68	0.67	27.01	1.27
HLY 25	0.25	0.82	8.48 (± 0.77)	76.01	0.75	3.88	0.63
	0.75	0.78	1.13 (± 0.28)	71.50	0.66	4.76	0.78
	1.25	0.80	–	55.35	0.56	10.02	0.90
	1.75	0.76	–	53.18	0.58	9.50	0.89
	2.5	0.74	–	52.74	0.56	9.94	0.79
	3.5	0.72	–	58.16	0.60	5.63	0.77
	5.5	0.72	–	53.52	0.42	4.12	0.27
	7.5	0.72	–	44.89	0.47	5.38	0.37
	9.5	0.72	–	46.18	0.55	2.09	0.00
†HLY 26	0.25	0.69	13.66 (± 0.84)	81.74	5.35	3.79	0.71
	0.75	0.69	0.62 (± 0.17)	96.44	4.42	3.83	0.79
	1.25	0.67	0.45 (± 0.13)	64.75	0.75	3.15	0.53
	1.75	0.66	–	61.44	0.75	3.81	0.96
	2.5	0.63	–	58.68	0.67	1.94	0.24
	3.5	0.64	–	76.35	0.75	7.42	0.70
	5.5	0.64	–	82.83	0.89	19.26	1.05
	7.5	0.64	–	91.21	0.91	20.56	2.46
	9.5	0.64	–	89.89	1.00	7.99	0.18
†HLY 32	0.25	0.79	15.43 (± 0.10)	166.79	1.97	3.81	3.67
	0.75	0.84	2.72 (± 0.13)	220.53	5.61	92.39	10.76
	1.25	0.81	2.01 (± 0.10)	245.26	2.00	94.44	8.28
	1.75	0.77	1.29 (± 0.09)	150.14	0.73	113.04	7.18
	2.5	0.74	–	158.20	0.84	129.68	6.62
	3.5	0.71	–	126.65	0.73	134.73	5.57
	5.5	0.67	–	106.29	0.75	72.49	5.01
	7.5	0.61	–	85.91	0.60	37.63	6.89
	9.5	0.62	–	89.03	0.51	38.91	5.80
†HLY 35	0.25	0.72	5.00 (± 0.46)	102.74	1.97	5.64	0.90
	0.75	0.64	1.62 (± 0.28)	101.35	1.80	4.29	3.65
	1.25	0.62	0.80 (± 0.16)	106.88	1.22	5.02	5.27
	1.75	0.59	1.25 (± 0.20)	116.19	2.15	3.50	6.89
	2.5	0.53	–	108.64	0.82	9.49	9.17
	3.5	0.56	–	95.92	0.60	15.26	7.54
	5.5	0.55	–	109.32	0.40	59.34	3.68
	7.5	0.51	–	68.03	0.40	–	–
	9.5	0.52	–	55.76	0.42	–	–
†HLY 39	0.25	0.68	6.04 (± 0.56)	92.56	2.69	4.27	1.51
	0.75	0.66	3.21 (± 0.42)	109.41	1.27	8.55	11.39
	1.25	0.66	1.55 (± 0.24)	113.61	1.82	35.70	20.02
	1.75	0.67	0.90 (± 0.20)	96.75	0.87	46.05	30.18
	2.5	0.68	–	91.95	0.84	61.36	27.38
	3.5	0.68	–	107.26	0.73	87.51	24.09

Table A1 (continued)

Station	Avg. depth (cm)	Porosity	Excess Th-234 (dpm g ⁻¹)	Fe concentration (μmol g ⁻¹)	Mn concentration (μmol g ⁻¹)	Pore water Fe (μM)	Pore water Mn (μM)
	5.5	0.66	–	80.97	0.62	183.34	13.66
	7.5	0.62	–	65.77	0.56	191.76	9.28
	9.5	0.59	–	69.15	0.51	–	–
HLY 54	0.25	0.73	10.56 (± 0.92)	120.22	1.86	–	–
	0.75	0.57	1.16 (± 0.20)	94.97	0.96	–	–
	1.25	0.55	0.51 (± 0.06)	92.91	0.64	–	–
	1.75	0.54	–	64.39	0.51	–	–
	2.5	0.51	–	55.80	0.56	–	–
	3.5	0.51	–	51.25	0.47	–	–
	5.5	0.50	–	64.23	0.49	–	–
	7.5	0.46	–	54.49	0.31	–	–
	9.5	0.47	–	48.74	0.53	–	–
HLY 58	0.25	0.66	3.43 (± 0.39)	73.52	0.89	–	–
	0.75	0.64	0.35 (± 0.14)	78.05	0.98	–	–
	1.25	0.50	0.85 (± 0.18)	58.02	0.56	–	–
	1.75	0.45	–	65.05	0.66	–	–
	2.5	0.46	–	55.88	0.62	–	–
	3.5	0.48	–	59.97	0.42	–	–
	5.5	0.41	–	50.96	0.31	–	–
	7.5	0.40	–	42.04	0.29	–	–
	9.5	0.41	–	44.93	0.36	–	–
†HLY 65	0.25	0.78	35.94 (± 1.81)	81.78	0.89	3.09	0.49
	0.75	0.72	9.88 (± 0.86)	78.82	0.49	3.35	0.71
	1.25	0.64	3.50 (± 0.48)	58.70	0.47	3.71	1.00
	1.75	0.63	1.30 (± 0.22)	60.88	0.53	7.39	1.36
	2.5	0.65	–	56.42	0.53	7.73	0.93
	3.5	0.62	–	55.94	0.47	17.66	0.75
	5.5	0.61	–	44.64	0.40	–	–
	7.5	0.64	–	43.92	0.29	–	–
	9.5	0.64	–	42.76	0.29	–	–
HLY 69	0.25	0.82	21.87 (± 1.92)	139.52	1.49	4.17	0.77
	0.75	0.78	7.28 (± 0.88)	128.35	0.75	4.06	1.44
	1.25	0.76	3.41 (± 0.49)	79.52	0.62	6.13	1.41
	1.75	0.74	–	75.98	0.67	31.98	1.46
	2.5	0.73	–	77.52	0.60	40.07	1.47
	3.5	0.73	–	74.85	0.64	59.85	1.37
	5.5	0.70	–	72.39	0.64	41.59	1.25
	7.5	0.67	–	63.51	0.67	25.16	0.84
	9.5	0.65	–	68.31	0.69	10.87	0.43
HLY 73	0.25	0.80	13.57 (± 1.02)	103.27	1.16	4.39	1.14
	0.75	0.77	0.91 (± 0.28)	100.42	1.04	5.37	2.43
	1.25	0.74	0.85 (± 0.28)	73.01	0.75	22.26	4.36
	1.75	0.73	–	66.20	0.71	16.51	4.20
	2.5	0.73	–	73.38	0.86	22.23	3.36
	3.5	0.72	–	76.32	0.73	50.79	1.72
	5.5	0.69	–	76.91	0.78	33.02	1.32
	7.5	0.67	–	64.39	0.75	33.17	1.09
	9.5	0.67	–	65.93	0.76	–	–
HLY 83	0.25	0.87	23.33 (± 1.91)	195.54	3.04	3.79	0.93
	0.75	0.81	6.57 (± 0.50)	163.56	1.16	7.91	3.04
	1.25	0.82	2.42 (± 0.31)	132.21	1.04	36.59	2.79
	1.75	0.80	–	129.47	1.07	71.13	3.22
	2.5	0.80	–	157.88	1.07	71.62	3.50
	3.5	0.80	–	150.15	1.06	71.62	3.75
	5.5	0.78	–	145.53	1.11	62.61	3.28
	7.5	0.76	–	150.42	1.06	66.00	3.22
	9.5	0.74	–	131.29	1.07	48.55	2.77
HLY 90	0.25	0.78	11.76 (± 0.78)	105.74	1.06	4.36	0.68
	0.75	0.77	1.52 (± 0.33)	117.45	0.78	2.98	0.95
	1.25	0.77	-0.33 (± 0.18)	90.84	0.66	5.64	1.42
	1.75	0.75	–	72.15	0.66	15.22	1.43
	2.5	0.71	–	66.04	0.67	19.02	1.73
	3.5	0.71	–	63.62	0.67	16.22	1.05
	5.5	0.68	–	63.80	0.69	13.65	1.07
	7.5	0.68	–	68.14	0.67	24.52	0.62
	9.5	0.67	–	74.01	0.80	24.28	0.00
HLY 92	0.25	0.83	19.41 (± 1.41)	193.02	3.64	3.01	1.05
	0.75	0.83	7.68 (± 0.81)	175.47	1.89	10.49	9.55
	1.25	0.78	4.99 (± 0.63)	121.93	0.84	52.96	5.38
	1.75	0.79	–	106.17	0.71	65.52	3.86
	2.5	0.77	–	115.36	0.67	91.32	3.00

Table A1 (continued)

Station	Avg. depth (cm)	Porosity	Excess Th-234 (dpm g ⁻¹)	Fe concentration (μmol g ⁻¹)	Mn concentration (μmol g ⁻¹)	Pore water Fe (μM)	Pore water Mn (μM)
	3.5	0.76	–	107.08	0.66	97.16	2.45
	5.5	0.68	–	94.57	0.64	71.19	1.88
	7.5	0.66	–	85.68	0.56	44.68	1.46
	9.5	0.63	–	94.85	0.62	40.93	1.09
HLY 93	0.25	0.74	4.46 (± 0.52)	104.74	1.64	0.00	3.89
	0.75	0.63	2.05 (± 0.40)	101.82	0.86	90.67	13.07
	1.25	0.61	1.09 (± 0.30)	111.06	1.07	102.25	10.25
	1.75	0.61	–	102.66	0.95	118.45	9.04
	2.5	0.62	–	103.86	0.86	156.88	7.06
	3.5	0.61	–	90.50	0.75	130.78	7.94
	5.5	0.57	–	99.11	0.87	157.92	8.80
	7.5	0.54	–	61.15	0.60	111.90	4.03
	9.5	0.55	–	56.53	0.56	0.00	1.47
†HLY 98	0.25	0.87	32.06 (± 1.71)	159.21	1.89	2.07	0.69
	0.75	0.84	4.58 (± 0.65)	175.52	1.47	2.29	3.31
	1.25	0.79	2.46 (± 0.46)	168.95	0.91	22.44	3.77
	1.75	0.76	–	128.23	0.71	47.13	1.99
	2.5	0.75	–	98.74	0.55	69.72	1.57
	3.5	0.73	–	96.48	0.73	77.27	1.82
	5.5	0.69	–	86.83	0.56	71.05	1.94
	7.5	0.68	–	79.02	0.56	60.73	1.69
	9.5	0.65	–	106.97	0.47	34.93	1.01
†HLY 116	0.25	0.79	15.78 (± 1.25)	119.63	0.86	4.65	0.61
	0.75	0.75	1.66 (± 0.35)	123.22	0.76	5.14	1.25
	1.25	0.74	2.30 (± 0.42)	81.24	0.47	8.23	1.48
	1.75	0.72	–	85.54	0.44	16.68	1.46
	2.5	0.56	–	88.12	0.49	19.88	1.14
	3.5	0.72	–	85.86	0.56	27.51	1.16
	5.5	0.68	–	100.85	0.47	10.79	0.48
	7.5	0.69	–	77.00	0.55	18.73	0.22
	9.5	0.68	–	74.85	0.47	16.70	0.31
†KNR 1	0.25	0.895	44.51 (± 3.35)	126.49	1.69	3.72	1.01
	0.75	0.905	10.77 (± 0.89)	120.48	1.58	3.59	1.01
	1.25	0.898	2.40 (± 0.40)	130.77	1.11	3.49	1.02
	1.75	0.879	–	120.73	1.07	3.65	1.05
	2.5	0.869	–	116.81	1.04	4.08	1.16
	3.5	0.855	–	109.97	1.04	3.59	1.11
	5.5	0.833	–	97.70	0.96	3.75	1.09
	7.5	0.833	–	101.39	0.98	4.96	1.44
	9.5	0.822	–	102.50	0.98	8.01	2.06
KNR 17	0.25	0.496	2.94 (± 0.34)	58.91	0.95	–	–
	0.75	0.472	1.10 (± 0.12)	64.25	0.42	–	–
	1.25	0.447	0.35 (± 0.13)	71.93	0.42	–	–
	1.75	0.423	–	66.29	0.31	–	–
	2.5	0.435	–	68.31	0.25	–	–
	3.5	0.444	–	48.65	0.20	–	–
	5.5	0.458	–	41.83	0.16	–	–
	7.5	0.467	–	44.71	0.22	–	–
	9.5	0.461	–	33.66	0.16	–	–
†KNR 22	0.25	0.861	13.15 (± 0.86)	111.02	1.06	3.41	4.64
	0.75	0.795	2.10 (± 0.29)	114.85	0.89	3.43	5.44
	1.25	0.778	2.05 (± 0.36)	101.69	0.76	2.40	3.05
	1.75	0.729	–	101.44	0.78	3.45	3.09
	2.5	0.709	–	81.44	0.66	11.33	3.01
	3.5	0.705	–	74.60	0.64	16.44	1.98
	5.5	0.662	–	68.40	0.47	6.48	1.38
	7.5	0.617	–	68.91	0.55	8.44	1.42
	9.5	0.626	–	80.51	0.64	5.58	1.61
†KNR 27	0.25	0.955	102.94 (± 7.87)	111.31	17.53	4.51	1.00
	0.75	0.922	9.01 (± 0.86)	115.44	6.53	3.91	1.23
	1.25	0.914	0.44 (± 0.30)	104.56	1.66	4.10	1.83
	1.75	0.917	–	132.96	4.48	3.99	2.33
	2.5	0.917	–	62.71	0.44	4.17	2.64
	3.5	0.912	–	58.77	0.46	6.22	2.84
	5.5	0.901	–	67.40	0.49	4.26	2.93
	7.5	0.893	–	61.06	0.53	4.11	3.34
	9.5	0.878	–	65.95	0.51	5.39	2.85
KNR 32	0.25	0.708	5.51 (± 0.54)	83.84	1.75	–	–
	0.75	0.546	1.04 (± 0.25)	84.27	1.05	–	–
	1.25	0.560	1.03 (± 0.21)	89.65	0.35	–	–
	1.75	0.534	–	81.91	0.23	–	–

Table A1 (continued)

Station	Avg. depth (cm)	Porosity	Excess Th-234 (dpm g ⁻¹)	Fe concentration (μmol g ⁻¹)	Mn concentration (μmol g ⁻¹)	Pore water Fe (μM)	Pore water Mn (μM)
	2.5	0.533	–	62.96	0.14	–	–
	3.5	0.547	–	57.87	0.23	–	–
	5.5	0.545	–	55.56	0.20	–	–
	7.5	0.529	–	56.77	0.40	–	–
	9.5	0.514	–	64.42	0.47	–	–
KNR 45	0.25	0.719	4.85 (± 0.37)	89.64	1.18	–	–
	0.75	0.548	0.92 (± 0.15)	85.81	0.80	–	–
	1.25	0.454	0.50 (± 0.15)	85.34	0.25	–	–
	1.75	0.451	–	76.94	0.05	–	–
	2.5	0.451	–	57.05	0.01	–	–
	3.5	0.464	–	46.30	0.03	–	–
	5.5	0.435	–	37.29	0.00	–	–
	7.5	0.412	–	39.00	0.02	–	–
	9.5	0.410	–	34.71	0.01	–	–
†KNR 53	0.25	0.953	63.91 (± 4.84)	156.30	16.83	3.50	0.74
	0.75	0.938	5.01 (± 1.20)	222.96	8.98	3.39	0.84
	1.25	0.933	14.53 (± 0.85)	242.52	1.87	3.44	1.56
	1.75	0.908	–	119.88	0.74	4.05	2.40
	2.5	0.924	–	90.70	0.52	3.59	3.72
	3.5	0.912	–	85.84	0.60	3.95	4.21
	5.5	0.902	–	74.34	0.51	3.79	5.47
	7.5	0.898	–	69.38	0.57	3.63	5.84
	9.5	0.889	–	70.82	0.69	3.88	5.84
KNR 60	0.25	0.523	4.11 (± 0.40)	29.37	0.17	–	–
	0.75	0.482	0.06 (± 0.19)	32.67	0.00	–	–
	1.25	0.462	–0.53 (± 0.13)	31.96	0.00	–	–
	1.75	0.444	–	39.03	0.00	–	–
	2.5	0.446	–	33.91	0.00	–	–
	3.5	0.431	–	30.62	0.00	–	–
	5.5	0.448	–	27.87	0.00	–	–
	7.5	–	–	28.93	0.00	–	–
	9.5	–	–	–	0.00	–	–
†KNR 67	0.25	0.923	23.82 (± 1.86)	106.61	28.57	3.86	0.67
	0.75	0.912	1.32 (± 0.59)	98.41	20.17	3.32	0.69
	1.25	0.907	–0.30 (± 0.53)	100.46	1.45	3.34	0.80
	1.75	0.906	–	66.14	0.88	3.42	2.80
	2.5	0.893	–	64.85	0.96	3.92	5.09
	3.5	0.886	–	72.90	1.06	3.66	7.08
	5.5	0.871	–	65.69	1.35	4.63	9.22
	7.5	0.869	–	48.71	1.16	9.12	10.96
	9.5	0.871	–	52.66	1.28	3.60	11.45
KNR 79	0.25	0.775	18.12 (± 1.27)	62.85	1.18	3.34	0.70
	0.75	0.687	2.78 (± 0.28)	65.94	0.86	3.25	0.95
	1.25	0.592	1.03 (± 0.20)	69.62	0.52	3.49	1.34
	1.75	0.586	–	54.65	0.38	91.35	4.32
	2.5	0.593	–	51.65	0.42	12.99	2.46
	3.5	0.592	–	37.03	0.32	7.86	1.73
	5.5	0.541	–	32.69	0.25	–	–
	7.5	0.545	–	35.67	0.27	–	–
	9.5	0.572	–	40.74	0.39	–	–
KNR 89	0.25	0.724	18.15 (± 1.37)	163.02	2.97	3.32	1.02
	0.75	0.608	5.72 (± 0.61)	158.53	1.08	7.64	4.87
	1.25	0.660	2.00 (± 0.24)	141.24	1.02	30.11	5.27
	1.75	0.604	–	142.60	0.99	35.49	4.72
	2.5	0.622	–	142.90	0.88	57.39	4.84
	3.5	0.613	–	119.20	0.80	47.77	4.31
	5.5	0.530	–	102.98	0.76	38.75	4.71
	7.5	0.559	–	103.87	0.71	12.58	2.83
	9.5	0.549	–	103.94	0.71	13.19	2.87
KNR 106	0.25	0.854	5.80 (± 0.51)	143.32	1.53	4.53	1.63
	0.75	0.833	1.86 (± 0.29)	139.49	1.52	5.77	4.20
	1.25	0.783	–0.56 (± 0.29)	145.77	1.40	–	–
	1.75	0.783	–	132.40	1.19	–	–
	2.5	0.728	–	133.99	1.18	23.25	3.58
	3.5	0.742	–	131.81	1.21	40.97	3.51
	5.5	0.731	–	104.08	0.97	36.66	3.53
	7.5	0.721	–	107.68	0.98	22.41	2.51
	9.5	0.719	–	120.91	1.12	14.08	2.43
KNR 113	0.25	0.691	9.40 (± 0.71)	56.10	0.67	–	–
	0.75	0.649	1.83 (± 0.28)	65.00	0.69	–	–
	1.25	0.627	0.74 (± 0.36)	58.18	0.53	–	–

Table A1 (continued)

Station	Avg. depth (cm)	Porosity	Excess Th-234 (dpm g ⁻¹)	Fe concentration (μmol g ⁻¹)	Mn concentration (μmol g ⁻¹)	Pore water Fe (μM)	Pore water Mn (μM)
	1.75	0.610	–	46.92	0.46	–	–
	2.5	0.600	–	38.54	0.49	–	–
	3.5	0.555	–	38.70	0.46	–	–
	5.5	0.562	–	40.81	0.46	–	–
	7.5	0.557	–	37.44	0.56	–	–
	9.5	0.541	–	41.76	0.55	–	–
KNR 115	0.25	–	–	71.16	1.07	–	–
	0.75	–	–	79.76	1.06	–	–
	1.25	–	–	72.40	1.16	–	–
	1.75	–	–	85.76	1.57	–	–
	2.5	–	–	90.21	0.71	–	–
	3.5	–	–	89.57	0.35	–	–
	5.5	–	–	42.39	0.25	–	–
	7.5	–	–	33.74	0.16	–	–
	9.5	–	–	39.23	0.35	–	–
KNR 122	0.25	0.812	9.08 (± 2.21)	105.18	0.98	7.10	3.05
	0.75	0.767	–	112.51	0.73	13.32	3.58
	1.25	0.742	1.63 (± 0.49)	120.19	1.04	27.79	3.11
	1.75	0.742	–	124.67	0.86	25.64	3.03
	2.5	0.732	–	95.68	0.91	8.04	1.93
	3.5	0.722	–	95.46	0.87	9.53	1.95
	5.5	0.711	–	77.68	0.87	–	–
	7.5	0.672	–	85.67	0.91	–	–
	9.5	0.657	–	79.86	0.84	–	–
†KNR 130	0.25	0.833	12.96 (± 2.56)	218.77	5.66	2.90	1.41
	0.75	0.729	8.34 (± 2.12)	241.81	4.40	3.79	8.27
	1.25	0.737	3.28 (± 1.19)	251.23	2.40	11.29	6.48
	1.75	0.733	–	217.23	1.73	14.82	5.67
	2.5	0.706	–	177.96	1.35	17.64	5.29
	3.5	0.705	–	194.27	1.46	11.57	3.94
	5.5	0.707	–	148.20	1.27	32.64	3.22
	7.5	0.688	–	152.85	1.22	30.84	3.26
	9.5	0.680	–	153.05	1.16	22.53	2.95
KNR 137	0.25	–	3.67 (± 0.42)	87.13	1.12	–	–
	0.75	–	2.29 (± 0.40)	96.19	0.97	–	–
	1.25	–	2.18 (± 0.36)	88.37	1.21	–	–
	1.75	–	–	107.33	1.55	–	–
	2.5	–	–	110.80	0.72	–	–
	3.5	–	–	111.30	0.43	–	–
	5.5	–	–	48.06	0.25	–	–
	7.5	–	–	38.30	0.18	–	–
	9.5	–	–	44.75	0.31	–	–
†KNR 140	0.25	0.701	6.70 (± 0.66)	102.57	1.71	6.75	25.93
	0.75	0.686	3.93 (± 0.52)	104.13	0.67	18.68	27.08
	1.25	0.662	1.65 (± 0.31)	114.35	0.84	8.12	17.09
	1.75	0.621	–	112.02	0.71	10.61	13.79
	2.5	0.596	–	116.20	0.80	12.17	9.52
	3.5	0.603	–	102.55	0.51	21.64	7.75
	5.5	0.548	–	93.72	0.56	21.39	5.79
	7.5	0.545	–	67.06	0.40	22.35	4.44
	9.5	0.528	–	52.59	0.35	–	–
†KNR 147	0.25	0.901	22.67 (± 1.85)	319.72	2.17	4.41	5.57
	0.75	0.871	10.43 (± 0.75)	350.86	1.44	8.64	4.15
	1.25	0.857	2.32 (± 0.49)	306.35	1.24	8.06	2.85
	1.75	0.832	–	242.24	1.15	9.86	2.14
	2.5	0.824	–	193.82	1.04	14.04	1.87
	3.5	0.822	–	180.30	1.09	25.30	1.75
	5.5	0.817	–	154.43	0.93	24.33	1.53
	7.5	0.798	–	161.54	0.93	24.44	1.45
	9.5	0.819	–	191.83	0.93	20.28	1.42

benthos, namely, the northern and middle-shelf regions. Likewise, in the deeper waters of the off-shelf region, where we expect correspondingly low OM fluxes to the sediments, we found the lowest rates of Fe oxide reduction, accounting for less than 5% of total OM remineralization.

Overall, the regional pattern observed in both average Fe reduction rates and the percentage of OM remineralized by Fe reduction is consistent with the hypothesis that the OM supply rate is important in regulating reduction rates. However, a select number of stations in the northern and middle regions had high

rates of sediment oxygen consumption with relatively low rates of Fe reduction (e.g.: HLY 32, HLY 98, KNR 45 and KNR 89). It is possible that oxygen consumption rates may under- or over-estimate total carbon oxidation due to the de-coupling of sedimentary remineralization pathways, as can happen under non-steady-state conditions. This could account for the weaker correlation found between these variables (Fig. 6); however, other factors may contribute to the variation in Fe reduction rates across the shelf.

The influence of biogenic sediment reworking on the transport of Fe oxides should also be considered, and is another plausible contributor to the observed variation in reduction rates. Deposit feeders, which move particles over rather large vertical distances, are likely responsible for most particle mixing and transport (Wheatcroft et al., 1990). As Fe reduction occurs deeper in the sediment, relative to Mn reduction, deposit feeders may be more influential in the cycling of Fe oxides. Bioturbation could potentially transport reduced Fe species adsorbed to particles at depth to the surface or mobilize particulate Fe phases from the surface to reduced sediments (Burdige, 2006). Furthermore, variation in bioturbation rates is influenced by benthic community structure. For instance, Shull (2001) demonstrated that the upward transport by *N. annulata* and *M. ambiseta*, as well as the upward and downward transport by maldanid polychaetes were most important in the quantification of overall bioturbation rates. The presence or absence of key organisms that may greatly influence particle-mixing may not necessarily correlate to oxygen consumption (Renaud et al., 2008), possibly explaining the weak correlation between Fe reduction rates and rates of oxygen consumption.

Addressing whether Fe reduction rates are capable of supplying Fe to surface waters, our findings suggest that sedimentary Fe reduction could indeed supply a significant fraction of bioavailable Fe to phytoplankton. Based on the mean rate of Fe reduction ($1.74 \text{ mmol m}^{-2} \text{ d}^{-1}$) and assuming an average rate of primary production of 250 g C yr^{-1} (Springer et al., 1996), as well as phytoplankton requirements of $0.01 \text{ mol Fe} : 106 \text{ mol C}$ (Brand, 1991), if less than one percent of soluble Fe^{2+} reduced in the sediment were to escape by diffusion or bioirrigation, that would be sufficient to support phytoplankton growth. Thus it is possible that wintertime water-column mixing, frontal mixing processes or mixing along isopycnals at the shelf break could transport diagenetically-derived Fe in shelf bottom waters to surface waters, alleviating Fe limitation of primary production across the shelf.

4.3. Manganese reduction

The reduction of Mn oxides tells a different story. First, there is a weaker cross-shelf trend, compared to Fe reduction rates. One plausible explanation is that Mn reduction rates were overestimated in the off-shelf region. Stations with very low bioturbation rates and shallow Mn oxide penetration depths tended to show high rates of Mn reduction. This is likely due to tracer dependence and the overestimation of bioturbation rates by ^{234}Th . Manganese reduction rates at these sites should be considered upper bounds. However, the weaker regional trend may also be partly due to calculated rates being so low in all regions. Also, the absence of any correlation between Mn reduction rates and sediment oxygen consumption rates points to a minor role played by Mn reduction in organic carbon oxidation. This is similar to patterns found by both Kostka et al. (1999) and Nickel et al. (2008), where Mn oxide reduction was negligible in Arctic and Barents Sea sediments.

Second, the lack of any regional difference in the fraction of total carbon oxidation coupled to Mn reduction could be explained by the very low concentrations of Mn oxides (Canfield et al., 2005). Excess Mn oxide surface concentrations were low across the shelf (Table 2) and were typically depleted within 2 cm of the sediment

surface. Thus, Mn oxide reduction is likely a minor pathway for OM remineralization in the southeastern Bering Sea as observed for other sub-arctic and arctic systems (Thamdrup, 2000; Vandieken et al., 2006).

5. Conclusions

The reduction of Fe oxides was found to be an important pathway of carbon oxidation in the southeastern Bering Sea, whereas Mn reduction was determined to be of minor importance. The highest percentages of OM remineralized by Fe were found in the northern and middle-shelf regions of the Bering shelf, which has been noted as having Fe-replete surface waters (Aguilar-Islas et al., 2007; Hurst et al., 2010). Given the relatively high rates of Fe reduction in this region and the extremely low percentage of reduced soluble Fe that would need to escape the sediment to support primary production, it may be that sedimentary reduction of Fe oxides is a significant source of bioavailable Fe to surface waters. Therefore, by possibly supplying a significant fraction of Fe to the water column, sedimentary Fe reduction may play an important role in regulating primary production in the southeastern Bering Sea.

Acknowledgments

We would like to thank the officers and crews of the U.S.C.G.C. *Healy* and the R/V *Knorr* for their efforts and assistance. This research was part of the Bering Ecosystem Study-Bering Sea Integrated Ecosystem Research Project (BEST-BSEIRP) and was funded by the National Science Foundation awards ARC0612380 and MRI0723234 to D.H.S., ARC0612436 to A.H.D., ARC-0732680 to S.B.M., and by North Pacific Research Board award NPRB-B56 to S. B.M. This is BEST-BSIERP Bering Sea Project contribution number 94 and NPRB publication number 419.

Appendix A

See Table A1.

References

- Aguilar-Islas, A.M., Hurst, M.P., Buck, K.N., Sohst, B., Smith, G.J., Lohan, M.C., Bruland, K.W., 2007. Micro- and macronutrients in the southeastern Bering Sea: insight into the iron-replete and iron-depleted regimes. *Prog. Ocean* 73, 99–126.
- Aller, R.C., 1994. The sedimentary Mn cycle in Long Island Sound: its role as intermediate oxidant and the influence of bioturbation, O_2 , and C_{org} flux on diagenetic reaction balances. *J. Mar. Res.* 52, 259–295.
- Aller, R.C., Cochran, J.K., 1976. $^{234}\text{Th}/^{238}\text{U}$ disequilibrium in near-shore sediment: particle reworking and diagenetic time scales. *Earth Planet. Sci. Lett.* 29, 37–50.
- Berelson, W., McManus, J., Coale, K., Johnson, K., Burdige, D., Kilgore, T., Colodner, D., Chavez, F., Kudela, R., Boucher, J., 2003. A time series of benthic flux measurements from Monterey Bay, CA. *Cont. Shelf Res.* 23, 457–481.
- Boudreau, B., 1997. *Diagenetic Models and Their Implementation*. Springer-Verlag, Berlin.
- Boudreau, B., 1998. Mean mixed depth of sediments: the wherefore and why. *Limnol. Oceanogr.* 43, 524–526.
- Brand, L.E., 1991. Minimum iron requirements for marine phytoplankton and the implications for the biogeochemical control of new production. *Limnol. Oceanogr.* 36, 1756–1771.
- Burdige, D.J., 1993. The biogeochemistry of manganese and iron reduction in marine sediments. *Earth-Sci. Rev.* 35, 249–284.
- Burdige, D.J., 2006. *Geochemistry of Marine Sediments*. Princeton University Press, Princeton, New Jersey 609.
- Burdige, D.J., 2012. Estuarine and coastal sediments – coupled biogeochemical cycling. In: Laane, R., Middelburg, J.J. (Eds.), *Treatise on Estuarine and Coastal Science*, vol. 5. Biogeochemistry Academic Press, pp. 279–316.
- Canfield, D.E., Thamdrup, B., Hansen, J.W., 1993. The anaerobic degradation of organic matter in Danish coastal sediments: Iron reduction, manganese reduction, and sulfate reduction. *Geochim. Cosmochim. Acta* 57, 3867–3883.

- Canfield, D.E., Thamdrup, B., Kristensen, E., 2005. The iron and manganese cycles. In: Southward, A.J., Tyler, P.A., Young, C.M., Fuiman, L.A. (Eds.), *Aquatic Geomicrobiology*. Elsevier Academic Press, San Diego, USA, pp. 269–312.
- Chase, Z., Johnson, K.S., Elrod, V.A., Plant, J.N., Fitzwater, S.E., Pickell, L., Sakamoto, C. M., 2005. Manganese and iron distribution off central California influenced by upwelling and shelf width. *Mar. Chem.* 95, 235–254.
- Cooper, L.W., Grebmeier, J.M., Larsen, I.L., Egorov, V.G., Theodorakis, C., Kelly, H.P., Lovvorn, J.R., 2002. Seasonal variation in sedimentation of organic materials in the St. Lawrence Island Polynya region, Bering Sea. *Mar. Ecol. Prog. Ser.* 226, 13–26.
- Coyle, K.O., Konar, B., Blanchard, A., Highsmith, R.C., Carroll, J., Carroll, M., Denisenko, S.G., Sirenko, B.I., 2007. Potential effects of temperature on the benthic infaunal community of the southeastern Bering Sea shelf: possible impacts of climate change. *Deep-Sea Res.* 54, 2885–2905.
- Davenport, E., Shull, D.H., Devol, A.H., 2012. Roles of sorption and tube-dwelling benthos in the cycling of phosphorus in Bering Sea sediments. *Deep-Sea Res. II* 65–70, 163–172.
- Danielson, S., Eisner, L., Weingartner, T., Aagaard, K., 2011. Thermal and haline variability over the central Bering Sea shelf: seasonal and interannual perspectives. *Cont. Shelf Res.* 31, 539–554.
- Elrod, V.A., Berelson, W.M., Coale, K.H., Johnson, K.S., 2004. The flux of iron from continental shelf sediments: a missing source for global budgets. *Geophys. Res. Lett.* 31, L12307.
- Emerson, S., Hedges, J., 2003. Sediment diagenesis and benthic flux. In: Mackenzie, F.T. (Ed.), *Sediments, Diagenesis, and Sedimentary Rocks Vol. 6 Treatise on Geochemistry* (Holland, H.D., Turekian, K.K. (Eds.)). Elsevier, pp. 293–319.
- Feely, R.A., Massoth, G.J., Paulson, A.J., 1981. Distribution and elemental composition of suspended particulate matter in Norton Sound and the northeast Bering Sea Shelf: Implications for Mn and Zn recycling in coastal waters. In: Hood, D. W., Calder, J.A. (Eds.), *Eastern Bering Sea Shelf: Oceanography and Resources*, Vol. 1. University of Washington, pp. 321–337.
- Froelich, P.N., Klinkhammer, G.P., Bender, M.L., Luedtke, N.A., Heath, G.R., Cullen, D., Dauphin, P., Hammond, D., Hartman, B., Maynard, V., 1979. Early oxidation of organic matter in pelagic sediments of the eastern equatorial Atlantic: suboxic diagenesis. *Geochim. Cosmochim. Acta.* 43, 1075–1090.
- Gordon, L.I., Jennings Jr., J.C., Ross, A.A., Krest, J.M., 1994. A suggested protocol for continuous flow automated analysis of seawater nutrients (phosphate, nitrate, nitrite and silicic acid) in the WOCE Hydrographic Program and the Joint Global Ocean Fluxes Study, WOCE Operations Manual. WHP Office Report WHPO 91-1. WOCE Report no. 68/91. Revision 1. Woods Hole, Mass.
- Grebmeier, J.M., McRoy, C.P., Feder, H.M., 1988. Pelagic-benthic coupling on the shelf of the northern Bering and Chukchi seas. I. Food supply source and benthic biomass. *Mar. Ecol. Prog. Ser.* 48, 57–67.
- Grebmeier, J.M., Overland, J.E., Moore, S.E., Farley, E.V., Carmack, E.C., Cooper, L.W., Frey, K.E., Helle, J.H., McLaughlin, F.A., McNutt, S.L., 2006. A major ecosystem shift in the northern Bering Sea. *Science* 311, 1461–1464.
- Hollander, M., Wolfe, D.A., 1973. *Nonparametric Statistical Methods*. Wiley, 526.
- Hood, D.W., 1981. Introduction. In: Hood, D.W., Calder, J.A. (Eds.), *The Eastern Bering Sea Shelf: Oceanography and Resources*, Vol. 1. University of Washington, pp. xiii–xviii.
- Horak, R.E.A., Whitney, H., Shull, D., Mordy, C., Devol, A.H., 2013. The role of sediments on the Bering Sea shelf N cycle: insights from measurements of benthic denitrification and benthic DIN fluxes. *Deep-Sea Res. II* 94, 95–105.
- Hunt, G.L., Stabeno, P., Walters, G., Sinclair, E., Brodeur, R.D., Napp, J.M., Bond, N.A., 2002. Climate change and control of the southeastern Bering Sea pelagic ecosystem. *Deep-Sea Res. II* 49, 5821–5853.
- Hurst, M.P., Aguilar-Islas, A.M., Bruland, K.W., 2010. Iron in the southeastern Bering Sea: elevated leachable particulate Fe in shelf bottom waters as an important source for surface waters. *Cont. Shelf Res.* 30, 467–480.
- Hutchins, D.A., Bruland, K.W., 1998. Iron-limited diatom growth and Si:N uptake ratios in a coastal upwelling regime. *Nature* 393, 531–564.
- Johnson, K.S., Chavez, F.P., Friederich, G.E., 1999. Continental-shelf sediment as a primary source of iron for coastal phytoplankton. *Nature* 398, 697–700.
- Kostka, J.E., Haefele, E., Viehweger, R., Stucki, J.W., 1999. Respiration and dissolution of iron(III)-containing clay minerals by bacteria. *Environ. Sci. Technol.* 33, 3127–3133.
- Lecroart, P., Olivier, M., Schmidt, S., Grémare, A., Anschutz, P., Meysman, J.R.F., 2010. Bioturbation, short-lived radioisotopes, and the tracer-dependence of biodiffusion coefficients. *Geochim. Cosmochim. Acta* 21, 6049–6063.
- Lomas, M.W., Moran, S.B., Casey, J.R., Bell, D.W., Tiahlo, M., Whitefield, J., Kelly, R.P., Mathis, J.T., Cokelet, E.D., 2012. Spatial and seasonal variability of primary production on the Eastern Bering Sea Shelf. *Deep-Sea Res. II* 65, 126–140.
- Meysman, F.J.R., Boudreau, B.P., Middelburg, J.J., 2003. Relations between local, nonlocal, discrete and continuous models of bioturbation. *J. Mar. Res.* 61, 391–410.
- Moore, J.K., Doney, S.C., Glover, D.M., Fung, I.Y., 2002. Iron cycling and nutrient: limitation patterns in surface waters of the world ocean. *Deep-Sea Res. II* 49, 463–507.
- Moran, S.B., Lomas, M.W., Kelly, R.P., Grandinger, R., Iken, K., Mathis, J.T., 2012. Seasonal succession of lower trophic level carbon partitioning in the eastern Bering Sea. *Deep-Sea Res. II* 65–70, 84–97.
- Nickel, M., Vandieken, V., Brüchert, V., Jørgensen, B.B., 2008. Microbial Mn(IV) and Fe(III) reduction in northern Barents Sea sediments under different conditions of ice cover and organic carbon deposition. *Deep-Sea Res. II* 55, 2390–2398.
- Phillips, E.J.P., Lovely, D.R., 1987. Determination of Fe(III) and Fe(II) in oxalate extracts of sediment. *Soil Sci. Soc. Am. J.* 51, 938–941.
- Renaud, P.E., Morata, N., Carroll, M.L., Denisenko, S.G., Reigstad, M., 2008. Pelagic-benthic coupling in the western Barents Sea: processes and time scales. *Deep-Sea Res. II* 55, 2372–2380.
- Revsbech, N.P., 1989. An oxygen microsensor with a guard cathode. *Limnol. Oceanogr.* 34, 474–478.
- Richter, R., 1952. Sediment-Gaseinien und sedifluktion überhaupt. *Notizbl. Hess. L. Amt. Bodenforsch.* 3, 67–81.
- Rho, T., Whitley, T.E., 2007. Characteristics of seasonal and spatial variations of primary production over the Southeastern Bering Sea shelf. *Cont. Shelf Res.* 27, 2556–2569.
- Rho, T., Whitley, T.E., Goering, J.J., 2005. Interannual variations of nutrients and primary production over the southeastern Bering Sea shelf during the spring of 1997, 1998, and 1999. *Oceanology* 45 (3), 402–416.
- Robbins, J.M., Lyle, M., Heath, G.R., 1984. A sequential extraction procedure for partitioning elements among co-existing phases in marine sediments. *Coll. Oceanogr. Oregon State Univ. Ref.* 84–3, 64.
- Roden, E.E., Wetzel, R.G., 2002. Kinetics of microbial Fe (III) oxide reduction in freshwater wetland sediments. *Limnol. Oceanogr.* 47, 198–211.
- Sambrotto, R.N., Mordy, C., Zeeman, S.I., Stabeno, P.J., Mackin, S.A., 2008. Physical forcing and nutrient conditions associated with patterns of Chl a and phytoplankton productivity in the southeastern Bering Sea during summer. *Deep-Sea Res. II* 55: 1745–1760.
- Schlitzer, R., 2008. Ocean Data View (<http://odv.awi.de>).
- Sharma, G.D., Wright, F.F., Burns, J.J., Burbank, D.C., 1974. Sea-surface circulation, sediment transport, and marine mammal distribution, Alaska continental shelf, prepared for Nat. Aeronautics and Space Admin., Goddard Space Flight Center, Greenbelt, MD, ERTS Final Reporter. U.S. Dept. Commerce Natl. Tech. Inf. Serv., E74-10711, 77 pp.
- Shull, D.H., 2001. Transition-matrix model of bioturbation and radionuclide diagenesis. *Limnol. Oceanogr.* 46, 905–916.
- Springer, A.M., McRoy, C.P., Flint, M.V., 1996. The Bering Sea Green Belt: Shelf-Edge Processes and Ecosystem Production. *Fish. Oceanogr.* 5, 205–223.
- Stabeno, P.J., Farley, E., Kachel, N., Moore, S., Mordy, C., Napp, J.M., Overland, J.E., Pinchuk, A.I., Sigler, M., 2012. A comparison of the physics of the northern and southern shelves of the eastern Bering Sea and some implications for the ecosystem. *Deep-Sea Res.* 65–70, 14–30.
- Stabeno, P.J., Hunt, G.L., 2002. Overview of the inner front and Southeast Bering Sea carrying capacity programs. *Deep-Sea Res. II* 49, 6157–6168.
- Stabeno, P.J., Bond, N.A., Kachel, N.B., Salo, S.A., Schumacher, J.D., 2001. On the temporal variability of the physical environment over the south-eastern Bering Sea. *Fish. Oceanogr.* 10, 81–98.
- Thamdrup, B., 2000. Bacterial manganese and iron reduction in aquatic sediments. In: Schink, B. (Ed.), *Advances in Microbial Ecology*, Vol. 6. Kluwer Academic, pp. 41–84.
- Vandieken, V., Nickel, M., Jørgensen, B.B., 2006. Carbon mineralization in Arctic sediments northeast of Svalbard: Mn(IV) and Fe(III) as principal anaerobic respiratory pathways. *Mar. Ecol. Prog. Ser.* 322, 15–27.
- Walsh, J.J., McRoy, C.P., 1986. Ecosystem analysis in the southeastern Bering Sea. *Cont. Shelf Res.* 5, 259–288.
- Wheatcroft, R.A., Jumars, P.A., Smith, C.R., Nowell, A.R.M., 1990. A mechanistic view of the particulate biodiffusion coefficient: step lengths, rest periods and transport directions. *J. Mar. Res.* 48, 177–207.



The role of sediments on the Bering Sea shelf N cycle: Insights from measurements of benthic denitrification and benthic DIN fluxes



Rachel E.A. Horak^{a,*}, Heather Whitney^a, David H. Shull^b, Calvin W. Mordy^c, Allan H. Devol^a

^a School of Oceanography, Box 355351, University of Washington, Seattle, WA 98195-5351, United States

^b Department of Environmental Sciences, Western Washington University, Bellingham, WA 98225-9181, United States

^c Joint Institute for the Study of the Atmosphere and Ocean, University of Washington, 3737 Brooklyn Ave. NE, Box 355672, Seattle, WA 98105-5672, United States

ARTICLE INFO

Available online 14 March 2013

Keywords:

Denitrification
Bering Sea shelf
Sediments
Nitrification
N* nitrogen cycle

ABSTRACT

Continental shelves are hotspots for sedimentary denitrification, and the loss of N through denitrification can limit primary production in ecosystems. Spatial and seasonal trends in sedimentary denitrification and benthic nutrient fluxes are poorly characterized in the highly productive Bering Sea shelf ecosystem. Through the Bering Sea Ecosystem Study (BEST) program, we measured benthic fluxes of N₂ and dissolved inorganic nitrogen (DIN: NH₄⁺ + NO₂⁻ + NO₃⁻), the extent of coupled sedimentary nitrification/denitrification, and the water column DIN deficit relative to phosphate, as indicated by a modified N* parameter (N**), on the Bering Sea shelf in the spring and summer 2009–2010. We found that sedimentary denitrification is widespread over the shelf, it is fueled mostly through coupled nitrification/denitrification, the net balance of sedimentary DIN flux is near zero over the shelf, and that the water column DIN deficit varies widely according to season and year. In the summer, N** in the surface layer appeared to be strongly affected by non-Redfieldian uptake of inorganic nutrients by phytoplankton in the spring bloom; in the winter, N** was strongly affected by sedimentary denitrification. Our findings indicate that the estimate of total N loss in Bering Sea shelf sediments should be revised upwards by at least 50% to 5.2–6.2 Tg N y⁻¹. In addition, sediments are not a significant source of remineralized N for primary production over the shelf; hence sedimentary denitrification exacerbates N-limitation of the ecosystem.

© 2013 Elsevier Ltd. All rights reserved.

1. Introduction

The Bering Sea hosts one of the most productive oceanic ecosystems and provides at least 50% of the U.S. commercial fishery industry (NRC, 1996; Sigler et al., 2010). The vast Bering Sea shelf covers 40% of the Bering Sea surface area, and it is characterized by seasonal sea ice cover that is particularly sensitive to interannual variability in climate (Hunt Jr. et al., 2002; Rho and Whitledge, 2007; Stabeno et al., 2007; Hunt Jr. et al., 2010). Recent studies in the Bering Sea indicate that the area is undergoing rapid change, and climate change effects on nutrient dynamics and the lower trophic levels in the ecosystem are poorly characterized (Grebmeier et al., 2006).

Sedimentary denitrification, that is, the anaerobic microbially mediated conversion of fixed N (nitrogen) to N₂ (gas), is an important sink of bioavailable N in the world ocean. Globally, continental shelves may be the largest sink of fixed N; Seitzinger

et al. (2006) estimated that sedimentary denitrification on continental shelves account for 44% of total global denitrification. As a large sink of fixed N, sedimentary denitrification can negatively influence primary production on many continental shelves (for example, Christensen et al., 1987; Fennel et al., 2006). Previous studies of sedimentary denitrification on the Bering Sea shelf are limited in spatial and temporal distribution, but they have indicated that denitrification is an important N cycle process on the shelf (Haines et al., 1981; Whitledge et al., 1986; Rowe and Phoel, 1992; Henriksen et al., 1993; Tanaka et al., 2004; Granger et al., 2011).

Water column nutrient concentrations on the Bering Sea shelf exhibit clear seasonal patterns and some interannual variability (Whitledge et al., 1986; Rho et al., 2005; Mordy et al., 2012). In the winter, nutrient concentrations are highest on the Bering Sea shelf, and the water column is mixed to the seafloor. In late spring or early summer, following sea ice retreat, the shelf experiences massive phytoplankton blooms, and the timing of these blooms is strongly dependent on the timing of winter sea ice retreat (Hunt et al., 2002; Stabeno et al., 2007). Following the spring bloom, a large part of the shelf (middle shelf, 50–100 m depth) becomes a two-layer system with a wind-mixed nutrient-deplete surface

* Corresponding author. Tel.: +1 206 543 0272; fax: +1 206 685 3351.

E-mail addresses: rahorak@uw.edu (R.E.A. Horak), hwhitney@uw.edu (H. Whitney), David.shull@wwu.edu (D.H. Shull), Calvin.w.mordy@noaa.gov (C.W. Mordy), devol@uw.edu (A.H. Devol).

layer and a nutrient-replete bottom layer (Mordy et al., 2012). Dissolved inorganic nitrogen (DIN: $\text{NH}_4^+ + \text{NO}_2^- + \text{NO}_3^-$) has been hypothesized to limit late spring and summer productivity on the eastern shelf because of the depletion of DIN in the mixed layer following a bloom event (Whitledge et al., 1988; Rho et al., 2005; Mathis et al., 2010). The concentration of PO_4^{-3} in the bottom layer of spring and summer are similar to the PO_4^{-3} concentration in the winter water column (Mordy et al., 2012). Seasonal variations and distributions of NO_2^- are rarely reported for the Bering Sea shelf, but are usually less than $0.7 \mu\text{M}$ (Granger et al., 2011). Water column NO_3^- is usually highest in the spring (pre-bloom) throughout the water column; in the summer and fall, deep water NO_3^- is usually somewhat depleted as compared with pre-bloom values, but is still at least $5 \mu\text{M}$ (Mordy et al., 2012). On the middle shelf, NH_4^+ concentrations are uncharacteristically high for a well-oxygenated oceanic water column. NH_4^+ concentrations are highest post-bloom (in summer, as compared to the winter) in the bottom layer (“cold pool”), and usually reach $4\text{--}8 \mu\text{M}$, but can be as high as $15 \mu\text{M}$ (Whitledge et al., 1986; Mordy et al., 2008; Granger et al., 2011; Mordy et al., 2012). Efflux of NH_4^+ from sediments following ammonification has been implicated as a cause of these elevated NH_4^+ concentrations (Whitledge et al., 1986; Rowe and Phoel, 1992; Granger et al., 2011). Granger et al. (2011) used a stable isotope approach to estimate that 50–95% of sediment-regenerated NH_4^+ is released into the water column, which could presumably be used to sustain primary production. However, experimentally determined benthic DIN fluxes over the entire Bering Sea shelf are lacking.

The ratio of water column DIN relative to PO_4^{-3} and its associated geochemical tracer N^* [$\text{N}^* = (\text{DIN} - 16 * \text{PO}_4^{-3}) + 2.9$] are commonly used to assess the degree of N deficiency or N excess in a water mass (Gruber and Sarmiento, 1997). Assuming that biomass and remineralization occurs in a N:P ratio = 16 (Redfield stoichiometry; Redfield, 1934, 1958), negative deviations in water column DIN relative to PO_4^{-3} (negative N^*) indicate regions of DIN loss or PO_4^{-3} input, while positive deviations (positive N^*) indicate regions of DIN input or PO_4^{-3} loss (Gruber and Sarmiento, 1997). Consequently, oceanic regions with very high N^* values generally have high inputs of N through N_2 -fixation (such as the North Atlantic), and oceanic regions with very low N^* values are generally regions of intense N loss through sedimentary or water column denitrification (such as the oxygen deficient zones in the Eastern Tropical Pacific; Gruber and Sarmiento, 1997; Codispoti et al., 2001; Deutsch et al., 2007). Several investigators have reported low water column DIN:DIP ratios (relative to Redfield DIN:DIP = 16) at discrete times in the year on the Bering Sea shelf, including April (Granger et al., 2011), August and September (Tanaka et al., 2004), late September (Mordy et al., 2010); only Mordy et al. (2012) has examined seasonal trends (along a 70 m isobath) in nutrient concentrations. To assess seasonal and inter-annual changes in the Bering Sea shelf N deficit, Mordy et al. (2010) established a regional N^* tracer (Codispoti et al., 2001) which accounts for N deficient waters entering the Bering Sea shelf.

Based on limited data sets, sedimentary denitrification has been implicated as the cause of low DIN:DIP ratios on the shelf (Tanaka

et al., 2004). However, the spatial extent, seasonal variability, and magnitude of shelf N loss is poorly constrained. Sedimentary N loss typically occurs through one of two pathways (or a combination of both): direct denitrification and coupled nitrification/denitrification. In direct denitrification, there is flux of NO_3^- into the sediments, and NO_3^- from the overlying water column is the substrate for N loss. In coupled nitrification/denitrification, reduced N-containing organic matter is remineralized to NH_4^+ , nitrified to NO_2^- or NO_3^- , and subsequently denitrified (through either anammox or canonical denitrification; in this paper, we do not differentiate anammox from canonical denitrification). This scenario is characterized by low DIN flux into and out of the sediments co-occurring with N_2 (gas) flux. Coupled nitrification/denitrification may be the dominant pathway of N loss on many continental shelves (Devol and Christensen, 1993; Seitzinger and Giblin, 1996). The pathway of sedimentary N loss on the Bering Sea shelf has not been determined by direct rate measurements over the entire shelf.

In the present study, we measured the role of sediments in remineralization of inorganic N and sedimentary N loss to elucidate sedimentary denitrification pathways and determine the degree to which sediments are a net source or sink of remineralized N to the water column. We also investigated seasonality in water column DIN:DIP ratios to assess the variability of nutrient limitation.

2. Methods

2.1. Study area

The data were collected on a series of 4 cruises from 2009 to 2010 (Table 1) as a part of the interdisciplinary Bering Sea Ecosystem Study (BEST) program. Each cruise sampled the Bering Shelf, from south of St. Lawrence Island to the Aleutian Islands, and from 180°E to 160°W . Hydrographic transects were repeated on each cruise (Fig. 1), except that ice cover prevented sampling on the inner shelf during the spring 2009 and the first 2010 cruise. Station depths ranged from 40 m (inner shelf) to 3500 m (deep, off-shelf).

2.2. Benthic fluxes

2.2.1. Sample collection

Sediment cores were collected with an Ocean Instruments MC 800 multicore, an eight-tube multi-corer that takes 10-cm diameter cores up to 40-cm in length while preserving the sediment–water interface. Bottom water was also collected at each station using a Niskin bottle attached to the multi-corer.

2.2.2. Whole-core incubation

Whole-core incubations were used to measure benthic dissolved inorganic nitrogen (DIN: $\text{NO}_3^- + \text{NO}_2^- + \text{NH}_4^+$) fluxes, aerobic respiration, and denitrification rates. The incubation set-up was the same as that described in Davenport et al. (2012) and modified by Esch et al. (2013). Briefly, 8-cm diameter sub-cores containing about 15 cm of sediment and 10 cm of overlying water were allowed to equilibrate for 24 h at in-situ temperatures (2°C cold van). Then, the overlying water was siphoned off from the core without disturbing the sediment, and it was replaced by niskin-collected bottom water. Cores were sealed with silicone (in 2009) or PVC (in 2010) closures in a manner that avoided trapped air bubbles. Benthic fluxes ($n=2$ or 3) were determined by monitoring nutrient concentration in the overlying water during a period of two to five days after sample collection. The closures contained both an inlet and an outlet. The inlet was connected to a reservoir filled with overlying water from the sample location. When samples were

Table 1
Listing of cruises, dates, and corresponding measurements for this study.

Cruise ID	Ship	Dates	Measurements	Conditions
HLY09-02	R.V. <i>Healy</i>	04/04/09–05/12/09	Sediment: DIN+O ₂ flux water column: nutrients	Ice on inner shelf
Knorr195-10	R.V. <i>Knorr</i>	06/14/09–07/13/09	Sediment: DIN+O ₂ flux water column: nutrients	Largely ice-free
TN249	R.V. <i>Thompson</i>	05/09/10–06/14/10	Sediment: N ₂ flux water column: nutrients	Late advance of sea ice
TN250	R.V. <i>Thompson</i>	06/16/10–07/14/10	Sediment: N ₂ flux water column: nutrients	Largely ice-free

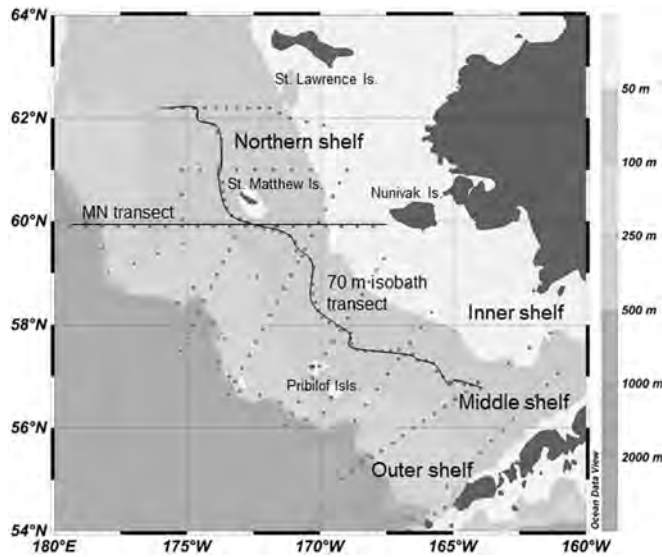


Fig. 1. Typical cruise track for the BEST program. This map is for Knorr 195-10. The MN line and 70 m isobath transects are highlighted.

drawn from the incubation core, the volume removed was replaced with water from the reservoir. All sampling was done without air contamination of the incubation cores.

Oxygen concentration in the overlying water of the incubation cores was measured using a PreSens Microx TX2 fiber optic oxygen meter combined with a flow-through PreSens optode. The optode was calibrated using air-equilibrated seawater and seawater deoxygenated with sodium sulfite. Five mL of overlying water was removed for the measurement. Aerobic respiration was calculated from the change in O_2 concentration during the 2–5 day incubation; we fitted the oxygen concentration for the time series to a 2nd order polynomial. In some instances, only two time points were available; in these cases, we used a two-point slope. This only affected station 35 for HLY0902 and stations 45, 60, and 89 for KN195-10. In a comparison of the 2nd order polynomial fit versus a 2-point linear fit, O_2 respiration calculated with a 2-point linear fit was almost always lower than that of the 2nd order polynomial fit (mean \pm 1 S.D.: 13.8% \pm 9.5%). We calculated the flux according to the formula:

$$J = \left\{ \frac{dc}{dt} \right\}_{t=0} * V * A^{-1} \quad (1)$$

where J is the O_2 flux ($\text{mmol m}^{-2} \text{d}^{-1}$), $\{dc/dt\}_{t=0}$ is the instantaneous change in O_2 concentration at $t=0$ ($\pm 0.4\%$ accuracy at 100% O_2 saturation), V is the volume of the overlying water in the flux core (m^3), and A is the surface area of the core (m^2). Using an error propagation approach, we estimated the maximum uncertainty in the J term to be 1.65%. We corrected the oxygen fluxes to account for the addition of reservoir water to the core incubation. Furthermore, in 2009, the silicone closures had a slow desorption of oxygen, and we corrected the oxygen flux data as previously presented (Davenport et al., 2012; Esch et al., 2013).

To measure DIN concentration, we used a SmartChem autoanalyzer (Westco Scientific) based on methods presented in Gordon et al. (1994). The uncertainty for DIN concentration is 1.1%. DIN fluxes were calculated from the change in nutrient concentration in the overlying water column during the initial part of the core incubation (within the first 2–2.5 days). Changes in nutrient concentration were fitted by linear regression and the flux was calculated according to Eq. (1).

During the 2010 cruises, we used two methods to directly measure sedimentary denitrification rates through dissolved $N_2:Ar$ ratios in the overlying water of the core. First, we measured N_2 , O_2 , and Ar concentrations with a membrane inlet mass spectrometer (MIMS), as described by Chang and Devol (2009) and Kana et al. (1994). The MIMS is a modification to that first described in Kana et al. (1994). Briefly, water from the core outlet was introduced into the vacuum line without alteration using a Rainin peristaltic pump with Viton tubing. Immediately after passing through the silicone capillary membrane inlet and before introduction to the mass spectrometer, the sample passed through a u-tube immersed in liquid N to remove water vapor and CO_2 . The sample was analyzed using a Pfeiffer Vacuum Balzers Prisma 200 quadrupole mass spectrometer. Gas ratios were determined when the signal stabilized after sample introduction to the vacuum line (between 2 and 10 min lapsed until the signal stabilized). We used the average $N_2:Ar$ ratio of 3–5 values recorded within one minute after signal stabilization; the variation among these measurements was always less than 0.1% and usually within 0.05%. The instrument was kept in the same 2 °C cold van for as the core incubations, and temperature was recorded

every hour to ensure that samples and standards were maintained at constant temperature. Salinity standards to calibrate MIMS gas ratios were air-equilibrated and made daily. We did not remove O_2 from the sample prior to introduction to the MIMS, which Eyre et al. (2002) claims can affect the $N_2:Ar$ ratio because of the creation of mass interferences by a combination of oxygen-containing ions. As noted in Chang and Devol (2009) and similar in response to Kana and Weiss (2004), the error in $N_2:Ar$ ratios attributable to O_2 in the sample with this MIMS instrument is 0.06%.

For the MIMS measurements, $N_2:Ar$ ratios were measured over a period of 1–5 days. During the entire whole core incubation, the overlying water column was continuously stirred. The incubation was terminated when the O_2 concentration dropped below 140 μM , which represented approximately 50% of the initial concentration. This ensured that gas ratio measurements were not altered by a change in microbial physiology following a decrease in O_2 concentrations.

Second, we collected and preserved water samples for $N_2:Ar$ ratios and quantification of the absolute N_2 flux from the beginning and end of the dedicated whole core incubations. These samples were collected after the initial equilibration (initial time point) and after 2–3 days of incubation (final time point). Samples of the overlying water were collected without introduction of atmosphere into pre-evacuated and $HgCl_2$ -poisoned 300 ml glass flasks (Emerson et al., 1999; Chang and Devol, 2009). Sample flasks were equipped with gas tight 9 mm-bore Louwers-Hapert single o-ring valves, and were returned to the University of Washington for analysis. Samples were weighed to determine water volume. Following equilibration with the headspace by rotating the flask in a constant temperature water bath for at least 16 h, we removed almost all of the water using a vacuum pump. A known amount of ^{36}Ar spike was added to the headspace gas in order to determine the absolute concentration of N_2 gas in each sample. Then, the headspace gas was pumped through liquid N traps to remove CO_2 and H_2O and cryogenically frozen into a steel finger immersed in liquid He. A Finnigan dual-inlet Delta XL Isotope Ratio Mass Spectrometer (IRMS) was used to measure the dissolved gas ratios (28:40, 29:28, 36:40, 32:40) relative to an in-house gas standard with known gas ratios (Emerson et al., 1999; Hamme and Emerson, 2002). We corrected the gas ratio data (with a series of $N_2:Ar$ gas samples containing different O_2 concentrations) in order to account for the effect of O_2 on the ionization efficiency of the other gases (Emerson et al., 1999; Chang and Devol, 2009). This IRMS procedure to measure gas ratios and absolute N_2 concentration has shown to be precise to 0.1%, which represents 0.5 μM error for a typical N_2 concentration of 500 μM (Emerson et al., 1999).

2.3. Water column nutrients

Samples for nutrient analysis were syringe-filtered using 0.45 μm cellulose acetate membranes, and collected in 30 ml acid-washed, high-density polyethylene bottles after 3 rinses. Samples were analyzed shipboard within 1–12 h of collection. NO_3^- , NO_2^- and NH_4^+ concentrations were determined using a combination of analytical components from Alpkem, Perstorp, and Technicon. We closely followed the WOCE-JGOFS standardization and analysis procedure specified by Gordon et al. (1994), including reagent preparation, calibration of labware, preparation of primary and secondary standards, and corrections for blanks and refractive index. We used the program Ocean Data View (Schlitzer, 2011) to visualize the distribution of water-column nutrients.

2.4. Calculations

The regional N^{**} tracer (Mordy et al., 2010) was used to determine the N deficit that results from the biogeochemical processes occurring solely in the eastern Bering Sea. This estimate of N^{**} in the Bering Sea was determined using data from the outer shelf and slope for reference. The revised offset (5.9) from the original N^* equation published by Gruber and Sarmiento (2.9; 1997) accounts for the fact that water that replenishes the Bering Sea Shelf is already deficient in N. Mordy et al. (2010) defined a Bering Sea N^{**} as

$$N^{**} = \text{DIN} - (\text{PO}_4^{3-} * 15.5) + 5.9, \quad (2)$$

where $\text{DIN} = [\text{NO}_3^-] + [\text{NO}_2^-] + [\text{NH}_4^+]$.

For the 2009 data, we also calculated the sedimentary denitrification rate through a mass balance approach (Devol and Christensen, 1993; Hartnett and Devol, 2003). For this, the denitrification rate (rate of removal of DIN) is the sum of the regenerated NH_4^+ produced by sedimentary aerobic respiration and the DIN flux (where net DIN flux into the sediment is positive and net DIN efflux is negative). Hence, when there was an efflux of DIN from the sediment, denitrification rate is the difference between the NH_4^+ produced by sedimentary aerobic respiration and the net DIN flux out of the sediment. We used a standard Redfield stoichiometry to convert the moles of O_2 respired to moles of regenerated NH_4^+ (106:16; Froelich et al., 1979). Thus, denitrification was calculated according to the following:

$$\text{Denitrification rate} = dO_2/dt(16/106) + \text{flux}(\text{DIN}), \quad (3)$$

where dO_2/dt = oxygen consumption rate and DIN flux is positive into the sediment.

3. Results

3.1. N_2 flux measurements of sedimentary denitrification rates

We measured N_2 flux with both IRMS and MIMS on cruise TN249 on 14 individual cores and compared the results between methods. There was no significant difference between the N_2 flux rates measured with both techniques (Wilcoxon signed-rank test, $p=0.12$, $n=14$) and there was a significant linear regression between both techniques ($R^2=0.68$, $p<0.01$, Fig. 2).

Active sedimentary denitrification was detected at all shelf, slope, and deep stations that were sampled (Fig. 3). The lower range of denitrification rates was similar between the TN249 and TN250 cruise, but during the TN249 cruise there were 2 stations that recorded dramatically higher denitrification rates with the IRMS technique (Fig. 3a; 57.00°N, 170.65°W: 4.06 $\text{mmol N m}^{-2} \text{d}^{-1}$; 59.89°N, 178.89°W: 2.51 $\text{mmol N m}^{-2} \text{d}^{-1}$). For both TN249 and TN250, there were no apparent trends in the distribution of sediment denitrification over the entire Bering Sea shelf (Fig. 3, Table 2). Denitrification rates on the middle shelf (depth 50–100 m) were comparable to those on the outer shelf (depth 100–200 m) for both cruises (Fig. 3). For TN250, denitrification rates were similar in range and distribution for the inner shelf stations (<50 m, $n=3$) compared to the remaining shelf stations (Fig. 3b, $n=13$). Also, we found no apparent differences in the magnitude and distribution of denitrification rates, regardless of technique, north and south of 60°N, the approximate latitude that physically separates the northern and southern shelves (Stabeno et al., 2006).

For both the MIMS and IRMS technique, the denitrification rates were similar in range and mean between the shelf (depth 47–208 m) and slope (depth 381–656 m) stations (Table 2). For cruise TN250, we compared denitrification rates in the deep Bering Sea (depth 1098–2789 m) and shelf (depth 40–149 m) stations. Rates were comparable between deep and shelf stations, although the range for the shelf stations was somewhat greater (Table 2).

3.2. Benthic DIN fluxes and calculated denitrification rates

For the HLY09-02 and Knorr 195-10 cruises, we used a whole-core incubation technique to measure sediment DIN and O_2 flux from shelf stations (depth 31–196 m), and we estimated rates of NH_4^+ regeneration and denitrification using a mass balance approach (Section 2.4). The station sampling date, depth, and location for these analyses can be found in Table 3.

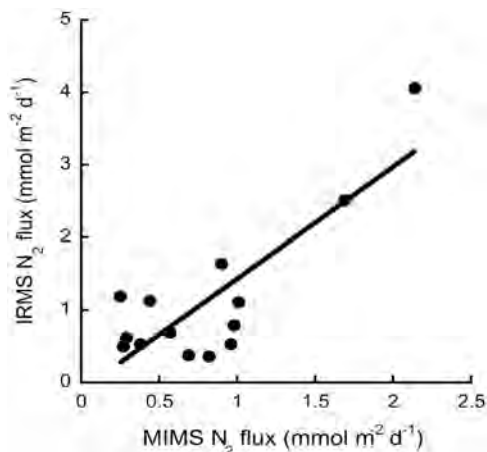


Fig. 2. Correlation (linear regression) of MIMS and IRMS N_2 flux measurements. Each data point represents measurements for both MIMS and IRMS from a single core. $R^2=0.68$, $p<0.01$.

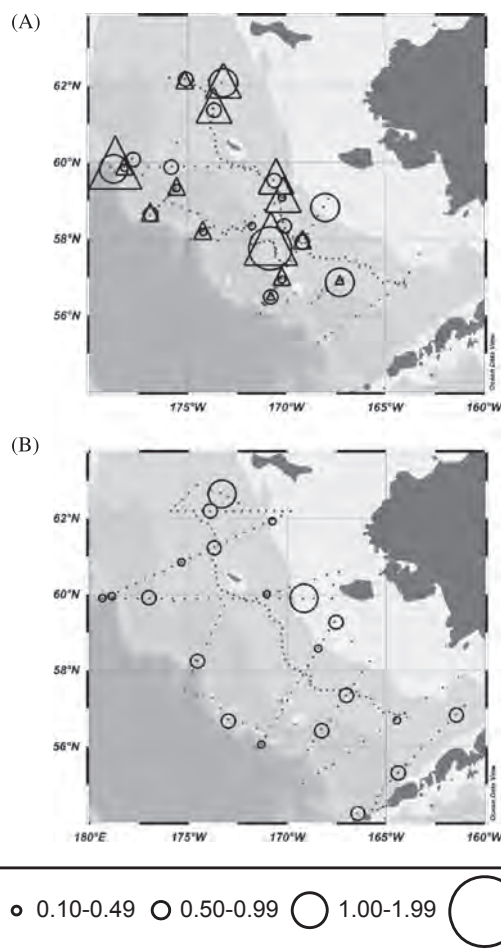


Fig. 3. Denitrification rates on the Bering Sea shelf in 2010. (A) TN249, late spring 2010 (B) TN 250, summer 2010. Rates of N_2 flux ($\text{mmol N m}^{-2} \text{d}^{-1}$) in whole core incubations were measured with isotope ratio mass spectrometry (triangles) and membrane inlet mass spectrometry (circles). Legend indicates the magnitude of the denitrification rate.

For the HLY09-02 cruise (spring 2009), DIN fluxes from cores were variable by station over the entire shelf, but mostly small (range: -0.28 to $0.22 \text{ mmol N m}^{-2} \text{d}^{-1}$; Table 4). NH_4^+ and NO_2^- fluxes were not consistently into or out of the sediments (Table 4). The shelf average flux for both NH_4^+ and NO_2^- was very small and not significantly different than 0 (Table 4). NO_3^- fluxes were out of the sediment for most stations (Table 4), and the shelf-wide sedimentary NO_2^- efflux average was also small ($-0.06 \pm 0.03 \text{ mmol N m}^{-2} \text{d}^{-1}$). The denitrification rate, calculated as the difference between the respiration-generated NH_4^+ flux and measured DIN flux, averaged $0.86 \pm 0.06 \text{ mmol N m}^{-2} \text{d}^{-1}$ (Table 4).

For the Knorr 195-10 cruise (summer 2009), more stations were a sink of DIN from the overlying water column than were a source of DIN to the water column (Table 4). However, similar to the spring measurements, the shelf-wide average for all three DIN fluxes was not significantly different from 0 (Table 4). The denitrification rate was on average higher in the summer than in the spring, although there was more variability among stations (Table 4; average: $1.19 \pm 0.12 \text{ mmol N m}^{-2} \text{d}^{-1}$).

3.3. Water column N deficit

3.3.1. 2009

The spatial distribution of N^{**} values in the water column over the Bering Sea shelf was dramatically different in the 2009 spring mixed water column as compared with the 2009 summer

Table 2
Bering Sea shelf, slope, and deep denitrification rates measured by N₂ flux.

Cruise	Method	Number of stations	N ₂ flux (mmol N m ⁻² d ⁻¹)	
			Range	Mean±1 SD
TN249	IRMS	Slope: 3	0.50–2.52	1.21±0.93
		Shelf: 14	0.34–4.06	1.09±1.13
TN249	MIMS	Slope: 3	0.27–1.69	0.75±0.66
		Shelf: 17	0.25–2.14	0.78±0.49
TN250	MIMS	Deep: 4	0.25–0.80	0.56±0.21
		Shelf: 17	0.23–1.27	0.62±0.30

Table 3
Listing of station sampling date, bottom depth, and location for whole core incubations.

Station	Date (mm/dd/yr)	Depth (m)	Lat. (°N)	Long. (°W)
HLY09–02				
3	04/05/2009	72	58.22	169.12
9	04/07/2009	31	59.96	169.90
17	04/09/2009	104	59.90	174.00
32	04/15/2009	81	62.20	175.14
35	04/16/2009	62	61.96	173.24
39	04/17/2009	53	61.93	171.22
54	04/21/2009	68	58.37	168.72
58	04/22/2009	69	57.45	169.77
65	04/24/2009	111	56.73	170.52
69	04/26/2009	135	59.56	175.20
73	04/27/2009	132	59.59	175.08
83	04/28/2009	95	60.81	174.39
90	04/30/2009	134	59.55	175.15
92	05/01/2009	75	61.57	173.71
93	05/02/2009	58	62.26	172.52
98	05/04/2009	82	62.18	175.15
116	05/06/2009	134	59.56	175.15
Knorr 195–10				
22	06/18/2009	113	56.13	166.13
32	06/20/2009	104	56.75	167.87
45	06/22/2009	70	57.90	169.24
60	06/25/2009	196	57.28	173.84
79	06/29/2009	121	57.16	172.65
89	06/30/2009	66	59.71	170.32
106	07/01/2009	105	59.90	173.99
122	07/05/2009	136	59.56	175.20
130	07/06/2009	65	61.00	171.76
140	07/07/2009	62	62.20	173.11

stratified water column (Fig. 4). Along both the 70 m isobath and MN line transects, spring N^{**} was always negative, and it sometimes approached $-10 \mu\text{mol N}$ (Fig. 4A and C). This sharply contrasts with the N^{**} distribution just one month later when mixed layer N^{**} values were positive over the majority of the shelf. For instance, along the 70 m isobath, positive N^{**} values could be found as deep as 20 m (Fig. 4B). Along the MN line, there were positive N^{**} values down to 75 m (Fig. 4D) and relatively small seasonal changes in deep water N^{**} values (see Mordy et al., 2012). In summer 2009, highly positive N^{**} in surface waters was found consistently offshore of the 70 m isobath and in the southeast (Fig. 6A). Depletion in surface DIP and DIN was evident shelf-wide (Fig. 6B and C).

3.3.2. 2010

Water column N^{**} values and distributions were different in summer 2010 compared to summer 2009. There was no evidence for positive N^{**} values in the mixed layer along the 70 m isobath in either cruise in 2010, except in the extreme southeast corner (Figs. 5 and 6D). Mixed layer N^{**} values for both summer 2010 cruises were similar to the spring 2009 water column and summer

2009 deep waters. During the TN250 cruise on the MN line, positive N^{**} values were recorded in approximately the same location as in summer 2009, but positive N^{**} was detected only to a maximum depth of 35 m (data not shown). On nearly the same calendar days in 2009, N^{**}, DIP, and DIN had a different distribution in 2010 (Fig. 6D–F). As discussed above, positive deviations in surface N^{**} after the seasonal bloom were much less common over the shelf and occurred mainly in two locations (on western MN line and in the southeast corner). DIP and DIN were generally not as highly depleted as in 2009, especially in the inner and middle shelf.

4. Discussion

4.1. Widespread sedimentary denitrification on the Bering Sea shelf

The mean sedimentary denitrification rates were similar for all 3 methods that we used to measure or estimate denitrification rates for this study (Table 5). Our rates are higher than most literature values of Bering Sea shelf denitrification (Table 5), but a direct comparison is complicated by the fact that previous studies used different techniques. Also, without a direct methods comparison, a comparison of rates is complicated by the fact that the Bering Sea is possibly undergoing rapid changes which may affect nitrogen biogeochemical cycling (Grebmeier et al., 2006). Our sedimentary denitrification measurements are higher than those of the deep (>2000 m) Bering Sea (Table 5; Lehmann et al., 2005), and slightly lower than measurements from the more productive Northern Bering Sea/Anadyr waters (Table 5; Lomstein et al., 1989; Henriksen et al., 1993). The average rate for this study is similar to other denitrification rates elsewhere on Arctic shelves: on the Western Arctic shelf, Devol et al. (1997) reported an average sedimentary denitrification rate of $1.3 \text{ mmol N}_2 \text{ m}^{-2} \text{ d}^{-1}$ and Chang and Devol (2009) recorded an average rate of $0.96 \text{ mmol N}_2 \text{ m}^{-2} \text{ d}^{-1}$ in the Chukchi Sea.

Discrete measurements of N₂ flux and mass balance estimates (based on DIN flux and O₂ consumption/NH₄⁺ regeneration) indicate no strong spatial trends in denitrification rates over the shelf. This is in contrast to the conclusions of Granger et al. (2011), the only other paper to date with an extensive survey of nitrogen cycling over the entire shelf. Granger et al. reported a decrease in NO₃⁻ towards inshore and the north and attributed this to increased sedimentary denitrification in these areas.

Because sedimentary denitrification is a heterotrophic process, rates may be expected to be higher post-bloom, when export of organic carbon should be higher than in pre-bloom conditions. In 2009, denitrification rates were determined in both pre-bloom (spring) and post-bloom (summer) conditions, and 3 stations were sampled in both seasons. Two of these stations (59.6°N, 175.2°W, HLY09–02 station 116, Knorr 195–10 station 122; 62.3°N, 172.5°W, HLY09–02 station 93 and Knorr 195–10 station 140) demonstrated higher average denitrification rates in the summer as compared to the spring, although these differences were not significant. The average denitrification rate on the shelf was higher in summer 2009 as compared with spring 2009; again, variability in measured rates preclude a statistical comparison. It is possible that temporal variability correlates with C export, which is predicted to be highly variable as well.

4.2. Benthic DIN fluxes

4.2.1. Exceptionally small DIN fluxes over the shelf

Based on limited direct measurements and modeling studies, previous workers have indicated that Bering Sea shelf sediments are a net source of NH₄⁺ and NO₃⁻ to the water column (Table 5;

Table 4

Measurements of sediment DIN flux, calculated NH_4^+ regeneration, and calculated denitrification rates from whole core incubations in 2009. For each station, measurements are mean and S.D. (parentheses), $n=2$ or 3. For DIN flux measurements, positive values indicate flux into the sediment. Spring/summer shelf averages are accompanied by standard errors.

Station	Sedimentary DIN flux ($\text{mmol N m}^{-2} \text{d}^{-1}$)			NH_4^+ regenerated ($\text{mmol N m}^{-2} \text{d}^{-1}$)	Denitrification rate ($\text{mmol N m}^{-2} \text{d}^{-1}$)
	NH_4^-	NO_2^-	NO_3^-		
HLY09-02					
3	0.16 (0.07)	0.01 (0.003)	-0.25 (0.03)	1.02 (<0.01)	0.94 (0.10)
9	0.06 (0.01)	0.01 (0.002)	-0.08 (0.04)	0.88 (0.12)	0.86 (0.15)
17	0.10 (0.10)	0.00 (0.001)	-0.00 (0.02)	0.55 (0.06)	0.64 (0.16)
32	-0.02 (0.04)	-0.01 (0.004)	0.06 (0.04)	0.61 (0.06)	0.64 (0.14)
35	0.01 (0.02)	0.00 (<0.00)	0.13 (0.05)	1.39 (0.32)	1.54 (0.38)
39	0.02 (0.01)	0.01 (<0.01)	-0.15 (0.06)	1.11 (0.64)	0.99 (0.70)
54	-0.08 (0.08)	-0.01 (<0.01)	0.07 (0.10)	1.19 (0.03)	1.17 (0.04)
58	-0.01 (0.02)	0.01 (0.01)	-0.28 (0.29)	0.90 (0.09)	0.62 (0.23)
65	0.22 (0.39)	0.04 (0.01)	-0.12 (0.10)	0.52 (0.01)	0.66 (0.48)
69	0.01 (0.01)	0.00 (<0.01)	0.14 (0.09)	0.62 (0.20)	0.76 (0.30)
73	0.00 (0.02)	0.00 (<0.01)	-0.08 (0.05)	0.77 (0.13)	0.69 (0.16)
83	0.18 (0.20)	0.00 (0.01)	-0.06 (0.01)	1.01 (0.12)	1.13 (0.06)
90	-0.03 (0.04)	0.01 (0.01)	-0.07 (0.04)	0.67 (0.06)	0.58 (0.01)
92	-0.05 (0.02)	0.00 (<0.01)	-0.16 (0.09)	0.87 (0.03)	0.66 (0.13)
93	0.01 (0.06)	-0.02 (0.02)	0.04 (0.11)	1.02 (0.29)	1.05 (0.09)
98	-0.05 (0.01)	0.03 (0.02)	-0.03 (0.13)	1.16 (0.09)	1.12 (0.01)
116	<0.01 (<0.00)	-0.03 (0.01)	-0.14 (0.10)	0.78 (0.08)	0.61 (0.01)
Spring shelf average (std. error)^a	0.02 (0.02)	0.00 (<0.01)	-0.06 (0.03)	0.88 (0.06)	0.86 (0.06)
Knorr 195-10					
22	0.08 (0.08)	0.01 (0.01)	0.40 (0.089)	1.08 (0.15)	1.56 (0.30)
32	0.01 (0.09)	0.01 (0.003)	0.24 (0.05)	0.90 (0.27)	1.16 (0.29)
45	0.09 (0.06)	0.00 (0.02)	0.27 (0.03)	1.35 (0.30)	1.70 (0.19)
60	-0.02 (0.33)	0.01 (0.01)	-0.06 (0.09)	0.68 (0.12)	0.61 (0.12)
79	0.06 (0.03)	0.00 (<0.01)	0.02 (0.03)	1.20 (0.12)	1.28 (0.16)
89	0.02 (0.01)	0.00 (0.00)	0.06 (0.02)	0.92 (0.04)	1.00 (0.07)
106	-0.10 (0.08)	0.00 (<0.01)	-0.60 (0.19)	1.38 (0.63)	0.67 (0.57)
122	0.10 (0.06)	0.00 (<0.01)	0.01 (0.04)	0.95 (0.27)	1.06 (0.24)
130	-0.14 (0.30)	0.00 (<0.01)	-0.08 (0.05)	1.93 (0.57)	1.71 (0.31)
140	-0.17 (0.04)	-0.01 (<0.01)	0.33 (0.06)	1.14 (0.32)	1.19 (0.26)
Summer shelf average (std. error)^a	0.00 (0.03)	0.00 (<0.01)	0.06 (0.09)	1.22 (0.13)	1.19 (0.12)

^a Seasonal shelf averages and standard errors were determined through linear mixed effect models for DIN Flux and NH_4 regeneration. Denitrification averages and standard errors were determined by the means of the station level results and standard errors of the means.

Whitledge et al., 1986; Rowe and Phoel, 1992; Granger et al., 2011). Based on a stable isotope study, Granger et al. (2011) named shelf sediments as the primary source of NH_4^+ to the NH_4^+ -rich (1–15 μM ; Whitledge and Luchin, 1999) cold pool over the middle shelf.

In this study, there was some variability in sedimentary DIN flux between replicates and among stations on the shelf, but shelf-wide, DIN flux was exceptionally low (Table 4). High small-scale variability (between replicate cores) in benthic flux measurements has commonly been reported in northern latitudes, including in the Bering sea (Whitledge et al., 1986; Lomstein et al., 1989; Rowe and Phoel, 1992), in the North Sea (Hall et al., 1996), and in Young Sound, Greenland (Rysgaard et al., 1998). The cause of such variability in parallel measurements is unclear from our data, but spatial variability of benthic invertebrates may be one contributing reason. Indeed, Lomstein et al. (1989) and Henriksen et al. (1993) suggested that DIN fluxes are strongly influenced by infaunal excretion and burrows in the Bering Sea-Anadyr waters and Alaska Coastal Water.

Even with variability among stations, sediment DIN fluxes were small compared to measurements by other workers on the Bering Sea shelf and in the Northern Bering Sea (Table 5). No stations had a NH_4^+ flux out of the sediments as high as that reported by Whitledge et al. (1986) ($-0.26 \text{ mmol N m}^{-2} \text{d}^{-1}$), and only 3 stations had a flux as high as that reported by Rowe and Phoel (1992) ($-0.10 \text{ mmol N m}^{-2} \text{d}^{-1}$). For the 10 stations that demonstrated NH_4^+ flux out of the sediment, the NH_4^+ efflux represented 2–15% of the sediment-regenerated NH_4^+ (remainder remineralized

as N_2 or NO_3^-). The shelf-wide average for NH_4^+ , NO_2^- , and NO_3^- in both seasons was not significantly different than 0 (Table 4, seasonal average ± 1 S.E.). With such low benthic DIN fluxes, remineralization from sediments is an unlikely source of NH_4^+ to the cold pool on the middle shelf in the spring and summer months, the typical months of NH_4^+ accumulation in the cold pool. We propose that a combination of a relatively long residence time (Coachman, 1986), ammonification of spring production (Whitledge et al., 1986), and slow nitrification are the leading contributing factors in the development of high NH_4^+ on the shelf.

4.2.2. Insignificant contribution of sediment-regenerated NH_4^+ to primary production

Since sediment DIN remineralization does not significantly contribute to the DIN inventory of the water column, the benthos cannot be a significant source of regenerated DIN for primary production. If we consider only the 10 out of 27 stations that did demonstrate NH_4^+ flux out of the sediments and propagate the average of the average flux for those 10 stations over the entire shelf, the contribution of sediment remineralization to the water column DIN inventory would represent 0.1–2.1% of N needed to support primary production on the Bering Sea shelf (106 mol C: 16 mol N phytoplankton uptake ratio; primary production 286 Tg C y^{-1} ; Brown et al., 2011). Laursen and Seitzinger (2002) found a similarly low contribution of remineralized DIN to primary production (1%) on the Mid-Atlantic Bight. A direct implication of

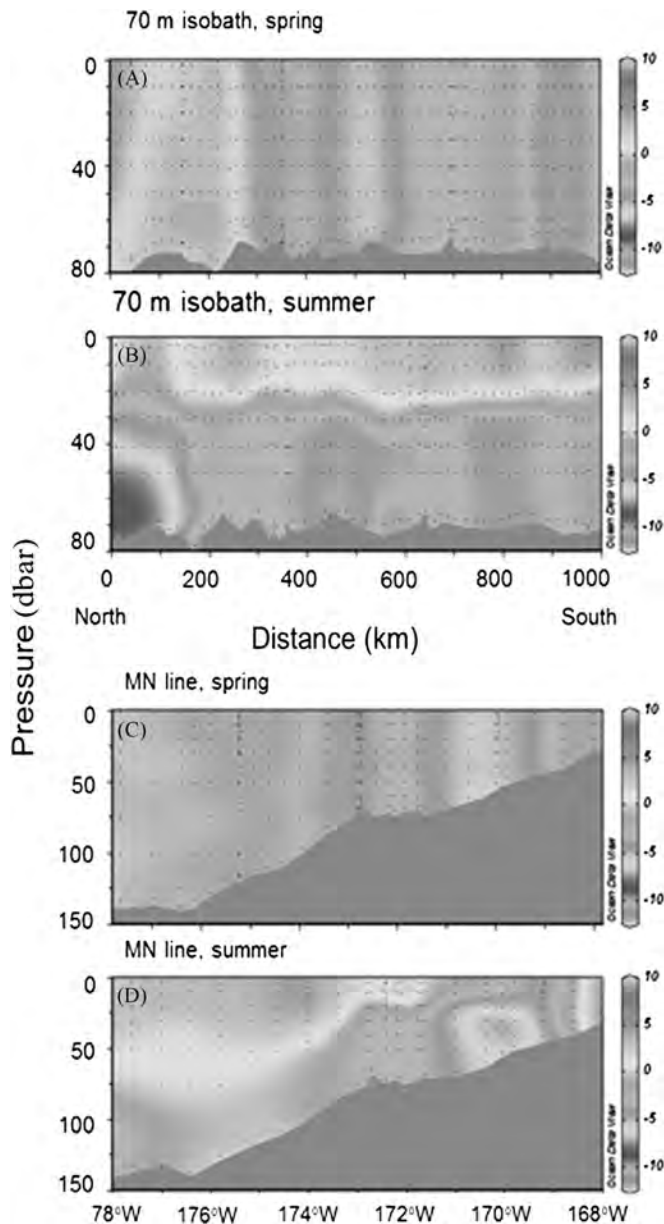


Fig. 4. Spring and summer comparison of water column N^{**} in 2009 along the 70 m isobath (A, B) and MN line (C, D). Scale bar indicates units of $\mu\text{mol kg}^{-1}$.

our benthic flux measurements is that most organic matter-N exported to the sediments is no longer available to primary production and Bering Sea shelf sediments are a stronger sink for water column fixed N than previously measured.

4.2.3. Extensive coupled nitrification/denitrification

Sedimentary N loss on the shelf consumes almost all sedimentary-regenerated N and through the coupled nitrification/denitrification pathway, rather than through direct denitrification (fueled by NO_3^- diffusion into sediments). The observation of very low DIN flux along with the observation of continuous denitrification co-occurring with O_2 consumption, and presumably NH_4^+ regeneration, implies that almost all organic material that is exported to sediments is denitrified or buried. Several studies of other polar continental shelves have demonstrated very low DIN effluxes and suggested that almost all of the sediment-regenerated N leaves sediments as N_2 gas, including studies in Svalbard, Norway (Blackburn et al., 1996; Glud et al., 1998) and in the

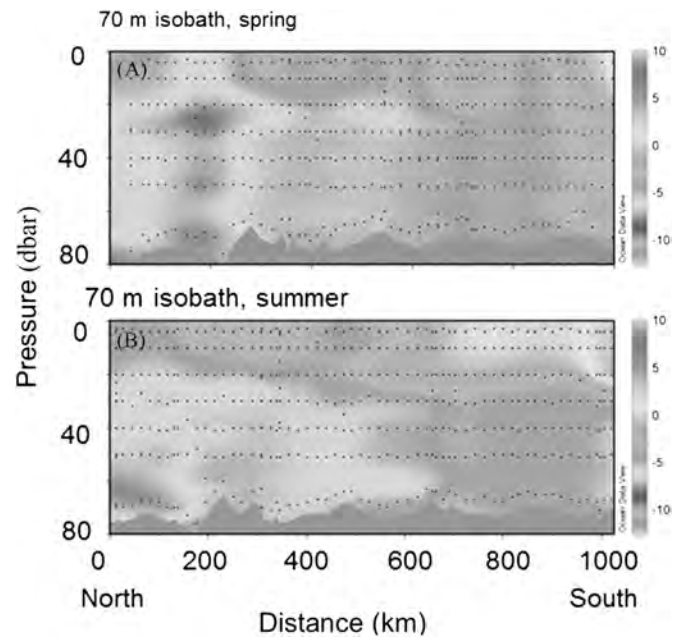


Fig. 5. N^{**} distribution in 2010 along the 70 m isobath during cruise TN249 (A) and TN250 (B). Scale bar indicates units of $\mu\text{mol kg}^{-1}$.

Beaufort and Chukchi Seas (Christensen, 2008). Coupled nitrification/denitrification has been shown to be a significant pathway of N loss on other continental margins, including in the Gulf of Maine (Christensen et al., 1987), eastern North Pacific (Devol and Christensen, 1993; Hartnett and Devol, 2003), North Atlantic and Mid-Atlantic Bight (Seitzinger and Giblin, 1996; Laursen and Seitzinger, 2002) and on the Western Antarctic Peninsula (Hartnett et al., 2008). In contrast, direct denitrification is the dominant N loss pathway in the deep Bering Sea (Lehmann et al., 2007).

Using a mass balance approach for each station, we estimated the importance of coupled nitrification/denitrification versus direct denitrification as pathways of sedimentary N loss. In the spring, only 5 stations demonstrated a net flux of NO_3^- into the sediments, and this flux could account for only 3.3–17.7% of the denitrification rate. More stations (7) in the summer demonstrated net NO_3^- diffusive flux into the sediments, but NO_3^- flux still only represented 1.8–25% of the substrate needed for denitrification at these stations. The remainder of the stations (12 in spring and 3 in summer) exhibited only coupled nitrification/denitrification. Collectively, our results indicate that coupled nitrification/denitrification is the dominant pathway to N loss on the Bering Sea shelf rather than direct denitrification. This agrees with previous studies about Bering Sea shelf sediments (Rowe and Phoel, 1992; Henriksen et al., 1993; Granger et al., 2011), although our study suggests a much higher dependence upon sedimentary coupled nitrification/denitrification than previous studies have predicted.

4.3. Water column N deficit

4.3.1. Interannual variability in N deficit

A comparison of mixed layer nutrients for summer 2009 and summer 2010 reveal different stages of the spring bloom on similar calendar days (Fig. 6). Below the mixed layer, the absolute value of N^{**} in the spring and in the summer are similar throughout the shelf in 2009 and 2010. After the onset of seasonal stratification in 2009 and 2010, surface water N^{**} differed from pre-bloom values both in absolute value and in distribution. The vast depletion of DIP and DIN and change in N^{**} in summer 2009 indicates the end of a spring bloom, the majority of which must

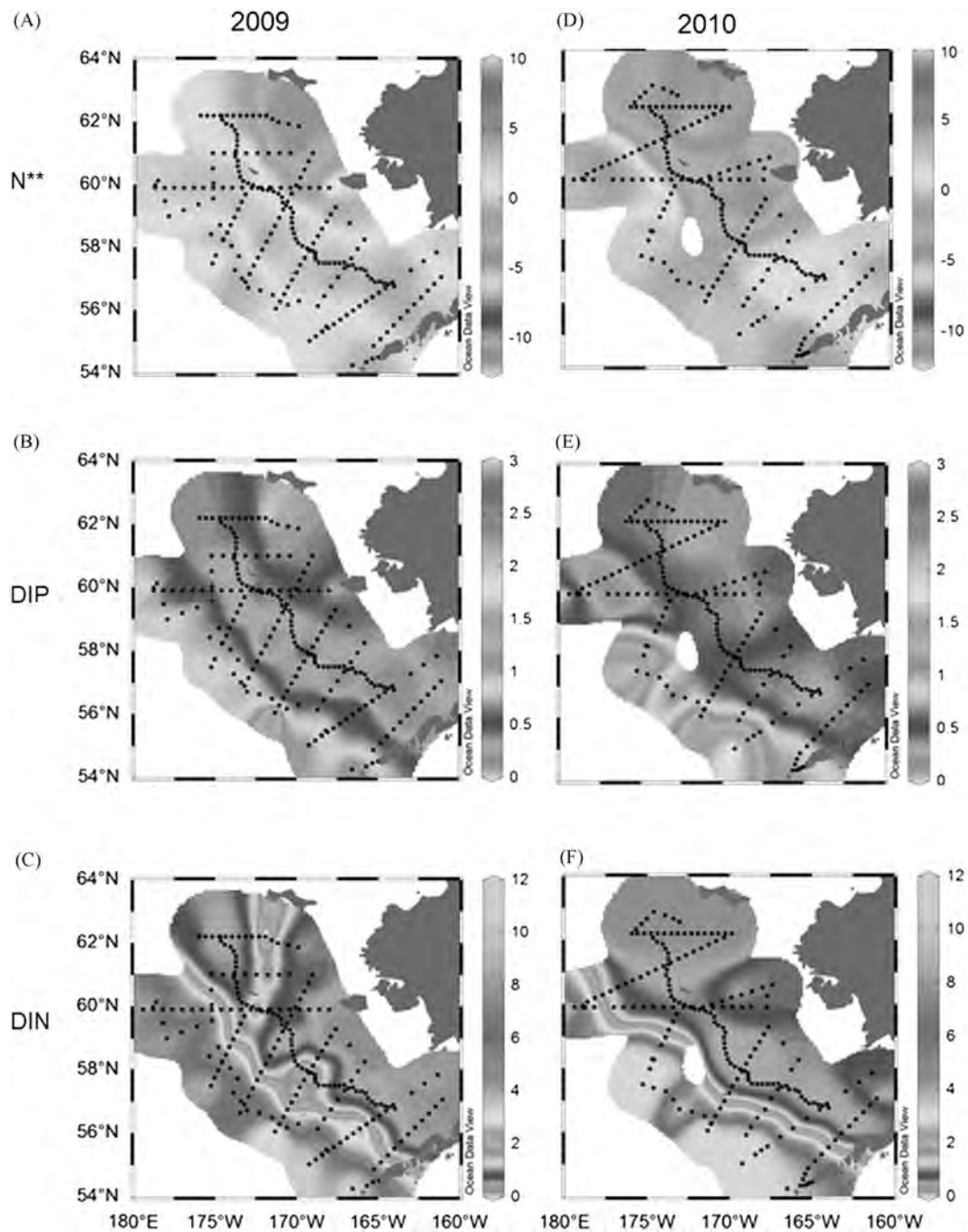


Fig. 6. Surface N^{**} (A, D), phosphate (B, E), and DIN (C, F) on the Bering Sea shelf in summer, 2009 and 2010. Scale bar indicates units of $\mu\text{mol kg}^{-1}$.

have taken place between the 2009 field expeditions (mid-May through mid-June). In contrast to 2009, 2010 was characterized a seasonally late advance of sea ice onto the shelf during May (Napp, 2010). Such a late season advance of ice is expected to bring about a later spring bloom. The depth profile of the 70 m isobath shows a contrast between summer 2009 (Fig. 4B) and summer 2010 (Fig. 5B): after the onset of seasonal stratification in 2010, none of the water column on the 70 m isobath exhibited a positive N^{**} . This contrasts sharply with the same transect a year earlier (Fig. 4B), 2008 (data not shown), and to a lesser extent, 2005 (Mordy et al., 2010), when positive N^{**} deviation over that of the winter N^{**} was found all along the 70 m isobath in the mixed layer. Positive N^{**} deviations did occur in the mixed layer in the southeastern shelf near the Aleutian Islands and on the western section of the MN line (Fig. 6D), but the trend was far from

widespread over the shelf. Stations on the MN line and 70 m isobath were sampled on approximately the same calendar dates (within one day) for the 2009 and 2010 summers, so the variability is not related to differences in sampling dates. Since sedimentary denitrification rates were comparable between 2009 and 2010, we do not suspect interannual differences in N^{**} to result from sedimentary denitrification. These annual differences in mixed layer DIN, DIP, and N^{**} may result from differences in timing of sea ice retreat and may be reflective of ecosystem response to interannual variability in weather conditions (Hunt et al., 2002).

4.3.2. The cause of positive surface N^{**} in 2009

The development of positive surface N^{**} between spring and summer 2009 was quite rapid; there was only one month between

Table 5

A comparison of Bering Sea shelf, northern Bering Sea, and deep Bering Sea benthic N fluxes. A negative DIN flux indicates flux from the sediment to the overlying water column.

Study area (Lat.–Long.)	Number stations	Method	Mean DIN Flux ($\text{mmol N m}^{-2} \text{d}^{-1}$)		Mean denitrification rate ($\text{mmol N m}^{-2} \text{d}^{-1}$)	BS shelf areal N loss (Tg N y^{-1})	Reference
			NH_4^+	NO_3^-			
Bering Sea Shelf							
56°N–57°N 165°W–172°W	3	^{15}N – NO_3^- tracer	ND	ND	0.20	0.50 ^a	Koike and Hattori (1979)
55°N–63°N 163°W–180°E	39	Acetylene blockage of N_2O Reduction	ND	ND	0.36	1.80 ^b	Haines et al. (1981)
56°N–58°N 162°W–170°W	7	Flux of NH_4^+ from box core incubation	–0.26	ND	ND	ND	Whitledge et al. (1986)
55.5°N–58.5°N 162°W–167°W	7	Sediment DIN flux + mass balance	–0.11	–0.38	0.58	3.56	Rowe and Phoel (1992)
55°N–59°N 166°W transect	9	Stoichiometric estimate using water column DIN, DIP	ND	ND	1.10	2.50 ^a	Tanaka et al. (2004)
54°N–63°N 160°W–180°E	15	IRMS, N_2 flux	N/A	N/A	Spring: 1.14	5.2–6.2	This study
	41	MIMS, N_2 flux	N/A	N/A	Spring: 0.62, Summer: 0.76		This study
	27	Sediment DIN flux + mass balance	Spring: 0.02, Summer: <0.01	Spring: –0.06, Summer: 0.06	Spring: 0.86, Summer: 1.19		This study
Northern Bering Sea							
Bering Sea/ Anadyr waters	20	DIN flux from whole core incubation	–0.70	–0.10	1.2	N/A	Lomstein et al. (1989)
Bering Sea/ Anadyr waters	9	DIN flux from whole core incubation	–0.99	0.10	1.35	N/A	Henriksen et al. (1993)
Deep Bering Sea							
Deep (>2000 m)	10	Water column NO_3^- deficit + sediment NO_3^- flux + isotopes	ND	0.05–0.14	0.23	N/A	Lehmann et al. (2005)
Deep (1098–2789)	4	MIMS, N_2 flux	N/A	N/A	0.56	N/A	This study

ND: no data available; N/A: not applicable.

^a Calculated denitrification for only half of the shelf.

^b Authors indicated gross N loss of 2.2 Tg N y^{-1} and 0.4 Tg N y^{-1} input from N_2 -fixation.

sampling efforts. Although we did not measure sedimentary denitrification in 2009 between those cruises, we did measure active sedimentary denitrification in May and June 2010, and those measurements were similar to 2009. Given the assumption of constant sedimentary denitrification for the month between cruises in 2009 and the observation that the positive increase in N^{**} occurred exclusively in the mixed layer, we do not believe that a decline in denitrification caused the strong positive N^{**} . There are several processes that could be responsible for the positive deviations in N^{**} : (1) riverine runoff, (2) atmospheric N deposition, (3) input of N from N_2 -fixation, and (4) non-Redfieldian uptake of nutrients by phytoplankton.

The shelf waters with the highest increase in N^{**} occur along the middle and outer shelf; without a similar increase on the inner shelf and the large distance between riverine sources and the middle shelf, it is unlikely that riverine runoff is a major cause of positive N^{**} deviations. Also, a comparison of N^{**} and salinity for summer 2009 did not show a trend of increasing N^{**} with decreasing salinity, as would be expected if riverine runoff were a major contributor to positive N^{**} deviations (data not shown). Also, there is not enough atmospheric deposition of nitrogen ($71\text{--}140 \text{ mg N m}^{-2} \text{ y}^{-1}$ Duce et al., 2008) to account for the increase in N^{**} during the month between sampling periods. Atmospheric deposition of N could for a maximum of 4% of the change in mixed layer integrated N^{**} from spring to summer.

Water column N_2 -fixation is a common cause of positive N^* in the tropical and subtropical ocean far away from land (Michaels et al., 1996; Gruber and Sarmiento, 1997). Haines et al. (1981)

measured a gross input of N to the Bering Sea shelf from sedimentary N_2 -fixation ($65.2 \mu\text{mol N m}^{-2} \text{ d}^{-1}$ or 0.4 Tg N y^{-1}), but a lack of N^{**} increase immediately above the sediments argues against sedimentary N_2 -fixation as a cause of positive N^{**} in the surface mixed layer. Also, a recent modeling study suggests that there is a lack of a significant population of diazotrophs in the Bering Sea (Monteiro et al., 2011). Although assays to directly detect diazotrophs (i.e. *nifH* molecular analyses) and N_2 -fixation rate measurements in the water column have not yet been published, N_2 -fixation is likely not a cause of positive N^{**} deviations in the surface waters.

In this study, the relatively quick development of positive N^{**} in the mixed layer co-occurring with the onset of the spring bloom and the rapid depletion of nutrients (especially DIN) in the mixed layer is best explained by non-Redfieldian nutrient uptake and remineralization by phytoplankton, specifically, low phytoplankton biomass N:P. Under rapid growth conditions, phytoplankton have higher cellular P requirements because of the need for P-rich RNA and other cellular reproductive machinery during exponential growth (Klausmeier et al., 2004). Seasonal Arctic and Antarctic diatom blooms have been shown to produce similar non-Redfieldian uptake dynamics, where N:P drawdown ratio was low and the result was an excess of PO_4^{-3} (Rubin et al., 1998; Arrigo et al., 1999; Green and Sambrotto, 2006; Mills and Arrigo, 2010; Deutsch and Weber, 2012). Based on nutrient drawdown ratios between seasons, recent research indicates that Bering Sea phytoplankton along the 70 m isobath drawdown N:P in an average ratio 10.0 ± 2.8 (range: 4.2–17.8; Mordy et al., 2012). This is very close to the diatom biomass N:P

ratio (11:1) that Weber and Deutsch (2010) predicted under peak diatom growth conditions through a Southern Ocean modeling study based on nutrient drawdown.

4.4. Total N loss in the Bering Sea resulting from sedimentary denitrification

We used spring and summer denitrification measurements (from IRMS, MIMS, and sediment DIN mass balance) and a Bering Sea shelf area of $1.2 \times 10^6 \text{ km}^2$ (Hunt Jr. et al., 2010) to calculate an annual N loss of 5.2–6.2 Tg N y^{-1} . Our results indicate that the previous estimate for Bering Sea shelf total areal N loss should be revised upwards by at least 50%; prior to this study, the highest reported estimate was 3.56 Tg N y^{-1} (Rowe and Phoel, 1992). Because our sampling effort in the deep basin was limited (4 stations along the margins), we used the annual N loss estimate of 1.27 Tg N y^{-1} from Lehmann et al. (2005) to calculate total denitrification in the Bering Sea basin. Taken together, N loss for the entire Bering Sea is 6.5–7.5 Tg N y^{-1} . Given an annual primary production of 286 Tg C y^{-1} for the Bering Sea (Brown et al., 2011) and a phytoplankton uptake ratio of 106 C:16 N, our estimate of sedimentary N loss can account for 15.1–17.4% of total N uptake by phytoplankton. Seitzinger and Giblin (1996) found a similar percentage of N removal by denitrification (13%) on the North Atlantic continental shelves, which was also mostly through coupled nitrification/denitrification. This estimate of sedimentary N loss represents a substantial portion of annual primary production in the Bering Sea.

5. Conclusions

This study is the most extensive field program to date that investigates the two major factors affecting the N deficit on the commercially important Bering Sea shelf, sedimentary denitrification and sedimentary DIN fluxes. In addition, this study is the first to examine seasonal and interannual changes in N deficit in light of the main process affecting its distribution, sedimentary denitrification. The summer positive increase in the Bering shelf-specific geochemical tracer N^{**} most likely indicates that phytoplankton on the shelf drawdown inorganic N and P in a ratio lower than Redfield. Interannual variation in water column N^{**} may reflect differences in the magnitude and fate of the spring bloom, which is related to the timing of sea ice retreat, and not differences in sedimentary denitrification. Sedimentary denitrification is an important sink of water column fixed N, as evidenced by the denitrification rate, the near zero sedimentary DIN flux, and very low N^{**} in the winter. Denitrification is fueled largely through coupled nitrification/denitrification, and not by diffusive NO_3^- flux at the sediment–water interface. Based on four separate assays to measure denitrification, we revise upwards the basin-wide estimate of N loss over the shelf to 5.2–6.2 Tg N y^{-1} and 6.5–7.5 Tg N y^{-1} for the entire Bering Sea. Given that extensive microbial nitrogen cycling on the shelf sediments causes the benthos to be a negligible source of remineralized N to the water column, sedimentary microbial activity over the entire shelf negatively regulates primary production on the Bering Sea shelf more strongly than previously recognized.

Acknowledgments

We would like to thank the Captains and crews of the USCGC *Healy*, R/V *Knorr*, and R/V *Thomas G. Thompson* for their efforts supporting this work. We thank Maggie Esch, Wendi Ruef, and Greg Brusseau for their assistance with sample collection in the

field. We are grateful to Clara Fuchsman and the University of Washington Stable Isotope Lab the IRMS analysis and the University of Washington Center for Statistical Consulting. We thank 2 anonymous reviewers for their thoughtful comments which greatly improved this manuscript. This work was part of the BEST-BSIERP Project, supported by NSF and NPRB. This publication was funded by NSF grants OCE-0612436 to AHD, ARC-0732430 and ARC-0732640 to CWM, and ARC-0612380 and MRI-0723234 to DHS. This research was partially funded by the Joint Institute for the Study of the Atmosphere and Ocean (JISAO) under NOAA Cooperative Agreement NA10OAR4320148. This is BEST-BSIERP Bering Sea Project publication number 88, contribution number 3828 to the NOAA Pacific Marine Environmental Laboratory, and 2024 to JISAO, and contribution EcoFOCI-0781 to NOAA's Fisheries-Oceanography Coordinated Investigations.

References

- Arrigo, K., Robinson, D., Worthen, D., Dunbar, R., DiTullio, G., VanWoert, M., Lizotte, M., 1999. Phytoplankton community structure and the drawdown of nutrients and CO_2 in the Southern Ocean. *Science* 283, 365–367.
- Blackburn, T., Hall, P., Hulth, S., Landen, A., 1996. Organic-N loss by efflux and burial associated with a low efflux of inorganic N and with nitrate assimilation in Arctic sediments (Svalbard, Norway). *Mar. Ecol. Prog. Ser.* 141, 283–293.
- Brown, Z., van Dijken, G., Arrigo, K., 2011. A reassessment of primary production and environmental change in the Bering Sea. *J. Geophys. Res. (C Oceans)* 116, C08014.
- Chang, B., Devol, A., 2009. Seasonal and spatial patterns of sedimentary denitrification rates in the Chukchi sea. *Deep Sea Res. (II Top. Stud. Oceanogr.)* 56, 1339–1350.
- Christensen, J., 2008. Sedimentary carbon oxidation and denitrification on the shelf break of the Alaskan Beaufort and Chukchi Seas. *Open Oceanogr. J.* 2, 6–17.
- Christensen, J., Murray, J., Devol, A., Codispoti, L., 1987. Denitrification in continental shelf sediments has major impact on the ocean nitrogen budget. *Glob. Biogeochem. Cy.* 1, 97–116.
- Coachman, L., 1986. Circulation, water masses, and fluxes on the southeastern Bering Sea shelf. *Cont. Shelf Res.* 5, 23–108.
- Codispoti, L., Brandes, J., Christensen, J., Devol, A., Naqvi, S., Paerl, H., Yoshinari, T., 2001. The oceanic fixed nitrogen and nitrous oxide budgets: moving targets as we enter the anthropocene? *Sci. Mar.* 65, 85–105.
- Davenport, E., Shull, D., Devol, A., 2012. Roles of sorption and tube-dwelling benthos in the cycling of phosphorus in Bering Sea sediments. *Deep Sea Res. (II Top. Stud. Oceanogr.)* 65–70, 163–172.
- Deutsch, C., Sarmiento, J., Sigman, D., Gruber, N., Dunne, J., 2007. Spatial coupling of nitrogen inputs and losses in the ocean. *Nature* 445, 163–167.
- Deutsch, C., Weber, T., 2012. Nutrient ratios as a tracer and driver of ocean biogeochemistry. *Annu. Rev. Mar. Sci.* 4, 113–141.
- Devol, A., Christensen, J., 1993. Benthic fluxes and nitrogen cycling in sediments of the continental margin of the eastern North Pacific. *J. Mar. Res.* 51, 345–372.
- Devol, A., Codispoti, L., Christensen, J., 1997. Summer and winter denitrification rates in western Arctic shelf sediments. *Cont. Shelf Res.* 17, 1029–1050.
- Duce, R.A., LaRoche, J., Altieri, K., Arrigo, K.R., Baker, A.R., Capone, D.G., Cornell, S., Dentener, F., Galloway, J., Ganeshram, R.S., Geider, R.J., Jickells, T., Kuypers, M. M., Langlois, R., Liss, P.S., Liu, S.M., Middleburg, J.J., Moore, C.M., Nickovic, S., Oschlies, A., Pedersen, T., Prospero, J., Schltzer, R., Seitzinger, S., Sorensen, L.L., Uematsu, M., Ulloa, O., Voss, M., Ward, B., Zamora, L., 2008. Impacts of atmospheric anthropogenic nitrogen on the open ocean. *Science* 320, 893–897.
- Emerson, S., Stump, C., Wilbur, D., Quay, P., 1999. Accurate measurement of O_2 , N_2 , and Ar gases in water and the solubility of N_2 . *Glob. Biogeochem. Cy.* 5, 49–69.
- Esch, M., Shull, D., Devol, A., Moran, B., 2013. Regional patterns of iron and manganese reduction rates in the shelf sediments of the southeastern Bering Sea. *Deep Sea Res. (II Top. Stud. Oceanogr.)*, 94, 80–94.
- Eyre, B., Rysgaard, S., Dalsgaard, T., 2002. Comparison of isotope pairing and N_2 :Ar methods for measuring sediment denitrification. *Estuaries* 25, 1077–1087.
- Fennel, K., Wilkin, J., Levin, J., Moisan, J., O'Reilly, J., Haidvogel, D., 2006. Nitrogen cycling in the Middle Atlantic Bight: results from a three-dimensional model and implications for the North Atlantic nitrogen budget. *Glob. Biogeochem. Cy.* 20, GB3007.
- Froelich, P., Klunkhammer, G., Bender, M., Luedtke, N., Heath, G., Cullen, D., Dauphin, P., Hammond, D., Hartman, B., Maynard, V., 1979. Early oxidation of organic matter in pelagic sediments of the eastern equatorial Atlantic: Suboxic diagenesis. *Geochim. Cosmochim. Acta* 43, 1075–1090.
- Glud, R., Holby, O., Hoffmann, F., Canfield, D., 1998. Benthic mineralization and exchange in Arctic sediments (Svalbard, Norway). *Mar. Ecol. Prog. Ser.* 173, 237–251.
- Gordon, L., Jennings Jr., J., Ross, A., Krest, M., 1994. A Suggested Protocol for Continuous Flow Automated Analysis of Seawater Nutrients (Phosphate, Nitrate, Nitrite and Silicic Acid) in the WOCE Hydrographic Program and the Joint Global Ocean Fluxes Study. WHP Operations and Methods, WOCE Hydrographic Program Office, Methods Manual 91-1, November.

- Granger, J., Prokopenko, M., Sigman, D., Mordy, C., Morse, Z., Morales, L., Sambrotto, R., Plessen, B., 2011. Coupled nitrification-denitrification in sediment of the eastern Bering Sea shelf leads to ^{15}N enrichment of fixed N in shelf waters. *J. Geophys. Res. Oceans* 116, c11006.
- Grebmeier, J., Overland, J., Moore, S., Farley, E., Carmack, E., Cooper, L., Frey, K., Helle, J., McLaughlin, F., McNutt, S., 2006. A major ecosystem shift in the Northern Bering Sea. *Science* 311, 1461–1464.
- Green, S., Sambrotto, R., 2006. Net community production in terms of C, N, P and Si in the Antarctic Circumpolar Current and its influence on regional water mass characteristics. *Deep Sea Res. (I Oceanogr. Res. Pap.)* 53, 111–135.
- Gruber, N., Sarmiento, J., 1997. Global patterns of marine nitrogen fixation and denitrification. *Glob. Biogeochem. Cy.* 11, 235–266.
- Haines, J., Atlas, R., Griffiths, R., Morita, R., 1981. Denitrification and nitrogen fixation in Alaskan continental shelf sediments. *Appl. Environ. Microbiol.* 41, 412–421.
- Hall, P., Hulth, S., Hulth, G., Landen, A., Tengberg, A., 1996. Benthic nutrient fluxes on a basin-wide scale in the Skagerrak (north-eastern North Sea). *J. Sea Res.* 35, 123–137.
- Hamme, R., Emerson, S., 2002. Mechanisms controlling the global oceanic distribution of the inert gases argon, nitrogen, and neon. *Geophys. Res. Lett.* 29, 2010.10.1029/2002GL015273.
- Hartnett, H., Boehme, S., Thomas, C., McMaster, D., Smith, C., 2008. Benthic oxygen fluxes and denitrification rates from high-resolution porewater profiles from the Western Antarctic Peninsula continental shelf. *Deep Sea Res. (II Top. Stud. Oceanogr.)* 55, 2415–2424.
- Hartnett, H., Devol, A., 2003. Role of a strong oxygen-deficient zone in the preservation and degradation of organic matter: a carbon budget for the continental margins of northwest Mexico and Washington State. *Geochim. Cosmochim. Acta* 67, 247–264.
- Henriksen, K., Blackburn, T., Lomstein, B., McRoy, C., 1993. Rates of nitrification, distribution of nitrifying bacteria and inorganic N fluxes in northern Bering-Chukchi shelf sediments. *Cont. Shelf Res.* 13, 629–651.
- Hunt Jr., G., Allan, B., Angliss, R., Baker, T., Bond, N., Buck, G., Byrd, G., Coyle, K., Devol, A., Eggers, D., Eisner, L., Feely, R., Fitzwater, S., Fritz, L., Gritsai, E., Ladd, C., Lewis, W., Mathis, J., Mordy, C., Mueter, F., Napp, J., Sherr, E., Shull, D., Stabeno, P., Stepanenko, M., Strom, S., Whittledge, T., 2010. Status and trends of the Bering Sea region, 2003–2008. In: McKinnell, S., Dagg, M. (Eds.), *Marine Ecosystems of the North Pacific Ocean, 2003–2008*. PICES Special Publication, pp. 196–267.
- Hunt Jr., G., Stabeno, P., Walters, G., Sinclair, E., Brodeur, R., Napp, J., Bond, N., 2002. Climate change and control of the southeastern Bering Sea pelagic ecosystem. *Deep Sea Res. (II Top. Stud. Oceanogr.)* 49, 5821–5853.
- Kana, T., Darkangelo, C., Hunt, M., Oldham, J., Bennett, G., Cornwell, J., 1994. Membrane inlet mass spectrometer for rapid high-precision determination of N_2 , O_2 , and Ar in environmental water samples. *Anal. Chem. (Wash.)* 66, 4166–4170.
- Kana, T., Weiss, D., 2004. Comment on “Comparison of isotope pairing and N:Ar methods for measuring sediment denitrification” by B.D. Eyre, S. Rysgaard, T. Dalsgaard, P. Bondo Christensen, 2002. *Estuaries* 25, 1077–1087. *Estuaries* 27, 173–176.
- Klausmeier, C., Litchman, E., Daufresne, T., Levin, S., 2004. Optimal nitrogen-to-phosphorus stoichiometry of phytoplankton. *Nature* 429, 171–174.
- Koike, I., Hattori, A., 1979. Estimates of denitrification in sediments of the Bering Sea shelf. *Deep-Sea Res* 26A, 409–415.
- Laursen, A., Seitzinger, S., 2002. The role of denitrification in nitrogen removal and carbon remineralization in Mid-Atlantic Bight sediments. *Cont. Shelf Res.* 22, 1397–1416.
- Lehmann, M., Sigman, D., McCorkle, D., Brunelle, B., Hoffmann, S., Kienast, M., Cane, G., Clement, J., 2005. Origin of the deep Bering Sea nitrate deficit: constraints from the nitrogen and oxygen isotopic composition of water column nitrate and benthic nitrate fluxes. *Glob. Biogeochem. Cy.*, 19.
- Lehmann, M., Sigman, D., McCorkle, D., Granger, J., Hoffmann, S., Cane, G., Brunelle, B., 2007. The distribution of nitrate $^{15}\text{N}/^{14}\text{N}$ in marine sediments and the impact of benthic nitrogen loss on the isotopic composition of oceanic nitrate. *Geochim. Cosmochim. Acta* 71, 5384–5404.
- Lomstein, B., Blackburn, T., Henriksen, K., 1989. Aspects of nitrogen and carbon cycling in the northern Bering Shelf sediment. I. The significance of urea turnover in the mineralization of NH_4^+ . *Mar. Ecol. Prog. Ser.* 57, 237–247.
- Mathis, J., Cross, J., Bates, N., Moran, S., Lomas, M., Mordy, C., Stabeno, P., 2010. Seasonal distribution of inorganic carbon and net community production on the Bering Sea shelf. *Biogeosciences* 7, 1769–1787.
- Michaels, A., Olson, D., Sarmiento, J., Ammerman, J., Fanning, K., Jahnke, R., Knap, A., Lipschultz, F., Prospero, J., 1996. Inputs, losses and transformations of nitrogen and phosphorus in the pelagic North Atlantic Ocean. *Biogeochemistry* 35, 181–226.
- Mills, M., Arrigo, K., 2010. Magnitude of oceanic nitrogen fixation influenced by the nutrient uptake ratio of phytoplankton. *Nat. Geosci.* 3, 412–416.
- Monteiro, F., Dutkiewicz, S., Follows, M., 2011. Biogeographical controls on the marine nitrogen fixers. *Glob. Biogeochem. Cy.* 25 (GB2), 003.
- Mordy, C., Cokelet, E., Ladd, C., Menzia, F., Proctor, P., Stabeno, P., Wisegarver, E., 2012. Net community production on the Middle Shelf of the Eastern Bering Sea. *Deep Sea Res. (II Top. Stud. Oceanogr.)* 65–70, 110–125.
- Mordy, C., Eisner, L., Proctor, P., Stabeno, P., Devol, A., Shull, D., Napp, J., Whittledge, T., 2010. Temporary uncoupling of the marine nitrogen cycle: accumulation of nitrite on the Bering Sea shelf. *Mar. Chem.* 121, 157–166.
- Mordy, C., Stabeno, P., Righi, D., Menzia, F., 2008. Origins of the subsurface ammonium maximum in the southeast Bering Sea. *Deep Sea Res. (II Top. Stud. Oceanogr.)* 55, 1738–1744.
- Napp, J., 2010. *The Bering Sea: Current Status and Recent Events*. vol. 18. PICES Press, Saanich, British Columbia, Canada, pp. 34–36.
- NRC, 1996. *The Bering Sea Ecosystem*. National Academy Press, Washington, D. C.
- Redfield, A., 1934. On the proportions of organic derivative in sea water and their relation to the composition of plankton. In: Daniel, R. (Ed.), *James Johnstone Memorial Volume*. University of Liverpool, pp. 176–192.
- Redfield, A., 1958. The biological control of chemical factors in the environment. *Am. Sci.* 46, 205–221.
- Rho, T., Whittledge, T., 2007. Characteristics of seasonal and spatial variations of primary production over the southeastern Bering Sea shelf. *Cont. Shelf Res.* 27, 2556–2569.
- Rho, T., Whittledge, T., Goering, J., 2005. Interannual variations of nutrients and primary productivity over the southeastern Bering Sea shelf during the spring of 1997, 1998, and 1999. *Oceanology* 45, 376–390.
- Rowe, G., Phoele, W., 1992. Nutrient regeneration and oxygen demand in Bering Sea continental shelf sediments. *Cont. Shelf Res.* 12, 439–449.
- Rubin, S., Takahashi, T., Chipman, D., Goddard, J., 1998. Primary productivity and nutrient utilization ratios in the Pacific sector of the Southern Ocean based on seasonal changes in seawater chemistry. *Deep Sea Res. (I Oceanogr. Res. Pap.)* 45, 1211–1234.
- Rysgaard, S., Thamdrup, B., Risgaard-Petersen, N., Fossing, H., Berg, P., Bondo Christensen, P., Dalsgaard, T., 1998. Seasonal carbon and nutrient mineralization in a high-Arctic coastal marine sediment, Young Sound, Northeast Greenland. *Mar. Ecol. Prog. Ser.* 175, 261–276.
- Schlitzer, R., 2011. *Ocean Data View*.
- Seitzinger, S., Giblin, A., 1996. Estimating denitrification in North Atlantic continental shelf sediments. *Biogeochemistry* 35, 235–260.
- Seitzinger, S., Harrison, J., Hobbie, J., Bouwman, A., Lowrance, R., Peterson, B., Tobias, C., Van Drecht, G., 2006. Denitrification across landscapes and waterscapes: a synthesis. *Ecol. Appl.* 16, 2064–2090.
- Sigler, M., Harvey, H., Ashjian, C., Lomas, M., Napp, J., Stabeno, P., Van Pelt, T., 2010. How does climate change affect the Bering Sea ecosystem? *EOS Trans. Am. Geophys. Union* 91, 457–458.
- Stabeno, P., Bond, N., Salo, S., 2007. On the recent warming of the southeastern Bering Sea shelf. *Deep Sea Res. (II Top. Stud. Oceanogr.)* 54, 2599–2618.
- Stabeno, P., Hunt Jr., G., Napp, J., Schumacher, J., 2006. Physical forcing of ecosystem dynamics on the Bering Sea shelf. In: Robinson, A., Brink, K. (Eds.), *The Global Coastal Ocean: Interdisciplinary Regional Studies and Syntheses, Part B*. Harvard University Press, pp. 1177–1212.
- Tanaka, T., Guo, L., Deal, C., Tanaka, N., Whittledge, T., Murata, A., 2004. N deficiency in a well-oxygenated cold bottom water over the Bering Sea shelf: influence of sedimentary denitrification. *Cont. Shelf Res.* 24, 1271–1283.
- Weber, T., Deutsch, C., 2010. Ocean nutrient ratios governed by plankton biogeography. *Nature* 467, 550–554.
- Whittledge, T., Bidigare, R., Zeeman, S., Sambrotto, R., Rascigno, P., Jensen, P., Brooks, J., Trees, C., Veidt, D., 1988. Biological measurements and chemical features in Soviet and United States regions of the Bering Sea. *Cont. Shelf Res.* 8, 1299–1319.
- Whittledge, T., Luchin, V., 1999. Summary of chemical distributions and dynamics in the Bering Sea. In: Loughlin, T., Ohtani, K. (Eds.), *Dynamics of the Bering Sea*. University of Alaska Sea Grant, Fairbanks, AK, pp. 217–250.
- Whittledge, T., Reebergh, W., Walsh, J., 1986. Seasonal inorganic nitrogen distributions and dynamics in the southeastern Bering Sea. *Cont. Shelf Res.* 5, 109–132.



Contents lists available at ScienceDirect

Deep-Sea Research II

journal homepage: www.elsevier.com/locate/dsr2

Hydrography and biological resources in the western Bering Sea



G.V. Khen*, E.O. Basyuk, N.S. Vanin, V.I. Matveev

Pacific Research Fisheries Center (TINRO-Center), 4, Shevchenko Alley, Vladivostok, 690091, Russia

ARTICLE INFO

Available online 18 March 2013

Keywords:

Western Bering Sea
Hydrology
Hydrochemistry
Interannual variability
Water exchange

ABSTRACT

The variability of temperature, salinity, dissolved oxygen and nutrients (phosphate and silicate) in the west Bering Sea in the Russian Exclusive Economic Zone (REZ) since 1950 and the influence of these factors on the distribution and dynamics of hydrobionts were studied. Since 1950, the sea surface temperature has been gradually increasing, although non-significant cooling occurred in the last decade. In contrast, in the 50–200 m depth range, the temperature has been cooling. During the last 60 years, the salinity decreased by 0.30, 0.06–0.10 and 0.04 at the sea surface, at the 100–200 m layer and at the depth of 500 m, respectively, resulting in a strengthening of the vertical stability and weakening of the vertical water exchange. As a consequence, the oxygen concentrations at depths down to 1000 m decreased during this period. Phosphate and silicate concentrations increased during the last 40 years. The water exchange with the North Pacific (based on the discharge through the Kamchatka Strait) from the mid-1960s to the early 1990s was 2–3-fold higher than in the 1950s or from the mid-1990s to 2010. During the periods of weakened water exchange, the herring population sharply increased, while during periods of strengthened water exchange, pollock biomass increased. The increase of codfishes, flounders and sculpin biomass at the sea shelf during the second half of the 20th century coincided with sea surface warming. Since 2007, the westward water transport from the Aleutian Basin was almost half that during 2002–06, while the northward stream from Near Strait noticeably increased. The populations of immature chum, sockeye and chinook in the REZ declined because of their weakened input from the US zone, and these species were distributed mainly in the northern and eastern Russian waters.

Taking into account the cooling since the middle of the last decade, the change in the intensity and direction of the Aleutian Low and Siberian High trends, and the westward shift of the Aleutian Low, one can hypothesize the possible return of the Bering Sea climate to the conditions of the 1960–80s and the corresponding response observed in ichthyofauna.

© 2013 Elsevier Ltd. All rights reserved.

1. Introduction

The Bering Sea is located at the northern edge of the North Pacific, in a region strongly affected by arctic air masses. An active water exchange with the North Pacific occurs through the numerous straits of the Aleutian Arc. A connection with the Arctic Ocean is maintained through the shallow (< 40 m) and narrow (85 km) Bering Strait, through which up to $0.2 \times 10^6 \text{ m}^3 \text{ s}^{-1}$ of arctic water input is possible (Coachman et al., 1975), which is < 1% of the volume of Pacific water entering from the south.

The hydrography of the Bering Sea is formed under the influence of ocean inflow of Pacific water and atmospheric and ice processes. River discharge mainly impacts the salt and density modes of the shelf.

The climate conditions of the Bering Sea that form its hydrography vary depending on the geographical location. In the

western Bering Sea, the well-expressed monsoon climate prevails, while the northern Bering Sea is under arctic influence (Starichenko and Botianov, 1999). The central (as far east as shelf break) and southern parts are influenced by inflow of Pacific.

Interannual changes in the hydrosphere of the Bering Sea are closely related to atmospheric processes and can be “cold” or “warm” depending on state of the Siberian High or Aleutian Low (Luchin et al., 1998, 2002; Varlamov et al., 1998). In different seasons, the pattern of interannual variations during the second half of the 20th century varies noticeably (Khen and Sorokin, 2008). In the cold half of the year, the sea surface temperature (SST) increased from 1950 until the beginning of the 1990s and steeply decreased in the subsequent decades. In summer, from the beginning of the recorded data until the 1980s, the SST decreases and then rises. At a depth of 30 m, which is below the summer mixed layer, two periods of cooling are marked: the first period ranged from the mid-1950s until the mid-1970s, and the second period ranged from the end of the 1970s until the mid-1990s (Luchin et al., 1998, 2002). During the interval between these periods, a steep warming (almost 5 °C over two years) related to

* Corresponding author. Tel.: +8 423 2604530; fax: +8 423 2300751.
E-mail address: gennady1@tinro.ru (G.V. Khen).

the famous “regime shift” in the North Pacific occurred (Minobe, 1997). The aforesaid is true for the whole Bering Sea basin.

The hydrophysical processes in the eastern and western parts of the sea are considered to be opposite to each other (Stabeno et al., 1999). The strengthening of the Pacific water input leads to the warming of the eastern part, but in the west, cooling occurs (Luchin et al., 2002). However, these conclusions were based on limited time intervals. Subsequent work (Ustinova et al., 2008) has shown a synchronous SST increase in both the eastern and western parts of the sea. Steep variations of the SST in both regions in the 1970s and at the turn of the century were also confirmed. In the eastern area that is under the direct influence of warm Pacific waters, the temperature is usually 0.5–1.0 °C higher than in the west. In the middle of the most recent decade, the SST difference changed sign, i.e., the western part of the sea became warmer than the eastern part due primarily to local cooling of the eastern Bering Sea (Khen et al., 2009).

Many important fishery species, such as walleye pollock, cod, salmon, herring, flounder, crab, shrimp, halibut and others are common in the eastern and western parts of the sea. Total fish biomass is noticeably greater in the eastern part of the Bering Sea than that in its western part, due to inflow of warm Pacific waters through the eastern Aleutian passes and extended shelf area (Shuntov et al., 1993).

However, the annual catch in the REZ is 430,000–680,000 mt, not including salmon (Artyukhin et al., 2010). The salmon catch (mainly pink salmon), which has a biannual periodicity, in recent years was 17,000 mt during the even years of 2008 and 2010, with a record value of 147,000 mt in 2009, an odd year (Shevlyakov et al., 2008, 2009, 2010). The biological resources in the western part of the sea, as elsewhere, are subject to strong interannual changes related to environmental variation, anthropogenic pressure and intrapopulation variations. The periods of the dominance of certain fish and other species are marked (Naumenko, 2001); the time intervals of the rise, stabilization and decrease of total catches have been examined (Zolotov and Balykin, 2010) and the dynamics of commercial invertebrates have been shown (Sliskin and Safronov, 2000; Naumenko et al., 2003). The influence of habitat on fish populations in the western part of the sea is still poorly studied. Although attempts to relate the productivity of herring generations with the temperature of the cold intermediate layer (Davydov, 1972), to reveal a connection between the change of the dominant species in catches and thermal conditions (Naumenko, 1996) and to disclose the dependence of navaga (*Eleginus navaga*) populations in the spawning areas on temperature and salinity (Tolstyak, 1990) were undertaken. Besides the 6–7 years periodicity in atmosphere and hydrosphere the similar variations in total catches in the REZ were also noted (Luchin et al., 1998) though none of above-mentioned relations were confirmed.

In this report, the results of an analysis of thermohaline and hydrochemical parameters collected during the past two decades in the western part of the Bering Sea, from the surface to a depth of 1000 m, are presented, and the possible influence of these factors on the distribution, migration and biomass of the dominant hydrobionts is examined.

2. Materials and methods

In this report, the archive of oceanographic data of the Pacific Fisheries Research Center (TINRO-Center) is used. This dataset is continually growing due to observations conducted annually aboard research vessels of the TINRO-Center during ichthyological surveys for the study of the biological resources in the upper pelagic zone and at the shelf and continental slope in the west Bering Sea. Samples of such cruises are shown in Fig. 1. During the

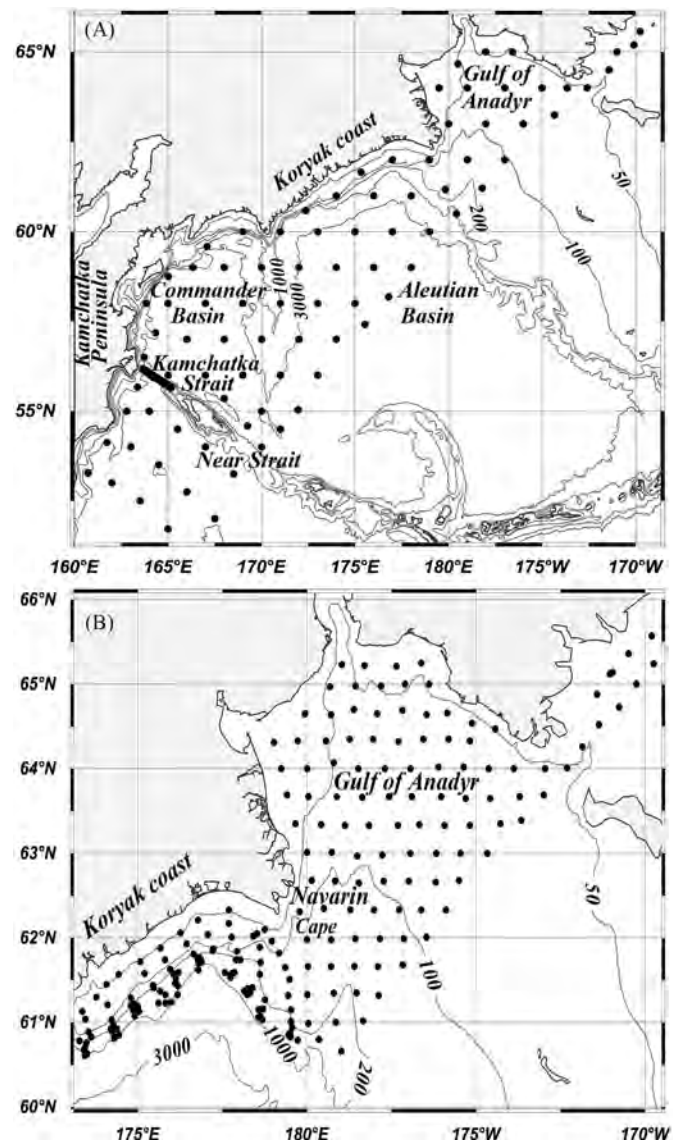


Fig. 1. Oceanographic stations in the TINRO-Center study area. (A)—survey for investigation of the epipelagic fish resources and (B)—investigation of the bottom fish resources.

past two decades, the cruises have become regular, permitting monitoring from the sea surface to a depth of 1000 m. Data from other Russian marine institutions were also used but form < 5% of the final dataset.

Anomalies of temperature and salinity for the warm half of the year were calculated relative to the norms taken from the World Ocean Atlas (Locarnini et al., 2010; Antonov et al., 2010, respectively). The comparability of our results with anomalies taken from the Climatic Atlas (Luchin et al., 2009) for the period from 1988–2004 was estimated by a superposition of the two arrays of anomalies.

Across Kamchatka Strait, where the main discharge of water from the Bering Sea occurs, a standard section consisting of 9 CTD stations was being sampled annually to estimate the interannual variability of the water exchange with the North Pacific. Up to the mid-1990s, this section was sampled irregularly, mainly to a depth of 500 m. In the last 15 years, the observations have been conducted to a depth of 1500 m. Relation between the geostrophic water transports relative to the 500 and 1500 db reference levels is sufficiently high (Khen and Zaachny, 2009), correlation coefficients by our calculations attains 0.91 ($r^2=0.82$).

To estimate the interannual variability of the SST in spring and summer, 10-day averaged data in $1 \times 1^\circ$ squares from the site of NEAR-GOOS (<http://goos.kishou.go.jp/rtrdb/usr>) were used. The variability of hydrochemical parameters is analyzed using the data from the TINRO expeditions from 1950 to 2009. The total number of stations with hydrochemical measurements after the raw material control is presented in Table 1. Additionally, data from the World Ocean Data Archive (Garcia et al., 2010a,b) were used. Because of data incompleteness, the interannual variability was considered using decadal averaging. Mean annual values for July–September of each year were calculated preliminary, then they were averaged for decades (for instance, 1950–59), with removing the values out of 2σ .

The data from “holey-sock” drogues at the depth of 40 m from the NOAA EcoFOCI site (http://www.ecofoci.noaa.gov/drifters/efoci_drifterData.shtml) were taken to draw the general scheme of the currents of the Bering Sea in summer and winter. A total of 510

trajectories with durations of sometimes more than two years were used. All drifters trajectories were examined carefully, and doubtful data were removed. Mean positions of drifters were calculated for 5-day intervals, then zonal and meridional components of current velocity (cm/s) and direction of the current vector (degrees from N) were determined for each 0.5×0.5 degree area from the difference between these positions. The calculations technique is described in detail by Stabeno and Reed (1994).

To reveal the possible links of salmon migration with circulation, the geostrophic currents relatively to the 1000 db reference level in the deep basin of the REZ were also calculated for the autumn surveys from 2002–10.

To analyze atmospheric processes, sea-level pressure maps obtained from the NOAA Climate Prediction Center (<http://www.cdc.noaa.gov/cgi-bin/>) were used.

3. Hydrography of the Bering Sea

3.1. Pattern of currents during warm and cold seasons

The overall pattern of the currents derived from the satellite-tracked drifters presented here (Fig. 2) confirms the general cyclonic circulation in the deep basin known from numerous previous works (Arsenev, 1970; Takenouti and Ohtani, 1974; Khen, 1989; Stabeno and Reed, 1994; Stabeno et al., 1999). Over the background of cyclonic rotation in winter, a wide current

Table 1

Number of stations with observations of main hydrochemical parameters in the south-western part of the Bering Sea (June–October).

Parameter	1950–59	1960–69	1970–79	1980–89	1990–99	2000–09	Total
Oxygen	173	635	1273	398	384	215	3078
Phosphate	54	36	72	66	168	205	601
Silicate	54	40	89	60	168	205	616

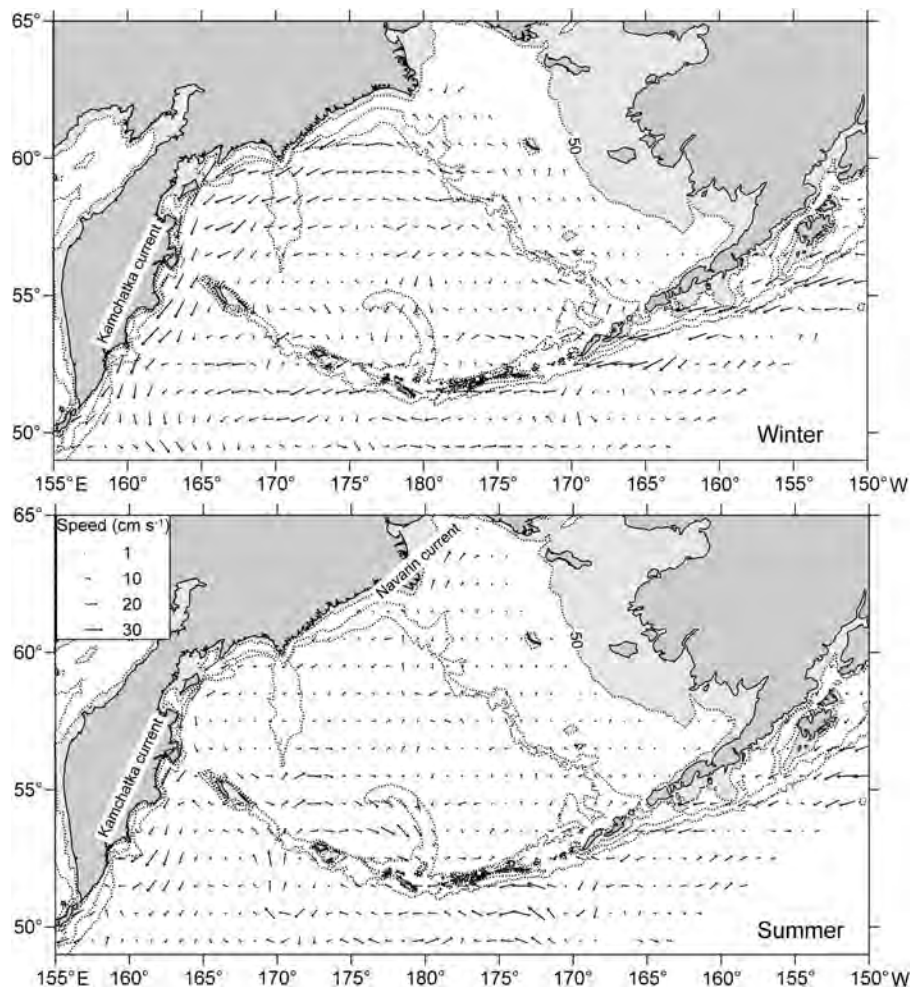


Fig. 2. Scheme of the Bering Sea currents in winter and in summer at a depth of 40 m based on the united data set of 510 “holey-sock” drifters for 1986–2007.

pattern at the north and west, caused by the action of strong northeasterly winds, is noticeable. In summer, the width of the currents is narrower and does not exceed the limits of the continental slope. The mean winter velocities in the sea in general are higher than the summer ones by more than 60%. Near the continental slope, the difference is greater; in winter the mean velocities attain $15\text{--}20\text{ cm s}^{-1}$ in the east and more than 30 cm s^{-1} in the west, whereas in summer, the mean velocities do not exceed 10 cm s^{-1} in the east. Along the west continental slope adjoining to the Kamchatka Peninsula, the velocities are up to 1.5–2 fold greater than those along the east slope during both winter and summer. The Kamchatka Current is well-expressed throughout the year, although it is noticeably weaker in summer. During that season, the geostrophic velocities (relative to 1500 db) are generally $5\text{--}10\text{ cm s}^{-1}$, although in the upper 200 m along the coast can reach as high as $15\text{--}20\text{ cm s}^{-1}$ (Khen and Zaichny, 2009). In summer, for most of the deep basin, the velocities are not high. Along the eastern slope, both cyclonic and anticyclonic eddies are being formed. The Navarin Current, transferring modified Pacific waters into Anadyr Bay, is noticeable only in summer, and in the cold season, it weakens or completely disappears because of strong northeasterly winds.

3.2. Temperature at the sea surface and in the cold intermediate layer

In May, the isotherms at the sea surface stretch from east to west according to the inflow of Pacific waters through the Aleutian Passes (Fig. 3). In the core of the cold intermediate layer, the longitudinal distribution is altered. Along the eastern slope, a tongue of warm water inflowing through the eastern straits is formed. This warm water separates two cold areas: an eastern region that occupies the shallow shelf and a western region covering most of the deep basin.

In summer at the sea surface, three warm areas are formed, in Commander Basin ($10\text{--}11.5\text{ }^{\circ}\text{C}$), around Bristol Bay ($9\text{--}10\text{ }^{\circ}\text{C}$) and,

in the north-east, Norton Sound ($9\text{--}11\text{ }^{\circ}\text{C}$). Both in the eastern and western parts of the sea, the SST increases shoreward, but near the Koryak coast, the SST decreases. Here, the divergence of the Slope Current results in upwelling of intermediate waters which leads to lowering of the SST by $1\text{--}2\text{ }^{\circ}\text{C}$ (Khen, 1989).

In summer in the cold intermediate layer, two cold areas formed from residual winter waters are distinguished. The first area adjacent to the St. Lawrence Island occupies the bottom layer; its temperature is well below $0\text{ }^{\circ}\text{C}$. Another area at the south-west over the Commander Basin, with a temperature of $1.0\text{--}1.5\text{ }^{\circ}\text{C}$, occupies depths of $130\text{--}150\text{ m}$. As in May, along the Slope Current, a tongue of warm waters separating the eastern and western cold areas is formed.

3.3. Interannual variability of SST in the southern part of the Bering Sea

In the specified squares (Fig. 3) of the southeastern and southwestern parts (Bristol Bay and Commander Basin, respectively), the SST both in spring and summer gradually rises from 1950 (Fig. 4). The rate of growth in both of the squares was practically matched. Over the background of general warming, three periods of cooling could be detected: the first one in the 1970s, the second at the turn of the century and the third since the middle of the last decade. The first cooling was stronger in Bristol Bay, and the second cooling period was approximately equal in both of the squares. The present-day cooling, when the temperature became below normal, affected Bristol Bay only. At the stationary biophysical mooring M2 in Bristol Bay (Hunt and Stabeno, 2002), the cooling in the $0\text{--}70\text{ m}$ layer began in 2006 (Coyle et al., 2011). In the southeast, the SST was not changed and stayed above normal.

The warming effect of the Pacific waters extending through the eastern Aleutian straits forms a positive difference of mean annual SST between Bristol Bay and Commander Basin. However, in the middle of the last decade, this difference abruptly changed sign, i.e., the south-western part of the sea became warmer than the

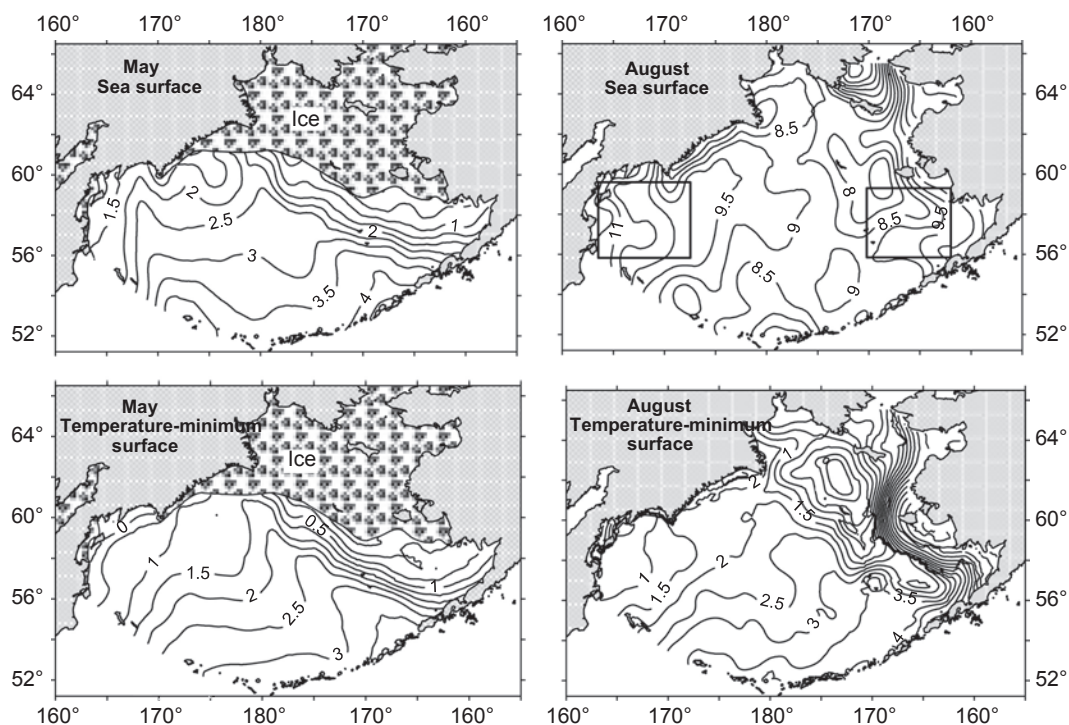


Fig. 3. Long-term (1950–2007, TINRO-Center data set) temperature at the sea surface and on temperature-minimum surface in spring (May) and summer (August). Squares in the southwestern and southeastern Bering Sea denote the areas, where the interannual variations of the SST anomalies are studied.

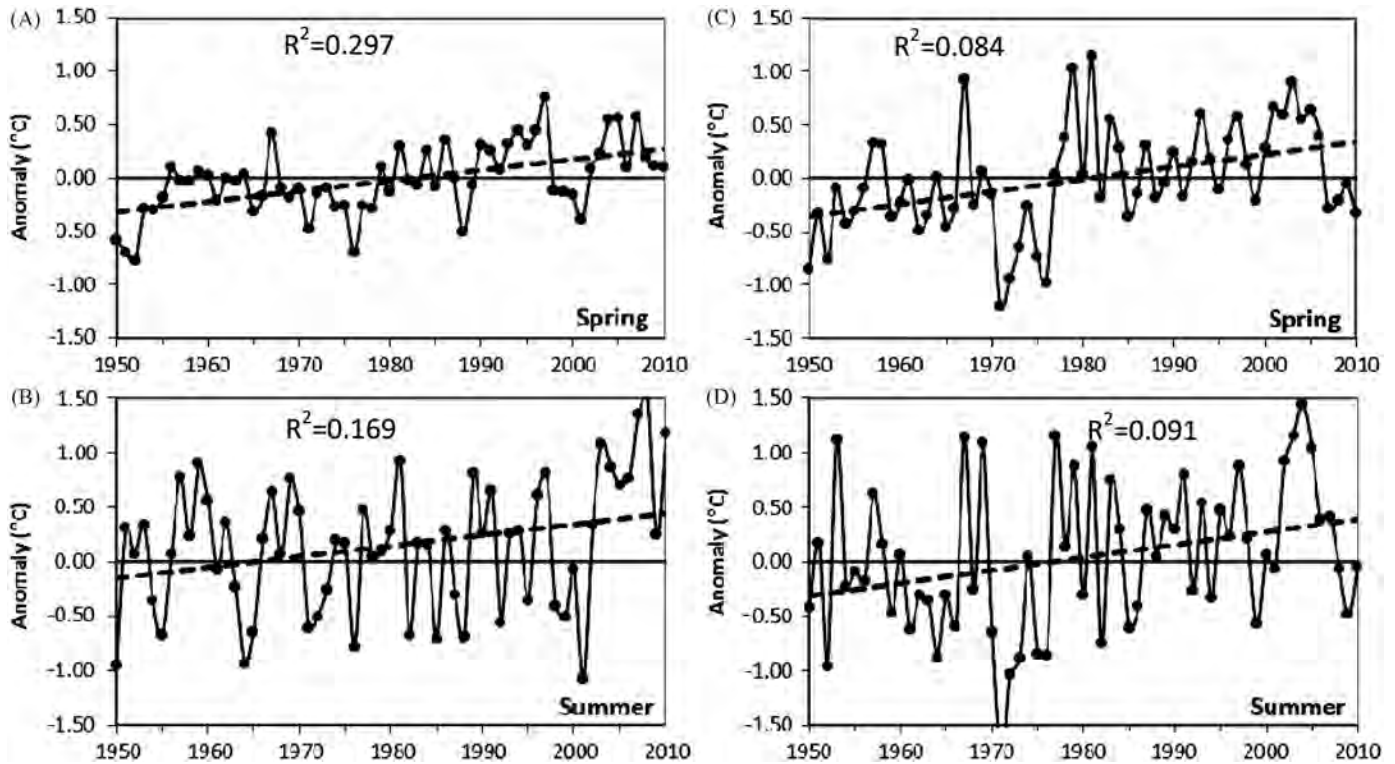


Fig. 4. Interannual variability of the SST anomalies in the southwestern (A, B) and in the southeastern (C, D) Bering Sea (see location at Fig. 3) in spring and summer.

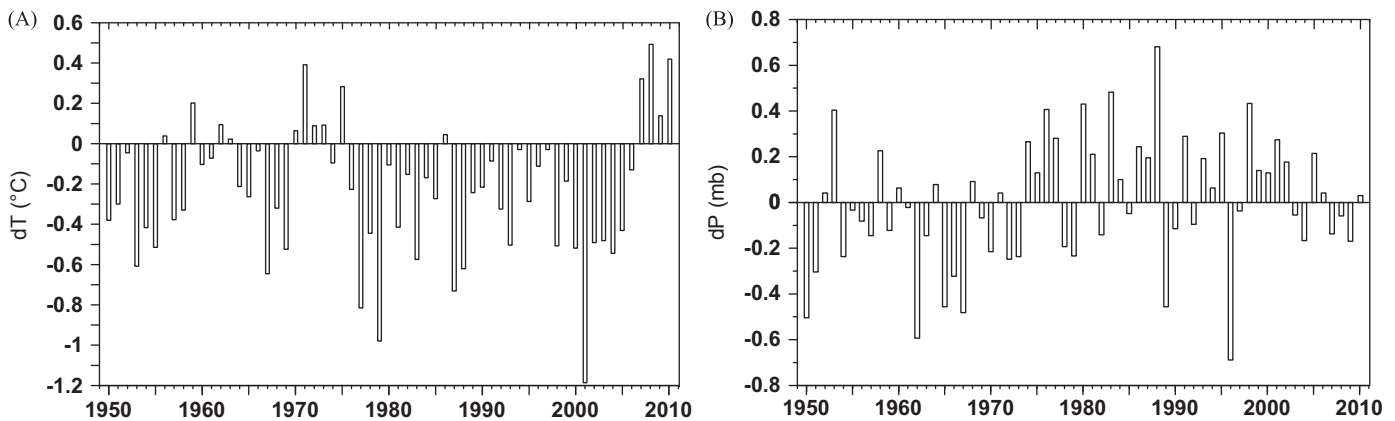


Fig. 5. Time series of difference of the annually averaged SST (A) and the sea level pressure (B) between the southwestern (Commander Basin) and southeastern (Bristol Bay) parts of the Bering Sea.

south-eastern part of the sea (Fig. 5A). Simultaneously, the difference of the sea level pressure between these areas also reversed. Obviously, these reversals are related to the westward shift of the Aleutian Low (Fig. 6) and to the changes of its intensity (Fig. 5B). Possible mechanism of Pacific water inflow variations depending on location of the Aleutian Low based on Sverdrup's dynamics will be shown below in Section 4.4.

Up to the mid-1970s, with a predominantly western location of the Aleutian Low, the SLP in the southwest was lower than that in the southeast. As a sequence, the recurrence of years with a positive difference of SST between the southwest and southeast during this period was higher. The present situation will possibly continue, and a reiteration of the synoptic and thermal conditions of the 1960–70s cannot be excluded.

4. Interannual variability in the western Bering Sea

4.1. Interannual variability of water temperature

Two time series show the water temperature changes in the western part of the sea from the surface to a depth of 800 m (Fig. 7). The first time series is taken from the Climate Atlas of the North Pacific Seas 2009 (Luchin et al., 2009); the second curve represents data of the TINRO-Center. Although the first curve is plotted using annual averages, the superposition of these curves for the period from 1988 to 2004 demonstrates their similarity, allowing the estimation of the real variability of temperature from 1950 to 2010. In general, at the sea surface, from 1950 to 2010 the temperature increases by 1.47 °C, whereas below the seasonal

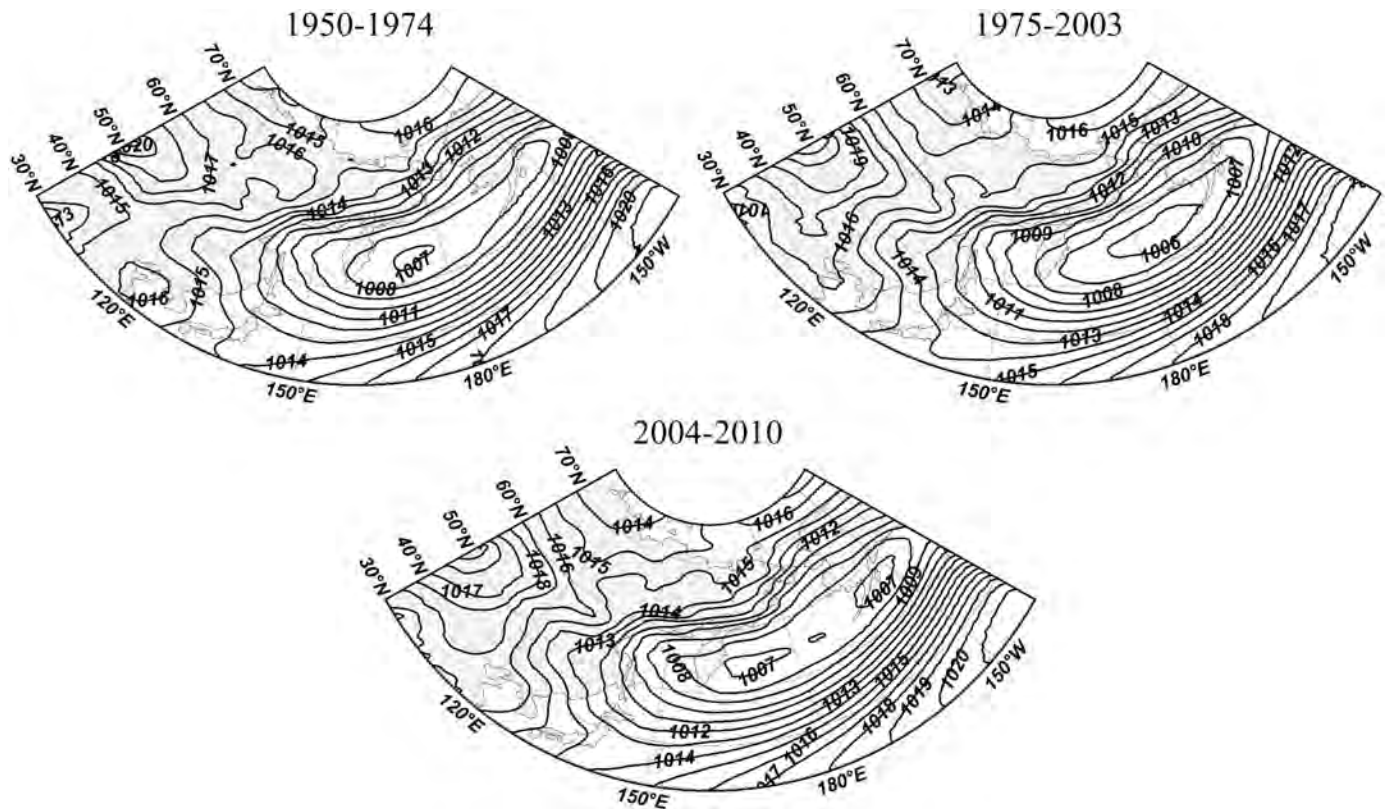


Fig. 6. Mean annual sea level pressure in the North Pacific for 1950–74, 1975–2003 and 2004–10 with the western, eastern and again western locations of the Aleutian Low.

thermocline, at the depths of 50, 100 and 200 m, the tendency is the opposite, i.e., in the layer containing the majority of the marine species, including many fishery species, at least from the middle of the 20th century, cooling occurs.

From 1950 to 2010, the temperature decreases by 0.7 °C, 0.07 °C and 0.14 °C at the depths of 50, 100 or 200 m, respectively. Over the background of the negative trend in the 50–200 m layer, the most noticeable temperature drops occur in the mid-1970s and at the turn of the century. The first case is more pronounced, when temperature was 1.5–2.0 °C below normal for three years in row from 1975 to 1977. The abrupt growth of temperature coincided with the famous climatic shift in the North Pacific, resulting in the accordance to climatic norms for the Bering Sea (Minobe, 1997; Hare and Mantua, 2000).

In the deeper part of the warm intermediate layer, at depths of 500 and 800 m, the interannual temperature variability has one peculiarity. Up to the mid-1960s, the temperature rises, after that time, the temperature stabilises for some years, and in the mid-1970s, like in the upper layers, it steeply drops. However, in contrast to the upper layers, the shift in the late 1970s does not occur, and the cold conditions remain until the beginning of the 1990s. During subsequent years, the temperature tends to increase, and in the second half of the last decade, the temperature reaches its maximum.

The cooling in recent years noted above in the eastern part of the sea (Fig. 3) is observed in deeper layers also, but the start of the cooling does not occur until 2006, 2008 and possibly 2010 for depths of 50–100 m, 200, 500 and 800 m, respectively. Apparently, the cause of the later cooling is related to regional changes in the atmosphere, in particular to the westward displacement (Fig. 6) and intensity (Fig. 5B) of the Aleutian Low. The abrupt temperature changes in the 1970s coincide with the Pacific decadal and Arctic oscillations (PDO and AO) (Stabeno and Overland, 2001; Hunt and Stabeno, 2002), and the changes at the turn of the century

coincide with the ENSO and Victoria patterns (Overland et al., 2008), i.e., the temperature changes are caused by global processes.

Longterm increase of SST and decrease of temperature in the subsurface layer resulted in a sharpening of the seasonal thermocline by more than 0.1 °C/m during the last 15 years, and the vertical temperature gradients in the thermocline reached 0.30–0.35 °C m⁻¹ in 2010 (Fig. 8). Along with that the thickness of the upper homogenous layer in summer (defined by depth where vertical gradient of temperature > 0.1 °C m⁻¹) has increased by almost 10 m. From the mid-1990s to the late 2000s, the thickness of that layer increased from 20–25 to 30 m. This is possibly important for salmon inhabiting the upper epipelagic zone.

4.2. Interannual variability of salinity

There is some difference in the salinity anomalies at the sea surface between the values calculated from the data of the Climatic Atlas (Luchin et al., 2009) and the TINRO-Center (Fig. 9). First, the anomalies are higher than those due to different methods of calculating these values (see Section 2). Below the surface layer, the time series are in general agreement, and the lack of coincidence is only observed in individual years. A common feature for all of the considered horizons is the salinity decrease during the last 60 years. For that period, the salinity decrease reaches up to 0.30, 0.06–0.10 and 0.04 at the sea surface, in the 100–200 m layer, and at the depth of 500 m, respectively. In the Bering Sea, the salinity dominates the control of the density (Miura et al., 2002.), and one can suppose that the greater salinity decrease at the sea surface than in the lower depths strengthens the vertical stability of the water column and results in a weakening of convection. The opposite trends of temperature at the sea surface and in the deep layers (growth and decrease, respectively) also strengthen the vertical stability.

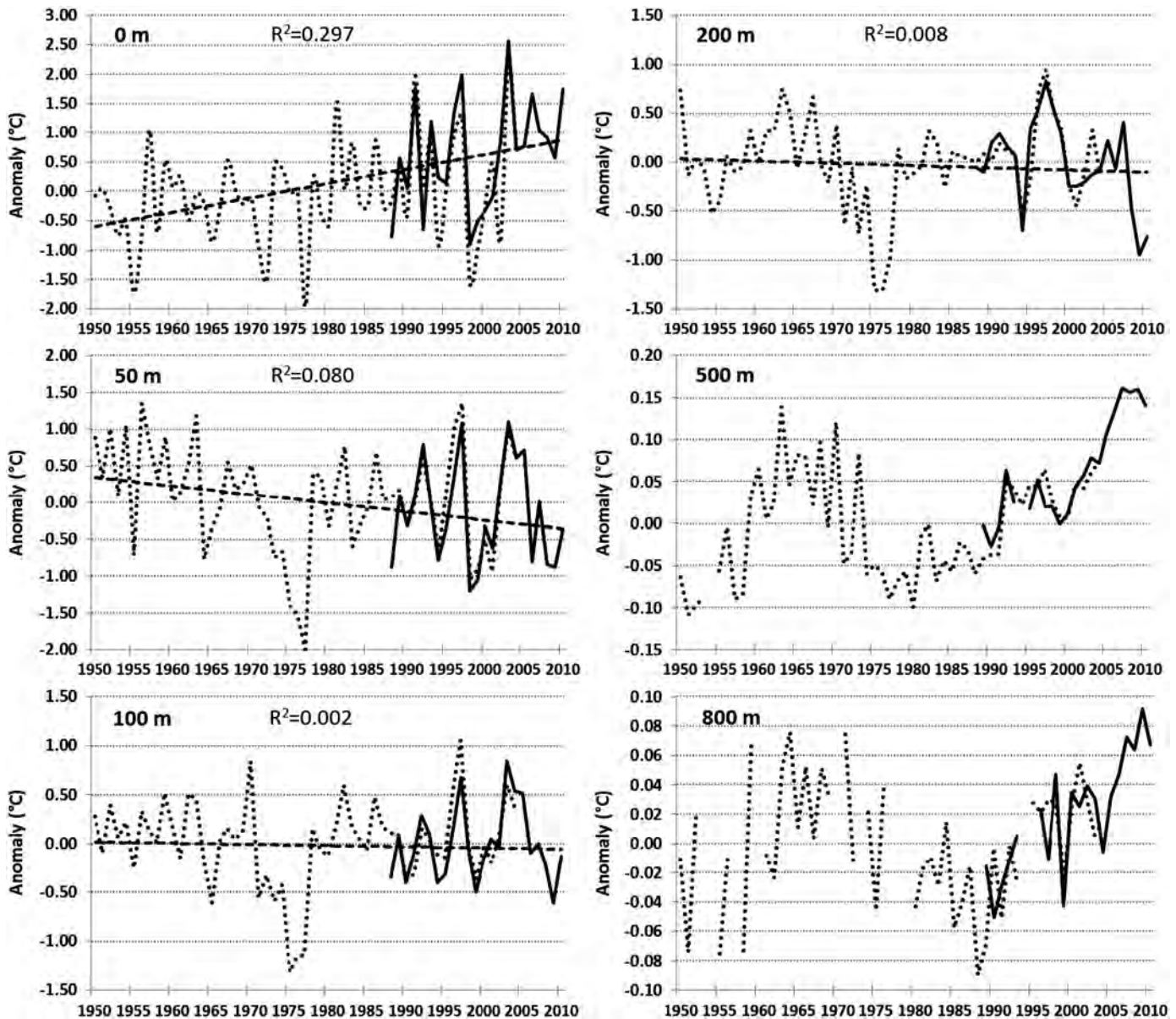


Fig. 7. Interannual variability of the temperature anomalies from the sea surface to a depth of 800 m. Dotted curves for the period of 1950–2004 (from Luchin et al., 2009), solid curves for 1986–2010 (based on the TINRO-Center data set).

4.3. Interannual variability of dissolved oxygen and nutrients

Dissolved oxygen (DO) and nutrients (Fig. 10) are important constituents of water-column productivity. During the second half of the 20th century, at the surface, the DO concentration has increased in spite of the temperature rise. During the most recent decade, when the temperature increase stopped, the DO concentration steeply decreased. The weak dependence of dissolved oxygen on temperature in the western Bering Sea in summer was also noted earlier by Sapozhnikov et al. (1995).

A weakening of the water exchange between upper and intermediate layers hampers the input of nutrients into the euphotic zone what results in decrease of new production there and reduces the convective transport of oxygenated (by photosynthesis) water to deeper horizons.

Apparently, such a situation was one of the causes of the oxygen decrease during the last 60 years in the intermediate layers (50–250 m). Using decadal data averaging, the changes at depths of 500 and 1000 m are difficult to detect. Nevertheless, the

oxygen decrease in the deep layers (800 and 1000 m) is evident from time series taken from the Climate Atlas (Luchin et al., 2009).

The main regularities of interannual variations observed for the DO are also typical for nutrients, phosphate and nitrate, but with an inverse tendency. In the surface layer, a rather stable decline of nutrient concentrations is noted, with the minimum in the 1990s. The high oxygen content and low concentration of nutrients in the upper layer during these years support a high biological productivity of the west Bering Sea.

Phosphate concentration beneath the upper layer from 1970s till now has increased by 1.2–1.4 times depending on depth. Silicate concentration during this period also increased by 1.1–1.3 times. Averaged values of phosphate and in particular silicate concentrations for 1950s and 1960s are doubtful, possibly a part of these data is erroneous (Ivanenkov, 1964). Now raw data for this period are mostly lost or not available for us, and we have limited number of observations (< 5 per year, Table 1), not enough for correct averaging.

Phosphate concentration is determined mainly by the phosphorus regeneration from organic remnants and is associated with

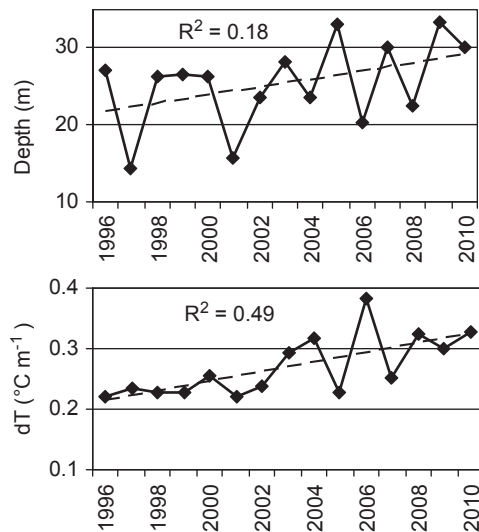


Fig. 8. Interannual variability of the thickness of the upper homogeneous layer (A) and the vertical temperature gradient in the seasonal thermocline (B).

zooplankton life cycle (Cushing, 1975). Increasing of phosphate concentration beneath upper layer during the last four decades is possibly related to growth of mean annual biomass of zooplankton since 1980s (Shuntov, 2009). Increasing of silicate concentration can be an evidence of diatom biomass growth.

4.4. Interannual variability of the Kamchatka Current

One of the important indices of variability in the Bering Sea is the recurring water discharge through the Kamchatka Strait. From 1950 to the mid-1960s, the water exchange in the 0–500 m layer was weak, and in the subsequent two decades, it has increased (Fig. 11). Since the early 1990s, the water discharge dropped again and reached a minimal level at the turn of the century (below $0.5 \times 10^6 \text{ m}^3 \text{ s}^{-1}$), an order of magnitude lower than in the mid-1960s and late 1980s.

During the last decade, the water exchange has gradually increased and in 2010 reached the mean long-term value of $2.2 \times 10^6 \text{ m}^3 \text{ s}^{-1}$. The extremely high water discharges from the mid-1960s to the early 1990s coincided with the western location or two-cored configuration of the Aleutian Low, and minimal water transport coincided with its eastern location (Fig. 12).

The transport of ocean currents in meridionally bounded oceans is determined by the wind stress *curl* rather than by the wind stress vector (Munk, 1950). So we calculated wind stress *curl* for the North Pacific onto a 2.5° latitude/longitude grid for two typical meteorological situations in winter (January–March) using the data of reanalysis (Kalnay et al., 1996). Sverdrup's (meridional) water transport through the latitude 56.25°N inside longitudes 164°E and 167.5°W was also computed. The calculated values are distinctly different for the years with western (1965) and eastern (2000) position of the Aleutian Low and are estimated as 25×10^6 and $18 \times 10^6 \text{ m}^3 \text{ s}^{-1}$, respectively.

In general for the Bering Sea (as in the most of the North Pacific subarctic area) in winter a positive wind *curl* prevails that causes the poleward Sverdrup transport. In examined cases the maximum of the wind *curl* was confined to the northern sector of the AL at latitude 56°N and was located at 171°E and 179°E for the western and eastern locations of the AL respectively. In order to agree with the wind stress *curl* conditions one can suppose the main flow from the North Pacific has to enter the Bering Sea through Near Strait in first and through the eastern Aleutian straits in latter case

with respective thermal consequences for the western or eastern parts of the sea.

In spring (March–May), the typical situations are similar but with lower gradients of atmospheric pressure and weaker winds, so the calculated Sverdrup's transport decreases by several times. These estimations are preliminary and need to be made more accurately in a future, but they support our suggestion about pattern of water exchange variation caused by the Aleutian Low shifts.

Taking into account the above-noted tendency of the westward displacement of the Aleutian Low, one can suppose that a further strengthening of the water exchange with the North Pacific is possible. During recent years the evident changes in tendencies of the sea-level pressure in the winter atmospheric centers of the North Pacific have taken place (Fig. 13). After a long period of the Aleutian Low deepening and Asian High weakening observed during the second half of the 20th century, during the last decade, the inverse process occurs, i.e., one can suppose the gradual return of the sea to the conditions of the 1960–1980s, when the enhanced water exchange was observed.

4.5. Interannual variability of the geostrophic currents in the western Bering Sea during the last decade

Detailed surveys in the western part of the Bering Sea conducted by researchers at the TINRO-Center during the last decade in the framework of the BASIS (The Bering-Aleutian Salmon International Survey) program (http://www.npafc.org/new/science_basis.html) revealed a year-to-year variability of the main streams there. At first, the common pattern includes the westward stream from the Aleutian Basin (Stabeno and Reed, 1994) and the northward stream from Near Strait (Khen, 1989). The convergence of these flows at the west continental slope forms the Kamchatka Current (Stabeno et al., 1999). From 2002 to 2006, the westward water transport prevailed ($4.6\text{--}5.8 \times 10^6 \text{ m}^3 \text{ s}^{-1}$ in the 0–1000 m layer, table 2). The meridional flow was weak (below $1.0 \times 10^6 \text{ m}^3 \text{ s}^{-1}$), and in 2006, it was quite unnoticeable. Since 2007, the northward inflow of the Pacific waters through Near Strait increased up to $1.6\text{--}2.0 \times 10^6 \text{ m}^3 \text{ s}^{-1}$, and the westward flow decreased by 1.5-fold.

The change of current intensity coincided in time with the beginning of the present cooling (Fig. 4) and with the change of the sign of the SST difference between the southeastern and southwestern parts of the sea (Fig. 5a). Possibly, the westward displacement of the Aleutian Low and its weakening leads to decrease of the Pacific water inflow through the eastern straits and to strengthening of the northward water transport from Near Strait. As a result, the cooling in the eastern part and maintenance of warm conditions in the west occurs.

5. Discussion

When comparing the interannual changes in the water environment with the main biological components of the west Bering Sea, one should bear in mind that the co-occurrences of these changes do not necessarily imply their close interdependence. Both the environment and animate nature can uniquely respond to a third factor, which can be of a planetary scale. Attempts to link the population dynamics with the climatic indices reflecting the planetary processes per se are numerous (e.g. Kawasaki et al., 1991; Klyashtorin and Lyubushin, 2005; Mantua et al., 1997). Sometimes the relations are successful and can be used for the long-term prediction of marine biological resources.

The most appropriate time scale for resource predictions is the decadal scale because the life span of many commercial fish

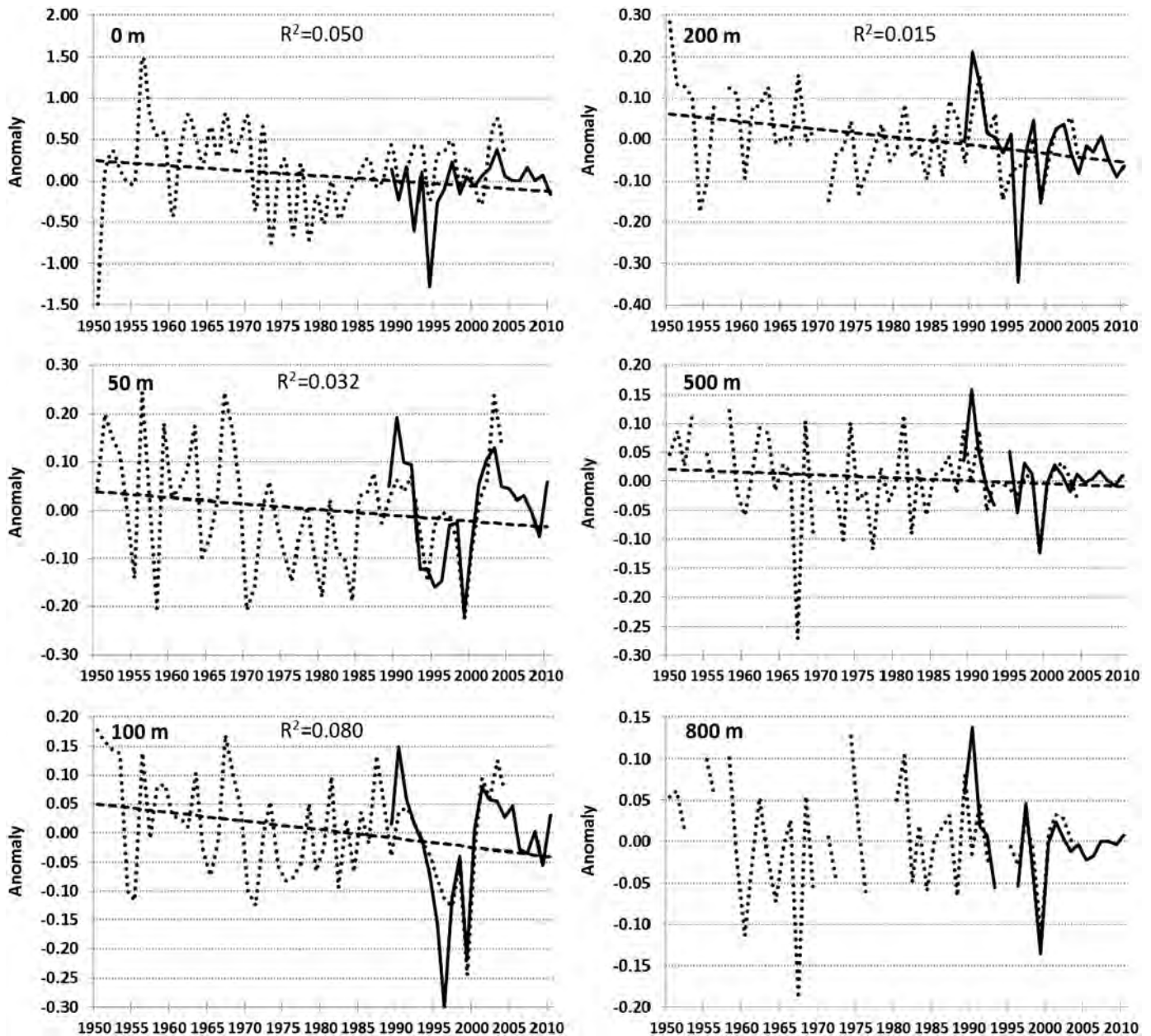


Fig. 9. Interannual variability of the salinity anomalies from the sea surface to a depth of 800 m in the deep area of the Russian EEZ. Dotted curves for the period of 1950–2004 (from Luchin et al., 2009), solid curves for 1986–2010 (based on TINRO-Center data set).

species is < 10 years, therefore long-term planetary processes are usually not highly important for these forecasts. One should take in account the regional processes in the environment compared to the habitat areas of the populations or communities of fishes. These regional processes are more significant for the formation of yield generations and do not always correspond to global changes. Further, we shall examine some cases of hydrobiont dynamics relating to regional processes (considered in Sections 3 and 4) affecting the water column of the western part of the Bering Sea.

5.1. Codfishes, flounders and sculpins at the sea shelf

During the second half of the last century, the SST in the western part of the Bering Sea increased (Fig. 4). In the middle of the first decade of the present century, the SST stabilized but had insignificantly decreased by the end of the decade.

The biomass of codfishes, flounders and sculpins at the sea shelf of the Karaginsky and Olyutorsky Bays during these years

(Zolotov and Balykin 2010, Fig. 14) varied synchronously with the SST changes, and even the decrease of biomass during the second half of the last decade coincided with the last cooling. However, one should not assume cause-and-effect relations between these factors. The pattern might just be one of the simple coincidences that are numerous in nature. Also, in the western part of the sea during the second half of the 20th century in the 50–200 m layer, where the specified fishes dwell, cooling has occurred that seems unfavorable for bottom inhabitants. The temperature of the surface layer is an important factor for the survival of the spawn and fry of some fish species, such as pollock and most flounders in particular, whose survival probability is determined by their breeding population. However, many species of sculpins, cods and northern two-lined flounder have bottom or bottom-pelagic spawning (Balykin et al., 2010), and in no way does the sea surface warming influence their juvenile survival.

Most likely, the SST rise and increase of biomass of the main ichthyofauna at the shelf of the western part of the sea during the

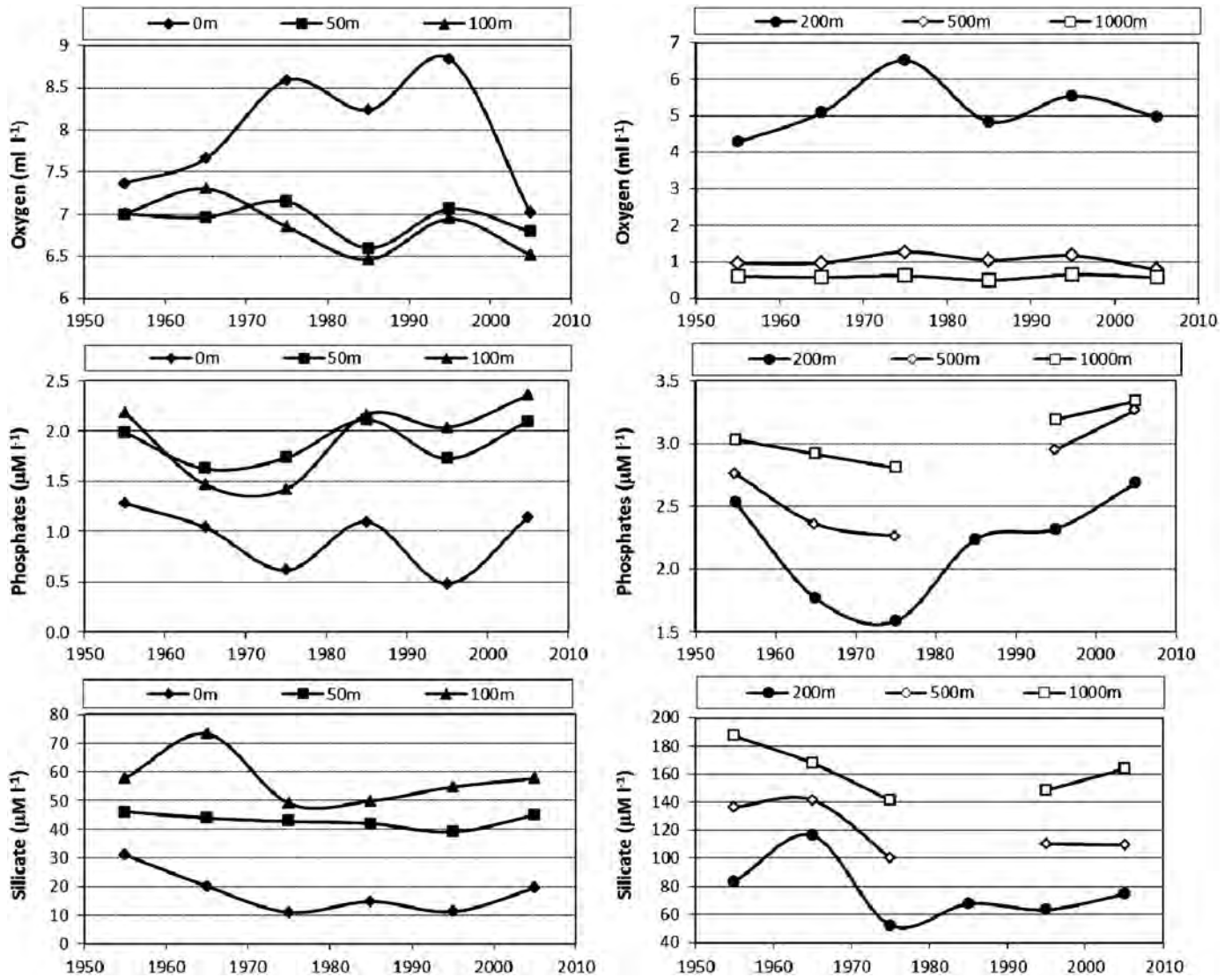


Fig. 10. Interdecadal variability of dissolved oxygen, phosphate and silicate at the sea surface, 50 and 100 m (left column), and at 200, 500 and 1000 m (right column).

second half of the 20th century are consequences of large-scale changes that occurred simultaneously in the water environment and throughout the trophic chain, from primary producers to nekton. The catches of pink salmon and sockeye near the east coast of Kamchatka during this period have also increased (Fig. 15), particularly in the late 1980s to the early 1990s. However, in this case, the salmon population growth corresponds to the total biomass increase throughout the North Pacific (Irvine and Fukuwaka, 2011), in the REZ in particular (Shuntov, 2009), and can be explained by the global warming of the climate (Klyashtorin and Lyubushin, 2005), which has primarily appeared since the 1980s.

5.2. Distribution and biomass of immature salmon

From 2002–06, the westward geostrophic currents prevailed, with the water outflow from Aleutian Basin into Commander Basin. From 2007–10, the northward stream from Near Strait into Commander Basin increased.

The spatial distributions of immature sockeye in early autumn (September to early October) during these years also differ. Until 2007, the main stock was concentrated in Commander Basin (Fig. 16), and a portion of the population left Bering Sea and came

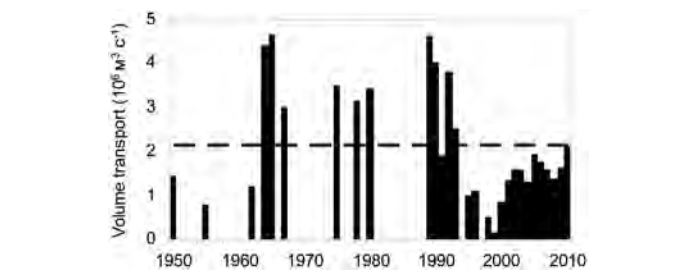


Fig. 11. Variability of the Kamchatka Current transport through the Kamchatka Strait in the 0–500 m layer in summer (10⁶ m³ s⁻¹).

into Pacific Ocean. With the weakening of the westward flow in 2007, the majority of the stock in early autumn remained in the Aleutian Basin. The lowered abundance of sockeye compared to preceding years might be a result of the strengthening of the northward flow from Near Strait. Since 2007, sockeye practically stopped coming into the ocean from the sea.

Decreases of the biomass of chum, sockeye and chinook (mainly their immature forms) in the REZ after 2006 (Table 3)

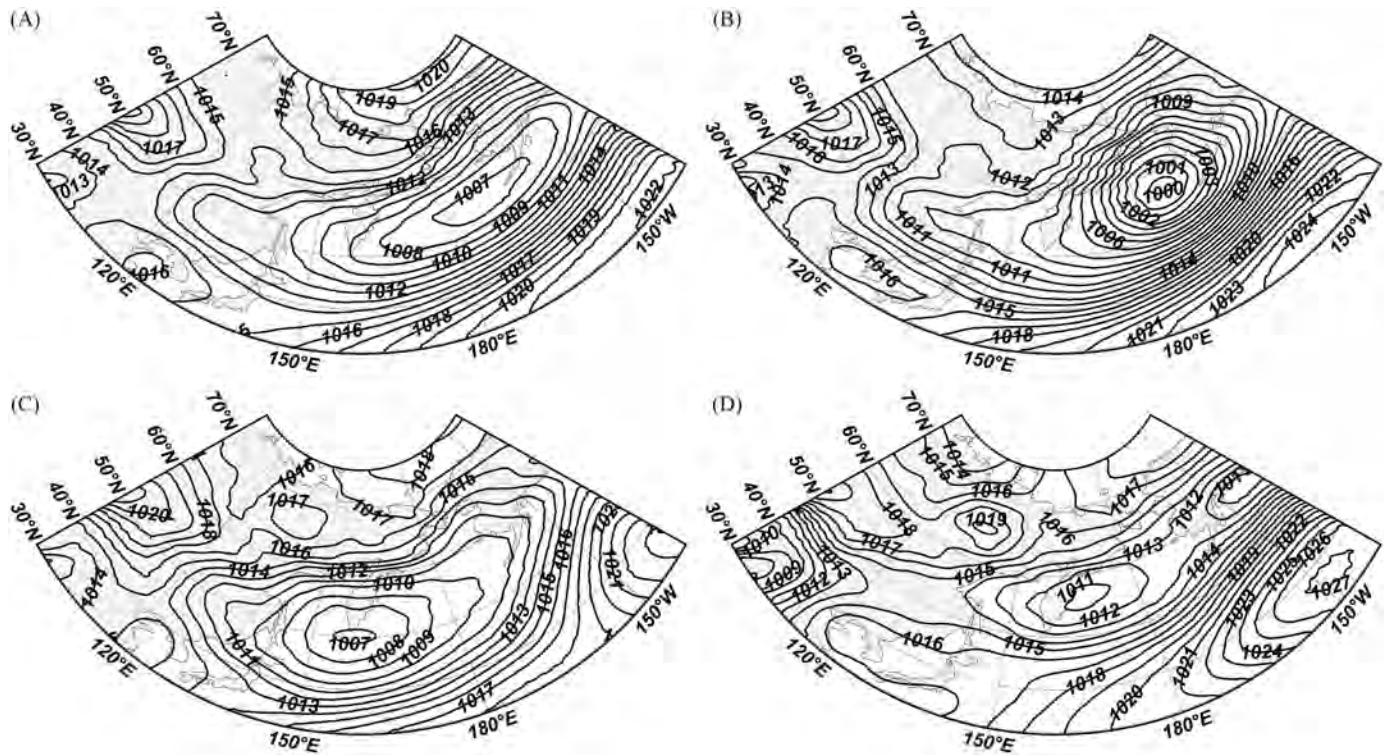


Fig. 12. Typical location and configuration of the Aleutian Low in March–May: averaged climatic (A), the eastern (B) and western (C) locations and a two-cored configuration (D).

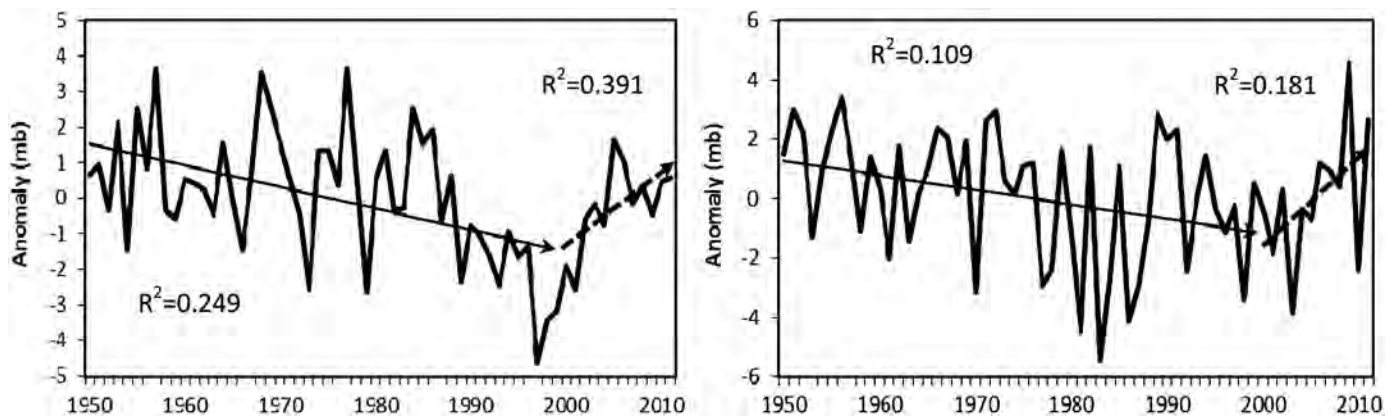


Fig. 13. Interannual variability of the sea level pressure anomalies in the centers of the Aleutian Low (A) and Siberian High (B) in winter. Solid line indicate the linear trends in 20th century. Dotted line indicate the linear trends in 21st century.

Table 2

Water transport ($10^6 \text{ m}^3 \text{ s}^{-1}$) from Aleutian Basin and Near Strait into Commander Basin in the 0–1000 m layer in September–October. In 2003, 2005 and 2009, the surveys were conducted in the summer (June–August), and those data were not considered.

From Aleutian Basin into Commander Basin	From Near Strait into Commander Basin
2002 5.8	0.4
2004 4.6	0.8
2006 5.0	0
2007 3.6	1.8
2008 3.2	1.6
2010 2.8	2.0

should also be noted. The main cause could be the decline of their biomass during recent years, but the US fishery statistics do not confirm this hypothesis (Table 4).

The chinook stock alone could be an exception because its catch since 2007 has decreased 1.5-fold in the US zone, but the biomass of this stock in the REZ has declined even more, over 3-fold. Evidently, the variations of currents can substantially influence the autumn migration of immature salmon from the US zone into the REZ.

5.3. Mesopelagic fishes and squid

Since 1950, the salinity of the water in the 0–1000 m layer gradually decreases. In the upper layer, the rate of lowering is one order of magnitude higher than that in the deep layers, so the vertical stability increases, and the exchange between surface and deep waters becomes weakened.

Along with the strengthening of vertical stability, the migration of mesopelagic fishes and squid from the intermediate layers to the surface has become more intense. Their biomass in the upper

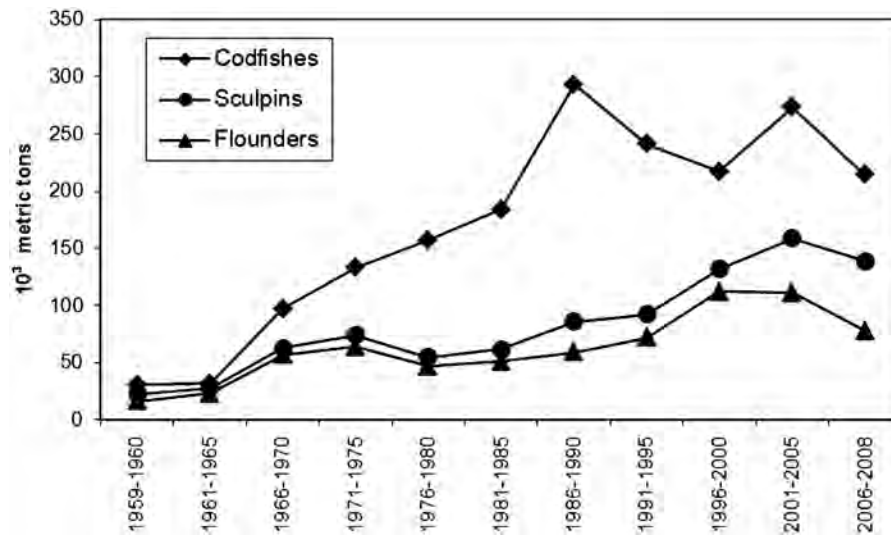


Fig. 14. Biomass (10^3 mt) of bottom fish groups (codfishes, sculpins and flounders) in the western part of the Bering Sea in 1959–2008 (Zolotov and Balykin 2010).

epipelagic zone (0–50 m) during last 20 years has noticeably increased (Table 5). The biomass of squid has increased by 3-fold, and the biomass of mesopelagic fishes has increased almost by an order and, in 2007, even by two orders due to a drastic increase of northern smoothtongue (*Leuroglossus schmidti*) and northern lampfish (*Stenobranchius leucopsarus*) fractions in catches (Glebov et al., 2007). Possibly the increase of stability along with the cooling in the active layer resulted in insufficient feeding conditions, and therefore the inhabitants of the active layer migrate to the surface waters. In contrast, the macroplankton that is the main prey component has noticeably increased in the upper layer from 519 mg m^{-3} in the 1980–90s to 928 mg m^{-3} in 1996–2006 (Shuntov, 2009), what could stimulate an active migration of mesopelagic fishes and squid into the surface layer.

5.4. Walleye pollock and herring

The water exchange with the North Pacific until the mid-1960s was weak, then during following 25 years, the water exchange remained high. In the early 1990s, the water discharge through the Kamchatka Strait dropped, and to date, the water exchange remains at a low level.

The interannual dynamics of pollock and herring stocks in the western part of the sea correspond to water exchange with the North Pacific. The relatively high biomass ($1.6\text{--}2.2 \times 10^6$ mt) of pollock was formed in the 1970–1980s (Fig. 17). In the early 1990s, along with the decrease of the water exchange, the population of pollock dropped to 0.6×10^6 mt and dropped to 0.1×10^6 mt during the period of the lowest water exchange at the turn of the century; to date, it remains at that low level. The population's moderate increase after 2005 coincided with the last strengthening of the Kamchatka Current up to the long-term values, and in later decades, the stock reached 0.4×10^6 mt. During the intense water exchange, herring was at a low abundance level, and its stock attained $0.09\text{--}0.2 \times 10^6$ mt, whereas with the Kamchatka Current weakening in the 1950s and at the turn of the century, the herring population increased up to $0.9\text{--}1.4 \times 10^6$ mt.

Traced during the recent years, the change of trends in the Aleutian Low, Asian High and Far East Depression, the westward displacement of the Aleutian Low and a possible return of the hydrography regime to the conditions of the 1970–80s can strengthen the Kamchatka Current as well as change the fish population and restore fishery activity.

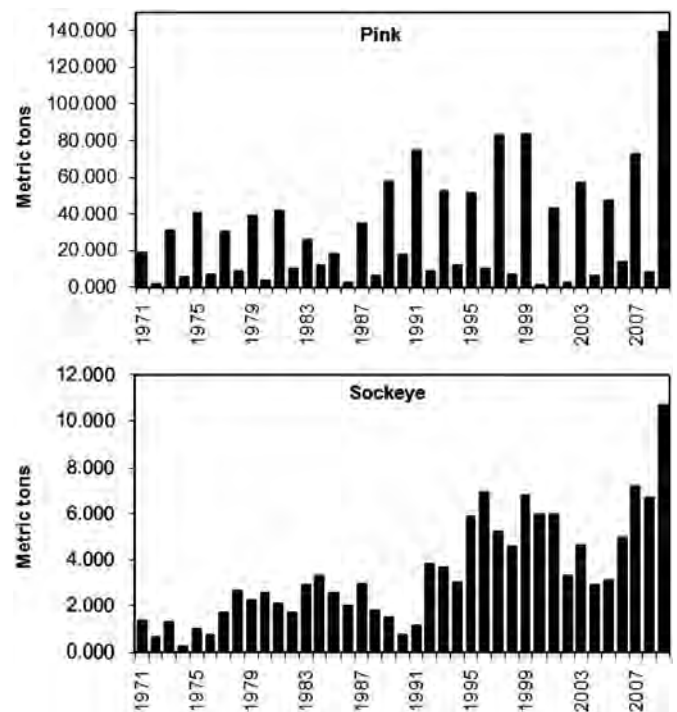


Fig. 15. Catches (mt) of pink and sockeye salmon off the eastern Kamchatka from 1971 to 2009.

6. Conclusion

Since middle of 20th century, noticeable changes in the Bering Sea oceanography occurred, related to both global processes and regional climate. Thus, the trend of SST increasing corresponds to planetary warming. On the other hand, the cooling started in 2006 in the east Bering Sea is a local event related to western shift of the Aleutian Low. In the western Bering Sea, the SST has not significantly changed in this period, but since 2007 the northward flow from Near Strait has strengthened and westward flow at the northern part of the deep basin has weakened. Noticeable regional changes of water exchange between the North Pacific and Bering Sea also occurred. Before the middle of 1960s the water exchange was weak, the transport of Kamchatka Current (relatively to 500 db) was below $2.2 \times 10^6 \text{ m}^3 \text{ s}^{-1}$, then the current strengthened

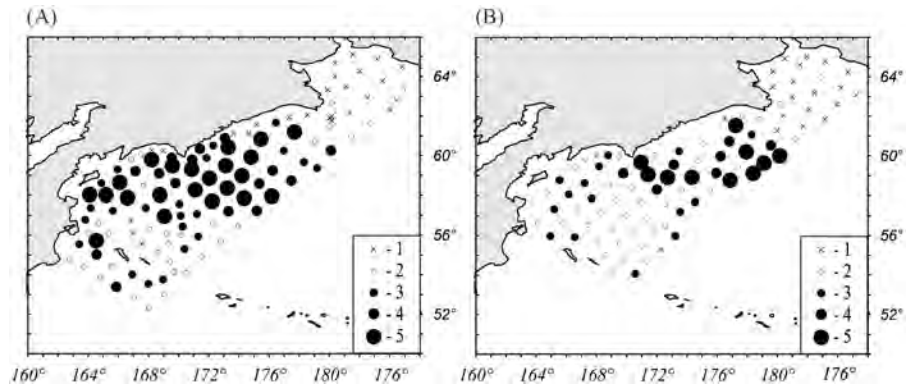


Fig. 16. Catches of immature sockeye salmon in the western Bering Sea during 24.08.2006–12.10.2006 (A) and 09.09.2008–13.10.2008 (B). (1) none; (2) < 100; (3) 100–250; (4) 250–500; (5) > 500 pieces per km².

Table 3

Annual biomass (in thousands of tons) of chum, sockeye and chinook salmon in the upper epipelagic layer (0–50 m) in the western Bering Sea during September and October (according to data from Shuntov and Temnykh, 2009).

	Chum	Sockeye	Chinook
2002–06	283.0	132.7	17.9
2007–09	178.8	62.8	5.5

Table 4

Mean US catches (in thousands of tons) of chum, sockeye and chinook in Alaskan waters.

	Chum	Sockeye	Chinook
2002–06	61.2	98.5	4.7
2007–09	61.8	115.5	2.9

Table 5

Biomass (in thousands of tons) of mesopelagic fishes and squid in the upper pelagic layer (0–50 m) in the Commander Basin in summer (Glebov et al., 2004, 2007, with additional data from I. Glebov).

	1991	1992	1993	1995	2003	2005	2007	2009
Mesopelagic fishes	4.6	1.5	13.2	9.0	15.8	14.8	150.9	40.9
Squid	70.0	5.1	95.0	48.1	99.3	203.7	243.3	231.2

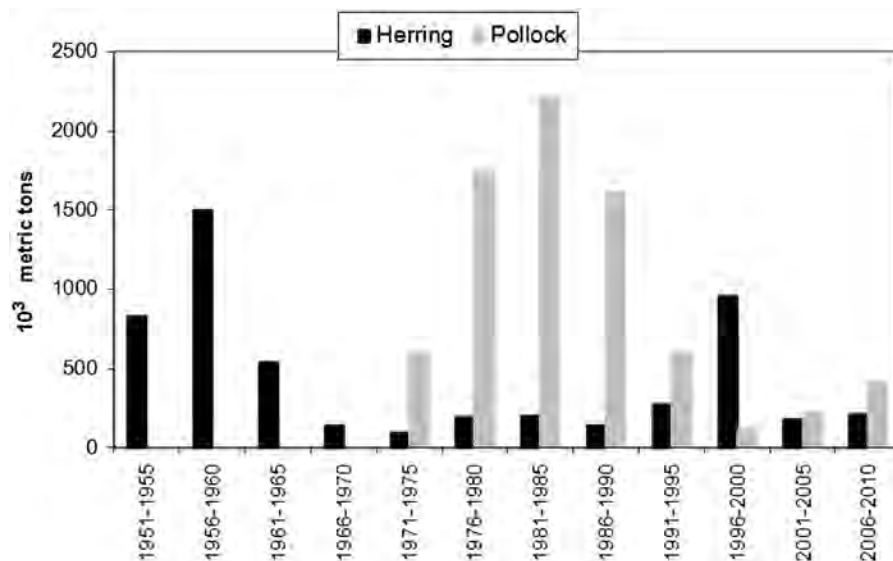


Fig. 17. Biomass of walleye pollock and Pacific herring in the western Bering Sea (Zolotov and Balykin, 2010).

and to the early 1990s its water transport exceeded $3.0 \times 10^6 \text{ m}^3 \text{ s}^{-1}$. However, it decreased again below $2.2 \times 10^6 \text{ m}^3 \text{ s}^{-1}$ in the last two decades.

Fish stocks of the west Bering Sea respond in various ways to variations of hydrography conditions. Total biomass of shelf fishes and total catches of salmon near the eastern coast of Kamchatka increased with the warming of the surface waters on second half of 20th century. The mechanism of this relationship is still unclear. Possibly, it is just coincidence of the variations in hydrosphere and biota. Variations of biomass of pollock and herring in the Bering Sea correspond to the water exchange with the North Pacific: biomass of pollock/herring grows/decreases with water exchange increasing and vice versa. Along with changes of intensity of westward and northward flows, immature sockeye and chinook stocks rearrange within the Russian EEZ occurs.

Acknowledgments

We thank professor V.P. Shuntov, Drs. O.S. Temnych, A.N. Zavolokin and I.I. Glebov, who provided their material on the dynamics and distribution of some of the fish species. We also acknowledge the officers, crews and scientific staff of the RV “TINRO” and “Professor Kaganovskiy” for assistance with the CTD casts and sample collection. This report is carried out as a part of the studies of the fishery resources of the Far-Eastern Seas annually confirmed by the Russian Federal Fisheries Agency.

References

- Antonov, J.I., Seidov, D., Boyer, T.P., Locarnini, R.A., Mishonov, A.V., Garcia, H.E., Baranova, O.K., Zweng, M.M., Johnson, D.R., 2010. World Ocean Atlas 2009. In: Levitus, S. (Ed.), NOAA Atlas NESDIS 69, vol. 2: Salinity. US Government Printing Office, Washington, D.C. 184 pp.
- Arsenev, V.S., 1970. Currents and Water Masses of the Bering Sea. Nauka, Moscow 135p. (in Russian).
- Artyukhin, Y.B., Balykin, P.A., Bonk, A.A., Karpenko, V.I., 2010. Fisheries and its environmental consequences. In: Makarevich, P.R. (Ed.), Current State of the Ecosystem of the western Bering Sea, Rostov-on-Don, Southern Scientific Centre, pp. 301–337 (in Russian).
- Balykin, P.A., Bonk, A.A., Zolotov, A.O., Tokranov, A.M., 2010. Marine fish. In: Makarevich, P.R. (Ed.), Current State of the Ecosystem of the Western Bering Sea, Rostov-on-Don, Southern Scientific Centre, pp. 160–240 (in Russian).
- Coachman, L.R., Aagard, K., Tripp, R.B., 1975. Bering Strait, The Regional Physical Oceanography. University of Washington Press, Washington 172p.
- Coyle, K.O., Eisner, L.B., Mueter, F.J., Pinchuk, A.I., Janout, M.A., Cieciel, K.D., Farley, E.V., Adreus, A.G., 2011. Climate change in the southeastern Bering Sea: impact on Pollock stocks and implications for the oscillating control hypothesis. *Fish. Oceanogr.* 20 (2), 139–156.
- Cushing, D.H., 1975. Marine Ecology and Fisheries. Cambridge University Press, 278 pp.
- Davydov, I.V., 1972. About oceanography basics of yield of single herring generations forming in the western part of the Bering Sea. *Izvestia TINRO* 82, 181–307. (in Russian).
- Garcia, H.E., Locarnini, R.A., Boyer, T.P., Antonov, J.I., Baranova, O.K., Zweng, M.M., Johnson, D.R., 2010a. World Ocean Atlas 2009. In: Levitus, S. (Ed.), NOAA Atlas NESDIS 70, vol. 3: Dissolved Oxygen, Apparent Oxygen Utilization, and Oxygen Saturation. US Government Printing Office, Washington, DC 344p.
- Garcia, H.E., Locarnini, R.A., Boyer, T.P., Antonov, J.I., Zweng, M.M., Baranova, O.K., Johnson, D.R., 2010b. World Ocean Atlas 2009. In: Levitus, S. (Ed.), NOAA Atlas NESDIS 71, vol. 4: Nutrients (phosphate, nitrate, silicate). US Government Printing Office, Washington, DC 398p.
- Glebov, I.I., Loboda, S.V., Vanin, N.S., 2007. Salmon in structure of nekton community of upper epipelagial of the western part of the Bering Sea in June–July 2007. In: Shuntov, V.P. (Ed.), Realization of “The concept of Far-Eastern Regional Program of the Pacific Salmon Studying”, Bull. 2. TINRO, Vladivostok, pp. 236–251. (in Russian).
- Glebov, I.I., Sviridov, V.V., Ocheretyanyi, M.A., Efimkin, A.Ya, Slabinskiy, A.M., Basyuk, E.O., 2004. Characteristic of nekton and plankton communities in upper epipelagial of the western part of the Bering Sea. *Izvestia TINRO* 139, 43–60. (in Russian, English Summary).
- Hare, S.R., Mantua, N.J., 2000. Empirical evidence for North Pacific regime shifts in 1977 and 1989. *Progr. Oceanogr.* 47 (2–4), 103–145.
- Hunt, L.G., Stabeno, P.J., 2002. Climate change and the control of energy flow in the southeastern Bering Sea. *Progr. Oceanogr.* 55 (1–2), 5–22.
- Irvine, J.R., Fukuwaka, M., 2011. Pacific salmon abundance trends and climate change. *ICES J. Mar. Sci.* 68 (6), 1122–1130, <http://dx.doi.org/10.1093/icesjms/fsq199>.
- Ivanenkov, V.N., 1964. Hydrochemistry of the Bering Sea. Nauka, Moscow 139p. (in Russian).
- Kalnay, et al., 1996. The NCEP/NCAR 40-year reanalysis project. *Bull. Amer. Meteor. Soc.* 77, 437–470.
- Kawasaki, T., Tanaka, S., Toba, Y., Taniguchi, A. (Eds.), 1991. Pergamon Press, Oxford 402p.
- Khen, G.V., 1989. Oceanographic conditions and Bering Sea biological productivity. In: Proceedings of the International Symposium on the Biology and Management of Walleye Pollock, University of Alaska Sea Grant, AK-SG-89-01, Fairbanks, pp. 31–52.
- Khen, G.V., Basyuk, E.O., Zuenko, Y.I., Ustinova, E.I., Figurkin, A.L., Shatilina, T.A., 2009. Peculiarities of hydrometeorological conditions in the Far-Eastern Seas in 2008–2009. *Quest. Fish. Oceanol.* 6 (N 2), 22–46. (in Russian).
- Khen, G.V., Zaochny, N.A., 2009. Variability of the Kamchatka Current transport and water properties in the Kamchatka Strait. *Izvestia TINRO* 158, 247–260. (in Russian, English Summary).
- Khen, G.V., Sorokin, Y.D., 2008. Seasonal features of the SST interannual changes in the North Pacific and its single areas. *Quest. Fish. Oceanol.* 5 (1), 164–183. (in Russian).
- Klyashtorin, L.B., Lyubushin, A.A., 2005. Cyclic Climate Changes and Fish Productivity. VNIRO Publishing, Moscow 235p. (in Russian, English Summary).
- Locarnini, R.A., Mishonov, A.V., Antonov, J.I., Boyer, T.P., Garcia, H.E., Baranova, O.K., Zweng, M.M., Johnson, D.R., 2010. World Ocean Atlas 2009. In: Levitus, S. (Ed.), NOAA Atlas NESDIS 68, vol. 1: Temperature. US Government Printing Office, Washington, DC 184 pp.
- Luchin, V.A., Kruts, A., Sokolov, O., Rostov, V., Rudykh, N., Perunova, T., Zolotukhin, E., Pishalnik, V., Romeiko, L., Hramushin, V., Shustin, V., Udens, Y., Baranova, O., Smolyar, I., Yarosh, E., 2009. Climatic Atlas of the North Pacific Seas 2009: Bering Sea, Sea of Okhotsk and Sea of Japan. In: Akulichev, V., Volkov, Yu., Sapozhnikov, V., Levitus, S. (Eds.), NOAA Atlas NESDIS, vol. 67. US Government Printing Office, Washington, DC, pp. 380. (CD Disc).
- Luchin, V.A., Semiletov, I.P., Weller, G.E., 2002. Changes in the Bering Sea region: the atmosphere–land–sea system in the second half of the twentieth century. *Progr. Oceanogr.* 55 (1–2), 23–44.
- Luchin, V.A., Saveliev, A.V., Radchenko, V.I., 1998. Long-range climatic waves in ecosystem of the western Bering Sea. Proceedings of the Arctic Regional Center, vol. 1, pp. 29–40. (in Russian).
- Munk, W.H., 1950. On the wind-driven ocean circulation. *J. Meteorol.* 7 (2), 79–93.
- Mantua, N.J., Hare, S.R., Zhang, Y., Wallace, J.M., Francis, R.C., 1997. A Pacific interdecadal climate oscillation with impacts on salmon production. *Bull. Am. Meteorol. Soc.* 78, 1069–1079.
- Minobe, S., 1997. Climate variability with periodicity of 50–70 years over the North Pacific and North America. In: Proceedings of CREAMS’97 (Circulation Research of the East Asian Marginal Seas), Fukuoka, 28–30 January 1997, pp. 149–152.
- Miura, T., Suga, T., Hanawa, K., 2002. Winter mixed layer and formation of dichothermal water in the Bering Sea. *J. Oceanogr.* 58, 815–823.
- Naumenko, N.I., 1996. Long-term fluctuations in the Ichthyofauna of the Western Bering Sea. In: Ecology of the Bering Sea: A Review of Russian Literature. Mathisen, O.A., Coyle, K.O., (Eds.), Alaska Sea Grant College Program Report No. 96-01, University of Alaska Fairbanks, pp. 143–158.
- Naumenko, N.I., 2001. Marine Herring Biology and Harvest in the Far East. Kamchatka Printing House, Petropavlovsk-Kamchatsky 330p. (in Russian).
- Naumenko, N.I., Lysenko, V.N., Fedotov, P.A., Kharlamov, V.I., Schaginyan, E.R., Bazin, A.G., 2003. Commercial invertebrates. In: Sinyakov, S.A. (Ed.), The State of Biological Resources of the North-West Pacific. North Pacific Publishers, Petropavlovsk-Kamchatsky, pp. 93–116. (in Russian).
- Overland, J., Rodionov, S., Minobe, S., Bond, N., 2008. North Pacific regime shifts: definition, issues and recent transitions. *Progr. Oceanogr.* 77, 92–102.
- Sapozhnikov, V.V., Arzhanova, N.V., Gruzhevich, A.K., Zubarevich, V.L., Karpushin, M.A., Mordasova, Y.V., Tolmachev, D.O., 1995. Hydrochemistry of the West Bering Sea, Complex Studies of the Bering Sea Ecosystem. VNIRO, Moscow, pp. 96–134. (in Russian).
- Shevlyakov, E.A., Dubynin, V.A., Erokhin, V.K., 2008. Characteristics of the coastal salmon fisheries in the Kamchatka region in 2008. In: Shuntov, V.P. (Ed.), Realization of “The concept of Far-Eastern Regional Program of the Pacific Salmon Studying”, Bull. 3. TINRO, Vladivostok, pp. 12–23.
- Shevlyakov, E.A., Erokhin, V.K., Dubynin, V.A., 2009. Characteristics of the coastal salmon fisheries in the Kamchatka region in 2009. In: Shuntov, V.P. (Ed.), Realization of “The concept of Far-Eastern Regional Program of the Pacific Salmon Studying”, Bull. 4. TINRO, Vladivostok, pp. 12–27. (in Russian).
- Shevlyakov, E.A., Dubynin, V.A., Erokhin, V.K., Pogodaev, E.G., 2010. Characteristics of the coastal salmon fisheries in the Kamchatka region in 2010. In: Shuntov, V.P. (Ed.), Realization of “The concept of Far-Eastern Regional Program of the Pacific Salmon Studying”, Bull. 5. TINRO, Vladivostok, pp. 12–29. (in Russian).
- Shuntov, V.P., 2009. State of biota and biological resources of marine macrosystems of the Far-Eastern Russian economic zone. In: Shuntov, V.P. (Ed.), Realization of “The concept of Far-Eastern Regional Program of the Pacific Salmon Studying”, Bull. 4. TINRO, Vladivostok, pp. 242–251. (in Russian).
- Shuntov, V.P., Volkov, A.F., Temnykh, O.C., Dulepova, E.P., 1993. In: Chigirinskiy, A.I. (Ed.), Pollock in the ecosystems of the Far-Eastern Seas. TINRO, Vladivostok, pp. 426. (in Russian).
- Shuntov, V.P., Temnykh, O.S., 2009. Record high salmon fishing season—2009. In: Shuntov, V.P. (Ed.), Realization of “The concept of Far-Eastern Regional Program of the Pacific Salmon Studying”, Bull. 4. TINRO, Vladivostok, pp. 3–11.
- Sliskin, A.G., Safronov, S.G., 2000. Commercial Crab Species of Kamchatka. North Pacific Publishers, Petropavlovsk-Kamchatsky 180 pp. (in Russian).

- Stabeno, P.J., Schumacher, J.D., Ohtani, K., 1999. The physical oceanography of the Bering Sea. In: Loughlin, T.R., Ohtani, K. (Eds.), *Dynamics of the Bering Sea*. University of Alaska Sea Grant College Program, Fairbanks, pp. 1–28.
- Stabeno, P.J., Overland, J.E., 2001. The Bering Sea shifts toward an earlier spring transition. *Eos Trans. Am. Geophys. Union* 82, 317–321.
- Stabeno, P.J., Reed, R.K., 1994. Circulation in the Bering Sea basin by satellite tracked drifters. *J. Phys. Oceanogr.* 24, 848–854.
- Starichenko, L.A., Botianov, V.A., 1999. Meteorology and climate. *Hydrometeorology and Hydrochemistry of the Seas: Bering Sea, N 1 Hydrometeorological Conditions*, vol. X. Hydrometeoizdat, Saint-Petersburg 20–63. (in Russian).
- Takenouti, A.Y., Ohtani, K., 1974. Currents and water masses in the Bering Sea: a review of Japanese works. In: *Oceanography of the Bering Sea: with emphasis on renewable resources*. Institute of Marine Science University of Alaska, Fairbanks, pp. 39–57.
- Tolstyak, A.F., 1990. Effects of some environmental factors on the stock abundance of Kamchatka saffron cod, *Biological Resources of the Shelf and Marginal Seas*. Nauka, Moscow, pp. 148–154. (in Russian).
- Ustinova, E.I., Glebova, S.Yu., Sorokin, D., 2008. Hydrometeorologic conditions of the Far-Eastern Seas and North-West Pacific in 2008. *Quest. Fish. Oceanol.* 5 (N 2), 48–67. (in Russian).
- Varlamov, S.M., Luchin, V.A., Semiletov, I.P., Pipko, I.I., Pugach, S.P., Dashko, N.A., Proshutinsky, A.Yu., Weller, G., 1998. On interannual variability in the Bering Sea: effects of winter meteorological conditions. In: Kozlov (Ed.), *Proceedings of the Arctic Regional Center "Climatic and interannual variability in the atmosphere-land-sea system in the American-Asian Sector of Arctic"*, 1, pp. 65–85. (in Russian).
- Zolotov, A.O., Balykin, P.A., 2010. Long-term changes in the ichthyocenoses of the south-western part of the Bering Sea, Rostov-on-Don, Southern Scientific Centre. In: Makarevich, P.R. (Ed.), *Current State of the Ecosystem of the western Bering Sea, Rostov-on-Don, Southern Scientific Centre*, pp. 241–255 (in Russian).



A multivariate analysis of observed and modeled biophysical variability on the Bering Sea shelf: Multidecadal hindcasts (1970–2009) and forecasts (2010–2040)



Albert J. Hermann^{a,*}, Georgina A. Gibson^b, Nicholas A. Bond^a, Enrique N. Curchitser^c,
Kate Hedstrom^d, Wei Cheng^a, Muyin Wang^a, Phyllis J. Stabeno^e, Lisa Eisner^f,
Kristin D. Cieciel^f

^a Joint Institute for the Study of the Atmosphere and Ocean, University of Washington, Seattle, WA 98195, USA

^b International Arctic Research Center, University of Alaska Fairbanks, Fairbanks, AK 99775, USA

^c Institute of Marine and Coastal Sciences, Rutgers University, New Brunswick, NJ 08901, USA

^d Arctic Region Supercomputing Center, Fairbanks, AK 99775, USA

^e Ocean Environment Research Division, NOAA/PMEL, Seattle, WA 98195, USA

^f Auke Bay Laboratories, NOAA, Juneau, AK 99801, USA

ARTICLE INFO

Available online 9 April 2013

Keywords:

USA

Alaska

Bering Sea

Modeling

ABSTRACT

Coupled physical/biological models can be used to downscale global climate change to the ecology of subarctic regions, and to explore the bottom-up and top-down effects of that change on the spatial structure of subarctic ecosystems—for example, the relative dominance of large vs. small zooplankton in relation to ice cover. Here we utilize a multivariate statistical approach to extract the emergent properties of a coupled physical/biological hindcast of the Bering Sea for years 1970–2009, which includes multiple episodes of warming and cooling (e.g. the recent cooling of 2005–2009), and a multidecadal regional forecast of the coupled models, driven by an IPCC global model forecast of 2010–2040. Specifically, we employ multivariate empirical orthogonal function (EOF) analysis to derive the spatial covariance among physical and biological timeseries from our simulations. These are compared with EOFs derived from spatially gridded measurements of the region, collected during multiyear field programs. The model replicates observed relationships among temperature and salinity, as well as the observed inverse correlation between temperature and large crustacean zooplankton on the southeastern Bering Sea shelf. Predicted future warming of the shelf is accompanied by a northward shift in both pelagic and benthic biomass.

© 2013 Elsevier Ltd. All rights reserved.

1. Introduction

1.1. The Bering Sea ecosystem

The hydrography and climatology of the Bering Sea result in a highly productive ecosystem, with huge populations of plankton, shellfish, finfish, marine birds and marine mammals. This ecosystem supports major fisheries. Such intense production derives in part from a broad shelf with strong tides, plentiful iron, and seasonal stratification, adjacent to a deep, macronutrient-rich basin. The southeastern shelf includes three biophysical domains: a well-mixed inner region (~0–50 m), a middle region which is well-mixed in the winter and has two distinct layers in the summer (~50–100 m), and an outer region which is more

gradually stratified (~100–200 m) (Coachman, 1986; Kachel et al., 2002). Within these regimes, the relative magnitude of pelagic vs. benthic pathways of carbon flux varies interannually, and is believed to be strongly influenced by the extent of seasonal ice through its effects on stratification (Hunt et al., 2002). Recent cooling trends in the Bering Sea (Stabeno et al., 2012a) have been documented by the Bering Sea Ecosystem Program (BEST), the Bering Sea Integrated Ecosystem Research Program (BSIERP), the US Bering-Aleutian Salmon International Survey (BASIS), and the North Pacific Climate Regimes and Ecosystem Productivity Program (NPCREP). The relative importance of pelagic vs. benthic pathways is likely to shift under the influence of global warming, partially through its impact on seasonal ice extent in the Bering Sea. Field data suggest that recent cold temperatures in the Bering Sea have led to an increase in large crustacean zooplankton, favored as food items by juvenile pollock in the fall season (Coyle et al., 2011).

The revised “oscillating control hypothesis” (OCH) of Hunt et al. (2011) relates temperature and seasonal ice cover in the

* Corresponding author at: Pacific Marine Environmental Laboratory, 7600 Sand Point Way NE, Seattle, WA 98115 USA. Tel.: +1 206 526 6495; fax: +1 206 526 6485.

E-mail address: albert.j.hermann@noaa.gov (A.J. Hermann).

southeastern Bering Sea to the production of zooplankton and fish. This revised hypothesis may be summarized as follows.

Under warm conditions, the seasonal ice cover melts early in the year (February–March). This releases freshwater at the surface, but there is too much mixing and not enough sunlight to support a phytoplankton bloom at this time. Instead, the bloom occurs later (May–June), due to thermal stratification of relatively warm waters. These conditions favor the growth of small neritic copepods, as compared to large crustacean zooplankton (LCZ) (mid- to large-sized copepods, e.g. *Calanus marshallae*, and euphausiids, e.g. *Thysanoessa rashii* and *Thysanoessa inermis*). In general, these warm conditions promote energy flow into the pelagic (vs. benthic) food chain.

Under cold conditions, the ice cover melts late in the year (March–April), and an early bloom (April–May) follows due to the enhanced stratification of the water column. These conditions do not necessarily impede the growth of small neritic copepods, but do enhance the production of larger copepods, which need the early bloom to recruit from nauplii to copepodites in the southeastern Bering Sea. Less of this spring production goes into the pelagic food chain, and more into the benthic food chain.

The OCH also includes the linkage of these lower trophic dynamics to fish recruitment. These will not be considered in this paper, since our model includes only physics through zooplankton. Future research with a model including fish (Aydin et al., unpublished) will address these issues.

1.2. The multivariate analysis

Coupled physical/biological models can be used to downscale global climate change to the ecology of subarctic regions, and to explore the bottom-up and top-down effects of that change on the spatial structure of subarctic ecosystems, such as those predicted by the OCH. If an ice-free Bering is fundamentally different from one with ice cover, we can expect biophysical “modes” to emerge in a statistical analysis of models and data. Other atmospheric factors, such as changing wind direction or the frequency of storms, could likewise be expected to have widespread impact on the system, and emerge as broad-scale patterns in multivariate analyses. In the present work, we focus on temperature effects.

A cursory analysis of ocean model output typically reveals broad-scale patterns which appear to strengthen and weaken synchronously with a major forcing variable. In addition, we may notice that certain physical and biological variables tend to rise and fall together. A formal statistical evaluation of model output can be used to quantify the response of single variables over the entire model domain. An analysis of the spatial covariance in gridded data is frequently accomplished using empirical orthogonal functions (EOFs), which compactly include most of the total variance of the system within a few dominant temporal and spatial modes (Preisendorfer, 1988). However, for a complex biophysical model, the covarying changes among different state variables of the system may be of even greater interest (Allen and Somerfield, 2009). With multivariate EOFs, we may examine the covariance structure not only across space and time, but also across state variables. The method deployed here is essentially a form of combined principal component analysis (CPCA; Bretherton et al., 1992). Where possible, a similar analysis can be applied to real data, as a stringent test of model (and data) performance. These methods will be explored more fully in Section 2.4.

1.3. Organization of this paper

We begin with a description of the methods used for the physical and biological modeling of this ecosystem, the data used for comparison with the models, and the statistical methods used

for the multivariate analysis of models and data. This is followed by a description of basic features of the model output as compared with data, a limited multivariate analysis over a 6-year period where both model and data overlap, and the more extensive multivariate analysis using multidecadal model runs.

2. Methods

2.1. The physical model

2.1.1. Model structure, forcing, and boundary conditions

The physical model used here is based on an implementation of the regional ocean modeling system (ROMS) for the Northeast Pacific (NEP-5) as described by Danielson et al. (2011; henceforth referred to as DCHWS). ROMS is a sigma-coordinate model with curvilinear horizontal coordinates; a description of basic features and implementation can be found in Haidvogel et al. (2008) and Shchepetkin and McWilliams (2005). The NEP-5 grid has approximately 10 km horizontal resolution, with 60 vertical levels. Fine-scale bathymetry is based on ETOPO5 and supplementary datasets as described in DCHWS; smoothing of that bathymetry was utilized for numerical stability. Any regions shallower than 10 m were set to be 10 m deep. Mixing is based on the algorithms of Large et al. (1994). Both ice (Budgell, 2005) and tidal dynamics are included in this model; the explicit inclusion of tidal flows allows tidally generated mixing and tidal residual flows to develop. Freshwater runoff was applied by freshening of the salinity field within a few gridpoints of the coastline, using the monthly runoff values of Dai et al. (2009). Bulk forcing, based on algorithms of Large and Yeager (2008), was used to relate winds, air temperature, relative humidity, and downward shortwave and longwave radiation to surface stress and the net transfers of sensible heat, latent heat, net shortwave and net longwave radiation through the sea surface. The simulation detailed in DCHWS covers the period 1970–2004, which includes substantial interannual and interdecadal variability.

For the present work we utilized three forcing datasets, with the intent of spanning the years 1970–2009 (hindcast) and 2010–2040 (forecast). The common ocean reference experiment reanalysis (CORE; Large and Yeager, 2008) was utilized for a hindcast of years 1969–2004. The climate forecast system reanalysis (CFSR; Saha et al., 2010) was utilized for a hindcast of years 2003–2009. The coupled global climate model (CGCM3) from the Canadian Centre for Climate Modelling and Analysis (Flato et al., 2000) was utilized for a forecast of years 2003–2040. Note that CORE is a global atmospheric reanalysis spanning 1950–2004, while CFSR is a coupled atmospheric and oceanic reanalysis spanning 1979–present. Use of the CORE product for most of our hindcast is based on the availability of CORE forcing variables for the earlier decades, as well as its broad acceptance within the oceanic community. CORE products were not available for years beyond 2005 at the time our analyses were begun, while CFSR products were not available for years before 1979; hence both were employed for different portions of our hindcast. Overlapping runs for 2003 and 2004 allowed a comparison of results using the two reanalyses; these were used to adjust CFSR for compatibility with CORE. Ultimately our “continuous” (i.e. concatenated) hindcast/forecast series was composed of the CORE results for 1970–2004, CFSR results for 2005–2009, and CGCM3 results for 2010–2040.

The CGCM3 forecast (specifically, CGCM3.1-t47, under emissions scenario A1B) is one of the Intergovernmental Panel on Climate Change (IPCC) models used to explore the coupled global atmospheric and oceanic response to anticipated changes in atmospheric CO₂. CGCM3 makes use of the same ocean component as that used in the earlier CGCM2 (Flato et al., 2000), but

employs a substantially updated atmospheric component. Hindcasts with the CGCM3 model have demonstrated fidelity to present mean conditions in the Bering Sea (Wang et al., 2010); hence it was selected as one of the several IPCC forecasts to use in downscaling runs. Note that whereas CORE and CFSR are reanalyses based on the data, the CGCM3 is a free-running forecast beyond 2001, and hence does not capture the details of inter-annual variability during 2003–present. This necessarily results in a degree of discontinuity between our CFSR and CGCM3 results at the beginning of 2010.

For CORE- and CFSR-based runs, we utilized 6-hourly values for wind speed, temperature, humidity and sea-level pressure, and daily average values for shortwave and longwave radiation (the model internally converts daily shortwave into instantaneous values). CORE provided monthly values for rainfall; for CFSR we used 6-hourly values. For CORE-based runs, the monthly runoff estimates of Dai et al. (2009), available for 1948–2007, were used near coastal boundaries. For CFSR, we utilized a monthly climatology of runoff values based on the Dai et al. (2009) timeseries. For CGCM3-based runs we utilized the available daily average values of all atmospheric forcing values, and the same runoff climatology as for CFSR. These attributes of the runs are summarized in Table 1.

A subset of the NEP-5 domain was utilized for our Bering Sea biophysical simulations; this grid is henceforth referred to as Bering10K. The domain is shown in Fig. 1. For the CORE-based hindcast, initial and lateral boundary conditions were obtained from the NEP-5 simulation of DCHWS (itself driven by CORE forcing, with initial and boundary conditions from the SODA v2.0.2 reanalysis, Carton and Giese, 2008). For the CFSR-based hindcast, hourly values from the CFSR ocean model (<http://nomads.ncdc.noaa.gov/data.php#cfs-reanal>) were filtered to 5-day averages for use as boundary conditions. This is the same time averaging used for the SODA BCs in DCHWS. For the CGCM3-based forecast, monthly averaged properties from CGCM3 ocean model were used as boundary conditions. All the boundary conditions were enforced using the hybrid nudging/radiation scheme of Marchesiello et al. (2001). The hindcast using CFSR boundary and atmospheric forcing, and the forecast using CGCM3, were both initialized in January 2003 from CORE output, so as to overlap the CORE hindcast during 2003–2004. After calibration of shortwave and longwave fluxes (see Section 2.1.2), no significant differences were found between the CORE and CFSR hindcasts of the Bering Sea during these 2 years. As in DCHWS, outflow through the Bering Strait was fixed to a value of 0.8 sv.

The full 60-level vertical resolution of Bering10K has been used for multiyear simulations of biophysical dynamics of the Bering Sea (Gibson et al., unpublished). Here, to facilitate the execution of long multidecadal biophysical runs, we have reduced the vertical resolution from 60 to 10 levels. We fully recognize the desirability of greater vertical resolution; the use of only 10 levels inevitably degrades the resolution of features such as the seasonal pycnocline and the subsurface chlorophyll maximum. However, as shown in the Results section, this reduced version still retains most of the essential physical and biological dynamics, as well as

model-generated relationships among physical and biological qualities. This makes it a very useful (albeit imperfect) tool to investigate the interannual variability of the entire system, the covariance among different elements of the system, and the spatial relationships of that covariance over multiple decades.

2.1.2. Calibration of the physical model

While our Bering10K physical model is very similar to that used in DCHWS, certain aspects were calibrated to better fit the observed temperature and salinity fields of the Bering Sea. These include the following:

1. Sensible and latent heat fluxes, calculated through the Large and Yeager (2009) algorithms, were increased by 25% each. This was found necessary to keep the water column from overheating during the summer months, in response to absorption by shortwave radiation (this bias was evident in both 60- and 10-layer versions of the model, e.g. see Fig. 8 of DCHWS). Reasonable justifications for this change include the extreme roughness of the sea surface in the Bering Sea, which could result in significant heat transfer due to sea spray (Andreas et al., 2008), and the fact that most bulk flux algorithms were initially developed using equatorial and mid-latitude data, rather than subpolar and polar data.
2. The latitude-dependent open-ocean albedo of the Bering Sea surface was increased from ~ 0.075 to ~ 0.15 . As in (1), this was found necessary to reduce excessive summer temperatures, which are largely driven by the shortwave flux. Reasonable justifications for this change include the prevalence of white-caps (which reflect sunlight) in the Bering Sea. In general, observed open-ocean albedo is higher at high latitudes than in the tropics (Large and Yeager, 2009). The adjustment of albedo,

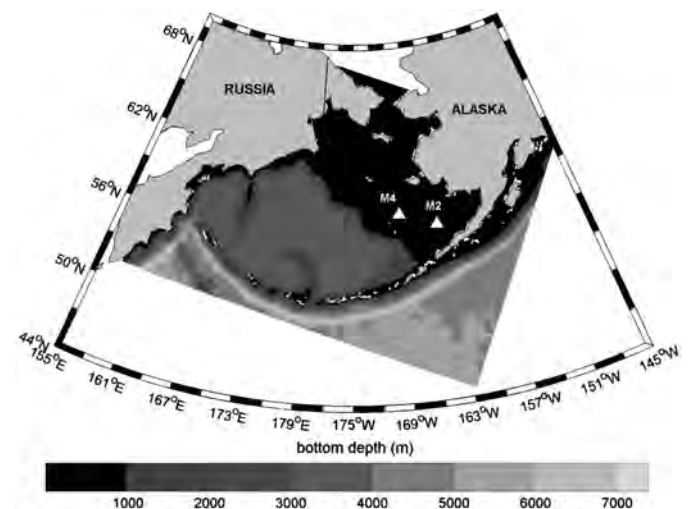


Fig. 1. Model domain with shaded bathymetry (m). The locations of biophysical moorings M2 and M4 are shown.

Table 1

Time resolution of forcing and boundary variables for the three runs. Tair=air temperature ($^{\circ}\text{C}$); Pair=sea level pressure (mb); Qair=specific humidity (kg kg^{-1}); swrad=shortwave radiation (W m^{-2}); lwrad=longwave radiation (W m^{-2}); Uwind, Vwind=eastward and northward wind velocity (m s^{-1}); Rain=rainfall (m s^{-1}); Runoff=coastal runoff (m s^{-1}); BCs=physical oceanic boundary conditions.

Run	Tair	Pair	Qair	swrad ^a	lwrad	Uwind, Vwind	Rain	Runoff ^b	BCs
CORE (1969–2004)	6 h	6 h	6 h	1 d ^a	1 d	6 h	1 mo	1 mo	5 d
CFSR (2003–2009)	6 h	6 h	6 h	1 d ^a	1 d	6 h	6 h	1 mo	5 d
CGCM3 (2003–2040)	1 d	1 d	1 d	1 d ^a	1 d	1 d	1 d	1 mo	1 mo

^a swrad is converted to instantaneous values (based on solar altitude) in ROMS.

^b CORE uses monthly runoff estimates; CFSR and CGCM3 use monthly climatology.

rather than incident shortwave radiation per se, was based on a comparison of shortwave measurements at station M2 with the downward shortwave forcing in CORE; the two were found in good agreement, i.e. CORE does not appear to overestimate shortwave as had been found with earlier NCEP results (Ladd and Bond, 2002). A second possible factor, which could reduce the conversion of incident shortwave radiation to heat in the water column, is the absorption of photons via the intense primary production of the Bering Sea. A rough calculation suggests this may be a significant loss (as much as 10 W/m² of energy in mid-summer), but further work is needed to quantify this term.

3. Sea surface salinity is relaxed to climatological values as in DCHWS, but with a slower timescale (in DCHWS 2 months; here 1 year), to allow more interannual variability.
4. Water column thickness in ROMS is limited to be no thinner than 0.1 m above the sea bottom, to ensure numerical stability.
5. A comparison of CFSR and CORE data for overlapping years revealed small differences in both shortwave and longwave components of the forcing. Based on a comparison of CORE and CFSR values for 2002–2006, the CFSR downward shortwave was attenuated by 10%, and the CFSR downward longwave was attenuated by 3%, prior to its use as atmospheric forcing.
6. The DCHWS model utilized a time-invariant river discharge, applied as a spatially dependent surface flux. Here, the monthly and interannually varying discharge values of Dai et al. (2009) were used for this purpose; these yield an improved fit with salinity data. Where data were not available (beyond 2004), a monthly climatology based on the available record was applied.

2.2. The biological model

The biological model used here is described in Gibson and Spitz (2011). Univariate comparisons with temperature and nutrient data will be described elsewhere (Gibson et al., unpublished). The major components of this model are: nitrate, ammonium, iron, small phytoplankton, large phytoplankton, microzooplankton, small copepods, large copepods (e.g. *Neocalanus* spp.), krill

(euphausiids), jellyfish, ice phytoplankton, iron, nitrate, ammonium, slow sinking detritus, fast sinking detritus, benthic detritus, and benthic infauna. These components are summarized in Fig. 2. While the present work concerns only the lower trophic level dynamics of the system, other simulations couple these with a size- and age-structured fish model (FEAST; Aydin et al., unpublished) to examine both top-down and bottom-up control of zooplankton.

As with surface salinity, a small relaxation term (1 year timescale) was utilized to guide iron, nitrate, and ammonium back to climatological profiles, to prevent spurious long-term drift. Such drift is due primarily to missing elements of the nitrogen and iron cycles, which are not closed in this model. A comparison of simulations with and without this relaxation term demonstrated no appreciable difference over a 4-year period; at the same time, this small corrective term proved essential for our multidecadal runs.

2.3. Observations compared with the model

Three types of data were compared with the model: Eulerian timeseries from biophysical moorings at stations M2 (56.87N, 164.05W) and M4 (57.85N, 168.87W) along the 70 m isobaths (mid-shelf, Fig. 1), spatially gridded velocities derived from drogued Lagrangian drifter data on the shelf, and spatially gridded hydrographic and chlorophyll data from repeated surveys.

The biophysical mooring data have been described in a series of papers by Stabeno et al. (2001, 2007, 2010, 2012a, 2012b). A nearly continuous multiyear series of temperature, salinity, and currents, spanning the water column, has been maintained at M2; similar (albeit less complete) series have been maintained at locations further north along the 70 m isobaths (e.g. M4). Winds and solar insolation have been measured continuously at M2 during many of these years. While salinometer data are sparser than thermistor data, the combined data were sufficient to generate estimates of water column stability. As in Ladd and Stabeno (2012), we used the potential energy anomaly ϕ , which is the amount of energy required to completely mix the water column (Simpson et al.,

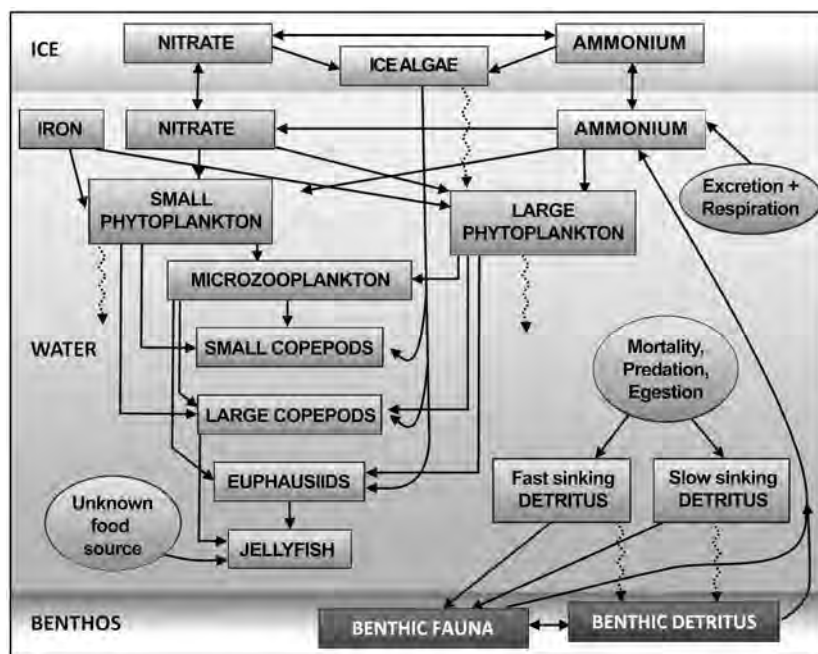


Fig. 2. Structure of the NPZ model used in this study (from Gibson and Spitz, 2011).

1978):

$$\phi = \frac{1}{h} \int_{-h}^0 (\rho - \bar{\rho}) g z \, dz; \quad \text{where } \bar{\rho} = \frac{1}{h} \int_{-h}^0 \rho \, dz. \quad (1)$$

The same formula was applied to model output, for comparison with the Ladd and Stabeno (2012) values at M2.

Based on time- and depth-averaged temperature at M2, the years are divided into three categories: cold (1995, 1997, 1999, 2007–2010); average (1996, 2000, 2006); and warm (1998, 2001–2005). This classification is based on Stabeno et al. (2012a). Using this classification of years, we compare measured velocities at M2 with their model equivalent at near-surface (10–15 m) and near-bottom (50–55 m) locations.

We also compare climatological velocities from drogued drifter data with their model equivalent on the Bering Sea shelf. Our basic methodology for drifter data is similar to that described in Stabeno and Reed (1994). Drifters were outfitted with holey-sock drogues and tracked via satellite. Data were available for years 1995–2006; hourly changes in drifter position were used to calculate the local velocity. Model climatology was derived from 1986 to 2004 of the CORE-forced hindcast. Both model and drifter data from May 15 to October 15 of each year were binned using the same, regular $0.5^\circ \times 0.5^\circ$ latitude–longitude grid. From the data, only those bins with a total of at least 200 hourly drifter observations were retained for comparison (note this can be from a single drifter over 200 h, or many drifters over shorter periods). Further, only those locations shallower than 200 m are compared; observations were too sparse beyond the shelf break to obtain stable mean values at the $0.5^\circ \times 0.5^\circ$ resolution, due to intermittent shelf-break eddies in both model and data.

Hydrographic surveys conducted under the BASIS program are used in the multivariate analysis. BASIS data include observations of temperature, salinity, nutrients, phytoplankton, zooplankton, and fish, obtained between mid-August and early October from 2002 to present. In the present work, we utilize only the temperature, salinity, and total chlorophyll data, which were available as gridded fields for years 2003–2009. The sampling grid covers the eastern Bering Sea shelf from 55N to 65N; grid spacing is approximately 55 km. Station locations and other details of BASIS methodology are described in Danielson et al. (2010, 2011).

2.4. The multivariate statistical analysis

While multivariate statistics are routinely applied to biological data, with few exceptions (e.g. Allen and Somerfield, 2009) they have not been applied to biophysical model output. Here we provide a brief description of our multivariate method and its potential value. In physical oceanography and meteorology, EOFs are used as a standard tool to relate change in one part of the fluid to changes in some other part—for example, a correlation in the rise and fall of SSH in different parts of the ocean, driven by broad-scale winds. EOFs are the most compact way of expressing the common variance of a collection of timeseries, as they are the eigenfunctions of the matrix of covariances among all the series (Preisendorfer, 1988). Typically they are applied using timeseries of a single variable at multiple locations:

$$T(x_1, t_1), T(x_1, t_2), T(x_1, t_3), \dots, T(x_1, t_N) \quad (2a)$$

$$T(x_2, t_1), T(x_2, t_2), T(x_2, t_3), \dots, T(x_2, t_N) \quad (2b)$$

$$T(x_M, t_1), T(x_M, t_2), T(x_M, t_3), \dots, T(x_M, t_N) \quad (2c)$$

In biology, principal component analysis is frequently used to establish the co-occurrence of species from a collection of

samples at one location:

$$N(x_1, t_1), N(x_1, t_2), N(x_1, t_3), \dots, N(x_1, t_N) \quad (3a)$$

$$P(x_1, t_1), P(x_1, t_2), P(x_1, t_3), \dots, P(x_1, t_N) \quad (3b)$$

$$Z(x_1, t_1), Z(x_1, t_2), Z(x_1, t_3), \dots, Z(x_1, t_N) \quad (3c)$$

or a set of multivariate observations scattered in space and time (e.g. Allen and Somerfield, 2009)

$$N(x_1, t_1), N(x_2, t_2), N(x_3, t_3), \dots, N(x_M, t_M) \quad (4a)$$

$$P(x_1, t_1), P(x_2, t_2), P(x_3, t_3), \dots, P(x_M, t_M) \quad (4b)$$

$$Z(x_1, t_1), Z(x_2, t_2), Z(x_3, t_3), \dots, Z(x_M, t_M) \quad (4c)$$

where N, P, Z represent three different biological properties, e.g. nutrients, phytoplankton, and zooplankton.

Note how in (3a)–(3c), the different variable types are analogous to the different spatial locations used in (2a)–(2c). In either case the fundamental goal is the same; to compactly describe the covariance among a collection of timeseries. To this end, a $N \times N$ matrix is constructed whose elements are the covariance (or correlation) of the i th series to the j th timeseries for all $i=1, \dots, N$ and $j=1, \dots, N$. The eigenvectors and eigenvalues of this matrix are derived; the eigenvectors are then interpreted as coupled modes of variability among the series. For EOF analysis, this results in an orthogonal set of spatial patterns (the “modes”) and an orthogonal set of timeseries (the principal components, i.e. PCs).

Since our aim here is the examination of coupled spatial modes of biophysical variability, we use a multivariate set of timeseries spanning the model domain:

$$\begin{aligned} &N(x_1, t_1), N(x_1, t_2), N(x_1, t_3), \dots, N(x_1, t_N) \\ &P(x_1, t_1), P(x_1, t_2), P(x_1, t_3), \dots, P(x_1, t_N) \\ &Z(x_1, t_1), Z(x_1, t_2), Z(x_1, t_3), \dots, Z(x_1, t_N) \\ &T(x_1, t_1), T(x_1, t_2), T(x_1, t_3), \dots, T(x_1, t_N) \\ &\dots\dots\dots \\ &N(x_M, t_1), N(x_M, t_2), N(x_M, t_3), \dots, N(x_M, t_N) \\ &P(x_M, t_1), P(x_M, t_2), P(x_M, t_3), \dots, P(x_M, t_N) \\ &Z(x_M, t_1), Z(x_M, t_2), Z(x_M, t_3), \dots, Z(x_M, t_N) \\ &T(x_M, t_1), T(x_M, t_2), T(x_M, t_3), \dots, T(x_M, t_N) \end{aligned}$$

Again, the intended product is the covariance structure of the coupled system—that is, which features of the biological and physical system covary, and what is the spatial structure of this covariance. At the outset, we expect that none of the multivariate modes from this analysis will explain as much of the variance contained a *single* variable, as can be explained through univariate EOF analysis. However, this approach is a useful way to summarize the spatial modes in which different hydrographic features and trophic levels rise and/or fall together, either through self-generated dynamics (e.g. phytoplankton decrease as zooplankton increase) or through a common driver (warmer temperatures lead to increased/decreased production of certain trophic levels in particular areas). For the Bering Sea, shifts to the north and/or inshore are of particular interest.

It is important in such an analysis to avoid the pitfall of quadrature. As an example, when control is neither fully top-down nor fully bottom-up, a biological system (real or modeled) may develop predator–prey cycles (and/or seasonal succession) which place predator and prey 90° out of phase with each other—that is, closely linked but perfectly uncorrelated. A simple example is a phytoplankton bloom followed with some time lag by zooplankton growth. To guard against this pitfall, we must take care to average over the timescale on which such cycles would occur. For the full multivariate analysis of Section 3.3.2, we use

multiyear timeseries composed of annual averages for each variable and location.

Note also the need for normalization of the timeseries prior to analysis; each variable is in different units, and we seek to give all of them an equal chance to contribute to the biophysical modes. Here, we proceed by normalizing each variable using its standard deviation over all space and time. This simultaneously eliminates units and emphasizes the relative change in each case. Once the EOFs are calculated on these normalized series, we de-normalize the results by multiplying back by the set of standard deviations. The results are then plotted using shading levels ranging from -1 to $+1$ s.d. of each variable. In this manner, we illustrate how strongly each of the variables has contributed to the coupled mode, relative to that variable's own total variance.

Many timeseries could be used as input for this type of multivariate analysis, up to the full 3D fields of every modeled variable, as well as the many fluxes among those variables. For the present investigation, we select some of the major scalar variables which are believed to play a role in the OCH, with a focus on temperature, ice, and zooplankton. We further limit our attention to 2D variables (e.g. ice cover), 2D slices from 3D variables (sea surface and sea bottom temperature), or vertical averages of 3D variables (e.g. zooplankton).

Two types of analysis were performed:

- 1) A direct comparison with BASIS data was carried out for sea surface temperature, sea bottom temperature, sea surface salinity and averaged phytoplankton in the upper 40 m. Model-equivalent values from the CFSR-forced hindcast were sampled at precisely the same locations and times as the BASIS data for this comparison (sampled days span mid-August–early October of each year). A carbon-to-chlorophyll ratio of 50:1 was assumed for this analysis, to convert chlorophyll values (from BASIS surveys) to large plus small phytoplankton biomass (from the model output). A summary of the variables used for this analysis is shown in Table 2. Extensive gridded data do not exist for other seasons, however, univariate comparisons with physical and biological have quantified the correspondence to observed temperature and nutrient fields in most areas (Gibson et al., unpublished).

Table 2

Variables used in the multivariate analysis of the BASIS data, and its model equivalent.

Surface temperature	SST	°C
Bottom temperature	SBT	°C
Surface salinity	SSS	psu
Phytoplankton (top 40 m ave)	PHYT	mg C m ⁻³

- 2) An extended multiyear analysis was carried out using annual averages of 15 properties from the model output, chosen to include features relevant to the OCH hypotheses (temperature, ice, nutrients, and multiple trophic levels). A summary of the variables used for these analyses is shown in Table 3. This more extensive multivariate analysis was applied to three different groupings of the simulation output: (1) a concatenated series of CORE (1970–2004) and CFSR (2005–2009) hindcasts; (2) last two decades of the CGCM3 forecast (2020–2040); (3) a concatenated series of CORE (1970–2004), CFSR (2005–2009) and CGCM3 (2010–2040).

After their de-normalization, the multivariate EOFs may be interpreted as coupled spatial patterns for each of the variables, describing how particular quantities rise and/or fall together. The principal component timeseries for that mode, multiplied by the de-normalized EOF, indicates a time history of rising/falling quantities in the domain, in the original units of the variable. A spatial map for temperature with both positive and negative values indicates that, for that particular multivariate EOF, some parts of the domain rise in temperature at the same time that other parts fall in temperature, e.g. those different regions are negatively correlated. In the same way, at a particular location, we may see that temperature has positive EOF value while salinity has a negative EOF value. This indicates that those variables are negatively correlated at that location. Further, we may observe that temperature has a positive EOF value at location A, while nitrate has a negative EOF value at location B. This indicates that temperature at location A is negatively correlated with nitrate at location B.

3. Results

3.1. 10-Level physical model performance

A detailed statistical analysis of the 60-level biophysical model performance has demonstrated significant model skill in capturing the spatial and temporal variability of both temperature and nitrate in the top 40 m of the water column (Gibson et al., unpublished). The broad structure and seasonality of the nutrient field are similar in both 60-layer and 10-layer models. A thorough assessment of the 60-level physical model on the NEP-5 grid is reported in DCHWS; these included a comparison of observed vs. modeled ice and tides. As described in Section 2, our physical model is similar in structure to that of DCHWS, albeit on a smaller grid (a subsection with the same horizontal resolution as the full NEP-5 grid), and with some modifications pertaining to surface

Table 3

Variables used in the multivariate analysis of the simulations.

Surface temperature	SST	°C
Bottom temperature	SBT	°C
Surface salinity	SSS	psu
Ice cover	ICECOVER	fractional area
Mixed layer depth	MLD	m (positive up coordinates; hence negative change denotes <i>deepening</i> MLD)
Vertical mixing (depth ave)	AKTS	m ² s ⁻¹
Nitrate+ammonium (depth ave)	NUT	mg N m ⁻³
Ice phytoplankton (surface layer ave)	ICEPHYT	mg C m ⁻³
Small plus large phytoplankton (depth ave)	PHYT	mg C m ⁻³
Microzooplankton (depth ave)	MZOO	mg C m ⁻³
Small copepods (depth ave)	COPE	mg C m ⁻³
Neocalanus (depth ave)	NCA	mg C m ⁻³
Euphausiids (depth ave)	EUP	mg C m ⁻³
Benthic detritus	BENDET	mg C m ⁻²
Benthic infauna	BENINF	mg C m ⁻²

heat flux. Here, we describe representative properties of the 10-level model, and their comparison with data. Our intent is to demonstrate that the 10-level model, while vertically coarse, captures enough of the essential physics and biology of the region

to be useful as a tool to explore relevant aspects of past and future interannual change. Ice and tidal results were in fact very similar to those of DCHWS; here instead we focus on velocity, temperature and salinity results.

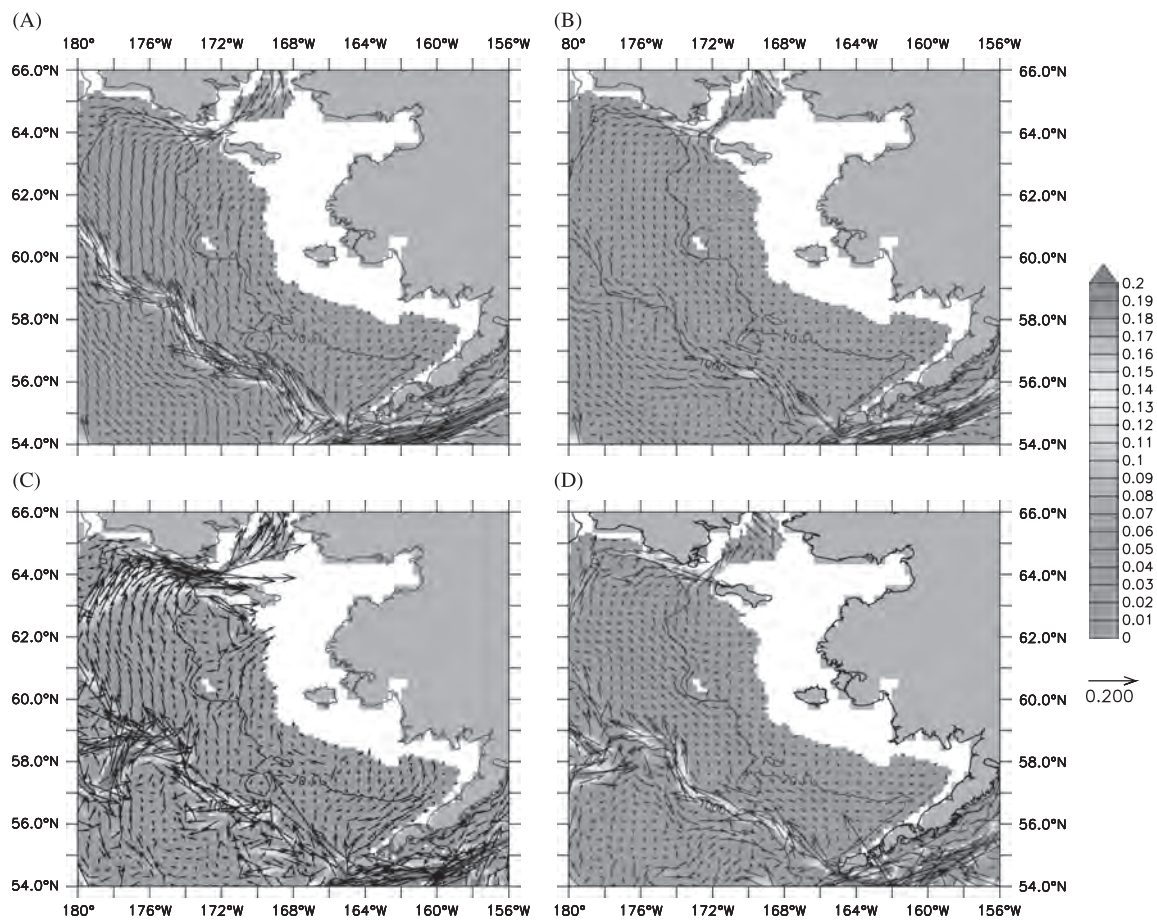


Fig. 3. Climatological and weekly averaged model velocities at 40 m, from a simulation of years 1970 to 2009. Speed is shaded (m s^{-1}). Upper panels show climatological January (A) and July (B) values; lower panels show a weekly average from January 2004 (C) and July 2004 (D). Bathymetric contours at 70 m and 1000 m depth are shown. (a) January climatology, (b) July climatology, (c) 11 Jan 2004 and (d) 11 July 2004.

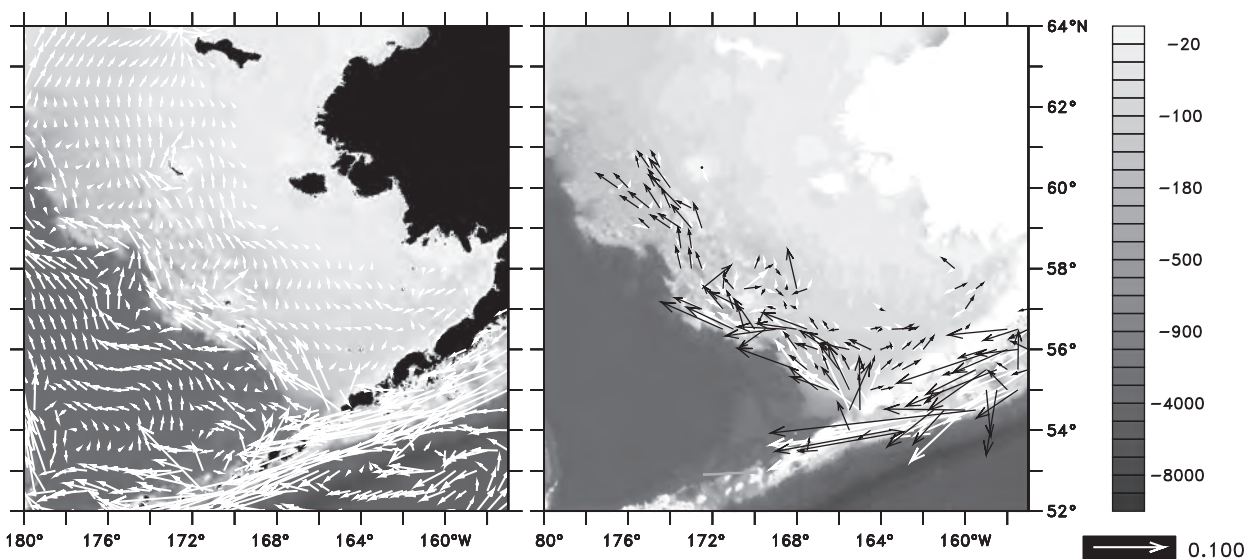


Fig. 4. Climatological modeled (red) vs. measured (black) summer (May 15–October 15) velocities at 40 m depth for the Bering Sea. Velocities are in m s^{-1} ; bathymetry is shaded (m). Measured values are derived from drogued drifter climatology. Left figure illustrates model vectors (red); right figure illustrates measured (black) and modeled (red) vectors, and excludes locations with no measurements. (For interpretation of the references to color in this figure caption, the reader is referred to the web version of this article.)

3.1.1. Climatological circulation

The climatological circulation of the model exhibits major observed circulation features between 54N and 66N: a vigorous flow along the southern boundary of the Aleutians and through Unimak Pass, and to the northwest along the shelf break (Fig. 3). Weaker but persistent flows are to the northwest on the Bering Sea shelf; these are strongest in winter. Weekly averaged velocities

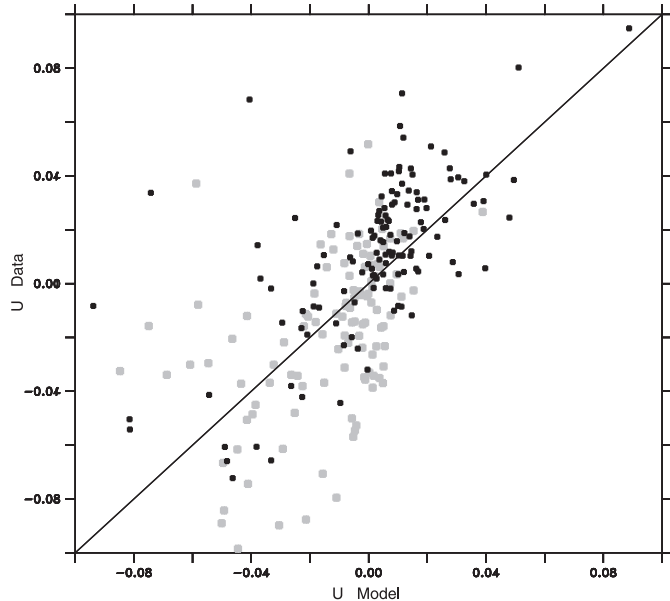


Fig. 5. Modeled (x-axis) vs. observed (y-axis) values for climatological summer eastward (red) and northward (blue) velocities at 40 m. Values are in $m\ s^{-1}$. The r -squared values are 0.54 and 0.70 for eastward and northward velocities, respectively. (For interpretation of the references to color in this figure caption, the reader is referred to the web version of this article.)

exhibit more detailed structures, such as 200-km eddies along the shelf break. Note how the climatological maps reveal strong northwestward flows along the 50 m and 100 m isobaths in winter; these correspond to frontal structures separating the inner/middle and middle/outer biophysical regimes of the Bering Sea (Coachman, 1986; Kachel et al., 2002).

3.1.2. Velocity climatology from drifters

In Fig. 4 we compare modeled and drifter-derived climatological velocities at 40 m depth for Bering Sea summer (May 15–October 15). Model-derived velocities are in conformance with the available data in most areas. A scatterplot compares observed climatological velocities with their equivalent from the 10-level model (Fig. 5). The r -squared values are 0.54 for the eastward and 0.70 for the northward velocities, respectively. There is a slight bias towards weaker velocities in the model as compared with data.

3.1.3. Mid-shelf velocity climatology

A comparison of measured climatological velocity by month at station M2 (from Stabeno et al., 2012a) with their model equivalent (Fig. 6) reveals a similar seasonal progression in both model and data, with a tendency to offshore flow during the summer. The observed and modeled summertime near-surface offshore flow is more pronounced during cold years (Stabeno et al., 2012a).

3.1.4. Mid-shelf hydrography at stations M2 and M4

Thermistor arrays at mid-shelf stations M2 and M4 allow a detailed comparison with model output. The CORE-driven hindcast, even with only 10 vertical levels, captures the basic seasonal and interannual trends as the data (Fig. 7). Seasonal creation of the thermocline in summer is followed by its destruction in the fall. The presence of ice in cold years is

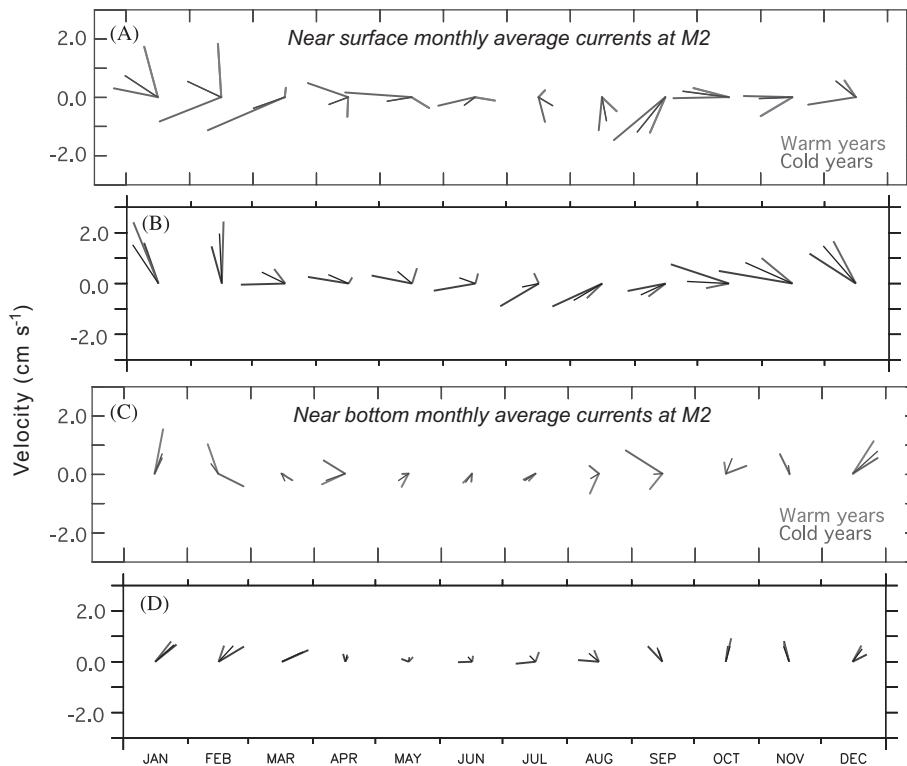


Fig. 6. Monthly velocity climatology at station M2, from observation and model. (A) Near-surface velocity from data; (B) near-surface velocity from model; (C) near-bottom velocity from data; (D) near-bottom velocity from model. Colors indicate averages from warm years only (red), cold years only (blue) and all years combined (black). (A) and (C) are adapted from Stabeno et al. (2012a). (a) surface data, (b) surface model, (c) bottom data and (d) bottom model. (For interpretation of the references to color in this figure caption, the reader is referred to the web version of this article.)

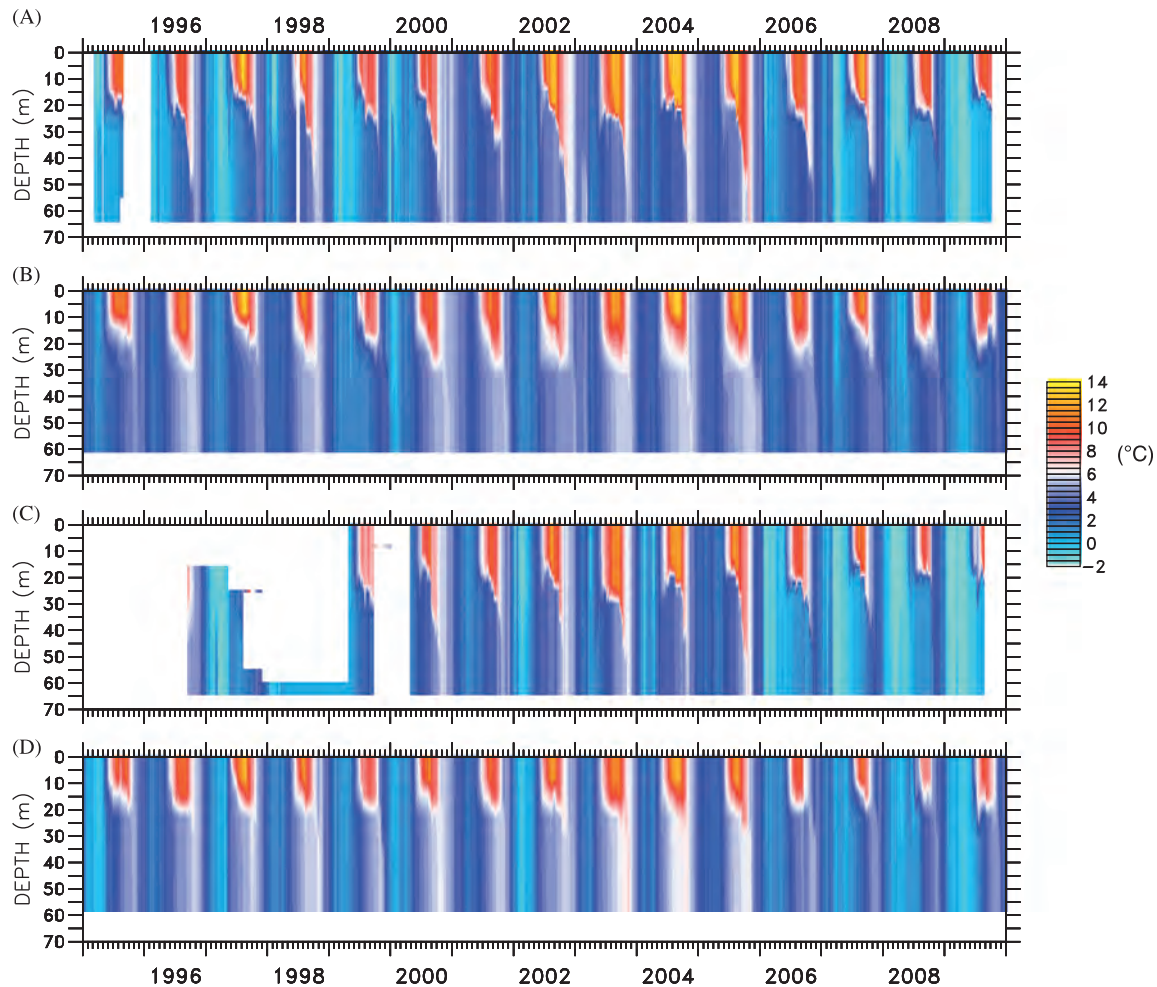


Fig. 7. Comparison of measured vs. modeled temperatures at stations M2 (A and B) and M4 (C and D). Units are °C. (a) M2 DATA, (b) M2 MODEL, (c) M4 DATA and (d) M4 MODEL.

associated with near-freezing temperatures which extend to the bottom (e.g. January–April 2009). The model exhibits similar patterns at slightly reduced amplitude. Depth-averaged temperatures are compared in Fig. 8. Model bias is smallest in summer; largest discrepancies are found in winter, where the model has a residual tendency to underestimate the areal extent of ice at both M2 and M4 (not shown). When ice coverage is not complete in a given grid cell, the average temperature there will be above freezing. A straightforward adjustment of the ice module can increase ice cover growth, as opposed to ice thickness growth, when new ice is formed; this has been applied to recent simulations and will be reported in a future paper.

Salinity at M2 and M4 has been more sparsely sampled than temperature. Rather than full vertical profiles, we compare salinity timeseries at two depths: 15 m and 55 m (Fig. 9). In both model and data, interannual variability is the dominant signal, and the residual between model and data at 15 m is frequently less than 0.1 psu. This is in fact within the accuracy of the salinometer itself. Note how the model generates a fresh, 20 m-deep surface layer in summer, especially during cold years.

The model likewise captures the essential seasonal and interannual patterns of stratification as expressed through the potential energy anomaly ϕ at station M2 (Fig. 10). Stratification increases rapidly in May and peaks around August. As with temperature itself, the model exhibits the same pattern as the data, but at slightly reduced amplitude.

3.2. Multidecadal behavior of the model

Before proceeding to the full multivariate analysis, we focus on two aspects of the interannual/interdecadal performance of the 10-level model: temperature and large crustacean zooplankton.

3.2.1. Mid-shelf temperature timeseries

Multidecadal timeseries of depth-averaged temperature at M2 from the model, based on each of the three forcing datasets (Fig. 11), exhibit marked interannual and interdecadal variability, with some pronounced changes corresponding with regime shifts of the larger North Pacific (e.g. the shift of 1976). The recent periods of warming (1999–2004) and cooling (2005–2009) (see Fig. 9) are clearly evident in the CORE and CFSR hindcasts. These two hindcasts overlap during 2003–2004; the time plots of temperature during those years show essentially identical results (and hence are difficult to distinguish as separate lines in Fig. 11). The CGCM3-based forecast indicates a slow warming trend, with the 5-year mean average gradually rising from ~ 3.75 °C to ~ 5.25 °C by the mid-2030s. Note how the CGCM3 forecast, down-scaled here beginning with year 2003, anticipated a colder series of years in 2003–2006 and a warmer series of years in 2006–2010 than were actually observed. This level of mismatch is in fact anticipated, as CGCM3 is a freely evolving coupled global air–sea simulation unconstrained by data; as such it manifests different interannual details than the real atmosphere and ocean.

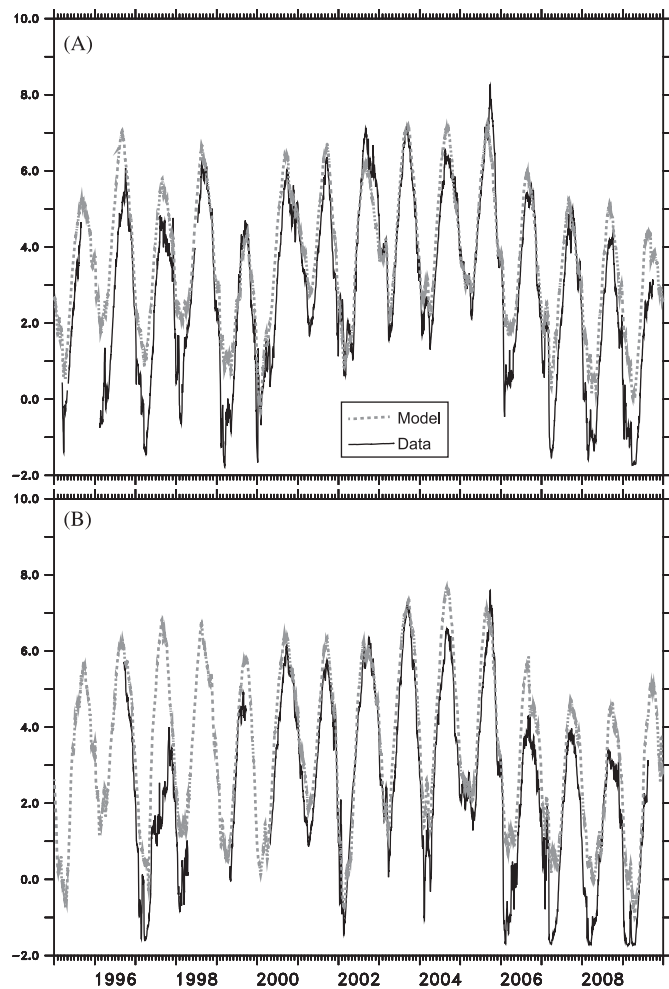


Fig. 8. Comparison of measured (black) vs. modeled (red) depth-integrated temperature at locations M2 (A) and M4 (B). Units are °C. (a) M2 depth-average T and (b) M4 depth-average T. (For interpretation of the references to color in this figure caption, the reader is referred to the web version of this article.)

3.2.2. Correlation with large crustacean zooplankton

Observations during the recent period of cooling in the Bering Sea suggest a tendency for large crustacean zooplankton (represented by euphausiids and neocalanus in the model) to covary inversely with temperature (Hunt et al., 2011; Coyle et al., 2011). This general tendency is apparent in the 10-level model results over all three simulation periods (Fig. 12), and is consistent with the detailed comparisons by region from the 60-level model during warm vs. cold years (Gibson et al., unpublished).

3.3. Results from multivariate analysis

As noted in the methods, the multivariate EOFs may be interpreted as coupled spatial patterns for each of the variables, describing how particular quantities, at particular locations, rise and/or fall together. Below we explore these patterns, and their amplitude through time.

3.3.1. Comparison with BASIS gridded data

The leading biophysical mode from the BASIS data exhibits a correlated fall in surface and bottom temperatures (SST, SBT) in the southeastern Bering Sea (Fig. 13). Higher sea surface salinity (SSS) is found along the 70 m isobaths during warmer years, and higher concentrations of phytoplankton (PHYT) are observed during those years. The leading biophysical mode from the corresponding model

output exhibits markedly similar patterns in SST, SBT and SSS during warm/cold years, but a much weaker (and even negative) correlation with PHYT. The temporal trend (first PC) of this mode is markedly similar between the model and data; in both cases the dominant signal reflects the cooling between 2005 and 2009. The conformance of the model/data SSS patterns is especially striking. The likely cause of this pattern is melt along the southern/offshore extent of the seasonal ice field, as suggested in the (univariate) salinity EOF analysis of Danielson et al. (2010, 2011). In the northeastern Bering Sea, ice is typically formed in the lee of headlands and islands and is advected south by the prevailing winds (Stabeno et al., 2010), hence serving as a net conveyor of freshwater to the south. In warm years, less ice is melted along the southeast segment of the 70 m isobath (the southerly/offshore extent of this ice field), and so the SSS is higher than in cold years at that location.

3.3.2. Full multivariate analysis of model output

The full multivariate analysis of model output yields a leading spatial mode where some variables rise in concert with others (e.g. SST and SSB), whereas others vary out of phase with each other (e.g. SST vs. ICECOVER). Biological variables such as EUP show marked spatial variance; positive/negative values on the inner/outer shelf indicate that EUP goes up on the inner shelf when it is falling on the outer shelf. Further, a comparison of EUP and SST maps reveals that outer shelf EUP go down when shelf-wide SST is rising. The leading biophysical mode is similar across all groupings of the model output (Figs. 14–16). In each case, SST, SBT and SSS exhibit similar trends and tendencies as in the BASIS data. For the mode using CORE and CFSR hindcasts (Fig. 14), and the mode using all three forcing datasets (Fig. 16), warmer SST, warmer SBT, and reduced ICECOVER co-occur in the south, but cooler temperatures are associated with this change in the north when all three datasets are included. Increased SSS is observed at the mean location of the ice edge; these are associated with enhanced mixing (AKT) and deepening of the MLD (note: both SSH and MLD are defined in meters above mean sea level, hence more negative values for MLD denote a deeper mixed layer). Reduced pelagic biomass (MZOO, COPE, NCA, EUP) is found on the outer shelf, while increased biomass of those terms is found both inshore and northward. EUP in particular exhibits a decrease in biomass during warm periods, as was seen in the direct scatterplot of these quantities at M2 (Fig. 12). This inverse correlation is likewise found in the 60-level output (Gibson et al., unpublished). A similar shift is observed in benthic detritus and benthic infauna, but has a more zonal alignment (i.e., benthic biomass shifts more directly to the north, as opposed to inshore). Dissolved inorganic nitrogen (NUT) shows a trend to lower values along the 70 m isobaths when temperatures are warm; changes in large plus small phytoplankton (PHYT) are less dramatic. The amplitude of this mode (the first PC) exhibits large changes in 1975–1980, 1999–2004, and 2005–2009. These latter two periods exhibit the same interannual trends as the depth-averaged temperature timeseries at M2 (Fig. 8).

The dominant mode obtained using only the last 20 years of CGCM3-driven results (Fig. 15) are similar to those of the CORE/CFSR analysis (Fig. 14), but emphasize primarily the coupling among hydrographic variables (SST, SBT, SSS, ICECOVER). The increase in mixing and deepening of MLD are more broadly spread along the outer shelf. NUT decreases in the south and increases in the north, while PHYT increases all along the 70 m isobath; its pattern is in fact similar to that of SSS. The patterns associated with the benthos and the zooplankton are weaker than in the hindcast, and, along with the pattern for ICECOVER, have been shifted north. This likely reflects the northerly shift of the seasonal ice edge under continued warming.

When the full concatenated series (CORE/CFSR/CGCM3) is used (Fig. 16), the largest jump in the PC occurs between the end of the CFSR segment and the beginning of the CGCM3 segment.

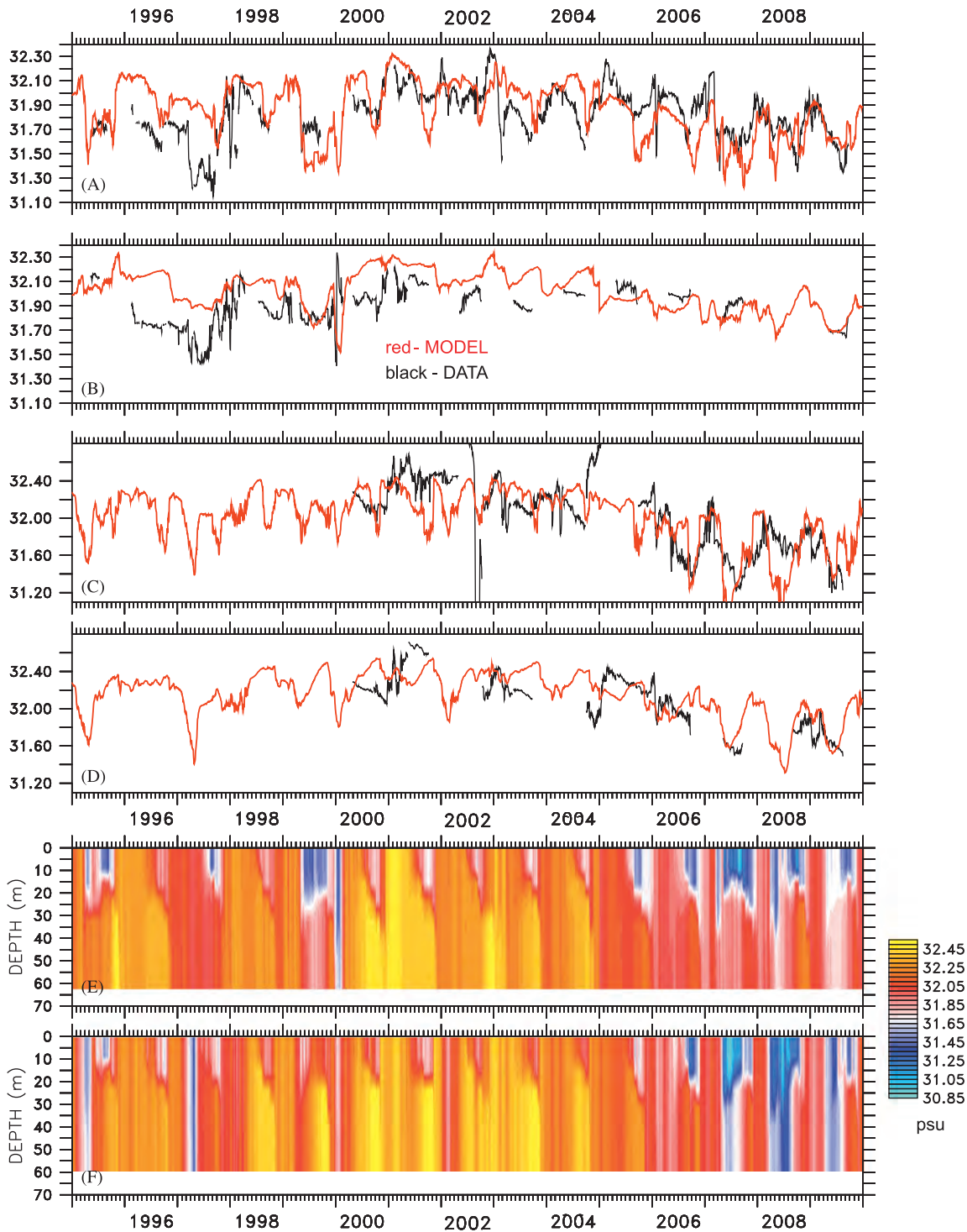


Fig. 9. Comparison of modeled vs. measured salinity at stations M2 (A and B) and M4 (C and D). Upper figures compare modeled (red) vs. measured (black) values at 15 m depth (A and B) and 55 m depth (C and D). Lower figures exhibit model values over all depths for M2 (E) and M4 (F). Units are psu. (a) M2 15 m, (b) M2 55 m, (c) M4 15 m, (d) M4 55 m, (e) M2 MODEL and (f) M4 MODEL. (For interpretation of the references to color in this figure caption, the reader is referred to the web version of this article.)

A north/south gradient in temperature (SST, SBT) is especially striking in the leading spatial mode, and emerges as well in difference maps between mean forecast and hindcast temperatures (not shown). Dissolved inorganic nitrogen (NUT) appears to contribute substantially to the dominant mode using this full concatenated series, and is positively correlated with temperature in most areas. Mixing (AKT) is diminished and the MLD shoals broadly across the shelf, in synchrony with the warmer temperature. An onshore and northward shift of pelagic and benthic biomass is once again evident, as in the analysis using CORE/CFSR only (Fig. 14).

4. Discussion

4.1. Alternate statistical approaches

It is worth considering what we gain by the CPCA analysis, that we could not learn from simple difference maps. We might see very similar patterns if we grouped the warm vs. cold years, and took the difference between those climatologies. While both approaches presume that temperature is a controlling variable, the present CPCA approach allowed its importance to more spontaneously emerge

from the analysis, without an a priori selection of temperature categories. Further analysis will help to specify which atmospheric variables (e.g. air temperature vs. shortwave radiation) play the largest role in controlling the temperature field.

In their comparison of multivariate methods, Bretherton et al. (1992) noted that the modes produced by CPCA may exhibit a bias towards spatial structures similar to those of the most energetic univariate EOFs. In the present case, this likely means a bias towards a mode which fits much of the SST and SBT data. This is acceptable in our case, as the original intent was to seek modes which correlate with temperature. However, it is worth noting that other methods compared in Bretherton et al. (e.g. coupled correlation analysis) might produce a significantly different result. Our present usage of CPCA does appear robust, insofar as the three different choices of timeseries produced similar results.

4.2. Discrepancies with data

The primary mode computed from BASIS data exhibits correlated physical/biological properties: warmer sea surface and sea bottom

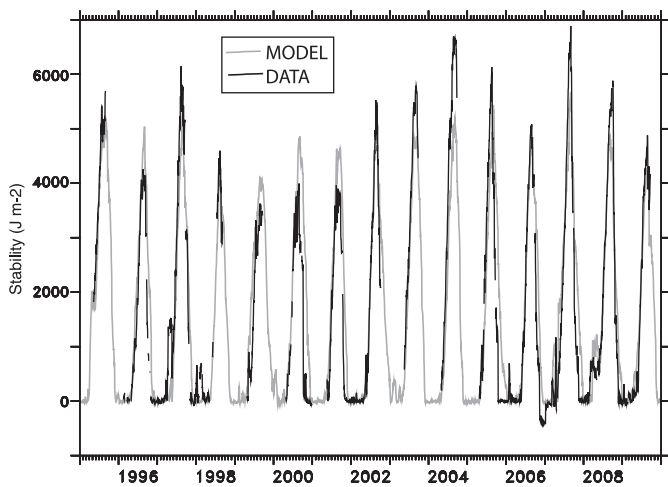


Fig. 10. Comparison of modeled (red) and measured (black) water column stability (J m^{-2}) at location M2. Measured values are from Ladd and Stabeno (2012). (For interpretation of the references to color in this figure caption, the reader is referred to the web version of this article.)

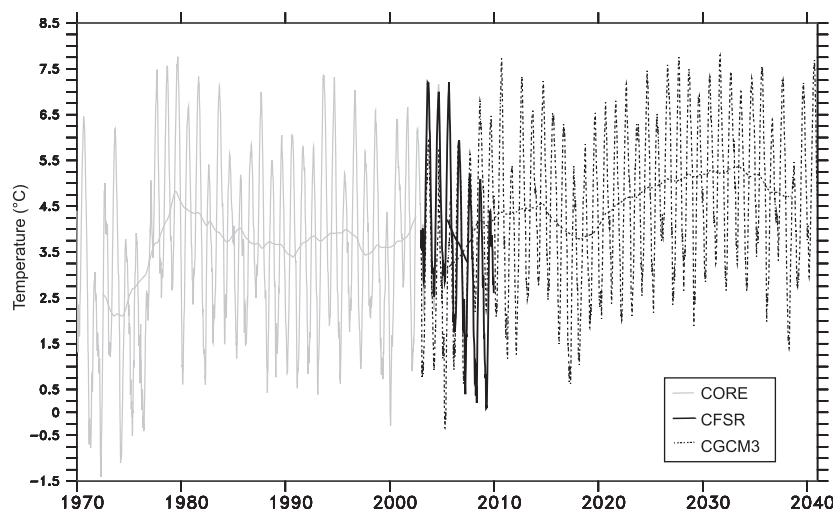


Fig. 11. Depth-averaged temperature at station M2 from model simulation using CORE hindcast forcing (black line), CFSR hindcast forcing (blue line), and CGCM3 forecast forcing (red line). Thin lines show weekly average values; thick line is 5-year running mean. Units are $^{\circ}\text{C}$. (For interpretation of the references to color in this figure caption, the reader is referred to the web version of this article.)

temperatures, increased sea surface salinity at mean location of the ice edge, and increased phytoplankton (or more specifically, chlorophyll) on the middle shelf. While physical variables in the leading mode from the model were very similar to their BASIS data counterparts, we failed to replicate the observed positive correlation of phytoplankton with temperature. This mismatch may be due to several factors, including a bias in the timing of the modeled fall bloom as compared with the measured fall bloom (Gibson et al., unpublished). The modes computed from the longer simulations, based on annual averages of scalar properties, do appear to exhibit a positive correlation between temperature and phytoplankton on the middle shelf. The strength of this correlation varies with the span of years chosen, and is strongest when the full concatenated series (CORE/CFSR/CGCM3) is used.

The model was calibrated to better fit summer temperatures, yet there was a residual tendency of the model to overestimate winter temperature and to underestimate ice cover. The ice model itself (Budgell, 2005) contains tunable parameters, such as the

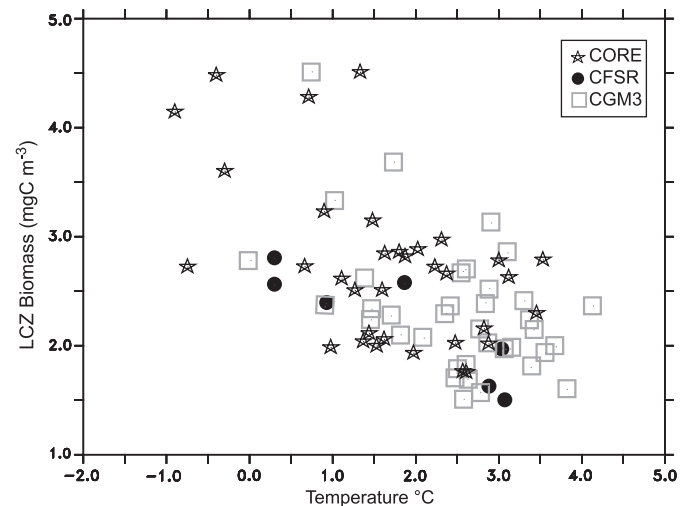


Fig. 12. Scatterplot of depth-averaged temperature ($^{\circ}\text{C}$) in spring vs. depth-averaged large crustacean zooplankton (LCZ, mg C m^{-3}) in fall at station M2, from model hindcasts and forecast. CORE, CFSR and CGM3 runs are marked with black, blue, and red stars, respectively. (For interpretation of the references to color in this figure caption, the reader is referred to the web version of this article.)

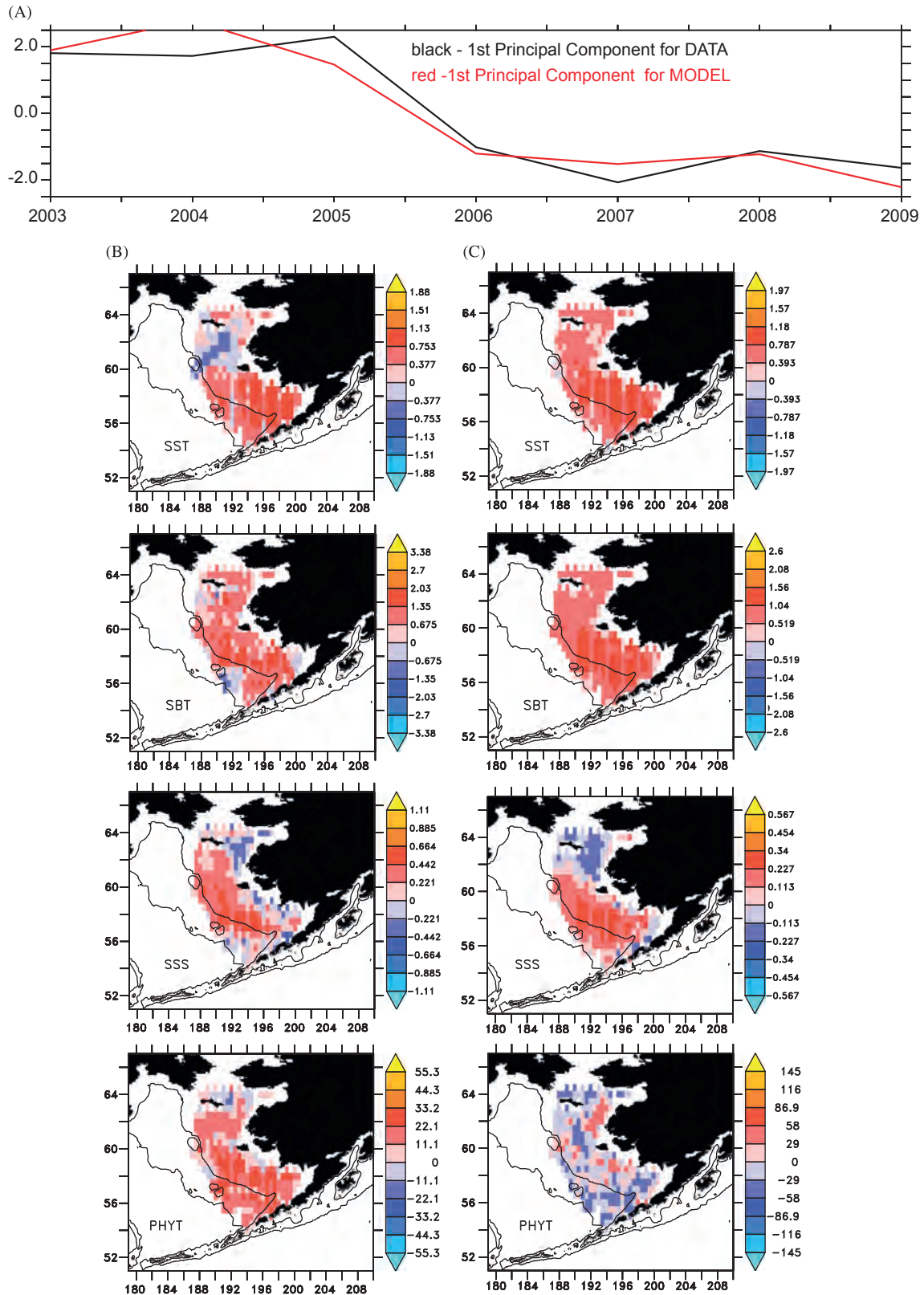


Fig. 13. Leading biophysical mode using gridded data and equivalent model output for the same variables. (A) First principal component for data (black line) and model (red line). The leading mode for data contains 43.0% of the total variance in its multivariate timeseries, and the leading mode for the model equivalent contains 49.6% of the variance in its multivariate timeseries. (B) Spatial loadings (EOFs) for each of the variables from BASIS data, converted back to their original units (listed in Table 2). Levels used for shading span -1 to $+1$ s.d. of each variable. Bathymetric contours at 70 m and 1000 m depth are shown. (C) Spatial loadings for each of the variables from the model, sampled at the same locations and times as the BASIS data. (a) PC1, (b) EOF1 for DATA and (c) EOF1 for MODEL. (For interpretation of the references to color in this figure caption, the reader is referred to the web version of this article.)

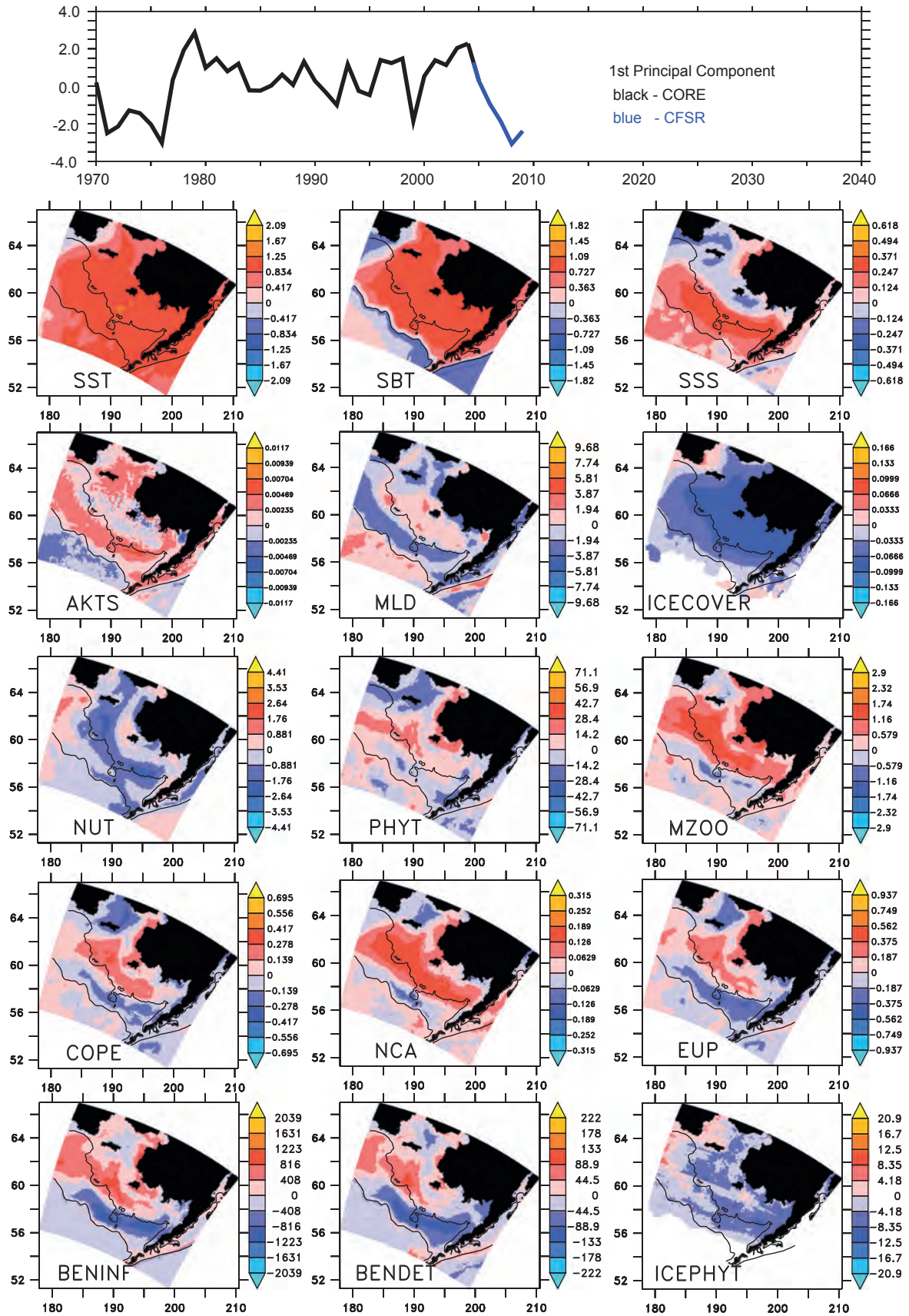


Fig. 14. Leading biophysical mode using model output from the combined CORE and CFSR hindcasts. Top figure shows the first principal component. Period of CORE (1970–2004, black line) and CFSR (2005–2009, blue line) hindcasts are indicated. This mode contains 15.1% of the total variance of the normalized timeseries. Panels exhibit the spatial loadings for each of the variables, converted back to their original units (listed in Table 3). Levels used for shading span -1 to $+1$ s.d. of each variable. Bathymetric contours at 70 m and 1000 m depth are shown. (For interpretation of the references to color in this figure caption, the reader is referred to the web version of this article.)

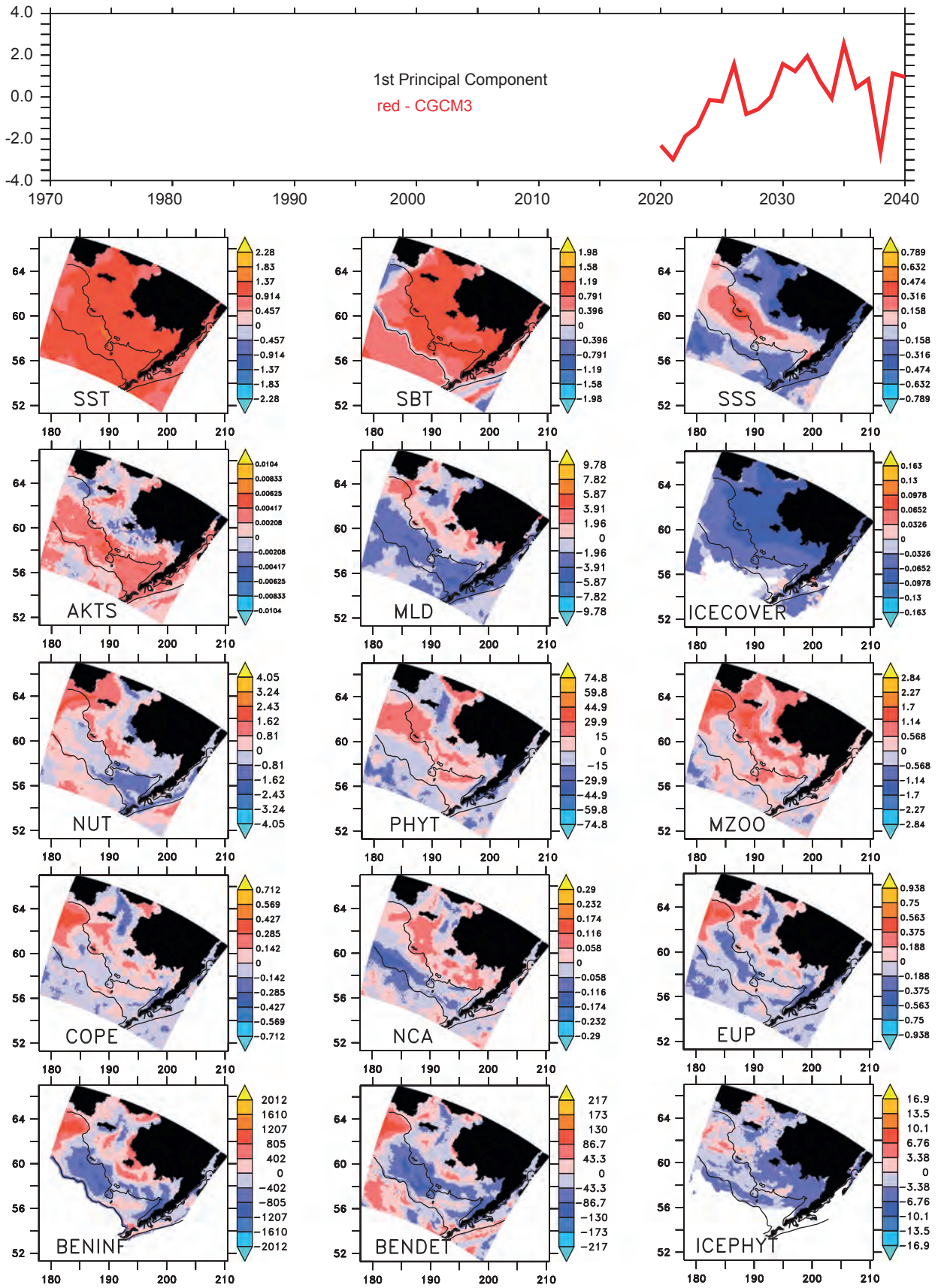


Fig. 15. Leading biophysical mode using only the last 20 years of the CGCM3 forecast (2020–2040). This mode contains 15.1% of the total variance of the normalized timeseries.

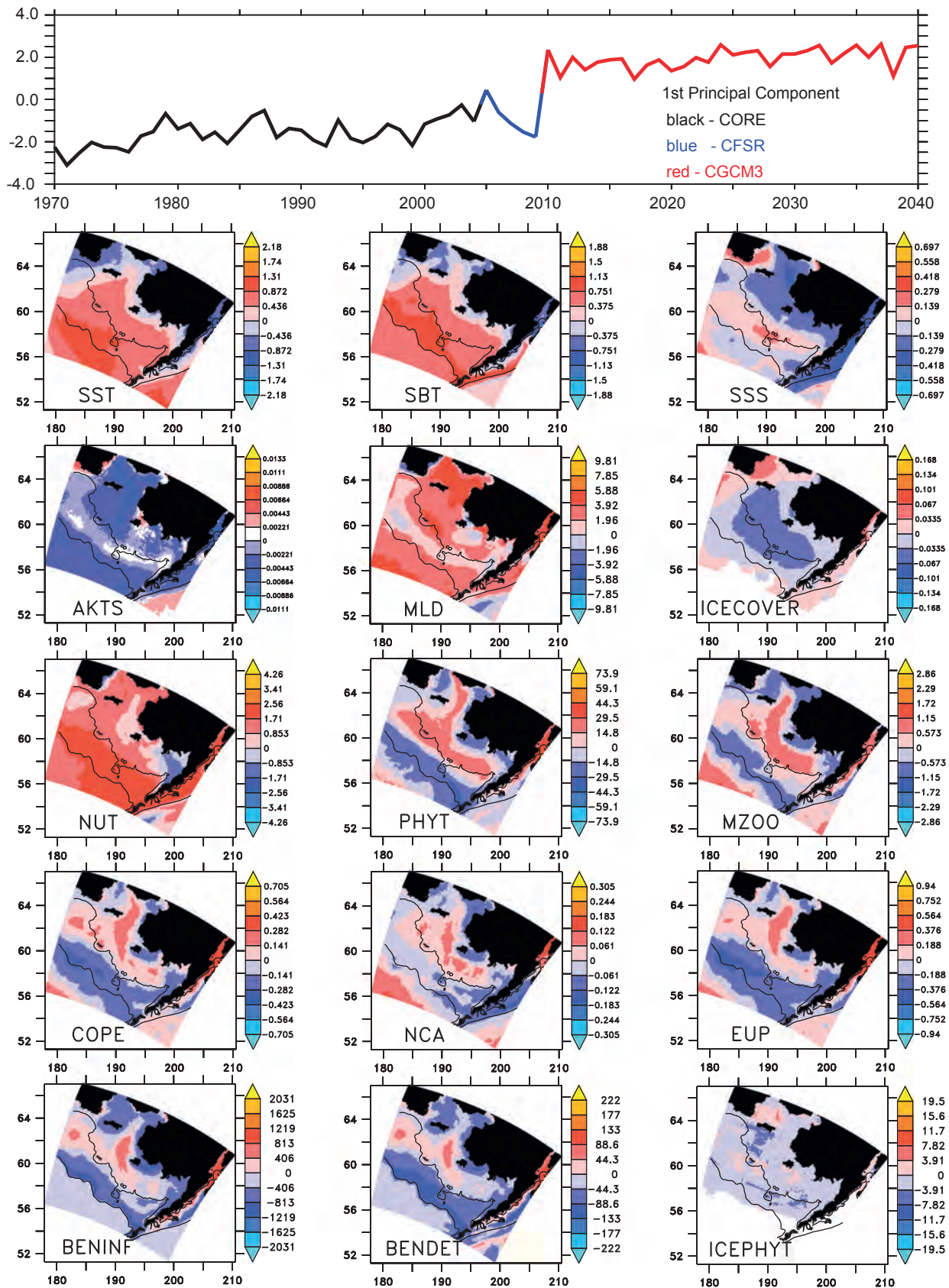


Fig. 16. Leading biophysical mode using a continuous series constructed from all three hindcasts: CORE (1970–2004, black line), CFSR (2005–2009, blue line) and CGCM3 (2010–2040, red line). This mode contains 21.5% of the total variance of the normalized timeseries. (For interpretation of the references to color in this figure caption, the reader is referred to the web version of this article.)

ratio of growth in ice area to growth in ice thickness when freezing takes place. These will be explored in future simulations.

4.3. Differences between hindcast and forecast runs

When the full concatenated series (CORE/CFSR/CGCM3) is used in the multivariate analysis (Fig. 16), the largest jump in the PC occurs between the end of the CFSR segment and the beginning of the CGCM3 segment. The series to either side of this jump are relatively flat. This may be due in part to the mismatch between what CGCM3 predicted for the 2003–2009 period, vs. what actually occurred; as a consequence the concatenated series includes a sharp jump in temperature between 2009 and 2010 (see Fig. 9). A second source of this discontinuity may be the fact that forcing datasets in hindcast vs. forecast periods are different in spatial and temporal resolution (see Table 1). Note in particular that CGCM3 winds were only available at daily time scales, whereas CORE and CFSR were available at 6-hourly time scales. The multivariate analysis attempts to capture variance in the most efficient manner, and this first mode may in fact be composed partly of the differences between these two datasets. As an example, if there were a bias towards a more northward ice edge in CGCM3, relative to CORE or CFSR, under equivalent atmospheric conditions, the leading EOF of the combined series would contain this change in bias.

4.4. Model results vs. the oscillating control hypothesis

As summarized in Section 1.1, the modified OCH of Hunt et al. (2011) predicts that cooler temperatures will lead to a larger biomass of large crustacean zooplankton, which in turn appear necessary (albeit not sufficient) for the successful recruitment of young walleye pollock. An earlier version of the OCH (Hunt et al., 2002) suggested that warmer temperatures should lead to greater production of both small and large copepods, but this was not borne out by data from the middle and outer shelf (Hunt et al., 2011). While we cannot address the fish-related elements (and associated bottom-up vs. top-down control scenarios) of the OCH in this version of the model, we can examine the conformance of our hindcast results (Fig. 14) to the relationships among lower trophic levels in the OCH.

Specifically, the modified OCH suggests the following should occur together in the eastern Bering Sea during a warm year: warmer SST, less ice, a later bloom of phytoplankton, and a higher ratio of pelagic to benthic production. Conversely, the following should occur in a cold year: cooler SST, more ice, an earlier bloom of phytoplankton, enhanced production of large crustacean zooplankton, and a lower ratio of pelagic to benthic production. The relationships in Fig. 14 are indeed suggestive of the modified OCH, but primarily on the middle and outer shelf. Note that all the zooplankton categories are enhanced/reduced on the inner shelf

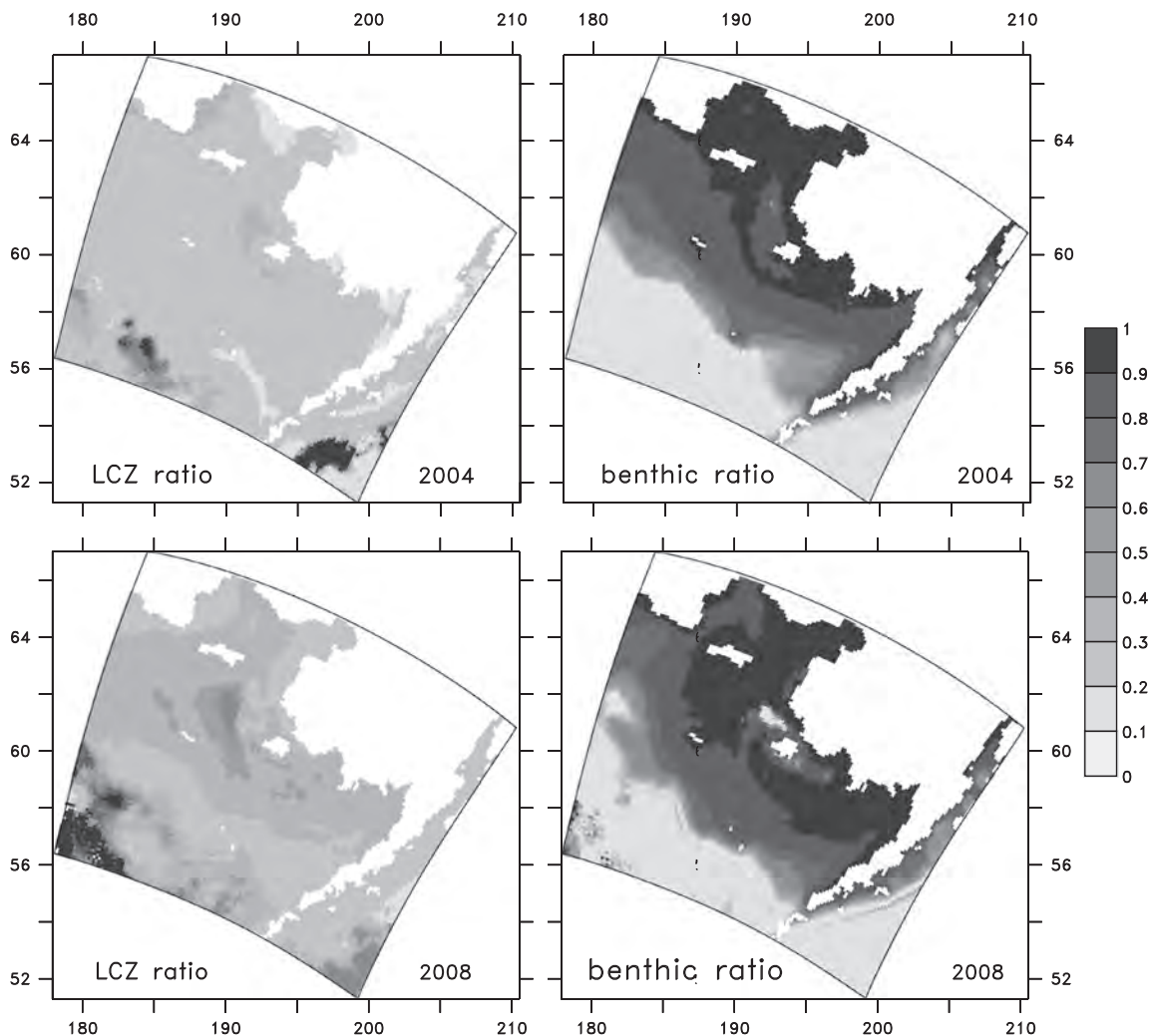


Fig. 17. Ratios of large crustacean zooplankton biomass to total zooplankton biomass (LCZ ratio), and benthic infauna biomass to total pelagic plus benthic biomass (benthic ratio), in warm (2004) vs. cold (2008) years, derived using the leading multivariate mode shown in Fig. 14.

(shoreward of the 70 m isobath) during warm/cold periods, while euphausiids and benthic biomass are significantly reduced/enhanced on the outer shelf during warm/cold periods. It would appear that for this model during 1970–2009, the inner shelf responds to higher temperatures by increasing zooplankton biomass across all size categories. By contrast, the middle and outer shelf respond to cold periods by enhancing euphausiid production (as in OCH) and enhancing benthic production (as in OCH), but only weakly enhancing small zooplankton.

A comparison of the patterns among variables in Fig. 14 suggests the following scenarios along the 70 m isobath during 1970–2009. In a cold year with more ice, lower salinity yields reduced mixing (as in Ladd and Stabeno, 2012, salinity stratification controls mixing over much of the shelf). Lower temperatures and enhanced ice cover (less light) yield lower pelagic production inshore, resulting in higher nutrient levels. Increased nutrients yield bigger zooplankton, and a shorter food chain. In a warm year, less ice results in higher salinity and enhanced mixing on the middle shelf. Higher temperatures and reduced ice cover (more light) lead to enhanced pelagic production which depletes nutrients, resulting in smaller zooplankton and a longer food chain. In each of these cases, the yearly average phytoplankton signal is modest (the timing of the bloom may shift, but that is not addressed by our analysis here).

We quantify some of these effects by reconstructing that portion of the original signal which consists of the temporal mean plus the correlated anomalies of the leading mode from the CORE/CFSR results (Fig. 14). For each variable, the anomalies are constructed by multiplying the PC timeseries by the EOF spatial patterns. Consider the case of a “warm” year (2004; PC value ~ 2.0) compared to a “cold year” (2008; PC value ~ -3.0). The EOF values on the southern, outer shelf (195E, 65 N) are approximately $+1\text{ }^{\circ}\text{C}$ for SST, -0.25 mg C m^{-3} for MZOO and -0.25 mg C m^{-3} for EUP. In 2008, our coupled multivariate signal consists of a 3° drop in SST, accompanied by a 0.75 mg C m^{-3} increase in MZOO, a 0.75 mg C m^{-3} increase in EUP, and a 1000 mg C m^{-3} increase in BENINF.

We add these anomalies to the temporal mean at each location, and subsequently compare the ratios of large crustacean zooplankton biomass to total zooplankton biomass (LCZ ratio), and benthic infauna biomass to total pelagic plus benthic biomass (benthic ratio). For the later ratio we distribute benthic biomass (BENINF) over the depth of the water column at each location (H):

$$\begin{aligned} \text{LCZ} &= \text{NCA} + \text{EUP} \\ \text{LCZ ratio} &= \text{LCZ} / (\text{LCZ} + \text{COPE} + \text{MZOO}) \\ \text{benthic ratio} &= (\text{BENINF} / \text{H}) / (\text{LCZ} + \text{COPE} + \text{MZOO} + (\text{BENINF} / \text{H})) \end{aligned}$$

In Fig. 17, we illustrate the results for warm (2004) vs. cold (2008) years. Both the LCZ ratio and the benthic ratio have increased in cold years. The LCZ ratio increases over the entire shelf, while the benthic ratio increases primarily on the outer, southern shelf. In this manner, the revised OCH is supported by the model all across the shelf, while an earlier version of the OCH (enhanced production of all sizes classes of zooplankton during warm periods; see Fig. 14) is supported by the model on the inner shelf alone. If COPE are included as part of the LCZ (not shown), the spatial pattern is shifted slightly, and the change in LCZ ratio is greater on the outer shelf, as compared with the version where $\text{LCZ} = \text{EUP} + \text{NCA}$ only.

5. Conclusions

A 10-level model of the Bering Sea captures key physical and biological dynamics of the region, and has been used to explore its multiyear and multidecadal variability. Model hindcasts and forecasts have been interpreted using a form of coupled principal

component analysis (CPCA). The leading mode of our CPCA analysis of biophysical model output for the Bering Sea exhibits correlated physical/biological properties with substantial inter-annual variability and a long-term warming trend. Several of the patterns observed conform to the revised oscillating control hypothesis (OCH). The following properties were observed:

- 1) All the zooplankton categories (microzooplankton, small copepods, neocalanus and euphausiids) exhibit similarities in spatial pattern, (positive correlation on the inner shelf, negative correlation on the outer shelf), but the relative magnitude of this response varies among small vs. large size classes.
- 2) Large crustacean zooplankton are negatively correlated with temperature on the outer, southwestern shelf, and positively correlated to temperature on the inner, northeastern shelf. Areas of positive correlation tend to correspond with those areas with greatest change in ice cover. As in the revised OCH, the ratio of large to total zooplankton is enhanced at lower temperatures. On the outer shelf, higher temperatures may be leading to reduced secondary production either through effects on stratification (and hence nutrient limitation), or through direct effects of temperature on growth, respiration, and vertical migration. Changes on the northern shelf may involve a complex interplay of light and nutrient limitation effects, as modulated by reduced ice cover. A closer examination of these relationships is warranted.
- 3) Salinity exhibits a strong signal at the mean location of the ice edge. As noted in Danielson et al. (2010, 2011), this likely due to the southward advection of freshwater in ice. In warm years there is less ice formation in the northeast (hence fresher there) and less ice melt at the southeastern extent of the ice (hence saltier there).
- 4) Benthos (benthic detritus and benthic infauna) and euphausiids are reduced on the middle and outer shelf with rising temperatures; this is correlated with a rise in both small and large zooplankton on the inner shelf. Under cold conditions, consistent with the OCH, the ratio of benthic to pelagic production appears to rise over most areas. A more explicit inclusion of production values (rather than biomass) will help to elucidate these factors.
- 5) Recent work by Danielson et al. (2012) underscores the importance of wind as a controlling variable which structures the Bering Sea system. In future multivariate analyses, we will utilize other groupings of variables, including the individual atmospheric forcing terms used by the model (winds and heat fluxes), to examine these relationships.

Acknowledgments

This research is contribution no. 3939 from NOAA/Pacific Marine Environmental Laboratory, and contribution ecoFOCI-0798 to NOAA's Ecosystems Fisheries Oceanography Coordinated Investigations. This publication is partially funded by the Joint Institute for the Study of the Atmosphere and Ocean (JISAO) under NOAA cooperative agreement NA10OAR4320148, contribution no. 2100. The research was generously supported by grants from the NSF sponsored Bering Sea Ecosystem Study (BEST) program (NSF-0732534), the North Pacific Research Board (NPRB) sponsored Bering Sea Integrated Ecosystem Research Program (BSIERP projects B52 and B70) and NOAA's North Pacific Climate Regimes and Ecosystem Productivity programs. This is BEST-BSIERP Bering Sea Project publication number 96 and NPRB publication number 418.

References

- Allen, J.I., Somerfield, P.J., 2009. A multivariate approach to model skill assessment. *J. Mar. Sys* 76 (1–2), 83–94.

- Andreas, E.L., Persson, P.O.G., Hare, J.E., 2008. A bulk turbulent air–sea flux algorithm for high-wind, spray conditions. *J. Phys. Oceanogr.* 38, 1581–1596.
- Aydin, K., Ortiz, I., Hermann, A.J. Climate to fisheries: high spatial resolution and bioenergetics in a multi-species vertically integrated model. Unpublished results.
- Bretherton, C.S., Smith, C., Wallace, J.M., 1992. An intercomparison of methods for finding coupled patterns in climate data. *J. Clim.* 5, 541–560.
- Budgell, W.P., 2005. Numerical simulation of ice–ocean variability in the Barents Sea region: towards dynamical downscaling. *Ocean Dyn.* 55, 370–387.
- Carton, J.A., Giese, B.S., 2008. A reanalysis of ocean climate using simple ocean data assimilation (SODA). *Mon. Wea. Rev.* 136, 2999–3017.
- Coachman, L.K., 1986. Circulation, water masses, and fluxes on the southeastern Bering Sea shelf. *Cont. Shelf Res.* 5 (1–2), 23–108.
- Coyle, K.O., Eisner, L.B., Mueter, F.J., Pinchuk, A.I., Janout, M.A., Ciciel, K.D., Farley, E.V., Andrews, A.G., 2011. Climate change in the southeastern Bering Sea: impacts on pollock stocks and implications for the oscillating control hypothesis. *Fish. Oceanogr.* 20 (2), 139–156.
- Dai, A., Qian, T., Trenberth, K.E., Milliman, J.D., 2009. Changes in continental freshwater discharge from 1948–2004. *J. Clim.* 22, 2773–2791.
- Danielson, S., Eisner, L., Weingartner, T., Aagaard, K., 2010. Thermal and haline variability over the central Bering Sea shelf: seasonal and inter-annual perspectives. *Cont. Shelf Res.* , <http://dx.doi.org/10.1016/j.csr.2010.12.010>.
- Danielson, S., Curchitser, E., Hedstrom, K., Weingartner, T., Stabeno, P., 2011. On ocean and sea ice modes of variability in the Bering Sea. *J. Geophys. Res.* 116, C12034, <http://dx.doi.org/10.1029/2011JC007389>.
- Danielson S., Hedstrom K., Aagaard K., Weingartner T., Curchitser E., 2012. Wind-induced reorganization of the Bering shelf circulation. *Geophys. Res. Lett.* 39, L08601, <http://dx.doi.org/10.1029/2012GL051231>.
- Flato, G.M., Boer, G.J., Lee, W.G., McFarlane, N.A., Ramsden, D., Reader, M.C., Weaver, A.J., 2000. The Canadian Centre for Climate Modelling and Analysis global coupled model and its climate. *Clim. Dyn.* 16, 451–467.
- Gibson, G.A., Hermann, A.J., Hedstrom, K., Curchitser, E.N. Response of euphausiid production to ‘cold’ and ‘warm’ years in the Bering Sea. Unpublished results.
- Gibson, G.A., Spitz, Y.H., 2011. Impacts of biological parameterisation, initial conditions, and environmental forcing on parameter sensitivity and uncertainty in a marine ecosystem model for the Bering Sea. *J. Mar. Syst.* 88, 214–231.
- Haidvogel, D.B., Arango, H., Budgell, W.P., Cornuelle, B.D., Curchitser, E., Di Lorenzo, E., Fennel, K., Geyer, W.R., Hermann, A.J., Lanerolle, L., Levin, J., McWilliams, J.C., Miller, A.J., Moore, A.M., Powell, T.M., Shchepetkin, A.F., Sherwood, C.R., Signell, R.P., Warner, J.C., Wilkin, J., 2008. Regional ocean forecasting in terrain-following coordinates: model formulation and skill assessment. *J. Comput. Phys.* 227, 3595–3624.
- Hunt Jr., G.L., Stabeno, P., Walters, G., Sinclair, E., Brodeur, R.D., Napp, J.M., Bond, N.A., 2002. Climate change and control of the southeastern Bering Sea pelagic ecosystem. *Deep-Sea Res.* 49 (26), 5821–5853, [http://dx.doi.org/10.1016/S0967-0645\(02\)00321-1](http://dx.doi.org/10.1016/S0967-0645(02)00321-1).
- Hunt Jr., G.L., Coyle, K.O., Eisner, L., Farley, E.V., Heintz, R., Mueter, F., Napp, J.M., Overland, J.E., Ressler, P.H., Salo, S., Stabeno, P.J., 2011. Climate impacts on eastern Bering Sea foodwebs: a synthesis of new data and an assessment of the oscillating control hypothesis. *ICES J. Mar. Sci.* 68 (6), 1230–1243, <http://dx.doi.org/10.1093/icesjms/fsr036>.
- Kachel, N.B., Hunt Jr., G.L., Salo, S.A., Schumacher, J.D., Stabeno, P.J., Whitedge, T.E., 2002. Characteristics and variability of the inner front of the southeastern Bering Sea. *Deep-Sea Res.* II 49 (26), 5889–5909, [http://dx.doi.org/10.1016/S0967-0645\(02\)00324-7](http://dx.doi.org/10.1016/S0967-0645(02)00324-7).
- Ladd, C., Bond, N.A., 2002. Evaluation of the NCEP/NCAR reanalysis in the NE Pacific and the Bering Sea. *J. Geophys. Res.* 107 (C10), 3158, <http://dx.doi.org/10.1029/2001JC001157>.
- Ladd, C., Stabeno, P.J., 2012. Stratification on the Eastern Bering Sea shelf revisited. *Deep-Sea Res.* II 65–70, 72–83.
- Large, W.G., McWilliams, J.C., Doney, S.C., 1994. Oceanic vertical mixing: a review and a model with a nonlocal boundary layer parameterization. *Rev. Geophys.* 32, 363–403.
- Large, W.G., Yeager, S.C., 2008. The global climatology of an interannually varying air–sea 1009 flux data set. *Clim. Dyn.* 33, 341–364.
- Marchesio, P., McWilliams, J.C., Shchepetkin, A., 2001. Open boundary conditions for long-term integration of regional oceanic models. *Ocean Model.* 3, 1–20.
- Preisendorfer, R.W., 1988. *Principal Component Analysis in Meteorology and Oceanography*. Elsevier, Amsterdam.
- Saha, S., et al., 2010. The NCEP climate forecast system reanalysis. *Bull. Am. Meteor. Soc.* 91, 1015–1057, <http://dx.doi.org/10.1175/2010BAMS3001.1>.
- Shchepetkin, A.F., McWilliams, J.C., 2005. The regional oceanic modeling system (ROMS): a split-explicit, free-surface, topography-following-coordinate oceanic model. *Ocean Model.* 9 (4), 347–404.
- Simpson, J.H., Allen, C.M., Morris, N.C.G., 1978. Fronts on the continental shelf. *J. Geophys. Res.* 83, 4607–4614.
- Stabeno, P.J., Reed, R.K., 1994. Circulation in the Bering Sea basin observed by satellite-tracked drifters: 1986–1993. *J. Phys. Oceanogr.* 24 (4), 848–854.
- Stabeno, P.J., Bond, N.A., Kachel, N.B., Salo, S.A., Schumacher, J.D., 2001. On the temporal variability of the physical environment over the south-eastern Bering Sea. *Fish. Oceanogr.* 10 (1), 81–98, <http://dx.doi.org/10.1046/j.1365-2419.2001.00157.x>.
- Stabeno, P.J., Bond, N.A., Salo, S.A., 2007. On the recent warming of the southeastern Bering Sea shelf. *Deep-Sea Res.* II 54 (23–26), 2599–2618, <http://dx.doi.org/10.1016/j.dsr2.2007.08.023>.
- Stabeno, P.J., Napp, J., Mordy, C., Whitedge, T., 2010. Factors influencing physical structure and lower trophic levels of the eastern Bering Sea shelf in 2005: sea ice, tides and winds. *Prog. Oceanogr.* 85 (3–4), 180–196, <http://dx.doi.org/10.1016/j.poccean.2010.02.010>.
- Stabeno, P.J., Kachel, N.B., Moore, S.E., Napp, J.M., Sigler, M., Yamaguchi, A., Zerbini, A.N., 2012. Comparison of warm and cold years on the southeastern Bering Sea shelf and some implications for the ecosystem. *Deep-Sea Res.* II 65–70, 31–45.
- Stabeno, P.J., Farley, E., Kachel, N., Moore, S., Mordy, C., Napp, J.M., Overland, J.E., Pinchuk, A.I., Sigler, M., 2012. A comparison of the physics of the northern and southern shelves of the eastern Bering Sea and some implications for the ecosystem. *Deep-Sea Res.* II, 65–70, 14–30.
- Wang, M., Overland, J.E., Bond, N.A., 2010. Climate projections for selected large marine ecosystems. *J. Mar. Syst.* 79 (3–4), 258–266, <http://dx.doi.org/10.1016/j.jmarsys.2008.11.028>.



Conceptual model of energy allocation in walleye pollock (*Theragra chalcogramma*) from age-0 to age-1 in the southeastern Bering Sea



Elizabeth C. Siddon^{a,*}, Ron A. Heintz^b, Franz J. Mueter^a

^a University of Alaska Fairbanks, School of Fisheries and Ocean Sciences, 17101 Pt. Lena Loop Road, Juneau, AK 99801, USA

^b Ted Stevens Marine Research Institute, Alaska Fisheries Science Center, National Marine Fisheries Service, National Oceanic and Atmospheric Administration, 17109 Pt. Lena Loop Road, Juneau, AK 99801, USA

ARTICLE INFO

Available online 8 December 2012

Keywords:

Walleye pollock (*Theragra chalcogramma*)
Larval fish
Bering Sea
Bioenergetics
Energy allocation
Recruitment

ABSTRACT

Walleye pollock (*Theragra chalcogramma*) support the largest commercial fishery in the United States and are an ecologically important component of the southeastern Bering Sea (SEBS) pelagic ecosystem. Alternating climate states influence the survival of walleye pollock through bottom-up control of zooplankton communities and possible top-down control of predator abundance. Quantifying the seasonal progression and spatial trends in energy content of walleye pollock provides critical information for predicting overwinter survival and recruitment to age-1 because age-0 walleye pollock rely on energy reserves to survive their first winter. Age-0 and age-1 walleye pollock were collected in the SEBS from May to September 2008–2010. Energetic status was determined through quantification of energy density (kJ/g) and proximate composition (i.e., % lipid, % moisture) with variation in energy density primarily driven by variability in % lipid. Energy densities remained relatively low during the larval phase in spring, consistent with energy allocation to somatic growth and development. Lipid acquisition rates increased rapidly after transformation to the juvenile form (25–40 mm standard length), with energy allocation to lipid storage leading to higher energy densities in late summer. This transition in energy allocation strategies is a physiological manifestation of survival constraints associated with distinct ontogenetic stages; a strategy favoring growth to escape size-dependent predation appears limited to larval development while juvenile fish allocate proportionally more mass to lipid storage in late summer. We propose that the time after the end of larval development and before the onset of winter represents a short critical period for energy storage in age-0 walleye pollock, and that overwinter survival depends on accumulating sufficient stores the previous growing season and consequently may be an important determinant of recruitment success.

© 2012 Elsevier Ltd. All rights reserved.

1. Introduction

Multiple factors during the early life stages of fishes result in variable recruitment success, including prey availability and environmental conditions (Cushing, 1982). Variability in the spatial and temporal overlap of predator and prey (match/mismatch hypothesis; Cushing, 1969, 1990), as well as differences in prey quality (Litzow et al., 2006; Sogard and Olla, 2000), affect fish growth and energy storage, which may directly affect differences in year-class success of many marine fish species, such as walleye pollock, *Theragra chalcogramma* (Hunt et al., 2011). In addition, cold water temperatures generally delay ontogenetic development of walleye pollock (Blood 2002; Smart et al., 2013) while also lowering routine metabolic

demands (Ciannelli et al., 1998). Such constraints affect larval fishes' ability to achieve sufficient size and energy reserves prior to their first winter (Heintz and Vollenweider, 2010; Sogard and Olla, 2000).

In high latitude systems, winter is a period of low light, cold temperatures, and reduced prey availability, and is therefore a significant source of mortality and determinant of recruitment success of marine fishes (Hurst, 2007). Overwintering survival is likely size-dependent because most sources of mortality tend to select against the smallest individuals (Bailey and Houde, 1989; Houde, 1987; Paul and Paul, 1999; Sogard and Olla, 2000). The 'critical size and period hypothesis' (Beamish and Mahnken, 2001) emphasizes the importance of increased body size in late summer and fall as indicative of winter survival (e.g., Moss et al., 2005). Lab studies have experimentally corroborated the effects of size on rates of energy depletion (Schultz et al., 1998), which are proportionally greater in smaller individuals (e.g., Atlantic silverside, *Menidia menidia*; Schultz and Conover, 1999 and

* Corresponding author. Tel.: +1 907 796 5460; fax: +1 907 796 5447.
E-mail address: ecsiddon@alaska.edu (E.C. Siddon).

walleye pollock; Kooka et al., 2007) due to higher weight-specific metabolism. Given the shorter growing season in high latitudes, marine fishes in these systems may have adapted to grow particularly fast in response to size-selective winter mortality (Conover, 1990).

Energy allocation strategies in larval and juvenile fish reflect competing physiological demands of somatic growth versus lipid storage (Post and Parkinson, 2001) and are a response to differing survival constraints. Somatic growth is important during the larval phase, as small fish are more susceptible to size-dependent predation. In contrast, lipid storage is important when fish face periods of food scarcity. By comparing the energy density and proximate composition (i.e., % lipid) of fish during early life stages, differing allocation strategies as well as the relative importance of these survival constraints can be identified. Fish with low energy density and % lipid values are allocating energy to growth and development; those with relatively high energy density and % lipid values are allocating proportionally more energy to storage.

Understanding variability of survival during the early life stages of commercially important species is pivotal to fisheries management in predicting year-class success (Megrey et al., 1996) and subsequent recruitment to the fishery. Numerous studies have established empirical links between recruitment and environmental variability (see Beamish and McFarlane, 1989), but incorporating the impacts of climate variability on survival into stock assessments requires knowledge of the mechanistic responses to alternate climate states (Hollowed et al., 2009). The energetic status of age-0 walleye pollock in late summer is increasingly recognized as a predictor of age-1 abundance during the following summer in the southeastern Bering Sea (SEBS; Heintz et al., this issue).

The Oscillating Control Hypothesis, initially proposed by Hunt et al. (2002), was revised (Hunt et al., 2011) based in part on new findings regarding the importance of energetic status to fish survival (Heintz et al., this issue). The OCH provides a theoretical framework within which to predict ecosystem responses to warm and cold regimes in the SEBS. In warm regimes with early ice retreat, stratified waters maintain production within the pelagic system (Walsh and McRoy, 1986), which was predicted to result in enhanced survival of species such as walleye pollock (Hunt and Stabeno, 2002; Mueter et al., 2006; Moss et al., 2009). However, recent data indicate that changes in prey composition and abundance during a warm regime may be detrimental to walleye pollock survival. Specifically, larger zooplankton taxa, such as lipid-rich *Calanus* spp., were less abundant during recent warm years, which resulted in reduced growth rates and lipid reserves of age-0 walleye pollock and may have increased their predation risk and decreased their overwinter survival (Coyle et al., 2011; Stabeno et al., 2012). In contrast, higher abundances of larger, lipid-rich zooplankton taxa during cold years, combined with lower metabolic demands, allowed age-0 walleye pollock to acquire greater lipid reserves by late summer, resulting in increased overwinter survival (Hunt et al., 2011).

Walleye pollock are major consumers of zooplankton at all life history stages (Aydin et al., 2007) with pronounced changes in prey preference throughout their early life (Ciannelli et al., 2004; Hillgruber et al., 1995; Kendall and Nakatani, 1992). Larvae begin diel vertical migration at approximately 10 mm standard length (SL; Kendall et al., 1994; Smart et al., 2013) with more pronounced vertical behavior and nocturnal feeding occurring at approximately 50 mm SL (Brodeur et al., 2000), coinciding with increased gape size and shifts to larger prey (i.e., euphausiids; Ciannelli et al., 1998). Ontogenetic changes in habitat preference (Brodeur et al., 2000) as well as visual acuity (Copp and Kovac, 1996) affect the vertical behavior of larval and juvenile fish. Walleye pollock are also an important forage species for other

predators, including arrowtooth flounder, *Atheresthes stomias*, Pacific cod, *Gadus macrocephalus*, skates, flathead sole, *Hippoglossoides elassodon*, Pacific halibut, *Hippoglossus stenolepis*, seabirds, and marine mammals (Aydin and Mueter, 2007). In addition, older age classes exhibit strong cannibalism on age-0 walleye pollock (Wespestad and Quinn, 1996), especially in warmer climate regimes (Hunt et al., 2011).

Despite the important role of walleye pollock in the SEBS pelagic ecosystem, and the relationship between age-0 energy density in late-summer and overwinter survival (Heintz et al., this issue), the energy allocation patterns during age-0 remain poorly understood. This paper describes larval and juvenile strategies for growth and energy storage in age-0 walleye pollock. By maximizing growth and transitioning through the larval period rapidly, larvae minimize exposure to size-dependent predation during this stage. However, overwinter survival is higher in fish that are both larger and have increased lipid reserves, indicating that energy allocation during the juvenile stage will favor lipid storage while also increasing fish size (i.e., critical size and period hypothesis; Beamish and Mahnken, 2001; Heintz and Vollenweider, 2010). We hypothesize that energy allocation strategies (i.e., favoring growth vs. storage) will differ seasonally among life stages and we tested this by contrasting body compositions of larval and juvenile fish. The goals of this study were to (1) describe cohort-specific patterns in energy density for walleye pollock from age-0 to age-1 and (2) describe seasonal patterns in energy allocation during larval and juvenile (age-0) development leading to estimates of energy levels prior to their first winter.

1.1. Study region

The SEBS is characterized by a broad (> 500 km) and shallow continental shelf that supports a highly productive ecosystem owing to on-shelf flow of nutrient-rich waters (Stabeno et al., 1999, 2001). Alternating climate states have resulted in periods of both warm and cold conditions in recent years. The most extensive ice cover and coldest water column temperatures since the early 1970s were observed beginning in 2007 and continued through at least the winter of 2010/2011 (Stabeno et al., 2012).

Current trajectories over the shelf are generally northward with the Bering Slope Current flowing along the shelf break and Alaska Coastal Current waters following either the 50 m or 100 m isobaths (Stabeno et al., 2001). The onset and location of fronts affect current trajectories (Kachel et al., 2002) and, therefore, transport pathways of larvae (Duffy-Anderson et al., 2006). The main spawning areas for walleye pollock over the SEBS shelf include north of Unimak Island and along the Alaska Peninsula and around the Pribilof Islands (Bacheler et al., 2010; Hinckley 1987). Larvae are generally advected northward over the shelf with slope-spawned larvae advected onto the shelf via the Bering Slope Current, as inferred from their spawning locations and summer distributions (Bacheler et al., 2010).

2. Materials and methods

2.1. Biological sampling

Age-0 and age-1 walleye pollock were collected from 13 research surveys conducted in the SEBS between May and September 2008–2010 (Table 1; Fig. 1). The geographic coverage varied across cruises. Sampling for age-0 fish is assumed to encompass the bulk of their distribution based on historical data (Bacheler et al., 2010), while age-1 fish were predominantly sampled from the outer shelf domain (between 100 and 200 m isobaths; Fig. 1). Gear type, mesh size, and sampling depth also

Table 1

Year, season, sampling dates, and gear used to collect age-0 and age-1 walleye pollock (*T. chalcogramma*). The mean (\pm standard error, *n*) energy density, % lipid, and standard length (mm) are shown for each cruise by age class.

Age-0							
Year	Season	Dates	Gear	Mesh size	Energy density (kJ/g)	% Lipid	Standard length (mm)
2008	Spring	May 12–21	Bongo	505 μ m		8.51 (0.94, 13)	5.67 (0.07, 274)
2008	Mid-summer	July 3–17	MOCNESS	505 μ m	17.99 (0.68, 6)	11.36 (0.45, 18)	10.61 (0.14, 168)
2008	Late-summer	September 7–30	Rope trawl	1.2 cm codend liner	23.35 (0.22, 37)	21.49 (0.82, 31)	62.7 (1.25, 102)
2008	Late-summer	September 9–20	Beam trawl	7 mm; 3 mm codend liner	22.36 (0.18, 34)		66.82 (1.34, 33)
2009	Mid-summer	June 14–July 12	MOCNESS	505 μ m	16.95 (0.68, 4)	8.34 (0.26, 89)	8.79 (0.14, 251)
2009	Late-summer	September 2–30	Rope trawl	1.2 cm codend liner	22.81 (0.14, 50)	17.98 (0.84, 46)	67.1 (1.08, 100)
2010	Spring	May 6–18	Bongo	505 μ m		2.15 (0.30, 22)	5.67 (0.05, 164)
2010	Mid-summer	June 16–July 14	MOCNESS	505 μ m	15.39 (0.88, 3)	6.0 (0.23, 66)	8.88 (0.14, 135)
2010	Late-summer	August 16–September 26	Rope trawl	1.2 cm codend liner	22.64 (0.11, 89)		59.8 (0.76, 104)
2010	Late-summer	September 2–15	Beam trawl	7 mm; 3 mm codend liner	22.43 (0.25, 34)		62.38 (1.9, 34)
Age-1							
2008	Summer	June 2–July 31	Methot trawl	2 \times 3 mm; 1 mm codend liner	23.13 (0.12, 49)	19.44 (0.52, 49)	132.46 (1.67, 49)
2009	Summer	June 9–August 7	Methot trawl	2 \times 3 mm; 1 mm codend liner	22.99 ^a (0.18, 34)	17.97 (1.0, 34)	138.45 (3.46, 34)
2009	Late-summer	September 2–30	Rope trawl	1.2 cm codend liner	23.51 ^a (0.34, 18)	18.8 (1.66, 18)	155.04 (6.23, 19)
2010	Summer	June 5–August 7	Methot trawl	2 \times 3 mm; 1 mm codend liner	24.41 (0.17, 34)	25.58 (0.72, 34)	148.25 (2.98, 34)

^a Energy density values were predicted from % lipid values based on the regression relationship: energy density = 20.1 + 0.76% lipid.

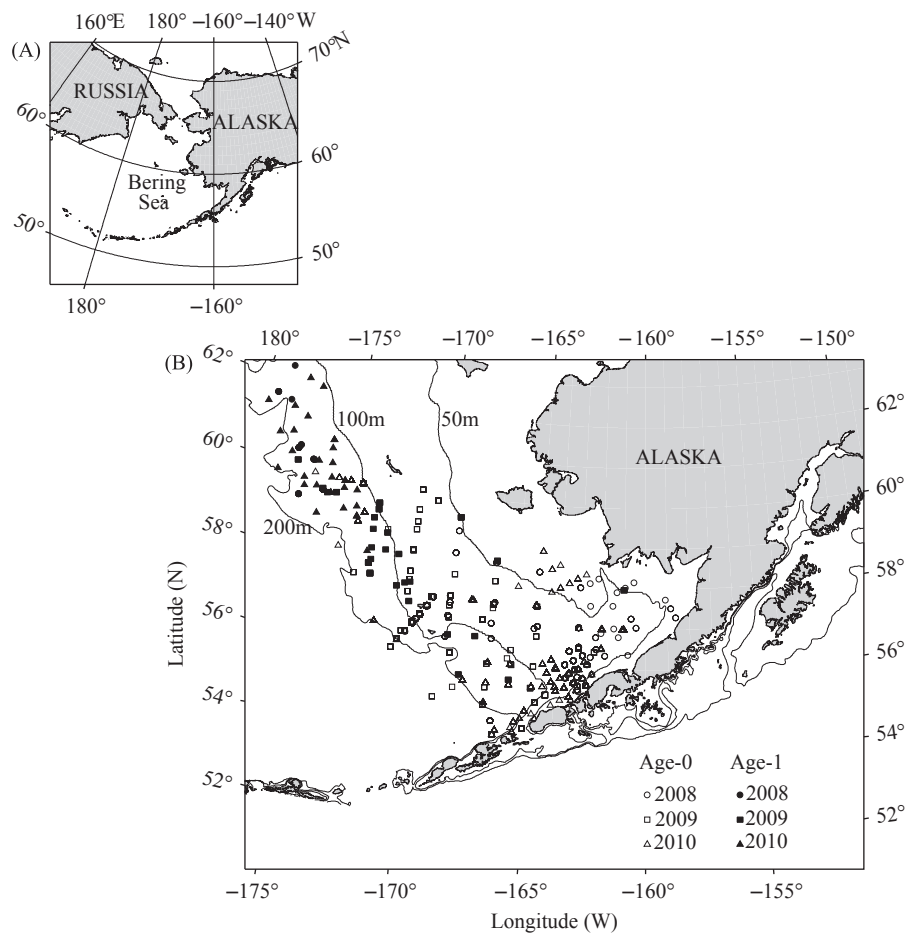


Fig. 1. (A) Map showing the location of the Bering Sea. (B) Map of the southeastern Bering Sea showing the location of sample collections by age class and year. Sampling for age-0 fish is assumed to encompass the bulk of their distribution based on historical data, while age-1 fish were predominantly sampled from the outer shelf domain (between 100 and 200 m isobaths). Depth contours are shown for the 50 m, 100 m, and 200 m isobaths.

varied across cruises to target the life stages occurring at the time of sampling (Table 1; Shima and Bailey, 1994).

Vertically integrated oblique bongo tows were made during spring cruises to a maximum depth of 300 m (or to within 10 m of the seafloor) to sample larval walleye pollock. During mid-summer, larval walleye pollock were sampled from the drogue net of the

MOCNESS (Multiple Opening/Closing Net and Environmental Sensing System), which was open during deployment, thereby providing vertically integrated samples to a maximum depth of 100 m (or to within 10 m of the seafloor). Bongo and MOCNESS sampling occurred 24 h a day, therefore it was assumed that vertically integrated sampling was not affected by diel vertical migrations of walleye

pollock. The ship speed was monitored and adjusted (1.5–2.5 knots) throughout all bongo and MOCNESS tows to maintain a wire angle of 45°. Surface and midwater rope trawls were used to sample age-0 and age-1 walleye pollock during late summer. Sampling was conducted during daytime only with the surface and midwater rope trawl sampling above and below the pycnocline, respectively, as determined by water column profiles of temperature and salinity obtained using a Sea-Bird SBE-911 CTD. Fish were predominantly observed and collected from surface waters in 2008 and from the surface and midwater in 2009; in 2010, only walleye pollock collected from surface rope trawls were used in the analyses in order to facilitate interannual comparisons across 2008–2010. In addition to the surface and midwater trawls, the beam trawl sampled near-bottom fishes during late summer as walleye pollock begin to descend in the water column. Methot trawls were used to target midwater walleye pollock from observed acoustics layers (Table 1). Beam and Methot trawl sampling occurred 24 h a day. For this study, we combined walleye pollock from different vertical layers, assuming that vertical differences in energy content are negligible.

After retrieval of the gear, walleye pollock were selected from the catch to represent the size range observed in each haul. Fish were flash frozen (−80 °C) for later chemical analysis at the Alaska Fisheries Science Center, NOAA (National Oceanic and Atmospheric Administration) in Juneau, Alaska, USA. Larvae were measured to the nearest 0.01 mm length (standard, fork, or total) while juvenile and age-1 fish were measured to the nearest mm fork length (FL). All lengths were converted to SL using established conversions for walleye pollock preserved by freezing (Buchheister and Wilson, 2005). Fish were classified as age-0 (larvae < 30 mm SL; juvenile > 30 mm and < 100 mm SL; Matarese et al., 1989) or age-1 (> 100 mm SL and < 200 mm SL) based on length-frequency distributions.

2.2. Chemical analysis

Stomach contents of fish > 8 mm SL were removed prior to chemical analysis so as not to affect estimates of energy density or % lipid.

2.2.1. Energy density

Energy density (ED; kJ/g dry mass) was estimated directly using bomb calorimetry or indirectly from estimates of % lipid (see Proximate composition). Larvae were dried in a drying oven (60 °C) to a constant weight and all data are presented on a dry mass basis. Homogenized tissue was pressed into a pellet form and a Parr Instrument 6725 Semimicro Calorimeter with 6772 Precision Thermometer and 1109A Oxygen Bomb was used to measure the energy released from combustion of the sample pellets. The minimum pellet weight was set at 0.025 g of dry material based on the limits of instrument detection; samples were composited within stations as needed to attain sufficient dry masses for larvae collected in spring and mid-summer. Juvenile and age-1 fish were dried to a constant weight at 135 °C using a LECO Thermogravimetric Analyzer (TGA) 601 or 701 which provided % moisture values used to convert wet mass to dry mass equivalents. The dried tissue was homogenized and processed using the bomb calorimeter as described above. Moisture analysis for juvenile and age-1 fish was replicated when sufficient sample mass was available to ensure the coefficient of variation (CV) for % moisture was less than 1 standard deviation (SD). When sufficient sample mass was not available, we relied on the CV for a reference material (dried adult walleye pollock homogenate) to obtain duplicate estimates of energy density or % moisture processed with each batch of fish ($n=17$ for energy density; $n=15$ for % moisture).

Quality assurance (QA) procedures for the bomb calorimeter included (1) duplicate tissue estimates (sample or walleye pollock reference material) to evaluate precision and (2) duplicate reference material (benzoic acid standard) to evaluate precision and accuracy. Predetermined limits for variation observed in QA samples were set, where precision estimates from duplicate tissue and reference samples must not vary by more than 1.5 SD or 15% CV and reference samples must not vary by more than 15% CV for accuracy. QA samples did not exceed these limits for any batch of samples used in this study.

2.2.2. Proximate composition

For larvae, a sulfo-phospho-vanillin (SPV) colorimetric analysis (Van Handel, 1985) was performed to determine % lipid composition, which is presented on a dry mass basis. Dried material was sonicated in 2:1 (by volume) chloroform:methanol solvent in glass centrifuge tubes for 60 min. Washes of 0.88% KCl and 1:1 (by volume) methanol:water were performed on the extracts as in the modified Folch extraction method (Vollenweider et al., 2011). Resulting chloroform extracts were evaporated in a LabConco RapidVap for 30 min at 40 °C and 250 mbar until reduced to approximately 1 ml in volume. Extracts were evaporated to dryness in 12 mm test tubes on a heating block at 75 °C and then allowed to cool. Concentrated sulfuric acid was added to the tubes prior to incubation at 100 °C for 10 min with subsequent cooling. The SPV reagent (1.2 mg/ml vanillin in 80% phosphoric acid) was added to each tube and allowed to develop for 10 min. Absorption was measured on an Agilent 8453 Spectrophotometer at 490 nm and extrapolated from species-specific calibration curves determined prior to analysis. For juvenile and age-1 fish, proximate composition analysis was performed as previously described (Vollenweider et al., 2011), with lipid extractions utilizing a Dionex ASE (accelerated solvent extractor) 200 and a modified Folch extraction procedure using a 2:1 (by volume) chloroform:methanol solvent mixture. Measurements of % lipid for juvenile and age-1 fish were converted to dry mass equivalents using estimates of % moisture obtained from the TGA (see above).

QA procedures for the SPV data included two blank runs to estimate background absorption, two method blank samples containing all analysis reagents but no lipid extract to evaluate contamination and reagent absorption, and two reference samples (adult walleye pollock homogenate) to examine precision and accuracy for each batch of 15 samples. Mean background absorbance was subtracted from sample absorbance values. Method blank samples had to be < 10 mg of lipid and walleye pollock reference samples had to vary by < 1 SD and be accurate within 15% of the established lipid value. ASE samples used similar QA criteria except that the method blank samples were allowed to be as high as 0.1 mg of lipid (due to much higher analyzed lipid masses).

To compare energy densities of walleye pollock from age-0 to age-1 for the cohort analysis, a linear regression was used to predict energy density estimates from % lipid values for age-1 fish collected during two cruises (summer 2009 Methot trawl and late-summer 2009 rope trawl surveys; Table 1). All age-1 fish processed for both energy density and % lipid ($n=83$) were used to develop a regression relationship, $ED=20.1+0.76*\% \text{ lipid}$ ($R^2=0.79$) that was used to predict energy density. The size of the fish used in the regression ranged from 109 to 194 mm SL. Direct estimates of energy density from the bomb calorimeter were used when available.

2.3. Statistical analysis

2.3.1. Cohort-specific patterns from age-0 to age-1

Cohort-specific patterns in energy density from age-0 to age-1 were examined to determine the extent of interannual variation

in the seasonal patterns using two complete cohorts. The 2008 cohort was sampled as age-0 fish in mid- and late-summer 2008, and as age-1 fish in summer and late-summer 2009. The 2009 cohort was sampled as age-0 fish in mid- and late-summer 2009, and as age-1 fish in summer 2010. Energy densities were compared between age-0 fish in mid-summer, age-0 fish in late-summer, and age-1 fish using separate one-way ANOVAs (analysis of variance).

2.3.2. Seasonal patterns in energy allocation of age-0 fish

Seasonal patterns in energy allocation during age-0 larval and juvenile development were analyzed using generalized additive mixed models (GAMMs) to identify the seasonal timing and size (i.e., length) at which walleye pollock shift energy allocation strategies from growth to lipid storage. These models do not specify a fixed functional form, but rather quantify the relationship between a set of predictors and the response variable through non-parametric smooth functions of the predictor variables. The optimum amount of smoothing was chosen by generalized cross-validation as implemented in the R package 'mgcv' (Wood, 2006).

Variability in energy density and % lipid during the larval and juvenile stages were modeled as a function of SL to estimate changes in energy allocation with fish size. Fish for which SL measurements were not available were removed from models ($n=5$ and 6 for energy density and % lipid, respectively). Models for energy density, % lipid, and SL included sampling date (date) to estimate seasonal trends, a year term to account for differences in the mean response among years, and a spatial smooth term (thin-plate regression spline fit to latitude and longitude) to describe and account for differences in the mean energy density, % lipid, or SL across stations and to reduce spatial autocorrelation. Based on residual diagnostics, estimates of energy density and % lipid identified as influential outliers ($n=5$ and 8 , respectively) were removed from further analyses; removing these outliers did not affect our conclusions. The sampling area differed among cruises as did the number of fish processed per station, therefore modeling approaches that accounted for spatial patterns and/or included a random station effect were compared using Akaike Information Criterion (AIC) (Akaike, 1973; Burnham and Anderson, 2002). The full models included station as a random effect to account for variability among stations (a_i), in addition to within-station residual variability (ε_{ik}):

$$y = \alpha + f_1(\text{SL}) + f_2(\text{date}) + f_3(\text{latitude, longitude})_k + Y_k + a_i + \varepsilon_{ik}$$

$$\text{SL} = \alpha + f_4(\text{date}) + f_5(\text{latitude, longitude})_k + Y_k + a_i + \varepsilon_{ik}$$

$$a_i \sim N(0, \sigma_a^2)$$

$$\varepsilon_{ik} \sim N(0, \sigma_\varepsilon^2)$$

where y is energy density or % lipid, f_1 , f_2 , and f_4 are smooth functions of the predictor variables, f_3 and f_5 are smooth spatial surfaces for a given year k (with degrees of freedom limited to five to restrict flexibility in the fitted surface), and Y_k is the year-specific intercept for year k . The random effects a_i and residuals ε_{ik} are assumed to be independent and normally distributed with mean 0 and variances σ_a^2 and σ_ε^2 , respectively.

Random effects and residuals from the models were examined for normality, homoscedasticity, and independence by plotting them against all relevant covariates and by examining spatial patterns in the random station effects by year. Each term in the full model was evaluated for significance and dropped from the model if it was not significant. Differences in spatial variability across years were evaluated by comparing the full model to a model that fit a single smooth spatial surface across years using

AIC. Residual diagnostics for all resulting best models showed no unusual trends and no evidence of remaining spatial autocorrelation; diagnostic plots are not presented.

3. Results

3.1. Biological sampling

A total of 1501 age-0 and age-1 walleye pollock collected from 13 cruises over the 3-year sampling period were measured for standard length with 341 estimates of energy density (kJ/g) from bomb calorimetry ($n=257$ age-0 including 13 composite samples, $n=84$ age-1) and 423 estimates of % lipid ($n=285$ age-0 including 41 composite samples, $n=135$ age-1) (Table 1). The overall mean energy density (\pm SE) of age-0 and age-1 walleye pollock was 22.43 ± 0.11 and 23.67 ± 0.12 (kJ/g dry mass), respectively, and overall mean % lipid (\pm SE) for age-0 and age-1 fish was 10.58 ± 0.40 and 20.53 ± 0.49 (on dry mass basis), respectively.

3.2. Cohort-specific patterns from age-0 to age-1

The 2008 and 2009 cohorts had similar seasonal patterns of energy density overall. Age-0 fish from both cohorts had low mean energy densities in mid-summer with no significant difference between cohorts (1-way ANOVA: $F_{(1,9)}=1.07$, $P=0.33$). There was a short period from mid-July to mid-September during which energy density rapidly increased by approximately 25% in late-summer 2008 and 2009 (Table 1, Fig. 2). Energy density of age-0 fish during late-summer 2008 was significantly higher during the rope trawl survey (mean sampling date=September 27) than the beam trawl survey (mean sampling date=September 9), with late-summer 2009 having an intermediate energy density (1-way ANOVA: $F_{(2,120)}=7.04$, $P<0.01$). Age-1 fish of both the 2008 and 2009 cohorts had energy densities similar to those of age-0 fish the previous year in late summer. However, the 2009 cohort had significantly greater energy density at age-1 than the 2008 cohort (1-way ANOVA: $F_{(2, 85)}=13.68$, $P<0.001$; Fig. 2).

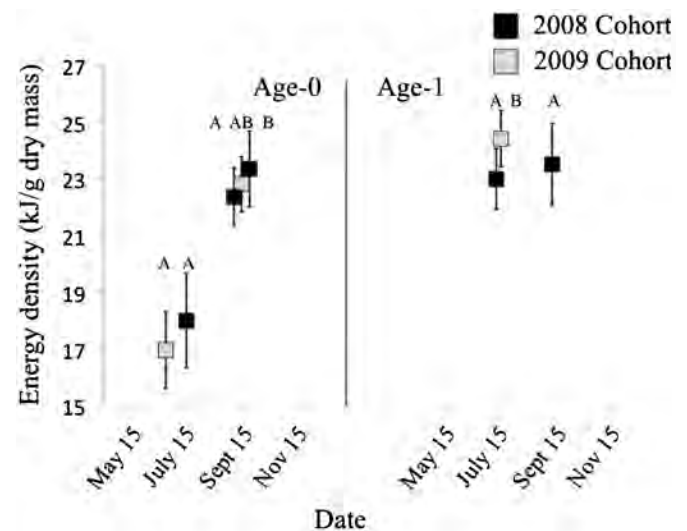


Fig. 2. Plot of energy density (kJ/g dry mass) for the 2008 and 2009 cohorts of walleye pollock (*T. chalcogramma*). Error bars are plotted as ± 1 standard deviation to show the variability in energy density estimates for each sampling interval. Different letters indicate significant differences in energy density within season. Note x-axis is mean sampling date across the age-0 and age-1 seasons.

3.3. Seasonal patterns in energy allocation of age-0 fish

Patterns in energy density, % lipid, and SL were described using unique combinations of explanatory variables. Variability in energy density was best explained by SL, a spatial smooth term, a random station effect, and year (adjusted $R^2=0.688$; $n=247$). Patterns in % lipid were best explained by SL, sampling date, a random station effect, and year (adjusted $R^2=0.847$; $n=271$) while patterns in SL were best explained by sampling date, a spatial smooth term, a random station effect, and year (adjusted $R^2=0.955$; $n=1365$; Table 2). The effect of fish length is difficult to separate from the seasonal pattern because SL is strongly correlated with sampling date in larvae that were measured for energy density ($r=0.56$) and for % lipid ($r=0.91$), although largely uncorrelated for juveniles (energy density $r=0.086$; % lipid $r=-0.35$). Therefore, for juveniles, we can statistically separate the apparent effects of size from the seasonal pattern of fish condition.

Patterns in energy density for larval walleye pollock had large uncertainty because samples had to be composited to acquire sufficient dry mass for analytical processing. Sampling date was not significant in the full model indicating that changes in energy density are primarily driven by changes in fish length rather than seasonal changes. For a given location and year, energy density was below average at small sizes, increased to above-average energy densities at around 55 mm, and reached an asymptote at approximately 75 mm SL (Fig. 3a). The spatial patterns in energy density varied significantly among years, although the relative

effect of sampling location was small compared to the importance of SL in explaining patterns of variability (e.g., small range of predicted values in Fig. 3b). Average energy density was highest in 2008, lowest in 2009, and intermediate in 2010 (Fig. 3c).

Percent lipid in larvae seems to decrease with increasing length up to 20 mm SL; patterns are uncertain for fish 20–40 mm SL due to lack of samples. In fish > 40 mm SL, % lipid increases linearly with increasing size (Fig. 4a). Lipid content increased linearly over time, although variability in these estimates was high (Fig. 4b). The magnitude of the effect of SL on lipid content was comparable to that of the seasonal effect, as indicated by the range in % lipid anomalies between Fig. 4a and b. The average % lipid of age-0 walleye pollock differed significantly from 2008 to 2010 (Fig. 4c), but we did not see a consistent trend in average energy density over the same time period (Fig. 3c). However, we do not have estimates of % lipid for all sampling periods in all years of the study, therefore we cannot fully address interannual differences in % lipid.

Walleye pollock lengths increased slowly during spring, but rapidly after approximately July 15. Fish lengths reached an

Table 2

Summary of generalized additive mixed model (GAMM) fits for energy density, % lipid, and standard length showing terms, coefficient estimates, standard error (SE) for fixed coefficients, degrees of freedom (d.f.; number of parameters for each term in the model, estimated for smooth terms), and P -values. P -values for parametric terms (intercept, year coefficients) based on t -test of the null hypothesis that the coefficient is equal to zero; for smooth terms (f_i) based on an approximate F -test (Wood, 2006); for random effects term (σ_a) based on likelihood ratio test. The intercept (α) corresponds to the 2008 means and the subsequent year effects (Y_k) correspond to the difference between that year's mean and the intercept; f_1 , f_2 , and f_4 are smooth terms (SL=standard length; date=sampling date); f_3 and f_5 are smooth spatial surfaces (lat=latitude; long=longitude) by year k , and ϵ_{ik} is within-station residual variability.

Model (adjusted R^2)	Term	Estimate	SE	d.f.	P -value
Energy density (0.688)					
	Intercept (α)	22.93	0.15	1	< 0.001
	Y_{2009}	-1.09	0.26	1	< 0.001
	Y_{2010}	-0.52	0.19	1	0.007
	f_1 (SL)			3.7	< 0.001
	f_3 (lat, long) ₂₀₀₈			2.9	< 0.001
	f_3 (lat, long) ₂₀₀₉			2	< 0.001
	f_3 (lat, long) ₂₀₁₀			2	0.16
	$\sigma(a_i)$	0.49		1	< 0.001
	$\sigma(\epsilon_{ik})$	0.71		1	
% Lipid (0.847)					
	Intercept (α)	13.22	0.50	1	< 0.001
	Y_{2009}	-2.65	0.59	1	< 0.001
	Y_{2010}	-5.50	0.69	1	< 0.001
	f_1 (SL)			3.9	< 0.001
	f_2 (date)			1	< 0.001
	$\sigma(a_i)$	1.58		1	< 0.001
	$\sigma(\epsilon_{ik})$	2.06		1	
Standard length (0.955)					
	Intercept (α)	20.53	1.22	1	< 0.001
	Y_{2009}	6.84	1.89	1	< 0.001
	Y_{2010}	2.1	1.65	1	0.2
	f_4 (date)			6.36	< 0.001
	f_5 (lat, long) ₂₀₀₈			2	< 0.001
	f_5 (lat, long) ₂₀₀₉			2.89	< 0.001
	f_5 (lat, long) ₂₀₁₀			2	0.46
	$\sigma(a_i)$	5.68		1	< 0.001
	$\sigma(\epsilon_{ik})$	3.79		1	

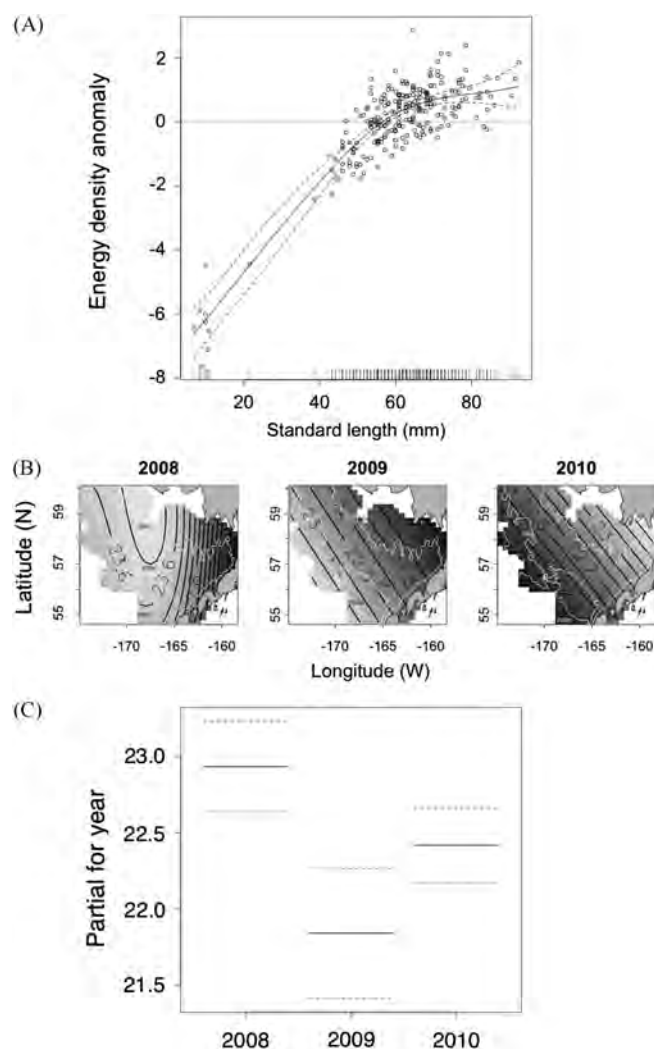


Fig. 3. Results from generalized additive mixed model (GAMM) regression analyses showing the estimated effects on energy density (kJ/g dry mass) of (a) standard length (SL; mm), (b) spatial location (by year), and (c) year for age-0 walleye pollock (*T. chalcogramma*). Dashed lines denote 95% confidence intervals in (a) and (c). Energy densities in (a) are plotted as anomalies because actual values depend on location and year. Spatial contours in (b) correspond to the estimated energy density for a fish of 60 mm SL on September 1. Depth contours are shown for the 50 m, 100 m, and 200 m isobaths. The partial fits by year (c) show the average energy density by year with other covariates fixed at their mean values.

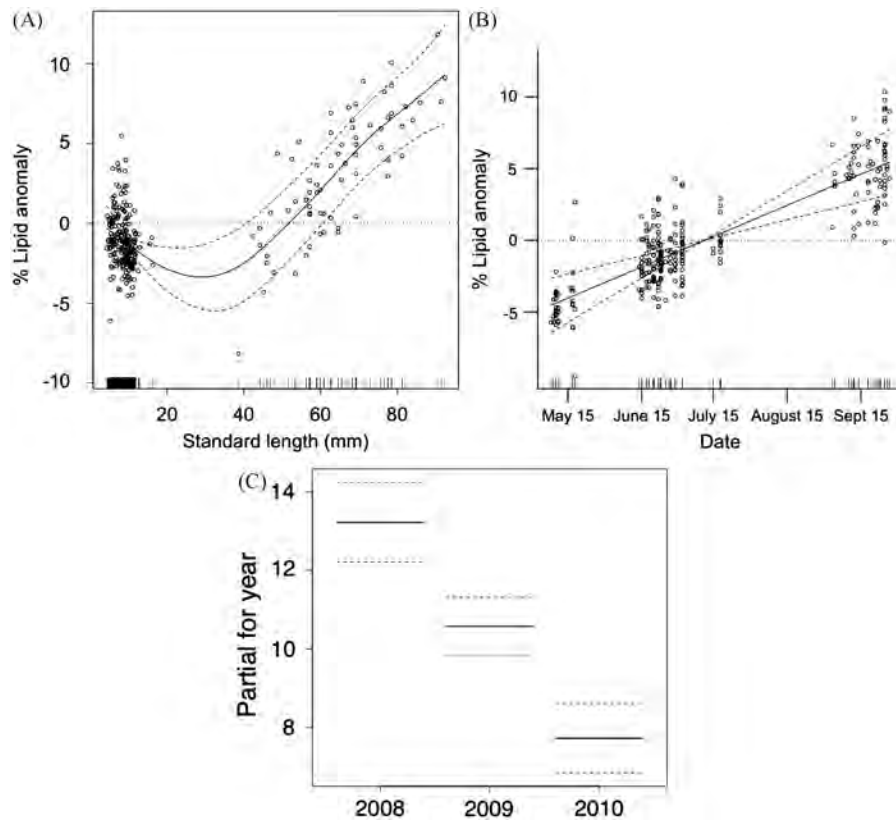


Fig. 4. Results from generalized additive mixed model (GAMM) regression analyses showing the estimated effects on % lipid (on a dry mass basis) of (a) standard length (SL; mm), (b) sampling date, and (c) year for age-0 walleye pollock (*T. chalcogramma*). Dashed lines denote 95% confidence intervals. % Lipid values in (a) and (b) are plotted as anomalies because actual values depend on sampling date and year. The range of y-axis values are comparable between (a) and (b), indicating SL and sampling date are similarly important in explaining variability in % lipid. The partial fits by year (c) show the average % lipid by year with other covariates fixed at their mean values.

asymptote in late summer, between approximately August 20 and September 15, before showing an increasing trend again over the remaining sampling period. Fish lengths were more variable in late summer than in spring and mid-summer (Fig. 5a). The spatial patterns in SL were inconsistent across years (plots not shown), but the seasonal changes in fish length were robust across years. The average SL of fish was lowest in 2008, highest in 2009, and intermediate in 2010 (Fig. 5b).

Patterns in average energy density and % lipid differed among years. Although changes in energy density are primarily driven by changes in % lipid, fish size (i.e., length) also contributes to total energy content. For example, fish in 2008 had high energy density and % lipid, but were smaller relative to fish in 2009 that had intermediate % lipid leading to lower overall energy density (Figs. 3c, 4c, and 5b).

4. Discussion

This study provides estimates of energy density and % lipid for age-0 and age-1 walleye pollock and proposes a conceptual model of how energy allocation strategies shift in age-0 walleye pollock during the larval and juvenile phases. This shift represents adaptations to survival constraints associated with distinct ontogenetic stages; a strategy favoring allocation to growth in order to escape size-dependent predation appears limited to larval development while juvenile fish (> 30 mm) adopt a strategy to increase lipid storage in late summer (Fig. 4a). This allocation strategy has potentially important consequences for overwinter survival (Post and Parkinson, 2001). For example, age-0 Pacific herring, *Clupea pallasii*, in Prince William Sound, Alaska, rely on energy stores for

overwinter survival (Norcross et al., 2001), impacting year-class success (Paul and Paul, 1998). In the SEBS, the energy density of walleye pollock in late summer is directly correlated with observed differences in year-class strength between alternating climate states (Hunt et al., 2011; Heintz et al., this issue). We propose that late summer (July–September) represents a critical period for energy storage in age-0 walleye pollock, and that overwinter survival is dependent on sufficient storage in the previous growing season and may be an important determinant of recruitment success.

Differences in energy storage result from differences in the quantity and quality of prey during the age-0 period (Heintz et al., this issue). Higher abundances of larger, lipid-rich zooplankton taxa during cold years, combined with lower metabolic demands, allow age-0 walleye pollock to acquire greater lipid reserves by late summer, resulting in increased overwinter survival (Hunt et al., 2011). In the cold years of 2006–2010, the zooplankton community over the Bering Sea shelf was dominated by large copepods (e.g., *Calanus marshallae*) and euphausiids (e.g., *Thysanoessa raschii*). Under warmer conditions (2002–2005), smaller zooplankton taxa were dominant (e.g., *Pseudocalanus* spp., *Acartia* spp., Coyle et al., 2011; Stabeno et al., 2012) and the lack of larger prey appeared to have limited growth and energy storage, leading to poor energy levels and reduced year-class recruitment. The limited availability of large zooplankton coincided with increased rates of cannibalism by older age classes of walleye pollock, as well as high predation rates by juvenile salmon, further reducing age-0 survival in warm years (Coyle et al., 2011). Hence, prey quality may be as important as the thermal regime for determining overwinter survival (Hurst, 2007), although prey availability and prey quality were closely linked to temperature conditions in recent years (Coyle et al., 2011).

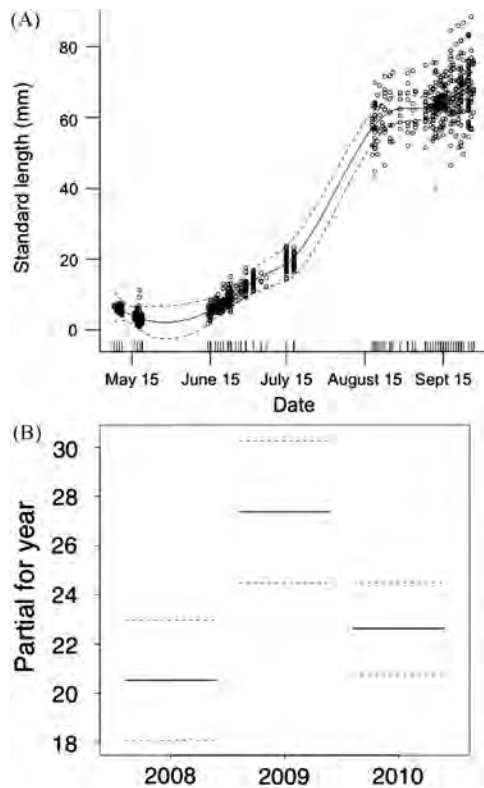


Fig. 5. Results from generalized additive mixed model (GAMM) regression analyses showing the estimated effects on standard length (SL; mm) of (a) sampling date and (b) year for age-0 walleye pollock (*T. chalcogramma*). Dashed lines denote 95% confidence intervals. The partial fits by year (b) show the average SL by year with other covariates fixed at their mean values.

The 2008 and 2009 cohorts showed similar seasonal patterns of energy density overall, with observed differences in late-summer age-0 fish likely reflecting the difference in mean sampling date between cruises; this highlights late summer as a period of rapidly increasing energy density in walleye pollock. Differences between the late-summer 2008 age-0 fish sampled during the rope trawl and beam trawl surveys could also be due to surface fishes (sampled by the rope trawl survey) having higher energy density than bottom-associated fishes (beam trawl survey). Energy densities are presumed to decrease during late winter when water column temperatures, prey availability, and feeding rates decrease, although patterns in energy density after late-summer sampling are unknown. Energy density of walleye pollock collected in southeastern Alaska continued to increase between September and December sampling intervals, but declined between December and March (Heintz and Vollenweider, 2010). Age-1 fish in the current study appear to achieve energy densities the following summer that are comparable to the preceding late-summer period. The 2009 cohort had significantly higher energy densities by age-1, which could be due to differential overwinter survival, reduced winter energy loss for the 2009 cohort leading to less of an energy deficit in spring 2010, and/or differences in prey availability for age-1 fish during their second summer. The 2009 cohort also likely experienced less intra-specific competition as the size of the 2009 year-class estimate remains well below the 2008 estimate (Ianelli et al., 2011).

During spring through mid-summer, low energy density and % lipid values indicate fish preferentially allocate energy to development (i.e., organogenesis) with little increase in overall fish growth during the larval stage. The decrease in lipid content with length as larvae increase from ~5 to 15 mm (Fig. 4a) likely reflects decreasing energy stores as larvae adapt to capturing prey and allocate energy to completion of larval development.

During summer, walleye pollock appear to be growing in length while also increasing lipid stores, although patterns are poorly defined due to lack of samples during this period. That said, late July–August may be a period when energetic demands are highest based on metabolic demands in warmer water temperatures (Ciannelli et al., 1998). The length at transformation from larval to juvenile form occurs at 25–40 mm SL (Brown et al., 2001; Matarese et al., 1989) and marks a threshold after which % lipid acquisition rates increased linearly with size, leading to higher energy density in late summer as energy was allocated to storage for overwinter survival. Our samples fall on either side of this size range, supporting the inference that fish below this length range (i.e., larvae) are allocating energy to development and fish above this length range (i.e., juveniles) favor energy storage relative to accumulation during the larval phase.

This study was conducted during three cold years in the SEBS (Stabeno et al., 2012), therefore delayed development times likely resulted in smaller fish sizes relative to warmer years (Smart et al., 2013). Age-0 juvenile walleye pollock reached an asymptotic length at approximately 60 mm SL in late summer, which may correspond to a shift in prey preferences with increasing gape size (i.e., switch to euphausiids; Brodeur, 1998; Sturdevant et al., 2001) and associated foraging capability (e.g., Ciannelli et al., 2002). However, there is potential confounding between sampling date, year, and gear type that could account for the observed patterns in fish length due to differences in sampling dates among years and the use of different gears with potentially different size selectivity. An asymptotic energy density occurred when fish reached approximately 75 mm SL, similar to that observed for walleye pollock near the Pribilof Islands (asymptotic energy density at 80 mm SL) during 1994–1996 and 1999, with 1995 and 1999 also being cold years (Ciannelli et al., 2002).

While our study focused on seasonal patterns in energy allocation, spatial patterns in the distribution and energetic condition of fish relative to prey may be equally important in determining recruitment success. Significant spatial patterns were observed among years in the best models for energy density and fish length; due to confounding between sampling location and date, we cannot statistically differentiate the relative effect of sampling location. However, the relative importance of the spatial smooth terms was minimal compared to the effect of other covariates in the best models. Therefore, we believe that the patterns observed in energy density as a function of standard length, and in length as a function of sampling date, are robust.

Age-0 walleye pollock in the Gulf of Alaska during late-summer experience spatially variable habitat conditions for growth due to differences in water temperature and prey (Mazur et al., 2007). Once larvae are capable of diel vertical migration, their position in the water column (i.e., above or below the pycnocline) also affects temperature-dependent metabolic rates, as well as trade-offs in foraging times versus predation risk (Sogard and Olla, 1996). As such, both the horizontal and vertical distributions of larvae affect their growth and energetic condition. Juvenile walleye pollock are capable of selecting habitat based on temperature, prey availability, and predator abundance (Kooka et al., 2007). Consequently, we plan to incorporate both local-scale environmental conditions and estimates of prey availability into a bioenergetics model to quantify fine-scale spatial variability in growth potential and to support the development of predictive models for recruitment success of walleye pollock in the SEBS.

5. Conclusions

Larval and juvenile walleye pollock face competing demands for available energy resources. We identified differing energy

allocation strategies indicating that distinct ontogenetic stages face different survival constraints. Larval fish favored allocation to somatic growth, presumably in order to escape size-dependent predation, while juvenile fish allocated energy to lipid storage in late summer. We propose that late summer (July–September) represents a critical period for energy storage in age-0 walleye pollock and that subsequent energy levels provide an early metric for the prediction of overwinter survival and recruitment success to age-1.

Acknowledgments

We thank the officers and crew of the NOAA ships Miller Freeman and Oscar Dyson, the USCG vessel Healy, and the R/Vs Knorr (WHOI) and Thompson (UW). Funding was provided through the North Pacific Research Board (NPRB) Bering Sea Integrated Ecosystem Research Program (BSIERP) and NOAA's North Pacific Climate Regimes and Ecosystem Productivity Program (NPCREP). NOAA's EcoFOCI, MACE, and BASIS programs kindly conducted additional sampling for this project. We thank Dr. Thomas Hurst, Dr. Matthew Wilson, and one anonymous reviewer for providing helpful comments that greatly improved the manuscript. This research is NPRB publication #360 and BEST-BSIERP Bering Sea Project #67. Fig. 1 courtesy of Ross Parnell-Turner, University of Cambridge. Reference to trade names does not imply endorsement by the National Marine Fisheries Service (NMFS), NOAA. The findings and conclusions in the paper are those of the authors and do not necessarily represent the views of the NMFS, NOAA.

References

Akaike, H., 1973. Information theory as an extension of the maximum likelihood principle. In: Petrov, B.N., Csaki, F. (Eds.), Second International Symposium on Information Theory. Akademiai Kiado, Budapest, pp. 267–281.

Aydin, K., Mueter, F.J., 2007. The Bering Sea – A dynamic food web perspective. *Deep-Sea Res. II* 54, 2501–2525.

Aydin, K., Gaichas, S., Ortiz, I., Kinzey, D., Friday, N., 2007. A Comparison of the Bering Sea, Gulf of Alaska, and Aleutian Islands Large Marine Ecosystems Through Food Web Modeling. NOAA Technical Memo, NMFS-AFSC-178, 298.

Bacheler, N.M., Ciannelli, L., Bailey, K.M., Duffy-Anderson, J.T., 2010. Spatial and temporal patterns of walleye pollock (*Theragra chalcogramma*) spawning in the eastern Bering Sea inferred from egg and larval distributions. *Fish. Oceanogr.* 19 (2), 107–120.

Bailey, K.M., Houde, E.D., 1989. Predation on early developmental stages of marine fishes and the recruitment problem. *Adv. Mar. Biol.* 25, 1–83.

Beamish, R.J., Mahnken, C., 2001. A critical size and period hypothesis to explain natural regulation of salmon abundance and the linkage to climate and climate change. *Prog. Oceanogr.* 49, 423–437.

Beamish, R.J., McFarlane, G.A. (Eds.), 1989. Effects of ocean variability on recruitment and an evaluation of parameters used in stock assessment models. *Can. Spec. Publ. Fish. Aquat. Sci.* 108.

Blood, D.M., 2002. Low-temperature incubation of walleye pollock (*Theragra chalcogramma*) eggs from the southeast Bering Sea shelf and Shelikof Strait, Gulf of Alaska. *Deep-Sea Res. II* 49, 6095–6108.

Brodeur, R.D., 1998. Prey selection by age-0 walleye pollock, *Theragra chalcogramma*, in nearshore waters of the Gulf of Alaska. *Environ. Biol. Fish.* 51, 175–186.

Brodeur, R.D., Wilson, M.T., Ciannelli, L., 2000. Spatial and temporal variability in feeding and condition of age-0 walleye pollock (*Theragra chalcogramma*) in frontal regions of the Bering Sea. *ICES J. Mar. Sci.* 57, 256–264.

Brown, A.L., Busby, M.S., Mier, K.L., 2001. Walleye pollock *Theragra chalcogramma* during transformation from the larval to juvenile stage: otolith and osteological development. *Mar. Biol.* 139, 845–851.

Buchheister, A., Wilson, M.T., 2005. Shrinkage correction and length conversion equations for *Theragra chalcogramma*, *Mallotus villosus* and *Thaleichthys pacificus*. *J. Fish Biol.* 67, 541–548.

Burnham, K.P., Anderson, D.R., 2002. Model Selection and Multi-Model Inference: A Practical Information-Theoretic Approach. Springer-Verlag, New York, NY 488.

Ciannelli, L., Brodeur, R.D., Buckley, T.W., 1998. Development and application of a bioenergetics model for juvenile walleye pollock. *J. Fish Biol.* 52, 879–898.

Ciannelli, L., Paul, A.J., Brodeur, R.D., 2002. Regional, interannual and size-related variation of age 0 year walleye pollock whole body energy content around the Pribilof Islands, Bering Sea. *J. Fish Biol.* 60, 1267–1279.

Ciannelli, L., Brodeur, R.D., Napp, J.M., 2004. Foraging impact on zooplankton by age-0 walleye pollock (*Theragra chalcogramma*) around a front in the southeast Bering Sea. *Mar. Biol.* 144, 515–526.

Conover, D.O., 1990. The relation between capacity for growth and length of growing season: evidence for and implications of countergradient variation. *Trans. Am. Fish. Soc.* 119 (3), 416–430.

Copp, G.H., Kovac, V., 1996. When do fish with indirect development become juveniles? *Can. J. Fish. Aquat. Sci.* 53, 746–752.

Coyle, K.O., Eisner, L.B., Mueter, F.J., Pinchuk, A.I., Janout, M.A., Cieciel, K.D., Farley, E.V., Andrews, A.G., 2011. Climate change in the southeastern Bering Sea: impacts on pollock stocks and implications for the Oscillating Control Hypothesis. *Fish. Oceanogr.* 20 (2), 139–156.

Cushing, D.H., 1969. The regularity of the spawning season of some fishes. *J. Cons. Int. Explor. Mer.* 33, 81–97.

Cushing, D.H., 1982. Climate and Fisheries. Academic Press, London, ISBN: 0-12-199720-0 373.

Cushing, D.H., 1990. Plankton production and year-class strength in fish populations: an update of the match/mismatch hypothesis. *Adv. Mar. Biol.* 26, 250–293.

Duffy-Anderson, J.T., Busby, M.S., Mier, K.L., Deliyannis, C.M., Stabeno, P.J., 2006. Spatial and temporal patterns in summer ichthyoplankton assemblages on the eastern Bering Sea shelf 1996–2000. *Fish. Oceanogr.* 15, 80–94.

Heintz, R.A., Vollenweider, J.J., 2010. Influence of size on the sources of energy consumed by overwintering walleye pollock (*Theragra chalcogramma*). *J. Exp. Mar. Biol. Ecol.* 393 (1–2), 43–50.

Heintz, R.A., Siddon, E.C., Farley, E.V., 2011. Climate-related changes in the nutritional condition of young-of-year (YOY) walleye pollock (*Theragra chalcogramma*) from the southeastern Bering Sea. *Deep-Sea Res. II*, this issue.

Hillgruber, N., Haldorson, L.J., Paul, A.J., 1995. Feeding selectivity of larval walleye pollock *Theragra chalcogramma* in the oceanic domain of the Bering Sea. *Mar. Ecol. Prog. Ser.* 120, 1–10.

Hinckley, S., 1987. The reproductive biology of walleye pollock, *Theragra chalcogramma*, in the Bering Sea, with reference to spawning stock structure. *Fish. Bull.* 85 (3), 481–498.

Hollowed, A.B., Bond, N.A., Wilderbuer, T.K., Stockhausen, W.T., A'mar, Z.T., Beamish, R.J., Overland, J.E., Schirripa, M.J., 2009. A framework for modelling fish and shellfish responses to future climate change. *ICES J. Mar. Sci.* 66 (7), 1584–1594.

Houde, E.D., 1987. Fish early life dynamics and recruitment variability. *Am. Fish. Soc. Symp.* 2, 17–29.

Hunt Jr., G.L., Stabeno, P.J., 2002. Climate change and the control of energy flow in the southeastern Bering Sea. *Prog. Oceanogr.* 55, 5–22.

Hunt Jr., G.L., Stabeno, P.J., Walters, G., Sinclair, E., Brodeur, R.D., Napp, J.M., Bond, N.A., 2002. Climate change and control of the southeastern Bering Sea pelagic ecosystem. *Deep-Sea Res. II* 49, 5821–5853.

Hunt Jr., G.L., Coyle, K.O., Eisner, L., Farley, E.V., Heintz, R., Mueter, F.J., Napp, J.M., Overland, J.E., Ressler, P.H., Salo, S., Stabeno, P.J., 2011. Climate impacts on eastern Bering Sea foodwebs: a synthesis of new data and an assessment of the Oscillating Control Hypothesis. *ICES J. Mar. Sci.* 68 (6), 1230–1243, <http://dx.doi.org/10.1093/icesjms/fsr036>.

Hurst, T.P., 2007. Causes and consequences of winter mortality in fishes. *J. Fish Biol.* 71, 315–345.

Ianelli, J.N., Honkalehto, T., Barbeaux, S., Kotwicki, S., Aydin, K., Williamson, N., 2011. Assessment of the walleye pollock stock in the Eastern Bering Sea. In: Stock Assessment and Fishery Evaluation Report for the Groundfish Resources of the Bering Sea/Aleutian Islands Regions. North Pacific Fishery Management Council, 605 W. 4th Ave., Suite 306, Anchorage, AK 99501. 118.

Kachel, N.B., Hunt Jr., G.L., Salo, S.A., Schumacher, J.D., Stabeno, P.J., Whitedge, T.E., 2002. Characteristics and variability of the inner front of the southeastern Bering Sea. *Deep-Sea Res. II* 49, 5889–5909.

Kendall Jr., A.W., Nakatani, T., 1992. Comparisons of early-life-history characteristics of walleye pollock *Theragra chalcogramma* in Shelikof Strait, Gulf of Alaska. *Fish. Bull.* 90, 129–138.

Kendall Jr., A.W., Incze, L.S., Ortner, P.B., Cummings, S.R., Brown, P.K., 1994. The vertical distribution of eggs and larvae of walleye pollock, *Theragra chalcogramma*, in Shelikof Strait, Gulf of Alaska. *Fish. Bull.* 92, 540–554.

Kooka, K., Yamamura, O., Nishimura, A., Hamatsu, T., Yanagimoto, T., 2007. Optimum temperature for growth of juvenile walleye pollock *Theragra chalcogramma*. *J. Exp. Mar. Biol. Ecol.* 347, 69–76.

Litzow, M.A., Bailey, K.M., Prah, F.G., Heintz, R., 2006. Climate regime shifts and reorganization of fish communities: the essential fatty acid limitation hypothesis. *Mar. Ecol. Prog. Ser.* 315, 1–11.

Matarese, A.C., Kendall Jr., A.W., Blood, D.M., Vinter, B.M., 1989. Laboratory Guide to Early Life History Stages of Northeast Pacific Fishes. NOAA Technical Report NMFS 80, 652.

Mazur, M.M., Wilson, M.T., Dougherty, A.B., Buchheister, A., Beauchamp, D.A., 2007. Temperature and prey quality effects on growth of juvenile walleye pollock *Theragra chalcogramma* (Pallas): a spatially explicit bioenergetics approach. *J. Fish Biol.* 70, 816–836.

Megrey, B.A., Hollowed, A.B., Hare, S.R., Macklin, S.A., Stabeno, P.J., 1996. Contribution of FOCI research to forecast of year class strength of walleye pollock in the Shelikof Strait, Alaska. *Fish. Oceanogr.* 5 (S1), 189–203.

Moss, J.H., Beauchamp, D.A., Cross, A.D., Myers, K.W., Farley Jr., E.V., Murphy, J.M., Helle, J.H., 2005. Evidence for size-selective mortality after the first summer of ocean growth by pink salmon. *Trans. Am. Fish. Soc.* 134, 1313–1322.

Moss, J.H., Farley, E.V., Feldman, A.M., Ianelli, J.N., 2009. Spatial distribution, energetic status, and food habits of eastern Bering Sea age-0 walleye pollock. *Trans. Am. Fish. Soc.* 138, 497–505.

- Mueter, F.J., Ladd, C., Palmer, M.C., Norcross, B.L., 2006. Bottom-up and top-down controls of walleye pollock (*Theragra chalcogramma*) on the Eastern Bering Sea shelf. *Prog. Oceanogr.* 68, 152–183.
- Norcross, B.N., Brown, E.D., Foy, R.J., Frandsen, M., Gay, S.M., Kline Jr., T.C., Mason, D.M., Patrick, E.V., Paul, A.J., Stokesbury, K.D.E., 2001. A synthesis of the life history and ecology of juvenile Pacific herring in Prince William Sound, Alaska. *Fish. Oceanogr.* 10 (S1), 42–57.
- Paul, A.J., Paul, J.M., 1998. Comparisons of whole body energy content of captive fasting age zero Alaskan Pacific herring (*Clupea pallasii* Valenciennes) and cohorts over-wintering in nature. *J. Exp. Mar. Biol. Ecol.* 226, 75–86.
- Paul, A.J., Paul, J.M., 1999. Interannual and regional variations in body length, weight and energy content of age-0 Pacific herring from Prince William Sound, Alaska. *J. Fish Biol.* 54, 996–1001.
- Post, J.R., Parkinson, E.A., 2001. Energy allocation strategy in young fish: allometry and survival. *Ecology* 82 (4), 1040–1051.
- Schultz, E.T., Conover, D.O., Ehtisham, A., 1998. The dead of winter: size-dependent variation and genetic differences in seasonal mortality among Atlantic silver-side (Atherinidae: *Menidia menidia*) from different latitudes. *Can. J. Fish. Aquat. Sci.* 55, 1149–1157.
- Schultz, E.T., Conover, D.O., 1999. The allometry of energy reserve depletion: test of a mechanism for size-dependent winter mortality. *Oecologia* 119, 474–483.
- Shima, M., Bailey, K.M., 1994. Comparative analysis of ichthyoplankton sampling gear for early life stages of walleye pollock (*Theragra chalcogramma*). *Fish. Oceanogr.* 3 (1), 50–59.
- Smart, T.L., Siddon, E.C., Duffy-Anderson, J.T., 2013. Vertical distributions of the early life stages of a common gadid in the eastern Bering Sea (*Theragra chalcogramma*, walleye pollock). *Deep-Sea Res. II*, 94, 201–210.
- Sogard, S.M., Olla, B.L., 1996. Food deprivation affects vertical distribution and activity of a marine fish in a thermal gradient: potential energy-conserving mechanisms. *Mar. Ecol. Prog. Ser.* 133, 43–55.
- Sogard, S.M., Olla, B.L., 2000. Endurance of simulated winter conditions by age-0 walleye pollock: effects of body size, water temperature and energy storage. *J. Fish Biol.* 56, 1–21.
- Stabeno, P.J., Schumacher, J.D., Ohtani, K., 1999. Physical oceanography of the Bering Sea. In: Loughlin, T.R., Ohtani, K. (Eds.), *The Bering Sea: A Summary of Physical, Chemical and Biological Characteristics and a Synopsis of Research*. North Pacific Marine Science Organization, PICES, pp. 1–28, Alaska Sea Grant Press.
- Stabeno, P.J., Bond, N.A., Kachel, N.B., Salo, S.A., Schumacher, J.D., 2001. On the temporal variability of the physical environment over the south-eastern Bering Sea. *Fish. Oceanogr.* 10 (1), 81–98.
- Stabeno, P.J., Kachel, N.B., Moore, S.E., Napp, J.M., Sigler, M., Yamaguchi, A., Zerbini, A.N., 2012. Comparison of warm and cold years on the southeastern Bering Sea shelf and some implications for the ecosystem. *Deep-Sea Res. II* 65–70, 31–45.
- Sturdevant, M.V., Brase, A.L.J., Hulbert, L.B., 2001. Feeding habits, prey fields, and potential competition of young-of-the-year walleye pollock (*Theragra chalcogramma*) and Pacific herring (*Clupea pallasii*) in Prince William Sound, Alaska, 1994–1995.
- Van Handel, E., 1985. Rapid determination of total lipids in mosquitoes. *J. Am. Mosq. Control Assoc.* 1 (3), 302–304.
- Vollenweider, J.J., Heintz, R., Schaufler, L., Bradshaw, R., 2011. Seasonal cycles in whole-body proximate composition and energy content of forage fish vary with water depth. *Mar. Biol.* 158, 413–427.
- Walsh, J.J., McRoy, C.P., 1986. Ecosystem analysis in the southeastern Bering Sea. *Cont. Shelf Res.* 5, 259–288.
- Wespestad, V.G., Quinn II, T.J., 1996. Importance of Cannibalism in the Population Dynamics of Walleye Pollock, *Theragra chalcogramma*. NOAA Technical Report NMFS, vol. 126, 212–217.
- Wood, S.N., 2006. *Generalized Additive Models: An introduction with R*. Chapman & Hall/CRC, Boca Raton, FL 422.



Contents lists available at ScienceDirect

Deep-Sea Research II

journal homepage: www.elsevier.com/locate/dsr2

Correlation between recruitment and fall condition of age-0 pollock (*Theragra chalcogramma*) from the eastern Bering Sea under varying climate conditions



Ron A. Heintz^{a,*}, Elizabeth C. Siddon^b, Edward V. Farley Jr.^a, Jeffrey M. Napp^c

^a NOAA, National Marine Fisheries Service, Alaska Fisheries Science Center, Auke Bay Laboratories, 17109 Pt. Lena Loop Rd., Juneau, AK 99801, USA

^b University of Alaska Fairbanks, School of Fisheries and Ocean Sciences, 17101 Pt. Lena Loop Rd., Juneau, AK 99801, USA

^c NOAA, National Marine Fisheries Service, Alaska Fisheries Science Center, 7600 Sand Point Way NE, Seattle, WA 98115, USA

ARTICLE INFO

Available online 9 April 2013

Keywords:

Pollock
Bering Sea
Recruitment
Climate change
Winter
Prey quality

ABSTRACT

Fishery managers require an understanding of how climate influences recruitment if they are to separate the effects of fishing and climate on production. The southeastern Bering Sea offers opportunities to understand climate effects on recruitment because inter-annual oscillations in ice coverage set up warm or cold conditions for juvenile fish production. Depth-averaged temperature anomalies in the Bering Sea indicate the past nine years have included three warm (2003–2005), an average (2006), and five cold (2007–2011) years. We examined how these climatic states influenced the diet quality and condition (size, energy density and total energy) of young-of-the-year (YOY) pollock (*Theragra chalcogramma*) in fall. The implications of fall condition were further examined by relating condition prior to winter to the number of age-1 recruits-per-spawner the following summer (R/S). The percentage of lipid in pollock diets was threefold higher in cold years compared with warm years, but stomach fullness did not vary. Consequently, fish energy densities were 33% higher in cold years ($P < 0.001$) than in warm years. In contrast, neither fish size ($P = 0.666$), nor total energy ($P = 0.197$) varied with climatic condition. However, total energy was significantly ($P = 0.007$) and positively correlated with R/S ($R^2 = 0.736$). We conclude that recruitment to age-1 in the southeastern Bering Sea is improved under environmental conditions that produce large, energy dense YOY pollock in fall.

Published by Elsevier Ltd.

1. Introduction

Fishery managers are limited in their ability to predict the number of young fish recruiting into fisheries because recruitment is the product of a linked series of complex and non-linear processes (e.g. Bailey et al., 2005). Most recruitment models rely on the number and fecundity of spawning females to project the future number of recruits. However, offspring must negotiate larval and prolonged juvenile stages prior to recruitment, so there is often little or no correlation between the number of spawners and subsequent recruits (e.g. Zheng, 1996). The problem of predicting recruitment may be exacerbated in the future because climate change will unpredictably alter the present interactions between the biotic and abiotic drivers. Consequently it is important that fishery managers develop a quantifiable and mechanistic understanding of how recruitment processes function under different climate conditions (Hollowed et al., 2009).

The southeastern Bering Sea can be viewed as a natural laboratory for understanding climate effects on fisheries recruitment. It occupies

a broad, flat continental shelf north of the Aleutian Islands on the western coast of Alaska. In spring, summer, and fall oceanographic fronts bound distinct hydrographic areas known as the inner, middle and outer domains. The southern extent of ice coverage in this area varies annually in response to atmospheric forcing. The sea ice undergoes periods of relatively little coverage (warm years) followed by periods of almost complete coverage (cold years). This oscillation influences the development of oceanographic fronts with a profound influence on the ecological processes within each domain. These effects of winter ice cover have been incorporated into the Oscillating Control Hypothesis (OCH) (Hunt et al., 2002), which predicts how warming temperatures will affect recruitment of walleye pollock (*Theragra chalcogramma*) in the southeastern Bering Sea. The pollock harvest there constitutes the largest fishery (by weight) in the United States. Consequently, pollock recruitment in the southeastern Bering Sea is the object of intense interest.

A recent revision of the OCH focuses on the relationship between the eastern Bering Sea zooplankton community and the timing of ice retreat in spring (Hunt et al., 2011). Early ice retreat in warm years results in an absence of large crustacean zooplankton over the middle shelf domain and favors communities comprised of small copepods such as *Pseudocalanus*, *Acartia*, *Oithona* and *Centropages*. Conversely, the zooplankton biomass over the middle

* Corresponding author. Tel.: +1 907 789 6058; fax: +1 907 789 6094.

E-mail address: ron.heintz@noaa.gov (R.A. Heintz).

shelf is dominated by medium-sized calanoids and euphausiids in cold years (Coyle et al., 2011; Hunt et al., 2011; Ressler et al., 2012; Stabeno et al., 2012). The species composition in cold years has been theorized to supply zooplanktivorous fishes with improved access to lipid and subsequently increased recruitment success (Moss et al., 2009).

Improved access to lipid-rich prey is important because young-of-the-year (YOY) pollock face severe energy deficits as they enter winter (e.g. Sogard and Olla, 2000). These energetic deficiencies are believed to account for winter mortality (Hurst, 2007), which can significantly reduce year class strength (Farley et al., 2007). High latitude fish need to satisfy those energy deficits with endogenous energy (Post and Parkinson, 2001) stored as lipid. The time window during which pollock can provision themselves with lipid occurs between the completion of metamorphosis in early August and the onset of oceanographic winter (Willson et al., 2011; Siddon et al., 2013). This highlights the importance of accessing lipid rich prey in late summer and early fall. Those individuals that can consume high lipid prey during this critical period should survive winter better than individuals consuming leaner prey.

The size of fish prior to winter is also an important determinant of winter survival. Observations of size-dependent mortality during winter for many freshwater and marine species have led to the so-called critical size hypothesis (Farley et al., 2007; Hurst, 2007). Empirical evidence suggests that mortality among high latitude fish in winter depends on size, with larger individuals having the greater chance of survival. Size-dependent mortality during winter has been described for silversides (*Menidia menidia*) (Conover, 1984), Pacific herring (*Clupea pallasii*) (Norcross et al., 2001), pollock (Sogard and Olla, 2000; Heintz and Vollenweider, 2010), pink (*Oncorhynchus gorbuscha*) (Moss, 2005) and sockeye (*O. nerka*) (Farley et al., 2011) salmon. Larger fish are thought to survive winter better than small fish because they have a greater capacity to store energy (Schultz and Conover, 1999). These data indicate that foraging conditions during the critical pre-winter period should be an important determinant to recruitment success because those conditions that allow fish to grow and store lipid will maximize winter survival. Yet, none of these studies has considered food quality as a factor contributing to winter survival.

We examine the hypothesis that YOY pollock are better prepared to survive winter in the eastern Bering Sea when they are able to forage on lipid-rich zooplankton communities characteristic of cold years. The objectives of this study were to understand how climatic conditions in the eastern Bering Sea influence the pre-winter condition of YOY pollock, and how that condition influences their winter survival. We compared the nutritional condition (size, energy density, total energy) of walleye pollock collected from warm and cold years to the percent lipid in their diets. Finally, the importance of fall condition is examined by correlating the pre-winter condition of YOY pollock with their winter survival, expressed as the number of age-1 recruits-per-spawner the following summer.

2. Materials and methods

2.1. Pollock collection and processing

Pollock were sampled during the Bering Aleutian Salmon International Survey (BASIS) conducted by the National Marine Fisheries Service each year between 2003 and 2011. Years were classified as warm (2003–2005), average (2006) or cold (2007–2011) based on ice coverage in March/April and the depth averaged temperature anomaly between April and October at mooring M2 following Stabeno et al. (2012). BASIS is a fisheries

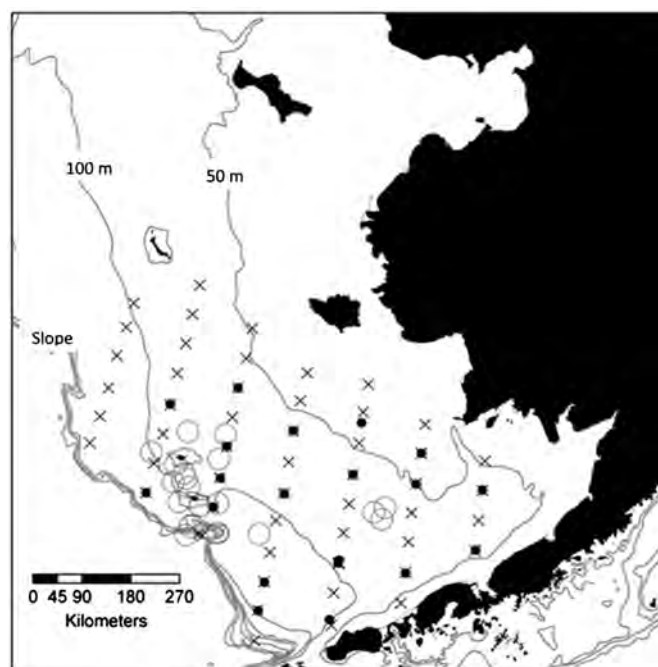


Fig. 1. Map of the eastern Bering Sea showing BASIS sampling stations (X's). Zooplankton were collected at stations identified with filled circles in 2009 and at stations identified by open circles in 2004.

oceanographic survey of the eastern Bering Sea that takes place between mid August and the end of September. Fish were collected by surface trawl during the day in a gridded series of 81 fixed stations (Fig. 1; Farley and Moss, 2009). Over the course of the study period the actual number of stations surveyed has varied due to weather and other constraints. However, the core areas where YOY pollock were historically caught have been sampled in all years. In this report we only consider fish sampled from surface trawls deployed south of 60° north latitude to maintain consistency between years.

YOY pollock < 100 mm total length, as delineated by Moss et al. (2009), were processed from each station. The total number caught was counted or estimated from subsamples of the total mass. The average weight of the YOY pollock at each station was recorded by dividing the total mass of YOY by the number of YOY in that mass. A subsample of up to 10 fish was retained to estimate diet composition. Another subsample of up to 15 fish was retained and frozen for calorimetry.

Fish collected for diet analysis were processed immediately on the vessel to estimate the average diet composition for each station. The stomach contents were removed from each fish, pooled into a common sample and weighed to estimate the average bulk mass of the stomach contents. The average stomach fullness at each station was recorded as the bulk stomach content mass divided by the total fish mass and multiplied by 100. The taxa comprising the bulk were identified to the lowest practical level and weighed. The percentage contribution of each taxon to the bulk weight was recorded. Diet compositions in warm and cold years have been described elsewhere (Moss et al., 2009; Coyle et al., 2011) and are only briefly reviewed here.

The energy density (kJ/g wet mass) of the YOY pollock from each cruise (2003–2011) was measured by bomb calorimetry. Samples for bomb calorimetry from a given station were stratified by length. They were dried, pulverized and combusted using a Parr 6725 semi-micro bomb calorimeter. Pulverized homogenates were pressed into pellets weighing at least 25 mg prior to combustion. Calorimetric data collected after 2007 were supplemented with

energy densities calculated from proximate compositions. Conversions to energy density from proximate composition relied on linear regressions relating percent lipid to energy density in samples for which both analyses had been performed. Details for the calorimetry and proximate analysis along with quality assurance protocols can be found in Siddon et al. (2013).

2.2. Collection and processing of zooplankton

The percent lipid of pollock prey items was estimated from zooplankton samples collected in a warm (2004) and cold (2009) year. Estimates of zooplankton percent lipid for the warm year come from samples collected between 26 July and 19 August on a survey centered near the Pribilof Islands. That survey also included a transect over the shelf break and a grid of stations centered on a mooring (M2) on the continental shelf (56.8°N 164°W) (Hunt et al., 2008; Fig. 1). During this survey, zooplankton samples were collected at night using the drogue net (150 μm mesh) of a MOCNESS with a nonfiltering cod end. The MOCNESS was fished obliquely from the surface to near bottom and prey species were sorted under a dissecting microscope on ice and then frozen and transported to the lab in liquid nitrogen. Estimates of zooplankton percent lipid for the cold year (2009) come from samples obtained during the BASIS survey between 30 August and 28 September. During this survey, zooplankton samples were collected using bongo nets (505 μm mesh) (Coyle et al., 2011) fished vertically from at most 100 m depth to the surface during the day. Zooplankton were sorted immediately after collection and representative individuals of each species were frozen in separate air tight vials and held at < -75 °C until they were processed in the laboratory.

Prey quality was measured in the laboratory as the percent lipid in the zooplankton wet mass. Zooplankton were gently blotted to remove liquid and weighed to the nearest 10 μg. When individuals were too small to weigh individually, the average wet mass was estimated from composited samples, weighed in bulk. Average mass was estimated by dividing the bulk weight by the number of individuals in the composite. Lipid was extracted from each sample using a modified Folch method. The minimum sample size for extraction was 25 mg (wet mass), which often required compositing 3–35 individuals. Samples were extracted using a solvent mixture of 2:1 chloroform:methanol in a Dionex Accelerated Solvent Extractor (ASE). See Siddon et al. (2013) for details on the extraction protocol and quality assurance procedures. Samples from 2004 that were < 25 mg were extracted in the same solvent mix using hand maceration. The extract was passed over a micro-column of sodium sulfate as a drying agent to remove tissue material. The same quality assurance methods and reference materials were used as those extracted using the ASE to ensure comparability.

2.3. Data analysis

2.3.1. Climate effects on prey quality

Climate effects on prey quality were examined by comparing the percent lipid of prey sampled from eastern Bering Sea in 2004 and 2009. The percent lipid of five species was measured in both years, *T. chalcogramma*, *Neocalanus cristatus*, *Calanus spp.*, *Thysanoessa inermis* and *Thysanoessa raschii*. We compared their percent lipid between years using a two-way ANOVA with year, species and their interaction as fixed factors. Assumptions regarding normality (Anderson Darling) and homogeneity of variance (*F* test) of the response variables relative to climatic state were tested prior to the analysis.

2.3.2. Climate effects on pollock diet

The diet compositions obtained in each survey year were combined with the percent lipid (wet mass basis) of the prey to estimate the average percent lipid of diets in warm, cold and average years. Percent fullness and dietary lipid of fish collected from the BASIS surveys in warm, cold and average years was compared using a one-way ANOVA. The average percent lipid of the diet (I_{st}) observed at each station (s) in a given year (t), expressed as the percent of ingested wet mass was calculated as

$$I_{st} = \sum_i^n P_{ist} L_{ic}$$

where P_{is} is the proportional contribution of prey type i at station s to the total mass ingested and L_{ic} is the percent lipid of prey type i under climate condition c . When only one lipid value was available it was used for both the warm and cold year diets. When diet could only be identified to taxon (i.e. genus, family or order), the overall average lipid value for that taxon was applied. We calculated the average dietary percent lipid for each year, \bar{I}_t , by weighting I_s by the catch at each station in year t (C_{ts}) to account for the highly variable number of fish caught at each station.

$$\bar{I}_t = \frac{\sum C_{ts} I_s}{\sum C_{ts}}$$

Estimates of fullness were also weighted by catch prior to analysis.

2.3.3. Climate effects on pre-winter condition

Climate effects on fish condition were examined by comparing the catch-weighted averages across years. Climate responses were examined using a one-way ANOVA. Climate classification was considered a fixed variable. The response variables included catch-weighted average weight, energy density and total energy. The latter response (i.e. kJ per fish) was estimated as the product of the catch-weighted average weight and catch-weighted average energy density for a given year. We used total energy based on the assumption that winter survival is optimized when fish can simultaneously accrete tissue mass and allocate energy to depot lipids. Assumptions regarding normality (Anderson Darling) and homogeneity of variance (*F* test) of the response variables relative to climatic state were tested prior to the analysis.

2.3.4. Influence of pre-winter condition on survival

We used regression analysis to evaluate the strength of the relationship of YOY condition in fall and subsequent survival to age-1. Survival of year class t (S_t) was indexed as the number of age-1 recruits (R_{t+1}) per female spawner (F_t) calculated as

$$S_t = \frac{R_{t+1}}{F_t}$$

using data provided in the Bering Sea Pollock Stock Assessment (Ianelli et al., 2011). The number of recruits-per-spawner (hereafter referred to as survival) was regressed against three indices of condition: catch-weighted average fish mass, catch-weighted energy density and total energy.

3. Results

3.1. Climate effects on prey quality

We estimated the percent lipid in 22 zooplankton taxa between our 2004 and 2009 collections, five of those taxa were sampled in both years (Fig. 2). The average percent lipid of zooplankton differed significantly between years ($F_{1,80}=12.59$, $p < 0.001$), and there was no interaction between species and year ($F_{1,80}=0.12$,

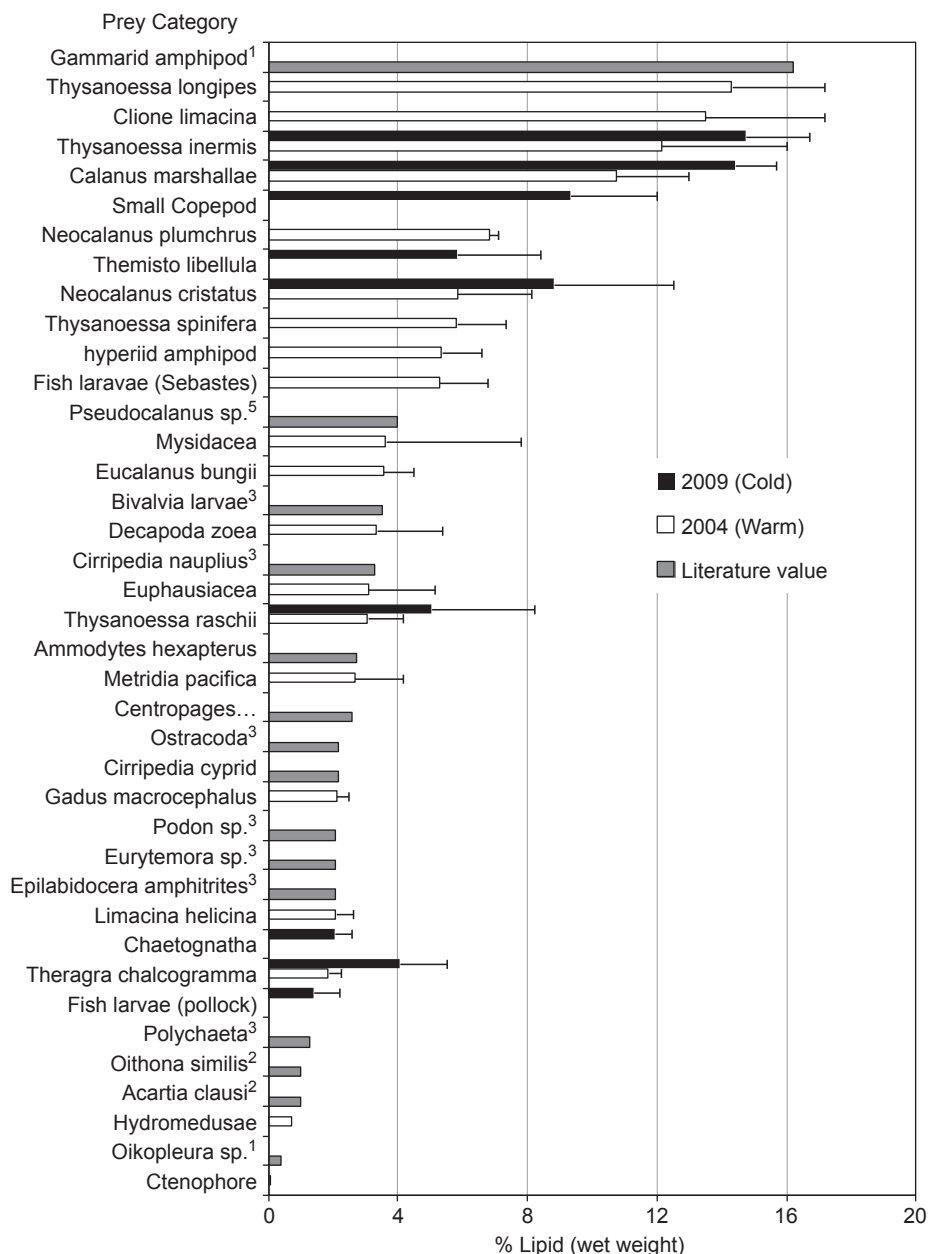


Fig. 2. Average percent lipid (± 1 S.D.) of prey consumed by YOY pollock in 2004 and 2009. Bar colors reflect year the sample was collected, open bars show prey collected in 2004, closed bars show prey collected in 2009, and gray bars reflect values taken from other sources: 1, Nomura and Davis (2005); 2, Yamamoto et al. (2008); 3, Foy and Paul (1999); 4, Lee et al. (2006) and 5, Peters (2006).

$p=0.890$). Prey species had higher percent lipid in the cold year compared with the warm year. This was true for the euphausiids, *T. raschii* and *T. inermis*, as well as teleosts such as pollock, which all increased in percent lipid by at least 21%. *Calanus spp.* increased in percent lipid by 37% between the warm and cold year and *N. cristatus* increased by 50%.

3.2. Climate effects on pollock diets

YOY pollock consumed a more diverse diet in warm years, but tended to have lower average fullness than in cold years. The diets of the fish sampled in 2004–2007 were previously reported by Moss et al. (2009), while those from 2003–2009 were reported by Coyle et al. (2011). The diets observed in 2010 and 2011 conformed to the previously described patterns. In general, diets were most diverse in warm years (Fig. 3), including many additional prey taxa not observed in cold years. The most frequent taxon in warm years

was *Pseudocalanus spp.*, (listed as “Small copepod” in Fig. 3), accounting for up to 60% of the ingested mass. In cold years *Pseudocalanus spp.* were also relatively frequent, but they made up a smaller proportion of the mass ingested because larger taxa were also ingested. The most frequent items in cold years were *Calanus spp.*, but euphausiids accounted for the majority of the mass. Despite the compositional differences between warm and cold years, stomach fullness remained constant ($F_{2,6}=1.52$, $p=0.293$). Although, the average fullness increased from $1.7 \pm 0.1\%$ (mean ± 1 S.E.) in the warm years to $2.2 \pm 0.4\%$ in the cold years due to

Pollock diets had a greater amount of lipid in cold years due to the larger contributions of *Calanus spp.* and euphausiids. Items typical of warm years, such as small copepods (including *Pseudocalanus spp.*), were intermediate in percent lipid (Fig. 2), but can also be seen in cold year diets. In contrast, *Calanus spp.* and euphausiids have higher percent lipid (Fig. 2), and were abundant in the diets of pollock sampled in cold years (Fig. 3). Consequently,

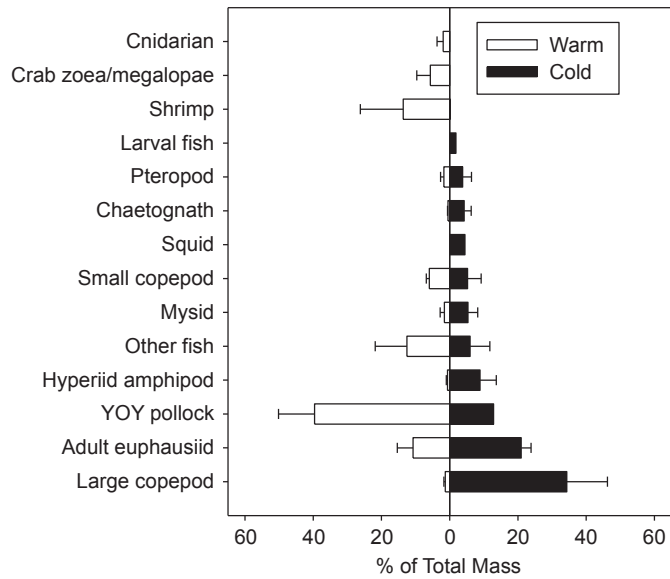


Fig. 3. Average percent composition (± 1 S.D.) of YOY pollock diets in warm (2003–2005) and cold (2007–2011) years. Each prey item is expressed as percent of total mass of prey examined within a year and averaged across the appropriate years. Only those prey items that averaged at least 1% of the mass examined are shown. Taxa have been combined to simplify presentation. For more detailed comparisons of diets in warm and cold years see Moss et al. (2009) and Coyle et al. (2011).

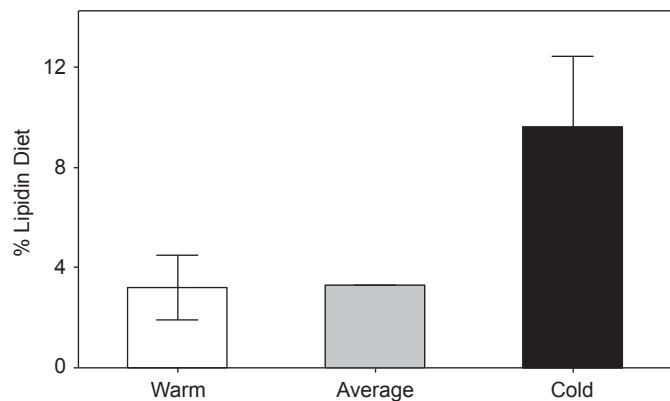


Fig. 4. Catch-weighted average ($\pm 95\%$ confidence interval) lipid content of YOY pollock diets in warm (2003–2005), average (2006) and cold (2007–2011) years.

pollock diets had significantly more lipid in the cold years than in the warm years ($F_{2,6}=12.84, p=0.007$), averaging about threefold greater (Fig. 4). The taxa in our collection were sufficient to describe the percent lipid of $>98\%$ of the mass observed in pollock stomachs from cold years. We had to supplement our collection of percent lipid with published values (Fig. 2) to account for the more diverse diets observed in warm years. Inclusion of published values allowed us to account for a median of $>90\%$ of the mass observed in those stomachs.

3.3. Climate effects on pre-winter condition

Neither the size nor the total energy content of pollock was influenced by climate, but there was an effect of climate on energy density. Pollock were slightly lighter in mass during the warm years averaging 1.97 ± 0.25 g compared with 2.35 ± 0.28 g in the cold years, but these differences were not statistically significant ($F_{2,5} > 0.43, p > 0.666$) (Fig. 5). In contrast, the catch-weighted average energy density was highly correlated with climatic condition ($F_{2,6}=35.38, p < 0.001$; Fig. 5B). Energy density in the cold

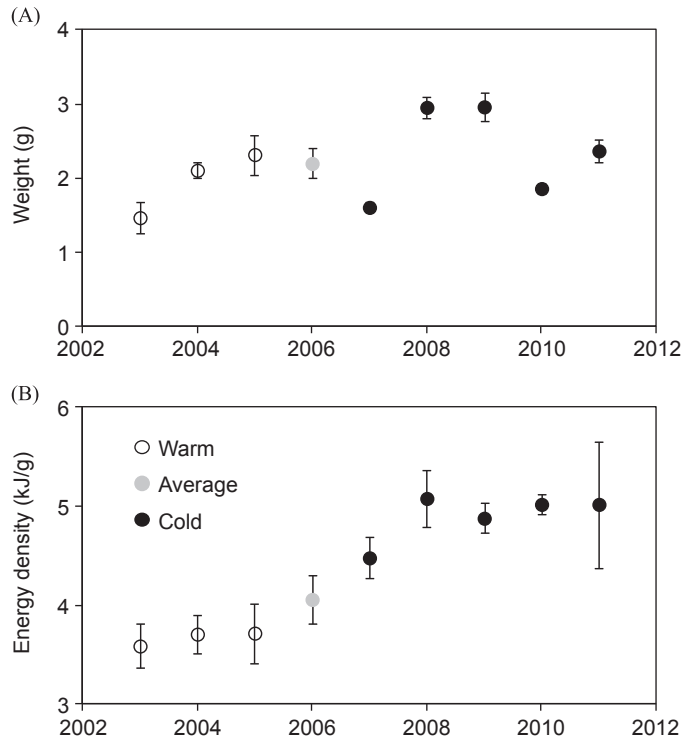


Fig. 5. Catch-weighted average weight (± 1 S.D.) (top panel) and energy density (bottom panel) of YOY pollock sampled from 2003 to 2011.

years (4.90 ± 0.11 kJ/g) was 33% greater than the warm years (3.67 ± 0.04 kJ/g). In contrast to the energy density, there was no relation between climate and the total energy content of YOY pollock ($F_{2,6}=2.16, p=0.197$). However, there was a trend of greater total energy in cold years (11.2 ± 1.5 kJ/fish) compared to warm years (7.3 ± 0.9 kJ/fish).

3.4. Influence of pre-winter condition on survival

Total energy was the best predictor of survival. The product of weight and energy density expressed as total energy was significantly ($F_{1,6}=16.77, p=0.006$) and positively ($r^2=0.736$) correlated with recruitment to age-1 (Fig. 6). Weight ($r^2=0.496$) and energy density ($r^2=0.677$) were also positively correlated with survival ($F_{1,6} > 5.92, p < 0.051$), but accounted for less of the variation in survival over the past nine years.

4. Discussion

These data demonstrate that the ability of YOY pollock to provision themselves prior to winter has direct bearing on their survival to age-1. Climate effects on prey field composition (Coyle et al., 2011) led to the consumption of high lipid diets in cold years. Fish that consumed high lipid diets had higher energy densities as a result of the increased level of lipid in their tissues (Anthony et al., 2000). The effect of consuming high lipid diets on body composition is well known (e.g. Arzel et al., 1994). In larval pollock high lipid diets may also increase survival by reducing activity costs (Davis and Olla, 1992). However, consuming high lipid diets did not guarantee survival in this study; fish also needed to reach sufficient size. This indicates the critical size hypothesis should be refined to reflect both the effects of large size late in the growing season and the availability of high lipid diets. The oceanographic conditions that produce large, energy dense fish are also those

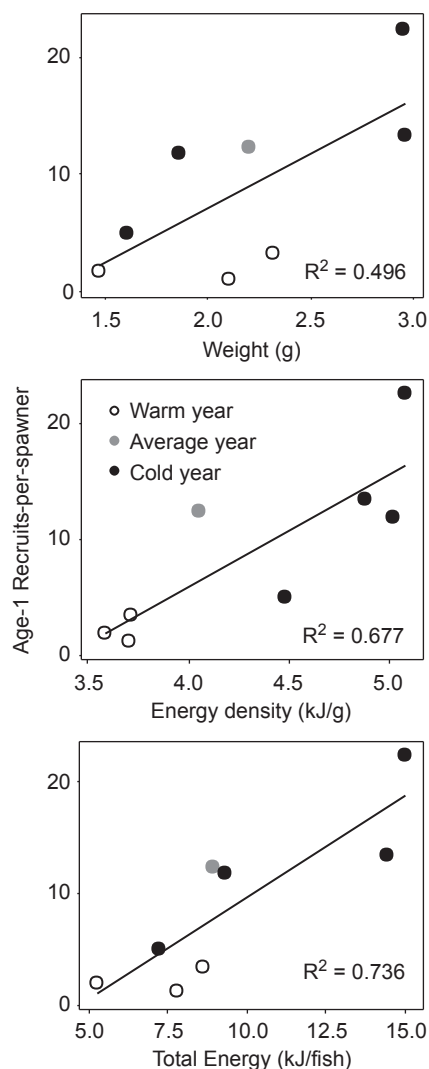


Fig. 6. Relationship between catch-averaged weight, energy density and total energy of YOY pollock with survival. Survival is estimated as the number of age-1 recruits per female spawner and was not available for 2011 year class at time of publication.

conditions likely to lead to increased winter survival of YOY pollock.

4.1. Climate impacts on food abundance and quality

Food limitation is often cited as a mechanism restricting production and recruitment in fish populations, but the data presented here indicate food quality is also important. Zooplankton biomass in cold years was twice that of warm years in the southeastern Bering Sea (Coyle et al., 2011), but pollock catch-per-unit-effort on BASIS surveys was lower in cold years (Hunt et al., 2011). This indicates the *per capita* availability of prey was likely much higher in cold years. Pollock consumption rates are higher at warm temperatures (Kooka et al., 2007) suggesting lower average stomach fullness in warm years reflected a density-dependent impact on foraging success. However, pollock in warm years would have had to ingest three times more food in warm years to ingest the same amount of lipid as fish in cold years. It is unlikely that pollock would be able to consume three times as much food in warm years if the food were available because maximum consumption rates only increase about twofold between 3 and 12 °C (Kooka et al., 2007).

The processes which led to the increased availability of high quality prey in cold years was augmented by the increased percent lipid found in specific prey taxa. Improved quality in *Calanus spp.* likely relates to mechanisms associated with their increased abundance such as improved coupling between spring blooms and metamorphosis (Baier and Napp, 2003) or reduced stratification and increased nutrient supply during summer (Coyle et al., 2011). However, it is possible that the climate related changes in food quality we observed are related to seasonal effects on lipid storage. Zooplankton sampled in 2009 were collected as much as six weeks later in the year than those in 2004 and the percent lipid of the specific prey increased by 20–65%. However this seasonal effect, if it exists, is only of marginal importance because the majority of the warm year diets were comprised of leaner prey taxa than in cold years.

4.2. Importance of winter

Larger fish can store proportionately more energy and they use it more slowly than smaller fish. This is because the allometry for lipid storage before winter has a steeper slope than the allometry for lipid depletion during winter (Schultz and Conover, 1999). Therefore, the correlation between pollock condition and their subsequent survival to age-1 was a product of both their size and energy density, which accounts for the relatively poor survival of the 2007 year class. Fish from the 2007 year class had high energy densities and consumed lipid-rich diets, but were relatively small in size. Consequently, their overall energy content was low at the onset of winter.

Conditions during the period in which pollock provision themselves for winter seem to have been more important in determining winter survival, than conditions earlier in summer. In warm years pollock may spawn earlier (Smart et al., 2012) and grow faster if food supplies are not limiting (Kooka et al., 2007). Warm conditions apparently led to improved larval survival and supported the production of YOY pollock as indicated by the catches-per-unit-effort during the late summer and early fall in the southeastern Bering Sea (Hunt et al., 2011). However, density dependence during the provisioning period may have ultimately limited the production of age-1 pollock. These observations suggest that winter survival in the Bering Sea determines recruitment to a greater extent than larval production, a process similar to that reported for pollock in the Gulf of Alaska (Bailey, 2000; Ciannelli et al., 2005).

Moderation of the severity of winters and a warming of the upper water column during winter are probable consequences of changing climate in southeastern Bering Sea. Over the past 30–40 years, the stormy spring-winter-fall period has decreased in length resulting in a longer summer stable period and decreased frequency of summer storms (Stabeno et al., 2012). These storms promote new production in the late summer/early fall and may prolong the period during which YOY pollock can find lipid-rich prey items. In addition, decreased ice cover in the southeastern Bering Sea during warm periods has been associated with a later spring phytoplankton bloom (Hunt et al., 2011; Stabeno et al., 2012). Thus increased water temperatures may present a threefold challenge to juvenile pollock; (1) low densities of lipid-rich prey in the late summer/early fall result in low lipid reserves, (2) higher temperatures result in higher basal metabolic costs, and (3) a delay in the production cycle the following winter/spring means the period without sufficient prey resources is longer.

4.3. Conclusion

These observations provide a quantitative basis for predicting recruitment as a function of environmental conditions. Estimates

of total energy in fall integrate the effects of climate, diet, growth, prey abundance and quality at the end of the first growing season. The effects of climate on diet quality and condition of YOY pollock are consistent with observations of an inverse relationship between late summer sea surface temperatures and survival (Mueter et al., 2011). These data further demonstrate how fishery managers can take a significant step towards an ecosystem-based approach by linking recruitment models to the environmental and biological parameters responsible for production.

Acknowledgments

We thank all of the people involved in collecting and sorting the samples used in this study. This includes the crews of numerous vessels. In addition it includes numerous students that have helped to sort, prepare and process samples in the laboratory. Collection of summer 2004 prey samples was supported by NSF Grant OPP-0327308 (to G.L. Hunt, Jr.) and NOAA's North Pacific Climate Regimes and Ecosystem Productivity (NPCREP) research program. This research is contribution NPRB 414, BEST-BSIERP 93, and EcoFOCI-0797 to NOAA's NPCREP Program. References to trade names do not imply endorsement by the National Marine Fisheries Service, NOAA. The findings and conclusions in this paper are those of the authors and even though NOAA reviewed the work and paid our salaries the views here do not represent those of NMFS or NOAA.

References

- Anthony, J.A., Roby, D.D., Turco, K.R., 2000. Lipid content and energy density of forage fishes from the northern Gulf of Alaska. *J. Mar. Biol. Ecol.* 248, 53–78.
- Arzel, J., Lopez, F.X.M., Métailler, R., Stéphan, G., Viau, M., Gandemer, G., Guillaume, J., 1994. Effect of dietary lipid on growth performance and body composition of brown trout (*Salmo trutta*) reared in seawater. *Aquaculture* 123, 361–375.
- Baier, C.T., Napp, J.M., 2003. Climate induced variability in *Calanus marshallae* populations. *J. Plankton Res.* 25, 771–782.
- Bailey, K.M., 2000. Shifting control of recruitment of walleye pollock *Theragra chalcogramma* after a major climatic and ecosystem change. *Mar. Ecol.-Prog. Ser.* 198, 215–224.
- Bailey, K.M., Ciannelli, L., Bond, N.A., Belgrano, A., Stenseth, N.C., 2005. Recruitment of walleye pollock in a physically and biologically complex ecosystem: a new perspective. *Prog. Oceanogr.* 76, 24–42.
- Ciannelli, L., Bailey, K.M., Chan, K., Belgrano, A., Stenseth, N.C., 2005. Climate change causing phase transitions of walleye pollock (*Theragra chalcogramma*) recruitment dynamics. *Proc. Royal. Soc. B* 272, 1735–1743.
- Conover, D.O., 1984. Adaptive significance of temperature-dependent sex determination in a fish. *Am. Nat.* 123, 297–313.
- Coyle, K.O., Eisner, L.B., Mueter, F.J., Pinchuk, A.I., Janout, M.A., Cieciel, K.D., Farley, E.V., Andrews, A.G., 2011. Climate change in the southeastern Bering Sea: impacts on pollock stocks and implications for the Oscillating Control Hypothesis. *Fish. Oceanogr.* 20 (2), 139–156.
- Davis, M.W., Olla, B.L., 1992. Comparison of growth, behavior, and lipid concentrations of walleye pollock *Theragra chalcogramma* larvae fed lipid-enriched, lipid-deficient and field collected prey. *Mar. Ecol.-Prog. Ser.* 90, 23–30.
- Farley, E.V., Moss, J.H., Beamish, R.J., 2007. A review of the critical size, critical period hypothesis for juvenile Pacific salmon. *North Pac. Anadromous Fish Comm. Bull.* 4, 311–317.
- Farley, E.V., Moss, J.H., 2009. Growth rate potential of juvenile chum salmon on the eastern Bering Sea shelf: an assessment of salmon carrying capacity. *North Pac. Anadromous Fish Comm. Bull.* 5, 265–277.
- Farley, E.V., Starovoytov, A., Naydenko, S., Heintz, R., Trudel, M., Guthrie, C., Eisner, L., Guyon, J.R., 2011. Implications of a warming eastern Bering Sea for Bristol Bay sockeye salmon. *ICES J. Mar. Sci.* 68, 1138–1146.
- Foy, R.J., Paul, A.J., 1999. Winter feeding and changes in somatic energy content of age-0 Pacific herring in Prince William Sound, Alaska. *Trans. Am. Fish. Soc.* 128, 1193–1200.
- Heintz, R.A., Vollenweider, J.J., 2010. Influence of size on the sources of energy consumed by overwintering walleye pollock (*Theragra chalcogramma*). *J. Exp. Mar. Biol. Ecol.* 393 (1–2), 43–50.
- Hollowed, A.B., Bond, N.A., Wilderbuer, T.K., Stockhausen, W.T., A'mar, Z.T., Beamish, R.J., Overland, J.E., Schirripa, M.J., 2009. A framework for modelling fish and shellfish responses to future climate change. *ICES J. Mar. Sci.* 66 (7), 1584–1594.
- Hunt Jr, G.L., Stabeno, P.J., Walters, G., Sinclair, E., Brodeur, R.D., Napp, J.M., Bond, N.A., 2002. Climate change and control of the southeastern Bering Sea pelagic ecosystem. *Deep-Sea Res. II* 49, 5821–5853.
- Hunt Jr, G.L., Stabeno, P.J., Strom, S., Napp, J.M., 2008. Patterns of spatial and temporal variation in the marine ecosystem of the southeastern Bering Sea, with special reference to the Pribilof Domain. *Deep-Sea Res. II* 55, 1919–1944.
- Hunt Jr, G.L., Coyle, K.O., Eisner, L.B., Farley, E.V., Heintz, R.A., Mueter, F., Napp, J.M., Overland, J.E., Ressler, P.H., Salo, S., Stabeno, P.J., 2011. Climate impacts on eastern Bering Sea foodwebs: a synthesis of new data and an assessment of the Oscillating Control Hypothesis. *ICES J. Mar. Sci.* (6), 1230–1243.
- Hurst, T.P., 2007. Causes and consequences of winter mortality in fishes. *J. Fish Biol.* 71, 315–345.
- Ianelli J.N., Honkalehto T., Barbeaux S., Kotwicki S., Aydin K., Williamson N. (2011) Assessment of the walleye pollock stock in the Eastern Bering Sea. In: Stock assessment and fishery evaluation report for the groundfish resources of the Bering Sea/Aleutian Islands regions. North Pacific Fishery Management Council, 605 W.4th Ave., Suite306, Anchorage, AK99501.
- Kooka, K., Yamamura, O., Nishimura, A., Hamatsu, T., Yanagimoto, T., 2007. Optimum temperature for growth of juvenile walleye pollock *Theragra chalcogramma*. *J. Exp. Mar. Biol. Ecol.* 347, 69–76.
- Lee, R.F., Hagen, W., Kattner, G., 2006. Lipid storage in marine zooplankton. *Mar. Ecol.-Prog. Ser.* 307, 273–306.
- Moss, J.H., 2005. Evidence for size-selective mortality after the first summer of ocean growth by pink salmon. *Trans. Am. Fish. Soc.* 134, 1313–1322.
- Moss, J.H., Farley, E.V., Feldman, A.M., Ianelli, J.N., 2009. Spatial distribution, energetic status, and food habits of eastern Bering Sea age-0 walleye pollock. *Trans. Am. Fish. Soc.* 138, 497–505.
- Mueter, F.J., Bond, N.A., Ianelli, J.N., Hollwed, A.B., 2011. Expected declines in recruitment of walleye pollock (*Theragra chalcogramma*) in the eastern Bering Sea under future climate change. *ICES J. Mar. Sci.* 68 (6), 1284–1296.
- Nomura T., Davis N.M. (2005) Lipid and moisture content of salmon prey organisms and stomach contents of chum, pink and sockeye salmon in the Bering Sea. North Pacific Anadromous Fish Commission Technical Report Number 6: 59–61.
- Norcross, B.L., Brown, E.D., Foy, R.J., Frandsen, M., Gay, S.M., Kline, T.C., Mason, D.M., Patrick, E.V., Paul, A.J., Stokesbury, K.D.E., 2001. A synthesis of the life history and ecology of juvenile Pacific herring in Prince William Sound, Alaska. *Fish. Oceanogr.* 10, 42–57.
- Peters, J. (2006) Lipids in key copepod species of the Baltic Sea and North Sea – implications for life cycles, trophodynamics and food quality. PhD Dissertation. University of Bremen.
- Post, J.R., Parkinson, E.A., 2001. Energy allocation strategy in young fish: allometry and survival. *Ecology* 82, 1040–1051.
- Ressler, P.H., De Robertis, A., Warren, J.D., Smith, J.N., Kotwicki, S., 2012. Developing an acoustic index of euphausiid abundance to understand trophic interactions in the Bering Sea ecosystem. *Deep-Sea Res. II* 65–70, 184–195.
- Schultz, E.T., Conover, D.O., 1999. The allometry of energy reserve depletion: test of a mechanism for size-dependent winter mortality. *Oecologia* 119, 474–483.
- Siddon, E.C., Heintz R.A., Mueter F.J., 2013. Conceptual model of energy allocation in walleye pollock (*Theragra chalcogramma*) from larvae to age-1 in the south-eastern Bering Sea. *Deep-Sea Res. II*, 94, 140–149.
- Smart, T.I., Siddon, E.C., Duffy-Anderson, J.T., Horne, J.K., 2012. Alternating temperature states influence walleye pollock early life stages in the southeastern Bering Sea. *Mar. Ecol.-Prog. Ser.* 455, 257–267.
- Sogard, S.M., Olla, B.L., 2000. Endurance of simulated winter conditions by age-0 walleye pollock: effects of body size, water temperature and energy stores. *J. Fish Biol.* 56, 1–21.
- Stabeno, P.J., Kachel, N.B., Moore, S.E., Napp, J.M., Sigler, M., Zerbini, A.N., 2012. Comparison of warm and cold years on the southeastern Bering Sea shelf and some implications for the ecosystem. *Deep-Sea Res. II* 65–70, 31–45.
- Willson, M.T., Mier, K., Dougherty, A., 2011. The first annulus of otoliths: a tool for studying intra-annual growth and size-at-age variability among walleye pollock (*Theragra chalcogramma*). *Env. Biol. Fish.* 92, 53–63.
- Yamamoto, T., Teruya, K., Hara, T., Hokazono, H., Hashimoto, H., Suzuki, N., Iwashita, Y., Matsunari, H., Furuita, H., Mushiaki, K., 2008. Nutritional evaluation of live food organisms and commercial dry feeds used for seed production of amberjack *Seriola dumerilii*. *Fish. Sci.* 74, 1096–1108.
- Zheng, J., 1996. Herring stock-recruitment relationships and recruitment patterns in the north Atlantic and northeast Pacific Oceans. *Fish. Res.* 26, 257–277.



Updated analysis of flatfish recruitment response to climate variability and ocean conditions in the Eastern Bering Sea



Thomas Wilderbuer^{a,*}, William Stockhausen^a, Nicholas Bond^b

^a Resource Ecology and Fisheries Management (REFM) Division, Alaska Fisheries Science Center, NMFS, NOAA, USA

^b Joint Institute for the Study of the Atmosphere and Ocean (JISAO), University of Washington, Seattle, WA, USA

ARTICLE INFO

Available online 14 March 2013

Keywords:

Advection
Flatfish
Recruitment
Climate changes

ABSTRACT

This study provides a retrospective analysis of the relationship between physical oceanography, biology and recruitment of three Eastern Bering Sea flatfish stocks: flathead sole (*Hippoglossoides elassodon*), northern rock sole (*Lepidopsetta polyxystra*), and arrowtooth flounder (*Atheresthes stomias*) during the period 1978–2005. Stock assessment model estimates of recruitment and spawning stock size indicate that temporal patterns in productivity are consistent with decadal scale (or shorter) patterns in climate variability, which may influence marine survival during the early life history phases. Density-dependence (through spawning stock size) was statistically significant in a Ricker stock-recruit model of flatfish recruitment that included environmental terms. Wind-driven advection of northern rock sole and flathead sole larvae to favorable nursery grounds was found to coincide with years of above-average recruitment. Ocean forcing of Bristol Bay surface waters during springtime was mostly on-shelf (eastward) during the 1980s and again in the early 2000s, but was off-shelf (westerly) during the 1990s, corresponding with periods of good and poor recruitment, respectively. Finally, the Arctic Oscillation was found to be an important indicator of arrowtooth flounder productivity. Model results were applied to IPCC (Intergovernmental Panel on Climate Change) future springtime wind scenarios to predict the future impact of climate on northern rock sole productivity and indicated that a moderate future increase in recruitment might be expected because the climate trends favor on-shelf transport but that density-dependence will dampen this effect such that northern rock sole abundance will not be substantially affected by climate change.

Published by Elsevier Ltd.

1. Introduction

Increasing attention has been focused on trying to understand the linkage between the variability in recruitment and the environment in marine fish and shellfish populations (ICES, 2011). Understanding these links will be essential to developing quantitative estimates of the impacts of climate change on these marine populations. The findings of how future climate change will impact marine populations would be useful to a broad spectrum of stakeholders, including those who rely on fish and shellfish resources for their businesses or communities, fishery managers who utilize forecasts to determine whether actions are needed to facilitate future sustainability, and conservation groups who seek to understand the risks and challenges that a changing climate may have on their species of interest. For fishery managers and analysts, such information linking climate and recruitment would provide the ability to produce more realistic forecasts of annual

production by including both environmental variability and biological controls in place of methods that are restricted to the use of random draws from historical distributions of recruitment.

The influence of climate forcing on flathead sole (*Hippoglossoides elassodon*), northern rock sole (*Lepidopsetta polyxystra*) and arrowtooth flounder (*Atheresthes stomias*) recruitment for the period 1978–1996 follows a pattern that is consistent with shifts of atmospheric forcing in the region (Wilderbuer et al., 2002). Here, we extend the analysis of Wilderbuer et al. (2002) through 2005 (last year of available recruitment estimates) to test whether the observed relationships still hold. We then examine potential future productivity of northern rock sole based on simulations of recruitment through 2050 using IPCC (Intergovernmental Panel on Climate Change) downscaled spring-time wind projections (Najac et al., 2009).

Flathead soles, northern rock soles and arrowtooth flounders are of both ecological and commercial importance in the Eastern Bering Sea. Ecologically, they occupy separate segments of the Bering Sea ecosystem. Northern rock soles consume benthic infauna (polychaetes as well as other marine worms), whereas arrowtooth flounders are a large piscivorous fish capable of consuming large amounts of juvenile pollock (Ianelli et al., 2010;

* Corresponding author. Tel.: +1 206 526 4224; fax: +1 206 526 6723.
E-mail address: tom.wilderbuer@noaa.gov (T. Wilderbuer).

Lang et al., 1995). Flathead soles consume both benthic and pelagic prey and have a broad diet, where fish consumption increases with predator length (Stockhausen et al., 2010). The northern rock sole commercial fishery is the second largest flatfish fishery in the United States, (averaging 50,000 metric tons (t) annually), and is highly prized for its roe (NPFMC, 2010). Flathead sole and arrowtooth flounder have a combined average catch of 17,500 t since 1995.

2. Rationale for analysis

After spawning of mature adults in late winter–early spring, the larvae of these species are subject to advection from wind, currents, and tidal forcing, as well as spatial and temporal variability in food sources, during April–June. During these months, or shortly thereafter, surviving larvae settle to the seafloor in nearshore nursery areas, where they metamorphose into the flatfish form and commence a benthic life style. These near shore nursery areas (including bays and estuaries) are important nursery habitats for the early-life history stages of flatfish species worldwide (Gibson, 1997; Norcross et al., 1996, 1999). The following indices reflect potential mechanisms that may underlay the apparent associations between the recruitment patterns of winter spawning flatfish and climate variability:

- 1) Average May sea surface temperature (SST) measured at St. Paul Island—a possible indicator of variability in larval food supply required for good survival which has been identified as a determinant of year-class productivity for rock sole (Fargo and McKinnell, 1989) and is linked to the timing of the spring bloom in the Bering Sea (Hunt and Stabeno, 2002).
- 2) Average annual Arctic Oscillation Index—an indicator of large scale ocean-atmosphere processes which partially determine local ocean conditions and is linked to the Aleutian low pressure center that has shown decadal oscillations and appears to be in-phase with time periods of favorable recruitment.
- 3) A near-surface drift pattern index that characterizes simulated trajectories as on-shelf, along-shelf or off-shelf based on April 1–June 30 wind-driven larval advection spatial patterns from a known spawning location on the Bering Sea shelf. These drift trajectories serve as an index of annual springtime advection to favorable nursery areas.
- 4) Estimated depth (m) and distance from land in nautical miles (nmi) at the June 30 endpoint of larval drift by the Ocean Surface Current Simulation (OSCURS) model (Ingraham and Miyahara, 1988). These metrics serve as measures of nearness to nursery areas at the time of settlement.

3. Methods

Recruitment estimates for Eastern Bering Sea flatfish are available from age-structured stock assessment models used in annual stock assessments for the Bering Sea/Aleutian Islands groundfish stocks (NPFMC, 2010). Data used in the stock assessments include fishery and NMFS trawl survey age and length compositions, as well as biomass estimates from trawl surveys and fishery catch information, to produce numerical population estimates of age-specific abundance from the 1970s to 2010. Estimates of age 1 (arrowtooth flounder and northern rock sole) and age 3 (flathead sole) recruitment and female spawning biomass are shown in Fig. 1 for 1978–2005. Recruitment estimates are only available for fish spawned through 2005, since they are not captured in the trawl survey until ages 4 or 5.

The OSCURS model was used to analyze advection of flatfish larvae from spawning areas to nursery grounds in a given year. Used in conjunction with known spatial and temporal locations of spawning flatfish, the OSCURS model calculates 24-hour water movement in the North Pacific Ocean and Bering Sea by converting the daily sea level pressure grid to wind direction and surface mixed layer current velocity and then adding the long term-geostrophic currents (Ingraham and Miyahara, 1988). The estimated center of spawning concentrations (Wilderbuer and Nichol, 2011) and the approximate larval duration of winter spawning flatfish were used to determine the starting point and duration for the wind drift surface current simulations. Based on commercial fishery locations when fleets were in pursuit of northern rock sole roe, simulations were started at 56°N, 164°W for a 90-day period from April 1 to June 30. End-points of the simulated drift were used as an estimator for location and settlement after 90 days. Annual springtime climate conditions were characterized according to the range of the ending longitude (L) for each larval drift simulation: (A) on-shelf drift ($L < 165^\circ\text{W}$), (B) along-shelf drift ($165^\circ\text{W} < L \leq 168^\circ\text{W}$), and (C) off-shelf drift ($168^\circ\text{W} \leq L$). To evaluate the effects of the environmental variables on estimated recruitment a nonlinear statistical model was employed. A Ricker stock recruitment curve with environmental factors was fitted for the stocks of the three flatfish species, as follows:

$$R = \alpha S e^{-\beta S + E_1 V_1 + E_2 V_2 \dots + E_7 V_7},$$

where R and S are recruitment and stock in millions and kilotons, respectively, α is a density-independent parameter, β is a density-dependent parameter, and V_1 through V_8 are the following environmental variables: V_1 , the ending larval drift depth (m); V_2 , the ending larval drift distance from land; V_3 , the Arctic Oscillation; V_4 , the Pribilof Islands SST; V_5 , the on-shelf winds (1 = drift endpoint east of 165° longitude, 0 otherwise); V_6 , the along-shelf winds (1 = drift endpoint between 165 – 168° longitude, 0 otherwise); and V_7 , the off-shelf winds (1 = drift endpoint west of 168° longitude, 0 otherwise). The Ricker model was chosen for this analysis because it provided the best fit to the stock-recruitment estimates.

We evaluated model suitability using Akaike's information criterion (AIC), an information theoretic model selection criterion (Akaike, 1973; Burnham and Anderson, 2002, 2004). Using AIC allows one to rank a set of alternative models based on the estimated Kullback–Liebler information (loss) associated with each model relative to the unknown truth (Burnham and Anderson, 2004). For any given model i , the associated AIC value (AIC_i) is given by

$$AIC_i = -2 \times \ln(L_i(\hat{\theta}_i|data)) + 2 \times K_i,$$

where $L_i()$ is the maximum likelihood for model i and K_i is the number of model parameters. AIC thus applies a principle of parsimony to model selection by providing a balance between fitting the data and model complexity. Model selection using AIC consists of ranking the set of candidate models based on their AIC values, with the model having the smallest AIC value being the “best”.

Because the AIC value for any particular model is not interpretable (it is much affected by sample size and contains arbitrary constants), it is important to rescale them to

$$\Delta_i = AIC_i - AIC_{\min},$$

where AIC_{\min} is the minimum AIC value in the set of candidate models. This rescaling results in the best model having $\Delta_i = 0$, while the rest have positive values. Δ_i represents the information loss associated with using model i rather than the best model. The transformation $\exp(-\Delta_i/2)$ provides the likelihood of the model, given the data (Akaike, 1981). The relative likelihood of model i versus model j is given by $\exp(-(\Delta_i - \Delta_j)/2)$, and is termed the

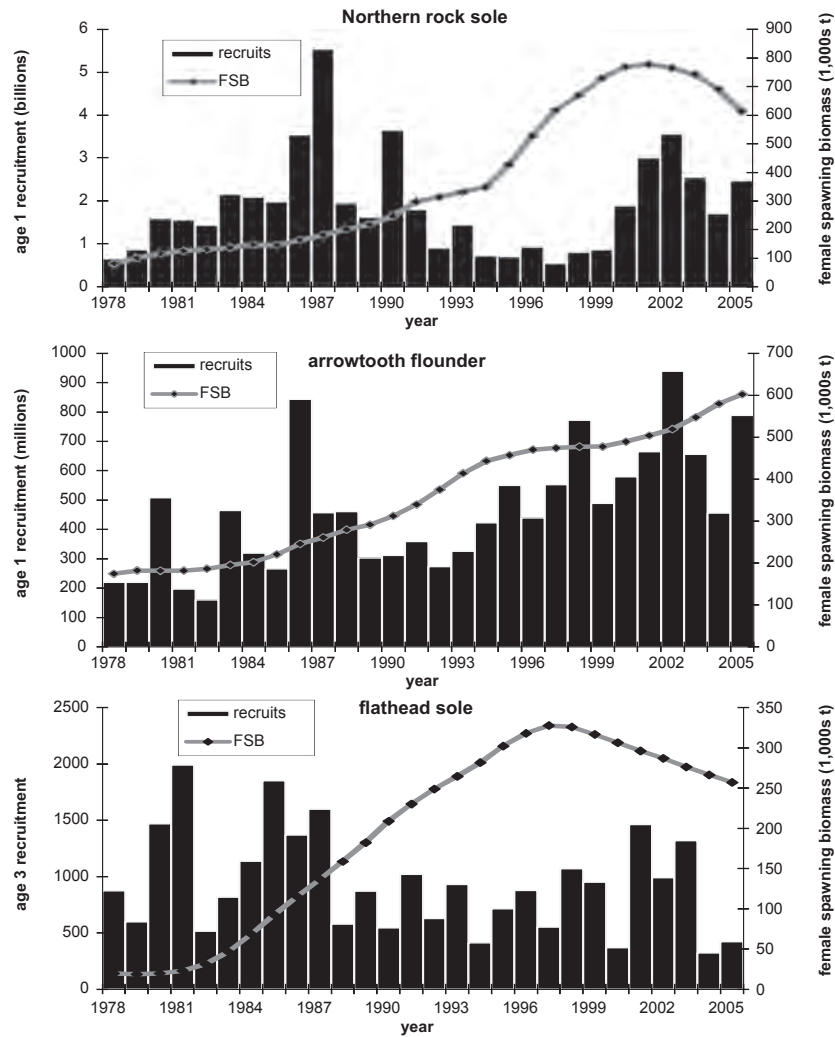


Fig. 1. Stock assessment model estimates of recruitment and female spawning biomass (FSB) for three eastern Bering Sea flatfish species.

evidence ratio or model odds. If the evidence ratio is very large (e.g., ratio > 150), then model *j* is a poor model relative to model *i*. The rescaled AIC values can also be normalized such that they sum to 1 and can be treated as probabilities:

$$w_i = \frac{\exp(-\Delta_i/2)}{\sum_j \exp(-\Delta_j/2)},$$

where w_i , also called Akaike weights, are useful in evaluating the weight of evidence in favor of model *i* being the best model in the set of candidate models. The model odds (evidence ratios: w_i/w_j) are independent of the set of candidate models, while the w_i 's depend on the set, because they sum to 1. Here, we used both the model probabilities (w_i 's) and the model odds, relative to the model with smallest AIC, to evaluate model suitability.

The flatfish species with the strongest association between recruitment strength and springtime wind regime was then used in a projection model with downscaled global climate model output to model future recruitment productivity. The climate models used in this analysis are model simulations of global climate which were conducted for the IPCC Fourth Assessment Report. The IPCC produced 23 different coupled atmosphere–ocean general circulation models to forecast future climate under common CO₂ emission scenarios. Hollowed et al. (2009) presented a protocol designed for using these simulations towards the projection of environmental factors known or suspected to be important to fisheries. The method relies on critical evaluation of

the models' 20th century hindcast simulations. The first step is to consider the degree to which each available model replicates the spatial pattern, temporal scale and magnitude of variance associated with the leading mode of variability in North Pacific SST (i. e., the Pacific Decadal Oscillation (PDO)). The top 12 models most successful at replicating the historical PDO (Overland and Wang, 2007) were selected. In particular, as detailed in Hollowed et al. (2009), we then used the projections from these models to create weighted ensemble means and estimates of uncertainties for individual parameters in specific regions. As long as the physical environmental controls for a specific population or region are reasonably well known, and forecasts appear reliable, this approach should provide plausible calculations of flatfish productivity trends. It should be considered as complementary to direct simulations (Aquad et al., 2006), in which climate scenarios are used to force regional ocean numerical models, which in turn are linked to biological models (i.e., dynamical downscaling).

Following the framework for projecting environmental indicators outlined above, spring wind and the associated advection on the Bering Sea shelf were estimated from a weighted ensemble of the IPCC model output. The various IPCC models used (those that captured the PDO trend as described above) were rated based on how well their hindcasts for the latter half of the 20th century matched observations. The two specific criteria for this rating were the IPCC model's ability to reproduce the overall mean April–June winds on the southeast Bering Sea shelf, and the interannual

variance in the seasonal mean winds. The weights for each model were then used to form a projection of the seasonal mean winds, and the attendant variance or uncertainty, out to 2050 and converted to ending longitude of surface-drifting larvae. The result using this approach features a slight tendency towards increased shoreward transports through the first half of the 21st century, with substantial variability on top of this weak trend (Fig. 2).

Based on the results from the IPCC climate models (Fig. 2), the future production of northern rock sole was projected for the period 2010–2050 using the aforementioned Ricker stock recruit model with environmental variables. This allowed for estimates of annual variability in future springtime climate (i.e., wind direction and subsequent larval drift) as well as variability in recruitment under projected future climate conditions as follows: First, three climate conditions were characterized according to the range of the ending longitude as described above. Then, for each projected year, the corresponding predicted mean drift longitude and variance from the IPCC model results were used (Fig. 2) to draw a sample drift longitude from a normally-distributed population. Next, the climate condition corresponding to the sample longitude was identified based on the limits described above and the probability of occurrence for each climate condition was computed (Fig. 3) using bootstrap sampling with replacement.

Recruitment for each future year was assigned from the Ricker stock recruitment curve with environmental factors as described above. An age-structured projection model was then run configured as follows: the projections begin with the age-specific schedules of numbers, body mass (g), fishery selectivity, natural mortality, and proportion mature as estimated in a recent stock assessment (Wilderbuer and Nichol, 2009). Fishing mortality followed the North Pacific Fishery Management Council harvest control rule without considering market or other factors (e.g., by catch limits) which typically limit catches (NPFMC, 2010). Future recruitment was drawn from the stock–recruit curve depending on the IPCC predicted future springtime wind regime and the model estimate of female spawning biomass with lognormal variability ($\sigma=0.6$) assumed. One hundred stochastic recruitment scenarios were then generated from each of 100 future climate scenarios up to the year 2050.

4. Results

Spawner recruit modeling results indicate that the density-dependent β term provides a better fit than any particular environmental variable; the probability was >99% that the

standard Ricker model (with α and β only) was the correct model when compared to models that estimated α and a single environmental parameter (Table 1). This is primarily because low-to-moderate levels of spawning biomass for these stocks was associated with high recruitment (the 1980s) while higher levels of spawning biomass were associated with lower recruitment (the 1990s). An examination of recruitment and springtime wind patterns indicates that the environment may have played a major role in the reproductive success of these species over decadal time periods. Modeling results indicate that adding the environmental data to the standard Ricker model after the inclusion of the density-dependent β term identified spring wind pattern as an important explanatory variable for northern rock soles and the Arctic Oscillation and springtime winds for arrowtooth flounders. For flathead soles, no single environmental variable was as important in terms of explaining recruitment variability compared to the other two species, although spring wind pattern was the variable of greatest importance among those considered here.

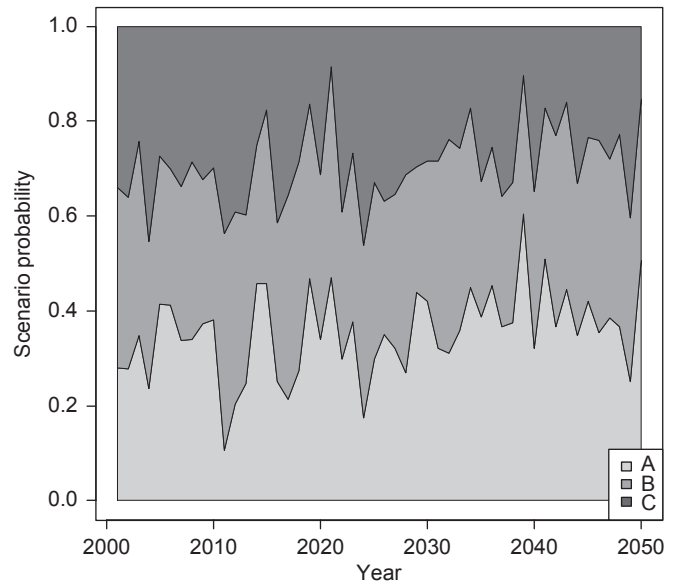


Fig. 3. Cumulative probability of future spring climate conditions based on 20,000 bootstrap samples per year. (A) On-shelf winds; (B) mid-shelf winds; and (C) off-shelf winds.

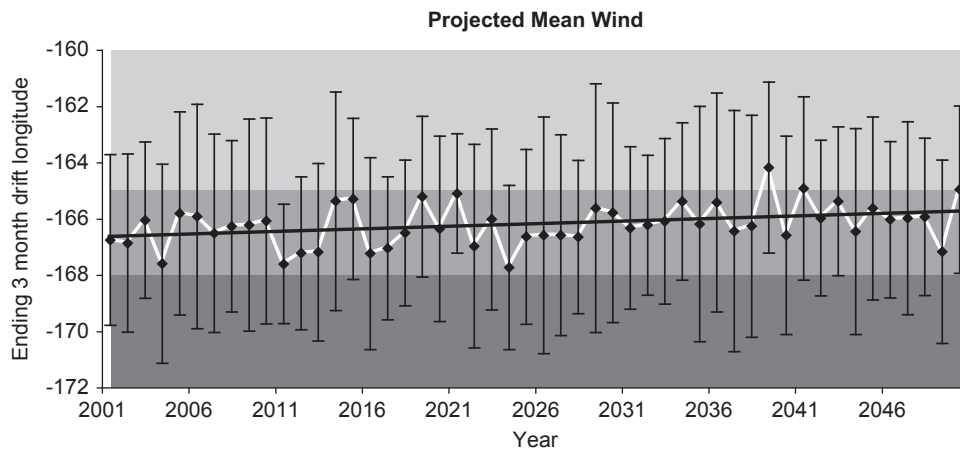


Fig. 2. Predicted mean and standard deviation of the longitudinal endpoint of projected larval drift from spring winds for 2001–2050. Color shading reflects classification of projected endpoints according to spring climate condition: on-shelf wind drift (light shading), off-shelf wind drift (dark shading), and across-shelf wind drift (gray shading).

Findings of strong density-dependence in autocorrelated recruitment time-series could be a symptom of the non-independence of successive years of estimated female spawning biomass and recruitment. Differences in Bering Sea springtime climate occurring on a decadal (or other) scale may also contribute to these patterns in recruitment. Simulations of ocean surface current trajectories indicate differences in springtime drift patterns that may determine flatfish larval advection to favorable nursery areas. From 1980 to 1989 the April 1–June 30 surface current pattern over the Bering Sea shelf was generally on-shelf or along-shelf (except for 1984 and part of 1985), whereas for the years 1990–1999 the pattern was more consistently off-shelf (except 1994, 1998 and 1999, Fig. 4). On- and along-shelf patterns persisted again from 2001 to 2006, with the exception of 2005, where winds were again predominately off-shelf. Average estimated recruitment for the three flatfish species was higher for the years with on-shelf currents relative to years with off-shelf currents; being 50% greater for northern rock sole and flathead sole and 11% higher for arrowtooth flounder.

The return to more consistently on-shelf transports during 1999–2006 was associated with the overall distribution in anomalous sea level pressure (SLP) shown in Fig. 5. The spatial scale of this SLP perturbation was > 1000 km, similar to those in the 1980s and 1990s (Wilderbuer et al., 2002). It is these kinds of long-term and large-scale features that can be predicted, at least in principle, by current generation climate models.

Given this indication that the environment has played a significant role in the reproductive success of these species, spawner–recruit relationships were fit for years consistent with each oceanic springtime wind regime (Fig. 6). Higher recruitment levels are estimated for northern rock soles from years with both on-shelf and across-shelf winds, and flathead sole and arrowtooth flounder curves were higher in on-shelf years, indicating that the environment is linked to the productivity of these stocks.

Since the relationship between springtime wind patterns and recruitment strength was found to be highest for northern rock sole, the Ricker spawner–recruit model with environmental variables was applied to downscaled IPCC estimates of future springtime wind direction over the Bering Sea shelf to provide predictions of their future productivity. In the IPCC downscaled climate models for the Bering Sea, the temporal trend in probability of occurrence of each future climate scenario followed a pattern similar to that of the mean ending longitude of larval drift (Fig. 2). These results imply that a moderate recruitment increase over time might be expected because the trend indicates more frequent occurrence of the on-shelf climate condition which on average corresponds to stronger year-class strength (Fig. 3A). However, when the recruitment projection model includes the

density-dependent effects from the stock-recruitment model and the environmental effects, the trend toward larger recruitments with time is much reduced (Fig. 7). These results indicate that climate change impacts on northern rock sole production will be relatively minor, at least regarding hypothesized effects changes in patterns of springtime larval advection.

5. Discussion

A possible outcome of revisiting past analyses with an updated time series is that correlations and relationships that were observed in the past may not hold with an extended data set (Brodeur et al., 2002, 2008). In the case of this updated analysis, incorporation of the stock assessment estimates of recruitment and female spawning biomass through 2005 has produced results consistent with the earlier analysis. Namely, density-dependence still dominates the Ricker fit to the estimates, on-shelf and across-shelf winds are positively correlated with northern rock sole year-class strength (and to a lesser extent flathead sole) and the Arctic Oscillation is important for arrowtooth flounder. Other research has focused on relating temporal shifts in oceanographic forcing to the variability in spawning biomass and recruitment to distinguish those effects from density-dependent factors (Bakun, 1996; Clark et al., 1999; Wilderbuer et al., 2002).

Four hypotheses are presented to reconcile alternating cycles of synchronous strong and weak recruitment with environmental conditions for three winter-spawning Bering Sea flatfish. Although the relationship between spawning stock size and recruitment was the dominant factor in this type of analysis, springtime wind direction was also found to coincide with years of high recruitment for northern rock soles, and to a lesser extent flathead soles, and the Arctic Oscillation and springtime winds were important for arrowtooth flounders. Strong year classes have been found to correspond to years when the on-shelf and/or across-shelf advection was predominately eastward or northeastward toward the nearshore nursery areas which extend around Bristol Bay. Other Bering Sea fish and invertebrate stocks have also exhibited periodic and autocorrelated trends in recruitment success that have been linked to the environment. Examples are king crab stocks (Zheng and Kruse, 2000), Tanner crabs (Rozenkranz et al., 1998), Pacific halibuts (Clark et al., 1999) and walleye pollocks (lanelli et al., 2011; Mueter et al., 2011).

The Arctic Oscillation is related to annual ice extent and the subsequent formation of the cold pool (waters less than 2 °C.) on the Bering Sea shelf each summer from the maximum ice extent the previous winter (Stabeno et al., 2001). Arrowtooth flounders typically avoid these cold waters (Spencer, 2008) and their

Table 1

Results of the Ricker spawner recruit model fit to the environmental data hypothesized to influence recruitment estimates for northern rock soles, flathead soles and arrowtooth flounders (Bolded cells indicate most important effects).

Model	Northern rock sole		Flathead sole		Arrowtooth flounder	
	Probability	Odds	Probability	Odds	Probability	Odds
α and depth	0.001		0		0	
α and distance	0.001		0		0	
α and arctic oscillation	0.001		0		0	
α and sea surface temperature	0.001		0		0	
α and springtime wind pattern	0.002		0		0	
α and β (density dependence)	0.993		1		1	
α and β (density dependence) and depth	0.08	1.2	0.11	1.1	0.16	2.5
α and β (density dependence) and distance	0.09	1.3	0.05	1.2	0.06	1.0
α and β (density dependence) and arctic oscillation	0.10	1.5	0.11	2.5	0.35	5.6
α and β (density dependence) and sea surface temperature	0.12	1.8	0.13	2.7	0.06	1.0
α and β (density dependence) and springtime wind pattern	0.61	9.1	0.17	3.1	0.30	4.7

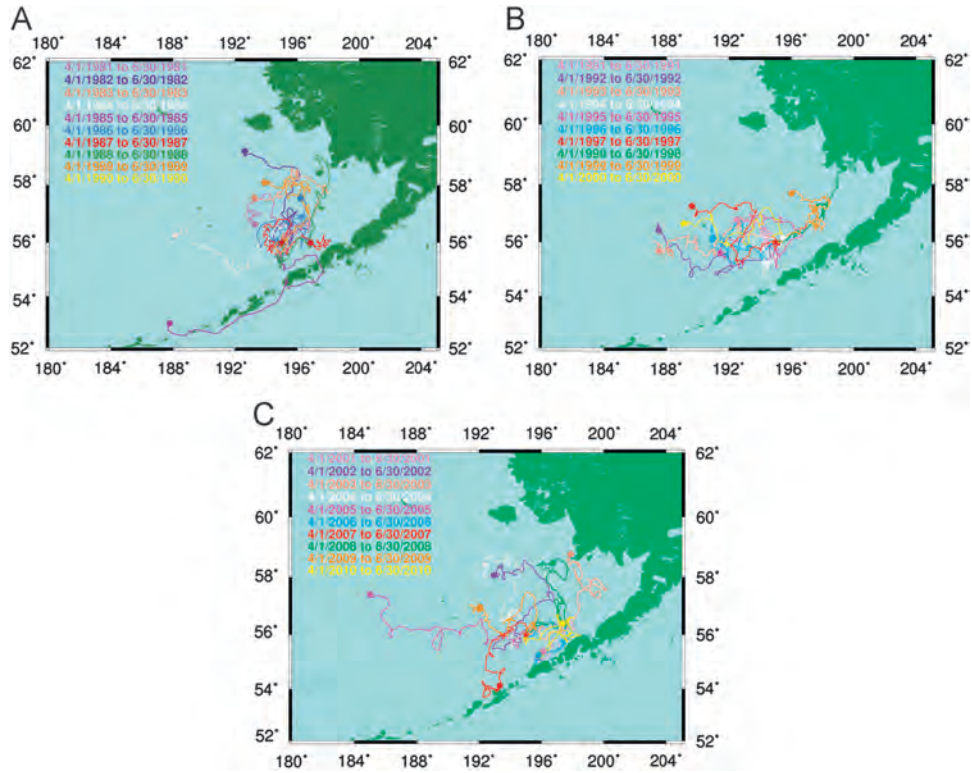


Fig. 4. (A) Ocean Surface Current model results for 1981–1990, (B) Ocean Surface Current model results for 1991–2000 and (C) Ocean Surface Current model results for 2001–2010.

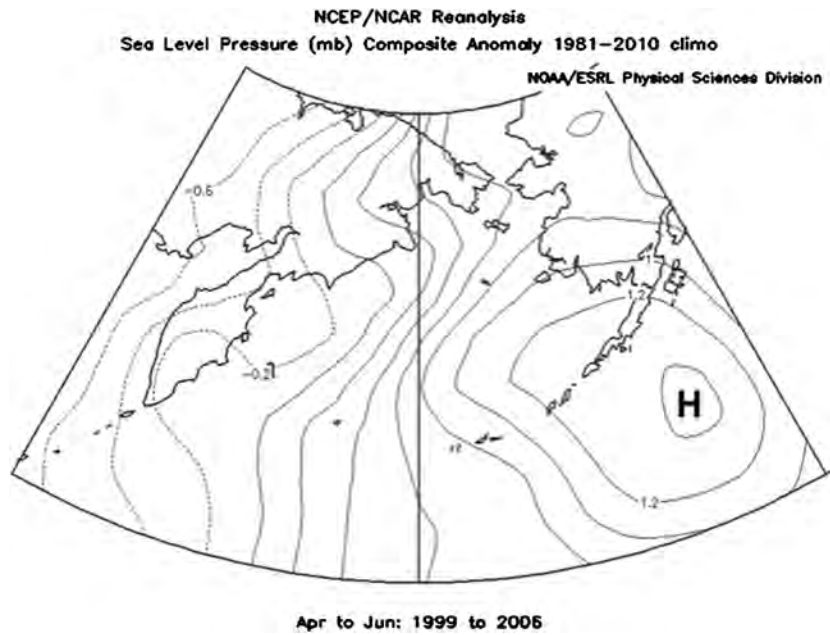


Fig. 5. Sea level pressure (mb) composite anomalies for the Bering Sea for April–June 1999–2006.

distribution also may be influenced by the distribution of their prey (juvenile pollock). However, it is uncertain how this characteristic is linked to recruitment success but may have implications for settlement patterns as they relate to increased survival. A source of additional uncertainty in this study regarding arrowtooth flounder is the April 1–June 30 time period used to assess larval drift. Doyle et al. (2009) reported that the peak timing of larval fish occurrence in Gulf of Alaska ichthyoplankton surveys was in January and February with lesser amounts in March–June, suggesting that the time-period selected here was more appropriate for northern rock

soles and flathead soles but did not match well the peak larval advection period for arrowtooth flounders.

May SST, thought to be representative of the annual availability of larval food through the timing of the spring bloom, was only found to be of limited importance in this analysis. The importance of the availability of larval food at the time of first feeding has been shown to be critical for anchovy (Lasker, 1975) and is also most likely true for Alaska flatfish. However, our characterization of the mis-match of larval food at the essential time for these species from the use of May SST was probably too coarse an approach.

Improved knowledge of the annual variability in phytoplankton bloom dynamics over finer scales would be required to understand how this factor relates to year-class strength.

The simulation methods presented here allow for the opportunity to project Bering Sea winds for the next four decades where the magnitude of the projected changes in the cross-shelf winds are

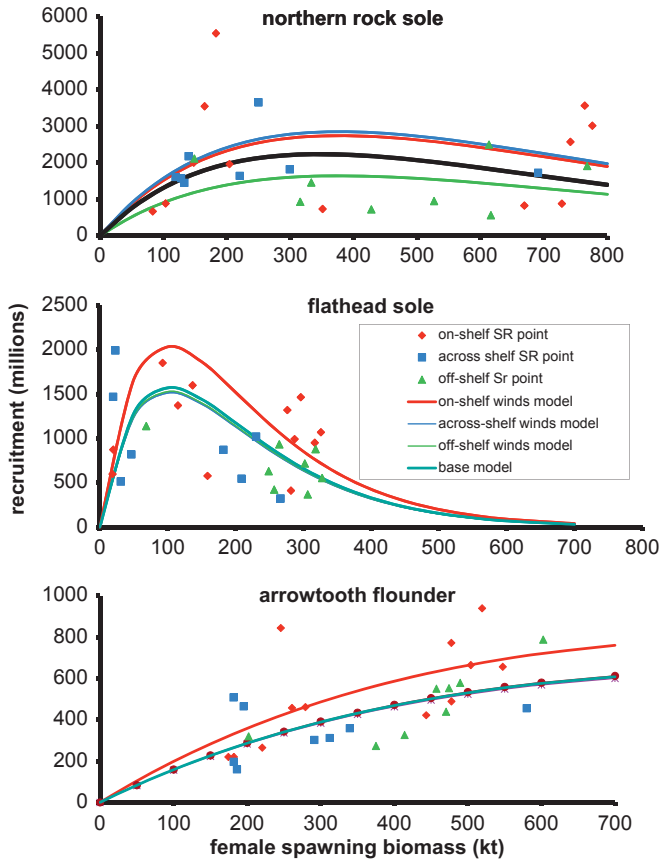


Fig. 6. Ricker model fit to spawner-recruit estimates for the three springtime climate conditions (on-shelf, across-shelf and off-shelf) for northern rock sole, flathead sole and arrowtooth flounder.

comparable to the decadal variations observed in the 20th century. Results from the IPCC climate simulations indicate a future climate trend favoring on-shelf winds which could promote a modest increase in the median productivity of northern rock sole, with a high amount of variability in the projection. Adding a stock–recruitment relationship with recruitment variability resulted in recruitment simulations with more variability and lacked the trend toward more favorable recruitment because density dependence appears strong for northern rock soles. This suggests that incorporating the relationship between spawning stock biomass and subsequent recruitment in the projections has a dampening effect on the future estimates compared to assuming recruitment is independent of spawning biomass and largely a function of the environment.

The key uncertainties in these projections are the characterizations of future springtime winds (climate models) and the interpretation of climatic state and its linkage to the stock–recruit relationship. The climate models may tend to underestimate the degree to which consecutive yearly runs of favorable or unfavorable conditions occur on decadal or smaller time scales (Overland et al., 1999). Autocorrelated patterns of this sort can have large impacts on the population dynamics of fish and invertebrate stocks. Although this effect may be present in some of the individual model runs produced, we do not rely on individual realizations to forecast the implications of future climate change but instead use the composite of many realizations to generalize future impacts. In addition, the climate models are reliant upon the model assumptions set forth in the AR4 report (IPCC, 2007) regarding future emission scenarios. The extent to which these assumptions will be validated over the next 40 years is unknown. Additionally, the oceanographic response to climate is also uncertain and can potentially give conflicting results. Regarding the interpretation of springtime Bering Sea winds as they relate to future recruitment, the process is undoubtedly more complicated than offered here and include, in addition to larval advection: predation and starvation (Cushing, 1975), changes in the duration of the larval pelagic stage brought on by changes in sea surface temperature (Van der Veer et al., 2000), and changes in annual spawning distributions (Rijnsdorp et al., 2009). These processes were not explicitly included in the projection model used in this analysis but may be considered as part of the added recruitment variability (i.e., σ_R).

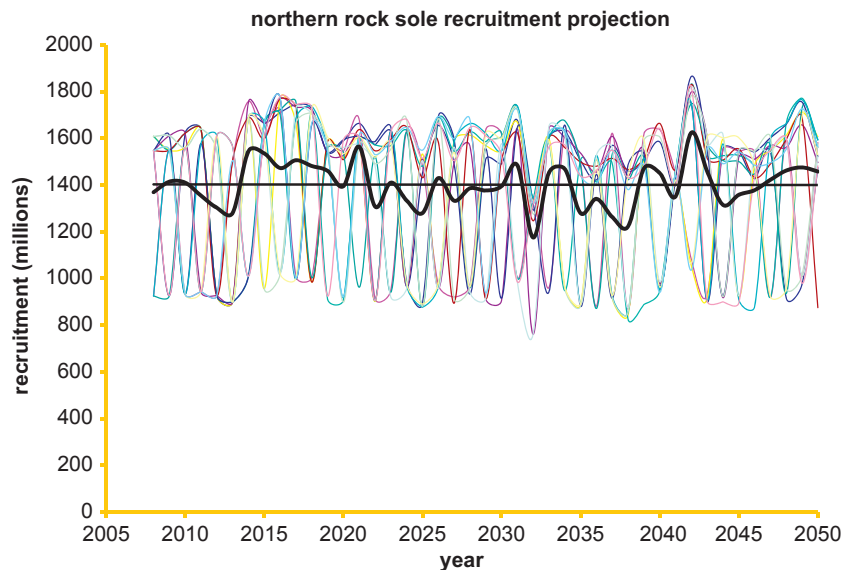


Fig. 7. Projected northern rock sole recruitment through 2050 using IPCC (Intergovernmental Panel on Climate Change) climate scenarios and Ricker stock recruitment formulation which relates recruitment to wind direction and spawning stock size. The thick black line is annual mean of 10,000 model realizations, and the straight black line is the trend line fit to the annual means. Thin colored lines represent some selected individual model realizations.

The mechanisms that affect species productivity and are also related to climate change are typically poorly understood and hard to predict (Francis et al., 1998). Cases where mechanisms have been linked to productivity or growth suggest that future climate change is bound to affect some species in an adverse manner while others may benefit. Mueter et al. (2011) found that walleye pollock productivity is negatively correlated with increasing sea surface temperatures, and ice-associated species are predicted to vacate some current habitat as it becomes less favorable as they move poleward in warming conditions (ACIA, 2005). In contrast, Nye et al. (2009) compared the distributional responses of 36 fish stocks in the Northeast Atlantic Ocean over the past 40 years in relation to temperature changes and found that many sub-arctic species expanded their range northward with increasing temperatures as more favorable habitats became available with warming. Although there are large uncertainties in the future springtime wind direction in the Bering Sea, the northern rock sole example suggests a species which may not be substantially impacted by future climate change—at least in regard to the effects of that change on patterns of springtime larval advection through the end of our projections.

Acknowledgments

The authors thank Jim Ianelli for his assistance in coding the population dynamics projection model and Neal Williamson, Paul Spencer, James Lee, Mike Sigler and two anonymous reviewers for their thoughtful reviews of the manuscript. This manuscript has been assigned NPRB no. 365 and BEST-BSIERP Bering Sea Project no. 69. The findings and conclusions in the paper are those of the authors and do not necessarily represent the views of the National Marine Fisheries Service, NOAA.

References

- ACIA, 2005. Arctic Climate Impact Assessment. Cambridge University Press 1042.
- Akaike, H., 1973. Information theory as an extension of the maximum likelihood principle. In: Petrov, B.N., Csaki, F. (Eds.). Proceedings of the Second International Symposium on Information Theory, Akademiai Kiado, Budapest pp. 267–281.
- Akaike, H., 1981. Likelihood of a model and information criteria. *J. Econometrics* 16, 3–14.
- Auad, G., Miller, A., Di Lorenzo, E., 2006. Long-term forecast of oceanic conditions off California and their biological implications. *J. Geophys. Res.* 111, C09008, <http://dx.doi.org/10.1029/2005JC003219>.
- Bakun, A., 1996. Patterns in the ocean. Ocean processes and marine population dynamics. California Sea Grant/CIB, p. 323.
- Brodeur, R.D., Sugisaki, H., Hunt Jr., G., 2002. Increases in jellyfish biomass in the Bering Sea: implications for the ecosystem. *Mar. Ecol. Prog. Ser.* 233, 89–103.
- Brodeur, R.D., Decker, M., Ciannelli, L., Purcell, J., Bond, N., Stabeno, P., Acuna, E., Hunt Jr., G., 2008. Rise and fall of jellyfish in the eastern Bering Sea in relation to climate regime shifts. *Prog. Oceanogr.* 77, 103–111.
- Burnham, K.P., Anderson, D.R., 2002. Model Selection and Multimodel Inference: A Practical Information: Theoretical Approach, 2nd ed. Springer-Verlag, New York.
- Burnham, K.P., Anderson, D.R., 2004. Multimodel inference: understanding AIC and BIC in model selection. *Socio. Methods Res.* 33, 261–304.
- Clark, W.G., Hare, S.R., Parma, A.M., Sullivan, P.J., Trumble, R.J., 1999. Decadal changes in growth and recruitment of Pacific halibut (*Hippoglossus stenolepis*). *Can. J. Fish. Aquat. Sci.* 56, 242–252.
- Cushing, D.H., 1975. Marine Ecology and Fisheries. Cambridge University Press, Cambridge/New York.
- Doyle, M.J., Picquelle, S.J., Mier, K.L., Spillane, M.C., Bond, N., 2009. Larval fish abundance and physical forcing in the Gulf of Alaska, 1981–2003. *Prog. Oceanogr.* 80, 163–187.
- Fargo, J., McKinnell, S., 1989. Effects of temperature and stock size on year-class production for rock sole (*Lepidopsetta bilineata*) in northern Hecate Strait, British Columbia. In: Beamish, R.J., McFarlane, G.A. (Eds.). Effects of ocean variability on recruitment and an evaluation of parameters used in stock assessment models. *Can. Spec. Pub. Fish. Aquat. Sci.* (108) pp. 327–333.
- Francis, R.C., Hare, S.R., Hollowed, A.B., Wooster, W.S., 1998. Effects of interdecadal climate variability on the oceanic ecosystems of the NE Pacific. *Fish. Oceanogr.* 6, 1–21.
- Gibson, R.N., 1997. Behavior and distribution of flatfishes. *J. Sea Res.* 37, 241–256.
- Hollowed, A.B., Bond, N.A., Wilderbuer, T.K., Stockhausen, W.T., A'Mar, Z.T., Beamish, R.J., Overland, J.E., Schirripa, M.J., 2009. A framework for modeling fish and shellfish responses to future climate change. *ICES J. Mar. Sci.* 66 (7), 1584–1594.
- Hunt, G.L., Stabeno, P.J., 2002. Climate change and the control of energy in the southeastern Bering Sea. *Prog. Oceanogr.* 55, 5–22.
- Ianelli, J.N., Hollowed, A.B., Haynie, A.C., Mueter, F.J., Bond, N.A., 2011. Evaluating management strategies for eastern Bering Sea walleye pollock (*Theragra chalcogramma*) in a changing environment. *ICES J. Mar. Sci.* 68 (6), 1297–1304.
- Ianelli, J.N., Barbeaux, S., Honkelato, T., Kotwicki, S., Aydin, K., Williamson, N., 2010. Assessment of the walleye Pollock stock in the eastern Bering Sea. In: Stock Assessment and Fishery Evaluation Report for the groundfish resources of the Eastern Bering Sea and Aleutian Islands. North Pacific Fisheries Management Council pp. 53–156 (Section 1).
- ICES, 2011. Climate change effects on fish and fisheries: forecasting impacts, assessing ecosystem responses, and evaluating management strategies. *ICES J. Mar. Sci.* 68 (6), 983–1372.
- IPCC, 2007. Climate change 2007: synthesis report. Contribution of Working Groups I, II and III to the fourth Assessment Report of the Intergovernmental Panel on Climate Change. In: Pachauri, R.K., Reisinger, A., Core Writing Team (Eds.). IPCC, Geneva, Switzerland. p. 104.
- Ingraham, W.J., Jr., Miyahara, R.K., 1988. Ocean surface current simulations in the North Pacific Ocean and Bering Sea. (OSCURS-numerical model), U.S. Department of Commerce, NOAA Technical Memorandum, NMFS F/NWC-130. p. 155.
- Lang, G.M., Livingston, P.A., Miller, B.S., 1995. Food habits of three congeneric flatfishes: yellowfin sole *Pleuronectes asper*, rock sole *P. bilineatus*, and Alaska plaice *P. quadrituberculatus*, in the eastern Bering Sea. In: Proceedings of the International Symposium on North Pacific flatfish, Alaska Sea Grant college Program, AK-SG-93-04, Anchorage, AK pp. 225–245.
- Lasker, R., 1975. Field criteria for survival of anchovy larvae: the relation between inshore chlorophyll maximum layers and successful first feeding. *Fish. Bull. U.S.* A 73, 453–462.
- Mueter, F.J., Bond, N.A., Ianelli, J.N., Hollowed, A.B., 2011. Expected declines in recruitment of walleye Pollock (*Theragra chalcogramma*) in the eastern Bering Sea under future climate change. *ICES J. Mar. Sci.* 68 (6), 1284–1296.
- Najac, J., Boe, J., Terray, L., 2009. A multi-model ensemble approach for assessment of climate change impact on surface winds in France. *Clim. Dyn.* 32, 615–634, <http://dx.doi.org/10.1007/s00382-0080440-4>.
- Norcross, B., Holladay, B., Dressel, S., Frandsen, M., 1996. Recruitment of juvenile flatfishes in Alaska: habitat preferences near Kodiak Island, University of Alaska, Coastal Marine Institution, Vol. 1 final study report, OCS Study MMS 96-003.
- Norcross, B., Blanchard, A., Holladay, B.A., 1999. Comparison of models for defining flatfish nursery areas in Alaskan waters. *Fish. Oceanogr.* 8 (1), 50–67.
- NPFMC North Pacific Fisheries Management Council, 2010. Stock assessment and fishery evaluation document for groundfish resources in the Bering Sea/Aleutian Islands Region as projected for 2001. North Pacific Fishery Management Council, P. O. Box 103136, Anchorage, Alaska, 99510.
- Nye, J.A., Link, J.S., Hare, J.A., Overholtz, W.J., 2009. Changing spatial distribution of fish stocks in relation to climate and population size on the Northeastern United States continental shelf. *Mar. Ecol. Prog. Ser.* 393, 111–129.
- Overland, J.E., Adams, J.M., Bond, N.A., 1999. Decadal variability of the Aleutian low and it's relation to high latitude circulation. *J. Clim.* 12, 1542–1548.
- Overland, J.E., Yang, M., 2007. The Arctic climate paradox: the recent decrease of the Arctic Oscillation. *Geophys. Res. Lett.* 34 (L06701), 5.
- Rijnsdorp, A.D., Peck, M.A., Engelhard, G.H., Millmann, C., Pinnegar, J.K., 2009. Resolving the effect of climate change on fish populations. *ICES J. Mar. Sci.* 66 (7), 1570–1583.
- Rozenkranz, G.E., Tyler, A.V., Kruse, G.H., Niebauer, H.J., 1998. Relationship between wind and year-class strength of tanner crabs in the Southeastern Bering Sea. *Alaska Fish. Res. Bull.* 5, 18–24.
- Spencer, P.D., 2008. Density-independent and density-dependent factors affecting temporal changes in spatial distributions of eastern Bering Sea flatfish. *Fish. Oceanogr.* 17, 396–410.
- Stabeno, P.J., Bond, N.A., Kachel, N.B., Salo, S.A., Schumacher, J.D., 2001. On the temporal variability of the physical environment over the south-eastern Bering Sea. *Fish. Oceanogr.* 10 (1), 81–98.
- Stockhausen, W.T., Nichol, D.G., Lauth R., Wilkins, M., 2010. Assessment of the flathead sole in the Bering Sea and Aleutian Islands. In: Stock Assessment and Fishery Evaluation Report for the groundfish resources of the Eastern Bering Sea and Aleutian Islands. North Pacific Fishery Management Council, Anchorage, AK, 869–968 (Section 8).
- Van der Veer, H., Berghahn, W.R., Miller, J.M., Rijnsdorp, A.D., 2000. Recruitment in flatfish, with special emphasis on North Atlantic species: progress made by the Flatfish Symposia. *ICES J. Mar. Sci.* 57, 202–215.
- Wilderbuer, T.K., Hollowed, A.B., Ingraham, W.J., Spencer, P.D., Connors, M.E., Bond, N.A., Walters, G.E., 2002. Flatfish recruitment response to decadal climatic variability and ocean conditions in the eastern Bering Sea. *Prog. Oceanogr.* 55, 235–247.
- Wilderbuer, T.K., Nichol, D.G., 2009. Northern rock sole. In: Stock Assessment and Fishery Evaluation Report for the groundfish resources of the Eastern Bering Sea and Aleutian Islands. North Pacific Fishery Management Council, Anchorage, AK, 707–776 (Section 7).
- Wilderbuer, T.K., and Nichol, D.G. 2011. Northern rock sole. In: Stock Assessment and Fishery Evaluation Report for the groundfish resources of the Eastern Bering Sea and Aleutian Islands. North Pacific Fishery Management Council, Anchorage, AK, 813–888 (Section 8).
- Zheng, J., Kruse, G.H., 2000. Recruitment patterns in Alaska crabs in relation to decadal shifts in climate and physical oceanography. *ICES J. Mar. Sci.* 57, 18–24.



Historical growth of Bristol Bay and Yukon River, Alaska chum salmon (*Oncorhynchus keta*) in relation to climate and inter- and intraspecific competition



Beverly A. Agler^{a,*}, Gregory T. Ruggerone^b, Lorna I. Wilson^a, Franz J. Mueter^c

^a Alaska Department of Fish and Game, Mark, Tag, and Age Laboratory, Division of Commercial Fisheries, 10107 Bentwood Place, Juneau, AK 99801, United States

^b Natural Resources Consultants, Inc., 4039 21st Ave West, Suite 404, Seattle, WA 98199, United States

^c University of Alaska, School of Fisheries and Ocean Sciences, 17101 Point Lena Loop Road, Juneau, AK 99801, United States

ARTICLE INFO

Available online 14 March 2013

Keywords:

Growth
Salmon fisheries
Climatic changes
Sea surface temperature

ABSTRACT

We examined Bristol Bay and Yukon River adult chum salmon scales to determine whether climate variability, such as changes in sea surface temperature and climate indices, and high pink and Asian chum salmon abundance reduced chum salmon growth. Annual marine growth increments for 1965–2006 were estimated from scale growth measurements and were modeled as a function of potential explanatory variables using a generalized least squares regression approach. First-year growth of salmon originating from Bristol Bay and the Yukon River showed increased growth in association with higher regional ocean temperatures and was negatively affected by wind mixing and ice cover. Third-year growth was lower when Asian chum salmon were more abundant. Contrary to our hypothesis, warmer large-scale sea surface temperatures in the Gulf of Alaska were also associated with reduced third-year growth. Negative effects of high abundances of Russian pink salmon on third-year growth provided some evidence for interspecific interactions, but the effects were smaller than the effects of Asian chum salmon abundance and Gulf of Alaska sea surface temperature. Although the relative effects of Asian chum salmon and sea surface temperature on the growth of Yukon and Bristol Bay chum salmon were difficult to untangle, we found consistent evidence that high abundances of Asian chum salmon contributed to a reduction in the growth of western Alaska chum salmon.

© 2013 Elsevier Ltd. All rights reserved.

1. Introduction

Growth affects survival and age-at-maturation of Pacific salmon (*Oncorhynchus* spp.) in general and chum salmon (*O. keta*) in particular (e.g., Farley et al., 2007a; Healey, 1986; Martinson et al., 2008; Ruggerone et al., 2007). Faster growing salmon may be better able to avoid predators, and larger body size may provide juvenile salmon with the lipid stores necessary to survive during the winter when prey availability is low (Beamish and Mahnken, 2001; Farley et al., 2007b, 2011). Salmon growth and survival have been shown to co-vary with climate during the period of this study from the mid-1960s to the mid-2000s (Farley et al., 2007b; Ruggerone et al., 2005, 2007), when the North Pacific Ocean experienced climate shifts (Hare and Mantua, 2000; Mantua et al., 1997). Ocean regime shifts in 1976–1977 and in 1989 led to changes in abundances of salmon stocks from different parts of the Eastern North Pacific Ocean and Bering Sea (Anderson and Piatt, 1999; Hare and Mantua, 2000; Mantua et al., 1997).

Growth and productivity of chum salmon may be affected by interactions with Asian pink salmon (*O. gorbuscha*) populations, which are characterized by differences in the abundance of odd- and even-year populations. Interspecific competition for food and density-dependent growth effects have been observed when stocks originating from Asia and western Alaska intermingle and feed in offshore waters (Myers et al., 2004; Ruggerone and Nielsen, 2004; Ruggerone et al., 2003). Pink salmon may be competitively dominant over other salmon species in the North Pacific Ocean and Bering Sea because they are highly abundant, grow rapidly, and prefer high energy prey that is also consumed by other salmon species (Davis et al., 2004). It has been hypothesized that biennially-cycling pink salmon abundance inhibited growth and survival of sockeye (*O. nerka*), chum and Chinook (*O. tshawytscha*) salmon during odd-numbered years in the western Bering Sea. Chum salmon growth and survival may be inhibited by pink salmon through competition for similar prey (Kaeriyama et al., 2004). Productivity of chum salmon was negatively correlated with pink abundance, although the effect of pink salmon was less than the effect of Asian chum salmon abundance (Ruggerone et al., 2011). Researchers have also suggested that increased pink salmon abundance altered the feeding and distribution of chum salmon on the

* Corresponding author. Tel.: +1 907 465 3498; fax: +1 907 465 2765.
E-mail address: bev.agler@alaska.gov (B.A. Agler).

high seas (Azumaya and Ishida, 2000; Kaeriyama et al., 2004; Myers et al., 2004).

Intraspecific competition may lead to density-dependent growth in Pacific salmon (Ishida et al., 1993; Peterman et al., 1998; Ruggerone et al., 2003). Salmon are migratory, and competition may occur among conspecifics originating from distant locations (Pyper and Peterman, 1999). Since 1980, approximately 3.1 billion hatchery chum salmon were released annually from Asian and North American hatcheries (Ruggerone et al., 2010). Increasing hatchery production of chum salmon since the 1970s has led to concerns about possible effects of hatchery populations on wild salmon in the marine environment (Cooney and Brodeur, 1998; Holt et al., 2008). Hatchery chum production has been associated with a significant reduction in the growth of Asian chum salmon (hatchery and wild) and in delayed age-at-maturation (Ishida et al., 1993; Kaeriyama et al., 2007a; Zavolokin et al., 2009). Wild chum populations may compete for food with abundant hatchery populations. Myers et al. (2004) hypothesized that Asian chum salmon, including abundant hatchery stocks, competed with western Alaska chum salmon for food, due to their overlapping distributions with western Alaska chum. Hatchery and wild chum salmon from North America (central and southeast Alaska stocks) may also compete with wild chum salmon from western Alaska, but they are less abundant than Asian fish and do not overlap with western Alaska salmon to the same extent (Beacham et al., 2009; Myers et al., 2007; Urawa et al., 2009). Thus, competition among chum salmon for food may lead to reduced growth and survival (Ruggerone et al., 2011; Zaporozhets and Zaporozhets, 2004).

Growth of salmon scales provides an index of annual and seasonal growth of salmon at sea (Fisher and Pearcy, 2005; Fukuwaka and Kaeriyama, 1997). Several recent studies have used scales to examine similar issues with salmon (e.g., sockeye, Chinook; Kaeriyama et al., 2007b; Martinson et al., 2008; Ruggerone et al., 2005; Zavolokin et al., 2009). This paper is part of a broad study to compare marine growth of western Alaska chum salmon with Asian chum salmon abundance to determine whether growth within the North Pacific Ocean varied in response to climate change and inter- and intraspecific competition. We tested the following hypotheses: (1) growth of Bristol Bay and Yukon River, Alaska chum salmon is related to climate variability (e.g., changes in sea surface temperature (SST), North Pacific Index, etc.) and (2) high Russian pink and Asian chum salmon abundance reduces the growth of Bristol Bay and Yukon River chum salmon. We used historical chum salmon scale collections from Bristol Bay (age 0.3, 1965–2006; age 0.4 1966–2006) and Yukon River (age 0.3, 1965–2006; age 0.4, 1967–2006) to reconstruct seasonal and annual scale growth of chum salmon. These data were compared with several explanatory variables, large-scale climate indices, the abundance of Asian chum salmon, and the alternating year pattern of pink salmon abundance, which provided a natural experimental control.

2. Methods

2.1. Study Area

Scales were collected annually by personnel from Alaska Department of Fish and Game (ADF&G) following established

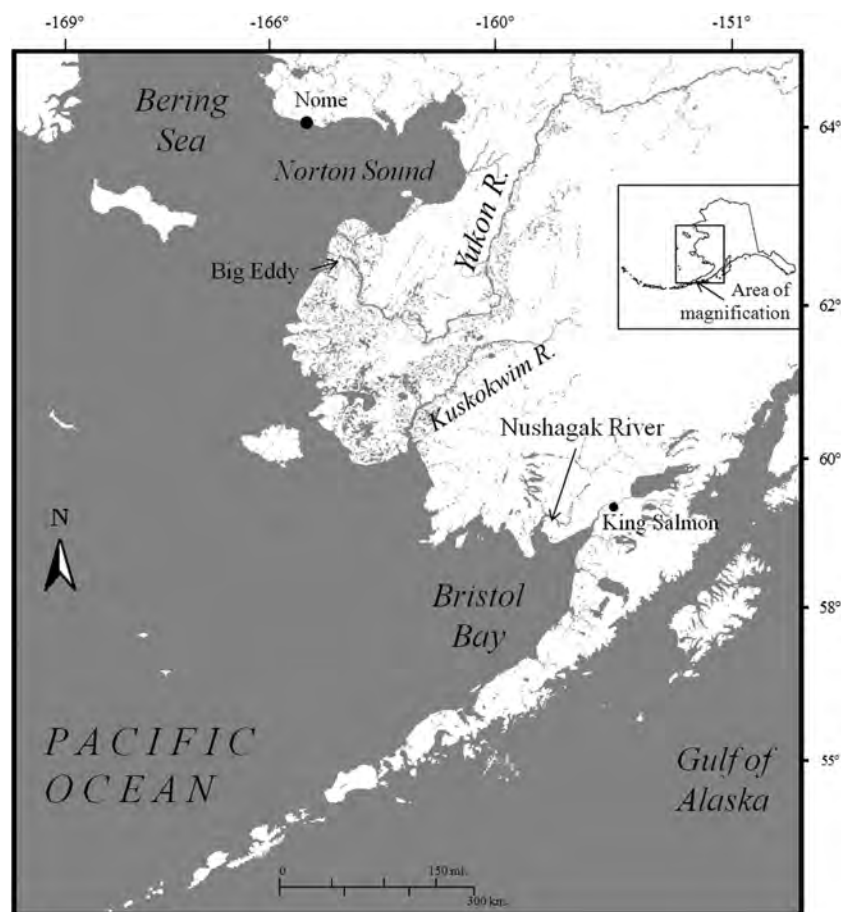


Fig. 1. Map of the study area. Scales were collected annually during the commercial chum fisheries in the Nushagak District of Bristol Bay, Alaska. The Nushagak District is located at the mouth of the Nushagak River. Scales were also collected annually during commercial and test fisheries from Big Eddy at the mouth of the Yukon River, Alaska.

protocols. Two western Alaska chum salmon populations (Bristol Bay and Yukon River) were the focus of this study. Bristol Bay scales were collected from mixed species commercial fisheries near the mouth of the Nushagak River where it flows into Bristol Bay (Fig. 1), and Yukon River scales were collected from commercial and test fisheries in the lower river.

2.2. Scale sampling

Age was designated using European notation. Chum salmon spend minimal time in freshwater and three to four winters at sea before returning to the natal stream to spawn. Thus, an age 0.3 fish spent 0 winters in freshwater followed by three winters at sea (Fig. 2). In actuality, this fish would be 4 years old when the winter spent as an embryo in gravel was included.

Acetate impressions of adult chum salmon scales were obtained from the ADF&G regional archive in Anchorage, Alaska. Only age 0.3 and 0.4 fish, the dominant age groups, were used in this study. In Bristol Bay, we obtained samples from 1965 to 2006 for age 0.3 fish and from 1966 to 2006 for age 0.4 fish, and in the Yukon River we obtained samples from 1965 to 2006 for age 0.3 fish and from 1967 to 2006 for age 0.4 fish. Yukon River fish were captured with 14 cm (85%) and 22.6 cm (15%) mesh size drift gillnets; whereas, the mesh size of the drift gillnets used in Bristol Bay was not recorded. Images of scales were selected for measurement when: (1) the reader agreed with the age determination

previously made by ADF&G; (2) the scale shape indicated the scale was collected from the preferred area of the body (Koo, 1962); (3) circuli and annuli were clearly defined and not affected by regeneration or resorption along the measurement axis; and, (4) the scale was from a fish collected between 5 June and 26 July. We sampled scales across the run from 15 June to 15 July to capture potential timing-related differences in returning salmon, but in some years samples sizes were not sufficient; in which case, sampling was extended to achieve the minimum sample size.

Scale measurements were collected using procedures described by Hagen et al. (2001). A digital microfiche reader was used to scan the scale from the acetate impressions, and the image was stored as a high resolution digital image (3360×4425 pixels). This image provided a view of the entire scale and enough pixels between the narrow circuli for accurate measurements of circulus spacing. A digital LCD flat panel monitor and Optimas 6.5 image processing software were used to measure the scale with a customized program. Scales were measured from the focus to the edge along the longest axis. The distance (resolution ~0.0017 mm/pixel) between each pair of circuli was measured within each growth zone from the scale focus to the outer edge of the first ocean annulus (SW1) then from the outer edge of SW1 to the edge of the second ocean annulus (SW2) until the edge of the scale was attained (Fig. 2). Data were stored in a Microsoft Access database by growth zone and linked to the age, sex, and length data by a fish identification number. In most years, 25 male and

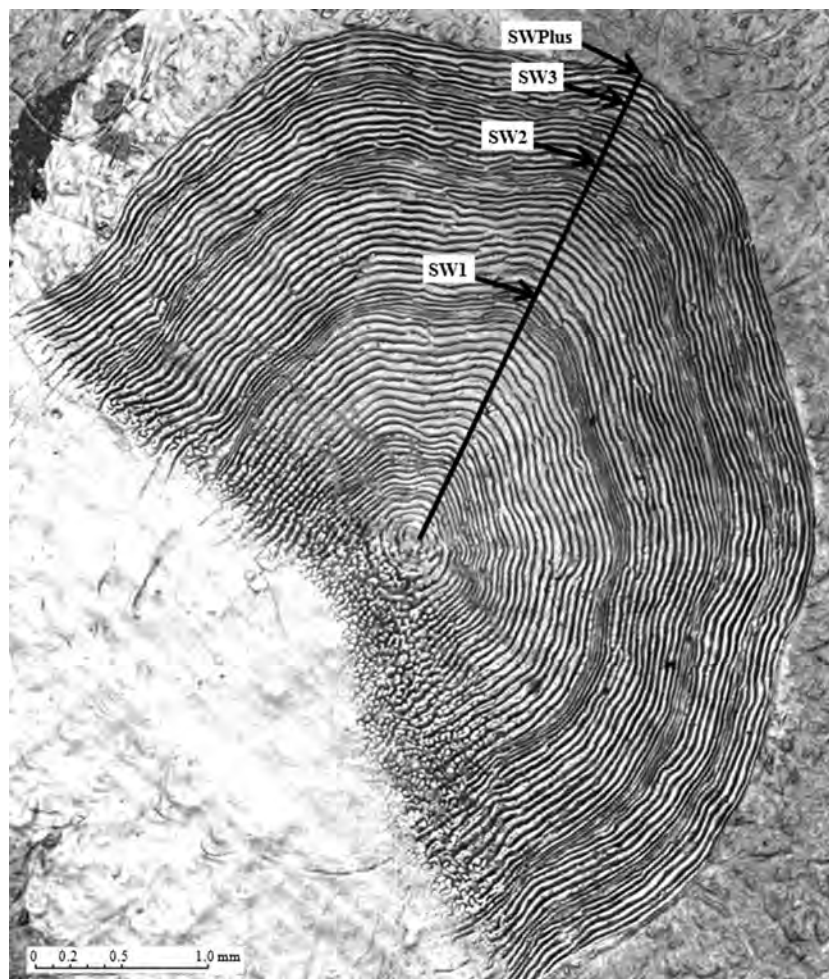


Fig. 2. Example of a chum salmon scale. This is an age 0.3 chum salmon scale with the annuli marked by seasonal growth zones SW1, SW2, etc. SW is an abbreviation for saltwater, indicating the fish is in marine waters. The numbers 1, 2, etc. indicate the number of years at sea. We used the longest axis to measure scales.

25 female scales were measured. Previous scale studies indicated 40–50 scales were sufficient to provide an accurate estimate of the mean (Briscoe, 2004; Zimmermann, 1991).

We focused on two growth zones: the first marine (SW1) and the third marine years (SW3, Fig. 2). The SW1 zone was chosen because it has been hypothesized that growth in the early marine period was critical to the survival of an individual fish (Beamish and Mahnken, 2001). The SW3 zone was chosen because it has been hypothesized that if a fish did not reach a certain size, it remained in marine waters another year and returned the next summer as an age 0.4 fish (Helle, 1979). If it reached this “critical” size, it returned to spawn as an age 0.3 fish.

Scales were collected from fish during the year of maturation. Growth data (SW1 and SW3) were paired with the corresponding year of environmental data. For example, an age 0.4 fish that returned in 2006 was conceived in 2001, emerged from the gravel and spent its first year at sea in 2002 and its third year at sea in 2004, hence environmental data for 2002 were compared with SW1 growth, and data from 2004 were compared with SW3 growth.

2.3. Explanatory variables

Pink salmon have a 2-year life cycle that created an alternating-year pattern of abundance, and Russian pink salmon populations were dominated by odd-year adult pink salmon. We used population abundances of Russian pink salmon because they were the dominant pink salmon population in the western North Pacific Ocean and Bering Sea. In addition, Russian pink salmon were correlated with Alaska pink salmon populations ($p < 0.001$), thus the effects could be similar. Total Russian pink (*Pinks_t*, 1952–2007) and Asian chum salmon abundances were obtained from Ruggerone et al., 2010) and were updated with North Pacific Anadromous Fish Commission data. We calculated a 4-year moving average of Asian chum salmon abundance (*Asian chums_t*) to coincide with the 4- to 5-year life cycle pattern that dominates North Pacific chum salmon.

We used a “winter index” of the Pacific Decadal Oscillation (PDO_t) or an average of the monthly PDO indices from November of the previous year through March of the current year (Mantua 2001). These months were chosen because conditions during this time likely determine the amount of winter mortality of salmon, and both western Alaska and Asian fish overwinter in the Gulf of Alaska and central North Pacific Ocean. We extracted SST data from global monthly temperatures on a $2^\circ \times 2^\circ$ grid available from the National Oceanic and Atmospheric Administration’s (NOAA) Climate Data Center. To compare SSTs with SW1 growth, we averaged temperatures from areas corresponding with juvenile chum salmon distribution during the first summer (*Local SST_t*, Appendix A). Growth in the SW3 zone was compared to average annual SSTs within the Gulf of Alaska, corresponding to the approximate distribution of chum salmon after the third growing season (*GOA Annual SST_t*). We averaged SSTs within a $10^\circ \times 30^\circ$ box (48–58°N, 130–160°W) over the Gulf of Alaska at year t .

We used several climate indices for the North Pacific to examine whether they might be indicative of salmon growth and improve model fit. The North Pacific Index (*NPI_t*) at year t is the area-weighted sea level pressure over the region 30–65°N, 160°E–140°W. The Aleutian Low Pressure Index (*ALPI_t*) is the relative intensity of the Aleutian Low pressure system of the North Pacific (December through March in year t). The effect of the El Niño–Southern Oscillation (*ENSO_t*) on the northern hemisphere reaches its maximum during the boreal winter, and we used the mean December–January values of the multivariate ENSO index from the NOAA Earth System Research Laboratory Physical Science Division. El Niño episodes occur every 4–5 years and can last up to 12–18 months

(Wolter and Timlin, 1998). The Arctic Oscillation Index (*AO_t*) examines how atmospheric pressure fluctuates between positive and negative phases. The AO was most variable during the winter, thus, it captured characteristics when fish may not have enough fat reserves to survive. We used two wind mixing indices: *MayMix_t* measured in m^3/s^3 at year t from the vicinity of St. Paul Island, Alaska, and *JJMmixM2_t* measured at Mooring 2 (57°N, 164°W) in m^3/s^3 . We used wind mixing indices because they provide an estimate of the rate of mixing at the base of the upper mixed layer, an area in the ocean important to juvenile salmon. The average ice concentration in the Bering Sea at year t was represented by *Ice Cover_t*. The amount of ice cover has been shown to affect the spring plankton bloom, which may be important to juvenile salmon (Hunt et al., 2002; Moss et al., 2009). The Bering Sea level pressure winter index (*BSLPw_t*) represents deviations from the mean value of sea level pressure average over the Bering Sea (55–65°N, 170°E–160°W) December through March (Appendix A).

Air temperatures (*Local Air Temp_t*) from the nearest city to the site (Nome, Alaska for Yukon River and King Salmon, Alaska for Nushagak River) were used as a proxy for coastal SST and river temperatures. SST data nearshore were not always complete, and river temperatures may affect timing of seaward migration and subsequent growth, especially for a long river such as the Yukon River, which is 3190 km in length. We obtained air temperatures from western Alaska from the Weather Underground website (Appendix A). Air temperatures were averaged for winter (November–March), summer (May–September), and annually and were compared with first-year growth. All explanatory variables were normalized or “scaled” to the standard deviation using the ‘base’ package in R version 2.9.2 (R Development Core Team, 2009). A value of one is one standard deviation from the long-term mean. This allowed us to directly compare the magnitudes of the estimated effects.

2.4. Analyses and models

We examined relationships between chum salmon growth and the explanatory variables using correlation analysis followed by multiple linear regression. First, we computed Pearson’s correlations among explanatory variables to assess multi-collinearity. We also computed Pearson’s correlations between growth and explanatory variables to identify important variables (Tables 1 and 2).

Table 1
Pearson’s correlations comparing marine scale growth of Yukon River, Alaska age 0.3 (1965–2006) and age 0.4 (1967–2006) chum salmon during the first (SW1) and third (SW3) year at sea with several explanatory variables (Appendix A). Correlations significant at the 95% confidence level are shown in bold.

Variable	Age 0.3		Age 0.4	
	SW1	SW3	SW1	SW3
Pinks	—	−0.179	—	−0.223
ALPI	0.293	−0.137	0.385	−0.180
PDO	0.169	−0.124	0.053	−0.196
Asian chum	—	−0.263	—	−0.326
YR sum SST	0.358	—	0.281	—
YR ann SST	0.169	—	0.203	—
GOA ann SST	—	−0.294	—	−0.435
GOA sum SST	—	−0.217	—	−0.362
Ice cover	−0.190	0.004	0.017	−0.006
AO	−0.045	−0.150	−0.061	−0.136
NPI	−0.176	0.081	−0.251	0.155
ENSO	0.139	0.087	0.134	0.029
BSLP winter	−0.236	0.059	−0.090	0.068
MayMix	−0.225	0.005	−0.262	0.077
Nome winter air	0.257	—	0.137	—
Nome ann air	0.542	—	0.308	—
Nome sum air	0.539	—	0.381	—

Table 2

Pearson's correlations and comparing marine scale growth of Bristol Bay, Alaska age 0.3 (1965–2006) and age 0.4 (1966–2006) chum salmon during the first (SW1) and third (SW3) year at sea with explanatory variables (Appendix A). Correlations significant at the 95% confidence level are shown in bold.

Variable	Age 0.3		Age 0.4	
	SW1	SW3	SW1	SW3
Pinks	—	-0.139	—	-0.248
ALPI	0.518	-0.144	0.454	-0.175
PDO	0.383	-0.127	0.305	-0.103
Asian chum	—	-0.332	—	-0.375
BB ann SST	0.779	—	0.750	—
BB sum SST	0.738	—	0.696	—
GOASumSST	—	-0.138	—	-0.271
GOAAnnSST	—	-0.250	—	-0.362
IceCover	-0.256	-0.011	-0.205	0.016
AO	0.214	-0.124	0.311	-0.095
NPI	-0.416	0.095	-0.366	0.115
ENSO	0.145	0.081	0.122	0.146
BSLP winter	-0.327	0.112	-0.367	0.032
MayMix	-0.163	0.005	-0.215	-0.018
K. salmon win air	0.334	—	0.399	—
K. salmon ann air	0.611	—	0.610	—
K. salmon sum air	0.605	—	0.583	—

Results were used to select a subset of variables for the regression models. We modeled chum salmon growth as a function of the selected variables using a general regression approach:

$$y = X\beta + \varepsilon \tag{1}$$

where y was observed growth (SW1 or SW3), X was a matrix of explanatory variables, and ε were the residuals. Because the time series nature of the data and preliminary analyses suggested the residuals were autocorrelated, we used generalized least squares (GLS) regression to allow for autocorrelation in the residuals. Generalized least squares regression is a technique for estimating unknown parameters in a linear regression model, and GLS is often applied when the variances of the observations are unequal (heteroscedastic) or when there is correlation among observations. To account for time-series dependence in the residuals, we used a generalized variance-covariance structure that modeled the dependence as an auto-regressive process of order p , where p was assumed to be between 1 and 6 to span the generation time of chum salmon. We fit each full model assuming that residuals were independent and used a backward stepwise approach, choosing the model with the lowest Akaike Information Criterion (AIC) by at least four points as the best submodel (Burnham and Anderson, 2004). We chose the most parsimonious model, if differences in AIC were small, or whenever the larger model was deemed biologically unrealistic. Plots of the residuals of the reduced final model were examined for normality and influence of outliers. The model was weighted by the number of scales measured per year to account for unequal sample sizes among years. In the Yukon River, we measured >25 scales per gender per age each year, but in Bristol Bay, there were not enough samples for age 0.3 fish in 1966, and for age 0.4, we had reduced sample sizes in 1969, 1970, 1975, 1977, 1980, and 2000. For Bristol Bay age 0.4 fish, we examined the model with all years and removed 1975 from the model due to its influence as an outlier, probably due to sample size. All model parameters were estimated via maximum likelihood estimation using the 'nlme' package (Pinheiro and Bates, 2000) in R version 2.9.2 (R Development Core Team, 2009).

2.4.1. SW1 model

The SW1 models focused on explanatory variables that might influence early marine growth in chum salmon, such as wind mixing and regional SST. Effects of density dependence on SW1

growth were not examined because few Alaskan chum overlap with highly abundant Asian chum and pink salmon during the first year at sea, and because abundances of western Alaska chum and pink salmon are relatively small. Because there were no differences by gender in first-year growth, we combined the data for SW1, giving us larger sample sizes (≥ 50 in most years). Based on Pearson's correlations and simple linear regressions, we developed a full model that we applied to both systems:

$$SW1_t = \alpha + \beta_1(local\ SST_t) + \beta_2(ALPI_t) + \beta_3(NPI_t) + \beta_4(MayMix_t) + \beta_5(IceCover_t) + \beta_6(localAirTemp_t) + \varepsilon_t \tag{2}$$

where the terms are defined in Appendix A.

2.4.2. SW3 model

The SW3 models focused on comparison of growth with density dependence, competition, SST, and gender differences. To test for interactions between pink or Asian chum salmon abundance and third-year growth, we compared SW3 growth with pink and Asian chum salmon abundances. To examine effects of SST on growth, we included the GOA Annual SST, and one climate index, the NPI. From our exploratory data analysis, there appeared to be an interaction between pink salmon and Asian chum salmon abundance. In addition, it has been suggested that pink salmon abundance altered the feeding and distribution of chum salmon on the high seas (Azumaya and Ishida, 2000; Kaeriyama et al., 2004; Myers et al., 2004). Because of uncertainty about this interaction, we chose to examine the model with and without the interaction. We also included separate intercepts by gender in these models to account for the observed larger mean size of males:

$$SW3_t = \alpha + \beta_1(Pinks_t) + \beta_2(Asian\ Chums_t) + \beta_3(GOA\ Annual\ SST_t) + \beta_4(NPI_t) + \beta_5(Pinks_t:AsianChums_t) + Gender_k + \varepsilon_t \tag{3}$$

where the terms are defined in Appendix A.

2.4.3. Other analyses

We examined whether total mean scale radius was a good predictor of average adult fish length (mm) using the following linear model:

$$L_t = \alpha + \beta_1(R_t) \tag{4}$$

where L_t was mean adult length at year t , and R_t was mean scale radius at year t .

All response variables (SW1 and SW3) were plotted and examined for normality and outliers. Shapiro-Wilk tests for normality were used to assess the normality of the response variables. The response variables were plotted by odd and even year of growth to determine whether there was an odd-even year effect due to pink salmon abundance. We compared mean annual growth between odd and even years using Student's t -test. Differences in growth by gender were examined by comparing annual mean male and female growth using a Welch Two Sample t -test.

3. Results

The results of Pearson's correlations between growth and explanatory variables indicated that there was some collinearity in the explanatory variables, particularly the air temperature and SST measures were all significantly and positively correlated ($r=0.39-0.88$). Temperature measures were inversely correlated with ice cover ($r=-0.35$ to -0.58). In addition, Russian pink and Asian chum abundance were correlated with each other ($r=0.66$, $p<0.001$) and with most SST and air temperatures measures ($0.34-0.60$). We found very few significant correlations with the

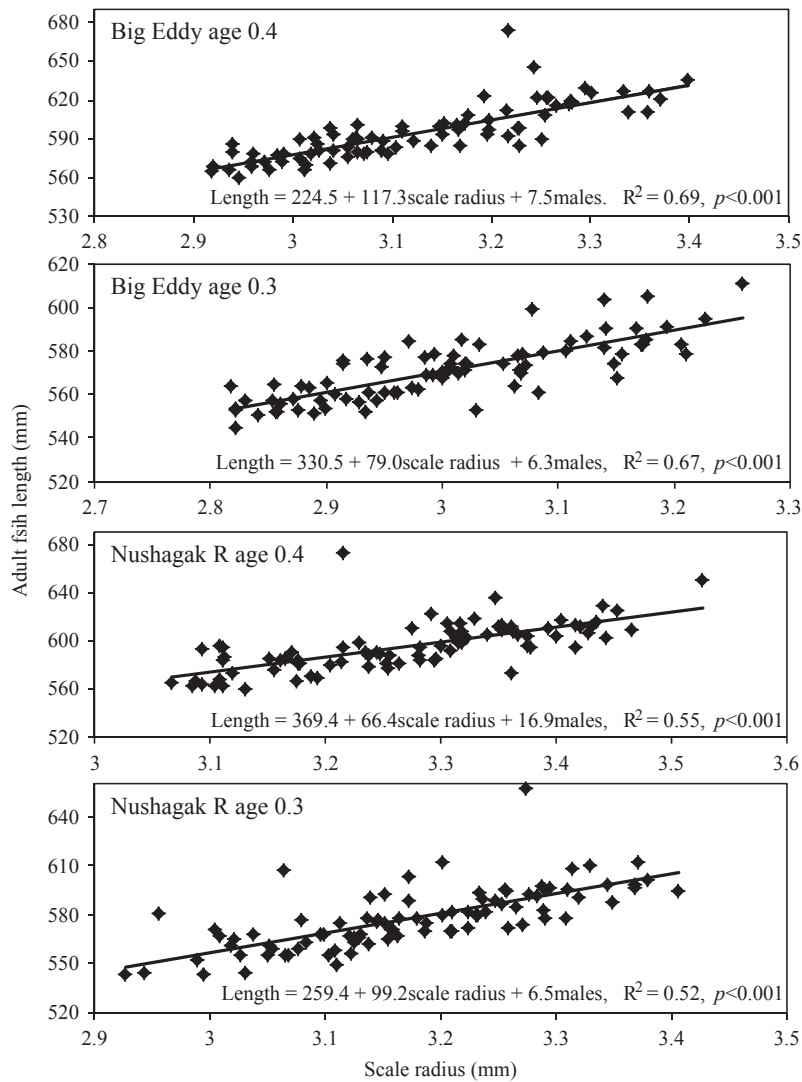


Fig. 3. Mean adult fish length (mm, mid-eye to fork of tail) compared to mean scale growth (mm, radius) for chum salmon from Big Eddy, Yukon River and Nushagak River, Bristol Bay, Alaska.

first-year growth of Yukon River salmon and the explanatory variables, which contrasted greatly with Bristol Bay fish (Tables 1 and 2). Growth of Bristol Bay and Yukon River salmon were correlated by age and zone ($r=0.38\text{--}0.87$; $p<0.05$).

Adult fish length was positively related to total scale growth for both ages in both populations (Fig. 3; Yukon River: age 0.3, $R^2=0.69$; age 0.4, $R^2=0.67$; Bristol Bay: age 0.3, $R^2=0.55$; age 0.4, $R^2=0.52$). Scale growth explained 52–69% of the variability in fish length depending on stock and age.

Normalized time series plots of first- and third-year growth showed no apparent pattern related to the odd–even year abundance of Asian pink salmon (Figs. 4 and 5). All plots showed changes in growth around the 1976–1977 regime shift. For example, Bristol Bay age 0.3 first-year growth increased and third-year growth decreased in the mid-1970s, corresponding to the PDO and the ocean regime shift (Fig. 4). When we compared odd- to even-year growth, we found that none of the comparisons were significant at $p<0.05$.

3.1. Gender

Third-year growth, scale radius, and fish length were significantly larger for males (Welch two-sample t -test, $p<0.005$) for both age classes (age 0.3 and 0.4 fish) and populations. In contrast,

first-year growth did not differ significantly between males and females ($p>0.4$).

We found that for most populations and ages the third-year growth of females was significantly less than that of males, as indicated by negative model coefficients (Tables 3 and 4, Figs. 6 and 7). The difference between genders tended to be more pronounced for age 0.3 than for age 0.4 salmon. Some values were positive for Bristol Bay age 0.4 fish, indicating females grew faster than the late maturing males during the third year of growth. This contradicted previous work examining seasonal growth in Bristol Bay using different methods (Agler, 2012). Breeding males are larger than females, and this appeared to be when size differentiation occurred (Agler, 2012).

3.2. Yukon River

3.2.1. SW1 growth

For age 0.3 fish, single-variable regressions indicated that Nome annual air temperature and local SST had significant positive effects ($p<0.02$), and NPI, BSLP winter index, wind mixing, and ice cover ($p<0.05$) had significant negative effects on first-year growth of age 0.3 Yukon River chum salmon. ALPI had marginally significant positive effects on first-year growth of age 0.3 fish (Fig. 6; $p=0.051$). For age 0.4 fish, we found that ALPI, Nome annual air temperature, and local

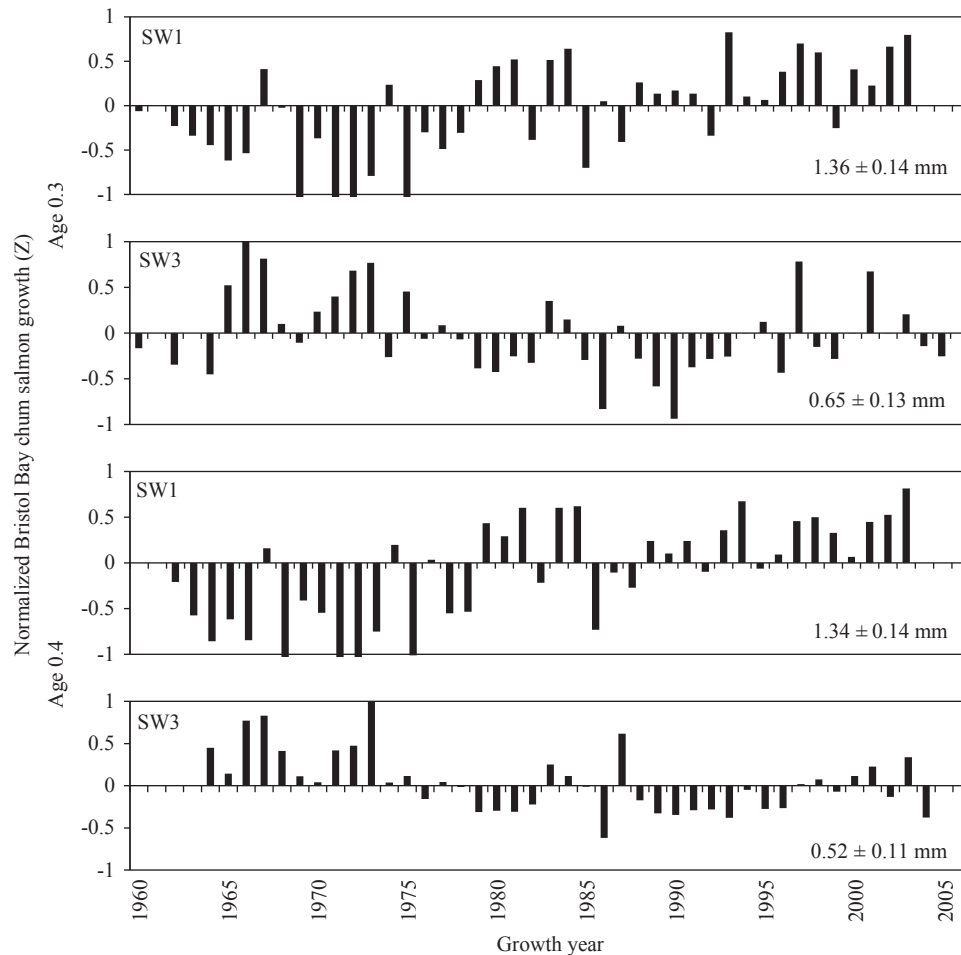


Fig. 4. Mean annual growth of age 0.3 and 0.4 Nushagak River, Bristol Bay, Alaska chum salmon during first (SW1) and third (SW3) growth years 1961–2006. Un-weighted mean \pm 1 SD during each life stage is shown.

SST had significant positive effects ($p < 0.05$); however, the May mixing index had significant negative effects ($p = 0.022$) and NPI had marginally significant negative effects on first-year growth (Fig. 6; $p = 0.055$).

The best multivariate model for first-year growth of age 0.3 fish showed that the May mixing index had negative effects and Nome annual air temperature had positive effects (Table 3). For age 0.4 fish, the best model indicated that local sea surface temperature had positive effects and the May mixing and ice cover indices had negative effects on first-year growth of Yukon River chum salmon (Table 3). The autoregressive terms for all models were negative and fell between -0.256 and -0.450 , implying that following a year with good growth, growth was reduced in following years (i.e. 1, 2, 3, or 4 years later, depending on the autoregressive term).

3.2.2. SW3 growth

Correlations and single variable regressions indicated that Asian chum salmon abundance and GOA SST had significant negative correlations with both ages of third-year marine growth of Yukon River chum salmon (Fig. 7; $p < 0.05$). ENSO had significant positive effects on both ages ($p < 0.05$), and pink salmon abundance had marginally significant negative effects on age 0.4 fish ($p = 0.081$).

The best multivariate regression (Table 4) for age 0.3 Yukon River fish suggested negative effects of pink salmon abundance, Asian chum salmon abundance, GOA SST, and NPI on third-year growth and included the pink: Asian chum interaction. For age 0.4 fish, the final model indicated that GOA SST had significant negative effects on third-year growth. Asian chum and pink salmon abundance were negatively correlated with growth of age 0.4 fish in the single-

variable model, but they did not contribute additional information to the multivariate model when GOA SST was included (Fig. 7). For each system and age, we compared the observed growth with the predicted values as a means to show variability in the relationships (Fig. 8). The autoregressive terms vacillated from negative to positive for age 0.3 fish (-0.64 to 0.01), and there were none for age 0.4 fish.

3.3. Bristol Bay

3.3.1. SW1 growth

For age 0.3, the results of the single variable regressions indicated that ALPI, annual air temperature, and local SST had significant positive effects, and NPI and a wind mixing index had significant negative effects on first-year growth of Bristol Bay chum salmon (Fig. 6; $p < 0.05$). The BSLP winter ($p = 0.052$) and ice cover ($p = 0.062$) indices showed marginally significant negative effects on first-year growth. For age 0.3 fish, the best multivariate model indicated that local SST and the ice cover index had significantly positive effects on first-year growth (Table 3).

For age 0.4, the results of the single variable regressions indicated that ALPI, annual air temperature, and local SST had significant positive effects ($p < 0.001$), and NPI and the May wind mixing index had significant negative effects on the first-year growth (Fig. 6; $p < 0.03$). Ice cover showed marginally significant effects on first-year growth ($p = 0.089$). For age 0.4 fish, the best multivariate model indicated that local SST had significant positive effects, and the May wind mixing index showed detectable negative effects on first-year growth of Bristol Bay chum salmon (Table 3).

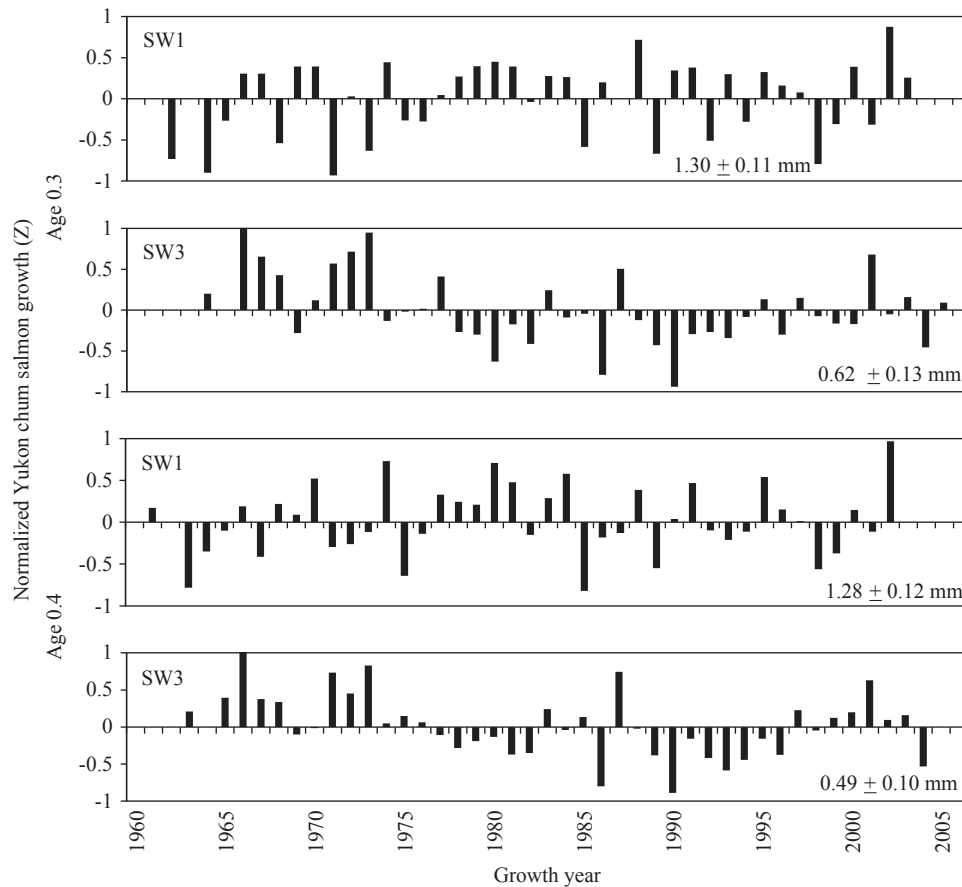


Fig. 5. Mean annual growth of age 0.3 and 0.4 Big Eddy, Yukon River, Alaska chum salmon during first (SW1) and third (SW3) growth years 1961–2006. Un-weighted mean ± 1 SD during each life stage is shown.

Table 3

Best regression models (based on AIC) relating first-year growth (SW1) for Yukon River, Alaska age 0.3 (1965–2006) and age 0.4 (1967–2006) and for Bristol Bay age 0.3 (1965–2006) and age 0.4 (1966–2006) chum salmon to explanatory variables. *P* values are listed below each coefficient. *b*=intercept.

Systems	Age	AR	<i>b</i>	Model coefficients			
				SST	Ice	MayMix	Air temp
Bristol Bay	0.3	3	0.564	0.172	0.020		
	0.4	0	0.578	<0.001	0.030	-1.895	
Yukon River	0.3	4	1.301			0.044	0.025
	0.4	1	1.300	0.016	-0.016	0.014	<0.001
				0.031	0.033	0.018	

3.3.2. SW3 growth

The results of the single variable regressions indicated that Asian chum salmon abundance and PDO had significant negative effects ($p < 0.05$), while pink salmon abundance had marginally significant negative effects ($p = 0.096$) on third-year growth of Bristol Bay age 0.3 chum salmon (Fig. 7). We also found that NPI had significant positive effects on third-year growth of age 0.3 chum salmon ($p = 0.015$). For age 0.4 fish, ENSO had significant positive effects ($p = 0.050$), and GOA SST, pink and Asian chum salmon abundance showed significant negative effects on third-year growth (Fig. 7; $p < 0.03$).

The best multivariate model for age 0.3 Bristol Bay fish (Table 4) indicated that pink salmon abundance, Asian chum salmon abundance, GOA SST, and NPI had negatively significant effects on

third-year growth. The interaction of pinks and Asian chums had a significant positive relationship with SW3 growth. For age 0.4 fish, the best multivariate model indicated that pink and Asian chum salmon abundance had significant negative effects, and the pink:Asian chum salmon interaction had a significant positive relationship with third-year growth (Table 4). The autoregressive terms for age 0.3 fish were negative (-0.14 to -0.44), implying that following a year with good growth, growth was reduced in following years (i.e. 1, 2, or 3 years later). The autoregressive terms for age 0.4 fish were positive (0.13–0.42).

4. Discussion

Overall, we found that warmer regional temperatures, increased wind mixing of the water column, and less ice cover significantly enhanced first-year growth of chum salmon originating from Bristol Bay and Yukon River. We also found that reduced third-year growth of chum salmon was significantly correlated with increased Asian chum salmon abundance, and pink salmon abundance also influenced third-year growth but to a lesser extent. In contrast with our hypothesis that warmer temperatures in the Gulf of Alaska would increase growth, we found that warmer large-scale SSTs from the Gulf of Alaska were associated with reduced third-year growth of chum salmon.

Enhanced first-year growth was associated with local SST and/or regional air temperature in both populations. After the 1976–1977 regime shift, SSTs in coastal areas warmed (Hare et al., 1999; Mantua et al., 1997), and this may have contributed to the positive correlation between first-year growth and SST. Overall, first-year growth was negatively correlated with NPI, and positively

Table 4

Best regression models (based on AIC) relating third-year growth (SW3) for Yukon River, Alaska age 0.3 (1965–2006) and age 0.4 (1967–2006) and for Bristol Bay age 0.3 (1965–2006) and age 0.4 (1966–2006) chum salmon to explanatory variables. *P* values are listed below each coefficient. *b*=intercept. Int.=pink:Asian chum.

Systems	Age	AR	<i>b</i>	Model coefficients					
				Pinks	Chums	SST	NPI	Int.	Gender
Bristol Bay	0.3	3	1.326	-0.002	-0.005	-0.046	-0.015	2.8E-05	-0.048
				<0.001	<0.001	0.004	0.010	<0.001	<0.001
Yukon River	0.3	4	0.726	-0.001	-0.004	-0.042	-0.042	1.2E-05	-0.055
				0.046	<0.001	<0.001	0.001	0.007	<0.001
Yukon River	0.3	3	1.309	-0.002	-0.004	-0.042	-0.042	-0.061	-0.015
				<0.001	<0.001	0.001	0.001	<0.001	<0.001
	0.4	0	0.944			-0.051			-0.033
						<0.001			0.002

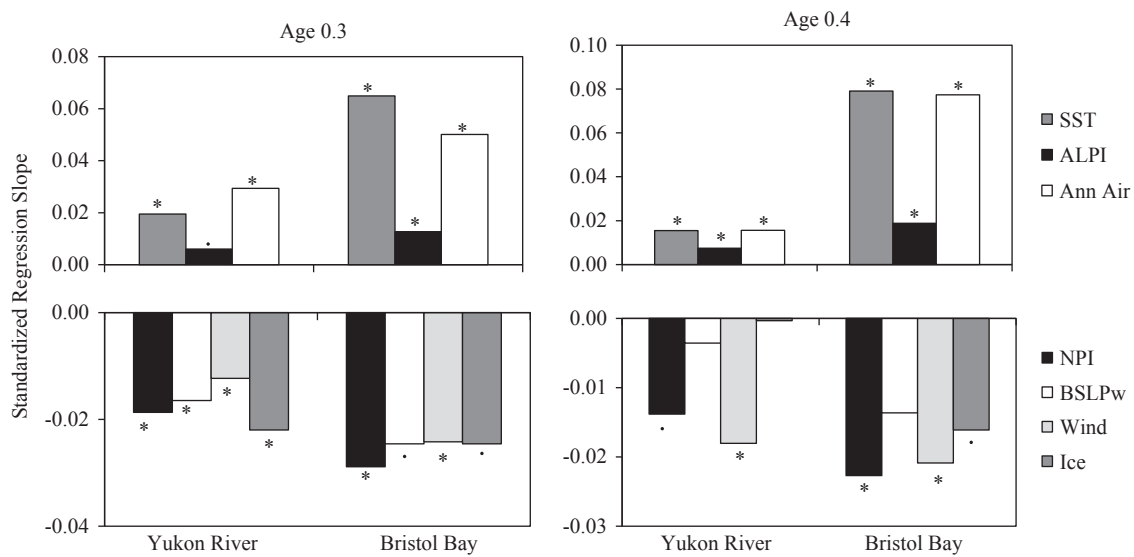


Fig. 6. Model coefficients from single-variable regressions (fit by generalized least squares) relating first-year (SW1) growth of chum salmon from Yukon River age 0.3 (1965–2006) and age 0.4 fish (1967–2006) and Bristol Bay age 0.3 (1960–2006) and age 0.4 fish (1966–2006) to explanatory variables. An asterisk (*) represents *p*<0.05, and a dot (·) represents *p*<0.1.

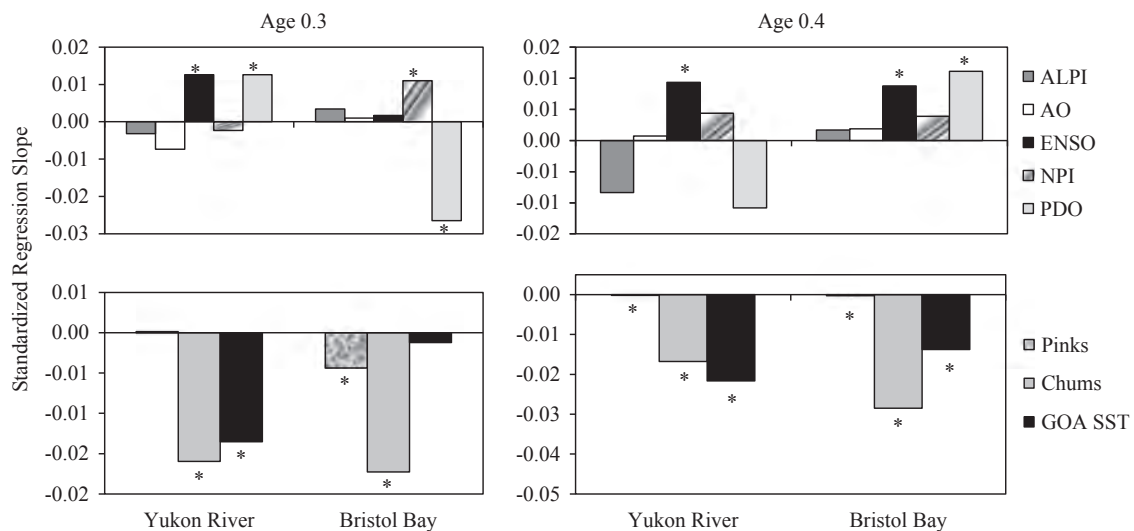


Fig. 7. Model coefficients from single-variable regressions (fit by generalized least squares) relating third-year (SW3) growth of chum salmon from Yukon River age 0.3 (1965–2006) and age 0.4 fish (1967–2006) and Bristol Bay age 0.3 (1960–2006) and age 0.4 fish (1966–2006) to explanatory variables. An asterisk (*) represents *p*<0.05, and a dot (·) represents *p*<0.1.

correlated with ALPI. Including the North Pacific Index improved the fit of some models, thus it might be useful in improving salmon forecasting models. Increased ice cover always showed negative effects on first-year growth in the single variable

regressions (Fig. 7) and was part of the final models for age 0.4 Yukon River and age 0.3 Bristol Bay fish. Thus, varying ice cover in recent years may have had significant effects on juvenile salmon growth and salmon abundance. Farley and Moss (2009)

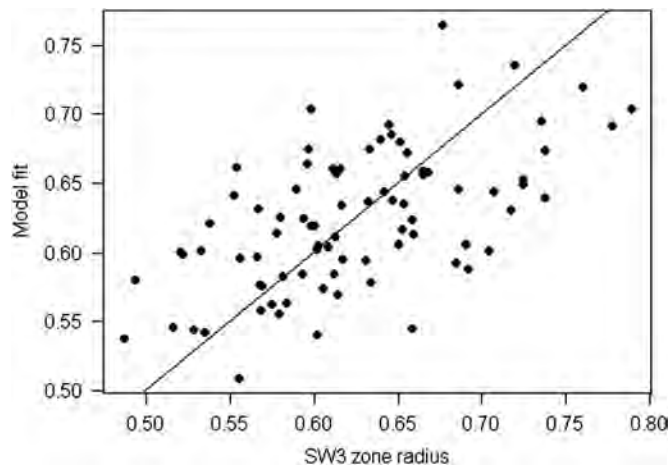


Fig. 8. Representative scatter plot comparing of observed third-year growth with predicted values for age 0.3 Big Eddy, Yukon River, Alaska chum salmon.

reported that the relative abundance of juvenile chum salmon in the southeastern Bering Sea (Kuskokwim River south to the Alaska Peninsula) was less during cold years or years with greater ice cover.

The only environmental variables that had significant effects on third-year growth were NPI, ENSO, and PDO. All were correlated with GOA SSTs and not all were correlated with all populations and ages. Enhanced third-year growth was associated with ENSO for all but Bristol Bay age 0.3 fish. We hypothesized that warmer temperatures in the Gulf of Alaska would increase marine growth of western Alaska chum salmon, and Gulf of Alaska temperatures significantly affected marine growth of both ages of Bristol Bay and Yukon River chum salmon, but the model coefficients were negative. This finding contradicted our hypothesis. We found that warmer SSTs, which typically promote salmon growth in northern regions, coincided with reduced chum salmon growth in western Alaska. Although this appears counterintuitive, Ruggerone et al. (2011) also found that adult length-at-age was negatively correlated with SST. We suggest two possible explanations. First, density-dependent effects due to the abundance of hatchery chum salmon may have overwhelmed the favorable growing conditions associated with warm SSTs. We found consistent negative relationships between Asian chum salmon abundance and the four chum growth indices in both the single-variable and multivariate regression models. Only age 0.4 Yukon chum did not show a negative relationship with Asian chum in the multivariate model, probably because SST explained more of the growth variability. GOA SST was found to be correlated with Asian chum abundance ($r=0.60$, $p<0.001$). Alternatively, the negative correlation we observed between cooler SSTs and chum salmon growth might reflect greater wind mixing and vertical fluxes of nutrients to the euphotic zone (Mueter et al., 2002a, 2002b). Due to this increased mixing cooler SSTs can be associated with greater lower-trophic level production or a preponderance of lipid-rich sub-arctic species, creating a better prey base for chum salmon.

We hypothesized that Russian pink salmon abundance inhibited the growth of western Alaska chum salmon during the third year at sea. Studies of sockeye salmon also found a negative effect of the abundance of pink salmon during the second and third year at sea. These effects began immediately after peak prey availability in spring and continued to the end of the growing season (Ruggerone et al., 2005). Although we found consistent evidence of interspecific interactions due to the effect of the abundance of Russian pink salmon on third-year growth, the effects were smaller than the effects of Asian chum salmon abundance and GOA SST. This finding

probably reflects the greater influence of intraspecific versus interspecific competition for prey.

Researchers have suggested that Asian chum salmon shift their spatial distribution from the Bering Sea to the North Pacific Ocean in years when pink salmon abundance is high (Azumaya and Ishida, 2000; Ogura and Ito, 1994). Azumaya and Ishida (2000) found that there was no significant relationship between growth of chum salmon and abundance of pink salmon, suggesting that growth of chum salmon during marine life was more affected by intraspecific interactions than interspecific interactions. If pink salmon showed increased productivity and abundance, it is possible that this forced more chum salmon into the Gulf of Alaska where SSTs were associated with greater wind mixing and vertical fluxes of nutrients and increased lower-trophic level production. In addition, chum salmon have a unique gut architecture, which allows them to eat a diverse diet. In comparison with sockeye salmon, which are sympatric with Asian pink salmon and share similar prey, chum salmon are more omnivorous. When pink salmon abundance increased, chum salmon were able to “prey switch” and forage on lower quality prey, such as gelatinous zooplankton, including amphipods, euphausiids, pteropods, and copepods (Andrievskaya, 1966; Davis et al., 2000, 2004). Prey switching might permit chum salmon to survive and possibly increase in abundance when prey productivity was low, unlike sockeye salmon, whose growth and survival have been reduced in odd years due to competition with abundant pink salmon (Ruggerone et al., 2003, 2005).

Most intermingling of North American and Asian chum salmon occurs when Asian fish extend their range into the Gulf of Alaska during their second and third winters at sea (Fukuwaka et al., 2007a, 2007b; Myers et al., 2004; Urawa, 2003; Urawa et al., 2004, 2009). We found that the abundance of Asian chum salmon was negatively correlated with the growth of both ages of Yukon River and Bristol Bay chum salmon. Asian chum salmon abundance had more of an effect on the growth of age 0.3 than age 0.4 fish. Age 0.3 is the predominant age group of Asian chum salmon (Kaeriyama, 1989), and may have contributed to this age-related effect. Competition among conspecifics for prey items would likely be greater among those from the same age group. To return 1 year earlier, age 0.3 fish must grow faster to attain the length necessary to reproduce 1 year prior to age 0.4 fish, and competition may have its greatest effect when potential growth rates is highest. Age 0.4 fish have another year to feed in the ocean and “catch up” to reach the minimum size needed for reproduction.

These findings were consistent with results from Norton Sound chum salmon (Ruggerone et al., 2011; G. Ruggerone, NRC, Inc., personal communication). They found that second-year scale growth, length-at-age, and survival of chum salmon were negatively correlated with abundance of Asian chum salmon. Although we did not examine second-year chum growth, Western Alaska chum salmon inhabit the Gulf of Alaska and North Pacific Ocean during the second and third years of growth and are affected by similar ocean conditions. Production of adult hatchery chum salmon from Asia increased rapidly beginning in 1970, and numbers of hatchery chum salmon have exceeded total production of wild adult salmon in the North Pacific Ocean since the mid-1980s. Asian hatchery chum salmon, at approximately two billion juveniles per year (Ruggerone et al., 2010), are currently the dominant chum salmon stock in the Bering Sea and North Pacific Ocean (Urawa et al., 2001, 2009). A future step would be to examine our second-year growth data to see if we can determine when these interactions began.

Asian chum salmon are currently the dominant chum salmon stock in the Bering Sea and North Pacific Ocean (Ruggerone et al., 2010). Because most of the Asian chum salmon were hatchery-raised, there is a great deal of controversy about whether hatchery salmon affect wild salmon. Our results indicate significant

Table A1
Explanatory variables used in generalized least squares regressions (GLS) to compare with first and third-year growth of western Alaska and Asian chum salmon.

Variable	Name	Description	Source
NPI_t	North Pacific index	Area-weighted sea level pressure over the region 30–65°N, 160°E–140°W	http://www.cgd.ucar.edu/cas/jhurrell/npindex.html
$ALPI_t$	Aleutian low pressure index	Relative intensity of the Aleutian low pressure system of North Pacific (December–March). A positive index value reflects a relatively strong or intense Aleutian low	http://www.pac.dfo-mpo.gc.ca/science/species-especies/climatology-ie/cori-irco/alpi/index-eng.htm
$Local\ Air\ Temp_t$	Local air temperature	Temperatures averaged as winter (November–March), summer (May–September) and annually	http://www.wunderground.com/
$Nome$	Yukon River	Nome, AK airport, National Weather Service	http://www.wunderground.com/
$K. Salmon$	Bristol Bay	King Salmon, AK airport, National Weather Service	http://www.wunderground.com/
May/Mix_t	Wind mixing index	Measured in m^3/s^2 at year t in the vicinity of St. Paul Island, Alaska from 1950 to 2010	http://www.beringclimate.noaa.gov/index.html
$Ice\ Cover_t$	Average ice concentration	Average ice concentration in the Bering Sea in a $2^\circ \times 2^\circ$ box (56–58°N, 163–165°W) from 1 January to 31 May. Ice Cover represented normalized anomalies by year	http://www.beringclimate.noaa.gov/index.html
PDO	1960–2008	Winter index, average of monthly PDO indices from November to March	http://jisao.washington.edu/pdo/PDO.latest
AO_t	Arctic oscillation index	Leading mode of empirical orthogonal function analysis of monthly mean during the period 1979–2000. Largest variability during cold season	http://www.ncdc.noaa.gov/oa/ncdc.html
$Local\ SST_t$	Local sea surface temperature	Used a $2^\circ \times 2^\circ$ grid examined winter (December–March) and summer (May–September)	NOAA Climate Data Center
$YR\ SST_t$	Yukon River	Mean temperature 62–66°N latitude and 160–166°W longitude	
$BB\ SST_t$	Bristol Bay	Mean temperature 56–60°N latitude and 160–180°W longitude	
$GOA\ SST_t$	SST	Gulf of Alaska annual SSTs from a $10^\circ \times 30^\circ$ box (48–58°N, 130–160°W) at year t . Winter and summer above	
$GOA\ SST_t$	SST	Gulf of Alaska annual SSTs from a $10^\circ \times 30^\circ$ box (48–58°N, 130–160°W) at year t . Winter and summer above	
$Pinkst_t$	Pink salmon abundance	Represents the total abundance of Russian pink salmon at year t	Ruggerone et al. (2010)
$Asian\ chums_t$	Asian chum salmon abundance	A 4-year moving average of the Asian chum salmon abundance at year t (catch and escapement in millions of fish). Used 4-year moving average because it corresponded with chum salmon life cycle	Ruggerone et al. (2010)
$ENSO_t$	El Niño/So. oscillation index	Used the mean December–January values of the multivariate ENSO index	http://www.npafic.org/new/index.html
$JJ/MixM2_t$	Wind mixing index	Wind mixing index at Mooring 2 (57°N, 164°W) in m^3/s^2 from June to July 1950–2010	http://www.ncdc.noaa.gov/oa/ncdc.html
BSI/Pw_t	Bering Sea level pressure winter index	Deviations from the mean of sea level pressure average over the Bering Sea (55–65°N, 170°E–160°W) December through March	http://www.ncdc.noaa.gov/oa/ncdc.html

negative effects on growth of western Alaska chum salmon due to the abundance of Asian chum salmon. Determination of how detrimental these effects are to the chum population is a future exercise. In recent decades, researchers have raised concerns about density-dependent effects on salmon due to increased hatchery production, questioning whether there are limits to the carrying capacity of the North Pacific Ocean (Cooney and Brodeur, 1998; Holt et al., 2008). Although our findings are based on correlation analyses, which do not conclusively demonstrate cause and effect, they are consistent with other investigations and they support concerns raised about the capacity of the ocean to support wild salmon along with increasing numbers of hatchery salmon. Salmon, originating from distant regions and adjacent continents, share a common food resource and due to distributional overlap in the North Pacific Ocean and Bering Sea, they likely compete for prey leading to reduced growth and possibly survival.

The Gulf of Alaska is part of a dynamic ecosystem, and several of the explanatory variables used in the models are “autocorrelated.” It is possible that the dynamic nature of the ecosystem created additional levels of complexity necessitating the importance of the multiplicative and additive effects in the full models. Some would suggest that these effects lead to spurious results, while others point out that these were interactions among a complex, dynamic ecosystem. Overall, it appeared that SST, regional air temperature, May wind mixing, and ice cover influenced first-year scale growth of Bristol Bay and Yukon River chum salmon. Although Russian pink salmon abundance, the North Pacific Index, and Gulf of Alaska sea surface temperature influenced the third-year growth of Bristol Bay and Yukon River chum salmon, the abundance of Asian chum salmon appeared to have the most consistent, negative effect on growth of western Alaska chum salmon.

Acknowledgments

This investigation was funded by the AYK Sustainable Salmon Initiative (Projects 45677 and 45164) as Historical Analyses of AYK and Asian Chum Salmon, phase one and two, and by the North Pacific Marine Research Program (Project SFOS 99-188). We appreciate the efforts to gather and measure scales by many unknown ADF&G staff, as well as: D. Folletti, J. Baker, J. Cashen, J. Chesmore, S. Hinton, M. Lovejoy, A. Norman, W. Rosky, and W. Whelan. We also received support from a number of ADF&G staff, including: L. Brannian, D. Evenson, E. Volk, L. Dubois, H. Krenz, T. Baker, F. West, L. Fair, D. Oxman, T. Frawley, and W. Johnson. E. Siddon and J. Richar developed the SST program as part of a University of Alaska, Fairbanks graduate class. Constructive comments on the paper were provided by Drs. W. Smoker, P. Hagen, G. Kruse as well as C. Robinson and E. Volk. Two anonymous reviewers provided helpful suggestions. Use of any trade names or products is for descriptive purposes only and does not imply endorsement of the US Government. The statements, findings, conclusions, and recommendations are those of the author(s) and do not necessarily reflect the views of the AYK Sustainable Salmon Initiative, the North Pacific Marine Research Program, or the Alaska Department of Fish and Game.

Appendix A

See Table A1.

References

Agler, B., 2012. Growth of Western Alaska and Asian Chum Salmon (*Oncorhynchus keta*) in Relationship to Climatic Factors and Inter- and Intraspecific Competition. Ph.D. Thesis., University of Alaska, Fairbanks.

- Anderson, P.J., Piatt, J.F., 1999. Community reorganization in the Gulf of Alaska following ocean climate regime shift. *Marine Ecol. Prog. Ser.* 189, 117–123.
- Andrievskaya, L.D., 1966. Food relationships of the Pacific salmon in the sea. *Vopr. Ikhtiol.* 6, 84–90.
- Azumaya, T., Ishida, Y., 2000. Density interactions between pink salmon (*Oncorhynchus gorbuscha*) and chum salmon (*O. keta*) and their possible effects on distribution and growth in the North Pacific Ocean and Bering Sea. *North Pac. Anadr. Fish Comm. Bull.* 2, 165–174.
- Beacham, T.D., Candy, J.R., Sato, S., Urawa, S., Le, K.D., Wetklo, M., 2009. Stock origins of chum salmon (*Oncorhynchus keta*) in the Gulf of Alaska during winter as estimated with microsatellites. *North Pac. Anadr. Fish Comm. Bull.* 5, 15–23.
- Beamish, R.J., Mahnken, C., 2001. A critical size and period hypothesis to explain natural regulation of salmon abundance and the linkage to climate and climate change. *Prog. Oceanogr.* 49, 423–437.
- Briscoe, R.J., 2004. Factors Affecting Marine Growth and Survival of Auke Creek, Alaska Coho Salmon (*Oncorhynchus kisutch*). MS Thesis, University of Alaska, Fairbanks.
- Burnham, K.P., Anderson, D.R., 2004. Understanding AIC and BIC in model selection. *Sociol. Method Res.* 33, 261–304.
- Cooney, R., Brodeur, R.D., 1998. Carrying capacity and North Pacific salmon production: stock-enhancement implications. *Bull. Mar. Sci.* 62, 443–464.
- Davis, N.D., Aydin, K.Y., Ishida, Y., 2000. Diel catches and food habits of sockeye, pink, and chum salmon in the Central Bering Sea in summer. *North Pac. Anadr. Fish Comm. Bull.* 2, 99–109.
- Davis, N.D., Fukuwaka, M., Armstrong, J.L., Myers, K.W., 2004. Salmon food habits studies in the Bering sea, 1960 to Present. *North Pac. Anadr. Fish Comm. Tech. Rep.* 6, 24–29.
- Farley Jr., E.V., Moss, J.H., 2009. Growth rate potential of juvenile chum salmon on the Eastern Bering Sea Shelf: an assessment of salmon carrying capacity. *North Pac. Anadr. Fish Comm. Bull.* 5, 265–277.
- Farley Jr., E.V., Murphy, J.M., Adkison, M.D., Eisner, L.B., Helle, J.H., Moss, J.H., Nielsen, J., 2007a. Early marine growth in relation to marine-stage survival rates for Alaska sockeye salmon (*Oncorhynchus nerka*). *Fish. Bull.* 105, 121–130.
- Farley, E.V., Moss, J.H., Beamish, R.J., 2007b. A review of the critical size, critical period hypothesis for juvenile Pacific salmon. *North Pac. Anadr. Fish Comm. Bull.* 4, 311–317.
- Farley Jr., E.V., Starovoytov, A.N., Naydenko, S.V., Heintz, R., Trudel, M., Guthrie, C., Eisner, L., Guyon, J., 2011. Implications of a warming eastern Bering Sea for Bristol Bay sockeye salmon. *ICES J. Mar. Sci.* 68, 1138–1146.
- Fisher, J.P., Percy, W.G., 2005. Seasonal changes in growth of coho salmon (*Oncorhynchus kisutch*) off Oregon and Washington and concurrent changes in the spacing of scale circuli. *Fish. Bull.* 103, 34–51.
- Fukuwaka, M., Kaeriyama, M., 1997. Scale analyses to estimate somatic growth in sockeye salmon, *Oncorhynchus nerka*. *Can. J. Fish. Aquat. Sci.* 54, 631–636.
- Fukuwaka, M., Azumaya, T., Nagasawa, T., Starovoytov, A.N., Helle, J.H., Saito, T., Hasegawa, E., 2007a. Trends in abundance and biological characteristics of chum salmon. *North Pac. Anadr. Fish Comm. Bull.* 4, 35–43.
- Fukuwaka, M., Sato, S., Takahashi, S., Onuma, T., Sakai, O., Tanimata, N., Makino, K., Davis, N.D., Volkov, A.F., Seong, K.B., 2007b. Winter distribution of chum salmon related to environmental variables in the North Pacific. *North Pac. Anadr. Fish Comm. Tech. Rep. No.* 7, pp. 29–30.
- Hagen, P.T., Oxman, D.S., Agler, B.A., 2001. Developing and deploying a high resolution imaging approach for scale analysis. *North Pac. Anadr. Fish Comm. Doc.* 567, 1–11.
- Hare, S.R., Mantua, N.J., 2000. Empirical evidence for North Pacific regime shifts in 1977 and 1989. *Prog. Oceanogr.* 47, 103–145.
- Hare, S.R., Mantua, N.J., Francis, R.C., 1999. Inverse production regimes: Alaska and west coast Pacific salmon. *Fisheries* 24, 6–14.
- Healey, M.C., 1986. Optimum Size and Age at Maturity in Pacific Salmon and Effects of Size-Selective Fisheries. *Can. J. Fish. Aquat. Sci.* 89, pp. 39–52.
- Helle, J.H., 1979. Influence of Marine Environment on Age and Size at Maturity, Growth, and Abundance of Chum Salmon, *Oncorhynchus keta* (Walbaum), from Olsen Creek, Prince William Sound, Alaska. Ph.D. Thesis., Oregon State University, Corvallis.
- Holt, C.A., Rutherford, M.B., Peterman, R.M., 2008. International cooperation among nation-states of the North Pacific Ocean on the problem of competition among salmon for a common pool of prey resources. *Mar. Policy* 32, 607–617.
- Hunt Jr., G.L., Stabeno, P., Walter, G., Sinclair, E., Brodeur, R.D., Napp, J.M., Bond, N.A., 2002. The Eastern Bering Sea: evidence for change and a new hypothesis linking ecosystem control and climate. *Deep-Sea Res. II* 49, 5821–5853.
- Ishida, Y., Ito, S., Kaeriyama, M., McKinnell, S., Nagasawa, K., 1993. Recent changes in age and size of chum salmon (*Oncorhynchus keta*) in the North Pacific Ocean and possible causes. *Can. J. Fish. Aquat. Sci.* 50, 290–295.
- Kaeriyama, M., 1989. Comparative morphology and scale formation in four species of *Oncorhynchus* during early life. *Ichthyl. Res.* 35, 445–452.
- Kaeriyama, M., Nakamura, M., Edpalina, R.R., Bower, J.R., Yamaguchi, H., Walker, R. V., Myers, K.W., 2004. Change in feeding ecology and trophic dynamics of Pacific salmon (*Oncorhynchus* spp.) in the central Gulf of Alaska in relation to climate events. *Fish. Oceanogr.* 123, 197–207.
- Kaeriyama, M., Yatsu, A., Kudo, H., Saitoh, S., 2007a. Where, when, and how does mortality occur for juvenile chum salmon *oncorhynchus keta* in their first ocean year? *North Pac. Anadr. Fish Comm. Tech. Rep. No.* 7, pp. 52–55.
- Kaeriyama, M., Yatsu, A., Noto, M., Saitoh, S., 2007b. Spatial and temporal changes in the growth patterns and survival of Hokkaido chum salmon populations in 1970–2001. *North Pac. Anadr. Fish Comm. Bull.* 4, 251–256.

- Koo, T.S.Y., 1962. Age designation in salmon. In: Studies of Alaska Red Salmon. University of Washington Publications in Fisheries, New Series, vol. 1, pp. 37–48.
- Mantua, N.J., 2001. The Pacific decadal oscillation. In: McCracken, M.C., Perry, J.S. (Eds.), The Encyclopedia of Global Environmental Change, The Earth System: Physical and Chemical Dimension of Global Environmental Change, pp. 592–594.
- Mantua, N.J., Hare, S.R., Zhang, Y., Wallace, J.M., Francis, R.C., 1997. A Pacific interdecadal climate oscillation with impacts on salmon production. *Bull. Am. Meteorol. Soc.* 78, 1069–1079.
- Martinson, E.C., Helle, J.H., Scarnecchia, D.L., Stokes, H.H., 2008. Density-dependent growth of Alaska sockeye salmon in relation to climate-oceanic regimes, population abundance, and body size, 1925 to 1998. *Mar. Ecol. Prog. Ser.* 370, 1–18.
- Moss, J.H., Murphy, J.M., Farley Jr., E.V., Eisner, L.B., Andrews, A.G., 2009. Juvenile pink and chum salmon distribution, diet, and growth in the Northern Bering and Chukchi Seas. *North Pac. Anadr. Fish Comm. Bull.* 5, 191–196.
- Mueter, F., Pyper, B.J., Peterman, R.M., Wood, C.C., Blackbourn, D.J., 2002a. Opposite effects of sea-surface temperature on survival rates of pacific salmon from northern and southern areas. *North Pac. Anadr. Fish Comm. Tech. Rep. No. 4*, pp. 22–23.
- Mueter, F.J., Peterman, R.M., Pyper, B.J., 2002b. Opposite effects of ocean temperature on survival rates of 120 stocks of Pacific salmon (*Oncorhynchus* spp.) in northern and southern areas. *Can. J. Fish. Aquat. Sci.* 59, 456–463.
- Myers, K.W., Walker, R.V., Davis, N.D., Armstrong, J.L., 2004. Diet Overlap and Potential Feeding Competition Between Yukon River Chum Salmon and Hatchery Salmon in the Gulf of Alaska in Summer. High Seas Salmon Research Program, Fisheries Research Institute, School of Aquatic and Fishery Sciences, University of Washington, Seattle.
- Myers, K.W., Klovach, N.V., Gritsenko, O.F., Urawa, S., Royer, T.C., 2007. Stock-specific distributions of asian and north american salmon in the open ocean, inter-annual changes, and oceanographic conditions. *North Pac. Anadr. Fish Comm. Bull.* 4, pp. 159–177.
- Ogura, M., Ito, S., 1994. Change in the known ocean distribution of Japanese chum salmon, *Oncorhynchus keta*, in relation to the progress of stock enhancement. *Can. J. Fish. Aquat. Sci.* 51, 501–505.
- Peterman, R.M., Pyper, B.J., Lapointe, M.F., Adkison, M.D., Walters, C.J., 1998. Patterns of covariation in survival rates of British Columbian and Alaskan sockeye salmon (*Oncorhynchus nerka*) stocks. *Can. J. Fish. Aquat. Sci.* 55, 2503–2517.
- Pinheiro, J., Bates, D., 2000. Mixed-Effects Models in S and S-Plus, 528.
- Pyper, B.J., Peterman, R.M., 1999. Relationship among adult body length, abundance, and ocean temperature for British Columbia and Alaska sockeye salmon (*Oncorhynchus nerka*), 1967–1997. *Can. J. Fish. Aquat. Sci.* 56, 1716–1720.
- R Development Core Team, 2009. A Language and Environment for Statistical Computing. R Foundation for Statistical Computing, Vienna.
- Ruggerone, G.T., Nielsen, J.L., 2004. Evidence for competitive dominance of pink salmon (*Oncorhynchus gorbuscha*) over other salmonids in the North Pacific Ocean. *Rev. Fish Biol. Fish.* 14, 371–390.
- Ruggerone, G.T., Zimmermann, M., Myers, K.W., Nielsen, J.L., Rogers, D.E., 2003. Competition between Asian pink salmon (*Oncorhynchus gorbuscha*) and Alaskan sockeye salmon (*O. nerka*) in the North Pacific Ocean. *Fish. Oceanogr.* 12, 209–219.
- Ruggerone, G.T., Farley, E., Nielsen, J., Hagen, P., 2005. Seasonal marine growth of Bristol Bay sockeye salmon (*Oncorhynchus nerka*) in relation to competition with Asian pink salmon (*O. gorbuscha*) and the 1977 ocean regime shift. *Fish. Bull.* 103, 355–370.
- Ruggerone, G.T., Nielsen, J.L., Bumgarner, J., 2007. Linkages between Alaskan sockeye salmon abundance, growth at sea, and climate, 1955–2002. *Deep-Sea Res. II* 54, 2776–2793.
- Ruggerone, G.T., Peterman, R.M., Dorner, B., Myers, K.W., 2010. Magnitude and trends in abundance of hatchery and wild pink salmon, chum salmon, and sockeye salmon in the North Pacific Ocean. *Mar. Coast. Fish.* 2, 306–328.
- Ruggerone, G.T., Agler, B.A., Nielsen, J.L., 2011. Evidence for competition at sea between Norton Sound chum salmon and Asian hatchery chum salmon. *Environ. Biol. Fish.* 92, 1–15.
- Urawa, S., 2003. Stock identification studies of high seas salmon in japan: a review and future plan. *North Pac. Anadr. Fish Comm. Tech. Rep. No. 5*, pp. 9–10.
- Urawa, S., Ueno, Y., Ishida, Y., Seeb, L.W., Crane, P.A., Abe, S., Davis, N.D., 2001. A migration model of japanese chum salmon during early ocean life. *North Pac. Anadr. Fish Comm. Tech. Rep. No. 2*, pp. 1–2.
- Urawa, S., Azumaya, T., Crane, P.A., Seeb, L.W., 2004. Origins and distribution of chum salmon in the central bering sea. *North Pac. Anadr. Fish Comm. Tech. Rep. No. 6*, pp. 67–70.
- Urawa, S., Sato, S., Crane, P.A., Agler, B., Josephson, R., Azumaya, T., 2009. Stock-specific ocean distribution and migration of chum salmon in the bering sea and north pacific ocean. *North Pac. Anadr. Fish Comm. Bull. No. 5*, pp. 131–146.
- Wolter, K., Timlin, M.S., 1998. Measuring the strength of ENSO—how does 1997/98 rank? *Weather* 53, 315–324.
- Zaporozhets, O.M., Zaporozhets, G.V., 2004. Interaction between hatchery and wild Pacific salmon in the Far East of Russia: a review. *Rev. Fish Biol. Fish.* 14, 305–319.
- Zavolokin, A.V., Zavolokina, E.A., Khokhlov, Y.N., 2009. Changes in size and growth of Anadyr chum salmon (*Oncorhynchus keta*) from 1962–2007. *North Pacific Anadromous Fish Comm. Bull.* 5, 157–163.
- Zimmermann, M., 1991. Trends in Freshwater Growth of Sockeye Salmon (*Oncorhynchus nerka*) from the Wood River Lakes and Nushagak Bay, Alaska. M.S. Thesis, University of Washington, Seattle.



Contents lists available at ScienceDirect

Deep-Sea Research II

journal homepage: www.elsevier.com/locate/dsr2

Does location really matter? An inter-colony comparison of seabirds breeding at varying distances from productive oceanographic features in the Bering Sea



Ann Harding^{a,*}, Rosana Paredes^b, Robert Suryan^c, Daniel Roby^b, David Irons^d, Rachael Orben^e, Heather Renner^f, Rebecca Young^g, Christopher Barger^g, Ine Dorresteijn^g, Alexander Kitaysky^g

^a Alaska Pacific University, Environmental Science Department, 4101 University Drive, Anchorage, AK 99508, USA

^b US Geological Survey-Oregon Cooperative Fish and Wildlife Research Unit, Department of Fisheries and Wildlife, 104 Nash Hall, Oregon State University, Corvallis, OR 97331-3803, USA

^c Hatfield Marine Science Center, Oregon State University, 2030 S.E. Marine Science Dr. Newport, OR 97365, USA

^d US Fish and Wildlife Service, 1011 East Tudor Road, MS 341, Anchorage, AK 99503, USA

^e Ocean Sciences Department, University of California Santa Cruz, Long Marine Lab, 100 Shaffer Road, Santa Cruz, CA 95060, USA

^f Alaska Maritime National Wildlife Refuge, US Fish and Wildlife Service, 95 Sterling Highway, Homer, AK 99603, USA

^g Department of Biology and Wildlife, Institute of Arctic Biology, University of Alaska Fairbanks, Irving 311, Fairbanks, AK 99775, USA

ARTICLE INFO

Available online 14 March 2013

Keywords:

Corticosterone
Diving
GPS-tracking
Prey
Provisioning
Shelf-break
Stress

ABSTRACT

Central place foragers, such as breeding seabirds, need to commute between their nests and foraging grounds, thus close proximity of the breeding colony to productive oceanographic features might be beneficial for seabird reproduction. We tested this hypothesis by investigating the at-sea foraging and breeding behavior of thick-billed murres (*Uria lomvia*) nesting at three colonies (Bogoslof, St. Paul, and St. George Islands) in the Bering Sea located at different distances from the productive continental shelf-break. We found that distances to feeding areas differed only during night trips among colonies. St. Paul murres foraged entirely on the shelf, whereas St. George murres commuted to the continental shelf-break at night and foraged on the shelf during the day. Bogoslof murres foraged in oceanic waters in close proximity to the colony. Murres breeding at the both Pribilof colonies spent less time attending nests and had higher levels of stress hormone corticosterone compared to murres breeding at Bogoslof, although chick-provisioning rates and fledging success were similar among the three colonies. Lower nest attendance and higher corticosterone suggest lower food availability in the Pribilof domain compared to the Bogoslof region. Murres breeding at the Pribilofs used different foraging strategies to buffer effects of food shortages on their reproduction: flight costs associated with longer distance night trips at St. George were presumably balanced by benefits of higher density and/or more lipid rich prey in the continental shelf-break regions, whereas the additional distance of St. Paul from the continental shelf-break may have outweighed any energetic gain. Murres exhibited a remarkable degree of plasticity of foraging strategies in response to changes in their food availability, but the breeding success of murres did not reflect either food limitations or the colony proximity to productive oceanographic features.

© 2013 Elsevier Ltd. All rights reserved.

1. Introduction

Central place foragers commute between their breeding location and foraging grounds to provision offspring (Orians and Pearson, 1979). The amount of food and frequency of meals that can be delivered to offspring is limited both by distance to food

patches and the amount of time spent foraging within those patches. There is a tradeoff between the time and energetic costs of travel and the energy acquired whilst foraging: Foraging theory predicts that animals should travel the minimum distance to meet energy requirements (Schoener, 1971), and are expected to travel longer distances only if the net energy gain (e.g., due to high-quality, abundant, or easier to capture prey) is higher in distant areas than that in closer areas (Houston and McNamara, 1985; Kacelnik and Cuthill, 1990).

According to Optimal Foraging Theory, foraging behavior should ultimately maximize fitness (Emlen, 1966; McArthur and

* Correspondence to: Alaska Pacific University, Environmental Science Department, 4101 University Drive, Anchorage, AK 99508, USA.
Tel.: +1 907 424 5201.

E-mail address: a.m.a.harding@gmail.com (A. Harding).

Pianka, 1966). Parents may therefore feed their offspring higher value prey items than they consume themselves because of the nutritional requirements of growth and development (Forero et al., 2002). It may also benefit central place foragers with limited ability to carry and transport prey to deliver fewer, high quality meals to their offspring while feeding on prey of more variable quality because of the costs of transporting food items (e.g., Davoren and Burger, 1999).

The availability of prey to marine predators is highly variable in time and space. Diel vertical migrations of oceanic prey species can result in large temporal patchiness of food availability, with prey brought close to the surface during the night (Moku et al., 2000). Prey are distributed over a large range of spatial scales (Maravelias et al., 1996), with aggregations often described by a nested hierarchical patch structure (Fauchald and Erikstad, 2002; Kotliar and Wiens, 1990; Russell et al., 1992). At larger scales, schools or swarms of prey are often concentrated into patches associated with specific marine habitat requirements, spawning migrations, or meso-scale oceanographic features such as fronts or eddies linked to strong bathymetric relief or circulation patterns (Mackas et al. 2005; Polovina et al., 2001). Seabirds in temperate, sub-arctic and polar regions are strongly attracted to these mesoscale patches, concentrating their foraging near major oceanographic features such as shelf edges and fronts, where prey are abundant and predictable over extended time periods (Hamer et al., 2009; Skov et al., 2008; Weimerskirch, 2007). In contrast, the predictability of prey in oceanic waters is presumably lower, and seabirds show relatively little fidelity to particular feeding locations (Weimerskirch, 2007). Thus, for many seabirds, the proximity of a breeding colony to spatially and temporally predictable high-quality foraging habitats may be important to successfully rear their chicks.

Close proximity to predictable foraging habitat may be especially important for energetically constrained species with high travel costs. Murres (*Uria* spp.) have elevated flight costs compared to other seabird species because of their small wing area and high wing loading (Pennycuik, 1987), and energy expenditure has been shown to increase with foraging distance (Gaston, 1985a). Murres typically deliver only one prey item at a time to their chick (Houston, 2002), and both frequency of chick meal delivery and chick fledging mass may be limited by the amount of time and energy expended on foraging trips (Davoren and Montevecchi, 2003; Houston et al., 1996). Although both parents share chick-provisioning duties, trip duration and distance is also constrained by the need for one member of the pair to be present with the chick at all times to prevent predation and exposure to poor weather conditions (Birkhead and Nettleship, 1981). Flexible time budgets allow murres to maintain chick-feeding rates (Piatt et al., 2007) and breeding success (Kitaysky et al., 2000) at fairly constant rates over a range of foraging conditions, by allocating more time to foraging when conditions are poor (Harding et al., 2007). However, very little is known about how foraging distances vary under different conditions of food availability (e.g., Wilson et al., 2005). While at-sea surveys are useful for broad-scale measures of abundance and foraging distribution (Clarke et al., 2003; Trathan et al., 1998), birds enumerated in these surveys can include a high proportion of non-breeding individuals (Davoren et al., 2003), and it is impossible to determine breeding location when multiple colonies are within commuting distance. A few studies have estimated commuting distances from flight durations obtained by time-depth data loggers (Takahashi et al., 2008; Watanuki et al., 2001), but little is known about actual foraging areas and habitat use of individuals (Benvenuti et al., 1998).

We examined how proximity of the breeding colony to particularly productive oceanographic habitats influences the

foraging behavior and breeding performance of thick-billed murres (*Uria lomvia*) by studying three Bering Sea colonies located at varying distances from productive oceanographic features. A previous study has shown that breeding thick-billed murres can forage up to distances of 168 km from their colony (Benvenuti et al., 1998). Bogoslof Island is an oceanic colony, surrounded by deep waters ca. 30 km north of the Aleutian shelf-break, whereas the two Pribilof Islands are located in the shallow waters of the middle domain of the continental shelf, but at different distances from the continental shelf-break; St. George is located ca. 30 km from the continental shelf-break, while St. Paul is located ca. 90 km away (Fig. 1). Both the continental shelf-break and the Aleutian shelf-break are characterized by elevated productivity, and provide important foraging grounds for seabirds in the Bering Sea (Ladd et al., 2005; Schneider, 1982; Springer et al., 1996). Although murre diets have been quantified at the three colonies (e.g., Iverson et al., 2007; Renner et al., 2012; Sinclair et al., 2008), very little is known about where murres from these colonies forage (Kokubun et al., 2008; Takahashi et al., 2008). Moreover, although there is evidence that Pribilof murres sometimes forage on the shelf, these data are restricted to very few years and the availability of shelf-based prey varies greatly among years (Sinclair et al., 2008).

The Bering Sea has experienced climate shifts in recent decades (Hare and Mantua, 2000), with ocean conditions oscillating between regimes of predominately warm or cold temperatures. Such regimes have been shown to affect the abundance and quality of forage fish and invertebrates (Litzow et al., 2006). Annual variation in oceanographic conditions around the Pribilofs has been shown to influence seabirds breeding on the islands, with higher levels of nutritional stress of piscivorous seabirds during cold years attributed to poor foraging conditions on the continental shelf (Benowitz-Fredericks et al., 2008; Satterthwaite et al., 2012). Key forage fish species, such as the juvenile walleye pollock (Sinclair et al., 2008), are less abundant on the continental shelf during cold years because they either disperse or travel deeper to avoid cold waters (Hollowed et al., 2012). We studied birds in 2009, which was characterized by cold oceanographic

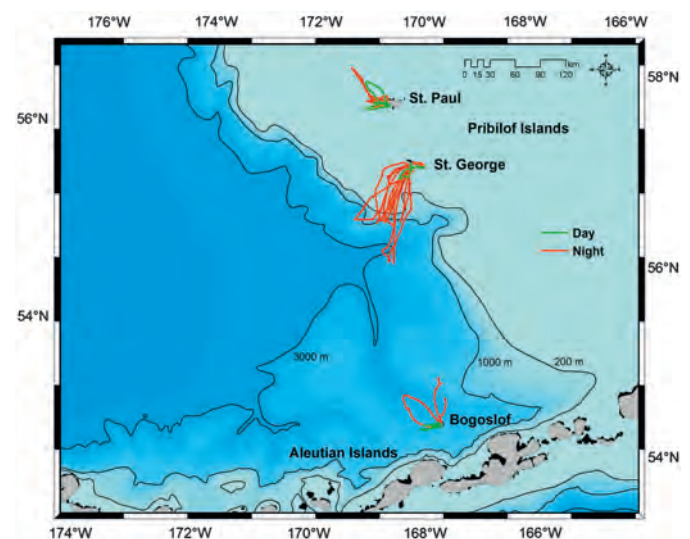


Fig. 1. Study sites in the southeastern Bering Sea. Of the Pribilof Islands, St. George is closest to the continental shelf break-slope (200–1000 m isobaths), known as the Bering Sea green belt (see Study System), compared to St. Paul. Bogoslof Island is closed to the shelf break-slope of the Aleutian Islands. Day (green) and night (red) foraging trips of thick-billed murres obtained by GPS tracking are shown for each colony (St. George $n=11$ individuals, St. Paul $n=15$, Bogoslof $n=18$).

conditions (Stabeno et al., 2012), providing a good opportunity to examine the importance of accessibility to the shelf-edge for Pribilof birds during years when food availability on the shelf is poor.

Species have different abilities to respond to changes in foraging conditions, and the sensitivity of different parameters therefore differ in their sensitivity to changes in food availability among species (Piatt et al., 2007). The closely related common murre has been shown to buffer chick-feeding rates and fledging success across a wide range in food availability by reallocating discretionary time spent at the colony to foraging effort (Harding et al., 2007; Piatt et al., 2007). Reproductive performance is therefore not a good indicator of foraging conditions (Kitaysky et al., 2000), whereas the behavior of adults (colony nest-attendance; Harding et al., 2007), and blood levels of stress hormones (Kitaysky et al., 2007) have been shown to be directly related to changes in the availability of food resources to chick-rearing murrens.

The steroid hormone corticosterone (CORT) plays an important role in an individual's adaptive response to environmental stress (Romero et al., 2000; Wingfield et al., 1998). Individuals have been shown to respond to a number of stressors such as challenging environmental conditions, parasites, and predators by increasing secretion of CORT (e.g., Raouf et al., 2006; Romero et al., 2000). Levels have also been shown to be elevated during food shortages (Kitaysky et al., 1999a, 1999b, 2007, 2010), and in individuals in poor body condition (Kitaysky et al., 1999b; Romero and Wikelski, 2001; but see Schultner et al., 2013). Studies of seabirds have shown that the secretion of CORT is largely driven by changes in food (Benowitz-Fredericks et al., 2008; Kitaysky et al., 1999b, 2007, 2010), and a strong negative correlation between CORT and fish abundance has been demonstrated in a number of seabird populations, including common murrens (*Uria aalge*; Kitaysky et al., 2007). Baseline concentrations of CORT increase in a matter of days in response to food limitation (Kitaysky et al., 2007; 2010), and a number of seabird studies have used CORT as an index of the nutritional status of individuals (e.g., Dorresteyn et al., 2012; Satterthwaite et al., 2010; Schultner et al., 2013; Welcker et al., 2009).

We tested the hypothesis that close proximity of the breeding colony to a productive oceanographic feature is beneficial for breeding murrens. We used GPS loggers to determine the foraging location of murrens from each colony, and examined how differences in foraging habitat and foraging distance from the colony affect diet, diving behavior, parental time budgets, breeding success, and the nutritional status of parents.

We predicted that breeding murrens from Bogosof would commute to the Aleutian shelf-break, and that murrens from St. George and St. Paul would commute to the continental shelf-break. Given the energetic and time constraints associated with a longer commute to foraging grounds, we further predicted that St. Paul murrens would experience greater food limitation and spend less time at the colony. Previous tagging studies were done with large seabirds and marine mammals (Le Boeuf et al., 2000; Ryan et al., 2004); this is the first study to use GPS receivers on a smaller diving and flying seabird. We used CORT concentrations in blood plasma as a measure of the energy balance of parents breeding at each colony, and define nutritional stress as when food resources are in lower supply than optimal.

2. Methods

2.1. Study system

A shelf-break bisects the Bering Sea, separating the shallow continental shelf from the deep waters of the basin hydrographic

domain. The edge of the continental shelf has been described as the Bering Sea Green Belt, with the highly productive habitat resulting from physical processes such as crosswise circulation and eddies in the Bering Slope Current, tidal mixing, and advection and upwelling that bring nutrients into the euphotic zone (Coachman and Walsh, 1981; Schumacher and Reed, 1992; Springer et al., 1996). Primary productivity at the shelf break is approximately 60–270% higher than that in the outer shelf and ocean domains (Springer and McRoy, 1993; Springer et al., 1996). High productivity along the shelf break supports large numbers of zooplankton, fish and squid (Radchenko, 1992; Sinclair and Stabeno, 2002), which in turn attracts high numbers of marine mammals and seabirds (Piatt and Springer, 2003; Schneider, 1982). Further south, the Aleutian Islands form the border between the Bering Sea and the North Pacific Ocean, and the combination of strong currents, abrupt topography and distinct water masses from the two separate water basins promotes high primary productivity and also sustains large numbers of predators (Ladd et al. 2005; Springer et al., 1996).

We studied thick-billed murrens breeding at three Bering Sea colonies in 2009. The colonies are located in contrasting oceanographic environments. Bogoslof Island (53°55' 38" N, 168°02' 04" W) is situated 30 km north of the Aleutian Chain, adjacent to Aleutian passes and surrounded by deep oceanic waters (1000–2000 m), whereas the two Pribilof Islands are located on the continental shelf and are surrounded by shallower water (100–200 m; Fig. 1). The continental shelf-break is therefore within foraging range of murrens from both Pribilof Islands, but is located much nearer to St. George (56°36' 20" N, 169°33'35"W; 30 km) than St. Paul (57°7' 30" N, 170°17' 3" W; 90 km).

2.2. Field methods

Field work encompassed the period from pre-lay through to the end of chick-rearing (Bogoslof field work=June 21–Sept 2; median hatch date 21 July (range=13 Jul–31 Jul, $n=48$ nests); St. George field work=May 16–Sept 8; median hatch date 27 Jul (range=12 Jul–12 Aug, $n=169$ nests); St. Paul field work=25 May–1 Sept; median hatch date 2 Aug (range=20 Jul–24 Aug, $n=142$ nests)).

2.2.1. Instruments

We opportunistically selected thick-billed murrens that were rearing chicks 5–15 days old throughout the chick-rearing period, catching them at the nest-site using a telescoping noose-pole (Hogan, 1985). Captures of birds on the Pribilofs were distributed throughout the daylight hours, whereas Bogoslof murrens were primarily captured at dawn to maximize the chance of recording active foraging behavior during the battery life of the GPS (see below). Instruments were only deployed on one member of a breeding pair at a time. At initial capture, each bird was weighed (± 1 g) and one or two instruments were attached; a Time-Depth Recorder (TDR), and a GPS (Table 1). Both instruments were

Table 1
Summary statistics of GPS deployment and logger fate at three Bering Sea colonies, n =individual.

	St. Paul	St. George	Bogoslof
GPS deployed	27	28	32
Birds recaptured	20	20	30
GPS units recovered	20	17	25
GPS units with sufficient data for analysis	15	11	18
GPS lost prior to recapture	3	10	5
Bird fledged prior to recapture	1	0	1
Bird abandoned/nest failed	1	7	1

attached to birds on St. George and Bogoslof, but only GPSs were deployed at St. Paul. The TDR was attached to a plastic leg band (Protouch) using zip-ties, and the GPS logger attached to the central back feathers using black Tesa tape® (Paredes et al., 2005). GPS loggers were waterproofed prior to attachment using shrink heat tubing (4FT IC8725 3/4 inches clear; Frigid North, AK, USA), heated to mould tightly around the logger and minimize buoyancy. Handling time took ca. 10–15 min, and less than 20 min in all cases. Recapture efforts started approximately 24 h post-deployment, and birds were recaptured on average after 39 h (Bogoslof mean=30 h; St. George mean=59 h; St. Paul mean=31 h; Table 1). Upon recapture, all instruments were removed, and body mass was measured again. All individuals were banded with a unique USFWS metal band prior to release.

Lotek TDRs LAT 2500 (mass=3.6 g, dimensions=8 × 35 mm) recorded depth and time every 1 s, with an absolute pressure accuracy of +/-1% of full scale. Two types of TechoSmart GPS loggers with rechargeable batteries were used. The Gipsy-3 (flat antennae: dimensions 41 × 14 × 7 mm; total mass=10 g), with a 250 mA battery was used on Bogoslof, whereas the TechnoSmart Gipsy-2 (flat antenna: dimensions 23 × 15 × 6 mm; total mass=10–14 g), with a 250–500 mA battery, was used on the two Pribilof Islands. Latitude and longitude were recorded at intervals of 1–2 s for > 95% of positions acquired. Longer time gaps where satellite reception was lost, however, did occur and varied by island, thereby affecting deployment duration (acquiring satellite signal reception requires more battery power than simply recording positions) and the resolution of tracks. GPS units used at St. Paul provided the highest resolution tracks with a mean of 32 positions per minute (range 0.2–58) and mean recording duration of 16 h [41 maximum] before recovery, followed by St. George (12 positions per minute [0.3–60], 21 h [75]) and Bogoslof (9 positions per minute [1–34], 11 h [25]). Therefore, a greater number of complete long duration foraging trips (e.g., overnight trips) were recorded at the Pribilof Islands than on Bogoslof.

2.2.2. Chick diet

Murres bring a single prey item to their chick, usually held in line with the bill and with a proportion of the prey visible for identification. Identification methods were of three types: all-day watches dedicated to observations of chick diet (St. Paul), ancillary observations made during all-day adult time-budget watches (all three islands), and targeted periods of time dedicated to the digital photography of prey loads using a digital SLR camera [Canon 500 mm F4, usually with a 1.4 extender (Bogoslof)]. Photographic sessions on Bogoslof were conducted between 0800–2100 Alaska-time, and we therefore restrict the comparison of chick diet among colonies to prey delivered during this time period. A telescope with a 20–60 zoom lens or 10 × 42 binoculars were used to identify prey items during the observations sessions; photographed prey were viewed and identified on a computer screen. All prey were identified to the lowest possible taxonomic level and visually assigned to a size category. The three size categories were (S) smaller, (L) larger, or (M) equal to the gape length of the parent.

2.2.3. Adult diet

Diet samples of breeding adult murres were obtained using the water off-loading (lavage) method described in detail by Wilson (1984) and for murres by Ito et al. (2010), with the process repeated twice to ensure as complete emptying of the stomach as possible (Neves et al., 2006). Both GPS birds and non-GPS birds were lavaged, and GPS birds were only sampled during their second capture. Total numbers of birds diet-sampled at each

island were: St. Paul $n=50$, St. George $n=55$, Bogoslof $n=34$, and captures were distributed evenly during day-light hours. Diet results are presented as percent occurrence (defined as the percentage of samples containing at least one item of a given prey type).

2.2.4. Parental time Budgets

We measured parental attendance and chick-feeding rates (feeds h^{-1}) at each of the three colonies. Individually marked chick-rearing parents were observed on plots containing 7–13 breeding pairs of murres from sunrise to sunset, during 3–4 observation-days at each of the three colonies. Observation-days were scheduled to sample the early (1–3 August), middle (6–9 August) and late (12–15 August) parts of the chick-rearing phase to control for any change in provisioning behavior with chick age (Birkhead and Nettleship, 1987). Where possible we observed the same nest-sites across chick-rearing, although constraints placed by the need of simultaneous observation of GPS-tagged and untagged birds resulted in fewer observation days at some nests because tagged individuals differed among observation days and observed nests had to be in one field of view.

Parent's arrival and departure time at the colony were noted, along with the time of food delivery to chicks. Attendance was measured in bird-minutes per hour (Harding et al., 2007). For example, where one brooding parent attended its nest for a full hour, and the off-duty partner attended for half of that hour, we calculated 90 bird-minutes of attendance for that hour. Fewer than 60 bird-minutes of attendance would mean that the egg or chick was left unattended for some period of time.

2.2.5. Corticosterone

We sampled circulating levels of baseline CORT from breeding adults during the chick-rearing period at each colony to infer the energy balance of parents (St. Paul $n=85$; St. George $n=72$; Bogoslof $n=44$). These included samples from the initial capture of individuals deployed with GPS units at St. Paul ($n=16$) and St. George ($n=13$). All birds were sampled according to a standardized technique (Benowitz-Fredericks et al., 2008), with a blood sample (< 500 μ l) collected within three minutes of capture. After blood collection, all samples were centrifuged, and plasma was preserved frozen for later analysis at the University of Alaska Fairbanks.

2.2.6. Fledging success

Fledging success (number of chicks fledged per nests with chicks) was determined at each colony from data recorded during regular observations of sites with eggs (Byrd et al., 2008a; Harris and Wanless, 1988). A minimum of six plots were selected at scattered locations at each colony, and each plot was comprised of 20–30 nests. Nests were checked every 3–6 days, and chicks were considered to have fledged if they disappeared from the nest-site more than 15 d after hatching (Byrd et al., 2008a; Gaston and Jones, 1998).

2.2.7. Instrument effect

We examined: (a) to what extent the instruments may have distorted the normal behavior of the bird, and (b), whether the effect of the device varied among colonies. First, incidences of abandonment and chick-loss post GPS deployment were examined. Second, we examined the effect of instrumentation on behavior by directly observing GPS-tagged birds, and comparing attendance and chick-feeding rates of those birds with controls on the Pribilof colonies (we were unable to observe GPS-tagged birds on Bogoslof due to nesting locations, which were not visible from land). Third, we determined how instrumentation affected the

physiology of individuals, by (a) comparing changes in mass between tag deployment and recapture at each colony, and (b) comparing changes in baseline CORT levels between deployment and recapture on St. Paul and St. George only. Levels of circulating CORT have been used previously to index the extra energy cost associated with instrumentation (e.g., Takahashi et al., 2008), consequently we collected blood samples from individuals at both initial capture for tagging and recapture.

2.3. Laboratory analysis

CORT concentrations (ng mL^{-1} of plasma) were measured using radioimmunoassays. Each sample was equilibrated with 2000 cpm of tritiated CORT prior to extraction with 4.5 mL distilled dichloromethane. After extraction, percent tritiated hormone recovered from each individual sample (average hormone recovery was $> 87\%$) was used to correct final CORT concentrations. Samples (in duplicates) were reconstituted in PBSG buffer and combined with antibody and radiolabel in a radioimmunoassay. Dextran-coated charcoal was used to separate antibody-bound hormone from unbound hormone. All samples were analyzed in five different assays; sensitivity of the assays was 7.8 pg per tube, and inter-assay variation was less than 6 %.

2.4. Statistical analysis

Location data from GPS units were used to determine foraging range and maximum distance from the colonies. We first used a forward-backward speed filter (McConnell et al., 1992) with a maximum speed of 80 km/h (Croll et al., 1991) to cull erroneous positions ($< 5\%$ of locations were removed), leaving over 1 million locations from 44 individuals. Not all birds were equipped with dive loggers to identify known foraging activity, therefore we developed criteria to define a foraging trip based on activities of birds carrying dive loggers and direct observations of adults returning with prey to provision chicks. According to these criteria, a bird needed to depart a 50 m buffer around the nest site (selected based on accuracy of GPS position fixes and proximity of nesting location to the ocean) for a minimum of 10 min (the mean minimum duration among islands of a foraging trip resulting in the feeding of a chick during provisioning rate observations) to be included in analyses of foraging activity. We measured the straight-line distance between the nest site and the most distant location of the each central-place trip. In situations where a complete round-trip was not recorded because of GPS failure, we still included the maximum distance estimate in our analysis if the individual began returning to the colony (to within 75% of the maximum distance). The one exception to this rule was that all night trips of birds from Bogoslof ($n=5$) were included, even if the GPS failed before the bird began returning to the colony. Most GPS units at Bogoslof stopped recording (due to lower battery capacity from a shore-based, photovoltaic powered charging system) before an entire night foraging trip could be obtained. Therefore, values for Bogoslof represent a minimum estimate of distance traveled from the colony. An overnight trip was defined as beginning on one calendar day and returning the next. Differences in trip distance were examined with a General Linear Model (GLM), with colony, time (day or night), and the interaction between colony and time as factors; and Tukey tests were used for post-hoc comparisons.

We used data from dive loggers to compare maximum depth [per dive] between islands (St. George and Bogoslof) and day vs. night foraging. Although the loggers were set to begin recording at 5 m, the delay in instrument reaction time resulted in the first depth of a dive sometimes recorded as 7 m if the bird dived rapidly past the 5 m threshold for initiating depth recording.

A dive was therefore classified as descending greater than 7 m for > 3 s (based on an approximate descent rate of 1.1 m/s) and < 4.45 min (the maximum dive duration based on visual review of dive profiles). Night dives were defined as occurring between evening and morning nautical twilight when the center of the sun is < 12 degrees below the horizon and no visible sunlight remains. Day dives occurred between sunrise and sunset and crepuscular dives were between nautical twilight and sunrise or sunset. The sun zenith for each location was calculated with the sun position program written in Matlab (Vincent Roy, The MathWorks.com\usersforum) using the latitude and longitude of each island and compared to the United States Naval Observatory solar table to verify accuracy.

The proportion of squid vs. fish in chick diet and the relative importance of squid, fish and euphausiid (% occurrence) in adult diet were compared among colonies using a Chi-square test. We compared time spent at the colony (attendance) and chick-feeding rates obtained from observations among colonies using a GLM, with colony as a factor. Circulating levels of baseline CORT were compared among colonies with an ANOVA, with colony as a factor, and Tukey multiple comparisons were used as post-hoc tests. Similarly, fledging success was compared among colonies with an ANOVA, where average value per plot ($n=6$ plots at Bogoslof; 12 at St. Paul, and 10 on St. George) was used as a sampling unit, and colony as a factor.

To examine the effect of GPS loggers on the behavior of birds observed at the colony, we compared attendance and chick-feeding rates between simultaneously observed GPS and control nests using a GLM, with colony (St. George or St. Paul) and GPS (1 or 0) as treatment effects. During prior tests we found no significant effect of nest on either of these parameters, and therefore used nest-day as the sample unit for all subsequent analyses. To determine whether partners were compensating for the reduced performance of the GPS birds (Paredes et al., 2005), we compared the chick-feeding rates of GPS birds and their partner using a paired *t*-test. The mass of birds at deployment of GPS (hereafter 'initial capture') differed significantly among colonies ($F_{2,88}=21.64$, $P < 0.001$), with St. Paul birds heavier than either St. George or Bogoslof (St. Paul mean = 1104.9 ± 15.3 g, $n=27$; St. George mean = 987.6 ± 10.9 g, $n=28$; Bogoslof mean = 1018.9 ± 11.6 g, $n=34$). To compare changes in body mass during deployment among islands we therefore used mass change as a percentage of mass at initial capture (only birds where GPS loggers remained successfully attached for full deployment were included in this analysis) a GLM was used, with colony as a factor, and the total number of hours deployed included as a covariate. A two-way ANOVA was used to compare mean dive depth between time of day (day, night, and crepuscular) and colony (Bogoslof and St. George). Dive data were log-transformed prior to analysis, and Bonferroni post-hoc multiple comparison tests used. A separate paired *t*-test was used to compare levels of circulating CORT between initial capture and recapture at St. Paul and St. George. CORT data were log-transformed prior to analysis to attain normal distribution.

GPS tracking and dive data were processed using custom programs written in Matlab. Statistical tests were performed in Minitab and SPSS. Statistical significance was assumed at $P < 0.05$. Unless otherwise indicated, values reported are means ± 1 S.E.

3. Results

3.1. Foraging location

St. George birds foraged on the shelf during the day and on the continental shelf-break and the basin at night. There was less

noticeable diurnal difference in the foraging location of murres breeding at St. Paul and Bogoslof: the majority of St. Paul birds foraged on the shelf to the NW of the island, and Bogoslof birds all foraged in the deep water over the basin (Fig. 1). Mean trip

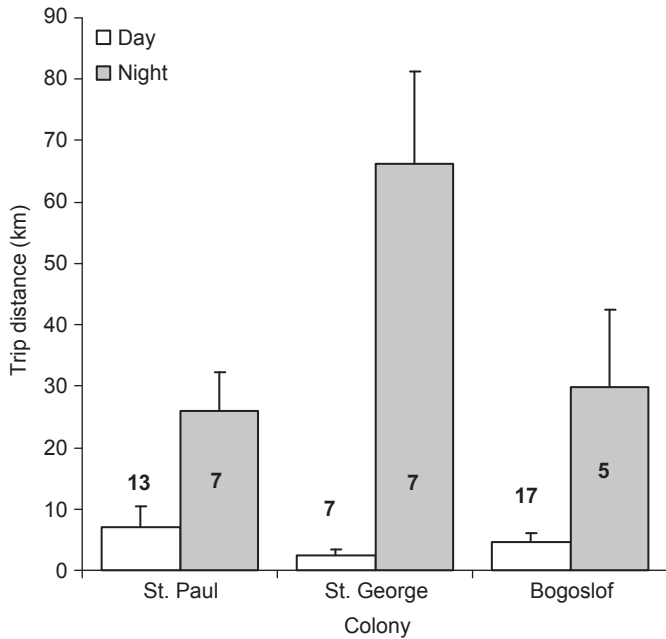


Fig. 2. Trip distances (mean ± 1 SE) of thick-billed murres conducted during the day and night hours at three Bering Sea colonies in 2009 (n=individual birds).

Table 2

Dive depths (m) conducted during the day, night, and crepuscular hours at Bogoslof and St. George Islands in 2009. Minimum depth used to classify a dive was set at 7 m. Values presented are means among individuals, n=individual.

	St. George			Bogoslof		
	Night	Day	Crepuscular	Night	Day	Crepuscular
n	11	15	15	12	25	18
mean	9.68	48.71	16.67	10.22	57.27	16.58
SE	0.43	4.31	1.69	0.50	4.86	1.18
min	8.25	27.74	8.71	7.50	21.61	8.15
Max	12.84	83.52	30.03	13.30	105.74	28.94

distance (km) differed significantly among the three colonies ($F_{2,50}=4.50$, $P=0.016$), with time (day or night; $F_{1,50}=45.19$, $P<0.001$), and the interaction between colony and time ($F_{2,50}=6.54$, $P=0.003$). Overall, distances were longer on St. George than either St. Paul or Bogoslof, but there was no difference between St. Paul and Bogoslof (Tukey post-hoc tests $P<0.05$: St. George mean=34.4 ± 11.4 km, n=14; St. Paul mean=13.68 ± 3.69 km, n=20; Bogoslof mean=10.26 ± 3.73 km, n=22), and trips conducted during the night were longer than those conducted during the day (Tukey post-hoc tests $P<0.05$: night mean=41.87 ± 7.84 km, n=19; day mean=5.00 ± 1.42 km, n=37). St. George night trips were significantly longer than both the day trips on St. George and the day and night trips on St. Paul and Bogoslof (Tukey post-hoc tests $P<0.05$; Fig. 2), but there was no significant difference in day trip length among colonies.

3.2. Dive depth

A total of 10,002 dives from 42 birds were recorded; 5533 dives from 26 birds at Bogoslof, and 4469 from 16 birds at St. George. There was no significant difference in mean dive depth between islands ($F_1=0.84$, $P=0.361$), but dive depth differed significantly between the three time periods (day, night, and crepuscular; $F_2=194.01$, $P<0.001$), with deeper dives conducted during the day, shallower dives at night, and dives of intermediate depth during the crepuscular hours (Table 2; Fig. 3). The majority of dives performed during the night were less than 20 m deep at both islands, whereas mean maximum depth per individual conducted during the day ranged from 22–106 m (Table 2; Fig. 3). The maximum dive depth recorded was 142 m from a bird at Bogoslof.

3.3. Chick diet

A total of 712 prey items were observed at the three colonies, and, out of these, 465 (65%) were visible for some kind of identification. The remaining 35% were either not identified because the prey were obscured from view or the delivery was too fast. The proportion of fish vs. squid in chick diet differed among the colonies ($\chi^2=152.61$, $df=2$, $P<0.001$; Table 3): Bogoslof chicks were fed primarily squid, whereas St. Paul chicks received mostly fish. St. George chicks ate about 75% fish and 25% squid. A more detailed breakdown of percentage prey composition is shown in Table 3. The relative proportion of identified fish (at least to family level) was similar on St. George and St. Paul

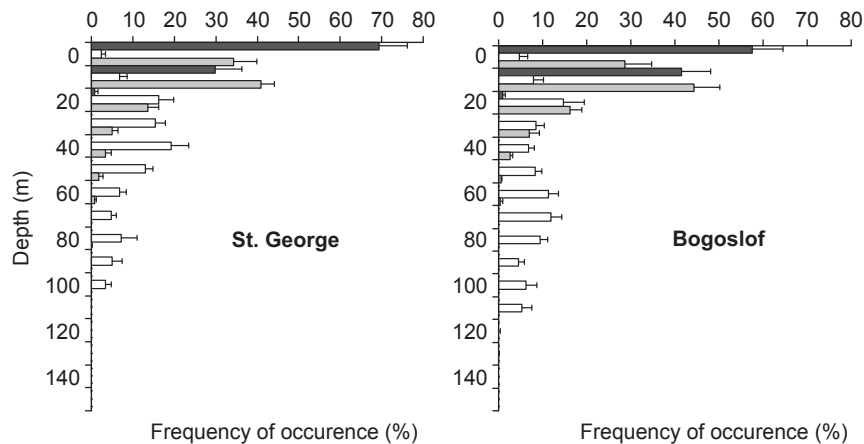


Fig. 3. Frequency of dive depths conducted during the day (white bars) night (black bars) and crepuscular (gray) hours on Bogoslof and St. George. Bins are lower edge, e.g. 0=0–10, and minimum depth used to classify a dive was 7 m. Values are means (± 1 SE) among individuals (Bogoslof night n=12 individuals, day n=25, crepuscular n=18; St. George night n=11, day n=15, crepuscular n=15).

Table 3

Percent prey composition of chick diet (n =prey items) and percent occurrence (defined as the percentage of samples containing at least one prey type) of prey composition of adult (n =lavage samples) diet of thick-billed murres breeding on three Bering Sea islands in 2009. Dominant prey taxa are shown in bold.

Chick diet		Adult diet					
Colony	St. Paul	St. George	Bogoslof	St. Paul	St. George	Bogoslof	
n	110	206	149	48	30	21	
Fish spp	Myctophid		0.5	6.6	2.08		
	Sandfish		0.5				
	Sand lance	1.9	1.0				
	Searcher				2.08		
	Smelt		1.0	0.7			
	Unid. Gadid	4.7	0.5		16.67	3.33	4.8
	Pollock				72.92	23.33	9.5
	Flatfish	1.9	4.0				
	Greenling		1.0				
	Eelpout/Prickleback	18.9	6.9		10.42		
	Sculpin		4.0				
	Gunnel			0.7			
	Unidentified fish	70.8	45.5	3.9	4.17	6.67	
	Invert spp	Squid	1.9	34.7	85.5	4.16	76.67
Euphausiids						3.33	19.05
Polychaete					22.17		
Themisto					2.08	3.33	
Amphipod							
Unid.						2.08	
Mollusc							
Unidentified invert		0.5	2.6				

(70–72% of fish); the majority of identified fish at St. Paul were eelpouts (*Zoarcidae*) and pricklebacks (*Stickleidae*), whereas a higher diversity of fish species was identified at St. George.

A total of 563 prey items (Bogoslof $n=166$, St. George $n=280$, St. Paul $n=117$) were categorized into three broad prey sizes: smaller than the parent's gape length (S), the same length as the gape (M), and longer than gape length (L). There were no small prey observed on Bogoslof ($M=23\%$, $L=77\%$ of diet samples), whereas both St. George ($S=26\%$, $M=31\%$, and $L=43\%$) and St. Paul ($S=27\%$, $M=9\%$, and $L=64\%$) birds delivered a wider range of prey sizes.

Squid were primarily large at Bogoslof ($B=19\%$, $L=81\%$, $n=130$); of mixed size at St. George ($B=31\%$, $L=39\%$, $S=30\%$, $n=130$), and the single squid observed at St. Paul was large. A similar pattern was observed with unidentified fish relatively large at Bogoslof ($B=20\%$, $L=80\%$, $n=5$), and of more mixed sizes at the two Pribilof Islands (St. George: $B=35\%$, $L=48\%$, $S=17\%$, $n=91$; St. Paul: $B=7\%$, $L=59\%$, $S=34\%$, $n=71$).

3.4. Adult diet

Adult diet reflected both day and night-time foraging, however, there may be a sampling bias associated with trip duration, with soft-bodied prey collected at night (longer trip duration) likely to be underestimated to a larger extent because of the longer time duration between prey ingestion and lavage. The relative importance of fish, squid and euphausiids (% occurrence; see methods) in adult diet differed among colonies ($\chi^2=228.29$, $df=2$, $P < 0.001$); parents on St. Paul fed mostly on fish (primarily juvenile walleye pollock, *Theragra chalcogramma*, 93%), whereas

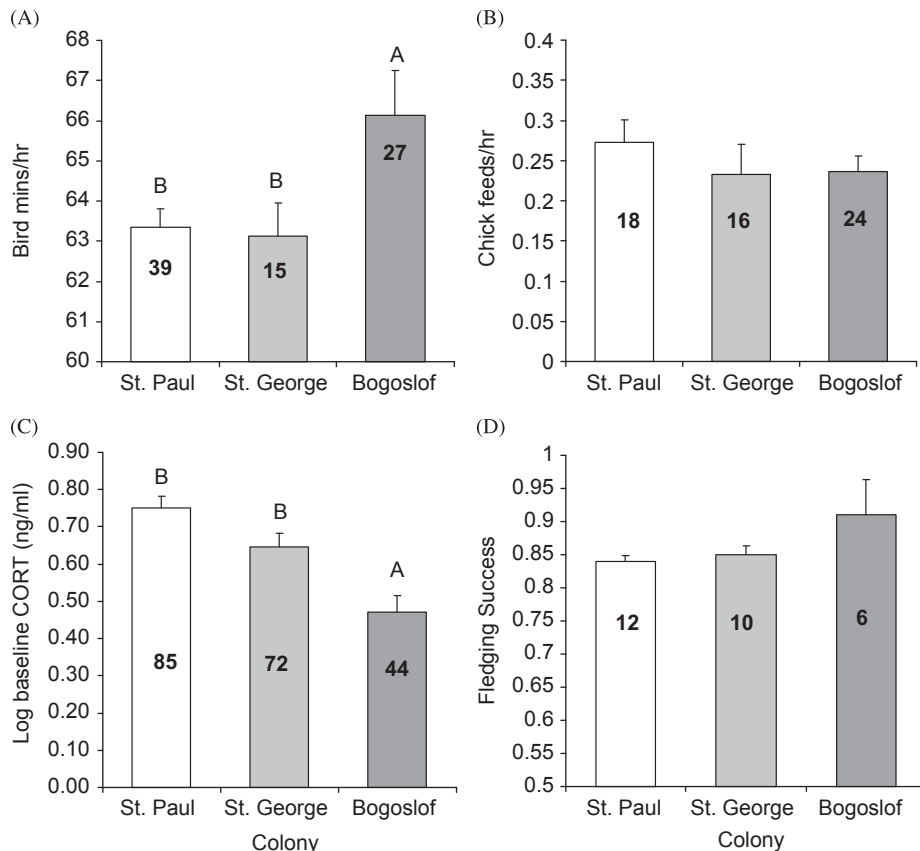


Fig. 4. Mean (± 1 SE) colony attendance (A: n =nest day), chick-feeding rates (B: n =nest day), circulating levels of corticosterone (C: n =individual), and fledging success (D: n =plot) of thick-billed murres breeding on St. Paul, St. George, and Bogoslof. Means with different letters are significantly different ($P < 0.05$).

squid dominated the diet on both St. George (77%) and Bogoslof (90%), and euphausiids were most common at Bogoslof (20%). Pollock was the dominant identified fish species in the diet at both Pribilof Islands (Table 3), and lab dissection of undigested pollock suggests that the ingested polychaete worms were internal fish parasites.

3.5. Parental time budgets

Nest attendance differed between colonies ($F_{2,80}=4.25$, $P=0.018$), with birds spending more time at their nest at Bogoslof than either of the two Pribilof Islands (Bogoslof mean = 66 ± 1.11 min h^{-1} , $n=27$; St. George mean = 63 ± 0.81 min h^{-1} , $n=15$; St. Paul mean = 63 ± 0.47 min h^{-1} , $n=39$; Fig. 4). There was no difference in chick-feeding rates among colonies ($F_{2,57}=0.64$, $P=0.529$; Fig. 4); chicks at all three colonies received the equivalent of 3–4 meals in a 16 h day.

3.6. Corticosterone

CORT levels differed among colonies ($F_{2,198}=12.12$, $P<0.001$). CORT levels at Bogoslof (log transformed mean = 0.47 ± 0.046 ng ml^{-1} , $n=44$) were lower than both St. George (mean = 0.65 ± 0.036 ng ml^{-1} , $n=72$) and St. Paul (mean = 0.75 ± 0.033 ng ml^{-1} , $n=85$), but there was no difference in CORT levels between the two Pribilof Islands (Tukey multiple comparison test $P>0.05$; Fig. 4).

3.7. Fledging success

Fledging success did not differ significantly among the three colonies ($F_{2, 25}=1.39$, $P=0.267$); and it was high at all three colonies (St. George = 0.85 ± 0.01 , $n=10$ plots; St. Paul = 0.84 ± 0.01 , $n=12$ plots; Bogoslof = 0.91 ± 0.05 , $n=6$ plots; Fig. 4).

3.8. Effect of GPS loggers

Eighty-seven GPS loggers were deployed at the three colonies (Table 1); 70 of these birds were recaptured. Of the 17 loggers not retrieved, nine (10%) were on birds that abandoned their nests after the instrument deployment and eight (9%) birds fledged their chicks during the instrument deployment. A total of 44 GPS deployments resulted in usable data [see Methods] for foraging trip analysis (Table 1). These deployments recorded a total of 93 trips (Bogoslof $n=33$, St. George $n=28$, St. Paul $n=32$). There was a significant effect of GPS on the attendance of birds at St. Paul and St. George (logger effect: $F_{1,70}=10.44$, $P=0.002$), but no significant difference between the two colonies (logger effect \times colony interaction: $F_{1,70}=0.26$, $P=0.614$). Birds at control nests spent more time at the colony than birds at nests where one member of the pair was instrumented (control mean = 63.29 ± 0.41 bird min h^{-1} , $n=54$ nest-days; GPS nest mean = 60.33 ± 0.68 bird min h^{-1} , $n=17$ nest-days). Chick-feeding rates did not differ significantly between control and instrumented nests at the Pribilofs ($F_{1,51}=2.66$, $P=0.109$: controls = 0.25 ± 0.28 feeds h^{-1} , $n=34$; instrumented = 0.17 ± 0.05 , $n=18$), or between the two colonies ($F_{1,51}=0.00$, $P=0.970$). Within nests of instrumented birds, there was no significant difference in chick-feeding rates between the GPS bird and their uninstrumented partner (Paired t -test: $T = -1.11_{16}$, $P=0.282$).

Mass change during deployment, calculated as a percentage of mass at initial capture upon recapture, differed significantly among the three colonies ($F_{2,63}=4.00$, $P=0.023$), but did not change with the duration of deployment ($F_{1,63}=2.06$, $P=0.157$). St. George birds lost a higher percentage of their initial body mass

than birds from St. Paul and Bogoslof (St. George mean = $-5.25 \pm 1.04\%$, $n=18$; St. Paul mean = $-1.47 \pm 0.90\%$, $n=20$; Bogoslof mean = $-3.89 \pm 0.85\%$, $n=25$).

CORT levels of birds at initial capture and subsequent recapture were determined on St. Paul and St. George colonies only (see Methods). There was no significant difference in circulating levels of CORT between the two colonies ($F_{1,58}=0.00$, $P=0.982$), capture period (initial capture and recapture: $F_{1,58}=1.10$, $P=0.298$), or the interaction between colony and capture period ($F_{1,58}=0.01$, $P=0.923$).

4. Discussion

Our main results can be summarized as: (a) murre nesting at St. Paul did not commute to the continental shelf-break, and instead foraged entirely on the shelf, whereas murre nesting at St. George commuted to the continental shelf-break at night, and foraged on the shelf during the day. Bogoslof murre foraged entirely over the basin relatively close to the colony, and did not commute to the Aleutian shelf-break, (b) levels of food limitation at the two Pribilof Islands were similar, and higher than those at Bogoslof Island, and (c) murre at the Pribilofs spent less time at the colony than Bogoslof birds, but there was no difference in colony attendance between St. George and St. Paul. Below, we discuss these results under four broad categories: (1) Foraging behavior, (2) Diet, (3) Colony attendance, and (4) Instrument effects and performance.

4.1. Foraging behavior

Contrary to our predictions, birds on St. Paul foraged entirely on the shelf instead of traveling further distances to the continental shelf-break. St. George birds only traveled to continental shelf-break waters at night, and Bogoslof birds fed entirely in the basin rather than along the Aleutian shelf-break. Although there were technical limitations with the Bogoslof GPS tags, distances estimated from temperature-depth-recorders (much smaller Cefas tags, weight ~ 2.7 g) deployed in the same study year by a simultaneous study were also short (ca. 17 km; C. Barger Unpubl. data). CORT levels suggest that foraging conditions were relatively good at Bogoslof, whereas birds at the two Pribilof Islands were experiencing similar high levels of food limitation. To put our 2009 CORT results into context, the lowest CORT levels (indicative of favorable foraging conditions) in chick-rearing thick-billed murre recorded on St. Paul were in 2005 (0.27 ± 0.09 ng/ml; Kitaysky et al. Unpubl. data), on St. George in 2003 (0.33 ± 0.03 ng/ml; Benowitz-Fredericks et al., 2008), and on Bogoslof in 2008 (0.37 ± 0.05 ng/ml; Barger and Kitaysky, 2012). CORT levels in 2009 on St. Paul and St. George were therefore ~ 2 times higher than the lowest values recorded at these islands. These results have important implications at both the individual and population level, as elevated levels of CORT reduce survival in a number of seabird species, including murre (Kitaysky et al., 2007; Satterthwaite et al., 2010).

Even if it is more profitable to feed in a certain area, murre parents need to balance the costs of longer flight with either more abundant or higher quality prey. Given energetic and time limitations associated with high flight costs and the need for parents to feed their chick 3–5 times per day (Croll et al., 1991), parents may be constrained to feed in less “profitable” areas closer to the colony. Although oceanic domains are thought to be relatively low in productivity (Springer and McRoy, 1993; Springer et al., 1996), deep-water prey are usually high quality, and may be very concentrated near the surface at night due to diel vertical migration even if total productivity of the water column is

relatively low. Vertically migrating fish, squid, and zooplankton species that live in deep basin waters tend to store large energy reserves so they can fast for extended periods and maintain near neutral buoyancy over a wide range of depths and pressures (Moku et al., 2000; Visser and Jonasdottir, 1999). The diet of seabirds that forage over deep water basins usually include species with relatively high energy densities, such as northern lampfish (*Stenobrachius leucopsarus*), and northern smoothtongue (*Leuroglossus schmidti*; Iverson et al., 2007; Lance and Roby, 2000). Lipid values of individual species have also been shown to vary among habitats, and a recent study on the energy density of forage fish and invertebrates in the southeastern Bering Sea has shown that the lipid values in squid varied from 9–52%, with energy values higher in the slope region than over the shelf (Whitman, 2010). Therefore, the prey species available in the deep basin waters around Bogoslof and off the shelf near the Pribilofs were of substantially higher quality than those available on the shelf. Distances traveled by Bogoslof birds at night were equivalent to the distance to the Aleutian edge, suggesting that prey profitability was higher in the deeper basin waters than along the chain. Although we recorded very few night trips on Bogoslof, a simultaneous study on the diet (measured by stable isotopes) and foraging behavior (measured by temperature depth recorders) supports our findings, showing that thick-billed murrens on Bogoslof were eating squid and euphausiids, and conducting relatively short-distance trips from the colony (ca. 17 km; C. Barger Unpubl. data). Interestingly, the day-time foraging locations of Bogoslof birds also suggest that energy gained from prey in the basin outweighed any benefits associated with traveling further distances to the Aleutian chain, despite the absence of diurnal vertical migration. Further study is now required to understand the day-time availability of basin-based prey. St. George birds were able to forage in the basin at night, when they were free from day-time chick-provisioning constraints, but it was energetically unfeasible for St. Paul birds to make the long commute to the basin, despite the higher quality prey available in the basin.

Birds on both St. George and St. Paul foraged on the shelf during the day, despite evidence of energy limitation. These results suggest that it was energetically beneficial for birds at both islands to forage closer to the colony when feeding their chick. Perhaps food availability on the shelf in 2009 was sufficient to outweigh the additional energetic and time costs associated of commuting to the continental shelf-break/basin, and/or chick provisioning requirements confined day-time foraging trips. Certainly, previous studies have shown that Pribilof murrens sometimes forage on the shelf in frontal areas associated with tidal currents and bottom topography (Decker and Hunt, 1996; Kokubun et al., 2008), with foraging efforts often focused below the thermocline in stratified water (Kokubun et al., 2008; Takahashi et al., 2008).

Interestingly, when experiencing similar levels of food limitation, St. Paul and St. George birds employed different behavioral strategies. St. George birds traveled longer distances to forage at the continental shelf-break and in the basin at night, but these flight costs were presumably balanced by the benefits of feeding on higher density prey aggregations, and/or more lipid rich prey (squid) than birds on St. Paul (Pollock; Van Pelt et al., 1997). The energy value of squid has been shown to vary among species, and even be similar to pollock (Logerwell and Schaufler, 2005). However, a recent study has shown that squid in the Southeastern Bering Sea have higher energy value than the Gulf of Alaska (Van Pelt et al., 1997; Whitman, 2010), with squid caught on these surveys having higher total energy value per individual (19.26 kJ) than northern lampfish (11.37 kJ; Heppel and Benoit-Bird unpubl. Data).

Although St. George and St. Paul are situated close to each other, the two Pribilof Islands have different habitat availability

(Schneider and Hunt, 1984). The closer proximity of St. George to the continental shelf-break may buffer birds from changes in food availability on the shelf, whereas birds on St. Paul may be more vulnerable to climate effects on food resources in the shelf regions (Byrd et al., 2008a, 2008b). There is accumulating evidence for changes in biological communities associated with ecosystem shifts in the Bering Sea (Grebmeier et al., 2006), and it has been suggested that the prolonged regimes observed during the last decades may be detrimental to populations of seabirds and northern fur seals (*Callorhinus ursinus*) breeding at the Pribilof Islands (Stabeno et al., 2012). Piscivorous birds on the Pribilofs have been shown to experience greater food limitation during cold years (Kitaysky, Unpubl. data; Benowitz-Fredericks et al., 2008; this study; Satterthwaite et al., 2012), and a recent analysis of the relationship between environmental variables, productivity and CORT levels of seabirds suggests a potential decline of both Pribilof colonies if current cold conditions persist in the North Pacific (Satterthwaite et al., 2012). Although there were relatively cold conditions for the Bering Sea in 2009 (Stabeno et al., 2012) and murrens breeding on both Pribilof Islands were more food-limited (higher CORT and lower co-attendance compared to Bogoslof), St. Paul birds were able to attain a similar level of energy balance as birds on St. George. However, this might not always be the case, for example if foraging conditions on the shelf deteriorate further, the additional distance to the productive continental shelf-break may be cost-prohibitive for murrens to reproduce successfully on St. Paul Island. Conditions on St. Paul have certainly been shown to be poorer than St. George at least in some years, with higher CORT levels (Benowitz-Fredericks et al., 2008) and lower chick-feeding rates (Kitaysky et al., 2000).

Interestingly, there was very little difference in the distance of foraging trips conducted during the day among the three colonies, with birds feeding on average ca 5 km from a colony. Birds at all three colonies traveled further distances at night, and this pattern was most pronounced on St. George. Many species of seabird alternate short foraging trips (which maximize food delivery to their offspring) with longer self-feeding foraging trips (to replenish their own energy reserves; Chaurand and Weimerskirch, 1994; Weimerskirch et al., 1994). In murrens, the distance of trips conducted during the day might be limited by the need to provision the chick a total of 3–4 meals day⁻¹ during daylight hours and the necessity for one parent to brood the chick continuously. In this study, we observed a large diurnal/nocturnal difference in foraging range, with birds at all three colonies conducting longer trips at night. Although there is some evidence that murrens conduct both long and short trips under certain environmental conditions (Benvenuti et al., 1998; Watanuki et al., 2001), further study is required to examine differences between day and night trip distances and the variability in night behavior under different environmental conditions and among colonies at different latitudes.

Birds at both St. George and Bogoslof conducted shallower dives at night, and the frequency of these shallow dives may even be underestimated because logger-settings prevented the recordings of depths less than 7 m (see Methods). Thick-billed murrens on St. George have previously been shown to dive to depths no deeper than 5 m during the period of darkness, with dive depths becoming deeper as the sun rose (Takahashi et al., 2008). Shallow night dives most likely reflect a greater abundance of prey in the epipelagic layer due to diel vertical migration (Katugin and Zuev, 2007; Kooyman et al., 1992), lower light conditions for pursuit hunting, or both. A recent Bering Sea study linking observations of murrens with the vertical accessibility and availability of their prey clearly shows that murrens were conducting shallower dives at night in response to the diel migration of prey (Benoit-Bird et al., 2011). Some of the day-time foraging behavior will reflect dives

for larger prey located at depth for chick provisioning (Ito et al., 2010); however, the majority of the dives conducted during the day were probably dedicated to self-feeding. Piatt et al. (2007) estimated that relatively little extra food-energy is required for murre parents to feed their chick: i.e., based on measurements of field metabolic rates (FMR; Gabrielsen, 1994) and assimilation efficiency (87%; Romano et al., 2006), murre parents need to capture about 512 g of fish (at 5.0 kJ g^{-1} wet mass), the equivalent of about 49% of their body mass. Despite this large daily food requirement for self-maintenance, raising a single chick only increases a parent murre food demands by about 8%, which might explain why we did not observe inter-colony differences in chick feeding rates.

4.2. Diet

Inter-colony differences in diet reflect the differences in foraging habitat. Our data indicated that Bogoslof birds were both self-feeding and provisioning their chick primarily on squid caught in the basin. Although squid are common mesopelagic prey in the Bering Sea that migrate to the upper 200 m at night (Sinclair et al., 1999), their predominance in both adult and chick diet on Bogoslof suggests availability at depths ≤ 100 m during daylight hours. Squids of the family Gonatidae dominate the epipelagic cephalopod assemblages in the western Bering Sea. The majority of squid found in the top 50 m of the water column are at early stages of their development, and may have a limited ability to conduct diel vertical migration (Katugin and Zuev, 2007). Squid are a significant source of prey for many seabird species (see Croxall and Prince, 1996 for a review), and more study is required on species identification, their availability in the water column, and their nutritional value to seabirds. The occurrence of euphausiids in the adult diet (but not in chick diet) on Bogoslof supports the predictions of Central Place Foraging Theory (Orians and Pearson, 1979), with parents minimizing transport costs by provisioning prey items to their offspring that are larger and energetically richer than prey they ingest themselves (e.g. Gaston and Hipfner, 2000).

Chick diet on St. Paul reflects the birds' relatively near-shore foraging behavior, with an abundance of pricklebacks and eelpouts (both benthic species), whereas St. Paul murre parents fed primarily on the (pelagic) pollock that were available on the shelf to the NW of the island in 2009 (Janelli et al., 2009). Diet at St. George was intermediate between St. Paul and Bogoslof, presumably reflecting the proximity of the island to both shelf and basin habitats. Parents were primarily foraging at night on or near the continental shelf-break, an area of high production where both squid and fish are known to concentrate and at least one important squid species (*Berryteuthis magister*) spawns (Sinclair and Stabeno, 2002; Sinclair et al., 2008). However, both the dominance of squid in parental diet and their presence in chick diet suggests that a good proportion of squid were caught on the shelf during the day. The relatively high diversity of fish delivered to chicks at St. George could reflect the high diversity of local marine habitat (Sinclair et al., 2008), lower abundance of prey in general (Schoener, 1971), or a greater ability to identify fish by observers at the colony.

A total of 99 (71%) of the 139 collected lavage samples had prey remains. The number of empty samples differed among colonies; only 4% were empty on St. Paul, while 40% were empty on St. George, and 38% on Bogoslof. Differences in numbers of empty samples either reflect variation in sampling effectiveness among field-workers (which is unlikely because all field crews received training and followed the same lavage protocol), or differential digestion rates for different prey species (Furness et al., 1984; Wilson et al., 1985), the effect of meal size on

digestion rates (Neves et al., 2006), and time of ingestion relative to water flushing (Neves et al., 2006). Certain prey species, such as euphausiids, may be underestimated with this method because hard parts of prey are relatively resistant to digestion compared to soft-bodied prey, whereas cephalopods, in particular, may be overestimated due to the persistence of beaks in the stomach (Furness et al., 1984). Although methods in our study were similar among colonies, the shorter duration of GPS deployment and distance of trips at night on St. Paul and Bogoslof may have resulted in a greater probability of recovering soft-bodied prey species than on St. George. This potential sampling bias may partly explain the higher proportion of squid in the diet of St. George adults than St. Paul, however, the difference is likely to be real because chicks on St. George were also fed more squid, and previous studies have shown that both seabirds and northern fur seals (*Callorhinus ursinus*) on St. George generally consume more squid than St. Paul (Sinclair et al., 2008). Given constraints with differential digestion time of prey, stable isotope analysis may be a more appropriate method to quantify adult diet (Barger and Kitaysky, 2012), although it would be impossible to distinguish between adult diet collected during day and night trips with this method.

4.3. Colony attendance

Murre parents have highly flexible time budgets, and have been shown to buffer chick-feeding rates and breeding success over a range of food availabilities, by allocating more time to foraging when conditions are poor (Harding et al., 2007). Our results support the flexible time budget hypothesis, with parents at both Pribilof Islands experiencing relatively poor foraging conditions, but maintaining similar chick-provisioning rates and fledging success by spending more time foraging than Bogoslof birds. However, this flexibility is not without its potential long-term costs, and high levels of CORT (Brown et al., 2005; Kitaysky et al., 2007, 2010; Romero and Wikelski, 2001), and increased parental effort (Golet et al., 1998) may be detrimental to adult survival. Although colony attendance differed among colonies by only 3 min h^{-1} , this translates to an extra 48 min in a 16 h day diverted to foraging. Harding et al. (2007) showed that provisioning rates are a non-linear function of colony attendance in the closely related common murre. In this study, chick-feeding rates plateaued at 4.3 meals $16 \text{ h}^{-1} \text{ day}$ over a wide range in the amount of time parents spent at the colony. Only when attendance dropped below 63 bird min day^{-1} —equivalent to the non-brooding parent spending less than 50 min day^{-1} at the colony—did provisioning rate diminish. These results suggest that attendance levels at the Pribilofs (63 min) may be at or near this lower threshold, and chick-feeding rates may start to decrease if foraging conditions deteriorate further.

Discretionary time spent at the colony and the relatively low CORT levels of parents on Bogoslof suggests that food in the basin may have been higher density and/or higher quality than on the shelf near the Pribilof Islands. However, although parents on Bogoslof had discretionary time available at the colony, they did not increase their provisioning rates. Perhaps there is little benefit for parents to feed offspring more than 3–4 meals day^{-1} . Murre fledgling survival may not be as closely linked to condition at colony departure as in other species because chicks leave the colony at only 15–30% adult body mass, and are fed at sea by the male parent for an extended period of time (Gaston, 1985b). Certainly, wild murre chicks have been shown to consume under their maximum limit (Harris and Wanless, 1995). Alternatively, murre parents may have limited ability to increase parental effort (Erikstad et al., 1997; Kitaysky et al., 2000; but see Paredes et al., 2005). Or, chick feeding rates may be constrained by the need for

parents to spend time at the colony, with colony attendance by both parents more important on Bogoslof because of the presence of predatory glaucous-winged gulls *Larus glaucescens* (Martindale, 1982), whereas there are almost no avian predators on the Pribilof Islands. Although more complete data are needed on fish identification and the nutritional value of squid, the higher proportion of larger prey items on Bogoslof Island suggests chicks were receiving more energy than chicks on the Pribilofs despite the similarity in provisioning rates among colonies. However, given that common murre chicks have been shown to survive on much less energy than that required for optimal growth (Benowitz-Fredericks and Kitaysky, 2005), it is not surprising that presumed differences in chick daily energy intake among colonies were not translated into measures of fledging success.

4.4. Instrument effects and performance

Although GPS locations obtained in this study were frequent enough to estimate and compare maximum foraging distances among islands, deploying GPS loggers on a small diving and flying bird proved challenging. Several loggers were pecked off or damaged during deployment, and GPS loggers stopped recording data when birds were diving. The variation in gap duration presumably reflected both differences in dive duration and the time required for GPS units to reacquire satellite reception.

There is increasing evidence that data loggers can affect the behavior of birds (e.g., Passos et al., 2010; Wilson et al., 2002). GPS units used in this study weighed between 10–14 g, and total instrumentation weight, including TDR (3.6 g), bands and tesa tape (4 g) was therefore about 20–21 g or approximately 2% of the average initial mass of GPS birds in this study (mean = 1033.86 ± 8.89 g, $n=87$). Although this mass is below the suggested threshold of 3% body mass (Philips et al., 2003), and light compared to other loggers previously used on murre (see Takahashi et al., 2008 for summary), the necessity of a back-attachment is not ideal for diving birds and will have increased the effect of drag whilst underwater (Tremblay et al., 2003). Thus, whilst it is unlikely that instrumentation had no effect, it is important to determine (a) to what extent the instruments distorted the normal behavior of the bird, and (b), whether the effect of the device varied among colonies.

Evidence of an effect of instrumentation on individual behavior is mixed. GPS birds were observed provisioning their chick, the vast majority of GPS nests successfully reared a chick, and the comparison of baseline CORT between deployment and recapture suggested negligible short-term physiological effect. However, parents at instrumented nests spent more time away from the colony, and feeding rates suggests some reduction in chick provisioning by the instrumented birds and compensatory behavior by their partners (Paredes et al., 2005). Dives conducted by birds on St. George and Bogoslof were similar to those previously recorded for the species (Hedd et al., 2009; Takahashi et al., 2008). Furthermore, although, birds at all three colonies lost mass during deployment on average, mass loss during the breeding season may be an adaptive adjustment for reducing flight costs and increasing foraging efficiency (Croll et al., 1991), and we have no measure of mass loss on control (non-tagged) birds to determine logger effect.

Evidence on whether the effect of the device varied among colonies is also unclear. The effect of instrumentation on chick-feeding rates and attendance did not differ between St. George and St. Paul, and changes in CORT during deployment were similar between the two colonies. However, overall, 10% of nests where GPS loggers were deployed failed post-deployment, but this percentage was higher on St. George (25%) than both St. Paul (4%) and Bogoslof (3%), despite the similarity in fledging success

among islands. St. George birds also lost the highest percentage of their initial body mass. Longer night foraging distances in combination with the dual instrument deployment (GPS and TDR) and lighter body mass of birds on St. George may explain why nest failure, recapture time, and loss of body mass during deployment were higher at St. George compared to those at St. Paul. While levels of abandonment in this study were not significant at a population level, more thorough tests are required to truly determine the influence of tags on the behavior of this species. Such tests could include the comparison of CORT and mass change between tagged and non-tagged birds over the same time period, and comparing the flight distance and dive behavior estimated from birds deployed with GPS units versus small time-depth recorders attached to the leg.

4.5. Conclusions

Foraging strategies of marine predators have been shown to vary both among species and populations (Lewis et al., 2001), and the comparison of foraging behavior under different environmental conditions can help disentangle the various life-history, ecological and physical constraints on foraging behavior. Our study suggests that murre may have more flexibility to adjust foraging distances at night rather than changing their behavior during the day when chicks need frequent provisioning. Further study is now needed to examine variability in day and night-time behavior over a range of environmental conditions, and determine whether monitoring night behavior would provide a better indication of local prey availability than conventionally measured day trips.

Murre exhibited remarkable plasticity in foraging strategy among breeding colonies, even between the two colonies situated within commuting distance of each other. This flexibility appears key for allowing thick-billed murre to nest successfully in a wide range of colony environments. However, this flexibility is not without its potential long-term costs on adult survival, and even a small change in adult survival of long-lived species will have a large effect on population size (Doherty et al., 2004). Our results also suggest that the relative importance of productive oceanographic features for foraging seabirds varies according to the location of the colony and general productivity of the local area. Foraging theory predicts that individuals should travel the minimum distance to meet energy requirements (Schoener, 1971), and Bogoslof birds were able to maintain a high energy balance by foraging entirely in the deep oceanic waters surrounding the colony. Further work is needed to assess whether productivity in basin waters surrounding Bogoslof is influenced by passes in the Aleutian Chain that promote high productivity through powerful tidal mixing and the upwelling of nutrients (Mordy et al., 2005). Although colony proximity to important oceanographic features did not totally explain inter-colony differences in food limitation in 2009, the closer proximity of St. George to the continental shelf-break and access to higher energy basin-based prey may be an important buffer in years when food supply on the shelf is poor (Byrd et al., 2008b).

Acknowledgment

This publication number is NPRB #377 BEST-BSIERP Bering Sea Project #76. We are indebted to B. Battaile, D. Cushing, B. Drummond, T. Harten, D. Kildaw, R. Marshall, R. Massengale, R. Papish, T. Vergoz, J. Warzybok, A. Will, and S. Youngren for their dedication and skill in the field, A. Will and B. Battaile for designing the observation data-base, R. and J. Irons for assistance with pressure testing the GPS casing, E. Kitaiskaia for conducting

hormonal analysis, and K. Turco for her invaluable expertise and patience with the lavage analysis. Many thanks to G. Dell’Omo (Technosmart) and Mike Vandertillaart (Lotek) for their technical support throughout the season. We thank K. Holser (St. George Island Institute), P. Wohl and A. Purcella (Northern Forum), P. Zavadil and D. Lestenkof (Aleut Community of St. Paul Island), S. Mercuri (Tribal Council St. George Island), K. Brennehan, J. Reed, L. Spitler, J. Williams, and the crews of the *MV Tiglax* and Miss Alyssa for crucial logistical and financial support. We are grateful to stimulating discussions with other members of the BSIERP projects led by A. Trites, S. Hepell, K. Benoit-Bird, and K. Kuletz. All procedures have been approved by the Institutional Animal Care and Use Committee, University of Alaska, Fairbanks, and conducted under IACUC permit #2009008. This study was funded by NPRB, BSIERP Project B63 and B77 to D.B. Irons, D.D. Roby, and A.S. Kitaysky, and Project B65 to H.M. Renner and G.V. Byrd.

References

- Barger, C.P., Kitaysky, A.S., 2012. Isotopic segregation between sympatric seabird species increases with nutritional stress. *Biol. Lett.* 8, 442–445.
- Benoit-Bird, K.J., Kathy, K., Hepell, S., Jones, N., Hoover, B., 2011. Active acoustic examination of the diving behavior of murre foraging on patchy prey. *Mar. Ecol. Prog. Ser.* 443, 217–235.
- Benowitz-Fredericks, Z.M., Kitaysky, A.S., 2005. Benefits and costs of rapid growth in common murre chicks *Uria aalge*. *J. Avian Biol.* 36, 287–294.
- Benowitz-Fredericks, Z.M., Shultz, M.T., Kitaysky, A.S., 2008. Stress hormones suggest opposite trends of food availability for planktivorous and piscivorous seabirds in two years. *Deep-Sea Res. II* 55, 1868–1876.
- Benvenuti, S., Bonadonna, F., Dall’Antonia, L., Gudmundsson, G., 1998. Foraging flights of breeding thick-billed murre (*Uria lomvia*) as revealed by bird-born direction recorders. *Auk* 115, 57–66.
- Birkhead, T.R., Nettleship, D.N., 1981. Reproductive biology of thick-billed murre (*Uria lomvia*): an inter-colony comparison. *Auk* 98 (2), 258–269.
- Birkhead, T.R., Nettleship, D.N., 1987. Ecological relationships between common murre, *Uria aalge*, and thick-billed murre, *Uria lomvia*, at the Gannet Islands, Labrador. III. Feeding ecology of the young. *Can. J. Zool.* 65, 1630–1637.
- Brown, C.R., Brown, M.B., Raouf, S.A., Smith, L.C., Wingfield, J.C., 2005. Effects of endogenous steroid hormone levels on annual survival in cliff swallows. *Ecology* 86, 1034–1046.
- Byrd, G.V., Schmutz, J.A., Renner, H.M., 2008a. Contrasting population trends of piscivorous seabirds in the Pribilof Islands: A 30-year perspective. *Deep-Sea Res. II* 55, 1846–1855.
- Byrd, G.V., Sydeman, W.J., Renner, H.M., Minobe, S., 2008b. Responses of piscivorous seabirds at the Pribilof Islands to ocean climate. *Deep Sea Res. II* 55, 1856–1867.
- Chaurand, T., Weimerskirch, H., 1994. The regular alternation of short and long foraging trips in the blue petrel *Halobaena caerulea*: a previously undescribed strategy of food provisioning in a pelagic seabird. *J. Anim. Ecol.* 63, 275–282.
- Clarke, E.D., Spear, L.B., McCracken, M.L., Marques, F.F.C., Corchers, D.L., Buckland, S.T., Ainley, D.G., 2003. Validating the use of generalized additive models and at-sea surveys to estimate size and temporal trends in seabird populations. *J. Appl. Ecol.* 40, 278–292.
- Coachman, L.K., Walsh, J.J., 1981. A diffusion model of cross-shelf exchange of nutrients in the Southeastern Bering Sea. *Deep Sea Res.* 28, 819–846.
- Croll, D.A., Gaston, A.J., Noble, D.G., 1991. Adaptive loss of mass in thick-billed murre. *Condor* 93, 496–502.
- Croxall, J.P., Prince, P.A., 1996. Cephalopods as prey. 1. Seabirds. *Philos. Trans. R. Soc. B* 351, 1023–1043.
- Davoren, G.H., Burger, A.E., 1999. Differences in prey selection and behavior during self-feeding and chick provisioning in rhinoceros auklets. *Anim. Behav.* 58, 853–863.
- Davoren, G.K., Montevecchi, W.A., 2003. Consequences of foraging trip duration on provisioning behavior and fledging condition of common murre *Uria aalge*. *J. Avian Biol.* 34, 44–53.
- Davoren, G.K., Montevecchi, W.A., Anderson, J.T., 2003. Distributional patterns of a marine bird and its prey: habitat selection based on prey and conspecific behavior. *Mar. Ecol. Prog. Ser.* 256, 229–242.
- Decker, M.B., Hunt Jr., G.L., 1996. Foraging by murre (*Uria* spp.) at tidal fronts surrounding the Pribilof Islands, Alaska, USA. *Mar. Ecol. Prog. Ser.* 139, 1–10.
- Doherty, P.F., Schreiber, E.A., Nichols, J.D., Hines, J.E., Link, W.A., Schenck, G.A., Schreiber, R.W., 2004. Testing life history prediction in a long-lived seabird: a population matrix approach with improved parameter estimation. *Oikos* 105, 606–618.
- Dorresteyn, I., Kitaysky, A.S., Barger, C., Benowitz-Fredericks, Z.M., Byrd, G.V., Shultz, M., Young, R., 2012. Climate affects food availability to planktivorous least auklets *Aethia pusilla* through physical processes in the southeastern Bering Sea. *Mar. Ecol. Prog. Ser.* 454, 207–220.
- Emlen, J.M., 1966. The role of time and energy in food preference. *Am. Naturalist* 100, 611–617.
- Erikstad, K.E., Asheim, M., Fauchald, P., Dahlhaug, L., Tveraa, T., 1997. Adjustment of parental effort in the puffin; the roles of adult body condition and chick size. *Behav. Ecol. Sociobiol.* 40, 95–100.
- Fauchald, P., Erikstad, K.E., 2002. Scale-dependent predator-prey interactions: the aggregative response of seabirds to prey under variable prey abundance and patchiness. *Mar. Ecol. Prog. Ser.* 231, 279–291.
- Forero, M.G., Hobson, K.A., Bortolotti, G.R., Donazar, J.A., Bertellotti, M., Blanco, G., 2002. Food resource utilization by the Magellanic penguin evaluated through stable-isotope analysis: segregation by sex and age and influence on offspring quality. *Mar. Ecol. Prog. Ser.* 234, 289–299.
- Furness, B.L., Laugsch, R.C., Duffy, D.C., 1984. Cephalopod beaks and studies of seabird diets. *Auk* 101, 619–620.
- Gabrielsen, G.W., 1994. Energy Expenditure in Arctic Seabirds. Ph.D. Thesis. University of Tromsø, Norway.
- Gaston, A.J., 1985a. Energy invested in reproduction by thick-billed murre (*Uria lomvia*). *Auk* 102, 447–458.
- Gaston, A.J., 1985b. Development of the young in the Atlantic Alcidae. In: Nettleship, T.R., Birkhead, T.R. (Eds.), *The Atlantic Alcidae*. Academic Press, Toronto, pp. 319–354.
- Gaston, A.J., Jones, I.L., 1998. *The Auks*. Oxford University Press, Oxford.
- Gaston, A.J., Hipfner, J.M., 2000. Thick-billed Murre (*Uria lomvia*). In: Poole, A. (Ed.), *The Birds of North America Online*. Cornell Lab of Ornithology, Ithaca.
- Golet, G.H., Irons, D.B., Estes, J.A., 1998. Survival costs of chick-rearing in black-legged kittiwakes. *J. Anim. Ecol.* 67, 827–841.
- Grebmeier, J.M., Overland, J.E., Moore, S.E., Farley, E.V., Carmack, E.C., Cooper, L.W., Frey, K.E., Helle, J.H., McLaughlin, F.A., McNutt, S.L., 2006. A major ecosystem shift in the Northern Bering Sea. *Science* 311, 1461–1464.
- Hollowed, A.B., Barbeaux, S.J., Cokelet, E.D., Farley, A., Kotwicki, S., Ressler, P.H., Spital, C., Wilson, C.D., 2012. Effects of climate variations on pelagic ocean habitats and their role in structuring forage fish distributions in the Bering Sea. *Deep Sea Res. II* 65–70, 230–250.
- Hamer, K.C., Humphreys, E.M., Magalhães, M.C., Garthe, S., Hennicke, J., Peters, G., Grémillet, D., Skov, H., Wanless, S., 2009. Fine-scale foraging behavior of a medium-ranging marine predator. *J. Anim. Ecol.* 78, 880–889.
- Harding, A.M.A., Piatt, J.F., Schmutz, J.A., Kettle, A.B., Shultz, M., Van Pelt, T.I., Kettle, A.B., Speckman, S.G., 2007. Prey density and the behavioural flexibility of a marine predator: the common murre (*Uria aalge*). *Ecology* 88 (8), 2024–2035.
- Hare, S.R., Mantua, N.J., 2000. Empirical evidence for North Pacific regime shifts in 1977 and 1989. *Prog. Oceanogr.* 47, 103–1445.
- Harris, M.P., Wanless, S., 1995. The food consumption of young common murre (*Uria aalge*) in the Wild. Colonial Waterbirds 18, 209–213.
- Harris, M.P., Wanless, S., 1988. The breeding biology of Guillemots *Uria aalge* on the Isle of May over a six year period. *Ibis* 130, 172–192.
- Hedd, A., Regular, P.M., Montevecchi, W.A., Buren, A.D., Burke, C.M., Fifield, D.A., 2009. Going deep: common murre dive into frigid water for aggregated, persistent and slow-moving capelin. *Mar. Biol.* 156, 741–751.
- Hogan, G.G., 1985. Noosing adult cormorants for banding. *N. Am. Bird Bander* 10, 76–77.
- Houston, A.I., 2002. Prey size of single-prey loaders as an indicator of prey abundance. *Ecol. Lett.* 3 (1), 5–6.
- Houston, A.I., McNamara, J.M., 1985. A general theory of central-place foraging for single-prey loaders. *Theor. Popul. Biol.* 28, 233–262.
- Houston, A.I., Thompson, W.A., Gaston, A.J., 1996. The use of a time and energy budget model of a parent bird to investigate limits to fledging mass in the thick-billed murre. *Funct. Ecol.* 10, 432–439.
- Ito, M., Takahashi, A., Kokubun, N., Kitaysky, A.S., Watanuki, Y., 2010. Foraging behavior of incubating and chick-rearing thick-billed murre *Uria lomvia*. *Aquat. Biol.* 8, 279–287.
- Iverson, S.J., Springer, A.M., Kitaysky, A.S., 2007. Seabirds as indicators of food web structure and ecosystem variability: qualitative and quantitative analysis using fatty acids. *Mar. Ecol. Prog. Ser.* 352, 235–244.
- Janelli, J.N., Barbeaux, S., Honkalehto, T., Kotwicki, S., Aydin, K., and Williamson, N., 2009. Chapter 1 & 1B. Assessment of walleye Pollock in the Eastern Bering Sea and Bogoslof Region. In: *Stock Assessment and Fishery Evaluation Report for the Groundfish Resources of the Bering Sea/Aleutian Islands Regions*. North Pacific Fishery Management Council, Anchorage, AK, p. 47–234.
- Kacelnik, A., Cuthill, I., 1990. Central place foraging in starlings (*Sturnus vulgaris*). II. Food allocation to chicks. *J. Anim. Ecol.* 59, 655–674.
- Katugin, O.N., Zuev, N.N., 2007. Distribution of cephalopods in the upper epipelagic northwestern Bering Sea in autumn. *Rev. Fish Biol. Fish.* 17, 283–294.
- Kitaysky, A.S., Piatt, J.F., Wingfield, J.C., Romano, M., 1999a. The adrenocortical stress-response of black-legged kittiwake chicks in relation to dietary restrictions. *J. Comp. Physiol. B* 169, 303–310.
- Kitaysky, A.S., Wingfield, J.C., Piatt, J.F., 1999b. Dynamics of food availability, body condition and physiological stress response in breeding Black-legged Kittiwakes. *Funct. Ecol.* 13, 577–584.
- Kitaysky, A.S., Hunt, G.L., Flint, E.N., Rubega, M.A., Decker, M.B., 2000. Resource allocation in breeding seabirds: responses to fluctuations in their food supply. *Mar. Ecol. Prog. Ser.* 283, 283–296.
- Kitaysky, A.S., Piatt, J.F., Wingfield, J.C., 2007. Stress hormones link food availability and population processes in seabirds. *Mar. Ecol. Prog. Ser.* 352, 245–258.
- Kitaysky, A.S., Piatt, J.F., Hatch, S.A., Kitaiskaia, E.V., Benowitz-Fredericks, Z.M., Shultz, M.T., Wingfield, J.C., 2010. Food availability and population processes: severity of nutritional stress during reproduction predicts survival of long-lived seabirds. *Funct. Ecol.* 24, 625–637.

- Kokubun, N., Iida, K., Mukai, T., 2008. Distribution of murre (*Uria* spp.) and their prey south of St. George Island in the southeastern Bering Sea during the summers of 2003–2005. *Deep-Sea Res. II* 55, 1827–1836.
- Kooyman, G.L., Cherel, Y., Le Mayo, Y., Croxall, J.P., Thorson, P.H., Ridoux, V., Kooymann, C.A., 1992. Diving behavior and energetics during foraging cycles in king penguins. *Ecol. Monogr.* 62, 143–163.
- Kotliar, N.B., Wiens, J.A., 1990. Multiple scales of patchiness and patch structure: a hierarchical framework for the study of heterogeneity. *Oikos* 59, 243–260.
- Ladd, C., Jahncke, J., Hunt Jr., G.L., Coyle, K.O., Stabeno, P.J., 2005. Hydrographic features and seabird foraging in Aleutian Passes. *Fish Oceanogr.* 14 (Suppl. 1), 178–195.
- Lance, B.K., Roby, D.D., 2000. Diet and postnatal growth in red-legged and black-legged kittiwakes: an interspecies cross-fostering experiment. *Auk* 117, 1016–1028.
- Le Boeuf, B.J., Crocker, D.E., Costa, D.P., Blackwell, S.B., Webb, P.M., Houser, D.S., 2000. Foraging ecology of northern elephant seals. *Ecol. Monogr.* 70, 353–382.
- Lewis, S., Sherratt, T.N., Hamer, K.C., Wanless, S., 2001. Evidence of intra-specific competition for food in a pelagic seabird. *Nature* 412, 816–819.
- Litzow, M.A., Bailey, K.M., Prael, F.G., Heintz, R., 2006. Climate regime shifts and reorganization of fish communities: the essential fatty acid limitation hypothesis. *Mar. Ecol. Prog. Ser.* 315, 1–11.
- Logerwell, E.A., Schaufler, L.E., 2005. New data on proximate composition and energy density of Steller sea lion (*Eumetopias jubatus*) prey fills seasonal and geographic gaps in existing information. *Aquat. Mammals* 31, 62–82.
- Mackas, D.L., Tsurumi, M., Galbraith, M.D., Yelland, D.R., 2005. Zooplankton distribution and dynamics in a North Pacific Eddy of coastal origin: II. Mechanisms of eddy colonization by and retention of offshore species. *Deep-Sea Res. II* 52, 1011–1035.
- Maravelias, C.D., Reid, D.G., Simmonds, E.J., Haralabous, J., 1996. Spatial analysis and mapping of acoustic survey data in the presence of high local variability: geostatistical application to North Sea herring (*Clupea harengus*). *Can. J. Fish. Aquat. Sci.* 53, 1497–1505.
- Martindale, S., 1982. Nest defense and central place foraging: a model and experiment. *Behav. Ecol. Sociobiol.* 10, 85–89.
- McArthur, R.H., Pianka, E.R., 1966. Optimal use of a patchy environment. *Am. Naturalist* 100, 603–609.
- McConnell, B.J., Chambers, C., Fedak, M.A., 1992. Foraging ecology of southern elephant seals in relation to the bathymetry and productivity of the Southern Ocean. *Antarct. Sci.* 4, 393–398.
- Moku, M., Kawaguchi, K., Watanabe, H., Ohno, A., 2000. Feeding habits of three dominant myctophid fishes, *Diaphus theta*, *Stenobrachius leucopsarus* and *S. nannochir*, in the subarctic and transitional waters of the western North Pacific. *Mar. Ecol. Prog. Ser.* 207, 129–140.
- Mordy, C.W., Stabeno, P.J., Ladd, C., Zeeman, S., Wisegarver, D.P., Salo, S.A., Hunt Jr., G.L., 2005. Nutrients and primary production along the eastern Aleutian Island Archipelago. *Fish. Oceanogr.* 14, 55–76.
- Neves, V.C., Bolton, M., Monteiro, L.R., 2006. Validation of the water offloading technique for diet assessment: an experimental study with Cory's shearwaters (*Calonectris diomedea*). *J. Ornithol.* 147, 474–478.
- Orians, G.H., Pearson, N.E., 1979. On the theory of central place foraging. In: Horn, D.J., Mitchell, R.D., Stairs, G.R. (Eds.), *Analysis of Ecological Systems*. Ohio State University Press, Columbus, Ohio, USA, pp. 154–177.
- Paredes, R., Jones, I.L., Boness, D.J., 2005. Reduced parental care, compensatory behavior and reproductive costs experienced by female and male thick-billed murre equipped with data loggers. *Anim. Behav.* 69, 197–208.
- Passos, C., Navarro, J., Giudici, A., González-Solis, J., 2010. Effects of extra mass on the pelagic behavior of a seabird. *Auk* 127, 100–107.
- Pennycook, C.J., 1987. Flight of auks (alcidae) and other northern seabirds compared with southern procellariiformes: Ornithodolite observations. *J. Exp. Biol.* 128, 335–347.
- Philips, R.A., Xavier, J.C., Croxall, J.P., 2003. Effects of satellite transmitters on albatross and petrels. *Auk* 120, 1082–1090.
- Piatt, J.F., Springer, A.M., 2003. Advection, Pelagic Food webs and the biogeography of seabirds in Beringia. *Mar. Ornithol.* 31, 141–154.
- Piatt, J.F., Harding, A.M.A., Shultz, M., Speckman, S.G., Van Pelt, T.I., Drew, G.S., Kettle, A.B., 2007. Seabirds as indicators of marine food supplies: cairns revisited. *Mar. Ecol. Prog. Ser.* 352, 221–234.
- Polovina, J.J., Howell, E., Kobayashi, D.R., Seki, M.P., 2001. The transition zone chlorophyll front, a dynamic global feature defining migration and forage habitat for marine resources. *Prog. Oceanogr.* 49, 469–483.
- Radchenko, V.I., 1992. The role of squids in the pelagic ecosystem of the Bering Sea. *Oceanology* 32, 1093–1101.
- Raouf, S.A., Smith, L.C., Brown, M.B., Wingfield, J.C., Brown, C.R., 2006. Glucocorticoid hormone levels increase with growth size and parasite load in cliff swallows. *Anim. Behav.* 71, 39–48.
- Renner, H.M., Mueter, F., Drummond, B.A., Warzybok, J.A., Sinclair, E.H., 2012. Patterns of change in diets of two piscivorous seabird species during 35 years in the Pribilof Islands. *Deep-Sea Res. II* 65–70, 273–291.
- Romano, M.D., Piatt, J.F., Roby, D.D., 2006. Testing the junk-food hypothesis on marine birds: effects of prey type on growth and development. *Waterbirds* 29, 407–516.
- Romero, L.M., Wikelski, M., 2001. Corticosterone levels predict survival probabilities of Galapagos marine aguanas during El Niño events. *Proc. Natl. Acad. Sci.* 98, 7366–7370.
- Romero, L.M., Reed, M.J., Wingfield, J.C., 2000. Effects of weather on corticosterone responses in wild free-living passerine birds. *Gen. Comp. Endocrinol.* 118, 113–122.
- Ryan, P.G., Petersen, S.L., Peters, G., Grémillet, D., 2004. GPS tracking a marine predator: the effects of precision, resolution and sampling rate on foraging tracks on African Penguins. *Mar. Biol.* 145 (2), 215–223.
- Russell, R.W., Hunt, G.L., Coyle, K.O., Cooney, R.T., 1992. Foraging in a fractal environment: spatial patterns in a marine predator-prey system. *Landscape Ecol.* 7, 195–209.
- Satterthwaite, W.H., Kitaysky, A.S., Hatch, S.A., Piatt, J.F., Mangel, M., 2010. Unifying quantitative life history theory and field endocrinology to assess prudent parenthood in a long-lived seabird. *Evol. Ecol. Res.* 12, 779–792.
- Satterthwaite, W.H., Kitaysky, A.S., Mangel, M., 2012. Linking climate variability, productivity and stress to demography in a long-lived seabird. *Mar. Ecol. Prog. Ser.* 454, 221–235.
- Schneider, D.C., 1982. Fronts and seabird aggregations in the southeastern Bering Sea. *Mar. Ecol. Prog. Ser.* 10, 101–103.
- Schneider, D.C., Hunt, G.L., 1984. A comparison of seabird diets and foraging distribution around the Pribilof Islands, Alaska. In: Nettleship, D.N., Sanger, G.A., Springer, P.F. (Eds.), *Marine Birds: Their Feeding Ecology and Commercial Fisheries Relationships*. Special Publication, Canadian Wildlife Service, Ottawa, pp. 86–95.
- Schoener, T.W., 1971. Theory of feeding strategies. *Annu. Rev. Ecol. Syst.* 2, 369–404.
- Schultner, J., Kitaysky, A.S., Welcker, W., 2013. Fat or lean: adjustment of endogenous energy stores to predictable and unpredictable changes in allostatic load. *Funct. Ecol.* 27, 45–55.
- Schumacher, J.D., Reed, R.K., 1992. Characteristics of currents over the continental slope of the eastern Bering Sea. *J. Phys. Oceanogr.* 97, 9423–9433.
- Sinclair, E.H., Balanov, A.A., Kubodera, T., Radchenko, V.I., Fedorets, Y.A., 1999. Distribution and ecology of mesopelagic fishes and cephalopods. In: Loughlin, T.R., Ohtani, K. (Eds.), *Dynamics of the Bering Sea*. University of Alaska Sea Grant, Fairbanks, Alaska, pp. 485–508 99775–5040.
- Sinclair, E.H., Stabeno, P.J., 2002. Mesopelagic nekton and associated physics of the southeastern Bering Sea. *Deep-Sea Res. II* 49, 6127–6145.
- Sinclair, E.H., Vlietstra, L.S., Johnson, D.S., Zeppelin, T.K., Byrd, G.V., Springer, A.M., Ream, R.R., Hunt, G.L., 2008. Patterns in prey use among fur seals and seabirds in the Pribilof Islands. *Deep-Sea Res. II* 55, 1897–1918.
- Skov, H., Humphreys, E., Garthe, S., Geitner, K., Hamer, K., Hennicke, J., Parner, H., Grémillet, D., Wanless, S., 2008. Application of habitat suitability modelling to tracking data of marine animals as a means of analyzing their feeding habitats. *Ecol. Model.* 212, 504–512.
- Springer, A.M., McRoy, C.P., 1993. The paradox of pelagic food webs in the northern Bering Sea-III. Patterns of primary production. *Cont. Shelf Res.* 13, 575–599.
- Springer, A.M., McRoy, C.P., Flint, M.V., 1996. The Bering Sea Green Belt: shelf-edge processes and ecosystem production. *Fish. Oceanogr.* 5, 205–223.
- Stabeno, P.J., Kachel, N.B., Moore, S.E., Napp, J.M., Sigler, M., Yamaguchi, A., Zerbini, A.N., 2012. Comparison of warm and cold years on the southeastern Bering Sea shelf and some implications for the ecosystem. *Deep-Sea Res. II* 65–70, 31–45.
- Takahashi, A., Matsumoto, K., Hunt, G.L., Shultz, M.T., Kitaysky, A.S., Sato, K., Iida, K., Watanuki, Y., 2008. Thick-billed murre use different diving behaviors in mixed and stratified waters. *Deep-Sea Res. II* 55, 1837–1845.
- Trathan, P.N., Murphy, E.J., Croxall, J.P., Everson, I., 1998. Use of at-sea distribution data to derive potential foraging ranges of macaroni penguins during the breeding season. *Mar. Ecol. Prog. Ser.* 169, 262–275.
- Tremblay, Y., Cherel, Y., Oremus, M., Tveraa, T., Chastel, O., 2003. Unconventional ventral attachment of time-depth recorders as a new method for investigating time budget and diving behavior of seabirds. *J. Exp. Biol.* 206, 1929–1940.
- Van Pelt, T.I., Piatt, J.F., Lance, B.K., Roby, D.D., 1997. Proximate composition and energy density of some North Pacific forage fishes. *Comp. Biochem. Physiol. A* 118, 1393–1398.
- Visser, A., Jonasdottir, S., 1999. Lipids, buoyancy and the seasonal vertical migration of Calanus finmarchicus. *Fish. Oceanogr.* 8, 100–106.
- Watanuki, Y., Mehlum, F., Takahashi, A., 2001. Water temperature sampling by foraging Brünnich's guillemots with bird-borne data loggers. *J. Avian Biol.* 32, 189–193.
- Weimerskirch, H., 2007. Are seabirds foraging for unpredictable resources? *Deep-Sea Res. II* 54, 211–223.
- Weimerskirch, H., Chastel, O., Ackermann, L., Chaurand, T., Cuenot-Chaillet, F., Hindermeier, X., Judas, J., 1994. Alternate long and short foraging trips in pelagic seabird parents. *Anim. Behav.* 47, 372–476.
- Welcker, J., Harding, A.M.A., Kitaysky, A.S., Speakman, J.R., Gabrielsen, G.W., 2009. Daily energy expenditure increases in response to low nutritional stress in an Arctic-breeding seabird with no effect of mortality. *Funct. Ecol.* 107, 1–97.
- Whitman, L.D., 2010. Variation in the Density of Forage Fishes and Invertebrates from the Southeastern Bering Sea. M.Sc. Thesis. University of Oregon. USA.
- Wilson, R.P., 1984. An improved stomach pump for penguins and other seabirds. *J. Field Ornithol.* 55 (1), 109–112.
- Wilson, R.P., La Cok, G.D., Wilson, M.P., Mollagee, F., 1985. Differential digestion of fish and squid in jackass penguins *Spheniscus demersus*. *Ornis Scand.* 16, 77–79.

- Wilson, R.P., Grémillet, D., Syder, J., Kierspel, M.A.M., Garthe, S., Weimerskirch, H., Schäfer-Neth, C., Scolaro, J.A., Bost, C.-A., Plötz, J., Nel, D., 2002. Remote-sensing systems and seabirds; their use, abuse and potential for measuring marine environmental variables. *Mar. Ecol. Prog. Ser.* 228, 241–261.
- Wilson, R.P., Scolaro, J.A., Grémillet, D., Kierspel, M.A.M., Laurenti, S., Upton, J., Gallelli, H., Quintana, F., Frere, E., Müller, G., Straten, M.T., Zimmer, I., 2005. How do magallanic penguins cope with variability in their access to prey? *Ecol. Monogr.* 75, 379–401.
- Wingfield, J.C., Maney, D.L., Breuner, C.W., Jacobs, J.D., Lynn, S., Ramenofsky, M., Richardson, R.D., 1998. Ecological basis of hormone-behavior interactions: the “Emergency Life History Stage”. *Am. Zool.* 38, 191–206.



Contents lists available at ScienceDirect

Deep-Sea Research II

journal homepage: www.elsevier.com/locate/dsr2

Linking food availability, body growth and survival in the black-legged kittiwake *Rissa tridactyla*



Simone Vincenzi^{a,b,*}, Marc Mangel^{b,c}

^a MRAG Americas, POB 1410, Capitola, CA 95010, USA

^b Center for Stock Assessment Research and Department of Applied Mathematics and Statistics, University of California, Santa Cruz, CA 95064, USA

^c Department of Biology, University of Bergen, P.O. Box 7803, 5020 Bergen, Norway

ARTICLE INFO

Available online 14 March 2013

Keywords:

Black-legged kittiwake *Rissa tridactyla*

Patch dynamics

Nestling growth

Fledging age

ABSTRACT

Population dynamics of black-legged kittiwakes *Rissa tridactyla* in Bering Sea colonies are likely to increasingly experience climate-induced changes in the physical environment. Since adult kittiwakes are central place foragers with high energy requirements, increased variability of forage patch dynamics, as predicted for polar regions, may influence both quantity and quality of food available and consequently alter the population dynamics of kittiwake colonies. Here, we describe, conceptualize, and model the effects of environment and energy resources on kittiwake growth, fledging age (from 35 to 50 days) and survival from hatching up to first breeding (post-hatching productivity). For our life-history model, we use a von Bertalanffy growth function for body growth in mass. We model nestling mortality as a function of somatic growth, in order to account for oxidative damage and trade-offs in the allocation of resources, and energy available, since low food availability increases the risk of chicks' starvation and predation risk. In the case of a good environment (i.e., high food availability), the best strategy (i.e., highest post-hatching productivity) is to grow fast (about 18.6 g d⁻¹) and to spend a moderately long time in the nest (up to 45 days), while in the case of a poor environment the best strategy is to grow fast (about 18 g d⁻¹) and leave the nest soon (35–40 days). Different ages at first breeding do not change the optimal strategies. We discuss the implications of optimal growth strategy in terms of evolution of life histories in kittiwakes and how our work, coupled with models of post-breeding survival and reproductive dynamics, could lead to the development of a full life-history model and the exploration of future evolutionary trajectories for traits like body growth and age at first breeding.

© 2013 Elsevier Ltd. All rights reserved.

1. Introduction

Understanding and predicting the temporal and spatial dynamics of populations is a fundamental issue in ecology. In the Bering Sea, populations of seabirds (the black-legged kittiwake *Rissa tridactyla* and the thick-billed murre *Uria lomvia*) are either declining (St. Paul) or are stable (St. George) on the Pribilof Islands and are increasing at Bogoslof Island (Byrd et al., 2008). The three islands have peculiar environmental conditions: St. Paul is a shelf colony that is closest to the maximum edge of the winter ice; St. George is located near the shelf edge, and Bogoslof is an oceanic colony. One of the hypotheses concerning these differences is that the population dynamics of seabirds in these colonies are affected by climate-induced changes in the physical environment, which controls forage patch dynamics (i.e., spatial or temporal heterogeneity of food availability) and thus may alter both quantity and

quality of food for seabirds (Ciannelli et al., 2005; Byrd et al., 2008; Coyle et al., 2011). However, how individual and population dynamics of seabirds will change in response to climate change is still unclear.

Models building from the effects of the behavior of individuals on their survival, growth and reproductive success, to the outcomes emerging at the population level, have already shown particular promise in explain observed temporal patterns of population dynamics and predicting consequences of alteration of climate, and habitat and food availability (Hollowed et al., 2009; Jenouvrier et al., 2009; Barbraud et al., 2011; Wolf et al., 2010; Jenouvrier and Visser, 2011; Jenouvrier et al., 2012; Satterthwaite et al., 2012).

Recently, different studies have investigated the post-fledging survival and reproductive behavior of seabirds using long-term datasets and novel statistical methods (e.g., Steiner et al., 2010; Aubry et al., 2011; Desprez et al., 2011). However, less attention has been given to the nestling phase and its carry-over effects to the subsequent life stages. It is well known that early environmental influences are more likely to lead to irreversible or at least less reversible modification of phenotypes (e.g., West-Eberhard, 2003).

* Correspondence to: Center for Stock Assessment Research, National Marine Fisheries Service, 110 Shaffer Road, Santa Cruz, CA 95060, USA

E-mail address: simon.vincenzi@gmail.com (S. Vincenzi).

Harsh environmental conditions can have important consequences for survival and life-history traits of seabirds, and this may depend on the life-stages at which the individuals are exposed to them (Starck and Ricklefs, 1998 ch. 14). In particular, when sub-optimal or harsh conditions are experienced during the developmental stage, they may not only have immediate effects on the organism, but can have long-lasting consequences (Metcalf and Monaghan, 2001). In seabirds, based on both observations and experiments, this corresponds to the time before fledging (e.g., Cam and Aubry, 2011; Coulson, 2011). Cam and Aubry (2011) provided a critical analysis on whether there is evidence of long-term fitness consequences of early conditions in long-lived birds and they concluded that whether early conditions have long-term fitness consequences is still ambiguous.

In seabirds, although heavier fledglings may be more likely to survive, growth in mass (we will use mass and weight interchangeably in this work) is only one component of nestling development that might affect juvenile survival. For example, in addition to being more likely to survive to recruitment, larger and better-developed seabird fledglings might be younger at recruitment (Sedinger and Flint, 1995 for Black Brant *Branta bernicla*). This correlation suggests that mass at fledging reflects the quality of the individual (Ludwigs and Becker, 2006) or conditions at recruitment (Sedinger and Flint, 1995), or both. If slower growth or low fledgling mass results in decreased condition later in life (Metcalf and Monaghan, 2001), then light and/or small fledglings may be constrained or restrain themselves from breeding at an early age (Curio, 1983). However, there are trade-offs in the allocation of resources. For instance, the development of the immune system is probably energetically costly (e.g., Moreno, 2003), and an individual may be forced to trade the costs of immune suppression against allocation of energy to growth.

However, understanding the response to climate change, and the effects of temporal variability in food availability, requires conceptualizing and modeling the effects of environment on chicks' growth and survival and the carry-over effects of the early life history decision on organism's fitness. That is the focus of this paper.

2. Material and methods

We focus on the black-legged kittiwake *Rissa tridactyla* and from now on we will refer to it simply as the kittiwake. We limit our analysis to the prebreeding (i.e., immature) phase.

2.1. Species description

Seabirds are extremely *K*-selected species: adult (i.e., post-breeding) survival is generally high, and annual reproductive output is low. Many species delay first breeding until several years old.

Kittiwakes occur in both the North Atlantic Ocean and North Pacific Ocean and present differences in life histories and demographic traits according to a latitudinal gradient (Coulson, 2011). Most of the information both at the population and individual level comes from colonies living in the North Atlantic (Coulson, 2011), while less information is available for colonies of the North Pacific (but see Kitaysky et al. 2000; Piatt, 2002). However, most of the life histories can be considered equivalent for the scope of the present work and thus in general we do not explicitly differentiate between them.

The kittiwake is a pelagic seabird wintering at sea whose adults usually come back annually to breed on vertical cliffs on the coastline. Individuals show high overall site fidelity. Breeders tend to lay one- or two-egg clutches in Alaska, while in North Atlantic

colonies three-egg clutches can be observed (Coulson, 2011), and chicks remain in the nest until nearly adult size.

The food of breeding kittiwakes has been shown to vary markedly from year to year both in quality and quantity (Jodice et al., 2008).

2.2. Overview of kittiwake life cycle

2.2.1. Nestling phase

The weight of kittiwake chicks at the time of hatching is around 33 g (Coulson, 2011), for colonies of North Shield, UK; 33.3 ± 2.0 g, (Bech et al., 1984), for colonies of Svalbard, Norway; 30 g, (Maunder and Threlfall, 1972), for colonies of Gull Island, Newfoundland; 35–40 g, (Merkling et al., 2012), for colonies of Middleton Island, Alaska). The maximum (peak) weight of the chick coincides with the approach of fledging and is similar to the weight of adults (peak weight is about 96% of adult weight according to Maunder and Threlfall (1972)). Kittiwakes reach peak weight some days before fledging, and they have lost around 10% of it at fledging (Coulson, 2011). For kittiwakes in the North Shields (UK), Coulson (2011) found that between 75 and 300 g the growth rate (g d^{-1}) was virtually constant for an individual and averaged for males 16.7 g d^{-1} , with maximum growth around 18 g d^{-1} . Kitaysky et al. (2000) found that mean growth rates (6–22 days post-hatch) of kittiwakes breeding on the Pribilofs (Alaska) varied between 13 and 16.7 g d^{-1} . Piatt (2002) found growth rates at Gull and Barrens colonies (Alaska) between 16 and 18 g d^{-1} . On the contrary, chicks at the Chisik colony (Alaska) grew substantially slower ($11\text{--}14 \text{ g d}^{-1}$) and they were portably strongly food-limited. For kittiwakes living in Middleton Island (Alaska, US), maximum body growth of male chicks (i.e., maximum slope of the growth curve) in 2006–2009 was between 20 and 22 g d^{-1} with peak mass around 450 g (Merkling et al., 2012). Females grow more slowly than males and reach a lower peak mass before fledging (Coulson, 2011; Merkling et al., 2012).

Seabirds experiencing harsh conditions during development, such as high parasite load, severe weather or low food availability, may exhibit smaller mass at fledging or independence, lower survival probability in the first year after fledging, and lower reproductive success (Braasch et al., 2009 for common terns *Sterna hirundo*; Cam and Aubry, 2011 provide a review for seabirds).

Fledging success (fraction of hatched chick successfully fledging) is generally high for kittiwakes, and is in part a consequence of the greater safety from predators arising from cliff-nesting. Over a 30-year period, Coulson and Thomas (1985) found fledging success consistently greater than 80% for colonies in the North Shields, UK. Hamer et al. (1993) found for kittiwake colony of Sumburgh Head (Shetland, England) in 1990 and 1991 a fledging success of 0% and 85%, respectively. Gill et al. (2002) found fledging success of about 50% for kittiwakes laying eggs in Middleton Island (Alaska). However, Barrett and Runde (1980) found fledging successes as low as 20% in some Norwegian colonies. Kitaysky et al. (2010) found that fledging success was consistently low on Duck Island (Cook Inlet, Alaska) from 1996 to 2000, ranging from 0 to 3.6%, and likely to be caused by low food availability.

Time at fledging is variable in kittiwakes and it has been linked to post-fledging survival (Cam et al., 2003), although it is not clear whether it is a direct effect of it or a longer developmental period allows for a greater body size or mass at fledging. According to data reported in Coulson (2011) for North Shields colonies, the number of days from fledging to hatching was from 35 to 50 days, with an average of 41.5 days. Similar results were reported by Coulson and White (1958), Maunder and Threlfall (1972), Mulard and Danchin (2008) and Merkling et al. (2012).

2.2.2. Post-fledging

Very little is known about the behavior and risk of mortality of kittiwakes during their pelagic pre-reproductive period. However, the main causes of death for kittiwakes during the pelagic phase are likely to be starvation and disease (Coulson, 2011).

A positive relationship between condition or weight at the time of fledging and post-fledging survival has been reported for a variety of bird species (e.g., Kremenetz et al., 1989; Tinbergen and Boerlijst, 1990; Gaston, 1997), but there are also species where no such relationships was observed (e.g. Kersten and Brenninkmeijer, 1995; Olsson, 1997).

Here, we provide a simple quantitative framework to analyze how food availability, body growth during the nestling phase, length of the developmental period (fledging time or age) may interact to define post-hatching productivity of kittiwakes. Since the effort required to monitor seabirds' population is enormous due to their peculiar life cycle, we also want to provide additional information to biologists on the traits and parameters most critical for seabirds' individual dynamics along with predictions to be empirically tested.

2.3. The model

We use a simple life-history model to illustrate how, conditioned on the energy available for the chick, body growth rate in weight during development and length of developmental period (i.e. fledging age, in days since hatching) may determine productivity of kittiwakes. We divide the life history of the kittiwake in two phases: a nestling phase and pre-breeding (i.e., immature) phase. To simplify the model, we consider a single male kittiwake hatching in a nest (singleton). The nestling environment is characterized by a measure of energy available E , which has immediate effects on fledging weight and mortality during the nestling phase. Starck and Ricklefs (1998 ch. 17) suggest that the logistic, Gompertz, and von Bertalanffy growth models are appropriate to describe body growth in mass during the nestling phase. The body growth rate of chicks during the linear phase of growth is a parameter commonly used to examine spatial and temporal effects of changes in food availability on the reproductive performance of seabirds. Clearly, body growth is not a single trait, but it is the outcome of a complex suite of behavioral, morphological and physiological processes.

2.3.1. Body growth

We use the von Bertalanffy growth model to describe the nestling growth in body mass of chicks, since its parameters can be more readily interpreted in term of bio-energetic determinants than those of the other growth models (Mangel, 2006). In the von Bertalanffy model, the growth in weight W ($\frac{dW}{dt}$ in weight time⁻¹) results from the difference between anabolism, which is proportional to $EW^{\frac{2}{3}}$, and catabolism, which is proportional to kW , where E is the coefficient of anabolism and k the coefficient of catabolism (i.e. cost of growing):

$$\frac{dW}{dt} = EW^{\frac{2}{3}} - kW \tag{1}$$

According to Eq. (1), the individual will reach an asymptotic weight $(\frac{E}{k})^{\frac{3}{2}}$.

If W_0 is the weight of chick at age 0, k is the von Bertalanffy growth parameter (it is a rate, but not a growth rate since the unit of measure is t^{-1}), and E can be interpreted as a measure of the energy to be available to the chick during the nestling period (Mangel, 2006) (Fig. 1), the weight of chick at time t , W_t , is equal to:

$$W_t = \left[\left(\frac{E}{k} \right) \left(1 - \exp\left(-\frac{k}{3}t\right) \right) + W_0^{\frac{1}{3}} \exp\left(-\frac{k}{3}t\right) \right]^3 \tag{2}$$

For simplicity, we did not model the residual body growth after fledging and we assumed that weight at fledging remained constant through the lifetime of the bird (Maunder and Threlfall, 1972; Helfenstein et al., 2004). In addition, to simplify the model we did not include the loss of weight after it peaks before fledging.

2.3.2. Nestling mortality

Juvenile mortality risk is typically modeled as an increasing function of body growth rate to reflect the conflict between reaching a large body size and using calories and nutrients for maintenance and development of other functions (e.g., immune system, repair).

We model the daily rate of mortality m_N during the nestling period N having contribution from different components. First, there is a baseline of mortality characterized by rate m_0 . Second, we include a component $m_E(E)$ related to the energy available during the nestling period. Third, we include a component $m_G(G)$ related to body growth representing: (a) the conflict between somatic growth and development of other functions, and (b) oxidative damage. Therefore:

$$m_N = m_0 + m_E(E) + m_G(G) \tag{3}$$

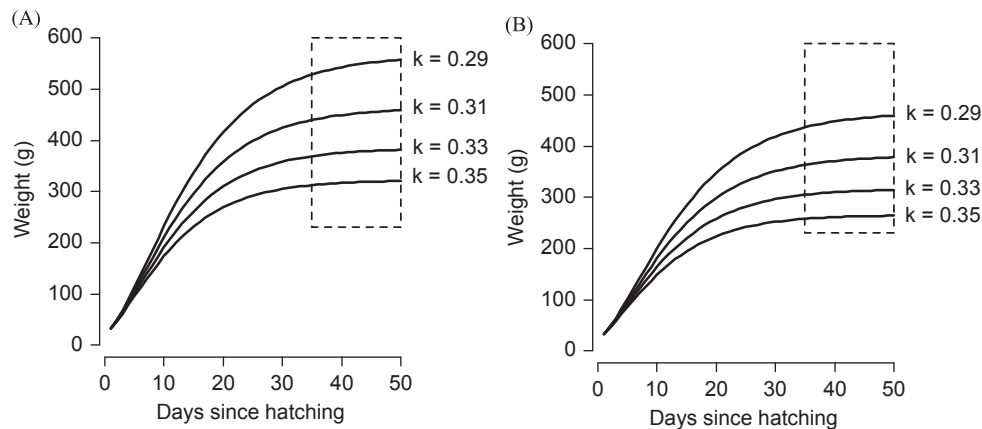


Fig. 1. von Bertalanffy growth curves where weight (g) of kittiwake chick at time t (d) is $W_t = \left[\left(\frac{E}{k} \right) \left(1 - \exp\left(-\frac{k}{3}t\right) \right) + W_0^{\frac{1}{3}} \exp\left(-\frac{k}{3}t\right) \right]^3$, with (A) $E=2.4$, (B) $E=2.25$, with k varying from 0.29 to 0.35 t^{-1} . The rectangle identifies a window of opportunity for fledging. The chick must trade-off the time in the nest, where body growth is possible, but potentially the mortality rate is higher, and fledging (equivalent to independence in our model), after which the risk mortality is usually lower, but there is virtually no body growth. In our model, post-fledging mortality decreases with increasing weight at fledging.

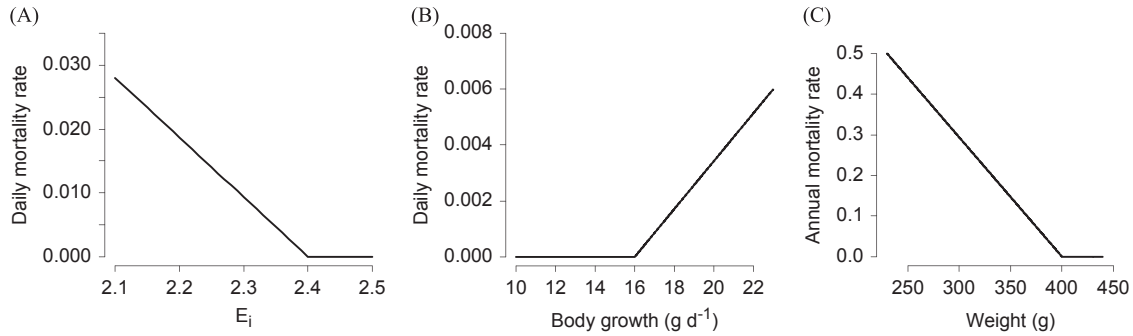


Fig. 2. Functional forms for (A) daily mortality period in the nestling phase related to energy available (i.e., risk of death for starvation or increased predation risk due to low attendance of parents), (B) daily mortality rate in the nestling phase related to growth (i.e., oxidative damage and/or incomplete development) and (C) annual mortality rate related to weight of kittiwake for the pre-breeding phase.

where G is the mean realized growth rate (g d^{-1}) between day 5 and 15 of the growth period (i.e., where growth is approximately linear, Fig. 1, Coulson, 2011; Merckling et al., 2012), depending on both E and k . In Fig. 2, we show the functional forms of $m_E(E)$ and $m_G(G)$.

We assume that mortality increases with a reduction of energy both for direct effects (starvation risk), and indirect effects, such as an increase in predation risk when parents are at sea more frequently due to food scarcity (Fig. 2a). We assume that mortality increases with increasing growth rate (Fig. 2b). This may be interpreted as physiological damage due to oxidative stress (Halliwell and Gutteridge, 1999). In addition, the rate of development of certain body structures may constrain the growth rates of other structures or functions or induce costs related to rapid growth (Starck and Ricklefs, 1998). Similarly, rapid growth may result in compromised morphology, such as suboptimal body proportions, increased fluctuating asymmetry, and skeletal deformities (see Arendt, 1997, for a general review; Starck and Ricklefs, 1998 ch. 12, specifically for birds).

Assuming that survival at hatching is 1, t_F is the number of days from hatching to fledging (i.e., fledging age), and that E and k are time-independent, survival to fledging $S(F)$ is:

$$S(F) = \exp(-m_N t_F) = \exp\{-[m_0 + m_E(E) + m_G(G)]t_F\} \quad (4)$$

Days from hatching to fledging can vary from 35 to 50 days (Coulson, 2011). Although kittiwakes reach independence some days after fledging (approximately 11 days, Mulard and Danchin, 2008), to simplify the model we consider the fledging age equal to the time of independence. Thus, in our model there is a window of opportunity for fledging (Fig. 1). It is clear that the chick must trade-off the time in the nest, where body growth is possible, but potentially the mortality rate is higher, and fledging, after which the risk mortality is usually lower, but body growth basically stops.

2.3.3. Post-fledging mortality

We model post-fledging and pre-breeding mortality $m_{PF}(a)$, where age a ranges from 0 to 6, as:

$$m_{PF}(a) = m_A(a) + \frac{m_W(W_F)}{l(a)}. \quad (5)$$

where W_F is mass at fledging, $m_W(W_F)$ is a decreasing function of W_F (Fig. 2c), $m_A(a)$ is the age-dependent mortality rate and $l(a)$ is an increasing function of age representing “learning” or “experience”. In our model, learning or experience allow the mortality due to low body weight to decrease with age. Studies provide some evidence of a higher risk of mortality in the first year after independence (Callum and Coulson, 1990), and it is likely that during that first days and months after leaving the nest higher body mass, and a consequent higher resistance to starvation, may be particularly favorable.

We parameterized the models using a pattern-oriented procedure (Grimm et al., 2005) and data from Coulson (2011), Desprez et al. (2011) and Merckling et al. (2012) for male kittiwakes.

2.3.4. Productivity

Post-hatching productivity $\phi(k, t_F | \alpha)$ (from now on simply productivity) is the survival from hatching to age at first breeding α , where age at first breeding is fixed and thus not a results of the dynamics that the model describes. With $\alpha=0$, productivity is equal to $S(F)$. If $\alpha \geq 1$:

$$\phi(k, t_F | \alpha) = S(F) \prod_{a=0}^{\alpha-1} \exp[-m_{PF}(a)] \quad (6)$$

Therefore, given E defining energy/food available for kittiwakes related to food availability, and age at first breeding α , we explore the productivity of kittiwakes with different von Bertalanffy growth parameter k and days spent in the nest t_F (i.e. fledging age).

3. Results

The parameter space for this model is rich (Table 1) and a full exploration of the model is clearly beyond the scope of this work. Hence, we present the results of a number of particular cases to illustrate the main insights that the model provides for the link between food availability, body growth and productivity.

We fix body weight at hatching at 33 g. We use numerical simulations to find the combinations of von Bertalanffy coefficients E and k (Eq. (2)) that allow body growth rates and mass at fledging to be comparable to what is observed in nature (Fig. 1). Body growth in mass rapidly increases a few days after hatching and then approaches a plateau in the time window for fledging. With increasing von Bertalanffy growth parameter k , both growth rate G and asymptotic weight $(\frac{E_i}{k})^3$ decrease, and the growth plateau is approached earlier (Fig. 1).

When feeding conditions are good (“good environment”, $E_i=2.4$), there is no mortality due to starvation and/or low attendance of parents increasing predation. Growing fast comes at a cost (Fig. 2b) and the survival probability of fast growers (low k values) is lower than for slow growers (high k values) and decreases with fledging age (Fig. 3).

Apart from the extreme case of very fast growth and prolonged nestling phase (i.e., top left of Fig. 3a), survival probabilities are consistently greater than 0.65. On the contrary, when feeding conditions are not optimal (“bad environment”, $E=2.25$), survival probabilities to fledging are flat over different values of k , that is, basically independent of the rate of body growth, and increase with fledging age (Fig. 3b).

Table 1

Values and description of the parameters used in the model.

Parameter	Value	Description
E_i	2.1–2.4	Energy/food available in the environment
k	0.29–0.39	von Bertalanffy growth parameter (t^{-1})
t_F	35–50	Fledging date or age (d)
m_0	0.004	Base daily mortality rate in the nestling phase (t^{-1})
m_E	0.028	Daily Mortality due to starvation and/or low attendance of parents when energy is minimum (t^{-1}) (see Fig. 2)
m_G	0.006	Daily Mortality rate due to fast growth (oxidative damage and/or incomplete development) in the nestling phase when growth is maximum (t^{-1}) (see Fig. 2)
m_W	0.5	Annual mortality rate related to weight in the post-fledging phase when weight is minimum (t^{-1}) (see Fig. 2)
$m_A(0)$	0.3	Age-specific post-fledging mortality
$m_A(1)$	0.2	
$m_A(2)$	0.2	
$m_A(3)$	0.2	
$m_A(4)$	0.3	
$m_A(5)$	0.3	
$l(0)$	1	Age-specific factor related to “experience” or “learning” of the Kittiwake
$l(1)$	2	
$l(2,3,4,5,6)$	3	
α	3–5	Age at first breeding (y)

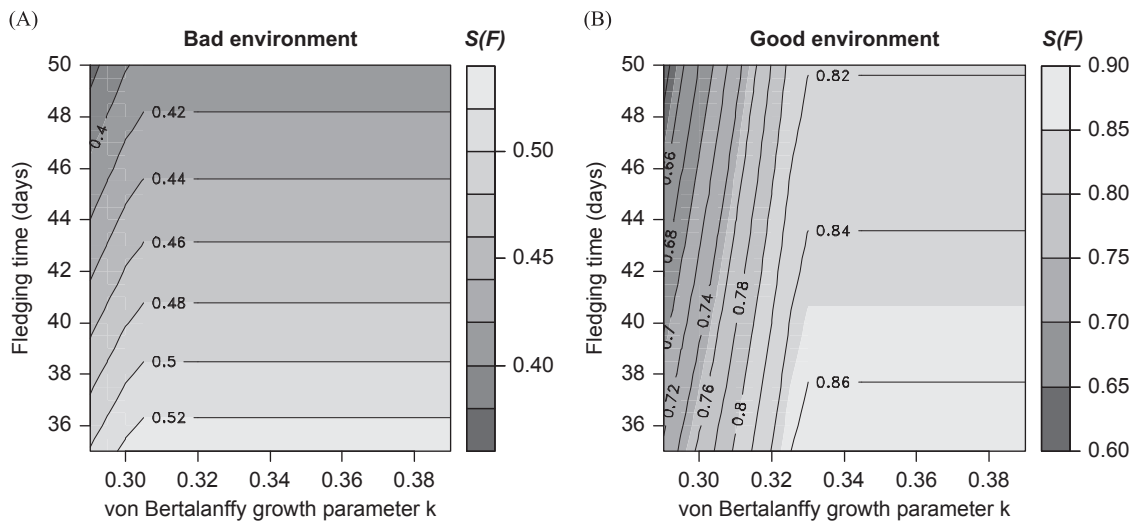


Fig. 3. Survival up to fledging $S(F)$ with different von Bertalanffy growth parameter k (from 0.29 to 0.39) and time at fledging (from 35 to 50 days since hatching), with (A) bad environment ($E_i=2.25$) and (B) good environment ($E_i=2.4$). Body growth G in $g\ d^{-1}$ (mean body growth between days 5 and 15 since hatching) increases with decreasing values of k . The range of survival is different in the two plots for easier interpretation of results.

However, the picture changes when we consider productivity, that is survival from hatching to age at first breeding (Fig. 4). In the case of good environment, maximum productivity is reached by kittiwakes that grew moderately fast during the nestling phase for between 35 and 45 days, thus reaching a weight at fledging of about 450 g (Fig. 2c and Table 2). This allows the individual to pay lower mortality costs than faster growers and to be able to reach an optimal weight (i.e., for which no post-fledging mortality costs are paid) at fledging. The same picture is basically conserved when the age at first breeding is either 3 (Fig. 4a) or 5 years old (Fig. 4b), with individuals growing slowly during the nestling phase displaying the minimum productivity.

When feeding conditions during the nestling phase induce energy-dependent mortality (Fig. 2a), individuals with the faster growth during the nestling phase, but with the shortest length of time spent in the nest, have the highest productivity when first breeding is either at age 3 or 5 (Fig. 4c,d, Table 2). Those individuals can thus reach the optimal weight at fledging and at the same time pay lower costs due to the poor environment during nestling. Clearly, this depends on the relative costs of growing too fast, that is of increasing oxidative damage and/or allocating a

suboptimal amount of resources to the development or use of other function, and of spending time in a poor environment with consequent risks of starvation or predation. When survival post-fledging does not depend on body weight at fledging ($m_W = 0$), the patterns of survival at fledging of Fig. 3a and b are conserved post-fledging.

4. Discussion

The intuition emerging from our results is that in the case of good environment it pays to grow fast and to spend a moderately long time in the nest, while in case of poor environment the best strategy is to grow fast and leave the nest soon. In this case, growth refers to the value of the parameter k of the von Bertalanffy model, since the realized growth in $g\ d^{-1}$ depends on both k and E . Our model provides predictions that can be empirically tested (Table 2). As chicks’ growth rates are often used as a proxy of food availability, in order to avoid circular reasoning predictions may be more rigorously tested using experimental setups in which food availability is manipulated (Gill et al., 2002).

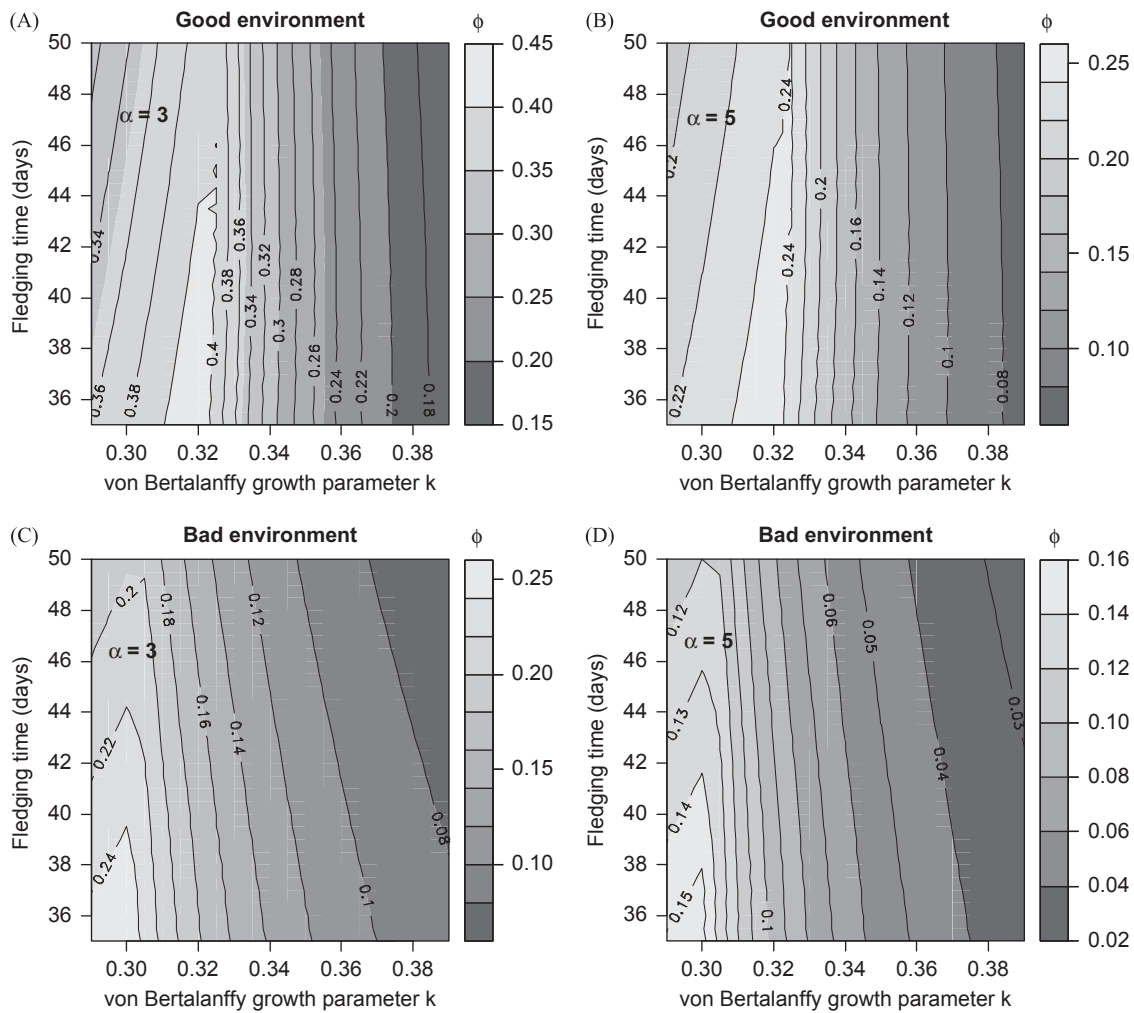


Fig. 4. Productivity $\phi(k, t_F(\alpha))$ (i.e., survival from hatching up to age at first breeding α) with (A) and (B) good environment ($E_i=2.4$), and (C) and (D) bad environment ($E_i=2.25$), where age at first breeding α is 3 or 5 years old. The range of productivity is different in the two plots for easier interpretation of results.

Table 2

Predictions of the model that can be empirically tested. Male (singleton) chicks are predicted to have a slightly slower realized growth during the linear growth phase (between day 5 and 15) in a bad (i.e. non-optimal) environment than in a good environment and a similar peak mass before fledging. Kittiwakes are predicted to fledge (slightly) sooner when conditions are bad.

Predicted trait	Good environment	Bad environment
Growth in mass during the linear phase (g d^{-1})	18.62	17.99
Peak mass (g)	440–454	440–450
Fledging age (d)	35–45	35–40

According to our modeling results, prolonging the nestling phase often decreases productivity of kittiwakes and a different age at first breeding does not change the optimal body growth strategies (Fig. 4). Cam et al. (2003) found that longer developmental time increased fitness in kittiwakes living in colonies in Brittany, France. They used length of the rearing period as a surrogate for parental effort, but since they did not control for either fledging weight or body growth, we are unable to tease apart the different contribution of somatic growth and parental effort on fitness. Similarly, Coulson (2011) found an apparent (i.e. birds can survive, but fly to other colonies or not be observed) important effect of nestling body growth rate on post-fledging survival. When growth rate was higher, so was the proportion of birds that survived to return at the

colony at least a couple of years later. However, since the effect of growth rate was not estimated controlling for body size at fledging, we are unable to determine whether the apparent lower survival was directly related to growth rate or to a lower body mass at independence.

The decreasing productivity with increasing fledging age we predict is a consequence both of the relative importance of growth-dependent and -independent costs of body growth and the reduced opportunity to grow larger when the chick enters the time window for fledging. In particular, while some growth in the window time for fledging is possible when the von Bertalanffy k is low (and thus both realized body growth and asymptotic weight are larger, Fig. 1), in the other cases (i.e., increasing values of von Bertalanffy k) the plateau in body growth is basically reached when the chick enters the time window for fledging. This is especially true when the environment is poor (Fig. 1b); with scarce feeding opportunities and with low body growth the chick can never reach the minimum body fledging weight that allows it not to pay post-fledging survival costs. However, since there are no costs for slow growth, we observe a fledging success of slow-growing chicks equal (Fig. 3a) or greater (Fig. 3b) than that of fast-growing chicks. Equal survival of slow- and fast-growing chicks has been observed in kittiwakes (e.g., Coulson and Porter, 1985), but in other birds a decreasing survival with depressed body growth in the nest has been reported (Starck and Ricklefs, 1998 ch. 14), mostly due to starvation. However, other studies found

that faster growth can make chicks more susceptible to starvation (Lack, 1968; Starck and Ricklefs, 1998), and that a trade-off between growth rate and energy supply may guide the evolution of nestling growth.

The literature contains conflicting evidence concerning implications of food availability, body growth and body size for survival during the nestling phase. According to Coulson and Porter (1985), for kittiwakes in the North Shields (UK) the risk of dying during the nestling phase progressively declined with the age of the chicks and three-quarters of the deaths occurred during the first two weeks of life. Coulson and Porter (1985) did not find any evident correlation between growth rate in mass and fledging success. The most frequent cause of death for chicks in the North Shields (UK) was associated with hatching and the transition by the parents from incubating to brooding; no predation was observed. The mortality rates of chicks declined as their food requirements increased, suggesting that food shortage experienced by the parents was not a major cause of the chicks' deaths. For Kittiwake populations living in Norwegian islands, Barrett and Runde (1980) found that on one island (Runde) the majority of chicks that died were lighter at the time of death than those which survived 30 days or more. On the contrary, in the islands Hekkingen and Runneskholmen chicks that died weighed nearly the same as, and some were even heavier than the average surviving chick.

However, food shortage is considered to have been the cause of mortality, acting both directly and indirectly. The direct effect was through starvation, and the indirect effect was through an unusually low adult attendance at nests with chicks. Nest attendance is normally 100% during nestling period, but chicks may be left unattended when food availability is low and more feeding flights are required (Coulson, 2011).

According to life-history theory (e.g., Roff, 2002), in general body growth rates and size-at-age are expected to be subject to strong directional selection, since both survival and reproductive success are usually positively correlated with body size at different life-stages in a variety of taxa. However, body growth commonly occurs at rates lower than the physiological maximum (Arendt, 1997), thus implying that (a) growth rates are optimized rather than maximized and (b) slower growth could be favored under certain conditions. Realized growth rate thus results from a compromise between the costs and advantages of growing rapidly, and the optimal rate of growth is not equivalent to the maximum rate.

From a modeling perspective, in the case of an increasing risk of starvation for both fast- and slow-growing chicks, we can substitute the linearly increasing function (after a threshold) of body growth during the nestling phase (Fig. 2b) with a quadratic function increasing mortality costs for both slow- and fast-growing chicks. This will decrease the fledging survival of slow-growing chicks (Fig. 3), but it will not substantially change the general patterns of post-fledging survival, since chicks growing relatively faster show the maximum productivity (Fig. 4).

Longitudinal studies of kittiwake populations have revealed a great diversity in individual life histories within populations and large amounts of phenotypic variation among individuals for traits such as survival, sexual maturity and reproductive output, and reproductive behavior (e.g., skipped breeding) (e.g., Aubry et al., 2011; Coulson et al., 2011). The concept of "quality" (of parents, eggs or offspring) has been used to explain these large differences in individual life-histories and lifetime reproductive success and the concept is now pervasive in studies of the individual dynamics of seabirds (Steiner et al., 2010; Vergara et al., 2010; Coulson et al., 2011; Cam and Aubry, 2011). Since the concept of quality is still ill-defined (e.g., Moreno 2003) and often leads to circular and/or *a posteriori* arguments (e.g., high quality birds defined as birds with

high reproductive success and viceversa), we do not model possible differences in "quality". The relationship between body growth, length of the nestling period and time-dependent mortality in kittiwakes has not yet been resolved. Determining whether the responses of a growing organism are adaptive is central for an understanding of evolutionary processes and for the prediction of future demographic and life-history responses. Starck and Ricklefs (1998) noted that it is important to distinguish between variation in growth and maturation imposed by the environment and those that are induced (i.e., adaptive) in response to environmental cues. Imposed variation may happen when a decrease in food supply during development leads to a stunted, poorly performing individual (Monaghan, 2008; Starck and Ricklefs, 1998). On the contrary, maternal androgen deposition in eggs provides a flexible mechanism the developmental and/or body growth trajectories to prevailing environmental conditions, thus producing different phenotypes (reviewed in Groothuis et al., 2005). In a variety of bird species including seabirds, androgens enhance the frequency of begging display. In manipulative experiments with physiological levels of androgen (i.e., in a range found in nature), chicks from yolks with higher levels of androgens grew relatively fast in terms of body mass and tarsus length (Groothuis et al., 2005). From an adaptive point of view, under poor food conditions mothers may benefit from producing offspring that stimulate paternal feeding by enhanced begging. However, androgen-induced faster growth might be at the expense of the development of immune function – while preserving the development of skeleton and nervous system – especially when resources are limited and thus the problem of resource allocation is more urgent (Groothuis et al., 2005).

Thus, we predict that it is adaptive in a poor environment to induce a fast body growth in chicks (Fig. 4c and d) in order to reach a fledging weight that allows not to pay size-related post-fledging costs, while at the same time fledging early. This picture holds when we assume that the mother has a reasonably accurate knowledge of the energy available for the chick. This assumption motivates some evolutionary considerations. Although body growth in weight ($g\ d^{-1}$) changes through development (Fig. 1), we assumed that the growth strategy (k) is fixed for the whole growth period and there are no day-to-day changes in the availability of food. It is clear that the relative inflexibility of the body growth strategy is adaptive when the environment is stable and/or when the expected environment and the realized environment coincide, since maintaining growth plasticity is costly for the organism (Auld et al., 2010). However, the variability of both within- and between-years food availability in polar regions like the Bering Sea is predicted to increase with climate change, and this will increase the probability of a mismatch between prediction of environment/resources made by the parents or the chick and actual environment/resources, thus theoretically favoring the evolution of more flexible growth strategy.

Flexible growth rates can be adaptive when food availability fluctuates stochastically. Such flexibility increases the chances of survival chances during food shortages, and the appropriate – in terms of timing and magnitude – induced response when a chick is confronted by a food shortage depends on the severity, duration and predictability of the deprivation. Most seabirds depend on food resources that are intrinsically highly unpredictable with large temporal and spatial variation (Lack, 1968; Schultner et al., 2013). However, it is difficult to determine the immediate and delayed costs of a flexible growth strategy (i.e., costs of adaptive phenotypic plasticity, Auld et al., 2010), the existence of reaction norms (that is, genotype X environment interactions, Davidowitz and Nijhout, 2004), and for how long during development the flexibility can be maintained without compromising other functions.

Other factors may complicate of our adaptive view of this situation. First, singletons are rare in kittiwakes (Coulson, 2011) and this may reduce the correlation between the fitness of any single chick and parents' fitness. For example under food restriction, while a single chick may be better served by growing rapidly (Fig. 4c and d), parents are predicted to increase their fitness by reducing the whole growth of the brood in order to reduce the total food requirement (Starck and Ricklefs, 1998). Siblicide, as mediated by food supply, is an important aspect of kittiwake behavior and survival during chick-rearing (Braun and Hunt, 1983). For example, when two or more chicks are produced, androgen concentrations in the yolk increase over the laying order (Groothuis et al., 2005). The later hatched chick competes with older and bigger siblings for food and care (i.e., warmth) provided by the parents. An increase of yolk androgen levels over the laying sequence may function as a maternal tool to diminish the disadvantage of being a late chick, since it may increase begging behavior and thus solicit paternal feeding. In addition, higher androgen levels are predicted to induce a preferential allocation of energy from immune function to growth, adaptively increasing the probability of survival when the chick is the younger sibling.

An opposite pattern of androgen concentration in the yolk (i.e., decreasing with hatching order) can also be adaptive, since it leads to an increased variance in size and growth within the brood that allows parents, in case of food shortage, to sacrifice the smallest chicks before overinvesting in them (Starck and Ricklefs, 1998).

However, adjustments in chick development (growth and time spent in the nest) as well other post-hatching dynamics would likely be of relatively minor importance for the viability of colonies as kittiwakes respond to changes in their food supply.

Hatch et al. (1993) found for Pacific colonies that only 65% of nest-building black-legged kittiwakes produce eggs in an average year, although in the most productive years the mean increases to 80%, and the highest single rate observed was 97%. When colonies fail, that is when the number of chicks fledged per pair is smaller than 0.1, two-thirds of the potential productivity of pairs is removed by a combination of non-breeding and reduced clutch sizes.

Our model of early growth and post-fledging survival, coupled with available models of post-breeding survival and reproductive dynamics (e.g., Desprez et al., 2011; Satterthwaite et al., 2012), allows the development of a full life-history model to explore how environmental processes and heterogeneity in food availability can create different selective environments for body growth, length of developmental period and age at sexual maturation (Vincenzi et al., 2012). This life-history model could also be spatially-explicit to take into account the colony structure, density-dependent processes and the arrival of migrants from other colonies (Coulson, 2011).

Acknowledgments

BEST-BSIERP Bering Sea Project publication number 90 NPRB publication number 409. This work was supported by funding from the North Pacific Research Board (BEST-BSIERP project B74) and by the Center for Stock Assessment Research (CSTAR), a partnership between the Fisheries Ecology Division, NOAA Fisheries, Santa Cruz and the University of California Santa Cruz and partially supported by NSF grant EF-0924195 to MM.

References

Arendt, J.A., 1997. Adaptive intrinsic growth rates: an integration across taxa. *Q. Rev. Biol.* 72, 149–177.

- Aubry, L.M., Cam, E., Koons, D.N., Monnat, J.-Y., Pavard, S., 2011. Drivers of age-specific survival in a long-lived seabird: contributions of observed and hidden sources of heterogeneity. *J. Anim. Ecol.* 80, 375–383.
- Auld, J.R., Agrawal, A., Relyea, R., 2010. Re-evaluating the costs and limits of adaptive phenotypic plasticity. *P. R. Soc. B Biol. Sci.* 277, 503–511.
- Barbraud, C., Rivalan, P., Inchausti, P., Nevoux, M., Rolland, V., Weimerskirch, H., 2011. Contrasted demographic responses facing future climate change in Southern Ocean seabirds. *J. Anim. Ecol.* 80, 89–100.
- Barrett, R.T., Runde, O.J., 1980. Growth and survival of nestling Kittiwakes *Rissa tridactyla* in Norway. *Ornis Scand.* 11, 228–235.
- Bech, C., Martini, S., Brent, R., Rasmussen, J., 1984. Thermoregulation in newly hatched black-legged kittiwakes. *The Condor* 86, 339–341.
- Braasch, A., Schauroth, C., Becker, P.H., 2009. Post-fledging body mass as a determinant of subadult survival in Common Terns *Sterna hirundo*. *J. Ornithol.* 150, 401–407.
- Braun, B.M., Hunt, G.L., 1983. Brood reduction in black-legged kittiwakes. *The Auk* 100, 469–476.
- Byrd, G., Schmutz, J., Renner, H., 2008. Contrasting population trends of piscivorous seabirds in the Pribilof Islands: a 30-year perspective. *Deep-Sea Res.* 55, 1846–1855.
- Callum, T.S., Coulson, J.C., 1990. Reproductive success of Kittiwake gulls, *Rissa tridactyla*. In: Clutton-Brock, T.H. (Ed.), *Reproductive Success: Studies of Individual Variation in Contrasting Breeding Systems*. University of Chicago Press, Chicago, Illinois 548p.
- Cam, E., Monnat, J.-Y., Hines, J.E., 2003. Long-term fitness consequences of early conditions in the kittiwake. *J. Anim. Ecol.* 72, 411–424.
- Cam, E., Aubry, L., 2011. Early development, recruitment and life history trajectory in long-lived birds. *J. Ornithol.* 152, 187–201.
- Ciannelli, L., Bailey, K.M., Chan, K.-S., Belgrano, A., Stenseth, N.C., 2005. Climate change causing phase transitions of walleye pollock (*Theragra chalcogramma*) recruitment dynamics. *P. R. Soc. B Biol. Sci.* 272, 1735–1743.
- Coulson, J.C., 2011. *The Kittiwake*. Poyser, London, UK.
- Coulson, J.C., White, E., 1958. The effect of age on the breeding biology of the kittiwake *Rissa tridactyla*. *Ibis* 100, 40–51.
- Coulson, J.C., Porter, J.M., 1985. Reproductive success of the Kittiwake: the roles of clutch size, chick growth rates and parental quality. *Ibis* 127, 450–466.
- Coulson, J.C., Thomas, C.S., 1985. Changes in the biology of the kittiwake *Rissa tridactyla*: A 31-year study of a breeding colony. *Journal of Animal Ecology* 54, 9–26.
- Coyle, K.O., Eisner, L.B., Mueter, F.J., Pinchuk, A.I., Janout, M.A., Cieciel, K.D., Farley, E.V., Andrews, A.G., 2011. Climate change in the southeastern Bering Sea: impacts on pollock stocks and implications for the oscillating control hypothesis. *Fish. Oceanogr.* 20, 139–156.
- Curio, E., 1983. Why do young birds reproduce less well? *Ibis* 125, 400–404.
- Davidowitz, G., Nijhout, H.F., 2004. The physiological basis of reaction norms: the interaction among growth rate, the duration of growth and body size. *Integr. Comp. Biol.* 44, 443–449.
- Desprez, M., Pradel, R., Cam, E., Monnat, J.-Y., Gimenez, O., 2011. Now you see him, now you don't: experience, not age, is related to reproduction in kittiwakes. *P. Roy. Soc. B Biol. Sci.* 278, 3060–3066.
- Gaston, A.J., 1997. Mass and date at departure affect the survival of Ancient Murrelet *Synthliboramphus antiquus* chicks after leaving the colony. *Ibis* 139, 673–678.
- Gill, V.A., Hatch, S.A., Lanctot, R.B., 2002. Sensitivity of breeding parameters to food supply in Black-legged Kittiwakes *Rissa tridactyla*. *Ibis* 144, 268–283.
- Grimm, et al., 2005. Pattern-oriented modeling of agent-based complex systems: lessons from ecology. *Science*, 987–991.
- Groothuis, T.G.G., Müller, W., von Engelhardt, N., Carere, C., Eising, C., 2005. Maternal hormones as a tool to adjust offspring phenotype in avian species. *Neurosci. Biobehav. Rev.* 29, 329–352.
- Halliwell, B., Gutteridge, J.M.C., 1999. *Free Radicals in Biology and Medicine*. Oxford University Press Midsomer Norton, Avon, England.
- Hamer, K.C., Monaghan, P., Uttley, J.D., Walton, P., Burns, M.D., 1993. The influence of food supply on the breeding ecology of Kittiwakes *Rissa tridactyla* in Shetland. *Ibis* 135, 255–263.
- Hatch, et al., 1993. Status and ecology of kittiwakes in the North Pacific. In: Vermeer, K., et al. (Eds.), *The Status, Ecology, and Conservation of Marine Birds of the North Pacific*.
- Helfenstein, F., Danchin, E., Wagner, R.H., 2004. Assortative mating and sexual size dimorphism in black-legged kittiwakes. *J. Avian Biol.* 27, 350–354.
- Hollowed, A.B., Bond, N.A., Wilderbuer, T.K., Stockhausen, W.T., A'mar, Z.T., Beamish, R.J., Overland, J.E., Schirripa, M.J., 2009. A framework for modelling fish and shellfish responses to future climate change. *ICES J. Mar. Sci.* 66, 1584–1594.
- Jenouvrier, S., Caswell, H., Barbraud, C., Holland, M., Stroeve, J., Weimerskirch, H., 2009. Demographic models and IPCC climate projections predict the decline of an emperor penguin population. *PNAS* 106, 1844–1847.
- Jenouvrier, S., Visser, M.E., 2011. Climate change, phenological shifts, eco-evolutionary responses and population viability: toward a unifying predictive approach. *Int. J. Biometeorol.* 55, 905–919.
- Jenouvrier, S., Holland, M., Stroeve, J., Barbraud, C., Weimerskirch, H., Serreze, M., Caswell, H., 2012. Effects of climate change on an emperor penguin population: analysis of coupled demographic and climate models. *Glob. Change Biol.* 18, 2756–2770.
- Jodice, P.G.R., Roby, D.D., Turco, K.R., Suryan, R.M., Irons, D.B., Piatt, J.F., Shultz, M.T., Roseneau, D.G., Kettle, A.B., 2008. Growth of black-legged kittiwake *Rissa*

- tridactyla* chicks in relation to delivery rate, size, and energy density of meals. *Mar. Ornithol.* 114, 107–114.
- Kersten, M., Brenninkmeijer, A., 1995. Growth, fledging success and post-fledging survival of juvenile oystercatchers *Haematopus ostralegus*. *Ibis* 137, 396–404.
- Kitaysky, A.S., Hunt, G.L., Flint, E.N., Rubega, M.A., Decker, M.B., 2000. Resource allocation in breeding seabirds: responses to fluctuations in their food supply. *Mar. Ecol. Progr. Ser.* 206, 283–296.
- Kitaysky, A.S., Piatt, J.F., Hatch, S.A., Kitaiskaia, E.V., Benowitz-Fredericks, Z.M., Shultz, M.T., Wingfield, J.C., 2010. Food availability and population processes: severity of nutritional stress during reproduction predicts survival of long-lived seabirds. *Funct. Ecol.* 24, 625–637.
- Krementz, D.G., Nichols, J.D., Hines, J.E., 1989. Postfledging survival of European Starlings. *Ecology* 70, 646–655.
- Lack, D., 1968. *Ecological Adaptations for Breeding in Birds*. Methuen, London.
- Ludwigs, J.-D., Becker, P.H., 2006. Individual quality and recruitment in the common tern *Sterna hirundo*. *Acta Zool. Sin.* 52, 96–100.
- Mangel, M., 2006. *The Theoretical Biologist's Toolbox: Quantitative Methods for Ecology and Evolutionary Biology*. Cambridge University Press, Cambridge, UK.
- Maunder, J.H., Threlfall, W., 1972. The Breeding Biology of the black-legged Kittiwake in Newfoundland. *The Auk* 89, 789–816.
- Merkling, T., Leclaire, S., Danchin, E., Lhuillier, E., Wagner, R.H., White, J., Hatch, S.A., Blanchard, P., 2012. Food availability and offspring sex in a monogamous seabird: insights from an experimental approach. *Behav. Ecol.* 23, 751–758.
- Metcalfe, N.B., Monaghan, P., 2001. Compensation for a bad start: grow now, pay later? *TREE* 16, 254–260.
- Monaghan, P., 2008. Early growth conditions, phenotypic development and environmental change. *Philos. Trans. R. Soc. B* 363, 1635–1645.
- Moreno, J., 2003. Lifetime reproductive success in seabirds: interindividual differences and implications for conservation. *Sci. Mar.* 67, 7–12.
- Mulard, H., Danchin, É., 2008. The role of parent–offspring interactions during and after fledging in the black-legged Kittiwake. *Behav. Processes* 79, 1–6.
- Olsson, O., 1997. Effects of food availability on fledging condition and post-fledging survival in king penguin chicks. *Polar Biol.* 18, 161–165.
- Piatt, J.F., 2002. Response of seabirds to fluctuations in forage fish density. Final Report to Exxon Valdez Oil Spill Trustee Council (Restoration Project 00163M) and Mineral Management Service (Alaska OCS Region). Alaska Science Center, US Geological Survey, Anchorage, Alaska.
- Roff, D.A. 2002. *Life History Evolution*. Sinauer, Sunderland, Massachusetts.
- Satterthwaite, W.H., Kitaysky, A.S., Mangel, M., 2012. Linking climate variability, productivity and stress to demography in a long-lived seabird. *MEPS* 454 221:235.
- Sedinger, J.S., Flint, P.L., 1995. Environmental influence on life-history traits: growth, survival, and fecundity in Black Brant (*Branta bernicla*). *Ecology* 76, 2404–2414.
- Schultner, J., Kitaysky, A.S., Welcker, J., Hatch, S., 2013. Fat or lean: adjustment of endogenous energy stores to predictable and unpredictable changes in allostatic load. *Funct. Ecol.* 27, 45–55.
- Starck, J.M., Ricklefs, R.E., 1998. *Avian Growth and Development*. Oxford University Press, New York, New York, United States.
- Steiner, U.K., Tuljapurkar, S., Orzack, S.H., 2010. Dynamic heterogeneity and life history variability in the kittiwake. *J. Anim. Ecol.* 79, 436–444.
- Tinbergen, J.M., Boerlijst, M.C., 1990. Nestling weight and survival in individual great tits (*Parus major*). *J. Anim. Ecol.* 59, 1113–1127.
- Vergara, P., Fargallo, J.A., Martínez-Padilla, J., 2010. Reaching independence: food supply, parent quality, and offspring phenotypic characters in kestrels. *Behav. Ecol.* 21, 507–512.
- Vincenzi, S., Crivelli, A.J., Giske, J., Satterthwaite, W.H., Mangel, M., 2012. Selective consequences of catastrophes for growth rates in a stream-dwelling salmonid. *Oecologia* 168, 393–404.
- West-Eberhard, M., 2003. *Developmental plasticity and evolution*. Oxford University Press, Oxford, UK.
- Wolf, S.G., Snyder, M.A., Sydeman, W.J., Doak, D.F., Croll, D.A., 2010. Predicting population consequences of ocean climate change for an ecosystem sentinel, the seabird Cassin's auklet. *Glob. Change Biol.* 16, 1923–1935.



Vertical distributions of the early life stages of walleye pollock (*Theragra chalcogramma*) in the Southeastern Bering Sea



T.I. Smart^{a,*}, E.C. Siddon^b, J.T. Duffy-Anderson^c

^a School of Aquatic and Fishery Sciences, University of Washington, Seattle, WA 98195, USA

^b Fisheries Division, School of Fisheries and Ocean Sciences, University of Alaska Fairbanks, Juneau, AK 99801, USA

^c RACE Division, Recruitment Processes Program, Alaska Fisheries Science Center, NOAA Fisheries, Seattle, WA 98115, USA

ARTICLE INFO

Available online 14 March 2013

Keywords:

Theragra chalcogramma
Vertical distribution
Bering Sea
Walleye pollock

ABSTRACT

The present study examines vertical distributions of the early life stages of walleye pollock (*Theragra chalcogramma*) in the Southeastern Bering Sea to assess ontogenetic and diel vertical migration in relation to development and habitat. Walleye pollock demonstrated a decrease in the depth of occurrence following hatching, indicating an ontogenetic change in vertical distribution. Eggs occurred deepest in the water column and early juveniles occurred shallowest. Vertical distributions were related to the date of collection, water column depth, and thermocline depth. Non-feeding stages (eggs and yolk sac larvae, <4.5 mm standard length [SL]) did not exhibit diel vertical migration. Feeding larvae exhibited diel vertical migration, although patterns varied between two feeding stages. Preflexion stage larvae (4.5–9.9 mm SL) were concentrated between 10 and 20 m during the day and deeper at night. Postflexion stage larvae (flexion and postflexion, 10.0–24.5 mm SL) underwent regular diel migrations (0–20 m, night; 10–40 m, day). Low sample sizes limited our ability to assess diel vertical migration in early juveniles, but this stage tends to occur in the upper 20 m of the water column, regardless of time of day. These results suggest that vertical distributions and diel migration potentially are driven by prey availability at sufficient light levels for preflexion larvae to feed and a trade-off between prey access and predation risk for postflexion larvae. Vertical distributions of eggs and preflexion larvae varied with habitat examined (on the continental shelf versus over the continental slope). Vertical distributions of walleye pollock eggs, yolk sac larvae, and preflexion larvae in the Bering Sea are different from distributions in other ecosystems, which can impact transport and modeling efforts.

© 2013 Elsevier Ltd. All rights reserved.

1. Introduction

Information on vertical distributions of early life history stages of fishes is critical for accurate modeling of larval transport to nursery habitats as transport can differ depending on vertical position in the water column (Fiksen et al., 2007; Kristiansen et al., 2009; Miller, 2007; Stenevik et al., 2003; Tanaka, 1991). Ontogenetic vertical migration (OVM) is a pattern in which vertical distribution changes with stage of development. Typically, OVM involves a shoaling in the depth of occurrence as eggs and larvae develop, which allows larvae to exploit high food concentrations and fast currents in surface waters (Fortier and Leggett, 1983; Hare and Govoni, 2005; Norcross and Shaw, 1984). Often OVM is accompanied by increasing complexity of vertical behaviors, such as responsiveness to changes in light intensity (Hare and Govoni,

2005; Heath et al., 1988). Diel vertical migration (DVM) is a behavioral trend in which depth of occurrence changes with time of day and light intensity. DVM typically is exhibited by feeding stages. Larval fish are visual predators, consuming a variety of zooplankton, and as such will orient themselves in the water column to overlap with prey vertical distribution and with light levels sufficient to facilitate feeding (Heath et al., 1988; Porter et al., 2005). Larval fish also are preyed upon by a variety of visual predators and may move down to darker depths during the day time to avoid predation (Hunter and Sanchez, 1976; Yamashita et al., 1985). Regular DVM is the pattern in which larvae move deeper in the water column during the day to avoid visual predators and shallower at night to feed upon zooplankton in surface waters (Kerfoot, 1985; Ohman, 1990). Reverse DVM is the pattern in which larvae migrate to the surface during the day and migrate to depth at night, often as a response to tidal currents or the presence of non-visual predators.

The continental shelf and shelf break areas of the Southeastern Bering Sea (SEBS) are important spawning and nursery grounds for commercially valuable pelagic and demersal fishes, such as walleye

* Corresponding author. Current address: Marine Resources Research Institute, Charleston, SC 29422, USA.

E-mail address: smartt@dnr.sc.gov (T.I. Smart).

pollock (*Theragra chalcogramma*, Matarese et al., 2003). The shelf in the SEBS is very broad (~300 nmi), providing a wide area of shallow habitat for developing larvae and juveniles. Walleye pollock spawn in several areas near islands in the SEBS, along the Alaska Peninsula, and in deep-water canyons along the continental slope (Bacheler et al., 2010; Hinckley, 1987). Coupled with the locations of spawning, the dominant currents in the SEBS can deliver walleye pollock early life stages to several different habitats over the continental shelf and slope, each with unique hydrographic and biological characteristics (Coachman, 1986; Stabeno et al., 2001). A coastal domain (<50 m water depth) surrounds all islands and the Alaska mainland and peninsula. The coastal domain is well-mixed. The middle shelf domain (50–100 m water depth) is strongly stratified in summer and characterized by a pool of cold (<2 °C) bottom water in summer that is detrimental to the development of larvae (Napp et al., 2000). The coastal and middle domains are habitat for several species of copepod whose naupliar stages are preferred prey items for larval walleye pollock (Coyle et al., 2011; Hillgruber et al., 1995). The outer shelf domain (100–200 m water depth) is an area of intermittent upwelling in spring and summer, high productivity, strong stratification, and abundant potential predators (Coyle et al., 2011; Hunt et al., 2002; Springer et al., 1996). The slope domain (>200 m water depth) adjoins the Aleutian Basin and is predicted to provide lower growth potential to larvae due to lower prey availability and temperature (Napp et al., 2000). Among the hydrographic domains, walleye pollock larvae are exposed to depth strata with distinct flow regimes, thermal regimes, predation pressures, and prey availability.

Although walleye pollock spawn in a variety of habitats and water depths in the North Pacific, ontogenetic and diel vertical migrations are known for relatively few areas and we have limited knowledge of how habitat interacts with vertical distributions. Vertical distributions have been studied most extensively in the Gulf of Alaska (GOA). In the GOA, walleye pollock early life stages undergo OVM. Eggs occur between 150 and 200 m depth (Kendall et al., 1994), yolk sac larvae rise gradually to the surface where feeding larvae are found above the thermocline (Davis and Olla, 1994), and juveniles are primarily pelagic (Brodeur and Wilson, 1996; Laurel et al., 2007). By comparison, in the shallow-water Funka Bay, Japan, eggs and larvae are found at depths less than 50 m with no indication of OVM (Kamba, 1977; Kendall et al., 1987). In the laboratory, regular DVM is initiated once GOA larvae reach 6 mm standard length (SL) and are feeding (Davis and Olla, 1994; Olla and Davis, 1990a). Kendall et al. (1994) found limited DVM in feeding larvae in Shelikof Strait, while larvae in Auke Bay, Alaska, responded to patches of copepod nauplii with regular DVM (Haldorson et al. 1993). Juvenile walleye pollock undergo regular DVM in the western GOA (Brodeur and Rugen, 1994; Olla and Davis, 1990b).

Our knowledge of vertical distributions of SEBS walleye pollock early life stages is limited relative to the GOA (but see Brase, 1996; Hillgruber et al., 1995; Walline, 1981). Egg distribution over the basin is much deeper (400–500 m) than over the shelf (≤ 100 m) (Nishiyama et al., 1986; Serobaba, 1974). Juvenile walleye pollock near the Pribilof Islands undergo regular DVM (similar to the western GOA), presumably in response to prey movement (Schabetsberger et al., 2000). There is currently no assessment of OVM or DVM in SEBS walleye pollock early life stages other than this example. The preferred prey of SEBS larvae, copepod eggs and nauplii, can be found in surface waters and are unlikely to undergo DVM themselves. Fish larvae in the SEBS are exposed to a variety of visual predators (e.g. walleye pollock, Pacific cod) that could drive DVM (Ohman, 1990). Fundamental differences in walleye pollock early life ecology exist between the GOA and SEBS (Bailey, 1989; Duffy-Anderson et al., 2003; Kendall et al., 1994), and it is likely that there are differences in vertical position as well. These differences may be critical, especially in efforts to model transport and habitat use in the SEBS.

The purposes of the present study were: (1) to describe the stage-specific vertical distribution patterns of the early life stages of walleye pollock in the SEBS and (2) to examine potential drivers of differences in distribution such as physical forcing, ontogeny, and trade-offs for survival. To this end, we examined the vertical distribution among life stages for evidence of ontogenetic vertical migration, we compared vertical distributions of each stage among time of day to test for diel vertical migration, and we assessed the interactions between the physical water column and habitat and vertical distribution patterns.

2. Materials and methods

2.1. Study area

The SEBS is bordered to the east by Alaska, to the south by the Alaska Peninsula and eastern Aleutian Islands, to the west by the Aleutian Basin, and to the north by Nunivak Island. Walleye pollock spawning areas included in this study were north of Unimak Island (Bering Canyon), the Alaska Peninsula and near the Pribilof Islands and Pribilof Canyon (Fig. 1). Shelf domains include the coastal domain (<50 m), the middle domain (50–100 m), the outer shelf domain (100–200 m), and the slope domain (depths >200 m, Fig. 1, Coachman, 1986; Stabeno et al., 2001).

2.2. Sampling for Ichthyoplankton vertical distributions

Vertical distributions were determined from depth-specific densities (number per 1000 m³ of water sampled) derived from sampling with a 1 m⁻² Multiple Opening and Closing Net and Environmental Sensing System (MOCNESS, 333 or 505 μ m mesh equipped with a flow meter to estimate volume filtered by each net). The larger mesh size was used when large phytoplankton blooms were present and clogged the smaller mesh. In a comparative study, Wiebe et al. (1976) found no difference in catchability for walleye pollock early life stages between the two mesh sizes so samples were pooled across mesh size. Walleye

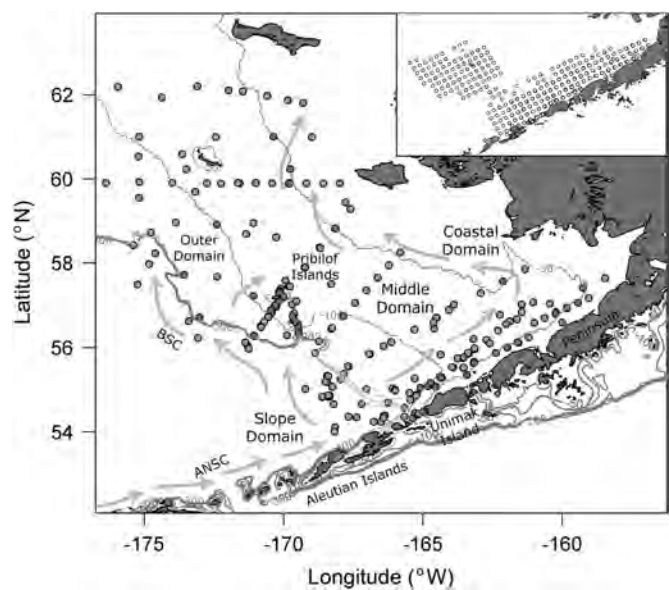


Fig. 1. Vertical distribution tows collected by MOCNESS (gray circles) from 1992 to 2009. Major currents (gray arrows) in this area include the Bering Slope Current (BSC) and the Aleutian North Slope Current (ANSC). Gray lines indicate the 50, 100, 200, and 1000 m isobaths. Walleye pollock spawning areas include the Alaska Peninsula, Bering Canyon (west of Unimak Island), and Pribilof Canyon (south of the Pribilof Islands). Hydrographic domains include three shelf domains (outer, middle, and coastal) and one off-shelf domain (slope). Inset: neuston samples (open circles) collected in 2003 and 2005–2009.

Table 1

Sampling for vertical distribution of walleye pollock (*Theragra chalcogramma*) in the southeastern Bering Sea 1992–2009.

Year	Cruise	Date range (month/day)	MOCNESS tows	CWMD tows	High-resolution tows	Neuston tows
1992	2MF92	4/16–4/22	20	6	0	0
1993	3MF93	4/17–4/28	17	4	0	0
1994	4MF94	4/16–4/27	9	5	0	0
1995	6MF95	4/23–4/30	5	2	2	0
	7MF95	5/5–5/16	9	3	3	0
1996	10MF96	9/7–9/15	21	19	18	0
1997	9MF97	9/11–9/17	13	2	2	0
1999	1MF99	4/17–4/18	6	6	6	0
2003	4MF03	5/18–5/24	9	9	9	53
2005	5MF05	5/10–5/18	20	20	20	71
2006	3MF06	5/9–5/18	12	12	10	90
	6MF06	9/11–9/22	9	9	6	86
2007	4MF07	5/8–5/17	2	2	2	83
2008	1MF08	2/19–2/26	8	8	8	0
	3DY08	5/12–5/21	7	7	7	64
	2HE08	7/3–7/17	44	44	0	0
2009	3DY09	5/8–5/17	2	2	2	77
	1KN09	6/13–7/10	91	91	0	0

1–3 cruises each year conducted MOCNESS tows with a wide range of depth intervals (MOCNESS tows), tows with depth intervals less than 20 m used for catch-weighted mean depths (CWMD tows), tows with depth intervals of 10 m (high-resolution tows), and/or neuston tows.

pollock early life stages were collected in MOCNESS tows in 13 years between 1992 and 2009 (Table 1) by NOAA's Fisheries-Oceanography Coordinated Investigations (FOCI) program. A tow is defined as the unit of sampling with multiple nets within a given tow. Concentration records were divided into stages based on standard length and developmental attributes outlined in the Ichthyoplankton Information System (<http://access.afsc.noaa.gov/ichthyo/index.cfm>). Catches were divided into five life stages: eggs, yolk sac larvae (<4.5 mm SL), preflexion larvae (4.5–9.9 mm SL), postflexion larvae (10.0–24.9 mm SL), and early juveniles (25.0–64.9 mm SL). MOCNESS tows are not ideal for sampling the very surface of the water column, which can contain buoyant eggs. To supplement the information derived from MOCNESS tows, egg densities from Sameoto neuston tows (30×50 cm² mouth opening, 333 or 505 μm mesh), which fished the upper 25 cm of the water column, also were examined in 2003 and 2005–2009.

Temperature and density data were derived from vertical CTD (Sea Bird 19 or 25, Sea-Bird Electronics, Bellevue, Washington, USA) profiles collected concurrently with ichthyoplankton samples from 2002 to 2009. Prior to 2002, CTD vertical profiles matching ichthyoplankton tows in space and time were obtained from the EPIC data archive maintained by the Pacific Marine Environmental Laboratory (<http://www.epic.noaa.gov/epic/>). Thermo- and pycnocline depths were extracted from CTD casts for each MOCNESS tow. The thermo- and pycnocline depths were defined as the depth at which the greatest rate of change in temperature or density occurred (Coyle and Pinchuk, 2005). Only thermocline depth was examined because pycnocline depth was correlated with thermocline depth. Years were assigned to either cold or warm temperature categories based on May sea surface temperature anomalies (see Smart et al., 2012, for details) to test for differences in vertical distribution with prevailing annual conditions in the study area.

2.3. Ontogenetic vertical migration

Net depth intervals of MOCNESS tows were inconsistent across years and cruises, ranging from 10-m to 100-m intervals. Tows with net depth intervals greater than 20-m in the upper 50 m of the water column were removed from analysis. For the remaining tows, we converted depth-specific concentrations of each stage to

catch-weighted-mean depths (CWMD) to provide a comprehensive view of vertical distribution. CWMD was calculated by the following equation:

$$CWMD = \frac{\sum_{i=1}^n x_i d_i}{\sum_{i=1}^n x_i} \quad (1)$$

where x_i is the concentration of each stage at each depth interval i , d_i is the midpoint of each depth interval, and n is the total number of depth intervals in each tow. CWMDs were compared by a two-way analysis of covariance (ANCOVA) with stage and temperature category as fixed factors and day of year (DOY), thermocline depth (m), and bottom depth (m) as covariates (Sokal and Rohlf, 1995). The concentration of eggs in neuston tows was compared by one-way ANCOVA with temperature category as a fixed factor and thermocline depth and bottom depth as covariates. Neuston samples were collected primarily during two weeks in May, so we did not examine DOY as a covariate.

2.4. Diel vertical migration

Tows that sampled in 10-m net depth intervals in the upper 50 m of the water column (high-resolution tows) were used to examine diel vertical migration behavior of early life stages. Depth strata of high-resolution tows were 0–10 m, 10–20 m, 20–30 m, 30–40 m, 40–50 m, 50–100 m, 100–200 m, and 200–300 m. Concentrations collected at each depth strata varied widely among samples and tows. Depth-specific concentrations from high-resolution tows were standardized among tows by conversion to the proportion of the total concentration in each tow collected at each depth stratum to remove any effect of differences in concentration among domains, years, or times of day. Each tow was assigned to either day time or night time (time of day, TOD) based on time and date of collection (Brodeur and Rugen, 1994). Tows collected in February between 0900 and 1900 were considered day time tows and tows collected between 1900 and 0900 were considered night time tows, in April and May, day time was 0630–2130 and night time was 2130–0630, and in September day time was 0700–2100 and night time was 2100–0700. Dusk and dawn categories were not used because there was no replication available for these time periods. Each tow also was assigned to a shelf domain to compare distributions among habitats.

The effects of depth stratum, TOD, and domain on proportion of each stage were examined using generalized additive mixed models (GAMMs) with TOD as a fixed factor, depth stratum and domain as continuous covariates, and tow as a random variable (Zuur et al., 2009). Temperature and bottom depth were initially examined as continuous covariates but were not chosen during the model fitting process. Models were fitted by comparing Akaike's Information Criterion values and removing non-significant variables until the best fit model was selected (Akaike, 1974). The negative binomial error distribution was a better fit to the data compared to other alternatives, such as the Poisson, Gaussian, and lognormal distributions. Interactions between depth stratum and TOD were included to test for diel vertical migration. Interactions between depth stratum and domain were included to test for differences in vertical distributions among areas or habitats.

3. Results

3.1. Sampling for ichthyoplankton vertical distributions

Catches ranged from no early life stages collected to depth-specific concentrations of up to 540,000 individuals 1000 m⁻³. Over 200,000 walleye pollock eggs, 34,000 larvae, and 125 early juveniles were collected by MOCNESS sampling since 1992.

3.2. Ontogenetic vertical migration

Walleye pollock CWMD and variability in CWMD decreased with ontogeny (Tables 2 and 3). CWMD was influenced by DOY, bottom depth, and thermocline depth. CWMD of all stages decreased with DOY (Table 3). CWMD of all stages except postflexion larvae increased with bottom depth (Table 3). CWMD of all stages except early juveniles increased with thermocline depth (Table 3). There was no difference in stage-specific CWMD or overall CWMD with temperature category. Eggs were collected at higher densities in surface neuston tows in cold years than in warm years (Table 4).

3.3. Diel vertical migration

There was no evidence of DVM in walleye pollock eggs (Table 5, Fig. 2), but the domain in which they were collected interacted with the depth stratum in which proportion of total egg concentration was highest (Table 5, Fig. 3). Eggs were found ≤ 30 m in all three shelf domains but ≥ 100 m over the slope. Walleye pollock eggs occurred throughout the water column, but proportion of concentration was higher in the upper 20 m or below 100 m relative to the middle of the water column. There was no difference in yolksac larval depth distribution between TODs (Table 5, Fig. 4). There were not enough replicate samples in multiple domains to assess for yolksac larvae. Yolksac larvae occurred at depths less than 100 m, and proportion of concentration was highest from 10–40 m relative to other depth strata.

For the two feeding larval stages, differences evidence for DVM were found. Preflexion larval depth distribution differed between TODs although the level of significance was marginal (Table 5, Fig. 5). Overall, preflexion larvae were shallower and more concentrated in the day time than at night time. Preflexion larvae were shallower over the shelf (10–20 m) than over the slope (20–30 m, Fig. 6). The interactions between depth strata and TOD were significant for postflexion larvae (Table 5). Postflexion larvae exhibited regular DVM; deeper during the day (10–40 m) than at night (0–20 m, Fig. 7). Domain did not interact with depth

Table 2
Ontogenetic vertical distributions.

	Eggs	Yolksac larvae	Preflexion larvae	Postflexion larvae	Early juveniles
Mean	33.1	29.3	21.5	20	18.5
Std. Dev.	46.7	15.4	11.4	10.1	8.9

Summary of catch-weighted-mean depths (m; mean and standard deviations [Std. Dev.]) of walleye pollock (*Theragra chalcogramma*) early life stages in the South-eastern Bering Sea.

Table 3
Ontogenetic vertical distribution analyses.

Factor	df	SS	MS	F	p
Stage	4	1.05×10 ⁴	2.60×10 ³	2.743	0.029
Temperature	1	3.00×10 ²	3.00×10 ²	0.314	0.575
Stage×Temperature	4	1.14×10 ³	2.84×10 ²	0.299	0.878
DOY	1	1.76×10 ⁴	1.76×10 ⁴	18.592	< 0.001
Bottom depth	1	1.14×10 ⁴	1.14×10 ⁴	11.991	0.001
Thermocline depth	1	9.09×10 ³	9.09×10 ³	9.577	0.002
Error	340	3.23×10 ⁵	9.49×10 ²		

Comparisons of catch-weighted-mean depths of walleye pollock (*Theragra chalcogramma*) early life stages and the physical characteristics that influence them. Degrees of freedom (df), sum of squares (SS), mean squares (MS), and f-ratios (F) are shown for all stages. P-values (p) in bold were significant at $\alpha=0.05$.

Table 4
Ontogenetic vertical migration.

Factor	df	SS	MS	F	p
Temperature	1	4.03×10 ⁹	4.03×10 ⁹	5.745	0.017
Bottom depth	1	1.04×10 ⁹	1.04×10 ⁹	1.481	0.224
TC depth	1	1.12×10 ⁹	1.12×10 ⁹	1.598	0.207
Error	513	3.60×10 ¹¹	7.02×10 ⁸		

Comparisons of walleye pollock (*Theragra chalcogramma*) egg densities in the surface neuston layer and the physical characteristics that influence them. Degrees of freedom (df), sum of squares (SS), mean squares (MS), and f-ratios (F) are shown. P-values (p) in bold were significant at $\alpha=0.05$.

Table 5
Diel vertical distributions.

Stage	Factor	df	F	p
Eggs	Depth	2.85	19.3	< 0.001
	TOD	1	0.6	0.439
	Domain	1	9.65	0.002
	Depth×TOD	3.91	3.88	0.1
	Depth×Domain	8	8.25	0.001
Yolksac larvae	Depth	2.72	8.08	0.001
	TOD	1	0.11	0.738
	Depth×TOD	4.1	2.48	0.349
Preflexion larvae	Depth	2.84	23.4	< 0.001
	TOD	1	0.34	0.561
	Domain	1	0.17	0.678
	Depth×TOD	3.26	7.12	0.034
	Depth×Domain	4.21	3.89	0.046
Postflexion larvae	Depth	2.42	6.67	0.001
	TOD	1	0.04	0.847
	Domain	1	0.56	0.455
	Depth×TOD	2.78	4.48	0.014
	Depth×Domain	2.65	2.01	0.131
Early juvenile	Depth	2.49	3.39	0.03
	TOD	1	0.01	0.951
	Domain	1	0.01	0.963
	Depth×TOD	2.83	2.44	0.144
	Depth×Domain	2.63	0.65	0.616

Generalized additive mixed models for differences in proportion of total density of walleye pollock (*Theragra chalcogramma*) early life stages among depth strata (Depth), times of day (TOD), and domains. Degrees of freedom (df) or estimated degrees of freedom, f-ratios (F), and p-values (p). P-values in bold were significant at $\alpha=0.05$.

stratum for postflexion larvae (Fig. 8). Proportion of postflexion larval concentration was highest above 30 m and lowest below 30 m relative to other strata.

Sample sizes for early juveniles were low relative to the other stages. Early juveniles tended to occur deeper at night than during the day, but the interaction between TOD and depth strata was not significant (Table 5, Fig. 9). Early juvenile vertical distribution was not affected by domain (Fig. 10). Early juveniles occurred at depths less than 100 m with greatest concentration from 0 to 20 m.

4. Discussion

Ontogenetic and diel vertical migrations have adaptive significance for planktonic organisms, including optimal transport, energy conservation, access to prey, and avoidance of predators (Fortier and Leggett, 1983; Hare and Govoni, 2005; Hunter and Sanchez, 1976). For walleye pollock in the SEBS, spawning occurs in either deep-water canyons or over the shelf, eggs are buoyant, and juveniles are abundant over the shelf. Here, prey concentrations are highest in the upper water column and visual predators occur in the water column and near the benthos. Based on these

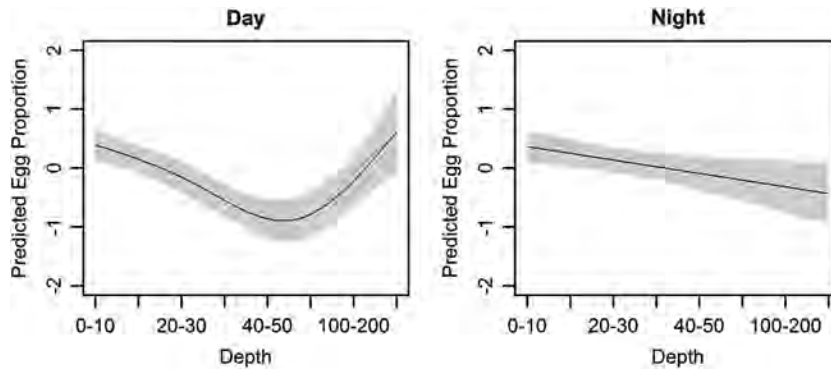


Fig. 2. Vertical distribution of southeastern Bering Sea walleye pollock (*Theragra chalcogramma*) eggs during day and night from high-resolution MOCNESS tows. Line represents predicted proportions for each depth interval with 95% confidence intervals (shaded area).

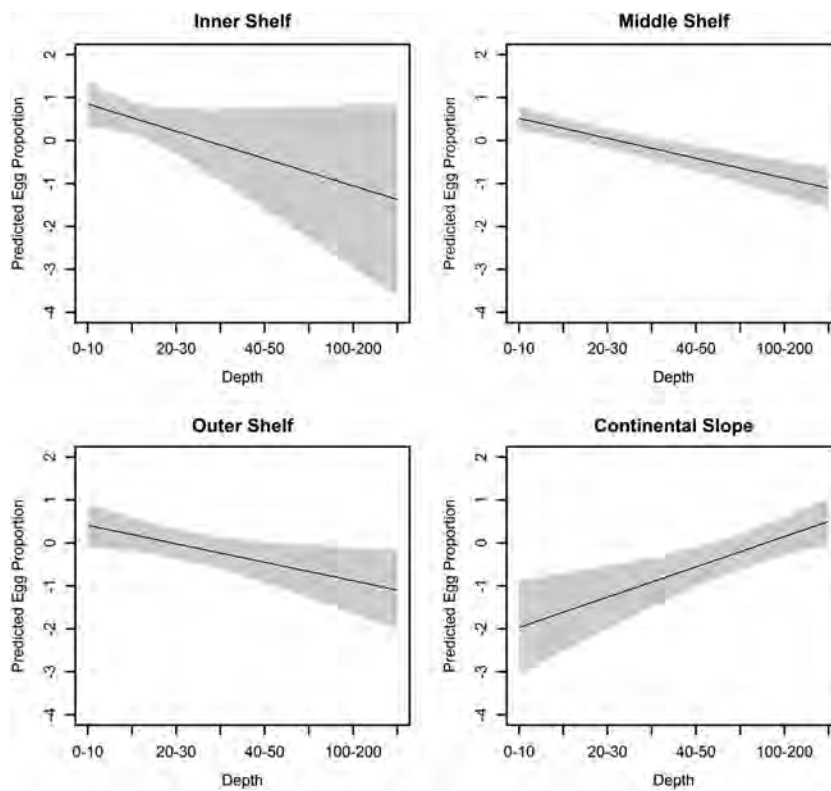


Fig. 3. Vertical distribution of southeastern Bering Sea walleye pollock (*Theragra chalcogramma*) eggs among domains from high-resolution MOCNESS tows. Line represents predicted proportions for each depth interval with 95% confidence intervals (shaded area).

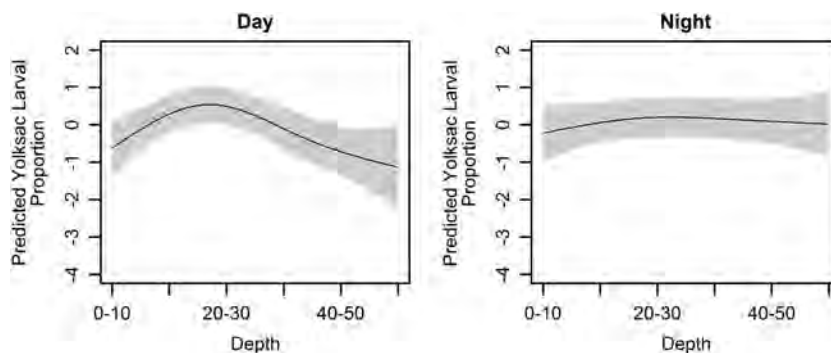


Fig. 4. Vertical distribution of southeastern Bering Sea walleye pollock (*Theragra chalcogramma*) yolk sac larvae during day and night from high-resolution MOCNESS tows. Line represents predicted proportions for each depth interval with 95% confidence intervals (shaded area).

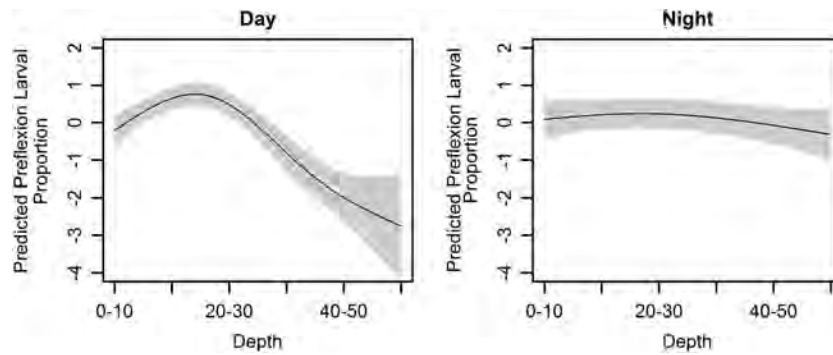


Fig. 5. Vertical distribution of southeastern Bering Sea walleye pollock (*Theragra chalcogramma*) preflexion larvae during day and night from high-resolution MOCNESS tows. Line represents predicted proportions for each depth interval with 95% confidence intervals (shaded area).

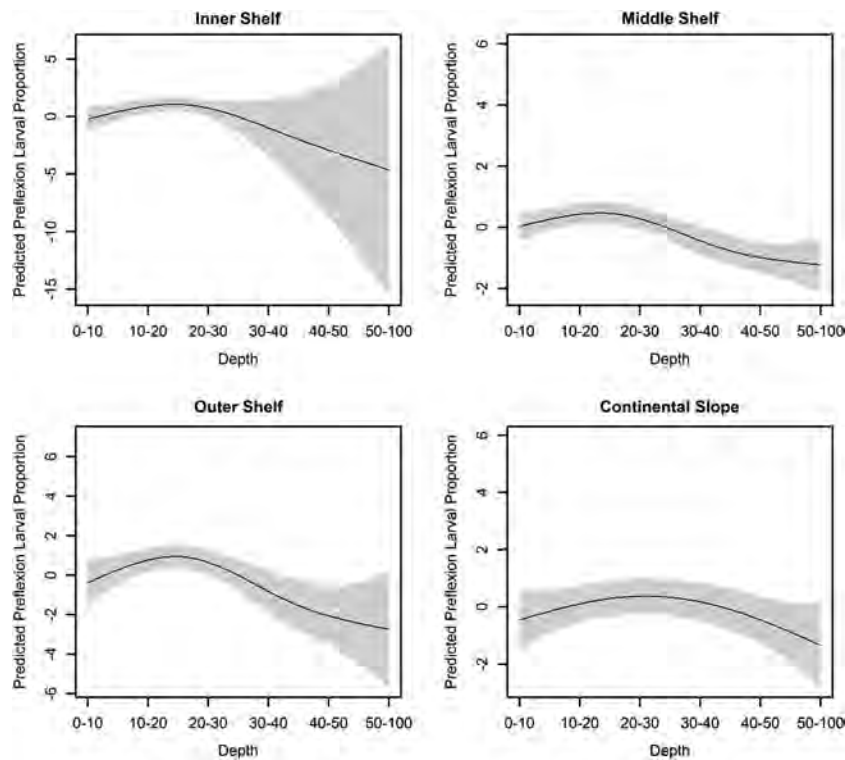


Fig. 6. Vertical distribution of southeastern Bering Sea walleye pollock (*Theragra chalcogramma*) preflexion larvae among domains from high-resolution MOCNESS tows. Line represents predicted proportions for each depth interval with 95% confidence intervals (shaded area).

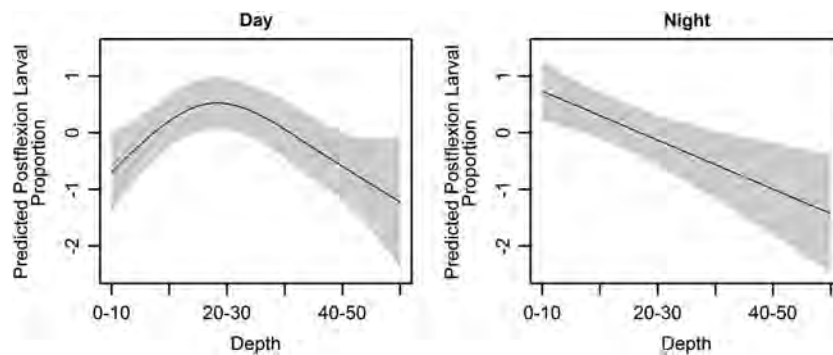


Fig. 7. Vertical distribution of southeastern Bering Sea walleye pollock (*Theragra chalcogramma*) postflexion larvae during day and night from high-resolution MOCNESS tows. Line represents predicted proportions for each depth interval with 95% confidence intervals (shaded area).

characteristics, we would expect vertical migration strategies that maximize on-shelf transport from spawning grounds over the basin or retention over the shelf, such as a decrease in depth of occurrence to provide access to prey and minimize predation risk,

such as OVM and regular DVM (Kerfoot, 1985). For walleye pollock early life stages in the SEBS, depth distribution became shallower and variability in depth distributions decreased with ontogeny supporting OVM, similar to the GOA but unlike Funka Bay.

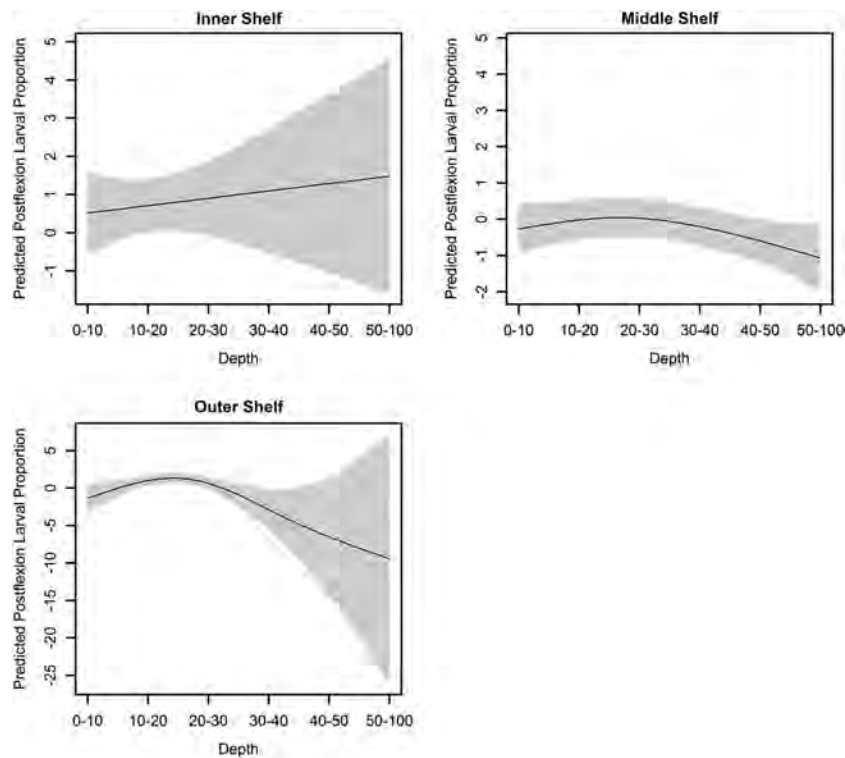


Fig. 8. Vertical distribution of southeastern Bering Sea walleye pollock (*Theragra chalcogramma*) postflexion larvae among domains from high-resolution MOCNESS tows. Line represents predicted proportions for each depth interval with 95% confidence intervals (shaded area).

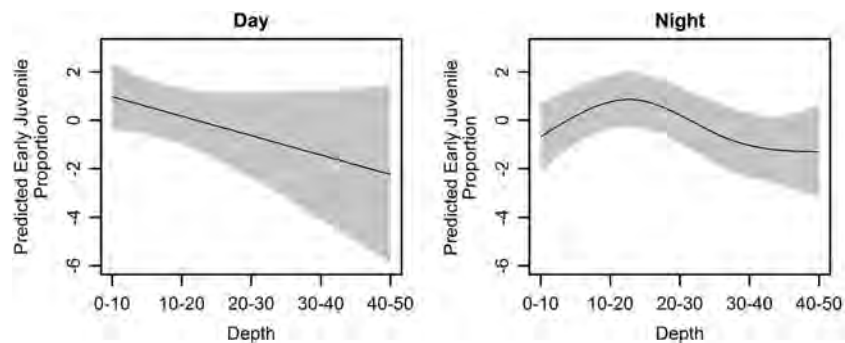


Fig. 9. Vertical distribution of southeastern Bering Sea walleye pollock (*Theragra chalcogramma*) early juveniles during day and night from high-resolution MOCNESS tows. Line represents predicted proportions for each depth interval with 95% confidence intervals (shaded area).

Weighted mean depths decreased with the progression of summer as stratification tended to increase. Weighted mean depths also decreased as bottom depth decreased and as the thermocline depth decreased (except juveniles), suggesting that distributions mirror the breadth of the available water column. Two of the five early life stages examined exhibited evidence of DVM: reverse in preflexion larvae and regular in postflexion larvae. These two stages are active feeders, while eggs and yolk sac larvae are nonmotile or weak swimmers and would not be expected to exhibit distribution patterns typically associated with active behaviors. Sample sizes for early juveniles were too small to assess DVM adequately.

OVM in walleye pollock provides several advantages for the early life stages. First, the majority of eggs over the slope were found deeper than 40 m, where they are exposed to the deep water Aleutian North Slope Current through Bering Canyon or the Bering Slope Current through Pribilof Canyon. Eggs spawned offshore, therefore, can be transported onto the shelf by these currents rather than advected further over the Aleutian Basin by cyclonic flow above these currents (Reed and Stabeno, 1999). Second, high

egg densities were observed in the neuston layer over the shelf in cold years when surface temperatures were comparable to temperatures below in deep water in warm years (Stabeno et al., 2012), allowing for extended development times and, by extension, the potential for increased time for on-shelf transport in cold years, regardless of the vertical position. High egg densities in the surface layer in cold years could be the result of a passive rise to the surface in the absence of a distinct density structure in the water column or the result of delayed hatching at low temperatures. Third, yolk sac larvae in the cooler waters below 20 or 30 m depth will conserve energy and extend the period of time before yolk reserves are exhausted and exogenous feeding must begin, which can be advantageous if larvae have not been transported far enough over the shelf to where prey are available. Fourth, following the rise to the upper 20 m of the water column, feeding larvae have access to prey in the upper water column (Coyle and Pinchuk, 2005) and warmer water, both of which reduce development time.

DVM typically is exhibited by feeding stages reacting to changes in time of day and light intensity, and walleye pollock conform to this pattern. As expected, neither eggs nor yolk sac

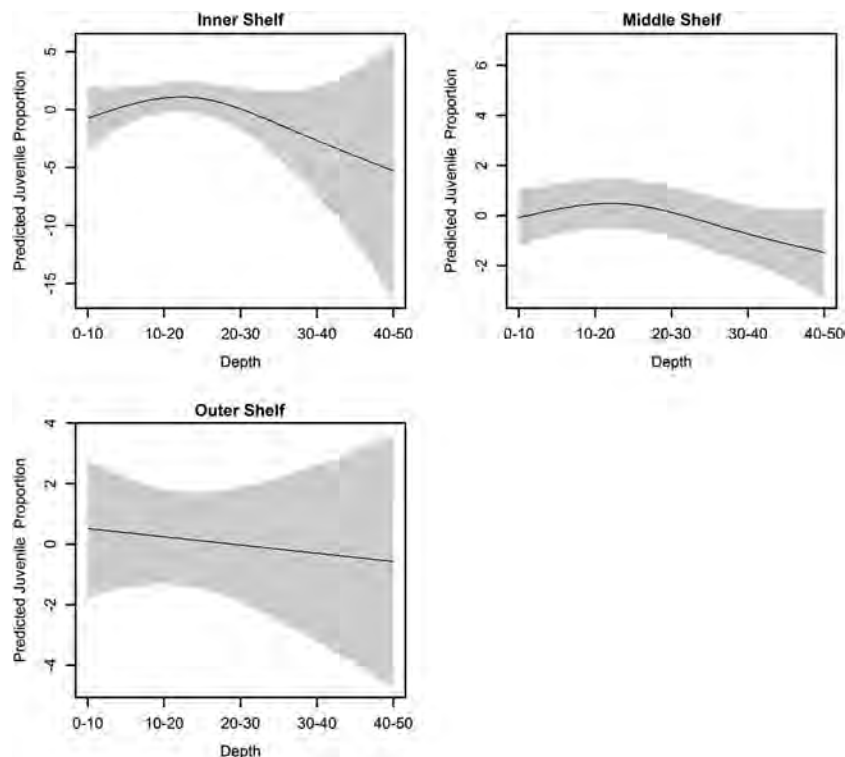


Fig. 10. Vertical distribution of southeastern Bering Sea walleye pollock (*Theragra chalcogramma*) early juveniles among domains from high-resolution MOCNESS tows. Line represents predicted proportions for each depth interval with 95% confidence intervals (shaded area).

larvae exhibited a pattern consistent with DVM. Vertical distributions of nonmotile or nonfeeding stages are driven generally by physics such as buoyancy or passive mixing. These two early stages displayed passive patterns which also suggests that diel differences in vertical distribution exhibited by feeding stages was driven by behavior rather than by diel changes in the physical water column. In preliminary analyses, we found no differences in the thermocline depth between day and night. Surprisingly, we were unable to conclude that early juvenile walleye pollock undergo DVM, although they tended to be deeper at night in the few tows in which they were collected. There is evidence from both laboratory (Sogard and Olla, 1996) and field (Bailey, 1989) studies that vertical migration in shorter juveniles (<60 mm) in the GOA is weak and the migration to deeper layers intensifies as the fish gain locomotory and sensory capabilities. Schabetsberger et al. (2000) documented DVM in juvenile walleye pollock between 30 and 92 mm SL near the Pribilof Islands. The juveniles in the present study were all shorter than 65 mm SL, supporting that DVM in these shorter fish is weak in the SEBS and consistent with the previous findings in the GOA. However, we were unable to address any impacts of predator presence or net avoidance in the current study.

Walleye pollock feeding larvae appear to take advantage of surface food concentrations, as they primarily occurred shallower than 30 or 40 m at the onset of feeding. We did not have samples to determine directly the vertical distributions of the preferred prey items, copepod eggs and nauplii. Walleye pollock undergo a transition from predominantly day time feeding as larvae (Canino and Bailey, 1995) to nocturnal feeding as juveniles (Brodeur et al., 2000). This is allowed by increased visual acuity and sensitivity to light with ontogeny (Carvalho et al., 2004; Miller et al., 1993). Preflexion larval distributions were consistent with reverse DVM (up during the day, down at night) and postflexion larvae underwent regular DVM (down and variable during the day, up at night), suggesting that different trade-offs between prey access, predator

avoidance, and perhaps physical forces could be acting on the two stages. Other studies have found that copepod nauplii do not undergo diel vertical migrations (Haldorson et al., 1993; Irigoien et al., 2004). By moving into surface waters during the day when light levels are high and where their preferred prey likely occur (Brase, 1996; Hillgruber et al., 1995), preflexion larvae could have higher success capturing prey since visual acuity is low relative to later stages. Postflexion larvae would have higher capture success in surface waters at night at reduced light levels than preflexion larvae because of their improved visual acuity. Postflexion larvae are large enough to be of interest to visual predators such as older age class walleye pollock (Juanes, 2003), which could lead to the pattern of avoiding surface waters during the day. Alternately, postflexion larvae in surface waters during the day may have been better able to avoid our collection gears due to their visual acuity and swimming abilities.

Walleye pollock vertical distributions vary among habitats both in the SEBS and the GOA. Forward et al. (1996) found three different patterns of vertical distribution for Atlantic menhaden (*Brevoortia tyrannus*) in three separate studies and suggested that vertical behaviors are flexible in order to incorporate necessary trade-offs that vary between ecosystems or habitats. Eggs in the SEBS were concentrated either below 100 m (slope) or in the upper 30 m (shelf domains), indicative of where they were spawned and probably their buoyancy (Kendall and Nakatani, 1992). SEBS yolksac larvae were concentrated around 30 m. In the GOA, eggs are spawned at or below 150 m, followed by an increase in depth prior to hatching (Kendall et al., 1994). GOA yolksac larvae remain at depths >150 m for several more days. One obvious difference between these systems is the depth of the water column and depth of spawning activity. Olla et al. (1996) proposed that remaining at the spawning depth in the GOA provided a predator refuge for eggs and yolksac larvae, an option that is not available in most of the SEBS habitats due to their relatively shallow water column. SEBS preflexion larvae underwent reverse DVM in most habitats and no DVM in the coastal domain. DVM is

either regular or absent for preflexion larvae in the GOA (Davis and Olla, 1994; Olla and Davis, 1990a). In the shallow-water coastal domain, the stimulus to move up during the day (e.g. sufficient light for hunting) may not be in place for SEBS preflexion larvae because sufficient light levels are available throughout the shallow (≤ 50 m) water column (Kendall and Nakatani, 1992). Similar to larvae in the GOA, coastal domain SEBS preflexion larvae also could respond to very high light levels at the surface during the day with negative phototaxis (Olla and Davis, 1990a). Postflexion larvae in the SEBS undergo regular DVM, in accordance with behavior observed near Auke Bay, Alaska, GOA (Haldorson et al., 1993). In Auke Bay, larvae migrated in response to the trade-off between the vertical distribution of nauplii and avoidance of predators. For postflexion larvae, visual predators occur in all areas in which this stage was collected and the same potential predators occur in the SEBS, suggesting that the trade-off between feeding and predation risk could be a common factor across habitats and ecosystems for this stage. We did not find support for DVM in SEBS early juveniles most likely due to small sample sizes, but juveniles undergo regular DVM in the GOA (Brodeur and Rugen, 1994; Olla and Davis, 1990b) and larger juveniles near the Pribilof Islands in the SEBS undergo regular DVM in response to prey movement (Schabetsberger et al., 2000).

Smart et al. (2012) found shifts in the spatial distributions of walleye pollock larvae and juveniles between cold years and warm years. The authors hypothesized that spatial shifts were driven by changes in area-specific mortality or transport. Satellite-tracked drifters and hydrographic models show high variation in on- and off-shore transport among years (Danielson et al., 2011; Stabeno et al., 2012), which could be linked to temperature conditions (Sohn et al., 2010) and might explain the differences in spatial distribution. Annual differences in vertical distributions could impact the amount of transport off-shore if larvae respond to variations in conditions with adjustments in their vertical distributions (Napp et al., 2000). We found no support for differences in vertical distributions related to categorizing years as either cold or warm.

5. Conclusions

Current speeds in the SEBS middle shelf tend to be slow relative to other spawning areas for walleye pollock (<5 cm s^{-1} , Napp et al., 2000). Because of these slow speeds, the probability of retention over the spawning grounds is high. Some off-shelf spawning grounds such as Bering Canyon may not have the highest growth potential, thus selection for an ontogenetic migration toward the surface where transport onto the shelf would be enhanced is likely in the SEBS. Walleye pollock early life stages underwent ontogenetic vertical migration and feeding stages were found in the upper portion of the water column where prey availability is high typically. Feeding larvae also exhibited diel vertical migrations that suggest trade-offs occurred between access to prey and exposure to predators. Characteristics of the habitat and ecology of each stage suggested that some determinants of vertical distribution are common between the SEBS and GOA (i.e. prey, light levels, predators) while others are not (i.e. depth refuges, spawning depth). Several hypotheses developed for the SEBS have linked variation in recruitment to the level of overlap between juveniles and their predators or juveniles and their prey, which in turn may be related to the extent and direction of transport. For example, Wespestad et al. (2000) found that strong year classes were linked to high spatial segregation of juveniles and cannibalistic older age classes. The authors proposed that juvenile distribution was closely tied to the transport and distribution of eggs and larvae. One way to address the connection between these various life stages is to model transport. Our results

clearly demonstrated that pollock larvae are not passive particles, early life stages are not distributed randomly throughout the water column, and vertical distributions from the GOA are not comparable to all stages in the SEBS. Accurate modeling needs to account for variation in vertical distribution and behavior among stages and habitats, and these data are now available for the SEBS.

Acknowledgments

Thanks to the members of NOAA's Ecosystems and Fisheries Oceanography Coordinated Investigations (EcoFOCI) who were involved in the collection and processing of the ichthyoplankton samples. This research was supported by the Bering Sea Integrated Ecosystem Research program (BSIERP) of the North Pacific Research Board and the North Pacific Climate Regimes and Ecosystem Productivity (NPCREP) program of the National Oceanographic and Atmospheric Administration. This paper is EcoFOCI Contribution no. N754—RAOA—N789, BEST-BSIERP Publication no. 89, and NPRB Publication no. 407. We appreciate comments by Jeffrey Napp, Morgan Busby, Thomas Hurst, and three anonymous reviewers.

References

- Akaike, H., 1974. A new look at the statistical model identification. *IEEE Trans. Autom. Control* 19, 716–723.
- Bacheler, N.M., Ciannelli, L., Bailey, K.M., Duffy-Anderson, J.T., 2010. Spatial and temporal patterns of walleye pollock spawning in the eastern Bering Sea inferred from egg and larval distributions. *Fish. Oceanogr.* 19, 107–120.
- Bailey, K.M., 1989. Interaction between the vertical distribution of juvenile walleye pollock *Theragra chalcogramma* in the eastern Bering Sea and cannibalism. *Mar. Ecol. Prog. Ser.* 53, 205–213.
- Brase, A.L.J., 1996. Temporal Variation in Feeding of Larval Walleye Pollock (*Theragra chalcogramma*) in the Southeastern Bering Sea shelf region. M.Sc. Thesis, University Alaska, Fairbanks, AK.
- Brodeur, R.D., Rugen, W.C., 1994. Diel vertical distribution of ichthyoplankton in the northern Gulf of Alaska. *Fish. Bull.* 92, 223–235.
- Brodeur, R.D., Wilson, M.T., 1996. A review of the distribution, ecology, and population dynamics of age-0 walleye pollock in the Gulf of Alaska. *Fish. Oceanogr.* 5, 148–166.
- Brodeur, R.D., Wilson, M.T., Ciannelli, L., 2000. Spatial and temporal variability in feeding and condition of age-0 walleye pollock (*Theragra chalcogramma*) in frontal regions of the Bering Sea. *ICES J. Mar. Sci.* 57, 256–264.
- Canino, M.F., Bailey, K.M., 1995. Gut evacuation of walleye pollock larvae in response to feeding conditions. *J. Fish. Biol.* 46, 389–403.
- Carvalho, P.S.M., Noltie, D.B., Tillitt, D.E., 2004. Biochemical, histological and behavioural aspects of visual function during early development of rainbow trout. *J. Fish Biol.* 64, 833–850.
- Coachman, L.K., 1986. Circulation, water masses, and fluxes on the southeastern Bering Sea shelf. *Cont. Shelf Res.* 5, 23–108.
- Coyle, K.O., Pinchuk, A.I., 2005. Seasonal cross-shelf distribution of major zooplankton taxa on the northern Gulf of Alaska shelf relative to water mass properties, species depth preferences and vertical migration behavior. *Deep-Sea Res. II* 52, 217–245.
- Coyle, K.O., Eisner, L.B., Mueter, F.J., Pinchuk, A.I., Janout, M.A., Cieciel, K.D., Farley, E. V., Andrews, A.G., 2011. Climate change in the southeastern Bering Sea: impacts on pollock stocks and implications for the oscillating control hypothesis. *Fish. Oceanogr.* 20, 139–156.
- Danielson, S., Eisner, L., Weingartner, T., Aagaard, K., 2011. Thermal and haline variability over the central Bering Sea shelf: Seasonal and interannual perspectives. *Cont. Shelf Res.* 31, 539–554.
- Davis, M.W., Olla, B.L., 1994. Ontogenetic shift in geotaxis for walleye pollock, *Theragra chalcogramma*, free embryos and larvae: potential role in controlling vertical distribution. *Environ. Biol. Fishes.* 39, 313–318.
- Duffy-Anderson, J.T., Ciannelli, L., Honkalehto, T., Bailey, K.M., Sogard, S.M., Springer, A.M., Buckley, T., 2003. Distribution of Age-1 and Age-2 Walleye Pollock in the Gulf of Alaska and Eastern Bering Sea: Sources of Variation and Implications for Higher Trophic Levels. Institute of Marine Research, Bergen Norway, Postboks 1870 Nordnes N-5817.
- Fiksen, O., Jørgensen, C., Kristiansen, T., Vikebo, F., Huse, G., 2007. Linking behavioral ecology and oceanography: larval behaviour determines growth, mortality and dispersal. *Mar. Ecol. Prog. Ser.* 347, 195–205.
- Fortier, L., Leggett, W.C., 1983. Vertical migrations and transport of larval fish in a partially mixed estuary. *Can. J. Fish. Aquat. Sci.* 40, 1543–1555.
- Forward Jr., R.B., Tankersley, R.A., Burke, J.S., 1996. Endogenous swimming rhythms of larval Atlantic menhaden *Brevoortia tyrannus* Latrobe: Implications for vertical migration. *J. Exp. Mar. Biol. Ecol.* 204, 195–207.

- Haldorson, L., Prichett, M., Paul, A.J., Ziemann, D., 1993. Vertical distribution and migration of fish larvae in a Northeast Pacific bay. *Mar. Ecol. Prog. Ser.* 101, 67–81.
- Hare, J.A., Govoni, J.J., 2005. Comparison of average larval fish vertical distributions among species exhibiting different transport pathways on the southeast United States continental shelf. *Fish. Bull.* 103, 729–736.
- Heath, M.R., Henderson, E.W., Baird, D.L., 1988. Vertical distribution of herring larvae in relation to physical mixing and illumination. *Mar. Ecol. Prog. Ser.* 47, 211–228.
- Hillgruber, N., Haldorson, L.J., Paul, A.J., 1995. Feeding selectivity of larval walleye pollock *Theragra chalcogramma* in the oceanic domain of the Bering Sea. *Mar. Ecol. Prog. Ser.* 120, 1–10.
- Hinckley, S., 1987. The reproductive biology of walleye pollock, *Theragra chalcogramma*, in the Bering Sea, with reference to spawning stock structure. *Fish. Bull.* 85, 481–498.
- Hunt, G.L., Stabeno, P.J., Walters, G., Sinclair, E., Brodeur, R.D., Napp, J.M., Bond, N.A., 2002. Climate change and control of the southeastern Bering Sea pelagic ecosystem. *Deep-Sea Res. II* 49, 5821–5853.
- Hunter, J.R., Sanchez, C., 1976. Diel changes in swim bladder inflation of the larvae of the northern anchovy *Engraulis mordax*. *Fish. Bull.* 74, 847–855.
- Irigoin, X., Conway, D.V.P., Harris, R.P., 2004. Flexible diel vertical migration behaviour of zooplankton in the Irish Sea. *Mar. Ecol. Prog. Ser.* 267, 85–97.
- Juanes, F., 2003. The allometry of cannibalism in piscivorous fishes. *Can. J. Fish. Aquat. Sci.* 60, 594–602.
- Kamba, M., 1977. Feeding habits and vertical distribution of walleye pollock, *Theragra chalcogramma* (Pallas), in early life stage in Uchiura Bay, Hokkaido. *Res. Inst. North Pac. Fish. Spec. vol.*, 175–197, Hokkaido University.
- Kendall Jr., A.W., Clarke, M.E., Yoklavich, M.M., Boehlert, G.W., 1987. Distribution, feeding, and growth of larval walleye pollock, *Theragra chalcogramma*, from Shelikof Strait, Gulf of Alaska. *Fish. Bull.* 85, 499–521.
- Kendall Jr., A.W., Incze, L.S., Ortner, P.B., Cummings, S.R., Brown, P.K., 1994. The vertical distribution of eggs and larvae of walleye pollock (*Theragra chalcogramma*) in Shelikof Strait, Gulf of Alaska. *Fish. Bull.* 92, 540–554.
- Kendall Jr., A.W., Nakatani, T., 1992. Comparisons of early-life-history characteristics of walleye pollock *Theragra chalcogramma* in Shelikof Strait, Gulf of Alaska and Funka Bay, Hokkaido. *Japan. Fish. Bull. U.S.* 90, 129–138.
- Kerfoot, W.C., 1985. Adaptive value of vertical migration: Comments on the predation hypothesis and some alternatives. *Contrib. Mar. Sci.* 27, 91–113.
- Kristiansen, T., Joergensen, C., Lough, R.G., Vikeboe, F., Fiksen, O., 2009. Modeling rule-based behavior: habitat selection and the growth-survival trade-off in larval cod. *Behav. Ecol.* 20, 490–500.
- Laurel, B.J., Stoner, A.W., Ryer, C.H., Hurst, T.P., Abookire, A.A., 2007. Comparative habitat associations in juvenile Pacific cod and other gadids using seines, baited cameras and laboratory techniques. *J. Exp. Mar. Biol. Ecol.* 351, 42–55.
- Matarese A.C., Blood, D.M., Picquelle, S.J., Benson, J.L., 2003. Atlas of abundance and distribution patterns of ichthyoplankton from the northeast Pacific Ocean and Bering Sea ecosystems based on research conducted by the Alaska Fisheries Science Center (1972–1996). NOAA Prof Pap NMFS No. 1, NOAA, Seattle, WA.
- Miller, T.J., Crowder, L.B., Rice, J.A., 1993. Ontogenetic changes in behavioural and histological measures of visual acuity in three species of fish. *Environ. Biol. Fish.* 37, 1–8.
- Miller, T.J., 2007. Contribution of individual-based coupled physical-biological models to understanding recruitment in marine fish populations. *Mar. Ecol. Prog. Ser.* 347, 127–138.
- Napp, J.M., Kendall, A.W., Shumacher, J.D., 2000. A synthesis of biological and physical processes affecting the feeding environment of larval walleye pollock (*Theragra chalcogramma*) in the eastern Bering Sea. *Fish. Oceanogr.* 9, 147–162.
- Nishiyama, T., Hirano, K., Haryu, T., 1986. The early life history and feeding habits of larval walleye pollock *Theragra chalcogramma* (Pallas) in the southeast Bering Sea. *INPFC Bull.* 45, 177–227.
- Norcross, B.L., Shaw, R.F., 1984. Oceanic and estuarine transport of fish eggs and larvae: a review. *Trans. Am. Fish. Soc.* 113, 153–165.
- Ohman, M.D., 1990. The demographic benefits of diel vertical migration by zooplankton. *Ecol. Monogr.* 60, 257–281.
- Olla, B.L., Davis, M.W., 1990a. Effects of physical factors on the vertical distribution of larval walleye pollock *Theragra chalcogramma* under controlled laboratory conditions. *Mar. Ecol. Prog. Ser.* 63, 105–122.
- Olla, B.L., Davis, M.W., 1990b. Behavioral responses of juvenile walleye pollock *Theragra chalcogramma* Pallas to light, thermoclines and food: Possible role in vertical distribution. *J. Exp. Mar. Biol. Ecol.* 135, 59–68.
- Olla, B.L., Davis, M.W., Ryer, C.H., Sogard, S.M., 1996. Behavioural determinants of distribution and survival in early stages of walleye pollock, *Theragra chalcogramma*: a synthesis of experimental studies. *Fish. Oceanogr.* 5, 167–178.
- Porter, S.M., Ciannelli, L., Hillgruber, N., Bailey, K.M., Chan, K.-S., Canino, M.F., Haldorson, L.J., 2005. Environmental factors influencing larval walleye pollock *Theragra chalcogramma* feeding in Alaskan waters. *Mar. Ecol. Prog. Ser.* 302, 207–217.
- Reed, R.K., Stabeno, P.J., 1999. The Aleutian north slope current. In: Loughlin, T.R., Ohtani, K. (Eds.), *Dynamics of the Bering Sea*. University of Alaska Sea Grant, Fairbanks AK-SF-99-03.
- Schabetsberger, R., Brodeur, R.D., Ciannelli, L., Napp, J.M., Swartzman, G.L., 2000. Diel vertical migration and interaction of zooplankton and juvenile walleye pollock (*Theragra chalcogramma*) at a frontal region near the Pribilof Islands, Bering Sea. *ICES J. Mar. Sci.* 57, 1283–1295.
- Serobaba, I.I., 1974. Spawning ecology of the walleye pollock, *Theragra chalcogramma*, in the Bering Sea. *J. Ichthyol.* 14 (544), 5–52.
- Smart, T.I., Duffy-Anderson, J.T., Horne, J.K., Farley, E.V., Wilson, C.D., Napp, J.M., 2012. Influence of environmental conditions on walleye pollock eggs, larvae, and juveniles in the southeastern Bering Sea. *Deep-Sea Res. II* 65–70, 196–207.
- Smart, T.I., Duffy-Anderson, J.T., Horne, J.K., 2012. Alternating temperature states influence walleye pollock early life stages in the southeastern Bering Sea. *Mar. Ecol. Prog. Ser.* 455, 257–267.
- Sogard, S.M., Olla, B.L., 1996. Food deprivation affects vertical distribution and activity of a marine fish in a thermal gradient: potential energy-conserving mechanisms. *Mar. Ecol. Prog. Ser.* 133, 43–55.
- Sohn, D., Ciannelli, L., Duffy-Anderson, J.T., 2010. Distribution and drift pathways of Greenland halibut (*Reinhardtius hippoglossoides*) during early life stages in the eastern Bering Sea and Aleutian Islands. *Fish. Oceanogr.* 19, 339–353.
- Sokal, R.R., Rohlf, F.J., 1995. *Biometry: The Principles and Practice of Statistics in Biological Research*. W.H. Freeman and Co., New York.
- Springer, A., McRoy, C.P., Flint, M., 1996. The Bering Sea Green Belt: shelf-edge processes and ecosystem production. *Fish. Oceanogr.* 5, 205–223.
- Stabeno, P.J., Bond, N.A., Kachel, N.B., Salo, S.A., Schumacher, J.D., 2001. On the temporal variability of the physical environment over the south-eastern Bering Sea. *Fish. Oceanogr.* 10, 81–98.
- Stabeno, P.J., Moore, S., Napp, J., Sigler, M., Zerbini, A., 2012. Comparison of warm and cold years on the southeastern Bering Sea shelf and some implications for the ecosystem. *Deep-Sea Res. II* 65–70, 31–45.
- Stenevik, E.K., Skogen, M., Sundby, S., Boyer, D., 2003. The effect of vertical and horizontal distribution on retention of sardine (*Sardinops sagax*) larvae in the Northern Benguela—observations and modelling. *Fish. Oceanogr.* 12, 185–200.
- Tanaka, Y., 1991. Change of specific gravity of fish eggs and larvae and their distribution and movement in relation to current structure. In: Kawai, E. (Ed.), *Current and Life—Lecture of Fisheries Oceanography*. Kyoto University Press, Kyoto, pp. 60–78.
- Walline, P.D., 1981. Hatching dates of walleye pollock (*Theragra chalcogramma*) and vertical distribution of ichthyoplankton from the Eastern Bering Sea, June–July 1979. NWAFC Processed Report 81-05. NOAA Fisheries, Department of Commerce.
- Wespestad, V.G., Fritz, L.W., Ingraham, W.J., Megrey, B.A., 2000. On relationships between cannibalism, climate variability, physical transport, and recruitment success of Bering Sea walleye pollock (*Theragra chalcogramma*). *ICES J. Mar. Sci.* 57, 268–274.
- Wiebe, P.H., Burt, K.H., Boyd, S.H., Morton, A.W., 1976. A multiple opening/closing net and environmental sensing system for sampling zooplankton. *J. Mar. Res.* 34, 313–326.
- Yamashita, Y., Kitagawa, D., Aoyama, T., 1985. Diel vertical migration and feeding rhythm of the larvae of the Japanese sand-eel *Ammodytes personatus*. *Bull. Jpn. Soc. Sci. Fish.* 51, 1–5.
- Zuur, A.F., Ieno, E.N., Walker, N., Saveliev, A.A., Smith, G.M., 2009. *Mixed Effects Models and Extensions in Ecology* with R. Springer, New York, NY574.



Summer distributions of forage fish in the eastern Bering Sea



Sandra L. Parker-Stetter^{a,*}, John K. Horne^a, Edward V. Farley^b, David H. Barbee^{a,1},
Alexander G. Andrews III^b, Lisa B. Eisner^b, Jennifer M. Nomura^a

^a School of Aquatic and Fishery Sciences, University of Washington, Box 355020, Seattle, WA 98195-5020, USA

^b Ted Stevens Marine Research Institute, Alaska Fisheries Science Center, 17109 Pt Lena Loop Road, Juneau, AK 99801, USA

ARTICLE INFO

Available online 25 April 2013

Keywords:

Bering Sea
Forage fish
Walleye pollock
Pacific cod
Capelin
Distribution

ABSTRACT

Juvenile and small adult fish, typically called forage fish, are an important but poorly studied part of the eastern Bering Sea (EBS) ecosystem. Acoustic and trawl data from a non-target survey were used to evaluate distributions of capelin (*Mallotus villosus*), age-0 Pacific cod (*Gadus macrocephalus*), and age-0 walleye pollock (*Theragra chalcogramma*, herein pollock) in 2006–2010. Within the surface zone (15 m to ~35 m, evaluated 2006–2010), capelin occurred throughout the EBS but primarily in the middle shelf. Capelin were also present in the midwater zone (~35 m to 0.5 m off-bottom) in both 2009 and 2010 (evaluated 2009–2010), and resulted in water column zone (15 m to 0.5 m off-bottom) distributions that differed from surface zone characterizations. Age-0 Pacific cod occurred primarily in the surface zone of the middle and outer shelf regions in all years. As midwater and surface zone age-0 Pacific cod were often coincident, water column zone distributions in 2009–2010 were similar to surface zone distributions. Age-0 pollock were found in the EBS surface zone in all years, primarily in the middle and outer shelf regions. High densities of age-0 pollock occurred in the midwater zone in 2006–2007 and 2009–2010. Water column zone distributions of age-0 pollock were similar to surface zone distributions in 2006–2007, but differed in 2009–2010 due to low numbers of age-0 pollock in the surface zone and presence of high densities in the midwater zone of the outer shelf region. While general patterns in capelin distribution in the surface zone were similar between the present and the previous studies, the acoustic-trawl characterization suggested that capelin densities were high in the middle shelf region. As expected, surface zone distributions of age-0 Pacific cod and age-0 pollock were similar to previous characterizations. Observed high densities of midwater age-0 pollock have not been described by previous studies. Annual abundance indices based on bottom or surface trawl data alone will not be sufficient in all years. Data and conclusions from non-target surveys may be constrained compared to dedicated survey efforts, but can provide baseline distributions, potential abundance indices, and insight for planning future research.

© 2013 Elsevier Ltd. All rights reserved.

1. Introduction

Juvenile and small pelagic adult fish, commonly referred to as forage fish, are a critical component of the eastern Bering Sea (EBS) ecosystem (Springer and Speckman, 1997), yet our understanding of their distributions and dynamics is incomplete. Implementation of ecosystem-based approaches to fisheries management (Pikitch et al., 2004; Livingston et al., 2005; Pikitch et al., 2012) and future predictions of biological response to climate change in the EBS

(e.g. Mueter and Litzow, 2008) will require comprehensive distribution and abundance data for this important trophic guild.

Unlike commercially-important fish populations, information on EBS forage fish has typically been extracted from large-scale surveys designed to sample other species. Recent data sources have included systematic bottom or surface trawl surveys (e.g. Moss et al., 2009; Hollowed et al., 2012; Hurst et al., 2012), midwater trawl surveys (e.g. Traynor and Smith, 1996), or opportunistic data collected during other assessments (e.g. Bakkala et al., 1985; Walters et al., 1988). While these data can be used to derive abundance or biomass indices, surveys using fixed-opening trawl gear only sample a portion of the water column, may not sample the bulk of forage fish distribution (Hollowed et al., 2012), and cannot typically adapt to compensate for vertical and/or horizontal changes in fish distributions related to environmental conditions.

An alternate sampling strategy combines active acoustics with trawling to map distributions and estimate abundances of pelagic

* Corresponding author. Tel.: +1 205 221 5459; fax: +1 206 685 7471.

E-mail addresses: slps@uw.edu (S.L. Parker-Stetter), jhorne@uw.edu (J.K. Horne), ed.farley@noaa.gov (E.V. Farley), binkt@uw.edu (D.H. Barbee), alex.andrews@noaa.gov (A.G. Andrews III), lisa.eisner@noaa.gov (L.B. Eisner), jmnomura@uw.edu (J.M. Nomura).

¹ Present address: Kongsberg Underwater Technology Inc., 19210 33rd Ave W, Suite A, Lynnwood, WA 98036, USA.

or semi-demersal fish species. An example of this approach by Hollowed et al. (2012) examined the distribution of age-1 walleye pollock (*Theragra chalcogramma*, herein pollock) in the EBS. Echosounders continuously sample the water column along the survey vessel's path and trawl samples are used to verify species compositions and to provide length frequency distributions. Large geographic ranges and systematic transect designs typical of acoustic-based surveys also ensure that variations in vertical and/or horizontal distributions can be detected over time or if environmental conditions change.

Dedicated acoustic assessments of forage fish species in the EBS have not been conducted, but acoustic data collected during non-target surveys can be used to increase knowledge of forage fish distributions. Analyses using acoustic and trawl data from non-target surveys may be constrained compared to those from dedicated survey efforts, but can provide an analytic starting point and a baseline for evaluating future research and appropriate survey designs.

This study was undertaken to characterize late-summer distributions of three forage fish species in the EBS using non-target acoustic and trawl survey data from 2006–2010. In some cases, surface trawl data from the existing survey have been used to evaluate EBS forage fish (e.g. Moss et al., 2009; Hollowed et al., 2012; Hurst et al., 2012). We build on these results by using acoustic data collected continuously between trawl stations and by evaluating densities within and below the surface trawl zone. Our specific objectives were to: (1) use acoustics and trawling to characterize spatial distributions of capelin (*Mallotus villosus*), age-0 Pacific cod (*Gadus macrocephalus*), and age-0 pollock, and (2) to compare acoustic characterizations with previously published distributions.

2. Methods

2.1. Survey design

Data were collected during the 2006–2010, mid-August to early-October Bering-Aleutian Salmon International Survey (BASIS) research surveys in the EBS (Fig. 1). The BASIS survey was initially designed as a systematic surface trawl survey to sample salmon species (*Oncorhynchus* spp.) throughout the EBS (Helle et al., 2007). In 2008 through 2010, the addition of active acoustics, limited midwater trawling on acoustic targets, and modifications to survey transect sampling enabled estimates of forage fish densities throughout the water column. Archived acoustic data from 2006–2007 (see Farley et al., 2009 for survey description) were also used in this study, but trawling during those survey years was limited to surface waters.

The spatial extent and timing of the surveys (Fig. 1), and the resolution of surface trawl stations sampled varied among years (Fig. 2) due to variation in available funding and ship time. During 2006, 2007, and 2010, surface trawl stations were spaced ~35 nautical miles (nmi, 1 degree longitude, 0.5 degree latitude) (Fig. 2). During the 2008 and 2009 surveys, BASIS stations were spaced ~65 nmi (2 degrees of longitude) in the east–west direction and ~35 nmi (0.5 degree latitude) in the north–south direction. The range of sampling dates also varied across years, with the 2008 and 2009 surveys starting in September rather than the more typical mid- to late-August start date in other years (Table 1). Survey operations occurred from approximately 0630 to 2200 Alaska Daylight Time (ADT).

BASIS surveys generally sampled in waters with bottom depths ranging from 25 to 400 m, with bottom depths during the truncated 2008 survey limited to 25 to 100 m (Fig. 1). Based on supplementary information in Sigler and Harvey (2013), the

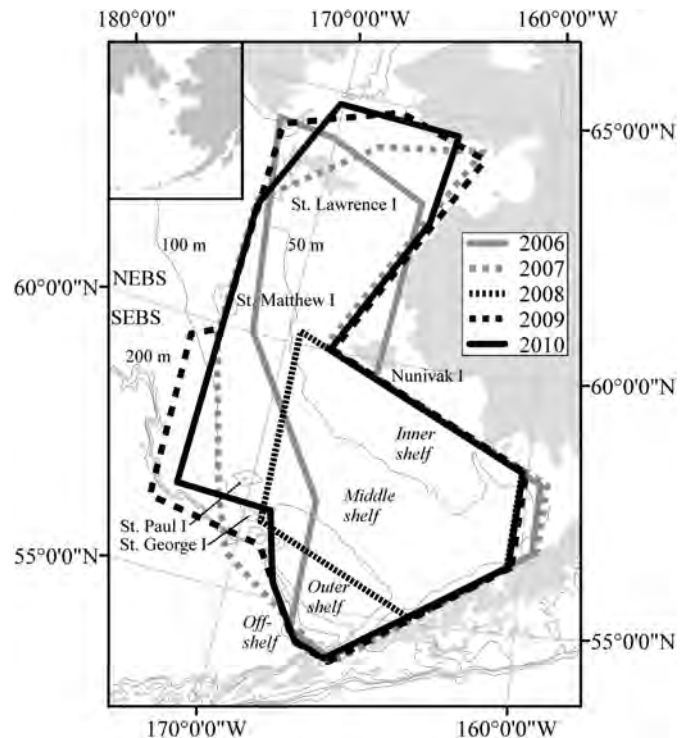


Fig. 1. Survey extents for 2006–2010. Bathymetric contours and the corresponding shelf regions referred to in the text are labeled. Inset map shows the location in Alaska, USA.

survey area included stations and transects within the inner shelf (< 50 m bottom depth range), inner front (transition zone between the inner and middle shelf regions), middle shelf (50–100 m), middle front (transition zone between the middle and outer shelf regions), outer shelf (100–200 m), and a small portion of the shelf break and off-shelf (> 200 m) regions. For brevity, north of 60°N is referred to as the North EBS (NEBS) and south of 60°N is referred to as the South EBS (SEBS, Fig. 1).

2.2. Acoustic data collection

Acoustic data were collected from three different chartered fishing vessels in 2006–2010 using hull-mounted Simrad ES60 echosounders (Kongsberg Maritime) operating at 38 kHz (Table 1). In 2008–2010, acoustic data were also collected from the NOAA ship *Oscar Dyson*'s Simrad EK60 split-beam echosounders (18, 38, 70, 120, and 200 kHz) mounted on a 3 m retractable centerboard that extends transducer faces to 9.15 m below the water surface. Only 38 kHz data were used in these analyses. All split-beam ES38-B kHz transducers had 7° beamwidths (measured at half power points) and the single-beam ES38-200 had a 13° beamwidth. All acoustic data were collected using a pulse duration of 1.024 ms and a ping rate of 1 pulse/s. Data from chartered fishing vessels were collected at speeds of 3.1 to 4.6 m/s (6–9 kt). Data from the *Oscar Dyson* were collected at speeds of 5.1 to 6.2 m/s (10–12 knots). All echosounders were calibrated prior to and/or following each survey using reference sphere methods described in Foote et al. (1987).

2.3. Trawling and target identification

Fish were sampled using a Cantrawl 400/601 rope trawl (20–25 m vertical opening, 1.2 cm cod-end liner) equipped with 5 m alloy trawl doors (for details see Farley et al., 2009). Three types of trawls were performed: standard BASIS surface trawls,

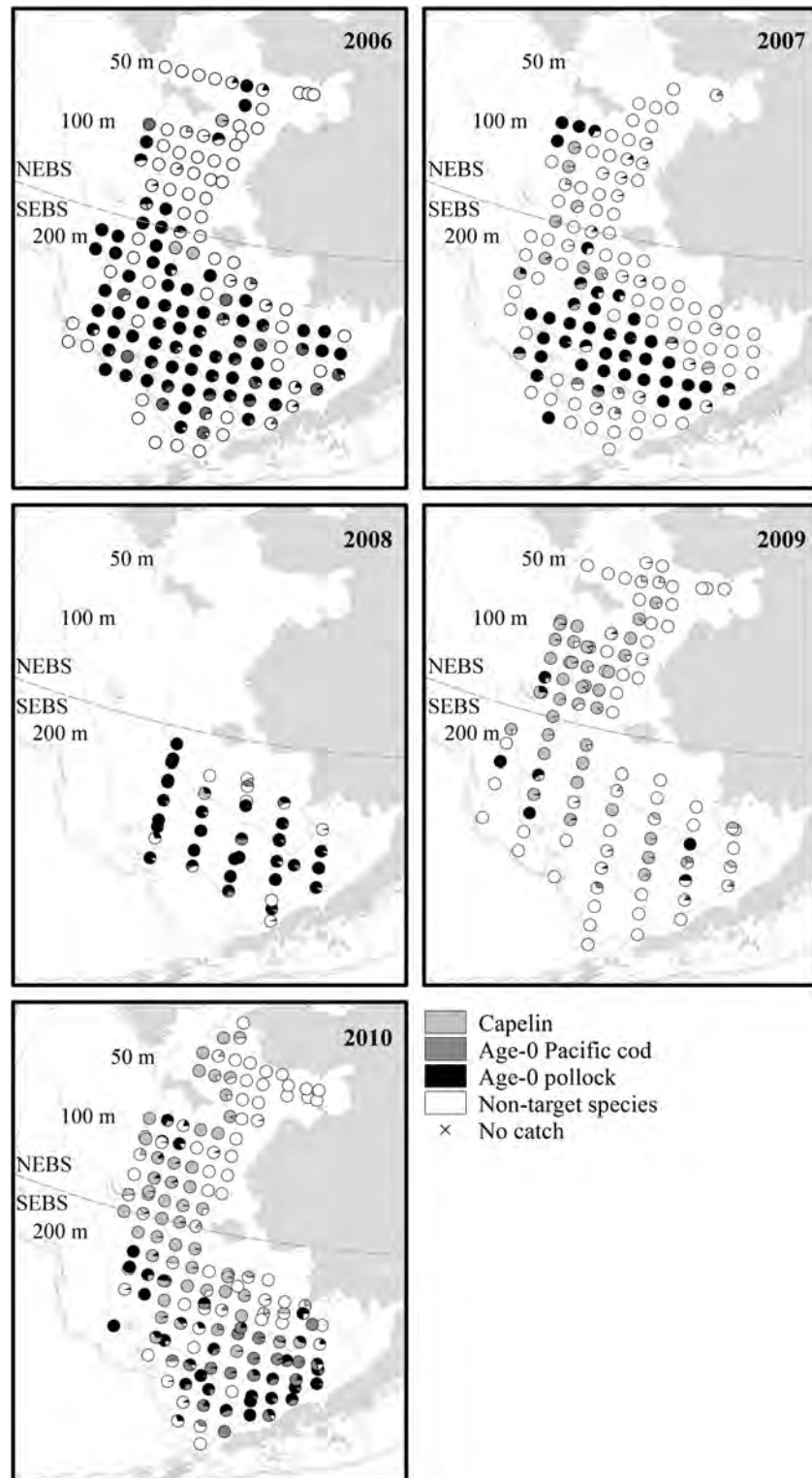


Fig. 2. Catch composition for trawls that sampled the surface zone in 2006–2010. Proportional catches of focal and non-target species are shown.

surface target identification trawls, and midwater target identification trawls. Three to four BASIS surface trawls were performed per day during daylight hours. A single midwater or surface target identification trawl was typically performed each day.

For standard BASIS surface trawls (2006–2010) and surface target identification trawls (2008–2010), floats were attached to the headrope of the Cantrawl to ensure the headrope remained at or near the surface. The duration of BASIS surface trawls was

30 min once the net was fishing. Surface target identification trawl times varied from 5 to 30 min. Autonomous depth loggers (Vemco Minilog-TD and Wildlife Computers Mk9) were deployed on the head and footrope during all net deployments in 2009–2010 to verify fishing depths and net openings. Based on headrope/footrope measurements taken from the *Oscar Dyson* in 2010, the average maximum footrope depth during fishing was 35 m. BASIS surface trawls occurred at regularly spaced stations. Surface target

Table 1

Survey dates, vessel, Simrad transducer model, transducer input power (Power, W), and amount of acoustic transect data (Dist, nmi) for 2006–2010 surveys.

Year	Dates	Vessel	Transducer	Power (W)	Dist (nmi)
2006	5–21 September	<i>Sea Storm</i>	ES38-B	1000	952.5
2006	21 August–4 September	<i>Northwest Explorer</i>	ES38-B	2000	816.0
2007	16 August–3 October	<i>Sea Storm</i>	ES38-200	1000	3142.5
2008	11–27 September	<i>Oscar Dyson</i>	ES38-B	2000	885.5
2009	3–28 September	<i>Oscar Dyson</i>	ES38-B	2000	1286.0
2009	1–13 September	<i>Epic Explorer</i>	ES38-B	2000	761.0
2010	18 August–16 September	<i>Oscar Dyson</i>	ES38-B	2000	1577.0
2010	6 September–5 October	<i>Epic Explorer</i>	ES38-B	2000	1476.0

identification trawl locations were selected based on observed echosounder patterns.

Midwater target identification trawls (2008–2010) were used to identify observed acoustic patterns below the vertical sampling range of the surface trawl. For midwater trawls, floats were removed and net depth and opening were monitored in real time using a Simrad FS70 sonar attached to the headrope of the trawl. Midwater trawl times varied between 5 and 57 min depending on fish densities observed on the echosounder and headrope sonar displays. Midwater target identification trawls were conducted at locations with bottom depths sufficient to safely trawl and selected based on echosounder patterns. Contamination of midwater trawl catch by surface species was assumed negligible.

Trawl catches were sorted to species, weighed, and sampled for length frequency distributions. If catch weight was 1 t (t) or less, the entire catch was processed. If the catch weight exceeded 1 t, then the entire catch was weighed and a ~1 t subsample was randomly selected for sampling. Fork lengths of at least 50 individuals from each species or age-group (i.e. juvenile or adult) were measured to the nearest mm. Catches were divided into four classes: capelin, age-0 Pacific cod, age-0 pollock, and non-target fish species. Proportional catch composition was calculated for each trawl by dividing the number of fish in each class by the total number of non-salmonid fish in the catch.

2.4. Acoustic data analysis

2.4.1. Acoustic data processing

Acoustic data analysis was restricted to the use of 38 kHz data as the chartered fishing vessels were typically equipped with only 38 kHz echosounders (Table 1). Echoview 4.70 (Myriax Pty Ltd) was used to process all acoustic data. The ES60 triangle wave error was removed prior to data processing (Keith et al., 2005). In the SEBS, sound speeds and absorption coefficients were set at 1470 m/s and 0.00998 dB/m. In the NEBS, where water column properties were more variable, sound speed and absorption coefficients were calculated using CTD data (range 1473–1482 m/s, 0.00992–0.00986 dB/m). Noise spikes and empty pings, where a transmitted pulse was not received due to vessel motion, were manually removed. Vessel noise levels (range –145 to –113 dB re 1 m⁻¹ @ 1 m across vessels and years) were estimated using passive data collections and removed from the acoustic data using linear subtraction (Watkins and Brierley, 1996; Korneliusson, 2000). Data cells that did not meet a 6 dB signal-to-noise ratio threshold were also removed from the analysis. Acoustic data near evening or morning crepuscular periods were only included if echogram patterns were consistent with daytime data. Across years, 73% to 100% of the acoustic transect data were collected during the daytime.

Data within 15 m of the surface were excluded from analysis to account for maximum transducer depth (9.15 m on the *Oscar Dyson*) and twice the near-field range of the 38 kHz transducers

(2 × 2.54 m). The seafloor was initially detected using the bottom detection algorithm in Echoview and then manually corrected. All data within 0.5 m of the corrected bottom were excluded from the analysis.

In 2008–2010, acoustic transect data between north–south BASIS stations in the SEBS and between east–west stations in the NEBS were used in analyses. In 2006 and 2007, when acoustic data collection was not included in the survey design and data quality was variable, any acoustic data (north–south or east–west) which had low vessel noise spikes in the water column were included in the analysis.

2.4.2. Depth zones

Patterns observed on the echosounder were combined with trawl sampling and bottom depth ranges to divide the study area into surface, midwater, and whole water column depth zones. These zones, while selected to facilitate data analysis, also enable comparisons between this study and previous characterizations of forage fish distributions.

The “surface zone” (15 to ~35 m, herein surface zone) was sampled by BASIS surface and surface target identification trawls. The upper edge of the surface zone was set to 15 m based on acoustic near-field constraints (Section 2.4.1). In the stratified middle, outer, and off-shelf regions, high backscatter values were observed in an acoustically-detected shallow layer (c.f. Woillez et al., 2012) typically associated with the mixed layer at 20 to 30 m depth (Ladd and Stabeno, 2012). The base of this acoustically-detected layer was set as the lower edge of the surface zone. A semi-automated edge detection routine, consisting of a 0.5 m vertical by 10 ping horizontal resample window, a –75 dB re 1 m⁻¹ (herein dB, MacLennan et al., 2002) S_{θ} minimum threshold, a Sobel edge detection operator (Gonzalez and Woods, 2007), and manual correction by an analyst were used to define the lower edge of the layer. When no layer was detected, the lower edge of the surface zone was set at 35 m based on the mean maximum fishing depths of the surface trawl (Section 2.3). In much of the inner shelf, fish were dispersed between the surface and the bottom. Therefore this region was considered to be effectively sampled by the surface trawl, with the acoustic upper edge set to 15 m and the lower edge set to 0.5 m from the bottom (Section 2.4.1). Acoustic estimates within the surface zone enable a comparison with previous characterizations of forage fish distributions based on surface trawl data.

The “midwater zone” (herein midwater zone), sampled using only midwater trawls, was defined from the lower edge of the surface zone to 0.5 m from the acoustically-detected bottom (Section 2.4.1). As no midwater trawling was performed in 2006 and 2007, midwater zone fish density estimates in those years were not possible for any species except age-0 pollock (see Section 2.4.6). In this analysis, midwater trawl catches were considered to be representative of species composition and length distributions within sampled regions and observed backscatter patterns. Sections of acoustic transects with backscatter patterns that were

Table 2Target strength (TS, dB) to length (L , cm) relationships used to proportion acoustic backscatter. Species or group scientific names are given in Section 3.1.

Species or group	TS Equation (dB)	Source
Arctic cod	$8.03 \log_{10} L - 60.78$	Parker-Stetter et al. (2011)
Atka mackerel	$20 \log_{10} L - 83.2$	Gauthier and Horne (2004)
Bering wolfish	$20 \log_{10} L - 67.4$	Foote (1987), general physoclist
Capelin	$20 \log_{10} L - 70.3$	Guttormsen and Wilson (2009)
Ninespine stickleback	$20 \log_{10} L - 67.4$	Foote (1987), general physoclist
Pacific cod	$20 \log_{10} L - 66.0$	Rose and Porter (1996), <i>Gadus morhua</i>
Pacific herring	$20 \log_{10} L - 65.1$	Gauthier and Horne (2004)
Pacific sand lance	$20 \log_{10} L - 89.3$	Yasuma et al. (2009), <i>Ammodytes personatus</i>
Pacific sandfish	$20 \log_{10} L - 67.4$	Foote (1987), general physoclist
Prowfish	$20 \log_{10} L - 67.4$	Foote (1987), general physoclist
Rainbow smelt	$23.4 \log_{10} L - 68.7$	Peltonen et al. (2006), <i>Osmerus eperlanus</i>
Rockfish unidentified	$20 \log_{10} L - 67.7$	Kang and Hwang (2003), <i>Sebastes schlegeli</i>
Saffron cod	$8.03 \log_{10} L - 60.78$	Parker-Stetter et al. (2011), <i>Boreogadus saida</i>
Threespine stickleback	$20 \log_{10} L - 67.4$	Foote (1987), general physoclist
Walleye pollock	$20 \log_{10} L - 66.0$	Traynor (1996)

inconsistent with trawl sampled patterns were designated “unknown” and excluded from calculations. Unknown regions typically included near- or on-bottom aggregations that could not be sampled with the trawl, or midwater zone backscatter patterns consistent with sampled jellyfish. Acoustic estimates within the midwater zone represent a depth zone that has not been characterized in previous surface trawl studies and provides a comparison for previous studies using bottom trawl data.

The “water column zone” (herein water column zone) was defined from 15 m below the surface to 0.5 m above the acoustically-detected bottom (Section 2.4.1). This zone combined information from the surface and midwater zones for all species in 2009–2010 (water column zone = surface zone + midwater zone). If backscatter from the midwater zone was classified as unknown, no water column zone estimate was made. Acoustic water column zone estimates provide a full water column distribution of pelagic forage fish that has not been previously reported.

2.4.3. Data threshold

To select appropriate volume backscatter thresholds (i.e. minimum S_v values) that included forage fish and excluded jellyfish, sections of acoustic data from the 2008 field season were used as training sets to determine backscatter characteristics of forage fish (based on age-0 pollock) and jellyfish (dominated by *Chrysaora melanaster*). Acoustic target strengths of jellyfish species found in the northeast Pacific have not been fully documented. Using trawl catches to guide selection, regions of echograms that contained dense surface zone age-0 pollock ($n=52$ regions), surface zone jellyfish ($n=99$), or midwater zone jellyfish ($n=23$) were identified. S_v values from samples within each section were exported and a negative log likelihood function was used to generate a mean and standard deviation of S_v values for surface zone age-0 pollock (-51.2 ± 9.7 dB) and jellyfish (-82.8 ± 8.6 dB), and midwater zone jellyfish (-86.3 ± 12.7 dB). Fitted curves, based on the negative log likelihood, for the three groups intersected at -67 dB. The -67 dB threshold was validated using data from 2009. Standard scores (i.e. z-scores) were used to compare areas of curves above or below the -67 dB intersection: 5.2% of the age-0 pollock occurred below the -67 dB intersection and 3.3% of the surface zone jellyfish and 6.4% of the midwater zone jellyfish occurred above the -67 dB intersection. The fish minimum S_v threshold was set at -67 dB in all data sets. Backscatter < -67 dB was removed from the analysis to exclude jellyfish.

2.4.4. Horizontal distribution of fish backscatter

Fish area backscatter values (s_A , m^2/nmi^2 , MacLennan et al., 2002) for surface zone and midwater zones were integrated and

exported at the -67 dB threshold in 0.926 km (0.5 nmi) horizontal bins. Backscatter above -67 dB, but classified as unknown, was also exported to evaluate the amount of unclassified backscatter in the analysis. No additional vertical binning was applied. The average bottom depth within each 0.5 nmi bin was calculated.

2.4.5. Acoustic species proportions

A trawl-derived acoustic species proportion was calculated for each trawl using surface and/or midwater trawl catches. All pelagic species captured in the trawl were included in the calculations except salmon (*Oncorhynchus* spp., primarily juvenile, few immature or adult) and adult Pacific herring (*Clupea pallasii*). These two groups were excluded as they were considered to be within the 15 m acoustic surface exclusion zone (Section 2.4.1) and not measured by the echosounder. As a check on this assumption, trawl catches from 12 paired surface and sub-surface (headrope 8 to 18 m) trawls during the 2008–2010 surveys were compared. Salmon were captured in 9 surface trawls, but in 0 sub-surface trawls. In the same 12 paired trawls, adult Pacific herring were captured in 5 surface trawls, but in 0 sub-surface trawls. Multiple analyst inspection of acoustic data in regions with high surface trawl catches of salmon or adult Pacific herring suggested that findings from the paired trawls were representative of the broader survey area.

For all pelagic species captured in trawls, an acoustic target strength was calculated from its measured length using a target strength versus length equation from the literature (Table 2). For fish lacking a species-specific equation it was necessary to use an equation from a similar species or a generalized equation. Target strength (TS, dB re $1 m^2$, herein dB, MacLennan et al., 2002) to length (L , cm) equations were identified for all non-salmonid fish captured in trawls (Table 2). The target strength (dB) for each fish was calculated and converted to linear echo amplitude (σ_{bs} , m^2 where $\sigma_{bs} = 10^{(TS/10)}$, MacLennan et al., 2002)

Linear echo amplitudes were summed for each trawl (i.e. sum of σ_{bs} for all species, total echo amplitude) and for each species within the trawl (i.e. sum of σ_{bs} for each species, species echo amplitude). The trawl-derived acoustic species proportion for each trawl was then calculated by dividing the species echo amplitude by the total echo amplitude for the trawl.

2.4.6. Trawl assignments

Fish backscatter within each 0.5 nmi horizontal acoustic bin was assigned the trawl-derived acoustic species proportion from the nearest trawl location using a nearest neighbor function

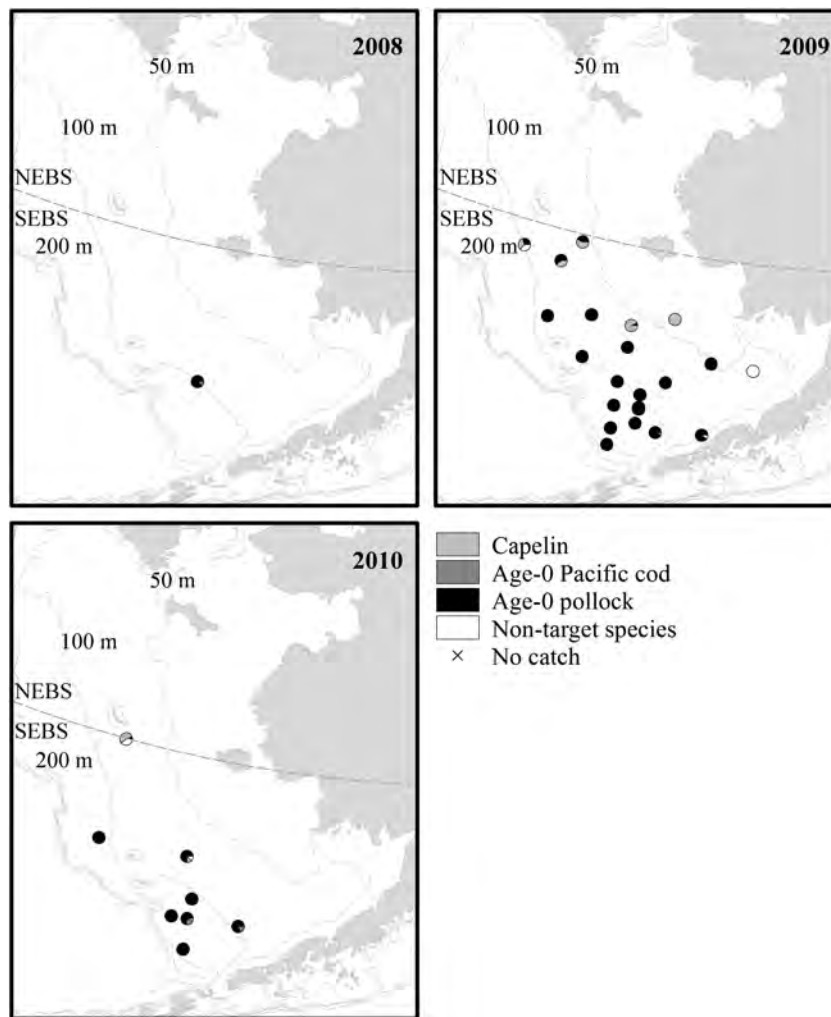


Fig. 3. Catch composition for trawls that sampled the midwater zone in 2008–2010. Proportional catches of focal and non-target species are shown.

(ArcMap 10.0, ESRI Inc.). Only trawls that sampled the surface zone or midwater zone were used to partition backscatter within that zone. Since no midwater trawling was performed in 2006 or 2007, and only a single midwater trawl was performed in 2008, it was not possible to estimate midwater zone densities of capelin or age-0 Pacific cod. As midwater zone age-0 pollock were found in large aggregations in 2009–2010, scrutiny by three analysts was used to identify “analyst-based pollock” (herein analyst-based pollock) midwater zones in 2006–2008 that were consistent with echosounder patterns from 2009–2010. This approach assumed that echosounder patterns from 2009 and 2010 were representative of previous years and that if not, the introduced bias was small and consistent.

2.4.7. Species densities

Species backscatter (s_A) within 0.5 nmi horizontal bins was calculated by multiplying the total fish s_A in each 0.5 nmi bin (Section 2.4.4) by its assigned trawl-derived acoustic species proportion (Sections 2.4.5, 2.4.6). This was then used to calculate final densities (fish/nmi²) by dividing the species s_A in each 0.5 nmi bin by a mean echo amplitude (σ_{sp} , m²; derived from σ_{bs} through the equation $\sigma_{sp} = 4\pi\sigma_{bs}$, MacLennan et al., 2002) for that species (Section 2.4.5). Mean echo amplitudes were calculated for each year, to account for potential inter-annual differences in fish length, and were weighted by length measurements from trawl catches. Densities were calculated for the surface zone, midwater zone, and water column zone (surface zone+midwater zone).

2.4.8. Species distributions

Distributions of density (fish/nmi²) in surface zones were plotted for capelin, age-0 Pacific cod, and age-0 pollock for 2006 to 2010. Midwater zone and water column zone densities were plotted for capelin and age-0 Pacific cod in 2009–2010. Midwater zone and water column zone densities were plotted for age-0 pollock in 2006–2008 using analyst-based pollock and for 2009–2010 from acoustic data validated using midwater trawl samples. Within the stratified middle, outer, and off-shelf regions, water column zone results were only plotted when estimates were available for both the surface zone and the midwater zone.

Minimum, maximum, and mean density values were calculated to facilitate comparisons among years and depth zones. For consistency among years, calculations were restricted to 0.5 nmi bins with bottom depths ranging from 20 to 200 m. Maximum density values were identified for all years (2006–2010) and depth zones (surface, midwater, water column). Minimum values were identified for the surface zone in all years (2006–2010), but for midwater and water column zones in only 2009–2010 as analyst-based pollock estimates in 2006–2008 were biased against low densities. Mean densities, standardized by bottom depth, were generated for the same zones and years in a three-step calculation. First, the bottom depths within all 0.5 nmi horizontal bins (Section 2.4.4) were classified into 10 m bottom depth categories. Second, a mean for each bottom depth category was calculated. Finally, the mean density was calculated by averaging the bottom depth category means. This standardization was necessary as sampling

effort across bottom depths was unequal within and among years. While this approach standardized for sampling effort, it did not account for differences in survey extent, such as the limited spatial distribution of acoustic data in 2006 or the lack of transects in bottom depths > 105 m in 2008, or for potential shifts in species' distributions outside the surveyed area.

2.4.9. Percentage of fish in the surface zone

The percentage of fish in the surface zone was calculated for middle, outer, and off-shelf using 0.5 nmi bins that had density estimates for both the surface zone and the midwater zone. Percentage of shallow fish was calculated by dividing the density of fish in the shallow zone by the density of fish in the water column zone and multiplying by 100. Calculations were not performed for 0.5 nmi bins where midwater zone backscatter was classified as unknown or for bins where the water column zone density of the species of interest was zero. The mean percentage of fish in the surface zone was only calculated for 2009 and 2010, as analyst-based pollock estimates in 2006 and 2007 were biased high. Percentages of surface zone fish were mapped to facilitate spatial comparisons. For comparison, values for the inner shelf, where the percentage of surface zone fish was analytically-defined at 100% (Section 2.4.2), were also mapped.

3. Results

3.1. Trawling results

Four-hundred and eighty-one trawls were used to characterize species proportions and lengths in the surface zone in 2006–2010, with 65 in 2006, 114 in 2007, 41 in 2008, 104 in 2009, and 157 in 2010 (Fig. 2). Additional BASIS surface trawls were conducted in 2006 ($n=86$) and 2007 ($n=17$), and are shown in Fig. 2 to illustrate patterns in species distribution, but were not used in the acoustic analysis as they were outside the area where acoustic data were available. 2008 had the highest mean surface zone catches of jellyfish in the SEBS east of 170°W (mean \pm 1 standard deviation, 305 ± 883 kg/30 min tow, $n=39$) in the five data years, and was used to develop the volume backscatter threshold to exclude jellyfish. Jellyfish mean catches were a factor of 2 to 6 lower in all other years. Non-target fish species were captured in the trawls in all years: Atka mackerel (*Pleurogrammus monopterygius*), Bering wolfish (*Anarhichas orientalis*), Pacific sand lance (*Ammodytes hexapterus*), Pacific sandfish (*Trichodon trichodon*), prowlfish (*Zaprora silenus*), rainbow smelt (*Osmerus mordax dentex*), threespine stickleback (*Gasterosteus aculeatus aculeatus*), and age-1+ pollock. Additional non-target fish species were found only in some years, likely influenced by survey extent: Arctic cod (*Boreogadus saida*, 2006, 2010), age-1+ Pacific cod (2006, 2007), ninespine stickleback (*Pungitius pungitius*, 2006, 2007, 2009), juvenile rockfish (*Sebastes* spp., 2006–2009), adult rockfish (2010), and saffron cod (*Eleginus gracilis*, 2006, 2007, 2009, 2010) (Fig. 2). Of the trawl locations and catches shown in Fig. 2, BASIS surface trawl results for fish have been summarized for some years (Moss et al., 2009; Hollowed et al., 2012; Hurst et al., 2012).

A total of 31 trawls were used to characterize species proportions and lengths in the midwater zone in 2008–2010, with 1 in 2008, 22 in 2009, and 8 in 2010 (Fig. 3). Limited midwater trawling effort in 2008 resulted from a compressed survey effort and a lack of midwater zone targets. In 2010 few trawls in the midwater zone were performed due to a lack of midwater zone targets. Age-0 pollock dominated the midwater catches, with non-target species including age-1+ pollock (2009), prowlfish (2009), and Pacific sandfish (2009, 2010). Midwater zone jellyfish catches were similar to or less than surface catches in 2009 and 2010.

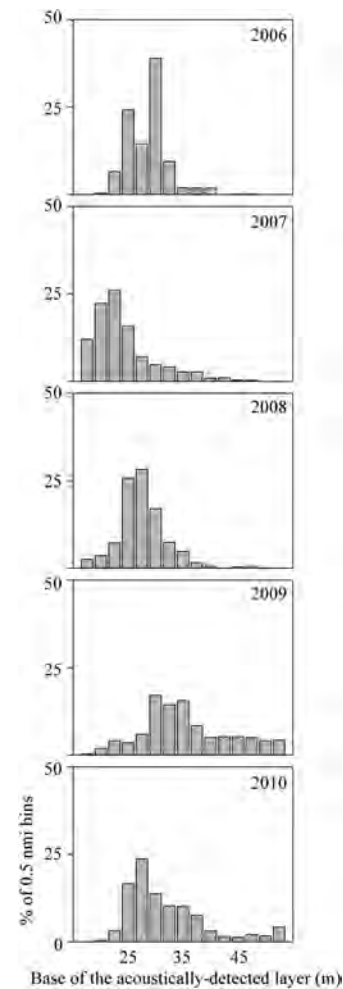


Fig. 4. Distribution of the depth of the base of the acoustically-detected layer in 2006–2010.

3.2. Acoustic general results

A total of 11,028.5 nmi (20,425 km), equivalent to 22,057 0.5 nmi horizontal bins, of acoustic transect data were collected in 2006–2010 (Table 1). The 2006 and 2007 data quality was variable, with sections of data omitted due to the presence of vessel noise spikes. The smallest acoustic dataset occurred during 2008 and did not include bottom depths > 105 m. Although 2006 had 1768.5 nmi of data, the entire study area is not represented as acoustic data were not recorded during sections of the survey. The number of 0.5 nmi bins that contained unknown backscatter in the midwater zone was 1093 (63% of all 0.5 nmi bins with a midwater zone, 2006), 2421 (81%, 2007), 1026 (100%, 2008), and 1998 (80%, 2010). Backscatter (s_A) values within these cells ranged from 1–14,637 (2006), 0.1–5486 (2007), 1–3226 (2008), and 0.1–2659 m^2/nmi^2 (2010). Of those cells containing unknown backscatter, the entire midwater zone was classified as unknown in 993 (2006), 2411 (2007), 1026 (2008), and 1633 (2010) 0.5 nmi bins. A total of 1286 regions within 0.5 nmi horizontal bins were identified as analyst-based pollock (743 in 2006, 543 in 2007, and 0 in 2008) and used in further analysis. The base of the acoustically-detected layer varied among years, from just below the 15 m acoustic surface exclusion line to a maximum of > 50 m (Fig. 4). Using only those 0.5 nmi horizontal bins where the layer was detected, and excluding those that were assigned to 35 m in the absence of a layer, 96% (2006, $n=716$ total layer observations), 95% (2007, $n=1759$), 97% (2008, $n=1026$), 63% (2009, $n=1505$), and 78% (2010, $n=1826$) of layer depths were less

than or equal to the 35 m mean maximum footrope depth of the surface trawl (Fig. 4).

3.3. Forage fish densities and distributions

3.3.1. Capelin

Capelin were distributed across the surface zone of the study area in all years, but were primarily found in the middle shelf in the SEBS and the inner and middle shelves in the NEBS (Fig. 5). In all years, capelin were not detected in the surface zone of the outer shelf. In years with sampling in both the NEBS and SEBS, capelin were located in both regions. The highest single estimate of capelin density in the surface zone (1.10×10^8 fish/nmi²) occurred in the middle shelf in 2009. Mean surface zone densities during 2009 and 2010 (49,644 and 85,045 fish/nmi²) were higher than in 2006–2008 (5844–11,230 fish/nmi², Fig. 5).

Capelin occurred in the midwater zone out to the off-shelf region in 2009 and 2010, with the highest densities in the outer shelf region (Fig. 6). No direct comparison of 2009 and 2010 distributions is possible as large sections of the 2010 midwater zone were classified as unknown. The mean midwater zone density of capelin was higher in 2009 (76,263 fish/nmi²) than in 2010 (10,687 fish/nmi², Fig. 6).

Combining the surface and midwater zone estimates, high water column zone densities of capelin were found in the middle and outer shelf regions in 2009 (Fig. 7). While the 2010 distribution map is incomplete, high densities in that year also occurred in the middle, outer, and off-shelf regions (Fig. 7). The highest single water column zone density estimate (1.10×10^8 fish/nmi²) for capelin occurred at the same location as the highest surface zone estimate in 2009. The mean water column zone densities of capelin were similar between 2009 (118,732 fish/nmi²) and 2010 (116,421 fish/nmi², Fig. 7).

3.3.2. Age-0 Pacific cod

Age-0 Pacific cod in the surface zone were distributed across a wide range of bottom depths, with middle and outer shelf regions containing the highest densities (Fig. 8). While some age-0 Pacific cod were estimated in the NEBS, higher and more consistent surface zone densities occurred in the SEBS. The highest single surface zone density of age-0 Pacific cod (7.48×10^7 fish/nmi²) was observed in 2006 near the inner front. Age-0 Pacific cod were scarce in 2009 (Fig. 8). The highest surface zone mean density of age-0 Pacific cod occurred in 2010 (426,548 fish/nmi²), with the lowest in 2007 (9667 fish/nmi², Fig. 8).

In the midwater zone, age-0 Pacific cod occurred primarily at the middle front or outer shelf region in 2009 (Fig. 6). While the 2010 midwater zone data are incomplete, high densities of age-0 Pacific cod were also found in the same regions. Mean midwater zone age-0 Pacific cod densities were higher in 2010 (120,888 fish/nmi²) than in 2009 (495 fish/nmi², Fig. 6).

Combining surface and midwater zone density estimates, age-0 Pacific cod water column zone distributions in 2009 and 2010 were similar to surface zone distributions, with the highest densities occurring in the outer shelf and lower densities in the middle shelf (Fig. 7). As high densities of age-0 Pacific cod in the 2010 water column zone were observed on either side of unknown regions (where the midwater zone was classified as unknown), it is possible that the distribution was continuous across that area (Fig. 7). The highest single water column zone density of age-0 Pacific cod (3.19×10^7 fish/nmi²) occurred in the outer shelf in 2010. Mean water column zone densities of age-0 Pacific cod were higher in 2010 (610,310 fish/nmi²) than in 2009 (64,177 fish/nmi², Fig. 7).

3.3.3. Age-0 pollock

Age-0 pollock within the surface zone were widely distributed in the survey area during all years, with the highest densities in the SEBS (Fig. 9). The maximum single age-0 pollock surface zone density observation (5.77×10^7 fish/nmi²) occurred in the middle shelf in 2006. The highest mean surface zone density for age-0 pollock was in 2006 (785,652 fish/nmi²), with the lowest occurring in 2009 (13,109 fish/nmi², Fig. 9). Surface zone densities of age-0 pollock were similar in 2007, 2008, and 2010.

Age-0 pollock occurred in the midwater zone of the study area in 2006 (analyst-based pollock), 2007 (analyst-based pollock), 2009, and 2010 (Fig. 10). No analyst-based pollock regions were detected in the limited 2008 study area, but were observed in deeper water outside the study area (Parker-Stetter, unpublished data). The highest single density of midwater zone age-0 pollock was measured in the middle shelf in 2007 (1.15×10^8 fish/nmi²) northwest of St. Paul Island. Mean densities for midwater zone age-0 pollock were similar in 2009 (994,788 fish/nmi²) and 2010 (972,078 fish/nmi², Fig. 10).

While maps of age-0 pollock water column zone distributions are fractured by unknown midwater zone data regions in 2006, 2007, and 2010 (Fig. 11), additional information can be gained from this partial dataset. In 2006 and 2007, water column zone distributions were similar to surface zone distributions as age-0 pollock in the surface zone were often coincident with midwater zone age-0 pollock (Fig. 11). The presence of high densities of midwater zone pollock in 2009 and 2010 weight the water column zone distributions to the outer and off-shelf regions (Fig. 11). The highest single water column zone estimate of age-0 pollock occurred in 2007 (1.15×10^8 fish/nmi²), at the same location as the highest midwater zone density estimate. Mean water column zone densities of age-0 pollock were similar between 2009 (949,519 fish/nmi²) and 2010 (1.13×10^6 fish/nmi², Fig. 11).

3.4. Percentage of fish in the surface zone

Capelin were primarily found in the surface zone of the middle shelf in 2009 (mean 65%) and 2010 (mean 92%, Fig. 12). All capelin in the outer and off-shelf regions were observed in the midwater zone. With the exception of the off-shelf region in 2009, some age-0 Pacific cod were located in the surface zone of all shelf regions in 2009 and 2010 (17–100%, Fig. 12). More age-0 Pacific cod were located in the surface zone during 2010 than 2009. Age-0 pollock distribution patterns were similar to those of age-0 Pacific cod, but with lower overall percentages of fish in the surface zone (Fig. 13). Some fish were found in all regions of the surface zone in 2009–2010 (8–48%) with the exception of the off-shelf region in 2009 (Fig. 13). More age-0 pollock were located in the surface zone in 2010 (26–48%) than during 2009 (0–18%). Distributions and proportions of analyst-based pollock in 2006 and 2007 were similar, with low percentages in the surface zone of the outer shelf region (Fig. 13).

4. Discussion

This study provides annual estimates of densities and distributions of important EBS forage fish species in 2006 through 2010 using acoustic-trawl data collected during an existing survey. Even though acoustic transect layouts and midwater trawling strategies did not conform to a traditional acoustic survey design, distributions derived from these surveys are believed to be representative and can be used to compare observed distributions to those reported in previous studies.

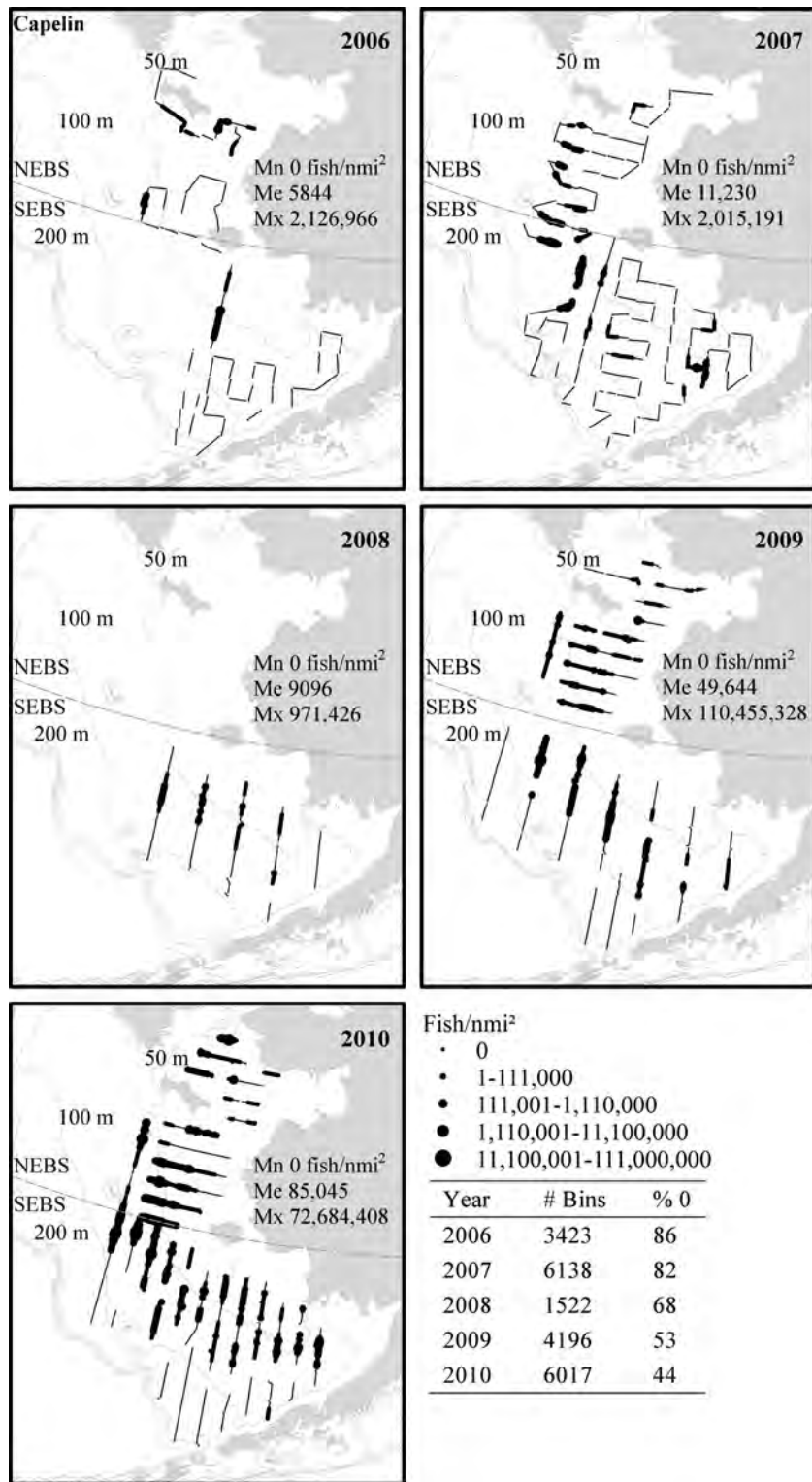


Fig. 5. Surface zone densities (fish/nmi²) of capelin in 2006–2010. Minimum (Mn), mean (Me), and maximum (Mx) densities, based on 20–200 m bottom depths, are shown. The number of 0.5 nmi bins (#) and % zero values (% 0) used in the calculations of Mn, Me, and Mx are listed in the inset table.

Capelin were located in the surface zone in the inner and middle shelf regions in all years, with the highest densities in the SEBS. Resulting distributions were generally similar between the acoustic-trawl data in this study and characterizations based on bottom trawl (Hollowed et al., 2012) data, with the notable exception that highest capelin densities in the SEBS during 2007, 2009, and 2010 typically occurred in the middle and not the inner shelf. While the difference in locations, and associated water

depths, may be attributed to differences in sampling dates (May–July for bottom trawl, August–October for acoustic-trawl), distributions of capelin based on “thermal gateways” predict high capelin densities to occur in the middle shelf during cold conditions (Ciannelli and Bailey, 2005), such as those during the present study and 2007–2009 in the Hollowed et al. (2012) study. Differences in distributions characterized using acoustic-trawl (i.e. surface and midwater) and bottom trawl data may be due to

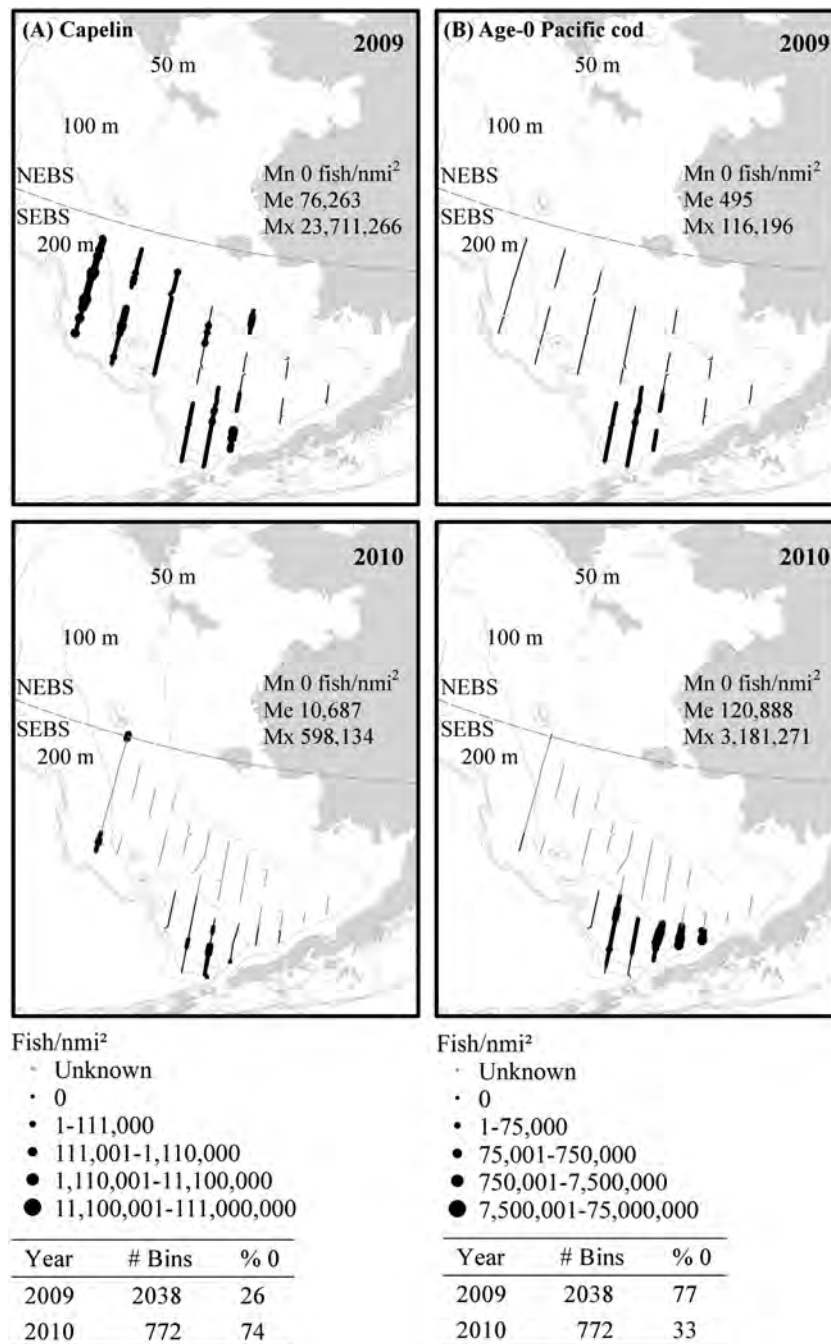


Fig. 6. Midwater zone densities (fish/nmi²) of (A) capelin and (B) age-0 Pacific cod in 2009 and 2010. Sections of transects classified as unknown are identified. Minimum (Mn), mean (Me), and maximum (Mx) densities and inset table as in Fig. 5.

the proportion of the water column sampled and location of gear relative to capelin vertical distribution. In the inner shelf region, fish were typically distributed throughout the water column, potentially within the sampling range of bottom trawls. In contrast, in the middle, outer, and off-shelf regions, capelin were located predominantly within the surface zone and would only be sampled by a bottom trawl during deployment and retrieval. Acoustic-trawl data used in this study would exclude capelin within 0.5 m of the bottom, which could result in density estimates of capelin being biased low within the inner shelf. This potential bias cannot be quantified with our data. Capelin in the midwater zone occurred over a larger area in 2009 than in 2010. As a result, capelin water column zone distributions differed from

surface zone distributions and from bottom trawl characterizations (Hollowed et al., 2012).

Age-0 Pacific cod were primarily distributed in the surface zone of the middle and outer shelf regions in the SEBS. The surface zone distribution of age-0 Pacific cod has also been evaluated using BASIS surface trawl data (Hurst et al., 2012). Distribution patterns in the two studies were expected to be similar as the same surface trawl data were used to partition surface acoustic backscatter at, and between, surface trawl stations in the present study. Analysis of the surface trawl (Hurst et al., 2012) and the acoustic-trawl data identified low-density, limited distributions of age-0 Pacific cod in 2007 and 2009. The reduced spatial extent of surface zone age-0 Pacific cod in 2008 (Hurst et al., 2012) may be due to the limited

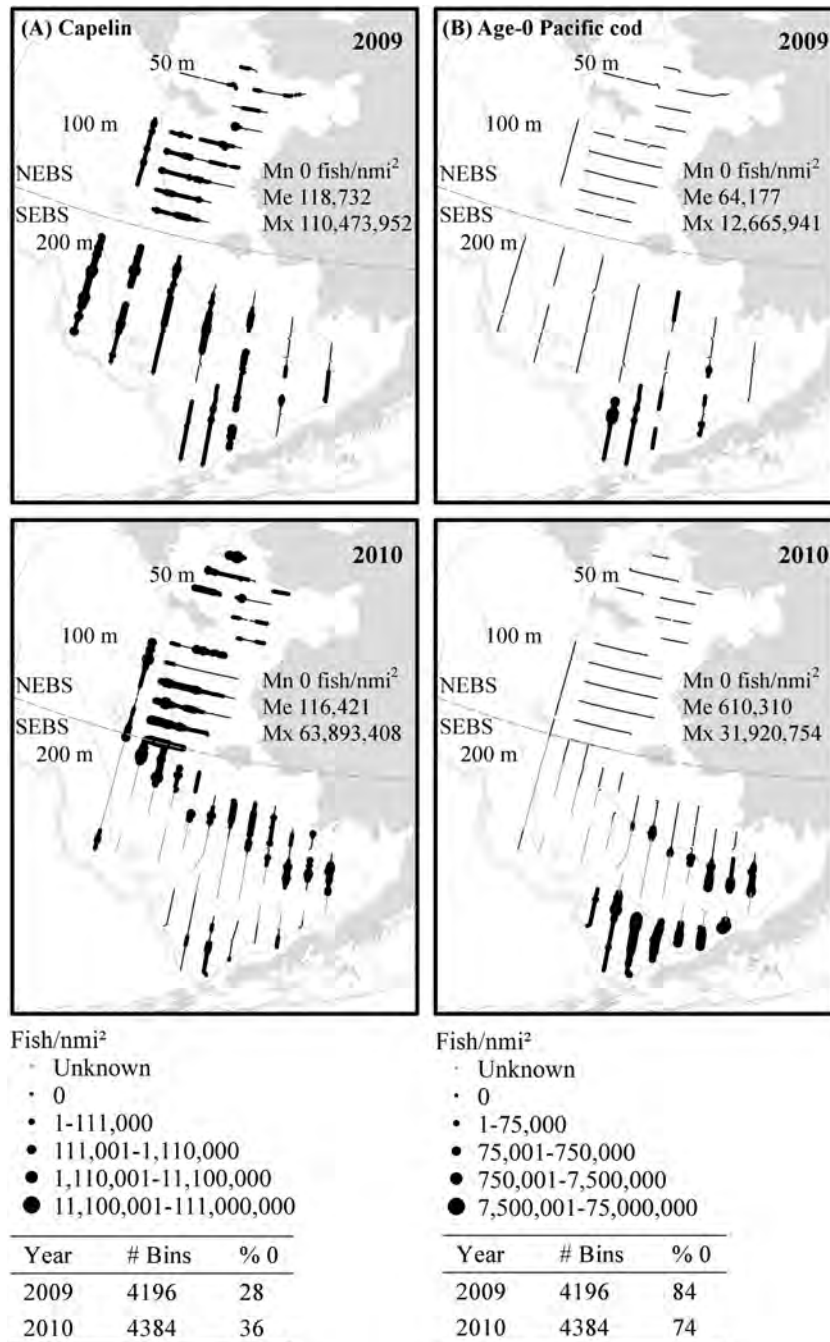


Fig. 7. Water column zone densities (fish/nmi²) of (A) capelin and (B) age-0 Pacific cod in 2009 and 2010. Bins where a water column zone estimate could not be made (midwater zone was unknown) are identified. Minimum (Mn), mean (Me), and maximum (Mx) densities and inset table as in Fig. 5.

survey area that year. In contrast age-0 Pacific cod densities in 2010, which were not evaluated in Hurst et al. (2012), were the highest observed in all study years. The observed distribution in 2010 was more similar to 2006 than any other year in the present study. In this study, midwater zone age-0 Pacific cod contributed to water column zone densities in a limited area during 2009 and 2010. As high densities of fish in the midwater zone typically occurred at the same location as high densities in the surface zone, the resulting water column zone maps are similar to those generated using surface zone data only. There is limited previous information on age-0 Pacific cod distribution in the SEBS, but shallow (typically < 40 m below the surface) trawls targeting age-0 pollock, also contained up to 5% age-0 Pacific cod in the

catch and age-0 Pacific cod were often spatially coincident with age-0 pollock (Bakkala et al., 1985; Walters et al., 1988).

Distribution maps characterized age-0 pollock densities as being highest in the stratified middle and outer shelf regions in all years. While the area around the Pribilof Islands has frequently been associated with high densities of age-0 pollock (e.g. Walters et al., 1988; Traynor and Smith, 1996; Swartzman et al., 2005), results from the present study suggest that high age-0 pollock densities were also observed on transects throughout the SEBS in all study years. Our findings support observations that age-0 pollock in surface waters were more abundant in layers within the middle and outer shelf regions (Bakkala et al., 1985; Moss et al., 2009; Hollowed et al., 2012) than in the inner shelf

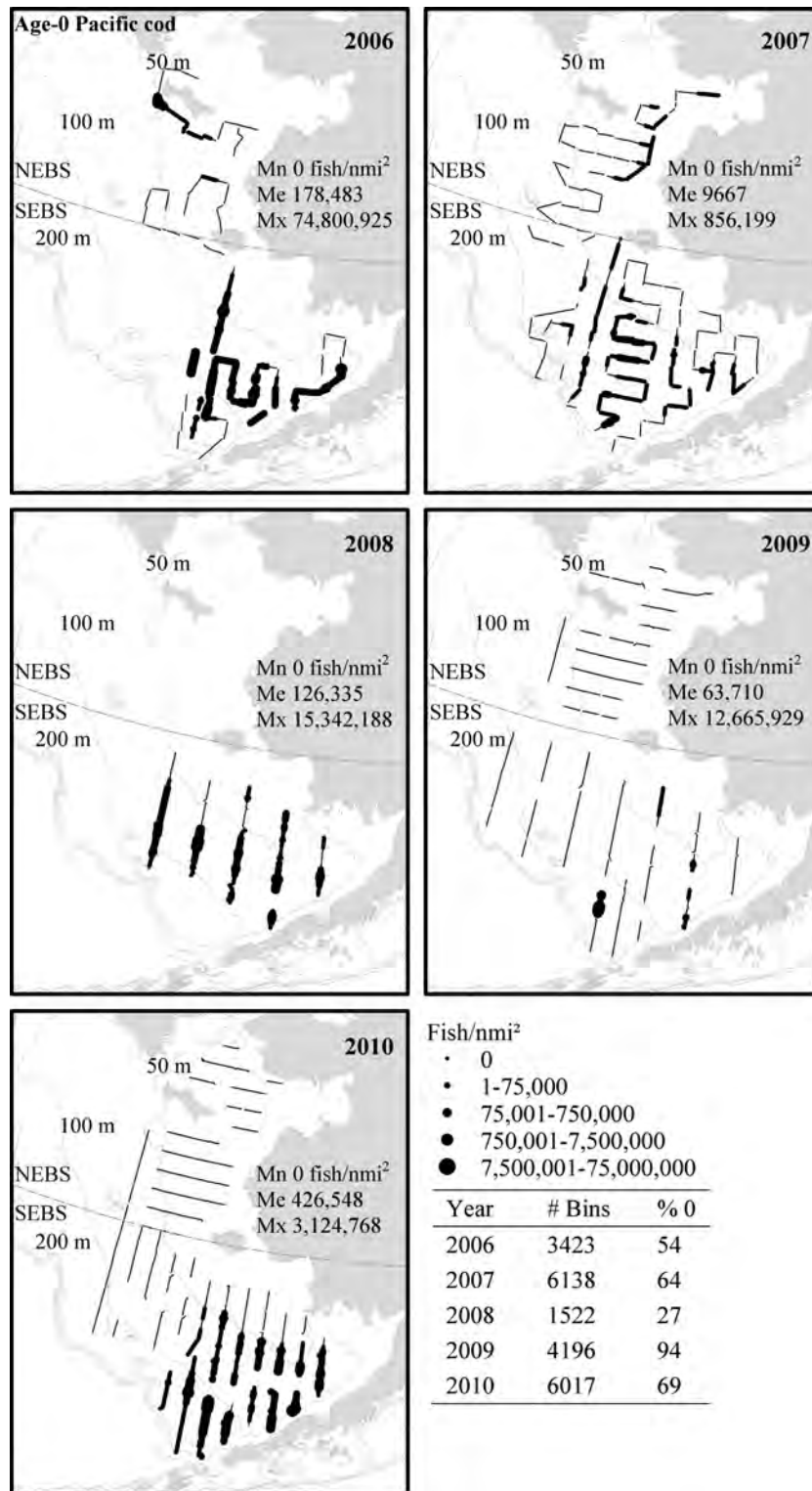


Fig. 8. Surface zone densities (fish/nmi²) of age-0 Pacific cod in 2006–2010. Minimum (Mn), mean (Me), and maximum (Mx) densities and inset table as in Fig. 5.

(Miyake et al., 1996; Swartzman et al., 2005). While age-0 pollock densities in surface waters have been described as being typically highest in water <120 m deep (e.g. Bakkala et al., 1985; Walters et al., 1988), we observed age-0 pollock out to the shelf break (i.e. 200 m isobath) in 2006, 2007, and 2010. As the same surface trawl data were used to partition surface zone acoustic backscatter in the present study as in previous studies (Moss et al., 2009; Hollowed et al., 2012), distribution patterns near surface trawl

stations were expected to be similar. The acoustic-trawl data collected between stations suggested that surface zone age-0 pollock distributions were generally continuous throughout the surveyed area, but that densities could vary by an order of magnitude between surface trawl stations. Our approach cannot account for potential shifts in species composition between stations as species composition was assigned to acoustic data based on the nearest trawl station. Net-based

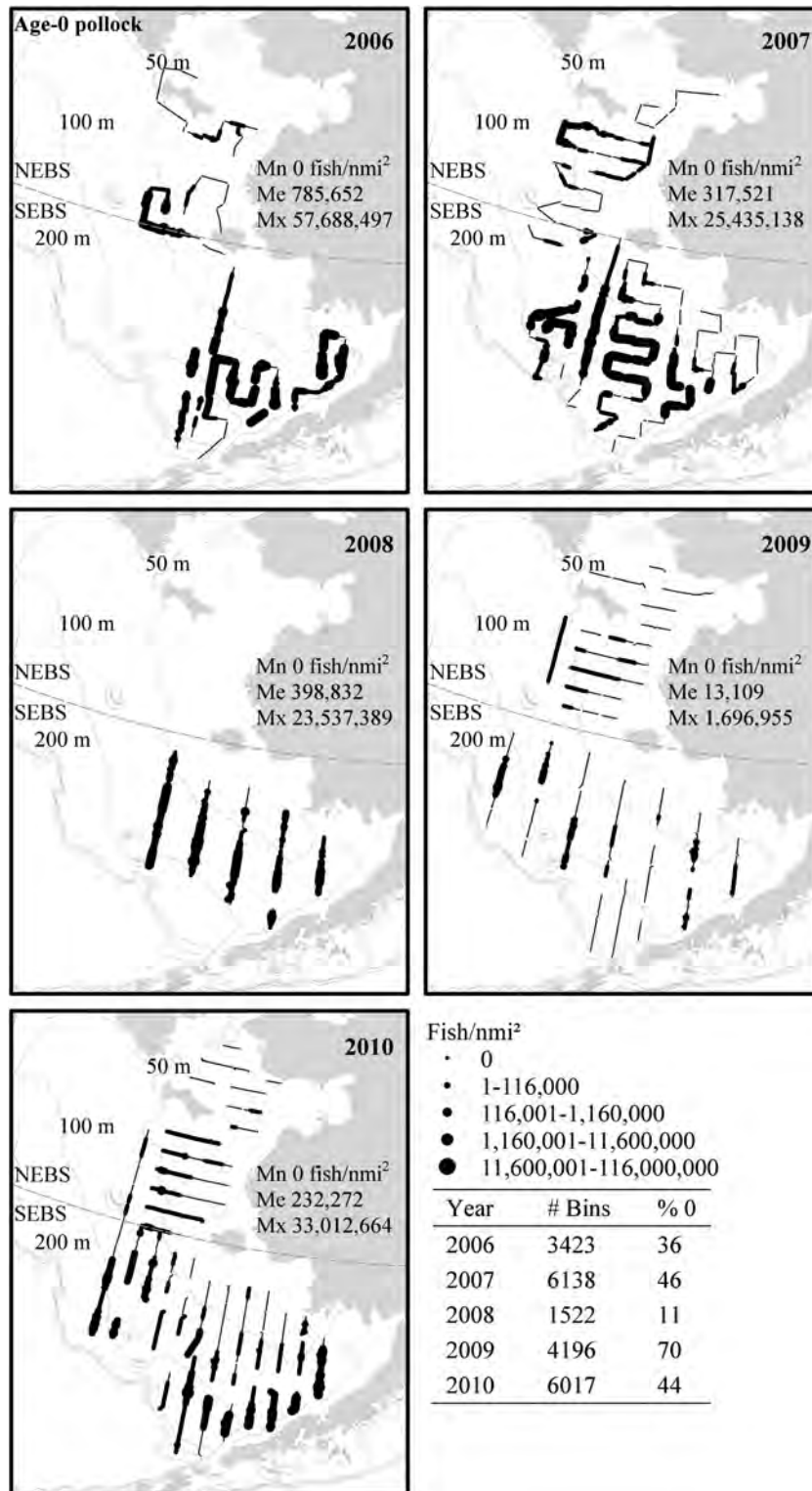


Fig. 9. Surface zone densities (fish/nmi²) of age-0 pollock in 2006–2010. Minimum (Mn), mean (Me), and maximum (Mx) densities and inset table as in Fig. 5.

abundance indices that interpolate densities between stations may not account for spatial heterogeneity within the survey area domain.

While high densities of age-0 pollock were observed and captured in the surface zone, the present study suggested that fish in the midwater zone were also an important component of water column zone densities. High densities of midwater zone age-0 pollock occurred in 2006 and 2007 (analyst-based

evaluation) and in 2009 and 2010 (survey data). As estimated midwater zone densities frequently exceeded surface zone estimates, the water column zone distribution maps of age-0 pollock differed from those generated using surface zone data only, and from other characterizations using only surface trawl data (e.g. Moss et al., 2009; Hollowed et al., 2012). In 2006, 2007, and 2010, midwater zone age-0 pollock increased overall water column zone densities, particularly in the outer and off-shelf regions. In 2009, a

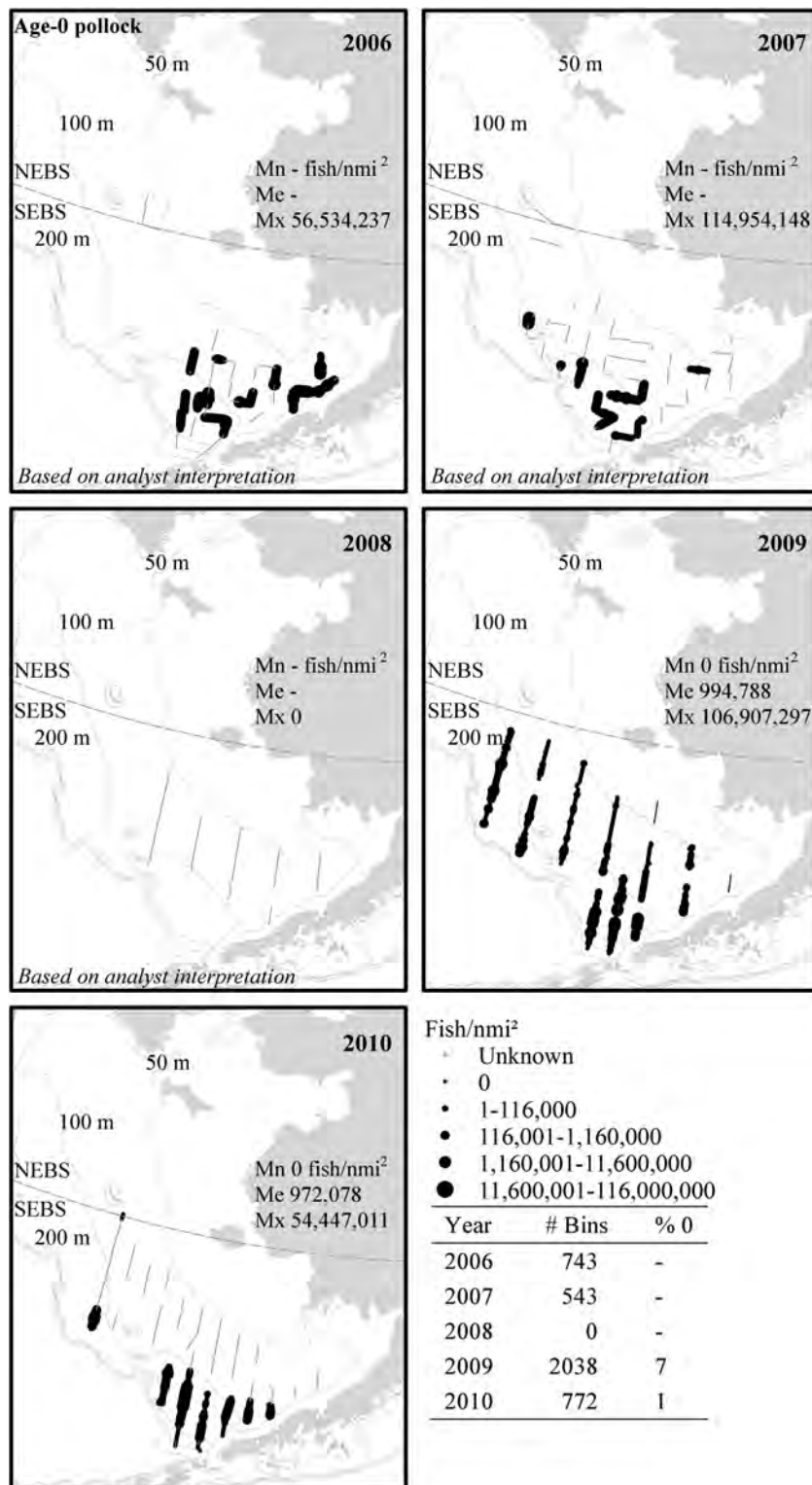


Fig. 10. Midwater zone densities (fish/nmi²) of age-0 pollock in 2006–2010. Sections of transects classified as unknown are identified. When calculated, minimum (Mn), mean (Me), and maximum (Mx) densities and inset table as in Fig. 5.

year with very low densities of surface zone age-0 pollock, midwater zone fish dominated the water column zone distribution. It is important to note that although age-0 pollock densities in surface waters may decrease in cold relative to warm years (as defined in Brodeur et al., 2002a; Moss et al., 2009), water column zone densities may remain stable in deeper water due to the presence of midwater zone age-0 pollock.

The presence of midwater zone age-0 pollock has been noted in previous studies, with position in the water column attributed to differences in fish lengths. During the day, fish shorter than 60 mm have been caught in shallow water, within or near the pycnocline (Bailey, 1989; Swartzman et al., 1999; Swartzman et al., 2002). Larger fish were typically located below the pycnocline, often migrating to the surface at night (Bailey, 1989; Swartzman et al.,

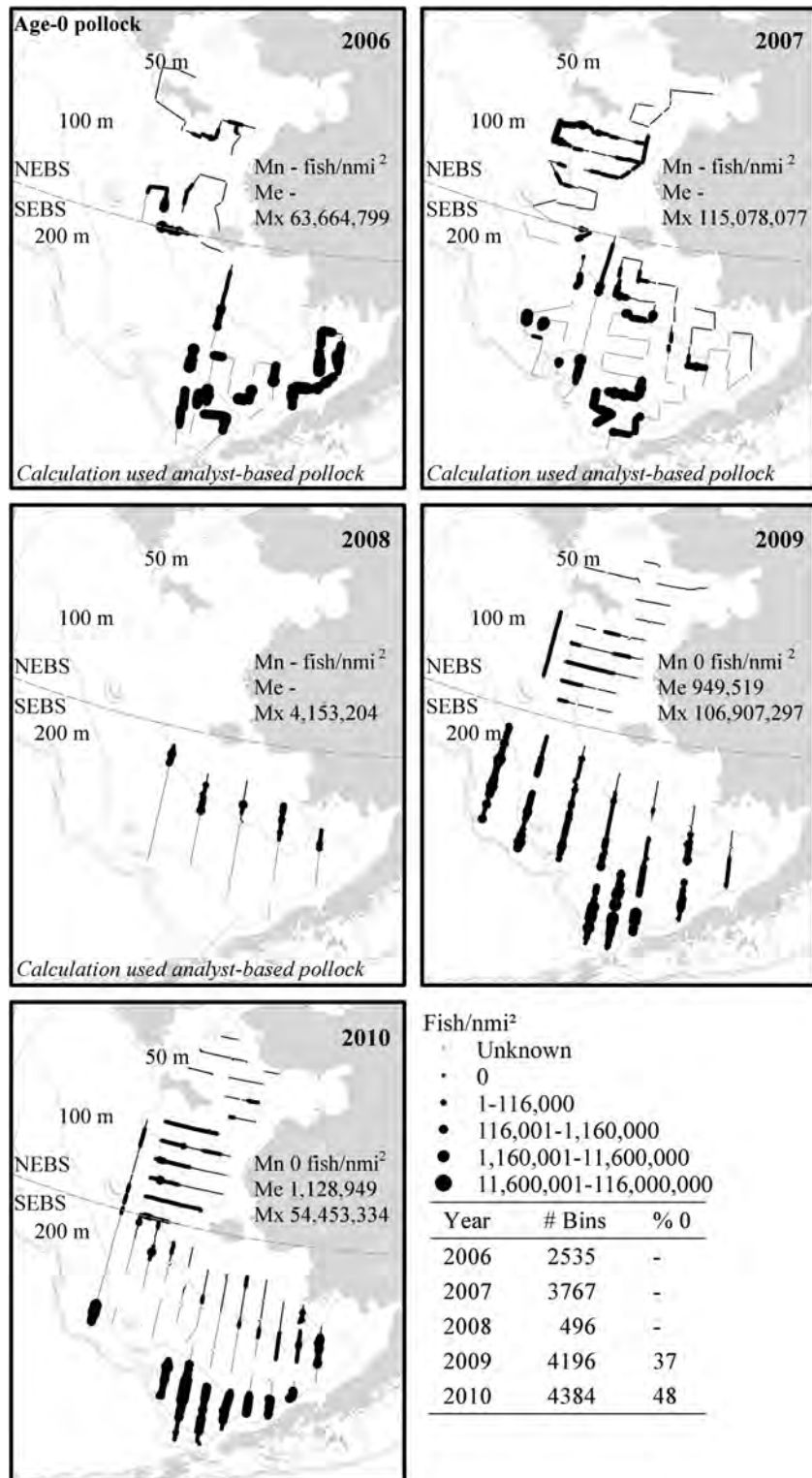


Fig. 11. Water column zone densities (fish/nmi²) of age-0 pollock in 2006–2010. Bins where a water column zone estimate could not be made (midwater zone was unknown) are identified. When calculated, minimum (Mn), mean (Me), and maximum (Mx) densities and inset table as in Fig. 5.

2002). Miyake et al. (1996) hypothesized that age-0 pollock inhabit progressively deeper water as length increases. Brodeur and Wilson (1996) observed that the mean depth of capture for age-0 pollock in the Gulf of Alaska increased from July/August to October. Only Tang et al. (1996), working in the Aleutian basin and not on the EBS shelf, observed all age-0 pollock (with a mean body

length of 40.2 mm) in deep water during the day migrated to the surface at night. We observed age-0 pollock above/within (surface zone) and below (midwater zone) the pycnocline, often in the same location. While age-0 pollock lengths varied spatially, the largest fish were not typically found at the deepest depths, and lengths of surface zone and midwater zone fish were similar

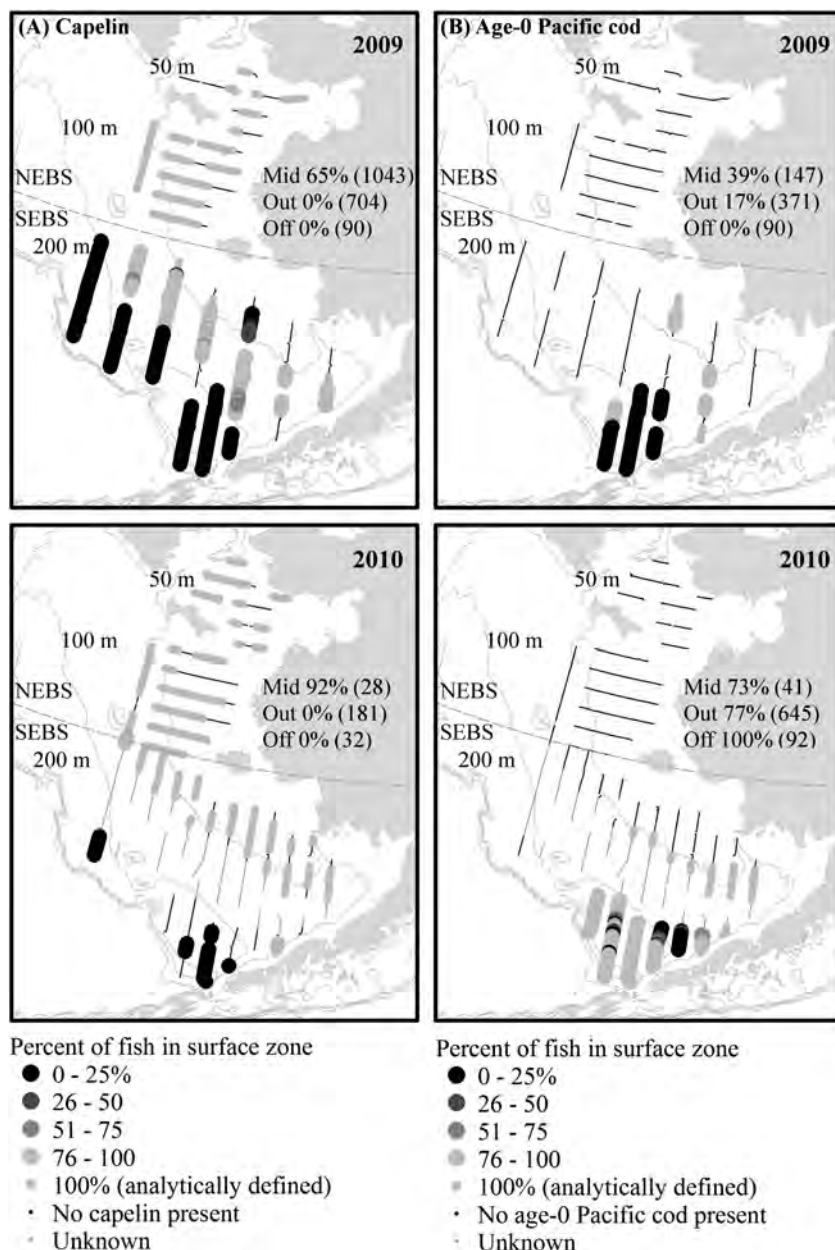


Fig. 12. Percentage of (A) capelin and (B) age-0 Pacific cod in the surface zone in 2009 and 2010. Inner shelf bins, where the percentage is analytically defined at 100%, are shown for reference. Mean percentages for middle (Mid), outer (Out), and off-shelf (Off) regions are given with number of 0.5 nmi bins included in the calculation (#).

(Parker-Stetter, unpublished data). This observation suggests that the explanation for the vertical location of age-0 pollock in the SEBS is more complex than length alone.

The acoustically-detected layer was a consistent feature in all 2006–2010 datasets. The location of the layer was related to the oceanographic mixed layer depth (i.e. depth of the top of the pycnocline) through the function: acoustically-detected layer depth base = $0.81 \times \text{mixed layer depth} + 10.32$ ($R^2 = 0.59$, $n = 670$, Parker-Stetter unpublished data). The 10.32 intercept approximates the upper limit of the 2 to 8 m late-summer pycnocline thickness range for 2006–2010 in the southern Bering Sea (Stabeno et al., 2012a). The pycnocline is a strong density gradient that separates surface and bottom water masses, each with different temperature, salinity, nutrients, and chlorophyll-a properties (Kachel et al., 2002). The aggregation of organisms near or within the pycnocline may be due to increased concentrations of phytoplankton or zooplankton prey. Using samples in June and July from the SEBS, Woillez et al. (2012) describe this layer as

containing pollock and euphausiids, likely jellyfish, and potentially fish larvae or macroplankton. Trawl samples in August to October suggested that the layer primarily contained larval and age-0 fish, age-1+ forage fish, and jellyfish. The potential contribution of macrozooplankton could not be evaluated. As suggested in Woillez et al., 2012, a dedicated effort is needed to determine the composition and relative abundance of organisms within the layer.

Recognizing that all sampling gears and survey designs can bias data, we examine potential biases and caveats associated with our effort to characterize forage fish distributions. We consider the results from the present study to be robust and that any biases in the data do not obfuscate observed distribution patterns. As this work serves as an initial assessment of forage fish distributions in the EBS, discussion of assumptions and potential biases is prudent and will inform future use of these data and the design of additional studies.

The use of a single acoustic frequency for data collection necessitated a simplified analytic scheme that may have

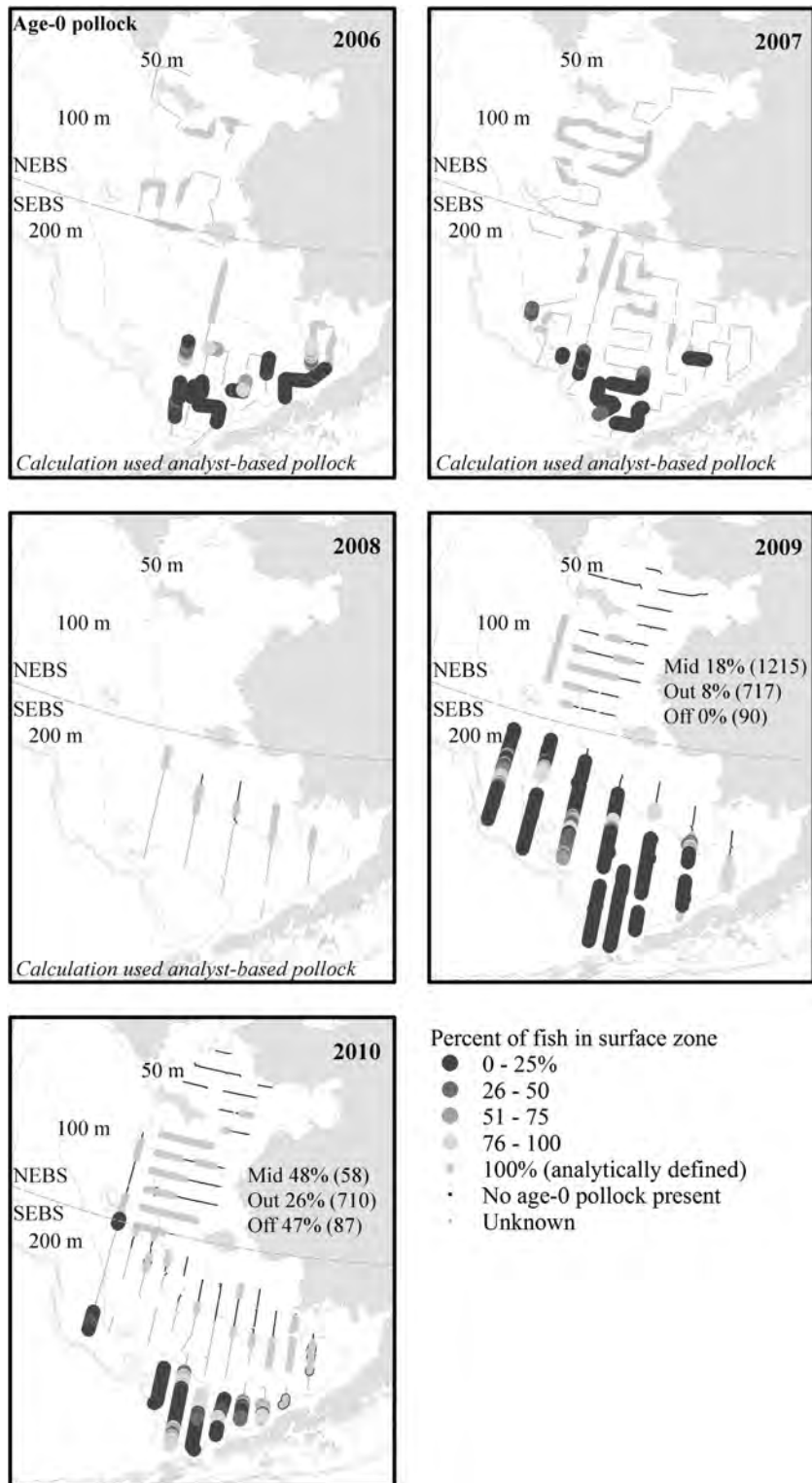


Fig. 13. Percentage of age-0 pollock in the surface zone in 2006–2010. Inner shelf bins, where the percentage is analytically defined at 100%, are shown for reference. Mean percentages for middle (Mid), outer (Out), and off-shelf (Off) regions are given with number of 0.5 nmi bins included in the calculation (#) are shown when calculated.

introduced bias from non-target organisms such as jellyfish. In the eastern Bering Sea jellyfish wet weight biomass can be more than 2 orders of magnitude greater than that of age-0 pollock (Schabetsberger et al., 2000; Brodeur et al., 2002b), and age-0 pollock are sometimes observed to be in association with the jellyfish, swimming among their tentacles during the day (Brodeur 1998). To minimize the contribution of jellyfish backscatter, the

present study used areas of dense age-0 pollock and jellyfish backscatter in the development of our empirically-based -67 dB minimum threshold. Previous studies of jellyfish within the genus *Chrysaora* have reported mean in situ target strengths at 38 kHz in the range of -63.9 dB (Graham et al., 2010) to -65.5 dB (Brierley et al., 2004) with potential changes > 10 dB due to variation in shape and orientation during swimming. This target strength

variability complicates the selection of a single volume backscatter threshold. By limiting the analysis to strong backscatter regions, our intention was to bias fish estimates low. In cells where jellyfish backscatter exceeded the -67 dB threshold, that backscatter would have been included as fish backscatter and biased fish density estimates high. In contrast, in cells with low densities of fish and corresponding backscatter values less than -67 dB, those fish would have been excluded from the analysis, biasing fish density estimates low. As an additional filter, acoustic cells suspected of containing high jellyfish backscatter, based on scrutiny by three analysts, were labeled unknown and removed from the analysis. Jellyfish backscatter may also have been included in analyst-based pollock classifications for 2006–2008 survey data. If analyst-based classifications were incorrect, then spatial distribution of midwater zone age-0 pollock may be biased. The magnitude of the bias associated with jellyfish inclusion or fish exclusion cannot be quantified with available data, particularly since trawl retention of jellyfish and the vertical distribution of jellyfish are unknown. As the biomass and potentially packing densities of jellyfish in the EBS vary annually and may be influenced by sampling gear (e.g. Cieciel et al., 2012; Lauth and Hoff, 2012), testing the validity of a single volume backscatter threshold to exclude backscatter from jellyfish will require a dedicated study conducted across a range of jellyfish densities. We recommend that future projects focus on this issue using multi-frequency acoustic data and directed trawl samples to quantitatively evaluate the contribution of jellyfish to regions of backscatter that contain forage fish.

As target strength to length relationships were not available for all species of forage fish, it was necessary to use non-target equations in our analysis. The use of generalized equations or those from similar species may bias target strength estimates and the resulting acoustic partitioning, but were necessary when species-specific equations were not available. In some cases, equations were developed using larger specimens than those in the present study. Depending on the mismatch between the species or length range, the use of non-target, target strength to length equations may bias fish estimates low or high. In our approach, which used target strengths and trawl catch to proportion acoustic energy, an underestimate of the target strength of one species will affect density estimate of other species in the sample. In other words, the total acoustic proportions for a trawl sum to one, so underestimating one causes another to be overestimated. The potential for bias introduced by using non-target equations cannot be quantified. Dedicated development of target strength to length equations for EBS forage fish species is a daunting, but necessary analytic need for accurate density estimates.

Two assumptions enabled the use of surface trawl data as species verification samples for the partitioning of acoustic backscatter in the surface zone. With the exception of salmon and adult Pacific herring, it was assumed that fish in the surface zone were equally available to the echosounder below 15 m. This assumption was checked using surface and sub-surface paired trawls and inspection of acoustic echograms. If this assumption was not met, acoustic species composition could be biased and densities may be erroneously estimated for species caught in surface trawls, but not measured by the echosounder. If fish were vertically stratified within the surface zone, and the surface trawl did not sample the entire zone, then species proportions used in the acoustic analysis would be biased toward the shallowest species. We also assumed that contamination of surface trawl catches by fish below the acoustically-detected layer was negligible. No paired trawls were performed to validate this assumption as there was typically little backscatter immediately below the acoustically-detected layer on which to trawl. Visual inspection of echograms suggested that negligible contamination of surface trawls by

midwater fish was likely a valid assumption. If this assumption was not met, then acoustic species compositions could be biased. Validation of these assumptions would require an analysis using fine-scale, depth-stratified trawling.

We assumed that trawl data adequately sampled forage fish species composition and length distributions. Retention of specific species or a restricted length range by a net may lead to selectivity biases (e.g. Nakashima, 1990; Godo and Sunnana, 1992; Williams et al., 2011). This assumption is common in trawl-based analyses and affects acoustic-based surveys using trawl catches to validate backscatter patterns. We did not assume that surface trawl data were representative of abundance, but that catch compositions were proportional to abundance. If the trawl did not proportionally sample species composition and lengths, then acoustic density estimates may be biased toward lengths or species that were captured in the trawl. This assumption could not be tested. Normal distributions of fish lengths and the retention of macrozooplankton (e.g. amphipods) suggest that the assumption was reasonable; however, estimates of species compositions and lengths from the trawl are uncertain. The catch composition of a similar midwater trawl was shown to be biased toward larger animals (Williams et al., 2011). A dedicated study of selectivity by the Cantrawl, as has been done for the Aleutian wing trawl (Williams et al., 2011), is needed to validate this assumption and to improve confidence in forage fish density estimates.

Time constraints during BASIS surveys limited the number of midwater trawls used to verify species composition and sample fish length distributions in 2008–2010. Areas where non-sampled midwater zone backscatter patterns did not match backscatter patterns that were sampled were classified as unknown and removed from analyses. While this approach reduced the size of midwater zone acoustic datasets (e.g. no midwater zone estimate for 2008), it increased our confidence in species backscatter allocations based on available trawl data. Although visual classification of acoustic data is less desirable than validation using direct samples, comparisons of midwater zone age-0 pollock distributions across years are possible, given appropriate caveats. Future efforts to estimate midwater forage fish densities will require additional trawling effort for target verification, and depth-stratified trawling to validate assumptions about distribution homogeneity.

Although the present study surveyed much of the EBS shelf, the sample domain may not have included the entire range of forage fish distributions. Studies have reported observations of age-0 pollock in both shallower (e.g. Wilson et al., 1996) and deeper (e.g. Tang et al., 1996) water depths than those sampled in the present study. As densities of capelin, age-0 Pacific cod, and age-0 pollock in this study generally tapered off before the ends of survey transects were reached, it is likely that the 2006–2010 surveys covered a representative range of depths occupied by these species. Failure to capture the entire distributional range would result in a biased (low or high) estimate of mean density and a biased characterization of spatial distribution.

Despite the fact that survey durations ranged from 17 (2008) to 49 (2007, 2010) days, all distribution data were treated as a snapshot of forage fish densities in the southeastern Bering Sea. This assumption implies that there was no directional movement by fish that resulted in an over- or underestimate of any fish density (Simmonds and MacLennan, 2005). As the range of sampling dates varied across years, we also assumed that no date-related temporal changes in horizontal distributions or ontogenetic shifts in vertical distribution affected density estimates between years. This assumption is consistent with other fixed-date surveys.

The 2006–2010 surveys coincided with a period of average (2006) and cold (2007–2010) ocean temperatures in the eastern

Bering Sea (Stabeno et al., 2012b). A comparison of fish vertical and horizontal densities across years suggested that temperature-related conditions may have influenced horizontal and vertical distributions. As predicted by “thermal gateways” (Ciannelli and Bailey, 2005), capelin were widely distributed in the surface zone and had the highest densities in the coldest years, 2009 and 2010. Both surface zone age-0 Pacific cod and age-0 pollock were absent from much of the surveyed areas in 2009, a year in which the temperature in the top 20 m was the coldest of the 2006–2010 period (Stabeno et al., 2012b). In 2010, surface zone age-0 pollock were concentrated near the Alaska Peninsula and Unimak Island rather than spread between the 50–100 m contours as they were in 2006–2008 and during the 2004–2005 warm years (Moss et al., 2009; Hollowed et al., 2012). Despite the limited midwater zone observations, the highest densities of age-0 pollock, which dominated the biomass in 2009 and 2010, were found in deeper waters of the SEBS, likely outside the extensive cold pool (Stabeno et al., 2012b). As distributions may be related to water temperatures, observed forage fish distributions in the present study are thought to reflect average and cold year conditions, and may not be representative of distributions during warm years.

Shifts in vertical and/or horizontal distributions by Bering Sea forage fish in response to water temperature or other climate-related conditions must be considered when planning surveys and/or analyzing existing data. While the present study did not include acoustic data from warm years, we would predict that if forage fish vertical distribution shifts shallower in the water column, then acoustic-based abundance indices may be biased low. Reduction of the acoustic exclusion zone below 15 m reduces this potential bias. Given observed changes in the depth of the acoustically-detected layer within and across years, surface trawl-based indices of abundances may be biased. Similarly, the presence of high densities of midwater age-0 pollock suggest that surface trawl data alone will not characterize their abundance and may not sample the bulk of the biomass in some years. This discrepancy is predicted to be most severe during cold water conditions such as those observed in 2009 and 2010. The integration of acoustic and trawl sampling is recommended to ensure accurate characterization of forage fish species throughout the water column (e.g. McQuinn et al., 2005).

Understanding horizontal and vertical distributions of forage fish is needed to effectively manage the Bering Sea ecosystem. Baseline distribution patterns from the present study quantify the 2006–2010 range of spatial distributions and densities under cold and average water temperatures. When combined with previous observations during warm years, it is possible to begin to evaluate potential influences of climate-related physical and biological factors on distributions, recruitment, and potential competition among forage fish species in the EBS.

Acknowledgments

The authors thank the Chief Scientists, scientific staff, Captains, and crews on the *Epic Explorer*, *Northwest Explorer*, *Sea Storm*, and the NOAA ship *Oscar Dyson* during 2006–2010. We also thank the NOAA-MACE program (Seattle, WA) for use of equipment and software during 2008–2010 and for providing calibration data for scientific echosounders. The NOAA-FEDZ Laboratory (Juneau, AK) is gratefully acknowledged for their assistance in species identification. We thank Jeff Napp (NOAA), Alex De Robertis (NOAA) and four anonymous reviewers for constructive comments that improved the final product. The findings and conclusions in this paper are those of the authors and do not necessarily represent the views of the National Marine Fisheries Service, NOAA. Reference to trade names does not imply endorsement by the National

Marine Fisheries Service, NOAA. This paper is NPRB publication number 420 and BEST-BSIERP Bering Sea Project publication number 97.

References

- Bailey, K.M., 1989. Interaction between the vertical distribution of juvenile walleye pollock *Theragra chalcogramma* in the eastern Bering Sea, and cannibalism. *Mar. Ecol. Prog. Ser.* 53, 205–213.
- Bakkala, R.G., Traynor, J.J., Teshima, K., Shimada, A.M., Yamaguchi, H., 1985. Results of Cooperative US–Japan Groundfish Investigations in the Eastern Bering Sea During June–November 1982. NOAA Technical Memorandum. NMFS F/NWC-87. U.S. Department of Commerce, 448 pp.
- Brierley, A.S., Axelsen, B.E., Boyer, D.C., Lynam, C.P., Didcock, C.A., Boyer, H.J., Sparks, C.A.J., Purcell, J.E., Gibbons, M.J., 2004. Single-target echo detections of jellyfish. *ICES J. Mar. Sci.* 61, 383–393.
- Brodeur, R.D., Wilson, M.T., 1996. A review of the distribution, ecology and population dynamics of age-0 walleye pollock in the Gulf of Alaska. *Fish. Oceanogr.* 5, 148–166.
- Brodeur, R.D., 1998. In situ observations of the association between juvenile fishes and scyphomedusae in the Bering Sea. *Mar. Ecol. Prog. Ser.* 163, 11–20.
- Brodeur, R.D., Wilson, M.T., Ciannelli, L., Doyle, M., Napp, J.M., 2002a. Interannual and regional variability in distribution and ecology of juvenile pollock and their prey in frontal structures of the Bering Sea. *Deep-Sea Res. II* 49, 6051–6067.
- Brodeur, R.D., Sugisaki, H., Hunt Jr., G.L., 2002b. Increases in jellyfish biomass in the Bering Sea: implications for the ecosystem. *Mar. Ecol. Prog. Ser.* 233, 89–103.
- Ciannelli, L., Bailey, K.M., 2005. Landscape dynamics and resulting species interactions: the cod-capelin system in the southeastern Bering Sea. *Mar. Ecol. Prog. Ser.* 291, 227–236.
- Cieciel, K., Gann, J., Eisner, L., 2012. Trends in jellyfish bycatch from the Bering Aleutian Salmon International Survey (BASIS). In: Zador, S. (Ed.), *Ecosystem Considerations 2012. Stock Assessment and Fishery Evaluation Report*. North Pacific Fishery Management Council, Anchorage, Alaska, pp. 117–118.
- Farley Jr., E.V., Murphy, J., Moss, J., Feldmann, A., Eisner, L., 2009. Marine ecology of western Alaska juvenile salmon. In: Krueger, C.C., Zimmerman, C.E. (Eds.), *Pacific Salmon: Ecology and Management of Western Alaska's Populations*, 70. American Fisheries Society, Symposium, Bethesda, Maryland, pp. 307–329.
- Foote, K.G., Knudsen, H.P., Vestnes, G., MacLennan, D.N., Simmonds, E.J., 1987. Calibration of Acoustic Instruments for Fish Density Estimation: A Practical Guide. ICES Cooperative Research Report no. 144.
- Foote, K.G., 1987. Fish target strengths for use in echo integrator surveys. *J. Acoust. Soc. Am.* 83, 981–987.
- Gauthier, S., Horne, J.K., 2004. Acoustic characteristics of forage fish species in the Gulf of Alaska and Bering Sea based on Kirchhoff-approximation models. *Can. J. Fish. Aquat. Sci.* 61, 1839–1850.
- Godø, O.R., Sunnana, K., 1992. Size selection during trawl sampling of cod and haddock and its effect on abundance indices at age. *Fish. Res.* 13, 293–310.
- Gonzalez, R.C., Woods, R.E., 2007. *Digital Image Processing*, 3rd edition Prentice Hall, New Jersey.
- Graham, T.R., Harvey, J.T., Benson, S.R., Renfree, J.S., Demer, D.A., 2010. The acoustic identification and enumeration of scyphozoan jellyfish, prey for leatherback sea turtles (*Dermochelys coriacea*), off central California. *ICES J. Mar. Sci.* 67, 1739–1748.
- Guttormsen, M.A., Wilson, C.D., 2009. In situ measurements of capelin (*Mallotus villosus*) target strength in the North Pacific Ocean. *ICES J. Mar. Sci.* 66, 258–263.
- Helle, J., Farley, E., Murphy, J., Feldmann, A., Cieciel, K., Moss, J., Eisner, L., Pohl, J., Courtney, M., 2007. The Bering-Aleutian Salmon International Survey (BASIS). NOAA AFSC Quarterly Report. January–February–March 2007. U.S. Department of Commerce, pp. 1–5.
- Hollowed, A.B., Barbeaux, S., Farley, E., Cokelet, E.D., Kotwicki, S., Ressler, P.H., Spital, C., Wilson, C., 2012. Effects of climate variations on pelagic ocean habitats and their role in structuring forage fish distributions in the Bering Sea. *Deep-Sea Res. II* 65–70, 230–250.
- Hurst, T.P., Moss, J.H., Miller, J.A., 2012. Distributional stability of 0-group Pacific cod (*Gadus macrocephalus*) in the eastern Bering Sea under variable recruitment and thermal conditions. *ICES J. Mar. Sci.* 69, 163–174.
- Kachel, N.B., Hunt Jr., G.L., Salo, S.A., Schumacher, J.D., Stabeno, P.J., Whitedge, T.E., 2002. Characteristics and variability of the inner front of the southeastern Bering Sea. *Deep-Sea Res. II* 49, 5889–5909.
- Kang, D., Hwang, D., 2003. Ex situ target strength of rockfish (*Sebastes schlegeli*) and Red Sea bream (*Pagrus major*) in the Northwest Pacific. *ICES J. Mar. Sci.* 60, 538–543.
- Keith, G.J., Ryan, T.E., Kloser, R.J., 2005. ES60adjust.jar. CSIRO Marine and Atmospheric Research.
- Korneliusson, R.J., 2000. Measurement and removal of echo integration noise. *ICES J. Mar. Sci.* 57, 1204–1217.
- Ladd, C., Stabeno, P., 2012. Stratification on the eastern Bering Sea shelf revisited. *Deep-Sea Res. II* 65–70, 72–83.
- Lauth, R., Hoff, G., 2012. Jellyfish—Eastern Bering Sea. In: Zador, S. (Ed.), *Ecosystem Considerations 2012. Stock Assessment and Fishery Evaluation Report*. North Pacific Fishery Management Council, Anchorage, Alaska, pp. 116–117.
- Livingston, P.A., Aydin, K., Boldt, J., Ianelli, J., Jurado-Molina, J., 2005. A framework for ecosystem impacts assessment using an indicator approach. *ICES J. Mar. Sci.* 62, 592–597.

- MacLennan, D.N., Fernandes, P.G., Dalen, J., 2002. A consistent approach to definitions and symbols in fisheries acoustics. *ICES J. Mar. Sci.* 59, 365–369.
- McQuinn, I.H., Simard, Y., Stroud, T.W.F., Beaulieu, J.-L., Walsh, S.J., 2005. An adaptive, integrated “acoustic-trawl” survey design for Atlantic cod (*Gadus morhua*) with estimation of the acoustic and trawl dead zone. *ICES J. Mar. Sci.* 62, 93–106.
- Miyake, H., Yoshida, H., Ueda, Y., 1996. Distribution and abundance of age-0 juvenile walleye pollock, *Theragra chalcogramma*, along the Pacific coast of southeastern Hokkaido, Japan. In: Brodeur, R., Livingston, P.A., Loughlin, T.R., Hollowed, A.B. (Eds.), NOAA Technical Report. NMFS 126. U.S. Department of Commerce, pp. 3–10.
- Moss, J.H., Farley Jr., E.V., Feldmann, A.M., Ianelli, J.C., 2009. Spatial distribution, energetic status, and food habits of eastern Bering Sea age-0 walleye pollock. *Trans. Am. Fish. Soc.* 138, 497–505.
- Mueter, F.J., Litzow, M.A., 2008. Sea ice retreat alters the biogeography of the Bering Sea continental shelf. *Ecol. Appl.* 18, 309–320.
- Nakashima, B.S., 1990. Escapement from a Diamond-IX midwater trawl during acoustic surveys for capelin (*Mallotus villosus*) in the Northwest Atlantic. *ICES J. Mar. Sci.* 47, 76–82.
- Parker-Stetter, S.L., Horne, J.K., Weingartner, T.J., 2011. Distribution of polar cod and age-0 fish in the U.S. Beaufort Sea. *Polar Biol.* 34, 1543–1557.
- Peltonen, H., Malinen, T., Tuomaala, A., 2006. Hydroacoustic in situ target strength of smelt (*Osmerus eperlanus* (L.)). *Fish. Res.* 80, 190–195.
- Pikitch, E.K., Santora, C., Babcock, E.A., Bakun, A., Bonfil, R., Conover, D.O., Dayton, P., Doukakis, P., Fluharty, D., Heneman, B., Houde, E.D., Link, J., Livingston, P.A., Mangel, M., McAllister, M.K., Pope, J., Sainsbury, K.J., 2004. Ecosystem-based fishery management. *Science* 306, 346–347.
- Pikitch, E., Boersma, P.D., Boyd, I.L., Conover, D.O., Cury, P., Essington, T., Heppell, S.S., Houde, E.D., Mangel, M., Pauly, D., Plagányi, É., Sainsbury, K., Steneck, R.S., 2012. Little Fish, Big Impact: Managing a Crucial Link in Ocean Food Webs. Lenfest Ocean Program, Washington, D.C. 108.
- Rose, G.A., Porter, D.R., 1996. Target-strength studies on Atlantic cod (*Gadus morhua*) in Newfoundland waters. *ICES J. Mar. Sci.* 53, 259–265.
- Schabetsberger, R., Brodeur, R.D., Ciannelli, L., Napp, J.M., Swartzman, G.L., 2000. Diel vertical migration and interaction of zooplankton and juvenile walleye pollock (*Theragra chalcogramma*) at a frontal region near the Pribilof Islands, Bering Sea. *ICES J. Mar. Sci.* 57, 1283–1295.
- Sigler, M., Harvey, R., 2013. Introduction to the Bering Sea Project. *Deep-Sea Res. II*, 94, 2–6.
- Simmonds, J., MacLennan, D., 2005. *Fisheries Acoustics: Theory and Practice*. Blackwell Science Ltd, United Kingdom.
- Springer, A.M., Speckman, S.G., 1997. A Forage Fish is What? Summary of the Symposium. Forage Fishes in Marine Ecosystems. Alaska Sea Grant College Program. University of Alaska Fairbanks, vol. 97-01, pp. 773–805.
- Stabeno, P.J., Farley Jr., E.V., Kachel, N.B., Moore, S., Mordy, C., Napp, J.M., Overland, J.E., Pinchuk, A.L., Sigler, M.F., 2012a. A comparison of the physics of the northern and southern shelves of the eastern Bering Sea and some implications for the ecosystem. *Deep-Sea Res. II* 65–70, 14–30.
- Stabeno, P.J., Kachel, N.B., Moore, S.E., Napp, J.M., Sigler, M., Yamaguchi, A., Zerbini, A.N., 2012b. Comparison of warm and cold years on the southeastern Bering Sea shelf and some implications for the ecosystem. *Deep-Sea Res. II* 65–70, 31–45.
- Swartzman, G., Brodeur, R., Napp, J., Hunt, G., Demer, D., Hewitt, R., 1999. Spatial proximity of age-0 walleye pollock (*Theragra chalcogramma*) to zooplankton near the Pribilof Islands, Bering Sea, Alaska. *ICES J. Mar. Sci.* 56, 545–560.
- Swartzman, G., Napp, J., Brodeur, R., Winter, A., Ciannelli, L., 2002. Spatial patterns of pollock and zooplankton distribution in the Pribilof Islands, Alaska nursery area and their relationship to pollock recruitment. *ICES J. Mar. Sci.* 59, 1167–1186.
- Swartzman, G., Winter, A., Coyle, K., Brodeur, R., Buckley, T., Ciannelli, L., Ianelli, J., Macklin, A., 2005. Relationship of age-0 pollock abundance and distribution around the Pribilof Islands, to other shelf regions of the eastern Bering Sea. *Fish. Res.* 74, 273–287.
- Tang, W., Jin, X., Li, F., Chen, J., Wang, W., Chen, Y., Zhao, X., Dai, F., 1996. Summer distribution and abundance of age-0 walleye pollock, *Theragra chalcogramma*, in the Aleutian Basin. In: Brodeur, R., Livingston, P.A., Loughlin, T.R., Hollowed, A.B. (Eds.), NOAA Technical Report. NMFS 126. U.S. Department of Commerce, pp. 35–46.
- Traynor, J.J., 1996. Target-strength measurements of walleye pollock (*Theragra chalcogramma*) and Pacific whiting (*Merluccius productus*). *ICES J. Mar. Sci.* 53, 253–258.
- Traynor, J.J., Smith, D., 1996. Summer distribution and abundance of age-0 walleye pollock, *Theragra chalcogramma*, in the Bering Sea. NOAA Technical Report. NMFS 126. U.S. Department of Commerce, pp. 57–59.
- Walters, G.E., Teshima, K., Traynor, J.J., Bakkala, R.G., Sassano, J.A., Halliday, K.L., Karp, W.A., Mito, K., Williamson, N.J., Smith, D.M., 1988. Distribution, Abundance, and Biological Characteristics of Groundfish in the Eastern Bering Sea Based on Results of the US–Japan Triennial Bottom Trawl and Hydroacoustic Surveys During May–September, 1985. NOAA Technical Memorandum. NMFS F/NWC-154. U.S. Department of Commerce, 400 pp.
- Watkins, J.L., Brierley, A.S., 1996. A post-processing technique to remove background noise from echo integration data. *ICES J. Mar. Sci.* 53, 339–344.
- Williams, K., Punt, A.E., Wilson, C.D., Horne, J.K., 2011. Length-selective retention of walleye pollock, *Theragra chalcogramma*, by midwater trawls. *ICES J. Mar. Sci.* 68, 119–129.
- Wilson, M.T., Brodeur, R.D., Hinckley, S., 1996. Distribution and abundance of age-0 walleye pollock, *Theragra chalcogramma*, in the western Gulf of Alaska during September 1990. In: Brodeur, R., Livingston, P.A., Loughlin, T.R., Hollowed, A.B. (Eds.), NOAA Technical Report NMFS 126. U.S. Department of Commerce, pp. 11–24.
- Wuillez, M., Ressler, P.H., Wilson, C.D., Horne, J.K., 2012. Multifrequency species classification of acoustic-trawl survey data using semi-supervised learning with class discovery. *J. Acoust. Soc. Am.* 131, EL184–EL190.
- Yasuma, H., Nakagawa, R., Yamakawa, T., Miyashita, K., Aoki, I., 2009. Density and sound-speed contrasts, and target strength of Japanese sandeel *Ammodytes personatus*. *Fish. Sci.* 75, 545–552.



Detecting temporal trends and environmentally-driven changes in the spatial distribution of bottom fishes and crabs on the eastern Bering Sea shelf



Stan Kotwicki^{*1}, Robert R. Lauth¹

Resource Assessment and Conservation Engineering Division, Alaska Fisheries Science Center, National Marine Fisheries Service, NOAA, 7600 Sand Point Way NE, Seattle, WA 98115, USA

ARTICLE INFO

Available online 14 March 2013

Keywords:

Spatial distribution
Population shift
Cold pool
Bottom fish
Crab
Bering Sea shelf

ABSTRACT

This study uses a 30-year time series of standardized bottom trawl survey data (1982–2011) from the eastern Bering Sea shelf to model patterns of summer spatial distribution for various bottom fishes and crabs in response to changes in the areal extent of the cold pool, time lag between surveys, and fluctuations in population abundance. This investigation is the first to include data for the 2006–2010 cold period and to use between-year comparisons of local and shelf-wide spatial indices to test specific responses to three different isothermal boundaries within the cold pool. Distributional shifts in population varied considerably among species and directional vectors for some species were greater in magnitude to the east or west than to the north or south; however, in general, eastern Bering Sea shelf populations shifted southward in response to the increasing cold pool size, and after accounting for differences in temperature and population abundance, there was still a temporal northward shift in populations over the last three decades despite the recent cooling trend. Model results for local and shelf-wide indices showed that survey time lag and cold pool extent had a greater effect on spatial distribution than population abundance, suggesting that density-independent mechanisms play a major role in shaping distribution patterns on the eastern Bering Sea shelf. The area enclosed by the 1 °C isotherm most commonly affects both local and shelf-wide spatial indices suggesting that 1 °C is a more important boundary for describing temperature preferences of eastern Bering Sea bottom fishes and crabs than is the 2 °C isotherm used for designating the physical boundary for the cold pool.

Published by Elsevier Ltd.

1. Introduction

The distributions of bottom fishes and crabs on the eastern Bering Sea continental shelf are affected by many different biotic and abiotic factors. A subsurface layer of cold water (< 2 °C) known as the “cold pool” (Stabeno et al., 2001) is a major abiotic factor affecting the distribution of fish populations on the eastern Bering Sea shelf (Spencer, 2008; Stabeno et al., 2012a; Wyllie-Echeverria and Wooster, 1998). Retreating seasonal ice and the diminishing areal extent of the summer cold pool during a warm period lasting from 2000 through 2005 was related to a community-wide northward shift in bottom fishes and invertebrates (Mueter and Litzow, 2008). Studies have focused primarily on climate change and a general warming trend as the mechanism for shelf-wide temporal shifts in the eastern Bering Sea. From 2006 to 2010, the eastern Bering Sea shelf environment entered into a relatively cold period when the spatial extent of winter sea ice and the summer cold pool both increased

(Sigler et al., 2011; Stabeno et al., 2012a,b). This is the first investigation to include an analysis of data for the 2006–2010 cold period to determine if increases in the size of the summer cold pool reversed the northward temporal shift in populations on the eastern Bering Sea shelf, and to investigate more specifically how distributions may be affected by three different isothermal boundaries within the cold pool.

A fundamental problem to studying ecological processes is that they are variable over a range of different spatial, temporal, and organizational scales (Ciannelli et al., 2008; Levin, 1992). Spatial analyses of bottom fishes and crabs on the eastern Bering Sea shelf are complex because the physical and biological processes are dynamic, and the organisms, as well as the cold pool, are not homogeneously distributed in space and time along latitudinal or longitudinal axes or gradients. This makes direct comparisons between years or over the scale of the entire eastern Bering Sea shelf difficult. Moreover, studies focusing on population shifts have lacked spatially-explicit information about how a species is likely to respond to different temperature levels within the cold pool. Interannually, the spatial extent of the cold pool varies substantially during the late spring and summer period. During warm

^{*} Corresponding author. Tel.: +1 206 526 6614; fax: +1 206 526 6723.

E-mail address: Stan.Kotwicki@noaa.gov (S. Kotwicki).

¹ Equal authorship.

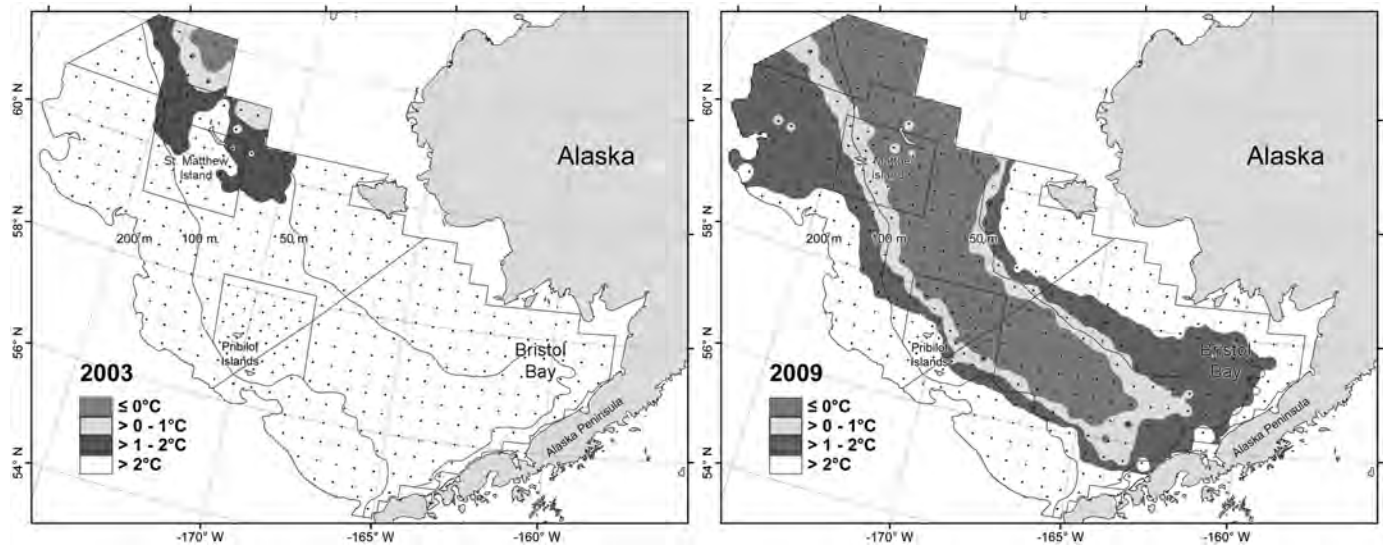


Fig. 1. Variation in the extent of the summer cold pool during a warm year (2003) and a cold year (2009) on the eastern Bering Sea shelf as measured during bottom trawl surveys. Also shown are the 50-m, 100-m, and 200-m isobaths, survey stratum boundaries, and sampling stations (dots).

years, the extent of the cold pool can be restricted to the northern shelf, which contrasts sharply to cold years when the extent of the cold pool can extend down the middle shelf as far as the Alaska Peninsula and eastward into Bristol Bay (Fig. 1). Between warm and cold periods, there is also spatial heterogeneity in the size and shape of the two-dimensional areas bounded within the 0, 1, and 2 °C isotherms. Given the large variability in the hydrographic structure and extent of the cold pool, one might expect corresponding changes in local spatial patterns within a population, as well as distribution shifts in the combined population, especially for migratory temperate species having a low tolerance for water temperatures typically observed within the cold pool (−1.7 to +2 °C).

This study uses a 30-year time series of standardized bottom trawl survey data (1982–2011) from the eastern Bering Sea shelf to model between-year responses of spatial distribution indices for selected bottom fishes and crabs against between-year differences in the areal extent of the cold pool using three different isothermal boundaries. There are other factors besides changes in temperature that can affect distribution, including natural fluctuations in population abundance (Spencer, 2008) and the temporal autocorrelation of spatial patterns (Pyper and Peterman, 1998) also known as the time lag effect; i.e., snapshots of a spatial distribution for a particular species that are closer in time may be more similar than those separated by longer periods of time. Hence, in addition to temperature, we investigate variability in spatial distribution patterns due to between-year changes in population abundance as well as the time lag between survey years.

The temporal scale we used was limited to the available survey data, but to determine if processes shape local patterns of distribution differently than shelf-wide patterns of distribution, we chose two indices as dependent variables in the model: (1) a shelf-wide index comparing between-year responses of population centers across the eastern Bering Sea shelf, and (2) a spatially-explicit local index comparing between-year responses of abundance location-by-location. A generalized additive model (GAM) framework was used to model responses using the two spatial indices for all possible survey year combinations. The basic thesis is that these models will explain the observed variability in spatial distribution of populations at shelf-wide and local levels, and determine the relative contribution of a changing cold pool, fluctuating population abundance, and time lag between surveys to the distributional changes observed in various bottom fishes and crabs on the eastern Bering Sea shelf.

2. Methods

2.1. Surveys

Since 1982, the National Marine Fisheries Service (NMFS) (NMFS, 2012) eastern Bering Sea shelf standardized bottom trawl survey has been conducted annually using chartered commercial fishing vessels to sample stations within a systematic grid design consisting of ten strata and 356 fixed stations (Fig. 1). In 1987, an additional two strata with 20 fixed stations were added to the northwestern most part of the shelf. The inner, middle, and outer shelf strata have different hydrographic structure and circulation and are nominally delineated by the 50, 100, and 200-m isobaths (Coachman, 1986) and a diagonal line across the middle of the shelf delineates regions of the survey area that were originally established to separate different southern and northern populations of principal bottom fishes and crabs (Pereyra et al., 1976). Strata in the vicinity of St. Matthew Island and the Pribilof Islands are sampled at a higher density than the other strata. All bottom trawl surveys were conducted within the same 3-month time period (May–August) using standardized gear and methods (Stauffer, 2004). Survey catch data were standardized to catch per unit of effort (CPUE) for each station by dividing total catch weight (kg) by the area-swept for each survey trawl haul in hectares (ha). The mean CPUE for each taxa in each stratum was weighted by the proportion of the total stratum area and then summed for all strata to obtain population abundance (*ABUND*) for each year. Bottom water temperatures were recorded at each station by deploying an expendable bathythermograph from the survey vessel (1982–1991) or by attaching a digital thermometer to the trawl headrope (1992–2011). Station bottom temperatures were weighted by stratum area before calculating an average survey bottom temperature. Linear regression analyses were used to test for significance of trends in total cold pool area (< 2 °C) and average survey bottom temperature over time. ArcMap² v9.3 was used to plot trawl station bottom temperatures by year and to generate isotherms in one degree intervals within the standard survey area using the inverse distance-weighted squared interpolation method.

² Mention of trade names or commercial companies is for identification purposes only and does not imply endorsement by the National Marine Fisheries Service, NOAA.

An Albers Equal Area Conic projection was used to calculate the area within the polygons generated from the 0, 1, and 2 °C isotherms.

The primary criterion for selecting the taxa used in the analysis (Table 1) was that bottom trawl abundance for a taxon had to be a credible index of abundance over time. Excluded taxa failed to meet this criterion for a variety of reasons: (1) bottom trawl not designed for quantitative sampling of pelagic species, (2) historical changes in the specificity and consistency of field identifications (Stevenson and Hoff, 2009), (3) historical changes in the consistency of subsampling rare or singular species from large catches, and (4) rare or patchily distributed species with insufficient data for analyses. Accordingly, Alaska skate (*Bathyrāja parmifera*) and northern rock sole (*Lepidopsetta polyxystra*) were combined into the broader taxonomic groups *Bathyrāja* spp. and *Lepidopsetta* spp., respectively. In both cases, the other species combined into these taxonomic groups had overlapping spatial distributions, but composed only a small percentage of the total abundance within

Table 1

List of taxa considered for the analysis. An “*” next to the common name indicates that the taxa was included in the analysis and a number in the last column indicates the rationale (see below) for those taxa excluded from the analysis.

Common name	Scientific name	Exclusion
Skates*	<i>Bathyrāja</i> spp.	
Arrowtooth flounder*	<i>Atheresthes stomias</i>	
Kamchatka flounder*	<i>Atheresthes evermanni</i>	2,4
Greenland turbot*	<i>Reinhardtius hippoglossoides</i>	
Pacific halibut*	<i>Hippoglossus stenolepis</i>	
Flathead sole*	<i>Hippoglossoides elassodon</i>	
Bering flounder*	<i>Hippoglossoides robustus</i>	
Rex sole*	<i>Glyptocephalus zachirus</i>	
Yellowfin sole*	<i>Limanda aspera</i>	
Longhead dab*	<i>Limanda proboscidea</i>	
Sakhalin sole	<i>Limanda sakhalinensis</i>	4
Starry flounder*	<i>Platichthys stellatus</i>	
Rock sole*	<i>Lepidopsetta</i> spp.	
Alaska plaice*	<i>Pleuronectes quadrituberculatus</i>	
Sawback poacher	<i>Leptagonus frenatus</i>	2,3
Sturgeon poacher*	<i>Podothecus accipenserinus</i>	
Bering poacher	<i>Ocella dodecahedron</i>	4
Pacific sand lance	<i>Ammodytes</i> spp.	1
Searcher	<i>Bathymaster signatus</i>	3,4
Pacific herring	<i>Clupea pallasii</i>	1
Yellow Irish lord	<i>Hemilepidotus jordani</i>	4
Butterfly sculpin*	<i>Hemilepidotus papillio</i>	
Warty sculpin	<i>Myoxocephalus verrucosus</i>	2
Great sculpin	<i>Myoxocephalus polyacanthocephalus</i>	2
Plain sculpin	<i>Myoxocephalus jaok</i>	2
Spinyhead sculpin	<i>Dasycottus setiger</i>	3,4
Bigmouth sculpin	<i>Hemitripterus bolini</i>	3
Pacific sandfish	<i>Trichodon trichodon</i>	4
Pacific cod*	<i>Gadus macrocephalus</i>	
Arctic cod	<i>Boreogadus saida</i>	1,2
Saffron cod	<i>Eleginus gracilis</i>	4
Walleye pollock*	<i>Theragra chalcogramma</i>	
Whitespotted greenling	<i>Hexagrammos stelleri</i>	3,4
Eulachon	<i>Thaleichthys pacificus</i>	1
Capelin	<i>Mallotus villosus</i>	1
Rainbow smelt	<i>Osmerus mordax</i>	1
Marbled eelpout	<i>Lycodes rarioides</i>	2,4
Wattled eelpout*	<i>Lycodes palearis</i>	
Shortfin eelpout*	<i>Lycodes brevipes</i>	
Decorator crab	<i>Oregonia gracilis</i>	2
Tanner crab*	<i>Chionoecetes bairdi</i>	
Snow crab*	<i>Chionoecetes opilio</i>	
Helmet crab	<i>Telmessus cheiragonus</i>	4
Red king crab*	<i>Paralithodes camtschaticus</i>	
Blue king crab*	<i>Paralithodes platypus</i>	
Horsehair crab	<i>Erimacrus isenbeckii</i>	4

1. Bottom trawl not designed for quantitative sampling of pelagic species.
2. Historical changes in the specificity and consistency of field identifications.
3. Historical changes in the consistency of subsampling rare or singular species.
4. Rare or patchily distributed species with insufficient data for spatial analyses.

that group in any given year (< 5%). Flathead sole (*Hippoglossoides elassodon*) and Bering flounder (*H. robustus*) are difficult to differentiate; however, their zoogeography differs (Mecklenburg et al., 2002) and there was a concerted effort to separate the two species since 1982, so the two species were analyzed separately. Two other similar species, arrowtooth flounder (*Atheresthes stomias*) and Kamchatka flounder (*A. evermanni*) were not identified separately in the survey until 1992, so the analysis for arrowtooth flounder was confined to the 1992–2011 time period. A separate analysis for Kamchatka flounder was not conducted due to insufficient data.

2.2. Spatial indices

Two spatial indices were used for analyzing pairwise comparisons among all bottom trawl survey years: the global index of collocation (*GIC*) and the local index of collocation (*LIC*; Bez, 2007). The *GIC* and *LIC* provide different ways of quantifying the degree of similarity in a population's spatial distribution between years. The *GIC* indicates whether a population center of abundance has shifted between years using a pairwise comparison of center of gravity (*CG*) within a large geographical area taking into account the respective dispersion of that population in each of those years. In contrast, the *LIC* measures variability in local spatial distribution patterns between years using a location-by-location pairwise comparison of standardized catch.

Indices for both the *GIC* and *LIC* range from 0 to 1 with higher values indicating greater between-year similarity in the spatial distribution of an organism. Fig. 2 is a set of hypothetical grids to

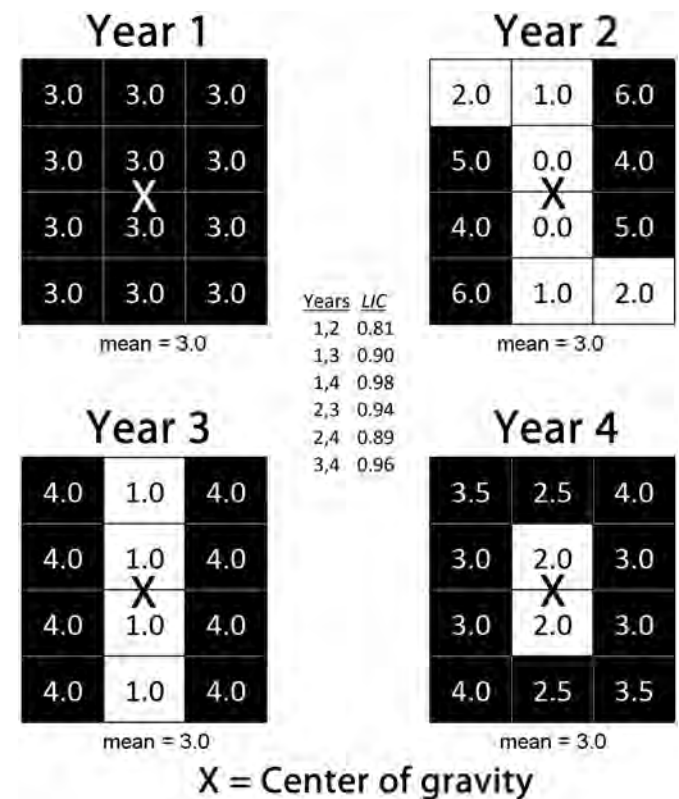


Fig. 2. Set of hypothetical grids illustrating different kinds of spatial variability. Numbers inside each grid cell represent an organism's abundance. White grid cells illustrate how an environmental feature such as temperature (e.g., cold pool ≤ 2.0 °C) might also vary at the same time. Regardless of the obvious heterogeneity within the grid cells, all 4 years have an identical center of gravity (*CG*) indicating no changes to the spatial distribution. In contrast, a grid cell-by-grid cell comparison using the local index of collocation (*LIC*) between years indicates changes in spatial distribution.

illustrate the difference between the *LIC* and the *GIC* and to underscore the importance of different kinds of spatial variability when choosing a metric for investigating distributional change. Suppose each grid cell represents an organism's abundance sampled annually during the same season in 4 consecutive years. White grid cells illustrate how an environmental feature such as temperature (e.g., cold pool ≤ 2.0 °C) might also vary at the same time. All 4 years have the same *CG*; hence, $\Delta CG=0$ and the calculated values of *GIC* for all six between-year comparisons are equal to 1 indicating no changes to the spatial distribution. In contrast, the between-year comparisons for *LIC* are grid cell-by-grid cell; hence, the calculated values of *LIC* are all different and are less than 1 indicating that the spatial distribution pattern between years has changed.

The *GIC* and the *LIC* were calculated using data from the 30-year NMFS eastern Bering Sea shelf standardized bottom trawl survey, which resulted in up to 435 pairwise comparisons of all the different year \times year combinations for each taxon. The *GIC* (1) compares the similarity in the *CG* for each pairwise year combination. The value of dispersion *I* (2) accounts for the variance for all weighted positions around the *CG*. The *GICs* were calculated using the fixed set of stations common to all survey years ($n=356$).

$$GIC = 1 - \frac{\Delta CG^2}{\Delta CG^2 + I_1 + I_2}, \quad (1)$$

where ΔCG is the distance in kilometers (km) between the *CGs* for a given pair of years (see details below) and I_1 is the dispersion for year one and I_2 for year two.

$$I = \frac{\sum_{i=1}^n (\Delta CG)^2 z_i}{\sum_{i=1}^n z_i} \quad (2)$$

The CG_{lat} (latitude) and CG_{long} (longitude) for each survey year and taxon were calculated by weighting the latitude (lat_i) or longitude ($long_i$) by the taxon density at each station (z_i) and dividing their respective sums by the sum of all z_i s by year (3). The (CG_{lat} , CG_{long}) was plotted by year for selected taxa.

$$CG_{lat} = \frac{\sum_{i=1}^n lat_i z_i}{\sum_{i=1}^n z_i} \quad CG_{long} = \frac{\sum_{i=1}^n long_i z_i}{\sum_{i=1}^n z_i} \quad (3)$$

The ΔCG was calculated for each pairwise comparison of years using radians in the formula for the great-circle distance where R is the mean radius of the earth (6,371 km).

$$\Delta CG = \arccos(\sin(CG_{lat_1}) * \sin(CG_{lat_2}) + \cos(CG_{lat_1}) * \cos(CG_{lat_2}) * \cos(CG_{long_1} - CG_{long_2})) * R \quad (4)$$

Variability in local spatial patterns of distribution were measured using the *LIC* (5), which makes pairwise comparisons at each survey station between years, where

$$LIC = \frac{\sum_{i=1}^n z_{i1} z_{i2}}{\sqrt{\sum_{i=1}^n z_{i1}^2} \sqrt{\sum_{i=1}^n z_{i2}^2}}, \quad (5)$$

where z_{i1} and z_{i2} are the organism densities by taxon at station i for each set of paired years. Survey catch data from all 376 stations were included for calculating the *LIC* if they were available. The *GICs* and *LICs* were pooled for all years by taxa to calculate a range, mean, and standard deviation for each.

2.3. Model

A GAM was used to investigate how the *GIC* and the *LIC* responded to the between-year absolute differences in the areal extent (ΔCPA_T) of the cold pool (ΔCPA_T) at a threshold temperature T (°C), the absolute difference in population abundance ($\Delta ABUND$), and the time lag ($\Delta YEARS$) by taxon. For simplicity, absolute differences in predictor variables will be referred to as “differences” in the remainder of the paper. The GAMs were run using the “mgcv” package in R (Wood, 2006) with the smoothing spline protocol (Wood, 2003). The basic form of the GAM used in the analysis was:

$$LIC \text{ or } GIC \sim s(\Delta CPA_T) + s(\Delta ABUND) + s(\Delta YEARS) + factor(VESSEL) + factor(YEAR1),$$

where s indicates variables fitted with a cubic spline and $factor$ indicates categorical variables.

To investigate more specific responses to a range of cold pool bottom temperatures, backward variable selection was performed for three different temperature thresholds: CPA_0 , CPA_1 , and CPA_2 °C, where a temperature threshold defines the two-dimensional boundary within the cold pool. Factors representing survey *VESSEL* and the first year of the comparison pair (*YEAR1*) were included in the model to account for the random or systematic errors that were considered to be artifacts of sampling methodology such as vessel or skipper effects (Munro, 1998; von Szalay and Brown, 2001), survey timing, and technology creep (Zimmermann et al., 2003).

Because the data used in the modeling were not completely independent (e.g., the *LIC* derived from a comparison between 1982 and 1983 was not independent of the *LIC* derived from a comparison between 1982 and 1984), we could not use the P -values provided by the mgcv package. Instead we derived P -values from the delete-d jackknife variance estimates around predictions, which is preferable to the delete-one jackknife because it produces a consistent variance estimate (Shao, 1989). A backward variable elimination was performed using jackknife-derived p -values by eliminating one variable at a time. The variable with the largest P -value was eliminated first and the jackknife was then repeated to estimate new p -values for the reduced model. This process was continued until remaining P -values for all variables were $P < 0.01$. A more stringent $P < 0.01$ was chosen instead of $P < 0.05$ to minimize the possibility of a Type I error. Confidence bounds around predictions were also estimated using model predictions from the jackknife. Among the different temperature models the final one was chosen based on the lowest generalized cross-validation (GVC) score (Wood, 2006). The time lag variable was used to account for any temporal trends that may be present in the survey time series and residuals from the final models were inspected visually using a linear modeling and smoothing spline to ensure the absence of temporal autocorrelation and linear or non-linear trends in the residuals.

Our null hypothesis was that there was no relationship between the interannual differences in local or shelf-wide patterns of spatial distribution by taxon and the interannual differences observed in the predictor variables. Rejection of the null hypothesis implies that a predictor variable has an effect on the spatial index, and thus affects the spatial distribution of a taxon. For example, if the magnitude of the difference in $\Delta ABUND$ is negatively correlated with a spatial index (i.e., greater $\Delta ABUND$ corresponds to decreasing similarity of the spatial index) then the population abundance influences the spatial distribution.

To illustrate effects on the *GIC*, plots of spatial distribution by taxon were made for ΔCPA_T , $\Delta ABUND$ and $\Delta YEARS$ if they were significant. As a proxy for each significant effect, median values among all years for each of the predictor variables by taxon were

used as cut-off values to subdivide all 30 years of the catch data into “cold” and “warm” years (ΔCPA_T), “high” and “low” abundance years ($\Delta ABUND$), and “early” and “recent” years ($\Delta YEARS$). A mean CG was taken for each pooled set of data and a great-circle distance (4) and bearing (6) between mean CGs (ΔCG) were calculated for each of the significant predictor variables. Radian values from the bearing calculation (θ) were converted to degrees and modular arithmetic was used to transform negative degree values to make them positive

$$\theta_{\Delta CG} = a \tan 2(\sin(CG_{long_2} - CG_{long_1}) * \cos(CG_{lat_2}), \cos(CG_{lat_1}) * \sin(CG_{lat_2}) - \sin(CG_{lat_1}) * \cos(CG_{lat_2}) * \cos(CG_{long_2} - CG_{long_1})) \quad (6)$$

The ΔCG s were plotted by taxa for each significant predictor variable to compare their relative effects on the shelf-wide spatial distribution, where distance represents magnitude and bearing represents direction of the ΔCG in response to the predictor variable. A more detailed examination of spatial analyses was done for three taxa of particular interest to the Bering Sea Integrated Ecosystem Research Program (BSIERP) because of their important role in the eastern Bering Sea ecosystem: arrowtooth flounder, Pacific cod (*Gadus macrocephalus*), and walleye pollock (*Theragra chalcogramma*). To illustrate effects on the LIC for these taxa, plots of spatial distribution were made for ΔCPA_T , $\Delta ABUND$ and $\Delta YEARS$ if they were significant. Again, as a proxy for each significant effect, median values among all years for each of the predictor variables by taxon were used as cut-off values to categorize the catch data (see above). ArcMap was used to produce inverse distance-weighted squared interpolation plots of mean CPUE by category and by taxon.

3. Results

3.1. Survey bottom temperatures and extent of cold pool

Mean survey bottom temperatures and areal extent of the cold pool showed considerable interannual variability from 1982 to 2011 (Fig. 3). The coldest survey year in 1999 resulted in the largest deviation from the mean and the largest areal extent of

cold pool in the time series (393,595 km²). This extremely cold year was followed by a 5-year period (2001–2005) with above average survey bottom temperatures. The areal extent of cold pool was at its minimum size (48,000 km²) during the warmest survey year (2003). The CPA_0 °C was absent (1996) or generally small during years when the mean survey bottom temperature was above the long-term mean (Fig. 3). From 2005 to 2006, the warm trend reversed and there was a sharp decline in the mean bottom temperature, coinciding with colder than average survey bottom temperatures for a 5-year period (2006–2010). In 2011, the cold pool decreased in size, especially the CPA_0 °C, resulting in a mean survey bottom temperature that was slightly above the 30-year mean. For the 30-year period, regression analyses showed an increasing trend in total cold pool area ($P=0.37$) and a decreasing trend in mean survey bottom temperature ($P=0.26$), but neither were significant.

3.2. Model results

The LICs generally had lower similarities and greater variability than GICs for all taxa (Table 2). The mean LIC ranged from 0.32 to 0.78 compared to the mean GIC which ranged from 0.83 to 0.98, and standard deviations were on average 2.5 times greater for LIC than GIC. Also, the highest GIC for every taxon was 1.0, compared to the highest LIC values which varied from 0.67 to 1.0.

The $\Delta YEARS$ was a significant effect for most LICs (86%) and GICs (82%) with the dominant trend being decreasing similarity in spatial indices with increasing $\Delta YEARS$ (Table 2). The LIC was significantly affected by the areal extent of the cold pool for a majority of taxa (77%), compared to about half (55%) for the GIC (Table 2). The ΔCPA_1 °C most frequently affected both LIC and GIC (61%), followed by ΔCPA_0 °C (23%) and ΔCPA_2 °C (16%). The $\Delta ABUND$ was a significant effect for a greater percentage of the LIC models (59%) than for the GIC models (41%), with most taxa showing decreasing similarity with the LIC and variable trends in similarity with the GIC (Table 2).

The GIC for all taxa except longhead dab showed a significant response to at least one of the predictor variables (Table 2),

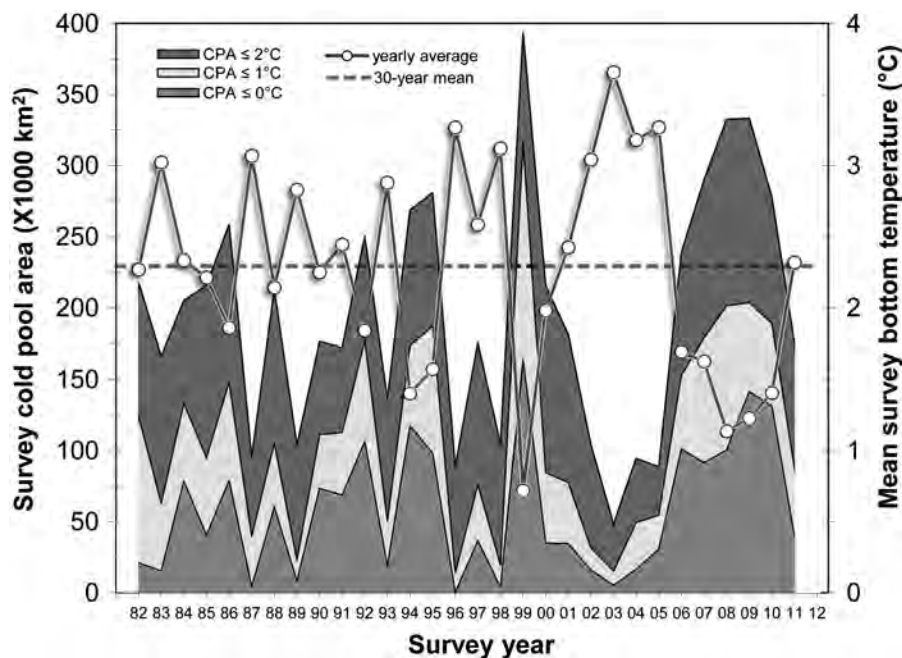


Fig. 3. Annual variation in the average survey bottom temperature, the 30-year mean survey bottom temperature, and the area (km²) of the cold pool (CPA_T) for three different isothermal boundaries, 0, 1, and 2 °C.

Table 2

Range, average, and standard deviation of local (*LIC*) and global (*GIC*) collocation indices and general additive model results of and indices of collocation for selected taxa from the eastern Bering Sea shelf. Predictor variables include pairwise interannual comparisons of survey cold pool area (ΔCPA_T) within isothermal boundaries of $-0, 1,$ and 2°C , abundance ($\Delta ABUND$), and survey time lag ($\Delta YEARS$). The level of significance for listed predictor variables is < 0.01 . Dashes indicate that the variable dropped out from the model during the selection process, and “d”, “n”, and “i” indicate whether trend in the response variable was decreasing, neutral or increasing, respectively.

Common name	LIC								GIC							
	Min.	Max.	Avg.	SD	Trend ΔCPA_T	Trend $\Delta ABUND$	Trend $\Delta YEARS$	Deviance explained (%)	Min.	Max.	Avg.	SD	Trend ΔCPA_T	Trend $\Delta ABUND$	Trend $\Delta YEARS$	Deviance explained (%)
Skates	0.19	0.72	0.49	0.11	d 1°	d	d	69.6	0.79	1.00	0.97	0.03	n 1°	–	d	76.6
Arrowtooth flounder	0.27	0.84	0.64	0.13	d 1°	d	–	56.6	0.88	1.00	0.98	0.02	d 1°	–	–	39.7
Greenland turbot	0.26	0.83	0.54	0.11	d 1°	–	d	48.1	0.60	1.00	0.93	0.08	–	n	d	67.2
Pacific halibut	0.23	0.71	0.46	0.09	d 2°	d	d	41.9	0.80	1.00	0.97	0.03	n 1°	–	i	66.9
Flathead sole	0.08	0.85	0.44	0.16	–	d	d	67.3	0.85	1.00	0.97	0.04	–	d	d	30.6
Bering flounder	0.04	0.84	0.46	0.15	d 0°	–	d	48.0	0.71	1.00	0.92	0.06	d 2°	d	n	48.5
Rex sole	0.38	0.99	0.78	0.13	d 0°	–	d	60.4	0.84	1.00	0.97	0.03	i 0°	i	i	52.6
Yellowfin sole	0.35	0.87	0.59	0.09	d 2°	i	d	58.3	0.88	1.00	0.98	0.02	–	–	d	51.6
Longhead dab	0.09	0.92	0.57	0.16	–	d	d	41.7	0.58	1.00	0.93	0.08	–	–	–	64.4
Starry flounder	0.03	0.84	0.37	0.18	d 0°	–	n	55.9	0.44	1.00	0.90	0.12	d 1°	–	n	76.9
Rock sole	0.28	0.91	0.57	0.12	d 1°	d	d	62.7	0.69	1.00	0.96	0.05	n 1°	–	n	87.4
Alaska plaice	0.21	0.82	0.53	0.13	d 2°	–	d	43.7	0.83	1.00	0.97	0.03	–	–	d	23.1
Sturgeon poacher	0.07	0.89	0.46	0.17	–	–	d	61.9	0.51	1.00	0.91	0.09	d 1°	–	d	65.2
Butterfly sculpin	0.01	1.00	0.46	0.25	n 1°	–	–	43.8	0.47	1.00	0.84	0.13	–	i	–	49.4
Pacific cod	0.12	0.80	0.37	0.12	d 1°	d	n	54.8	0.81	1.00	0.97	0.03	–	i	d	58.3
Walleye pollock	0.08	0.67	0.32	0.10	–	d	–	37.0	0.74	1.00	0.95	0.05	d 0°	–	d	36.8
Wattled eelpout	0.08	0.71	0.38	0.13	d 0°	–	d	53.4	0.56	1.00	0.90	0.10	n 1°	i	n	39.0
Shortfin eelpout	0.00	0.85	0.48	0.19	d 1°	d	d	62.1	0.09	1.00	0.85	0.21	n 1°	–	–	66.3
Tanner crab	0.09	0.89	0.36	0.17	d 1°	i	d	55.3	0.55	1.00	0.92	0.08	–	i	n	81.1
Snow crab	0.08	0.73	0.43	0.11	i 1°	d	d	47.5	0.66	1.00	0.95	0.06	–	–	n	48.5
Red king crab	0.03	0.95	0.38	0.19	d 2°	d	d	53.4	0.45	1.00	0.91	0.10	d 0°	–	n	61.6
Blue king crab	0.03	0.97	0.44	0.22	–	–	d	54.9	0.31	1.00	0.83	0.18	–	n	d	51.2

indicating a community shift in the shelf-wide distribution of demersal fauna on the eastern Bering Sea shelf. The $\Delta YEARS$ was significant for a majority of taxa (82%), and compared to the temperature and abundance effects, the ΔCG for early relative to recent years showed the largest magnitude of displacement (mean = 45 km) and the broadest range of directional shifts with 18 of the 22 taxa undergoing a northward shift (Table 3; Fig. 4a). The effect of increasing ΔCPA_T on ΔCG fell along a southeast to northwest axis and had a mean displacement of 34 km southward (Table 3; Fig. 4b). Changes in abundance had the smallest effect on ΔCG , with a mean displacement of 23 km along a relatively narrow southeast–northwest axis (Fig. 4c).

3.3. Selected species

Walleye pollock: The shelf-wide distribution of pollock decreased in similarity with both an increase in $\Delta CPA_{-0^\circ\text{C}}$ and $\Delta YEARS$ (Table 2). The cold year CGs were generally west of warm year CGs along a southeast–northwest axis (Fig. 5) resulting in a mean CG for cold years that shifted 42 km toward the shelf edge (262°; Table 3). Among the 8 years with the most northerly distribution (latitude $> 58^\circ 05' \text{N}$), four of those years, 1999 and 2008–2010, were the coldest in the survey time series (Fig. 5). The pollock population had a mostly southeastern distribution during early years, but switched to a more northwestern distribution during recent years, shifting 50 km to the northwest (309°; Table 3; Fig. 5). For pollock, similarities in local distribution patterns were not significantly affected by ΔCPA_T at any temperature, but there was decreasing similarity with increasing $\Delta ABUND$ (Table 2; Fig. 6). During high abundance years, pollock are spread further across the middle and inner shelf, and there were higher densities along the northwest outer shelf east of Zhemchug Canyon, in the vicinity of the Pribilof Islands, and north of Unimak Island and the Alaska Peninsula (Fig. 6).

Pacific cod: The shelf-wide distribution of Pacific cod was significantly affected by $\Delta ABUND$ and $\Delta YEARS$, but not ΔCPA_T (Table 2). There was a decreasing similarity in the *GIC* with increasing $\Delta YEARS$, and the years 2000–2008 generally had a lower abundance and more northwestern CGs than other years (Fig. 7). With the increasing abundance of Pacific cod starting in 2009, the CGs shifted southeast (Fig. 7). The direction of the ΔCG was similar between high and low abundance years and between early and recent years (Table 3; Fig. 7).

The similarity in local distribution patterns were significantly affected by all three predictors: $\Delta CPA_{-1^\circ\text{C}}$, $\Delta ABUND$, and $\Delta YEARS$ (Table 2). For the *LIC*, the similarity between spatial distributions decreased with increased differences in both $\Delta CPA_{-1^\circ\text{C}}$ and $\Delta ABUND$ (Fig. 8). There was also a decrease in similarity with $\Delta YEARS$ up to 10 years after which similarity generally increased, but not consistently. In the cold, high abundance, and early years, numerous concentrated pockets of Pacific cod were spread across the shelf including the north side of Bristol Bay. In general, the highest densities of Pacific cod were observed outside the 1°C isotherm, and except during the cold years, a dense pocket of Pacific cod ($> 80 \text{ kg/ha}$) was present at the northern end of St. Matthew Island (Fig. 8; top).

Arrowtooth flounder: Both the *GIC* and *LIC* indices decreased significantly with an increase in $\Delta CPA_{-1^\circ\text{C}}$, and similarity in local distribution patterns also decreased with an increase in $\Delta ABUND$ (Table 2). The ΔCG from warm to cold years shifted 36 km to the southeast (Table 3; Fig. 9). Arrowtooth flounder were absent or densities were generally below 1 kg/ha inside the 1°C isotherm boundary (Fig. 10). During the cold and high abundance years, densities were higher on the outer shelf near Pribilof Canyon and north of Unimak Island. During the warm and high abundance years, the distribution of arrowtooth flounder expanded to occupy most of the northern middle shelf and a greater proportion of the inner shelf (Fig. 10).

Table 3

The distance and bearing associated with a change in the center of gravity (ΔCG) by species for warm relative to cold years, high relative to low abundance years, and early relative to recent years are shown to illustrate the magnitude and direction of the predictor variables ΔCPA_T (cold pool area at isotherm temperature T), $\Delta ABUND$ (change in abundance), and $\Delta YEARS$ which had a significant effect on the global index of collocation (GIC).

Species	Approximated predictor variable	ΔCG distance (km)	ΔCG bearing (deg)
Skates	ΔCPA_{1°	30	196
	$\Delta YEARS$	61	28
Arrowtooth flounder	ΔCPA_{1°	36	136
	$\Delta ABUND$	16	147
Greenland turbot	$\Delta YEARS$	24	336
	ΔCPA_{1°	35	119
Pacific halibut	$\Delta YEARS$	54	306
	$\Delta ABUND$	33	131
Flathead sole	$\Delta YEARS$	90	301
	ΔCPA_{2°	37	205
Bering flounder	$\Delta ABUND$	20	135
	$\Delta YEARS$	21	45
Rex sole	ΔCPA_{0°	6	264
	$\Delta ABUND$	17	294
Yellowfin sole	$\Delta YEARS$	22	132
	$\Delta YEARS$	19	85
Starry flounder	ΔCPA_{1°	21	116
	$\Delta YEARS$	35	20
Rock sole	ΔCPA_{1°	31	161
	$\Delta YEARS$	42	316
Alaska plaice	$\Delta YEARS$	21	52
	ΔCPA_{1°	5	244
Sturgeon poacher	$\Delta YEARS$	36	230
	$\Delta ABUND$	13	334
Butterfly sculpin	$\Delta ABUND$	32	292
	$\Delta YEARS$	40	303
Pacific cod	ΔCPA_{0°	42	262
	$\Delta YEARS$	50	309
Walleye pollock	ΔCPA_{1°	79	296
	$\Delta ABUND$	16	296
Wattled eelpout	$\Delta YEARS$	113	112
	ΔCPA_{1°	54	128
Shortfin eelpout	$\Delta YEARS$	42	211
	$\Delta ABUND$	35	152
Tanner crab	$\Delta YEARS$	57	303
	ΔCPA_{0°	31	240
Snow crab	$\Delta YEARS$	11	90
	$\Delta YEARS$	68	337

4. Discussion

4.1. Community level effects

Studies have shown that both density-independent and density-dependent factors can affect bottom fish distribution (Ciannelli et al., 2008; Spencer, 2008). The prevalence of the time lag variable in our study suggests that some unknown combination of density-independent and density-dependent factors, other than temperature or population abundance specifically, have the most influence on the spatial distribution of species. Density-independent environmental factors are frequently attributed to the effects of climate change as approximated by water temperature (e.g., Mountain and Murawski, 1992; Swain, 1999; Spencer, 2008); however, distribution shifts can also result from changes in other density-independent biological factors such as migrations involving ontogeny, spawning, and feeding (Nichol, 1998; Ernst et al., 2005; Kotwicki et al., 2005; Sohn et al., 2010), in situ light conditions (Kotwicki et al., 2009), primary production patterns, or fishing pressure (Garrison and Link, 2000). Additionally, density-dependent factors such as food availability (e.g., Dorn, 1995; Nøttestad et al., 1999) and competition between species or predation (Ciannelli et al., 2008), are also mechanisms that can affect spatial distribution patterns.

The change in area occupied by the cold pool was the second most common significant effect, suggesting that it is an important mechanism affecting spatial patterns of distribution on the eastern Bering Sea shelf. The cold pool affected local distribution patterns for a higher percentage of taxa (77%) than shelf-wide patterns (55%) indicating that distributional changes due to temperature are more frequently contained within certain areas of the eastern Bering Sea shelf rather than involving distributional shifts for the entire population. Our analyses show that increasing cold pool size is partly responsible for driving the short-term interannual variability in both local and shelf-wide spatial distribution patterns. The cold pool area enclosed by the 1 °C isotherm was the temperature threshold most commonly affecting both spatial indices, suggesting that 1 °C is a more important boundary for describing temperature preferences of eastern Bering Sea bottom fishes and crabs than is the 2 °C isotherm commonly used for designating the cold pool boundary (e.g., Stabeno et al., 2001).

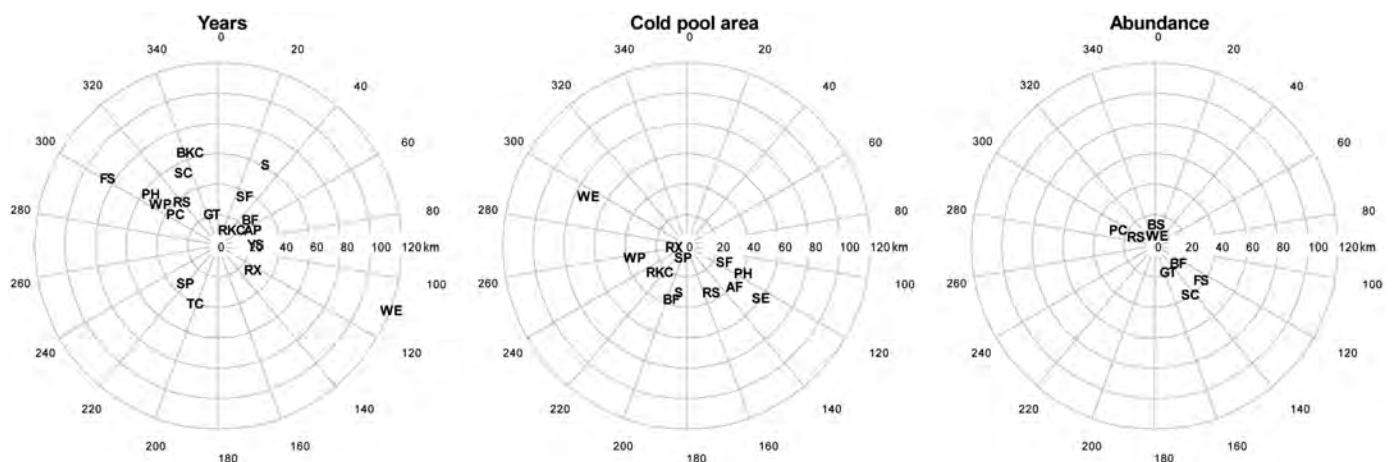


Fig. 4. Relative shifts in the centers of gravity for species that had statistically significant effects in the GAM models for: (a) time lag (early vs. recent years; early years are set to be in the center of the graph), (b) cold pool area (warm vs. cold years; warm years are set to be in the center of the graph), and (c) abundance (low vs. high relative abundance years; low abundance years are set to be in the center of the graph). Alaska plaice (AP), arrowtooth flounder (AF), Bering flounder (BF), blue king crab (BKC), butterfly sculpin (BS), flathead sole (FS), Greenland turbot (GT), Pacific cod (PC), Pacific halibut (PH), red king crab (RKC), rex sole (RX), rock sole (RS), shortfin eelpout (SE), skates (S), snow crab (SC), starry flounder (SF), sturgeon poacher (SP), Tanner crab (TC), walleye pollock (WP), wattled eelpout (WE), yellowfin sole (YS).

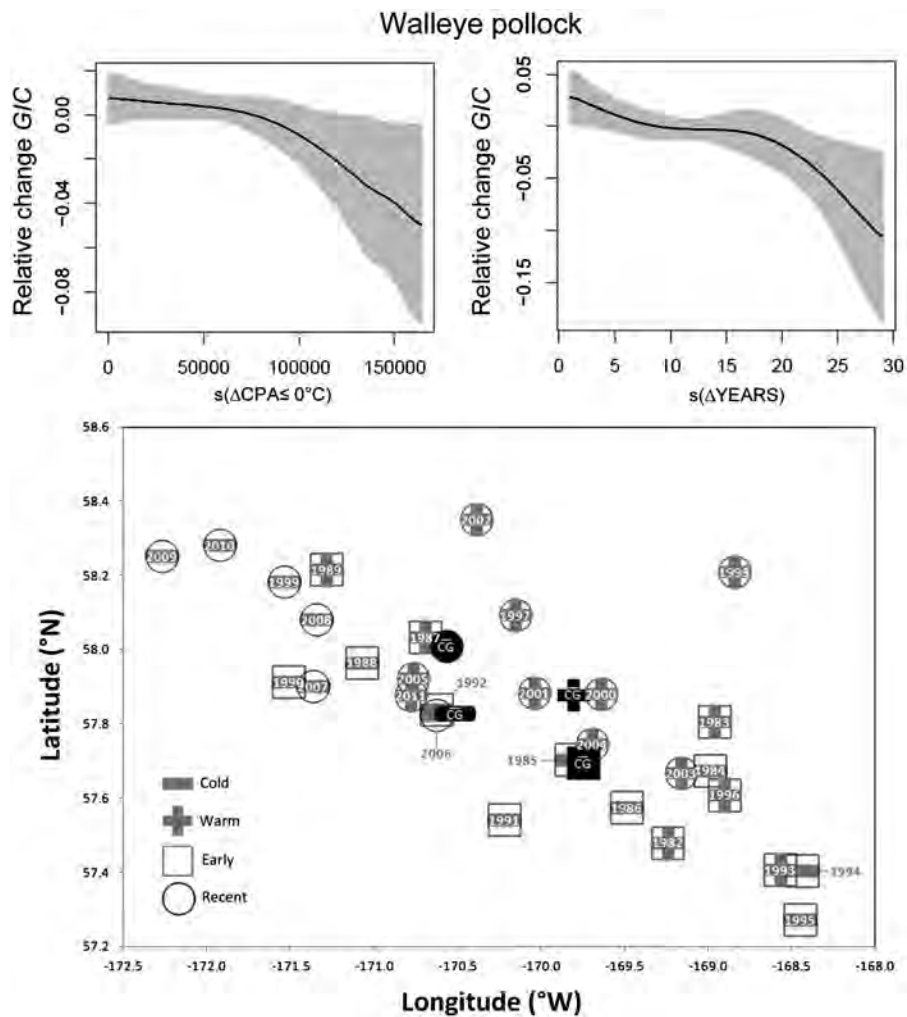


Fig. 5. GAM results for walleye pollock with 99% confidence intervals (gray) showing a. decreasing trend in the global index of collocation (*GIC*) with increasing $\Delta CPA_{\leq 0^{\circ}C}$ and $\Delta YEARS$ (top). The center of gravity for the walleye pollock population by year during cold (minus) and warm (plus) years, early (square) and recent (circle) years, and their respective means (CG; below).

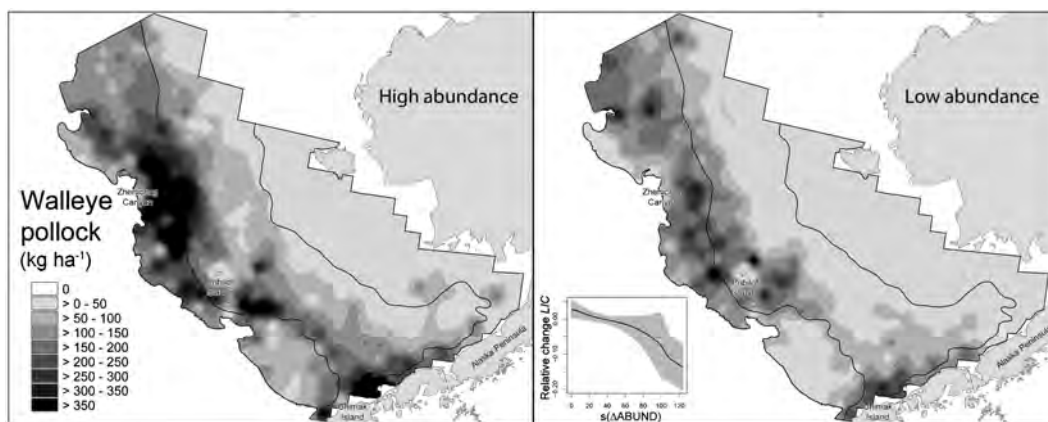


Fig. 6. Variability in the spatial distribution of walleye pollock during the high and low abundance years illustrating the decreasing similarity in the local index of collocation (*LIC*) associated with an increased change in abundance ($\Delta ABUND$). The gray shaded area represents the 99% confidence intervals.

Changes in spatial distribution of many fish populations are attributed to warmer temperatures associated with climate change (Perry et al., 2005; Mueter and Litzow, 2008; Nye et al., 2009). Twelve of the 14 taxa that were found to have a northward displacement in the Mueter and Litzow (2008) study were also found to have a northward displacement in our study, and four taxa that were found to have a southward displacement in that

study were also found to have a southward displacement in our study; however, the temporal northward shift detected in this study was attributed to a time lag effect that is not directly related to cold pool temperatures or population abundance. There was no long-term trend in the declining size of the cold pool detected on the EBS shelf over the last 30 years, and despite inclusion of recent data from the extended cold period from 2006 to 2010, we still

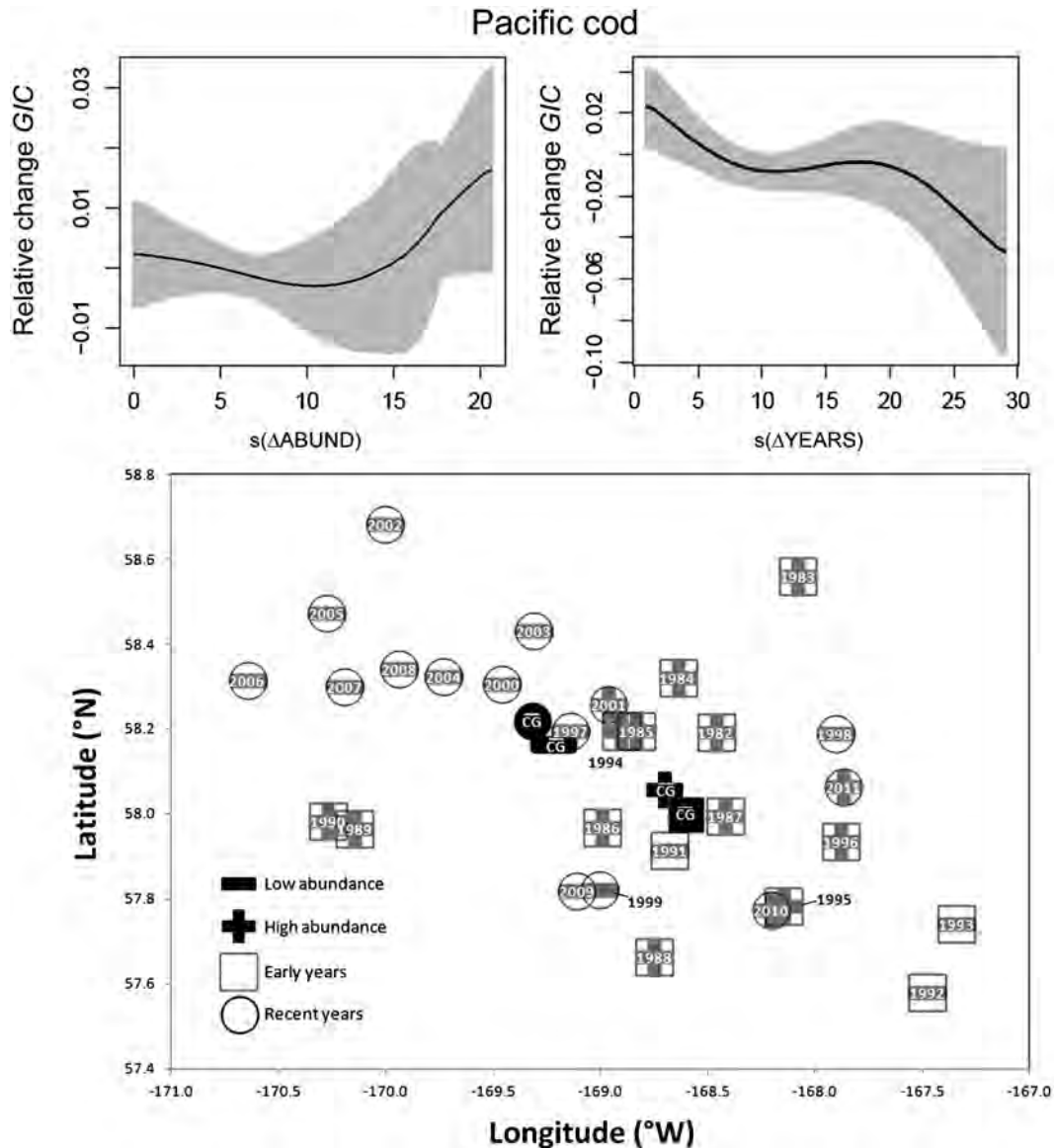


Fig. 7. GAM and center of gravity results for Pacific cod. See Fig. 5 for details with the exception that the plus signs represent high abundance years and the minus signs represent low abundance years.

observed a temporal northward shift. The patterns observed in this study do not support the thesis that a general warming trend on the eastern Bering Sea shelf was the primary mechanism for the temporal northward distributional shift that was proposed in a previous study by Mueter and Litzow (2008). Nevertheless, the short-term interannual variability in spatial patterns do appear to respond to fluctuations in the area occupied by the cold pool, suggesting that populations will indeed respond similarly to decreasing cold pool extent over the long-term by shifting northward. Predictions for the next half-century are that winter ice cover and a summer cold pool will persist on the northern Bering Sea shelf and continue to act as a barrier to northward migration of subarctic species (Sigler et al., 2011; Stabeno et al., 2012a).

We also looked at the spatio-temporal displacement of populations in all directions rather than just along a north-south axis. Directional vectors representing temporal shifts in populations varied considerably by response variable and among taxa suggesting a variety of species-specific biological or environmental mechanisms or perhaps different responses to the same mechanism. In response to changing cold pool size, vectors for some taxa were greater in magnitude to the east–west than to the north–south

suggesting that cross-shelf expansion or contraction of populations on the eastern Bering Sea shelf are affected by interannual variation of the hydrographic boundaries imposed by the cold pool.

Another possible mechanism for the northward temporal displacement is disproportional commercial fishing effort on the southeastern Bering Sea shelf. Commercial fishing can impact fish distribution and can change community structure (Garrison and Link, 2000; Ciannelli et al., in press). There is a major fishing port in close proximity to the Bering Sea shelf located in Dutch Harbor, Alaska. Among all U.S. fishing ports, Dutch Harbor was ranked number one in total commercial fishery landings for most of the past 20 years with annual totals ranging from 230 to 413 thousand metric tons (National Marine Fisheries Service, 2012). Practical considerations such as winter ice cover and regional management closures (e.g., Abbott and Haynie, 2012), or financial incentives such as travel time and fuel costs, may favor fishable waters closer to Dutch Harbor and result in disproportionate fishing pressure on the southeast portion of the shelf. Ten of the 22 taxa investigated here have been, or continue to be, targeted by a commercial fishery on the Bering Sea shelf, and 8 of the 10 commercially exploited taxa show a northward temporal displacement. The

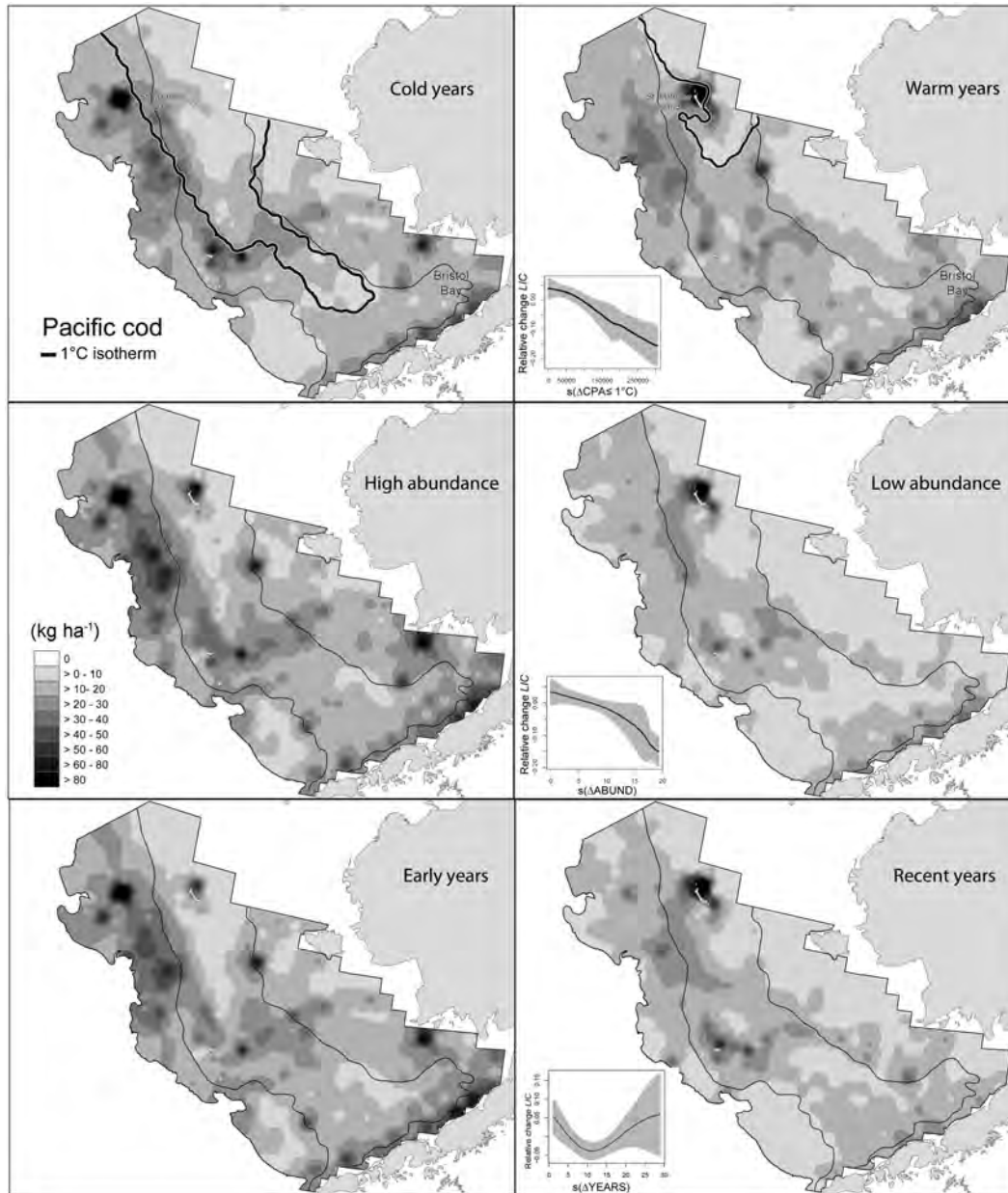


Fig. 8. Variability in the spatial distribution of Pacific cod during cold and warm years (upper panels), high and low abundance years (middle panels) and early and late years (bottom panels) to illustrate the decreasing similarity of the local index of collocation (*LIC*) to the effects of increasing $\Delta CPA_{1^\circ C}$ and $\Delta ABUND$ and the neutral response to $\Delta YEARS$. The gray shaded area represents the 99% confidence interval.

largest trawl fishery on the Bering Sea shelf by weight is walleye pollock, and the relative commercial fishing effort between the southeast and northwest shelf varies by season and by year (Bailey, 2011; Pfeiffer and Haynie, 2012). Another major trawl fishery for yellowfin sole and rock sole catches a majority of their annual quota on the southeastern shelf (Wildebuer and Nichol, 2011; Wildebuer et al., 2011). Commercial harvest of king crabs (*Paralithodes* spp.) occurred around the Pribilof Islands and St. Matthew Island until the late 1990s; however, population declines in both areas resulted in closures that are still in effect (Gish, 2010; Gaeuman, 2012). The only remaining major commercial harvest of king crab on the southeastern Bering Sea shelf is for red king crab (*Paralithodes* spp.) in Bristol Bay where populations have also declined dramatically (Dew and McConnaughey, 2005). Historical area- and species-specific commercial fishery data are available and can be used to investigate how disproportional fishing effort on the southeastern Bering Sea shelf during the last 30 years is a

contributing factor to the apparent northward temporal shift in bottom fish and crab populations.

Fluctuations in population abundance affected local distribution patterns (59%) more often than shelf-wide patterns (41%). Population growth creates greater competition for resources, forcing animals within a population to spread more into outlying areas (Swain and Wade, 1993; Atkinson et al., 1997). In the 1980s, there was rapid growth in the populations of several eastern Bering Sea flatfish species, which corresponded to significant increases in the dispersion of those species (McConnaughey, 1995). Increases in the population abundance of “arrowtooth flounder” (combined *Atheresthes stomias* and *A. evermanni*) and rock sole (*Lepidopsetta* spp.) on the eastern Bering Sea shelf were shown to be strongly related to increased spatial coverage of their populations, while increases in the area occupied by the cold pool have been associated with decreased spatial coverage of these species (Spencer, 2008).

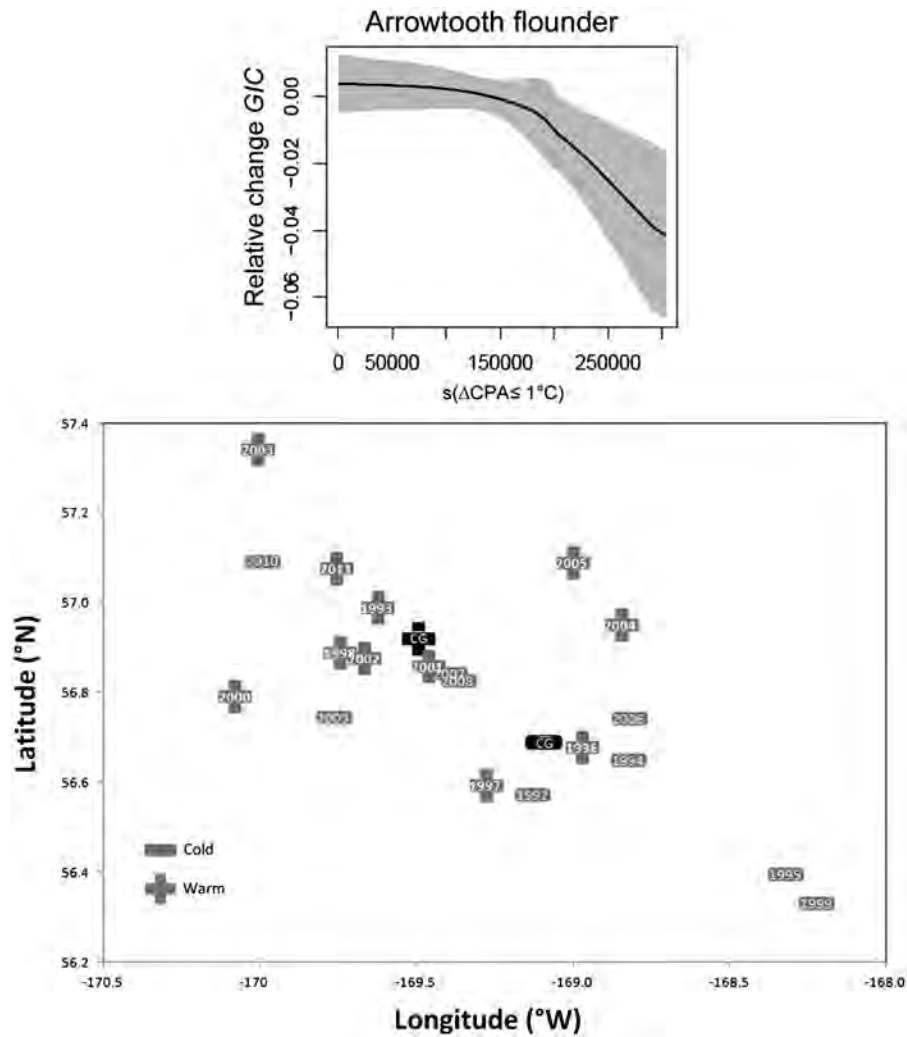


Fig. 9. GAM and center of gravity results for arrowtooth flounder. See Fig. 5 for details.

An easily overlooked factor that could have affected spatial distribution patterns for many of the species we investigated from the eastern Bering Sea shelf is immigration to and emigration from other areas outside the survey area. The geographical distributions of a number of the species we investigated are contiguous with other areas of the Bering Sea for which there is insufficient data to include in this analysis. The shelf extends hundreds of kilometers to the north where there is a significant biomass of Alaska plaice (*Pleuronectes quadrituberculatus*), yellowfin sole (*Limanda aspera*), and snow crab (*Chionoecetes opilio*), and along the outer shelf, deeper living species such as arrowtooth flounder and Greenland turbot (*Reinhardtius hippoglossoides*) can inhabit both the shelf and slope regions (Lauth, 2011).

4.2. Implication for studies of spatial dynamics in the eastern Bering Sea ecosystem

Spatial relationships in relation to environmental factors are key components in constructing models of marine ecosystems (Rose et al., 2010). Accounting for environmental factors in spatial dynamics studies can be challenging, especially in cases like the eastern Bering Sea, where spatial data for many stocks is limited to summer months when feeding migrations predominate. Spatial data from winter or early spring, when many bottom fishes are spawning (e.g., Nichol, 1998) might show entirely different trends in relation to environmental factors. Although this study lacks data

on intra-annual or seasonal variability, we attempted to capture more interannual variability by quantifying similarities in summer fish distribution between all possible survey year combinations. The modeling framework used in this study could be extended to address more specific questions regarding the spatial dynamics of the Bering Sea ecosystem. Data from the survey time series could be categorized into functional groups based on life history stage, feeding guilds, or some other criterion to investigate environmental responses to cannibalism, predator–prey relationships, or interspecies competition. Catch data categorized by age or size could be used for analyzing processes that may shape spatial recruitment patterns (Petitgas et al., 2009) or segregation of different age groups (Wuillez et al., 2007). The analysis could also be expanded to include other environmental variables such as bottom type (McConnaughey and Smith, 2000; McConnaughey and Syrjala, 2009), cold pool volume or thermocline depth (Swartzman et al., 1994).

4.3. Choice of predictors

We believe the approach and model are robust for detecting temporal trends and environmentally-driven changes in the spatial distributions of bottom fish and crab populations on the eastern Bering Sea shelf. The model incorporates more variability than previous studies by comparing similarities between the predictor and response variables for all possible survey year

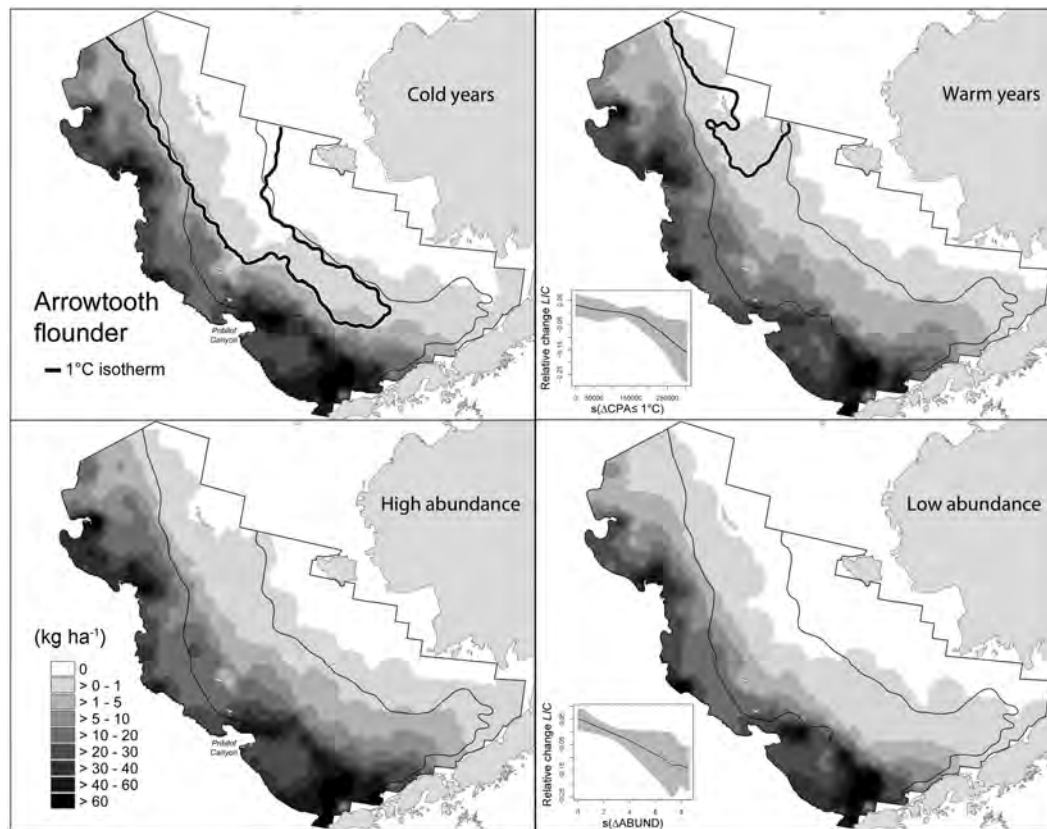


Fig. 10. Variability in the spatial distribution of arrowtooth flounder during cold and warm years and the high and low abundance years to illustrate the decreasing similarity of the local index of collocation (*LIC*) to the effects of increasing ΔCPA_1 °C and $\Delta ABUND$. The gray shaded area represents the 99% confidence interval.

combinations rather than comparing similarities for only two populations (e.g., Syrjala, 1996) or a linear trend in the time series. For modeling spatial variability, we chose only taxa that we felt provided a consistent index of abundance over the 30-year time series. We also chose response variables for detecting differences in both local and shelf-wide spatial patterns of distribution. Moreover, we also considered magnitude and distance in the spatio-temporal displacement of populations for each of the predictors. Three predictors were chosen for investigating local and shelf-wide spatial patterns: (1) the areal extent of the cold pool at three different temperature levels, (2) population abundance, and (3) time lag in survey years. These variables were chosen because other studies have suggested that they affect spatial distribution (Kotwicki et al., 2005; Mueter and Litzow, 2008; Spencer, 2008), and because data for all three were available from the eastern Bering Sea time series. Temperature and population abundance are often cited by other researchers as important in determining the distribution of a species (e.g., Ciannelli et al. 2008; Spencer, 2008). The third, time lag in survey years, is also very important because through covariation it incorporates temporal trends about other factors in the eastern Bering Sea marine ecosystem that are dynamic and unrelated to temperature or population abundance. We also used spatial indices that measured general similarity in the distribution, but did not require assumptions about the direction of the temporal displacement (e.g., Mueter and Litzow, 2008).

In contrast to the previous studies, we evaluated three different temperature levels to model temperature effects on bottom fish and crab distributions. Past studies have used mean temperature over the eastern Bering Sea shelf area (Mueter and Litzow, 2008), or the proportion of the area that was covered by the cold pool defined as the area where bottom temperature was below a single threshold (e.g., < 2 °C; Spencer, 2008). Although both of these

metrics are adequate indicators of the general bottom temperature conditions over the eastern Bering Sea shelf, neither provides a direct measure of the extent of the cold pool. Moreover, different fish taxa have different temperature preferences (Scott, 1982) and an arbitrary choice of one temperature level may not be adequate to assess the effect of the cold pool on specific bottom fish or crab distributions. Thus, we chose a more explicit model that was allowed to choose a best fit to the data using three different temperature levels.

Acknowledgments

We thank the legions of people for their extraordinary efforts to create and maintain the eastern Bering Sea shelf bottom trawl survey time series. This includes survey gear specialists, data managers, survey support and administrative staff, captains and crews of chartered fishing vessels, and most important, survey participants from within our own ranks at the AFSC, as well as scores of others representing too many organizations to list. We also thank Matt Baker, Dan Nichol, Dave Somerton, Paul Spencer, Paul von Szalay, Duane Stevenson, and four anonymous reviewers whose valuable comments greatly improved the quality of this manuscript. The findings and conclusions in this paper are those of the authors and do not necessarily represent the views of National Marine Fisheries Service, NOAA. This is BEST-BSIERP Bering Sea project publication number 80 and NPRB publication number 395.

References

- Abbott, J.K., Haynie, A.C., 2012. What are we protecting? Fisher behavior and the unintended consequences of spatial closures as a fishery management tool. *Ecol. Appl.* 22, 762–777.

- Atkinson, D.B., Rose, G.A., Murphy, E.F., Bishop, C.A., 1997. Distribution changes and abundance of northern cod (*Gadus morhua*), 1981–1993. *Can. J. Fish. Aquat. Sci.* 54 (Suppl. 1), 132–138.
- Bailey, K.M., 2011. An empty donut hole: the great collapse of a North American Fishery. *Ecol. Soc.* 16 (2), 28.
- Bez, N., 2007. Transitive geostatistics and statistics per individual: a relevant framework for assessing resources with diffuse limits. *J. Soc. Fr. Stat.* 148, 53–75.
- Ciannelli, L., Fauchald, P., Chan, K., Agostini, V., Dingsor, G., 2008. Spatial fisheries ecology: recent progress and future prospects. *J. Mar. Systems* 71 (3–4), 223–236.
- Ciannelli, L., Fisher, J.A.D., Skern-Mauritzen, M., Hunsicker, M.E., Hidalgo, M., Frank, K., Bailey K.M. Theory, consequences and evidence of eroding population spatial structure in harvested marine fishes. *Mar. Ecol. Prog. Ser.*, in press.
- Coachman, 1986. Circulation, water masses, and fluxes on the southeastern Bering Sea shelf. *Cont. Shelf Res.* 5, 23–108.
- Dew, C.B., McConnaughey, R.A., 2005. Did trawling on the brood stock contribute to the collapse of Alaska's king crab? *Ecol. Appl.* 15, 919–941.
- Dorn, M.W., 1995. The effects of age composition and oceanographic conditions on the annual migration of Pacific whiting, *Merluccius productus*. *CalCOFI Rep.* 36, 97–105.
- Ernst, B., Orensanz, J.M., Armstrong, D.A., 2005. Spatial dynamics of female snow crab (*Chionoecetes opilio*) in the eastern Bering Sea. *Can. J. Fish. Aquat. Sci.* 62, 250–268.
- Garrison, L.P., Link, J.S., 2000. Fishing effects on spatial distribution and trophic guild structure of the fish community in the Georges Bank region. *ICES J. Mar. Sci.* 57, 723–730.
- Gaeuman, W., 2012. 2011 Saint Matthew Island blue king crab assessment. In: Stock Assessment and Fishery Evaluation Report for the King and Tanner Crab Fisheries of the Bering Sea and Aleutian Islands Regions, pp. 491–552 (Chapter 6). Available from the North Pacific Fishery Management Council, 605 West 4th Avenue, Suite 306, Anchorage, AK 99501.
- Gish, R.K., 2010. The 2008 Pribilof District king crab survey. Alaska Dep. Fish Game, Fishery Management Report 10-07, p. 72.
- Kotwicki, S., Buckley, T.W., Honkalehto, T., Walters, G., 2005. Variation in the distribution of walleye pollock (*Theragra chalcogramma*) with temperature and implications for seasonal migration. *Fish. Bull. U.S.* 103, 574–587.
- Kotwicki, S., De Robertis, A., von Szalay, P., Towler, R., 2009. The effect of light intensity on the availability of walleye pollock (*Theragra chalcogramma*) to bottom trawl and acoustic surveys. *Can. J. Fish. Aquat. Sci.* 66, 983–994.
- Lauth, R.R., 2011. Results of the 2010 eastern and northern Bering Sea continental shelf bottom trawl survey of groundfish and invertebrate fauna. NOAA Tech. Rep. NMFS-AFSC-227, U.S. Dep. Commer, 256 pp.
- Levin, S.A., 1992. The problem of pattern and scale in ecology. *Ecology* 73, 1943–1947.
- McConnaughey, R.L., 1995. Changes in geographic dispersion of eastern Bering Sea flatfish associated with changes in population size. In: Baxter, B.R. (Ed.), Proceedings of the International Symposium on North Pacific Flatfish. Alaska Sea Grant Report No. 95-04, Fairbanks, pp. 385–405.
- McConnaughey, R.A., Smith, K.R., 2000. Associations between flatfish abundance and surficial sediments in the eastern Bering Sea. *Can. J. Fish. Aquat. Sci.* 57, 2410–2419.
- McConnaughey, R.A., Syrjala, S.E., 2009. Statistical relationships between the distributions of groundfish and crabs in the eastern Bering Sea and processed returns from a single-beam echosounder. *ICES J. Mar. Sci.* 66, 1425–1432.
- Mecklenburg, C.W., Mecklenburg, T.A., Thorsteinson, L.K., 2002. Fishes of Alaska. American Fisheries Society, Bethesda, MD 1037 pp.
- Mountain, D.G., Murawski, S.A., 1992. Variation in the distribution of fish stocks on the northeast continental shelf in relation to their environment, 1980–1989. *ICES Mar. Sci. Symp.* 195, 424–432.
- Mueter, F.J., Litzow, M.A., 2008. Sea ice retreat alters the biogeography of the Bering Sea continental shelf. *Ecol. Appl.* 18, 309–320.
- Munro, P.T., 1998. A decision rule based on the mean square error for correcting fishing power differences in trawl survey data. *Fish. Bull. U.S.* 96, 538–546.
- National Marine Fisheries Service, 2012. Fisheries of the United States, 2011, 124 p. Fisheries Statistics Division, National Marine Fisheries Service, NOAA, 1315 East-West Highway, Silver Spring, MD 20910-3282.
- Nichol, D.G., 1998. Annual and between-sex variability of yellowfin sole, *Pleuronectes asper*, spring–summer distributions in the eastern Bering Sea. *Fish. Bull. U.S.* 96, 547–561.
- Nøttestad, L., Giske, J., Holst, J.C., Huse, G., 1999. A length-based hypothesis for feeding migrations in pelagic fish. *Can. J. Fish. Aquat. Sci.* 56 (Suppl.), 26–34.
- Nye, J.A., Link, J.S., Hare, J.A., Overholtz, W.J., 2009. Changing spatial distribution of Northwest Atlantic fish stocks in relation to temperature and stock size. *Mar. Ecol. Prog. Ser.* 393, 111–129.
- Pereyra, W.T., Reeves, J.E., Bakkala, R.G., 1976. Demersal fish and shellfish resources of the eastern Bering Sea in the baseline year 1975. NNAFSC Processed Report, 619 pp. Available from Alaska Fish. Sci. Cent., NOAA, Natl. Mar. Fish. Serv., 7600 Sand Point Way NE, Seattle, WA 98115-6349.
- Perry, A.L., Low, P.J., Ellis, J.R., Reynolds, J.D., 2005. Climate change and distribution shifts in marine fishes. *Science* 308 (5730), 1912–1915.
- Petitgas, P., Goarant, A., Masse, J., Bourriau, P., 2009. Combining acoustic and CUFES data for the quality control of fish-stock survey estimates. *ICES J. Mar. Sci.* 66, 1384–1390.
- Pfeiffer, L., Haynie, A.C., 2012. The effect of decreasing seasonal sea-ice cover on the winter Bering Sea pollock fishery. *ICES J. Mar. Sci.* 69, 1148–1159.
- Pyper, B.J., Peterman, R.M., 1998. Comparison of methods to account for autocorrelation in correlation analyses of fish data. *Can. J. Fish. Aquat. Sci.* 55, 2127–2140.
- Rose, K.A., Icarus Allen, J., Artioli, Y., Barange, M., Blackford, J., Carlotti, F., Cropp, R., Daewel, U., Edwards, K., Flynn, K., Hill, S.L., HilleRisLambers, Huse, G., Mackinson, S., Megrey, B., Moll, A., Rivkin, R., Salihoglu, B., Schrum, C., Shannon, L., Shin, Y., Smith, S.L., Smith, C., Solidoro, C., St. John, M., Zhou, M., 2010. End-to-end models for the analysis of marine ecosystems: challenges, issues, and next steps. *Mar. Coastal Fish.* 2, 115–130.
- Scott, J.S., 1982. Depth, temperature and salinity preferences of common fishes of the Scotian Shelf. *J. Northwest Atl. Fish. Sci.* 3, 29–40.
- Shao, J., 1989. The efficiency and consistency of approximations to the jackknife variance estimators. *J. Am. Stat. Assoc.* 84, 114.
- Sigler, M.F., Renner, M., Danielson, S.L., Eisner, L.B., Lauth, R.R., Kuletz, K.J., Logerwell, E.A., Hunt Jr., G.L., 2011. Fluxes, fins, and feathers: relationships among the Bering, Chukchi, and Beaufort Seas in a time of climate change. *Oceanography* 24 (3), 250–265.
- Sohn, D., Ciannelli, L., Duffy-Anderson, J.T., 2010. Distribution and drift pathways of Greenland halibut (*Reinhardtius hippoglossoides*) during early life stages in the eastern Bering Sea and Aleutian Islands. *Fish. Oceanogr.* 19 (5), 339–353.
- Spencer, P.D., 2008. Density-independent and density-dependent factors affecting temporal changes in spatial distributions of eastern Bering Sea flatfish. *Fish. Oceanogr.* 17 (5), 396–410.
- Stabeno, P.J., Farley, E., Kachel, N., Moore, S., Mordy, C.W., Napp, J.M., Overland, J.E., Pinchuk, A.I., Sigler, M.F., 2012a. A comparison of the physics of the northern and southern shelves of the eastern Bering Sea shelf and some implications for the ecosystem. *Deep-Sea Res. II* 65–70, 14–30.
- Stabeno, P.J., Kachel, N.B., Moore, S.E., Napp, J.M., Sigler, M., Zerbini, A.N., 2012b. Comparison of warm and cold years on the southeastern Bering Sea shelf and some implications for the ecosystem. *Deep-Sea Res. II* 65–70, 31–45.
- Stabeno, P.J., Bond, N.A., Kachel, N.B., Salo, S.A., 2001. On the temporal variability of the physical environment over the south-eastern Bering Sea. *Fish. Oceanogr.* 10, 81–98.
- Stauffer, G., 2004. NOAA protocols for groundfish bottom trawl surveys of the nation's fishery resources. U.S. Dep. Commer., NOAA Tech. NMFS-SPO-65, 205 pp.
- Stevenson, D.E., Hoff, G.R., 2009. Species identification confidence in the eastern Bering Sea shelf survey (1982–2008). AFSC Processed Rep. 2009-04, 46 pp. Alaska Fish. Sci. Cent., NOAA, Natl. Mar. Fish. Serv., 7600 Sand Point Way NE, Seattle, WA 98115, USA.
- Swain, D.P., 1999. Changes in the distribution of Atlantic cod (*Gadus morhua*) in the southern Gulf of St. Lawrence—effects of environmental change or change in environmental preferences? *Fish. Oceanogr.* 8, 1–17.
- Swain, D.P., Wade, E.J., 1993. Density-dependent geographic distribution of Atlantic cod (*Gadus morhua*) in the southern Gulf of St. Lawrence. *Can. J. Fish. Aquat. Sci.* 50, 715–733.
- Swartzman, G., Stuetzle, W., Kulman, K., Powojowski, M., 1994. Relating the distribution of pollock schools in the Bering Sea to environmental factors. *ICES J. Mar. Sci.* 51 (4), 481–492.
- Syrjala, S.E., 1996. A statistical test for a difference between the spatial distributions of two populations. *Ecology* 77, 75–80.
- von Szalay, P.G., Brown, E., 2001. Trawl comparisons of fishing power differences and their applicability to National Marine Fisheries Service and Alaska Department of Fish and Game trawl survey gear. *Alaska Fish. Res. Bull.* 8 (2), 85–95.
- Wildebuer, T.K., Nichol, D.G., 2011. Assessment of the northern rock sole stock in the Bering Sea/Aleutian Islands. In: Stock Assessment and Evaluation Report for the Groundfish Resources of the Bering Sea/Aleutian Islands Regions, pp. 813–888 (Chapter 8). Available from the North Pacific Fishery Management Council, 605 West 4th Avenue, Suite 306, Anchorage, AK 99501.
- Wildebuer, T.K., Nichol, D.G., Ianelli, J., 2011. Assessment of yellowfin sole stock in the Bering Sea/Aleutian Islands. In: Stock Assessment and Evaluation Report for the Groundfish Resources of the Bering Sea/Aleutian Islands Regions, pp. 583–668 (Chapter 4). Available from the North Pacific Fishery Management Council, 605 West 4th Avenue, Suite 306, Anchorage, AK 99501.
- Wuillez, M., Poulard, J.-C., Rivoirard, J., Petitgas, P., Bez, N., 2007. Indices for capturing spatial patterns and their evolution in time, with an application to European hake (*Merluccius merluccius*) in the Bay of Biscay. *ICES J. Mar. Sci.* 64, 537–550.
- Wood, S.N., 2003. Thin plate regression splines. *J. R. Stat. Soc. B* 65, 95–114.
- Wood, S.N., 2006. Generalized Additive Models; an Introduction with R. CRC/Chapman & Hall, Boca Raton, Florida.
- Wyllie-Echeverria, T., Wooster, W.S., 1998. Year-to-year variations in Bering Sea ice cover and some consequences for fish distributions. *Fish. Oceanogr.* 7, 159–170.
- Zimmermann, M., Wilkins, M.E., Weinberg, K.L., Lauth, R.R., Shaw, F.R., 2003. Influence of improved performance monitoring on the consistency of a bottom trawl survey. *ICES J. Mar. Sci.* 60, 818–826.



Cetacean distribution and abundance in relation to oceanographic domains on the eastern Bering Sea shelf, June and July of 2002, 2008, and 2010



Nancy A. Friday^{a,*}, Alexandre N. Zerbini^{a,b}, Janice M. Waite^a, Sue E. Moore^c, Phillip J. Clapham^a

^a National Marine Mammal Laboratory, Alaska Fisheries Science Center, National Marine Fisheries Service, National Oceanic and Atmospheric Administration, 7600 Sand Point Way NE, Seattle, WA 98115-6349, USA

^b Cascadia Research Collective, 218½ W 4th Avenue, Olympia, WA 98501, USA

^c Marine Ecosystems Division, Office of Science and Technology, National Marine Fisheries Service, National Oceanic and Atmospheric Administration, 7600 Sand Point Way NE, Seattle, WA 98115-6349, USA

ARTICLE INFO

Available online 14 March 2013

Keywords:

Abundance
Cetacean
Distribution
Eastern Bering Sea shelf
Spatial variations
Temporal variations

ABSTRACT

As part of the Bering Sea Project, cetacean surveys were conducted to describe distribution and estimate abundance on the eastern Bering Sea shelf. Three marine mammal observers conducted visual surveys along transect lines sampled during the Alaska Fisheries Science Center walleye pollock assessment survey in June and July of 2008 and 2010. Distribution and abundance in 2008 and 2010 (cold years) are compared with results from a similar survey conducted in 2002 (a warm year), as the only three years that the entire survey area was sampled; patterns largely match those previously observed. Abundance estimates for comparable areas in 2002, 2008 and 2010 were as follows: humpback whales (*Megaptera novaeangliae*): 231 (CV=0.63), 436 (CV=0.45), and 675 (CV=0.80); fin whales (*Balaenoptera physalus*): 419 (CV=0.33), 1368 (CV=0.34), and 1061 (CV=0.38); minke whales (*Balaenoptera acutorostrata*): 389 (CV=0.52), 517 (CV=0.69), and 2020 (CV=0.73); Dall's porpoise (*Phocoenoides dalli*): 35,303 (CV=0.53), 14,543 (CV=0.32), and 11,143 (CV=0.32); and harbor porpoise (*Phocoena phocoena*): 1971 (CV=0.46), 4056 (CV=0.40), and 833 (CV=0.66). It should be noted that these abundance estimates are not corrected for biases due to perception, availability, or responsive movement. Estimates for humpback, fin and minke whales increased from 2002 to 2010, while those for harbor and Dall's porpoise decreased; trends were significant for fin whales. It is likely that changes in estimated abundance are due at least in part to shifts in distribution and not just changes in overall population size. Annual abundance estimates were examined by oceanographic domain. Humpback whales were consistently concentrated in coastal waters north of Unimak Pass. Fin whales were broadly distributed in the outer domain and slope in 2008 and 2010, but sightings were sparse in 2002. Minke whales were distributed throughout the study area in 2002 and 2008, but in 2010 they were concentrated in the outer domain and slope. In 2002, Dall's porpoise were sighted on the western edge of the middle domain and in the outer domain and slope, but shifted west out of the middle domain in 2008 and 2010. In 2002 and 2008, harbor porpoise were consistently found in the middle domain with scattered sightings in the outer domain and slope. In 2010, there was a multi-species aggregation between Navarin and Pervenets canyons.

Published by Elsevier Ltd.

1. Introduction

The eastern Bering Sea (EBS) shelf is a highly productive ocean region, which supports large-scale commercial fishing and regional community-based subsistence activities, and also sustains numerous seabirds and marine mammals. The EBS responds rapidly to changes in the physical environment at seasonal, interannual, and

decadal time scales (Napp and Hunt, 2001; Stabeno et al., 2007, 2012b). Because it is such an important ecosystem and is sensitive to climate change, the U.S. National Science Foundation's Bering Ecosystem Study (BEST) and the North Pacific Research Board's (NPRB) Bering Sea Integrated Ecosystem Research Program (BSIERP) combined to form the Bering Sea Project to study the impacts of climate change and dynamic sea ice cover on the ecosystem of the EBS (Wiese et al., 2012). As part of the Bering Sea Project, we collected cetacean sightings data to assess distribution, estimate abundance, and estimate trends in abundance of cetaceans, particularly fin (*Balaenoptera physalus*) and humpback (*Megaptera novaeangliae*) whales, on the eastern Bering Sea shelf.

* Corresponding author. Tel.: +1 206 526 6266; fax: +1 206 526 6615.

E-mail addresses: Nancy.Friday@noaa.gov (N.A. Friday), Alex.Zerbini@noaa.gov (A.N. Zerbini), Janice.Waite@noaa.gov (J.M. Waite), Sue.Moore@noaa.gov (S.E. Moore), Phillip.Clapham@noaa.gov (P.J. Clapham).

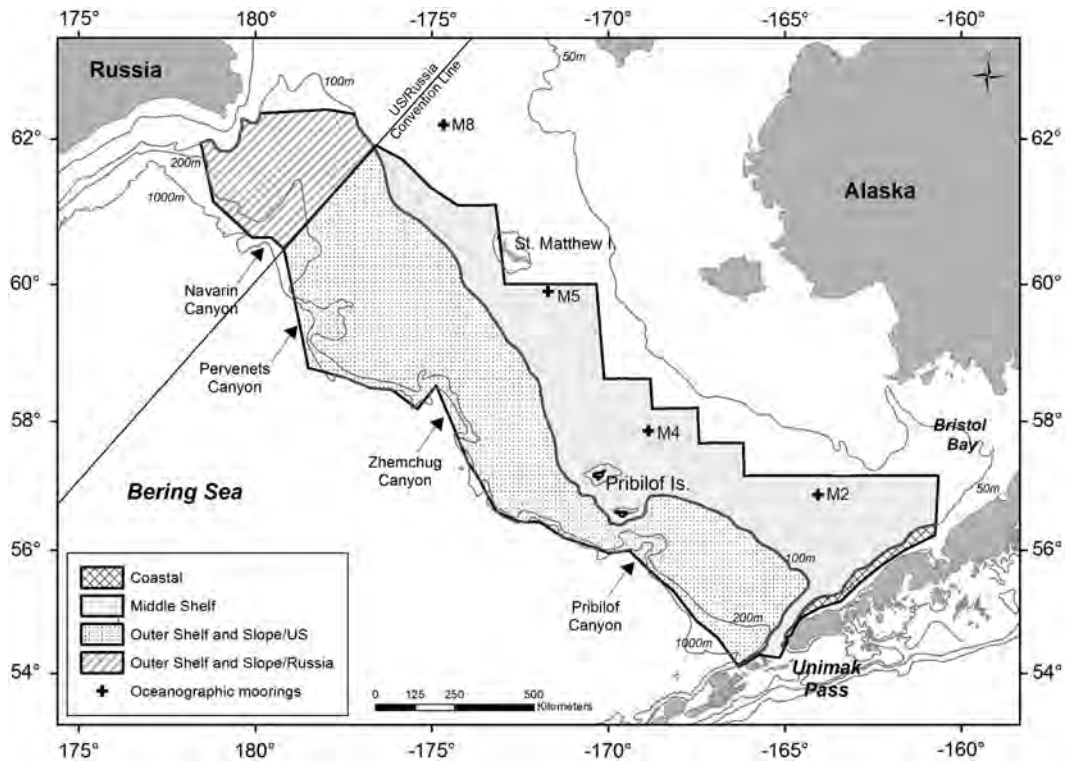


Fig. 1. Map of the study area and oceanographic domains. Also indicated are the NOAA's oceanographic moorings: M2, M4, M5, and M8.

The extent and duration of sea ice over the EBS shelf is largely controlled by atmospheric forcing and is a driving factor for many of the characteristics observed on the EBS shelf (Stabeno et al., 2007, 2012a) including the overall summertime productivity of the EBS ecosystem (Hunt et al., 2002, 2010, 2011; Stabeno et al., 2001, 1998). A revised Oscillating Control Hypothesis predicts that late sea ice retreats are associated with early, ice-associated spring blooms, which results in higher abundance of the medium sized, lipid-rich shelf copepod *Calanus* spp. and euphausiids *Thysanoessa raschii* and *T. inermis*. Availability of these zooplankton prey is critical for a strong pollock year class and for other planktivores such as baleen whales. In contrast, early sea ice retreats are associated with late spring blooms in warmer water, which lead to lower abundance of *Calanus* and *Thysanoessa* spp. (Hunt et al., 2011; Hunt and Stabeno, 2002; Stabeno et al., 2001). The frequency and duration of summer storms also affects the EBS shelf ecosystem (Sambrotto et al., 1986). Summer storms temporarily weaken the pycnocline and bring nutrients from the deep water into the upper water layer (Sambrotto et al., 1986; Whitley et al., 1986) where it is available for phytoplankton production. However, a balance between storm mixing and stratification is needed for blooms where storms increase mixing and phytoplankton production, but water column stratification and stability is high enough that phytoplankton remain above the compensation depth (Coyle et al., 2008).

The EBS shelf is comprised of three oceanographic domains, separated by fronts or transition zones, as described by Coachman (1986): coastal (shore to the 50 m isobath), middle shelf (50–100 m), and outer shelf (100–180 m) (Fig. 1). The inner front (50 m) divides the coastal and middle domains, and the middle front (100 m) divides the middle and outer shelf domains. A salinity front at the shelf break (180 m) divides the outer domain from the slope waters. Each domain has defining characteristics in terms of their summer structure and zooplankton composition (Cooney and Coyle, 1982; Coyle et al., 1996; Coyle and Pinchuk, 2002; Hunt et al., 2002; Smith, 1991; Smith and Vidal, 1986). The coastal domain is characterized by

a single well-mixed layer or two weakly stratified layers. The middle domain is a strongly stratified two-layer system: a wind-mixed surface layer and a nutrient rich, tidally-mixed lower layer. The coastal and middle domains are populated by shelf zooplankton species such as *Thysanoessa raschii*, *Pseudocalanus* spp., *Acartia* spp., and *Calanus marshallae*, but biomass is lower in the coastal domain than the middle domain (Napp et al., 2002). The outer domain has a wind-mixed surface layer and a tidally-mixed bottom layer with a transition layer in between, and is populated by oceanic zooplankton species such as *Thysanoessa inermis*, *Neocalanus plumchrus*, *Neocalanus cristatus*, *Eucalanus bungii*, and *Metridia pacifica*.

Environment has a profound effect on summer zooplankton composition in the middle domain. Coyle et al. (2008) found that the zooplankton composition shifted from large to small species and the water column stability increased three-fold when comparing a colder year, 1999, to a warmer year, 2004. Stabeno et al. (2012b) examined water temperature and temperature anomalies on the southeastern Bering Sea shelf at mooring M2 from 1995 to 2010. They were able to assign years to three categories: cold (1995, 1997, 1999, and 2007–2010), average (1996, 2000, and 2006) and warm (1998 and 2001–2005). Stabeno et al. (2012b) also examined interannual variability in sea ice cover at M2 during the same time period. They found three different temporal patterns in the variability of sea ice extent: high interannual variability (1995–1999), low variability with minimal ice coverage (2000–2006), and low variability with maximum ice coverage (2007–2010). They described a relationship between the species and abundance of zooplankton and the warm/cold year category; this relationship was less evident during periods of high interannual variability. Stabeno et al. (2012b) also found that the relative abundance of fin whales sighted during aerial surveys was 7–12 times higher in 1999, a cold year, compared to 2002, a warm year, suggesting that feeding conditions were better in cold conditions.

Since cetacean distribution in high latitudes is assumed to be driven primarily by the distribution of their prey, cetaceans are

indicators of variability of zooplankton and forage fish prey. We expect cetacean distribution to change temporally and spatially with the composition and energetic value of the zooplankton and forage fish communities. Therefore, the differences in zooplankton community among the domains should be reflected in the distribution of cetaceans. If climate change shifts the pattern of variability toward prolonged periods of warmer conditions, this could have a profound effect on the composition of the lower trophic levels, which could then affect the abundance and distribution of upper trophic level species, including cetaceans.

Historical information on the distribution and abundance of cetacean species on the EBS shelf is limited. Leatherwood et al. (1983) conducted aerial surveys in the Bering Sea in the early 1980s, but they did not estimate abundance. Brueggeman et al. (1987) conducted aerial surveys in 1985 in the southeastern Bering Sea and estimated abundance for two areas divided along the 165°W longitude line; the North Aleutian Basin to the east and the St. George Basin to the west. Because surveys to determine distribution and abundance in the EBS are costly, the Alaska Fisheries Science Center's (AFSC) National Marine Mammal Laboratory (NMML) teamed with the Center's Resource Assessment and Conservation Engineering (RACE) Division to conduct visual surveys for cetaceans during RACE's biennial echo integration-trawl survey for walleye pollock on the EBS shelf (Friday et al., 2012; Moore et al., 2000, 2002; Tynan, 2004; Waite et al., 2002). Biologists from NMML were able to join the RACE surveys in 1997, 1999, 2000, 2002, 2004, 2008, and 2010, providing an opportunity to describe cetacean distribution and calculate abundance over a broad area of the EBS shelf. It was possible to place observers on the entire acoustic trawl survey in only 2002, 2008, and 2010, the last two surveys being part of the Bering Sea Project.

Friday et al. (2012) presented cetacean distribution and estimates of abundance by species and oceanographic domain for the 1999, 2000, 2002, and 2004 surveys. They found that the abundance of baleen whales tended to be greater in cold years (1999) than warm years (2002 and 2004), but no clear relationship was found for porpoise in regard to warm and cold years. Here, we compared the distribution and abundance of cetaceans on the EBS shelf in a warm year (2002) to two cold years (2008 and 2010), allowing us to compare estimates of abundance and to determine if the distribution patterns reported in Friday et al. (2012) persist.

2. Materials and methods

Visual surveys for cetaceans were conducted as a secondary study in association with the RACE echo integration-trawl (EIT) surveys for walleye pollock in June and July of 2002, 2008 and 2010 (Table 1). Because of the time constraints and requirements of the EIT surveys (e.g., maintaining the trackline during echo integration and conducting fish trawls to verify acoustic backscatter), visual surveys for cetaceans were conducted along the EIT transect lines in passing model only. Searches for cetaceans were conducted from the flying bridge of the NOAA ship *Miller Freeman* in 2002 and the NOAA ship *Oscar Dyson* in 2008 and 2010 at a platform height of 12 m and 15.5 m, respectively, above the sea surface and a survey speed of 18.5–22 km/h (10–12 kts). North-south transect lines were spaced 37 km apart and defined by the historical acoustic survey for walleye pollock. In 2008 and 2010, AFSC received permission to survey on the Russian side of the U.S./Russia Convention Line resulting in a 10% increase in the survey area in these years. Realized visual survey effort varied due to weather conditions, and the requirements of the pollock survey. Survey effort was divided into on-effort (during transect legs) and

Table 1

Sighting effort by year and domain: area (km²) covered in each domain and on-effort (km) surveyed.

Domain	Area (km ²)		Effort (km)		
	2002	2008/2010	2002	2008	2010
Dates			6/6–7/28	6/3–7/30	6/6–8/5
Coastal	5097	5097	43	43	26
Middle shelf	150,749	150,749	1623	1092	353
Outer shelf U.S.	181,906	181,906	2086	1693	1015
Outer shelf Russian	0	33,531	0	424	245
Total on-effort	337,752	371,283	3752	3253	1638

additional-effort (other times when the survey protocol was being used, such as transit to, from, and between transect legs).

Standard line transect survey protocols were followed with two observers using Fujinon¹ 25 × (Big Eye) reticle binoculars at port and starboard stations on the flying bridge. The port observer scanned for cetaceans from 10° right to 90° left of the trackline, and the starboard observer from 10° left to 90° right. A third observer focused on the trackline, but scanned the entire 180° area forward of the ship by eye or Fujinon 7 × 50 reticle binoculars and recorded data in a laptop computer using the program WINCRUZ (available at: <http://swfsc.noaa.gov/textblock.aspx?Division=PRD&ParentMenuId=147&id=1446>). Effort data included date, time, latitude and longitude of the vessel, an observers' code, and observer positions. Environmental variables relating to sightability were recorded (e.g., sea state, glare, visibility, etc.). Species, radial distance (calculated from reticles in the binoculars), angle relative to the ship's heading (measured with an angle board or an angle ring on the binocular mount), group size (estimated number of animals in the sighted group), and sighting method (whether a sighting was made with the Big Eye binoculars or not) were recorded for each sighting. For group size, "best", "high" and "low" estimates were made by the observer who sighted the group; best estimates of group size were used in this analysis. Sighting effort was suspended when the sea state was estimated to be above Beaufort 5.

The study area was post-stratified into three oceanographic domains, separated by two fronts (Coachman, 1986): the coastal domain (shore to inner front), middle shelf domain (inner front to middle front), and outer shelf domain (middle front to western edge of the survey area) (Fig. 1). Although the locations of the inner and middle fronts vary, we have used standard front locations along the 50 m and 100 m isobaths, respectively, to demarcate the domains (Coachman, 1986). Using isobaths as proxies for the fronts is a common procedure and allows the cetacean abundances, and not just the densities, to be compared between years. The slope is separated from the outer shelf domain by a salinity front at the shelf break (200 m), but was combined with the outer shelf domain (combination is hereafter referred to as the outer stratum) for this analysis because the zooplankton communities are similar and only the eastern edge of the slope was sampled. In 2008 and 2010, the outer stratum was divided at the U.S./Russia Convention Line creating an outer U.S. stratum, matching 2002, and an outer Russian stratum. Cetacean distribution, sighting rates, and abundances were examined by oceanographic domain to investigate possible trends in species occurrence and density.

Abundance estimates were computed using conventional (CDS) and multi-covariate (MCDS) distance sampling methods

¹ Reference to trade names does not imply endorsement by the National Marine Fisheries Service, NOAA.

Table 2

Number of groups sighted (with the total number of animals in parentheses) during on-effort and additional-effort survey modes by year.

	On-effort			Additional-effort		
	2002	2008	2010	2002	2008	2010
Mysticetes						
Humpback whale	6 (14)	16 (30)	7 (12)	12 (38)	29 (94)	24 (99)
Fin whale	16 (48)	47 (137)	33 (70)	12 (25)	25 (51)	23 (39)
Sei whale	0 (0)	1 (1)	0 (0)	0 (0)	0 (0)	1 (1)
Minke whale	12 (13)	4 (5)	19 (28)	10 (11)	2 (2)	2 (2)
Gray whale	0 (0)	0 (0)	0 (0)	0 (0)	1 (7)	0 (0)
Odontocetes						
Sperm whale	2 (3)	1 (1)	0 (0)	0 (0)	3 (4)	5 (7)
Baird's beaked whale	0 (0)	0 (0)	0 (0)	0 (0)	2 (11)	1 (3)
Stejneger's beaked whale	0 (0)	0 (0)	0 (0)	1 (2)	0 (0)	0 (0)
Killer whale	8 (124)	21 (143)	10 (38)	12 (85)	9 (33)	9 (51)
Pacific white-sided dolphin	0 (0)	0 (0)	0 (0)	0 (0)	0 (0)	2 (19)
Dall's porpoise	108 (535)	64 (298)	41 (141)	72 (348)	106 (529)	46 (175)
Harbor porpoise	49 (73)	47 (99)	8 (16)	8 (10)	9 (15)	1 (1)
Unidentified sightings						
Un-ID large whale	3 (3)	33 (49)	8 (9)	7 (27)	20 (27)	8 (8)
Un-ID baleen whale	6 (13)	10 (11)	26 (32)	10 (14)	1 (1)	21 (29)
Un-ID small whale	9 (9)	6 (6)	0 (0)	2 (4)	1 (1)	0 (0)
Un-ID dolphin/porpoise	24 (42)	32 (53)	6 (9)	17 (33)	13 (23)	5 (16)
Un-ID cetacean	4 (5)	7 (7)	3 (3)	1 (1)	2 (5)	4 (7)

(Buckland et al., 2001, 2004) as implemented in the Mark-Recapture Distance Sampling (mrds) package (Laake et al., 2012) for R (R Development Core Team, 2012). To increase the sample size when fitting the detection function, sightings from 2002, 2008 and 2010 were combined with three other data sources: (1) additional-effort sightings from the transit legs which were not part of the uniform coverage of the study area, (2) sightings from similar surveys on the EBS shelf on the NOAA ship *Miller Freeman* from early June to early July in 2000 and 2004 and from early July to early August in 1999 (Friday et al., 2012), and (3) a similar echo integration-trawl survey for walleye pollock on the NOAA ship *Miller Freeman* in the Gulf of Alaska in June and July of 2003 (Guttormsen and Yassenak, 2007) that used the same survey protocols. Sightings from these additional data sources were collected using the same visual observation protocols as the on-effort sighting, thus species should have the same probability of sighting. Including these additional data sources improves the fit of the detection function and improves the precision of the resulting estimates. To improve the fit of the detection functions, the perpendicular distance data for minke whales (*Balaenoptera acutorostrata*) were truncated at 2 km and were binned, and the perpendicular distance data for fin whales, Dall's porpoise (*Phocoenoides dalli*), and harbor porpoise (*Phocoena phocoena*) were truncated at 7, 5, and 4.5 km, respectively, but were not binned. It was not necessary to truncate or bin the perpendicular distance data for humpback whales. Two numeric covariates (sea state and group size) and two factor covariates (vessel and sighting method) were explored. Including the ship covariate accounted for differences in sightability between the NOAA ship *Miller Freeman* and the NOAA ship *Oscar Dyson*, if such differences were significant, so that comparisons could be made between vessels/years. To improve model fitting for species with a few outlying large groups, estimates of group size were transformed. The square root of group size was used for humpback and minke whales, and Dall's porpoise group sizes were divided by the maximum group size. Hazard-rate and half-normal models were fit with and without covariates, but without interactions, resulting in 32 proposed models for each species. Interactions might improve the fit of the detection functions, but are not merited by the sample sizes and would not

greatly improve the precision of the density and abundance estimates given the other sources of variability.

The best-fit detection probability model was selected using Akaike's Information Criteria (AIC) (Burnham and Anderson, 2002). Models with $\Delta AIC \leq 2$ are considered well-supported by the data and are presented here for comparison, but density and abundance were computed with the best-fit model. On-effort sightings were separated by oceanographic domain and year for estimating group size, sighting rates, density, and abundance; additional-effort sightings were not used for these estimates. Because of the limitations of the survey, data were not collected to determine animals missed on the trackline (perception bias) or animals submerged when the ship passed (availability bias). Therefore, corrections were not made for these biases and $g(0)$, the sighting probability on the trackline, was assumed to be 1.0. This assumption likely causes underestimation of small cetaceans and minke whales (Barlow, 1995). However, estimates of fin and humpback whales are likely accurate because $g(0)$ was estimated as close to unity for ship surveys on comparable vessels in the North Pacific (Barlow, 1995; Calambokidis and Barlow, 2004). Estimates were not corrected for responsive movement (avoidance of, or attraction to, the vessel), which is an important factor in estimating abundance of some cetacean species (e.g., Dall's porpoise; Turnock and Quinn, 1991).

Annual rates of change were estimated for each species by fitting an exponential growth model to the log of the abundance estimates for the U.S. area only because they were comparable across years. The abundance in the starting year, the annual rate of change, and a term for additional variance were estimated by maximum likelihood methods, and the 95% confidence intervals for the rate of change were estimated using likelihood profiling (Branch, 2007; Hilborn and Mangel, 1997). The negative log likelihood was minimized using the optim function in R (R Development Core Team, 2012).

3. Results

The transect survey effort ranged from 1638 km in 2010 to 3752 km in 2002 (Table 1). Distribution patterns were examined

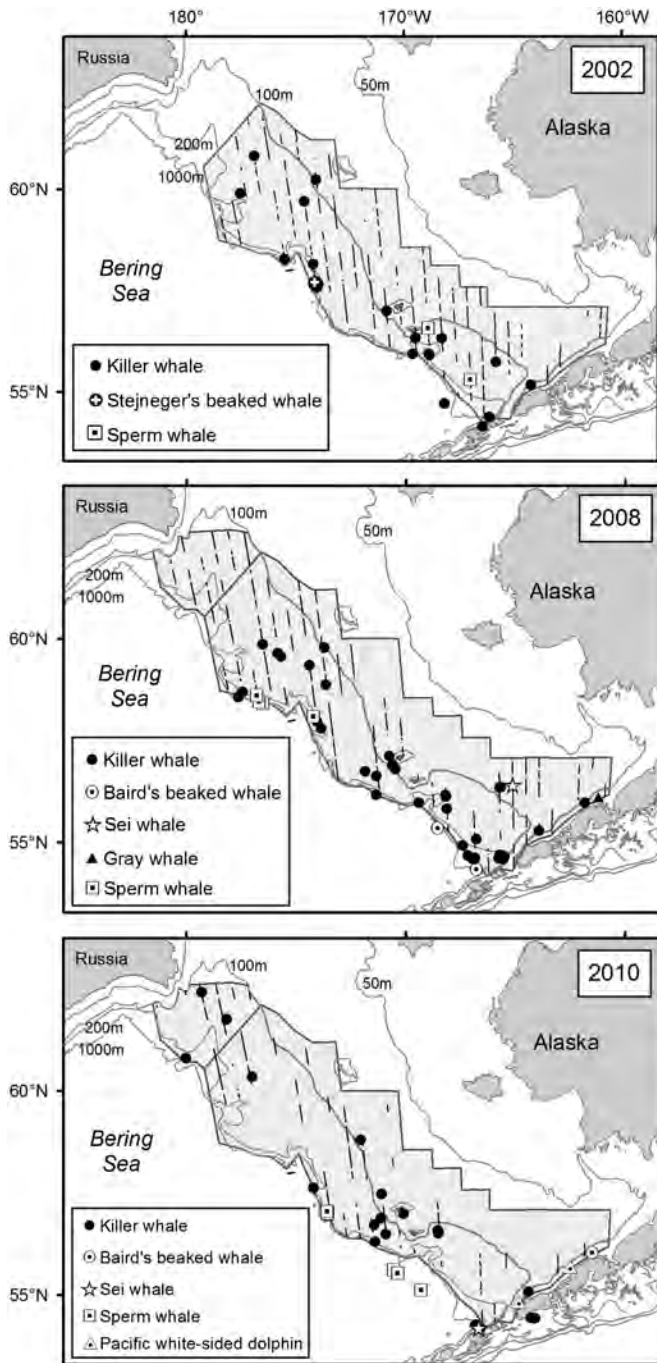


Fig. 2. Sightings of sei, gray, sperm, Baird's beaked, Stejneger's beaked, and killer whales by year; all sightings are plotted.

and abundance estimated for species with five or more sightings per year: humpback, fin, and minke whales, and Dall's and harbor porpoise (Table 2). Killer whales (*Orcinus orca*) also had five or more sighting per year and are widely distributed (Table 2, Fig. 2), but were excluded from further analysis because sightings were not identified to ecotype ("resident", "transient" or "offshore"; Ford et al., 2000). Other species sighted less frequently include sei (*Balaenoptera borealis*), gray (*Eschrichtius robustus*), sperm (*Physeter macrocephalus*), Baird's beaked (*Berardius bairdii*), and Stejneger's beaked (*Mesoplodon stejnegeri*) whales, and Pacific white-sided dolphins (*Lagenorhynchus obliquidens*), as well as sightings that were not identified to species (Table 2, Fig. 2). Fin

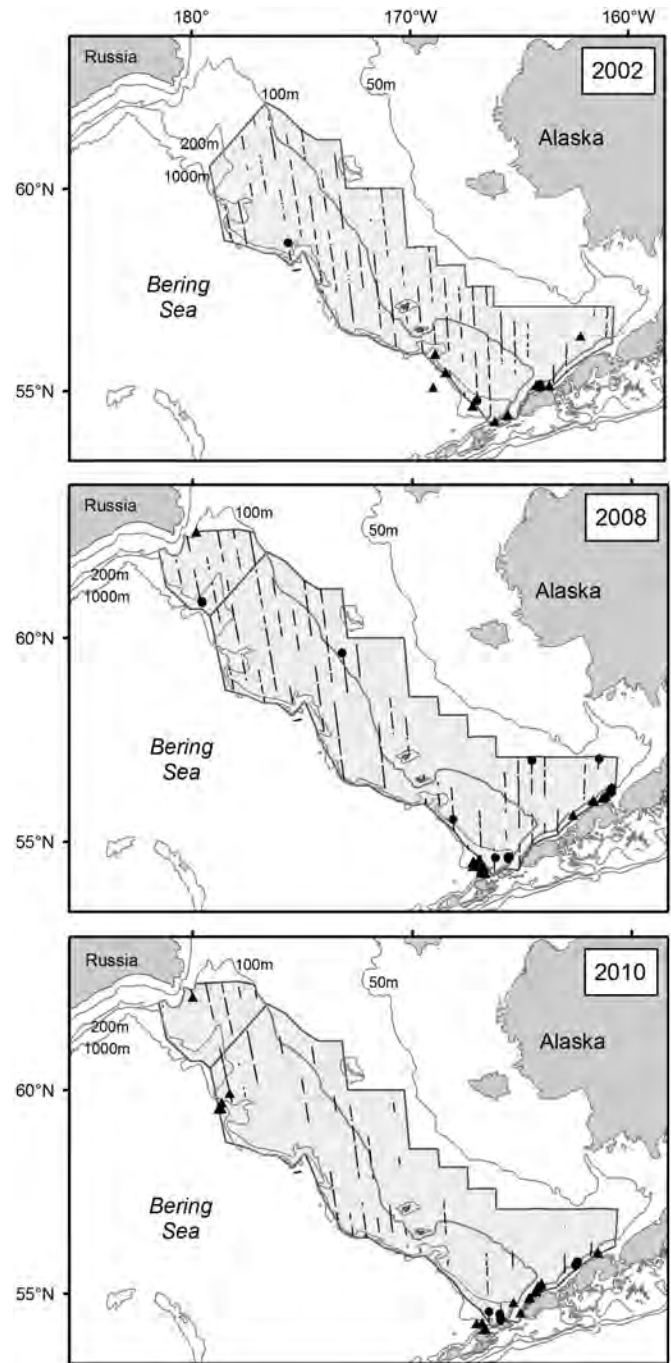


Fig. 3. Sightings of humpback whales by year. On-effort sightings are indicated by circles (●) and additional-effort and off-effort sightings are indicated by triangles (▲).

whales were the most common large whale and Dall's porpoise were the most common small cetacean sighted in all years (Table 2).

3.1. Distribution

Distribution patterns for each species were similar among years, although differences in realized sampling effort in some regions of the study area confound interannual comparisons. Humpback whales were consistently concentrated in coastal waters north of Unimak Pass and along the Alaska Peninsula, with only scattered sightings along the slope (Fig. 3). Fin whales were well distributed

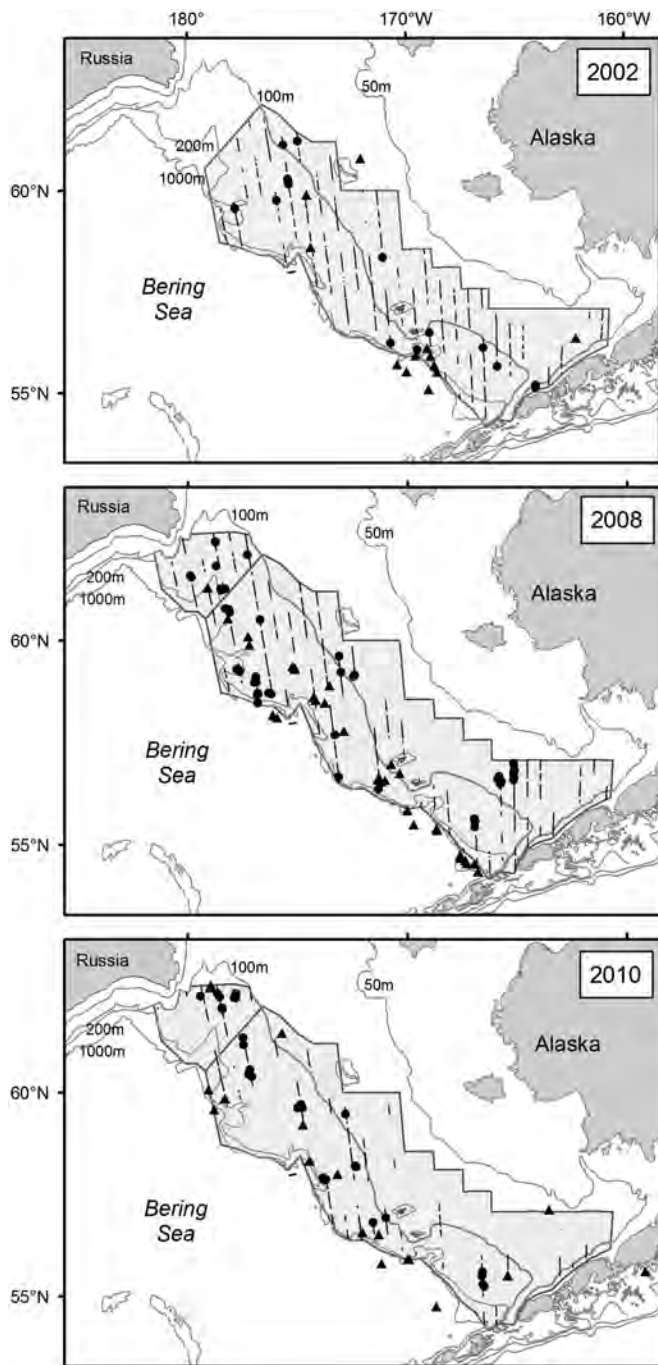


Fig. 4. Sightings of fin whales by year. On-effort sightings are indicated by circles (●) and additional-effort and off-effort sightings are indicated by triangles (▲).

in the outer stratum in all years, but were sparse in 2002, except for a cluster of sightings around Pribilof Canyon (Fig. 4). There were scattered sightings in the middle domain in all years and a cluster of sightings around 57°N, 165°W in 2008. In 2008 and 2010, fin whales were sighted in the Russian waters of the outer stratum indicating that the extension of the survey area over the U.S./Russia Convention Line may include more of the important habitat for fin whales. Overall, the distribution of humpback and fin whales seems to be consistent among all three years, with increased number of sightings of these species in 2008 and 2010 compared to 2002.

The distributions of minke whales and porpoise were more variable. Minke whales were seen throughout the study area in all

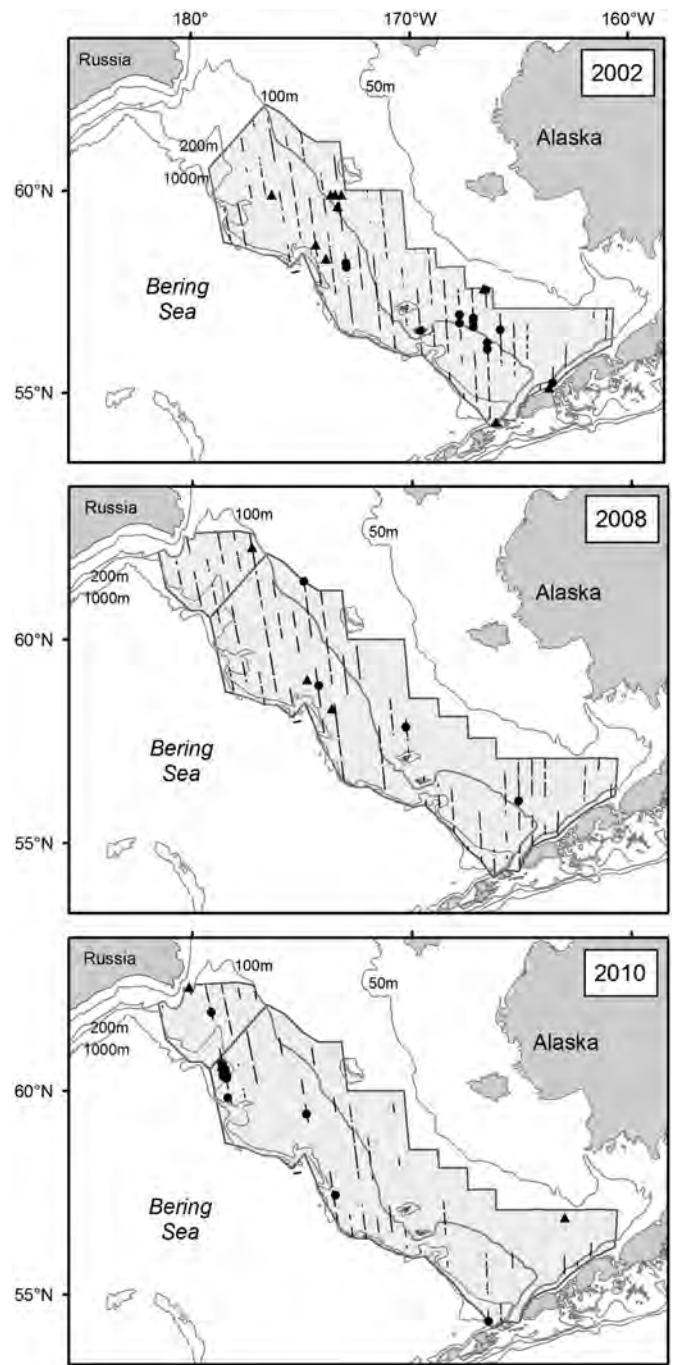


Fig. 5. Sightings of minke whales by year. On-effort sightings are indicated by circles (●) and additional-effort and off-effort sightings are indicated by triangles (▲).

domains (Fig. 5). In 2002 and 2008, sightings were scattered, while in 2010, sightings were concentrated in the outer stratum in Navarin Canyon. There were roughly equal numbers of sightings in 2002 and 2010, but few in 2008. The area east of the Pribilof Islands was an area of high sightings in 2002, but was not well sampled in 2008 and 2010. Dall's porpoise were sighted on the western edge of the middle domain along the 100 m isobath and in the outer stratum in 2002, while in 2008 and 2010, all of the on-effort and most of the additional-effort sightings occurred in the outer stratum (Fig. 6). In 2002, harbor porpoise were found in the middle domain, east of the Pribilof Islands, with scattered sightings in the outer stratum (Fig. 7). In 2008, harbor porpoise

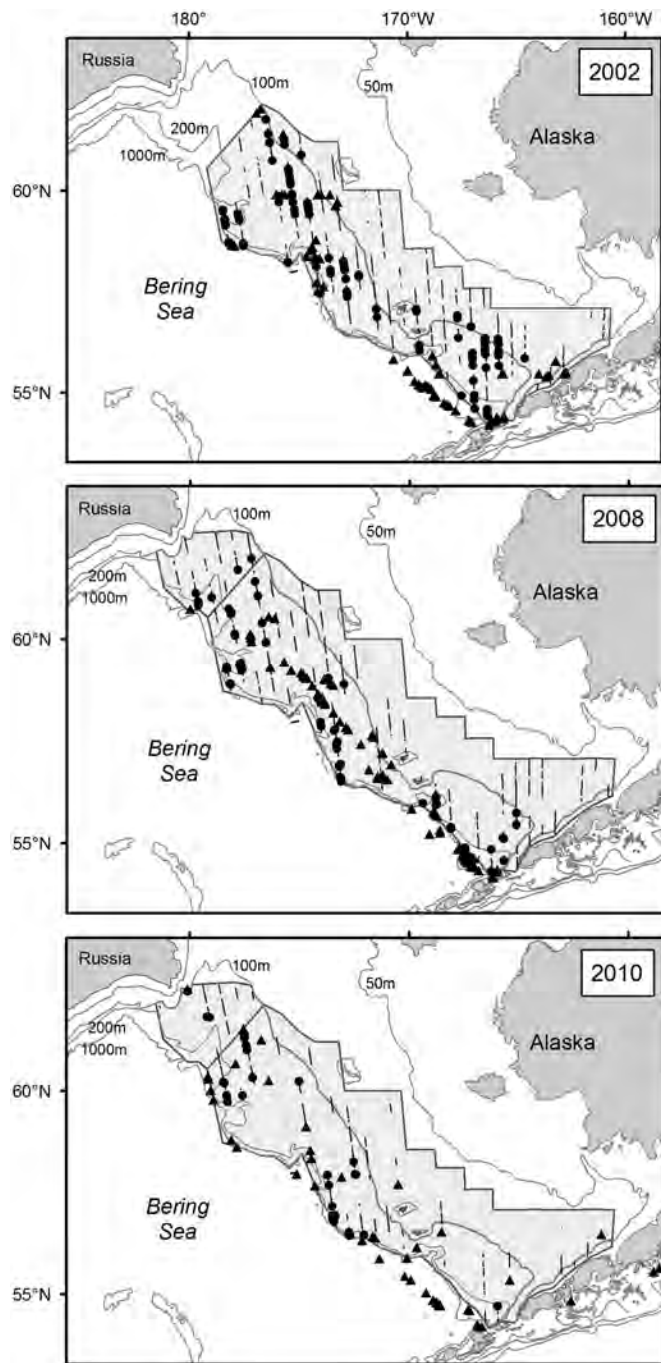


Fig. 6. Sightings of Dall's porpoise by year. On-effort sightings are indicated by circles (●) and additional-effort and off-effort sightings are indicated by triangles (▲).

were found in the middle domain and outer stratum. In 2010, there were very few harbor porpoise sightings, and they all occurred in the outer stratum, with most around Pervenets and Navarin Canyons. In 2010, there was an atypical multi-species mix, including sightings of fin, humpback, and minke whales and Dall's and harbor porpoise between Navarin and Pervenets Canyons.

3.2. Abundance

The detection functions for the best-fit models (minimum AIC) for each species are illustrated in Fig. 8. All well-supported models

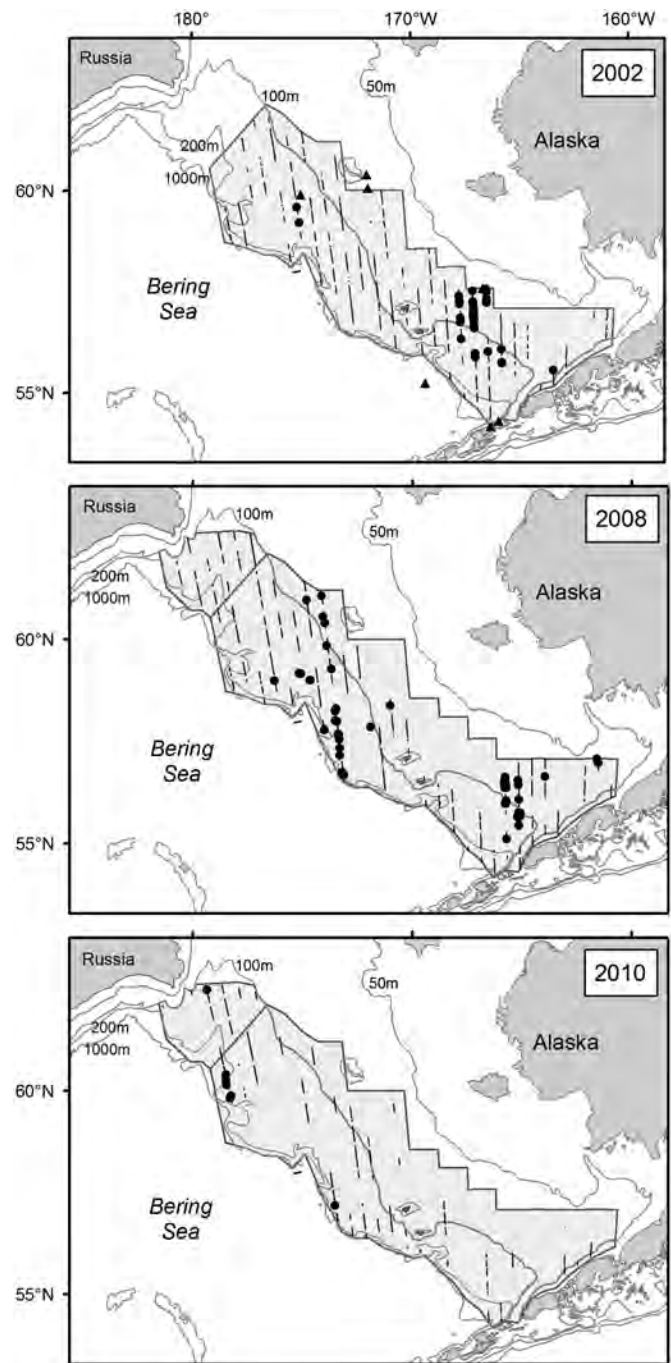


Fig. 7. Sightings of harbor porpoise by year. On-effort sightings are indicated by circles (●) and additional-effort and off-effort sightings are indicated by triangles (▲).

for the detection function ($\Delta AIC \leq 2$) are presented in Table 3. Although the covariates in the well-supported models varied by species, the sighting method covariate was included in all well-supported models. The sea state covariate was included in all well-supported models for fin whales, Dall's porpoise and harbor porpoise. The need to truncate the minke whale data at 2 km from the trackline may have made sea state less important in this analysis even though sea state is often a factor for minke whales. Encounter rate, group size, density and abundance were estimated using the best-fit detection function model and are presented in Tables 4 and 5 for each species by year and oceanographic domain. General patterns for each species are discussed below.

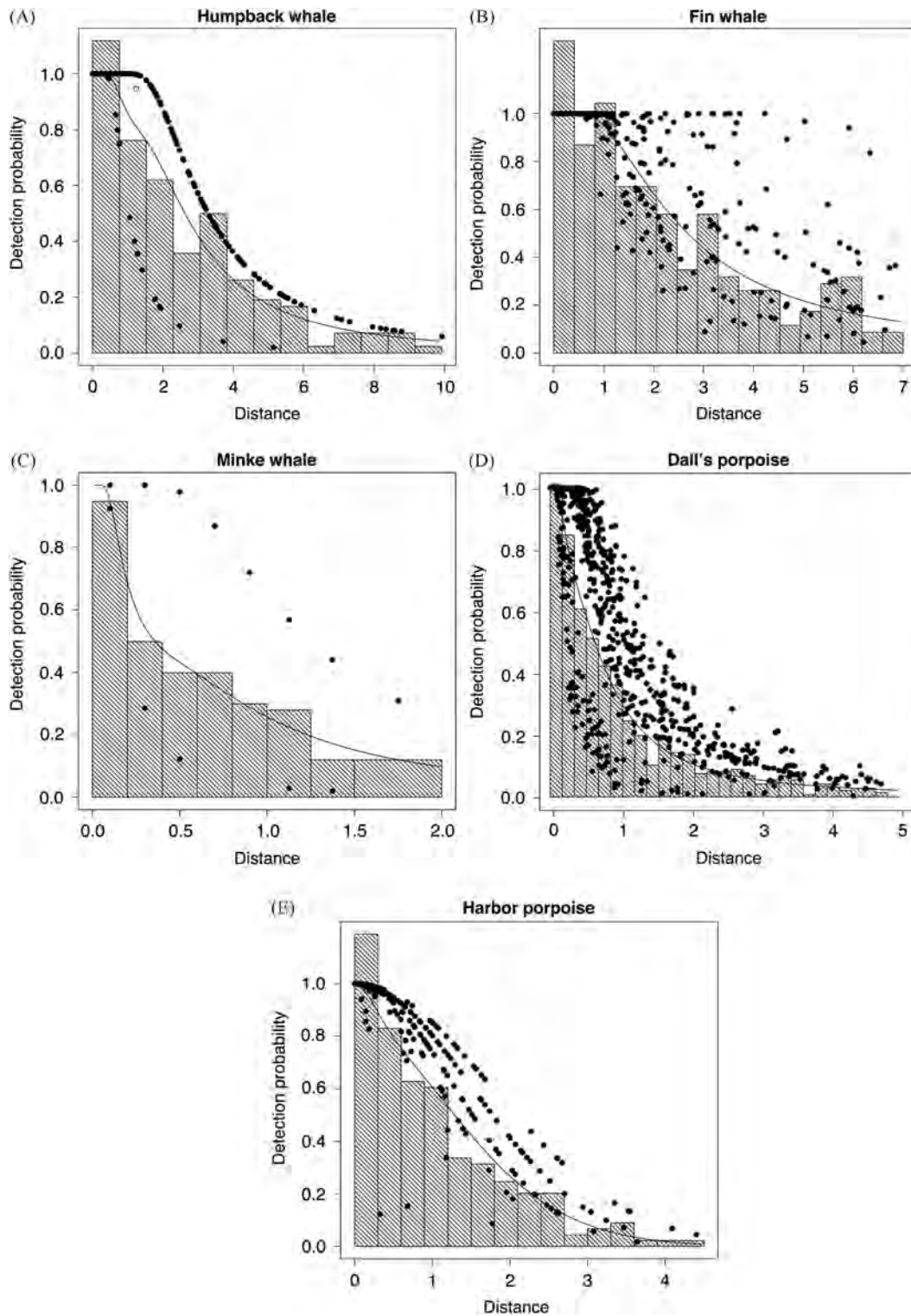


Fig. 8. Histograms of perpendicular distance (km) and fitted detection functions for best-fit model selected by Akaike's Information Criteria (dots represent detection probability for each individual sighting) for (A) humpback whales, (B) fin whales, (C) minke whales, (D) Dall's porpoise, and (E) harbor porpoise.

Estimated encounter rates for humpback whales were highest in the coastal domain, and were higher in 2008 and 2010 than in 2002, but group sizes were similar across years and oceanographic domains (Table 4). Density was highest for humpback whales in the coastal domain in all years: 0.029 whales/km² (CV=0.89) in 2002, 0.032 (CV=0.73) in 2008, and 0.029 (CV=0.95) in 2010 (Table 5). Domain-specific estimates were relatively imprecise (CVs > 0.7) due to small sample sizes, but

yearly estimates are more precise than the corresponding domain-specific estimates. Point estimates of yearly abundance in the U.S. section of the study area increased from 231 (CV=0.63) in 2002 to 672 (CV=0.80) in 2010, but the three estimates are not significantly different from each other.

Estimated encounter rates for fin whales were higher in 2008 and 2010 than in 2002, except in the coastal domain, but group sizes were smaller in 2010 (Table 4). In 2008 and 2010, fin whale

Table 3

Summary of model selection for well-supported models, with $\Delta AIC \leq 2$ compared to the best-fit model, proposed to fit perpendicular distance data for humpback, fin, and minke whales and Dall's and harbor porpoise.

Model, covariates	ΔAIC	w_i	Par. no.	P	CV
Humpback whales					
hz, method	0.00	0.243	3	0.33	0.10
hz, ship+method	0.04	0.238	4	0.31	0.11
hz, ship+sea state+method	1.95	0.091	5	0.30	0.11
hz, size+method	1.97	0.091	4	0.33	0.10
hz, sea state+method	2.00	0.089	4	0.33	0.10
Fin whales					
hz, sea state+size+method	0.00	0.283	5	0.47	0.08
hz, sea state+size	0.64	0.205	4	0.47	0.08
hn, sea state+size+method	1.48	0.135	4	0.50	0.04
hz, ship+sea state+size+method	2.00	0.104	6	0.47	0.08
Minke whales					
hz, method	0.00	0.228	3	0.33	0.30
hz, ship+method	0.58	0.171	4	0.32	0.32
hz, size+method	1.03	0.136	4	0.30	0.44
hz, ship+size+method	1.32	0.118	5	0.26	0.52
hz, sea state+method	1.70	0.098	4	0.33	0.32
hz, ship+sea state+method	2.00	0.084	5	0.31	0.36
Dall's porpoise					
hz, ship+sea state+size+method	0.00	0.571	6	0.19	0.06
Harbor porpoise					
hn, sea state+method	0.00	0.364	3	0.32	0.07
hn, ship+sea state+method	0.57	0.273	4	0.32	0.07
hn, sea state+size+method	2.00	0.134	4	0.32	0.07

hz—hazard rate, hn—half-normal, ship—vessel covariate, sea state—Beaufort numeric covariate, size—group size covariate, method—sighting method covariate, w_i —Akaike weight, P —average detection probability, CV—coefficient of variation of the average detection probability.

densities were highest in the outer stratum, with Russian waters in 2010 being the highest: 0.004 whales/km² (CV=0.48) in U.S. waters in 2008, 0.005 (CV=0.57) in Russian waters in 2008, 0.005 (CV=0.42) in U.S. waters in 2010, and 0.012 (CV=0.68) in Russian waters in 2010 (Table 5). In 2002, densities were highest in the coastal domain (0.009 whales/km², CV=0.89). Abundance was highest for fin whales in the U.S. waters of the outer stratum in all years: 295 whales (CV=0.41) in 2002, 802 (CV=0.48) in 2008 and 911 (CV=0.42) in 2010. Yearly abundances in the U.S. section of the study area were higher in 2008 (1368 whales, CV=0.34) and 2010 (1061 whales, CV=0.38) than in 2002 (419 whales, CV=0.33).

Minke whales were encountered at a higher rate in 2010 than in 2002 and 2008, but the oceanographic domains where they were seen varied among the years (Table 4). Minke whales were generally sighted as single animals except for 2010 when there were seven sightings of pairs and a sighting of a group of three in the outer stratum (Table 4). The highest density and highest abundance were found in the U.S. waters of the outer stratum in 2010 (0.011 whales/km², 2020 whales, CV=0.73, Table 5). The yearly abundance in the U.S. section of the study area was highest in 2010 (2020 whales, CV=0.73) and low, but not significantly different, in 2002 and 2008 (389, CV=0.52 and 517, CV=0.69, respectively).

Estimated encounter rates for Dall's porpoise were highest in the U.S. outer stratum, but were generally consistent across years (Table 4). Group sizes were similar across years and oceanographic domains (Table 4). The highest density and highest abundance of Dall's porpoise were found in the U.S. waters of

the outer stratum in 2002 (0.175 porpoise/km², 31,868 porpoise, CV=0.58, Table 5). In 2008 and 2010, Dall's porpoise densities and abundances were also highest in the outer stratum: 0.080 porpoise/km² and 14,543 porpoise (CV=0.32) in U.S. waters in 2008, 0.077 porpoise/km² and 2570 porpoise (CV=0.60) in Russian waters in 2008, 0.061 porpoise/km² and 10,143 porpoise (CV=0.32) in U.S. waters in 2010, and 0.010 porpoise/km² and 333 porpoise (CV=0.72) in Russian waters in 2010. The yearly abundance in the U.S. section of the study area was highest in 2002 (35,303 porpoise, CV=0.53) and low in 2008 and 2010 (14,543 porpoise, CV=0.32 and 11,143 porpoise, CV=0.32, respectively).

Estimated encounter rates for harbor porpoise were generally higher in 2002 and 2008 than in 2010, but group sizes were similar across years and oceanographic domains (Table 4). The highest density and highest abundance of harbor porpoise were found in the U.S. waters of the outer stratum in 2008 (0.013 porpoise/km², 2421 porpoise, CV=0.60, Table 5). The middle domain in 2002 and 2008 also had relatively high densities and abundances (0.010 porpoise/km², 1479 porpoise, CV=0.58 and 0.011 porpoise/km², 1635 porpoise, CV=0.41, respectively). Yearly abundance in the U.S. section of the study area was lowest in 2010 (833 porpoise, CV=0.66) and higher, but not significantly different, in 2002 and 2008 (1971 porpoise, CV=0.46, and 4056 porpoise, CV=0.40, respectively).

3.3. Annual rate of change

The estimated annual rate of change in abundance of humpback (12.0%, 95% CI=−9.8% to 34.0%), fin (14.0%, 95% CI=1.0 to 26.5%), and minke (15.6%, 95% CI=−6.2% to 38.6%) whales increased between 2002 and 2010. The increase for fin whales is statistically significant, while those for humpback and minke whales are not. In contrast, the estimated annual rate of change in abundance of Dall's (−14.4%, 95% CI=−29.0% to 1.0%) and harbor (−0.7%, 95% CI=−33.6% to 24.9%) porpoise decreased during this same period; neither are statistically significant.

4. Discussion

This paper provides a broad-scale assessment of cetacean distribution and abundance in the EBS and compares results over a nine-year period. Overall, distribution patterns for each species largely match those previously reported (Friday et al., 2012). Humpback whales were consistently concentrated 'on the margins' of the study area: northern Alaska Peninsula (along the 50 m and 100 m isobaths), Aleutian Islands, the coastal waters north of Unimak Pass, southeastern middle domain near Bristol Bay, and Pervenets Canyon (Fig. 3). Humpback distribution north of the Alaska Peninsula corresponds with the middle and inner fronts, which are areas of nutrient upwelling (Kachel et al., 2002) and potential prey aggregation. Ortiz et al. (this issue) characterized this area north of the Alaska Peninsula as having high fishing activity; another indication that this is a highly productive area. Fin whales were consistently distributed both in the 'green belt' of the outer stratum, an area of high productivity along the edge of the EBS continental shelf (Springer et al., 1996), and in the middle domain (Fig. 4). Minke whales were scattered throughout the study area except for 2010, when they were concentrated mainly in the outer stratum (Fig. 5). In 2002, Dall's porpoise were sighted on the western edge of the middle domain and in the outer stratum, but shifted west out of the middle domain in 2008 and 2010 (Fig. 6). In 2002 and 2008, harbor porpoise were consistently found in the middle domain with scattered sightings in the outer stratum (Fig. 7).

Table 4

Number of sightings (*n*), encounter rates (ER, #/km), encounter rate coefficient of variation (ER CV), estimated group size (ES), and estimated group size coefficient of variation (ES CV) for humpback, fin, and minke whales and Dall's and harbor porpoise by domain and year.

Domain	2002					2008					2010				
	<i>n</i>	ER	ER CV	ES	ES CV	<i>n</i>	ER	ER CV	ES	ES CV	<i>n</i>	ER	ER CV	ES	ES CV
Humpback whales															
Coastal	4	0.0929	0.88	2.5	0.20	5	0.1157	0.73	2.2	0.09	3	0.1155	0.95	2.0	0.29
Middle	0	–	–	–	–	3	0.0027	0.57	2.0	0.50	1	0.0028	1.09	3.0	0.00
Outer U.S.	2	0.0010	0.66	2.0	0.00	6	0.0035	0.74	1.8	0.26	3	0.0030	0.75	1.0	0.00
Outer Russia	–	–	–	–	–	2	0.0047	0.90	1.0	0.00	0	–	–	–	–
Fin whales															
Coastal	2	0.0464	0.88	2.0	0.00	0	–	–	–	–	0	–	–	–	–
Middle	3	0.0018	0.53	2.3	0.38	15	0.0137	0.50	2.7	0.17	2	0.0057	0.68	1.0	0.00
Outer U.S.	10	0.0048	0.35	3.3	0.22	22	0.0130	0.42	3.1	0.24	17	0.0168	0.40	1.9	0.12
Outer Russia	–	–	–	–	–	8	0.0189	0.51	2.9	0.19	10	0.0409	0.53	1.7	0.09
Minke whales															
Coastal	0	–	–	–	–	0	–	–	–	–	0	–	–	–	–
Middle	5	0.0031	0.63	1.0	0.00	3	0.0027	0.50	1.0	0.00	0	–	–	–	–
Outer U.S.	3	0.0014	0.68	1.0	0.00	0	–	–	–	–	10	0.0099	0.77	1.6	0.14
Outer Russia	–	–	–	–	–	0	–	–	–	–	1	0.0041	0.83	1.0	0.00
Dall's porpoise															
Coastal	0	–	–	–	–	0	–	–	–	–	0	–	–	–	–
Middle	16	0.0099	0.36	3.9	0.15	0	–	–	–	–	0	–	–	–	–
Outer U.S.	90	0.0431	0.16	5.1	0.15	57	0.0337	0.30	4.6	0.07	38	0.0374	0.34	3.4	0.07
Outer Russia	–	–	–	–	–	7	0.0165	0.43	5.3	0.24	2	0.0082	0.70	4.0	0.00
Harbor porpoise															
Coastal	0	–	–	–	–	0	–	–	–	–	0	–	–	–	–
Middle	38	0.0234	0.64	1.4	0.10	21	0.0192	0.53	1.7	0.10	0	–	–	–	–
Outer U.S.	10	0.0048	0.50	1.9	0.18	24	0.0142	0.53	2.5	0.10	7	0.0069	0.83	2.1	0.26
Outer Russia	–	–	–	–	–	0	–	–	–	–	1	0.0041	0.83	1.0	0.00

A greater diversity of cetacean sightings in Navarin and Pervenets Canyons was observed in 2010 compared to the earlier years (Figs 3–7). Species not seen (minke whales and harbor porpoise) or rarely seen (humpback whales) there in earlier years were conspicuously abundant. In addition, species commonly reported there before (Dall's porpoise and fin whales) were also present in large numbers. This region was also used by a humpback whale satellite-tagged near Unalaska Island that moved north across the Bering Sea shelf (Zerbini et al., 2011). The high abundance and diversity of cetaceans suggest that these submarine canyons can be important habitats for cetaceans in the Bering Sea outer shelf domain and slope.

Abundance estimates for 2002 are consistent with those published by Friday et al. (2012) (Table 5), with the abundance of fin and minke whales greater in cold years (2008 and 2010) than in a warm year (2002). This is consistent with a fine-scale comparison of fin whale occurrence on the middle shelf between a cold year (1999) and a warm year (2002), which found that the group and individual encounter rates were 7–12 times higher in the cold year (Stabeno et al., 2012b). Conversely, the finding that the abundance of humpback whales was greater in the cold years of 2008 and 2010 is counter to that reported in Friday et al. (2012), who found the highest abundance of humpback whales in the warm year of 2004. These differences in abundance with whether a year is warm or cold are likely related to interannual differences in prey availability (Friedlaender et al., 2006; Ressler et al., 2012; Stabeno et al., 2012b). If the majority of the important habitat for humpback whale is outside the study area, it may be more difficult to accurately determine patterns in abundance. If these surveys and those of Friday et al. (2012) are only observing the margins of humpback whale habitat, the relationships found may be artificial. Surveying more of the habitat is necessary to determine if there is a relationship between humpback whale abundance and whether a year is warm or cold, and what that relationship is.

The estimated rates of increase for humpback, fin, and minke whales presented here are likely a combination of changes in distribution and changes in population size. Rates of increase of humpback whales in the North Pacific have been estimated from sightings survey data and from mark-recapture data and range from 4.9% to 7% (Calambokidis et al., 2008; Mobley et al., 2001; Zerbini et al., 2006), with a single higher estimate of 10% from Mizroch et al. (2004). Zerbini et al. (2010) examined plausible rates of increase for humpback whales using Monte Carlo simulations to compute a distribution of rates taking into account uncertainty in biological parameter estimates and proposed that 11.8%, the 99% quantile of their results, as the maximum plausible rate of increase for humpback whales. There is less information on the rate of increase of fin whales in the North Pacific. Zerbini et al. (2006) reported a 4.8% rate of increase for fin whales in the coastal waters of the Aleutian Islands and the Alaska Peninsula for the summer of 2001 to 2003. Rates of increase range from 3.5% to 7.1% for fin whales in the California Current depending on the time period (Moore and Barlow, 2011). There is no information on rates of increase for minke whales (IWC, 2010) and no information on maximum plausible rates of increase for fin whales or minke whales. Given estimated rates of increase for humpback and fin whales and what we know about the biological characteristics of humpback, fin, and minke whales, it is likely that changes in abundance in the study area are due at least in part to changes in distribution and not just to changes in overall population size.

Although Friday et al. (2012) did not find a clear relationship between the abundance of Dall's or harbor porpoise and whether a year was warm or cold year, the abundance of Dall's porpoise declined from 2002 to 2010, although the abundance estimates are not significantly different from each other and the estimated rate of decline was not significant. The pattern for harbor porpoise was more complex with an increase between 2002 and 2008 followed by a decline in 2010 below the 2002 estimate. It is unclear what could be contributing to these decreases in

Table 5

Number of sightings (*n*), estimated density (*D*, #/km²), estimated abundance (*N*), coefficient of variation (CV), and 95% confidence interval (95% CI) for humpback, fin, and minke whales and Dall's and harbor porpoise by domain and year.

Domain	2002					2008					2010				
	<i>n</i>	<i>D</i>	<i>N</i>	CV	95% CI	<i>n</i>	<i>D</i>	<i>N</i>	CV	95% CI	<i>n</i>	<i>D</i>	<i>N</i>	CV	95% CI
Humpback whales															
Coastal	4	0.0288	147	0.89	6–3672	5	0.0316	161	0.73	21–1258	3	0.0287	146	0.95	5–4341
Middle	0	–	–	–	–	3	0.0007	103	0.74	25–419	1	0.0031	462	1.12	65–3280
Outer U.S.	2	0.0005	84	0.78	20–355	6	0.0009	172	0.77	41–721	3	0.0004	67	0.76	16–279
Outer Russia	–	–	–	–	–	2	0.0006	20	0.90	3–141	0	–	–	–	–
Total	–	–	–	–	–	16	0.0004	456	0.43	191–1086	7	0.0006	675	0.80	150–3040
Total—U.S. only	6	0.0002	231	0.63	39–1370	14	0.0004	436	0.45	177–1073	7	0.0006	675	0.80	150–3040
Fin whales															
Coastal	2	0.0088	45	0.89	2–1084	0	–	–	–	–	0	–	–	–	–
Middle	3	0.0005	80	0.57	26–242	15	0.0038	565	0.47	220–1451	2	0.0010	151	0.71	37–605
Outer U.S.	10	0.0016	295	0.41	130–669	22	0.0044	802	0.48	311–2069	17	0.0050	911	0.42	386–2151
Outer Russia	–	–	–	–	–	8	0.0050	168	0.57	43–650	10	0.0122	409	0.68	85–1975
Total	–	–	–	–	–	45	0.0014	1535	0.31	827–2851	29	0.0014	1470	0.34	746–2896
Total—U.S. only	15	0.0004	419	0.33	219–802	37	0.0013	1368	0.34	695–2692	19	0.0010	1061	0.38	493–2283
Minke whales															
Coastal	0	–	–	–	–	0	–	–	–	–	0	–	–	–	–
Middle	5	0.0012	176	0.65	51–604	3	0.0034	517	0.69	146–1831	0	–	–	–	–
Outer U.S.	3	0.0012	213	0.75	54–841	0	–	–	–	–	10	0.0111	2020	0.73	520–7855
Outer Russia	–	–	–	–	–	0	–	–	–	–	1	0.0069	231	0.94	37–1436
Total	–	–	–	–	–	3	0.0005	517	0.69	146–1831	11	0.0021	2251	0.68	633–8003
Total—U.S. only	8	0.0004	389	0.52	147–1030	3	0.0005	517	0.69	146–1831	10	0.0019	2020	0.73	520–7855
Dall's porpoise															
Coastal	0	–	–	–	–	0	–	–	–	–	0	–	–	–	–
Middle	16	0.0228	3434	0.46	1385–8515	0	–	–	–	–	0	–	–	–	–
Outer U.S.	90	0.1752	31,868	0.58	10,738–94,581	57	0.0799	14,543	0.32	7598–27,837	38	0.0613	11,143	0.32	5788–21,451
Outer Russia	–	–	–	–	–	7	0.0766	2570	0.60	650–10,161	2	0.0099	333	0.72	64–1742
Total	–	–	–	–	–	64	0.0158	17,113	0.29	9524–30,748	40	0.0106	11,476	0.31	6060–21,732
Total—U.S. only	106	0.0327	35,303	0.53	12,989–95,946	57	0.0135	14,543	0.32	7598–27,837	38	0.0103	11,143	0.32	5788–21,451
Harbor porpoise															
Coastal	0	–	–	–	–	0	–	–	–	–	0	–	–	–	–
Middle	38	0.0098	1479	0.58	483–4531	21	0.0108	1635	0.41	706–3788	0	–	–	–	–
Outer U.S.	10	0.0027	492	0.63	147–1643	24	0.0133	2421	0.60	754–7769	7	0.0046	833	0.66	230–3018
Outer Russia	–	–	–	–	–	0	–	–	–	–	1	0.0017	58	0.84	9–373
Total	–	–	–	–	–	45	0.0038	4056	0.40	1844–8920	8	0.0008	891	0.62	263–3015
Total—U.S. only	48	0.0018	1971	0.46	798–4870	45	0.0038	4056	0.40	1844–8920	7	0.0008	833	0.66	230–3018

abundance. There was a westward shift towards deeper water in the distribution of Dall's porpoise from 2002 to 2010 (Fig. 6) and a lack of sightings of harbor porpoise in 2010 (Fig. 7), which could indicate that the important habitat for these species has shifted outside the study area in colder years. Both species feed on forage fishes such as herring and capelin, and Dall's porpoise often forage on mesopelagic fishes and squid found in the deeper waters of the outer stratum (Aydin et al., 2007; Fiscus and Jones, 1999; Gearin et al., 1994; Perez, 1990).

Although the trend analyses were only significant for fin whales, the pattern of abundance increased for all three baleen whales and declined for porpoise with the shift from warm to cold years. These patterns could be significant for ecosystem management and important when predicting changes in cetacean distribution with climate change. Quantitative models are being developed which will integrate data on oceanographic conditions, cetacean sightings, and prey fields and may shed light on whether preferred habitat shifted outside the study area in warm years for mysticetes and in cold years for odontocetes. Such studies will be important for managing cetacean species as large positive and negative deviations from the mean trend in temperature are expected in the future (Overland et al., 2012). The possible decline in porpoise, particularly Dall's porpoise, also indicate the need for additional studies of porpoise to determine if there is a decline in population abundance, a shift in distribution, or a combination of both.

Ressler et al. (2012) examined euphausiid biomass from acoustic surveys in 2004 and from 2006 to 2010, and found an increase in biomass during cold years. Ohashi (2013) studied summer zooplankton from 1994 to 2009 and found that the biomass and abundance of both copepods and chaetognaths were higher in cold years than warm years. Stabeno et al. (2012b) report that year-class strength for walleye pollock and Pacific cod improved during cold periods, and Hollowed et al. (2012) found that the distribution of age-1 pollock varied between cold and warm years. When examining ecosystem considerations for fisheries stock assessment reports, Zador and Gaichas (2010) found that the mean biomass of zooplankton and pelagic foragers increased in the EBS from 2005 to 2010. However, the connection between abundance and warm/cold periods may be more complex than simple temperature anomalies. Coyle et al. (2008) describe a shift from larger to smaller zooplankton taxa between 1999 and 2004 and proposed that this shift was caused by high water column stability in 2004. Ladd and Stabeno (2012) found that the strength of summer stratification and depth-averaged temperature were not correlated. They propose that this decoupling of stratification and temperature complicated forecasting the ecosystem because projections of a warmer climate will not automatically imply higher stratification.

As with other cetacean sighting surveys conducted in conjunction with standard acoustic fish stock assessment surveys (Friday et al., 2012; Moore et al., 2000, 2002; Tynan, 2004; Waite et al., 2002), observers could not break trackline for species

identification. Therefore, the sample sizes for individual species were relatively small and sample sizes for unidentified groups were relatively high (Table 2). However, combining sampling effort for fish and cetacean surveys provided a cost-effective mechanism for describing cetacean distribution and abundance over a broad area of the EBS shelf. In addition, the 2008 and 2010 surveys collected a wide array of interdisciplinary data as part of the Bering Sea Project. Survey timing was consistent across years, varying by not more than a week, and we do not expect these small differences to affect the results. However, we do not know the extent to which cetacean distribution is influenced by inter-annual variability in environmental features (e.g., the timing of sea ice retreat). When examining the abundance estimates, care must be taken to note the CVs and not just the point estimates because some estimates were very imprecise. We emphasize that these abundance estimates were uncorrected for: (1) perception bias (animals missed on the trackline), (2) availability bias (animals submerged when the ship passed), and (3) responsive movement. The magnitude of the resulting biases varies by species; they are probably small for fin and humpback whales but could be larger for minke whales and for Dall's and harbor porpoise (Barlow, 1995; Palka and Hammond, 2001; Turnock and Quinn, 1991). Availability bias is unlikely to be an issue for the species in this study since this bias typically affects long-diving species such as sperm and beaked whales. Examining the detection functions, there is no evidence of negative responsive movement, even for minke whales and harbor porpoise which often show ship avoidance. The degree of ship attraction for Dall's porpoise is variable by geographic region and possibly other factors. The detection function for Dall's porpoise in this study may show evidence of ship attraction. However, even if these estimates are biased due to responsive movement, they would still be useful as relative abundance estimates. Potential biases are the same for the current surveys as for past surveys and are discussed further in Friday et al. (2012). Even with these caveats, the results presented here were unique because they portray cetacean distribution, and provide estimates of abundance and trend, in a standardized way such that comparisons can be made among oceanographic domains on the EBS shelf over a nine-year time span. This information is critical for management under the Marine Mammal Protection Act and under the Endangered Species Act (for fin and humpback whales) and will be important when predicting and interpreting the effects of climate change on the eastern Bering Sea shelf.

Although combining cetacean surveys with pollock stock assessment research provides a relatively inexpensive mechanism for estimating cetacean distribution and abundance, conflicting priorities often require that cetacean surveys be curtailed. We have noted that the vessel surveys presented here may not have captured all of the important habitat for humpback whales and for Dall's porpoise. The June–July timing of these surveys may also not be optimal for some species. Acoustic detections of fin, humpback, and North Pacific right whales (*Eubalaena japonica*) at NOAA moorings, M2 (57°N, 164°W), M4 (58°N, 169°W), and M5 (60°N, 172°W), indicate that the abundances of these species may peak in late summer and fall, after the pollock stock assessment survey has been completed (Stafford and Mellinger, 2009; Stafford et al., 2010). Dedicated cetacean surveys could be scheduled to coincide with peak cetacean abundance, as indicated by acoustic detections, and designed to capture the geographic range of target cetacean species, including the slope and basin regions. Dedicated surveys would also provide the additional staff needed to collect the data necessary to estimate correction factors and more flexibility to confirm species identification and group sizes. Sampling effort should also be increased to improve precision for better estimation and management. The estimates

presented here can be used as references to compute the additional effort required to reach more desirable levels of precision (e.g. $CV < 0.3$) in abundance estimates. Such surveys, combined with measures of local hydrography and prey field, should be the goal of future cetacean assessments.

Acknowledgments

We thank Patti Haase, Amy Kennedy, Doug Kinzey, Ernesto Vazquez Morquecho, Laura Morse, Stephanie Norman, Paula Olson, Desray Reeb, Kim Valentine, Bridget Watts, and Suzanne Yin for their expertise and dedication during the long hours of visual survey. We greatly appreciate the extra effort of the observers who acted as cetacean cruise leaders: Norman and Kinzey in 2002, Yin and Morse in 2008 and Yin and Olson in 2010. We also thank Gary Stauffer, former RACE Division Director, and Russell E. Nelson, Jr., current RACE Division Director, who graciously provided ship access and encouragement, without which there would be no data. The flexibility and assistance of the captains and crew of the NOAA ship *Miller Freeman* and NOAA ship *Oscar Dyson* contributed to the success of this research. AFSC survey Chief Scientists Alex DeRobertis, Taina Honkalehto, Paul Walline, and Neal Williamson allowed cetacean research opportunities when practical. Thanks also to the entire RACE scientific crew for their flexibility and support. The thoughtful reviews of Megan Ferguson and Ivonne Ortiz are greatly appreciated. Funding for this research was provided by NOAA/AFSC/NMML in 2002 and the North Pacific Research Board in 2008 and 2010. This research was conducted under MMPA Permit nos. 782-1438 and 782-1719 issued by the National Marine Fisheries Service. This is NPRB publication number 368 and BEST-BSIERP Bering Sea Project publication number 70. The views expressed herein are those of the authors and do not reflect the views of NOAA.

References

- Aydin, K., Gaichas, S., Ortiz, I., Kinzey, D., Friday, N., 2007. A comparison of the Bering Sea, Gulf of Alaska, and Aleutian Islands large marine ecosystems through food web modeling. U.S. Department of Commerce, NOAA Technical Memorandum NMFS-AFSC-178, 298pp.
- Barlow, J., 1995. The abundance of cetaceans in California waters. Part I: ship surveys in summer and fall of 1991. *Fish. Bull.* 93, 1–14.
- Branch, T.A., 2007. Abundance of Antarctic blue whales south of 60°S from three complete circumpolar sets of surveys. *J. Cetacean Res. Manage.* 9, 253–262.
- Brueggeman, J.J., Green, G.A., Grotefendt, R.A., Chapman, D.G., 1987. Aerial surveys of endangered cetaceans and other marine mammals in the northwestern Gulf of Alaska and southeastern Bering Sea. Report on Contract no. 85-ABC-00093. Minerals Management Service and NOAA Office of Oceanography and Marine Assessment, Alaska Office (OCSEAP Research Unit 673), 949 East 36th Avenue, Anchorage AK 99508. 129pp.
- Buckland, S.T., Anderson, D.R., Burnham, K.P., Laake, J.L., Borchers, D.L., Thomas, L., 2001. Introduction to Distance Sampling: Estimating Abundance of Biological Populations. Oxford University Press, New York City, New York, USA.
- Buckland, S.T., Anderson, D.R., Burnham, K.P., Laake, J.L., Borchers, D.L., Thomas, L., 2004. Advanced Distance Sampling: Estimating Abundance of Biological Populations. Oxford University Press, New York City, New York, USA.
- Burnham, K.P., Anderson, D.R., 2002. Model Selection and Multi-Model Inference: A Practical Information Theoretic Approach. Springer, New York City, New York, USA.
- Calambokidis, J., Barlow, J., 2004. Abundance of blue and humpback whales in the eastern North Pacific estimated by capture-recapture and line-transect methods. *Mar. Mammal. Sci.* 20, 63–85.
- Calambokidis, J., Falcone, E.A., Quinn, T.J., Burdin, A.M., Clapham, P.J., Ford, J.K.B., Gabriele, C.M., LeDuc, R., Mattila, D., Rojas-Bracho, L., Straley, J.M., Taylor, B.L., Urbán, R., Weller, D., Witteveen, B.H., Yamaguchi, M., Bendlin, A., Camacho, D., Flynn, K., Havron, A., Huggins, J., Maloney, N., 2008. SPLASH: structure of populations, levels of abundance and status of humpback whales in the North Pacific. Final Report for Contract AB133F-03-RP-00078. 58 pp (Available from: <http://www.cascadiaresearch.org/SPLASH/SPLASH-contract-Report-May08.pdf>).
- Coachman, L.K., 1986. Circulation, water masses, and fluxes on the southeastern Bering Sea shelf. *Cont. Shelf Res.* 5, 23–108.

- Cooney, R.T., Coyle, K.O., 1982. Trophic implications of cross-shelf copepod distributions in the southeastern Bering Sea. *Mar. Biol.* 70, 187–196.
- Coyle, K.O., Chavtur, V.G., Pinchuk, A.I., 1996. Zooplankton of the Bering Sea: a review of Russian-language literature. In: Mathiesen, O.A., Coyle, K.O. (Eds.), *Ecology of the Bering Sea: A Review of the Russian Literature*. Alaska Sea Grant Pub, 96-01, Fairbanks, AK, pp. 97–133.
- Coyle, K.O., Pinchuk, A.I., 2002. The abundance and distribution of euphausiids and zero-age pollock on the inner shelf of the southeast Bering Sea near the Inner Front in 1997–1999. *Deep-Sea Res. II* 49, 6009–6030.
- Coyle, K.O., Pinchuk, A.I., Eisner, L.B., Napp, J.M., 2008. Zooplankton species composition, abundance and biomass on the eastern Bering Sea shelf during summer: the potential role of water-column stability and nutrients in structuring the zooplankton community. *Deep-Sea Res. II* 55, 1775–1791.
- Fiscus, C.H., Jones, L.L., 1999. A note on cephalopods from the stomachs of Dall's porpoise (*Phocoenoides dalli*) from the northwestern Pacific and Bering Sea, 1978–1982. *J. Cetacean Res. Manage.* 1, 101–107.
- Ford, J.K.B., Ellis, G.M., Balcomb, K.C., 2000. Killer whales: The Natural History and Genealogy of *Orcinus orca* in British Columbia and Washington State. University of British Columbia Press, Vancouver.
- Friday, N.A., Waite, J.M., Zerbini, A.N., Moore, S.E., 2012. Cetacean distribution and abundance in relation to oceanographic domains on the eastern Bering Sea shelf: 1999–2004. *Deep-Sea Res. II* 65–70, 260–272.
- Friedlaender, A.S., Halpin, P.N., Qian, S.S., Lawson, G.L., Wiebe, P.H., Thiele, D., Read, A.J., 2006. Whale distribution in relation to prey abundance and oceanographic processes in shelf waters of the western Antarctic Peninsula. *Mar. Ecol. Prog. Ser.* 317, 297–310.
- Gearin, P.J., Melin, S.R., DeLong, R.L., Kajimura, H., Johnson, M.A., 1994. Harbor porpoise interactions with a chinook salmon set-net fishery in Washington State. *Rep. Int. Whaling Commn. special issue* 15, 427–438.
- Guttormsen, M.A., Yasenak, P.T., 2007. Results of the 2003 and 2005 echo integration-trawl surveys in the Gulf of Alaska during summer, Cruises MF2003-09 and OD2005-01. AFSC Processed Report no. 2007-04, Alaska Fisheries Science Center, NOAA, National Marine Fisheries Service, 7600 Sand Point Way NE, Seattle, Washington, 98115. 61 pp.
- Hilborn, R., Mangel, M., 1997. *The Ecological Detective*. Princeton University Press, Princeton, New Jersey, U.S.A.
- Hollowed, A.B., Barbeaux, S.J., Cokelet, E.D., Farley, E., Kotwicki, S., Ressler, P.H., Spital, C., Wilson, C.D., 2012. Effects of climate variations on pelagic ocean habitats and their role in structuring forage fish distributions in the Bering Sea. *Deep-Sea Res. II* 65–70, 230–250.
- Hunt Jr., G.L., Allen, B.M., Angliss, R.P., Baker, T., Bond, N., Buck, G., Byrd, G.V., Coyle, K.O., Devol, A., Eggers, D.M., Eisner, L., Feely, R., Fitzgerald, S., Fritz, L.W., Gritsai, E.V., Ladd, C., Lewis, W., Mathis, J., Mordy, C.W., Mueter, F., Napp, J., Sherr, E., Shull, D., Stabeno, P., Stepanenko, M.A., Strom, S., Whitley, T.E., 2010. Status and trends of the Bering Sea region, 2003–2008. In: McKinnell, S.M., Dagg, M.J. (Eds.), *Marine Ecosystems of the North Pacific Ocean, 2003–2008*. North Pacific Marine Science Organization, Sidney, British Columbia, Canada, pp. 196–267.
- Hunt Jr., G.L., Coyle, K.O., Eisner, L., Farley, E.V., Heintz, R., Mueter, F., Napp, J.M., Overland, J.E., Ressler, P.H., Salo, S., Stabeno, P.J., 2011. Climate impacts on eastern Bering Sea food webs: a synthesis of new data and an assessment of the Oscillating Control Hypothesis. *ICES J. Mar. Sci.* 68(6), 1230–1243.
- Hunt Jr., G.L., Stabeno, P.J., 2002. Climate change and the control of energy flow in the southeastern Bering Sea. *Prog. Oceanogr.* 55, 5–22.
- Hunt, G.L., Stabeno, P., Walters, G., Sinclair, E., Brodeur, R.D., Napp, J.M., Bond, N.A., 2002. Climate change and control of the southeastern Bering Sea pelagic ecosystem. *Deep-Sea Res. II* 49, 5821–5853.
- IWC, 2010. Report of the Interseasonal Workshop on MSYR for Baleen Whales. *J. Cetacean Res. Manage.* 11, 493–508.
- Kachel, N.B., Hunt Jr., G.L., Salo, S.A., Schumacher, J.D., Stabeno, P.J., Whitley, T.E., 2002. Characteristics and variability of the inner front of the southeastern Bering Sea. *Deep-Sea Res. II* 49, 5889–5909.
- Laake, J., Borchers, D., Len, T., Miller, D., Bishop, J., 2012. Mark-recapture distance sampling (mrds). R package, version 2.0.5.
- Ladd, C., Stabeno, P., 2012. Stratification on the eastern Bering Sea shelf revisited. *Deep-Sea Res. II* 65–70, 72–83.
- Leatherwood, S., Bowles, A.E., Reeves, R.R., 1983. Endangered whales of the eastern Bering Sea and Shelikof Strait, Alaska: results of aerial surveys, April 1982 through April 1983 with notes on other marine mammals seen. *Hubbs-Sea World Research Institute. Technical Report no.* 83-159/December 1983, 320 pp.
- Mizroch, S.A., Herman, L.M., Straley, J.M., Glockner-Ferrari, D.A., Jurasz, C., Darling, J., Cerchio, S., Gabriele, C.M., Salden, D.R., Von Ziegler, O., 2004. Estimating the adult survival rate of Central North Pacific humpback whales (*Megaptera novaeangliae*). *J. Mammal.* 85, 963–972.
- Mobley Jr., J., Spitz, S., Grottefendt, R., 2001. Abundance of humpback whales in Hawaiian waters: results of 1993–2000 aerial surveys. Report to the Hawaiian Islands Humpback Whale National Marine Sanctuary, 16pp.
- Moore, J.E., Barlow, J., 2011. Bayesian state-space model of fin whale abundance trends from a 1991–2008 time series of line-transect surveys in the California Current. *J. Appl. Ecol.* 48, 1195–1205.
- Moore, S.E., Waite, J.M., Friday, N.A., Honkalehto, T., 2002. Cetacean distribution and relative abundance on the central-eastern and the southeastern Bering Sea shelf with reference to oceanographic domains. *Prog. Oceanogr.* 55, 249–261.
- Moore, S.E., Waite, J.M., Mazzuca, L.L., Hobbs, R.C., 2000. Mysticete whale abundance and observations of prey associations on the central Bering Sea shelf. *J. Cetacean Res. Manage.* 2, 227–234.
- Napp, J.M., Baier, C.T., Brodeur, R.D., Coyle, K.O., Shiga, N., Mier, K., 2002. Interannual and decadal variability in zooplankton communities of the south-east Bering Sea shelf. *Deep-Sea Res. II* 49, 5991–6008.
- Napp, J.M., Hunt Jr., G.L., 2001. Anomalous conditions in the south-eastern Bering Sea 1997: linkages among climate, weather, ocean, and biology. *Fish. Oceanogr.* 10, 61–68.
- Ohashi, R., 2013. Interannual changes in the zooplankton community structure on the southeastern Bering Sea shelf during summers of 1994–2009. *Deep-Sea Res. II* 94, 44–56.
- Ortiz, I., Francis, W., Greig, A. Marine regions of the eastern Bering Sea. *Deep-Sea Res. II* (this issue).
- Overland, J.E., Wang, M., Wood, K.R., Percival, D.B., Bond, N.A., 2012. Recent Bering Sea warm and cold events in a 95-year perspective. *Deep-Sea Res. II* 65–70, 6–13.
- Palka, D.L., Hammond, P.S., 2001. Accounting for responsive movement in line transect estimates of abundance. *Can. J. Fish. Aquat. Sci.* 58, 777–787.
- Perez, M.A., 1990. Review of marine mammal population and prey information for Bering Sea ecosystem studies. U.S. Department of Commerce, NOAA Technical Memorandum NMFS F/NWC-186, 81 pp.
- R Development Core Team, 2012. R: a language and environment for statistical computing. R Foundation for Statistical Computing, Vienna, Austria. ISBN 3-900051-07-0, URL <<http://www.R-project.org/>>.
- Ressler, P.H., De Robertis, A., Warren, J.D., Smith, J.N., Kotwicki, S., 2012. Developing an acoustic index of euphausiid abundance to understand trophic interactions in the Bering Sea ecosystem. *Deep-Sea Res. II* 65–70, 184–195.
- Sambrotto, R.N., Niebauer, H.J., Goering, J.J., Iverson, R.L., 1986. Relationships among vertical mixing, nitrate uptake, and phytoplankton growth during the spring bloom in the southeast Bering Sea middle shelf. *Cont. Shelf Res.* 5, 161–198.
- Smith, S.L., 1991. Growth, development and distribution of the euphausiids *Thysanoessa raschi* (M. Sars) and *Thysanoessa inermis* (Krøyer) in the south-eastern Bering Sea. *Polar Res.* 10, 461–478.
- Smith, S.L., Vidal, J., 1986. Variations in the distribution, abundance, and development of copepods in the southeastern Bering Sea in 1980 and 1981. *Cont. Shelf Res.* 5, 215–239.
- Springer, A.M., McRoy, C.P., Flint, M.V., 1996. The Bering Sea green belt: shelf-edge processes and ecosystem production. *Fish. Oceanogr.* 5, 205–223.
- Stabeno, P.J., Bond, N.A., Kachel, N.B., Salo, S.A., Schumacher, J.D., 2001. On the temporal variability of the physical environment over the south-eastern Bering Sea. *Fish. Oceanogr.* 10, 81–98.
- Stabeno, P.J., Bond, N.A., Salo, S.A., 2007. On recent warming of the southeastern Bering Sea shelf. *Deep-Sea Res. II* 55, 2599–2618.
- Stabeno, P.J., Farley Jr., E.V., Kachel, N.B., Moore, S., Mordy, C.W., Napp, J.M., Overland, J.E., Pinchuk, A.I., Sigler, M.F., 2012a. A comparison of the physics of the northern and southern shelves of the eastern Bering Sea and some implications for the ecosystem. *Deep-Sea Res. II* 65–70, 14–30.
- Stabeno, P.J., Kachel, N.B., Moore, S.E., Napp, J.M., Sigler, M., Yamaguchi, A., Zerbini, A.N., 2012b. Comparison of warm and cold years on the southeastern Bering Sea shelf and some implications for the ecosystem. *Deep-Sea Res. II* 65–70, 31–45.
- Stabeno, P.J., Schumacher, J.D., Davis, R.F., Napp, J.M., 1998. Under-ice observations of water column temperature, salinity and spring phytoplankton dynamics: eastern Bering Sea shelf. *J. Mar. Res.* 56, 239–255.
- Stafford, K.M., Mellinger, D.K., 2009. Analysis of acoustic and oceanographic data from the Bering Sea, May 2006–April 2007. *North Pacific Research Board Final Report* 719, 23 pp.
- Stafford, K.M., Moore, S.E., Stabeno, P.J., Holliday, D.V., Napp, J.M., Mellinger, D.K., 2010. Biophysical ocean observation in the southeastern Bering Sea. *Geophys. Res. Lett.* 37, L02606, 1–4.
- Turnock, B.J., Quinn II, T.J., 1991. The effect of responsive movement on abundance estimation using line transect sampling. *Biometrics* 47, 701–715.
- Tyman, C.T., 2004. Cetacean populations on the SE Bering Sea shelf during the late 1990s: implications for decadal changes in ecosystem structure and carbon flow. *Mar. Ecol. Prog. Ser.* 272, 281–300.
- Waite, J.M., Friday, N.A., Moore, S.E., 2002. Killer whale (*Orcinus orca*) distribution and abundance in the central and southeastern Bering Sea, July 1999 and June 2000. *Mar. Mammal. Sci.* 18, 779–786.
- Whitley, T.E., Reeburgh, W.S., Walsh, J.J., 1986. Seasonal inorganic nitrogen distribution and dynamics in the southeastern Bering Sea. *Cont. Shelf Res.* 5, 109–132.
- Wiese, F.K., Van Pelt, T.I., Wiseman Jr, W.J., 2012. Bering Sea linkages. *Deep-Sea Res. II* 65–70, 2–5.
- Zador, S.G., Gaichas, S., 2010. Ecosystem Considerations for 2011. Appendix C of the BSAI/GOA Stock Assessment and Fishery Evaluation Reports. Technical Report, North Pacific Fishery Management Council, AK 99501.
- Zerbini, A.N., Clapham, P., Kennedy, A.S., Geyer, Y., 2011. Individual variation in movements of humpback whales (*Megaptera novaeangliae*) satellite-tracked in the Bering Sea during summer. 2011 Alaska Marine Science Symposium Book of Abstracts. NOAA Alaska Fisheries Science Center, Seattle, Washington, USA, Anchorage, Alaska, USA, p. 160.
- Zerbini, A.N., Clapham, P.J., Wade, P.R., 2010. Assessing plausible rates of population growth in humpback whales from life-history data. *Mar. Biol.* 157, 1225–1236.
- Zerbini, A.N., Waite, J.M., Laake, J.L., Wade, P.R., 2006. Abundance, trends and distribution of baleen whales off western Alaska and the central Aleutian Islands. *Deep-Sea Res. I* 53, 1772–1790.



Northern fur seals augment ship-derived ocean temperatures with higher temporal and spatial resolution data in the eastern Bering Sea



Chad A. Nordstrom^{a,b,*}, Kelly J. Benoit-Bird^c, Brian C. Battaile^a, Andrew W. Trites^{a,b}

^a Marine Mammal Research Unit, Fisheries Centre, University of British Columbia, AERL, 2202 Main Mall, Vancouver, BC, Canada V6T 1Z4

^b Department of Zoology, University of British Columbia, #2370–6270 University Boulevard, Vancouver, BC, Canada V6T 1Z4

^c College of Earth, Ocean, and Atmospheric Sciences, Oregon State University, 104 CEOAS Administration Building, Corvallis, OR 97331, USA

ARTICLE INFO

Available online 19 March 2013

Keywords:

Bio-logging
Spatial interpolation
Data-interpolating variational analysis
Northern fur seal
Callorhinus ursinus
USA
Alaska
Eastern Bering Sea

ABSTRACT

Oceanographic data collected by marine vertebrates are increasingly being used in biological and physical studies under the assumption that data recorded by free-ranging animals are comparable to those from traditional vertical sampling. We tested this premise by comparing the water temperatures measured during a 2009 oceanographic cruise with those measured during 82 foraging trips by instrumented northern fur seals (*Callorhinus ursinus*) in the eastern Bering Sea. The animal-borne data loggers were equipped with a fast-response temperature sensor and recorded 6492 vertical profiles to depths ≥ 50 m during long distance (up to 600 km) foraging trips. Concurrent sampling during the oceanographic cruise collected 247 CTD casts in the same 5-week period. Average temperature differences between ship casts and seal dives (0.60 ± 0.61 °C), when the two were within 1 day and 10 km of each other ($n=32$ stations), were comparable to mean differences between adjacent 10 km ship casts (0.46 ± 0.44 °C). Isosurfaces were evaluated at region wide scales at depths of 1 m and 50 m while the entire upper 100 m of the water column was analyzed at finer-scales in highly sampled areas. Similar patterns were noted in the temperature fields produced by ships or seals despite the differences in sampling frequency and distribution. However, the fur seal dataset was of higher temporal and spatial resolution and could therefore be used to visualize finer detail with less estimated error than ship-derived data, particularly in dynamic areas. Integrating the ship and seal datasets provided temperature maps with an unprecedented combination of resolution and coverage allowing fine-scale processes on-shelf and over the basin to be described simultaneously. Fur seals ($n=65$ trips) also collected 4700 additional profiles post-cruise which allowed ≥ 1 °C warming of the upper 100 m to be documented through mid-September, including regions where ship sampling has traditionally been sparse. Our data show that hydrographic information collected by wide-ranging, diving animals such as fur seals can contribute physical data comparable to, or exceeding those, of traditional sampling methods at regional or finer scales when the questions of interest coincide with the ecology of the species.

© 2013 Elsevier Ltd. All rights reserved.

1. Introduction

Traditional oceanographic sampling has been increasingly supplemented with data collected by free-ranging marine vertebrates (Biuw et al., 2007; Boyd et al., 2001; Charrassin et al., 2002; Lydersen et al., 2004; Roquet et al., 2009; Simmons et al., 2010). Animal-borne sensors have gathered large numbers of high-resolution vertical profiles over wide areas and long time periods but with an inherently different sampling strategy than the

regularized data collection protocols (e.g. transects) generally used by ships, moorings or satellites. Despite temporal and spatial differences in sampling, oceanographic data collected by animals have contributed to models of ocean heat flux, predictions of frontal strength, and deep-water turnover estimates (Boehme et al., 2008; Charrassin et al., 2008; Costa et al., 2008; Grist et al., 2011). Technical validations of the tags have been performed in the field and the lab (Roquet et al., 2011; Simmons et al., 2009), but to date there have been no large scale comparisons of data derived from *in-situ* platforms employing standard data collection techniques with those from animal-borne instruments sampling according to highly individualized spatiotemporal use. Animal-borne sensors can be powerful tools to collect habitat data, but only if the data can be assumed to be, at minimum, comparable to habitat descriptions previously obtained from more

* Corresponding author. Tel.: +1 604 822 6557; fax: +1 604 822 8180.

E-mail addresses: c.nordstrom@fisheries.ubc.ca (C.A. Nordstrom), b.battaile@fisheries.ubc.ca (K.J. Benoit-Bird), kbenoit@coas.oregonstate.edu (B.C. Battaile), a.trites@fisheries.ubc.ca (A.W. Trites).

traditional ocean profiling techniques, and this has yet to be examined on a large scale.

The eastern Bering Sea is a hydrographically complex region north of the Aleutian arc comprising a broad, shallow (<200 m) continental shelf with a deep oceanic basin (>3000 m) separated by a narrow shelf break (Fig. 1). The region is a seasonally productive high-latitude system where the coupling of physical and biological processes supports large aggregations of sea-birds and marine mammals (Hunt Jr. and Stabeno, 2002; Sinclair et al., 2008). Well described temperature domains at the mesoscale are defined by the major isobaths, although at the sub-mesoscale (<10 km) conditions can be highly dynamic (Stabeno et al., 2001, 2008; Sullivan et al., 2008). For example, the middle continental shelf (50 to <100 m) typically consists of two well-structured temperature layers compared to the three diffuse layers on the outer shelf (100 to <200 m) with the transition between the two relatively coincident with the 100 m isobaths. In addition, a bottom layer of water <2 °C (cold-pool) remnant from sea ice melt occupies the middle-shelf, but its extent shifts inter-annually (Stabeno et al., 2001). Eddies, meanders of the major northward currents, and disturbances created by bottom topography all introduce fine-scale variability within the region's large expanse (Ladd et al., 2012; Okkonen et al., 2004; Schumacher and Stabeno, 1994; Stabeno and van Meurs, 1999).

Northern fur seals (*Callorhinus ursinus*) are apex predators in the Bering Sea with an ecology that makes them well-suited

platforms for fine-scale sampling across varied habitats and large distances. These small otariids return from the open North Pacific to islands in the Bering Sea to breed, give birth and rear pups for 4 months each summer. During this period, lactating females intersperse wide-ranging (up to 600 km) foraging trips at-sea with nursing bouts ashore (Gentry, 1998). As a result, complete data records can be recovered following foraging trips instead of necessitating the use of sub-sampled data typically relayed through satellites, thereby facilitating examination of fine-scale oceanographic data from complex environments. Lactating northern fur seals also employ multiple foraging strategies (Goebel et al., 1991) and exhibit a large degree of inter-individual difference in terms of where animals travel in search of prey. While females appear to show some fidelity to areas where they previously foraged (Call et al., 2008; Robson et al., 2004), they do not appear to target specific foraging grounds as commonly seen in other species (e.g., Campagna et al., 2001; Chilvers et al., 2005; Lea et al., 2008; Trathan et al., 2006; Weise et al., 2010). From a sampling perspective, the routes used by the fur seals appear almost random at the island population level. This fine-scale heterogeneous sampling, in conjunction with their wide-ranging movements and predictable returns to the rookery for instrument recovery, should make the northern fur seal an excellent animal platform from which to study the physical parameters of the eastern Bering Sea. Reciprocally, a greater understanding of

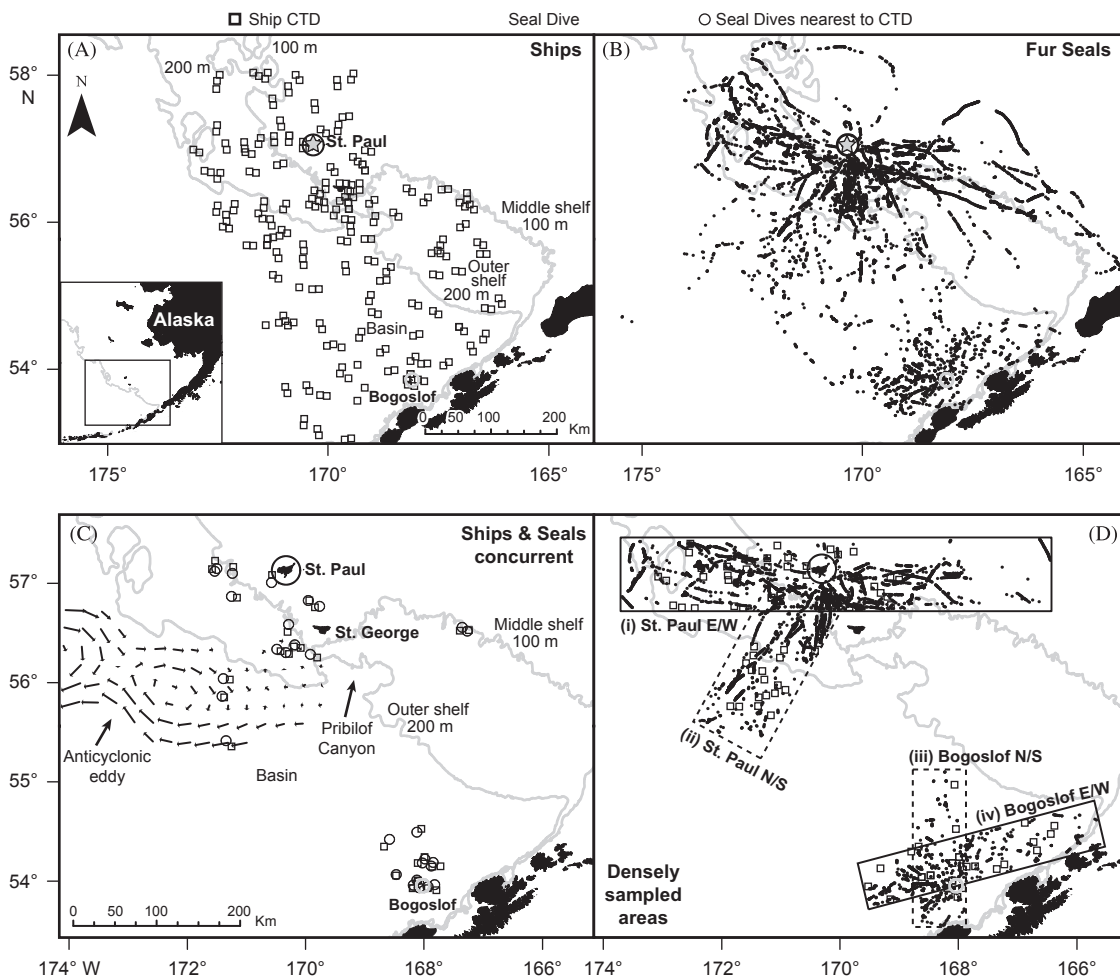


Fig. 1. Sampling stations with ocean temperature profiles ≥ 50 m in the eastern Bering Sea: (A) ship CTD casts ($n=247$) from July 18 to August 14, 2009; (B) fur seal dives from July 15 to September 17, 2009 ($n=11,192$); (C) concurrent CTD casts (open squares) and seal dives (open circles) within 10 km and 1 day of each other ($n=32$); and (D) delineated sub-regions where ships (open squares) and seals (black circles) sampled most frequently. The 200 m isobaths marks the approximate location of the shelf-break dividing the Bering Sea basin (west) from the continental shelf (east).

fine-scale oceanography could lead to insights into the ecology of the northern fur seal (e.g., Nordstrom et al., 2012; Sterling, 2009).

The overall objective of the study was to compare the upper water temperatures collected by ships with similar data collected by northern fur seals in the eastern Bering Sea. More specifically, we deployed fast-response temperature sensors (thermistors) on 31 northern fur seals concomitantly with ship-board sampling designed to support ecological studies of upper trophic predators. This provided a unique opportunity to collect point-sampled oceanographic data from different platforms operating independently and simultaneously over the same geographical region. Not only could the information be compared to examine differences between ship and fur seal collections but the data could also be combined to describe the oceanography of the region more completely. Our goals were to (1) compare water temperatures measured during a 2009 oceanographic cruise with those from instrumented fur seals, (2) evaluate interpolated temperature maps derived from each data source, and (3) describe summer conditions in the eastern Bering Sea using the novel, integrated dataset.

2. Materials and methods

2.1. Ship sampling

The goal of the sampling program was to describe the distributions and habitat conditions of forage fish and krill that were likely to support upper predators such as fur seals and seabirds from colonies in the eastern Bering Sea during the summer. The survey was therefore designed to collect data within 200 km of the Pribilof Islands and 200 km north–northwest of Bogoslof Island where major colonies were located to examine the consequences of variation in prey and oceanography on the at-sea distribution of predators. The area between St. Paul Island (57.1°N, 170.3°W) and Bogoslof Island (53.9°N, 168.0°W) was sampled from July 18th to August 14th, 2009 from chartered fishing vessels (the 43 m FV 'Frosti' and the 32 m FV 'Goldrush'). Prey sampling consisted of a series of 10 km long transects (trawls) and physical oceanographic sampling consisted of paired stations at the beginning and end of each transect. A total of 247 stations were distributed over three, hydrographically distinct zones (Coachman, 1986): middle shelf with bottom depths between 50 and 100 m (45 stations); outer shelf with bottom depths between 100 and 200 m (81 stations); and slope/basin with depths greater than 200 m (121 stations) (Benoit-Bird et al., 2011). The first station in each pair was randomly located as was the orientation to the next station. Transects were not allowed to cross region boundaries or other transects (Fig. 1A). Note that odd numbers of stations represent data loss from individual instrument deployments but at least one profile was collected for each transect.

A CTD (conductivity, temperature, and depth) profile was conducted at each station (at the beginning and end of each 10-km transect). A Sea-Bird SBE19plus CTD was guided by a real time remote pressure sensor (Simrad PI60) and lowered to a depth of 100 m or 5 m from the bottom if the sea floor was < 100 m from the surface. Each CTD was also equipped with a dissolved oxygen sensor, a transmissometer within the visible spectrum for most fish, and a fluorometer. Data were low pass filtered, aligned to account for instrument lags, and edited for loops (to account for ship heaving) before the raw data were converted to variables of interest using factory calibrations.

2.2. Seal sampling

Lactating fur seals at St. Paul Island (Reef rookery, $n=44$ females) and Bogoslof Island ($n=43$ females) were instrumented

with Mk10-F GPS enabled time-depth recorders equipped with fast-response thermistors (Wildlife Computers, WA, USA) from July 11th to September 19th, 2009. Each GPS tag ($102 \times 60 \times 31$ mm³) was paired with a VHF transmitter ($45 \times 31 \times 15$ mm³) to assist with instrument recovery (Advanced Telemetry Systems, MN, USA). The archival Mk10-F tags recorded depth (0.5 m resolution), external temperature (0.52 s response, 0.05 °C resolution, 0.1 °C accuracy, Hill *pers. comm.*), and light level once per second. Fastloc™ GPS fixes were attempted every 15 min while the animal was at the surface.

Females on St. Paul Island were tagged at Reef rookery because fur seals from this location have been shown to forage in all hydrographic domains around the island (Robson et al., 2004). Instruments were deployed on fur seals from 3 rookeries on Bogoslof Island with different geographic orientations to ensure tracks were representative for the island. Seals were captured using a mobile blind (July) or via hoop-net (August–September). Individual females were chosen based on size and the presence of a healthy pup and/or adequate milk production. These criteria increased the likelihood that females would return to the rookery for instrument recovery and redeployment. Animals were physically restrained using custom restraint-boards and neoprene wraps to allow devices to be glued to the dorsal pelage along the seal's midline using 5-min epoxy (Devcon®, MA, USA). Hoop-netted females were weighed (± 0.1 kg, mean=39.2 kg) using an MSI-7200 Dyna-Link digital scale (Measure Systems International, Seattle, WA). Standard lengths (± 1 cm, mean=121.4 cm) and girths (± 1 cm, mean=81.1 cm) were also measured whenever possible for all animals but were generally more challenging to obtain from the mobile blind. Animals were recaptured, physically restrained, re-measured, and devices were removed following foraging trips (deployment interval=5–39 days, mean=14 d). Capture teams based on each island redeployed instruments on successive animals after the data were recovered to increase the sample size of tagged individuals.

Profiles collected from fur seals were divided into 2 time periods: (1) July 15–August 15 (to match the ship cruise), and (2) from August 16 to September 17 (post-cruise until the last profile). The tag's salt-water switch was used to determine the start and end of each foraging trip in conjunction with GPS fixes. GPS locations were filtered to remove points requiring unlikely average travel speeds (> 3 m/s) by calculating the running mean of speed using the previous and next locations for each fix. Tracks were linearly interpolated between points as temporal resolution was generally very high (mean=17.4 post-filtered locations per day) (Tremblay et al., 2006). GPS points were rarely removed (99% of at-sea locations were retained) and those that were eliminated tended to be gross anomalies (e.g., basin wide movements within hours).

Dive data were zero-offset corrected using Wildlife Computer's DAP program (v.2.063) with dives defined as those reaching at least 5 m. Each dive was enumerated and broken into descent, bottom, or ascent portions using 80% of the maximum dive depth as the transition points. Maximum depth (m) was recorded and dives > 50 m were retained for comparison with ship profiles. Locations for the start and end of each dive were determined by matching the dive times to the interpolated track via the tag's clock (Fig. 1B).

The Mk10 external temperature data were processed according to validations conducted by Simmons et al. (2009). Briefly, external temperature readings were aligned with the depth sensor by applying a 1-s time lag and corrected by subtracting 0.05 °C. Seal dives were binned at 1-m intervals and temperature values were interpolated using a hermite spline. As most seals dived at < 1 m/s, temperature measures were averaged more often than interpolated for a given depth.

2.3. Satellite altimetry

Supplementary data describing the positions of mesoscale eddies and other submesoscale fronts over the basin on July 29 were also considered. These data provided a snapshot of frontal activity at the mid-point of the composite temperature maps and provided context for the patterns observed over the basin. Maps of sea-surface height (SSH) and geostrophic current anomalies were created from merged, delayed-time (corrected) satellite altimetry distributed by Aviso, France (<http://www.aviso.ocea.nobs.com>). The positions of fine-scale fronts were then estimated from 4-day maps of surface Lagrangian coherent structures (e.g. transport barriers, filament edges, or eddy boundaries). These 4-day maps were in turn derived from the geostrophic current anomalies using the finite-size Lyapunov exponent (FSLE) method which is well suited to study the properties of transport in fluid flow (Boffetta et al., 2001; d'Ovidio et al., 2004). Low FSLE values coincide with areas of low dispersion rates (e.g. eddy cores) while regions of large Lyapunov exponents are associated with areas of high dispersion such as the outer part of eddies and strong fronts (d'Ovidio et al., 2004; Resplandy et al., 2009). We contoured the FSLE values at 0.2 FSLE/d to reproduce the edges of the strongest fronts which was suitable for comparison with the aggregated temperature data.

2.4. Creation of datasets

Composite temperature maps for the study region were created by gridding the point-sample data collected by ships and seals. All maps of isosurfaces and vertical cross-sections were interpolated using the data-interpolating variational analysis (DIVA) method (Brasseur et al., 1996; Rixen et al., 2000; Troupin et al., 2010) as implemented in the Ocean Data View (v.4.4.2) software package (Schlitzer, 2011a, <http://odv.awi.de>). The DIVA algorithm is akin to optimal interpolation techniques but incorporates directional constraints and barriers such as bottom topography. Any re-created field is sensitive to correlation length (the range over which fluctuations in one region of space influence those in another) and, as with other gridding algorithms, the smoothness of the estimated field is controlled by adjusting the correlation length (Schlitzer, 2011b). Larger values allow for the assimilation of data from points further apart and result in smoother fields but at the expense of potentially losing fine-scale detail. The correlation length is set as the percent of x (e.g. longitude) and y or z (e.g. latitude or depth) in Ocean Data View therefore the areal extent of each surface was fixed prior to gridding. For example, we set a correlation length of 1% over a depth range of 110 m for all cross-sections to consistently allow each sample to influence the gridded value of vertically neighboring samples out to 1.1 m. Correlation lengths are reported as percentages with their equivalent linear distance in km.

2.4.1. Maps of isosurfaces

Separate temperature isosurfaces were generated from data collected across the region by ships or by seals for the area covering 174.25–164.0°W by 58.75–53.25°N using Ocean Data View at the default projection. Maps were created at 1 m and 50 m depth slices. This allowed us to estimate temperature at layers routinely sampled by both platforms across the entire sampling region. The 1 m depth slice was specifically chosen as a proxy for sea-surface temperature (SST) so it could be used as a stand-alone product for a region subject to extensive, satellite obscuring cloud cover while also easing potential comparison with other studies of marine predators that make use of satellite derived SST. The 50 m slice was chosen as it allowed us to

describe temperatures in a relatively less variable layer and use fur seal dives across the region as they rarely dove > 50 m when over the Bering Sea basin.

Datasets were later merged and isosurfaces at 1 and 50 m were again produced using integrated data from ships and seals. This allowed us to describe the eastern Bering Sea using all available data for the period of July 15–August 15. All isosurface maps were generated using a conservative correlation length of 1.3% (7.5 km latitude \times 8.3 km longitude) which was based on the 10 km separation between nearest ship casts.

2.4.2. Vertical cross-sections

Finer spatial scale cross-sections were interpolated from complete CTD profiles and from entire fur seal dives in sub-regions that were sampled most often (Fig. 1D) during 6-week blocks. This allowed us to examine the variability of the water column in highly sampled regions as described by either platform and to examine seasonal changes in temperature between two time-periods using data collected by the fur seals. Vertical cross-sections were generated using either 1% of longitude (3.0 km, sub-region i) or 2% (4.4 km, sub-region ii–iv) of latitude/longitude depending on the sampling density. Correlation length was kept consistent for ship and seal data within a sub-region and a correlation length of 1% (1.1 m) was used for depth in all cross-sections.

2.4.3. Error fields

The spatial distribution of analysis error is of interest when estimating a continuous spatial field in that it provides a relative measure of where one can have more or less confidence in the resulting map. Briefly, the analysis (DIVA interpolation) was applied on a vector containing the covariances of the data locations where the error needed to be calculated. DIVA, as enabled within Ocean Data View, employed a basic or poor man's error field (Barth et al., 2010; Troupin et al., 2010) which substituted a vector of values with constant variance for calculations performed by the analyzed field. This allowed the error to be assessed in all locations with the same analysis which in turn allowed for relatively rapid computation at the expense of underestimating true error (Troupin et al., 2012). As such, the error maps produced in these analyses should be considered minimum estimates of total error.

Errors estimates produced for the interpolated temperature fields incorporated instrument error (inherently as the values are considered anomalies against a constant background field) and sampling distribution error. Ocean Data View used the error estimates to restrict mapping to areas with error values below a user defined tolerance. The default quality limit of 0.25 was used as it produced relatively contiguous temperature maps without extrapolating estimates beyond the sampling region (errors are presented as the standard deviation relative to the field variance). This created irregularly shaped temperature maps and often produced “gaps” within isosurfaces/cross-sections but it retained only those estimates with errors below the defined threshold. The poor man's error field can be considered an efficient way to assess data coverage and determine which regions of the analysis cannot be trusted, however; other detailed analyses (such as the creation of climatologies) should make use of alternative methods to generate less optimistic error fields (Troupin et al., 2012).

2.5. Analysis techniques

2.5.1. Comparing in-situ temperatures

Temperatures from CTD casts and the corresponding nearest seal dives were directly compared at 1, 25, 50, 75, and 100 m

(as dives permitted) when they co-occurred within 10 km and 24 h (Fig. 1C). Previous, side-by-side validations have shown good agreement between the thermistor in the Mk10 and CTD sensor (Simmons et al., 2009). Temperature values from data-loggers were regressed against CTD values at paired depths and summary statistics were calculated for absolute differences using the *R* software package (R Development Core Team, 2009). All reported values include \pm standard deviation unless otherwise noted.

2.5.2. Comparing temperature isosurfaces

We compared maps of isosurfaces in 5 specific ways by (1) qualitatively assessing broad temperature patterns, (2) quantitatively examining fits and errors within surfaces (two methods), and (3) quantitatively comparing interpolated values between surfaces (two methods).

First, regional temperature maps were examined visually to assess how features such as the cold pool and transitions along the isobaths compared between maps produced from ship or seal data. Second, we measured the quality of each interpolated surface via cross-correlation (estimated goodness of fit) using *a priori* estimates of correlation length and signal-to-noise ratio generated by the DIVA fit routine (Barth et al., 2010). Third, error estimates obtained for individual surfaces from Ocean Data View were mapped using ArcGIS 9.3.1 software for additional within surface assessment.

Fourth, we directly compared temperature/error estimates extracted from ship and seal isosurfaces at 1 km intervals along a 300 km transect across the continental shelf (173.35–166.0°W at 51.1°N) and along a 235 km transect from the basin across the shelf-break to St. Paul Island (55.5–57.1°N; 172.0–170.3°W). Extracted transects were placed along the mid-line of densely sampled sub-regions (Fig. 1D). Fifth, regional surface maps were contrasted using a difference surface and a normalized difference surface for each depth slice that we generated by overlaying the ship derived field on the seal derived field and subtracting them. The normalized difference surface examined where differences between the fields was larger than the estimated errors and was defined as:

$$\text{Normalized difference} = \frac{\text{Ship temperature} - \text{Seal temperature}}{\sqrt{(\text{ship error}^2 + \text{seal error}^2)}} \quad (2.1)$$

where ship error and seal error are the standard deviations relative to the field variance of the respective surfaces.

2.5.3. Comparing vertical sections

Difference cross-sections were created from seal derived data for each of the 4 sub-regions by overlaying fields from July–August 15 with those from August 15–September and subtracting their gridded values. We calculated the standard deviation of the gridding errors over the section and doubled that value (2x SD) to obtain a threshold above which any temperature changes were likely to reflect actual differences between time periods as opposed to artifacts of the gridded interpolation. Further summary statistics on smaller patches within the difference section were calculated in Ocean Data View.

3. Results

3.1. Ship sampling

Temperatures ranged from -0.10 °C (measured in the cold-pool to the north-east of St. Paul Island) to 10.57 °C (measured at 1 m along the shelf break to the south-west of St. Paul Island). While stations were selected randomly within the study area, they were relatively well distributed at the regional scale (Fig. 1A) compared to the clumped, non-random distribution exhibited by the fur seals (Fig. 1B). The delineated sub-regions in Fig. 1D

covered 30.8% of the area sampled by ships and incorporated 36% of all ship casts, further highlighting the relatively even spatial sampling achieved by the ships within the study region.

3.2. Seal sampling

St. Paul Island ($n=44$) and Bogoslof Island ($n=41$) fur seals completed 147 foraging trips (July–August, $n=82$; August–September, $n=65$) recording at least one 50 m temperature profile (Table S1). Fur seals collected 11,192 profiles to depths ≥ 50 m during foraging dives at-sea between July 15th and September 17th, 2009 (July–August, $n=6492$; August–September, $n=4700$; Fig. 1B). Recorded temperatures ranged from -0.80 °C (in the cold pool east of St. Paul Island) to 10.45 °C (in the 1 m surface waters along the 100 m isobath south-east of St. Paul Island).

Profiles were collected relatively evenly between the middle domain ($n=3497$), the outer domain ($n=4060$), and the slope/basin ($n=3635$) of the eastern Bering Sea. Dives were nonetheless clumped within regions as the sub-regions delineated in Fig. 1D encompassed 21.6% of the area sampled by fur seals yet incorporated 50.9% of all sampling dives > 50 m.

St. Paul Island fur seals foraged widely as expected, radiating in all directions from the island with a notable concentration of southward trips. Seals originating from St. Paul Island traveled farther, were at-sea longer, and dove > 50 m more regularly (Nordstrom et al., 2012) and in doing so collected more profiles ($n=9325$) than seals from Bogoslof Island ($n=1867$). Some trips from St. Paul Island were restricted to the continental shelf and sampled the middle and outer shelf domains only while trips that reached the basin sampled all three hydrographic zones as they had to cross the shelf to reach the slope and basin regions.

Bogoslof Island fur seals did not pass through the Aleutian island chain but constrained their foraging trips primarily to the Bering Sea basin with occasional dives along the continental margins. Fewer sampling dives, generally restricted to the basin or slope regions, were recorded despite the greater number of trips performed by fur seals from Bogoslof Island. This was to be expected given Bogoslof Island's location over the basin when coupled with their shorter trips and their propensity for shallow diving (Nordstrom et al., 2012).

3.3. Comparing in-situ temperature

Seal dives ≥ 50 m coincided spatially and temporally with ship-borne CTD casts (within 10 km and 24 h of each other) on 48 occasions. Of these, 32 unique casts were directly compared to the nearest seal dive (Fig. 1C) as depths permitted (e.g. Fig. 2). Overall there was good agreement between paired ship casts and seal dives (e.g. Fig. 2A–C) when comparing absolute temperature differences at pre-determined depths (median=0.32, mean=0.60 \pm 0.61 °C). Differences were comparable to sequential CTD casts (within 10 km of each other) at those same depths ($n=120$ pairs, median=0.36 median, mean=0.46 \pm 0.44 °C)

Regression analysis of paired temperature values ($n=87$ pairs) showed significant correlations between values recorded from either platform ($F_{1,85}=516.1$, $p < 0.001$, adj. $R^2=0.87$; Fig. 3) and confidence intervals (95%) showed little uncertainty about predicted values. Most points were within 0.6 °C (the mean absolute difference between temperature pairings) of predicted values, particularly when temperatures were < 4 and > 8 °C which was typical of stable water masses well below or above the thermocline respectively.

3.4. Comparing temperature isosurfaces

Each of the five different methods used to compare interpolated temperature surfaces illustrated that those created from the

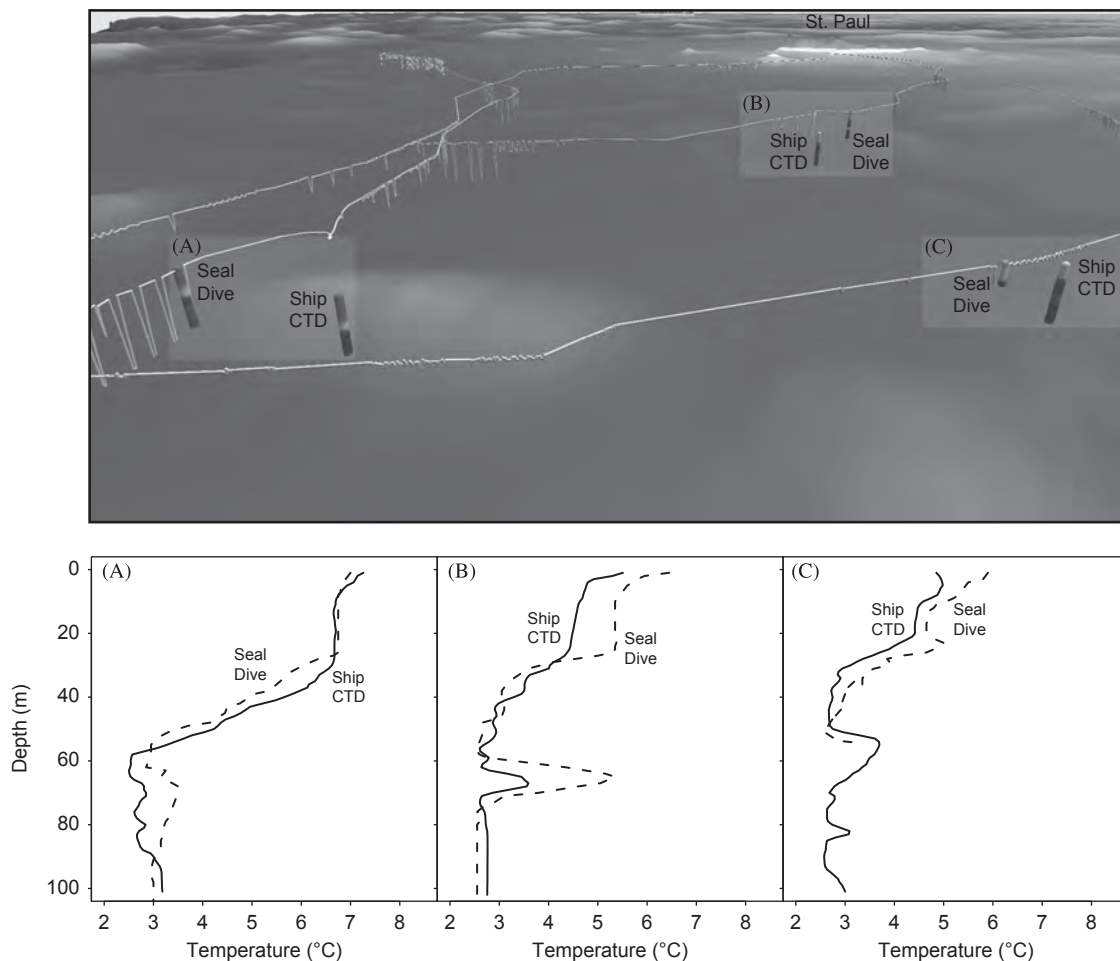


Fig. 2. Examples of paired temperature profiles collected by concurrent ship CTD casts and instrumented northern fur seals when sampling occurred within 10 km and 24 h. The upper panel depicts 3 pairs of *in-situ* profiles (colored vertical lines) on the continental shelf south of St. Paul I. White lines: fur seal surface track and additional dives. The lower panels compare the temperature-depth profiles from each ship cast (solid lines) and fur seal dive (dashed lines) pairing respectively (A: Dive SP09-0207 vs. CTD-34; B: Dive SP04B-0072 vs. CTD-32; C: Dive SP06-1466 vs. CTD-36).

seal data were equivalent or exceeded those produced from ship data in terms of areal coverage, detail, or quality.

3.4.1. Qualitative comparisons

Seal derived temperature fields at depths of 1 m and 50 m were qualitatively very similar to fields generated by standard CTD profiling despite obvious differences in the extents of the areas sampled (Fig. 4). The CTD data provided a nearly contiguous surface from north of St. Paul Island to south of Bogoslof Island thanks to the relatively even distribution of sampling stations over the study area. In contrast, seal surfaces were irregularly shaped polygons as they were generated from clumped sampling dives restricted along widely dispersed foraging tracks. While we did not detect any overlap in the foraging areas between the two different fur seal populations (St. Paul Island and Bogoslof Island), a sufficient number of sampling dives existed along the periphery of each fur seal range to bridge the surface into a collective whole rather than generating disjointed maps around each island. Instrumented seals provided highly detailed temperature data over a large expanse of the eastern Bering Sea with the early summer surfaces (Fig. 4C and D) providing more coverage over the continental shelf east of the Pribilofs while later summer surfaces were more contiguous over the basin (Fig. 4E and F).

Isosurfaces from both ships and seals highlighted similar features at the regional scale including cooler waters ($\sim 3\text{--}4\text{ }^{\circ}\text{C}$) surrounding the Pribilof Islands' at 1 m depth from July through August (Fig. 4A and C). They also delineated the cold-pool (waters $< 2\text{ }^{\circ}\text{C}$) north and east of the archipelago at 50 m although seals did not sample north of St. Paul Island until late August (Fig. 4F). Both data collection platforms also revealed a band of cool water ($\sim 2.5\text{ }^{\circ}\text{C}$; light-blue in Fig. 4) extending along the 100 m isobath across the outer shelf south and west of St. George Island.

Seal derived temperature surfaces showed greater spatial variability than ship derived surfaces and revealed finer scale heterogeneity of temperature within areas both on and off the continental shelf (Fig. 4A–D). For example, the large numbers of samples taken on the shallow plateau between St. Paul and St. George Islands showed that well-mixed waters at 1 m surrounded and connected both islands despite intrusions of warmer surface waters. Seals also revealed greater temperature fluctuations along the 100 and 200 m isobaths (particularly around the Pribilof Canyon) as well north and west of Bogoslof Island.

Isosurfaces from later summer (Fig. 4E and F), when only seals were sampling, showed generalized warming at both 1 and 50 m, however the cold pool appeared to remain relatively stationary. Waters at 1 m around the Pribilofs increased to $\sim 7\text{--}8\text{ }^{\circ}\text{C}$ and the outer shelf west of St. George Island increased to $\sim 9\text{--}10\text{ }^{\circ}\text{C}$. The band of cool water at 50 m in the outer shelf persisted, however;

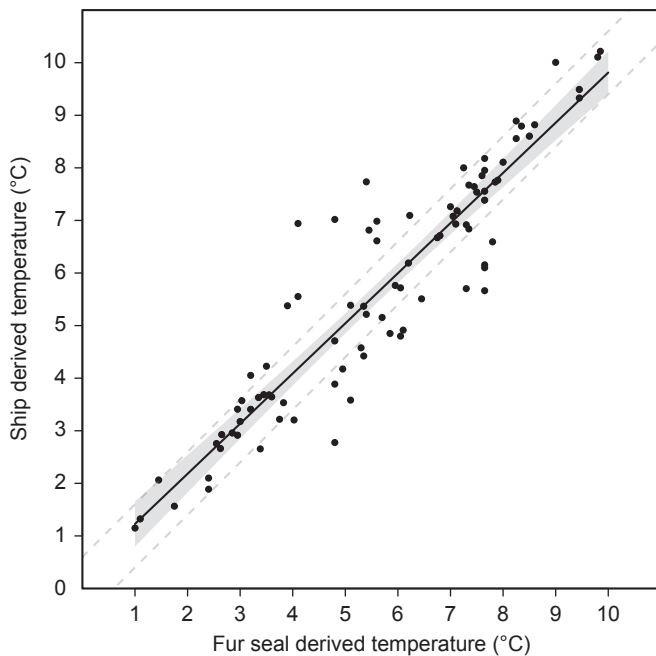


Fig. 3. Regression of temperature (°C) values collected at 1, 25, 50, 75, and 100 m by instrumented northern fur seals (when dives permitted) in relation to the nearest ship CTD cast within 10 km and 1 day (see Fig. 2.1C). Shading: 95% model confidence interval; gray dashed lines: ± 0.6 °C from 1 to 1 line (mean absolute difference between temperature pairings). There are 87 points comparing 32 stations/dives as collected by 20 individual fur seals.

it was less continuous as 4–5 °C water intersected it along the shelf-break.

3.4.2. Quantitative comparisons within surfaces

Results from DIVA cross-correlations (interpolated surface values correlated with observed temperature values) indicated a relative high-quality of fits ranging from 0.80 to 0.94 (where min=0 and max=1). Seal temperature surfaces at 1 m had better fits (July–August=0.89, August–September=0.94) than the 1 m ship surface while the ship surface fit was better (0.90) than the respective seal fits at 50 m (July–August=0.80, August–September=0.86). The July–August seal surfaces generated the highest (1 m field) and lowest (50 m field) statistical fits.

Isosurface error fields derived from ships and seals were notably different both in the distribution and the relative amount of error within the temperature surfaces (e.g. Fig. 5). Given that surfaces were masked, all resulting polygons were ringed with relatively large errors resulting from the cut-off at 0.25. The ship error field contained wide areas of relatively large errors (> 0.20) and the surface itself was pocked with small zones where the errors exceeded the threshold (Fig. 5A). In contrast, seal error fields generally comprised contiguous areas of relatively low error (< 0.10). Rare exceptions occurred in areas where the temperatures were interpolated between the southern limits of fur seal tracks from St. Paul Island and the northern extent of trips from Bogoslof Island (Fig. 5C and E) or in areas sampled by a lone fur seal. Overall, the ship surface had a greater degree of estimated error (median=0.08; Fig. 5B) compared to either seal surface (medians=0.02–0.03; Fig. 5C and F). Error fields were nearly identical at 1 m and 50 m highlighting the major role sampling distribution plays on mapping error.

3.4.3. Quantitative comparisons between surfaces

Extracted values from isosurfaces highlighted that both ship and seal maps tracked temperature changes across hydrographic

domains (Fig. 6). However, seal derived temperature estimates revealed finer details in the field compared to the smoothed estimates obtained from sparser ship data. The amount of error associated with the seal estimates was also noticeably less than ship estimates on both transects and at both 1 m and 50 m depths. Errors within transects from ship surfaces were not restricted to the terminuses, where increased error was expected as they coincided with the isosurface edge (due to the aforementioned error mask cutoff), but instead flared intermittently throughout the extracted length.

Difference surfaces highlighted areas where interpolated fields from ships and seals diverged (Fig. 7A and B) and summarized the magnitude of the discrepancies (Fig. 7C and D). Raw differences between 1 m surfaces ranged from -5.1 (where ship fields were cooler) to $+4.8$ °C (where ship fields were warmer) but 50% of the differences were within -0.17 and 1.13 °C (interquartile range). The largest raw differences occurred around St. George Island: (1) south along the 100 m isobath and over the Pribilof Canyon; (2) northeast on the 50 m plateau, and (3) west along the 200 m isobath (Fig. 7A). The raw differences approximated a normal distribution but overall the ship temperature surface was slightly warmer than the seal surface (median= 0.40 ± 1.14 °C).

Normalized differences between 1 m surfaces highlighted the inconsistencies remaining between temperature fields after attempting to account for the error within the respective ship and seal surfaces. Normalized differences between -1 and 1 indicated where fields were consistent within the estimated errors while differences < -1 (cooler) and > 1 (warmer) indicated where the fields were notably different. Half of the differences were within -0.17 and 1.23 (interquartile range) and again the ship surface was slightly warmer than seal surface (median= 0.36 ± 3.22). Large differences were again apparent around St. George coinciding with the previously described band of cooler water south and west of the island and with cooler but variable surface waters on the plateau of the Pribilof archipelago. Additionally, a narrow band north-east of Bogoslof Island was identified as a dissimilar zone (Fig. 7B).

3.5. Comparing vertical sections

Ship derived temperature cross-sections showed less detail and covered less area than those derived from seals (e.g. Figs. 8 and 9) in areas highly sampled by both platforms (Fig. 1D). Nonetheless, the cross-sections generated near Bogoslof Island (e.g. Figs. S1 and S2) and St. Paul Island tracked similar large scale shifts in the water column. For example, both ship (Fig. 8A) and seal (Fig. 8B) sections documented the abrupt transition from a weakly stratified 3-layer water column typical of the outer domain, to the strongly stratified 2-layer water column characteristic of the middle-domain (although the seal section was more informative thanks to increased sampling due east of St. Paul Island). Increased sampling by seals also made it possible to properly co-locate a shift in water column structure with the shelf-break south-west of St. Paul Island (Fig. 9B) as opposed to the same shift being documented more inshore on the outer shelf when using ship data (Fig. 9A). Had ships been sampling this area using a continuous transect (more traditional in physical oceanography), then the cross-sections would be more synoptic and the returned data would match the spatial scale of the survey design (but at the cost of being able to generate regional isosurfaces).

Fur seals documented the warming of the eastern Bering Sea in all hydrographic regions due to continued sampling following the end of the ship cruise (e.g. Figs. 8C and 9C). The sub-region bracketing St. Paul Island from east to west warmed unevenly in patches. On average, temperatures in the top 40 m increased over the outer shelf (mean= 0.61 ± 1.04 °C, max= 4.30 °C), around St. Paul Island (mean= 1.06 ± 1.46 °C, max= 5.30 °C) and over the

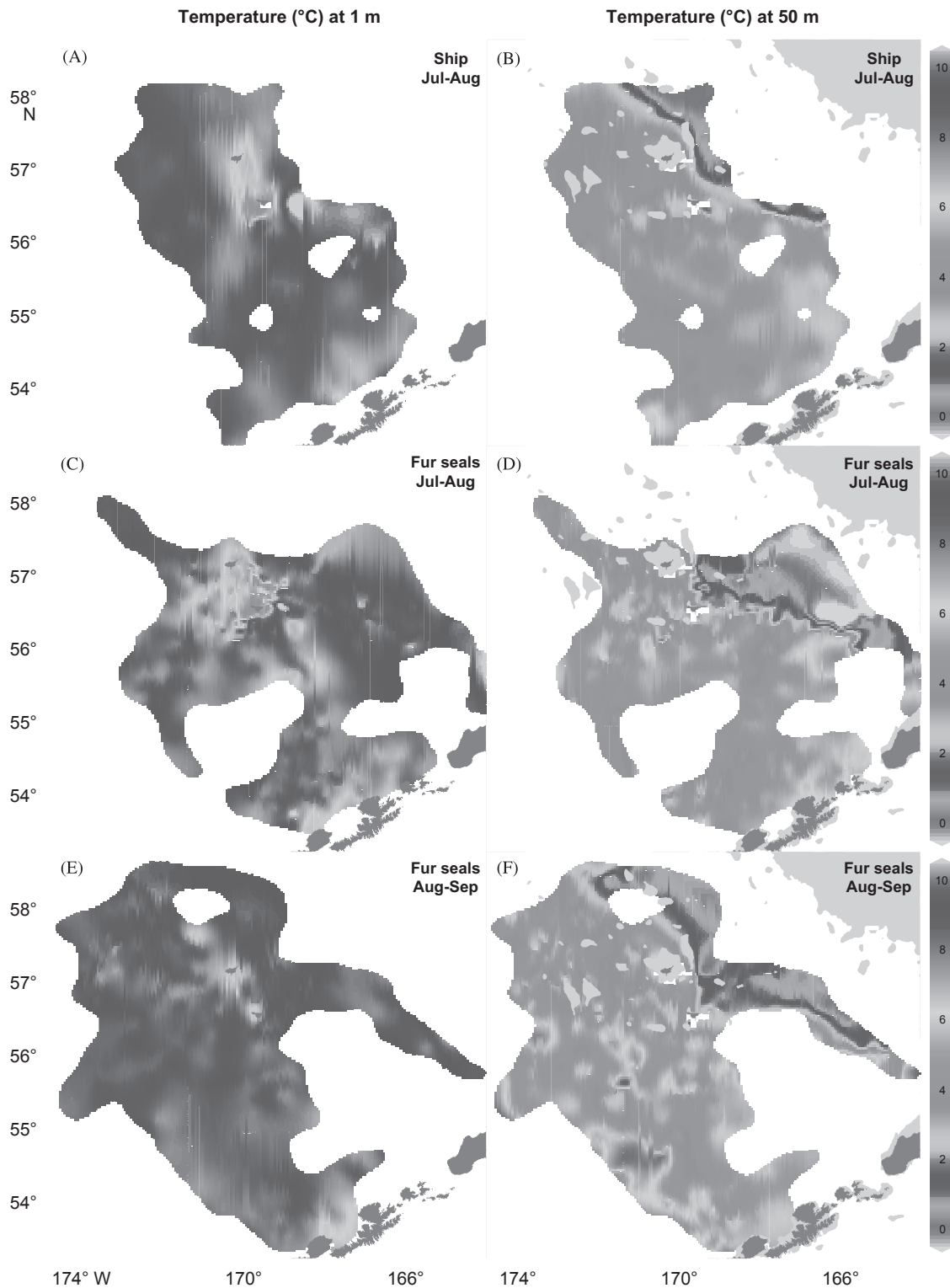


Fig. 4. Comparing interpolated temperature surfaces ($^{\circ}\text{C}$) of the eastern Bering Sea at 1 m and 50 m generated by ship CTD (panels A, B) or instrumented northern fur seal data (panels C, D) during July 15–August 15, 2009. Fur seals continued to collect data from August 16–September 17, 2009 (panels E, F).

middle shelf east of St. Paul Island to 167.25°W (mean = $1.56 \pm 1.84^{\circ}\text{C}$, max = 6.20°C) with the strongest changes typically occurring at the thermocline suggesting a deepening of the mixed layer (Fig. 8D). The region east of 167.25°W was not used in the domain average as the extreme cooling of the thermocline appears to be a sampling artifact, possibly the result of a limited number of seal dives at the outer limits of the delineated sub-region (Fig. 1D).

The sub-region intersecting the Bering Sea shelf and basin on a roughly north to south line also showed signs of warming with the most dramatic increases occurring on the outer shelf to depths of 100 m (mean = $1.7 \pm 1.11^{\circ}\text{C}$, max = 5.25°C ; Fig. 9D).

Seal dives over the basin south-west of St. Paul Island (Fig. 9B and C) occurred within a persistent anticyclonic eddy (Nordstrom et al., 2012; Paredes et al., 2012) and they recorded $\sim 7^{\circ}\text{C}$ water,

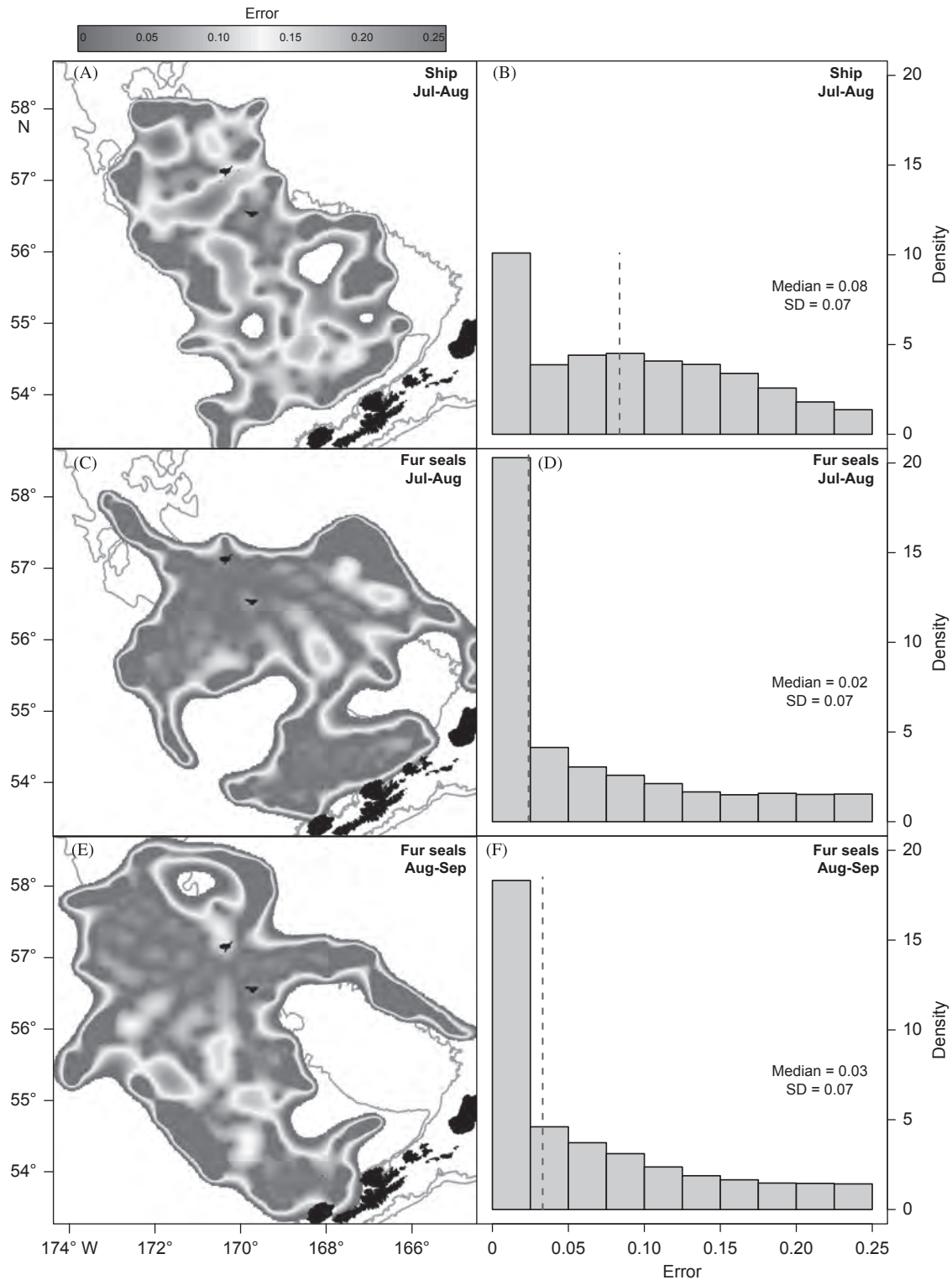


Fig. 5. Comparing temperature error fields in the eastern Bering Sea at 1m generated by ship CTD (panels A,B) or instrumented northern fur seal data (panels C,D) during July 15–August 15, 2009. Fur seals continued to collect data from August 16–September 17, 2009 (panels E,F). Median error levels of each surface are highlighted with a dashed line. Note: errors > 0.25 are masked from the analysis.

more typical of waters at 20 to 30 m depth, being drawn to the surface and segmenting the $\sim 9^\circ\text{C}$ surface waters from 55.5 to 56.25°N. The regularized, banded pattern was similar to the concentric ridges commonly observed in altimeter data (e.g., Fig. 1C) and was notable particularly during the July to mid-August period when the eddy was strongest. The same pattern was not detected using the coarser ship data (Fig. 9A).

3.6. Merged (ship and seal) isosurfaces

Given that temperature fields were similar at the regional scale, we integrated data collected by both platforms to produce isosurfaces that combined the sampling breadth of ships with the sampling resolution of fur seals (Fig. 10). Fine-scale temperature details were retained, and in some cases were enhanced, in the

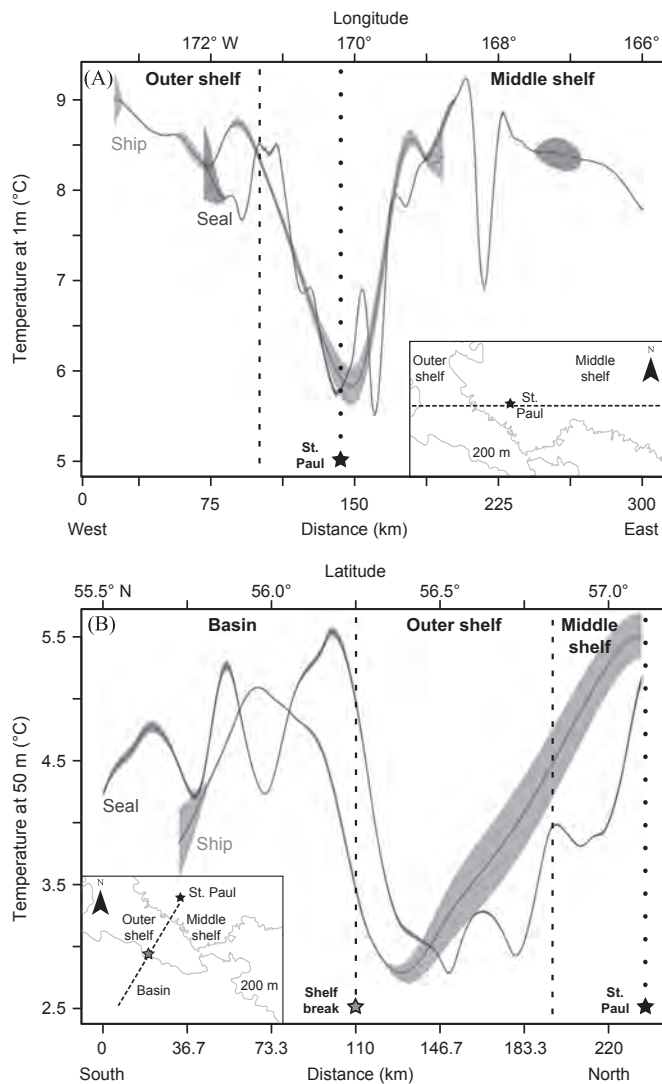


Fig. 6. Temperatures estimates ($^{\circ}\text{C}$, solid lines) and associated errors (ribbons) extracted from July to August isosurfaces (Figs. 4 and 5) at 1 m intervals across the continental shelf of the eastern Bering Sea at 1 m depth (panel A) and from St. Paul I. south across the shelf-break to the basin at 50 m depth (panel B). Blue lines: ship derived surface; red lines: seal derived surface; dashed lines: isobath location; dotted line: St. Paul location. Isosurfaces were sampled along the mid-line of densely sampled sub-regions (insets, Fig. 1D i and ii). Note the relatively smoothed temperatures and wider-errors from ship-derived estimates compared to those from instrumented seals. (For interpretation of the references to color in this figure legend, the reader is referred to the web version of this article.)

resulting maps. For example, a cluster of CTD casts north of St. Paul Island linked previously disparate bands of $\sim 2.5^{\circ}\text{C}$ water collected by fur seals on the east and west sides of the Pribilofs' (Fig. 4D) into a coherent ribbon surrounding the islands at 50 m (Fig. 10B). Those same casts better-defined the position of the cold-pool north of the Pribilof plateau.

Merged temperature maps also documented the cores of both anticyclonic and cyclonic eddies over the basin (Fig. 10). Anticyclonic (clockwise rotation) eddies commonly entrain warmer surface waters to deeper depths while cyclonic (counter-clockwise) eddies tend to transport colder water to the surface and this pattern has been documented in the southern Bering Sea (Mizobata et al., 2002) and the nearby Gulf of Alaska (Ladd et al., 2005). Temperature gradients at 1 m depth were too small in regional maps to adequately define these features from

temperature only (e.g. Fig. 10C); however, that was not the case at 50 m depth. A warm temperature anomaly near the center of the persistent eddy south-west of St. Paul Island was delineated (Fig. 10B i) as was an extension of the same feature that bordered the shelf-break farther east (Fig. 10B ii). Two cold temperature anomalies (assumed to be within cyclonic eddies) were also outlined over the central basin, albeit less sharply (Fig. 10B iii and iv). The temperature anomalies were confirmed as eddy cores by plotting the positions of encircling fronts which were derived from satellite altimeter measures of sea-surface height (Fig. 10D). Interestingly, plotting a simple sea-surface height anomaly for the same date places the temperature anomalies closer to eddy edges but this may be due to the lower spatial resolution of the coarser altimeter data. Nonetheless, it was possible to associate the temperature anomalies with sea-surface rotation for three of four eddies (Fig. 10B and D, i–iii), and in these cases the warm eddy cores were correctly associated with an anticyclonic rotation while the cold-core aligned with a cyclonic circulation. The fine-scale surface fronts did not perfectly enclose eddy cores although this was not to be expected given the fronts were highly dynamic and a single snapshot was overlaid on a month-long temperature composite.

4. Discussion

We used *in-situ* profiles, regional isosurfaces, error maps, difference surfaces, and vertical cross-sections to compare temperature data collected from ship-based CTDs with those collected by free-ranging, instrumented northern fur seals. Data from casts and dives relatively concurrent in time and space were similar as were regional temperature maps depicting well-described temperature structure in the eastern Bering Sea. Maps produced using fur seal data included more detail, less estimated error, and provided an additional 5-week period than those available from ship data generated with the study's sampling design. Maps produced using the integrated dataset preserved the fine-scale detail in the fur seal data while improving coverage due to the improved distribution of the ship stations, particularly north of St. Paul Island and over the basin. We propose that diving predators such as fur seals can provide high quality physical data products to support studies of their own ecology and to answer hydrographic questions provided that the instrumented species lend themselves to the questions of interest.

4.1. Comparing *in-situ* temperatures

Temperature profiles taken *in-situ* in a variety of hydrographic regions were strikingly similar regardless of whether thermistors were carried by ships or seals, particularly since the recordings could be separated by as much as 10 km and 24 h (e.g. Fig. 2). Relationships were similarly tight when ship derived temperatures were regressed against seal derived temperatures (Fig. 3). A nearly 1:1 relationship was found (slope=0.95) with only 13% error which suggested instrument performance was similar after binning temperature values to 1 m. Profiled readings between 4 and 8 $^{\circ}\text{C}$ were the most variable when compared likely because these temperatures were typical of the mid-water column where rapid shifts associated with the thermocline were more common and where temperature-depth pairings would be more affected than those well above or below the thermocline. Slight changes in the location and/or timing of the measurements, inherent to the paired ship casts and seal dives, likely contributed real temperature differences between sampling and would exacerbate instrument differences between readings.

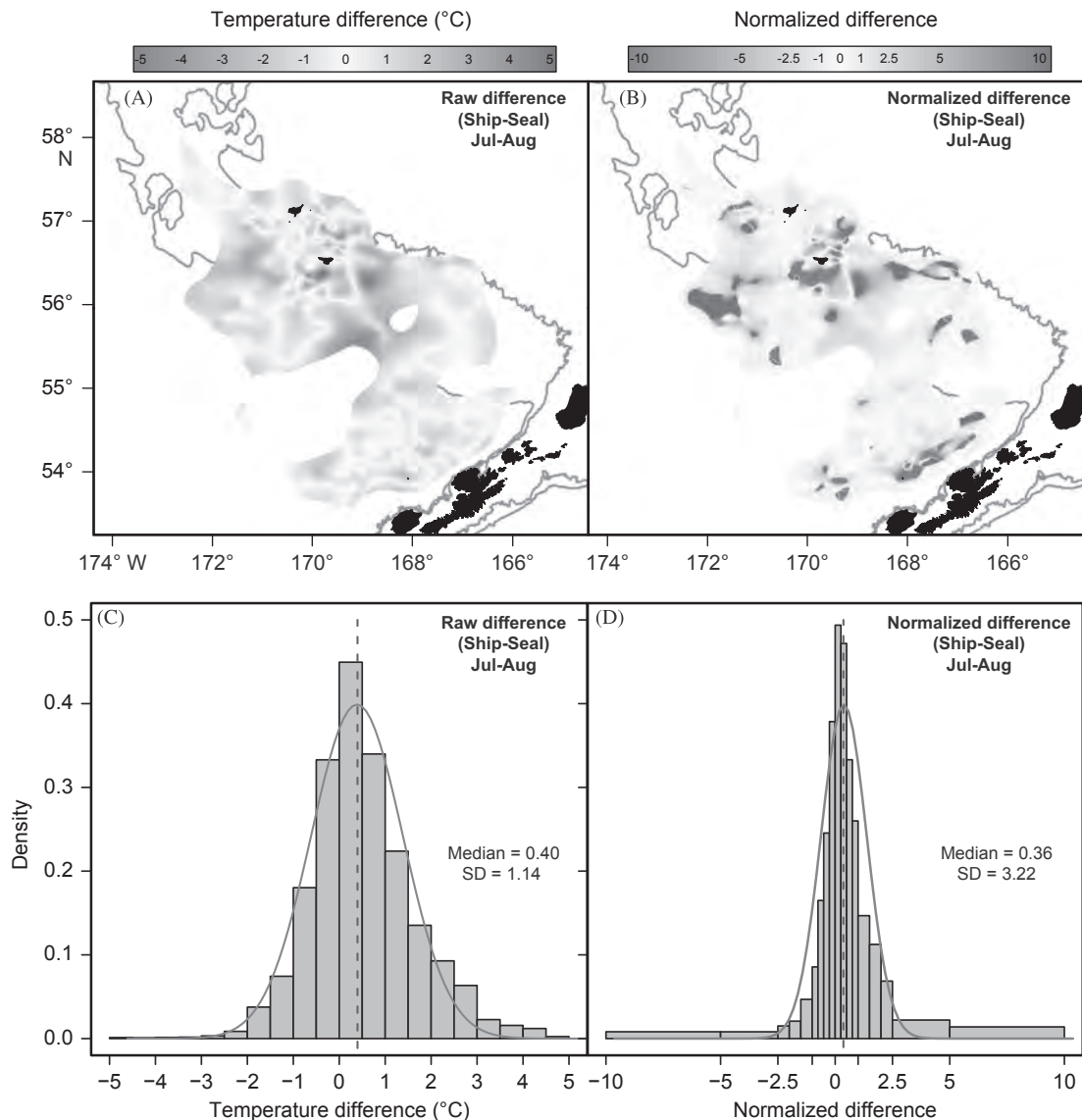


Fig. 7. Interpolated surfaces and histograms describing the differences between temperature fields generated at 1 m by ship CTD and instrumented northern fur seals in the eastern Bering Sea from July 15–August 15, 2009. Temperature ($^{\circ}\text{C}$) differences resulting from subtracting the seal surface (Fig. 4C) from the ship surface (Fig. 4A) are described in panels A and C while normalized differences (where temperature differences are corrected for error estimates) are depicted in panels B and D. Note: normalized differences between -1 and 1 indicate where fields are consistent within the estimated errors (yellows) and differences < -1 and > 1 indicated where the fields are notably different (blues and reds). (For interpretation of the references to color in this figure legend, the reader is referred to the web version of this article.)

4.2. Comparing temperature isosurfaces

Each surface polygon was the product of the correlation length, the specified error limit, and the sampling distribution. Correlation lengths and the error cut-off were kept consistent leaving the data coverage as the factor responsible for the different shapes and resolutions of the temperature surfaces. Regional maps were qualitatively similar where coverage was similar; however, fur seal isosurfaces revealed greater detail, particularly over the shelf region. For example, fur seals sampled the plateau between the Pribilofs intensively as they departed and returned to the rookery revealing chaotic, well-mixed surface waters in the early portion of the study followed by wide-spread warming up to 6°C in some areas as the summer progressed. Fur seals also traced a cool ($\sim 3^{\circ}\text{C}$) band of water along the 100 m isobath at 50 m depth that persisted throughout the study period. The band bifurcated east of St. George Island to surround the Pribilofs and may form part of a persistent front enveloping the islands (Kowalik and Stabeno, 1999; Sullivan et al., 2008) during summer months.

The benefits of high-resolution sampling were most apparent in areas that were highly physically dynamic. Given these areas typically coincided with known bathymetric features on-shelf, they are generally predictable and could be targeted in advance for additional study. Near-real time satellite altimetry and satellite-linked drifters have also been used successfully to direct detailed sampling in more pelagic environments (e.g., Ladd et al., 2005, 2012; Whitney and Robert, 2002). Future hydrographic work supporting upper trophic level studies, similar to the cruises in this study, could benefit from incorporating highly adaptive sampling schemes that would allow for additional casts or for towed CTD sampling in dynamic areas which would be akin to the fur seal sampling we observed in the study. Changes to physical sampling protocols could also be extended to net tows, acoustic sampling, or other biological collections to better describe relationships between prey and their environment at the finer scales at which predators commonly exploit them.

Goodness of fit and error estimates provided a quantitative assessment of the within surface variability for each individual

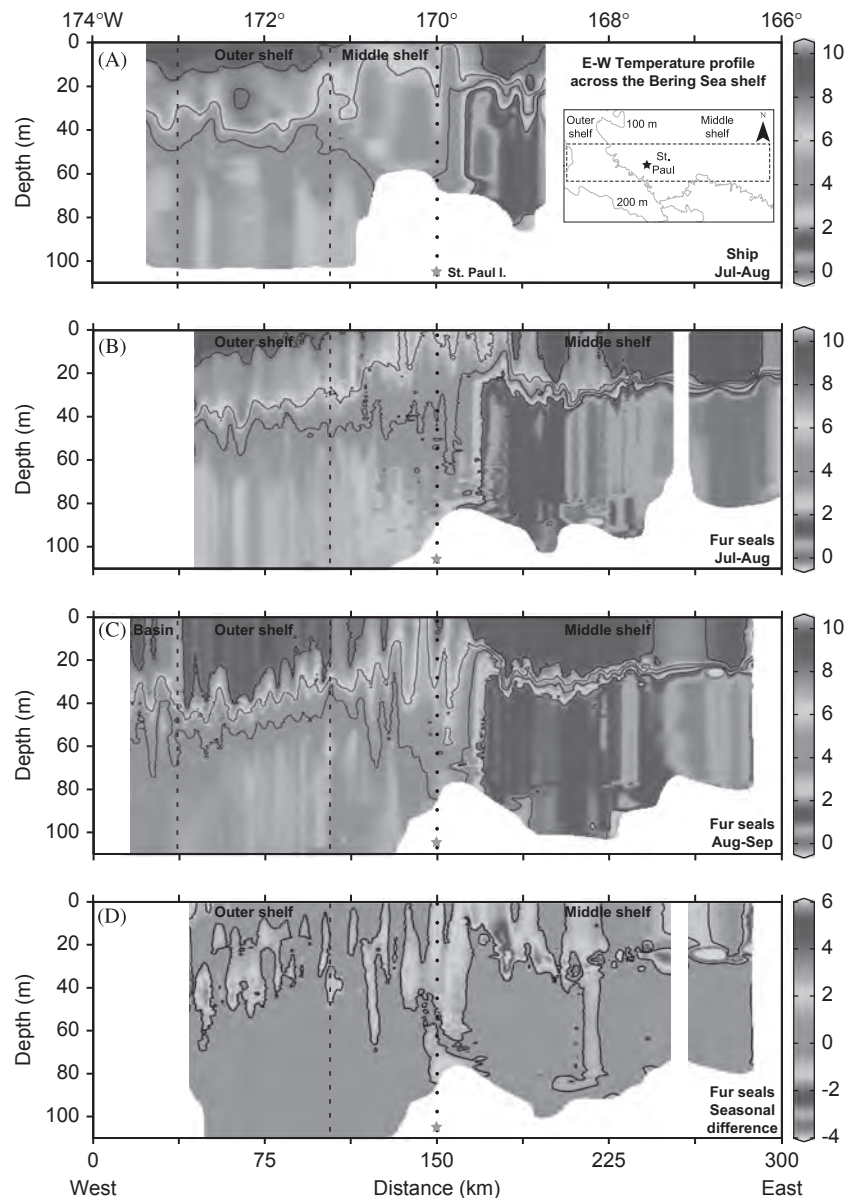


Fig. 8. Comparing interpolated temperature ($^{\circ}\text{C}$) cross-sections along a band across the eastern Bering Sea shelf bisecting St. Paul I. (see inset and Fig. 1D i) generated by ship CTD (panel A) or instrumented northern fur seals (panel B) from July 15 to August 15, 2009. Fur seals also collected data from Aug 16–Sep 17, 2009 (panel C) and the difference section (panel D) shows the patchy increase in temperature through to late summer in the upper 40 m of the water column (changes $> 1^{\circ}\text{C}$ are contoured in panel D). Dashed lines: isobath locations; dotted line: St. Paul location.

isosurface. The DIVA fit cross-correlation values have been shown to be overly optimistic for fields fit with the poor-man's error routine (Troupin et al., 2010) such as those used in this study but we restricted them to relative comparisons only. The error estimates within the interpolated temperature fields depended on two factors: the data coverage (again) and instrument error. The ship-board CTD's were more precise and more accurate instruments than the Mk-10 thermistors despite post-deployment corrections and limited sensor drift on the tags over time (Simmons et al., 2009). There was also more inherent variability within the 24 multi-purpose recorders deployed on seals than the two dedicated instruments deployed by the vessels. Given that error on data was negligible for ship instruments, the larger errors within the ship derived isosurfaces were primarily driven by their relatively limited sampling (Fig. 6).

High-resolution sampling by seals was also responsible for revealing finer temperature fluctuations (with less estimated error), than ship measures along identical transects extracted from temperature maps. The extracted data was predisposed to

contain less error than other areas of the maps as transects were placed along the center line of sub-regions previously identified as highly sampled areas for both platforms. Data extracted from alternative transects could show ships and seals as having similar temperature resolution and/or error rate depending on the placement. However, we observed subtle variations in temperature, an improved alignment of temperature with mapped isobaths, and limited error on the estimates in seal data both across the shelf near St. Paul Island (Fig. 6A) and across multiple domains (Fig. 6B) which were likely typical given the sheer number of seal samples in most areas.

The difference surfaces were difficult to interpret as the underlying sampling was not identical between ships and seals. Notable inconsistencies remained between the datasets despite 61% of the values in the normalized surface falling within -1 and $+1$ (indicating little difference). Outstanding differences could be related to the aforementioned instrument error of the tags, to sampling bias by fur seals, or to differences in the sampling time

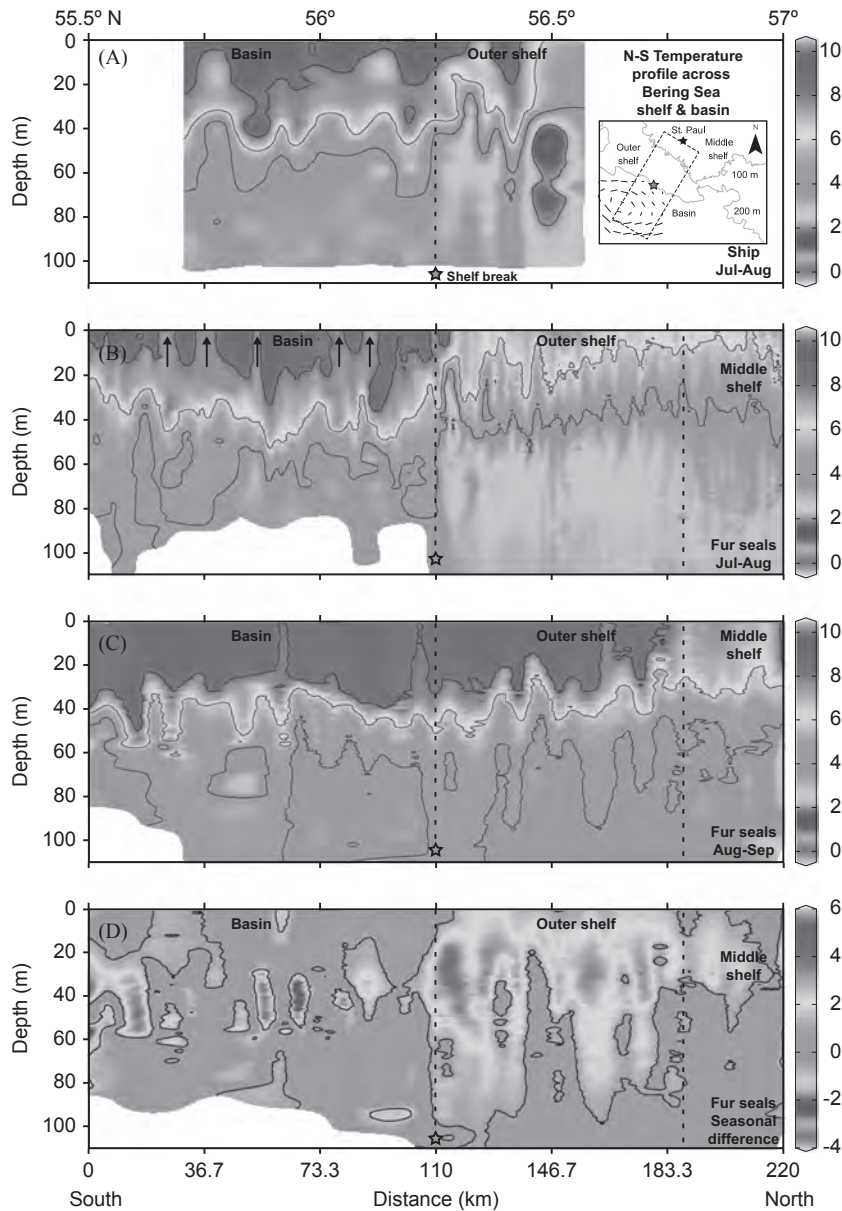


Fig. 9. Comparing interpolated temperature ($^{\circ}\text{C}$) cross-sections along a band from St. Paul I. (on-shelf) southwest to an area over the eastern Bering Sea basin within an eddy (see inset and Fig. 1D ii) generated by ship CTD (panel A) or instrumented northern fur seals (panel B) from July 15 to August 15, 2009. Fur seals also collected data from August 16–Sep 17, 2009 (panel C) and the difference section (panel D) shows the warming in the upper 40–60 m of the water column north of the shelf-break (located at $\sim 56.25^{\circ}$; changes $> 1^{\circ}\text{C}$ are contoured in panel D). Dashed lines: isobath locations; black arrows (panel B): temperature banding possibly due to concentric eddy currents.

of particular locations. Fur seal dives showed remarkable heterogeneity in their locations both between individuals and within seals tracked over multiple trips thereby limiting their sampling bias. Most discrepancies $\pm 3^{\circ}\text{C}$ were however, consistent with dynamic regions such as along isobaths, over canyons, and in areas of high vertical mixing (Fig. 7) which would be sensitive to differences in sampling time.

Both ships and seals detected spatial variability in temperature within dynamic areas at the regional scale but the specific boundaries placed by the spatial interpolations were strongly affected by the nearest casts or dives. Our composite maps (generated over a month) were presented as static snapshots but such temporally aggregated data would clearly mute dynamics occurring on a finer time scale which would be exacerbated in areas of rapid flux. The large inconsistencies remaining in the difference surfaces were not indicative of measures taken at the same time/locations (see Section 2.5.1

In-situ temperature comparisons) but rather we suspect they were the result of differences between predicted surfaces generated from datasets with very different spatial and temporal sampling strategies.

4.3. Comparing vertical sections

Seals recorded 4700 additional temperature profiles ≥ 50 m deep after the completion of the 5-week ship cruise which permitted us to examine sub-regions sampled most often at a finer-scale and over two time periods. The upper water column over much of the middle shelf, the waters surrounding St. Paul Island itself, and over the outer shelf experienced a warming and deepening of the mixed surface layer (e.g. Fig. 8B–D). Despite the lack of salinity measures, dramatic warming and increased structuring of the previously cooler and moderately mixed outer shelf waters was also documented south-west of St. Paul Island

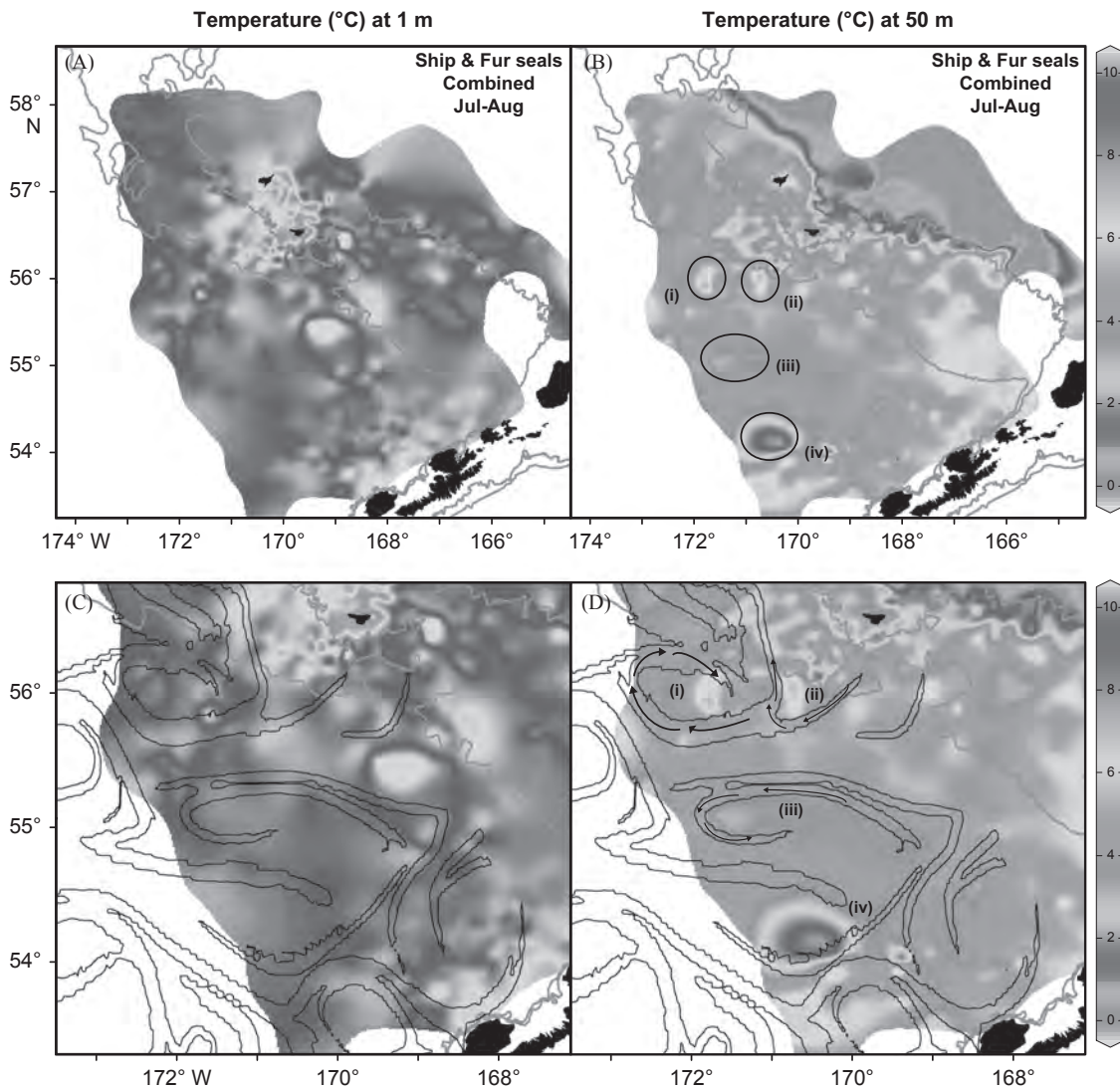


Fig. 10. Integrated temperature surfaces ($^{\circ}\text{C}$) of the eastern Bering Sea at 1 m (panels A and C) and 50 m (panels C and D) generated by combining and interpolating ship CTD data with instrumented northern fur seal data from July 15 to August 15, 2009. Contoured surface fronts (black lines, 0.2 FSLE/d) overlaid in panels C and D are derived from geostrophic current data from July 29, 2009. Anomalous warm and cold cores of confirmed anticyclonic (i, ii) and cyclonic (iii only) eddies are circled in panel B with rotational arrows added in panel D for emphasis.

(e.g. Fig. 9B–D). Fur seal derived observations agree with those from a recent study where the spatial distributions of stratification generally reflect the traditional boundaries of the middle and outer shelf domains (Ladd and Stabeno, 2012). However, the data were unique in that they track the development of stratification over a large area on the outer shelf and within the Pribilof domain as opposed to describing fully established stratification in the early fall.

Seals repeatedly sampled an anticyclonic eddy situated beyond the shelf-break and we suspect the temperature banding observed in the upper 20 m was indicative of concentric eddy currents drawing cooler waters to the surface (Fig. 9B). Spatial or temporal variability in the amalgamated seal dives could produce similar patterns to those observed, although the data in this area are generally synoptic as the sub-region coincides with a travel corridor from the rookery to the eddy and feeding trips averaged just over a week. However, we cannot confirm our suspicion without the density contours typically used to define eddies spawned in the Gulf of Alaska (Janout et al., 2009; Ladd et al., 2009, 2005). Similar temperature banding was not observed

within Bering eddies sampled on transects with stations > 10 km apart (Ladd et al., 2012; Mizobata et al., 2006), suggesting that finer scale CTD sampling, perhaps at 1 km intervals, would be required to detect such features from ships. The cooler intrusions were noted with less frequency and the upper 20 m was more homogenous (Fig. 9C) as the eddy core abutted the shelf break and began to wane in September.

Fur seals tracked temperature changes throughout the study period highlighting sometimes dramatic increases in specific locales. Longitudinal temperature records within a 2-month span (outside of mooring data) are relatively rare for most of the region as fisheries-based surveys rarely repeat transects. Recurring, short-term sampling of the basin, the slope, and even the outer shelf has been absent due to survey designs which are focused on the shallow continental shelf whereas moorings have been difficult to place in depths even approaching 200 m (but see Stabeno et al., 2009). The repeated measurements collected by fur seals across the region were therefore relatively unique and documented the continued warming of much of the eastern Bering, particularly the outer shelf waters to 100 m, over a relatively short span.

4.4. Merged (ship and seal) isosurfaces

The hybrid mapping approach using ships and seals appeared to balance the strengths and weaknesses of each data collection platform. Ship sampling locations could be chosen in advance within pre-defined regions creating a relatively well-distributed but small dataset to describe a large and varied oceanographic area. Fur seal sampling locations were entirely opportunistic (from a data collection perspective) but frequent dives from a large number of wide-ranging individuals created a large but occasionally clumped dataset describing the eastern Bering Sea. Merging data collected from ships and seals thereby produced temperature maps of the upper surface waters with an unparalleled combination of coverage and resolution, particularly beyond the 200 m isobath. Many studies have examined the water properties of the Bering Sea but have been typically confined to a limited area, feature, or transect. In contrast, the merged maps provided a contiguous view of some ephemeral summer processes as varied as the presence of the Pribilof front, the extent of the cold-pool, and the onset of stratification over the shelf while also delineating eddy cores over the basin.

Merging the ship and seal collected datasets provided the most complete temperature description of the region and highlights how traditional oceanographic measurements and animal-borne sampling can complement one another. For example, anomalous warm waters linked with anticyclonic eddies were evident at 50 m in the merged temperature record that were either poorly defined (seals only) or absent entirely (ships only) in the July–August isosurfaces derived from a single platform. Anomalous cold waters associated with cyclonic eddies were less defined as the surrounding waters were similarly cool and they were sampled less frequently resulting in a more diffuse definition of the core proper. In all cases, the addition of CTD profiles, taken in a more regular pattern over the basin, provided the missing data required to definitively isolate eddies from the background field. Supplemental ship-casts were not available, but were also less necessary to identify features over the basin during the August–September time period when fur seals increased their sampling in the area (e.g. Fig. 4F).

The observations we made from the merged regional maps were not novel and specific features may not have been recognized if not for the variety of oceanographic work previously conducted on smaller scales in various domains across the region. Well-mixed surface waters around the Pribilofs, the inner Pribilof front, the expansive cold-pool, and temperature domains delineated along major isobaths were all observed over the continental shelf while a high-degree of eddy activity was concurrently observed over the basin. The physical processes observed here all require continued dedicated study using a variety of *in-situ* and remote-sensing tools; however, the combination of ship and seal temperature data provided a unique snapshot of the processes at work across the whole of the southeastern Bering Sea and this hybrid approach may be applicable to a variety of oceanographic scenarios.

4.5. Considerations

Cost could be a determining factor when considering any combination of traditional and bio-logging data collection. While each situation will be unique, the operational costs of ship-sampling and fur seal sampling were very similar for this study. A range of financial assumptions were used in our estimates but cost differences were within 10% under any given scenario. Ship sampling involved fixed start-up costs but also high-constant operating costs (ship time fees) so the longer the sampling period, the greater the expense. In contrast, seal sampling also had fixed

startup costs (bio-logging instruments) but negligible operating costs. The comparisons only cover the overlapping 5-week sampling period from July–August 2009, after which ship costs would begin to outpace the expense required to maintain field crews. The disparity would continue to grow for multi-year sampling programs, even with the relatively high logistical costs of sub-polar field camps, as many times instruments can be recovered whereas ships must be re-chartered.

4.6. Limitations

The fast-response thermistor was the only oceanographic quality sensor onboard the fur seal borne packages which restricted the comparison with ships to temperature only. Ships carried a wide variety of instrumentation, thereby allowing them to sample additional physical and biological characteristics of the water column which can in turn help draw connections with other levels of the ecosystem, including top predators. Other tags exist that can alternatively include conductivity sensors or fluorometers (e.g. Sea Mammal Research Unit's CTD-SRDL) although their increased size restricts them to deployments on marine animals larger than small otariids such as female northern fur seals. Animal-borne sensors must also be minimized and hardened to withstand the rigors of the deployment which typically results in reduced sampling rates, response time, and resolutions.

Our study had a relatively large sample size (87 females) and the tagging effort focused on deployments that would maximize the spatial coverage at-sea yet there were areas that remained under sampled by fur seals. Obvious gaps included north of St. Paul Island and over the central basin, particularly in the July–August period. Deploying instruments on the northern rookeries would certainly improve sampling north of St. Paul Island as females there show high site fidelity to the shelf areas north of the island. In contrast, little could be done to improve central basin coverage as animals from Reef rookery (the study deployment site) typically forage over the central basin more than any other group of female fur seals. Female northern fur seals are known to be relatively shallow, nocturnal divers which limited their sampling primarily to the upper water column at night. Near surface (1 m) temperature recorded by the fur seals could therefore be slightly biased towards cooler values due to sampling after dark; however, a third of ship sampling was also conducted after sunset so discrepancies between isosurfaces were unlikely to have been driven by photoperiod. Sampling the upper 100 m was expected, but the number of fur seal dives deeper than 50 m decreased rapidly (n dives ≥ 75 m=5620; ≥ 100 m=2456) and became increasingly constricted to the outer shelf south of St. Paul Island. The comparisons we could make with ships and the extent to which we could describe the vertical structure of the Bering Sea was therefore limited. This was particularly evident for fur seals instrumented on Bogoslof Island as the majority of their dives were generally < 30 m. The physical limitations of the tags and the biological characteristics of the target species must be weighed alongside a project's goals and budget to determine whether bio-logging would be appropriate for any given application. In our case, a large number of northern fur seals were able to record a single environmental variable (temperature) extensively across a vast area and over an extended time period.

4.7. Conclusions and future research

Northern fur seals instrumented in the study collected high-quality temperature profiles at unprecedented spatial resolution in the upper water column of the eastern Bering Sea. They collected 26-times as many profiles as the ships over the same 5-week period and produced interpolated maps with finer detail

and less estimated error than similar surfaces produced by standard CTD casts. Inconsistencies between regional maps typically occurred in isolated clumps along isobaths or in high-mixing areas where subtle differences in the plotting of abrupt temperature shifts led to large differences in raw and normalized difference surfaces. Fur seals repeatedly sampled a range of hydrographic regions throughout their nursing period which tracked the continued warming of the upper water column in areas, such as the outer shelf, where longitudinal sampling within a season has been logistically challenging. Areas sampled intensively by fur seals were, by definition, biologically relevant areas to top predators and typically occurred where water masses mixed which were difficult to sample via ship. For example, some individuals repeatedly sampled temperatures within an anticyclonic eddy south-west of St. Paul Island and appeared to reveal subtle temperature intrusions associated with the eddy's concentric currents when the eddy was at peak strength. Integrated temperature maps simultaneously depicted phenomenon previously described in separate studies on-shelf or over the basin and therefore provided unbroken coverage over most of the region with high-resolution data clustered in dynamic areas.

Annual groundfish surveys collect hydrographic data according to a fixed grid across the majority of the eastern shelf and could be better informed about the finer-scale ocean characteristics between broadly spaced stations by incorporating data from free-ranging fur seals. Instrumenting animals from the north-east rookeries of St. Paul Island would provide the most value in that regard given their general fidelity to the shelf region. We recommend deploying multifunction instruments with environmental sensors in lieu of standalone time-depth recorders during future telemetry studies of northern fur seals whenever possible to increase the value of the data returned. In particular, sub-adult males have received little attention and their larger size would allow for deploying a complete CTD sensor suite (e.g., SMRU CTD-SRDL). Such a study would provide ecological insights into another sex class in addition to producing more informative hydrographic data.

Our animal-borne dataset benefitted by deploying a large number of instruments from two widely separated sources (i.e. rookeries) on a species with wide ranging foraging trips in order to match the vessels' sampling distribution and to compensate for the limited individual sampling at depths > 50 m. Northern fur seals also exhibited a high-dive frequency and were relatively non-selective in their foraging distribution at-sea (from a population sampling perspective). This produced a dataset with limited bias in terms of coverage which may not be true for other pinnipeds which show fidelity to highly specific areas (although these species would be well-suited to track changing oceanographic conditions in particular locales over time). Clearly, care must be taken to match the characteristics of potential instrument carriers with the data requirements in any bio-logging study. Our data show that hydrographic information collected by wide-ranging, diving animals such as fur seals can provide physical data products comparable to, and exceeding those provided by traditional sampling methods at regional or finer scales when the questions of interest coincide with the ecology of the species.

Acknowledgments

All animal procedures were conducted under the National Oceanographic and Atmospheric Administration (NOAA) permit no. 14,329 and abided by the guidelines of the Committee on Animal Care at the University of British Columbia (permit no. A09–0345). We thank S. Heppell, the captains, and the crews of

the *M/Vs Frosti* and *Goldrush* for their assistance in collecting the ship-board CTD data. We are also indebted to A. Baylis, J. Gibbens, R. Marshall, R. Papish, A. Will, and C. Berger for assistance with animal captures and instrument deployment. Thanks to A. Thomas for suggesting the Ocean Data View software used heavily in this work, to R. Pawlowicz for advice on comparing temperature fields, and to J.-M. Beckers for advice on accessing DIVA error estimates in ODV. C. Cotté calculated the FSLE for our study. Altimeter products were produced by Ssalto/Duacs and distributed by Aviso, with support from CNES. Two anonymous referees provided constructive criticism on an earlier version of the manuscript. This study was conducted as a part of the BEST-BSIERP “Bering Sea Project” funded jointly by the US National Science Foundation and the North Pacific Research Board. This is NPRB Publication Number 411 and BEST-BSIERP Bering Sea Project publication number 91.

Appendix A. Supplementary materials

Supplementary data associated with this article can be found in the online version at <http://dx.doi.org/10.1016/j.dsr2.2013.03.022>.

References

- Barth, A., Alvera-Azcárate, A., Troupin, C., Ouberdous, M., Beckers, J.-M., 2010. A web interface for gridding arbitrarily distributed *in situ* data based on Data-Interpolating Variational Analysis (DIVA). *Adv. Geosci.* 28, 29–37.
- Benoit-Bird, K.J., Kuletz, K., Heppell, S., Jones, N., Hoover, B., 2011. Active acoustic examination of the diving behavior of murre foraging on patchy prey. *Mar. Ecol. Prog. Ser.* 443, 217–235.
- Biuw, M., Boehme, L., Guinet, C., Hindell, M., Costa, D., Charrassin, J.B., Roquet, F., Bailleul, F., Meredith, M., Thorpe, S., Tremblay, Y., McDonald, B., Park, Y.H., Rintoul, S.R., Bindoff, N., Goebel, M., Crocker, D., Lovell, P., Nicholson, J., Monks, F., Fedak, M.A., 2007. Variations in behavior and condition of a Southern Ocean top predator in relation to *in situ* oceanographic conditions. *Proc. Natl. Acad. Sci., USA* 104, 13705–13710.
- Boehme, L., Meredith, M.P., Thorpe, S.E., Biuw, M., Fedak, M., 2008. Antarctic Circumpolar Current frontal system in the South Atlantic: monitoring using merged Argo and animal-borne sensor data. *J. Geophys. Res.* 113, C09012.
- Boffetta, G., Lacorata, G., Redaelli, G., Vulpiani, A., 2001. Detecting barriers to transport: a review of different techniques. *Phys. D: Nonlinear Phenom.* 159, 58–70.
- Boyd, I.L., Hawker, E.J., Brandon, M.A., Staniland, I.J., 2001. Measurement of ocean temperatures using instruments carried by Antarctic fur seals. *J. Mar. Syst.* 27, 277–288.
- Brasseur, P., Beckers, J.-M., Brankart, J.M., Schoenauen, R., 1996. Seasonal temperature and salinity fields in the Mediterranean Sea: climatological analyses of a historical data set. *Deep-Sea Res.* I 43, 159–192.
- Call, K.A., Ream, R.R., Johnson, D.S., Sterling, J.T., Towell, R.G., 2008. Foraging route tactics and site fidelity of adult female northern fur seal (*Callorhinus ursinus*) around the Pribilof Islands. *Deep-Sea Res.* II 55, 1883–1896.
- Campagna, C., Werner, R., Karesh, W., Marin, M.R., Koontz, F., Cook, R., Koontz, C., 2001. Movements and location at sea of South American sea lions (*Otaria flavescens*). *J. Zool.* 255, 205–220.
- Charrassin, J., Park, Y., Maho, Y., Bost, C., 2002. Penguins as oceanographers unravel hidden mechanisms of marine productivity. *Ecol. Lett.* 5, 317–319.
- Charrassin, J.B., Hindell, M., Rintoul, S.R., Roquet, F., Sokolov, S., Biuw, M., Costa, D., Boehme, L., Lovell, P., Coleman, R., Timmermann, R., Meijers, A., Meredith, M., Park, Y.H., Bailleul, F., Goebel, M., Tremblay, Y., Bost, C.A., McMahon, C.R., Field, I.C., Fedak, M.A., Guinet, C., 2008. Southern Ocean frontal structure and sea-ice formation rates revealed by elephant seals. *Proc. Natl. Acad. Sci., USA* 105, 11634–11639.
- Chilvers, B.L., Wilkinson, I.S., Duignan, P.J., 2005. Summer foraging areas for lactating New Zealand sea lions *Phocarcos hookeri*. *Mar. Ecol. Prog. Ser.* 304, 235–247.
- Coachman, L.K., 1986. Circulation, water masses, and fluxes on the southeastern Bering Sea shelf. *Cont. Shelf Res.* 5, 23–108.
- Costa, D.P., Klinck, J.M., Hofmann, E.E., Dinniman, M.S., Burns, J.M., 2008. Upper ocean variability in west Antarctic Peninsula continental shelf waters as measured using instrumented seals. *Deep-Sea Res.* II 55, 323–337.
- d'Ovidio, F., Fernández, V., Hernández-García, E., López, C., 2004. Mixing structures in the Mediterranean Sea from finite-size Lyapunov exponents. *Geophys. Res. Lett.* 31, L17203.
- Gentry, R.L., 1998. Behavior and Ecology of the Northern Fur Seal. Princeton University Press, Princeton, New Jersey, U.S.A..

- Goebel, M.E., Bengtson, J.L., DeLong, R.L., Gentry, R.L., Loughlin, T.R., 1991. Diving patterns and foraging locations of female northern fur seals. *Fish. Bull.* 89, 171–179.
- Grist, J.P., Josey, S.A., Boehme, L., Meredith, M.P., Davidson, F.J.M., Stenson, G.B., Hammill, M.O., 2011. Temperature signature of high latitude Atlantic boundary currents revealed by marine mammal-borne sensor and Argo data. *Geophys. Res. Lett.* 38, L15601.
- Hunt Jr., G.L., Stabeno, P.J., 2002. Climate change and the control of energy flow in the southeastern Bering Sea. *Prog. Oceanogr.* 55, 5–22.
- Janout, M.A., Weingartner, T.J., Okkonen, S.R., Whitledge, T.E., Musgrave, D.L., 2009. Some characteristics of Yakutat Eddies propagating along the continental slope of the northern Gulf of Alaska. *Deep-Sea Res. II* 56, 2444–2459.
- Kowalik, Z., Stabeno, P.J., 1999. Trapped motion around the Pribilof Islands in the Bering Sea. *J. Geophys. Res.* 104, 25667–625,684.
- Ladd, C., Crawford, W.R., Harpoil, C.E., Johnson, W.K., Kachel, N.B., Stabeno, P.J., Whitney, F., 2009. A synoptic survey of young mesoscale eddies in the Eastern Gulf of Alaska. *Deep-Sea Res. II* 56, 2460–2473.
- Ladd, C., Kachel, N.B., Mordy, C.W., Stabeno, P.J., 2005. Observations from a Yakutat eddy in the northern Gulf of Alaska. *J. Geophys. Res.* 110, C03003.
- Ladd, C., Stabeno, P.J., 2012. Stratification on the Eastern Bering Shelf revisited. *Deep-Sea Res. II*, in press.
- Ladd, C., Stabeno, P.J., O'Hern, J.E., 2012. Observations of a Pribilof eddy. *Deep-Sea Res. I* 66, 67–76.
- Lea, M.A., Guinet, C., Cherel, Y., Hindell, M., Dubroca, L., Thalmann, S., 2008. Colony-based foraging segregation by Antarctic fur seals at the Kerguelen Archipelago. *Mar. Ecol.-Prog. Ser.* 358, 273–287.
- Lydersen, C., Anders Nost, O., Kovacs, K.M., Fedak, M.A., 2004. Temperature data from Norwegian and Russian waters of the northern Barents Sea collected by free-living ringed seals. *J. Mar. Syst.* 46, 99–108.
- Mizobata, K., Saitoh, S.I., Shiimoto, A., Miyamura, T., Shiga, N., Imai, K., Toratani, M., Kajiwara, Y., Sasaoka, K., 2002. Bering Sea cyclonic and anticyclonic eddies observed during summer 2000 and 2001. *Prog. Oceanogr.* 55, 65–75.
- Mizobata, K., Wang, J., Saitoh, S.I., 2006. Eddy-induced cross-slope exchange maintaining summer high productivity of the Bering Sea shelf break. *J. Geophys. Res.*, 111.
- Nordstrom, C.A., Battaile, B.C., Cotté, C., Trites, A.W., 2012. Foraging habitats of lactating northern fur seals are structured by thermocline depths and submesoscale fronts in the eastern Bering Sea. *Deep-Sea Res. II*.
- Okkonen, S.R., Schmidt, G.M., Cokelet, E.D., Stabeno, P.J., 2004. Satellite and hydrographic observations of the Bering Sea 'Green Belt'. *Deep-Sea Res. II* 51, 1033–1051.
- Paredes, R., Harding, A.M.A., Irons, D.B., Roby, D.D., Suryan, R., Orben, R.A., Renner, H., Young, R., Kitaysky, A., 2012. Proximity to multiple foraging habitats enhances seabirds' resilience to local food shortages. *Mar. Ecol. Prog. Ser.* 471, 253–269.
- R Development Core Team, 2009. R: A language and environment for statistical computing., 2.10.1 ed. R Foundation for Statistical Computing, Vienna, Austria.
- Resplandy, L., Lévy, M., d'Ovidio, F., Merlivat, L., 2009. Impact of submesoscale variability in estimating the air-sea CO₂ exchange: results from a model study of the POMME experiment. *Global Biogeochem. Cycles* 23, 017, GB1.
- Rixen, M., Beckers, J.-M., Brankart, J.M., Brasseur, P., 2000. A numerically efficient data analysis method with error map generation. *Ocean Modell.* 2, 45–60.
- Robson, B.W., Goebel, M.E., Baker, J.D., Ream, R.R., Loughlin, T.R., Francis, R.C., Antonelis, G.A., Costa, D.P., 2004. Separation of foraging habitat among breeding sites of a colonial marine predator, the northern fur seal (*Callorhinus ursinus*). *Can. J. Zool.* 82, 20–29.
- Roquet, F., Charrassin, J.-B., Marchand, S., Boehme, L., Fedak, M., Reverdin, G., Guinet, C., 2011. Delayed-mode calibration of hydrographic data obtained from animal-borne satellite-relay data loggers. *J. Atmos. Oceanic Technol.* 28, 787–801.
- Roquet, F., Park, Y.-H., Guinet, C., Bailleul, F., Charrassin, J.-B., 2009. Observations of the Fawn Trough Current over the Kerguelen Plateau from instrumented elephant seals. *J. Mar. Syst.* 78, 377–393.
- Schlitzer, R., 2011a. Ocean Data View 4.4.1 <<http://odv.awi.de>>, 27568 Bremerhaven, Germany.
- Schlitzer, R., 2011b. Ocean Data View 4.4.1 User's manual, 27568 Bremerhaven, Germany.
- Schumacher, J.D., Stabeno, P.J., 1994. Ubiquitous eddies in the eastern Bering Sea and their coincidence with concentrations of larval pollock. *Fish. Oceanogr.* 3, 182–190.
- Simmons, S., Tremblay, Y., Costa, D., 2009. Pinnipeds as ocean-temperature samplers: calibrations, validations, and data quality. *Limnol. Oceanogr.: Meth.* 7, 648–656.
- Simmons, S.E., Crocker, D.E., Hassrick, J.L., Kuhn, C.E., Robinson, P.W., Tremblay, Y., Costa, D.P., 2010. Climate-scale hydrographic features related to foraging success in a capital breeder, the northern elephant seal *Mirovunga angustirostris*. *Endangered Species Res.* 10, 233–243.
- Sinclair, E.H., Vlietstra, L.S., Johnson, D.S., Zeppelin, T.K., Byrd, G.V., Springer, A.M., Ream, R.R., Hunt Jr., G.L., 2008. Patterns in prey use among fur seals and seabirds in the Pribilof Islands. *Deep-Sea Res. II* 55, 1897–1918.
- Stabeno, P.J., Bond, N.A., Kachel, N.B., Salo, S.A., Schumacher, J.D., 2001. On the temporal variability of the physical environment over the south-eastern Bering Sea. *Fish. Oceanogr.* 10, 91–98.
- Stabeno, P.J., Kachel, N., Mordy, C., Righi, D., Salo, S., 2008. An examination of the physical variability around the Pribilof Islands in 2004. *Deep-Sea Res. II* 55, 1701–1716.
- Stabeno, P.J., Ladd, C., Reed, R.K., 2009. Observations of the Aleutian North Slope Current, Bering Sea, 1996–2001. *J. Geophys. Res.* 114, C05015.
- Stabeno, P.J., van Meurs, P., 1999. Evidence of episodic on-shelf flow in the southeastern Bering Sea. *J. Geophys. Res.* 104, 29715–29720.
- Sterling, J.T., 2009. Northern fur seal foraging behaviors, food webs, and interactions with oceanographic features in the eastern Bering sea, School of Aquatic and Fishery Sciences. PhD Thesis, University of Washington, Seattle, p. 233.
- Sullivan, M.E., Kachel, N.B., Mordy, C.W., Stabeno, P.J., 2008. The Pribilof Islands: Temperature, salinity and nitrate during summer 2004. *Deep-Sea Res. II* 55, 1729–1737.
- Trathan, P.N., Green, C., Tanton, J., Peat, H., Poncet, J., Morton, A., 2006. Foraging dynamics of macaroni penguins *Eudyptes chrysolophus* at South Georgia during brood-guard. *Mar. Ecol. Prog. Ser.* 323, 239–251.
- Tremblay, Y., Shaffer, S.A., Fowler, S.L., Kuhn, C.E., McDonald, B.I., Weise, M.J., Bost, C.-A., Weimerskirch, H., Crocker, D.E., Goebel, M.E., Costa, D.P., 2006. Interpolation of animal tracking data in a fluid environment. *J. Exp. Biol.* 209, 128.
- Troupin, C., Machín, F., Ouberdous, M., Sirjacobs, D., Barth, A., Beckers, J.-M., 2010. High-resolution climatology of the northeast Atlantic using data-interpolating variational analysis (DIVA). *J. Geophys. Res.* 115, C08005.
- Troupin, C., Barth, A., Sirjacobs, D., Ouberdous, M., Brankart, J.-M., Brasseur, P., Rixen, M., Alvera-Azcárate, A., Belounis, M., Capet, A., Lenartz, F., Toussaint, M.-E., Bekers, J.-M., 2012. *Ocean Modell.* 52–53, 90–101.
- Weise, M.J., Harvey, J.T., Costa, D.P., 2010. The role of body size in individual-based foraging strategies of a top marine predator. *Ecology* 91, 1004–1015.
- Whitney, F., Robert, M., 2002. Structure of Haida eddies and their transport of nutrient from coastal margins into the NE Pacific Ocean. *J. Oceanogr.* 58, 715–723.



Continuity and change in subsistence harvests in five Bering Sea communities: Akutan, Emmonak, Savoonga, St. Paul, and Togiak



James A. Fall ^{a,*}, Nicole S. Braem ^b, Caroline L. Brown ^b, Lisa B. Hutchinson-Scarborough ^a, David S. Koster ^a, Theodore M. Krieg ^c

^a Division of Subsistence, Alaska Department of Fish and Game, 333 Raspberry Road, Anchorage, AK 99518, USA

^b Division of Subsistence, Alaska Department of Fish and Game, 1300 College Road, Fairbanks, AK 99701, USA

^c Division of Subsistence, Alaska Department of Fish and Game, PO Box 1030, Dillingham, AK 99576, USA

ARTICLE INFO

Available online 14 March 2013

Keywords:

Bering Sea
Akutan
Emmonak
Savoonga
St. Paul
Togiak
Subsistence
Hunting
Fishing

ABSTRACT

To document and quantify subsistence harvests of fish and wildlife resources, and provide topics for subsequent key respondent interviews to collect local and traditional knowledge (LTK) about the Bering Sea ecosystem, comprehensive household harvest surveys were conducted in four Bering Sea Alaska Native communities: Akutan, Emmonak, Savoonga, and Togiak. In a fifth community, St. Paul, annual programs to document two key subsistence resources, fur seals and sea lions, continued. Surveys documented relatively high and diverse subsistence harvests, consistent with earlier research that demonstrated the continuing economic, social, and cultural importance of subsistence uses of wild resources. The research also found differences in subsistence use patterns compared to previous years' studies, such as harvest levels, harvest composition, and diversity of resources used, although differences between study years were not uniform across communities. Survey respondents, as well as key respondents in subsequent interviews, identified a complex range of personal, economic, and environmental factors when comparing subsistence uses in the study year with other years, such as increasing costs of fuel and purchased food, commercial fisheries harvests and bycatch, more persistent storms and less predictable winds, and reduced sea ice. Such conditions affect resource abundance and locations as well as access to fish and wildlife populations, and may shape long-term trends. So far, as in the past, families and communities have adapted to changing economic, social, and environmental conditions, but the future is less clear if such changes intensify or accelerate. Local community residents should be essential partners in future efforts to understand these complex processes that affect the natural resources of the Bering Sea.

© 2013 Elsevier Ltd. All rights reserved.

1. Introduction

For many centuries, Alaska Native communities have depended upon the natural resources of the Bering Sea (Dumond, 1984). Their survival is linked directly to the availability of fish and wildlife, effective harvest technologies, and detailed environmental knowledge accumulated across generations and applied through direct experience. In the early 21st century, these communities' ways of life were based on a mixed subsistence/cash economy that blended harvest and use of traditional foods with adaptations to a rapidly changing and interconnected world.

In 2007, the North Pacific Research Board (NPRB) launched the "Bering Sea Integrated Ecosystem Research Program" (BSIERP) in

partnership with the National Science Foundation's "Bering Ecosystem Study" (BEST); joined together, these two programs form the integrated "Bering Sea Project". This comprehensive 5-year study sought a multi-disciplinary understanding of the implications of climate change for the highly productive and seasonally ice-covered eastern Bering Sea ecosystem (North Pacific Research Board (2008):3). BSIERP was guided by five hypotheses that addressed ecosystem changes and their consequences, focusing on variation in seasonal sea ice as an ecosystem driver North Pacific Research Board (2012).

BSIERP's research plan included human communities as a part of the Bering Sea ecosystem subject to environmental change, and also recognized these communities' residents as important sources of information about local conditions and processes. Therefore, documenting subsistence harvests and "local and traditional knowledge" (LTK) became a component of BSIERP and the Bering Sea Project. The NPRB Science Plan (North Pacific Research Board (2005):144) defines LTK as "information, understanding, and wisdom accumulated over time based on experience

* Corresponding author. Tel.: +1 907 267 2359; fax: +1 907 267 2450.

E-mail addresses: jim.fall@alaska.gov (J.A. Fall),

Nicole.braem@alaska.gov (N.S. Braem), caroline.brown@alaska.gov (C.L. Brown),

lisa.hutchinson-scarbrough@alaska.gov (L.B. Hutchinson-Scarborough),

david.koster@alaska.gov (D.S. Koster), theodore.krieg@alaska.gov (T.M. Krieg).

and often shared within a group or community.” BSIERP’s LTK component had four specific objectives:

1. Document, characterize, and quantify local harvest practices, such as species harvested, harvest quantities, search areas, and timing of harvests, and changes thereto, in order to better understand the relationship between Bering Sea communities and the Bering Sea ecosystem.
2. Document and characterize local understanding of Bering Sea ecosystem structure and function to allow comparison with biological understanding and sharing of knowledge between both ways of knowing.
3. Integrate the results of (1) and (2) across the communities involved, identifying key similarities and differences as well as regional trends or associations with particular environmental features.
4. Incorporate the results of (1), (2), and (3) into ecosystem models and other syntheses developed through BSIERP.

This paper summarizes findings directly linked to Objective 1, the documentation of subsistence harvest patterns, changes to these patterns, and comments household survey respondents offered about their subsistence uses of natural resources. To provide context to the survey findings, the paper also summarizes some findings from subsequent key respondent interviews, and

provides a sample of excerpts from these interviews. Huntington et al. (2013) addresses Objectives 2, 3, and 4, including more detail about key respondents’ observations about environmental conditions, natural resource populations, and ecosystem processes. Fienup-Riordan, Brown, and Braem (2013) provide a more detailed discussion of LTK observations from the residents of Emmonak, one of the five study communities.

Although the LTK component had the potential to address most BSIERP hypotheses, it was most relevant to those concerning the distribution and abundance of species (Hypotheses 2a, 2d, 3a, 4a, and 4b North Pacific Research Board (2012)). The LTK component directly addressed Hypothesis 5b, which states:

5. Climate-ocean conditions will change and thus affect the abundance and distribution of commercial and subsistence fisheries. Specifically:

b. For subsistence users, these changes will lead to: (1) greater reliance on owners of larger vessels that can travel farther to harvest and distribute subsistence goods, (2) decreased consumption of species with decreased local abundance, and (3) adoption of new species into the diet as these species colonize local areas North Pacific Research Board (2012).

Five communities participated in this LTK component of the BSIERP project (Fig. 1). They were chosen to represent a range of association with sea ice, and because subsistence harvest data from earlier studies were available for each. From south to north, the study

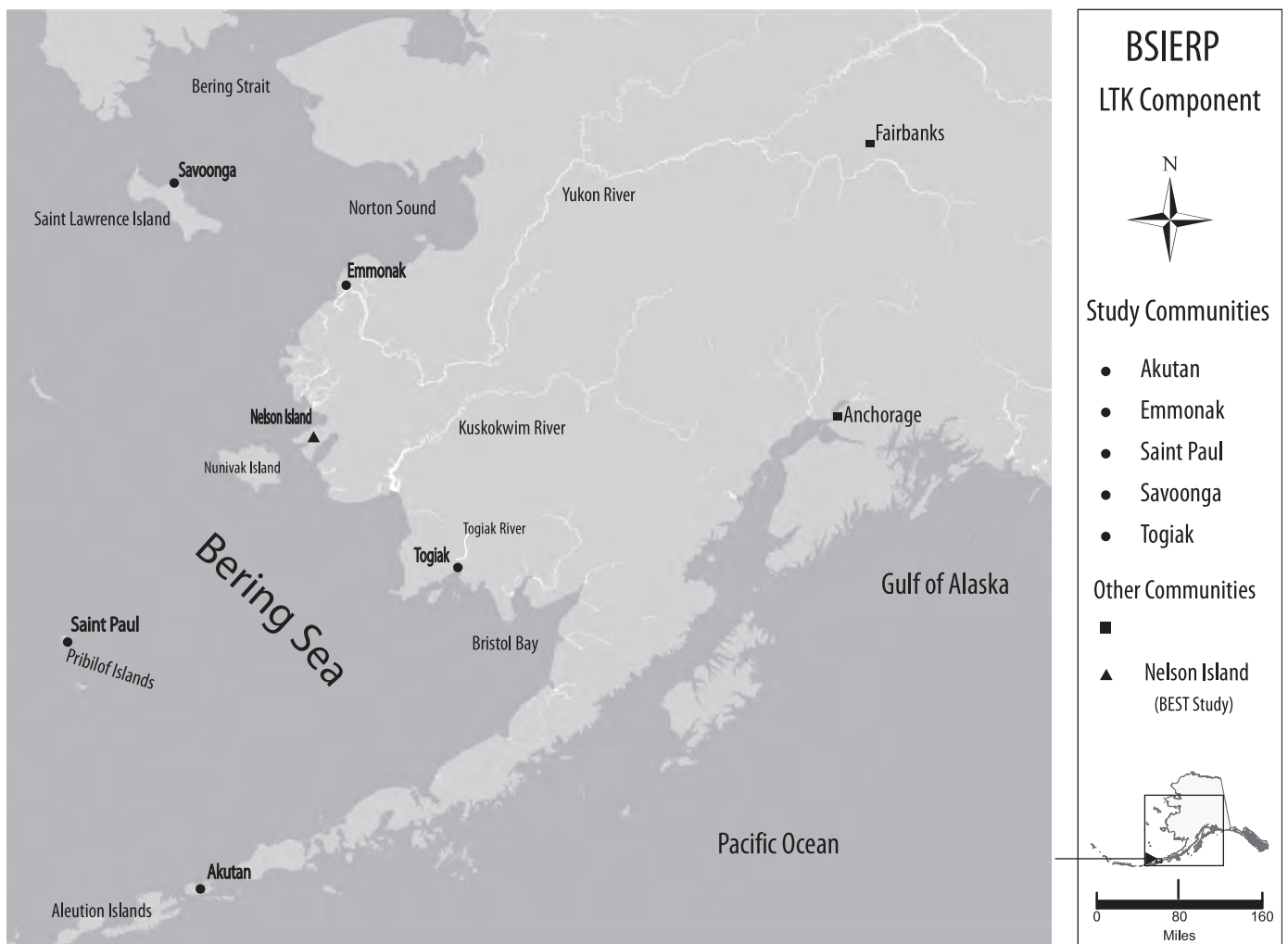


Fig. 1. Study communities.

communities were Akutan, St. Paul, Togiak, Emmonak, and Savoonga. These communities also represent linguistic and cultural diversity, with two Aleut (also known as “Unangan”) communities (Akutan and St. Paul), two Central Yup’ik communities (Togiak and Emmonak), and a Siberian Yupik community (Savoonga). In addition, several Central Yup’ik communities of Nelson Island participated in the BEST component of the Bering Sea Project, and provided LTK about changing ocean conditions, weather, and climate (Fienup-Riordan and Reardon, 2012). Harvest surveys were not conducted in the Nelson Island communities, and study findings for these communities are not addressed in this paper.

2. Methods

Our study plan noted that exact methods for documenting subsistence patterns could vary by community, based in part on community preferences and size. The common goal was to compare results with previous harvest survey work, and to provide quantitative data to contribute to modeling and to serve as a basis for additional LTK research through key respondent interviewing, such as reasons for differences between study years, in a subsequent phase of the project (Huntington et al., 2013).

The Division of Subsistence, Alaska Department of Fish and Game (ADF&G), had lead responsibility for conducting household harvest surveys as the primary tool to document subsistence patterns in Akutan, Emmonak, and Togiak. Kawerak Inc. assisted Savoonga with the harvest survey in that community, using data gathering and data analysis methods similar to those employed by ADF&G (Tahbone and Trigg 2011). St. Paul, through its Ecosystem Conservation Office, continued its harvest monitoring programs for fur seals, sea lions, and reindeer, but chose not to conduct a household harvest survey (Lestenkof et al., 2011).

A key feature of the BSIERP LTK component was the formation of a Regional Advisory Board (RAB), composed of representatives of each partner organization and the study communities. The RAB served as a forum for discussion and decision-making about all aspects of the project, including study designs, scheduling, and review of findings. A Community Advisory Board (CAB) was also formed in each of the five study communities to provide guidance to the project at the community level. Each CAB had the opportunity to review the study findings and draft final reports.

The project was guided by the research principles adopted by the Alaska Federation of Natives (1993) and the Office of Polar Programs of the National Science Foundation (2012). These principles emphasize community approval of research designs, informed consent of participants, anonymity of study participants, community review of draft study findings, and the provision of study findings to each study community upon completion of the research.

2.1. Methods: Akutan, Emmonak, and Togiak

The primary method for collecting information about contemporary subsistence harvests and uses in Akutan, Emmonak, and

Togiak was a systematic household survey. The survey followed procedures established in previous projects by the Division of Subsistence and its research partners in about 200 communities throughout the state (Fall, 1990). Information was collected for a 12-month study year, corresponding to calendar year 2008. Key topics for data collection during the household surveys included the following:

1. Subsistence harvest and use information.
 - a. Whether the household used, attempted to harvest, harvested, received, or gave away each wild resource.
 - b. Harvest quantities in numbers of animals, buckets, gallons, or other appropriate units.
 - c. Households’ assessments of uses and harvests in the study year compared to other recent years, and reasons for differences.
 - d. Harvest locations in the study year.
 - e. Individual involvement in subsistence activities, including the involvement of children.
2. Demographic information, including, for each household member, age, sex, ethnicity, birthplace, and length of residency in the community.
3. Employment and cash income, including jobs held by household members, occupational type, employer type, earned cash income, and other income.

Teams of researchers consisting of Division of Subsistence staff and local research assistants administered the surveys during face-to-face interviews in the study communities. A detailed training manual guided the orientation of local researchers and administration of the survey instrument.

The goal was to interview a representative random sample of households in Togiak and Emmonak; their relatively large populations precluded targeting census samples. Because of its small size, a census sample was attempted in Akutan. Participation was voluntary. Table 1 summarizes sample achievement. In total, 225 households were surveyed, including 36 in Akutan (90% of all resident households), 109 in Emmonak (a 61% random sample), and 80 in Togiak (a 43% random sample). Surveys took place in Togiak in February 2009, in Akutan in late March and early April 2009, and in Emmonak in April 2009.

All data were coded by Division of Subsistence staff following standardized codebook conventions to facilitate data entry. The division’s information management section set up database structures within an MS SQL Server to hold the survey data. The database structures included rules, constraints, and referential integrity to insure that data were entered completely and accurately. All data were entered twice, and compared programmatically for inconsistent data entry. After data were entered and confirmed, information was processed with the Statistical Package for the Social Sciences (SPSS). Initial processing included standardized logic checks of the data. Harvest data collected as

Table 1
Sample achievement, BSIERP comprehensive household harvest surveys.

	Akutan	Emmonak	Togiak	Savoonga
Study year	2008	2008	2008	2009
Number of households in the community	40	179	188	140
Interview goal ^a , number of households	40	91	80	84
Number of households interviewed	36	109	80	82
Percentage of households interviewed	90.0%	60.9%	42.6%	58.6%

^a Random samples selected in Emmonak and Togiak

numbers of animals, or in gallons or buckets, were converted to pounds usable weight using standard factors.

SPSS was also used for analyzing the survey information. Analysis included review of raw data frequencies, cross tabulations, table generation, estimation of population parameters, and calculation of confidence intervals for the harvest estimates.

Harvest estimates and responses to all questions were calculated based upon the application of weighted means (Cochran 1977). These calculations are standard methods for extrapolating sampled data. As an example, the formula for harvest expansion is

$$H_i = \bar{h}_i S_i \quad (1)$$

where

$\bar{h}_i = (h_i/n_i)$ (mean harvest per returned survey),

H_i = the total harvest (numbers of resource or pounds) for the community I,

h_i = the total harvest reported in returned surveys,

n_i = the number of returned surveys, and

S_i = the number of households in a community.

As an interim step, the standard deviation (SD), or variance (V; which is the SD squared), was also calculated with the unexpanded data. The standard error (SE), or SD, of the mean was also calculated for each community. In this paper, the relative precision of the mean is reported as a confidence limit (CL), expressed as a percentage. Once the standard error was calculated, the CL was determined by multiplying the SE by a constant that reflected the level of significance desired, based on a normal distribution. The constant for 95% confidence limits is 1.96. Though there are numerous ways to express the formula below, it contains the components of an SD, V, and SE.

Relative precision of the mean (CL%):

$$CL\% (\pm) = \frac{t_{\alpha/2} \times (s/\sqrt{n}) \times (\sqrt{N-n}/N-1)}{\bar{x}} \quad (2)$$

where

s = sample standard deviation,

n = sample size,

N = population size, and

$t_{\alpha/2}$ = Student's t statistic for alpha level ($\alpha=0.95$) with $n-1$ degrees of freedom.

Complete study findings for Akutan, Emmonak, and Togiak appear in Fall et al. (2012), a volume of the Division of Subsistence *Technical Paper Series*. Reports in the *Technical Paper Series* are available online at www.adfg.alaska.gov/sf/publications/. Survey data at the community level also appear in the Community Subsistence Information System database, online at www.adfg.alaska.gov/sb/CSIS/.

2.2. Methods: Savoonga

The Native Village of Savoonga contracted with the Kawerak Inc. Subsistence Resources Program to conduct the subsistence household survey. Kawerak Inc. is the Alaska Native regional nonprofit corporation for the Bering Strait area. The survey instrument was based on the form developed by the Division of Subsistence, and data analysis methods were similar to those described above for Akutan, Emmonak, and Togiak. A 60% sample of Savoonga's 140 households was attempted; 82 household were surveyed for a 58.6% sample (Table 1; Tahbone and Trigg 2011: 4–8). The study year was 2009.

2.3. Methods: St. Paul

The Ecosystem Conservation Office (ECO) of the Aleut Community of St. Paul Island monitors annual subsistence harvests of northern fur seals and Steller sea lions. The tribal government organizes subsistence fur seal hunting through a co-management agreement with the National Marine Fisheries Service. Sea lion hunters report harvests and animals that are struck and lost within 24 h to the ECO (Lestenkof et al., 2011:10–11). Also, for BSIERP, the ECO interviewed 11 St. Paul residents about LTK and environmental observations. No household harvest surveys were conducted in St. Paul.

3. Results

3.1. Findings: Akutan

The community of Akutan is located on Akutan Island in the eastern Aleutian Islands. In 2008, the community had 81 inhabitants living in 40 households; 81% of the population was Alaska Native, primarily Aleut (Unangan). Akutan is the location of a large seafood processing plant that provided group quarters housing for 937 seasonal employees in 2010 Alaska Department of Labor and Workforce Development (ADLWD) (2012a); this population was not part of the target sample for this project because it is not resident year-round and does not engage in subsistence hunting and fishing while present in Akutan.

Based on household survey results, in 2008, residents of Akutan harvested an estimated 26,909 lb of wild fish, game, and plants (usable weight), an average of 673 lb per household and 327 lb per capita ($\pm 3.8\%$) (Table 2). By category, most of the harvest was fish: 45% salmon and 25% other fish (primarily halibut, Dolly Varden, and Pacific cod). Other harvests included marine invertebrates (octopus, chitons, crabs, clams, sea urchins) (10%), marine mammals (harbor seal, sea lion, fur seal) (8%) (Fig. 2), wild plants (5%), land mammals (feral cattle) (5%), and birds and eggs (3%). All households in Akutan used wild foods in 2008; 97% participated in hunting, fishing, and gathering; 100% received gifts of wild foods; and 86% shared their harvests with other households (Table 2).

Research by the Division of Subsistence has found that subsistence harvesting in Alaska's rural communities tends to be specialized, with a minority of households accounting for most harvests and sharing these harvests with others. Commonly, about 30% of households produce about 70% of the harvest (Wolfe et al., 2010). In 2008, subsistence harvests in Akutan were quite specialized, with 71% of the harvests taken by just 11% of the households.

Involvement of households in commercial fishing is often associated with high levels of production of fish and wildlife resources for subsistence uses in rural Alaska communities (Wolfe et al., 2010). Such households possess, or have access to, the equipment, skills, knowledge, labor, and cash needed to harvest wild foods. Therefore, tracking the role of commercial fishing in local economies is potentially instructive for understanding trends in subsistence harvests and uses. Of all Akutan's households, 33% were involved in commercial fishing in 2008. These households averaged harvests 941 lb of wild foods, compared to 583 lb for other households. Because of the relatively small number of commercial fishing households, however, they accounted for just 35% of the total community harvest, and differences in the harvests between these two groups were not statistically significant (Table 3).

Commercial fishing played an important role in the local economy of Akutan in 2008, although in terms of participation

Table 2
Selected study findings, household harvest surveys.

	Akutan	Emmonak	Togiak	Savoonga				
Study year	2008	2008	2008	2009				
Population	82	788	801	695				
% Alaska native	81.1%	97.9%	94.1%	99.5%				
Percentage of households								
Using wild resources	100%	100%	98%	NA				
Attempting to harvest wild resources	97%	95%	96%	NA				
Harvesting wild resources	94%	94%	96%	NA				
Receiving wild resources	100%	96%	94%	NA				
Giving away while resources	86%	84%	90%	NA				
Subsistence harvests, lb per person and percent of total harvest								
Salmon	146.2	44.7%	191.5	39.7%	106.0	34.9%	10.5	1.2%
Other fish	80.4	24.6%	83.2	17.3%	63.4	20.9%	38.7	4.4%
Marine invertebrates	34.2	10.5%	0.1	0.0%	9.8	3.2%	0.9	0.1%
Land mammals	14.8	4.5%	126.0	26.1%	52.0	17.1%	18.7	2.1%
Marine mammals	26.2	8.0%	54.9	11.4%	31.9	10.5%	779.9	87.6%
Birds and eggs	9.9	3.0%	14.9	3.1%	17.2	5.7%	35.5	4.0%
Wild plants	15.5	4.7%	11.2	2.3%	23.2	7.6%	5.9	0.7%
All wild resources	327.3		481.8		303.5		890.2	
Subsistence harvests, mean lb per household	672.7		2121.8		1293.7		4418.2	
Average number of types of resources								
Used per HH	17.0		21.5		27.1		NA	
Attempted per HH	9.5		17.2		17.8		NA	
Harvested per HH	8.8		15.4		16.3		NA	
Received per HH	11.5		11.2		15.7		NA	
Given away per HH	7.7		9.0		11.9		NA	

NA=data not available.

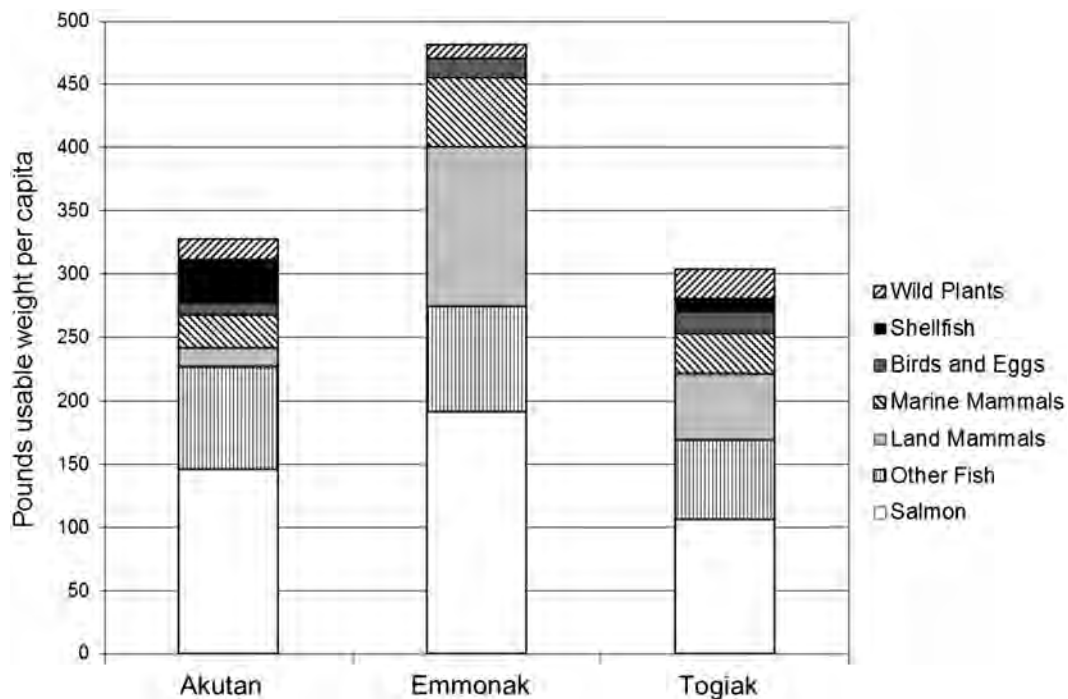


Fig. 2. Harvests of wild resources, lb usable weight per capita, by resource category, study communities, 2008.

Table 3
Comparison of subsistence harvests by households involved in commercial fishing and other households, 2008.

	Households involved in commercial fishing		Other households		t	Sig	
	Mean harvest (all resources)	% of community total	Mean harvest (all resources)	% of community total			
Akutan	941	35.0%	583	65.0%	-1.237	0.225	No
Emmonak	2676	67.1%	1492	32.9%	-3.301	0.001	Yes
Togiak	1519	85.5%	679	14.5%	-2.592	0.011	Yes

and, less so, of income, the role was diminished compared to 1990 (Table 4). Commercial fishing jobs (this does not include processing jobs) represented 19% of all jobs held by Akutan residents in 2008, compared to 37% of all jobs in 1990. Of all Akutan households with any cash employment, 35% in 2008 and 75% in 1990 had members involved in commercial fishing. Of all Akutan adults who had employment in 2008, 30% worked in commercial fishing jobs (about 18 individuals), compared to 44% (44 individuals) in 1990. Commercial fishing jobs produced 26% of the earned income and 22% of all income in Akutan in 2008; in 1990, 35% of earned income and 29% of all income derived from commercial fishing.

No Akutan residents have owned limited entry permits for salmon fishing since 1989 (when one resident owned a permit). Regarding commercial halibut fishing (primarily with longlines), since the late 1980s, about seven Akutan residents have held commercial halibut permits. Income data related to commercial halibut fishing are limited due to confidentiality rules. For four available years in the early 1980s, Akutan permit holders reported no income from halibut fishing. For five available years from 1988 through 1994, the annual total gross income was \$37,749 for all seven permittees. Gross income was notably higher for the two most recent years for which data are available (2005 and 2006) at an annual average of \$181,164 Commercial Fisheries Entry Commission (CFEC) (2012).

Estimated subsistence harvests in Akutan for 2008 were 29% lower than the only previous estimate of 461 lb per capita ($\pm 21.3\%$) for 1990 (Fig. 3). There was also a difference in the composition of the harvest: as a portion of the total harvest,

salmon increased from 26% to 45%, while marine mammals decreased from 23% to 8% (Fig. 4A).

The range of subsistence uses in Akutan was also lower in 2008 than in 1990. In 1990, 27 kinds of resources were used by at least 50% of Akutan households. In 2008, without exception, the percentage of households using these resources dropped (Fig. 5). For 20 resources, the decline was 25% or more, including 41% less households using sea lion, 51% less using Pacific cod, 44% less using scoters, 47% less using harlequin ducks, 65% less using eiders, 44% less using mallards, and 25% less using puffins. In 1990, the average household in Akutan used 31 kinds of wild foods, compared to 17 kinds in 2008.

Salmon was the only resource category for which the majority of surveyed Akutan households (53%) said their subsistence uses were lower in 2008 than in “other recent years” (approximately the last 5 years). For the other categories, most households said uses were about the same or had increased (Table 5). Respondents were asked to provide a reason if they indicated that their subsistence uses of a resource category had changed in 2008 compared to other recent years. In most cases (54%), they cited “personal reasons,” such as being too busy working, personal preferences, or a change in household composition. Factors related to climate or weather figured in 15% of the cases of lower subsistence uses. In about 20% of the cases, respondents cited lower populations of a resource as the reason (Fig. 6A). On the other hand, more abundant resource populations accounted for 36% of the cases of higher subsistence uses, primarily because Akutan respondents said that 2008 was a good year for berries.

Table 4
Role of Employment in Commercial Fishing, Akutan, Emmonak, and Togiak, 2008 and previous study year.

	Akutan		Emmonak ^a	Togiak	
	1990	2008	2008	1999	2008
Of all jobs, percentage involved with commercial fishing	37.0%	18.9%	28.9%	50.2%	40.2%
Percentage of all households with commercial fishing employment	72.3%	33.3%	53.2%	69.8%	72.5%
Percentage of all employed households with commercial fishing employment	75.0%	35.2%	63.7%	78.7%	81.7%
Percentage of all employed adults with commercial fishing employment	44.4%	29.6%	42.1%	64.8%	52.0%
Percentage of all income from jobs derived from commercial fishing jobs	34.7%	25.9%	21.7%	28.6%	32.3%
Percentage of all income derived from jobs with commercial fishing	29.0%	22.3%	10.5%	19.6%	20.7%

^a No previous study with comparable data is available for Emmonak.

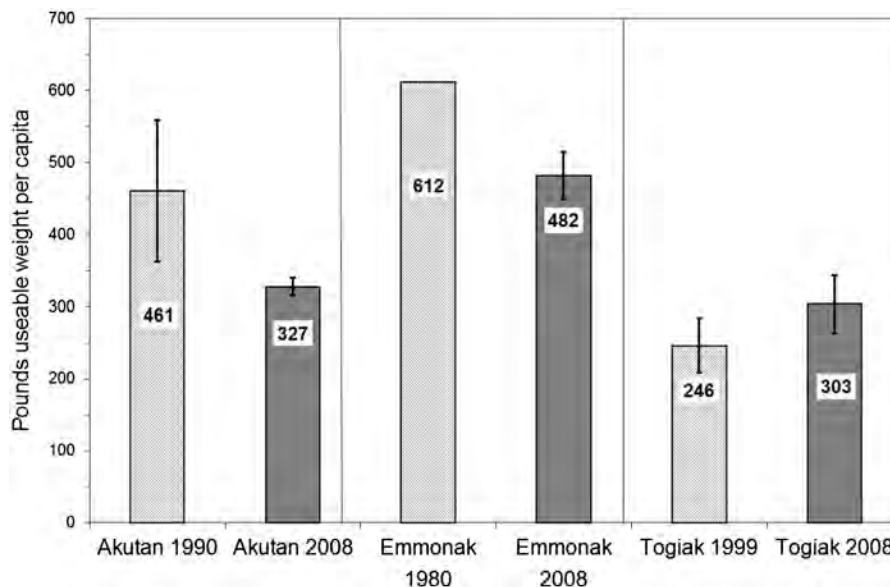


Fig. 3. Akutan, Emmonak, and Togiak: total subsistence harvests, lb per person, 2008 and previous study years.

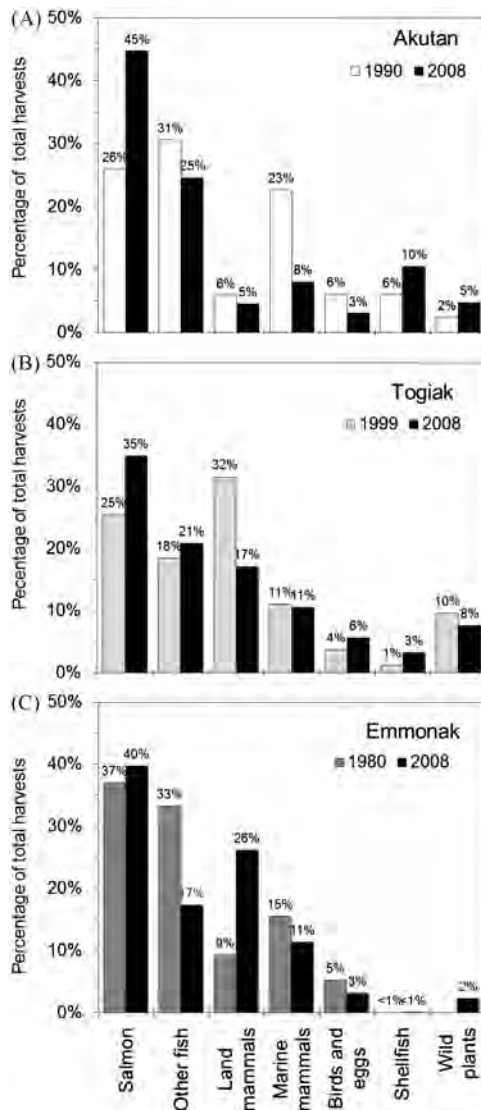


Fig. 4. Percentage of total resource harvest by category for (A) Akutan, 1990 and 2008; (B) Togiak, 1999 and 2008; and (C) Emmonak, 1980 and 2008.

Personal factors, such as investing in the purchase of a skiff or taking more interest in harvests, accounted for 32% of the cases of higher uses. In 28% of the cases of higher uses, Akutan respondents cited factors related to climate or weather as the cause; again, this was primarily related to a good berry crop resulting from adequate snow and rainfall (Fig. 6B).

Key respondent interviews conducted in Akutan as a follow up to the household surveys identified several themes related to changing subsistence harvest patterns in the community (see Huntington et al., 2013; Fall et al., 2012; and Hunn and Sepez 2010 for more details). Some themes addressed environmental conditions. For example, key harvesters reported that storms are more frequent and less predictable than in the past, perhaps over the last decade. These irregular weather patterns create difficulties for traveling long distances, especially in skiffs, thereby affecting access to subsistence resources. A major hunter and fisher in the community commented:

[There is an] indication that storms are more frequent and less predictable. For example, the usual pattern, up to a few years ago, would be a big storm with lots of wind that would stay a few days, then would clear for a few days before the next would come.

Lately, [the] last couple of years, the storms seem to come back-to-back and are mixed with each other. This makes it harder for locals to get out and hunt because the storms make the sea too dangerous. [This is] also evident by the “Goose” [float plane] going more and more days without being able to come to Akutan than [in] the past.

Hunters reported that changing wind patterns result in reduced predictability for hunting birds. One man said, “Wind patterns have changed and birds are not showing up in the usual places that they used to be hunted. They will haul up in other places or get blown elsewhere.”

Sea lion populations are down despite less hunting. One Akutan hunter stated that the major Cape Morgan haulout population of sea lions on the south shore of Akutan Island declined precipitously since the late 1960s, from some 75,000 to just about 2500 in 2010. Akutan residents point to predation by killer whales as a cause of such declines. In contrast, they report that harbor seals remain abundant, and are even increasing, because, more so than sea lions, they are able to escape killer whales by finding refuge in shallower waters among rocks near shore.

Also, the primary hunters and fishermen in Akutan with larger boats face increasing fuel costs; therefore they have tried to find efficiencies by fishing locally and limiting search time by only harvesting resources when someone “places an order,” for example for a seal; or by removing resources and incidental harvests from local commercial fisheries instead of making individual subsistence fishing trips.

In addition, Akutan respondents pointed to Bering Sea commercial fisheries and, especially, bycatches in these fisheries, as causes of lower populations of halibut and cod. Regarding halibut, Akutan subsistence and commercial fishers cited climate factors and commercial fishing as reasons for changes in local halibut stocks. They commented in 2008 that the average size of halibut in their harvests has declined in the recent past, saying that the larger halibut are living in deeper waters and not moving into the shallower areas in the summer, perhaps due to warmer ocean temperatures. They also reported that there are fewer larger halibut available for harvest and fishers are now taking the smaller “hatchery” halibut, a term they use to describe small halibut from a nursery location where they remain until large enough to be on their own. They worry that if the larger breeding fish are depleted, and the smaller fish are being overharvested, this could have long-term detrimental effects on the availability of halibut for harvest for subsistence uses as well as for the commercial fishery.

An Akutan key respondent noted that fishers check halibut stomach contents carefully to determine what they are eating and thus where they are most likely to be found. He also described how halibut are pushed into deeper water by concentrations of spawning Atka mackerel, particularly south of Akun Strait. Local halibut fishers cooperate to locate the best fishing areas.

Akutan respondents also reported that pollution by the local fish processing plant has resulted in scarcities of fish and marine invertebrates in Akutan Bay. In September 2011, the Environmental Protection Agency fined the processor for pumping fish waste into the bay and creating dead zones that suffocated sea life (Hopkins, 2011).

3.2. Findings: Togiak

Togiak is located at the mouth of the Togiak River, in the western Bristol Bay area. The community had 801 residents in 2008, 94% of whom were Alaska Native, primarily Central Yup'ik.

In 2008, residents of Togiak harvested an estimated 243,208 lb of wild fish, game, and plants (usable weight), an average of 1294 lb per household and 303 lb per capita ($\pm 13.2\%$) (Table 2).

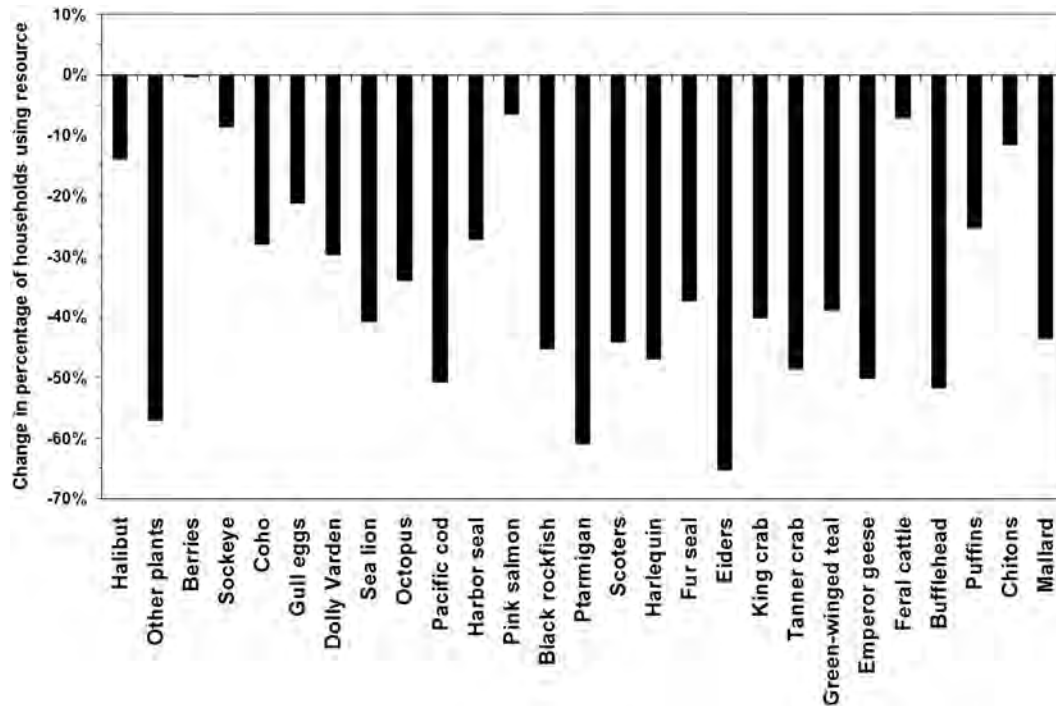


Fig. 5. Difference in percentage of Akutan households using resources, 1990 and 2008.

Table 5

Evaluation of subsistence harvests and uses compared to other recent years.

Categories ^a	Akutan			Emmonak			Togiak		
	Less (%)	Same (%)	More (%)	Less (%)	Same (%)	More (%)	Less (%)	Same (%)	More (%)
Salmon	53	38	9	36	46	18	47	33	20
Other fish	13	71	16	32	56	12	32	51	17
Large game				18	55	27	42	43	15
Small game				53	42	5	36	50	14
Marine mammals	36	60	4	45	48	7	41	47	12
Migratory birds	33	53	13	37	54	10	40	44	16
Other birds				33	61	6	29	55	16
Bird eggs	32	60	8	30	64	6	26	63	10
Shellfish	28	72	0				25	58	17
Wild Plants	24	47	29	29	49	21	31	56	14
All resources ^b				35	41	24	33	38	28

^a Does not include responses for categories usually harvested or used by less than 25 of the households.

^b Evaluations of “all resources” not elicited for Akutan.

By category, most of the harvest was fish: 35% salmon and 21% other fish (primarily herring spawn on kelp, herring, Dolly Varden, rainbow smelt, and northern pike). Other categories included land mammals (moose, caribou) (17%), marine mammals (harbor seal, spotted seal, walrus) (11%), wild plants (8%), birds and eggs (6%), and marine invertebrates (cockles, clams) (3%) (Fig. 2). In 2008, 98% of Togiak households used wild resources, 96% participated in harvest activities, 94% received gifts of wild resources, and 90% gave some portion of their harvests to other households (Table 2).

As in Akutan, a relatively small percentage of Togiak households harvested most of the subsistence resources in 2008: 31% of the households took 70% of the harvest. Most Togiak households (73%) were involved in commercial fishing in 2008, an activity which was associated with high levels of subsistence harvest in the community (Table 3). Commercial fishing households averaged subsistence harvests of 1519 lb and accounted for 85% of the community total, compared to 679 lb and 15% for other households. This difference was statistically significant.

Commercial fishing played an important role in the local economy of Togiak in 2008, as it did in the previous study year of 1999. Commercial fishing jobs (this does not include processing jobs) represented 40% of all jobs held by Togiak residents in 2008, compared to 50% of all jobs in 1999 (Table 4). For Togiak households with any cash employment, 82% in 2008 and 79% in 1999 had members involved in commercial fishing. Of all Togiak adults who had employment in 2008, 52% worked in commercial fishing jobs (about 181 individuals), compared to 65% (195 individuals) in 1999. Commercial fishing jobs produced 32% of the earned income and 21% of all income in Togiak in 2008; in 1999, 29% of earned income and 20% of all income derived from commercial fishing.

Fig. 7 shows trends in the number of limited entry permits for commercial salmon set gillnet and drift gillnet fishing held by Togiak residents from 1980 through 2010. Overall, the total dropped from an annual average of 134 permits in the 1980s to 122 permits in the 2000s; the total of 115 permits owned in 2010 was the lowest for the 31 year period. Losses of drift gillnet permits accounted for this entire decline—Togiak residents

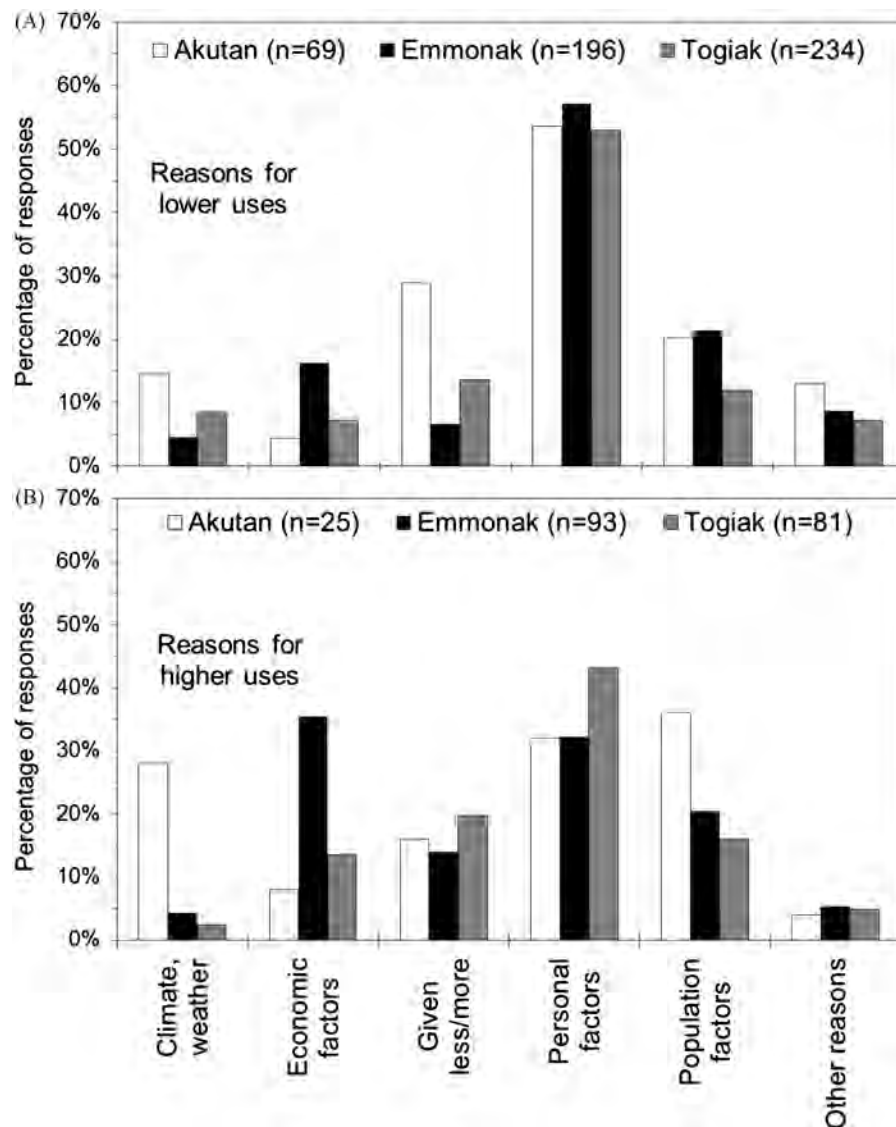


Fig. 6. Reasons in 2008 for (A) lower uses of categories of subsistence resources and (B) higher uses of categories of subsistence resources.

owned an annual average of 84 Bristol Bay drift gillnet permits in the 1980s and 61 on average in the 2000s, with the 53 owned in 2010 the lowest in the 31 year period. However, Togiak residents owned more set gillnet permits in the 2000s (an annual average of 61) compared to the 1980s (an average of 49 permits) Commercial Fisheries Entry Commission (CFEC) (2012).

Overall, gross earnings by Togiak residents who owned Bristol Bay set gillnet and drift gillnet commercial salmon permits declined from an annual average of about \$4.01 million in the 1980s to about \$3.76 million in the 1990s and \$2.41 million in the 2000s. However, since hitting a nadir of about \$700,000 in 2002, gross earnings by Togiak commercial salmon fishers have steadily risen, with an annual average of \$3.17 million from 2006 to 2010 compared to \$1.49 million on average for 2001 through 2005 Commercial Fisheries Entry Commission (CFEC) (2012).

Togiak's 2008 subsistence harvest of wild foods was 23% higher than the only previous estimate, 246 lb per capita ($\pm 15.3\%$) in 1999 (Fig. 3). There was a notable difference in the composition of the harvest: as a portion of the total harvest, salmon increased from 25% to 35%, while land mammals decreased from 32% to 17% (Fig. 4B). With just two years of comprehensive data, it is not possible to determine if this difference represents a real change or year-to-year

variations in harvests. As noted below, key respondent interviews added a longer time perspective for understandings trends in Togiak's subsistence harvests.

According to survey results, the diversity of subsistence uses in Togiak was higher in 2008 than in 1999. In 1999, 19 kinds of resources were used by at least 50% of Togiak households (Fig. 8). In 2008, the percentage of households using these resources increased, except for smelt (down 3%) and walrus (down 1%). For 12 resources, the increase was 25% or more, including 38% more households using Chinook salmon, 39% more using moose, 28% more using harbor seal, 30% more using herring spawn on kelp, 38% more using murre eggs, and 36% more using gull eggs. In 1999, the average household in Togiak used 17 kinds of wild foods, compared to 27 kinds in 2008.

For all subsistence resources combined, 33% of Togiak households reported that their uses were lower in 2008 than in "other recent years," while 28% said they were higher and 38% said they were about the same. For no category did a majority of Togiak households report lower uses; the largest percentages were salmon (47% with lower uses), large game (42%), marine mammals (41%), and migratory birds (40%) (Table 4).

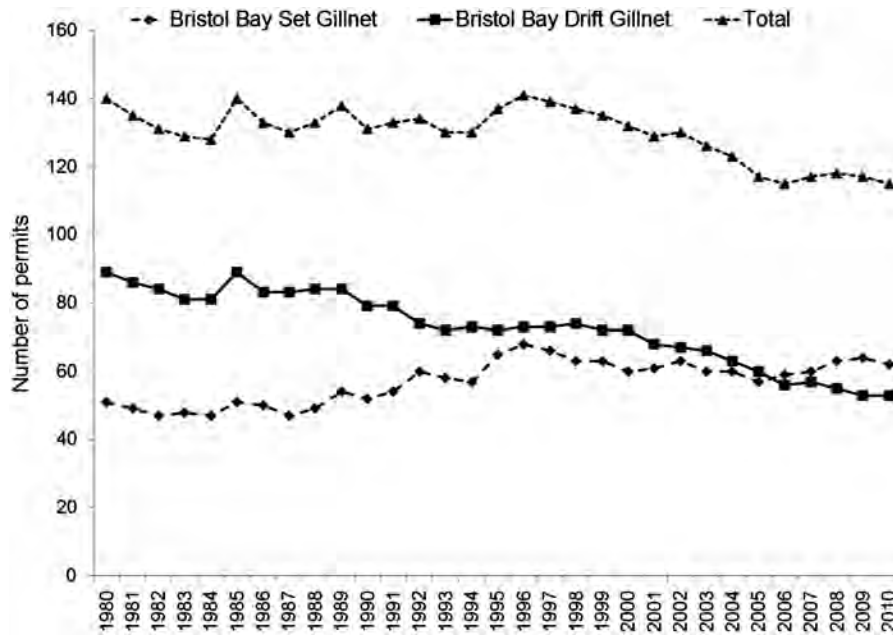


Fig. 7. Number of Bristol Bay commercial set gillnet and drift gillnet permits held by Togiak residents, 1980–2010.

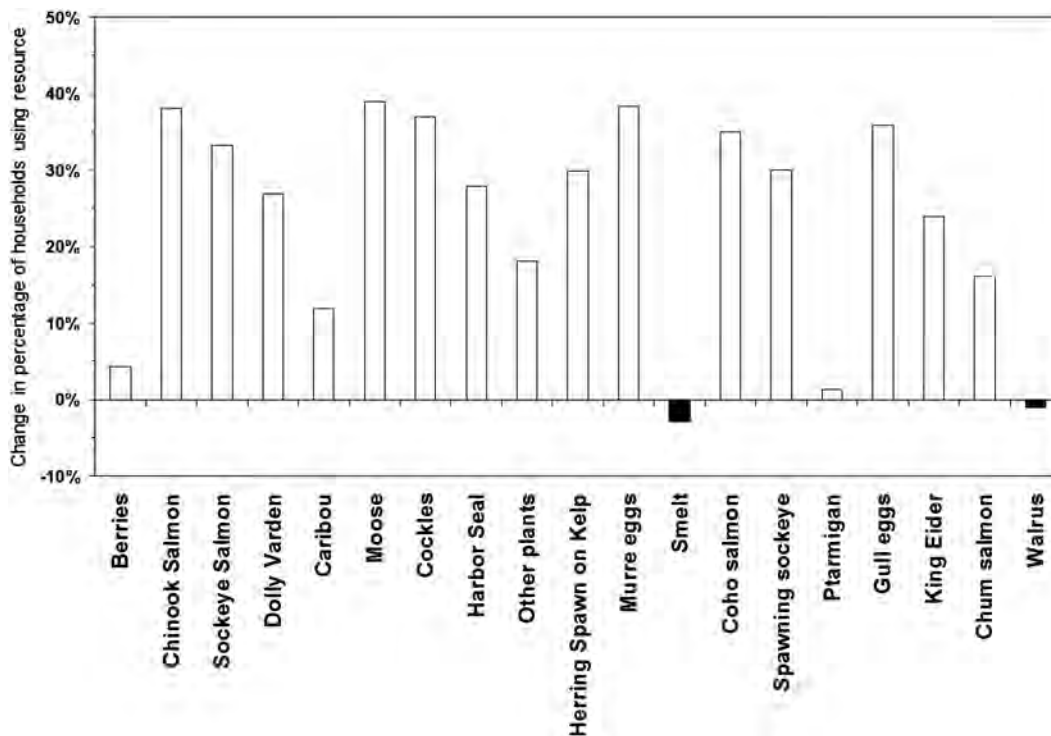


Fig. 8. Difference in percentage of Togiak households using resources, 1999 and 2008.

Surveyed Togiak households cited “personal factors” in 53% of the cases of lower subsistence uses in 2008. Ranking a distant second was less sharing (14% of cases). Reduced populations of resources were cited as the cause of lower uses in 12% of the cases, and in about 9% of the cases, respondents cited factors related to climate or weather (Fig. 6A). Personal factors also accounted for the most cases of higher levels of use in Togiak in 2008 (43%), followed by more sharing (20% of cases), higher populations of resources (16%), and economic factors (such as needing to harvest more wild foods due to increasing costs of food

in stores) (14%) (Fig. 6B). The following comments by survey respondents provide some examples.

- We used more subsistence resources because of our growing family.
- We used more subsistence resources because of the [poor] economy.
- Our children grew so we needed more [subsistence foods]. They were able to help me out more.

Prices [in the store] went up and we like to eat subsistence foods. Subsistence is good food. It's what we eat and thrive on and it gets me out of the house. My shooting improves when the prices go up.

We needed more subsistence foods because our family is growing and my parents want me to get foods for them too. We're trying to eat more subsistence foods so we don't have to buy expensive store-bought foods.

When asked directly during the survey if fuel costs affected their subsistence hunting and fishing, 75% of the Togiak respondents said yes. One person explained: "I spent less time running around. I had to concentrate on key points [i.e., locations] where it is good to get what's needed."

Subsequent key respondent interviews in Togiak explored reasons for possible changes in subsistence patterns, providing a longer time perspective than the two surveys from 1999 and 2008. These interviews identified a general theme of decline of many species of importance to subsistence uses, such as bearded seal, ringed seal, herring, herring spawn, capelin, king eiders, murre, long tailed ducks, shorebirds, common eider, snow goose, cormorant, arctic terns and other gulls, halibut, and Chinook salmon. Togiak respondents noted that, in addition to their general abundance, the timing of arrival of animals, birds, and fish, as well as their migration routes, pupping locations, haul outs, and nesting locations, are keys to subsistence harvest success. Narratives also emphasized the importance of "forage fish" (herring, smelt, capelin) both as human food and as food for other resources; their decline affects timing, migration routes, and abundance of other resources.

Togiak key respondents recognized two general causes of changes in subsistence resources: (1) environmental changes related to "climate change" or "warming" that they did not attribute to a broader cause; and (2) over-commercial fishing, causing depletions, especially of forage fish, as well as other human activities resulting in "disturbance," for example of marine mammals.

In commenting on climate-related changes, Togiak respondents noted that warming has resulted in less extensive sea ice and shore fast ice and more rapid disappearance of ice in spring, probably because it is not as thick as in the past. This change has especially affected opportunities to hunt bearded seals and ringed seals, with increasingly difficult access and reduced presence of marine mammals. "Ice seals" were important subsistence resources at Togiak in the 1980s and before (Wolfe et al., 1984:331–332, 403). Wolfe et al. (1984:331) noted that, at Togiak, "seals, particularly bearded and ringed, are commonly hunted during winter. These seals migrate into the area with the formation of the sea ice." However, Togiak's ice seal harvests have declined substantially over the last several decades. Estimated harvests were low in both survey years: 23 bearded seals ($\pm 129\%$) in 1999 and just 5 ($\pm 80\%$) in 2008. No ringed seals were reported harvested for 1999; the estimate was 9 ($\pm 69\%$) ringed seals in 2008. Thus the changes observed by Togiak hunters evidently began several decades ago, prior to the systematic collection of any harvest data.

According to Togiak hunters, seals remember their birth locations and return to them annually. With less ice and thinner ice, bearded and ringed seals are not pupping in bays near Togiak and therefore seals are not returning to the area. For example, a key respondent who is an active marine mammal hunter noted that while he was growing up at Togiak in the 1970s, during spring and until the end of May, ice was abundant in Togiak Bay. He observed the weather changing in the early part of the 1980s. When he started hunting seals, *maklaks* (bearded seals) were plentiful, but now he sees them infrequently. Togiak residents

used to hunt *maklak* in February and March and some of them in April but the ice melts rapidly now, disappearing in April. This hunter noted:

[There is] no place for the mother [bearded seal] to give birth, because they usually give birth on the ice, they follow the ice. We hardly catch any bearded seals during spring [now].

In Togiak Bay (near Togiak) there are hardly any bearded seals [now]. They stay further down behind Summit Island, on the south side of Summit Island and from there to Tongue Point in deeper water. They hardly come in the bay closer to Togiak. Whenever we want to hunt bearded seals we go down by Summit Island. I always go down by Summit and look around. It seems like bearded seals usually stay in deeper water, not in the shallow parts.

He also noted that bearded seals are associated with ringed seals (*nayiq*), "those small seals."

I call them their *iluraqs* [cousins] because whenever there are *nayiqs*, the bearded seal will also be around somewhere nearby. Mostly the ringed seals are in Togiak Bay [in the shallower areas] because their main diet is smelts and tomcod. Ringed seals are found in front of the rivers where smelt go in, like Togiak, Ungalikthluk, Guik, Matogak, and Osviak rivers because their diet is smelts. But bearded seal are mostly in deeper water [and] sometimes they go in the bay closer to Togiak.

Additionally, Togiak respondents stated that changes in ice conditions as well as less predictable weather and more frequent storms have reduced the window of opportunity for travel to access wild resource populations. A respondent explained how such changes have affected spring walrus hunting.

During spring we usually harvest walrus while they're on the ice. That's our number one rule that elders tell us, not to shoot them in the water, they'll sink. Walrus are like a rock in the water. That's why in the fall we try to hunt them while they're on the beach. Whenever we see them on the beach we try to hunt them. Seems like my uncle use to say while he was growing up walrus use to come in this bay too [Togiak Bay near Togiak] in front of the Togiak River. But now there's hardly any walrus that goes in this bay [closer to Togiak] I haven't seen any in the bay close to Togiak since like [the] 80s [and the] 90s, but further down in [Hagemester] Strait, and further down where there's ice.

Togiak key respondents also commented on changes to important subsistence resources that they attribute to human actions. A very active harvester described changes to Chinook salmon.

What I recollect is that king salmon enter Togiak Bay on the west side. They swim with the Kuskokwim fish and they split with them at Cape Newenham. The kings start showing up first in the Asigyukpak and Osviak area. After that they start showing up in this bay (near Togiak). Quinhagak starts catching kings the early part of June and they start showing up one or two weeks later in Togiak Bay. The population of king salmon is really going down and I don't know what's wrong. Maybe it is the trawler bycatch, it seems like it's affecting us in this bay too. There used to be lots of king salmon when there

weren't any trawlers like in the 1970s and early 80s. The run would go from June to around the Fourth of July, there would be lots of king salmon returning to the Togiak Bay, but now not that much. Last year (2009) the kings were real small, there weren't any of those big kings that we use to catch, there were just small kings and there weren't very many. Maybe the trawlers are affecting the fish that are bound for Togiak Bay because we've been conserving on commercial fishing for kings for maybe 20 years and the numbers are still going down. We use small mesh, ADF&G restricts us to 5 and 3/8 in. mesh, we don't even use king salmon nets anymore for commercial fishing. During spring people subsistence fish for king salmon, our main diet in the spring, we make dried strips. For subsistence we set nets farther out [from Togiak] in Togiak Bay, and I usually drift in the [Togiak] river for king salmon too.

Another man commented on the former abundance of herring and herring spawn.

Herring would spawn on points where kelp is growing extending from Rocky Point all the way to Kulukak and other areas but they don't spawn near fresh water where the rivers are. Herring spawn in the areas where there are rocks that the kelp grow on like on Hagemester and Summit islands, all the way around to Cape Newenham and even inside Chagvan Bay. The herring spawn in the grass in Nanvak Bay and the brant geese are waiting there to fly on to the north. In Nanvak Bay when the tide goes out after the herring have spawned, I have observed what I thought might be 75–80,000 birds in the mudflats where the grass is. It is solid with birds eating the eggs.

He added that, formerly, the kelp was thick with two inches of spawn. Even the tops of the rocks were covered with kelp, making it difficult to walk because they were so slippery. But he commented:

It's not like that anymore. Probably 20 years from now if they keep letting them purse seine there will be no more herring. Then those purse seiners will move out. That's the reason why hardly anyone from Togiak commercial fishes for herring.

Togiak elders report that herring return in two runs or "batches." In the past, "it looked like the ocean was smoking when the first batch [run] was spawning." The "second batch" was even larger. However, the commercial seiners fish for herring commercially on the first run's spawn and Togiak people feel they should wait until the second spawn. In their view, that is why there is not as much spawn on kelp today.

Another man commented on the widespread declines in various subsistence resources that he attributes to the commercial herring fishery and the decline of the abundance of herring as a forage fish.

After the commercialization of herring, seems like the numbers of geese, and whales, seals, sea lions went way down. My grandpa used to take my grandma and me, when I was about 9 or 10 years old, to hunt squirrels on the other side of the bay from Togiak near where Twin Hills is today. When my grandpa was taking us across Togiak Bay with a skiff, it seemed like we were hitting bottom with the prop but when I looked back there were herring flying up from the prop because there were so many herring.

I remember going hunting at the Anchor Point area when the herring were spawning. We would see hundreds of seals all over and herds of sea lion families, like four or five to a group, little groups here and there. I believe that's how sea lions hunt, is in a group. Now-a-days it is rare to see that many sea lions. Now we just see one big bull and one sea lion when we're going west to hunt. Early before the herring start showing up, we start seeing one or two sea lions coming this way, probably from the Cape Newenham area.

Emperor geese like to feed on the herring roe. I remember my grandpa commenting that the geese are fatter after herring season. That's when my grandpa preferred to do his geese hunting, when the birds were nice and fat, not skinny.

I remember that all kinds of whales used to come around. I think they were fin whales, and humpback whales, and gray whales, and those big ones, I think they were blue whales. The [air released from the] blowhole seemed to take forever for it to go out, at least that's how I thought it was.

A theme in Togiak key respondent interviews was that various species of birds were more abundant in the past. One hunter said:

In the past there used to be a whole bunch of tents on Tongue Point where people went to hunt eiders in the spring. The eiders used to fly through Hagemester Strait—but now they fly through or south of the other islands east of Hagemester, and along the east side and south of Hagemester Island. We used to be able to see the reflection of the king eiders on the water because there were so many of them way out on the horizon—they were like clouds between High Island and Hagemester—there's not as many like that anymore. We used to hunt them and bring them back to Togiak in our skiffs to share with those that couldn't get out.

Togiak respondents blamed the decline in eiders in part on the reduction in populations of "forage fish," such as herring and capelin, caused by commercial fishing.

Another hunter cited the growth of the commercial herring fishery in Togiak Bay as a cause of reduced local seal populations.

There used to be lots of seals in the bay in spring time when the herring would start spawning. But now days there are just a few seals. Even the *maklak* seals, we hardly see any when we go hunting.

Another elder told a story of his former experience at Metervik Bay. When the herring hit there were so many seals that when the breeze was blowing in from the ocean you could smell their breath—"that's a lot of seals," he said.

Finally, key respondents in Togiak highlighted key principles of human conduct for subsistence activities. A central value is showing "respect" for animals. As two respondents put it:

My grandparents used to tell me that the things I got from this land and water don't belong to me. It was given to me to use and to respect it all the time.

The first rule from my grandpa is take only what you can use, even if there is abundance of whatever take only what you can use, what you can handle. Never waste, and respect the animals, so, like with the fish, they can come back year after year after year.

In the traditional Yup'ik world view as expressed at Togiak, showing respect to animals entails nonwasteful harvest and use,

appropriate disposal of bones, providing a “drink of water” to the harvested animal, and using proper butchering techniques. A principle underlying these rules is that the spirits of animals are aware of how their remains are treated and how people speak about them, and will withhold themselves from being harvested if offended.

3.3. Findings: Emmonak

Emmonak is located on the lower Yukon River, in western Alaska, about 12 miles upriver from the Bering Sea. In 2008, the community had 788 residents, 98% of whom were Alaska Native, mostly Central Yup'ik.

In 2008, residents of Emmonak harvested an estimated 379,803 lb of wild fish, game, and plants (usable weight), an average of 2122 lb per household and 482 lb per capita ($\pm 6.8\%$) (Table 2). By category, most of the harvest was fish: 40% salmon and 17% other fish (primarily sheefish, whitefish, pike, and burbot). Land mammals, primarily moose, were also significant, at 26% of the total harvest, and marine mammals (mostly bearded seal, spotted seal, beluga, and ringed seal) contributed 11%. Other categories included birds and eggs (3%), wild plants (2%) and marine invertebrates (less than 1%) (Fig. 2). On average, Emmonak households used 22 different kinds of wild foods in 2008. All Emmonak households used wild resources in 2008, while 95% attempted harvests, 96% received wild foods as gifts, and 84% gave wild foods to other households (Table 2).

As in Akutan and Togiak, a relatively small percentage of Emmonak's households accounted for most of the subsistence harvest in 2008: 34% of the households took 70% of the harvest. As in Togiak, involvement in commercial fishing was associated with high levels of subsistence harvest in Emmonak (Table 3). Commercial fishing households (53% of all households) averaged subsistence harvests of 2676 lb and accounted for 67% of the community total, compared to 1492 lb and 33% for other households. This difference was statistically significant.

A notable difference between the results of household surveys conducted in Emmonak in 1980 and 2008 involved major changes in the economic role of commercial fishing. Commercial fishing in 1980 for communities in the lower Yukon including Emmonak “represented the largest and most consistent source of money... and comprised 45.8 percent of their annual monetary income, or \$8026 per household” (Wolfe 1981:92). Adjusted for inflation and for the consumer price index in Anchorage, this would be equivalent to about \$18,908 in 2011 Alaska Department of Labor and Workforce Development (ADLWD) (2012b). By contrast, average income earned by an individual engaged in commercial salmon fishing in the Lower Yukon in 2008 totaled only \$1479 (Wolfe et al., 2009); no directed commercial fishing for Chinook salmon took place in 2008 due to conservative management actions on the Yukon River.

Despite these changes, commercial salmon remained important to Emmonak's local economy in 2008. According to household survey results, in 2008, 29% of all jobs held by Emmonak residents involved commercial fishing (Table 4). About 42% of employed adults in Emmonak held commercial fishing jobs, and these jobs produced about 22% of earned income and 10% of all income for the community in 2008. The number of Emmonak residents holding limited entry permits for commercial gillnet fishing for salmon in the Lower Yukon River has been relatively steady since 1980, with annual averages of 102 permit holders in the 1980s, 98 permit holders in the 1990s, and 97 permit holders from 2000 through 2010. However, Emmonak residents' annual gross earnings in this fishery dropped from \$895,828 in the 1980s to \$735,565 in the 1990s and \$289,143 in the 2000s Commercial Fisheries Entry Commission (CFEC) (2012).

The 2008 estimated subsistence harvest of wild foods was 21% lower than the only previous estimate for Emmonak, 612 lb per capita in 1980 (Fig. 3). However, the 1980 household sample may have been biased towards more actively harvesting households (Wolfe 1981:128). There was a difference in the composition of the harvest between the 2 study years: as a portion of the total harvest, fish other than salmon decreased from 33% in 1980 to 17% in 2008, while land mammals (primarily moose) increased from 9% in 1980 to 26% in 2008 (Fig. 4C).

In the view of 35% of surveyed Emmonak households, their subsistence uses overall in 2008 were lower than in other recent years; 41% of households said uses were about the same and 24% said uses were higher (Table 5). Only for small game did a majority of Emmonak households report lower uses (53%), although 45% reported lower uses of marine mammals.

As in Akutan and Togiak, personal factors accounted for the largest number of cases of lower subsistence uses in Emmonak in 2008 as reported in the survey (57%) (Fig. 6A). Lower populations of resources were cited in 21% of the cases and economic factors, primarily the higher cost of fuel, in 16%. However, economic factors ranked first as a cause of higher levels of use (36%) (Fig. 6B). Respondents linked an increased need to harvest wild resources to higher costs of food and home heating oil. Personal factors ranked second (32%) and in 20% of the cases, Emmonak respondents cited higher populations of resources as leading to higher harvests. These latter cases mostly involved the increased populations of moose along the lower Yukon River, linked to improved habitat and an 8-year moratorium on hunting (between 1988 and 1995) (Perry 2010).

When asked directly in the survey if fuel costs affected their subsistence hunting and fishing, 89% of the Emmonak respondents said yes. Most said that high fuel costs limited their subsistence activities. Many commented on both the need to harvest subsistence foods and the high costs of traveling to hunt and fish. One person remarked: “We're in a disaster situation because of gas prices and fuel costs. Without subsistence we wouldn't make it.”

Key respondent interviews in Emmonak are discussed in more detail in Fienup-Riordan, Brown, Braem (2013) and Huntington et al. (2013). Following are several observations and themes from these interviews that place the just discussed harvest data in a more long-term perspective.

Emmonak fishers recognize certain wind conditions as a natural indicator of salmon behavior (Moncrieff et al., 2009). In their view, wind conditions affect which mouth of the river the salmon enter, and therefore people use the wind to guide where they set their nets. However, residents have observed that the frequency of storms has increased, and these storms generally come from the south. Northern and western winds bring abundant salmon into the south mouth, closest to Emmonak. But, according to local knowledge, with a south wind, salmon enter the north mouth of the Yukon River and bypass Emmonak.

Also, salmon runs have been declining over the last several years, though the reasons for this change are not fully understood. Fishers, managers, and scientists have suggested various causes, from changing environmental conditions in the Bering Sea to commercial groundfish bycatches. Also, increasingly complex regulations intended to protect the salmon runs have placed additional pressure on subsistence harvesting, with subsistence openings not always occurring during optimal processing times.

In key respondent interviews, Emmonak residents described a dramatically and rapidly changing local environment:

The ice used to be very thick, those days, very thick in those days because it used to be very, very cold. Now, we have very mild winters. The elders have noticed that quite a bit. They

have been telling us from way back, way, way back that this is going to actually happen. I don't know how in the world they know. Even my uncle, he is 93 year old, he say, those days he used to hear elders saying, "How come the world, our environment is changing?" They already know. They already know it is going to change.

These changes affect local residents' predictive understanding and capabilities as well as their actual hunting, fishing, and gathering practices.

For example, changing ice conditions may have modified Emmonak's harvest and use of marine mammals (see also Fienup-Riordan et al., 2013). Emmonak hunters note that with milder winters, sea ice is thinner and more dangerous. As a percentage of Emmonak's total subsistence harvest, marine mammal harvests were slightly higher in 1980 at 15% compared to 2008 at 11%. At the species level, however, bearded seals were harvested in greater numbers and ringed seals in lower numbers in 2008 compared to 1980, reflecting a shift in the composition of marine mammal harvests in the community. Estimated bearded seal harvests number 39 seals in 1980, compared to 198 in 1998, 72 in 1999, and 136 in 2008. In contrast, harvests of ringed seals totaled 139 in 1980 and 151 in 1998, compared to 66 in 1999 and 28 in 2008 (Fig. 9; Wolfe, 1981, Coffing et al., 1998; Coffing et al., 1999). The causes of this change are uncertain, and might be related to changes in ice formation, the costs of hunting, changes in transmission of hunting knowledge, or all of these factors. However, most marine mammal hunting in 2008 occurred in the fall in open water, focusing on bearded seals; in contrast, there was little spring hunting in 2008, when traditionally ringed seals were taken in association with sea ice in lead areas. In 2008, many key respondents commented on the dangers of hunting on the ice. According to one respondent,

Timing of *qamigar* ("to go seal hunting with a small sled and kayak in spring" [Jacobson 1984:310]) is changing. When I was young, before snowmachines came around, my dad and his friends used to get up very early in the morning like 3–4 in the morning start preparing to get their dogs ready and their grubs

ready because they have to go maybe 20–30 miles out to find the water. They have to go very, very early in the morning. Early in morning, that's when the seals are more active, you know, and you more chance of catching the seals early, early in the morning. In afternoon and evening they start getting more careful. So early in the morning is the best time.

Emmonk hunters also noted the technological changes which have allowed people to make day hunting trips rather than staying out at seal camp, an important setting where people build their knowledge of ice.

Them days, when I was growing up, them, my folks used to hunt seals. They don't hunt them in the fall time. Cause too far, too much ice. And they hunt what they have around that area. At winter time they go out, they look at the clouds, when open water, that's when they go out. Dog team. Take 'em all day to get down there and when they get down there they overnight, 2–3 nights on top of the ice. Now, let's go. Zip. Zip down, zip back. We got fast machines. Nobody overnights no more. Nowadays. Some of them even go in the afternoon down the coastline.

Additionally, it is difficult to evaluate climate related change in isolation from other kinds of changes being experienced by Emmonak residents, a point Emmonak residents themselves made during interviews. For example, one man observed,

But now, now since we don't use dog teams anymore, we switch to snowmachines and those travel 40–50 miles an hour and it doesn't take an hour or two to travel from our village to go down to the open water. A lot of times, these younger people miss out, they actually miss out on the seals when they are more active early, early in the morning...a lot has changed on our traditional way of hunting or gathering. Ice conditions have changed a lot...the ice out there in the Bering Sea is a lot thinner. You don't see no big thick ice. There used to be

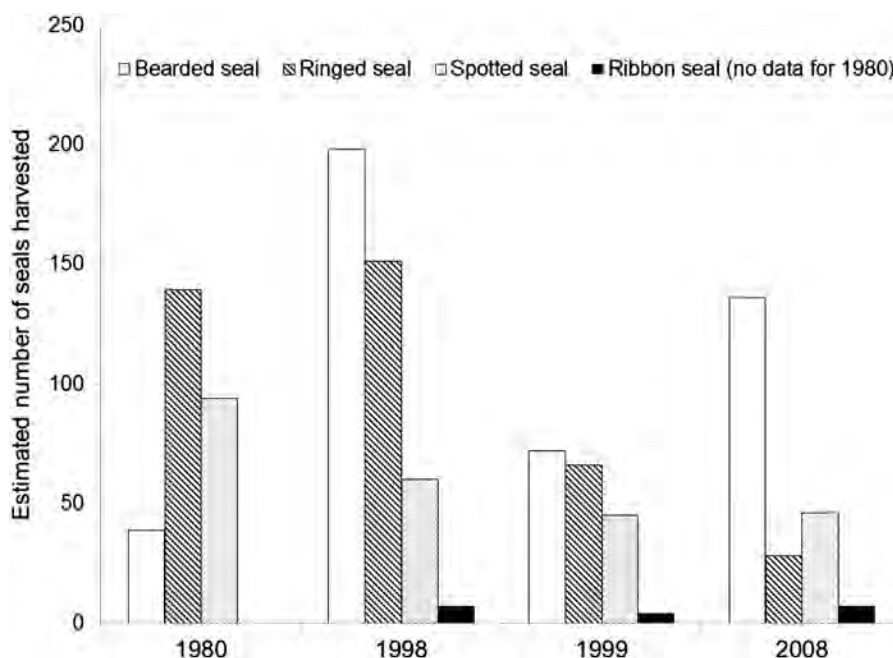


Fig. 9. Emmonak: estimated harvests of ice seals, 1980, 1998, 1999, and 2008.

a bunch of big icebergs out there where they pile up and you don't see as much as before...it's not more dangerous. It's the way people, their attitude has changed. They're not as careful as before. Just like the change between the dog team and the snowmachine and everything else too. Our younger people don't know the weather. They can't tell how it is going to be if they look, they don't know how to tell the weather no more. A lot of times they get lost or get hurt. They're more prone to accidents and to get lost. Right now we depend on GPS [global positioning system]. That's good, that's a lot of change, on the other hand, those years before GPS came around, the people that go out hunting they have to know the weather.

Thus, Emmonak residents remind researchers to consider what Moerlein and Carothers (2012) call the “total environment of change,” in order to assess and understand their observations of climate change and the implications of these changes for their subsistence practices. Correspondingly, as many Emmonak respondents also noted, ecological or environmental change is not necessarily remarkable in itself, nor is the need to adapt. Change is a constant.

3.4. Findings: Savoonga

Savoonga is located on St. Lawrence Island in the northern Bering Sea. In 2009, the community had 695 inhabitants, 99.5% of whom were Alaska Native, primarily Siberian Yupik.

In 2009, Savoonga residents harvested an estimated 618,669 lb of wild resources (usable weight), 4419 lb per household and 890 lb per capita (a confidence limit was not reported for total harvests) (Table 2). The range of resources used for subsistence was wide, with over 17 species of fish, shellfish, birds, marine mammals, and plants used by more than 25% of the households. However, marine mammals composed 88% of the total harvest as estimated in usable pounds, consisting primarily of three species: walrus (46%), bearded seal (20%), and bowhead whale (14%). Other harvested categories were: fish other than salmon (4%), birds and eggs (4%), land mammals (1%), salmon (1%), wild plants (less than 1%), and marine invertebrates (less than 1%) (Tahbone and Trigg 2011). The composition of Savoonga's subsistence

harvest was broadly similar in 2006: marine mammals, 81%; birds and eggs, 8%; land mammals, 4%; fish other than salmon, 4%; salmon, 2%; wild plants, 1%, and marine invertebrates, less than 1% (Ahmasuk and Trigg 2007).

Of the 79 Savoonga households that responded to the question, 53% reported that, overall, their subsistence uses were about the same in 2009 as in other recent years; 35% said uses were less and 11% uses were higher (Tahbone and Trigg 2011:59). Of all harvesters, 81% said higher fuel costs affected subsistence activities. In interviews conducted by Huntington et al. (2013), key respondents generally reported that, overall, subsistence resources were abundant and healthy near Savoonga.

As documented by the US Fish and Wildlife Service's marking and tagging program (Benter, 2011), subsistence walrus harvests at Savoonga are highly variable from year to year (Fig. 10). From 1989 to 2011, reported harvests ranged from 148 walruses in 1994 to 849 walruses in 2000. For the entire 23-year period, the average annual harvest was 457 animals. Reported harvests were lower from 1989 to 1999, at an annual average of 372 walruses, compared to 2000 to 2011, with an average of 536 walruses. The annual average for the most recent 5-year period (2007–2011) was 578 walruses.

3.5. Findings: St. Paul

The community of St. Paul is located on St. Paul Island in the central Bering Sea. The community had a population of 479 in 2010, 87% Alaska Native, primarily Aleut (Unangan). As noted, a comprehensive harvest survey was not conducted in St. Paul as part of the BSIERP project. Rather, the community's Ecosystem Conservation Office (ECO) continued in-season monitoring of subsistence harvests of fur seals and sea lions (Lestenkof et al., 2011). Also, annual estimates of subsistence halibut harvests by St. Paul residents since 2003 are available based on mailed surveys administered by ADF&G through a grant from NMFS (Fall and Koster 2012).

A comprehensive survey for 1994 conducted by ADF&G estimated per capita subsistence harvests at St. Paul at 267 lb per person (Alaska Department of Fish and Game (ADF&G), 2012).

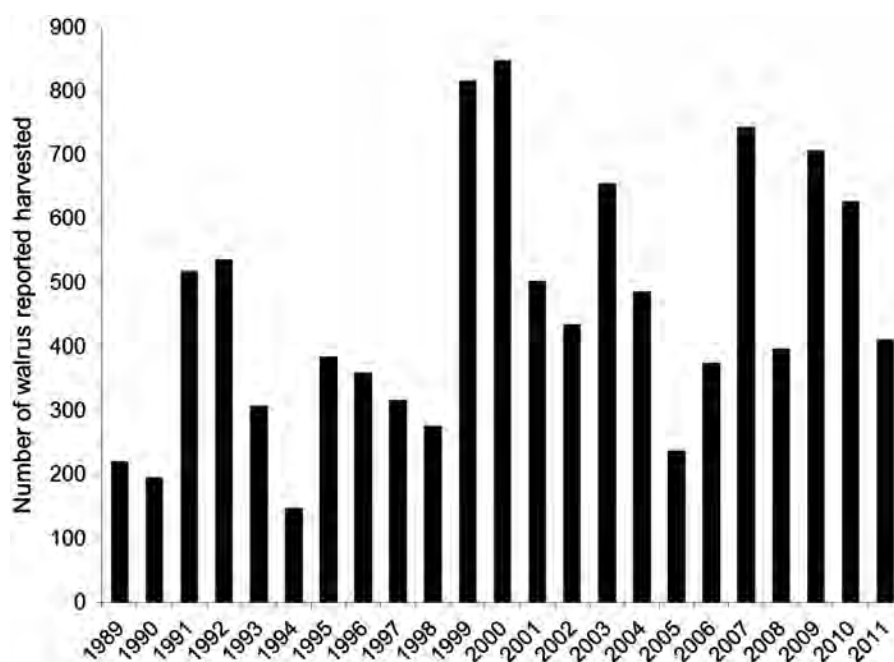


Fig. 10. Reported subsistence harvests of walrus, Savoonga, 1989–2011.

Table 6

Estimated subsistence harvests of fur seals, sea lions, and halibut, St. Paul, 1990–2010.

Sources: Lestenkof et al., 2011; Wolfe et al., 2009; Fall and Koster 2012; Alaska Department of Fish and Game (ADF&G) (2012); National Oceanic and Atmospheric Administration (NOAA) (2008), (2012).

Year	Number of animals			Usable lbs			Per capita lbs		
	Fur seal	Sea lion	Halibut	Fur seal	Sea lion	Halibut	Fur seal	Sea lion	Halibut
1990	1077			21,217			27.8		
1991	1644			32,387			47.8		
1992	1480	162		29,156	32,400		40.8	45.4	
1993	1518			29,905			42.5		
1994	1610	141	1167	31,717	28,200	37,450	64.4	57.3	75.8
1995	1263	54		24,881	10,720		32.9	14.2	
1996	1588	28		31,284	5640		42.0	7.6	
1997	1153	26		22,714	5180		30.0	6.8	
1998	1297	41		25,551	8200		34.7	11.1	
1999	1000	10		19,700	2000		29.3	3.0	
2000	747	12		14,716	2400		27.7	4.5	
2001	597	12		11,761	2400		22.5	4.6	
2002	548	18		10,796	3600		20.5	6.8	
2003	522	13	1010	10,283	2600	19,744	19.6	5.0	37.7
2004	493	9	518	9712	1800	8012	20.4	3.8	16.9
2005	466	19	377	9180	3800	7835	19.6	8.1	16.7
2006	396	20	435	7801	4000	5971	17.4	8.9	13.3
2007	272	22	901	5358	4400	11,342	12.5	10.3	26.5
2008	328	20	294	6462	4000	4607	15.0	9.3	10.7
2009	355	18	398	6994	3600	7280	15.9	8.2	16.6
2010	357	15	485	7033	3000	10,139	14.7	6.3	21.2
Annual averages									
1990s	1363	66	1167	26,851	13,191	37,450	36.9	18.1	75.8
2000s	462	16	552	9100	3236	9366	19.0	6.8	20.3
2006–10	342	19	503	6730	3800	7868	15.1	8.5	17.7

Three resources composed 87% of the harvest: halibut (from all sources: subsistence long lines, removal from commercial harvests for home use, and rod and reel) (39%), fur seals (27%), and sea lions (21%). By resource category, the 1994 subsistence harvest in St. Paul was 48% marine mammals, 44% fish other than salmon, 3% land mammals (reindeer), 2% wild plants, 1% salmon, and 1% marine invertebrates.

Annual monitoring programs have documented declining subsistence harvests at St. Paul since 1994 but more stable harvests in the 2000s (Table 6). Annual fur seal harvests averaged 1363 animals in the 1990s but only 462 seals annually in the 2000s; the recent (2006–2010) annual average subsistence harvest is 342 fur seals. For sea lions, subsistence harvests averaged 66 animals annually in the 1990s and 16 annually in the 2000s, with the recent 5-year annual average at 19 sea lions. The single subsistence harvest estimate for halibut in the 1990s was 1167 fish, compared to an annual average since 2003 of 552 halibut and since 2006 of 503 halibut. Subsistence harvests of these 3 key resources provided an annual average of 130.8 lb of wild food per person in the 1990s and 41.3 lb per person on average from 2006–2010, a decline of 68%.

Interviews conducted by the St. Paul's ECO with 11 community residents explored local and traditional knowledge regarding natural resources. Respondents reported observations of lower fur seal populations and fewer young fur seals, which some attributed to reduced fish populations or predation by killer whales (Lestenkof et al., 2011:16). However, orders for fur seals for subsistence use placed with tribal harvesters have declined, suggesting that reduced interest in using fur seal meat, rather than a declining population of fur seals, may account for lower harvests (Lestenkof et al., 2011:29). Concerning halibut, observations included fewer halibut, smaller halibut, and halibut further off shore making them more difficult to harvest by subsistence fishers with small boats. Respondents cited harvests in the

commercial halibut fishery and bycatch in other commercial fisheries as possible explanations for changes in the halibut population (Lestenkof et al., 2011:17). The interviews did not systematically record observations specifically about Steller sea lions.

4. Discussion

The results of the household surveys demonstrate the continuing importance of wild resource harvests in the study communities. Virtually all households used wild foods in the study year, and large percentages participated in resource harvests and shared these harvests. Harvests were diverse, consisting of a variety of fish, land mammals, marine mammals, marine invertebrates, birds and eggs, and wild plants.

The US Department of Agriculture estimated that on average, Americans consumed 224.4 lb of meat, fish, and poultry per capita in 2008 (out of a total annual food consumption of 1911 lb per person) United States Census Bureau (2011). Excluding plants, subsistence harvests documented in this study provided food at 125% of this national consumption level in Togiak, 139% in Akutan, 210% in Emmonak, and 394% in Savoonga. These harvests provided 171% of daily protein requirements (51 g/day) (United States Department of Agriculture (2011):76) in Togiak, 190% in Akutan, 287% in Emmonak, and 538% in Savoonga. With daily caloric requirements at 2250 Kcal/day (United States Department of Agriculture (2011); 14), subsistence harvests (excluding plants) provided 27% of this requirement in Togiak, 30% in Akutan, 46% in Emmonak, and 86% in Savoonga.

Nevertheless, comparisons of harvest data across study years combined with key respondents' observations suggest that subsistence harvest patterns have changed in the study communities over the last several decades. These changes were not uniform

across communities. Harvest quantities and diversity were lower in Akutan in 2008 than in 1990, the only previous year for which comprehensive survey data are available. In contrast, harvests were higher and diversity of uses greater in Togiak in 2008 than in the previous study year of 1999. Shifts in harvest composition occurred: Emmonak harvested more moose and less nonsalmon fish, more bearded seals but less ringed seals; Togiak harvested less moose and caribou and more salmon; and Akutan's harvests of marine mammals dropped while salmon harvests increased. At St. Paul, where multiple years of data are available for fur seals, sea lions, and halibut, subsistence harvests for these three key resources have declined since the early 1990s.

Survey respondents offered a range of personal, economic, and environmental explanations for changes they have experienced. Personal and economic factors dominated their explanations of changes in 2008 compared to other recent years. However, interviews with key respondent, perhaps because of the greater time depth and broader experience applied to their observations, identified other factors that are shaping trends over a longer time frame. These explanations are complex and multifaceted.

For example, at Akutan, respondents cited the effects of persistent storms and shifting winds that restrict travel and reduce the predictability of the locations of key resources. They also commented on the effects of bycatches in Bering Sea commercial fisheries on marine resource abundance. Emmonak respondents are also experiencing shifting winds and persistent storms, as well as unpredictable and unstable sea ice. They cite a combination of environmental and resource management factors, including bycatches in Bering Sea commercial fisheries, that negatively affect salmon, still their most important subsistence and commercial resource. Togiak respondents, too, point to both environmental changes and more immediate human-caused factors for declining resources. There as well, weather is more unpredictable, compressing the time available for some seasonal activities, especially in spring, and shifting the location of resources. As in Emmonak, ice conditions have likely caused a change in Togiak's uses of marine mammals. But Togiak respondents also voiced concern about the effects of commercial fisheries on subsistence resources.

An important hypothesis tested in the BEST-BSIERP Bering Sea Project proposed that with changing abundance and distribution of subsistence resources in the Bering Sea, communities will become more dependent on owners of large boats to travel further to harvest subsistence resources, and that there will be a shift in the composition of subsistence harvests to reflect changing species availability. The household surveys found evidence of specialization in subsistence harvests, associated in part with involvement in commercial fishing in Togiak and Emmonak. However, the study found no evidence that harvesters are traveling further to locate scarce resources. Indeed, in Akutan, owners of larger commercial fishing boats reported adapting to rising fuel costs by developing harvest efficiencies that involved fewer and shorter trips. High fuel costs also affected subsistence harvests in Emmonak, Togiak, and Savoonga. The household harvest surveys and key respondent interviews, and the harvest monitoring programs in St. Paul, supported the second part of the hypothesis by documenting shifts in the size and composition of subsistence harvests that can in part be linked to changes in resource abundance and distribution. But these shifts are likely also linked to other causes not directly tied to resource abundance, such as impediments to access caused by thinning ice or changing and unpredictable weather patterns, or commercial fisheries harvests and bycatches and other human-caused disturbances to natural resource populations. Also, as demonstrated by the surveys and interviews, subsistence harvests are shaped by a variety of other

economic and cultural factors, such as changing involvement in commercial fisheries and increasing costs of fuel and equipment.

Survey participants' and key respondents' observations of several decades of changing weather and other environmental conditions correspond with data summarized by Stabeno et al. (2012a) documenting a period of high year-to-year variability of the extent of sea ice in the southwestern Bering Sea from 1972–2000, followed by a 5-year warm period with low ice extent from 2001–2005 and a 4-year cold period with extensive sea ice from 2007–2010. This research, undertaken as part of the Bering Sea Project, recorded differences in wind directions in spring between warm and cold years which were associated with the extent of sea ice; additionally, ocean currents were more variable in warm years (Stabeno et al., 2012a:38–39). These findings may reflect local residents' reports of increasing difficulties in forecasting weather with consequent implications for access to harvest areas, as well as observations of reduced sea ice over much of the last several decades at Togiak and Emmonak. Also, Bering Sea Project findings show that recruitment of pollock and Pacific cod was below average in the warm years of 2001–2005, which was likely due to reduced populations of zooplankton. Reduced prey may also explain fewer sightings of fin whales on the southeastern Bering Sea shelf in warm years compared to cold years (Stabeno et al., 2012a:41). These findings are consistent with reports of key respondents, especially at Togiak, of reduced populations of fish, birds, and marine mammals that they explain at least in part as a consequence of a changing climate. Also, Stabeno et al. (2012b) note potentially different effects on the ecosystems of the southern and northern Bering Sea if warming continues, with the southern Bering Sea warming while the northern Bering Sea remaining cold. This geographic difference may correspond with the more prominent theme of changing conditions and reduced resources in the more southern study communities of Akutan and Togiak in comparison with Savoonga, a difference that may increase with time. For additional discussion of potential links between the findings of the BSIERP LTK research and other component of BSIERP, see Huntington et al. (2013).

5. Conclusions

In short, subsistence hunting, fishing, and gathering remain nutritionally, economically, culturally, and spiritually essential to individual and community well-being in the five study communities of Akutan, Emmonak, Savoonga, St. Paul, and Togiak. Access remains a key to hunting and fishing success. Access is shaped by environmental factors, such as abundance, distribution, weather, ice, and travel conditions. It is also affected by economic factors such as costs of equipment and fuel. Residents of the study communities continue to demonstrate considerable flexibility in their subsistence activities on an annual and long-term basis.

Indeed, northern peoples have always faced a great deal of variability in their physical, economic, and political environments. Consequently, the capacity to adapt to change is an important part of their cultures (e.g. Berkes and Jolly 2001). In this study, key respondents observed that change itself is not remarkable, but constant.

As keen and systematic observers of their environment, subsistence hunters, fishers, and gatherers tend to see the world "holistically" or "ecologically." As this project has illustrated, through both structured surveys and key respondents interviews, residents of Bering Sea communities seek understanding of the connections between physical and biological components of the world they experience through all the seasons and across years and generations. There appeared to be a consensus that the ecosystem is changing physically and biologically. There also appears to be a consensus that

economic, social, and cultural changes are taking place as well. Overall, the residents of these Bering Sea study communities have been able to respond to these changes so far, but the future is less clear if such changes intensify or accelerate. Clearly, the residents of Bering Sea communities should be essential partners in future efforts to understand the complex processes that affect the natural resources of their homeland.

Acknowledgments

First, we thank the tribal governments of each study community for their approval to conduct the research. Hundreds of individuals took the time to be interviewed; without their participation, this project would not have been possible.

We thank the North Pacific Research Board for funding the LTK component of the BSIERP project. We also thank the Regional Advisory Board and the five Community Advisory Boards for their support, guidance, and comments.

This is NPRB Publication no. 400. This project was part of the Bering Sea Integrated Ecosystem Research Program, and this paper is BEST-BSIERP Publication no. 84.

References

- Ahmasuk, A., Trigg, E., 2007. A Comprehensive Subsistence Use Study of the Bering Strait Region. A Report to the North Pacific Research Board. Kawerak, Inc. Nome, Alaska.
- Alaska Department of Fish and Game (ADF&G), 2012. Community Subsistence Information System. <<http://www.adfg.alaska.gov/sb/CSIS/>> (Accessed 24.2.12).
- Alaska Department of Labor and Workforce Development (ADLWD), 2012a. Demographic profile for Akutan city. Research and Analysis Section. <<http://live.laborstats.alaska.gov/cen/dp.cfm>> (Accessed 24/2/12).
- Alaska Department of Labor and Workforce Development (ADLWD), 2012b. Consumer Price Index Inflation and Deflation Calculators. <<http://labor.alaska.gov/research/cpi/inflationcalc.htm>>. (Accessed February 2012).
- Alaska Federation of Natives, 1993. Guidelines for research. <<http://www.ankn.uaf.edu/iks/afnguide.html/>> (Accessed 24.2.12).
- Benter, B., December 7 2011. Personal communication regarding subsistence harvests of walrus at Savoonga, Alaska. US Fish and Wildlife Service, Marine Mammal Marking and Tagging Program, Anchorage, Alaska.
- Berkes, F., Jolly, D., 2001. Adapting to climate change: social-ecological resilience in a Canadian Western Arctic community. *Conserv. Ecol.* 5 (2), 18.
- Cochran, W.G., 1977. *Sampling Techniques*, 3rd edition John Wiley & Sons, New York.
- Coffing, M., Scott, C.L., Utermohle, C.J., 1998. The subsistence harvests of seals and sea lions by Alaska Natives in three communities of the Yukon-Kuskokwim Delta, Alaska, 1997–98. Alaska Department of Fish and Game. Division of Subsistence Technical Paper no. 255, Juneau.
- Coffing, M., Scott, C.L., Utermohle, C.J., 1999. The subsistence harvests of seals and sea lions by Alaska Natives in three communities of the Yukon-Kuskokwim Delta, Alaska, 1998–99. Alaska Department of Fish and Game. Division of Subsistence Technical Paper no. 257, Juneau.
- Commercial Fisheries Entry Commission (CFEC), 2012. Fishery Statistics—Participation and Earnings. <www.cfec.state.ak.us>.
- Dumond, D.E., 1984. Prehistory of the Bering Sea Region. In: Damas, D. (Ed.), *Handbook of North American Indians*, vol. 5. Smithsonian Institution, Washington, pp. 94–105, Arctic.
- Fall, J.A., 1990. The division of subsistence of the Alaska Department of Fish and Game: an overview of its research program and findings: 1980–1990. *Arctic Anthropology* 27 (2), 68–92.
- Fall, J.A., Koster, D., 2012. Subsistence Harvests of Pacific Halibut in Alaska, 2010. Alaska Department of Fish and Game. Division of Subsistence Technical Paper no. 367, Juneau.
- Fall, J.A., Brown, C.L., Braem, N.S., Hutchinson-Scarborough, L.B., Koster, D.S., Krieg, T.M., Slayton, L., 2012. Subsistence Harvests and Use in Three Bering Sea Communities, 2008: Akutan, Emmonak, and Togiak. Alaska Department of Fish and Game. Division of Subsistence Technical Paper no. 371, Juneau.
- Fienup-Riordan, A., Reardon, A., 2012. *Ellavut: Our Yup'ik World and Weather: Continuity and Climate Change on the Bering Sea Coast*. University of Washington Press, Seattle.
- Fienup-Riordan, A., Brown, C.L., Braem, N.M., 2013. The value of ethnography in times of change: the story of Emmonak. *Deep-Sea Res. II*, 94, 301–311.
- Hopkins, K., September 29 2011. Seafood Processor Agrees to \$2.5 Million Pollution Fine. Anchorage Daily News.
- Hunn, E., Sepez, J., 2010. Draft Akutan Field Report for the Local and Traditional Knowledge Component of the Bering Sea Integrated Ecosystem Research Program. University of Washington and National Oceanographic and Atmospheric Administration (NOAA), Seattle.
- Huntington, H.P., Braem, N.M., Brown, C.L., Hunn, E., Krieg, T.M., Lestenkof, P., Noongwook, G., Sepez, J., Sigler, M.F., Wiese, F.K., Zavadil, P., 2013. Local and traditional knowledge regarding the Bering Sea ecosystem: selected results from five indigenous communities. *Deep-Sea Res. II*, 94, 323–332.
- Jacobson, S. A. 1984. *Yup'ik Eskimo Dictionary*. Alaska Native Language Center, University of Alaska. Fairbanks.
- Lestenkof, P.M., Zavadil, P.A., Zacharof, S.M., Melovidov, E.M., 2011. Subsistence Harvest Monitoring Results from 1999 to 2010 and Local and Traditional Knowledge Interview Results for St. Paul, Alaska. A Report to the North Pacific Research Board. Aleut Community of St. Paul Island, Alaska. Tribal Government Ecosystem Conservation Office.
- Moerlein K., C. Carothers. 2012. Total environmental change: impacts of climate change and social transition on subsistence fisheries in northwest Alaska. *Ecology and Society* 17(1):10.
- Moncrieff, C., Brown, C., Sill, L., 2009. Arctic Yukon Kuskokwim sustainable salmon initiative project final product: natural indicators of salmon run abundance and timing, Yukon River. Anchorage, AK: Yukon River Drainage Fisheries Association, Fairbanks, Alaska. Alaska Department of Fish and Game. Division of Subsistence.
- National Oceanic and Atmospheric Administration (NOAA), 2008. Marine Mammals: Subsistence Taking of Northern Fur Seals. Harvest Estimates. Federal Register, vol. 73, no. 107, Tuesday, June 3, 2008. Proposed Rules. <<http://www.gpo.gov/fdsys/pkg/FR-2008-06-03/pdf/E8-12323>>.pdf (Accessed 24.2.12).
- National Oceanic and Atmospheric Administration (NOAA), Thursday, February 9 2012. Marine Mammals: Subsistence Taking of Northern Fur Seals. Harvest Estimates. Federal Register, vol. 77, no. 27. Rules and Regulations. <<http://www.fakr.noaa.gov/frules/77fr6682.pdf>> (Accessed 24.2.12).
- National Science Foundation, 2012. Principles for the Conduct of Research in the Arctic. Prepared by the Interagency Social Science Task Force, Office of Polar Programs. <<http://www.nsf.gov/od/opp/arctic/conduct.jsp>> (Accessed 24.2.12).
- North Pacific Research Board, 2005. Science Plan. North Pacific Research Board: Anchorage.
- North Pacific Research Board, 2008. Understanding Ecosystem Processes in the Bering Sea: Bering Sea Integrated Ecosystem Research Program. Anchorage: North Pacific Research Board. Bering Sea Project Program Office.
- North Pacific Research Board, 2012. Bering Sea Integrated Ecosystem Research Program (BSIERP): Hypotheses. <<http://bsierp.nprb.org/focal/hypotheses.html>> (Accessed 24.2.12).
- Perry, P., 2010. Unit 18 Moose Management Report. Moose Management Report of Survey and Inventory Activities 1 July 2007–30 July 2009. In: Harper, P. (Ed.), Alaska Department of Fish and Game, Juneau, AK, pp. 271–281.
- Stabeno, P.J., Kachel, N.B., Moore, S.E., Napp, J.M., Sigler, M., Yamaguchi, A., Zergini, A.N., 2012a. Comparison of warm and cold years on the southeastern Bering Sea shelf and some implications for the ecosystem. *Deep-Sea Res. II* 65–70, 31–45.
- Stabeno, P.J., Farley, E.V., Kachel, N.B., Moore, S., Mordy, C.W., Napp, J.M., Overland, J.E., Pinchuk, A.L., Sigler, M.F., 2012b. A comparison of the Physics of the northern and southern shelves of the eastern Bering Sea and some implications for the ecosystem. *Deep-Sea Res. II* 65–70, 14–30.
- Tahbone, S.T., Trigg, E.W., 2011. 2009 Comprehensive Harvest Survey, Savoonga, Alaska. A Report to the North Pacific Research Board, Kawerak, Inc. Nome, Alaska.
- United States Census Bureau, 2011. The 2011 Statistical Abstract. Health and Nutrition: Food Consumption and Nutrition. Table 212 and Table 213. <http://www.census.gov/compendia/statab/cats/health_nutrition/food_consumption_and_nutrition.html> (Accessed 10.9.11).
- United States Department of Agriculture, 2011. Dietary Guidelines for Americans. Center for Nutrition Policy and Promotion. <<http://www.cnpp.usda.gov/Publications/DietaryGuidelines/2010/PolicyDoc/PolicyDoc.pdf>> (Accessed 2.24.12).
- Wolfe, R.J., 1981. Norton Sound/Yukon Delta Sociocultural Systems Baseline Analysis. Alaska Department of Fish and Game. Division of Subsistence Technical Paper no. 59, Juneau.
- Wolfe, R.J., Gross, J.J., Langdon, S.J., Wright, J.M., Sherrrod, G.K., L.J. Ellanna, V. Sumida, and P.J. Usher. 1984. Subsistence-Based Economies in Coastal Communities of Southwest Alaska. Alaska Department of Fish and Game Division of Subsistence Technical Paper no. 89, Juneau.
- Wolfe, R.J., Fall, J.A., Riedel, M., 2009. The subsistence harvest of harbor seals and sea lions by Alaska Natives in 2008. Alaska Department of Fish and Game. Division of Subsistence Technical Paper no. 347, Juneau.
- Wolfe, R.J., Scott, C.L., Simeone, W.E., Utermohle, C.J., Pete, M.D., 2010. The “Super-Household” in Alaska Native Subsistence Economies. Final Report to the National Science Foundation. ARC 0352611.



Mapping human interaction with the Bering Sea ecosystem: Comparing seasonal use areas, lifetime use areas, and “calorie-sheds”



Henry P. Huntington^{a,*}, Ivonne Ortiz^b, George Noongwook^c, Maryann Fidel^{d,h}, Dorothy Childers^e, Muriel Morse^f, Julia Beaty^g, Lilian Alessa^h, Andrew Kliskey^h

^a 23834 The Clearing Drive, Eagle River, AK 99577, USA

^b School of Aquatic and Fishery Sciences, University of Washington, BOX 355020, Seattle, WA 98195, USA

^c Savoonga Whaling Captains Association, Native Village of Savoonga, P.O. Box 202, Savoonga, AK 99766, USA

^d Aleut International Association, 333W. 4th Ave. Suite 301 Anchorage, AK 99501, USA

^e Alaska Marine Conservation Council, PO Box 101145, Anchorage, AK 99510, USA

^f 3240 Penland Parkway, #282, Anchorage, AK 99508, USA

^g 742 Woodland Ave., Old Town, ME 04468, USA

^h Resilience and Adaptive Management Group, University of Alaska Anchorage, 3211 Providence Drive, Anchorage, AK 99508, USA

ARTICLE INFO

Available online 7 March 2013

Keywords:

Calorie-shed
Subsistence use area
Bering Sea
Hunting
Fishing
Development

ABSTRACT

Alaska Native coastal communities interact with the marine environment in many ways, especially through the harvest of fish, marine mammals, and seabirds. The spatial characteristics of this interaction are often depicted in terms of subsistence use areas: the places where harvests and associated travel occur. Another way to consider the interaction is to examine the areas where harvested species range during their lifecycle or annual migratory path. In this paper, we compare seasonal subsistence use areas, lifetime subsistence use areas, and “calorie-sheds,” or the area over which harvested species range. Each perspective offers useful information concerning not only the nature of human–environment interactions but also the scope for potential conflict with other human activity and the means by which such conflicts could be reduced, avoided, or otherwise addressed. Seasonal subsistence use areas can be used to manage short-term activities, such as seasonal vessel traffic during community re-supply. Lifetime subsistence use areas indicate the area required to allow hunters and fishers the flexibility to adjust to interannual variability and perhaps to adapt to a changing environment. Calorie-sheds indicate the areas about which a community may be concerned due to potential impacts on the species they harvest.

© 2013 Elsevier Ltd. All rights reserved.

1. Introduction

Alaska Native communities on the islands and coast of the Bering Sea make extensive use of marine resources and may travel great distances to obtain them (e.g., Wolfe and Walker, 1987). Documenting these areas is of interest both to better understand patterns of human ecology (Ellanna et al., 1985) and to identify potential interactions or conflicts with other human activities such as shipping, industrial fishing, or offshore development (Stephen R. Braund and Associates, 2010; Tobias, 2009). In a time of rapid environmental change in the Bering Sea region, use areas can also give an indication of impacts on humans and also insight into the flexibility and adaptability required to

continue to thrive in a changing environment (Alessa et al., 2010; Fidel et al., 2012), including local evolving practices of resource management (Berkes, 1998).

Most studies of marine resource use areas have recorded the hunting, fishing, gathering, and traveling areas used over an individual's lifetime, which are then usually aggregated at the community level to create a map of the overall use area (e.g., Tobias, 2000, 2009). Some of these studies have segregated use areas by species, providing further insight into patterns on the land and sea (e.g., Freeman, 1976; Stephen R. Braund and Associates, 2011). Fewer studies have attempted to provide detailed breakdowns of seasonal patterns of use by species, showing seasonal and interannual variation in use areas (e.g., Fidel et al., 2012; Galganitis, 2010). The focus on use areas has also omitted consideration of the extent to which the harvested species move throughout the region, and thus the areas of the ocean upon which subsistence harvests draw, regardless of where the act of harvest occurs.

In this paper, we compare results from three studies that take different approaches to examining community interactions with

* Corresponding author. Tel.: +1 907 696 3564; fax: +1 907 696 3565.

E-mail addresses: hph@alaska.net (H.P. Huntington), ivonne@u.washington.edu (I. Ortiz), gnunguk@hotmail.com (G. Noongwook), maryann@bssn.net (M. Fidel), dorothy@akmarine.org (D. Childers), muriel.morse@gmail.com (M. Morse), juliabeaty@gmail.com (J. Beaty), adkliskey@uaa.alaska.edu (A. Kliskey).

their surroundings, using as our examples the maps made for three communities in on the Bering Sea coast of Alaska (Table 1). The three approaches we describe fall on a spectrum of mapping scales and techniques, each of which may be best suited for a particular purpose. Our intent is not an exhaustive review of various mapping methods, but rather the illustration of respective merits of different approaches and the introduction of the calorie-shed idea, to spur further thinking about the nature of human interactions with the environment at various scales and in various ways. The full range of approaches provides a way to systematize local knowledge and incorporate it with geo-spatial tools, which can lead to a number of benefits in understanding human–environment relationships and interactions (Anuchiracheeva et al., 2003; Lauer and Aswani, 2008).

At a short temporal scale and a fine geographical scale, mapping of use areas season by season provides insight into variability and also into the precise locations and times that subsistence users might be most sensitive to disruption by other activity or events. The seasonal maps presented here also include an evaluation of intensity of use, defined as the relative frequency that an area was used by respondents for subsistence. This can help set priorities for avoiding disturbance, such as identifying shipping routes that avoid most local hunting or fishing during the ice-free season.

At a broader scale, lifetime subsistence use area maps indicate the greater extent of travel, fishing, and hunting. Given the variability shown from season to season and year to year, these maps encompass the areas that a community may draw upon in any given year. The opportunity to use and keep using these areas is likely to contribute to the flexibility needed to adapt to variable or changing environmental conditions. Such areas, however, only show what has been done in the past. As equipment improves, for example more powerful outboard motors or the use of GPS to allow more confident navigation, use areas may expand if needed to access fish and animals. Other changes, however, may reduce the use area, for example the loss of sea ice may reduce spring travel on top of the ice, or higher gasoline prices may force people to stay closer to home.

At an even broader scale, the “calorie-shed” shows the where the food consumed in the community may have come from. Taking selected species from the list of those harvested in greatest quantities (Fall et al., 2013), we map the distribution and migrations of the species or population in question to determine the area of the ocean over which the food on one’s plate may have originated. The maps shown here are only the first-order approximation of the calorie-shed, in that they include only the species that are harvested and eaten, not the lower levels of the food web that produced those fish and animals. The calorie-sheds we have derived are also based only on a few species, and thus are more properly partial calorie-sheds. Nonetheless, the areal extent of even these example calorie-sheds indicate that the areas about which communities might reasonably be concerned, whether from impacts of environmental change or for the potential impact from other human activity, are indeed extensive.

Each perspective on human uses of the environment has its purpose, and it is not our intent to identify a preferred approach.

Instead, our comparison has two purposes. First, to show what each approach offers in order to allow better consideration of which is most appropriate in a given situation. Second, to introduce the concept of the calorie-shed and to place it in the context of the use-area mapping that has dominated the field to date. We begin by outlining the methods used for each approach, then continue with the results, including illustrative maps from each approach. The discussion explores the applications of the three approaches, with suggestions for future directions in research on the geographical dimensions of human interaction with ecosystems such as the Bering Sea.

This work arose as part of the Bering Sea Project, an ecosystem-scale interdisciplinary project funded by the North Pacific Research Board and the National Science Foundation (Sigler et al., 2010; Wiese et al., 2012). Discussions between Huntington and Ortiz about the distribution of subsistence species led to an invitation to two other research teams outside of the Bering Sea Project to collaborate on the analyses that are reported here. Connections of this type were a major goal of the interdisciplinary project, arising from collaborations developed among researchers over the course of their research and during the annual meetings of project researchers.

2. Methods

2.1. Seasonal subsistence use area mapping

Spatial data were collected as part of the Bering Sea Sub-Network (BSSN): A Distributed Human Sensor Array to Detect Arctic Environmental Change, a community-based, international research project. This five-year project was initiated to improve knowledge of environmental changes occurring in the Bering Sea enabling Arctic communities, governments and scientists to predict, plan and respond to these changes.

Data were collected by community research assistants using a standardized survey instrument consisting of three questionnaires, which included closed, open-ended, and multiple choice questions as well as a mapping component. Purposive sampling aimed at active harvesters was used to select participants. “Active harvesters” were defined as those who regularly engaged in hunting and fishing activities and had lived in the community for the previous 15 years. Community leaders, including the Tribal Council and the project’s local research assistants, identified active harvesters in each community according to these criteria.

In Gambell 95 respondents, or 58% of the 164 identified active harvesters (who in turn were 24% of the village population), provided input in the creation of these maps. In Togiak 103 respondents, or 46% of the 224 identified active harvesters (27% of the village population), provided input. These numbers reflect the total number of respondents who were interviewed from September 2009 to August 2010, although not all respondents had harvested the species addressed in this paper (Pacific walrus [*Odobenus rosmarus divergens*] for Gambell and sockeye salmon [*Oncorhynchus nerka*] for Togiak) during the specified seasons. The number of respondents providing input for each individual map is provided in the text of the map.

Table 1

Communities discussed in this paper. Population data are from the U.S. Census (2010). All three mapping approaches were used in each community, except Savoonga where no seasonal-use-area mapping was done.

Community	Population	Location	Cultural identity
Gambell	681	Island, northern Bering Sea	St. Lawrence Island Yupik
Savoonga	671	Island, northern Bering Sea	St. Lawrence Island Yupik
Togiak	817	Mainland, estuary, southeastern Bering Sea	Yup'ik

Respondents were interviewed twice a year for specified species and seasons. Each community identified the marine species which was considered most important to subsistence. In Gambell selected species included bowhead whale (*Balaena mysticetus*), Pacific walrus, three species of ice seals; bearded (*Erignathus barbatus*), spotted (*Phoca largha*), ringed (*Pusa hispida*), and Chinook salmon (*Oncorhynchus tshawytscha*). In Togiak selected species included Pacific walrus, harbor seal (*Phoca vitulina*), sockeye salmon, steelhead trout (*Oncorhynchus mykiss*) and smelt (*Thaleichthys pacificus*). Seasons were partitioned into six-month intervals, spring/summer (March–August) and fall/winter (September–February). Respondents were asked about harvests for the selected species that had occurred during the previous two seasons, for example if the interview was conducted in the fall or winter the respondent was asked about the harvests that had occurred during the previous spring or summer. They were asked to further identify the exact months or dates that the harvest occurred. Other questions elicited spatial information about any change in the location the harvest took place, travel to the location and new or unusual species observed at the location.

During interviews respondents circled areas on paper maps indicating where they went to harvest selected species during the previous season. The wording of this question was intended to capture where a person had searched and harvested. Distances traveled to common harvest locations varied in each community so maps were scaled accordingly. Respondents were provided with both a fine and broad scale maps. In Gambell maps were 1:400,000 and 1:1,500,000 and in Togiak maps were 1:175,000 and 1:825,000. Maps included major landmarks, rivers, lakes and a hillshade. Each paper map was digitized in ArcGIS 9.3.1 and joined with corresponding data from the survey questions. During the first year of this four-year project, a total of 239 drawn polygons were entered for Gambell and 346 for Togiak.

A kernel density analysis was used to aggregate harvest use areas. Spatial data were selected and isolated according to the season and species of the map being created. Since the size of individual polygons (drawn circles) varied, each polygon was given equal weight in the density analysis by using

$$X = C/A$$

where X equals the weighted value, C is a constant and A is the area of the polygon in m^2 . The resulting weighted value was used to convert the polygon to raster, then all rasters were added together. This layer was converted to a point layer using the value of each cell. Land areas greater than 1 km from shore and .5 km on either side of the rivers were excluded from analysis. Similarly, the seasonal maps from Gambell only display harvest use areas in Alaska (U.S.) waters. A kernel density analysis was run on the point layer using the default search radius. The resulting density classes are 10 equal intervals on a standardized scale representing the density of locations per unit area – effectively a dimensionless unit. For detailed methodology, see Alessa et al. (2008) and Fidel et al. (2012).

2.2. Lifetime subsistence use area mapping

A team from the Alaska Marine Conservation Council conducted the mapping project for the Bering Sea Elders Advisory Group in tribal communities from Kuskokwim Bay to Bering Strait. The purpose was to document the extent of areas used by Alaska Native communities along the Bering Sea coast for harvesting Pacific walrus, seals, whales, fish, and shellfish.

The maps selected for this paper are from interviews conducted in January 2010 in Gambell and Savoonga on St. Lawrence Island. Group mapping interviews were conducted with 5–7

experts in each village, who were selected by tribal officials for their knowledge and life experience. The groups of elders and active hunters were asked to draw the extent of their lifetime use area for walrus, seals, whales, and fish based on a common set of questions. The base map was the St. Lawrence Island section (including Russia and mainland Alaska for reference and landmarks) of NOAA chart #16006. Gambell and Savoonga data are combined because of an agreement with the participating tribes that data would be aggregated.

Small group interviews were used because the project was seeking very general spatial information, not specific details that might vary to a greater extent by individual respondent. The maps also incorporate lifetime data from an earlier period published by the Bering Straits Coastal Resource Service Area (1984). Interviews were conducted in English but the participants spoke among each other extensively in St. Lawrence Island Yupik and then provided answers in English to convey their collective knowledge of the general use area. GIS shapefiles were created using ArcGIS 9.3.1 and stored in a geodatabase. St. Lawrence Island tribes were sent draft maps that contained aggregated data from the two villages. These maps were reviewed by teams in each village and corrected with their suggested changes.

2.3. Species ranges for “calorie-sheds”

We chose the communities of Togiak, on the mainland, and Gambell and Savoonga, on St. Lawrence Island, as case studies to demonstrate the concept of calorie-sheds, because use area data from Togiak and from St. Lawrence Island were available to be analyzed together with harvest data collected during the Bering Sea Project (Fall et al., 2013). The species selected for the calorie-sheds shown here are not necessarily those harvested in greatest quantity, but are those that are important contributors to the diet for which range data were also available. The calorie-sheds represent the overlapping distribution of the marine/anadromous species harvested by a community. To illustrate the point, three species were selected for each community: pink salmon (*Oncorhynchus gorbuscha*), sockeye salmon, and harbor seal for Togiak; and pink salmon, Pacific walrus, and bowhead whale for Gambell and Savoonga. Distribution maps for each species were taken from both published literature and/or direct data; sources are summarized in Table 2.

For the Togiak calorie-shed, sockeye and pink salmon distributions are the ocean ranges of these species based on tag/release data for fish recovered in Bristol Bay/Aleutian Islands combined. These are recoveries of tagged fish reported to the former International North Pacific Fisheries Commission (INPFC) and to the North Pacific Anadromous Fish Commission (NPAFC). Data includes all coastal recoveries (1956–1995) of salmonids tagged with external (high-seas) tags during INPFC- and NPAFC-related tagging experiments in the North Pacific Ocean, and ocean recoveries (1980–1995) of coded-wire tagged salmonids released from Bristol Bay/Aleutian Islands as described in Myers et al. (1996). The area shown for harbor seals is the approximate distribution of the Bristol Bay stock, one of nine in Alaska as defined by genetic structure. The stock is nonmigratory (Allen and Angliss, 2011).

For the Gambell and Savoonga calorie-shed, the distribution of bowhead whales is that of the western Arctic or Bering Sea stock, including their summer in the Beaufort Sea, winter grounds in the Bering Sea, and migratory route through the Chukchi Sea (Allen and Angliss, 2011). The distribution for the Pacific walrus includes the aggregated distribution of males and females during summer and winter (Garlich-Miller et al., 2011). Pink salmon distribution represents the ocean range based on tag/release data for pink salmon from the North American stock. These are recoveries of

tagged fish reported to the former International North Pacific Fisheries Commission (INPFC) and to the North Pacific Anadromous Fish Commission (NPAFC). Data include all coastal recoveries (1956–1995) of salmonids tagged with external (high-seas) tags during INPFC- and NPAFC-related tagging experiments in the North Pacific Ocean, and ocean recoveries (1980–1995) of coded-wire tagged salmonids as described in Myers et al. (2007). Pink salmon distribution on the Bering Sea shelf is based on tag/release data and catch data of pink salmon as part of the Bering–Aleutian Salmon International Surveys (BASIS) (Ed Farley, unpublished data, Alaska Fisheries Science Center, NOAA, 2011).

3. Results

3.1. Seasonal subsistence use areas

Fig. 1 displays the seasonal harvest areas used by residents of Togiak for sockeye salmon. As expected, harvests during the summer were concentrated in Togiak Bay and near the mouth of Togiak River. In the fall, harvest areas coincide with seasonal

salmon runs moving up-river to Togiak Lake. No harvests were reported during winter and spring. These harvest activities are indicative of resource-maximizing and time-minimizing strategies found in many optimal foraging theories (Smith, 1991). The total area for salmon harvest use areas during the summer season was 2500 km², and fall was 2000 km².

Fig. 2 displays the seasonal harvest of Pacific walrus by the residents of Gambell. The spring walrus hunt included the greatest number of people ($n=25$) and encompassed the largest area when compared with the other seasons. The timing of the walrus hunt is consistent with Alaska Department of Fish and Game and U.S. Fish and Wildlife Service harvest data as compiled in Metcalf and Robards (2008). The extent of the harvest area varies. It is 18,800 km² in the spring, 12,200 km² in the summer, 250 km² in the fall and 1500 km² in the winter.

3.2. Lifetime subsistence use areas

Fig. 3 shows combined data from Gambell and Savoonga for lifetime use areas for Pacific walrus, gathered during the interviews

Table 2
Sources of information for species distribution maps.

Species	Source	
<i>Togiak</i>		
Pink salmon	Tag release data for Bristol Bay/Aleutian Islands	Myers et al. (1996)
Sockeye salmon	Tag release data for Bristol Bay/Aleutian Islands	Myers et al. (1996)
Harbor seal	Published report on harbor seal stock identity and distribution	Allen and Angliss (2011)
<i>Savoonga</i>		
Pink Salmon	Tag release data for central and western Alaska pink salmon catch data BASIS database	Myers et al. (2007) and Ed Farley, AFSC, (unpublished data, 2011)
Pacific walrus	Published report Status Review of Pacific Walrus by Biological Review Team	Garlich-Miller et al. (2011)
Bowhead whale	Published report Western Arctic or Bering Sea stock	Allen and Angliss (2011)

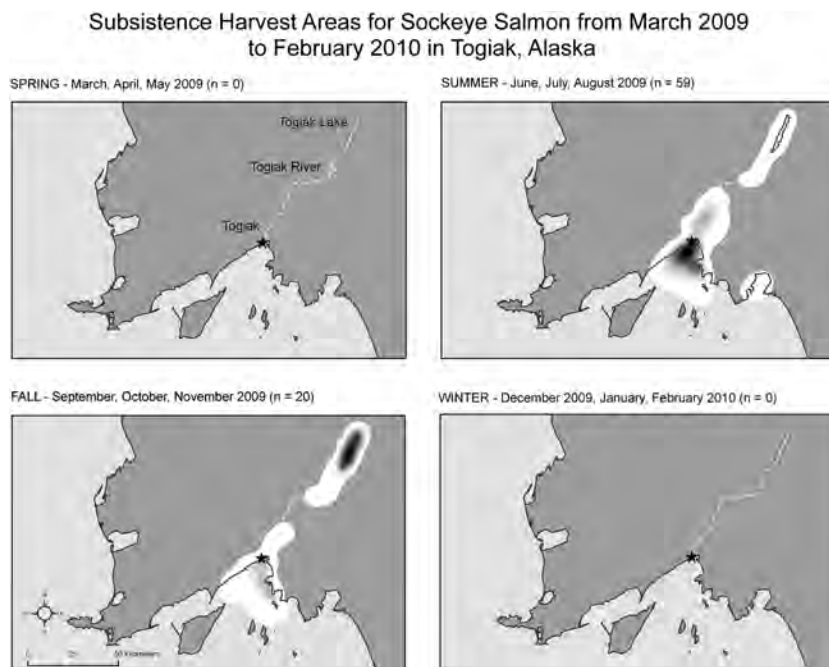


Fig. 1. The seasonal harvest areas for sockeye salmon used by residents of Togiak, Alaska in 2009–2010. Not all respondents harvested the specified species during each season displayed in this figure and Fig 2. The number of respondents per species and season is shown on each panel. Both figures display the intensity of subsistence activity on a dimensionless interval scale, whereby each grayscale step represents an equal step in activity level, with the greatest intensity shown in black. See Methods for more details.

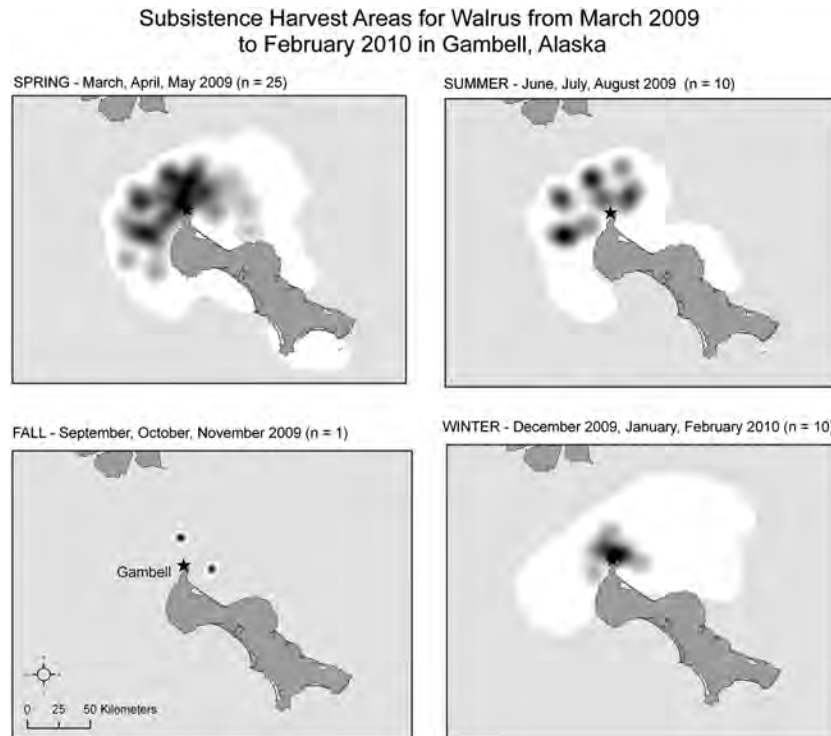


Fig. 2. The seasonal harvest areas for Pacific walrus for 2009–2010, as reported by residents of Gambell, Alaska. Not all respondents harvested Pacific walrus during each season displayed. The number of respondents per species and season is shown on each panel. Both figures display the intensity of subsistence activity on an interval scale, whereby each color step represents an equal step in activity level, with the greatest intensity shown in black.

described above and compared with similar data collected for the Bering Straits Coastal Resource Service Area (1984) in 1984. Although each data set represents lifetime use, the timeframes are different. Both sources were considered relevant to form a composite picture of the extensive area used over the course of a lifetime and to provide an indication of changes over time. The larger area shown from the 2010 interviews as compared with the 1984 results may reflect individual differences, technological improvements allowing hunters to travel farther, ecosystem changes requiring more extensive travel to find animals, or differences in how data were collected (detail on methods was not provided in the earlier source). Due to cooperative hunting and interaction between the two villages, the use area for Gambell is not appreciably different from that of Savoonga, so the comparison of use areas is reasonable. Lifetime use areas and calorie-shed maps include both Gambell and Savoonga, which is appropriate at that scale, while seasonal use areas are provided for Gambell only.

The Pacific walrus hunting area makes a useful comparison with the 2009–2010 seasonal Pacific walrus use areas for Gambell shown in Fig. 2, and the Pacific walrus calorie-shed for Gambell and Savoonga shown in Fig. 5. These temporal and spatial comparisons allow for better observations in the changes and adaptations in social foraging behaviors and practices (Smith and Winterhalder, 1981). It also covers all or nearly all of the area used for subsistence hunting of other marine species, and thus is a close approximation of the total lifetime subsistence use area for the marine environment. The lifetime subsistence use area for Pacific walrus from both communities, as documented in the Alaska Marine Conservation Council study, is 68,430 km².

3.3. Calorie-sheds

Fig. 4 shows the partial calorie-shed for Togiak. Salmon are highly migratory species spending several years in the ocean, mostly the North Pacific and Gulf of Alaska. In contrast, harbor seals are a nonmigratory species residing in the vicinity of the Bristol Bay

area year round. The area covered by sockeye salmon is about 5 million km², for pink salmon about 4.2 million km², and for harbor seals about 110,000 km². The overlap in range yields a total area of about 6.4 million km² for Togiak's three-species calorie-shed.

Fig. 5 shows the partial calorie-shed for Gambell and Savoonga. Bowhead whales and Pacific walrus spend part of the year in the Arctic Ocean, whereas salmon migrate southwards. Savoonga and Gambell thus lie at the crossroads of major marine migrations in the North Pacific region. The area covered by bowhead whales is about 1.5 million km², for walrus about 1.7 million km², and for pink salmon about 3.4 million km². The overlap in range yields a total area of about 5.2 million km² for Gambell and Savoonga's three-species calorie-shed.

The different locations of the St. Lawrence Island communities and of Togiak make them vulnerable to different though related potential impacts of climate change on arctic and subarctic populations. Togiak lies in the region of the southern marginal ice edge (Stabeno et al., 2012), whereby a decrease in ice extent might significantly impact the southern distribution limit of some species, such as walrus and ice seals, even if the overall abundance of these species were to stay the same. In contrast, Savoonga and Gambell are less susceptible to ice-edge effects but have a stronger reliance on arctic marine species and hence are more vulnerable to overall changes in abundance or adverse effects on the arctic feeding grounds for bowhead whales, Pacific walrus, and other marine mammals. Further analysis of the characteristics of the calorie-sheds and any changes thereto over time may shed light on impacts from and susceptibility to climate change.

4. Discussion

Human interactions with ecosystems are multi-faceted, from bare physical presence and location, through the use of ecosystem

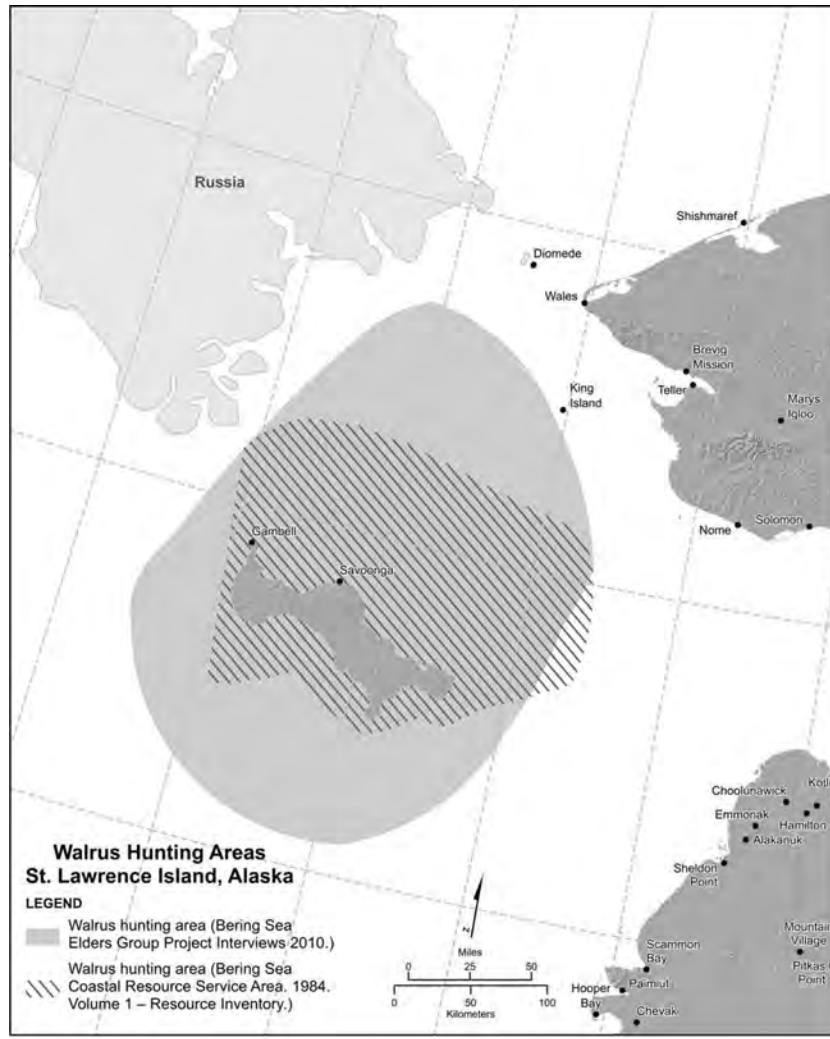


Fig. 3. Lifetime Pacific walrus use area map for St. Lawrence Island (Bering Straits CRSA 584 1984, and Alaska Marine Conservation Council project interviews, 2008–2011).

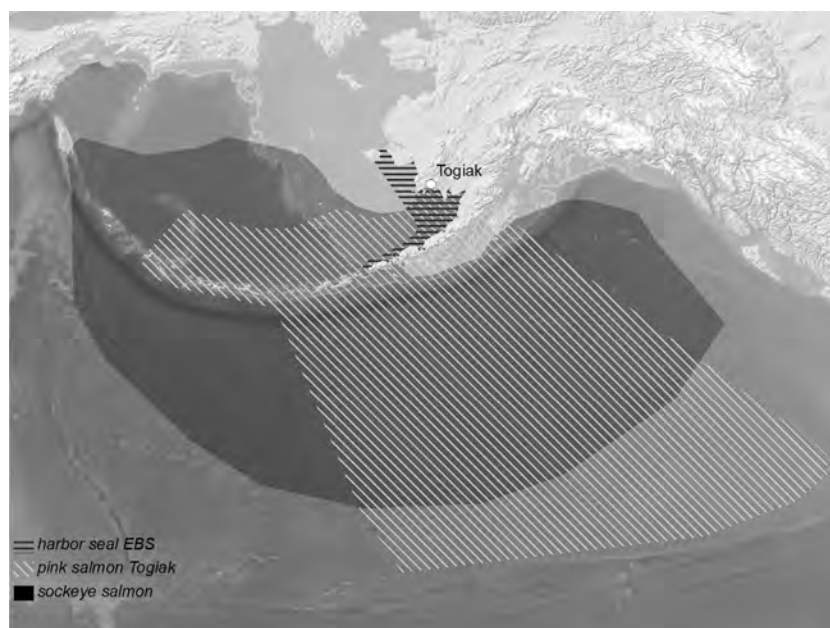


Fig. 4. Partial calorie-shed for Togiak based on the distribution of pink salmon, sockeye salmon, and harbor seal.

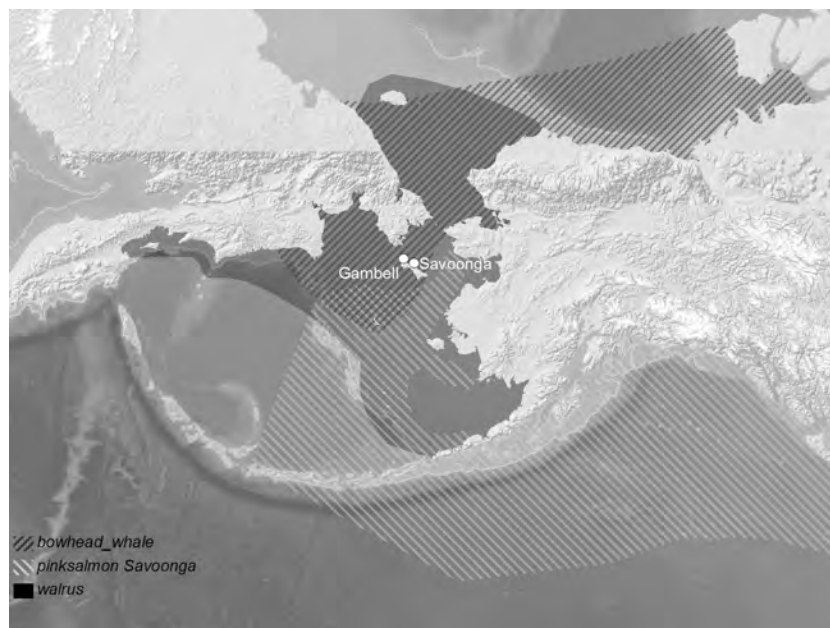


Fig. 5. Partial calorie-shed for Gambell and Savoonga based on the distribution of bowhead whales, Pacific walrus, and pink salmon.

services drawing on large areas (e.g., Costanza et al., 1997) or widely distributed impacts (e.g., Jackson et al., 2001), to simply appreciating the existence of species and places (e.g., Turpie, 2003). In assessing the geographical aspects of those interactions, various mapping techniques offer a variety of perspectives on the extent and nature of human use of the environment. These perspectives, in turn, offer insights into the ways in which environmental changes, anthropogenic or otherwise, can affect use patterns and potentially the well-being of the individuals, communities, or regions in question.

The three approaches presented in this paper focus on indigenous communities on the Bering Sea coast in Alaska. With no road network, the communities are isolated and typically at some distance from one another, although use areas may overlap with those of (relatively) nearby communities. Current interest in subsistence use areas and calorie-sheds stems largely from concerns about potential impacts from industrial activity and climate change. Industrial activity may cause disturbance to the species being harvested or to the harvesters themselves, and thus it is important to understand where local residents travel, hunt, and fish. Because the animals that are harvested range and migrate far beyond the local use area, it is also important for local communities to know whether and how industrial activity well beyond their region may affect the availability of prey species. The impacts of climate change may be more diffuse, but may still greatly affect hunting and fishing success through changes in distribution, abundance, and access. Furthermore, changes in distribution of prey species may affect the threats to which they are exposed during their annual migratory cycle. For the sake of simplicity, however, this discussion will focus on industrial impacts.

Each of the three approaches offers specific insights into various aspects of potential local impacts from industrial activity. Seasonal subsistence use areas, especially when mapped according to intensity, can be used to plan for and mitigate potential disturbances. For example, the arrival of annual re-supply barges will traverse use areas right to the community. Nonetheless, an awareness of local hunting and fishing patterns can help determine routes that will produce the least disturbance. The timing of barge arrival may depend on factors beyond local control, but

nonetheless, an awareness of seasonal variation in use areas or intensity can help in scheduling barge traffic or other such activity. Similarly, planning of shipping routes through the northern Bering Sea could benefit from input such as Fig. 2, suggesting that the east side of St. Lawrence Island may be preferable (at least for walrus hunters from the village of Gambell), or since shipping is concentrated during low ice or ice-free months, ships could avoid local impacts by staying well to the west and northwest of the island. Note that there are other considerations for shipping that could be informed by local expertise but are separate from conflicts with hunting areas (e.g., knowledge of dangerous currents), but those are not represented on these maps.

Lifetime subsistence use areas show the area in which industrial activity may affect local patterns to some extent at least. There is likely to be variability from year to year in use areas and patterns, depending on the conditions of that particular season and other factors. Thus, making plans on the basis of a single season's use area is shortsighted at best. The lifetime use areas show the larger area used over time to provide for the villages' needs, in which disturbances may affect community members at some point, even if not immediately or not in every year. For longer term disturbance, such as offshore installations or industrial fishing zones, the lifetime use areas may be a better indicator of potential conflicts than are the seasonal use maps, which in turn are more useful for finer-scale planning purposes. Creating an area of special protection or regulation may be appropriate based on the general lifetime use area maps, to minimize the potential for impacts over a longer period than, say, a single ship transit or season. Models of locally informed maps have proved successful in creating similar marine protected areas in Oceania (Aswani and Lauer, 2006; Lauer and Aswani, 2008).

Disturbance to hunters and fishers, however, is only one potential pathway for impacts. Disturbing the species being hunted or fished can also result in losses to the community. The calorie-shed offers a look at the larger area where industrial activity has the potential for disturbing subsistence patterns. The calorie-shed for Togiak, for example, indicates that the North Aleutian Basin, an area of oil and gas potential (Gautier et al., 2009), lies well within the range of species harvested in that

community. Similarly, the calorie-shed for Savoonga (which is likely to be identical or nearly so to the calorie-shed for Gambell, although the seasonal subsistence use areas will differ greatly; the lifetime use area map in Fig. 3 combines both communities) extends into the Chukchi and Beaufort Seas, another area of great interest in offshore oil and gas reserves (Gautier et al., 2009), and includes the Bering Strait, a major bottleneck for ship traffic into and out of the Arctic (AMSA, 2009). Thus, the calorie-sheds and the local knowledge represented within them help make the case that the communities in question have an interest in what occurs in those areas and should be part of discussions about risks, mitigation measures, and other features of exploration and development plans (Anuchiracheeva et al., 2003).

The methods for documenting subsistence use areas, though continuing to develop, are reasonably well established. The method for generating calorie-sheds is a new one, though in some respects a simple matter of combining subsistence harvest survey data (species and quantities harvested) with maps of the ranges of species or stocks from the area in question. Nonetheless, such range maps do not exist for many subsistence species, or lack the stock specificity needed to properly delimit the calorie-shed rather than including the entire range of the species. Furthermore, it would be ideal to be able to extend the calorie-shed down the food web, to understand where the primary productivity occurs that ultimately ends up as food consumed by people in the community. The biological data are not yet available to complete this analysis with any confidence, at least for the Bering Sea.

If these three tools offer promise for helping communities and others identify potential impacts and thus to find ways to prevent or mitigate those impacts, the proof of the concept will lie in actually using maps of this kind for that purpose. Providing such information in ways that are technologically and intellectually accessible, on a timeline that matches the need for information in various planning processes, will require further effort on all sides. Research studies can produce the underlying information, but effective communication and collaboration will be needed to place the results in the hands of those who can use them.

Acknowledgments

This paper combines findings from three separate research projects. For the work on the calorie-sheds and the impetus to place that work in a wider context, we thank the North Pacific Research Board for funding our work, and the leaders and researchers of the Bering Sea Project for their encouragement and support. We also thank the LTK Regional Advisory Board and its members for providing guidance and ideas for our project.

The lifetime subsistence mapping work was done by a team at the Alaska Marine Conservation Council including Dorothy Childers, Muriel Morse and Julia Beaty. The project was undertaken for the Bering Sea Elders Advisory Group, which is made up of 39 participating tribal governments from Kuskokwim Bay to the Bering Strait. We thank David Bill, Sr. and Fred Phillip, respectively chairman and executive director of the Bering Sea Elders Advisory Group, for their support. We also thank the many tribal administrators, other tribal office staff, and the elders, hunters and fishermen who supported the project interviews and review process in their villages. The full project report, entitled “The Northern Bering Sea: Our Way of Life,” is accessible at www.beringseaelders.org.

The seasonal subsistence mapping work was part of the Bering Sea Sub-Network (BSSN) – A Distributed Human Sensor Array to Detect Arctic Environmental Change, funded by the National Science Foundation through award number 856305 (Principal Investigator Lilian Alessa, Resilience and Adaptive Management

Group, University of Alaska Anchorage) and award number 856774 (Principal Investigator Victoria Gofman, Aleut International Association). GIS support came from UAA, RAM Group, special thanks to Brett Woelber and Leah Bower. Grace Beaujean from the RAM Group provided invaluable suggestions on the human ecology literature. The seasonal subsistence mapping work would not have been possible without the diligent help of community research assistants Olia Sutton and Margie Coopchiak from Togiak, and Bobbi Ann Slwooko and Joni Ungott from Gambell.

For all three projects, we thank all those who contributed or helped gather the information that is presented on the maps shown herein.

We also thank Tom Van Pelt for his editing and three anonymous reviewers whose constructive comments improved the manuscript considerably.

This is NPRB Publication No. 399. This project was part of the Bering Ecosystem Study – Bering Sea Integrated Ecosystem Research Program, and this paper is BEST-BSIERP Publication No. 83.

References

- Allen, B.M., Angliss, R.P., 2011. Alaska marine mammal stock assessments, 2010. U.S. Department of Commerce, NOAA Tech. Memo. NMFS-AFSC-223.
- Alessa, L., Kliskey, A., Brown, G., 2008. Social-ecological hotspots mapping: a spatial approach for identifying coupled social-ecological space. *Landsc. Urban Plan.* 85, 27–39.
- Alessa, L., Kliskey, A., Williams, P., 2010. Forgetting freshwater: the effect of modernization on water values in remote Arctic communities. *Soc. Nat. Resour.* 23, 254–268.
- AMSA, 2009. Arctic marine shipping assessment 2009 report. Arctic Council, Akureyri, Iceland.
- Anuchiracheeva, S., Demaine, H., Shivakoti, G.P., Ruddle, K., 2003. Systematizing local knowledge using GIS: fisheries management in Bang Saphan Bay, Thailand. *Ocean Coast. Manage.* 46, 1049–1068.
- Aswani, S., Lauer, M., 2006. Benthic mapping using local aerial photo interpretation in resident taxa inventories for designing marine protected areas. *Environ. Conserv.* 33, 263–273.
- Bering Straits Coastal Resource Service Area. 1984. Bering Straits CRSA, vol.1 – Resource Inventory. Northern Resource Management, Anchorage, Alaska.
- Berkes, F., 1998. Indigenous knowledge and resource management systems in the Canadian subarctic. In: Berkes, F., Folke, C., Colding, J. (Eds.), *Linking Social and Ecological Systems: Management Practices and Social Mechanisms for Building Resilience*. Cambridge University Press, Cambridge, pp. 98–128.
- Costanza, R., d’Arge, S., de Groot, R., Farber, S., Grasso, M., Hannon, B., Limburg, K., Naeem, S., O’Neill, R.V., Paruelo, J., Raskin, R.G., Sutton, P., van den Belt, M., 1997. The value of the world’s ecosystem services and natural capital. *Nature* 387, 253–260.
- Ellanna, L.J., Sherrod, G.K., Langdon, S.J., 1985. Subsistence mapping: an evaluation and methodological guidelines. Technical Paper 125. Division of Subsistence, Alaska Department of Fish and Game, Juneau, Alaska.
- Fall, J., et al., 2013. Subsistence harvests in the BSIERP communities, 94, 274–291.
- Fidel, M., Gofman, V., Kliskey, A., Alessa, L., Woelber, B., 2012. Subsistence density mapping brings practical value to decision-making. In: Carothers, C., Criddle, K.R., Chambers, C.P., Cullenberg, P.J., Fall, J.A., Himes-Cornell, A.H., Johnsen, J.P., Kimball, N.S., Menzies, C.R., Springer, E.S. (Eds.), *Fishing People of the North: Cultures, Economics, and Management Responding to Change*. Fairbanks, Alaska SeaGrant, pp. 193–210.
- Freeman, M.M.R., (Ed.), 1976. Inuit land use and occupancy project. 3 vols. Minister of Supply and Services Canada, Ottawa.
- Galganitis, M., 2010. Annual assessment of subsistence bowhead whaling near Cross Island, 2009: continuation of monitoring activities annual report. Applied Sociocultural Research, Anchorage.
- Garlich-Miller, J., MacCracken, J.G., Snyder, J., Meehan, R., Myers, M., Wilder, J.M., Lance, E., Matz, A., 2011. Status Review of the Pacific Walrus (*Odobenus rosmarus divergens*). U.S. Fish and Wildlife Service. <http://alaska.fws.gov/fisheries/mmm/walrus/pdf/review_2011.pdf> (accessed 3.03.11).
- Gautier, D.L., Bird, K.J., Charpentier, R.R., Grantz, A., Houseknecht, D.W., Klett, T.R., Moore, T.E., Pitman, J.K., Schenk, C.J., Schuenemeyer, J.H., Sorensen, K., Tennyson, M.E., Valin, Z.C., Wandrey, C.J., 2009. Assessment of undiscovered oil and gas in the Arctic. *Science* 324, 1175–1179.
- Jackson, J.B.C., Kirby, M.X., Berger, W.H., Bjorndal, K.A., Botsford, L.W., Bourque, B.J., Bradbury, R.H., Cooke, R., Eerlandson, J., Estes, J.A., Hughes, T.P., Kidwell, S., Lange, C.B., Lenihan, H.S., Pandolfi, J.M., Peterson, C.H., Steneck, R.S., Tegner, M.J., Warner, R.R., 2001. Historical overfishing and the recent collapse of coastal ecosystems. *Science* 293, 629–637.

- Lauer, M., Aswani, S., 2008. Integrating indigenous ecological knowledge and multi-spectral image classification for marine habitat mapping in Oceania. *Ocean Coast. Manage.* 51, 495–504.
- Metcalf, V., Robards, M., 2008. Sustaining a healthy human–walrus relationship in a dynamic environment: Challenges for comanagement. *Ecol. Appl.* 18 (2, Supplement), 148–256.
- Myers, K.W., Aydin, K.Y., Walker, R.V., Fowler, S., Dahlberg, M.L., 1996. Known ocean ranges of stocks of Pacific salmon and steelhead as shown by tagging experiments, 1956–1995. (NPFAC Doc 192) FRI-UW-9614. University of Washington, Fisheries Research Institute, Seattle.
- Myers, K.W., Klovach, N.V., Gritensko, O.F., Urawa, S., Royer, T.C., 2007. Stock-specific distributions of Asian and North American salmon in open ocean, interannual changes, and oceanographic conditions. *North Pac. Anadromous Fish Comm. Bull.* 4, 159–177.
- Sigler, M.F., Harvey, H.R., Ashjian, C.J., Lomas, M.W., Napp, J.M., Stabeno, P.J., Van Pelt, T.I., 2010. How does climate change affect the Bering Sea ecosystem? *Eos* 91, 457–458.
- Smith, E.A., 1991. *Inujjamiut Foraging Strategies: Evolutionary Ecology of an Arctic Hunting Economy*. Aldine De Gruyter, New York.
- Smith, E.A., Winterhalder, B., 1981. New Perspectives on Hunter-Gatherer Socioecology. In: Smith, E.A., Winterhalder, B. (Eds.), *Hunter-Gatherer Foraging Strategies: Ethnographic and Archeological Analyses*. The University of Chicago Press, Chicago, pp. 1–12.
- Stabeno, P.J., Kachel, N., Moore, S., Sigler, M.F., Yamaguchi, A., Zerbini, A.N., 2012. Comparison of warm and cold years on the southeastern Bering Sea shelf and some implications for the ecosystem. *Deep-Sea Res. II* 65–70, 31–45.
- Stephen R. Braund and Associates, 2010. Subsistence mapping of Nuiqsut, Kaktovik, and Barrow. MMS OCS Study Number 2009-003. Minerals Management Service, Anchorage, Alaska.
- Stephen R. Braund and Associates, 2011. Chukchi and Beaufort seas national pollutant discharge elimination system exploration general permits reissuance: report of traditional knowledge workshops – Point Lay, Barrow, Nuiqsut, and Kaktovik. Prepared for Tetra Tech. and the U.S. Environmental Protection Agency. March 11, 2011.
- Tobias, T.N., 2000. Chief Kerry's moose: a guidebook to land use and occupancy mapping, research design and data collection. Union of British Columbia Indian Chiefs and Ecotrust Canada, Vancouver.
- Tobias, T.N., 2009. Living proof: the essential data-collection guide for indigenous use-and-occupancy map surveys. Ecotrust Canada and Union of British Columbia Indian Chiefs, Vancouver.
- Turpie, J., 2003. The existence value of biodiversity in South Africa: how interest, experience, knowledge, income, and perceived level of threat influence local willingness to pay. *Ecol. Econ.* 46, 199–216.
- U.S. Census. 2010. <<http://www.census.gov/popfinder/>>, (accessed 15.10.12).
- Wiese, F.K., Wiseman, W.J., Van Pelt, T.I., 2012. Bering Sea linkages. *Deep-Sea Res. II* 65–70, 2–5.
- Wolfe, R.J., Walker, J., 1987. Subsistence economies in Alaska: productivity, geography and development impacts. *Arctic Anthropol.* 24 (2), 56–81.



The value of ethnography in times of change: The story of Emmonak[☆]



Ann Fienup-Riordan^{a,*}, Caroline Brown^b, Nicole M. Braem^b

^a Calista Elders Council, 9951 Prospect Dr., Anchorage, AK 99507, USA

^b Alaska Department of Fish and Game, Division of Subsistence, 1300 College Road, Fairbanks, AK 99701-1599, USA

ARTICLE INFO

Available online 8 April 2013

Keywords:

Bering Sea
Local and traditional knowledge
Alaska Natives
Subsistence
Ethnography

ABSTRACT

This paper considers the connections between the social science components of two major multi-disciplinary research projects recently carried out in the Eastern Bering Sea: The Bering Ecosystem Study Program (BEST) and the Bering Sea Integrated Ecosystem Research Program (BSIERP). Although the primary concern of the larger Integrated Bering Sea Project was oceanographic, a significant effort was made to understand the impacts of changes in the Eastern Bering Sea on coastal communities. We describe our complementary research in Emmonak in order to put the local and traditional knowledge (LTK) survey and interview data gathered during the BSIERP study into ethnographic and historical context to show how important time depth is in the interpretation of LTK. Taking examples from salmon fishing, seal harvesting, and local understandings of place, we argue that a comprehensive ethnographic approach, including both LTK and cultural history, is essential in understanding contemporary Bering Sea coastal communities.

© 2013 Elsevier Ltd. All rights reserved.

1. Introduction

Recent oceanographic drift buoy experiments in Kuskokwim Bay (Danielson et al., 2011), parallel the 100-years-previous drift of a young Yup'ik boy, Atertayagaq (lit., "Someone small who drifted away"), who was lost on the ice for three months and floated south from the Kuskokwim to the Aleutians. Elders still tell his story, sharing knowledge of ocean currents embedded in a dramatic tale of personal survival. Bringing these two together—Danielson's scientific observations and Yup'ik oral tradition—each informs the other (Fienup-Riordan and Rearden, 2012:10–25).

This paper likewise attempts to bring together two things—collaborative research carried out by the Calista Elders Council (CEC) (the primary heritage organization for southwest Alaska, representing the 1300 elders 65-years and older) under the BEST program and the LTK survey and interview work carried out under the BSIERP program. Until 2011, the BEST and BSIERP efforts were in different communities. Between 2006 and 2010, the CEC carried out fieldwork and topic-specific gatherings with Yup'ik elders and community members from the five Nelson Island communities of Newtok, Tununak, Toksook Bay, Nightmute, and Chefornak (Fienup-Riordan, 2010; Rearden and Fienup-Riordan, 2011). Between 2007 and 2012, the BSIERP team carried out harvest surveys and in-depth interviews with members of five Bering Sea coastal communities spread between St. Lawrence

Island and the Aleutians, including Savoonga, Emmonak, St. Paul, Togiak, and Akutan (see Huntington et al., 2013).

In January 2011, CEC completed collaborative ethnographic research on Nelson Island and thanks to continued National Science Foundation (NSF) support, moved 150 miles north to begin a major four-year cultural history project in four lower Yukon River communities. The largest of these communities is Emmonak (population 750), where the Alaska Department of Fish and Game (ADF&G) did both harvest surveys and in-depth interviews in 2009 and 2010 as part of the BSIERP effort and where CEC staff carried out fieldwork and topic-specific gatherings with elders and youth in March and August 2011 (Fig. 1).

The following pages will provide a brief ethnography of Emmonak as a way of putting the LTK research carried out under BSIERP into ethnographic and historical context to show how important time depth (ie. long-term participant observation) is in the interpretation of LTK. A primary critique of LTK studies has been the unfortunate decontextualization of local knowledge as pieces of information, wrenched from their cultural context and repackaged for an external forum such as management (Nadasdy, 2005). Classic anthropological fieldwork is by definition synthetic, and a good ethnography brings together all facets of people's lives. A community's economic, social, political, and spiritual activities are never discrete, and the unique cultural perspectives people bring to their circumstances are important in interpreting both their actions and their knowledge systems. Just as one needs to study biological characteristics of individual species as well as their ecological linkages to organisms within other trophic levels to understand the Bering Sea ecosystem as a whole, LTK in-depth

* Corresponding author. Tel:+907 346 2952.

E-mail addresses: riordan@alaska.net (A. Fienup-Riordan), caroline.brown@alaska.gov (C. Brown), nicole.braem@alaska.gov (N.M. Braem).

[☆]"Our subsistence way of life keeps us standing." John Phillip, January 2011:272.



Fig. 1. Aerial View of Emmonak. Alaska Department of Fish and Game.

survey information and more open-ended community driven cultural histories are two ways of looking at communities that when put together teach us more than the sum of their parts.

This paper combines the results of the survey and interview work carried out under BSIERP with elder observations recorded by CEC staff during fieldwork and topic-specific gatherings on the Yukon delta during 2011. The discussion also includes historical and comparative observations by the principal author based on her long-term relations with Yup'ik residents. The resulting ethnographic account of one coastal community—Emmonak—is put forward to illuminate the social and economic conditions facing many Alaskan coastal communities today. In doing so we will demonstrate the value of a comprehensive ethnographic perspective for a fuller understanding of the ways in which marine ecosystems matter to human communities. Our discussion takes examples from salmon fishing, social and environmental change, seal harvesting, and local understandings of place. These topics emerged as key themes in both interviews and elder gatherings. We discuss each topic in a narrative fashion—weaving together LTK survey data, observations by community members, historical information, and insights gained through long-term observation—to support our argument that an ethnographic perspective, involving cultural history as well as LTK research, is essential to understanding change in contemporary coastal communities.

2. Methods

For the purposes of this paper, local and traditional knowledge (LTK) refers to tacit knowledge embodied in life experiences and reproduced in everyday behavior and speech. As Cruikshank (2005:9) points out, “local knowledge has become a common-sense term, couched in acronyms like TEK (traditional ecological knowledge) or IK (indigenous knowledge), gaining new visibility in management science studies, but too often depicted as static, timeless, and hermetically sealed” (see also Fienup-Riordan, 1990:167–91; Nadasdy, 2005:114–46; Scott, 1996). Yup'ik knowledge is, first and foremost, dynamic, changing, and socially situated. As such it is best considered as a knowledge system embedded in a particular cultural context. The value of an ethnographic perspective is that it does not study isolated aspects of Yup'ik knowledge but attempts to provide a comprehensive and holistic view of Yup'ik cultural ecology (Fienup-Riordan and Rearden, 2012).

Local and traditional knowledge was passed on orally in the past; today it can be found in bilingual publications and on the web. In either case, experience and “best practices” are encoded in language, narrative, and social rules. Together, this body of knowledge becomes

the foundation for cultural identity. All components of this identity are subject to change over time, as culture change is the rule rather than the exception. In fact, in southwest Alaska, it is “traditional” to use the best technology available, e.g. to change. In a given situation change can be either positive or negative: it is not inevitably good or bad. One can view culture change as a negotiation process with creative, although not necessarily painless, outcomes. Instead of viewing individuals as responding to fixed cultural norms, in the last twenty years anthropologists have shifted their emphasis to understanding how people continually reshape their lives in the course of everyday experiences (Cruikshank, 1998; Fischer, 2007). Some argue that it is in the discontinuities between the values people hold and the continually shifting circumstances of everyday life that we find the primary driving forces of change (Fienup-Riordan, 2012:10).

Ethnography is a qualitative research method employed in the understanding of human society and culture, with culture defined as the system of symbols and meanings that guide the lives of a particular group of people. The field of socio-cultural anthropology pioneered ethnography as a means of gathering and synthesizing empirical data on human societies and cultures. Data collection is often done through a combination of participant observation, field notes, interviews, questionnaires, and archival research which aims to capture the social meanings and ordinary activities of community members—in short, the use of all known insider or local descriptions in order to constitute an “objective” outsider description (Sahlins, 2002). This combination allows for a more nuanced, in-depth portrait of people and their communities than any one method used in isolation would allow. Ethnography relies greatly on personal experience. Participation, rather than just observation, is essential to the process. Finally, ethnography typically attempts to be holistic, including the history, natural environment, and social, political, economic, and spiritual relations of a community (Geertz, 1973; Fabian, 2008).¹

Beginning in the mid-1980s cultural anthropology moved from a strictly interpretive ethnography, recognizing people as creative actors constructing their worlds, to ethnographic writing which drew attention to the place of the ethnographer, whose particular viewpoint in creating an ethnographic account makes claims to objectivity problematic (Clifford and Marcus, 1986; Marcus, 2008). Many contemporary authors thus endeavor to describe society and culture without denying the subjectivity of the people we work with or claiming absolute knowledge or objective authority. This new openness of anthropology to diverse points of view has also led to increased emphasis on collaboration in research and ethnographic writing. This paper's principal author, Fienup-Riordan, has worked as a cultural anthropologist among Yup'ik people in southwest Alaska since 1976, when she spent a year on Nelson Island carrying out fieldwork and beginning to learn the Yup'ik language. In 2000, she was asked by Calista Elders Council (CEC) director Mark John to work with CEC in their efforts to document Yup'ik traditional knowledge, and she has worked collaboratively with CEC staff, especially translator Alice Rearden, ever since.²

CEC's primary information gathering tool has been the topic-specific gathering. Staff pioneered this format working with elders between 2000 and 2005 during a major traditional knowledge

¹ The ethical dimensions of ethnographic research are central to the proper use of these methods, as laid out in the Arctic Social Sciences code of ethics (<http://www.mnh.si.edu/arctic/html/ethics.html>).

² Discussing Westbrook's (2008) book *Navigators of the Contemporary: Why Ethnography Matters* (2008), Krauss (2011:190) notes that the role of anthropology today is to identify, understand, and talk about complex, contemporary situations. He writes: “There is a great openness in this approach and attitude; it's postcritical, but not arbitrary; it's deeply democratic and as such almost antiscience. The anthropologist does not explain the world, as do many of his colleagues in science. Instead, he slowly unfolds complex arrangements, settings, and situations and makes them ‘conversational.’ This is a huge accomplishment.”

project funded by the NSF's Arctic Social Science program. We found that meeting with small groups of elder experts, accompanied by younger community members, for two- and three-day gatherings devoted to a specific set of questions was an effective and rewarding way of addressing topics. Unlike interviews, during which elders answer questions posed by those who often do not already hold the knowledge they seek, gatherings (like academic symposia) encourage elders to speak among their peers at the highest level (Fienup-Riordan, 2005b:4–9; Fienup-Riordan and Rearden, 2012:4–5).

CEC gatherings always take place in the Yup'ik language, Alice Rearden then creates detailed transcriptions and translations of each gathering, and we work together to turn these transcripts into both bilingual publications and accompanying English texts. To date CEC has produced four sets of "paired" books—one English for general and scholarly audiences and the other bilingual for community use (Andrew, 2008; Fienup-Riordan, 2005a, 2005b, 2007; Fienup-Riordan and Rearden, 2012; Meade and Fienup-Riordan, 2005; Rearden and Fienup-Riordan, 2011; Rearden et al., 2005). Quoted statements in this paper were recorded in Yup'ik during CEC topic-specific gatherings, and they are cited by speaker's name, CEC gathering date, and transcript page number.

In gatherings, elders speak about their past selectively, not comprehensively, and what is not said is often as significant as what is said. Long and careful listening to these conversations provides unique perspectives on Yup'ik knowledge (Fienup-Riordan, 2005b:1–41). In gatherings, elders teach not just facts, they teach listeners how to learn. They share not only what they know but how they know it and why they believe it is important to remember. Finally, CEC staff and Yup'ik community members value topic-specific gatherings not merely as tools for documentation but as contexts of cultural transmission. The gatherings themselves are meaningful events that enrich lives locally at the same time their documentation has the potential to increase cross-cultural understanding globally.

Adding another dimension to the knowledge shared during CEC's more open-ended topic-specific gatherings, Caroline Brown and Nikki Braem of the Division of Subsistence, Alaska Department of Fish and Game (ADF&G), carried out subsistence harvest surveys and in-depth interviews in Emmonak between 2009 and 2011 as part of the Bering Sea Integrated Ecosystem Research project (BSIERP). Harvest surveys can provide additional opportunities to explore social and environmental change over time by quantifying aspects of harvest and distribution practices that raise questions about how and why particular shifts occur. Follow-up in-depth interviews allowed researchers to contextualize these changes through the experiences and understandings of local actors. This surveying and interviewing research included local partnering through Community Advisory Boards (CAB). The CAB in Emmonak included five active subsistence hunters. The project was introduced to the CAB in January 2009 through a detailed presentation during which researchers discussed the project components and the survey protocol with CAB members. Researchers met with CAB members again at the beginning of the April 2009 survey implementation trip.

In April 2009, a research team of ADF&G staff traveled to Emmonak to conduct the survey over 11 days. Each ADF&G researcher worked with one of five Emmonak residents hired as local research assistants to review household lists and conduct the surveys. These teams worked together to document the harvests of each surveyed household, trading off roles such as asking questions and mapping land use areas. Teams used a survey instrument that included a core harvest module that collected, for example, the number of salmon or bearded seals harvested, along with basic information about sharing or distribution of the harvest. For some species, the survey also gathered information on seasonality of

harvest, sex of the animals, and units harvested. Surveys also collected demographic, economic, and harvest assessment data. Research teams mapped "search areas" (the entire area a household used to look for a particular species) and, in some cases, actual harvest areas. Ultimately, the teams surveyed 109 out of 179 total households, or 61% of the community. Once survey data were coded and entered, information was processed with the use of the Statistical Package for the Social Sciences (SPSS). Harvest estimates were calculated based upon the application of weighted means (Cochran, 1977).

Interviews were conducted during two separate trips (September 2010 and April 2011) to document local and traditional knowledge (LTK) and contextualize the survey results. Semi-structured interview questions were designed to elicit descriptions of hunting practices over time as well as observations about any changes in the distribution or health and abundance of particular species. When possible, researchers attempted to build on respondents answers to understand how Emmonak hunters and fishers made connections between different species and to the environment and other aspects of social life (sharing, etc) and what themes were most important in those connections or relationships. For example, discussions about salmon quickly led to insights regarding locally relevant intra-species variation (e.g. white noses and bluebacks) as well as discussions of the history of subsistence and commercial salmon fishing in light of changing abundance, fuel prices, management, and participation in the fishery by younger people. Finally, researchers asked respondents to provide explanatory information about particular trends in the harvest data that helped make sense of the estimates. For example, factors such as changes in bird migrations, shifting food preferences, technological advances, resource abundance, employment, and fuel prices all played roles in changing or consistent harvest estimates. Thirteen individuals were interviewed in 11 interviews, including 11 men and 2 elder women. Respondents ranged in age between 55 and 82. Most were active marine mammal hunters, fishers, or both.

3. Results and discussion

3.1. *Emmonak: a community in distress*

Emmonak is familiar to many Alaskans because of a January 2009 letter by local resident Nick Tucker in which he declared that the people of Emmonak were starving (Tucker, 2009a, 2009b). Tucker's five-page letter was first published in the local paper, *The Tundra Drums*, and quickly picked up by the Anchorage Daily News, radio and TV, and bloggers nationwide. In it, Tucker described the perfect storm that had created the disaster: a season with no commercial king salmon fishing (which along with public sector income is the foundation of the local economy)³; a cold snap that prevented fuel delivery; and subsequent rising fuel costs of up to \$7.25 for a gallon of gas and more than \$1000 a month per household for stove oil. Tucker wrote that that winter his family of ten was forced to choose between buying food or fuel. He then detailed the circumstances of two dozen other Emmonak families, equally desperate, in a village where in 2010 the annual per capita income was \$13,529, compared to \$30,726 in Alaska generally (Alaska Department of Labor 2010). The result was action—collections and food drives in Anchorage and the Lower Forty-eight, cash donations by dozens of individuals and organizations, airlifts of

³ The 2008 ADF&G survey found that income in Emmonak derived from the Alaska Permanent Fund dividend (33%), local government (15%), commercial fishing (11%), services (6%), public assistance (8%), social security (7.6%), and food stamps (5.5%).



Fig. 2. Plane unloading food supplies on the lower Yukon, 2009. US Fish and Wildlife Service.

supplies not just to Emmonak but to other lower Yukon communities, culminating in the visit of then governor Sarah Palin accompanied by evangelist Franklin Graham, head of Samaritan's Purse, who delivered 44,000 pounds of food (DeMarban 2009a, 2009b; Hopkins 2009a, 2009b) (Fig. 2).

The food and cash were needed and appreciated in these hard times. Yet moose (still in season) were spotted grazing near the runway when the planes landed bringing cans of Spam and boxes of Pilot Bread. Elders we work with at CEC were grateful, but they were also embarrassed. Note that Emmonak, in Yup'ik, means "blackfish," a tasty resource which along with moose and whitefish, are abundant for those with the ability to harvest them (Fig. 3). Some elders CEC staff worked with in spring 2011 denied that the people of Emmonak were starving, citing the piles of fish and meat Emmonak residents shared at that year's annual Potlatch (Fred Augustine and Edward Phillip, March 2011:1067). The 2008 ADF&G harvest survey supports this view, reporting per person harvests of 192 lb of salmon and 123 lb of moose, which 61% of households harvested and 95% of households used. When Fienup-Riordan called to check on food deliveries preceding the 2011 summer field season, elders were quick to reply, "Don't worry, you won't starve here!" Emmonak resident Ray Waska said simply, "Nick Tucker used the wrong word. He should have said hardship, not starvation."

Indeed, Emmonak is undergoing hard times, and a brief look at the community's history can help us understand why. Understanding this history also provides a context for what Emmonak elders, hunters, and residents say now about the changes they experience. While southwest Alaska generally was ignored by non-Native entrepreneurs at the turn of the century, this was not true of the lower Yukon. From the late 1800s supplies landed at St. Michael were shipped south along the coast and up the Yukon by stern wheeler and steamship as far as Nenana. Non-Natives also moved to the Yukon delta to exploit the salmon fishery, building canneries, salteries, stores, and post offices at central locations near the Yukon River's mouth (Fienup-Riordan, 2012:75–76, 80, 83).

Along with a cash economy and easier access to Western goods, contact also brought epidemic disruption far greater than that experienced in Bering Sea coastal communities to the south (Fienup-Riordan, 2012:13–14, 23–24). During both the 1900 and 1918 influenza pandemics, whole villages were wiped out, and orphans subsequently gathered at the St. Mary's Catholic Mission thirty miles south of present day Emmonak (Fienup-Riordan, 2012:26, 92). There children learned English which in adulthood



Fig. 3. Drying northern pike and blackfish in Emmonak, 2009. Caroline Brown.

they spoke to their own children, breaking the strength of the Yup'ik language so valued on Nelson Island and in lower Kuskokwim coastal communities (Fienup-Riordan, 2000:21).

Even with these changes, families continued to live scattered in hundreds of small seasonal camps and settlements, including from one to a dozen households (Fig. 4). In the early 1960s, however, the Bureau of Indian Affairs (BIA) built schools at four central locations on the lower Yukon—Kotlik, Emmonak, Alakanuk, and Nunam Iqua (Fig. 5). The law required parents to send their children to school, and people abandoned their camps and moved into town. These new villages ranged in size from 150 (Nunam Iqua) to 750 (Emmonak), small by modern standards but huge when compared to the tiny settlements of the past. This population concentration into central sites happened all across the Yukon-Kuskokwim delta, so that today only 57 villages remain of the thousands of tiny communities of fifty years before in an area the size of New York state (Fienup-Riordan, 1986, 1988) (Fig. 6).

People did not, however, abandon the subsistence resources land and sea provided. As a 2008 ADF&G survey shows, Emmonak residents continue to be heavily dependent on the harvest of a variety of subsistence resources, averaging 482 lb per person (Fall et al., 2013). In 2010, the average subsistence harvest was 316 lb per person for rural Alaska and 490 lb per person for western Alaska (Wade Hampton and lower Kuskokwim census areas). The average for urban Alaska is 23 lb per person (Alaska Department of Fish and Game 2012). Most subsistence resources continue to be plentiful on the Yukon delta. While salmon have declined, the delta wetlands support numerous species of whitefish in abundance. Also, tasty moose are moving onto the delta in staggering numbers. Thanks to an eight-year moratorium on hunting combined with warming climate and increasingly high habitat quality with the replacement of grassy banks by thick stands of willow and alder, moose numbers on the Yukon delta have risen from about 28 in 1992 to about 3300 in 2008, and now are among the highest densities of moose in Alaska. The worry today is not whether moose will colonize the delta but whether



Fig. 4. Historic Map of Yukon Delta settlements and seasonal camps, 1910. Jesuit Oregon Province Archives, Spokane, Washington.

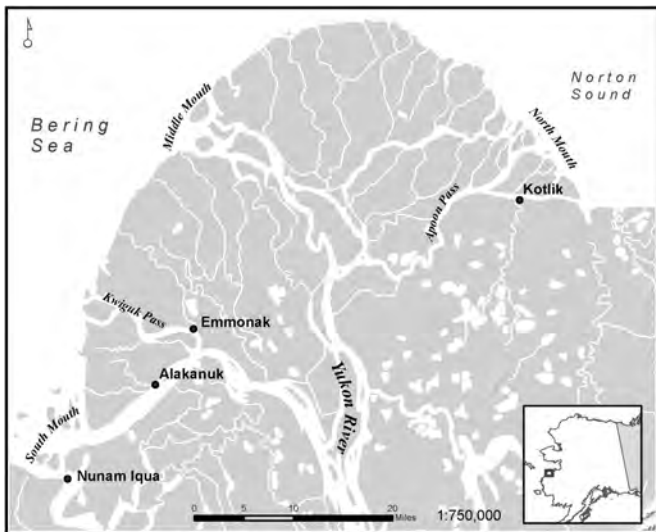


Fig. 5. Lower Yukon communities, CEC study 2011. Image by Nicole Braem.

the delta can continue to support these numbers without a population crash (Perry, 2010).

The problem for delta residents is not just the presence of subsistence resources but also access to them. In the past a man could set a fishtrap or snare within walking distance of his home. Ray Waska (March 2011) said that his father never went bird hunting, but merely kept a gun by his cabin door at spring camp and pointed it skyward when he wanted bird soup. Today a man



Fig. 6. Comparison of Yukon Delta region to New York state and the United States. Calista Corporation.

must often travel miles from home to harvest in the same rich wetlands his parents used. Because they use power boats, rifles, and snowmobiles, they must earn money for equipment and fuel by working within the local wage economy. People's success at the “traditional” acts of harvesting animals is directly tied to their ability to harvest cash. At a time when the market economy of southwest Alaska continues to struggle, hunting and fishing activities are often difficult to afford (Fienup-Riordan, 2012).

3.2. History of salmon fishing

A brief history of salmon harvesting in the lower Yukon illustrates this relationship and its role in the current resource-based, economic, and social challenges facing Emmonak people. In the 1950s, lower Yukon elders describe a summer season with nonstop fishing from June 1 through July 15, when an average annual take was 1200 king salmon. Each salmon, averaging 40 pounds, sold for 50 cents, and a man could bring in \$600 a season—enough to see him through the winter. However, king salmon runs have been declining over the last decade—the 2008 run was approximately 36% below the 2002–2007 average which itself was lower than previous averages. The reasons for this decline are not fully understood. Fishermen, managers, and scientists have suggested various causes from changing environmental conditions in the Bering Sea to over-exploitation as by-catch in the pollock fishery. While harvests of over 100,000 fish were common in the 1980s, the commercial harvest had dropped to around 60,000 by the late 1990s and has not existed since 2008 (Fall et al., 2012) (Fig. 7). Like all lower Yukon communities, the people of Emmonak were dependent on this commercial fishery; today it is gone, and nothing has replaced it. Chum salmon are still harvested commercially, but many fishermen note they often make no more than expenses.

It is not just the commercial harvests that are affected by these declines. The integration of the subsistence and commercial components of Emmonak's economy was first described by Robert Wolfe in the early 1980s (Wolfe 1982). As noted earlier, cash from participation in a market economy is funneled back into subsistence through the purchase of boats, motors, nets, guns, and gas that support harvesting activities, including longer stays at seasonal fish camps (see also Reedy-Maschner, 2009).

The absence of a commercial fishery to help fund fish camp activities along with the presence of seasonal employment that keeps families in the village and away from camp has led to a slow

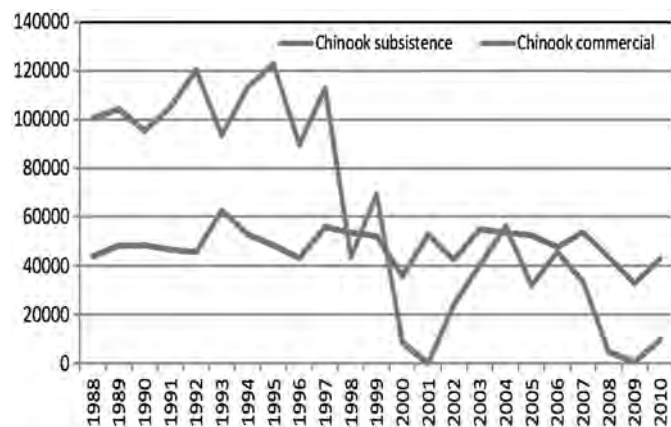


Fig. 7. Commercial and subsistence king salmon harvests, 1988 to 2010 (The United States and Canada Yukon River Joint Technical Committee (JTC), 2011).

attrition of fish camp residence. Also, the increasingly restrictive structure of fishing regulations, first to accommodate commercial and subsistence openings, and more recently to address declining Chinook (king) salmon runs, has further discouraged longer-term stays at fish camp. It is important to keep in mind that fish camp locations are not necessarily static; some are long-term fixed residences, while others can be temporary campsites used for a year or two before moving to another location. While not comprehensive in capturing all fish camps existing through time Fig. 8, depicting Emmonak fish camps in 1980 and 2007 shows a dramatic decline in camp use (Fig. 8). Declining camp residence has implications for the time spent out on the land necessary for successful subsistence harvesting activities as well as educating younger generations in proper ways to live. The decline in fish camps has coincided with a decline in fishing. While subsistence harvests of Chinook salmon by Emmonak residents have remained relatively stable over time in number of fish, Emmonak's population growth since 1980 suggests that people are using less Chinook salmon. Per capita levels of Chinook salmon harvests have fallen from 80 pounds per person in 1980 to 39 pounds in 2008.

At its base, the declining salmon runs are more than an environmental shift potentially related to changes in the Bering Sea. And the attendant crash of the commercial market is more than just an economic change represented by a loss of income. These losses require the community to respond to more than just a decline in an important food and income source. Because salmon are the foundation of an integrated socio-economic system, the effects of a declining salmon run cascade throughout village life.

3.3. Social and environmental change

The social consequences of the crash of the commercial salmon fishery, among other causes including language loss and cultural suppression, epidemic disruption, limited economic opportunities, and forced assimilation are the most troubling.⁴ Southwest Alaska has among the highest rates of suicide and domestic violence in the nation, and Yukon communities the highest among them (Alaska Injury Prevention Center, 2007). These rates gained national attention in 1987 when eight young men and women in Alakanuk (15 miles south of Emmonak) committed suicide in a little more than a year. Nine attempted suicides were also

⁴ The loss of dignity, issues of individual and cultural identity, and the history of multigenerational suffering associated with population loss and concentration are undeniable aspects of this complex contemporary situation (see Doak and Nachmann, 1987; Ducker 1996, 2000; Napoleon, 1996; Woisko, et al., 2007).

reported, and additional attempts probably went unreported (Fienup-Riordan, 2000:21).

In addition to death through suicide, high rates of alcoholism, child abuse, sexual assault, violent crime, and mental illness plague the region as a whole. During the 1980s, despite passage of the Alaska Native Claims Settlement Act (ANCSA) and all the state-funded schools and projects following the “Molly Hootch” decision,⁵ these rates increased rather than declined. After staying the same in the 1990s, suicide rates in rural Alaska have continued to stay high. Residents have repeatedly assessed recent suicides as a consequence of the conditions existing at the time. They maintain that although individuals are responsible for their own actions, they cannot be expected to act appropriately if they are not in control of their land and resources, language, and life. This assessment implies that a sector of the population has lost such a sense of control. Economic recessions past and present only make the situation worse.

An undercurrent of concern for environmental as well as social issues ran throughout our discussions with Yukon elders. Everything—rivers, lakes, wind, waves, snow, ice, plants, animals, and weather in every season—seems to be changing in southwest Alaska, as in other parts of the Arctic.⁶ Adding to the challenges presented by declining salmon runs and increasing fishing regulations, Emmonak fishermen observe that their summers are increasingly rainy, which interferes with optimal drying times, a main form of preserving salmon for winter storage. They also note that natural indicators, such as wind direction and plant growth used to predict salmon run timing and abundance, no longer hold (Moncrieff et al., 2009). After traveling through shrinking channels past dozens of newly formed sandbars at the Yukon River's mouth, Ray Waska (July 2011:191) noted, “Today the Yukon is no more Yukon. It's a newborn world.” (Fig. 9).

During topic-specific gatherings with Nelson Island elders, it was common to hear them repeat the well-known Yup'ik adage, “The world is changing following its people.” This adage captures the Yup'ik view that environmental change is directly related not just to human action—over-fishing, burning fossil fuels—but to human interaction. To solve the problems of global warming elders maintain that we need to do more than change our actions—reduce bycatch and carbon emissions. We need to correct our fellow humans. They encourage young people to pay attention to traditional rules for living, believing that if their values improve, correct actions will follow (Fienup-Riordan and Rearden, 2012:300–321).

When CEC began collaborative research with lower Yukon communities, CEC staff wondered if elders there would express themselves in the same way. We did, indeed, hear some say, “The world and its weather are changing following the people.” We also heard a significant variation: “They say people are changing following the fish.” As these fish-dependent coastal communities see changes in the timing and composition of annual runs, they experience new people moving into their communities and many young men and women moving away. Those who remain are different than their peers and ancestors. Given the longer contact history, few young people speak the Yup'ik language and many lack knowledge of the values, practices, and admonishments both Nelson Island and Yukon elders hold dear (Fig. 10).

⁵ In 1976 the “Molly Hootch” decision (Hootch v. Alaska State Operated School System, named for a Yup'ik student who sued the state for the right to be educated in her home village) mandated sweeping educational reform statewide. Local high schools were built in communities that previously had sent their children to boarding schools or outside the region and often the state.

⁶ The literature on climate change across the Arctic is extensive, including Huntington and Fox, 2005; Kolbert, 2006; Krupnik and Jolly, 2002; Laidler 2006; Oakes and Riewe, 2006.

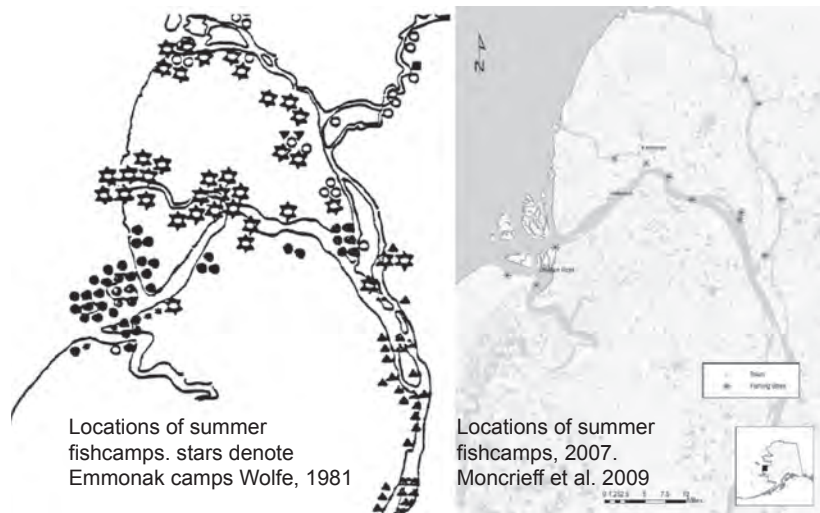


Fig. 8. Lower Yukon fish camp locations, 1980 and 2007 (Wolfe, 1981; Moncrieff et al., 2009).



Fig. 9. Ray Waska at the now-deserted village of Hamilton, where he was born and raised, July 2011. Ann Fienup-Riordan.



Fig. 10. Lawrence Edmund (Alakanuk), Eugene Pete (Nunam Iqua), and Mike Andrews, Sr. (Emmonak) attending a CEC topic-specific gathering in Anchorage, December 2011. Ann Fienup-Riordan.

3.4. Changes in seal harvesting patterns

Seal hunting provides a good example of this mix of environmental and social shifts that bear on how people use and relate to the land. ADF&G survey data showed that marine mammals comprise about 11% of the total subsistence harvest, down from about 15% in 1980. A comparison of results on a species level, however, suggests shifts in the patterns of seal harvest and use. Specifically, marine mammal harvests in Emmonak show a strong shift in 2008 toward harvesting bearded seals in greater numbers and fewer ringed seals relative to 1980. During the twelve month period between June 1980 and May 1981, hunters in Emmonak harvested an estimated 139 ringed seals and 39 bearded seals. Ringed seals were the largest portion of the community's total seal harvest by edible weight. Households harvested an estimated 19 pounds of ringed-seal meat per person, compared to an estimated 12 pounds of bearded-seal and spotted-seal meat respectively per person. The composition of the seal harvest was reversed in 2008, with hunters taking an estimated 136 bearded seals and 28 ringed seals. Correspondingly, the pounds per person harvest of bearded-seal meat doubled (to 24 pounds per person), while ringed-seal meat harvest (2 pounds per person) was just a fraction of the 1980 value (Wolfe 1981; Fall et al. 2012).

This shift in species composition hints at changes in harvest timing and location. In the 1980–81 harvest year, sealing occurred from late August until just before freeze-up in October and again in the spring. In the fall, the primary species harvested were spotted seals, which sometimes migrated in large numbers near the coast, along with juvenile bearded seal. Spring seal hunting typically began in March and April, although it might begin as early as January and February, at the edge of the land fast ice. Typically, small parties of hunters would travel by snowmachine directly out from the village until they came upon open leads. Hunting frequently occurred 20 to 30 miles from shore, and sometimes farther (Wolfe, 1981). While Wolfe (1981) did not break down harvest numbers by season, it seems likely that the greater harvest of ringed seals in 1980 were taken in the spring months, as they frequented lead areas. During a ADF&G interview, Emmonak hunter Ray Waska recalled: “Them days, when I was growing up, them - my folks used to hunt seals. They don't hunt them in the fall time. Cause too far, too much ice. And they hunt what they have around that area. At winter time they go out, they look at the clouds, when open water, that's when they go out. Dog team. Take 'em all day to get down there and when they get down there they overnight, 2–3 nights on top of the ice. Now, let's go.

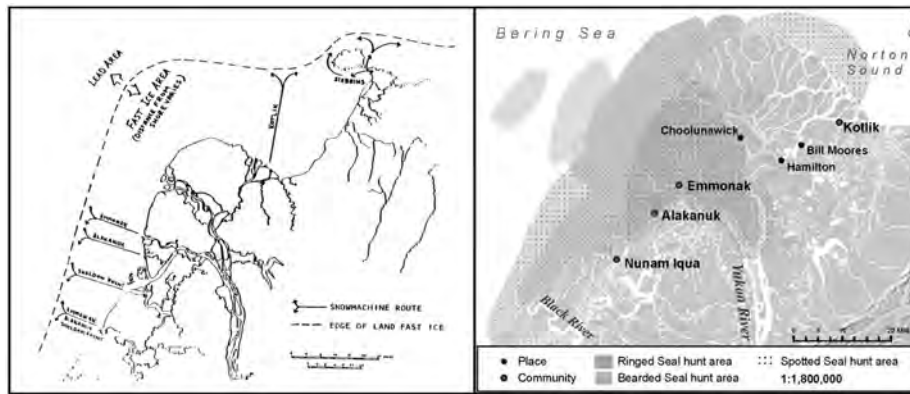


Fig. 11. Comparison of seal harvesting areas, 1980 and 2008 (Wolfe 1981; Fall et al., 2012).

Zip. Zip down, zip back. We got fast machines. Nobody overnights no more. Nowadays. Some of them even go in the afternoon down the coastline."

Changes in harvest locations between 1980 and 2008 may be related to the differences in seasonality of harvest and species harvested between 1980 and 2008. In 2008, the majority of the harvest occurred in the fall in open water near the coast or in-river, primarily where one would find bearded seals. Ringed seals may be less abundant, or the dramatic decrease in their harvest may reflect the timing of when hunters are going for seal (in the fall open water rather than at the leads of shorefast ice in spring.) Additionally, Wolfe (1981) reported that Emmonak hunters sometimes went out as far as 40 miles in the spring to get to open leads, while in 2008, hunters generally reported going out only 10 to 20 miles (Fig. 11).

Many factors likely contribute to this shift in seal hunting patterns, including changes in sea ice, increased hunting costs (particularly gas and equipment), technology, and changing social patterns of knowledge transmission. Many hunters commented on the dangers of hunting out on the ice, especially in spring. They also noted the technological changes which have allowed people to make day hunting trips rather than camping out on the ice, an important setting where people build their knowledge of ice and hunting. According to both hunters and elders, such knowledge is highly experiential; time and observation form the basis of their understandings of the intricacies of particular places. One hunter commenting on the pattern of declining spring seal hunting suggested that young men simply do not have the necessary ice and weather knowledge for spring hunting.

3.5. Local understandings of place: continuity and change

Despite concerns about changes in hunting practices and knowledge, the role of language in the lives of the younger people, and the various economic, environmental, and social changes experienced by Emmonak people, CEC gatherings with elders in Emmonak and on the lower Yukon generally reveal still vital and meaningful relations between local people and their coastal homes. We will give three final examples.

First, Yukon elders, like their Nelson Island counterparts (Rearden and Fienup-Riordan, 2011), were enthusiastic and dedicated to documenting traditional knowledge, especially place names. As Denis Sheldon (July 2011:272) said, "If our young people especially forget about the land and the names and the hunting places and those rivers, it's like they will lose some of their body parts. But if they learn more about their identity, their minds will be stronger." Lawrence Edmund (July 2011:271) agreed, "When they travel [without knowing place names], it's like they are lost [in a storm]." Unlike Nelson Island, however, where the majority of

names attached to points and historic sites, on the Yukon naming focused on routes in what Ray Waska described as the "highway of puzzles" that comprise the lowland delta. Moreover, whereas Nelson Island elders wanted young people to learn the Yup'ik names for places before they are forgotten, Yukon elders fear the new English names and nicknames youth are attaching to the old places, names like Ukulele and KK Slough, for Yuuqernarli and Qerqertulli which they cannot pronounce, Snotty Slough (for Kakegluk, literally "snot," for the mucus warriors observed floating downstream, so revealing their enemies' location), and Dusty, L.A. and Chinatown for Emmonak, Nunam Iqua, and Alakanuk. Young men use these names freely on the VHF radio, and elders hear them with dismay. Whereas for elders all places have names, young people know few places well. Today, they say, "they don't recognize places but only bump into things" (Mike Andrew, March 2011:580). According to Fred Augustine (March 2011:1042) good map work will save lives: "If these people do a good job recording [place names], the hardships that Yup'ik people will face in the future in this village won't be as severe. This is something to be grateful for."⁷

Along with their passion for communicating a coastal landscape rich in names and stories, elders communicated a deep spiritual connection to the land through word and deed. It was not unusual when out on the land for travelers to practice aviukar-yaraq, giving offerings of food and water to the ancestors buried in the land as well as to the land itself. During a trip to Nanvaruk, Ray Waska (July 2011:178) said: "The people of Nanvaruk here, according to Yup'ik custom, although they have died and are gone, they still feed people, they still provide for people. I'm usually skeptical of various traditions, but sometimes when I arrive at this place, I give them a little bit of water thinking about their old people, keeping in mind their souls and asking them to help me." (Fig. 12).

Traveling with elders and youth during July 2011, CEC staff often observed offerings made to the land itself. Paul Manumik (August 2011:651) explained: "Whenever we get to the tundra back here, into the old villages, Eugene Pete told us to always make an offering of food and water, especially water. So when you go berry picking you need to share your food with the land. And the land will give you back what the land has." Mike Andrew (March 2011:746) told the story of travelers with homebrew among their provisions, offering some to the land: "They say when they first drank, those people could feel the [homebrew] they drank. Then they say although they continued to drink, they couldn't get

⁷ Bethel Search and Rescue reports that although members have participated in thousands of rescue missions on the Yukon-Kuskokwim delta in the last two decades, more than 80 missing persons remain unaccounted for.



Fig. 12. Ray Waska, Peter Moore, and Mark John visiting Nanvaruk, July 2011. Ann Fienup-Riordan.

intoxicated. Then when it started to get dark, from that old village, those [dead] ones over there started making noise. [laughter] The ones over there were intoxicated, they were even singing, and they were very entertaining to listen to over there. Since that time, they never did that again.”

Animals may also be spoken to. Lawrence Edmund (July 2011:478) shared his experience camping across from a beaver den. When he was about to set his whitefish net, he spoke to the beavers: “I told them that I eat fish, that they eat willows, to leave that fishnet alone. After setting it, I left it. In the evening, two beavers started to swim not far from my net. I said, ‘They will cut it up.’ We woke in the morning and they were still swimming. I went to my fishnet and it wasn’t torn at all. I thought they heard me and obeyed since I’ve heard that these animals have ears through the land. Again, it didn’t touch my fishnet, but it caught many.”

Perhaps most moving are the ways lower Yukon residents are using their traditions to solve current social problems. An innovative program of suicide prevention, led by village elders and community members, is making use of traditional practices to rid their communities of suicide. Lawrence Edmund (July 2011:471) recalled how in the past ritual acts were done in fours, and in 2008 he and other elders met with students, having them stomp on the ground four times to take away death, then brush it away in four directions: “I said to them that our ancestors would have stopped that bad thing already upon seeing it. Since that time, they haven’t [committed suicide] up to this day. Indeed, I hope that they don’t. It was really bad during that time, and I was constantly worried, and afraid something would happen to my children. When they were extremely bad, [people died] every month, and two people would die from our community in one month, there were fourteen people who died in our community in one year.”

4. Conclusion

A photograph of dogs pulling a house across the ice in the spring of 1964, to found the new village of Toksook Bay on Nelson Island, captures what may be the single most important point to understand about Bering Sea coastal communities (Fig. 13). Villages like Emmonak may look fixed with their 200 frame houses and elaborate infrastructure of a state-owned airstrip, health clinic, two grocery stores, a large community center, public school, U.S. post office, several city and tribal government buildings, a seasonal ADF&G office, a small restaurant, and Kwik’pak, a

commercial fish processing plant. Yet their populations remain incredibly fluid, moving great distances for a wide range of harvesting (as well as educational, employment, and social) activities, and experiencing and responding to rapid and variable economic, political, social, and environmental changes.

As stated above, change is normal—the rule rather than the exception—in the course of human history. Yet the profound changes experienced by local communities during the last fifty years are unprecedented in Alaska, including the centralization of previously dispersed populations; the transformation of land ownership following the Alaska Native Claims Settlement Act in 1971; increased dependence on fossil fuels and new technologies; and the advent of formal education (Fienup-Riordan 2012:10–35). In his youth, men such as Ray Waska drove a dog team, harvesting hundreds of fish annually to feed them. Today he rides a high-powered snowmachine, runs a 220 hp motor on an aluminum skiff, and owns no dogs. His ties to the land and sea, however, remain strong. As he says (January 2011:240), “Where there’s food, I go see it.”

The question of sustainability immediately arises. With limited jobs and increasingly high cash needs associated with these harvesting activities, how can Ray Waska’s children and children’s children follow in his footsteps (Fig. 14)? Will they continue to value his way of life? Certainly the low number of salmon returning to the lower Yukon from the Bering Sea is exacerbating the economic downturn in Emmonak, but other important social and cultural shifts are at work, including the detachment of some youth from subsistence practices, as well as the prevalence of electronics, TV, etc. for entertainment. All these factors need to be understood in any evaluation of Emmonak’s ability to survive and thrive.

The present well-being of communities like Emmonak is absolutely tied to the health and marine resources of the Bering Sea but also to the larger global economy. The examples discussed above, including the history of salmon fishing, changes in seal hunting, and local understandings of place, all show that while Emmonak residents are experiencing environmental changes potentially related to weather or Bering Sea conditions, the ways

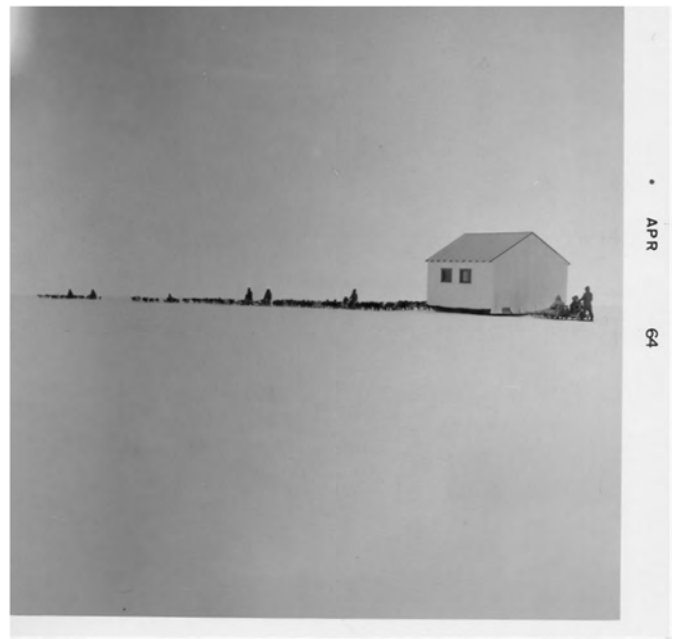


Fig. 13. Dogteam pulling houses over the ice from Nightmute to the new village site at Toksook Bay, April 1964. Jesuit Oregon Province Archives, Spokane, Washington.



Fig. 14. Ray Waska's grandson, Wayne Murphy, with his first seal, July 2011. Ann Fienup-Riordan.

they experience climate change are shaped by social and economic conditions as well as distinctly Yup'ik cultural perspectives.

Our experience is that local elders and knowledge holders want to collaborate with scientists to better understand their past and present to inform their future, as they did in CEC topic-specific gatherings and CAB meetings in Emmonak. The multiple viewpoints expressed in these contexts are critical for understanding this complex contemporary situation. To gain indigenous observations and information that will inform natural science research, LTK components are increasingly added to natural science studies. Yet, as previously stated, no oceanographer would try to understand the Bering Sea ecosystem as a whole without considering the biology of individual species and their linkages to other organisms. How can we then expect to understand coastal communities through LTK in isolation, without a fuller understanding of the historical and cultural context of the contemporary situation that ethnography can provide?

Though ethnography has been standard practice within anthropology for more than 150 years—in fact, pivotal in both defining and redefining the discipline throughout its history—social scientists in management sciences generally do not emphasize its value. Moerlein and Carothers (2012) note that environmental and social changes are inseparable and that “climate change is just one of many changes that have and are affecting the community.” They quote one informant as saying, “I think the world is changing,” followed by a combined list of environmental, social, and economic changes. As stated above (p. 6) working with Yup'ik elders in southwest Alaska we heard the same thing, but with a difference, in the oft repeated adage, “The world is changing, following its people.” In the last three words of this statement Yup'ik elders provide a link that expands on Moerlein and Carothers' analysis of residents' understandings of change: elders offer the explanation that the world is changing because humans are no longer treating each other with care and respect.

If we really want to understand community vulnerability and sustainability today, it is not sufficient to say that changes are taking place, even rapid change. We need to understand how community members interpret these changes—not just *what* is occurring but *why* people believe it to be so, not just what social and economic circumstances are in flux, but how these situations are perceived. Survey results alone cannot provide such an understanding. A holistic ethnographic approach, combining survey data with the insights of long-term observation and participation in community life, can help us move in that direction. Moerlein and

Carothers say as much in their concluding paragraph (emphasis added): “Within a science-based way of knowing, *ethnographic approaches that engage local perceptions of change* are necessary to generate meaningful understandings of total environments of change and to inform effective strategies of response.” We agree whole-heartedly with their conclusion, and hope that our definition and foregrounding of the concept of ethnography adds to the understanding of what form such an approach might take.⁸

Finally, the ethnographic approach sensitive to cultural history is not only of value in fully understanding LTK, but is also invaluable in informing other scientific studies contained within larger social-ecological research initiatives. For example the use of elder topic-specific gatherings, as described above, is both an effective and culturally appropriate forum for sharing information in Yup'ik coastal communities, “teaching listeners how to learn,” and demonstrating the embeddedness of knowledge systems. In fact, beginning in 2011 CEC has employed topic-specific gatherings to bring together elders and natural scientists in CEC's most recent environmental knowledge project to approach topics such as changes in sea ice, snow, and weather patterns collectively (Fienup-Riordan, in press). Like their Yup'ik partners, participating scientists indicated that they value these gatherings not only for the knowledge shared but for the relationships fostered among knowledge holders.

Coastal communities throughout Alaska, as elsewhere, are undergoing profound environmental, socioeconomic, and cultural changes related to their reliance on marine ecosystems and, increasingly, a global economy. Carried out in isolation, LTK research is limited in providing the insights we need to understand community vulnerability and sustainability. In bringing LTK research together with the vital context that ethnography provides, we have a powerful tool that can not only help natural and social scientists understand the unique cultural perspectives that underlie the actions and reactions of coastal residents, but give voice to community understandings of the world in which they live.

Acknowledgments

First and foremost, we are indebted to the men and women in lower Yukon communities who generously shared their knowledge. We have cited their contributions by name, CEC gathering date, and transcript page number. Fienup-Riordan is also grateful to the Calista Elders Council, especially Alice Rearden, Mark John, and the CEC's board of elders, who guide her work. Our ongoing work in lower Yukon communities would not be possible without the support of the National Science Foundation, both Polar Programs and the Bering Ecosystem Study Program (BEST), the North Pacific Research Board, and the Alaska Department of Fish and Game. Nikki Braem and Caroline Brown would like to thank Ted Hamilton, Michael Jimmy, and Dora Moore for their assistance in organizing local research and reviewing analyses. We also thank Seth Wilson and Robyn LaVine for assistance in data collection.

⁸ In his article “The Ends of Ethnography,” cultural anthropologist Marcus (2008:1) writes: “Anthropology is in good health mainly because of its past achievements concerning the study of difference and change in the world, and its accumulated knowledge and yes, wisdom about the work of culture(s) are not only very much needed...but this actual demand for anthropology (especially for the ethnographic gaze in various institutional settings and processes that are sensing problems in their confidence in purely rationalist and instrumental protocols but themselves do not have the means to act on these twinges of doubt) is also both acknowledged and manifest. In the US anthropology is enjoying a renewed relevance—but still in its long-established role as a ‘minor’ nonconformist outsider discipline.” In public anthropology in Alaska there is a crying need for this “outsider discipline” to move into the forefront, employing a time-honored tool—ethnography—to help us understand complex contemporary situations.

Finally, this paper benefitted from comments and additional information provided by BSIERP PI Henry Huntington, Jim Fall of the Alaska Department of Fish and Game, USFWS biologists Tom Doolittle and Spencer Rearden, volume editor Mike Sigler, as well as James Simon, Tom Van Pelt, and two anonymous reviewers.

References

- Andrew Sr., F., 2008. *Paitarkiukenka/My Legacy to You*. University of Washington Press, Seattle.
- Alaska Department of Fish and Game, Division of Subsistence, 2012. *Subsistence in Alaska: A Year 2010 Update*, Anchorage, AK.
- Alaska Department of Labor, 2010. *American Community Survey Site*. (<http://live.laborstats.alaska.gov/cen/acsarea.cfm>).
- Alaska Injury Prevention Center, 2007. *Suicide in Alaska*. Juneau, AK: Alaska State Department of Health and Social Services.
- Clifford, J., Marcus, G.E. (Eds.), 1986. *Writing Culture: The Poetics and Politics of Ethnography*. University of California Press, Berkeley.
- Cochran, W.G., 1977. *Sampling Techniques*, 3rd edition John Wiley & Sons, New York.
- Cruikshank, J., 1998. *The Social Life of Stories: Narrative and Knowledge in the Yukon Territory*. University of British Columbia Press, Vancouver.
- Cruikshank, J., 2005. *Do Glaciers Listen?: Local Knowledge, Colonial Encounters, and Social Imagination*. University of British Columbia Press, Vancouver.
- Danielson, S., Eisner, L., Weingartner, T., Aagaard, K., 2011. Thermal and haline variability over the Central Bering Sea Shelf: seasonal and interannual perspectives. *Cont. Shelf Res.* 31, 539–554.
- DeMarban, A., 2009a. Emmonak donations 'A Miracle of Caring'. *The Tundra Drums* (Bethel, AK) 36 (46), p. 1, 8.
- DeMarban, A., 2009b. Palin delivers food, touts resource jobs. *The Tundra Drums* (Bethel, AK) 36 (51), p. 1, 6.
- Doak, B., Nachmann, B., 1987. *Violent Deaths Among Young Adults in Southwest Alaska Villages: A Subgroup of Longitudinal Cohort Study*. Alaska Native Medical Center, Anchorage, Alaska.
- Ducker, J.H., 1996. Out of harm's way: relocating Northwest Alaska Eskimo 1907–1917. *Am. Indian Culture Res. J.* 20 (1), 43–71.
- Ducker, J.H., 2000. Curriculum for a new culture: a case study of schools and Alaska natives 1884–1947. *Pac. Northwest Q.* 91 (2), 71–83.
- Fabian, J., 2008. *Ethnography as Commentary: Writing from the Virtual Archive*. Duke University Press, Durham.
- Fall, J.A., Braem, N.M., Brown, C.L., Hutchinson-Scarborough, L.B., Koster, D.S., Krieg, T.M., 2013. Continuity and change in subsistence harvests in five Bering Sea communities: Akutan, Emmonak, Savoonga, St. Paul, and Togiak. *Deep Sea Research II* 94, 274–291.
- Fall, J., Brown, C.L., Braem, N., Hutchinson-Scarborough, L., Koster, D.S., Krieg, T.M., Slayton, L., 2012. *Subsistence Harvests and Uses in Three Bering Sea Communities, 2008: Akutan, Emmonak, and Togiak*. Alaska Department of Fish and Game, Division of Subsistence, Technical Paper no. 371, Anchorage.
- Fienup-Riordan, A., 1986. *When Our Bad Season Comes: A Cultural Account of Subsistence Harvesting and Harvest Disruption on the Yukon Delta*. Prepared for the Alaska Council on Science and Technology, Aurora vol. 1. Alaska Anthropological Association.
- Fienup-Riordan, A., 1988. *Alakanuk Village Description. Village Economics in Rural Alaska. Impact Assessment, Inc. U.S. Department of the Interior, Minerals Management Service. Alaska OCS Technical Report no. 132*.
- Fienup-Riordan, A., 1990. *Eskimo Essays: Yup'ik Lives and How We See Them*. Rutgers University Press, New Brunswick.
- Fienup-Riordan, 2000. *Hunting Tradition in a Changing World: Yup'ik Lives in Alaska Today*. Rutgers University Press, New Brunswick.
- Fienup-Riordan, A., 2005a. *Yup'ik Elders at the Ethnologisches Museum Berlin: Fieldwork Turned on Its Head*. University of Washington Press, Seattle.
- Fienup-Riordan, A., 2005b. *Wise Words of the Yup'ik People: We Talk to You because We Love You*. Lincoln: University of Nebraska Press.
- Fienup-Riordan, A., 2007. *Yuungnaqpiallerput/The Way We Genuinely Live: Masterworks of Yup'ik Science and Survival*. University of Washington Press, Seattle.
- Fienup-Riordan, A., 2010. *Yup'ik perspectives on climate change: the world is following its people. Étude/Inuit/Studies* 34 (1), 55–70.
- Fienup-Riordan, A., 2012. *Mission of Change in Southwest Alaska: Conversations with Father René Astruc and Paul Dixon on Their Work with Yup'ik People, 1950–1988*. University of Alaska Press, Fairbanks.
- Fienup-Riordan, A., *Linking Local and Global: Yup'ik Elders Working Together with One Mind*. *Polar Geography*, in press.
- Fienup-Riordan, A., Rearden, A., 2012. *Ellavut/Our Yup'ik World and Weather: Continuity and Change on the Bering Sea Coast*. University of Washington Press, Seattle.
- Fischer, M.J., 2007. *Culture and Cultural Analysis as Experimental Systems*. *Cultural Anthropology* 22 (1), 1–65.
- Geertz, C., 1973. *The Interpretation of Cultures*. Basic Books, New York.
- Hopkins, Kyle, 2009a. *Palin Visits Villages: Governor, Evangelist to Deliver Food*. Anchorage Daily News, Friday, February 20, p. A1, A12.
- Hopkins, Kyle, 2009b. *Worldwide Donations Find Way to Lower Yukon: Efforts from Alaska and Beyond Send Food, Cash to Villages*. Anchorage Daily News, Saturday, February 14, p. A1, A9.
- Huntington, H.P., Fox, S., 2005. *The changing Arctic: indigenous perspectives*. In: Symon, C., Arris, L., Heal, B. (Eds.), *Arctic Climate Impact Assessment*. Cambridge University Press, New York, pp. 61–98.
- Huntington, H.P., Braem, N.M., Brown, C.L., Hunn, E., Krieg, T.M., Lestenkof, P., Noongwook, G., Sepez, J., Sigler, M.F., Wiese, F.K., Zavadii, P., 2013. *Local and traditional knowledge regarding the Bering Sea ecosystem: Selected results from five indigenous communities*. *Deep-Sea Research II* 94, 323–332.
- Kolbert, E., 2006. *Field Notes from a Catastrophe: Man, Nature, and Climate Change*. Bloomsbury, New York.
- Krauss, W., 2011. *Review Essay: David Westbrook, Navigators of the Contemporary: Why Ethnography Matters* (University of Chicago Press, 2008), and Paul Rabinow and George E. Marcus. *Designs for an Anthropology of the Contemporary* (Duke University Press, 2008). *American Ethnologist* 38(1):187–90.
- Krupnik, I., Jolly, D. (Eds.), 2002. *The Earth is Faster Now: Indigenous Observations of Arctic Environmental Change*. ARCUS, Fairbanks, Alaska.
- Laidler, G., 2006. *Inuit and scientific perspectives on the relationship between sea ice and climate change: the ideal complement*. *Climate Change* 78 (2–4), 407–444.
- Marcus, G., 2008. *The ends of ethnography: social/cultural anthropology's signature form of producing knowledge in transition*. *Cultural Anthropol.* 23 (1), 1–14.
- Meade, M., Fienup-Riordan, A., 2005. *Ciuliamta Akluit: Things of Our Ancestors*. University of Washington Press, Seattle.
- Moerlein, K., Carothers, C., 2012. *Total environmental change: impacts of climate change and social transition on subsistence fisheries in Northwest Alaska*. *Ecol. Soc.* 17 (1), 10.
- Moncrieff, C., Brown, C., Sill, L., 2009. *Natural Indicators of Salmon Run Timing and Abundance, Yukon River. Yukon River Drainage Fisheries Association. Arctic-Yukon-Kuskokwim Sustainable Salmon Initiative*.
- Nadasdy, P., 2005. *Hunters and Bureaucrats: Power, Knowledge, and Aboriginal-State Relations in the Southwest Yukon*. University of British Columbia Press, Vancouver.
- Napoleon, H., 1996. *Yuuyaraq: The Way of the Human Being*. University of Alaska Fairbanks, Alaska Native Knowledge Network.
- Oakes, J., Riewe, R. (Eds.), 2006. *Climate Change: Linking Traditional and Scientific Knowledge*. Aboriginal Issues Press, Winnipeg, Manitoba, Canada.
- Perry, P., 2010. *Unit 18 Moose Management Report*. In: Harper, P. (Ed.), *Moose Management Report of Survey and Inventory Activities 1 July 2007–30 July 2009*. Juneau: Alaska Department of Fish and Game, pp 271–281.
- Rearden, A., Meade, M., Fienup-Riordan, A., 2005. *Yup'it Qanruyutait/Yup'ik Words of Wisdom*. University of Nebraska Press, Lincoln.
- Rearden, A., Fienup-Riordan, A., 2011. *Qaluyaaarmiuni Nunamtenek Qanemciput/Our Nelson Island Stories: Meanings of Place on the Bering Sea Coast*. University of Washington Press, Seattle.
- Reedy-Maschner, K., 2009. *Entangled livelihoods: economic integration and diversity in the Western Arctic*. *Alaska J. Anthropol.* 7 (2), 135–146.
- Sahlins, M., 2002. *Waiting for Foucault. Prickly Paradigm Press, Still, Chicago*.
- Scott, C., 1996. *Science for the West, Myth for the Rest? The Case of James Bay Cree Knowledge Construction*. In: Laura Nader (Ed.), *Naked Science: Anthropological Inquiry into Boundaries, Power, and Knowledge*. Routledge, London, pp. 69–86.
- The United States and Canada Yukon River Joint Technical Committee (JTC), 2011. *Yukon River Salmon 2010 Season Summary and 2011 Season Outlook. Regional Information Report no. 3A11-01*. Alaska Department of Fish and Game.
- Tucker, N.C., Sr., 2009a. *Fuel Crisis Devastating Families and Households*. January 10 Letter Circulated at a Meeting of Lower Yukon River villages in Emmonak, Alaska.
- Tucker Sr., N.C., 2009b. *An Alaska Village cries out for help*. *The Tundra Drums* (Bethel, AK) 36 (45), 5.
- Westbrook, D., 2008. *Navigators of the Contemporary: Why Ethnography Matters*. University of Chicago Press, Chicago.
- Wolfe, R., 1981. *Norton Sound/Yukon delta sociocultural systems baseline analysis*. ADF&G Division of Subsistence, Technical Paper no. 59.
- Wolfe, R., 1982. *The Subsistence Salmon Fishery of the Lower Yukon River*. ADF&G Division of Subsistence, Technical Paper no. 60.
- Wolsko, C., Lardon, C., Mohatt, G.V., Orr, E., 2007. *Stress, coping, and well-being among the Yupik of the Yukon-Kuskokwim Delta: the role of enculturation and acculturation*. *Int. J. Circumpolar Health* 66, 51–61.



The influence of wind and ice on spring walrus hunting success on St. Lawrence Island, Alaska



Henry P. Huntington^{a,*}, George Noongwook^b, Nicholas A. Bond^c, Bradley Benter^d, Jonathan A. Snyder^d, Jinlun Zhang^e

^a 23834 The Clearing Drive, Eagle River, AK 99577, USA

^b Savoonga Whaling Captains Association, Native Village of Savoonga, P.O. Box 202, Savoonga, AK 99769, USA

^c University of Washington/IJSAO, Box 355672, 3737 Brooklyn Avenue NE, Seattle, WA 98105, USA

^d U.S. Fish and Wildlife Service, Marine Mammals Management, 1011 East Tudor Road, Anchorage, AK 99508, USA

^e Applied Physics Laboratory, University of Washington, 1013 NE 40th Street, Seattle, WA 98105, USA

ARTICLE INFO

Available online 14 March 2013

Keywords:

Pacific walrus (*Odobenus rosmarus divergens*)

Hunting

St. Lawrence Island

Bering Sea

Winds

Sea ice

Generalized additive model (GAM)

ABSTRACT

St. Lawrence Island Yupik hunters on St. Lawrence Island, Alaska, take hundreds of Pacific walrus (*Odobenus rosmarus divergens*) each year. The harvest and associated effort (hunting trips taken), however, are variable from year to year and also from day to day, influenced by physical environmental factors among other variables. We used data from 1996 to 2010 to construct generalized additive models (GAMs) to examine several relationships among the variables. Physical factors explained 18% of the variability in harvest in Savoonga and 25% of the variability in effort; the corresponding figures for Gambell were 24% and 32%. Effort alone explained 63% of the harvest in Savoonga and 59% in Gambell. Physical factors played a relatively smaller role in determining hunting efficiency (walrus taken per hunting trip), explaining 15% of the variability in efficiency in Savoonga and 22% in Gambell, suggesting that physical factors play a larger role in determining whether to hunt than in the outcome of the hunt once undertaken. Combining physical factors with effort explained 70% of the harvest variability in Savoonga and 66% in Gambell. Although these results indicate that other factors (e.g. fuel prices, socioeconomic conditions) collectively cause a greater share of variability in harvest and effort than ice and wind, at least as indicated by the measures used as predictors in the GAMs, they also suggest that environmental change is also likely to influence future harvest levels, and that climate models that yield appropriately scaled data on ice and wind around St. Lawrence Island may be of use in determining the magnitude and direction of those influences.

© 2013 Elsevier Ltd. All rights reserved.

1. Introduction

Pacific walrus (*Odobenus rosmarus divergens*) hunting is vital to the well-being of the Yupik residents of St. Lawrence Island, Alaska (Fig. 1). In a 2009 subsistence harvest survey in Savoonga, the take of 962 walrus accounted for two-thirds of the weight of all the food harvested locally, and nearly three-quarters of the weight of the marine mammal harvest (Fall et al., 2013). Monitoring by the U.S. Fish and Wildlife Service (FWS), however, indicates that the number of walrus harvested each year in both Savoonga and Gambell, the two communities on the island, can vary by a factor of four or more (with 962 at the high end of the range). In interviews conducted as part of the local and traditional

knowledge (LTK) component of the Bering Sea Project (Wiese et al., 2012), elders and hunters in Savoonga indicated that ice conditions are a major influence on spring hunting success. FWS walrus harvest monitors further identified weather as a crucial factor in determining the ability of hunters to travel by boat and successfully harvest walrus (Garlich-Miller et al., 2011).

Using these observations as a starting point, we quantify the extent to which readily available remote sensing measures of ice concentration, wind speed, and wind direction (physical factors) explain the daily variation in walrus harvest level (harvest) and the number of hunting trips taken (effort) at Savoonga and Gambell for the period from 1996 to 2010, the degree to which effort explains the variation in harvest, the degree to which the number of walrus taken per trip (efficiency) is influenced by physical factors, and the degree to which physical factors and effort together explain harvest.

In a highly variable physical environment, hunting communities would not likely persist if they lacked the flexibility to adjust to a range of conditions. At the same time, a host of societal

* Corresponding author. Tel.: +1 907 696 3564; fax: +1 907 696 3565.

E-mail addresses: hph@alaska.net (H.P. Huntington), gnunguk@hotmail.com (G. Noongwook), nab3met@u.washington.edu (N.A. Bond), brad_benter@fws.gov (B. Benter), jonathan_snyder@fws.gov (J.A. Snyder), zhang@apl.washington.edu (J. Zhang).

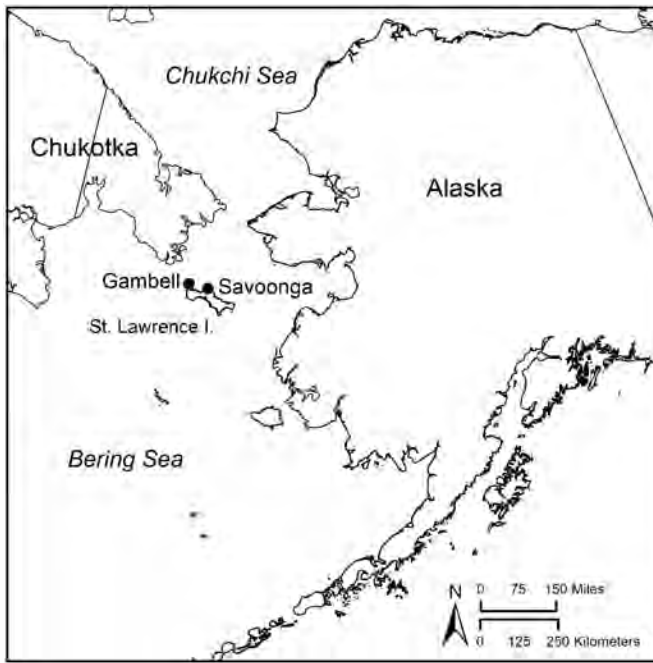


Fig. 1. Map of St. Lawrence Island and the eastern Bering Sea, showing the communities of Gambell and Savoonga.

factors also likely influence hunting success. Other physical conditions, such as fog, also hamper hunting, but are not readily reproduced in meteorological data or models. Finally, walrus hunting depends on the presence and abundance of walrus. Environmental conditions, therefore, establish a minimum threshold for hunting success. If hunters cannot travel upon the ocean, they cannot hunt. The ability to travel, however, means neither that hunters *will* go hunting, nor that they will succeed if they do. For these reasons, we did not expect to explain the majority of the interannual or daily variability in harvest levels. Instead, we sought only to identify the extent to which that variability can be attributed to ice and wind conditions, and then to further explore the relationship between effort and harvest.

Relatively few studies have quantitatively examined physical environmental factors as determinants of subsistence hunting success. Kapsch et al. (2010) examined the influence of ice concentration, wind speed and direction, visibility, and air temperature on spring walrus hunting success in the same communities, finding that the sea-ice concentration anomaly is a good predictor of the number of favorable hunting days. George et al. (2003) examined the influence of wind speed and direction on bowhead whale (*Balaena mysticetus*) harvests in Barrow, Alaska, finding that wind direction was the crucial variable in spring, largely because wind direction determined whether there was open water for whaling, whereas wind speed was most important in fall, when open water allowed waves to build up in high winds. Ashjian et al. (2010) confirmed that wind speed is crucial for fall whaling in Barrow, with 85% of whales harvested with wind speeds less than 6 m/s. These studies, however, primarily identified threshold environmental conditions. Our analysis goes a step further, describing functional relationships between harvests and environmental conditions taken, not one at a time, but as a suite of interacting factors.

The ability to assess correlations between harvest variability and physical environmental factors has the additional attraction of allowing an assessment of the likely impacts of changes in the physical environment. Climate change is having a marked impact on Arctic sea ice (e.g., Comiso et al., 2008; Hassol, 2004; Rothrock

et al., 1999; Stroeve et al., 2008) and may also currently affect weather patterns including wind conditions (e.g., Overland et al., 2008; Wendler et al., 2010). Projections of the distribution and frequency of future physical conditions can therefore help assess the degree and direction that climate change is likely to affect practices such as walrus hunting. Such projections are beyond the scope of this paper, but our results indicate some variables of interest and the scales at which they are relevant, which may help define the scope of climate-model downscaling (e.g., Najac et al. (2011) among others) and similar efforts in order to be most useful to hunting communities.

2. Methods

Our analysis draws upon many streams of data. We first describe each type of data and the methods by which it has been compiled, and then the statistical methods used to evaluate relationships among the quantitative data on walrus harvests, ice concentrations, and wind speed and direction. Most of our analyses examine 1996–2010 because that was the period for which data on all parameters was available. The analyses of harvest solely as a function of hunting effort and of hunting success (walrus taken per trip) considered the period 1992–2010 because hunting data were available for this longer period.

2.1. Local and traditional knowledge

Local and traditional knowledge (LTK) is defined by the North Pacific Research Board (2005: 144) as “an array of information, understanding, and wisdom accumulated over time based on experience and often shared within a group or community.” The primary method used to document LTK in this study was the semi-directive interview (Huntington, 1998). In this method, interviews are conducted with individuals or groups, addressing a set list of general topics, but no fixed order or questionnaire to follow. Instead, the respondent or respondents discuss the topic in a manner that makes sense to them, perhaps making connections with other ecosystem components or describing trends over time. The interviewer can intervene to keep the discussion on topic, to ask for more detail on various points, or to guide the respondent(s) toward items of particular interest. Six elder hunters were interviewed as a group in Savoonga over the course of 5 days in July 2009. Two members of the interviewer team were also from Savoonga and contributed their own observations and knowledge.

The discussions about ice conditions and walrus harvests were only a small part of the interview sessions. A report on the interviews will be placed in the Bering Sea Project Data Archive (<http://beringsea.eol.ucar.edu/>) at the conclusion of the project in 2013. The interviews were the catalyst for examining relationships between physical conditions and walrus harvests.

2.2. Walrus Hunting data

Spring walrus harvest data have been collected in Gambell and Savoonga since the 1960s. We utilized data collected from 1992 onward by the Walrus Harvest Monitoring Program (WHMP) operated by the U.S. Fish and Wildlife Service (Service). From 1992 until 2004, the harvest was monitored from mid April through late May or early June. This time period allowed the WHMP to gather harvest information on the majority of the spring hunt, when the bulk of the walrus are harvested in these villages. From 2005 through the present year, the project has been shortened to a 2- to 4-week period attempting to encompass the

peak of the harvest, with an emphasis on collection of biological samples used for walrus research and management.

Crews consisting of local monitors and Service biologists are responsible for keeping daily records of walrus hunting activity. An attempt to meet and interview each walrus hunting crew as they return is made in both communities. For each hunting crew, data are recorded on date of departure and return, distance traveled, number of walrus harvested, details about each walrus, and harvest location. If a boat stays out past midnight, harvest is recorded for the date the hunting trip started. Data on all walrus hunting trips are recorded, even if walrus are not harvested. With this information we are able to confidently know the days when hunting was attempted and when hunting was successful, when the WHMP was in operation. The data are stored in a database and error checked. Harvest statistics are mined from the database.

2.3. Ice concentration

Satellite ice concentration data were used to calculate daily mean sea ice coverage for ocean areas within 5, 10, 30, and 50 statute mile radii (8.05, 16.1, 48.3, and 80.5 km; miles were chosen as the unit because of the greater familiarity of Yupik hunters with miles) of Savoonga (63° 16' 34''N, 171° 42' 3''W) or Gambell (63° 16' 34''N, 171° 42' 3''W). The distances were chosen as simple increments of greater distance from the communities, but still within hunting distance. Daily passive microwave sea ice concentration data are from the National Snow and Ice Data Center (NSIDC; ftp site: <ftp://n4ftl01u.ecs.nasa.gov/SAN/OTHR/>). The daily NSIDC ice concentration data are first interpolated onto the BESTMAS (Bering Ecosystem Study Ice–Ocean Modeling and Assimilation System; Zhang et al. (2010)) model grid and then used for the analysis. All the model grid cells with their centers within the 5, 10, 30, and 50-mile radii from Gambell or Savoonga were used to calculate the mean ice coverage for the respective distance. Although the interpolated data do not have finer resolution than the NSIDC data, the use of the finer grid derived from the BESTMAS interpolation makes it simpler to define the regions within the four radii and to calculate the mean values within those regions. The resulting ice concentration values do not depend on the interpolation procedure.

2.4. Wind speed and direction

The wind data used in our analysis are from the North American Regional Reanalysis (NARR) data set (Mesinger et al., 2006). This data set was produced using the Eta numerical weather prediction (NWP) model and a data assimilation system incorporating available surface, upper-air, and satellite-based observations. The grid spacing is nominally 32 km and the output is available at 3-h intervals. An alternative for the present study would have been to use the hourly winds observed at Savoonga and Gambell, Alaska. We expect that the NARR winds (which take into account the underlying surface characteristics including the presence of sea ice as estimated from satellite) are more representative of conditions over the northern Bering Sea than the land-based observations at Savoonga and Gambell, although the hunters of course are using their own observations from the shore to determine whether to go out on the water. It should be noted that the land-based observations were incorporated as part of the data assimilation procedure, and serve to constrain the NARR output. The correspondence between the two data sets for the winds was evaluated quantitatively using data for Savoonga from the spring of 2008. The daily variations in the zonal and meridional winds at 1800 and at 2100 UTC (Coordinated Universal Time, or Greenwich Mean Time) from the two sources tracked one another; Pearson's correlation coefficients between the wind

components, and in the wind speed, are slightly above 0.6. The observed winds feature somewhat greater variability (e.g., higher peak speeds) than the NARR winds, as would be expected since the latter effectively includes some spatial smoothing. The validity of atmospheric reanalyses for characterizing the winds of the Bering Sea has been previously assessed. Using wind data from moored buoys that was not available for assimilation in the NCEP–NCAR Reanalysis, Ladd and Bond (2002) found that complex correlation coefficients between the measured and synthetic winds of about 0.9, with minimal systematic biases. It should be noted that the winds measured at the Savoonga and Gambell airports are subject to local (e.g., terrain) effects, and hence will not generally match the winds over the ocean. For the present study we considered the wind directions and speeds for the grid boxes over the ocean at Savoonga and Gambell at the times of 1800, 2100 and 0000 UTC (10 AM, 1 PM and 4 PM Alaska Daylight Time, respectively) for each day.

The weather station observations at Savoonga were used to evaluate the effects of fog on walrus hunting. These observations are at roughly 20 min intervals; the reported visibilities in miles from the reports closest in time to 1800 and 2100 UTC were used in analysis. As discussed in greater detail in Section 3, this variable was found to be a lesser environmental factor and therefore the present paper focuses on the ice and wind information.

2.5. Statistical analysis

A variety of approaches could be used to explore the relationships between physical environmental factors, namely ice concentrations and winds, and hunting effort, harvest, and hunting success. We chose to employ the generalized additive model (GAM) framework. This framework is akin to multiple linear regressions, but accounts for the potential of non-linear relationships between a predictand, in this case the number of walrus harvested, and each predictor. Examples of GAMs linking marine ecosystem variables to regional physical properties include Logerwell et al. (2003) and Brodeur et al. (2008), among others. The latter study, and in more detail, Hastie and Tibshirani (1990) and Wood (2004), summarize the characteristics of GAMs. A key point for the present study is that GAMs yield functional relationships between the predictand and predictors from the data itself, rather than from pre-conceived notions. The functions themselves range in complexity from linear to smooth cubic splines; the GAM is designed to seek as simple a set of relationships as possible that adequately fit the data. The R statistical software package (www.r-project.org) was used in the construction of the GAMs.

The first step in formulating the GAMs was to examine the relationships between harvest and effort and each physical factor individually. In general, in the GAM analysis the various ice concentrations and wind variables have statistically significant relationships with effort and harvest, but do not explain a large fraction of the variance in either. GAMs were then formulated using as predictors 3–4 variables expected to be complementary in terms of characterizing the ice and wind conditions each day. In particular, the GAMs were constructed with wind speeds and directions at only a single time of day because of the strong correspondence between the winds at one time with the other times during most days. The GAMs yield both functional relationships between each predictor and the effort or harvest, and information on model performance (percentage of explained variance, histograms of residuals or errors, etc.), as presented in the following section. We also used effort as a predictor of harvest, alone and in combination with the physical factors, and we used physical factors as a predictor of efficiency.

We carried out model tests for various sets of days. Our interest is in three types of days: all days with non-zero harvests, all days with non-zero effort, and all days during the periods of active hunting. The latter is defined as the stretch of days each season encompassing recorded trips, neglecting the periods of a week or more with only a trip or two that occurred in the early portions of some seasons. Most of our analyses used the latter set, which includes a mix of days with zero trips (and harvests), non-zero trips but zero harvests, and non-zero trips and harvests. The sets of days with non-zero trips are used to evaluate efficiency, defined as the ratio of the number of walrus harvested to the number of individual trips in that day. Their counterparts for the days of non-zero harvests formed the basis for experiments with log-normalized harvest as the predictand. Model runs were carried out using the data sets constructed for the hunting communities of both Savoonga and Gambell. These various experiments yielded similar results. The same sets of parameters tended to explain greater proportions of day-to-day variance in harvest, and the functional relationships from test to test resembled one another, with one exception noted below.

3. Results

3.1. Local and traditional knowledge

The LTK discussions about walrus and ice produced several insights regarding the relationships among walrus, wind, ice, and hunters' access, including:

- At a large scale, persistent northeast winds in winter create thin ice and open water (especially large polynyas in the lee of land such as St. Lawrence Island and parts of the mainland of Alaska and Chukotka), so in spring, the ice retreats quickly. This was the case in winter/spring 2008. Hunters know that winters with sustained northeast winds will result in rapid ice retreat the following spring when a south wind blows.
- In the winter of 2008–09, there was less northerly wind than during the previous winter and the sea ice stayed longer in spring, allowing for more marine mammal hunting.
- In more recent years, the ice is thinner than in the past and also softer so that it melts more quickly in spring. This may be a result of warmer winter weather, in which the ice does not

freeze as hard and the brine is not forced out as much, leaving saltier, softer ice.

- At the local scale in Savoonga, when the north wind blows in spring, sea ice packs in against the north side of the island, preventing Savoonga hunters from getting out in their boats.

Note that north winds during winter tend to produce relatively thin ice that breaks up and melts more quickly during spring across the northern Bering Sea, resulting in a shorter duration of ideal ice conditions for hunting. At the same time, north winds (especially during spring) have the localized effect of pushing the ice against the shore at Savoonga, preventing hunters from launching their boats. Even after the shore ice has broken up, north winds will push pack ice against the shore, reducing open water near the community and making boat travel difficult. (In Gambell, north winds also push ice against the north shore of the community, and west winds do the same on the west side, but Gambell has ocean access in two directions in contrast to Savoonga's one [BB and JS, personal observations].)

3.2. Harvest, effort, ice concentration, and wind

The data in these four categories are daily figures for the walrus taken in Savoonga or Gambell, the number of hunting trips made, the average ice concentrations within various radii from the village in question, and wind speed and direction at three times during the day at or near each location. Space prohibits a presentation of all years of daily data (over 40 days per year per community), but an example period is provided in Table 1.

3.3. Statistical relationships

In Savoonga, 430 days were analyzed, including 247 days with at least one trip made and 175 days with at least one walrus harvested. In Gambell, 419 days were analyzed, including 258 days with at least one trip, and 172 days with at least one walrus harvested. For the years 1992–1995, ice concentration data were unavailable, so analyses that include physical factors were conducted on fewer total days (see Table 2). Excluded from the analysis were days outside the main hunting period (e.g., periods over 7 days without harvest, or days with low harvest separated by more than a week from days with more substantial harvests) and the few days in the record for which harvests were reported without trips having been made (likely a result of observers

Table 1

Sample of the data on harvest (number of walrus taken), effort (number of trips taken), and physical factors (ice concentration at four radii, and wind direction and speed (m/s) at three times per day) used in the analysis of environmental influences on walrus harvests in Gambell and Savoonga. This example is for Savoonga, from May 2006.

Date	Harvest	Effort	5 mile ice concentration	10 mile ice concentration	30 mile ice concentration	50 mile ice concentration	1800 UTC wind direction	2100 UTC wind direction	0000 UTC wind direction	1800 UTC wind speed	2100 UTC wind speed	0000 UTC wind speed
12-May	0	0	0.544	0.544	0.541	0.494	149.664	156.24	165.707	6.07	6.219	7.263
13-May	0	0	0.533	0.533	0.533	0.471	176.097	171.264	176.979	6.771	6.531	5.792
14-May	74	21	0.375	0.371	0.345	0.277	156.095	156.213	138.885	3.837	4.098	2.66
15-May	0	0	0.291	0.286	0.244	0.181	148.118	132.472	108.184	4.293	4.649	4.073
16-May	0	0	0.253	0.247	0.213	0.163	117.835	121.162	118.825	8.066	7.688	7.077
17-May	0	0	0.238	0.237	0.227	0.188	105.256	112.721	110.891	5.962	6.211	4.921
18-May	43	22	0.215	0.215	0.209	0.173	110.67	126.984	121.765	4.219	3.676	3.2
19-May	0	9	0.26	0.258	0.229	0.179	132.851	128.273	83.589	3.77	2.506	2.87
20-May	0	6	0.258	0.253	0.201	0.138	303.679	301.019	277.681	6.129	6.065	5.607
21-May	104	28	0.251	0.246	0.199	0.15	239.511	216.419	193.904	2.752	2.133	2.559
22-May	0	0	0.197	0.192	0.147	0.107	261.919	260.898	263.078	3.767	3.55	2.355
23-May	101	26	0.202	0.198	0.163	0.124	261.458	252.883	239.279	2.25	2.727	0.989
24-May	0	0	0.137	0.137	0.132	0.107	252.172	248.853	257.54	3.01	3.824	4.59
25-May	5	2	0.152	0.149	0.12	0.085	249.888	248.286	252.604	4.682	4.496	6.87

Table 2

Summary of generalized additive model performance. All models are based on daily time series of harvest (number of walrus taken), effort (number of individual trips), and physical factors (ice at 5 nm scale, ice at 30 nm scale, wind speed and wind direction) except for the two entries indicating effort as the only predictor/independent variable. Efficiency is the number of walrus harvested per trip. The best predictor is the independent variable with the lowest p-value, taken in the context of the GAM. See text for details.

Model	Explained variance	Number of days analyzed	Best single predictor
Harvest at Savoonga, from physical factors only	0.18	348	Wind speed
Effort at Savoonga from physical factors only	0.25	348	Wind speed
Harvest at Savoonga, from effort only	0.63	430	Effort
Efficiency at Savoonga, from physical factors only	0.15	197	Ice_5
Harvest at Savoonga, from physical factors and effort	0.70	348	Effort
Harvest at Gambell, from physical factors only	0.24	311	Wind speed
Effort at Gambell, from physical factors only	0.32	311	Wind speed
Harvest at Gambell, from effort only	0.59	419	Effort
Efficiency at Gambell, from physical factors only	0.22	201	Ice_5
Harvest at Gambell, from physical factors and effort	0.66	311	Effort

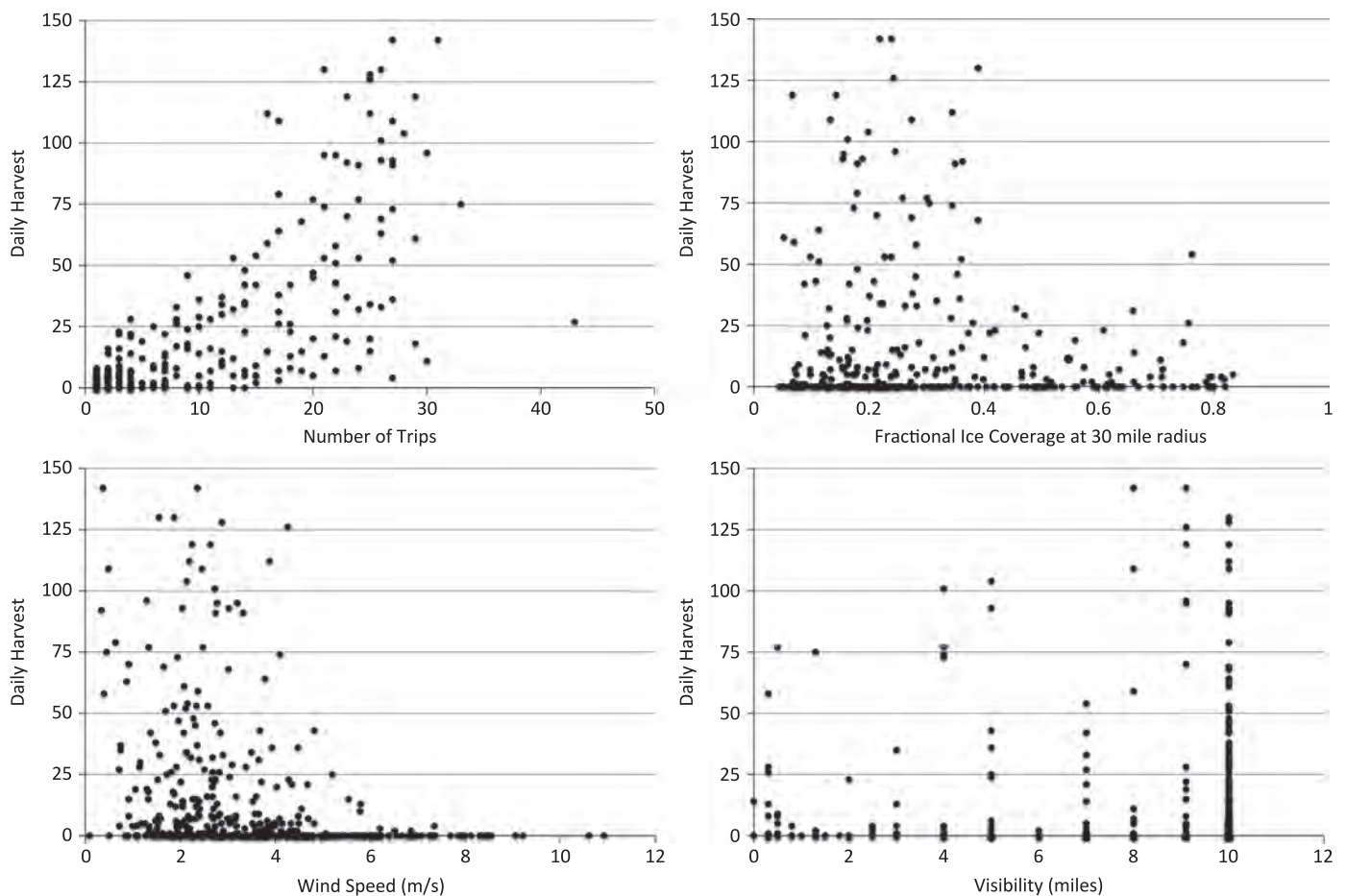


Fig. 2. Scatter plots of daily data showing walrus harvest vs. effort (upper left), ice concentration at the 30-mile radius (upper right), wind speed (lower left), and visibility (lower right) at Savoonga.

allocating overnight hunting trips to 1 day and the resulting harvest to another).

The first step in the GAM analysis was to examine individual relationships among the variables. Four examples are shown in Fig. 2, illustrating the types of data and the relationships among them that were incorporated into the GAMs. The correlation between harvest and effort is evident, as is a clear threshold effect at a wind speed of about 4.5 m/s. Ice concentration at the 30-mile radius suggests a threshold with some exceptions, but visibility indicates only a modest effect on highest harvests, though the number of days with harvests in good visibility is clearly higher.

The results from our evaluations of GAMs relating harvest and effort to ice concentrations and winds are summarized here. A variety of combinations of predictor variables, namely different scales for the ice concentrations and different times for the winds, were incorporated in GAM predictions of the Savoonga and Gambell harvests. From the perspective of the robustness of the results, an important outcome from these multiple tests is the consistency in the functional relationships identified by the GAMs. For the sake of brevity, we present below representative results from single combinations of variables for Savoonga and Gambell, and log-transformed harvests for Savoonga. A variety of GAM experiments were carried out; a measure of model skill

(explained variance) for each of these experiments is itemized in Table 2.

The GAM prediction of harvest at Savoonga considered all days during the active and reported periods of the hunting seasons. This formulation incorporates ice concentrations on the scales of 5 miles and 30 miles, and the wind speed and direction at 2100 UTC. There is a positive relationship between observed and predicted harvest values, but the physical factors only account for 18% of the observed variation in harvest. The same exercise was conducted for Gambell, with the difference that the 1800 UTC wind speed and direction were used because they yielded a slightly better fit than the 2100 UTC data. For Gambell, physical factors accounted for 24% of the observed variation in harvest.

Next, we predicted effort based on the same physical factors. The GAM explained 25% of the variability in effort in Savoonga and 32% in Gambell, an improvement over the ability to predict harvest, but still unable to account for a majority of the variability. A scatter plot of the observed (ordinate) versus modeled

(abscissa) effort and a histogram of residuals of model errors and at Savoonga are shown in Fig. 3.

We then examined the relationship between effort and harvest, since they are neither independent of one another nor equivalent. The correlation between effort as the independent variable and harvest as the depended variable was 63% in Savoonga and 59% in Gambell. This result raised the question of the influence of physical variables on efficiency, and the degree to which physical variables plus effort might together explain harvest variability.

The GAM experiment for the influence of physical variables on efficiency (walrus per trip) explained 15% of the variability in Savoonga and 22% in Gambell. These relatively low figures suggest that physical factors are most important in the decision to hunt or not to hunt, but that once a hunting trip is undertaken, physical factors are not a major influence on outcome.

We next considered harvest as a function of physical factors plus effort. The explanatory variables accounted for 70% of the variance in the daily harvest in Savoonga and 66% in Gambell. Fig. 4 shows a scatter plot of observed versus predicted harvests

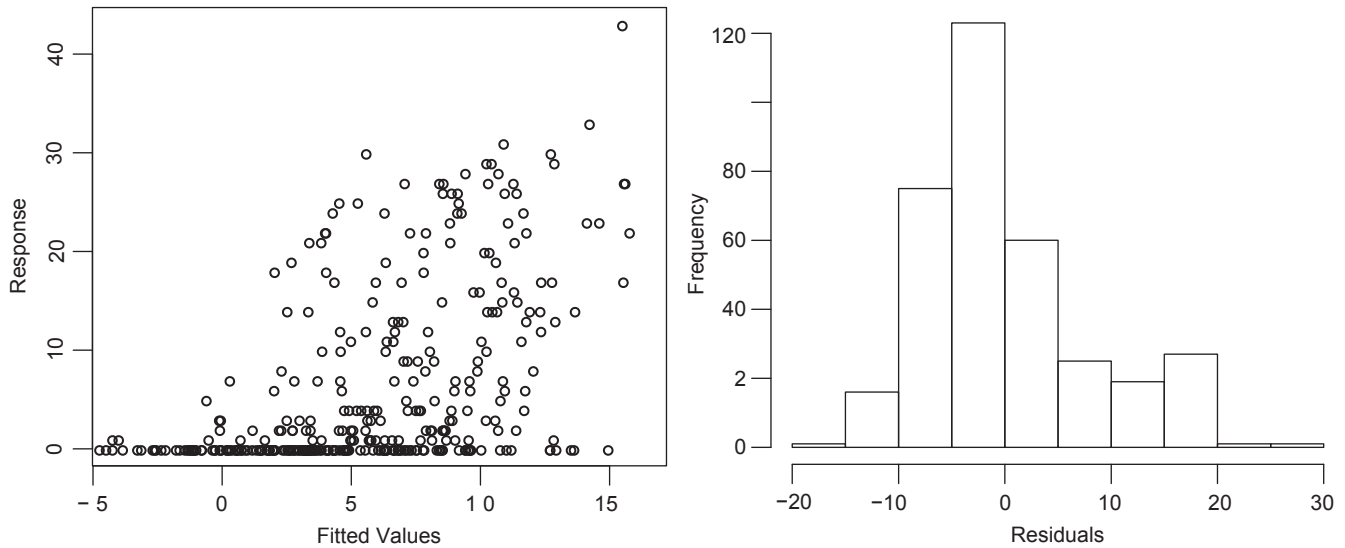


Fig. 3. Overall performance of basic GAM for Savoonga, predicting effort as a function of physical factors. Plot at left reflects distribution of observed (ordinate) versus modeled (abscissa) harvest totals for all non-zero harvest days. Histogram at right indicates the number of days with errors (observed-modeled) binned in multiples of 20 for the errors.

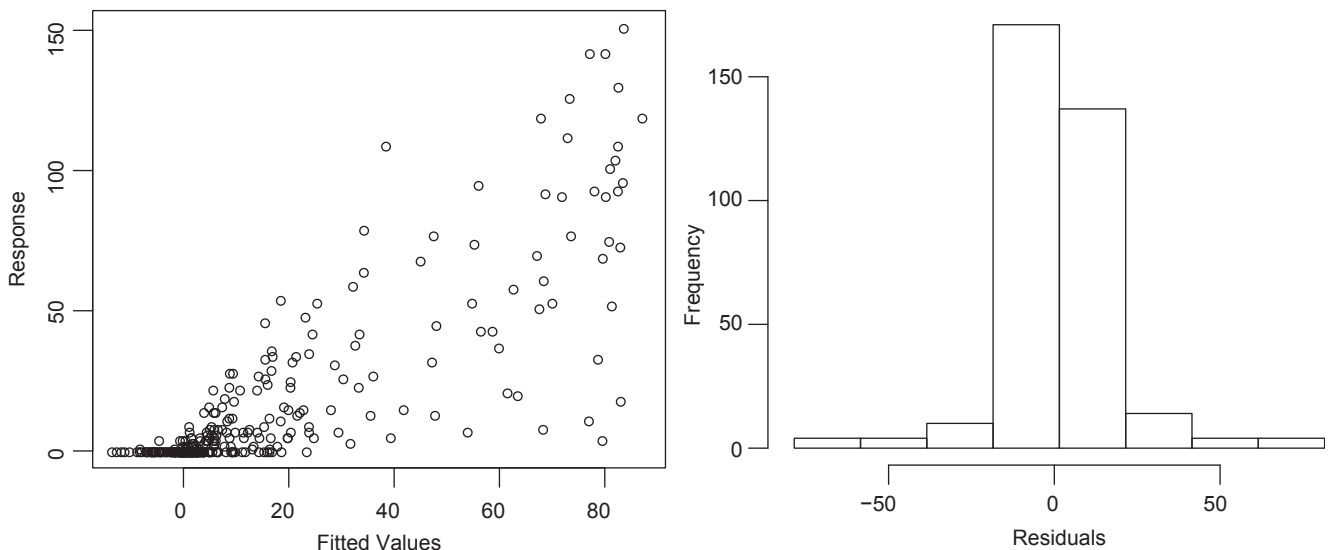


Fig. 4. As in Fig. 3, but for the GAM for Savoonga with effort and physical factors as the predictors and harvest as the predictand.

and the histogram of residuals of model errors for Savoonga, and Fig. 5 does the same for Gambell. Note the similarity in the character of the model residuals, and the systematic under-prediction of the higher harvest values.

The under-prediction of the magnitude of harvest on the most successful days led to a final GAM experiment. The highest predictions from the GAM are about 85 while the observations include a number of days with harvests exceeding 100 animals, and a peak of 151. The inability of the GAM to fit the extreme events is not surprising, but does beg the question of whether there is a more meaningful test of the relationship between harvest and physical variables plus effort. We attempted such a test using a GAM with the logarithm of the harvest values as the predictand, and only for the days with non-zero harvests. The log-transform effectively serves to lessen the influence of the days of extremely high harvest in the fitting of the model, relative to the model run with non-transformed harvest values. Such a transformation is often used, for example, in the formulation of stock-recruitment relationships for fisheries due to the occasional occurrence of very large year classes (e.g., Shelton, 1992). This GAM better replicated the harvests on the best days, but was slightly less skillful with both trips and physical factors used as predictors (61% for Savoonga vs. 70% for the non-transformed GAM, and 65% vs. 66% for Gambell).

It is worthwhile to examine the relationships that the GAM yields between predictors, i.e., number of trips, ice concentrations and winds, and predicted daily harvest values. Fig. 6 illustrates these relationships from the basic GAM for Savoonga. (Note that the relationships are determined by the GAM as a whole, and thus do not represent individual relationships between predictor and predictand.) There is a strong positive correspondence between daily harvests and number of trips (Fig. 6A), as would be expected. There was a roll-off in the predicted harvest for high values of trips, and greater uncertainty (Fig. 6A). It is unknown why, but the days with a large number of trips may include a high proportion of less skilled hunters, or more trips of shorter duration, and hence not necessarily more total time devoted to hunting. For whatever reason(s), a similar functional form was found in the equivalent GAM experiment for Gambell. Adding ice and wind variables as predictors resulted in 7% of additional explained variance for both Savoonga and Gambell. This value is not a true measure of the importance of environmental information to harvests, in that this information is not independent of the daily number of trips.

We now turn our attention to the functional forms of the environmental variables. As anticipated, ice concentrations on the 30-mile scale are inversely related to harvests (Fig. 6B) with a steeper drop-off in expected harvest at higher concentrations. A result that was unanticipated is that ice concentrations on the 5-mile scale are actually positively related to the harvest (Fig. 6C). Our interpretation of this result is that enhanced ice concentrations locally may help by reducing wave heights near shore, as long as there is enough open water on larger scales to minimize the prospect of getting trapped. It should be noted that the signal for the ice on the 5-mile scale is somewhat lower than that for the ice on the 30-mile scale; both have p -values less than 0.01.

The functional relationships for the wind direction and speed at 2100 UTC are illustrated in Fig. 6D and E, respectively. The GAM found that winds from the north to northeast, i.e., directions between near 0° and 50° , tended to be counter-productive in terms of harvests. The signal here is modest (note the difference in the scale on the ordinate versus its counterparts with respect to ice concentrations). The result for wind speed indicates that low wind speeds are highly favorable, and that higher wind speeds are unfavorable in an overall sense, but with large uncertainty. This large uncertainty is an artifact of the type of test that was carried out, at least in part. There were 40 days in the record for Savoonga during which the winds at 2100 UTC exceeded 6 m/s, and ice concentration values were available for use in the model. Trips were made on only five of these days. The average wind speed was 2.7 m/s for all the days with one or more trips out of Savoonga, and 4.5 m/s for those without, a divergence similar to that found by Kapsch et al. (2010), who also found that 69% of Savoonga's walrus were taken in winds 1–5 m/s. (Note that Kapsch used a different data set for winds, which reported higher wind speeds than the data we used; the pattern of wind and harvest in both cases is similar.)

The concept that strong winds are unfavorable is supported by the GAM for Gambell. In particular, the GAM yields a similar negative relationship between harvest and wind speed (Fig. 7A). There is a slightly greater tendency to hunt out of Gambell than out of Savoonga on days with higher wind speeds, but the success rate is still low. (This result is consistent with the fact that Gambell has access to the sea to the north and to the west, whereas Savoonga only has access to the north, providing no alternatives if the waves and/or ice are coming from that direction.) The GAM's fitting with respect to wind direction at Gambell is shown in Fig. 7B.

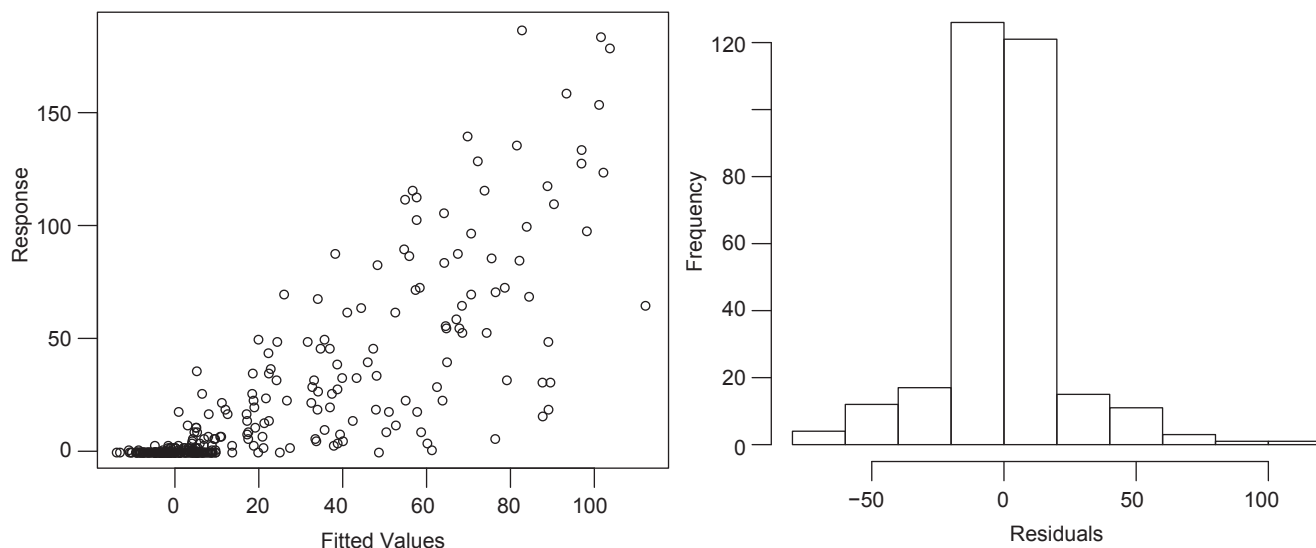


Fig. 5. As in Fig. 4, but for Gambell.

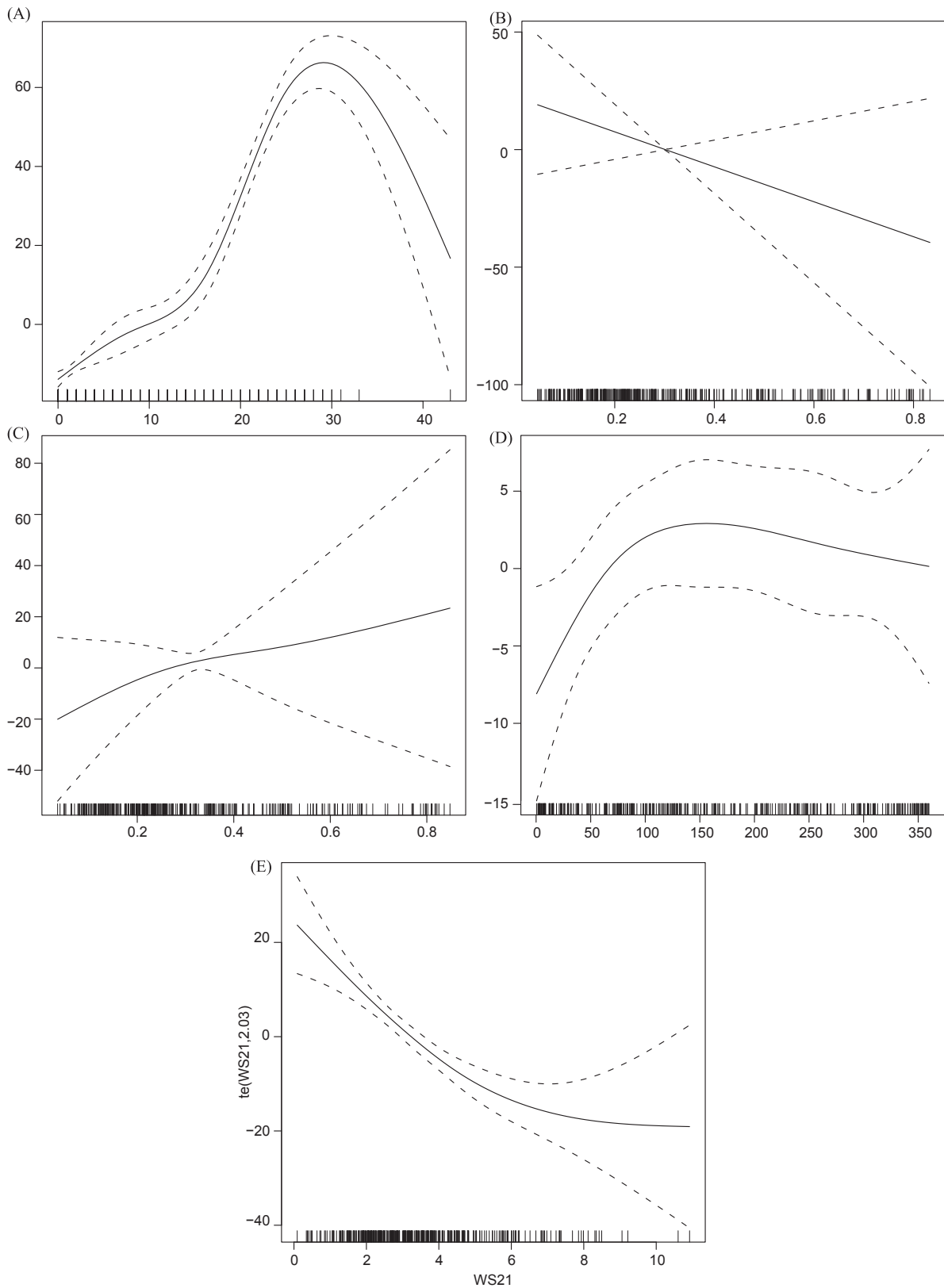


Fig. 6. (A) Fitted relationship on the effect of effort (abscissa) and harvest (ordinate, mean removed) from basic GAM for Savoonga. The solid line represents the model fit; the dashed lines encompass roughly 95% of the modeled values and hence are a representation of the confidence level in the model fit to this parameter. The individual values of the predictor are indicated along the bottom. (B) Fitted relationship between ice concentration on the 30-mile scale (abscissa) and harvest (ordinate, mean removed) from basic GAM for Savoonga. (C) Fitted relationship between ice concentration on the 5-mile scale (abscissa) and harvest (ordinate, mean removed) from basic GAM for Savoonga. (D) Fitted relationship between wind direction (abscissa) and harvest (ordinate, mean removed) from basic GAM for Savoonga. (E) Fitted relationship between wind speed (abscissa) and harvest (ordinate, mean removed) from basic GAM for Savoonga.

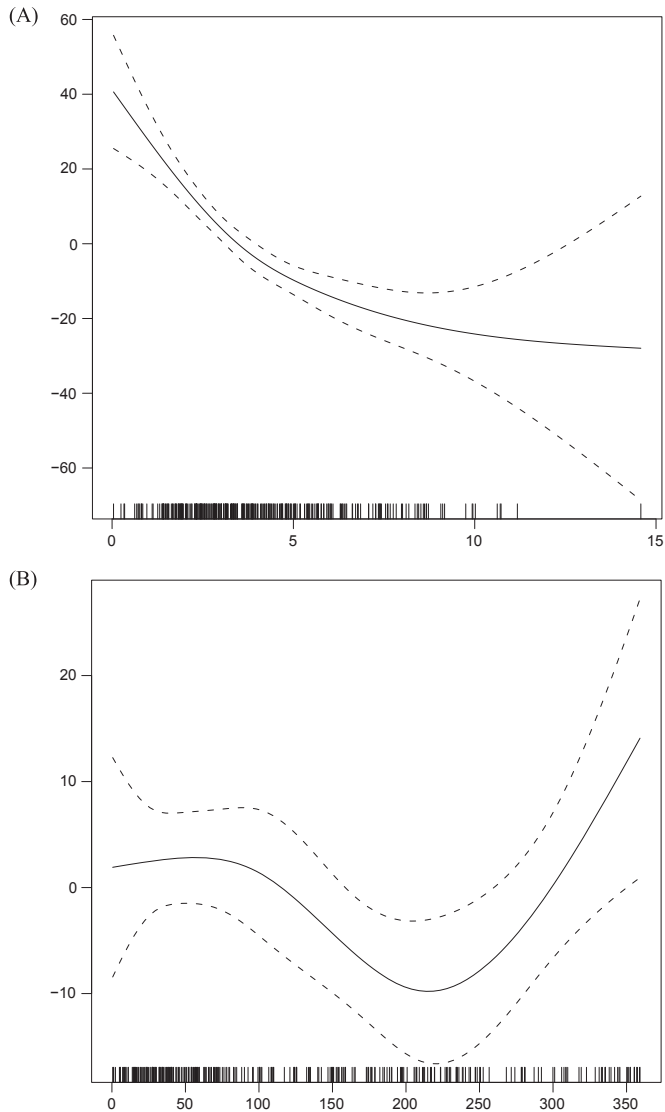


Fig. 7. (A) Fitted relationship between wind speed (abscissa) and harvest (ordinate) from basic GAM for Gambell. (B) Fitted relationship between wind direction (abscissa) and harvest (ordinate, mean removed) from basic GAM for Gambell.

The differences with its counterpart for Savoonga (Fig. 6C) are intriguing. In particular, wind directions from between about 160° and 260° , i.e., out of the south and southwest, tend to be unfavorable for Gambell while winds out of the north tend to be unfavorable for Savoonga. We suspect that this distinction can be attributed to contrasts in the nature and orientation of the coastlines at the two locations, and hence the direction of winds that would tend to close the leads in the ice near shore required for passage. Based on the various configurations of the GAM that were tested (not all of which are presented here), it seems to be the most consistent difference between the model results for the two communities, a difference also noted by Kapsch et al. (2010).

It is interesting to further consider GAM results regarding sea ice. In particular, the functional relationship between ice concentrations on the 10-mile scale and daily harvests at Savoonga (Fig. 8) indicates that moderate concentrations (~ 0.3) tend to yield the best conditions. This result may reflect elements of the relationships found for the ice on 5- and 30-mile scales, specifically that greater concentrations at the 5-mile scale and lower concentrations at the 30-mile scale tend to be associated with higher harvests, leaving the 10-mile scale in between. Our results

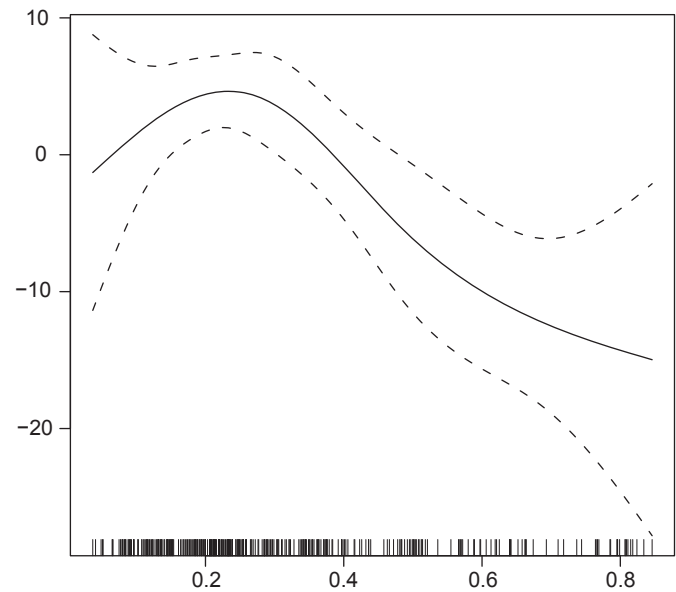


Fig. 8. Fitted relationship between ice concentration on the 10-mile scale (abscissa) and harvest (ordinate) from basic GAM for Savoonga.

are again similar to Kapsch et al.'s (2010) finding that 88% of walrus harvests occurred in ice concentrations less than 30% in a 75×75 km grid off each community, though our results offer additional insight into the form of the relationship between harvest and ice concentration at different radii from the community.

We also investigated the effects of visibility on walrus hunting out of Savoonga. The results from a series of GAM experiments yielded surprisingly little additional predictive skill (~ 1 – 2%) with respect to the number of trips or harvests. This can be explained in part by the lack of independence between the winds (especially direction) and visibilities, but in general, wind direction was a better predictor. In more quantitative terms, the GAM experiments yielded p -values of typically 0.1–0.3 for wind direction and about 0.5 for visibility, indicating that the statistical robustness of visibility as a predictor is minimal. The model runs did indicate that fewer trips, and smaller harvests, tend to be associated with lower visibilities, as expected. Kapsch et al. (2010) found that less than 5% or less of the walrus harvest took place on days with visibility less than 6 km, noting that fog is a major impediment to hunting (as also reported by St. Lawrence Island hunters). Our result likely indicates either that low visibility is not particularly prevalent (visibility is below Kapsch et al.'s threshold less than 18% of the time during the hunting season) and thus affects relatively few days, or that low visibility is correlated with wind direction and thus by itself adds little new information to the GAM, or both.

We recognize that other methods, e.g., regression trees, could be employed with our data sets. An evaluation of the relative benefits and drawbacks of different methods is outside the scope of this study. Given the consistency in the results from the tests that were carried out using a GAM, we expect that alternative approaches would yield similar results regarding the strength and nature of the relationships between hunting success and physical conditions.

4. Discussion

Establishing a quantitative relationship between human use of an ecosystem (walrus hunting) and physical conditions in that

ecosystem (ice and winds) offers insights regarding both traditional hunting practices and the ways in which those practices may be affected by climate and other environmental change. It is important to note, however, that many important variables are not included in this analysis. In particular, the distribution and abundance of walrus are also critical to a successful hunt. Although there is no particular reason to think that either has varied greatly enough (independent of ice concentrations) over the past two decades of spring hunting to have a major impact on hunting success (Chad Jay, personal communication, October 2011), changes in the walrus population or its migratory movements could clearly have an enormous impact on hunting success in the future. Local distribution patterns also affect hunting effort and outcomes. Reports of walrus close to the community, for example, can lead to hunters heading out even in marginal weather conditions or on a workday for those with regular employment.

Likewise, we have made no attempt to account for societal variables that might affect spring walrus hunting success, although it is highly likely that changes in equipment, employment, gasoline prices, and the like influence hunter decisions. Local rules are also a factor. Both Gambell and Savoonga have tribal ordinances limiting the take of walrus to four animals per hunting trip, though hunters can make multiple trips in a day if walrus are close (GN, personal observation). While such a rule might keep the actual harvest below the potential harvest, Gambell has taken up to 187 walrus in a single day and Savoonga up to 151, suggesting that hunters are capable of taking full advantage of optimal conditions when they occur, including making multiple trips when walrus are nearby.

With these qualifications in mind, we are still able to account for 25–32% of the daily variability in effort and 18–24% of the daily variability in harvest by considering three straightforward physical parameters: ice concentration, wind direction, and wind speed, readily available from remote sensing or reanalyses. Kapsch et al. (2010) took a different approach, identifying thresholds in ice concentration, winds, temperature, and visibility to determine optimal walrus hunting conditions for St. Lawrence Island. The findings of both studies are broadly consistent, that high ice concentrations and high wind speeds yield little effort or harvest, but our approach offers also a functional relationship between physical conditions and hunting. In other words, the GAM analysis allows a prediction of expected harvest under any combination of ice and wind conditions, whereas Kapsch et al.'s thresholds only indicate favorable or unfavorable conditions for single variables, without further differentiation and without combinations of variables. One difference between the studies is that our results suggest that low visibility, while it may restrict hunting, is not a major independent influence on either effort or harvest. Use of the GAMs allowed us to evaluate the combined influences of different factors in effort and harvest success, rather than being limited to separate analyses of each variable. Kapsch et al. also consider trends in suitable hunting conditions, a topic that is outside the scope of our analysis.

Although the strongest individual correspondence we found is between effort and harvest, the influence of physical factors on effort, harvest, and efficiency are not negligible. Perhaps more importantly, this result suggests an ability to say something meaningful about future walrus hunting by projecting changes in ice and winds in the northern Bering Sea. To date, most assessments of impacts on traditional hunting have been qualitative (e.g., Ford et al., 2006; Wenzel, 2009), often relying on past adaptations to evaluate a general degree of adaptability in Arctic communities. These evaluations, while useful in identifying potential problems, are often unable to identify or predict specific adaptations and adjustments by hunters, for example the

development of a fall whaling season in Savoonga in response to a delayed freeze-up (Noongwook et al., 2007).

By contrast, the identification of statistical relationships that connect readily available remote sensing and reanalysis data on ice and wind conditions with spring walrus hunting success offers specific and plausible targets for downscaling of global and regional climate models to project parameters that are now known to influence human behavior or human outcomes. Our evaluation is based on quantitative data (informed by qualitative insights into anticipated relationships between ice, wind, and hunting). The ability to predict physical conditions, however, does not necessarily equate to the ability to predict how hunters will be affected by those changes, nor how they might take advantage of new opportunities such as fall whaling in Savoonga. Nonetheless, the step from qualitative to quantitative relationships offers a way to connect numerical models with hunters' experiences and expectations.

That said, the example of walrus hunting in Gambell and Savoonga is an exceptional case. Few other harvest data sets include daily data over the course of two decades. Even for other communities in Alaska where walrus harvests are monitored by the U.S. Fish and Wildlife Service, the records were not long enough or the number of animals taken was too low to allow a similar analysis. Thus, our analysis offers a glimpse of what could be, but cannot be easily replicated for other species or other locations.

The fact that wind and ice only explain a certain portion of the variability in harvest indicates that many key variables are missing from the analysis. It is impossible to estimate how much additional variation is due to other environmental factors (e.g., walrus populations and distribution) and to societal factors (e.g., employment patterns, fuel prices, success of the spring bowhead whale hunt). Nonetheless, the persistence of human settlement on St. Lawrence Island, and the continued importance of walrus to sustaining those communities, indicates a high degree of reliability in walrus hunting. Despite environmental variability, hunters have been able to provide for their families year after year for a very long time. If key determinants of access such as wind and ice vary greatly from year to year but only account for a relatively small proportion of hunting variability, it seems reasonable to conclude that the skill and experience and adaptability of St. Lawrence Island hunters is a major contributor to their ability to thrive across a wide range of conditions.

Acknowledgments

This paper began with the insights of elders and hunters from Savoonga, Alaska, who patiently and generously shared their understanding of the Bering Sea ecosystem. We are grateful to Larry Kava, Raymond Toolie, Clarence Waghiyi, Chester Noongwook, Henry Noongwook, and Morris Toolie Sr. for their participation. We are also grateful to Sylvia Toolie, Preston Noongwook, and others in the community who helped guide the project and assist the visiting researchers during their time in Savoonga. We also thank the St. Lawrence Island hunters who have provided valuable harvest data for so many years and the local harvest monitors who collected the harvest data while spending endless hours on the beach awaiting the hunters' safe return. We are grateful to Tom Van Pelt, Chad Jay, Bruce Marcot, Quinn Smith, and the late Caleb Pungowiyi for joining the interviewing team. Winslow Hansen and James MacCracken provided constructive comments on an earlier draft, for which we thank them. Danielle Dickson made the map in Fig. 1, for which we are grateful.

We thank the North Pacific Research Board for funding our work, and the leaders and researchers of BEST-BSIERP for their

encouragement and support. We thank the BSIERP LTK Regional Advisory Board and its members for providing guidance and ideas for our project. J.Z. also thanks the National Science Foundation, whose grant ARC0611967 supports his work.

The findings and conclusions in this article are those of the authors and do not necessarily represent the views of the U.S. Fish and Wildlife Service.

This is NPRB Publication No. 394. This project was part of the Bering Ecosystem Study—Bering Sea Integrated Ecosystem Research Program, and this paper is BEST-BSIERP Publication No. 79.

References

- Ashjian, C.J., Braund, S.R., Campbell, R.G., George, J.C., Craig, Kruse, J., Maslowski, W., Moore, S.E., Nicolson, C.R., Okkonen, S.R., Sherr, B.F., Sherr, E.B., Spitz, Y.H., 2010. Climate variability, oceanography, bowhead whale distribution, and Īñupiat subsistence whaling near Barrow, Alaska. *Arctic* 63, 179–194.
- Brodeur, R.D., Decker, M.B., Ciannelli, L., Purcell, J.E., Bond, N.A., Stabeno, P.J., Acuna, E., Hunt Jr., G.L., 2008. Rise and fall of jellyfish in the eastern Bering Sea in relation to climate regime shifts. *Prog. Oceanogr.* 77, 103–111.
- Comiso, J.C., Parkinson, C.L., Gersten, R., Sock, L., 2008. Accelerated decline in the Arctic sea ice cover. *Geophys. Res. Lett.* 35, L01703, <http://dx.doi.org/10.1029/2007GL031972>.
- Fall, J., et al., 2013. Subsistence harvests in the BSIERP communities 94, 274–291.
- Ford, J.D., Smit, B., Wandel, J., 2006. Vulnerability to climate change in the Arctic: a case study from Arctic Bay. *Can. Glob. Environ. Chang.* 16, 145–160, <http://dx.doi.org/10.1016/j.gloenvcha.2005.11.007>.
- Garlich-Miller, J., MacCracken, J.G., Snyder, J., Meehan, R., Myers, M., Wilder, J.M., Lance, E., Matz, A., 2011. Status review of the Pacific walrus (*Odobenus rosmarus divergens*). U.S. Fish and Wildlife Service, Anchorage, Alaska <http://alaska.fws.gov/fisheries/mmm/walrus/pdf/review_2011.pdf>.
- George, J.C., Braund, S., Brower Jr., H., Nicolson, C., O'Hara, T., 2003. Some observations on the influence of environmental conditions on the success of hunting bowhead whales off Barrow, Alaska. In: McCartney, A.P. (Ed.), *Indigenous Ways to the Present: Native Whaling in the Western Arctic*. Canadian Circumpolar Institute and University of Utah Press, Edmonton and Salt Lake City, pp. 255–275.
- Hassol, S.J., 2004. *Impacts of a Warming Arctic: Arctic Climate Impact Assessment*. Cambridge University Press, New York.
- Hastie, T., Tibshirani, R., 1990. *Generalized Additive Models*. Chapman and Hall, London.
- Huntington, H.P., 1998. Observations on the utility of the semi-directive interview for documenting traditional ecological knowledge. *Arctic* 51, 237–242.
- Kapsch, M.-L., Eicken, H., Robards, M., 2010. Sea ice distribution and ice use by indigenous walrus hunters on St. Lawrence Island, Alaska. In: Krupnik, I., Aporta, C., Gearheard, S., Kielsen Holm, L., Laidler, G. (Eds.), *SIKU—Arctic Residents Document Sea Ice and Climate Change*. Springer, Berlin, pp. 115–144.
- Ladd, C., Bond, N.A., 2002. Evaluation of the NCEP–NCAR Reanalysis in the northeast Pacific and the Bering Sea. *J. Geophys. Res.* 107 (3158), <http://dx.doi.org/10.1029/2001JC001157>.
- Logerwell, E.A., Mantua, N., Lawson, P.W., Francis, R.C., Agostini, V.N., 2003. Tracking environmental processes in the coastal zone for understanding and predicting Oregon coho (*Oncorhynchus kisutch*) marine survival. *Fish. Oceanogr.* 12, 554–568.
- Mesinger, F., DiMego, G., Kalnay, E., Mitchell, K., Shafran, P.C., Ebisuzaki, W., Jović, D., Woollen, J., Rogers, E., Berbery, E.H., Ek, M.B., Fan, Y., Grumbine, R., Higgins, W., Li, H., Lin, Y., Manikin, G., Parrish, D., Shi, W., 2006. North American regional reanalysis. *Bull. Am. Meteor. Soc.* 87, 343–360.
- Najac, J., Lac, C., Terray, L., 2011. Impact of climate change on surface winds in France using a statistical–dynamical downscaling method with mesoscale modelling. *Int. J. Climatol.* 31, 415–430, <http://dx.doi.org/10.1002/joc.2075>.
- Noongwook, G., the Native Village of Savoonga, the Native Village of Gambell, Huntington, H.P., George, J.C., 2007. Traditional knowledge of the bowhead whale (*Balaena mysticetus*) around St. Lawrence Island, Alaska. *Arctic* 60, 47–54.
- North Pacific Research Board, 2005. *North Pacific Research Board Science Plan*. North Pacific Research Board, Anchorage.
- Overland, J., Turner, J., Francis, J., Gillett, N., Marshall, G., Tjernstrom, M., 2008. The Arctic and Antarctic: two faces of climate change. *EOS* 89, 19.
- Rothrock, D.A., Yu, Y., Maykut, G.A., 1999. Thinning of the arctic sea-ice cover. *Geophys. Res. Lett.* 26 (23), 3469–3472.
- Shelton, P., 1992. The shape of recruitment distributions. *Can. J. Fish. Aquat. Sci.* 49, 1754–1761.
- Stroeve, J., Serreze, M., Drobot, S., Gearhead, S., Holland, M., Maslanik, J., Meier, W., Scambo, T.S., 2008. Arctic sea ice extent plummets in 2007. *EOS* 89, 13.
- Wendler, G., Shulski, M., Moore, B., 2010. Changes in the climate of the Alaskan North Slope and the ice concentration of the adjacent Beaufort Sea. *Theo. Appl. Climatol.* 99, 67–74.
- Wenzel, G.W., 2009. Canadian Inuit subsistence and ecological instability—if the climate changes, must the Inuit? *Polar Res.* 28, 89–99, <http://dx.doi.org/10.1111/j.1751-8369.2009.00098.x>.
- Wiese, F.K., Wiseman, W.J., Van Pelt, T.I., 2012. Bering Sea linkages. *Deep-Sea Res.* II 65–70, 2–5.
- Wood, S.N., 2004. Stable and efficient multiple smoothing parameter estimation for generalized additive models. *J. Am. Stat. Assoc.* 99, 637–686.
- Zhang, J., Woodgate, R., Moritz, R., 2010. Sea ice response to atmospheric and oceanic forcing in the Bering Sea. *J. Phys. Oceanogr.* 40, 1729–1747, <http://dx.doi.org/10.1175/2010JP04323.1> 2010.



Local and traditional knowledge regarding the Bering Sea ecosystem: Selected results from five indigenous communities



Henry P. Huntington^{a,*}, Nicole M. Braem^b, Caroline L. Brown^b, Eugene Hunn^c, Theodore M. Krieg^d, Pamela Lestenkof^e, George Noongwook^f, Jennifer Sepez^{1,g}, Michael F. Sigler^h, Francis K. Wieseⁱ, Philip Zavadil^j

^a 23834 The Clearing Drive, Eagle River, AK 99577, USA

^b Alaska Department of Fish and Game, Division of Subsistence, 1300 College Road Fairbanks, AK 99701-1599, USA

^c Department of Anthropology, University of Washington, Seattle, WA 98195, USA

^d Alaska Department of Fish and Game, Division of Subsistence, P.O. Box 1030, Dillingham, AK 99576-1030, USA

^e Aleut Community of St. Paul Island Tribal Government, 460 W. Tudor Road, Ste 102, Anchorage, AK 99503, USA

^f Savoonga Whaling Captains Association, Native Village of Savoonga, P.O. Box 202, Savoonga, AK 99769, USA

^g Alaska Fisheries Science Center, National Oceanic and Atmospheric Administration, 7600 Sand Point Way, Seattle, WA 98115, USA

^h Alaska Fisheries Science Center, National Oceanic and Atmospheric Administration, 17109 Point Lena Loop Road, Juneau, AK 99801, USA

ⁱ North Pacific Research Board, 1007 W 3rd Avenue, Suite 100, Anchorage, AK 99501, USA

^j Aleut Community of St. Paul Island Tribal Government, P.O. Box 86, St. Paul Island, AK 99660, USA

ARTICLE INFO

Available online 2 May 2013

Keywords:

Bering Sea
Local and traditional knowledge
Alaska Natives
Subsistence
Hunting
Fishing

ABSTRACT

We documented local and traditional knowledge (LTK) about the Bering Sea ecosystem through interviews with Alaska Native elders, hunters, and fishers in the coastal communities of Akutan, St. Paul, Togiak, Emmonak, and Savoonga. Their observations describe a complex and changing ecosystem, with indications of divergent impacts of change in the south (many species in decline) and the north (a productive ecosystem). Observed changes in species abundance suggest that the marginal zone of maximum (March) sea-ice extent is experiencing the most rapid directional changes, including shifts in distribution of ice-associated species such as bearded seal (*Erignathus barbatus*). Causes of declines in other species such as northern fur seals (*Callorhinus ursinus*) and murrelets (*Uria* spp.) are harder to identify, and seabird abundance trends appear to vary greatly with location. Connections between the LTK findings and other research under the North Pacific Research Board and National Science Foundation's Bering Sea Project were modest due to mismatches in temporal and spatial scales of reference and the fact that LTK observations were not initially made with scientific relevance in mind. We found, however, the overall observations to be consistent with the emerging picture of high spatial variability in the Bering Sea ecosystem.

© 2013 Elsevier Ltd. All rights reserved.

1. Introduction

The Bering Sea ecosystem includes several indigenous peoples with rich traditions of observing and using their physical and biological environment (e.g., Johnson, 2003). The North Pacific Research Board and National Science Foundation's Bering Sea Project (Wiese et al., 2012) incorporated these human dimensions

in various ways, including research focused on five Alaska Native communities on the coasts and islands of the eastern Bering Sea. The community-based research effort had two foci: documenting subsistence harvests of marine species (Fall et al., 2013), and documenting local and traditional knowledge (LTK) about the marine ecosystem.

In this paper, we present selected results of the LTK interviews, emphasizing information related to some of the objectives and hypotheses of the Bering Sea Project (see Table 1). Our goal is threefold: first, to make available some of the ecological information gathered from interviews with knowledgeable residents of the five communities in which we worked; second, to assess how that information addresses the Bering Sea Project hypotheses, by itself and when taken in conjunction with results from other components of the project; and third, to offer conclusions regarding the utility of incorporating LTK in a major ecosystem research

* Corresponding author. Tel.: +1 907 696 3564; fax: +1 907 696 3565.

E-mail addresses: hph@alaska.net (H.P. Huntington), nicole.braem@alaska.gov (N.M. Braem), caroline.brown@alaska.gov (C.L. Brown), enhunn323@comcast.net (E. Hunn), theodore.krieg@alaska.gov (T.M. Krieg), pmllestenkof@tgsapi.com (P. Lestenkof), gnunguk@hotmail.com (G. Noongwook), Mike.Sigler@noaa.gov (M.F. Sigler), francis.wiese@nprb.org (F.K. Wiese), pazavadil@tgsapi.com (P. Zavadil).

¹ Retired.

Table 1

Bering Sea Project hypotheses addressed in this paper. (A full list of the hypotheses is available at http://doc.nprb.org/web/BSIERP/zzWebsite/focal/BSIERP_Conceptual_Framework_Hypotheses.pdf).

Hypothesis number	Hypothesis
1.b.	Reduced frequency and intensity of summer storms will reduce surface mixing and increase sea surface temperature, thereby increasing stratification.
2.b.	As heat content increases, the area suitable for spawning and foraging by subarctic species will expand northward and subarctic species will occupy areas formerly occupied by Arctic species.
3.a.	Competition with abundant, piscivorous fish species for forage species will lead to a decline in murre, kittiwakes and fur seals.
4.a.	Climate-ocean changes will displace predictably located, abundant prey (hot spots) necessary for successful foraging by central place (seabirds and fur seals while nurturing young) and hot spot (baleen whales, walrus) foragers.
4.b.	Central place foragers will shift their diet, foraging locations or rookery locations to increase foraging opportunities.

project of this kind, including suggestions for promising lines of further inquiry.

Local and traditional knowledge “refers to an array of information, understanding, and wisdom accumulated over time based on experience and often shared within a group or community” (NPRB, 2005: 144; see also Huntington, 1998, Berkes, 1999). Agrawal (1995) points out that neither LTK nor scientific knowledge can be treated as a uniform monolith of understanding or practice. Instead, both encompass a variety of methods, traditions, premises, and other characteristics that undermine any simple attempt to categorize and contrast different forms of knowing under only two headings. Agrawal does not, however, claim that different forms of knowledge are always compatible. Noongwook et al. (2007), for example, provide an example from the Bering Sea in which hunters’ knowledge of bowhead whale (*Balaena mysticetus*) behavior lies largely outside scientific understanding of whale cognition. In addition, while both the LTK and natural science projects within the Bering Sea Project relied on an inquiry-based approach, the modes of observation differed with the LTK observations largely relying on human senses and the natural science observations largely relying on instruments.

In the case of Bering Sea communities, interactions with scientists, directly and through media, such as television and newspaper, have long provided another source of information to their own observations of their environment. Thus, the data gathered via LTK interviews cannot be treated as an entirely independent stream of data from that generated by scientific methods, but nonetheless offer a distinct perspective on ecosystems processes and change based on continuous observations over a period far longer than the duration of any research project. A deeper comparative assessment of the nature of knowledge, whether local, indigenous, or scientific, is beyond the scope of this paper. We use the terms “LTK” and “scientific knowledge” or “natural science” to distinguish the data gathered from interviews with residents of the Bering Sea coast from the data gathered by other parts of the Bering Sea Project. This is not to imply that LTK does not share some characteristics of scientific research, but simply to avoid repeating lengthy descriptions or circumlocutions.

Within the Bering Sea Project, the LTK component aimed to gather information about trends in, and interactions among, physical and biological parameters of the Bering Sea ecosystem. This was done in part to provide another perspective on the topics being addressed by the natural science components of the project (e.g., Huntington et al., 2004a), and in part to secure substantive participation in the project by Bering Sea residents. The documentation of subsistence harvests (Fall et al., 2013) addressed the hypothesis that environmental change would impact Bering Sea communities. This paper, in contrast, focuses on the natural science hypotheses that guided the Bering Sea Project as a whole. Thus, despite employing methods more commonly associated with the social sciences, this paper is not a social science paper per se, but is intended as a contribution to the natural science

investigations under the Bering Sea Project. We acknowledge that our approach emphasizes LTK from an outside (etic) perspective, rather than from within the system in which the knowledge is generated, held, and used (an emic perspective; see Ingold and Kurtilla, 2000).

The five focal communities in this study were Akutan, St. Paul, Togiak, Emmonak, and Savoonga. They form a south–north transect in the eastern Bering Sea (Fig. 1) and were chosen in part because they have different degrees of exposure to sea ice and because subsistence harvest data have been collected for each community prior to the start of this project (Alaska Department of Fish and Game, Community Subsistence Information System). Akutan, St. Paul, and Savoonga are island communities. Togiak and Emmonak are on the mainland coast or estuaries and have long-standing patterns of marine resource use. Akutan and St. Paul are predominantly Aleut or Unangan villages, Togiak and Emmonak are Yup’ik, and Savoonga is St. Lawrence Island or Siberian Yupik. All engage in both commercial fishing and in subsistence hunting and fishing, though the economic significance of commercial fishing generally decreases as one moves northwards (Stevenson and Lauth, 2012). Subsistence harvest patterns are described in detail by Fall et al. (2013). Each community takes substantial quantities of wild meat and fish each year, indicating a strong degree of interaction with the local environment and thus a strong foundation for their LTK.

2. Methods

The primary method used to document LTK in this study was the semi-directive interview (Huntington, 1998), used in all communities except St. Paul where a formal questionnaire was used (see below). Semi-directive interviews are conducted with individuals or in groups, with a set of topics to be addressed, but no fixed order or questionnaire to follow. Instead, the respondent or respondents are allowed to discuss the topic in a manner that makes sense to them, perhaps making connections with other ecosystem components or describing trends over time. The interviewer can intervene to keep the discussion on topic, or to ask for more detail on various points, or to guide the respondent (s) toward items of particular interest. In each of the communities where this method was used, respondents were chosen based on their expertise about, and experience with, the marine environment, with the result that participants were predominantly older (> 50 years of age) men.

A disadvantage of this method is that the ensuing discussion has little structure, and thus compiling results from different interviews is not always straightforward. The advantages, however, are that the description of the ecosystem follows the respondent’s understanding, rather than any preconceived notions on the part of the interviewer, and thus that new insights are more likely to emerge because the interview format is flexible and open.

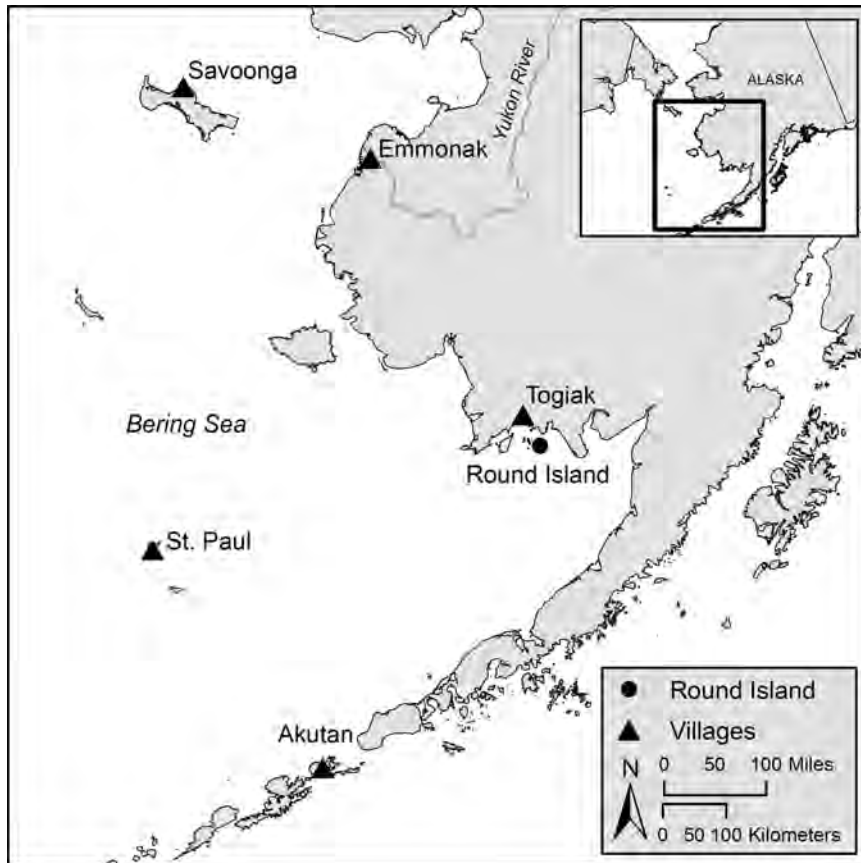


Fig. 1. Map of the Bering Sea, showing the five communities involved in the local and traditional knowledge component of the Bering Sea Project.

Table 2

Details of the interview procedures in each community (Household data from U.S. Census, 2010; Akutan's population is the number of permanent residents, excluding 937 workers at the cannery).

Community Population	Main interviewer(s)	Date(s) of interviews	Number of respondents
Akutan (90)	Jennifer Sepez Eugene Hunn Jennie Webster	September 2010	5 (plus many less formal discussions with additional community members)
St. Paul (479)	Emily Melovidov Philip Zavadil	2009	11 (individually)
Togiak (817)	Ted Krieg Josh Wisniewski	February 2010	11 (one individual, two pairs, one group of six)
Emmonak (762)	Nikki Braem, Caroline Brown Robbin Lavine Michael Jimmy	August 2010 April 2011	13 (individual or pairs)
Savoonga (671)	George Noongwook Henry Huntington Caleb Pungowiyi Chadwick Jay Bruce Marcot Tom Van Pelt	July 2009	8 (group)

Table 2 presents a summary of the interview details in each community. Some additional information was gathered during collection of harvest data (Fall et al., 2013), but this work was largely preparatory with regard to the documentation of LTK and is not included in Table 1.

The LTK interviews in St. Paul used a different method, the formal questionnaire, as chosen by the members of the community overseeing and conducting the research there. In contrast to the other communities, a range of demographic groups was targeted, including elders, fishers, hunters, young adults, and

youth. Interviewees were asked a series of pre-determined questions covering demographics, customary traditional practices, fisheries, environmental quality, seasonal cycles, northern fur seals (*Callorhinus ursinus*), other marine mammals, black-legged kittiwakes (*Rissa tridactyla*), thick-billed murre (*Uria lomvia*), other birds, halibut (*Hippoglossus stenolepis*), crab, other fish, ocean conditions, environmental-weather conditions, sea ice conditions, education and outreach, and general human impacts. Interviews were conducted at the Tribal Government office or in the respondent's home, and either audio or video recorded.

An in-depth comparison of methods is beyond the scope of this paper, but a few observations may be relevant for those planning similar studies in the future. The semi-directive interviews are harder to conduct and interpret, but in this case gathered a wider range of information, and thus may be of more use in a broad survey of ecological knowledge. The questionnaires require less skill to administer, and also allow for easier analysis. This method may thus be simpler in cases where the topics to be addressed are clearly defined beforehand. In both cases, the involvement of natural scientists in identifying topics to discuss and in interpreting the results is valuable for increasing the likelihood that the outcomes will be useful in a natural science-driven program such as the Bering Sea Project. In the Discussion, we note one approach that would draw on both methods as part of an iterative, rather than one-time, LTK documentation effort.

In addition to the interview methods themselves, the LTK work relied upon Community Advisory Boards, locally chosen individuals who helped steer the project in all locations, identify key topics to be discussed, and select potential respondents particularly knowledgeable on those topics. The selection of respondents thus was not arbitrary, but was intended to find those individuals who were locally regarded as experts on the marine ecosystem and its various components or, in the case of St. Paul, met other demographic criteria of interest. Thus, the LTK that was documented does not necessarily reflect a local consensus or represent typical local understanding, nor is it intended to reflect a community average achieved through a representative sample. Instead, it is intended to reflect what the locally recognized experts have to say about the ecosystem in which they have spent most of their lives.

3. Results

The LTK interviews were broad, covering a range of topics from environmental conditions to ecological relationships, from uses of animals to storage of meat to the means of showing respect to animals and the natural world. Detailed records for each community have been archived with other data in the Bering Sea Project Data Archive (<http://beringsea.eol.ucar.edu/>). Here, we highlight five different results related to four of the five main Bering Sea Project hypotheses (Table 1) and to overall patterns of change in the Bering Sea ecosystem. The Discussion section examines the light that the LTK findings shed on the hypotheses, and also compares the LTK results with the results of other lines of investigation within the Bering Sea Project or from the published literature. Fall et al. (2013) address impacts of ecosystem changes to subsistence use by hunters and fishers.

Statements in this section derive solely from the LTK interviews, unless otherwise noted. It is also essential to note that the lack of information on a particular point or from a particular community cannot be interpreted as a lack of change. Instead, it is simply “no data,” which could mean that no change has been seen, or that the topic did not arise during the interviews or was discussed inconclusively.

3.1. Changing weather

One respondent in Emmonak stated that summers used to be less stormy than they are now. Other respondents, however, noted that dry weather is needed to dry fish, and that recent summers have been rainier than usual, making fish drying difficult. Furthermore, they noted that in the past, windy periods lasting two to three days were cause for comment and complaint. In the past few years, however, winds have become more frequent, and almost every day has wind. September, for example, used to be reliably

calm, creating good conditions for hunting bearded seals (*Erigonathus barbatus*). This is no longer the case.

Respondents in St. Paul described warmer summers, longer and colder winters, and stronger storms in winter.

3.2. Shifts in species distribution

In the Togiak area, people noted that bearded seals have become less common. Some hunters attributed this to the effects of the Pacific herring (*Clupea pallasii*) fishery, but others to the loss of sea ice, which results in fewer seals being born in the area. Bearded seals are understood to return to the area of their birth, so if they are no longer being born in the Togiak area, they will not be present as adults either. The following is a compilation of statements from Togiak concerning bearded seals:

- In the enclosed area to the north of the spit on the west side of Hagemester Island there used to be lots of seals, there were so many seals there that the water used to be muddy. There used to be thousands of seal. There used to be so many that we did not know which one to shoot when we were hunting. They do not haul out any more like they used to.
- Fewer bearded seals are coming back now than in the past. They used to have babies in the Togiak Bay area and they would return to the same place that they were born. Lack of sea ice means they are not born in the Togiak area and therefore do not return there. Bearded seal used to go way up the Togiak River—the young bearded seals went up the river in the fall.
- Long ago there use to be big groups of bearded seals that would line up and space out for feeding, but you never see that anymore.
- Bearded seals can only be found on Hagemester side [south-west of Togiak]. They are not coming in closer to Togiak like they used to.
- Ringed seals (*Phoca hispida*) and bearded seals numbers are really low because the weather has changed and they are moving somewhere else.

In other communities and for other species, changes in abundance were described and, where present, often attributed to cyclic patterns in the environment. In Emmonak, for example, one respondent said that ecological change is not remarkable. It is a fact of life, as is the need to adapt to such change. In Savoonga, respondents noted that they have seen new songbirds, ones without Yupik names, but no other major shifts in species distribution.

3.3. Changes in abundance

The LTK interviews provided some observations of variations in population size over time, but most respondents attributed these primarily to cyclical patterns. For example, there is little evidence from the LTK interviews of long-term population declines in kittiwakes anywhere, or in murre other than in the Togiak area.

In Savoonga, respondents reported that in some years, the black-legged kittiwakes do not lay eggs. They noted no obvious environmental reason for this, but said that it is less frequent for kittiwakes not to lay eggs than it is for murre to experience die-offs, which themselves are not very frequent. The most recent seabird die-offs were in the late 1990s. They also reported in 2009 that the marine ecosystem in general seems to be healthy, with most or all species abundant.

In Togiak, respondents said that murre abundance has declined during their lifetimes, including a die-off in the mid-1990s. Murre are no longer as abundant on Black Rock, an outcrop in the waters between Togiak and Round Island, popular for hunting and egg gathering.

In St. Paul, two-thirds of respondents indicated seeing no change in black-legged kittiwake abundance.

Fur seals, on the other hand, are declining in St. Paul. Respondents listed predation on fur seals by killer whales (*Orcinus orca*) as one possible cause. There was, however, little information on changes in foraging or predation. Several respondents connected fur seal declines with less prey, noting declines in some birds and fish as well as the fur seals. The decline in prey was attributed to ecosystem change and to competition with commercial fisheries.

3.4. Reliability of “hot spots”

Respondents in Savoonga described “hot spots” around the island. Large aggregations of seabirds, seals, and minke whales (*Balaenoptera acuturostrata*) are often seen at sea. The Yupik word for “hot spots” translates as “cooking,” as they are all feeding together, usually on Pacific sand lance (*Ammodytes hexapterus*) or on “surf smelt” (*kegarangiiq* in Yupik; Badten et al., 2008 say the English or scientific name of this fish has not been determined. The fish are about four inches [10 cm] long, silver, and in cross-section are shaped like an inverted triangle). It was noted that the animals also eat small cod (*iqallugaq*; not clear which species is meant), capelin (*Mallotus villosus*, known locally as *sikaaq* and also “cigarfish”), and rainbow smelt (*Osmerus mordax*) and that overall there are many small fishes in the ocean and the animals will eat them all.

The comment was made that seabirds and marine mammals are intertwined around food, especially concentrations of food like sand lance schools. Because aggregations of small fishes move around, birds and marine mammals move with them. Residents, however, noted a few regular locations for such fishes, such as 20 miles (32 km) north of Eevwak Point (which is 5–6 miles, or 8–10 km, west of Savoonga) and also off Stolbi Rocks (1–2 miles, 2–3 km east of Savoonga). Fig. 2 shows the location of these “hot spots” as well as other patterns of aggregation or behavior in the St. Lawrence Island area.

Akutan respondents noted that fish follow forage fish, and birds and marine mammals follow the fish. Although no specific locations or patterns of forage fish aggregations were noted, respondents described changes in short-tailed shearwaters (*Puffinus tenuirostris*) foraging behavior in relation to a physically driven change in prey availability. Specifically, shearwaters and other birds used to feed on the surface, but in 1996 (a summer respondents noted was very warm) they started diving deep and staying under a long time; e.g., 2–3 min. In 1996, sea surface temperatures were notably warmer than in preceding years which likely explained why the shearwaters were forced to dive deeper to get their feed (e.g., Pacific sand lance, known locally as needlefish). Some birds died that year, apparently from starvation. “Hot spots” were not described in other communities.

3.5. Ecosystem perspectives

Respondents in all communities provided a detailed, complex description of their local ecosystems. Reduction of those descriptions to a few single indicators or evaluations of overall “ecosystem health” must therefore be done with caution. Nonetheless, there are some striking differences in the overall descriptions of the abundance and body condition of hunted animals across the south–north transect of the five study communities.

Akutan respondents noted that protected species are doing well. Killer whales, for example, are abundant, and thought to lead to major declines of species such as Steller sea lions (*Eumetopias jubatus*). Sea otters (*Enhydra lutra*), bald eagles (*Haliaeetus leucocephalus*), and eiders (*Somateria* spp.) are increasing or very abundant. The changes were ascribed largely to protective measures taken for those species. Other species declines that respondents described were confined primarily to changes in Akutan Bay, and largely attributed to pollution (especially fish waste) from the fish processing plant. A diesel spill on nearby Akun Island killed shellfish on the affected shoreline, but was similarly a local phenomenon.

The majority of St. Paul respondents rated the environmental quality of the surrounding waters as “very good,” with 64% indicating

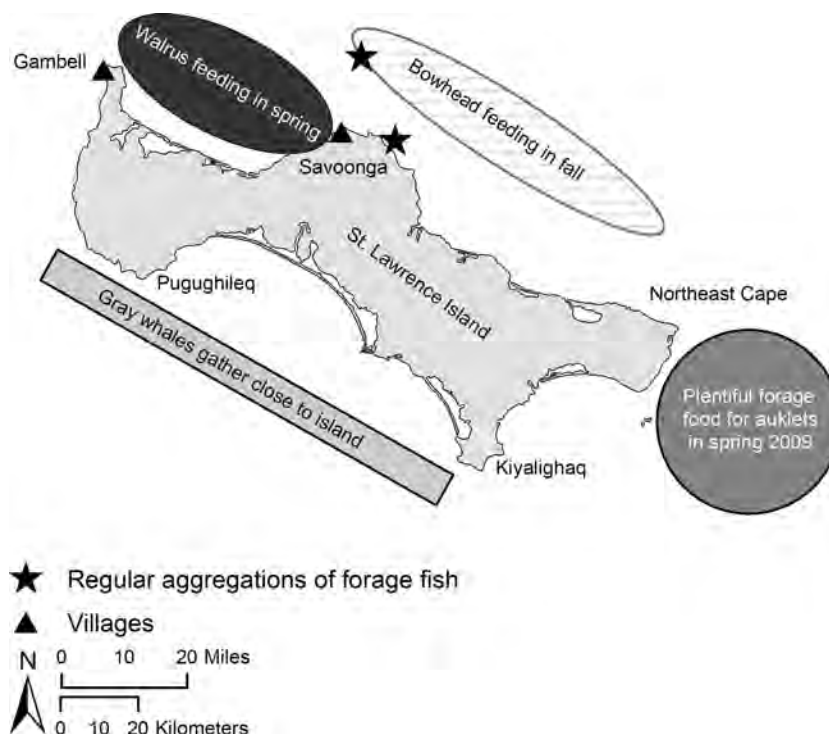


Fig. 2. “Hot spots” and other ecological features and aggregations in the St. Lawrence Island area.

no change and 27% reporting a decline. The decline in fur seals is perhaps the most obvious biological sign of ecosystem change, but the signal from other species is mixed. It is noteworthy that many observed changes had, in the view of the respondents, more to do with the state of commercial fisheries in the area (63% of respondents were commercial fishers), rather than with the background environmental conditions, although many noted changes in oceanographic and climatological variables.

Togiak's responses, in contrast, painted a general picture of decline in many species important to subsistence, including bearded seals, ringed seals, herring, herring spawn, king salmon (*Oncorhynchus tshawytscha*), red salmon (*O. nerka*), capelin, king eiders (*Somateria spectabilis*), common eiders (*S. mollissima*), murre (Uria spp.), long-tailed ducks (*Clangula hyemalis*), shorebirds, lesser snow geese (*Anser coerulescens coerulescens*), cormorants (*Phalacrocorax* spp.), arctic terns (*Sterna paradisaea*), gulls, Pacific halibut, and even larger whales (though these are not hunted in the Togiak area). These changes were ascribed to overfishing and/or climate change. Overfishing concerns focused primarily on herring since herring are seen as a crucial food item for many marine animals. Bottom trawling, too, was regarded as destructive, especially for the clam beds that Pacific walrus (*Odobenus rosmarus divergens*) depend upon. Walrus numbers at Round Island have been going down as the walrus population in the region decreases or moves elsewhere. The most visible indicator of climate change with extensive ecological repercussions in the Togiak area is that sea ice is thinner, and the ocean freezes later in the fall and melts sooner and more quickly in spring.

In Emmonak, the main concerns focused on king salmon and the perceived impacts from by-catch by offshore fishing fleets. Sea ice has gotten much thinner and is now typically four feet thick (1.2 m) rather than the six to eight feet (1.8–2.4 m) it used to be. As in Togiak, respondents have observed later freeze up and earlier ice break up. Winters are not as severe as they were. Hunting patterns have changed, partly as a result of changing ice, but also in response to technological change such as the use of snowmachines (snowmobiles) that allow hunting trips to be completed in a day, loss of knowledge for traveling over sea ice, the price of gasoline, and other societal factors such as work commitments. Summer water temperatures in the Yukon River and in the Bering Sea were reported as being warmer than they used to be. It was further noted that migratory birds are arriving later in the spring. Canada geese (*Branta canadensis*) used to arrive in March, and other birds in early April. Now, most birds do not arrive until the first week of May. There were, however, few descriptions of changes in animal abundance or distribution over time.

Savoonga reported that marine productivity is reliable and generally consistent around St. Lawrence Island. Conditions have been good in recent years, with fat walrus and abundant animals. Respondents noted that some species, such as walrus, murre, shearwaters, and crested auklets (*Aethia cristatella*), have occasional die-offs, but that these are not common and have not occurred recently. While they noted many changes, including declines in seal abundance at haulouts on the island, many were attributed to local causes (erosion of haulout sites or excessive noise by people) rather than broader ecosystem factors. Overall, the picture of the northern Bering Sea ecosystem was very positive, with little change in species abundance.

4. Discussion

The LTK results by themselves offer some insight into mechanistic relationships between species and species and their environment. Thus they address the Bering Sea Project hypotheses. Applying these observations directly to the hypotheses must be done with caution, however, as the hypotheses were generated during an extremely warm period in the Bering Sea in the early

2000s (Stabeno et al., 2012a) with an expectation, and model predictions, pointing to an increasingly warm climate in this area. Alas, the period of the Bering Sea Project field years was marked by cold water and extensive sea ice (Overland et al., 2012). Whereas this mismatch makes a direct “prove or disprove” of the natural science hypotheses difficult, the descriptions given by Bering Sea residents likely draw upon a lifetime or more of experience and observation, rather than just a few years' worth, and thus their observations and explanations may provide insights into the mechanisms regulating the Bering Sea marine ecosystem even if in the short-term they differ from observations derived from recent scientific study.

A comparison of LTK results with findings from other parts of the Bering Sea Project and from other scientific studies may also be illuminating, but should similarly be done with some caution. Time frame and spatial scales of reference are likely to differ (e.g., Huntington et al., 2004b), with local observations emphasizing local patterns, and broad-scale oceanographic investigations more likely emphasizing patterns across the Bering Sea. A comparison across the five communities offers some insight into such broader patterns, and is provided in the final part of the Discussion. Apparent disagreement between LTK results and scientific results, however, does not necessarily require judging one of them as “wrong” (Huntington et al., 2004a). Consistent results may increase confidence, but inconsistent results may point the way to new insights or promising new research ideas.

4.1. Changing weather

One of the core hypotheses of the Bering Sea Project states that: “Reduced frequency and intensity of summer storms will reduce surface mixing and increase sea surface temperature, thereby increasing stratification.”

As noted, this hypothesis was formulated as a prediction during a time of warming in the early 2000s (Stabeno et al., 2012a), whereas the LTK interviews and questionnaires were gathered during a period of extremely cold conditions (2006–2010). Given this juxtaposition, we anticipated observed weather patterns to differ from the ones predicted. Indeed, both Emmonak and St. Paul indicated stormier conditions in the recent cold years. A comparison of the warm years in the early 2000s to the colder years in the second half of the decade show increased abundance of large zooplankton in the later period (Coyle et al., 2011; Hunt et al., 2011). Thus, even though the LTK observations need not describe proper storms, but may simply indicate a change in everyday conditions, these observations do not falsify the hypothesis, and may indeed point to a way to use these local observations in an ecosystem productivity context.

Regarding stratification, the observation in Akutan about short-tailed shearwaters diving deeper to find their prey in warmer years (1996 vs. previous colder years) seems to directly corroborate the prediction of increased stratification during warm water periods, even though others have since demonstrated that stratification is not just a simple function of temperature (Ladd and Stabeno, 2012).

4.2. Shifts in species distribution

Another Bering Sea Project hypothesis states that: “As heat content increases, the area suitable for spawning and foraging by subarctic species will expand northward and subarctic species will occupy areas formerly occupied by Arctic species.” The Bering Sea Project study plan makes clear that this idea reflects particularly on fish species. While the period of intensive observations covered a cold period, there was sufficient information from previous warm periods to make contrasts relevant to the hypothesis.

Stabeno et al. (2012b), for example, found that the hypothesis may be true for the southern Bering Sea, where the differences in temperature and ice extent are greatest between warm and cold years, but that these changes may not occur in the northern Bering Sea, because this area is expected to remain cold despite potential future warming in the south. For birds and mammals, a further prediction about changes in distribution was made in the hypotheses: “Central place foragers will shift their diet, foraging locations or rookery locations to increase foraging opportunities.”

The Togiak observations of changes in bearded seal abundance and distribution and the general decline of a wide variety of other species of birds and fish are the most notable of the LTK results concerning these two hypotheses. Elsewhere, changes noted were either modest, regarded by locals as unremarkable, or not considered to be long-term secular trends, but rather cyclical patterns in the ecosystem.

The change in bearded seal abundance in the Togiak area appears to have occurred before the late 1990s. Subsistence harvest surveys were conducted there in 1999 and 2008, and neither found notable harvests of bearded seals. The extensive observations about bearded seals, however, strongly suggest that local hunters have had considerable experience with this species in the past. While hunters in our study attributed the decline in harvest to a decline in at least local abundance, another recent study looked specifically at LTK of seals in Togiak (Lori Quakenbush and Mark Nelson, Alaska Department of Fish and Game, pers. comm., 2011). That study found that, while bearded and ringed seals are not seen as commonly as they were before, it is unclear whether the change is due to an absolute change in abundance, or instead to reduced hunter access to the sea at times when these species are in the Togiak area. Reduced hunter access may be due to changes in sea ice, as noted in Emmonak, implicating the same underlying factor but via a different mechanism.

The observations from Togiak point to a possible response by bearded seal to diminished sea ice in the latter part of the 1990s and early 2000s at the southern edge of the marginal ice zone (Stabeno et al., 2012b). Neither Emmonak nor Savoonga indicated a decline in bearded seal abundance, suggesting that the change is more localized and perhaps only restricted to the southern Bering Sea. Although there is no direct evidence from the observations gathered through the interviews that persistently poor ice conditions lead to an eventual change in pupping grounds, Togiak hunters said that their understanding that bearded seals return to the areas where they were born was largely based on the behavior of other species such as salmon. As a result, the causal mechanism of reduced pupping habitat leading to fewer seals in the area must be regarded as speculative. Whether these changes are due to loss of ice cannot be determined at present. The alternative non-environmental explanation, that commercial fisheries have had negative impacts on bearded seal abundance and distribution, cannot be evaluated with the current state of scientific knowledge (Peter Boveng, Alaska Fisheries Science Center, pers. comm., 2011).

4.3. Changes in abundance

One Bering Sea Project hypothesis predicts: “Competition with abundant, piscivorous fish species for forage species will lead to a decline in murre, kittiwakes and fur seals.” The LTK findings do not describe causal mechanisms in any detail, but do report a decline in murre in the Togiak area and a decline in fur seals on St. Paul Island. The LTK results do include statements about changes in abundance of species other than seabirds and fur seals.

Kittiwakes and murre have been monitored by biologists at several sites throughout the Bering Sea since the 1980s (Dragoo et al., 2011). Black-legged kittiwakes at St. Paul Island showed a

population decline up to 1999, but have been increasing since then. Closer still to Togiak, at Cape Peirce, populations have declining since the early 1990s, although closest to Togiak, at Round Island, there is no trend since data collection began in the late 1990s.

Common (*Uria aalge*) and thick-billed murre at St. Paul have both been declining since about 1995. At Cape Peirce, there was no apparent change in common murre numbers during the 1990–97 period, then an abrupt decline and no apparent further change since then. Finally, the Round Island murre colony shows some evidence of an increase since monitoring began in the late 1990s, although with strong interannual variability. Although the LTK observations may not be based on the same sites as the systematic monitoring data, the general regional trends appear broadly consistent between the two data sources.

The declines reported for fur seals on St. Paul Island are consistent with regularly conducted population assessments, which indicate a continuous decline in pup production since at least 1998, and a general decline since at least the early 1970s (Towell et al., 2011). Predation and shifts in ecosystem conditions (perhaps exacerbated by commercial fisheries) resulting in less prey are the two possible explanations offered by St. Paul respondents. Although these observations do not speak to the idea that the decline is driven by competition from abundant, piscivorous fish, neither do they refute this concept.

The reports from Savoonga that the ecosystem is healthy and productive are inconsistent with other information gathered from St. Lawrence Island. The harvest survey conducted in Savoonga (Fall et al., 2013) found that many hunters reported having to travel farther to harvest marine mammals. Another study in Gambell, the other community on the island, also documented that hunters reported having to spend more time hunting in recent years (Gofman and Smith, 2011). The discrepancy may be due to the difference between hunting success, which depends on physical access and thus on ice and weather conditions, and biological well-being. A target species may be abundant and healthy, but out of reach. Alternatively, the differences may be due to sample bias. The LTK interviews in Savoonga targeted older, experienced hunters, many of whom may no longer be as personally active as younger members of the community. Or, their experience may be sufficient to compensate for recent changes in accessibility or availability of target species. The harvest surveys were a community-wide sample, and the Gambell study also included a demographically broader group than the Savoonga LTK interviews.

4.4. Reliability of “Hot Spots”

The Bering Sea Project hypothesis related to hot spots states that: “Climate-ocean changes will displace predictably located, abundant prey (hot spots) necessary for successful foraging by central place (seabirds and fur seals while nurturing young) and hot spot (baleen whales, walrus) foragers.” It is important here to distinguish between topographically driven hot spots, such as canyons that produce upwelling or regular polynyas, and ephemeral hot spots, such as ice edge blooms or current-driven concentrations of nutrients or prey, that may be more susceptible to change in place. The timing and intensity of productivity or aggregations may change in both cases. During the LTK interviews, hot spots per se were only described in Savoonga, where some were said to be regular features close to the island (Fig. 2). Respondents in Savoonga and Akutan also described aggregations of forage fish that attract marine mammals and seabirds. It was noted that these aggregations are observed regularly, but are not consistent or persistent in any one location.

No mention of trend in the frequency or magnitude of hot-spots was made, although the fact that they are consistent around Savoonga would appear to either speak against the hypothesized change in that area, or suggest that these hot spots are topographically driven and thus less susceptible to change. It should be noted that the forward-looking nature of the hypothesis means it is not synchronous with the time frame of the LTK observations, and the cold conditions during the study period may further confound a simple comparison. The observations from Savoonga that seabirds and marine mammals are abundant in the northern Bering Sea suggests either that foraging locations remain stable for these species or that changes are within the adaptive limits of their foraging behavior. For example, various studies (Piatt et al., 1990; Obst et al., 1995; Hunt, 1997) have found that least auklets (*Aethia pusilla*) exhibit considerable variation in foraging behavior, including distance traveled, which likely corresponds to differences in ocean patterns at various scales. The statements in St. Paul, on the other hand, that fur seal declines are due to fewer prey and thus changing foraging conditions is consistent with this hypothesis.

Observations of ephemeral hot spots that attract aggregations of birds, marine mammals, and fishes are consistent with scientific observations. Harrison (1979) noted feeding associations between gray whales (*Eschrichtius robustus*) and seabirds in the northern Bering Sea. Savoonga's observations mentioned minke whales specifically, but the basic idea is consistent. The observations from Akutan did not specify a whale species, but the idea is again consistent that whales and seabirds are often attracted to the same prey, and that disturbance of fishes by feeding whales might also provide foraging opportunities for birds. The area north of Akutan is well known for hot spots which appear to be topographically driven (e.g., Churnside et al., 2011).

4.5. Differences between Northern and Southern Bering Sea

The final category of results presented here is related to the emerging view from Bering Sea Project research that the northern and southern areas of the Bering Sea are undergoing very different patterns of physical change with consequent implications for ecosystem change (Stabeno et al., 2012b). The major reason for the different patterns appears to be sea ice. The southern Bering Sea is at the seasonal margin of sea ice extent, and thus most likely to see changes in the timing and extent of ice, a crucial ecotone. The northern Bering Sea, by contrast, remains firmly the domain of winter and spring sea ice. Observed changes in the distributions of many marine species in the southeastern Bering Sea (Mueter and Litzow, 2008) are not predicted to be matched in the near future by similar changes in the northern Bering Sea. This is in part due to the persistence of seasonal ice and associated pool of cold water (Mueter et al., 2011; Stabeno et al., 2012b).

In general terms, many of the LTK observations are consistent with the current scientific understanding that the southern Bering Sea is changing rapidly and experiencing negative impacts to many species, while the northern Bering Sea remains productive and healthy. Some specific observations, however, are either inconsistent with this idea, or reveal a different temporal or epistemological frame of reference. It is not possible at this time to tell the difference.

For example, statements by Akutan residents that Steller sea lion populations have had major declines is true in the long-term, but sites in the eastern Aleutian Islands area, including a site near Akutan, have been largely stable since the early 1990s (Fritz and Gelatt, 2011). Similarly, statements in Togiak about overfishing of herring and declines of salmon are not consistent with observations by the Alaska Department of Fish and Game (2011), which show consistent herring numbers since at least the early 1990s and healthy salmon runs in the last several years.

Togiak's concerns, however, stem from a traditional belief that allowing the first run of fish to spawn without being harvested is essential to the health of future runs. Their observations therefore emphasize the size of the first run and reflect a concern that any fishing is allowed on this run. Their baseline for observations of changes is the period prior to commercial fishing, and thus the major changes are not reflected in fisheries statistics that only include the commercial fishing era. In these cases, local residents may be reporting longer-term trends or smaller-scale locally important phenomena such as spawn-on-kelp rather than the absolute numbers of fish in the herring run, or may be reflecting a different understanding of ecological processes and species behavior.

5. Conclusions

The appropriate question to consider when summarizing the LTK results and then comparing them with the results of other lines of inquiry is not, "Is LTK right?", but rather, "Is the study of LTK useful?" The answer to that question will depend greatly on whom one means it to be useful to. We cannot speak on behalf of the communities and community members who took part in the study, and it would take a separate research effort to ask that question of them in a systematic way. We can, however, offer some comments on behalf of the Bering Sea Project research team, to consider whether the inclusion of a substantive LTK effort in a mostly natural science project is useful in terms of results and in terms of creating awareness that there is more than one point of view concerning the functioning and significance of the Bering Sea ecosystem.

Determining the correspondence between the LTK findings and current scientific understanding from other Bering Sea Project research and elsewhere is difficult as it is confounded by a mismatch in purpose, space and time. Studying an entire ecosystem requires selecting key species, processes, and locations as indicators or representatives of larger patterns. The LTK results are based on observations made for the purposes of hunting and fishing safety and success, and whereas people observe the environment in relation to these activities, they do not do so with the needs of outside researchers in mind. Thus, it is hardly surprising that the information available from LTK does not easily fit into the Bering Sea Project (or any other scientific) structure. The question of temporal frame of reference, noted in several sections of the Discussion, is one example. Hunters and fishers may note overall trends over the period of their activity (and perhaps beyond in the case of knowledge handed down from previous generations) and often include causal explanations, but they typically are less concerned with specific dates. Thus, creating a timeline as the basis for matching specific events (e.g., sea bird die-offs and an El Niño year) is problematic and the results of such an attempt by interviewers may remain unreliable.

Nevertheless, hunters and fishers pay close attention to the indicators and phenomena that matter to them. Their success and at times their lives depend on reliable, replicable understanding of the ecosystem (e.g., Noongwook et al., 2007). The observations summarized here offer a picture of the Bering Sea ecosystem at a broad level, with additional details from specific locales. The overall consistency between the two modes of understanding offers some encouragement to the overall conclusions drawn from both scientific and LTK investigations. A comparison of findings also points to the difference between general trends for a region (as defined and studied by a research project) and the relevant local impacts to communities that depend primarily on the local patterns of change. A healthy walrus population is a good thing, but if the distribution of walrus is not favorable to a community, the walrus harvest will be poor. Spatial scale is thus as important to consider as temporal scale when assessing how

LTK and scientific observations can benefit the individuals engaged in the pursuits that generate those observations (e.g., Huntington et al., 2004b).

The involvement of local residents in the Bering Sea Project, and the effort to document and analyze LTK have proved useful overall. The results led to interesting discussions among researchers (here including the community-based researchers, who took part in all the Bering Sea Project team meetings), spawned additional analyses and papers, and reminded us why the study of the Bering Sea ecosystem is important. Future efforts could benefit from aiming at greater correspondence between selected indicator species and the species that are of importance to local communities, from better defining the temporal and spatial scales of interest and that are likely to be of significance to both lines of investigation, and from greater interaction between community-based researchers and others as the LTK effort is shaped, conducted, and interpreted. A specific focus in future projects on study hypotheses in the elder interviews and subsistence surveys would align the scientific and LTK observations and through this pairing, likely strengthen our conclusions. The involvement of LTK holders in formulating hypotheses at the outset, or in reformulating hypotheses during the project, could also strengthen the connection between study goals and what LTK is likely to offer.

In addition, an iterative process of LTK documentation and joint analysis with other researchers would allow more systematic and detailed follow-up of key points emerging from the initial interviews. For example, the first round of interviews might use the semi-directive approach to take a broad look at ecosystem observations and understanding. A second round of interviews might use specific questions developed in collaboration with other members of the overall project team to explore key topics in greater depth and with more precision and consistency across individuals and communities. While such follow-up is beyond the scope of this project, several questions for additional study have arisen from our work (e.g., Huntington et al., 2004a). These include:

- What meteorological phenomena are important to coastal residents in summer, and how do these compare with the phenomena associated with “storms”? In other words, how do we compare local weather observations with the meteorological monitoring and modeling of interest to oceanographers and marine ecologists? The answers may help shed light on what exactly is changing and why it does or does not matter to local residents.
- What are the causes of changing bearded seal populations along the marginal ice edge? “Climate change” may be the root cause, but the mechanism remains unclear and may provide insight into the interaction between regional-scale processes (e.g., ice retreat) and local-scale ones (e.g., bearded seal pupping behavior and site fidelity).
- Are more experienced hunters better able to adapt to changing environmental conditions, thus experiencing fewer difficulties harvesting sufficient subsistence food than are less experienced hunters? The contradictory results from St. Lawrence Island suggest that experience may play a role in perception of ecosystem health and productivity, which in turn would suggest that the interpretation of LTK data from experienced elders should not be extrapolated without caution to the community as a whole.

We hope that the design of future research programs in the Bering Sea and elsewhere will benefit from the results and experience of this project and will have the ability to ask more detailed, specific questions such as these.

Acknowledgments

This paper would not have been possible without the patience and generosity of the many respondents who took part in the LTK interviews, and the commitment of many others in each community who guided the project and assisted the visiting researchers during their time there. In addition, other researchers helped identify topics, frame questions, or interpret results. Some of these researchers traveled to a community, in some cases participating in the interviews. These persons include Tom Van Pelt, the late Caleb Pungowiyi, Quinn Smith, Chad Jay, Bruce Marcot, and Nick Bond. Their support is greatly appreciated.

Several colleagues commented on earlier drafts or reviewed the results and helped place them in the context of other research for the Discussion section. We are grateful to Peter Boveng, Heather Renner, Kathy Kuletz, Lori Quakenbush, and Nick Bond for their insights and encouragement. James Lee reviewed the manuscript for consistency, and three anonymous reviewers provided constructive comments based on a careful reading of the manuscript, for which we are grateful. We thank Danielle Dickson for preparing the figures.

We thank the North Pacific Research Board for funding our work, and the leaders and researchers of Bering Sea Project for their encouragement and support. We thank the Bering Sea Project LTK Regional Advisory Board and its members for providing guidance and ideas for our project.

This is NPRB Publication No. 372. This project was part of the Bering Ecosystem Study—Bering Sea Integrated Ecosystem Research Program (“the Bering Sea Project”), and this paper is BEST-BSIERP Publication No. 74.

References

- Agrawal, A., 1995. Dismantling the divide between indigenous and scientific knowledge. *Dev. Change* 26 (3), 413–439.
- Alaska Department of Fish and Game, 2010. 2011 Togiak Herring Forecast. Alaska Department of Fish and Game, Anchorage. (http://www.adfg.alaska.gov/static/fishing/PDFs/commercial/2011_togiak_herring_forecast.pdf) (accessed 05.12.11).
- Badten, L.W., Kaneshiro, V.O., Oovi, M., Koonooka, C., Jacobson, S.A., 2008. St. Lawrence Island/Siberian Yupik Eskimo Dictionary. Alaska Native Language Center, University of Alaska Fairbanks, Fairbanks, Alaska. vol. 2.
- Berkes, F., 1999. *Sacred Ecology: Traditional Ecological Knowledge and Resource Management*. Taylor & Francis, Philadelphia.
- Coyle, K.O., Eisner, L.B., Mueter, F.J., Pinchuk, A.I., Janout, M.A., Cieciel, K.D., Farley, E.V., Andrews, A.G., 2011. Climate change in the southeastern Bering Sea: impacts on pollock stocks and implications for the oscillating control hypothesis. *Fish. Oceanogr.* 20, 139–156.
- Churnside, J.H., Brown, E.D., Parker-Stetter, S., Horne, J.K., Hunt Jr, G.L., Hillgruber, N., Sigler, M.F., Vollenweider, J.J., 2011. Airborne remote sensing of a biological hot spot in the southeastern Bering Sea. *Remote Sens.* 3, 621–637.
- Dragoo, D.E., Byrd, G.V., Irons, D.B., 2011. Breeding Status, Population Trends and Diets of Seabirds in Alaska, 2008. U.S. Fish and Wildlife Service, Homer, Alaska. (Report AMNWR 2011/07).
- Fall, J., et al., 2013. Subsistence Harvests in the BSIERP Communities, 94, 274–291.
- Fritz, L., Gelatt, T., 2011. Surveys of Steller sea lions in Alaska, June–July 2010. Memorandum for the Record, January 31, 2011. National Oceanic and Atmospheric Administration, Seattle, Washington. (<http://www.afsc.noaa.gov/nmml/PDF/SSL-Survey-memo-2010.pdf>) (accessed 05.12.11).
- Gofman, V., Smith, M., 2011. Bering Sea Sub-Network: Sharing Knowledge Pilot Phase Final Report (Aleut International Association). (CAFF Monitoring Series Report No. 2).
- Harrison, C.S., 1979. The association of marine birds and feeding gray whales. *Condor* 81, 93–95.
- Hunt Jr., G.L., 1997. Physics, zooplankton, and the distribution of least auklets in the Bering Sea—a review. *ICES J. Mar. Sci.* 54, 600–607.
- Hunt Jr., G.L., Coyle, K.O., Eisner, L.B., Farley, E.V., Heintz, R.A., Mueter, F., Napp, J.M., Overland, J.E., Ressler, P.H., Salo, S., Stabeno, P.J., 2011. Climate impacts on eastern Bering Sea food webs: a synthesis of new data and an assessment of the Oscillating Control Hypothesis. *ICES J. Mar. Sci.* 68, 1230–1243.
- Huntington, H.P., 1998. Observations on the utility of the semi-directive interview for documenting traditional ecological knowledge. *Arctic* 51, 237–242.
- Huntington, H.P., Callaghan, T., Fox, S., Krupnik, I., 2004a. Matching traditional and scientific observations to detect environmental change: a discussion on Arctic terrestrial ecosystems. *Ambio Spec. Rep.* 13, 18–23.

- Huntington, H.P., Suydam, R.S., Rosenberg, D.H., 2004b. Traditional knowledge and satellite tracking as complementary approaches to ecological understanding. *Environ. Conserv.* 31 (3), 177–180.
- Ingold, T., Kurtilla, T., 2000. Perceiving the environment in Finnish Lapland. *Body Soc.* 6 (3–4), 183–196.
- Johnson, T., 2003. The Bering Sea and Aleutian Islands: Region of Wonders. Alaska Sea Grant, Fairbanks.
- Ladd, C., Stabeno, P.J., 2012. Stratification on the Eastern Bering Sea shelf revisited. *Deep-Sea Res. II* 65–70 (2012), 72–83.
- Mueter, F.J., Litzow, M.A., 2008. Sea ice retreat alters the biogeography of the Bering Sea continental shelf. *Ecol. Appl.* 18 (2), 309–320.
- Mueter, F.J., Siddon, E.C., Hunt Jr., G.L., 2011. Climate change brings uncertain future for subarctic marine ecosystems and fishes. In: Lovecraft, A.L., Eicken, H. (Eds.), *North by 2020: Perspectives on Alaska's Changing Social-Ecological Systems*. University of Alaska Press, Fairbanks, Alaska, pp. 329–357.
- Noongwook, G., the Native Village of Savoonga, the Native Village of Gambell, Huntington, H.P., George, J.C., 2007. Traditional knowledge of the bowhead whale (*Balaena mysticetus*) around St. Lawrence Island. *Alaska Arct.* 60 (1), 47–54.
- NPRB (North Pacific Research Board), 2005. North Pacific Research Board Science Plan. North Pacific Research Board, Anchorage.
- Obst, B.S., Russell, R.W., Hunt Jr., G.L., Eppley, Z.A., Harrison, N.M., 1995. Foraging radii and energetic of least auklets (*Aethia pusilla*) breeding on three Bering Sea islands. *Physiol. Zool.* 68 (4), 647–672.
- Overland, J.E., Wang, M., Wood, K.R., Percival, D.B., Bond, N.A., 2012. Recent Bering Sea warm and cold events in a 95-year context. *Deep-Sea Res. II* 65–70, 6–13.
- Piatt, J.F., Roberts, B.D., Hatch, S.A., 1990. Colony attendance and population monitoring of least and crested auklets on St. Lawrence Island. *Alaska Condor* 92, 97–106.
- Stabeno, P.J., Kachel, N., Moore, S., Sigler, M.F., Yamaguchi, A., Zerbini, A.N., 2012a. Comparison of warm and cold years on the southeastern Bering Sea shelf and some implications for the ecosystem. *Deep-Sea Res. II* 65–70, 31–45.
- Stabeno, P.J., Farley, E., Kachel, N., Moore, S., Mordy, C., Napp, J.M., Overland, J.E., Pinchuk, A.I., Sigler, M.F., 2012b. A comparison of the physics of the northern and southern shelves of the eastern Bering Sea and some implications to the ecosystem. *Deep-Sea Res. II* 65–70, 14–30.
- Stevenson, D.E., Lauth, R.R., 2012. Latitudinal and temporal shifts in catch composition of bottom trawls conducted on the eastern Bering Sea shelf. *Deep-Sea Res. II* 65–70, 251–259.
- Towell, R., Ream, R., Bengtson, J., Sterling, J., 2011. 2010 Northern Fur Seal Pup Production and Adult Male Counts on the Pribilof Islands, Alaska. Memorandum for the Record. January 13, 2011. National Oceanic and Atmospheric Administration, Seattle, Washington. (<http://www.afsc.noaa.gov/nmml/pdf/2010-nfs-pup-estimates.pdf>) (accessed 05.12.11).
- U.S. Census. 2010. (<http://www.census.gov/popfinder/>) (accessed 15.10.12).
- Wiese, F.K., Wiseman, W.J., Van Pelt, T.I., 2012. Bering Sea linkages. *Deep-Sea Res. II* 65–70, 2–5.



Bathymetric and interspecific variability in maternal reproductive investment and diet of eurybathic echinoderms [☆]



David A.N. Ross ^a, Jean-François Hamel ^b, Annie Mercier ^{a,*}

^a Department of Ocean Sciences, Memorial University, St. John's (NL), Canada A1C 5S7

^b Society for the Exploration and Valuing of the Environment (SEVE), Portugal Cove-St. Philips (NL), Canada A1M 2B7

ARTICLE INFO

Available online 6 March 2013

Keywords:

Reproduction
Gonad index
Fecundity
Oocytes
Echinoderm
Sea star
Sea cucumber
Lipids
Fatty acids

ABSTRACT

While conditions in shallow-water and deep-sea environments differ markedly, it remains unclear how eurybathic species adapt their life histories to cope with these changes. The present study compared indicators of maternal reproductive investment of three common echinoderms collected shallower than 20 m and deeper than 850 m: *Cucumaria frondosa* (Holothuroidea), *Solaster endeca* and *Henricia sanguinolenta* (Asteroidea). Depth-specific and species-specific differences were found in gonad indices (GI), potential fecundity, oocyte size frequency, as well as lipid classes and fatty acids measured in gonad tissue and oocytes. The asteroids, *S. endeca* and *H. sanguinolenta*, exemplified the interspecific trade-off between size and number of oocytes: the former had fewer larger oocytes than the latter, with higher total lipid proportions in them. However, intraspecifically, larger oocytes found in deep specimens of *S. endeca* did not translate into lower fecundity but rather into a seemingly higher GI, indicating greater investment per oocyte without reducing fecundity. Oocytes were absent in specimens of *C. frondosa* sampled in deep water, suggesting delayed or impaired maturation at the limit of their depth tolerance. Analysis of *S. endeca* sterol proportions in gonads and oocytes across depths showed higher sterol input into oocytes in females from the deep. Gonads of *S. endeca* and *H. sanguinolenta* contained similar essential fatty acids, but showed significant differences in major fatty acids and some of the less dominant ones, indicating diet specificities. Analyses within *S. endeca* showed evidence of similar feeding mode (carnivory) at both depths, but suggested shifts in the diet or synthesis of fatty acids, presumably reflecting differences in available food sources and/or adaptations to their respective environments.

© 2013 Elsevier Ltd. All rights reserved.

1. Introduction

A relatively large number of marine macrobenthic species are known to occur across a wide range of depths (Gage and Tyler, 1992), yet, only a few studies have been made on the adaptations that underlie this ability (e.g. Féral et al., 1990). Compared with surface waters, the deep sea below 200 m is generally colder and more saline; receives little or no sunlight and is characterized by a gradient of increasing hydrostatic pressure (Stein, 2007; Townsend et al., 2006). Differences in environmental conditions between the shallow sub-littoral and bathyal depths are likely to influence the life histories of eurybathic taxa, including various aspects of their reproduction. The ability of a species to colonize different environments, including the deep sea, follows a gradient

from (1) areas where fully functional reproductive populations are maintained, to (2) the establishment of adult, but sterile, populations to (3) areas where larvae may occur but are unable to recruit (Bhaud, 2000). Food supply and temperature are among the key variables susceptible to modulate these reproductive processes (Giese et al., 1991; Mercier and Hamel, 2009).

A commonly studied effect of temperature on life-history traits is the inverse relationship between temperature and oocyte size (Moran and McAlister, 2009) initially documented by Thorson (1950) and Rass (1986). Thorson attributed the increased oocyte size to decreasing food availability with increasing latitude and depth, while Rass attributed the increased oocyte size to physiological changes in development due to temperature. Laptikhovskiy (2006) hypothesized that colder temperatures induce a non-proportional deceleration of different oogenesis stages, leading to a larger species-specific oocyte size. At colder temperatures yolk accumulates in greater amounts, in excess of what is needed by the embryo/larva, and may continue to feed the juvenile after metamorphosis (Lawrence and McClintock, 1994). Colder temperatures also lower metabolic demands of poikilothermic organisms, allowing deep-sea taxa to allocate more energy

[☆]This paper is part of the Volume 92, August 2013 Deep-Sea Biodiversity and Life History Processes special issue.

Abbreviations: RPF, relative potential fecundity; OPF, overall potential fecundity

* Corresponding author. Tel.: +1 709 864 2011.

E-mail address: amercier@mun.ca (A. Mercier).

into reproduction; it may allow them to produce larger oocytes without sacrificing fecundity (Laptikhovsky, 2006). Conversely, since the food supply in the deep sea is generally less consistent than in shallow waters (Rex, 1981), the effect of maternal nutrition on oocytes would imply that smaller oocytes should be produced to accommodate decreased nutritional input.

The quality and quantity of dietary intakes in echinoderms have a significant effect on the biochemical composition of gonads (Fernández, 1997; Hammer et al., 2006; Liyana-Pathirana et al., 2002). Therefore, it is likely that fatty acid composition of gonads will be different among species with different feeding and reproductive modes, and also across depths. Howell et al. (2003) confirmed that fatty acid biomarkers were significantly different among asteroids based on their known feeding mode. Differences may also occur in development pathways. Lecithotrophic species produce relatively few, large oocytes that contain enough nutrients for the non-feeding larvae to develop into juveniles, leading to substantial maternal investment per oocyte (Thorson, 1950). Various lecithotrophic echinoderms were found to meet the need for increased nutrients by increasing the percentage of lipids in the oocytes, specifically triacylglycerols and wax esters (Falkner et al., 2006; Prowse et al., 2008; Villinski et al., 2002). However, increased maternal provisioning is not systematically reflected in oocyte size. Although McEdward and Chia (1991) found a strong interspecific correlation between oocyte size and energy content in 5 asteroids and 2 holothuroids, several reports have shown no correlation between oocyte size and energy content intraspecifically (McEdward and Carson, 1987; McEdward and Chia, 1991; McEdward and Coulter, 1987). McEdward and Morgan (2001) found that differences in oocyte size reflect energy content when comparing between developmental modes, such as lecithotrophic versus planktotrophic, and pelagic versus brooded lecithotrophic larvae. However, fine scale comparisons show low confidence intervals relative to size range.

The present study focused on three eurybathic echinoderms, the sea stars *Solaster endeca* and *Henricia sanguinolenta* and the sea cucumber *Cucumaria frondosa*, collected both in the shallow subtidal zone and at bathyal depths > 850 m. To date, *H. sanguinolenta* has been reported to depths of 2400 m (Mah and Hansson, 2012), *S. endeca* to 400–500 m (Metaxas and Davis, 2005) and *C. frondosa* to 300 m or more (So et al., 2011). Females of each species from both shallow and deep habitats were examined and compared to identify trends in reproductive modes by examining gonad indices (GI), oocyte size frequency and potential fecundity. Lipid contents as well as fatty acid proportions in gonadal tissue and oocytes were compared where possible in shallow and deep specimens. The ultimate goal was to determine what effects depth would have on maternal reproductive investment in eurybathic echinoderms and whether trends could be related to dietary habits. We hypothesized that only a shift in diet would allow the maintenance of reproductive output at depth and, therefore, that species with less opportunistic diets would be more obviously affected by this factor.

2. Methods

2.1. Collection

Deep-sea specimens of *S. endeca*, *H. sanguinolenta* and *C. frondosa* were collected as by-catch during routine multi-species research surveys conducted by Fisheries and Oceans Canada (DFO) in October 2005 and November 2006 on the continental slope surrounding insular Newfoundland, eastern Canada. Surveys were conducted with the vessel CCGS *Teleost* using a Campellen 1800 trawl towed for 15 min on ~1.4 km of seafloor (gear opened and closed at depth). Specimens of *S. endeca*

(1143–1292 m) and *C. frondosa* (1214–1450 m) were obtained from depths exceeding their currently reported bathymetric range, whereas *H. sanguinolenta* (856–1230 m) was collected within its known distribution. All samples were vacuum packed and frozen at -20°C upon collection and transferred to the Ocean Sciences Centre (OSC) of Memorial University where they were kept frozen until processing. Shallow-water specimens were collected by divers at 3–18 m depth off the Avalon Peninsula (same season and general geographic area as deep-sea counterparts) and frozen at -20°C until processed.

2.2. Sample processing

This study was limited to females. Each individual was measured and weighed after removing excess ice and water. Size of *S. endeca* ($n=3$ individuals per depth) and *H. sanguinolenta* ($n=3$ per depth) was established using three separate measures of the radius, while three measures of total length (mouth–anus) and the mid-body circumference were recorded for *C. frondosa* ($n=3-4$ per depth). Still-frozen gonad samples ($n=3$ gonad samples per individual) were removed from each female, and transferred in pre-weighed lipid-cleaned 50-ml centrifuge tubes. These samples were immediately weighed and prepared for lipid extraction by preserving them in 8 ml of chloroform (CHCl_3), and placing them in a freezer at -25°C . The remaining gonads were weighed to calculate a gonad index (GI) as the ratio of total gonad wet weight to body wall wet weight (which included muscle bands and aquapharyngeal bulb in sea cucumbers). Oocytes were then extracted by dissecting gonads in seawater. Three 1-ml samples of extracted oocytes were prepared for lipid analysis as described above.

Fecundity was established using ovarian subsamples of known weight preserved in 4% formaldehyde. Oocytes were counted and imaged using a stereomicroscope (Nikon SMZ1500) coupled to a digital camera (Nikon DMX1200). Feret diameters were measured randomly in at least 140 oocytes. Relative potential fecundity (RPF) was calculated as the number of oocytes per gram of gonad and overall potential fecundity (OPF) by extrapolating the total number of oocytes per female.

2.3. Lipid and fatty acid analyses

Lipid analysis was performed on the two species of sea stars, given the absence of oocytes in deep-water sea cucumbers (preventing comparison with gamete-bearing conspecifics from the shallows). Extraction and analysis of lipids were based on standard methods (Parrish, 1999). Total lipids were extracted in chloroform:methanol (2:1). Lipid classes were determined using thin layer chromatography with flame ionization detection with a MARK VI Iatroscan (Iatron Laboratories, Tokyo, Japan). Lipids were separated in a 3 stage development system (Parrish, 1987). The first separation consisted of 2 developments in 99:1:0.05 hexane:diethyl ether:formic acid. The second separation consisted of a 40-min development in 79:20:1 hexane:diethyl ether:formic acid. The last separation consisted of 15-min developments in 100% acetone followed by 10-min developments in 5:4:1 chloroform:methanol:chloroform-extracted-water. After each separation, rods were scanned and data were processed using the PeakSimple Chromatography software (V3.67, SRI Inc).

For all samples, lipid extracts were transesterified using 14% BF_3 MeOH for 1.5 h at 85°C . The FAME were analyzed on a HP 6890 GC-FID equipped with an 7683 autosampler. The GC column was a ZB wax+ (Phenomenex, USA). The column length was 30 m with an internal diameter of 0.32 mm. The column temperature began at 65°C and held this temperature for 0.5 min. The temperature ramped to 195°C at a rate of $40^{\circ}\text{C}/\text{min}$, held for 15 min then

ramped to a final temperature of 220 °C at a rate of 2 °C/min. This final temperature was held for 0.75 min. The carrier gas was hydrogen flowing at a rate of 2 ml/min. The injector ramped from 150 °C to 250 °C at 120 °C/min. The detector temperature was 260 °C. Peaks were identified using retention times from standards purchased from Supelco: 37 component FAME mix, Bacterial acid methyl ester mix, PUFA 1 and PUFA 3. Chromatograms were integrated using the Varian Galaxie Chromatography Data System, version 1.9.3.2. The Iatroscan determined derivatization efficiency for the samples was 80%.

2.4. Statistical analysis

Measures of GI, RPF, OPF and oocyte size were compared based on depth (shallow, deep) and species (*S. endeca*, *H. sanguinolenta*, *C. frondosa*) using analyses of variance (ANOVA) or *t*-tests after verifying assumptions of normality and equal variance. Where test assumptions were not met, data were log-transformed. Post-hoc tests (Holm-Sidak) were used to compare specific groups where appropriate. Lipid classes in *S. endeca* were compared using ANOVA based on depth (shallow, deep) and tissue (gonads, oocytes), whereas lipid classes in gonads were compared based on depth and sea star species (*S. endeca*, *H. sanguinolenta*). In the few instances where assumptions for parametric tests were not met, even after transforming the data, Mann-Whitney rank sum tests were conducted. The significance level for all tests was set at $p < 0.05$ and data are expressed as mean \pm SD.

A hierarchical cluster analysis of fatty acid profiles was conducted based on Euclidean distance and complete linkage. Clusters were also investigated using similarity percentage (SIMPER) analysis. Finally, hierarchical clustering was performed as above to investigate similarities between shallow/deep *S. endeca* and 3 deep-sea carnivorous asteroids previously studied by Howell et al. (2003) using fatty acid data available for all samples.

3. Results

3.1. Gonad index (GI)

A two-way ANOVA on GI (depth \times species, log-transformed data) revealed a significant interaction of the factors ($F_{2,10}=7.33$, $p=0.011$) indicating the absence of a uniform bathymetric trend among species (Fig. 1). Pairwise tests, therefore, were conducted at the various levels of each factor.

A significantly higher GI was found in shallow (0.26 ± 0.10) than in deep (0.04 ± 0.01) specimens of *C. frondosa* ($p=0.009$; Fig. 1). However, it should be noted that only 2 out of 4 individuals obtained from the deep bathyal samples had gonads that could be weighed. The gonads in the remaining two specimens were too small for measuring. Comparing the components of the index revealed that the body wall of *C. frondosa* was significantly heavier ($t=10.2$, $df=3$, $p=0.002$) in shallow (64.3 ± 5.1 g) than in deep specimens (25.5 ± 0.9 g). The same trend occurred in the gonad (16.5 ± 6.4 g for shallow vs 0.91 ± 0.28 g for deep specimens; $t=3.3$, $df=3$, $p=0.047$) (Fig. 1, Table 1).

In contrast, the reverse trend was found in *S. endeca*, with a greater GI in deep (0.37 ± 0.19) than in shallow specimens (0.11 ± 0.04 ; Table 1). However, this difference was not significant ($p=0.060$). Similarly, bathymetry had no significant effect on the GI of *H. sanguinolenta* ($p=0.923$). The only significant interspecific difference in GI was found between specimens of *C. frondosa* and *S. endeca* collected in deep water ($p=0.012$; Fig. 1).

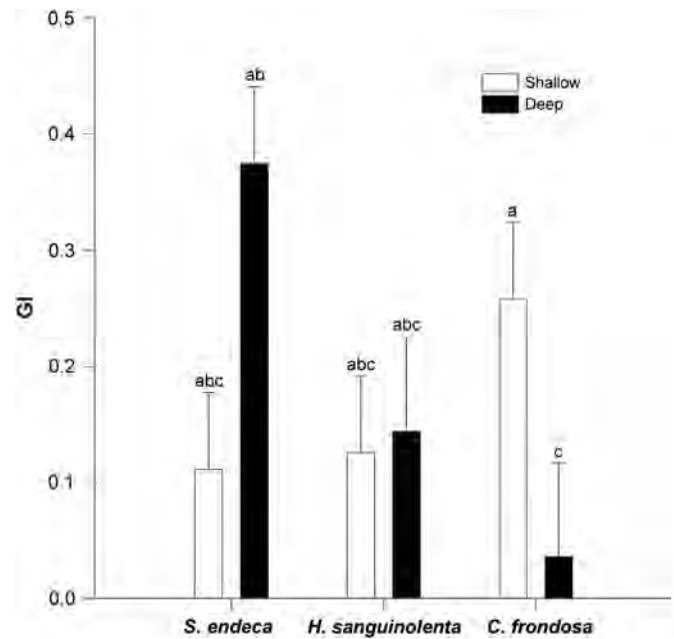


Fig. 1. Bathymetric trends in the gonad index (GI) of the sea stars *Solaster endeca* and *Henricia sanguinolenta*, and the sea cucumber *Cucumaria frondosa*. Data shown as mean \pm SD. Bars with different letters are significantly different (two-way ANOVA, Holm-Sidak, $p < 0.05$, on log-transformed data).

Table 1

Results of species-specific analyses across depths, where S means shallow, D means deep, '>' and '<' indicate a significant difference ($p < 0.05$), ' \geq ' and ' \leq ' indicate a non-significant trend ($p=0.05-0.06$), '=' indicates no significant difference ($p > 0.06$), and 'ND' is not determined.

Species	Gonad index (GI)	Fecundity (RPF)	Oocyte size	Total lipids	Triacylglycerol
<i>S. endeca</i>	S \leq D	S = D	S = D	S = D	S = D
<i>H. sanguinolenta</i>	S = D	S < D	S = D	S = D	S = D
<i>C. frondosa</i>	S > D	S > D ^a	S > D ^a	ND	ND

^a Inferred from the absence of oocytes in deep-water specimens.

3.2. Fecundity

Potential fecundity could not be compared statistically across depths in *C. frondosa* because no oocytes were found in the gonads of the deep-water specimens. For the sea stars, a two-way ANOVA (depth \times species) showed significant differences in relative potential fecundity (RPF) among species ($F_{1,7}=39.19$, $p < 0.001$), but no significant influence of depth ($F_{1,7}=2.32$, $p=0.171$) and no interaction between the factors ($F_{1,7}=5.02$, $p=0.060$). Post-hoc analysis showed that RPF (number of oocytes g^{-1} gonad) was significantly higher in *H. sanguinolenta* than in *S. endeca* in both shallow ($p=0.020$) and deep samples ($p < 0.001$; Fig. 2A). RPF was also greater in deep than in shallow *H. sanguinolenta* (shallow: 1712 ± 653 ; deep: 2844 ± 397 ; $p=0.040$). There was no difference between shallow and deep specimens of *S. endeca* (shallow: 812 ± 107 ; deep: 625 ± 38 ; $p=0.608$; Table 1).

Comparisons of overall potential fecundity (OPF) showed that it followed an interspecific trend opposite to that of RPF (Fig. 2B). As above, a two-way ANOVA (depth \times species, log-transformed data) showed significant differences among species ($F_{1,7}=43.06$, $p < 0.001$) but no influence of depth ($F_{1,7}=0.62$, $p=0.457$) and no interaction ($F_{1,7}=0.12$, $p=0.738$). OPF (oocytes female⁻¹) was significantly higher in *S. endeca* than in *H. sanguinolenta* in both shallow ($p=0.002$) and deep samples ($p=0.002$). The difference in

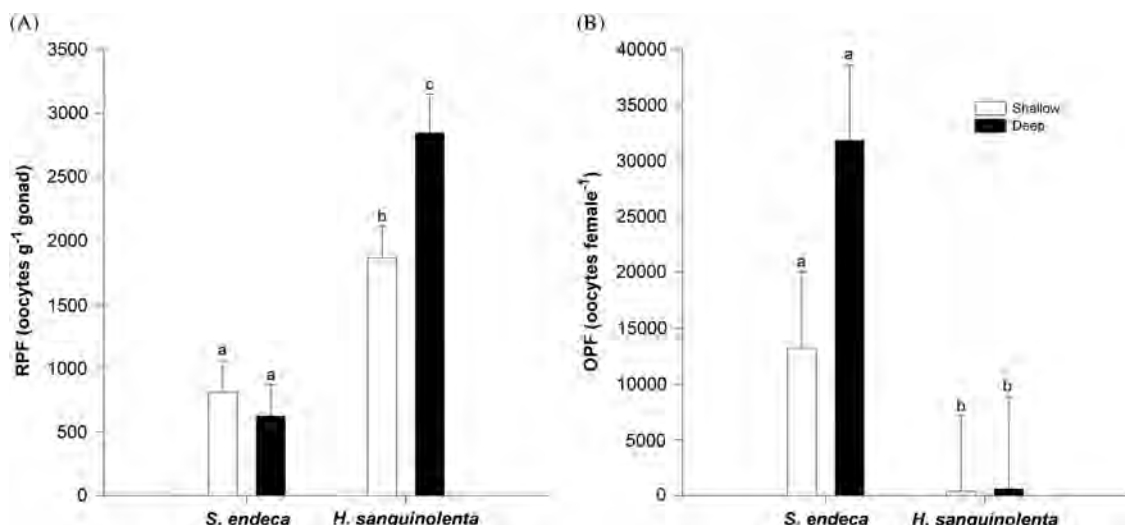


Fig. 2. Bathymetric trends in (A) relative potential fecundity (RPF; oocytes g⁻¹ gonad) and (B) overall potential fecundity (OPF; oocytes female⁻¹) in the sea stars *Solaster endeca* and *Henricia sanguinolenta*. Data shown as mean \pm SD. Bars with different letters are significantly different (two-way ANOVA, Holm-Sidak, $p < 0.05$, on log-transformed data for OPF).

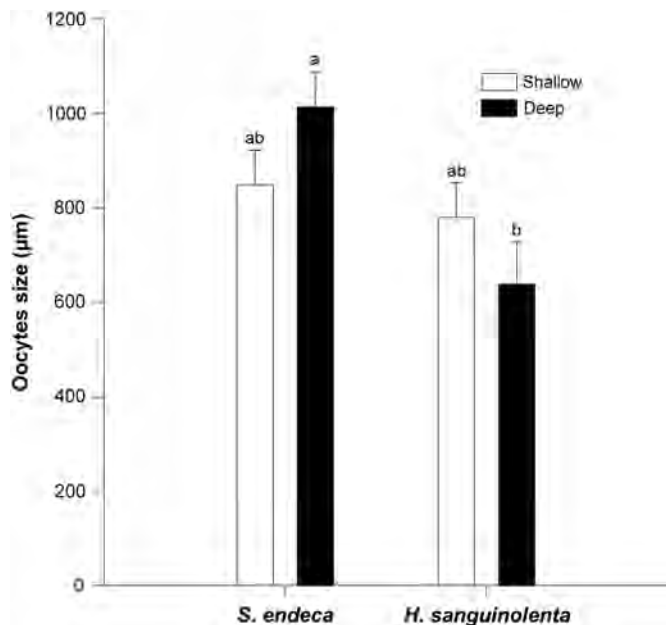


Fig. 3. Bathymetric trends in oocyte size (μm) in the sea stars *Solaster endeca* and *Henricia sanguinolenta*. Data shown as mean \pm SD. Bars with different letters are significantly different (two-way ANOVA, Holm-Sidak, $p < 0.05$).

OPF between shallow and deep specimens was not significant in *S. endeca* (shallow: $13,260 \pm 4893$; deep: $31,817 \pm 21,424$; $p = 0.423$) or in *H. sanguinolenta* (shallow: 383 ± 319 ; deep: 602 ± 693 ; $p = 0.777$).

3.3. Oocyte size

The bathymetric patterns exhibited by oocyte size followed inverse trends in the two sea stars studied (Fig. 3, Table 1). Oocytes from deep specimens seemed larger ($1014 \pm 323 \mu\text{m}$) than those from shallow specimens ($848 \pm 275 \mu\text{m}$) in *S. endeca*, whereas in *H. sanguinolenta* oocytes from shallow specimens seemed larger ($761 \pm 221 \mu\text{m}$) than those from deep specimens ($602 \pm 222 \mu\text{m}$); however, none of these differences were statistically significant (Fig. 3). Oocyte size in *S. endeca* was generally larger than in *H. sanguinolenta*, although statistical difference was

confined to deep-water comparisons ($p = 0.014$). A two-way ANOVA (species \times depth) showed a significant influence of species ($F_{1,7} = 8.11$, $p = 0.025$) but not depth ($F_{1,7} = 0.02$, $p = 0.884$) and no interaction ($F_{1,7} = 3.88$, $p = 0.090$). Oocyte size distributions (Fig. 4) illustrate a shift towards an increased frequency of larger oocytes in deep *S. endeca* specimens and smaller oocytes in deep *H. sanguinolenta*. In the sea cucumber *C. frondosa*, oocytes of shallow-water specimens were $432 \pm 101 \mu\text{m}$; oocytes were absent from deep-water specimens.

3.4. Lipid class analysis

The analysis of total lipids in sea stars revealed two significant differences. The gonad tissue of *S. endeca* had significantly more lipids ($643.6 \pm 203.9 \text{ mg g}^{-1}$) than the oocytes alone ($332.5 \pm 224.8 \text{ mg g}^{-1}$; two-way ANOVA, $F_{1,8} = 5.74$, $p = 0.044$), and more lipids than the gonad tissue of *H. sanguinolenta* ($61.0 \pm 66.8 \text{ mg g}^{-1}$; $F_{1,7} = 51.33$, $p < 0.001$, log-transformed data).

The proportion of free fatty acids was significantly greater in deep ($25.0 \pm 14.3\%$) than in shallow specimens ($11.0 \pm 4.7\%$; two-way ANOVA, $F_{1,7} = 10.65$, $p = 0.014$) (Table 2). Furthermore, the proportion of triacylglycerols was significantly greater in *S. endeca* ($64.4 \pm 10.6\%$) than in *H. sanguinolenta* ($17.2 \pm 25.5\%$; two-way ANOVA, $F_{1,7} = 17.16$, $p = 0.004$; Fig. 5). *H. sanguinolenta* appeared to have higher proportions of free fatty acids ($22.3 \pm 14.5\%$) than *S. endeca* ($13.3 \pm 9.1\%$), but the difference was not significant (two-way ANOVA, $F_{1,7} = 5.40$, $p = 0.053$).

For the analysis of *S. endeca* based on depth and tissue (Fig. 6), the proportion of sterols was significantly greater in gonads ($5.7 \pm 1.3\%$) than in oocytes ($3.5 \pm 2.3\%$; two-way ANOVA, $F_{1,8} = 6.54$, $p = 0.034$), and the trend towards more sterols in deep ($5.5 \pm 1.8\%$) than in shallow ($3.6 \pm 2.1\%$) specimens was found to be non-significant (two-way ANOVA, $F_{1,8} = 5.11$, $p = 0.054$). There were significantly more sterols in gonads ($5.5 \pm 0.3\%$) than oocytes ($1.8 \pm 0.9\%$) from shallow specimens ($p = 0.016$), and inversely more sterols in oocytes from deep ($5.2 \pm 2.0\%$) than from shallow ($1.8 \pm 0.9\%$) specimens ($p = 0.022$).

3.5. Fatty acid analysis

In both sea star species, 20:5n-3, 18:1n-7 and 20:4n-6 were the three most abundant fatty acids; and 16:0, 18:0,

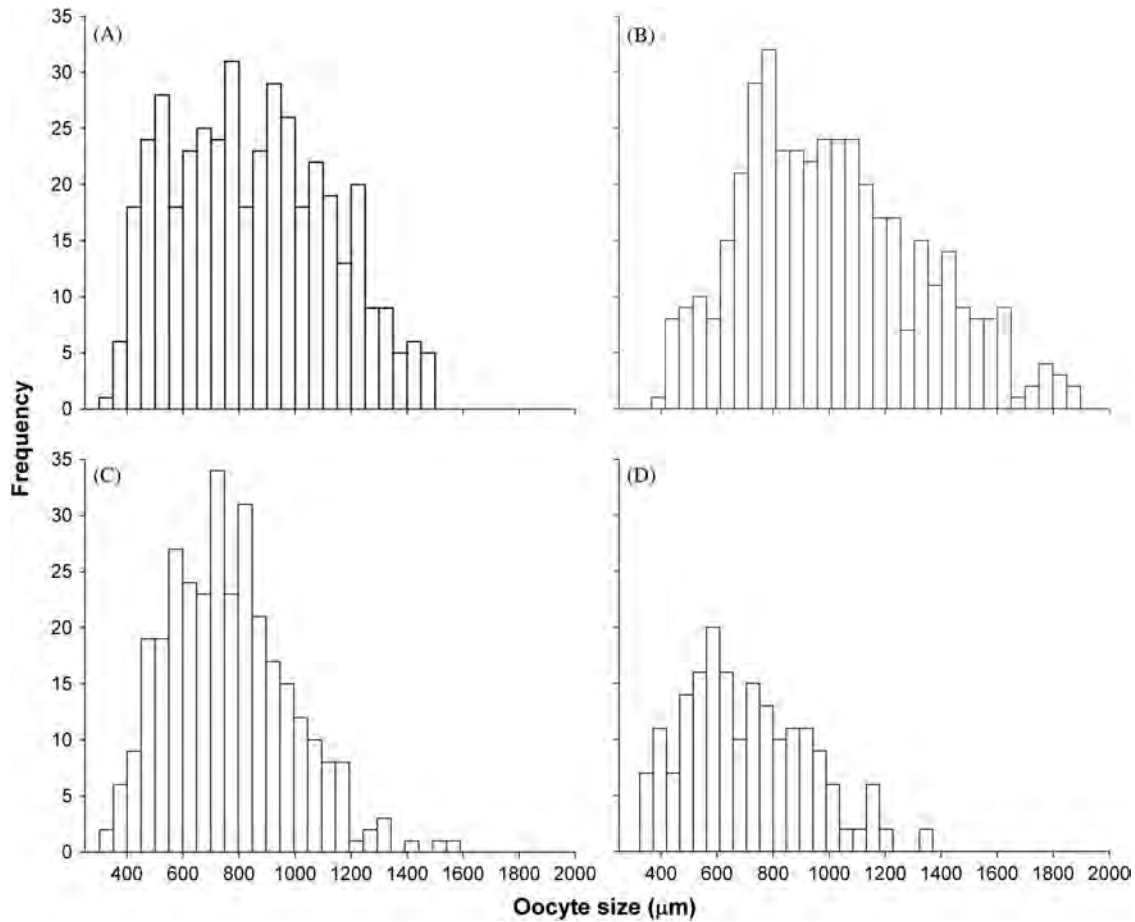


Fig. 4. Oocyte size distributions for (A) shallow-water *Solaster endeca*; (B) deep-water *S. endeca*; (C) shallow-water *Henricia sanguinolenta*; (D) deep-water *H. sanguinolenta*.

Table 2
Proportion of lipid classes (% of total lipids) in decreasing order of contribution (mean ± SD) in the gonads of *Solaster endeca* and *Henricia sanguinolenta*.

<i>S. endeca</i>		<i>H. sanguinolenta</i>	
Triacylglycerols	64.0 ± 11	Phospholipids	32.0 ± 24
Free fatty acids	13.0 ± 9	Free fatty acids	22.0 ± 15
Acetone mobile polar lipids	7.9 ± 3.4	Triacylglycerols	17.0 ± 26
Phospholipids	5.9 ± 2.4	Acetone polar mobile lipids	11.6 ± 4.4
Sterols	5.7 ± 1.3	Sterols	10.2 ± 7.1
Hydrocarbons	2.3 ± 1.6	Hydrocarbons	4.0 ± 4.1
Wax esters	0.4 ± 1.0	Wax esters	1.4 ± 3.2
Alcohols	0.1 ± 0.2	Alcohols	1.1 ± 2.4

20:1n-9 and 24:1 were also present in proportions > 1% in both species (Table 3).

The cluster analysis (Fig. 7A) showed a clear distinction between the fatty acid profiles of *S. endeca* and *H. sanguinolenta* and between shallow and deep *S. endeca* samples; however there was no distinction between fatty acid profiles of shallow and deep samples of *H. sanguinolenta* or between those of gonad tissue and oocytes in *S. endeca* at either depth. Comparing the fatty acid profiles of shallow and deep *S. endeca* against those of three deep-sea carnivorous asteroids studied by Howell et al. (2003) showed that deep *S. endeca* were more similar to shallow conspecifics than to other deep-sea species (Fig. 7B).

Similarity percentage (SIMPER) analyses identified fatty acids accounting for 90% of the differences between *S. endeca* and *H. sanguinolenta* gonad samples (Table 4) and between shallow

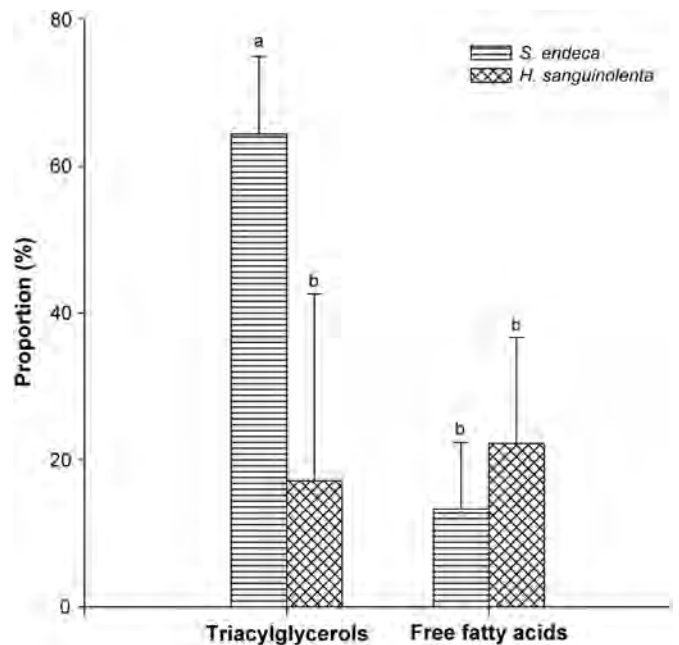


Fig. 5. Proportion (% of total lipids) of triacylglycerols and free fatty acids in the gonads of *Solaster endeca* and *Henricia sanguinolenta*. Data are mean ± SD. Bars with different letters are significantly different (two-way ANOVA, Holm-Sidak, $p < 0.05$).

and deep *S. endeca* gonad samples (Table 5). Between species: 24:1, 16:0, 20:1n-9, 22:1n-9, 22:1n-11, 17:1, ai15:0, 22:6n-3 and ai17:0 exhibited higher levels in *S. endeca*, while 20:5n-3,

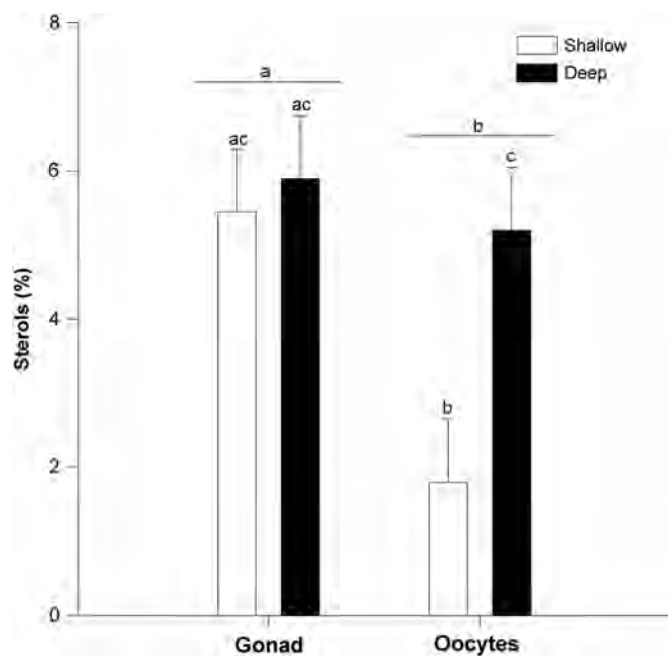


Fig. 6. Comparison of sterol proportions (% of total lipids) in *Solaster endeca*, showing the effect of depth and tissue. Data are mean \pm SD. Bars or groups of bars with different letters are significantly different (two-way ANOVA, Holm-Sidak, $p < 0.05$).

Table 3

Proportion (% of total fatty acids) of dominant fatty acids ($> 1\%$, mean \pm SD) in the gonads of *Solaster endeca* and *Henricia sanguinolenta*.

<i>S. endeca</i>		<i>H. sanguinolenta</i>	
20:5n-3	13.9 \pm 6.0	20:5n-3	18.4 \pm 6.9
20:4n-6	9.6 \pm 3.8	18:1n-7	14.8 \pm 5.2
18:1n-7	9.3 \pm 2.9	20:4n-6	11.9 \pm 4.0
24:1	5.8 \pm 1.8	18:0	6.7 \pm 3.3
16:0	4.4 \pm 1.0	20:2n-6	5.4 \pm 4.7
20:1n-9	4.4 \pm 0.9	18:3n-3	2.5 \pm 2.5
22:1n-9	1.9 \pm 0.6	20:1n-9	2.1 \pm 0.7
18:0	1.7 \pm 0.4	18:3n-4	1.4 \pm 1.3
22:1n-11	1.5 \pm 0.7	16:0	1.3 \pm 1.0
17:1	1.1 \pm 1.3	24:1	1.2 \pm 1.7
ai15:0	1.1 \pm 0.7	18:3n-6	1.1 \pm 0.6
22:6n-3	1.0 \pm 0.5		

18:1n-7, 18:0, 20:2n-6, 20:4n-6, 18:3n-3, 18:3n-6, 18:3n-4, 20:4n-3, i16:0 and 20:3n-6 were higher in *H. sanguinolenta*. Between depths in *S. endeca* gonads: 20:5n-3, 18:1n-7, 17:1, ai15:0, 20:1n-9, 22:1n-9 and ai17:0 exhibited higher levels in shallow samples, while 20:4n-6, 24:1, 16:0, i15:0, 22:1n-11, 18:0, 22:6n-3, 22:1n-7, i17:0 and 16:2n-4 were higher in deep samples.

A few significant differences were evident in comparisons of fatty acid classes and specific signatures in (1) *S. endeca* and *H. sanguinolenta* gonad samples and (2) shallow and deep *S. endeca* gonad samples. Between species: Σ MUFA and the zooplankton signature were higher in *S. endeca* ($t=5.61$ and 6.25 , $df=9$, $p < 0.001$), while Σ SAFA ($t=-3.80$, $p=0.004$), Σ PUFA ($U=0.00$, $p=0.004$) and terrestrial signature ($U=0.00$, $p=0.004$) were higher in *H. sanguinolenta*. Between depths in *S. endeca*: $\Sigma n-3$ and P/S ($t=-4.95$ and 5.83 , $df=4$, $p=0.002$ and 0.004) were higher in shallow specimens, while Σ SAFA and the zooplankton signature were higher in deeper specimens ($t=-4.95$ and -2.98 , $p=0.008$ and 0.041). No significant differences were found either between species or between depths in *S. endeca* for the ratio of DHA/EPA in gonad tissue. In all samples this ratio was well below 1 (< 0.21).

4. Discussion

While eurybathic macrobenthic species are not uncommon, the mechanisms that allow them to colonize a wide range of depths successfully remain poorly known. Comparisons are particularly scarce for ranges that extend from shallow to deep waters. The present study highlights differences in how certain echinoderms modulate reproductive investment in shallow subtidal (< 20 m) versus bathyal (> 850 – 1450 m) environments. The sea cucumber *C. frondosa* appears to have the weakest tolerance to depths; the rare specimens found at bathyal depths are clearly impacted by the effects of increasing depth, based on their thin body wall and small underdeveloped gonads. In contrast, the sea star *H. sanguinolenta* is more uniformly distributed between shallow and deep environments and has equally well developed reproductive tissues in both. *S. endeca* exhibits an intermediate adaptation state with increased reproductive investment at greater depth. Parallels can be drawn with the different feeding modes of the three species (strict planktivory, mixed planktivory/carnivory and strict carnivory, respectively). The lipid contents and fatty acid biomarkers found in the reproductive tissues of the two sea stars reflect both their specific diets and distinct reproductive modes (brooding vs broadcast spawning).

4.1. Reproductive traits

The GI was significantly higher in shallow-water than in deep-water specimens of *C. frondosa* by nearly an order of magnitude (0.26 vs 0.04). Both the body wall and gonad were also heavier in shallow specimens. The fact that the deep-water specimens examined had underdeveloped gonads suggests that depths > 1200 m are at the edge of the normal distribution of *C. frondosa* (which has not been explicitly reported at these depths before). In the literature, this commercial species is typically associated with depths between 10 and > 300 m without any specific lower limit (Coady, 1973; So et al., 2011; Therkildsen and Petersen, 2006). Its growth and reproductive output may be limited at greater depths due to reduced nutritional input, as suggested previously in other species (Rex and Etter, 1998; Rex et al., 2006). Hamel and Mercier (1998) have shown that the feeding behavior of *C. frondosa* is triggered by food (phytoplankton) availability, supporting this assumption. Furthermore, long periods of starvation are known to cause shrinkage of body wall and muscle bands in this species (Hamel and Mercier, 1996), similar to what was observed here in the deep specimens. Thus, smaller gonads and the absence of gametes in deep-water *C. frondosa* are likely to be caused by insufficient fresh phytoplanktonic resources at bathyal depths, resulting in these individuals having little or no reproductive capability. These sterile individuals may have developed from larvae originating from shallow-water populations (So et al., 2011) in a scheme consistent with the boundary of vegetative life presented by Bhaud (2000).

In contrast, a complete developmental cycle is possible in both sea stars (*S. endeca* and *H. sanguinolenta*) across their full depth range. However, the two species showed different trade-offs between relative fecundity and oocyte size. *S. endeca* produced marginally larger oocytes (848–1014 μ m) than *H. sanguinolenta* (706–761 μ m) at both depths and consequently there were fewer oocytes per gram of gonad in the former species. Interspecific (but not intraspecific) results are consistent with those obtained by Marshall et al. (2000) and Ito (1997) in other marine invertebrates, which showed a positive correlation between oocyte size and the average adult size. *S. endeca* had a mean body weight of 149 g for shallow and 126 g for deep specimens, and *H. sanguinolenta* of 1.8 g for shallow and 1.3 g for deep specimens (with no significant difference between depths for either species).

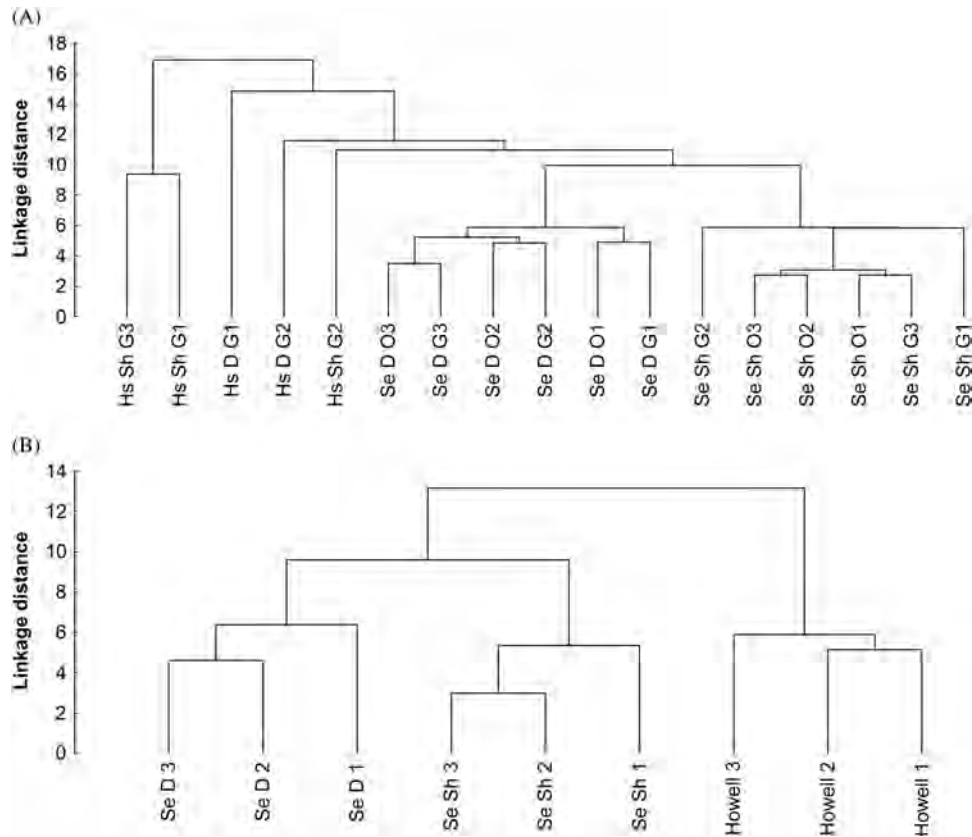


Fig. 7. (A) Cluster analysis of fatty acid profiles among samples in this study. (B) Cluster analysis of fatty acid profiles in *Solaster endeca* (gonad samples) and 3 carnivorous deep-sea asteroids studied by Howell et al. (2003). Hs=*Henricia sanguinolenta*, Se=*Solaster endeca*, Sh=shallow, D=deep, G=gonad, O=oocytes, Howell 1=*Dytaster grandis grandis*, Howell 2=*Bathybiaster vexillifer*, Howell 3=*Hymenaster membranaceus*.

Table 4

Summary of fatty acids accounting for 90% dissimilarity between the gonad tissues of *Solaster endeca* and *Henricia sanguinolenta*.

Fatty Acid	Proportion (%)		Average dissimilarity	Dissimilarity/SD	Contribution (%)	Cumulative (%)
	<i>S. endeca</i>	<i>H. sanguinolenta</i>				
20:5n-3	13.95	18.38	5.53	1.50	13.89	13.89
18:1n-7	9.29	14.84	4.32	1.25	10.85	24.74
18:0	1.68	6.67	3.67	2.10	9.21	33.95
20:2n-6	0.62	5.41	3.45	1.11	8.67	42.61
24:1	5.80	1.23	3.24	2.08	8.15	50.76
20:4n-6	9.60	11.86	3.14	1.41	7.87	58.63
16:0	4.40	1.34	2.17	2.27	5.45	64.08
18:3n-3	0.12	2.49	1.65	1.05	4.14	68.22
20:1n-9	4.39	2.09	1.63	2.12	4.09	72.32
22:1n-9	1.94	0.22	1.20	2.94	3.02	75.34
22:1n-11	1.49	0.26	0.87	1.74	2.19	77.53
17:1	1.13	0.66	0.75	1.14	1.89	79.41
18:3n-6	0.05	1.06	0.71	1.89	1.78	81.19
18:3n-4	0.48	1.36	0.65	0.74	1.64	82.83
20:4n-3	0.22	0.88	0.59	0.63	1.49	84.31
ai15:0	1.08	0.37	0.56	1.35	1.41	85.72
22:6n-3	1.03	0.39	0.55	1.73	1.39	87.11
ai17:0	0.89	0.46	0.45	1.43	1.13	88.25
i16:0	0.57	0.95	0.43	1.53	1.07	89.32
20:3n-6	0.03	0.62	0.41	1.32	1.03	90.35

The proportion of triacylglycerols and the total lipid contents of gonads were significantly higher in *S. endeca* (~64% and ~644 mg g⁻¹, respectively) than in *H. sanguinolenta* (~17% and ~61 mg g⁻¹), indicating a relationship between oocyte size and lipid content. Falkner et al. (2006) and Prowse et al. (2008) found that larger lecithotrophic eggs in an ophiuroid and some asteroids had higher total lipid densities, due largely to higher proportions

of triacylglycerols, the major energy storage molecule in lecithotrophic larvae. This supports the claim that higher proportions of triacylglycerols, and greater total lipid densities, are required by larger species to produce larger oocytes. This also supports the finding of Prowse et al. (2008), that broadcasted lecithotrophic eggs (such as in *S. endeca*) have significantly higher triacylglycerol proportions than in brooded eggs (such as in *H. sanguinolenta*).

Table 5Summary of fatty acids accounting for 90% of the dissimilarity between the gonad tissues of shallow and deep specimens of *Solaster endeca*.

Fatty acid	Proportion (%)		Average dissimilarity	Dissimilarity/SD	Contribution (%)	Cumulative (%)
	Shallow	Deep				
20:5n-3	19.14	8.76	8.08	4.05	27.60	27.60
20:4n-6	7.25	11.96	4.04	1.69	13.79	41.39
18:1n-7	11.72	6.85	3.80	3.06	12.99	54.38
24:1	5.60	6.01	1.68	2.17	5.72	60.11
16:0	3.55	5.25	1.33	2.57	4.55	64.66
17:1	1.74	0.52	1.18	1.24	4.02	68.68
ai15:0	1.74	0.42	1.03	6.51	3.52	72.20
20:1n-9	4.67	4.10	0.78	1.17	2.67	74.87
22:1n-9	2.44	1.44	0.78	3.65	2.67	77.54
ai17:0	1.33	0.44	0.70	3.51	2.38	79.91
i15:0	0.22	1.05	0.65	7.62	2.21	82.13
22:1n-11	1.09	1.88	0.62	1.04	2.10	84.23
18:0	1.39	1.98	0.46	3.04	1.57	85.80
22:6n-3	1.01	1.04	0.41	1.59	1.39	87.19
22:1n-7	0.30	0.83	0.41	2.65	1.39	88.57
i17:0	0.18	0.64	0.36	4.76	1.22	89.79
16:2n-4	0.33	0.76	0.34	3.90	1.15	90.95

There may also be a link with the diets of the two species: echinoderm-based vs sponge-based, respectively.

Consistent with the different reproductive traits evident above in the two sea star species, different intraspecific relationships between reproduction metrics and depth were also seen. Females of *H. sanguinolenta* had marginally smaller oocytes (mean of 706 vs 761 μm) and higher fecundity as RPF (2844 vs 1712 oocytes g^{-1} of gonad) deeper, with no difference in GI (0.14 and 0.13), indicating a trade-off between oocyte size and the number of eggs produced. This agrees with previous findings showing that decreased nutritional inputs at depth caused the production of smaller oocytes in deep-sea specimens compared with conspecifics from shallow waters (Laptikhovskiy, 2006). In contrast, Féral et al. (1990) showed reproductive traits such as oocytes size were independent of depth in the sea urchin *Brissopsis lyrifera* studied between 60 and 1000 m. In a study of the deep-water asteroid *Henricia lisa*, comparing samples from 600 and 1300 m, maximum oocyte size was also similar at both depths; however the GI was much lower in deeper specimens and female fecundity roughly five times higher in shallower specimens (Mercier and Hamel, 2008). The present study showed that females of *S. endeca* from the deep had marginally larger oocytes (mean of 1014 vs 848 μm), but no difference in either RPF or GI between depths. It suggests that *S. endeca* may be able to allocate more resources to oocyte production in the deep sea without sacrificing quantity, as also seen in the squid *Loligo gahi* by Laptikhovskiy et al. (2002). Although not significant, there was a graphical trend towards a higher GI in deep than in shallow *S. endeca*. This would allow *S. endeca* to produce equal numbers of larger oocytes in the deep by increasing the total weight of gonads (i.e. greater allocation to reproduction). Overall, this species appears to be well suited to bathyal depths, where water remains cold year round and where competition for prey may be lower than in the subtidal zone.

In *S. endeca*, there were more sterols in gonads than oocytes in shallow specimens, and inversely more sterols in oocytes from deep than from shallow specimens. The gonads of *S. endeca* showed no difference in sterol proportions between depths, whereas the proportion of sterols in the oocytes was significantly higher in deep than in shallow specimens. Robertson and Hazel (1995) found a strong positive correlation between environmental temperature and proportion of sterols (cholesterol) in a lipid membrane. However, it is unlikely that our data represent lipid proportions in membranes given the low ratio of phospholipids to triacylglycerols in *S. endeca* gonad (C. Parrish, pers. comm.).

The secondary function of sterols in asteroids was recently studied by Guenther et al. (2009), who found that they aid in chemical anti-fouling defences against organisms such as diatoms and bryozoans. Sterol results for *S. endeca* may thus reflect a contrast in the need for anti-fouling protection in adults and offspring as depth increases and substrata to colonize become scarcer, i.e. the bathyal zone in eastern Canada is dominated by soft bottoms (Baker et al., 2012).

4.2. Diets

High proportions of free fatty acids (FFAs) indicate phospholipid and triacylglycerol breakdown, high lipolytic and enzyme activity that can either be natural or due to sample treatment (Drazen et al., 2008). The fact that differences observed between shallow and deep specimens were not consistent across the two asteroid species minimizes the possibility that the results were biased by sample treatment. Nevertheless, it is possible that the significantly higher and more variable proportion of FFAs in deep specimens may partly result from a longer storage period before analysis for these samples. The highest FFA proportion occurred in deep *H. sanguinolenta* specimens ($36.9 \pm 5.5\%$), possibly indicating that the recorded triacylglycerol proportion is lower than what would have been found in fresh specimens. Furthermore, while dietary markers are now widely being used (e.g. Drazen et al., 2008; Howell et al., 2003) we recognize that they were primarily developed in epipelagic food webs and that interpretations in different systems must be made cautiously.

The gonads of *S. endeca* and *H. sanguinolenta* were both dominated by EPA, 18:1n-7 and ARA. High levels of EPA, an essential fatty acid in aquatic food webs (Parrish, 2009), indicate an abundance of diatoms in their diets, or in the diets of their prey. The latter is most likely for *S. endeca*, which is reported to feed on holothuroids (Gaymer et al., 2004) with herbivorous diets (Hamel and Mercier, 1998; Parrish, 2009). *H. sanguinolenta* is known to feed on sponges (Sheild, 1990; Sheild and Witman, 1993) and has been identified as a suspension feeder (Anderson, 1960; Rasmussen, 1965; as cited in Sheild and Witman, 1993), therefore accumulating EPA directly and through sponges (Thurber, 2007). The high level of EPA in both species is reflected in their low mean DHA/EPA ratios (< 1). The seemingly larger ratio in *S. endeca*, although not significant, may represent slight trophic magnification due to their strict carnivorous diet (Gaymer et al., 2004). Within *S. endeca* there was more EPA in the gonads of

shallow (19%) than deep (9%) specimens, with a parallel trend in $n-3$ fatty acid proportions (22% and 15%, respectively) since EPA comprised 61–85% of the $n-3$ fatty acids in its gonads. However, there was no variation of the DHA/EPA ratio with depth. This may indicate a similarity in available phytoplankton across depths (including phytodetritus in deeper areas) as also suggested by Féral et al. (1990) for *B. lyrifera*. Overall, the $n-3$ fatty acid proportions were relatively low in the gonads of both *S. endeca* and *H. sanguinolenta* when compared to other taxa (~27.5–41.0%), consistent with the findings of Copeman and Parrish (2003).

Copeman and Parrish (2003) and Joseph (1989) found that echinoderms (*Pteraster* sp., *Ophiura sarsi*, *Chiridota laevis*, *Ctenodiscus crispatus*) have unique fatty acid signatures with increased proportions of ARA and bacterial signatures (e.g. 18:1 $n-7$; Drazen et al., 2008), although bacterial signatures are typically lower in carnivores (Copeman and Parrish, 2003). The high bacterial signatures in *S. endeca* and *H. sanguinolenta* may come from their respective prey (Parrish, 2009; Thurber, 2007) and from complementary suspension feeding in *H. sanguinolenta* (Anderson, 1960; Rasmussen, 1965; as cited in Sheild and Witman, 1993), because high bacterial signatures are associated with non-selective detritivores (Shick et al., 1981).

The total proportions of saturated fatty acids (SAFAs) and polyunsaturated fatty acids (PUFAs) are indicative of diets centered on phytoplankton, algae and phytodetritus (Sargent et al., 1987; Volkman et al., 1989), while proportions of monounsaturated fatty acids (MUFAs) and zooplankton signature are indicative of predominantly carnivorous diets (Drazen et al., 2008). This distinction between the diets of *S. endeca* and *H. sanguinolenta* is clearly seen in gonad fatty acid profiles. The significantly larger proportions of MUFAs (47%) and zooplankton signature (25%) in *S. endeca* than *H. sanguinolenta* further highlight the strict carnivorous diet of *S. endeca* (Gaymer et al., 2004), while the significantly larger proportions of SAFAs, PUFAs and terrestrial plant signatures in *H. sanguinolenta* reflect its opportunistic suspension feeding (Anderson, 1960; Rasmussen, 1965; as cited in Sheild and Witman, 1993). Also, among the fatty acids contributing most to the dissimilarity between species 20:1 $n-9$, 22:1 $n-11$, ai15:0 and ai17:0 (indicating carnivory and bacteria; Drazen et al., 2008; Sargent et al., 1987) were more abundant in *S. endeca*, while 20:5 $n-3$, 18:3 $n-3$ and 18:3 $n-6$ (indicating suspension feeding; Parrish, 2009; Sargent et al., 1987; Volkman et al., 1989) were more abundant in *H. sanguinolenta*.

A total of 17 fatty acids were found to account for 90% of the dissimilarity across depths in the gonad tissue of *S. endeca*. In addition, three fatty acid classes (saturated FA, $n-3$ and zooplankton signature) and one ratio (P/S) showed significant differences across depths. EPA and $\Sigma n-3$ fatty acids were higher in shallow specimens, while 16:0, DHA and Σ SAFAs were higher in deep specimens, but all are consistent with phytoplankton, algae or phytodetritus in the diet (Parrish et al., 2005; Sargent et al., 1987; Volkman et al., 1989). In shallow specimens there was a higher ratio of P/S, which was used by Cripps and Atkinson (2000) to identify carnivory in krill, and deep *S. endeca* had a higher proportion of zooplankton signature. Although the latter is still consistent with carnivory, it may indicate a shift in prey type, perhaps from *C. frondosa* (a preferred prey in subtidal areas) to other more readily available species of echinoderms. Moreover, proportions of ai15:0, ai17:0 and 18:1 $n-7$ were greater in shallow specimens while i15:0 and i17:0 were more abundant in deep specimens, all of which indicate bacteria in the diet (Drazen et al., 2008; Sargent et al., 1987). It is therefore likely that diets differ with depth due either to a difference in local resources or to selectivity. The cluster analysis clearly highlighted this dissimilarity. Furthermore, analyzing similarity between shallow

and deep *S. endeca* gonads (present study) along with tissue samples from three deep-sea carnivorous asteroids (Howell et al., 2003) showed that the diet of deep *S. endeca* is more similar to shallow *S. endeca* than to other deep-sea asteroids. While methodological discrepancies cannot be ruled out, it suggests a difference between cold-adapted eurybathic species that occur from the surface to bathyal depths (like *S. endeca*) and species typical of the deep sea (900–4840 m; Howell et al., 2003).

4.3. Outlook

The diet of each species dictates what nutrients and lipids are available for incorporation into oocyte production, which may alter the optimal size (surface area to volume ratio) of oocytes or number per gonad unit (RPF). The strictly planktivorous *C. frondosa* apparently fails to invest in reproduction in deep locations where fresh phytoplankton is scarce. Results for *H. sanguinolenta* evoke a mixed diet with no clear bathymetric shift, although the increased number and smaller size of oocyte produced with depth may reflect a difference in nutritional input. Finally, the carnivorous *S. endeca* exhibits a clear bathymetric shift in diet. Does a shift in prey type at depth underlie the ability of *S. endeca* to maintain/increase oocyte size without significantly sacrificing fecundity? Are the somewhat larger oocytes in deep-water *S. endeca* made possible by the increased MUFA and zooplankton signature proportions? If so, divergent feeding modes might drive divergent reproductive modes. Alternatively, specific requirements for reproduction may modulate shifts in feeding modes.

Overall, diet appears to influence the lipid and fatty acid contents of gonads, especially since the proportions of sterols, EPA, $\Sigma n-3$, Σ SAFA, Σ PUFA and P/S were all contrary to what would be expected regarding membrane fluidity. The high triacylglycerol proportion in *S. endeca* provides an explanation for this, since membrane fluidity is usually only reflected in fatty acid proportions when the lipid sample is dominated by phospholipids (Chris Parrish, pers. comm.). A more exhaustive bathymetric analysis of *H. sanguinolenta* gonads, which were dominated by phospholipids, might help demonstrate how fatty acids change across depths to accommodate for environmental changes and membrane fluidity.

Acknowledgments

We thank B. Wigham and an anonymous reviewer for constructive comments on the manuscript. We also thank Z. Sun and S. Baillon for helping with various protocols, J. Wells and C. Parrish for lipid analyses, as well as Fisheries and Oceans Canada and the OSC Field Services for helping with sample collections. This research was partly supported by grants from the Natural Sciences and Engineering Research Council of Canada and Canada Foundation for Innovation to A.M.

References

- Anderson, J.M., 1960. Histological studies on the digestive system of a starfish, *Henricia*, with notes on Tiedemann's pouches in starfishes. *Biol. Bull.* 119 (3), 371–398.
- Baker, K.D., Wareham, V.E., Snelgrove, P.V.R., Haedrich, R.L., Fifield, D.A., Edinger, E.N., Gilkinson, K.D., 2012. Distributional patterns of deep-sea coral assemblages in three submarine canyons off Newfoundland, Canada. *Mar. Ecol. Prog. Ser.* 445, 235–249.
- Bhaid, M.R., 2000. Some examples of the contribution of planktonic larval stages to the biology and ecology of polychaetes. *Bull. Mar. Sci.* 67 (1), 345–358.
- Coady, L.W., 1973. Aspects of the Reproductive Biology of *Cucumaria frondosa* (Gunnerus, 1770) and *Psolus fabricii* (Düben and Koren, 1846) (Echinodermata:

- Holothuroidea) in Shallow Waters of the Avalon Peninsula, Newfoundland. M.Sc. Thesis, Memorial University of Newfoundland, St. John's.
- Copeman, L.A., Parrish, C.C., 2003. Marine lipids in a cold coastal ecosystem: Gilbert Bay. *Labrador. Mar. Biol.* 143 (6), 1213–1227.
- Cripps, G.C., Atkinson, A., 2000. Fatty acid composition as an indicator of carnivory in Antarctic krill, *Euphausia superba*. *Can. J. Fish. Aquat. Sci.* 57 (S3), 31–37.
- Drazen, J.C., Phleger, C.F., Guest, M.A., Nichols, P.D., 2008. Lipid, sterols and fatty acid composition of abyssal holothurians and ophiuroids from the North-East Pacific Ocean: food web implications. *Comp. Biochem. Physiol. B* 151 (1), 79–87.
- Falkner, I., Byrne, M., Sewell, M.A., 2006. Maternal provisioning in *Ophioneis fasciata* and *O. schayeri*: brittle stars with contrasting modes of development. *Biol. Bull.* 211 (3), 204–207.
- Féral, J.-P., Ferrand, J.-G., Guille, A., 1990. Macrobenthic physiological responses to environmental fluctuations: the reproductive cycle and enzymatic polymorphism of a eurybathic sea-urchin on the northwestern Mediterranean continental shelf and slope. *Cont. Shelf Res.* 10 (9–11), 1147–1155.
- Fernández, C., 1997. Effect of diet on the biochemical composition of *Paracentrotus lividus* (Echinodermata: Echinoidea) under natural and rearing conditions (effect of diet on biochemical composition of urchins). *Comp. Biochem. Physiol. A* 118 (4), 1377–1384.
- Gage, J.D., Tyler, P.A., 1992. *Deep-Sea Biology: A Natural History of Organisms at the Deep-Sea Floor*. Cambridge University Press, Cambridge, UK.
- Gaymer, C.F., Dutil, C., Himmelman, J.H., 2004. Prey selection and predatory impact of four major sea stars on a soft bottom subtidal community. *J. Exp. Mar. Biol. Ecol.* 313 (2), 353–374.
- Giese, A.C., Pearse, J.S., Pearse, V.B. (Eds.), 1991. *Reproduction of Marine Invertebrates*. Boxwood Press, Pacific Grove, CA, USA.
- Guenther, J., Wright, A.D., Burns, K., De Nys, R., 2009. Chemical antifouling defences of sea stars: effects of the natural products hexadecanoic acid, cholesterol, lathosterol and sitosterol. *Mar. Ecol. Prog. Ser.* 385, 137–149.
- Hamel, J.-F., Mercier, A., 1996. Evidence of chemical communication during the gametogenesis of holothurians. *Ecology* 77 (5), 1600–1616.
- Hamel, J.-F., Mercier, A., 1998. Diet and feeding behaviour of the sea cucumber *Cucumaria frondosa* in the St Lawrence Estuary, eastern Canada. *Can. J. Zool.* 76 (6), 1194–1198.
- Hammer, H., Hammer, B., Watts, S., Lawrence, A., Lawrence, J., 2006. The effect of dietary protein and carbohydrate concentration on the biochemical composition and gametogenic condition of the sea urchin *Lytechinus variegatus*. *J. Exp. Mar. Biol. Ecol.* 334 (1), 109–121.
- Howell, K.L., Pond, D.W., Billett, D.S.M., Tyler, P.A., 2003. Feeding ecology of deep-sea seastars (Echinodermata: Asteroidea): a fatty-acid biomarker approach. *Mar. Ecol. Prog. Ser.* 255, 193–206.
- Ito, K., 1997. Egg-size and -number variations related to maternal size and age, and the relationship between egg size and larval characteristics in an annual marine gastropod, *Halio japonica* (Opisthobranchia; Cephalaspidea). *Mar. Ecol. Prog. Ser.* 152 (1–3), 187–195.
- Joseph, J.D., 1989. Distribution and composition of lipids in marine invertebrates. In: Ackman, R.G. (Ed.), *Marine Biogenic Lipids, Fats and Oils*, vol. II. CRC Press, Boca Raton, FL, pp. 49–143.
- Laptikhovskiy, V., 2006. Latitudinal and bathymetric trends in egg size variation: a new look at Thorson's and Rass's rules. *Mar. Ecol. Prog. Ser.* 27 (1), 7–14.
- Laptikhovskiy, V.V., Arkhipkin, A.I., Middleton, D.A.J., Butcher, L.R., 2002. Ovary maturation and fecundity of the squid *Loligo gahi* on the southeast shelf of the Falkland Islands. *Bull. Mar. Sci.* 71 (1), 449–464.
- Lawrence, J.M., McClintock, J.B., 1994. Energy acquisition and allocation by echinoderms (Echinodermata) in polar seas: adaptations for success. *Echinoderms Through Time*. Balkema Press, Rotterdam, pp. 39–52.
- Liyana-Pathirana, C., Shahidi, F., Whittick, A., 2002. The effect of an artificial diet on the biochemical composition of the gonads of the sea urchin (*Strongylocentrotus droebachiensis*). *Food Chem.* 79 (4), 461–472.
- Mah, C., Hansson, H., 2012. *Henricia sanguinolenta*. In: Mah, C.L. (Ed.), *World Asteroidea Database*, accessed through: World Register of Marine Species at <<http://www.marinespecies.org/aphia.php?p=taxdetails&id=123974>> (accessed 02-01-2013).
- Marshall, D.J., Styan, C.A., Keough, M.J., 2000. Intraspecific co-variation between egg and body size affects fertilisation kinetics of free-spawning marine invertebrates. *Mar. Ecol. Prog. Ser.* 195, 305–309.
- McEdward, L.R., Coulter, L.K., 1987. Egg volume and energetic content are not correlated among sibling offspring of starfish: implications for life-history theory. *Evolution* 41 (4), 914–917.
- McEdward, L.R., Carson, S.F., 1987. Variation in egg organic content and its relationship with egg size in the starfish *Solaster stimpsoni*. *Mar. Ecol. Prog. Ser.* 37, 159–169.
- McEdward, L.R., Chia, F.-S., 1991. Size and energy content of eggs from echinoderms with pelagic lecithotrophic development. *J. Exp. Mar. Biol. Ecol.* 147 (1), 95–102.
- McEdward, L.R., Morgan, K.H., 2001. Interspecific relationships between egg size and the level of parental investment per offspring in echinoderms. *Biol. Bull.* 200 (1), 33–50.
- Mercier, A., Hamel, J.-F., 2008. Depth-related shift in life history strategies of a brooding and broadcasting deep-sea asteroid. *Mar. Biol.* 156, 205–223.
- Mercier, A., Hamel, J.-F., 2009. Endogenous and exogenous control of gametogenesis and spawning in echinoderms. *Adv. Mar. Biol.* 55, 1–302.
- Metaxas, A., Davis, J., 2005. Megafauna associated with assemblages of deep-water gorgonian corals in Northeast Channel, off Nova Scotia, Canada. *J. Mar. Biol. Assoc. UK* 85 (6), 1381–1390.
- Moran, A.L., McAlister, J.S., 2009. Egg size as a life history character of marine invertebrates: is it all it's cracked up to be? *Biol. Bull.* 216 (3), 226–242.
- Parrish, C.C., 1987. Time series of particulate and dissolved lipid classes during spring phytoplankton blooms in Bedford Basin, a marine inlet. *Mar. Ecol. Prog. Ser.* 35, 129–139.
- Parrish, C.C., 1999. Determination of total lipid, lipid classes, and fatty acids in aquatic samples. In: Arts, M., Wainman, B. (Eds.), *Lipids in Freshwater Ecosystems*. Springer-Verlag, New York, pp. 4–20.
- Parrish, C.C., Thompson, R.J., Deibel, D., 2005. Lipid classes and fatty acids in plankton and settling matter during the spring bloom in a cold ocean coastal environment. *Mar. Ecol. Prog. Ser.* 286, 57–68.
- Parrish, C.C., 2009. Essential fatty acids in aquatic food webs. In: Arts, M.T., Brett, M.T., Kainz, M.J. (Eds.), *Lipids in Aquatic Ecosystems*. Springer, New York, pp. 309–326.
- Prowse, T., Sewell, M., Byrne, M., 2008. Fuels for development: evolution of maternal provisioning in asterinid sea stars. *Mar. Biol.* 153 (3), 337–349.
- Rasmussen, B.N., 1965. On taxonomy and biology of the North Atlantic species of the asteroid genus *Henricia* Gray. *Medd. Dan. Fisk. Havunders.* 4, 157–213.
- Rass, T.S., 1986. Biogeographic rule of inverse relation between egg size and environmental temperature in poikilothermous animals (in Russian). *Trudy IOAN* 116, 152–168.
- Rex, M.A., 1981. Community structure in the deep-sea benthos. *Annu. Rev. Ecol. Syst.* 12 (1), 331–353.
- Rex, M.A., Etter, R.J., 1998. Bathymetric patterns of body size: implications for deep-sea biodiversity. *Deep-Sea Res. II* 45 (1–3), 103–127.
- Rex, M.A., Etter, R.J., Morris, J.S., Crouse, J., McClain, C.R., Johnson, N.A., Stuart, C.T., Deming, J.W., Thies, R., Avery, R., 2006. Global bathymetric patterns of standing stock and body size in the deep-sea benthos. *Mar. Ecol. Prog. Ser.* 317, 1–8.
- Robertson, J.C., Hazel, J.R., 1995. Cholesterol content of trout plasma membranes varies with acclimation temperature. *Am. J. Physiol.-Reg. I* 269 (5), R1113–R1119.
- Sargent, J.R., Parkes, R.J., Mueller-Harvey, I., Henderson, R.J., 1987. Lipid biomarkers in marine ecology. In: Sleight, M.A. (Ed.), *Microbes the Sea*. Ellis Horwood Limited, Chichester, UK, pp. 119–138.
- Sheild, C.J., 1990. Predation by the Sea Star, *Henricia sanguinolenta* (Echinodermata, Asteroidea), with Special Attention to its Effect on Sponges. MSc Thesis, Northeastern University, Boston, MA.
- Sheild, C.J., Witman, J.D., 1993. The impact of *Henricia sanguinolenta* (O. F. Mueller) (Echinodermata: Asteroidea) predation on the finger sponges, *Isodictya* spp. *J. Exp. Mar. Biol. Ecol.* 166 (1), 107–133.
- Shick, J.M., Edwards, K.C., Dearborn, J.H., 1981. Physiological ecology of the deposit-feeding sea star *Ctenodiscus crispatus*: ciliated surfaces and animal–sediment interactions. *Mar. Ecol. Prog. Ser.* 5, 165–184.
- So, J.J., Uthicke, S., Hamel, J.F., Mercier, A., 2011. Genetic population structure in a commercial marine invertebrate with long-lived lecithotrophic larvae: *Cucumaria frondosa* (Echinodermata: Holothuroidea). *Mar. Biol.* 158 (4), 859–870.
- Stein, M., 2007. Oceanography of the Flemish Cap and adjacent waters. *J. Northwest Atl. Fish. Sci.* 37, 135–146.
- Therkildsen, N.O., Petersen, C.W., 2006. A review of the emerging fishery for the sea cucumber *Cucumaria frondosa*: biology, policy, and future prospects. *South Pac. Comm. Beche-de-mer Inf. Bull.* 23, 16–25.
- Thorson, G., 1950. Reproductive and larval ecology of marine bottom invertebrates. *Biol. Rev.* 25, 1–45.
- Thurber, A.R., 2007. Diets of Antarctic sponges: links between the pelagic microbial loop and benthic metazoan food web. *Mar. Ecol. Prog. Ser.* 351, 77–89.
- Townsend, D.W., Thomas, A.C., Mayer, L.M., Thomas, M.A., Quinlan, J.A., 2006. Oceanography of the northwest Atlantic continental shelf (1, W). In: Robinson, A.R., Brink, K.H. (Eds.), *The Sea: The Global Coastal Ocean: Interdisciplinary Regional Studies and Syntheses*. Harvard University Press, Cambridge, MA, pp. 119–168.
- Villinski, J.T., Villinski, J.C., Byrne, M., Raff, R.A., 2002. Convergent maternal provisioning and life-history evolution in echinoderms. *Evolution* 56 (9), 1764–1775.
- Volkman, J.K., Jeffrey, S.W., Nichols, P.D., Rogers, G.I., Garland, C.D., 1989. Fatty acid and lipid composition of 10 species of microalgae used in mariculture. *J. Exp. Mar. Biol. Ecol.* 128 (3), 219–240.

C.A. Nordstrom, K.J. Benoit-Bird, B.C. Battaile and A.W. Trites	257	Northern fur seals augment ship-derived ocean temperatures with higher temporal and spatial resolution data in the eastern Bering Sea
J.A. Fall, N.S. Braem, C.L. Brown, L.B. Hutchinson-Scarborough, D.S. Koster and T.M. Krieg	274	Continuity and change in subsistence harvests in five Bering Sea communities: Akutan, Emmonak, Savoonga, St. Paul, and Togiak
H.P. Huntington, I. Ortiz, G. Noongwook, M. Fidel, D. Childers, M. Morse, J. Beaty, L. Alessa and A. Kliskey	292	Mapping human interaction with the Bering Sea ecosystem: Comparing seasonal use areas, lifetime use areas, and "calorie-sheds"
A. Fienup-Riordan, C. Brown and N.M. Braem	301	The value of ethnography in times of change: The story of Emmonak
H.P. Huntington, G. Noongwook, N.A. Bond, B. Benter, J.A. Snyder and J. Zhang	312	The influence of wind and ice on spring walrus hunting success on St. Lawrence Island, Alaska
H.P. Huntington, N.M. Braem, C.L. Brown, E. Hunn, T.M. Krieg, P. Lestenkof, G. Noongwook, J. Sepez, M.F. Sigler, F.K. Wiese and P. Zavadil	323	Local and traditional knowledge regarding the Bering Sea ecosystem: Selected results from five indigenous communities
D.A.N. Ross, J.-F. Hamel and A. Mercier	333	Bathymetric and interspecific variability in maternal reproductive investment and diet of eurybathic echinoderms